Membrane Science and Technology Series, 2

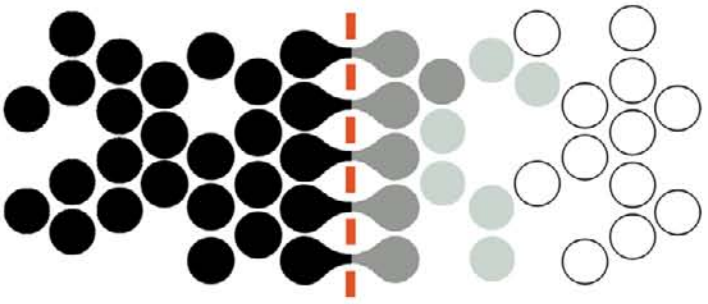

MEMBRANE SEPARATIONS TECHNOLOGY

PRINCIPLES AND APPLICATIONS

Edited by

R.D. NOBLE

S.A. STERN

ELSEVIER

MEMBRANE SEPARATIONS TECHNOLOGY
Principles and Applications

Membrance Science and Technology Series, 2

MEMBRANE SEPARATIONS TECHNOLOGY
Principles and Applications

Edited by

Richard D. Noble

Department of Chemical Engineering, University of Colorado, Boulder, CO 80309-0424,USA

and

S. Alexander Stern

Chemical Engineering and Materials Science Department, Syracuse University, Syracuse, NY 13244-1190, USA

ELSEVIER
Amsterdam - Boston - Heidelberg - London - New York - Oxford - Paris
San Diego - San Francisco - Singapore - Sydney - Tokyo

ELSEVIER SCIENCE B.V.
Sara Burgerhartstraat 25
P.O. Box 211, 1000 AE Amsterdam, The Netherlands

First edition 1995
Second impression 1999
Third impression 2003

Library of Congress Cataloging in Publication Data
A catalog record from the Library of Congress has been applied for.

British Library Cataloguing in Publication Data
A catalogue record from the British Library has been applied for.

ISBN: 0 444 81633 X

♾ The paper used in this publication meets the requirements of ANSI/NISO Z39.48-1992 (Permanence of Paper).
Printed in The Netherlands.

Preface

The field of membrane separation technology is presently in a state of rapid growth and innovation. Many different membrane separation processes have been developed during the past half century and new processes are constantly emerging from academic, industrial, and government laboratories. Microfiltration, which is very similar to conventional filtration, is probably the oldest and still the most widely used of these processes. Almost all other membrane separation processes found significant industrial applications only after the 'breakthrough' development of asymmetric polymer membranes by Loeb and Sourirajan in the early 1950s. Thus, ultrafiltration and reverse osmosis (sometimes called hyperfiltration) reached maturity in the 1960s, whereas membrane processes for the separation of gas mixtures started to be used on an industrial scale in the late 1970s and in the 1980s. Huge membrane plants for the separation of the uranium isotopes ^{235}U and ^{238}U by 'gaseous diffusion' were built in the United States much earlier, during the 1940s. However, the products of these plants were intended for military purposes.

Pervaporation and vapor permeation are the latest membrane separation processes to become economically competitive for some industrial applications. The first large-scale industrial pervaporation plant started operation in 1985 in Karlsruhe-Maxau (Germany) and another shortly thereafter in Betheniville (France). Both plants are being used for the dehydration of 94% ethanol. The first commercial vapor permeation plant, also designed for ethanol dehydration, became operative in September 1989 in Heilbron (Germany). Promising new applications are expected in future years for facilitated-transport membranes and catalytic membrane reactors.

While new membrane separation processes are being conceived with remarkable frequency, existing processes are also being constantly improved in order to enhance their economic competitiveness. Significant improvements are currently being made in many aspects of membrane separation technology: in the development of new membrane materials with higher selectivity and/or permeability, in the fabrication methods for high-flux asymmetric or composite membranes (whether in flat-sheet, hollow fiber, or tubular form), in membrane module construction and in process design (e.g., of hybrid separation processes).

Membrane separation technology is presently being used in an impressive variety of applications and has generated businesses totalling over one billion U.S. dollars annually. It is not surprising, therefore, that it has been the subject

of many monographs, books and review papers, and that an entire journal, the *Journal of Membrane Science* (Elsevier), is dedicated to it. The main objective of the present text is to present the principles and applications of a variety of membrane separation processes from the unique perspectives of investigators who have made important contributions to their fields. Another objective is to provide the reader with an authoritative resource on various aspects of this rapidly growing technology. The text can be used by someone who wishes to learn about a general area of application as well as by the knowledgeable person seeking more detailed information. The various chapters differ significantly in length, emphasis, and detail. No uniformity has been sought in the presentation of the subject matter or in nomenclature in order to preserve the perspective and personal style of the contributors. Also, very little editing has been done on the chapters whose authors used English as a second language, in order to avoid possible errors of interpretation or changes in emphasis.

The chapters in this text cover a wide variety of topics. Some of the authors have chosen to cover all aspects of certain membrane separation processes. Other authors have preferred to discuss specific topics in greater detail, such as process and module design, process economics, special applications of industrial or biotechnological interest, and emerging applications. It is hoped that the present text will not only provide readers interested in membrane separation technology with useful data and information, but also with the insights of well-known investigators who have contributed to its development and promise.

Contents

Chapter 6. ELECTRODIALYSIS AND RELATED PROCESSES
H. Strathmann

Chapter 12. GAS SEPARATION USING INORGANIC MEMBRANES
Klaas Keizer, Robert J.R. Uhlhorn and Ton J. Burggraaf

Chapter 13. ECONOMICS OF GAS SEPARATION MEMBRANE PROCESSES
Robert Spillman

List of contributors

Jose R. Alvarez
Department of Chemical Engineering, University of Oviedo, Oviedo, Spain

L. Boyadzhiev
Institute of Chemical Engineering, Bulgarian Academy of Sciences, Sofia, Bulgaria

Ton J. Burggraaf
University of Twente, Faculty of Chemical Technology, Laboratory of Inorganic Chemistry, Materials Science and Catalysis, P.O. Box 217, 7500 AE Enschede, The Netherlands

Y. Cen
Physikalisch-Chemisches Institut, Universität Heidelberg, Im Neuenheimer Feld 253, 69120 Heidelberg, Germany

Munir Cheryan
Department of Food Science, 103 Agricultural Bioprocess Laboratory, University of Illinois, Urbana, IL 61801, USA

Edward L. Cussler
Chemical Engineering and Materials Science Department, University of Minnesota, 421 Washington Ave. SE, Minneapolis, MN 55455, USA

William Eykamp
246 Pleasant Street, Arlington, MA 02174, USA

John L. Falconer
Department of Chemical Engineering, University of Colorado, Boulder, Colorado 80309-0424, USA

C.J.D. Fell
Centre for Membrane and Separation Technology, University of New South Wales, Kensington 2033, Australia

Klaas Keizer
University of Twente, Faculty of Chemical Technology, Laboratory of Inorganic Chemistry, Materials Science and Catalysis, P.O. Box 217, 7500 AE Enschede, The Netherlands

Z. Lazarova
Institute of Chemical Engineering, Bulgarian Academy of Sciences, Sofia, Bulgaria

R.N. Lichtenthaler
Physikalisch-Chemisches Institut, Universität Heidelberg, Im Neuenheimer Feld 253, 69120 Heidelberg, Germany

Stephen L. Matson
Arete Technologies Inc., 15 Withington Lane, Harvard, MA 01451, USA

M.H.V. Mulder
University of Twente, Faculty of Chemical Technology, P.O. Box 217, 7500 AE Enschede, The Netherlands

J. Néel
Ecole Nationale Supérieure des Industries Chimiques, B.P. 451, 1 rue Grandville, 54001 Nancy Cedex, France

Richard D. Noble
Department of Chemical Engineering, University of Colorado, Boulder, Colorado 80309-0424, USA

Bradley W. Reed
Hoechst Celanese Corporation, Separations Products Division, Charlotte, NC 28273, USA

Michael J. Semmens
Civil Engineering Department, University of Minnesota, Minneapolis, MN 55455, USA

Amitava Sengupta
Hoechst Celanese Corporation, 13800 South Lakes Drive, Charlotte, NC 28273, USA

Kamalesh K. Sirkar
Chemical Engineering, Chemistry and Environmental Science Department, New Jersey Institute of Technology, Newark, NJ 07102, USA

David P. Sperry
Department of Chemical Engineering, University of Colorado, Boulder, Colorado 80309-0424, USA

Robert Spillman
Amicon, Inc., 72 Cherry Hill Drive, Beverly, MA 01915, USA

H. Strathmann
University of Twente, Faculty of Chemical Technology, P.O. Box 217, 7500 AE Enschede, The Netherlands

Robert J.R. Uhlhorn
University of Twente, Faculty of Chemical Technology, Laboratory of Inorganic Chemistry, Materials Science and Catalysis, P.O. Box 217, 7500 AE Enschede, The Netherlands

Membrane Separations Technology. Principles and Applications
Edited by R.D. Noble and S.A. Stern

Chapter 1

Microfiltration and ultrafiltration

William Eykamp

246 Pleasant Street, Arlington, MA 02174, USA

1.1 INTRODUCTION

Membrane separation is practised on feed streams ranging from gases to colloids. Microfiltration (MF) membranes are used to retain colloidal particles as large as several micrometers. MF overlaps conventional filtration for separation of small particles. Gas separation membranes operate at the other extreme of molecular size. Molecules with a size of 0.3 nm, with a resolution in diameter of 0.02 nm are separated. The range of effective separation diameters of membrane applications is thus a ratio of about 10^4. Microfiltration membranes have the largest pores, and ultrafiltration (UF) membranes the next largest.

To the newcomer, UF and MF look similar, and in fact they are more alike than they are different. Because of their very different historical background, however, they remain very distinct to practitioners and to equipment and membrane manufacturers.

Membrane mediated fractionation, the separation of a stream into two fractions on the basis of molecular or particulate size, is the primary use of UF and is a significant application of MF. Both processes work primarily by size exclusion, permitting smaller species to pass through a membrane while larger ones are retained. Both processes were developed for, and find the vast preponderance of their applications in, aqueous separations. Microfiltration is also used in gas-phase filtration, and both processes have some non-aqueous liquid uses.

Membranes also compete with processes such as centrifugation and chromatography.

There are other membrane processes closely related to UF and MF. Hemodialysis, the artificial kidney, is the largest by far of all membrane applications.

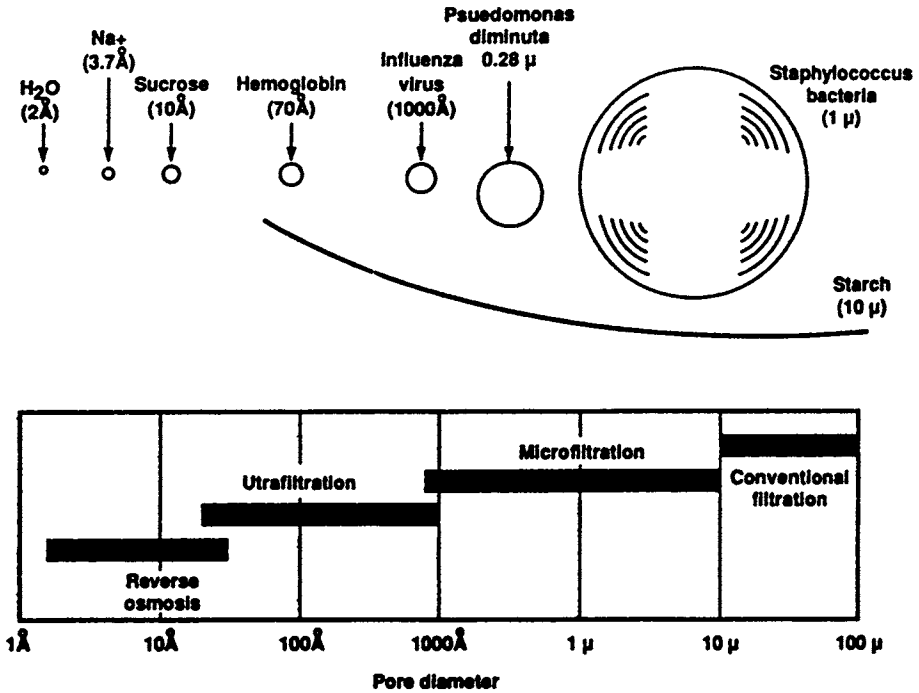

Fig. 1.1. Reverse osmosis, ultrafiltration, microfiltration and conventional filtration are all related processes differing principally in the average pore diameter of the membrane. Reverse osmosis membranes are so dense that discrete pores may not exist.

In many ways, the dialysis membrane is akin to a UF membrane, but the driving force for mass transfer is a concentration difference, while in UF and MF, the driving force is pressure. Hemodialysis is a relatively young separations application, but it is fully mature commercially. Membrane dialysis is established as a treatment for kidney failure in all industrialized countries. Prices and costs have dropped progressively; the industry has been "shaken out", and it is possible to purchase sterile membrane cartridges ready to attach to dialysis water and a patient for less than $\$14/m^2$.

Although the market for hemodialysis membranes is larger than the market for all other membrane separation processes combined, whether measured by area or by value, hemodialysis is outside the scope of this work. Interested readers may find more information in a recent book [1].

1.1.1 Historical

Microfiltration membranes are second only to dialysis as the oldest membrane application still practised commercially. Microfiltration grew out of the

discovery of nitrocellulose in 1846. Cellulose nitrate membranes were reported by Frick in 1855. Early cellulose nitrate membranes were prepared by dipping a test tube in a collodion solution [2]. Surprisingly, some of these early materials are still used today.

Membrane development continued for decades, mostly in Germany. Bechhold published means to vary pore size by varying polymer concentration in 1906. In 1918, Zsigmondy and Bachmann published means to make small quantities of "parchment-like" MF membrane, including a description of how to vary pore size. Zsigmondy, in 1922, got a U.S. patent on his invention made by exposing a thin coating of a nitrocellulose solution to humid air [3]. Sartorius started producing membranes commercially in 1927 [4]. Commercial development was very slow until shortly after World War II.

The discovery that propelled MF into large-scale commercial production was one attributed to Gertrude Mueller at the Hygiene Institute, University of Hamburg, that the micro flora from a large volume of water could be deposited intact on a small disk of microfiltration membrane. By culturing the membrane and counting the colonies, rapid and accurate determinations of the safety of drinking water could be made. This discovery was particularly important in post-war Germany, where much of the civil infrastructure was damaged [5].

Microfiltration technology was investigated by the U.S. Joint Intelligence Objectives Agency in their post-war assessment of German science and technology. The leading investigator was Alexander Goetz [6], who later developed his findings under contract with the U.S. Army. In 1950, the Lovell Chemical Company won a contract to develop Goetz' work further. A series of reports ranging from November 1950 through April 1954 chronicles the difficult transition of MF membranes from the laboratory to semicommercial production. The report of September 1951 is particularly interesting because it despairs of ever making large sheets of MF membrane. Glass plates, it says, are "too plastic" in large sizes to be kept flat. Membranes require a "precisely flat surface". Glass is subject to "cold flow". "Controls of great precision and nicety are so prerequisite to the making of a satisfactory MF that we strongly urge upon the Chemical Corps the concept that microfilters should not (and cannot) be a cheap item of manufacture comparable to filter paper. The day that expensive controls are abandoned for even normally careful standard production, the MF functional characteristics will be wholly undependable and the output will be rendered worthless as a reliable quantitative bacteriological tool." The report was signed by John R. Bush, who later bought the technology from Lovell and founded Millipore Corporation, now the world leader in microfiltration.

Reverse osmosis and ultrafiltration came much later in time. Curiously enough, neither developed from microfiltration. UF membranes were attempted in microfiltration firms, and some were made, but UF clearly is derived from RO in almost all important respects. The differences in the route of develop-

ment of MF and UF continues to divide the two fields to this day; firms outstanding in one field have little presence in the other, even though the two disciplines are now closely related technically.

The major problem that prevented microfiltration membrane technology from being extended to smaller and smaller pores was the one of throughput. As pore size decreases, so does the amount of fluid that may be pushed through the membrane. The problem may be illustrated by considering the equation for flow through a cylindrical pore in a membrane of a certain thickness:

$$q = \frac{\pi \Delta P d^4}{128 \mu t} \tag{1.1}$$

where q is the volumetric flowrate through the pore ($m^3 s^{-1}$), ΔP is pressure drop, pascals, d is pore diameter (m), μ is viscosity (Pa s m^{-2}), and t is the membrane thickness (m).

The throughput of a membrane, referred to as its flux, is the sum of the outputs of its pores. Flux, the symbol for which is usually J, is a velocity with units m s^{-1} but in practice it is more easily measured in $\mu m\ s^{-1}$. It is the average velocity for the entire membrane surface. In practice, flux is almost always reported as volume per area and time, with common units of l $m^{-2} h^{-1}$ or gal ft^{-2} day^{-1}.

For a membrane,

$$J = q \frac{N}{A} \tag{1.2}$$

where N is the number of pores in area A m^2.

From geometry, the number of uniform circular pores that will fit in a square is proportional to the inverse square of pore diameter.

$$\frac{N}{A} \propto d^{-2} \tag{1.3}$$

So, for constant pressure drop, fluid viscosity and membrane thickness,

$$J \propto d^{-2} \tag{1.4}$$

The pore size suitable for UF is of magnitude 10 nm; for MF, it is of magnitude 200 nm. Thus, a microfiltration membrane with high throughput will, if made as an UF membrane, have a throughput much less than 1% of the MF value. The UF throughput problem was trivial compared to that for reverse osmosis. Insofar as it is reasonable to speak of "pores" in an RO membrane, they would be smaller than those in a UF membrane by another order of magnitude. The problem was solved for RO with the invention of the skinned membrane (see below). The solution was quickly copied for UF, for it solved the UF flux problem. The RO membrane, not the MF membrane, is the direct predecessor of the UF membrane [7].

The RO membrane breakthrough occurred in 1959, with the invention at UCLA of the Loeb–Sourirajan membrane. Working with cellulose acetate, which Reid [8] had reported as having superior salt rejection properties, the inventors found a way to make an asymmetric membrane — a very thin skin integrally attached to an otherwise porous backing. In effect, they found a way to make the factor t in Eq. (1.1) very small without a negative impact on mechanical toughness or durability. High flux membranes thereby became possible.

While the group at UCLA pursued RO membranes as their principal thrust, a group under Alan Michaels, first at MIT, later at Amicon Corp., went after ultrafiltration membranes. Although many materials were tried for UF membranes, grades of cellulose acetate similar to those useful in RO would produce membranes with fairly good properties as ultrafilters. Because cellulosic polymers have chemical properties that limit their industrial suitability, Dorr-Oliver began a search for other polymers from which asymmetric UF membranes could be prepared — initially by sponsoring research at Amicon. The decade beginning in 1965 was one of explosive development activity in UF, both in membranes and in processes. Cellulose acetate membranes were soon displaced by a variety of noncellulosic membranes invented independently by several investigators within a short time span. Polyacrylonitrile UF membranes were discovered in a failed attempt to prepare an RO membrane, as described in a 1965 report [9]. Polysulfone membranes were first made as support films for RO membranes [10]. Polyvinylidene fluoride membranes were first made by accident [11].

1.2 THE MEMBRANE FILTRATION PROCESS

1.2.1 Crossflow

Conventional filtration processes operate in dead-end flow. That is the familiar filtration procedure, used for filtering a precipitate with filter paper or for straining spaghetti; the flow is normal to the face of the filter. Ultrafiltration is conventionally done in cross flow, with the principal flow parallel to the surface of the filter medium. Microfiltration is practised both ways. Crossflow operation is neither obvious nor difficult, and a good understanding of the reasons for its use is necessary for an understanding of membrane filtration.

One major difference in the operation of these two schemes is conversion per pass. In dead-end filtration, essentially all of the fluid entering the filter is either retained by the cake or emerges as permeate, so the conversion can approach 100%, all occurring in the first pass. For a crossflow filter, far more of the feed passes past the membrane than passes through it, and conversion per pass for a long string of filter elements in series is generally <20%. Recycle permits the ultimate conversion to be much higher.

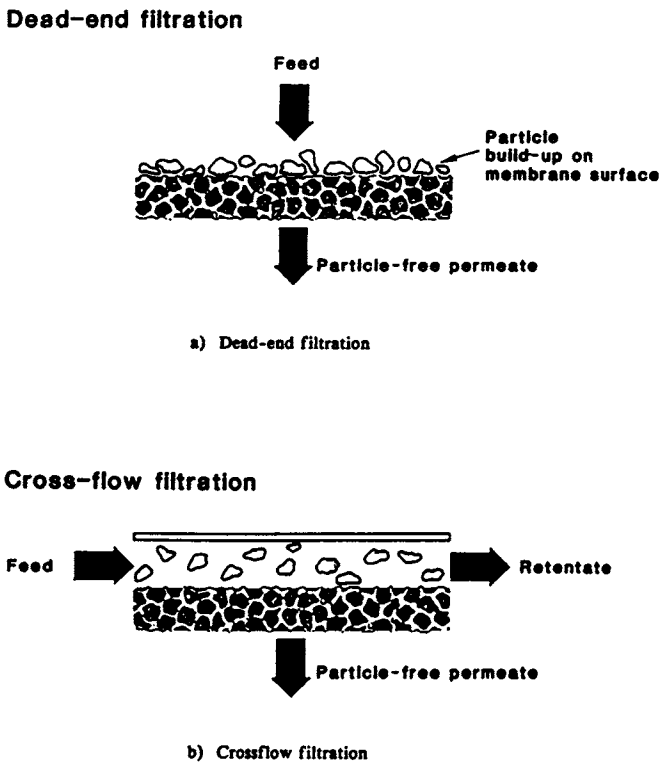

Fig. 1.2. Schematic representation of (a) dead-end and (b) crossflow microfiltration.

In crossflow, the fluid to be filtered is pumped across the membrane, parallel to its surface. Only a small fraction of the fluid actually passing across the membrane flows through it. By maintaining velocity across the membrane, material retained by the membrane is swept off its surface. Since there is little accumulation of retained material at the membrane surface, the membrane has less tendency to "blind", and output can be maintained at a level higher than is possible for the same system operating in dead-end flow. Crossflow is advantageous when the retained material is likely to plug the membrane.

1.2.2 Throughput and Driving Force

The resistance to flow through the filter in both crossflow filtration and dead-end filtration may be expressed as a sum of resistances:

$$J = \Delta p/R \qquad R = R_m + R_c \tag{1.5}$$

R is the total resistance to flow, R_m, the resistance of the membrane or other filter medium (e.g. filter cloth) and R_c, the cake resistance, boundary layer resistance,

etc. Neither of these terms is required to be constant, and in conventional dead-end filtration, R_c is always variable.

1.2.3 Conventional Filtration

For conventional filtration, the cake resistance term in Eq. (1.5) is written:

$$R_c = \mu\, \alpha'\, \Delta p^s\, (wV/A) \tag{1.6}$$

where A is area (m^2), V is the total volume of filtrate (m^3), Δp is pressure drop across the filter medium and cake (Pa), w is the mass of dry cake solids per volume of filtrate (kg m^{-3}), α' is a specific cake resistance (m kg^{-1}), μ is viscosity of the filtrate (Pa s), and s is the "cake compressibility". The term $\alpha'\Delta p^s$ is proportional to cake resistance. When $s = 0$, cake resistance is independent of pressure and flux is proportional to Δp. For totally compressible cakes, when $s = 1$, the flux of the filter can become independent of pressure, and does so for the usual condition, $R_c >> R_m$. This independence of pressure condition mimics the behavior of most crossflow membrane applications.

1.2.4 Crossflow Filtration

Equation (1.5) can be used to illustrate two limiting cases. First, in the absence of any filterable matter, there is no deposit on or accumulation at the membrane, so $R_c = 0$. R_m is the only resistance. In membrane filtration, that case is referred to as "water flux", a term used to describe the inherent porosity of a new membrane. Flux is proportional to pressure and inversely proportional to viscosity, so these are corrected to a standard basis to give a "standard water flux", a measure of the inherent porosity of a membrane.

The usual limiting case is one in which the membrane resistance is overwhelmed by the cake resistance, and membrane resistance may thus be neglected. Furthermore, as mentioned above, crossflow filtrations behave as if s were 1. The filtration rate is independent of pressure, demonstrated by experiment. Crossflow membrane filtration almost always behaves as if there were a cake and it were *totally* compressible. A normal operating curve of flux vs pressure for crossflow membrane filtration is given in Fig. 1.3. The left-most line is the water flux, where there are no filterable materials present. Flux is proportional to applied transmembrane pressure. The line represents Darcy's Law for flow through a porous medium.

The process flux lines show the normal operating condition of crossflow membrane operation for UF and MF. At low pressure, flux is proportional to pressure, although the proportionality constant is commonly less than for the pure water case. As pressure increases, a limiting case develops where a further increase in pressure produces no further increase in flux. This effect is consist-

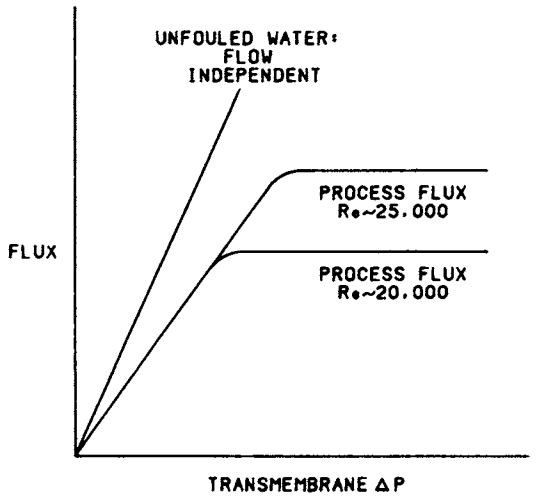

Fig. 1.3. When macrosolute is retained by a membrane, flux decreases until the process becomes pressure independent. Thereafter, increasing Reynolds number will increase the flux.

ent with the extreme possibility in dead-end filtration for a compressible cake ($s = 1$). Note, however, that the final flux is a function of the Reynolds number in the channel adjacent to the membrane. As $Re \rightarrow 0$ (no flow past the membrane), the crossflow filter becomes a dead end filter. Flux would be very much lower than the values shown in Fig. 1.3. These lines, part of a family of operating lines, represent the vast majority of crossflow UF and MF cases.

1.2.5 Mass Transfer

Why is flux flow-dependent? Consider the arrangement for crossflow operation. Fluid is flowing past the membrane at a velocity many orders of magnitude higher than the velocity through the membrane. (A typical flux may be 10 $\mu m\ s^{-1}$, and a typical crossflow rate might be 2 $m\ s^{-1}$.) The fluid moving perpendicular to the membrane carries with it material that will not pass through the membrane. It will accumulate at the surface of the membrane, as in the case of dead-end filtration; but the velocity of the stream parallel to the membrane will tend to redisperse the accumulated material.

Concentration polarization is the term used to describe the fact that since retained species accumulate near the membrane surface, their concentration there will be higher than it is in the bulk.

The filtration equation shows that filtration rate is inversely related to the amount of material accumulated at the filter surface. Mass transfer equations show that the rate of material redispersed is a function of concentration difference between the membrane surface and the bulk, among other factors.

1.2.6 Turbulent Mass Transfer

The vast majority of commercial UF and MF crossflow devices operate in turbulent flow. Figure 1.4 shows schematically how flow and mass transfer interrelate in turbulent flow. Recall that the transverse fluid velocity at the wall is always zero, and that the boundary layer thickness is defined as the location where 99% of the "action" takes place; outside the dynamic boundary layer we can assume plug flow (uniform velocity), and outside the concentration boundary layer we can assume uniform solute concentration in the bulk.

Also known is that the crossflow device truly operates at steady state in all practical cases. Some membrane systems run for months at constant flux. If there were accumulation of any species at the membrane, operation for more than a few hours at steady output would be impossible. The rate of the arrival of retained material at the membrane is thus equal to the rate of redispersion of the material already there. From this fact comes a simple but necessary concept: rate out = – rate in. The calculation of rates of dispersal from a more concentrated region to a less concentrated one is a much studied and solved problem

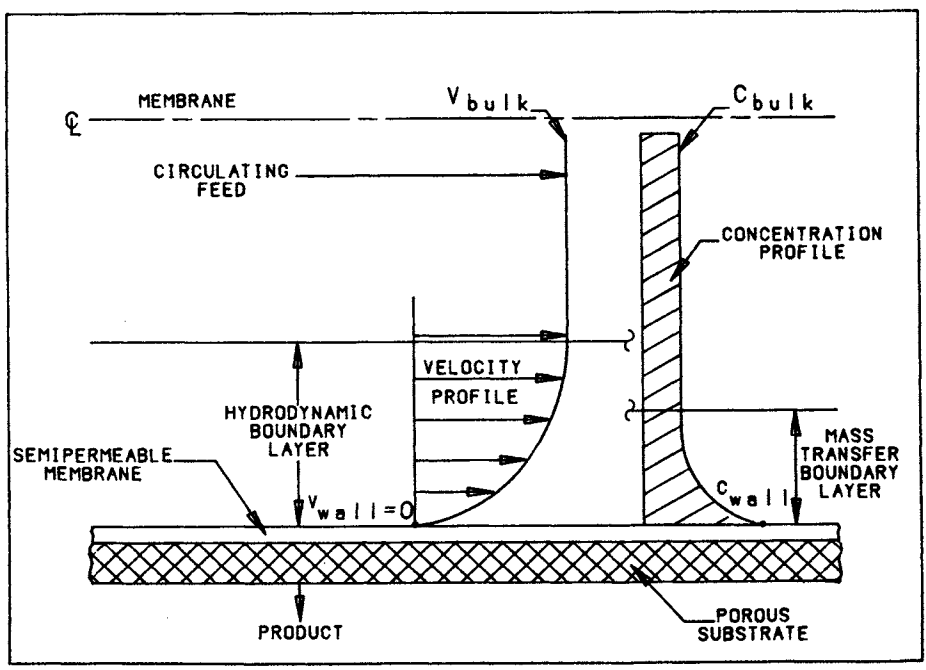

Fig. 1.4. Boundary layers in turbulent flow. Channel center line is at the top, flow is left to right, and a semi-permeable membrane is at the bottom. The hydrodynamic boundary layer shows velocity declining to zero at the membrane, while the concentration of retained material rises at the membrane.

in chemical engineering. Using those tools, one can predict the mass transfer coefficient, and thus the flux of a steady state membrane operating in crossflow.

An equation variously attributed to Dittus–Boelter and Desalius is:

$$Sh = 0.023\, Re^{0.8}\, Sc^{0.33} \tag{1.7}$$

where Sh is the Sherwood number, Re is the Reynolds number, and Sc is the Schmidt number.

$$Sh = kd_h/D \tag{1.8}$$

$$Re = Vd_h/\nu \tag{1.9}$$

$$Sc = \nu/D \tag{1.10}$$

where D is diffusivity ($m^2\ s^{-1}$), d_h is hydraulic diameter (m), k is the mass transfer coefficient ($m\ s^{-1}$), V is the velocity ($m\ s^{-1}$), and ν is kinematic viscosity ($m^2\ s^{-1}$).

It is easier to work with the Reynolds number when it is expressed as a function of the volumetric flow rate, Q. Hydraulic diameter, d_h is 4 Area/wetted perimeter. For cylindrical flow channels, $d_h = \pi d/4$, and for square pores, $d_h = d$. For this discussion, $d_h = d$ is assumed as a reasonable approximation.

Since the rate of arrival (fluid plus retained material for redispersal) is equal and opposite to the rate of re-dispersal of the retained material,

$$J \approx k \tag{1.11}$$

Combining these equations gives a general expression for flux in a turbulent flow membrane system:

$$J + B\frac{Q^{0.8}\, D^{0.67}}{d^{0.88}\, \nu^{0.55}} \tag{1.12}$$

where B is an experimental constant.

Please note that the exponent 0.8 on the term Q is predicted from heat and mass transfer experiments outside the membrane field. The exponent is often around 0.8 for membrane systems, but is sometimes very different. See further explanation below.

That flux is proportional to the rate of redispersion of retained material polarized at the membrane is accepted, experimentally verified fact. Why and how this happens is still controversial. The constancy of flux regardless of pressure has been known only slightly longer that the underlying reason for it has been in dispute. While the argument of total compressibility of the cake, which derives from classic filtration theory, may be reasonable for a concentrated protein solution, it does not seem appropriate for explaining the behavior of a latex composed of rigid spheres.

1.2.7 Turbulent Boundary Layer

What is going on next to the membrane? That is where the action is, where the results of system design and fluid properties are played out. The operating characteristics of an unfouled crossflow membrane are determined in a tiny slice of fluid just above the membrane.

Figure 1.5 shows a typical plot of experimental data in which, for each of the data lines shown, the stirring rate is held constant. The flux declines as log concentration rises. Plots like Fig. 1.5 may be made for most materials being ultrafiltered. Blatt [12] proposed that the macrosolute forms a new phase near the membrane — that of a gel or gel-like layer. The model was a good predictor of experimental data and has been widely used.

Other researchers had different ideas about the boundary layer. An explanation that fits the data well relies on osmotic pressure as the effect producing the reduction in flux.

The equation

$$J = \Delta P - \sigma \, \Delta \Pi \tag{1.13}$$

where Π osmotic pressure (Pa) is accepted for reverse osmosis. σ is the reflection coefficient, assumed to be unity for UF and MF. Boundary layer theory is used to predict the concentration at the membrane. The van't Hoff equation

$$\Pi = cRT \tag{1.14}$$

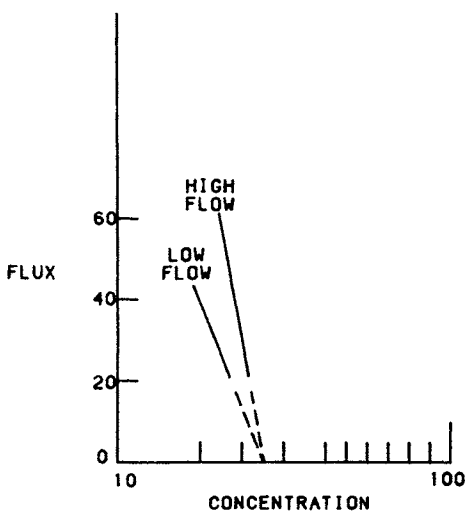

Fig. 1.5. Flux vs. log concentration. When extrapolated to zero flux, data from different flows have the same intercept.

where c is molar concentration, R is the gas constant, and T the absolute temperature, may be used to estimate the osmotic pressure corresponding to that concentration. Equation (1.14) is satisfactorily accurate for practical cases in reverse osmosis, but it does a poor job of predicting osmotic pressure in solutions of macromolecules. Early investigators in UF dismissed osmotic pressure as inapplicable in a solution whose molarity was measured in millimoles. That argument proved incorrect. Applying the empirical expression

$$\Pi(c) = \sum_{n=1}^{n=3} a_i c_i \tag{1.15}$$

where a_i are constants, it is possible to correlate experimental osmotic pressure data for macrosolutes and to predict the concentration at the membrane. Several investigators have found osmotic pressures high enough to resist the transmembrane driving force. Jonsson [13] has published some suggestive data, showing how an increase in transmembrane pressure can result in an increase in osmotic pressure even greater than the increase in applied pressure. If confirmed, this would result in a decrease in flux with increasing pressure. Several others have published data that support the osmotic pressure hypothesis more generally [14]. More recently [15], a new approach to the long sought goal of predicting flux *a priori* achieved some success. The model uses diffusivity determined in an ultracentrifuge and osmotic pressure experimentally determined by a membrane osmometer (for ovalbumin molecular weight 45,000 [16]) a 17% by weight solution had a 100 kPa osmotic pressure). Correcting for a loss of water flux produced by adsorption of the protein on the membrane (fouling), the authors get a good fit between predicted and measured flux. Additionally, a solution with the concentration at the membrane predicted from the plot shown in Fig. 1.5 did not exhibit the properties of a gel, although it was a viscous solution.

Other theories of the boundary layer exist, but they have not attracted adherents to date. In terms of predictive power, both the gel theory and the osmotic pressure theory provide a valuable framework for correlating data.

1.2.8 Effect of Flow on Flux

In most crossflow filtrations, diffusivity and kinematic viscosity are given properties of the feed, and are relatively constant. Since they are present in the equations as factors with fractional exponents, their numerical change is relatively small even if the values vary somewhat. Geometry within an experiment is fixed, so d is constant. A very useful equation comes from taking the logarithm of Eq. (1.12), then the partial derivative:

$$\left(\frac{\partial \log j}{\partial \log Q}\right)_{N,d,D} = m \tag{1.16}$$

Equation (1.16) is the basis for the ubiquitous plots of log J vs. log Q. Such plots are powerful tools in analyzing experimental data. The first point to examine is the slope of the log–log plot, m. For laminar flow, $m = 0.33$. For turbulent flow, the expected value in Eq. (1.12) is $m = 0.8$. It is important to determine the experimental value, both for design optimization and for prediction of long-term effects. Referring to Fig. 1.3, it is important that all values of flux be taken in the pressure independent region.

The known range of observed values of m in *well developed turbulent flow* is $0.8 < m < 2.0$.

The higher values are found especially in systems containing particles, usually large, dense particles. Polyvinyl chloride latex with particles over 0.5 μm diameter is a classic high-slope (m) case. True solutions of macromolecules behave as predicted, with the slope usually near $m = 0.8$.

The slope of the flux–flow line is an indicator of fouling (q.v.). In known turbulent flow, values of $m < 0.8$ are suspect *prima facie*. A decline in the value of m with time is the most sensitive indicator of fouling. While the slope is difficult to obtain unconfounded by changes in pressure, a well designed J vs. Q experiment yields results with good predictive value for fouling.

A special precaution when using spiral wound modules: DaCosta [17,18] found that while the pressure drop data in a spiral module behave as if the flow is turbulent, the mass transfer data are consistent with laminar flow.

1.2.9 Pressure Drop

A useful design equation, valid for smooth tubes with no significant entrance or exit expansions, where $10{,}000 < Re < 100{,}000$ is:

$$\Delta p \propto l\rho v^{0.25}\, d^{-4.75}\, Q^{1.75} \tag{1.17}$$

where l is the channel length.

For laminar flow, the more familiar equation is:

$$\Delta p = 128\, \mu l Q / l\, \pi d^4 \tag{1.18}$$

Equation (1.17) is very useful in the form:

$$\frac{\partial \log \Delta p}{\partial \log Q} = 1.75 \tag{1.19}$$

A plot of log delta p vs. log Q is helpful in establishing whether turbulent flow exists in the channel, and it is an excellent error check for pressure drop data.

Values of slope very different from 1.75 indicate either that the flow is not in the expected Reynolds number regime, that there are major changes in flow channel diameter, or usually, that the data contain error.

1.2.10 Energy Consumption

Combining Eqs. (1.12), (1.17) and (1.19) provides an interesting insight into system design. One economic factor of importance is energy consumed per unit permeated. The SI units for this are Pascals, but the units universally reported are kWh m^{-3}. When Eq. (1.17) is valid, energy is:

$$E = Q\Delta p \propto Q^{2.75} \tag{1.20}$$

where E is in Joules or in kW-h. Dividing by total permeate output, JA, recalling that $J \approx Q^m$,

$$V = JA \qquad E/V \propto Q^{2.75-m} \tag{1.21}$$

When m is low, say 0.8, there is a significant reduction in energy by designing at low flow rates, even though membrane area rises. But when m is high, the energy penalty for high flow, thus low area designs is low.

1.2.11 Laminar Mass Transfer

Some devices operate in laminar flow. While most capillary and ceramic monolith devices operate normally in turbulent flow, some do not, and for applications where the feed is viscous, Reynolds number can drop into the laminar regime even for diameters up to 5 mm.

For laminar flow, flow regimes up to a Reynolds number about 2200, an equation modified from Leveque's heat transfer formulation shows that for practical situations:

$$Sh = 1.62\left(\text{Re } Sc\,\frac{d}{l}\right)^{0.33} \tag{1.22}$$

Solving for k, which yields J:

$$k = 1.62\left(\frac{VD^2}{ld}\right)^{0.33} \tag{1.23}$$

$$J \propto \left(\frac{QD^2}{ld^3}\right)^{0.33} \tag{1.24}$$

The pressure drop equation was presented in Eq. (1.18).

Equation (1.24) shows that flux is proportional to the inverse cube root of channel length, and the reciprocal of channel height. An attractive module design would thus be short, very small pores. Practically, no economic way yet exists to manufacture such a design.

1.2.12 Other Depolarization Schemes

Equipment is now offered utilizing forces other than those derived from pressure to minimize polarization. Two of the newer ones are:

1.2.12.1 Taylor Vortex

One elegant way to decouple polarization from driving force is by using a rotating filter device. When fluid flows around a curve in a duct, or when fluid is confined between differentially rotating cylinders, secondary flows called Taylor Vortices are generated Using these secondary flows to minimize polarization provides a tool for membrane equipment design.

$$Ta = \frac{\omega R g}{\nu} \sqrt{g/R} \tag{1.25}$$

where Ta is the Taylor Number, R is the radius of the inner cylinder (m), g is the gap between inner and outer cylinders (m), and ω is the angular velocity of the rotating cylinder (radians s^{-1}).

In a detailed analytic and experimental paper, Holeschovsky and Cooney [19] find a flux equation for this device analogous to Eq. (1.10): the Sherwood number for a device utilizing Taylor vortices is:

$$Sh = C\, Ta^{0.5}\, Sc^{0.33} \tag{1.26}$$

where C is an experimental constant. For a fixed device on a given fluid, flux is predicted to be proportional to $\omega^{1/2}$.

1.2.12.2 Vibratory

Equipment may also move the membrane instead of the fluid. One firm mounts a membrane stack atop a resonant rotating spring, and literally shakes the stack to depolarize the membrane. No adequate theory is available to explain mass transfer in vibrating membrane systems. Summers [20] shows a correlation of mass transfer with the first power of shear rate over a narrow range of data and conditions. The first-order hypothesis is supported by other observations, but it must be regarded as unverified and preliminary.

1.3 SEPARATION MEMBRANES

There are many ways to make membranes that are useful in MF and UF, and there is an abundant literature describing membrane formation [21]. A general taxonomy is:

I. Membranes derived from microporous media
    Ceramics
    Sintered metal
    Sintered polymers
    Wound wire or fibre
II. Membranes derived from homogeneous solid films,
    Track-etched membranes
    Stretched polymers
    Aluminum derivatives
    Dense films (this is only for dialysis and gas membranes)
III. Membranes derived from heterogeneous solid films
    Leached glasses
    Extracted polymers
IV. Symmetric membranes derived from solution
    Leached membranes
    Thermally inverted solutions
V. Asymmetric structures derived from solution
    Loeb–Sourirajan membranes
VI. Asymmetric composite structures
    Dynamic membranes
    Thin film composites
    Coated structures
    Self-assembled structures

(I) Membranes in this group include membranes made from an assembly of small particles, either laid down in a bed, or sintered, with the pores being formed from the interstices between the solid particles. The simplest of this class of membrane is formed by sintering metal, metal oxide, graphite, ceramic or polymer [22]. Sintered membranes are used for MF and can be made to retain colloids with particle size of 0.1 μm. Silver, tungsten, stainless steel, glass, several ceramics and other materials are made into commercial membranes. Sintered metal may be coated by TiO_2 or zirconium oxide to produce MF and UF membranes. Fine wires or fibres can be wound such that their interstices have openings suitable for MF membranes.

Porous media illustrate the issue of what is and what is not a membrane. The definitions are arbitrary. Some media, such as diatomaceous earth deposited on

a screen, are within the definition of functional microfilters at the upper end of the range. Diatomaceous earth filter media are not considered to be membranes under any definition. However, dynamically formed membranes are generally regarded as true membranes. They are formed by depositing a material — hydrous zirconium oxide is the most common — onto a porous substrate in cross flow. Why is one a membrane and the other not? The dynamically formed membrane does not use the forming material as a filter aid, and once the membrane is formed, the filtration operation proceeds, usually in cross flow, very much the way any membrane operation is conducted. The fact that the membrane is deposited in cross flow rather than in dead-end flow is a further distinction. And, the ability to form dynamic membranes that have reasonable properties as reverse osmosis membranes confirmed the view that these devices were to be considered as membranes.

Membranes derived from microporous media may be uncharged or charged, symmetrical or asymmetric. The issue of charge is dominated by choice of material and by the usual rules of colloid chemistry. As illustrated in the case of ceramic membranes, surface charge may be a function of operating condition. Many microporous media membranes are symmetrical, but it is common to find several orders of magnitude difference in effective pore size when comparing the membrane surface to the support structure. Especially in the case of ceramic membranes, porous membranes are often constructed of layers of porous material of ever decreasing diameter, each applied and stabilized in turn, then acting as the support for the next finer layer.

Membranes derived from microporous media are generally used for MF. Attempts to decrease pore size down to the ultrafiltration range are achieving some success, and membranes exhibiting reasonable UF properties are now made from alpha and gamma alumina, zirconia and other vitreous materials.

(II) Homogeneous solid films constitute an important class of MF membranes. These are structures that contain pores or are a matrix whose openings are fixed. Stretched polymers, form a major part of this class. Semicrystalline polymers, if stretched perpendicular to the axis of crystallite orientation, may fracture in such a way as to make reproducible microchannels. Best known are Goretex® produced from Teflon®, and Cellguard ® produced from polyolefin. Stretched polymers have unusually large fractions of open space, featuring very high fluxes in certain applications, the microfiltration of gases, for example.

Track-etched polymers are cylindrical pore membranes. Originally, such membranes were made from mica on a very small scale. The membranes of commerce are made from polymers. A thin polymer film is first exposed to a collimated beam of radiation strong enough to break the polymer chains. The film is then etched in a bath which selectively attacks the damaged polymer. Successful implementation of the technique produces a film with roughly cylindrical pores, whose diameter may be varied by the intensity of the etching

step. Commercially available membranes have a narrow pore size distribution and are reportedly resistant to plugging. The membranes have low flux, because it is impossible to achieve high pore density without sacrificing size distribution. Using track-etched membranes, it is possible to prepare stunning photomicrographs of objects sitting on a well defined membrane surface, and they are often seen in that role.

These types encompass an incredible diversity of products. Perhaps their distinguishing characteristic is that they start from a homogeneous solid and end with a membrane with openings that are more consistent than not from one face of the membrane to the other.

A newer membrane form is prepared from a monolithic aluminum foil by electrolytic oxidation [23]. The homogeneous aluminum film is transformed through careful control of the electrochemical formation process into a highly asymmetric membrane with very uniform pores at a high area fraction. The resulting membranes are unusual in many ways; inorganic, asymmetric, high flux and brittle.

(III) Heterogeneous solid films may be extracted to form porous membranes with microfiltration properties. The most common are polymers extruded with high loadings of mineral or oil fillers, which are subsequently leached out. The common application for such materials is as battery separators, but some are employed as membranes. Inorganic glasses may be selectively extracted to produce porous structures having a spectrum of pore sizes. Metals may be made into membranes by selectively dissolving one phase. Coextrusion of two polymers followed by extraction of one is another variant [24].

(IV) Symmetrical phase inversion membranes are the most important commercial membranes produced today. They are the traditional mainstay of the microfiltration industry. There are two major variants in the method. The first, and most significant process involves preparing a concentrated solution of a polymer in a solvent. The solution is spread into a thin film, then precipitated through the addition of a non-solvent, usually water, sometimes from the vapor phase. The technique is impressively versatile, capable of producing fairly uniform membranes whose pore size may be varied within broad limits [25].

The second process is thermal precipitation. A solution of polymer in poor solvent is prepared at elevated temperature. A sudden drop in solution temperature causes the polymer to precipitate. The solvent is then washed out. Membranes may be spun or cast at high rates using thermal phase inversion.

(V) Asymmetric membranes derived from solution form the most important class of ultrafiltration membranes, and they are important in microfiltration. These membranes, often referred to as skinned membranes, divide two necessary functions of a membrane, allowing each to be optimized. First, there is the separating layer or skin. Separation is achieved here, and a high concentration of uniform pores is desired. Since the separation process is achieved at the

surface, and resistance to flow through a pore is proportional to the pore length, the universal rule is "thinner is better".

The second functional part of the membrane is the support. Its job is to provide mechanical support for the skin, and to make the membrane able to withstand handling and processing. Desirable characteristics include minimal resistance to flow, adequate resistance to compression in service and chemical inertness at least equal to the skin. It must also resist plugging by any particle able to pass through the skin.

The discovery of the asymmetric membrane by Loeb and Sourirajan was a major breakthrough in membrane technology, and the techniques in use today are derived from their early work. In its simplest form, a polymer is dissolved at about 20% solids in a water miscible solvent. The polymer solution is cast on a plate to form a thin film, which is then quenched in water. In normal practice, the skin forms on top, and immediately below it, the polymer forms a much more open porous support layer. Almost all commercial membranes are cast on fabric (sometimes called "casting paper"), a nonwoven polyester or polyolefin material. The substrate must also bond well to the fabric, which becomes a permanent part of the membrane structure. The skin is a small fraction of the finished membrane thickness.

(VII) Asymmetric composite structures are sometimes used for UF and MF. The oldest type is the dynamically formed membrane mentioned in the discussion under (I). Dynamic membranes do not normally require a membrane for a substrate. Porous materials derived from microporous media are commonly employed. Hydrous zirconium oxide is the favorite material, but others are cited in the literature. The major commercial manifestation of the technology uses porous carbon tubes for the substrate.

A few UF membranes are prepared by coating a previously prepared organic membrane with a topcoat. Extra uniform pore size distribution is one goal [26].

Self-assembled membranes are made from the natural membranes found on certain types of anachobacteria. Microporous membranes are coated with self-assembling fragments from these very unusual bacteria to form extremely uniform pore size distribution membranes. The bacteria grow in an extremely aggressive chemical environment, and the assembled membranes show excellent chemical resistance [27].

1.3.1 Membrane Ratings

Membranes are rated by the rate at which they produce permeate (*flux*), and the ability to discriminate between things they retain and things they pass. The flux issue is treated extensively above, but almost all MF and UF membranes are rated by their *water flux*, a value taken under standard conditions that has practically nothing to do with the flux found in actual operating conditions.

What the membrane holds back is described by three different words: retention, rejection, and reflection. For UF and MF, these terms are practically speaking synonymous. The choice between "rejection" and "retention" is largely dependent on the author's background. Reflection does have a special meaning in certain exotic applications.

By convention, retention is defined as:

$$R_i \equiv 1 - \frac{c_i\,(\text{permeate})}{c_i\,(\text{feed})} \tag{1.27}$$

where c is the concentration (weight, volume, conductivity, etc.) of the ith species. This definition is arbitrary in that by convention concentration is measured in the bulk of the feed, well distant from the membrane. Physically, the concentration that matters is that at the membrane surface, which can be quite different. The convention makes it much easier to do calculations about important things like yield, but it can be confusing.

1.3.1.1 Microfiltration

Only microfiltration membranes are easily tested by direct examination, as their pores can be observed by electron microscopy. Since the number of pores that may be observed directly by microscope is so small, microscopic pore-size determination is mainly useful for membrane research and verification of other pore-size-determining methods.

Large areas of microfiltration membrane can be tested and verified by a bubble test. Pores of the membrane are filled with liquid, then a gas is forced against the face of the membrane. The Young–Laplace equation relates the pressure required to force a bubble through a pore to its radius and the interfacial surface tension between the penetrating gas and the liquid in the membrane pore.

$$\Delta P = \frac{2\,\gamma \cos\,\theta}{r} \tag{1.28}$$

where γ is the surface tension (N m^{-1}), r is the pore radius (m), and P is pressure (in Pa). θ is the liquid–solid contact angle. For a fluid wetting the membrane perfectly, $\cos\,\theta = 1$. By raising the gas pressure on a wet membrane until the first bubble appears, the largest pore may be identified. This is a good test to run on a membrane apparatus used to sterilize a fluid, since bacteria larger than the identified largest pore (or leak) ought not to be able to penetrate the assembly. Pore size distribution may also be run by bubble point, but its most important function is to verify that all pores are smaller than a specific size. Bubble point testing is particularly useful in assembled microfilters, since the

membrane and all seals may be verified. Periodic testing insures that the assembly retains its integrity.

Diffusional flow of gas is a complication in large MF assemblies. It results from gas dissolving in pore liquid at the high pressure side, and desorbing at the low pressure side. In small area membrane tests it is generally unnoticed, but it can be a perturbing factor in larger assemblies. If the number of pores and the average pore length are known, the effect can be computed. It is easily distinguished from gas flow at the bubble point, although special protocols are used to insure that the apparatus meets the required level of bacterial reduction.

Membranes are further verified by challenge with microorganisms of known size — ability to retain all the organisms is proof that all pores are smaller than the organism. The best known microorganism for pore size determination is *Pseudomonas diminuta*, an asporogenous gram-negative rod with a mean diameter of 0.3 μm. Membranes with pore size smaller than that are used to ensure sterility in many applications. Leahy and Sullivan [28] provide details of validation procedures. Membranes may also be tested by latex particles.

There are a number of ASTM standard methods dealing issues of membrane testing. The one describing the bubble point method is ASTM F316-86, "Standard test method for pore size characteristics of membrane filters by bubble point and mean flow pore test." It is a method for individual membrane disks, not an entire apparatus, but the method includes corrections for diffusive flow and provides a good description of the technique. It also gives a method for determining pore size distribution. Goel et al. provide additional detail [29].

1.3.1.2 Ultrafiltration

Ultrafiltration membranes are not tested by bubble point. The pores are too small, so other means are used. Direct microscopic observation of the surface is difficult and unreliable. Because of their small size, the pores usually close when samples are dried for the electron microscope. Equation (1.28) also describes the force pulling a pore shut as it dries, and as r becomes very small, the force is enormous. Furthermore, its effect is greatest on the smallest pores. Critical point drying reduces γ to zero, and, although not without complications of its own, it has been used to produce a *few* good pictures. They are scattered exceptions in larger number of misleading photographs.

The best known method for UF membranes is molecular weight cutoff. Unfortunately, it is widely misunderstood and has been the cause of much error.

1.3.1.2.1 Molecular Weight Cutoff

The concept of molecular weight cutoff is deceptively simple. Ultrafilters retain soluble macromolecules, so why not measure their porosity by seeing

which molecules will pass through them? The concept of a "molecular weight cutoff" was conceived and introduced into commerce by Amicon Corporation in the mid 1960s. Some of the complications arising from the name were foreseen, others were not. To persons totally unfamiliar with ultrafiltration, MWCO communicated a new concept. The convention set by Amicon in the 1960s, now generally but not universally followed, is to define MWCO as the *molecular weight of the globular protein which is 90% retained by the membrane.*

In spite of decades of effort to narrow the distribution, most commercial membranes are not notably "sharp", so there is the complication that UF membranes have a distribution of pore sizes. That distribution may be polydisperse, and is in many successful commercial membranes. In the extreme case, picture a polydisperse membrane with most of its pores in one distribution and a few in another much larger distribution. The MWCO could fit between these distributions, so the membrane could have significant transport capacity for proteins above the "cutoff". Even for membranes with a normal distribution of pore size, the "90% point" is quite arbitrary.

For membranes with a perfectly monodisperse pore structure, there is the complication that membrane materials adsorb proteins, the adsorption is material specific and is dependent on concentration, pH, ionic strength, temperature, etc. Adsorption has two consequences: it changes the pore size and it removes protein from the permeate by adsorption in addition to that removed by "sieving". Porter [30] gives an old but illustrative table for adsorption of Cytochrome C on materials used for UF membranes, with values ranging from 1% to 25%.

Another complication, and source of considerable confusion, is that of marker size. UF membranes are basically size sensitive.. Polymeric markers are commonly employed. and polymers of the same molecular weight can have very different molecular size. To further complicate the picture, molecular shape can change in the vicinity of a membrane. Porter (1990) states that Dextran 250, a branched polysaccharide with molecular weight 250 kilodaltons passes through a 50 kD MWCO membrane. Linear molecules, such as polyacrylic acid, pass easily thorough membranes with MWCO far below their molecular weight.

To get a reproducible number for MWCO, many factors must be held constant. To the producer of membranes, that is easy enough, for by standardizing the test, he can have some assurance that the same membrane is being made in successive lots. Such standardized testing is also useful to a user of membranes, who has some assurance that a constant material is being supplied.

To test the membrane using protein, in keeping with the definition of MWCO, it is necessary to keep the concentration in the feed very low to prevent polarization effects which result in "auto filtration", the consequence of which would be to measure the boundary layer rather than the membrane itself. But

low concentration raises the specter of adsorption becoming important, perhaps dominant, in the retention measurement.

Because of the severe difficulties in testing with globular proteins, most membrane manufacturers use surrogate probes. Materials selected are ones for which the complications are minimized, the probe is simple, fast and cheap to detect, does not readily biodegrade, and with which the results, whatever they are, are reproducible. There is a good faith attempt to relate the findings back to globular protein, but the frustrations of the protein test sufficiently daunting to make the probe test the only test in many cases. And the convention adopted by manufacturer "A" may well be quite different from that adopted by manufacturer "B".

Severe misunderstanding arises when membrane users assume that MWCO means what it stands for. Further complications arise when users assume that a 50 kD membrane will separate a 25 kD material from a 75 kD material. If the lower molecular weight material is a branched polysaccharide, and the higher molecular weight material is a globular protein, and the solution is dilute and very well stirred, and the materials are right and the pH is correct etc. then there is a chance.

The existence of a gel-like layer at the membrane further complicates the ability of a UF membrane to fractionate polymers. Concentrated solutions of macromolecules, whether literally gel or not, are known to be highly entangled networks. How can a smaller polymer wiggle through a concentrated tangle of larger polymers and find the membrane pore through which it may theoretically fit? No matter what the true nature of the boundary layer, there is a "traffic jam" at the membrane surface with the cars just as stuck as the trucks. The rule of thumb is that for the separation to take place in UF with reasonable efficiency, there needs to be a factor of 10 in the ratio of the sizes of the materials separated. Kesting makes the same distinction about UF itself, saying that UF begins where the microsolute is 10 times as large as the solvent [31]. Much as we might wish otherwise, MWCO doesn't mean much more than a rough cut at relative pore size.

While MWCO is often misunderstood, the goal of separating macromolecules is well understood by industrial and academic researchers, and is the topic of ongoing research.

1.3.1.3 Complications from Fouling

Fouling is a major problem in all membrane operations. It causes significant problems in measuring and interpreting pore size in both MF and UF membranes. MF and UF membranes contain "pores", and for most membranes, they are not all of the same size. Fouling effects pores differently. Belfort [32] illustrates three cases affecting MF membranes to which needs to be added a fourth primarily affecting UF (Fig. 1.6).

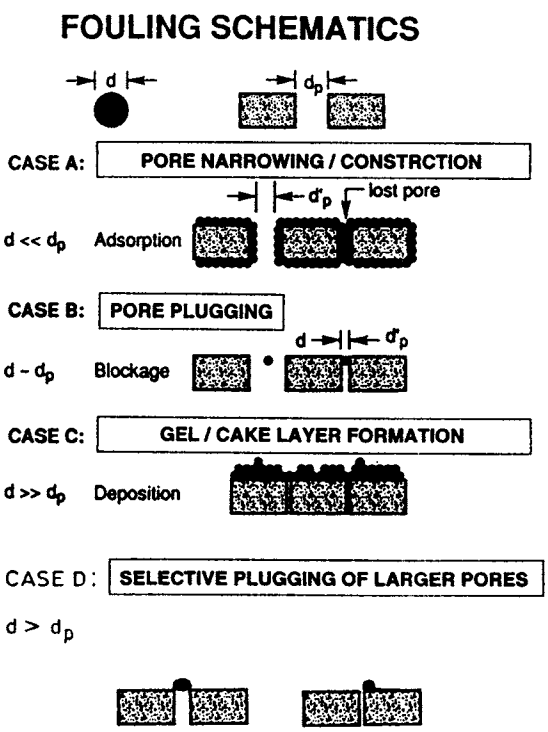

Fig. 1.6. Fouling Schematics (after Belfort). Case A: Particles plug smaller pores and narrow larger ones. Case B: Particles plug narrow pores. Case C: Particles form a layer on the membrane. Case D: Particles or debris plug largest pores.

Case A: Adsorption causes all pores to become smaller, and may result in the smallest pores plugging. In the case of a protein probe present in dilute solution, this fouling error would cause the test to understate the size of all pores, and could truncate the distribution on the low pore size end.

Case B: Pore plugging. In the absence of any adsorption, particles may plug pores. For the example shown, smaller pores would be expected to suffer disproportionately. Remember, the drawing is an artistic simplification. Pores are not created by precision drills in uniform materials. The entrance to a pore may be fairly sharp in a mica membrane exposed to radiation and etched by chemicals prepared by a careful chemist, but in the real world of membranes, pore openings are considerably less precise. Pore openings may be conical, they may be other shapes, and for many materials, "pore" is a tenuous concept. Nonetheless, to some degree the small openings are more susceptible to being plugged by small particles.

Case C represents the deposition of a material that supersedes the porous structure of the membrane. The membrane now becomes analogous to a precoat filter. Fouling is irreversible to the extent that the layer nearest the membrane

is probably adsorbed onto it. Throughout the layer, the binding may or may not be irreversible. At the fluid interface, quite a degree of dynamic reversibility remains. One may assume that in all cases, the effect is to shift the effective pore size downwards.

Case D is peculiar to membranes with small pores filtering particles much larger than the pores. An example is UF membranes processing electrodeposition paint, all of whose particles are much larger than most membrane pores. The effect is to plug the large holes, leaving the smaller ones. It is case B in reverse. The effect is to reduce the average pore diameter by affecting only the high end of the distribution.

Case D is familiar to operators of industrial equipment who often find that macroscopic seal leaks are effectively plugged by the gross debris in a feed stream.

1.3.1.3.1 Effects on Flux

Fouling affects flux dramatically. The pure water flux through a virgin UF membrane is commonly tenfold greater than the water flux after the membrane has been exposed to protein.

Flow will be laminar through a cylindrical pore because of the size. To summarize Eqs. (1.1)–(1.3), flux through a given area containing N cylindrical pores each having diameter d,

$$J = \frac{\pi \Delta P}{128 \mu t} \sum_{0}^{\infty} \frac{N_i}{A} d_i^4 \tag{1.29}$$

Reviewing the four cases of pore narrowing, Case B, in which smaller pores are plugged and larger ones are unaffected, will have the least impact on flux. Case A, narrowing of all pores and plugging of some of the smallest, will have a greater impact, because loss of some pore dimension is particularly important given the fourth power of diameter. Case C is a guess, as the porosity of a cake layer on the membrane can be anything. Case D results in a dramatic loss of throughput, because that form of plugging takes out the most productive pores.

1.3.1.3.2 Overall Effect on Retention

Passage of material through a pore obviously depends on how much is flowing and what that pore will pass. Big pores pass large quantities, but their retention is different from smaller pores. As a membrane fouls, the retention characteristics worked out for the virgin membrane will change, often dramatically.

A few general rules apply. Fouling processes that plug the smallest pores have little effect on retention. In theory they would be expected to lower retention somewhat, as the most retentive pores are plugged leaving the larger

less retentive ones, but the contribution of the smallest pores to overall output is normally low anyway. When fouling lowers retention it is probably because of the artifact resulting in the definition of retention: bulk concentration may be constant but concentration at the membrane may rise considerably due to fouling and the resulting impediment to back diffusion.

Fouling by almost any other mechanism raises retention. Either it substitutes a cake layer on top of the membrane, or it narrows pores, or it selectively plugs larger ones. It is poorly kept secret that many membranes do not do the job they are sold to do until they are a little bit fouled.

In an ideal world, membranes would contain a very high density of fully uniform cylindrical pores. It is perhaps instructive that in spite of the very creative effort invested in "sharp" membranes, their share of the overall membrane market is very small. Practically speaking, "ordinary" membranes have proven to be adequate for most separations.

1.4 MEMBRANE MODULES

In the discussion of the importance of the boundary layer, we saw that the output of a UF or MF membrane device is controlled by mass transfer at the membrane surface. There are special cases in which this generalization is not followed. One is the case where the solvent being processed is almost devoid of retained material. A second is the much more important case of fouling. Nevertheless, the way in which feed material is presented to the membrane is of critical importance. Ways to incorporate membrane area into subassemblies efficiently and economically is the objective of module design.

A requirement of a module is that it be easily removed and replaced. Membranes have finite lives. They still fall short of perfection in their manufacture. Module size must balance the probability of including a defective membrane, which naturally rises with module size, with the economy of installation and replacement which, up to a practical limit, improves with module size.

As membrane manufacture became more sophisticated, the probability of failure per unit area dropped dramatically. Therefore, the economics of module manufacture have pushed the membrane area per module up. Physical handling must be manageable, and the cost of special equipment for module replacement is an added capital cost, putting an upward limit on module size.

More important is how the module manages the fluid flow of the feed. Most crossflow membrane devices operate in turbulent flow, so designing for low energy consumption (important for both operating economics and capital cost) requires avoiding sudden expansions and contractions in conduit diameter, and avoiding small radius bends. Both these requirements are very demanding, and pose major challenges to the designer. For modules designed for laminar

flow, sudden changes in conduit diameter are far less important than the diameter of the smallest passage through which the fluid must flow. For any module, reliability is increased if stagnation points, where fibrous material and debris will accumulate, are minimized.

In spite of all their obvious shortcomings, spiral modules (see below) are widely used in both MF and UF, and their importance is both major and increasing.

1.4.1 Background

Because the demands are stringent, and because of the high rate of innovation in the membrane industry, module design diverged considerably before it started to converge on certain winning designs.

Early designs were 25 mm diameter tubes with the membrane cast inside (Abcor-Koch), capillaries (Amicon-Romicon) parallel plate designs (Dorr Oliver) and plate and frame devices (DDS). All of these had advantages, and each remains in the market. All have undergone development and refinement. While 25 mm tubes are still sold, the dominant polymeric tubular systems have 12 mm tubes. Ceramic devices usually have smaller channels, 4–6 mm diameter, and one new ceramic device has square cross section channels 1.9 mm on a side.

Large tubular membranes illustrate the extreme case of attention to fluid mechanics. The membranes were designed to have a diameter change only at the manifold, and then to have 50 m of tubular membrane joined by large radius return bends before the feed passed into the exit manifold. There were no stagnation points, and seals were made on the ends of the tubes to avoid diameter changes in the fluid path. The devices had wonderful hydraulic efficiency, about 90% of all the pressure drop occurred at a membrane surface, and they were remarkably resistant to fibres and debris. They were also bulky and expensive.

Membrane cassettes were at the other extreme. The fluid undergoes numerous direction reversals in very short radius turns. Significant pressure drop occurs in the inlet and outlet ports. But they are very compact and capable of automated manufacture.

Evolved versions of these extremes persist, but over 50% of the membrane area sold in crossflow applications is in spiral wound modules.

1.4.2 Spiral Wound

Spirals were not an early entry in UF or MF, they were invented in the early days of reverse osmosis [33] and found unsuitable for general UF. The unsatisfactory features were gradually designed out of the spiral, while the attractive attributes — compactness, ease and economy of manufacture and ease of

replacement — were maintained. The truly successful UF spiral required over a decade of constant improvement. Success inspired imitation, and there are now a number of manufacturers of spiral membranes offering a wide variety of membrane types, resulting in a competitive market for replacements and a decline in user's costs. For almost any new application, the spiral design must be inadequate in order for another design to prevail.

1.4.3 Capillary

Capillary devices, designed so that the process fluid flows inside the hollow fibre with the permeate flowing through the wall into a module housing seem a natural for process applications, but difficulties in the manufacture of modules plagued them for years. Their chief market niche today is in ultrapure water UF, where the open path for permeate is an advantage. Capillaries are used in many other applications.

In addition to the large volume capillary modules, there are two special variants. One, sold by Memtec (Australia) feeds the process stream on the shell side of the module with permeate exiting in the hollow fibre. This turns general design logic on its head, but it succeeds because of the innovation of pushing off the boundary layer accumulation of solids every few minutes with a blast of air pushed backwards through the membrane. The other variant (Mitsubishi Rayon Engineering) lets the fibres flop in the process stream because only the two ends are potted leaving numerous hairpin shaped membranes free to move in the fluid as it passes by.

1.4.3 Plate and Frame

Plate and frame devices are used in several applications. For most equipment, almost any flat sheet stock may be fit into a plate and frame device, which can have a favorable influence on the economics of membrane replacement.

1.4.4 Cartridges

For the applications where dead-end flow is appropriate, pleated cartridges are the usual answer. One firm reports a spiral run in dead-end flow, where in the early stages of filtration, some of the membrane area actually operates in cross flow.

A strong movement towards compact and energy-efficient design is apparent. Economics dictate that membrane equipment be compact to reduce the "footprint" on expensive industrial floor space, and improvements in design and membrane reliability make that possible.

1.5 FOULING

Fouling is the term used to describe the loss of throughput of a membrane device as it becomes chemically or physically changed by the process fluid (often by a minor component or a contaminant) [34]. Fouling is different from concentration polarization. Both reduce output, and their resistances are additive. Fouling can be thought of as the effect causing a loss of flux which cannot be reversed while the process is running. An increase in concentration or viscosity, or a decrease in fluid velocity, or, in some operating ranges, pressure, will cause a flux decline. Any of the declines from these causes are reversible by restoring concentration, velocity, etc. to prior values. Restoring prior conditions will not restore flux if a membrane is fouled. That is the best test of fouling.

Fouling is also distinct from membrane compaction, primarily a phenomenon resulting from irreversible creep in a membrane as a response to stress. This phenomenon is found in some reverse osmosis membranes, but at the pressures used in UF and MF, it may usually be ignored.

1.5.1 Prompt Fouling

There are several types of fouling. *Prompt fouling* is an adsorption phenomenon. It may occur so rapidly in an extreme case, that it may be observed by wetting a membrane with a process fluid without applying pressure. A marked decrease in water flux of the rinsed membrane indicates a strong likelihood of prompt fouling. It is thought to be caused by some component in the feed — protein is the most common cause — adsorbing on the surface of, and partially obstructing the passages through, the membrane. The effect occurs in the first seconds of an ultrafiltration, making it difficult to spot. In addition to lowering the flux of the membrane, this type of fouling raises the retention. The effect is very common, although not always recognized as such. Often, membranes are characterized after it has occurred [35]. In fact, some membranes are not commercially useful until prompt fouling has taken place. In principle, and usually, it is a negative effect.

1.5.2 Cumulative Fouling

Cumulative fouling is the slow degradation of membrane flux during a process run. It can reduce the flux to half its original value in minutes, or in months. It may be caused by minute concentrations of a poison, but is commonly the result of the slow deposition of some material in the feed stream onto the membrane. Usually, the deposition is followed by a rearrangement into a stable layer harder to remove. It is often related to prompt fouling, because the prompt fouling layer provides the foothold for a subsequent accumulation of foulant.

1.5.3 Destructive Fouling

Some fouling is totally irreversible. A substance present in the feed at low concentration having an affinity for the membrane is the usual culprit. Especially troublesome is a sparingly soluble substance at or near its saturation concentration. Such a material can slowly sorb in the membrane, and in the worst case, change the membrane's structure irreversibly. Antifoams are examples of a class of material responsible on occasion for destructive fouling. With the chemically robust membranes in use today, this effect is very unusual, unless a membrane feed has been contaminated with a damaging solvent.

1.5.4 Frequency of Fouling

Virtually all membranes in all commercial applications foul: "how fast" is an important economic issue. Proper cleaning generally restores output. Membrane producers and purveyors of cleaning agents devote considerable effort to finding safe, effective and economical means of returning the membranes to full productivity. Frequently, cleaning agents slowly damage membranes, making them more susceptible to future fouling. While there are totally benign cleaning agents for some types of fouling, the more common foulants such as those involving proteins require aggressive cleaning agents to keep the cleaning cycle short. It is said that the cleaning requirements for membranes are the major determinant of membrane life [36].

Just as fouling influences design, design influences fouling. Figure 1.3 shows the normal pressure–flux output curve for crossflow filtration. Operating in the region towards the right (high pressure) will produce fouling more quickly than operation around the knee of the curve [37]. The region to avoid is the high-pressure, low-flow regime. Experience indicates that thick, dense boundary layers promote fouling [38]. Dead-end filtration would be a worst-case operating condition.

Pressure driven equipment that operates membranes only in the low fouling region at or below the knee of the operating curve is very hard to design. Several firms are trying innovative approaches that decouple the pressure driving force from the membrane depolarizing force, such as by the use of vibration to promote mass transfer [39] the use of Taylor vortices [40] and the use of controlled permeate back pressure [41].

Fouling is the most important economic determinant of most crossflow membrane processes. Recently, researchers are finding ways to quantify results and publish meaningful papers on fouling. It is a particularly popular and important field with a rapidly expanding published information base.

1.6 APPLICATIONS

1.6.1 Microfiltration

The market for MF membranes and equipment is a billion dollar giant dwarfing all other membrane applications except hemodialysis. It is a market with outstanding competitors and large R&D budgets, with firms generally possessing excellent market research, marketing and management. Major market areas are: sterile filtration, medical applications, biotechnology and fluid purification.

Most of the microfiltration applications listed operate in dead-end flow. A few operate in cross flow. One important criterion for deciding whether crossflow is appropriate is the quantity of solids that must be retained by the microfilter. The higher the level of solids, the higher the likelihood that the crossflow filtration will be used.

Streams containing high loadings of solids (>0.5%) processed by membrane filters usually operate in crossflow. As discussed in the section on the boundary layer and concentration polarization, the limit to the rate at which a crossflow device produces permeate is the rate at which solids retained by the membrane can redisperse into the bulk feed flowing past the surface. A cursory analysis of the mass transfer equations shows that the molecular diffusivity of the retained material is a direct determinate of how fast it diffuses away from the surface. The colloidal material retained by a microfilter has a very low value of diffusivity. The redispersion rate of retained material is thus calculated to be very low. In fact, microfiltration rates are often quite high compared to UF, even at lower crossflow velocity. The answer seems to lie in a shear enhanced particle diffusivity which results in dramatically increased flux [42].

Membrane filters operating on feeds with lower loadings of solids (<0.5%) are generally operated in dead-end flow. Commonly, the surface of the membrane is protected by a guard filter which entrains most of the larger, easier to filter solids before they reach the membrane. The structure acts as a depth filter backed by a membrane filter.

Some of these devices are quite sophisticated, because both prefilter and membrane filter can be charged to give superior nonplugging characteristics. In some applications, these composite structural filters perform comparably to the outstanding characteristics of asbestos filters.

Fluids with low solids loadings (<0.1%) are almost always filtered in dead-end flow, where the membrane acts as an absolute filter as fluid passes directly through it. For some time, track-etched filters dominated this market. Now, other membranes compete successfully.

Membranes may be made with conical pores. When the small end of the cone is at the skin, the membrane is inherently nonplugging. In some low solids

loading applications, these membranes are run "upside down", that is, with the wide part of the cone towards the process stream. In this way, the cone serves as a trap for particles. This configuration mimics that of a structured filter, which wraps a coarse filter outside progressively finer filters. Although the membrane eventually plugs, its dirt-holding capacity is increased. This operating scheme is only appropriate where the load of material to be retained is quite low.

An especially important characteristic of a microfiltration membrane is uniform pores, with as many of them per unit area as possible, and with the thinnest possible layer in which these pores are at their smallest size.

Since a membrane will not reliably retain anything smaller than its largest pore, the largest pore determines the membrane retention rating. Smaller pores contribute far less flow: a pore 0.9 times as large as rated pore size contributes only two-thirds as much throughput. Pore length may be minimized by making the active layer in which the pores are at their minimum diameter as thin as possible. The importance of pore density in a dead-end filter will be apparent.

Many applications for microfiltration membranes are relatively small individual uses that add up to quite a large market.

In addition to those well-established applications, there is a major effort to introduce MF into a wide variety of process applications. These applications, while small in number at present, would each use large quantities of membrane. Their potential for growth is great, but it will take a very long time for them to eclipse the existing applications in importance.

Pharmaceutical

Pharmaceutical applications are a major market for microfiltration membranes [43]. Liquid products that contain macrosolutes are routinely sterilized by microfiltration membranes, particularly if they are heat labile. Parenterals, antibiotics, blood products and ophthalmic preparations are examples. For some applications, the membrane may be exotic — positively charged nylon membranes have replaced asbestos for many of the applications formerly requiring the unique properties of asbestos, including pharmaceutical applications and wine.

Sterile Filtration

Integrity testing of membranes and membrane assemblies is achieved by bubble-point testing, diffusional measurements and other means. The common arbiter of success is the ability to withstand challenge by *Pseudomonas diminuta*, a small gram-negative rod with a mean diameter of 0.30 μm, although its size varies with environmental influences [44].

Sterile filtration used in the pharmaceutical industry in the U.S. is governed by the Food and Drug Administration, which publishes regulations from time to time in the Code of Federal Regulations.

Medical applications include guarding against microbial and particulate contamination of fluids being injected into a patient or used in hemodialysis.

Microfiltration plays an extensive role in maintaining sterility in tissue culture and other aseptic media applications. In an unusual application of membranes, epithelial cells are grown directly on a microporous membrane, with the nutrients passing through the membrane [45].

Gas Phase

Sterile process filters for gas-phase use are important membrane applications in pharmaceutical, biotechnology and medical applications. For example, membranes are used on the vents of sterile water tanks to prevent microbial contamination as the water level is lowered. Similarly, membranes protect autoclaves and freeze-dryers during the admission of gas after the duty cycle. With autoclaves, the steam is usually filtered as well, often with the same membrane that filters the inlet air [46]. Another application is gas to blanket sterile packaging lines.

Vents on fermenters is another sterilizing application for gas microfilters. In many fermentations, large volumes of air are used to maintain the oxygen content of the fermentation process. It is usually necessary to insure that microorganisms from the fermentation be kept from the environment. Microfiltration membranes are used to capture any organisms that escape. Most vent applications require that the membrane withstand steam sterilization.

Wine

Most of the wine produced passes through a membrane. Membrane filtration has virtually replaced heat and chemical treatment because it does not affect organoleptic properties. Some spoilage organisms will pass a 1-μm filter, so the preferred membrane is 0.45 μm [47]. Sterilizing membranes are run in dead-end flow, making them very easily plugged by the colloidal material present in wine. Prefiltration is practised, occasionally as a built-in part of the membrane cartridge.

Semiconductor

Semiconductor fabrication is an important microfiltration market. According to Millipore, 58% of all integrated circuit defects result from contaminated process fluids. As line widths drop below 1 μm, contaminants in the 0.1-μm range are important. Even at extremely high purity levels, an impurity of 1 part

per billion translates into 2×10^{12} 0.1 μm particles per m^3 of a gaseous reactant. Water is another major concern: a silicon wafer is exposed to about 10 m^3 while it is being turned into chips [48]. Water for chip rinsing is treated exhaustively to remove ions and particles, yet even in the best systems, particle shedding from pipes, filters and fixtures is a constant problem.

Microfiltration and ultrafiltration membranes are widely used as final point of use devices to improve yields in chip manufacture [49]. For gases, membranes are more thorough than fiber HEPA and ULPA filters [50]. For liquids, the logic of passing water through a microfilter after it has passed through a reverse osmosis membrane rests on the observation that particles introduced by shedding and bacterial activity are generally large enough to be removed by a microfiltration membrane. The relatively large pores of the MF membrane simplify the equipment needed to utilize it at the point of use, since pressure is lower, and throughput is higher. Notwithstanding normal criteria (discussed above) final filters for water are normally operated in cross flow.

Miscellaneous

The quantity of MF membranes consumed in laboratory, manufacturing, and miscellaneous uses is very large. Another biotech application of microfiltration membranes is their use in blotting of proteins. Many references may be found in Ref. [51].

Diatomaceous Earth Replacement

One particularly attractive target for process microfiltration membranes is clarification processes now accomplished through the use of diatomaceous earth (D.E.). MF membranes are usually capable of doing the same job as D.E. filters, but they achieve higher clarity products and usually higher yield. These advantages are currently marginal in the biggest applications, with not enough economic incentive to achieve the displacement of installed D.E. filters. If disposal costs for spent D.E. continue to rise, and the economics of process microfiltration improve as volume grows, then there is a likelihood that MF will become preferred over D.E. filtration in new installations and will eventually displace it in existing applications.

Water and Wastewater

An emerging application for MF is in the treatment of wastewater, particularly municipal sewage. Capillary membranes operating with shell side feed, at very low crossflow velocities, are reported to give excellent clarity and sterility if backwashed frequently [52]. When operated in conjunction with high-speed

bioreactors, very low overall detention times with excellent removal of particulates including bacteria and viruses, is reported in pilot trials [53]. It is speculated that a major disadvantage of high throughput bioreactors, small biomass particle size, is eliminated by the use of membrane filters.

Concerns about parasites in drinking water may be translated into a significant increase in the use of microfiltration in drinking water.

1.6.2 Ultrafiltration

Ultrafiltration has the ability to separate soluble macromolecules from other soluble species. Some of its large applications take advantage of this property, but others do not.

Microfiltration Replacement

Many of the largest process uses of ultrafilters would seem to be more logical for microfiltration. Apple juice is ultrafiltered, yet the application is a straightforward replacement of diatomaceous earth to remove colloidal particles, which are clearly within the range of a microfiltration membrane. Similarly, electrocoat paint is a suspension of particulates within the MF range.

The glib answer is that UF works better. The reason is the deformable nature of particles that are retained. If the membrane pores are not much smaller than the size of an easily deformable particle, plugging will result. UF membranes for the two applications mentioned have pores that are a small fraction of the size of the retained material, the colloidal matter is very deformable, and, of critical importance, there is nothing of value that the UF membrane would retain and the MF membrane would pass. So although microfiltration is the obvious choice, ultrafiltration is the correct choice.

Electrocoat Paint

Recovery of electrocoat paint is economically the most important application of UF [54]. An efficient way of applying a corrosion-resistant coating on industrial metal is electrophoretic deposition of colloidal paint from an aqueous bath It is the prime coat (for automobiles) or a one-coat finish (appliances, coathangers, etc.). The metal object must be properly cleaned and "passivated". It is then immersed in a paint tank, attached to an electrode, and the paint is plated on. During the process, the paint film undergoes electroendosmosis, and it emerges from the tank already robust. It is still quite wet with droplets of uncoated paint, the "dragout". This dragout is quite valuable: in the automobile industry, its value per vehicle is around US$ 4. If the paint were to be left on the metal, the painted finish would be lumpy. If it were rinsed off with water, a

dilute stream would result, which is difficult to concentrate and expensive to treat in a waste plant. If the dragout can be rinsed off using a clean stream derived from the paint tank, recycling back to the tank for utilization of the paint is straightforward. Ultrafilters are used to produce this rinse stream in metal finishing applications worldwide. A large installation will contain 150 m^2 of membrane area and produce 3 $m^3\ h^{-1}$ of permeate.

Fractionation of Whey [55]

In the production of cheese and casein, about 90% of the volume of the milk fed to the process ends up as whey. The quantity of whey produced in the United States, a tiny fraction of world production, is about 25 million m^3 per annum. Formerly almost entirely wasted, almost half of the domestic whey is now processed in one way or another. UF is the means to produce high-value products, ranging from 35% protein powder (a skim milk replacement) to 80%+ protein products used as high-value, high functionality food ingredients. A large dairy ultrafilter operating on whey will contain 1800 m^2 of membrane and have a whey intake of 1000 m^3 per day.

Cheese Production

An emerging process for the production of cheese uses UF on the milk before cheese is made, rather than on the whey produced as a by-product of cheese. The process is proven for soft cheeses and is in commercial operation for cheese base, an intermediate in the production of several mass consumption cheese products. UF is now beginning to be used in the production of cheddar cheese as well. The process details are not vital for this discussion, but as a conservative average, the use of UF reduces the milk required to make cheese by 6%. This reduction is accomplished by concentrating the curd-forming solids which enables process modifications to capture the soluble proteins ("whey proteins") in the cheese curd instead of allowing them to pass into the whey.

Textile Sizing

In the knitting and weaving of textiles, a sizing material is commonly applied to the warp threads to lubricate them and protect them from abrasion. The sizing material is removed before fabric is dyed. Ultrafiltration provides an economical means to recover and reuse the sizing solution. Recovery of the sizing encourages the use of more expensive but more effective sizing agents, such as polyvinyl alcohol. Since desizing baths operate hot, it is necessary for the ultrafilter to withstand constant operation at 85°C. Some inorganic membranes have been used in this application, but polymeric membranes operating at low flux are often more economical because their lower power consumption more than compensates for their shorter life and consequent replacement cost.

A large size recovery plant has a membrane area of 10 000 m^2, and a feed rate of 60 m^3 per hour.

Oily Wastewater

In the metal-working industry, lubricants and coolants are used in metal cutting, rolling, drawing, etc. These are usually oil-in-water emulsions. Eventually, the coolant becomes contaminated, degraded or spent, and is discarded. In addition, parts that have been cooled or lubricated by the emulsions are generally washed, creating a dilute oily emulsion. The quantity of spent, dilute emulsion just from washing newly formed aluminum cans is over 8 $m^3\ h^{-1}$ per can line. Ultrafiltration is the principal technology employed to fractionate this waste into a permeate stream of water suitable for a municipal sewer, and an oily concentrate rich enough to support combustion or from which to recover oil.

Gelatin

Gelatin coming from the extractor is a dilute solution of soluble collagen. It is dried at about 30% total solids. The bulk of the water to be removed before the dryer may be evaporated or passed through a UF membrane. Because the membrane passes some of the salts along with the water, a subsequent ion exchange step is minimized when UF is used. Although ultrafiltration cannot concentrate the stream all the way to 30% solids, it can remove almost 90% of the water in the feed using less energy and with better economics than evaporation.

Juice

A significant fraction of all clarified apple juice produced in North America is passed through a UF membrane. The membrane process is rapidly displacing rotary vacuum filtration because of higher yield, better and more reliable quality and ease of operation. A major driving force is the elimination of the diatomaceous earth disposal problem.

Pulp and Paper

Lignosulfonates are recovered from spent sulfite liquor and from kraft black liquor in the pulp industry [56]. Recovered lignosulfonates are valued as dispersants, binders and for the production of vanillin.

Ultrafiltration is sometimes used to reduce color in caustic bleach effluents from the pulping process. Good color reductions are achieved, but the economic viability of the process is very location-specific. Both UF and MF are under development for the treatment of white water from paper-making machines. Pulp and paper applications are potentially among the largest uses for UF, but there is a long history of "almost successful" results to overcome.

1.7 ECONOMICS

Engineers designing crossflow membrane equipment into process flowsheets must balance capital cost and operating expense just as they do for other process equipment. For membrane equipment, the capital contributions and "typical" fraction of the total are:

Capital item	Percent of total capital
Pumps	30%
Replaceable membrane elements	20%
Housings for membranes	10%
Pipes, valves and framework	20%
Controls	15%
Other	5%

These numbers assume stainless fluid contact surfaces, painted steel framework, and automated operating and cleaning equipment.

Operating costs are dominated by capital charges in most cases. Firms demand short payback periods for membrane equipment, which means that capital charges are always the largest item. Naturally, this fact has a major influence on the design of membrane process equipment.

An example of the sub optimization, recall that previously flux J was shown to be proportional to Q^m where $0.8 < m < 2$. For most applications, m is closer to the lower limit than the higher one. Flux is conveniently measured in units such as 1 m^{-2} hr^{-1}, so for a specified output of product, increasing flux decreases membrane area.

Pressure drop in a well constructed turbulent flow system increases as $Q^{1.75}$. Energy increases as $Q^{2.75}$. Pump cost, defined broadly to include drivers and piping, is a function of both flow rate and power. As the broadly-defined pump cost goes down, more membrane area must be installed to compensate for the lower flux. Conversely, a high-power pumping package will give higher flux, and will require less membrane area [57]. Figure 1.7 shows the results of an actual calculation trading these two variables.

A volumetric flow rate of 1 represents the optimum for this particular calculation. At higher flow rates, the economics are dominated by pump costs. At very low flow rates, they are dominated by membrane costs. It is apparent that the incremental economics of pumps is different from the more nearly linear economics of adding more membrane area.

1.7.1 Energy

The optimum UF design commonly results in the dissipation of about 50 W m^{-2} at the membrane surface. After taking all the efficiencies into account in

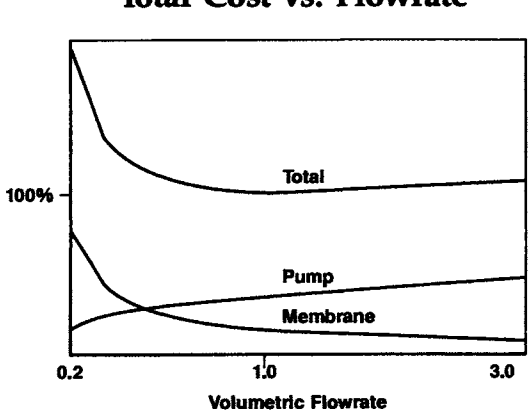

Fig. 1.7. Cost of membranes, system, and total system cost as a function of flowrate past the membranes. 1.0 on the abscissa is the optimum design point.

translating incoming electrical energy through wiring, driver, coupling, pump, pipe, valves, headers, etc., this energy must be divided by an efficiency factor of between 0.45 and 0.64 to account for actual energy employed. Actual energy required per unit of output may be obtained by dividing the total incoming energy by flux. A typical process flux might be 30 l $m^{-2} h^{-1}$. If the efficiency were 50%, the energy requirement would be 50 W $m^{-2}/0.50 \times 30$ l $m^{-2} h^{-1} = 3.3$ Watt-h $l^{-1} = 3.3$ kWh m^{-3}, the units used to describe energy requirement per unit permeated through the membrane. If cleaning is frequent, this energy may need to be adjusted upwards by 5% to take that component into account.

Operating economics, as has been stated, are dominated by capital cost. *Excluding capital charges*, the major operating cost elements are:

Item	Range of costs, % of total
Membrane replacement	35–50
Cleaning costs	35–12
Energy	15–20
Labor	15–18

Since all separation processes produce more than one stream, there may be downstream costs associated with a membrane separation by-product.

A more detailed analysis of economics may be found in Ref. [58].

REFERENCES

1 S.B. Kessler and E. Klein, Dialysis, Part III. In: W.S. Ho and K.K. Sirkar (Eds.), *Membrane Handbook*. Van Nostrand Reinhold, New York, 1992, Ch. 11–15.

2 R.E. Kesting, *Synthetic Polymeric Membranes*. New York, Wiley, 1985, p. 3.

3 R. Zsigmondy and W. Bachmann, *Anorg. Allegm Chem.*, 103 (1918) 119; R. Zsigmondy, *Filter for Ultramicroscopic Particles*, U.S. 1,421,341, 1922.

4 John Peterson, Millipore Corp., internal document.

5 M.C. Porter, *Handbook of Industrial Membrane Technology*. Noyes Publications, Park Ridge, NJ, 1990, p 61,

6 A. Goetz, *Microporous Filter Film on a Solid Support*. U.S. Patent 2,926,104, 1960.

7 As a historical fact, Elford apparently discovered asymmetric MF membranes far in advance of the discovery of skinned RO membranes. See W.J. Elford, Roy. Soc. Proc. B, 106 (1930) pp. 216.

8 C.E. Reid and E.J. Breton, *J. Appl. Polymer Sci.*, 1 (1959), 133–143.

9 Aerojet General, Report No. 3066 to the Office of Saline Water, Department of Interior, Contract No. 14-01-0001-435, 1965.

10 North Star Research and Develop Institute, Report No. 359 to the Office of Saline Water, Department of Interior, Contract No. 14-01-0001-1143, 1968.

11 Shmuel Sternberg, Private Communication.

12 W.F. Blatt, A. Dravid, A.S. Michaels and L. Nelsen, Solute Polarization and Cake Formation in Membrane Ultrafiltration: Causes, Consequences, and Control Techniques, in: J.E. Flynn (Ed.), *Membrane Science & Technology*. Plenum Press, New York, 1970, p. 47.

13 G. Jonsson, Boundary layer phenomena during ultrafiltration of dextran and whey protein solutions. *Desalination*, 51 (1984) 61–77.

14 Vincent L. Vilker et al., The osmotic pressure of concentrated protein and lipoprotein solutions and its significance to ultrafiltration. J. Membrane Sci., 20 (1984) 63–77.
D.R. Trettin and M.R. Doshi, Pressure-Independent Ultrafiltration — Is it Gel Limited or Osmotic Pressure Limited. In: A.F. Turbak (Ed.), *Synthetic Membranes, Vol. II*, ACS Symposium Series 154. American Chemical Society, Washington, 1981, pp. 373–409.
J.G. Wijmans et al., Flux limitation in ultrafiltration: osmotic pressure model and gel layer model. *J. Membr. Sci.*, 20 (1984) 115–124.
C. Tanford, *Physical Chemistry of Macromolecules*. Wiley, New York, 1961, Chap. 4.
W. Eykamp, Flux Limiting Step in Pressure-Driven Membrane Processes, in: S.L. Sandler and B.A. Finlayson (Eds.), *Chemical Engineering Education in a Changing Environment*. Am. Inst. Chemical Engineers, New York, 1988, pp. 403–415.
All recent values are higher than, but still in general agreement after correcting for molecular weight, with the classic Scatchard work on BSA. G. Stachard, Physical chemistry of protein solutions I. *J. Am. Chem. Soc.*, 68 (1946) 2315–2319 (1946); G. Stachard et al., Preparation and properties of serum and plasma proteins. VI. *ibid.*, 2320–2329; G. Stachard et al., Preparation and properties of serum and plasma proteins. VII. *ibid.*, 2610–2612.

15 H. Nabetani, M. Nakajima, A. Watanabe, S. Nakao and S. Kimura, Effects of osmotic pressure and adsorption on ultrafiltration of ovalbumin. *AIChE J.*, 36 (6) (1990) 907–915.

16 Tanford, *op. cit.* p. 215

17 A.R. DaCosta, *Fluid Flow and Mass Transfer in Spacer-filled Channels*. Ph.D. thesis submitted to the Department of Chemical Engineering and Industrial Chemistry, University of New South Wales, Sydney, Australia, 1993.

18 A.R. Da Costa, A.G. Fane, C.J.D. Fell and A.C.M. Franken, Optimal channel spacer design for ultrafiltration. *J. Membrane Sci.*, 62 (3) (1991), 275–291.
19 U.B. Holeschovsky and C.L. Cooney, Quantitative description of ultrafiltration in a rotating filtration device. *AIChE J.*, 37 (8) (1991) 1219–1226.
20 K.J. Summers, *Effects of Vibratory Enhanced Shear on Membrane Fouling*. M.S. thesis in the Department of Civil Engineering, Washington State University, in press
21 A fine review of membrane formation, plus an excellent source of references may be found in Heiner Strathmann's chapter in Porter's *Handbook of Industrial Membrane Technology, op. cit.*, Chap. 1.
22 H.P. Hsieh, *Inorganic Membranes*. American Institute of Chemical Engineers Symposium Series, 84, No. 261
23 W.R. Rigby, D.R. Cowieson, N.C. Davies and R.C. Furneaux, An anodizing process for the production of inorganic microfiltration membranes. *Trans. Inst. Metal Finishing*, 68 (3) (1990) 95–98.
24 R.D. Birch, and K.J. Artus, *Manufacture of Tubular Membranes from Aromatic Polyetherketone–Aromatic Polyether Sulfone Blends*. Eur. Pat. Appl. 417908, 1990.
25 H. Strathmann, Production of Microporous Media by Phase Inversion Processes, in: D.R. Lloyd (Ed.), *Materials Science of Synthetic Membranes*, ACS Symposium Series 269. American Chemical Society, Washington, 1985, pp. 165–195.
R.E. Kesting, Phase Inversion Membranes. *Ibid.*, pp. 131–164.
K. Kamide, and S.-I. Manabe, Role of Microphase Separation Phenomena in the Formation of Porous Polymeric Membranes. *Ibid.*. pp. 197–228.
W.C. Hiatt et al., Microporous Membranes via Upper Critical Temperature Phase Separation. *Ibid.*, pp. 229–244.
26 A.J. DiLeo and A.E. Allegrezza, Jr., U.S. Patent 5,017,292, 1991.
A.J. Dileo and A.E. Allegrezza, Jr., Validatable virus removal from protein solutions. *Nature*, 351 (May 1991) 420–421.
27 D. Pum, M. Sara and U.B. Sleytr, Structure, surface charge, and self-assembly of the S-layer lattice from *Bacillus coagulans* E38-66. *J. Bacteriology*, (Oct. 1989) 5296–5303.
U.B. Sleytr et al., Application potentials of two-dimensional protein crystals. *Philips Electron Optics Bull.*, 126, (ca. 1988) 9–14.
D. Pum et al., Use of two-dimensional protein crystals from bacteria for nonbiological applications, in press (1989) 7 pp.
U.B. Sleytr and M. Sara, Ultrafiltration membranes and supports for the immobilization of macromolecules from two-dimensional protein crystals. Paper presented at IMTEC 88, Sydney, (November 1988) 3 pp.
M. Sara and U.B. Sleytr, Production and characteristics of ultrafiltration membranes with uniform pores from two-dimensional arrays of proteins. *J. Membr. Sci.*, 33 (1987) 27–49.
28 T.J. Leahy and M.J. Sullivan, Validation of bacterial-retention capabilities of membrane filters. *Pharmaceutical Technol.*, 2 (11) (1978) 65.
29 V. Goel, M.A. Accomazzo, A.J. DiLeo, P. Meier, A. Pitt and M. Pluskal, in: W.S. Ho and K.K. Sirkar (Eds.),*Membrane Handbook*. Van Nostrand Reinhold, New York, 1992, pp. 506–527.
30 M.C. Porter, *Handbook of Industrial Membrane Technology*. Noyes Publications, Park Ridge, NJ, 1990, pp. 156–160.
31 R.E. Kesting, *op cit.* p. 63.
32 G. Belfort, J.M. Pimbley, A. Greiner and K.Y. Chung, Diagnosis of membrane fouling using a rotating annular filter, 1. *J. Membrane Sci.*, 77 (1993) 1–22.

33 J.C. Westmoreland, *Spirally Wrapped Reverse Osmosis Membrane Cell.* USP 3,367,504, 1968. Bray, D.T., *Reverse Osmosis Purification Apparatus.* USP 3,417,870, 1968.
34 G. Belfort and F.W. Altena, Toward an inductive understanding of membrane fouling. *Desalination,* 47 (1983) 105–127.
35 L.J. Zeman, Adsorption effects in rejection of macromolecules by ultrafiltration membranes. *J. Membr. Sci.,* 15 (1983) 213–230.
36 W. Eykamp and J. Steen, in: R.W. Rousseau (Ed.), *Handbook of Separation Process Technology.* Wiley, New York, 1987.
37 C.J.D. Fell, D.E. Wiley and A.G. Fane, *Optimisation of Module Design for Membrane Ultrafiltration.* World Congress III of Chemical Engineering, Tokyo, 1986.
38 E. Matthiasson, The role of macromolecular adsorption in fouling of ultrafiltration membranes, *J. Membr. Sci.,* 16 (1983) 23–36.
H. Reihanian, C.R. Robertson and A.S. Michaels, Mechanisms of polarization and fouling of ultrafiltration membranes by proteins. *J. Membr. Sci.,* 16 (1983) 237–258.
39 B. Culkin, Vibratory shear enhanced processing: an answer to membrane fouling? *Chem. Processing* (Jan 1991) 42–46.
B. Culkin, Vibratory Shear Enhanced Processing (V*SEP) Applied to Liquid–Solid Separations. Abstract for Fourth National Meeting, NAMS, San Diego, 1991.
40 K.H. Kroner and V. Nissinen, Dynamic filtration of microbial suspensions using an axially rotating filter. *J. Membr. Sci.,* 36 (1988) 85–100.
K. Kataoka, H. Doi, and T. Komai, Heat/mass transfer in Taylor vortex flow with constant axial flow rates. *J. Heat Mass Transfer,* 20 (1977) 57–63.
41 R.M. Sandblom, *Filtering Process.* U.S. Patent 4,105,547, 1978.
42 A.G. Fane, Ultrafiltration of suspensions. *J. Membrane Sci.,* 20 (1984) 249–259.
A.L. Zydney and C.K. Colton, A concentration polarization model for the filtrate flux in cross-flow microfiltration of particulate suspensions. *Chem. Eng. Commun.,* 47 (1986) 1–21.
43 T.H. Meltzer, *Filtration in the Pharmaceutical Industry.* Marcel Dekker, New York, 1987.
44 T.J. Leahy and M.J. Sullivan, Validation of bacterial-retention capabilities of membrane filters. *Pharmaceutical Technol.,* 2 (1978) 65.
45 A. Pitt and J. Gabriels, Epithelial cell culture on microporous membranes. *Am. Biotechnol. Lab.* (Sept–Oct 1986).
46 Anon, *Sterile Process Gas Technical Brief.* Millipore Corp. Bedford, MA, 1991.
47 P.M. Meier, Aseptic filling using membrane cartridge filtration. *Wine East Buyers' Guide,* 1988, pp. 15–17.
48 Millipore product bulletin PB003, Millipore Corp., Bedford, MA, (May) 1988.
49 D.L. Tolliver, Contamination control: new dimensions in VLSI manufacturing. *Solid State Technol.* (March 1984).
J.R. Monkoedki, Chemistry physics, and defect sources in semiconductor gas processes. *Microcontamination,* Feb–Mar 1985.
50 M.A. Accomazzo and D.C. Grant, Mechanisms and devices for filtration of critical process gases. *Special Technical Publ.* 975. ASTM, Philadelphia, 1987.
51 N. LeGendre, Immobilon-P transfer membrane: applications and utility in protein biochemical analysis. *BioTechniques,* 9 (Suppl.) (1990) 788–805.
52 V.P. Olivieri (deceased), G.A. Willinghan, J.C. Vickers and C. McGahey, Continuous microfiltration of secondary wastewater effluent. Presented at AWWA Membrane Processes Conf., Orlando, FL, March 1991.
53 Denis Haney, Memtec Ltd., private communication, 1991.

54 W. Eykamp and J.T. Selldorff, Ultrafiltration in electrocoating — from an equipment standpoint. *Electrocoat*, (April 27, 1971).
W.J. Allshouse and M. Fushijima, Improved product rinsing efficiency with multitubular ultrafiltration. *Electrocoat*, 84.
55 W. Eykamp, Ultrafiltration, in: *Membrane Separation Systems: A Research Needs Assessment*, U.S. Department of Energy, Office of Energy Research, Report DOE/ER/30133-H1 April, 1990, pp. 7-13–7-17.
56 P.H. Claussen, Ultrafiltration and Hyperfiltration in the Pulp and Paper Industry for By-Product Recovery and Energy Savings. Turbak, Vol. II *op. cit.* pp. 361–372.
57 W. Eykamp, *Ultrafiltration and Microfiltration.* A plenary lecture delivered at the Int. Congress on Membranes and Membrane Processes, Chicago, 1990.
58 W. Eykamp, in DOE/ER/30133-HI, *op. cit.* pp. 7-20–7-24.

Membrane Separations Technology. Principles and Applications
Edited by R.D. Noble and S.A. Stern

Chapter 2

Polarization phenomena and membrane fouling

M.H.V. Mulder

University of Twente, Enschede, The Netherlands

2.1 INTRODUCTION

In order to achieve a particular separation via a membrane process, the first step is to develop a suitable membrane. Membranes may differ significantly in structure and, consequently, in functionality. Roughly, the membranes can be classified in two main groups (depicted schematically in Fig. 2.1): porous membranes and nonporous membranes [1].

Porous membranes can be found in microfiltration and ultrafiltration — membrane processes that are used to concentrate or purify dilute (aqueous) solutions. Microfiltration is used to reject particles in the range 0.05–10 μm

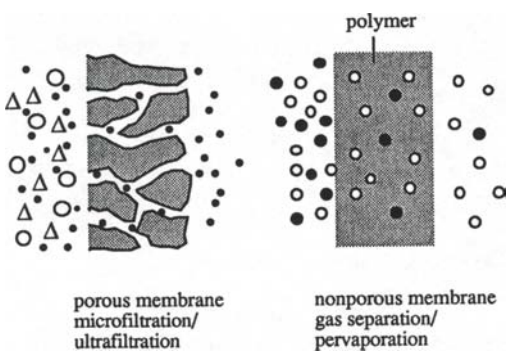

Fig. 2.1. Schematic drawing of a porous and a nonporous membrane.

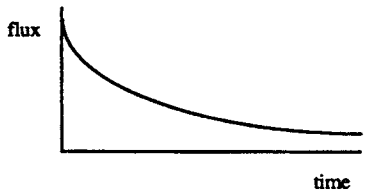

Fig. 2.2. Flux behavior as a function of time.

whereas in the case of ultrafiltration the size of the components to be rejected is in the range 1–50 nm. The transport of solvent is directly proportional to the applied pressure and models that can be used to describe the convective flow are the Kozeny–Carman and the Hagen–Poissueille equations. The membrane resistance is relatively low and, consequently, the pure solvent fluxes are high, greater than 500 l m^{-2} h^{-1} bar^{-1} for microfiltration and about 100–500 l m^{-2} h^{-1} bar^{-1} for ultrafiltration. In the case of nonporous membranes (gas separation and pervaporation) the resistance of the membrane is much higher and the fluxes are relatively low (for pervaporation fluxes are normally less than 1 l m^{-2} h^{-1}).

During an actual separation, the membrane performance (or better the system performance) may change with time, and often a typical flux–time behavior may be observed: the flux through the membrane decreases over time as shown schematically in Fig. 2.2.

The extent to which this phenomenon occurs is strongly dependent on the kind of separation problem involved. Especially in microfiltration and ultrafiltration, the flux decline is very severe with the process flux often being less than 5% of that of the pure-water flux. In contrast, the problem is less severe in gas separation and pervaporation.

Flux decline can be caused by several factors, such as concentration polarization, adsorption, gel-layer formation and plugging of the pores. All these factors induce additional resistances on the feed side to the transport across the membrane. The extent of these phenomena is strongly dependent on the types of membrane process and feed solution employed. Figure 2.3 provides a schematic representation of the various resistances that can arise. The flux through the membrane can be written as:

$$\text{flux} = \frac{\text{driving force}}{\text{viscosity} \cdot \text{total resistance}} \tag{2.1}$$

which in the case of pressure-driven processes such as microfiltration, ultrafiltration and hyperfiltration, becomes

$$J = \frac{\Delta P}{\eta R_{tot}} \tag{2.2}$$

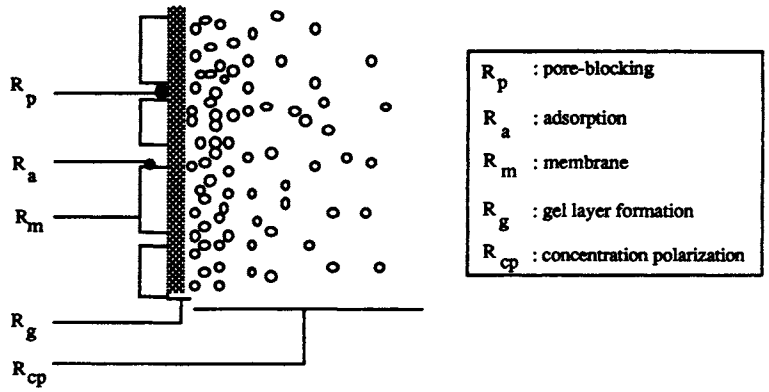

Fig. 2.3. Overview of various types of resistance towards mass transport across a membrane.

The various resistances depicted in Fig. 2.3 contribute to a different extent to the total resistance, R_{tot}. In the ideal case, only the membrane resistance R_m, is involved. Because the membrane has the ability to transport one component more readily than other components, or in some cases completely retain the solutes, there will be an accumulation of retained molecules near the membrane surface. This results in a highly concentrated layer near the membrane and this layer exerts a resistance towards mass transfer, i.e., the concentration polarization resistance, R_{cp}. Polarization phenomena always occur and are inherent to membrane separation processes. The concentration of the accumulated solute molecules may become so high that a gel-layer can be formed, which exerts the gel-layer resistance, R_g. This mainly happens when the solution contains proteins. With porous membranes it is possible for some solutes to penetrate into the membrane and block the pores, leading to the pore-blocking resistance, R_p. Finally, a resistance can arise due to adsorption phenomena, i.e., the adsorption resistance, R_a. Adsorption can take place upon the membrane surface as well as within the pores themselves. The adsorption process starts as soon as the membrane is in contact with the feed solution. In this respect adsorption is considered to be an equilibrium process. However, if pressure is applied at the feed side an additional deposition of (macromolecular) solutes may occur induced by the convective flow. In the first part of this chapter we will describe the influence of adsorption of solutes at the membrane surface due to interaction phenomena on the pure-water flux to clearly illustrate the extra resistance, which has already been exerted by this adsorbed layer. In discussing fouling, a classification must be made between porous membranes (see above) and non-porous membranes. Since the latter contain no pores (in this case it is better to speak of free volume) the blocking mechanism is absent. In addition, the type of feed stream (organic solvent and gas mixtures) means that gel-layer formation and adsorption is negligible. This means that in gas separation and perva-

poration the gel-layer resistance (R_g), the adsorption resistance (R_aa) and the pore-blocking resistance (R_p) do not have any effect and only the membrane resistance (R_m) and concentration polarization (R_{cp}) have to be taken into account.

Flux decline has a negative influence on the economics of a given membrane operation and, for this reason, measures must be taken to reduce its incidence. Some general methods for tackling this problem will become apparent when the principles of flux decline are discussed. However, it is first necessary to distinguish between concentration polarization and fouling, although both are not completely independent of each other since fouling can result from polarization phenomena. However, concentration polarization is a reversible phenomenon that occurs immediately when a process has been started and will reach an equilibrium value, whereas fouling is often an irreversible process that occurs in the long-term. It should be noted that another phenomenon, similar to concentration polarization, arises from heat transfer occurring in membrane distillation and thermo-osmosis. A temperature difference across the membrane being the driving force in these processes induces a heat flux through the membrane, which results in temperature polarization [2,3]. These phenomena will not be discussed in this chapter.

2.2 ADSORPTION

Adsorption already occurs before pressure has been applied and the membrane process has been started. As soon as the top surface of the membrane is in contact with the (macromolecular) solution, solute molecules will adsorb at the membrane surface due to physico-chemical interactions, e.g., hydrophobic interactions (dispersion forces), polar interactions (dipole–dipole and dipole–induced dipole forces) and charge transfer (hydrogen bonding). The nature of the membrane material, the type of solute, the solute concentration and, in the case of proteins, the ionic strength and pH are parameters that determine the extent of adsorption. Proteins especially tend to bind very severely to hydrophobic materials (polyethylene, polypropylene, polytetrafluoroethylene), which indicates that mainly hydrophobic forces are responsible. Since hydrophilic materials (cellulose esters, aliphatic polyamides) are less sensitive to adsorption, there is a clear trend to develop hydrophilic MF and UF membranes rather than hydrophobic ones. In addition, the chemical modification of the surface is a versatile tool to reduce fouling [5].

Many research activities have focused on adsorption, the adsorption mechanism, the reversibility of the process, and the influence of types of adsorbent and surface material [4–13]. The influence of the adsorbed layer on the pure-water flux can be demonstrated by some simple experiments [14,15]. After the

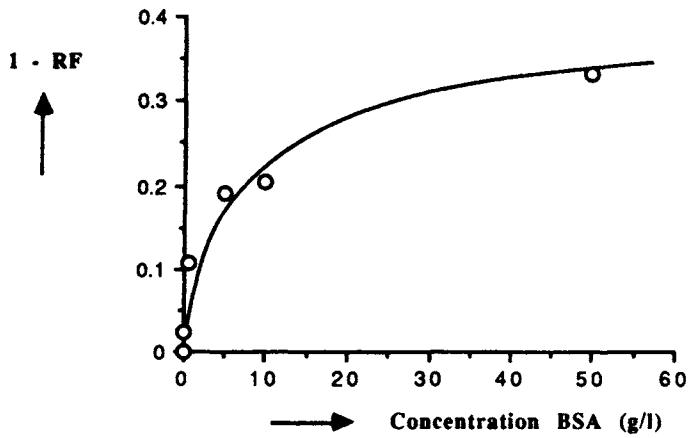

Fig. 2.4. Relative flux reduction (1 – RF) of pure water in post-treated PEI membranes as a function of the BSA concentration. Contact time: 16 h [14].

pure-water flux has been measured, the ultrafiltration membrane is immersed in a macromolecular solution (for instance a 0.5–10% solution of bovine serum albumin (BSA) in water) for a certain period of time. The membrane is then rinsed thoroughly with water and the pure-water flux is measured again. The relative permeate flux (RF) is defined as $RF = J_1/J_0$, with J_0 being the pure-water flux before BSA adsorption and J_1 the water flux after BSA adsorption. The relative flux reduction (RRF) is expressed as RRF = 1 – RF. Figure 2.4 gives the relative flux reduction of a polyetherimide (PEI) microfiltration membrane as a function of the BSA concentration (contact time in solution 16 h) [14]. From Fig. 2.4 it can be seen that after an initial sharp increase in flux reduction, a kind of plateau value is reached which for these specific membranes already amounts to a flux reduction of almost 40% for pure water. These adsorbed BSA molecules are not removed by thoroughly washing with water, which implies that to clean the membranes more severe means are required. In addition, these simple experiments clearly indicate the effect of adsorption on flux decline.

2.3 CONCENTRATION POLARIZATION

Membrane processes are used to accomplish a separation, which implies that the concentration of the solute in the permeate (c_p) is lower than the concentration in the bulk (c_b), which is in fact the basic concept of membrane separation. This is shown in Fig. 2.5.

The retained solutes can accumulate at the membrane surface where their concentration will gradually increase. Such a concentration build-up will generate a diffusive flow back to the bulk of the feed, but after a given period of time

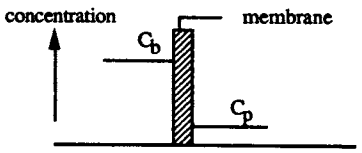

Fig. 2.5. Membrane separation: the basic concept.

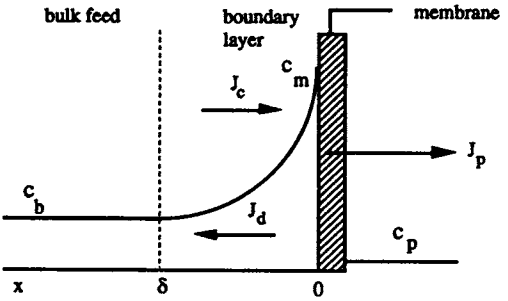

Fig. 2.6. Concentration polarization: concentration profile under steady-state conditions.

steady-state conditions will be established. The solute flow to the membrane surface due to convection flow will be balanced by the solute flux through the membrane plus the diffusive flow from the membrane surface to the bulk (it should be remembered that only concentration polarization phenomena are considered here with fouling being excluded). A concentration profile has now been established in the boundary layer (see Fig. 2.6). Steady-state conditions are reached when the convective transport of solute to the membrane is equal to the sum of the permeate flow plus the diffusive back-transport of the solute, i.e.,

$$J c + D \frac{\mathrm{d}\, c}{\mathrm{d}\, x} = J c_p \tag{2.3}$$

The boundary conditions are:

$$x = 0 \rightarrow c = c_m$$

$$x = \delta \rightarrow c = c_b$$

so that integration of Eq. (2.3) results in the well-known 'film–model' relationship.

$$\ln \frac{c_m - c_p}{c_b - c_p} = \frac{J \delta}{D} \tag{2.4}$$

or

$$\frac{c_m - c_p}{c_b - c_p} = \exp\left(\frac{J\,\delta}{D}\right) \tag{2.5}$$

The ratio of the diffusion coefficient D and the thickness of the boundary layer δ is called the mass-transfer coefficient k, i.e.

$$k = \frac{D}{\delta} \tag{2.6}$$

If we introduce the equation for the intrinsic retention:

$$R_{int} = 1 - \frac{c_p}{c_m} \tag{2.7}$$

then Eq. (2.5) becomes

$$\frac{c_m}{c_b} = \frac{\exp\left(\frac{J}{k}\right)}{R_{int} + (1 - R_{int}) \exp\left(\frac{J}{k}\right)} \tag{2.8}$$

The ratio c_m/c_b is called the concentration polarization modulus. This ratio increases (i.e., the concentration c_m at the membrane surface increases) with increasing flux J, with increasing retention R_{int} and with decreasing mass-transfer coefficient k.

When the solute is completely retained by the membrane ($R_{int} = 1.0$ and $c_p = 0$), Eq. (2.5) becomes

$$\frac{c_m}{c_b} = \exp\left(\frac{J}{k}\right) \tag{2.9}$$

This is the basic equation for concentration polarization, which illustrates in a simple form the two factors (the flux J and the mass-transfer coefficient k) and their origins (membrane part → J, hydrodynamics → k) responsible for concentration polarization. The mass-transfer coefficient depends strongly on the hydrodynamics of the system and can, therefore, be varied and optimized. The mass-transfer coefficient k is related to the Sherwood number (Sh), often represented as

$$Sh = \frac{k\,d_h}{D} = a\,Re^b\,Sc^c \tag{2.10}$$

where Re is the Reynolds number ($Re = \rho\,v\,d_h/\eta$), Sc the Schmidt number ($Sc = \nu/D$), ν the kinematic viscosity, ρ the density, d_h the hydraulic diameter, η the dynamic viscosity, v the flow velocity, D the diffusion coefficient, and a, b and c are adjustable parameters.

It can be seen that the mass-transfer coefficient k is mainly a function of the feed flow velocity (v), the diffusion coefficient of the solute (D), the viscosity, the density and the module shape and dimensions. These properties (diffusivity D, viscosity η and density ρ) hardly change in tangential direction. However, in normal direction, i.e., perpendicular on the feed stream, these properties may not be assumed to be constant due to concentration polarization. Because of the often high concentration gradients at the membrane wall the physical properties change so much that empirical mass-transfer correlations, in which these effects are not taken into account, are not able to describe mass transfer accurately. It should be realized that the classical mass-transfer relations have been developed for nonporous systems and not for membrane systems. In general the values in membrane processes are lower than predicted by the semiempirical relations. However, when particles are present in the feed stream the mass transfer is increased due to the tubular pinch effect, the particles are migrated from the membrane surface as a result of nonuniform shear forces near the membrane surface [41]. Many attempts have been made to correct the existing correlations and the large number of different equations makes it impossible to predict the mass-transfer coefficient accurately. An extended survey on mass-transfer correlations for turbulent flow has been given by Gekas et al. [16]. The semiempirical relationships frequently used are the Graetz–Leveque equation for laminar flow and the Deissler equation for turbulent flow.

Laminar flow conditions:

$$\text{tube: } Sh = 1.62\,(Re \cdot Sc \cdot d_h/L)^{0.33} \tag{2.11}$$

$$\text{channel: } Sh = 1.86\,(Re \cdot Sc \cdot d_h/L)^{0.33} \tag{2.12}$$

Turbulent flow conditions:

$$Sh = 0.023\,Re^{0.875}\,Sc^{0.25} \tag{2.13}$$

How can the extent of concentration polarization be reduced? This can be achieved both in terms of manipulating the flux J and the mass-transfer coefficient k; k is mainly determined by the diffusion coefficient and the flow velocity. Because the diffusivity of the solute(s) cannot be increased (only by changing the temperature), k can only be increased by increasing the feed velocity along the membrane and by changing the module shape and dimensions (decreasing the module length, changing the module design or increasing the hydraulic diameter). For a given module, the (cross-) flow velocity is a very important variable. However, there are other methods available for improving mass transfer besides increasing the flow velocity, for example, using turbulence

promoters, breaking the boundary layer (using corrugated membranes) or using a pulsating flow. An increase in the feed temperature will also generally reduce concentration polarization because of the increase in the mass-transfer coefficient (the diffusion coefficient of the retained solute will increase while the viscosity of the feed will decrease). However, an increase in feed temperature also causes an increase in the flux, which opposes the effect of the improved mass transfer. Table 2.1 summarizes the causes and consequences of concentration polarization in various membrane processes.

TABLE 2.1
Consequences of concentration polarization

Membrane operation	Influence	Origin
Hyperfiltration	moderate	k large
Ultrafiltration	strong	k small/J large
Microfiltration	strong	k small/J large
Gas separation	(very) low	k large/J small
Pervaporation	low	k large/J small
Electrodialysis	strong	–
Dialysis	low	J small

The effect of concentration polarization is very severe in microfiltration and ultrafiltration both because the fluxes (J) are high and the mass-transfer coefficients k ($= D/\delta$) are low as a result of the low diffusion coefficients of macromolecular solutes and of small particles, colloids and emulsions. Thus, the diffusion coefficients of macromolecules are of the order of 10^{-10} to 10^{-11} m^2 s^{-1} or less. The effect is less severe in reverse osmosis both because the flux is lower and the mass-transfer coefficient is higher. The diffusion coefficients of low-molecular weight solutes are roughly of the order of 10^{-9} m^2 s^{-1}. In gas separation and pervaporation, the effect of concentration polarization is low or can be neglected. The flux is low and the mass-transfer coefficient high in gas separation (the diffusion coefficients of gas molecules are of the order of 10^{-4} to 10^{-5} m^2 s^{-1}). The flux is also low in pervaporation, but the mass-transfer coefficient is smaller compared with gas separation and, hence, concentration polarization may become somewhat more serious. However, examples show that concentration polarization may become rate determining in pervaporation. When the concentration of the component in the feed, which permeates selectively, is very low and the selectivity is very high as in the removal of volatile organic components such as trichloroethylene from water, the effect can become especially severe. This specific application will be discussed later. Also,

in electrodialysis the effect of concentration polarization may become very severe and may limit the current density that can be applied. Also in this process, concentration polarization is the result of mass transfer but because this process is so specific these phenomena will not be discussed in this chapter (see for instance Ref. [1]).

Concentration polarization is generally not severe in dialysis because of the low fluxes involved (lower than in reverse osmosis) and also because the mass-transfer coefficient of the low-molecular solutes encountered is of the same order of magnitude as in hyperfiltration.

2.4 MODEL DESCRIPTION OF CONCENTRATION POLARIZATION

Generally, the pure-water flux through a membrane is directly proportional to the applied hydrostatic pressure according to

$$J = \frac{\Delta P}{\eta R_m} \tag{2.14}$$

where R_m is the hydrodynamic resistance of the membrane (Note that the hydrodynamic permeability L_p ($= 1/\eta \cdot R_m$) is often referred to as well).

The hydrodynamic resistance R_m is a membrane constant and does not depend on the feed composition or on the applied pressure. However, when solutes are added to the water the behavior observed is completely different, especially in microfiltration and ultrafiltration. When the pressure is increased the flux increases, but after a certain (minimum) pressure has been attained the flux does not increase further on increasing the pressure. This maximum flux is called the limiting flux, J_∞. Figure 2.7 shows that on increasing the feed concentration, but keeping the mass-transfer coefficient and the concentration at the membrane constant, the value of the limiting flux, J_∞, decreases. On the other hand, J_∞ increases when the mass-transfer coefficient k is increased at constant feed concentrations. When J in Eq. 2.9 is replaced by J_∞, it can be seen that the limiting flux depends on the concentration in the bulk of the feed, c_b and on the mass-transfer coefficient k.

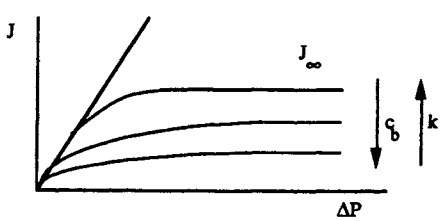

Fig. 2.7. The flux as a function of the applied pressure for different bulk concentrations c_b and different mass-transfer coefficients k.

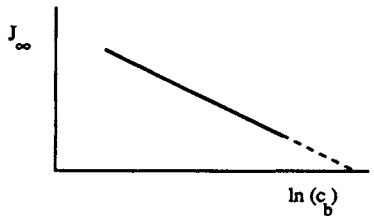

Fig. 2.8. Limiting flux (J_∞) plotted as a function of the logarithm of the bulk concentration.

$$J_\infty = k \ln \left(\frac{c_m}{c_b} \right) = k \ln c_m - k \ln c_b \tag{2.15}$$

If the results depicted in Fig. 2.7 are plotted as J_∞ versus ln (c_b), a straight line is obtained. This is shown in Fig. 2.8.

The behavior of the limiting flux depicted is typical for ultrafiltration and, to a lesser extent, for microfiltration. Whereas the flux increases with increasing pressure in reverse osmosis, the flux is invariant with pressure after an initial increase in ultrafiltration. In discussing these phenomena, it must be realized that the formal description of concentration polarization is the same for both ultrafiltration and reverse osmosis. However, the properties of concentrated macromolecular solutions, which appear in the boundary layer during ultrafiltration, are much more complex and less easy to describe than those of the concentrated solutions of simple salts encountered in reverse osmosis.

2.5 RESISTANCE MODELS

The flux in ultrafiltration can also be described by a resistances-in-series model, in which a resistance of a cake or of the boundary layer is in series with the membrane resistance. The flux can be described by

$$J_v = \frac{\Delta P}{\eta \, (R_m + R_{bl})} \tag{2.16}$$

In the *filtration model* the solute is considered to form a 'cake' or a deposition of particles at the membrane wall of constant concentration (see Fig. 2.9). This cake-filtration model is frequently used to determine a fouling index. The total boundary layer resistance (R_{bl}) is equal to r_c (the specific resistance of the cake) multiplied by l_c (the cake thickness).

$$R_{bl} = l_c \, r_c \tag{2.17}$$

The specific cake resistance is often expressed by the Kozeny–Carman relationship

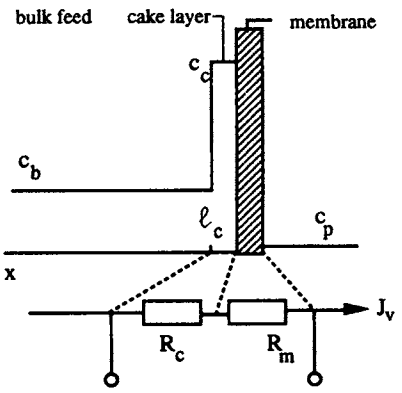

Fig. 2.9. Schematic representation of the cake-filtration model.

$$r_c = 180 \frac{(1-\varepsilon)^2}{[(d_s)^2 \varepsilon^3]} \tag{2.18}$$

where d_s is the 'diameter' of the solute particle and ε the porosity of the cake layer. The thickness l_c of the cake is equal to

$$l_c = \frac{m_s}{[\rho_s (1-\varepsilon) A]} \tag{2.19}$$

where m_s is the mass of the cake, ρ_s the density of the solute and A the membrane area. The effective thickness of the cake layer is in the order of several micrometers, which indicates that many monolayers ($\approx 100 - 1000$) of macromolecules are involved [20]. The thickness of the layer depends on the type of solute and especially on operating conditions and time. The growing layer of accumulates results in a continuous flux decline. The thickness of the cake layer can be obtained from a mass balance

$$c_b R V = c_m l_c A \tag{2.20}$$

Combination of Eqs. (2.16), (2.17) and (2.20) results in

$$\frac{1}{J} = \frac{1}{J_w} + \left(\frac{\eta c_b R r_{bl}}{\Delta P c_m} \right) \frac{V}{A} \tag{2.21}$$

where J_w is the pure-water flux. From unstirred dead-end filtration experiments it was shown that the reciprocal flux is indeed linearly related to the permeate volume V for various concentrations (c_b) and applied pressures (ΔP) as depicted schematically in Fig. 2.10.

The solution of Eq. (2.21) with $J = dV/Adt$ results in Eq. (2.22), which is the typical relationship for unstirred, dead-end filtration, showing that $V \approx t^{0.5}$.

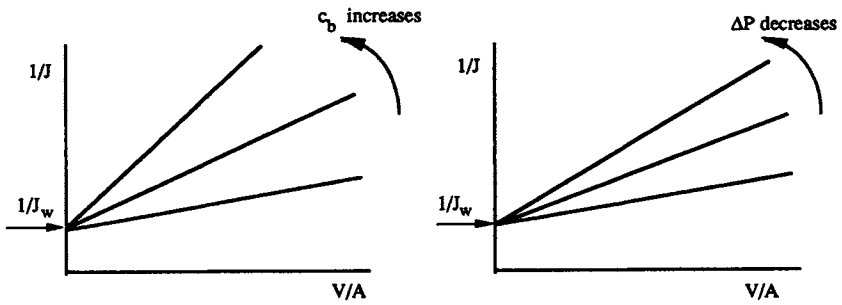

Fig. 2.10. Reciprocal flux as a function of the permeate volume for different concentrations (left) and applied pressures (right).

$$t = \frac{\eta\, c_b\, R\, r_{bl}}{\Delta P\, c_m} \left(\frac{V}{A}\right)^2 \tag{2.22}$$

Rewriting Eq. (2.22) in terms of the flux J, with $J = \mathrm{d}V/A\mathrm{d}t$ results in Eq. (2.23), which predicts that the flux declines as $t^{-0.5}$. This typical flux behavior is represented in Fig. 2.11.

$$J = \left(\frac{\Delta P\, c_m}{\eta\, c_b\, R\, c_b}\right)^{0.5} t^{-0.5} \tag{23}$$

The filtration model concept has been used for cross-flow and stirred and unstirred dead-end filtration of various solutes [17–20].

The *boundary layer resistance model* is another resistance model (see Fig. 2.12). The boundary layer can be considered as a concentrated solution through

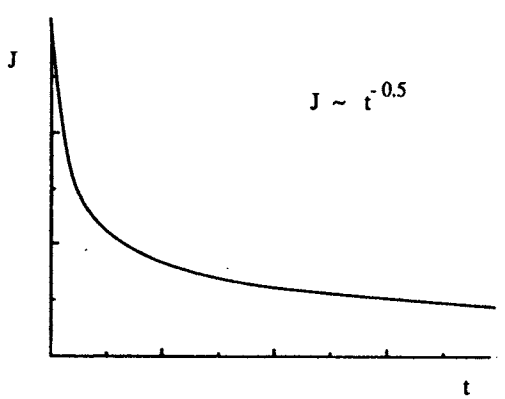

Fig. 2.11. Flux versus time according to Eq. (2.23).

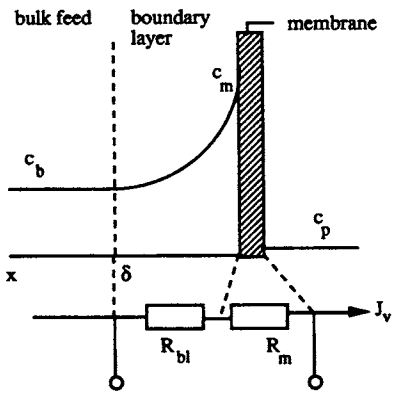

Fig. 2.12. Schematic representation of the boundary layer resistance model.

which solvent molecules permeate, with the permeability of this stagnant layer depending very much on the concentration and the molecular weight of the solute. The resistance exerted by this layer is far greater for macromolecular solutes (ultrafiltration) relative to low-molecular weight solutes (reverse osmosis). When the permeability of a solvent molecule in the boundary layer can be determined, the boundary layer resistance is also known. Since a correlation exists between the permeation of a solvent through a (stagnant) polymer solution and the sedimentation of polymer molecules (or molecules as small as sucrose) through a solvent, the permeability can be determined. This is shown schematically in Fig. 2.13. The permeability p is related to the sedimentation coefficient s via [21]

$$p = \frac{\eta\, s}{(1 - v_0/v_1)c} \tag{2.24}$$

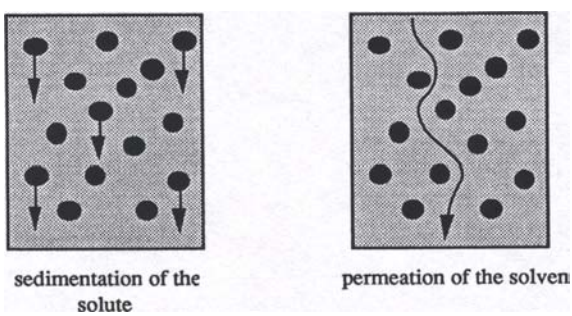

Fig. 2.13. Correlation between the sedimentation of a solute and the permeation of a solvent through a stagnant layer of solute molecules.

where v_0 and v_1 are the partial molar volume of the solvent and solute, respectively, and c is the solute concentration. The sedimentation coefficient s can be determined by ultracentrifugation. The specific resistance r_{bl} is equal to the reciprocal permeability p^{-1}.

The sedimentation coefficient is usually concentration dependent, which is expressed as

$$\frac{1}{s} = \frac{1}{s_o}(1 + k_1 c + k_2 c^2) \tag{2.25}$$

Assuming that the solute is completely retained by the membrane, the concentration of the solute in the boundary layer may be written as:

$$c(x) = c_b \exp\left(\frac{J x}{D}\right) \tag{2.26}$$

combination of Eqs. (2.24), (2.25) and (2.26) gives

$$R_{bl} = \frac{\left(1 \frac{v_1}{v_0}\right) D}{\eta s_o J}\left[(c_m - c_b) + \frac{k_1}{2}(c_m^2 - c_b^2) + \frac{k_2}{3}(c_m^3 - c_b^3)\right] \tag{2.27}$$

In deriving this equation it is assumed that the diffusion coefficient D is constant.

The resistance of the boundary layer R_{bl} can be calculated if ΔP, J, R_m, c_b, k, s and D are known. It is difficult to determine the exact value of the mass-transfer coefficient and an error in k has a large effect on the calculated R_{bl} since c_m is related to k via an exponential function.

2.6 GEL POLARIZATION MODEL

The gel polarization model is very similar to the film model. The solute concentration at the membrane surface may attain a very high value and a maximum concentration, the gel concentration (c_g) may be reached for a number of macromolecular solutes. The gel concentration depends on the size, shape, chemical structure and degree of solvation but is independent of the bulk concentration. The two phenomena, concentration polarization and gel formation are shown in Fig. 2.14.

The gel polarization model [22–24] is capable of describing the occurrence of limiting flux by assuming that $c_m \rightarrow c_g$. The limiting flux can now be described by

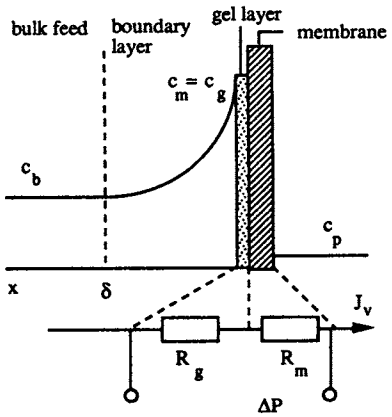

Fig. 2.14. Concentration polarization and gel-layer formation.

$$J_\infty = \frac{\Delta P}{\eta(R_m + R_g)} = k \ln\left(\frac{c_g}{c_b}\right) \tag{2.28}$$

If J_∞ is plotted as a function of ln (c_b) the result must be a straight line of slope $-k$ and the intercept on the abscissa ($J_\infty = 0$) will give the value of ln (c_g) (see Fig. 2.15). Although this model may be considered to be a significant contribution to the theory of concentration polarization and limiting flux behavior in ultrafiltration, some drawbacks should be mentioned. In the literature, data have indicated that the gel concentration c_g is not a constant but depends on the bulk concentration and the cross-flow velocity [25]. In addition, different authors have reported widely varying values for c_g for a given solute [26]. Furthermore, k is assumed to be constant whereas the diffusivity of the macromolecular solute is often concentration-dependent. Finally, although proteins form a gel readily, there are also many other macromolecular solutes, such as dextranes, that do not gel so easily even at very high concentrations. Despite these physical limitations it can still be considered as a very convenient and simple model.

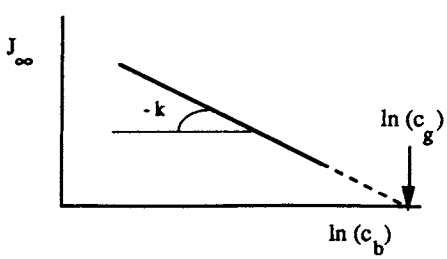

Fig. 2.15. Limiting flux (J_∞) plotted as a function of the logarithm of the concentration of the bulk feed.

2.7 OSMOTIC PRESSURE MODEL

Macromolecules are retained by the membrane in ultrafiltration whereas low-molecular-weight components permeate through freely. Because the main contribution to the osmotic pressure of a solution often arises from the low-molecular-weight solutes (the concentration of these being the same in the feed and permeate), the osmotic pressure of the retained macromolecules has been neglected in many cases.

However, for high flux values, high rejection levels and low mass-transfer coefficient values, the concentration of macromolecular solutes at the membrane surface can become quite high and hence, the osmotic pressure cannot be neglected. This has been commented upon by several investigators [27–33]. The dependence of the osmotic pressure of a macromolecular solution on the concentration is generally exponential rather than linear and can be described by

$$\pi = a \cdot c^n \tag{2.29}$$

where a is a constant and n is an exponential factor with a value greater than 1. Indeed, for semidilute or concentrated polymer solutions n will have a value of 2 or greater. For a number of macromolecular solutions the osmotic pressures are given for a solute concentration of 400 g/l (Table 2.2).

TABLE 2

Osmotic pressure of some macromolecular solutions at concentrations of 400 g/l

Solute	π (kPa)	Ref.
Dextran T 10	1300	26
Dextran T 70	710	23
BSA (pH: 5.4)	134	25
Whey proteins	650	26

If the osmotic pressure at the membrane surface is taken into account, the flux equation is then given by:

$$j = \frac{\Delta P - \Delta\pi}{\eta R_m} \tag{2.30}$$

Here, $\Delta\pi$ is the osmotic pressure difference across the membrane. The value of $\Delta\pi$ is determined by the concentration at the membrane surface c_m. Applying this osmotic pressure effect to the concentration at the membrane interface (c_m), and combining Eqs. (2.30) and (2.9), it is possible to calculate the flux assuming that the solutes are retained completely [27]:

$$J = \frac{\Delta P - a\, c_b^n \exp\left(\dfrac{n\,J}{k}\right)}{\eta\, R_m} \tag{2.31}$$

The derivative $\partial J/\partial \Delta P$ shows how the flux changes with increasing pressure

$$\frac{\partial J}{\partial \Delta P} = \left[\eta\, R_m + a\, c_b^n \frac{n}{k} \exp\left(\frac{n\,J}{k}\right)\right]^{-1} \tag{2.32}$$

Combining Eqs. (2.30) and (2.31) and substituting the result into Eq. (2.32) leads to

$$\frac{\partial J}{\partial \Delta P} = \left(\eta\, R_m + \frac{n}{k}\Delta\pi\right)^{-1} \tag{2.33}$$

or

$$\frac{\partial J}{\partial \Delta P} = \frac{1}{\eta\, R_m}\left(1 + \frac{\Delta\pi\, n}{\eta\, R_m\, k}\right) \tag{2.34}$$

From Eq. (2.34) it can be seen that two extremes may be distinguished:

$$\partial J/\partial \Delta P \rightarrow (\eta\, R_m)^{-1} \qquad \text{for } \Delta\pi \rightarrow 0$$

$$\partial J/\partial \Delta P \rightarrow 0 \qquad \text{for } \Delta\pi \text{ is very high}$$

These extremes have already been depicted in Fig. 2.7 as the pure-water flux and the limiting flux. The osmotic pressure model and the gel polarization model show the same flux–pressure relationship: as the pressure increases the flux approaches an asymptotic value. The concentration dependency also shows the same trend. In the gel polarization model, a plot of J versus $\ln(c_b)$ gives a straight line with a slope equal to $-k$. A similar J versus $\ln(c_b)$ relationship can be obtained from the osmotic pressure model. The derivative $\partial J/\partial \ln(c_b)$ shows how the flux changes with the bulk concentration c_b. From Eq. (2.31) the following relationship can be derived:

$$\frac{\partial J}{\partial \ln(c_b)} = -k\left(1 + \frac{R_m\, k\, \eta}{\Delta\pi\, n}\right)^{-1} \tag{2.35}$$

which shows that $\partial J/\partial \ln(c_b) \rightarrow -k$ for $(\Delta\pi \cdot n)/(\eta \cdot R_m \cdot k) >> 1$. Hence, the osmotic pressure model predicts a slope equal to $-k$ similar to that obtained from the gel polarization model.

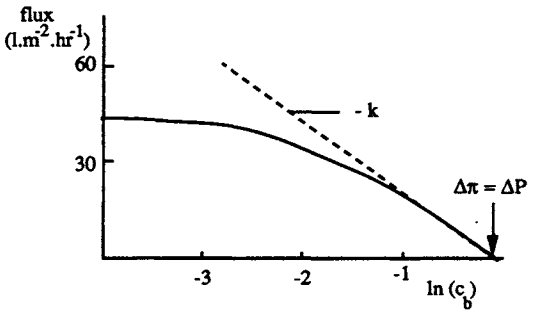

Fig. 2.16. A plot of the flux J_∞ as a function of the concentration in the bulk, c_b [33].

Figure 2.16 depicts a plot of the flux J_∞ as a function of the bulk concentration [33]. When $J_\infty = 0$, then $\Delta P = \Delta\pi$.

As has been pointed out by Wijmans, the boundary layer resistance model is equivalent to the osmotic pressure model [22]:

$$J_v = \frac{\Delta P}{\eta(R_m + R_{bl})} = \frac{\Delta P - \Delta\pi}{\eta R_m} \tag{2.36}$$

although independent measurements are essential for both models. However, for practical purposes, the osmotic pressure model is much easier to use.

2.8 CONCENTRATION POLARIZATION IN PERVAPORATION

From Table 2.1 it was argued that the effect of concentration polarization in pervaporation is small because the flux is relatively low and the mass-transfer coefficient is relatively high for the low-molecular-weight organic solvent mixtures. In general, this is indeed the case but special cases may exist where this does not count. One of these specific applications where the effect of concentration polarization may be very severe, the removal of trace organics from water [34–37], will be described here in more detail. In this case the concentration of the volatile organic component in water is very low (≈ 10–100 ppm) and the selectivity of the membrane is very high. As the diffusive transport through the membrane proceeds faster than the convective flow towards the membrane, the concentration of an organic component in the boundary layer will decrease. Steady-state conditions are reached when the convective and diffusive flow to the membrane are equal to the permeate flow. Figure 2.17 gives a schematic representation of the concentration profile of the preferentially permeating component.

The organic component flux can be represented by a resistance model in

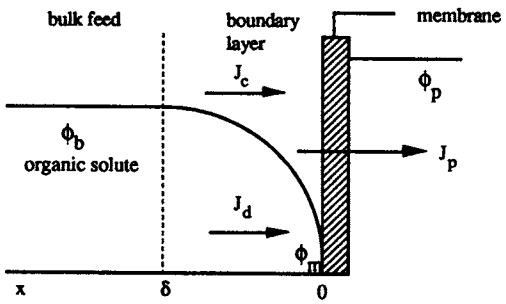

Fig. 2.17. Concentration profile for the preferentially permeating component under steady-state conditions.

which both the boundary layer resistance and the membrane resistance are in series. The component flux can be described in terms of the mass-tranfer coefficient and taking the boundary layer resistance into account the component flux is equal to

$$J_i = k_{ov}\,\Delta a_i \tag{2.37}$$

where k_{ov} is the overall mass-transfer coefficient and Δa_i the difference in activity of component i between feed and permeate. When the downstream pressure is very low the permeate activity approaches zero and using volume fractions instead of activities Eq. (2.38) becomes [37]

$$J_i = k_{ov}\,\phi_i^b \tag{2.38}$$

The overall mass-transfer coefficient (k_{ov}) can thus be determined from the bulk feed concentration (φ_i^b) and the steady-state permeate flux of component *i*. The reciprocal value of the overall mass-transfer coefficient is equal to the sum of the boundary layer resistance ($1/k_L$) and the membrane resistance ($1/k_m = l/P$)

$$\frac{1}{k_{ov}} = \frac{1}{k_L} + \frac{1}{k_m} = \frac{1}{k_L} + \frac{l}{P} \tag{2.39}$$

The boundary layer resistance for a given solution is mainly determined by the flow conditions and module design. With increasing flow velocity (increasing Reynolds number) the boundary layer resistance decreases and the membrane resistance becomes more dominant. The membrane resistance is directly proportional to the effective membrane thickness and inversely proportional to the component permeability. From Eq. (2.39) it can be seen that when the reciprocal of the overall mass-transfer coefficient is plotted as a function of the membrane thickness, a straight line should be obtained with the intercept being equal to the boundary layer resistance ($1/k_L$) and the slope equal to the reciprocal of the

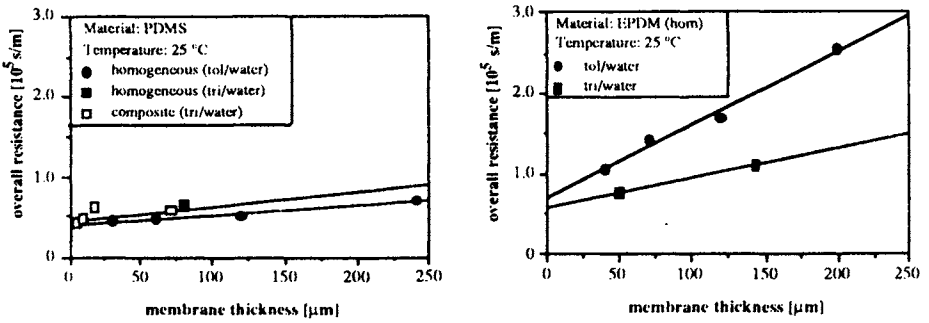

Fig. 2.18. Reciprocal of overall mass-transfer coefficient as a function of the membrane thickness for PDMS (left) and EPDM (right) [37].

permability coefficient (l/P). Figure 2.18 gives the reciprocal of the overall mass-transfer coefficient (k_{ov}) as a function of the membrane thickness with polydimethylsiloxane (PDMS) and ethylene propylene rubber (EPDM) as membrane materials and toluene and trichloroethylene as organic solutes in water at a concentration of 250 ppm (250 μg g^{-1}). The results clearly indicate the effect of the boundary layer resistance. Especially in the case of PDMS the membrane resistance can be neglected and the organic component flux is predominantly determined by the boundary-layer resistance. In the case of EPDM the membrane resistance becomes more important although here, the boundary layer resistance also contributes to a large extent to the total resistance. These results show very nicely that it is useless to reduce the elastomeric top-layer thickness. In order to improve the separation performance the emphasis must be focused on improving mass transfer in the liquid boundary layer (hydrodynamics and module design).

2.9 MEMBRANE FOULING

Fouling may be defined as the irreversible deposition of retained particles, colloids, macromolecules, salts, etc., at the membrane surface or inside the membrane at the pore wall, which causes a continuous flux decline (see Fig. 2.18). There is extensive literature on fouling [38–42]. Fouling occurs mainly in microfiltration/ultrafiltration where porous membranes are used, which are inherently susceptible to fouling. In the case of microfiltration the flux decline can reach values of more than 90% of the pure-water flux. The fouling behaviour in microfiltration is much more complex compared with ultrafiltration. In crossflow microfiltration a number of flux models are available to describe the flux decline. A good overview is given by Davis [42] in which a summary of all existing models is given. These models will not be described in this chapter and the reader is referred to Ref. [42].

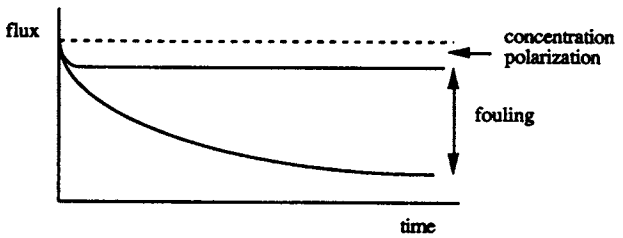

Fig. 2.19. Flux as a function of time. Concentration polarization and fouling can be distinguished.

In pervaporation and gas separation with dense membranes, fouling is virtually absent although concentration polarization occurs, as has been discussed in the previous section. The type of separation problem and the type of membrane used determine the extent of fouling. For this reason fouling phenomena will be described in relation to hyperfiltration, ultrafiltration and microfiltration. Roughly three types of foulant can be distinguished:

- organic precipitates (macromolecules, biological substances, etc.)
- inorganic precipitates (metal hydroxides, calcium salts, etc.)
- particulates

The phenomenon of fouling is very specific for a given application and is difficult to describe theoretically. Even for a certain solution, fouling will depend on the physical and chemical parameters such as concentration, temperature, pH, ionic strength or choice of membrane material. Since concentration polarization and fouling are inherently part of the microfiltration and ultrafiltration processes, it makes no sense to develop absolutely non-fouling membranes. However, it is possible to reduce fouling as much as possible and the methods necessary to achieve this will be discussed here. Fouling is very specific to a certain application and because of its complex nature it is hardly possible to describe a general theory. The most simple models that give a reasonable description are typically semiempirical. A very simple relationship, which has been widely used is,

$$J = J_0 t^n, \quad n < 0 \tag{2.40}$$

where J is the actual flux while J_0 is the initial flux and the exponent n is a function of the cross-flow velocity (see also Eq. (2.23)). There are a number of other (semi) empirical and more fundamental models that describe flux decline more or less satisfactorily and the reader is referred to the literature [44–50]. The disadvantage of these models is that they cannot be applied in general because of the complex nature of fouling. Therefore, methods to reduce fouling should be considered from case to case. However, reliable values of flux decline are necessary for process design. These values can be obtained from pilot-plant studies. Nevertheless, there is also a need for simple experiments. A measure

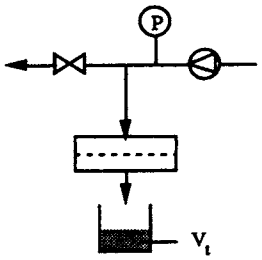

Fig. 20. Schematic drawing of a membrane fouling test apparatus.

of the fouling tendency can be obtained by performing "fouling tests", which can be carried out in an apparatus similar to that given in Fig. 2.20. These fouling tests are based on cake filtration. With the use of such an apparatus, the flux decline through a microfiltration membrane (pore sizes in the range from 0.1–1 μm) can be measured as a function of time under constant pressure, i.e., the cumulative permeate volume will be measured as a function of time. All types of solution can be used for this test, e.g., tap water, seawater and also solutions of suspensions or emulsions. Many parameters have been advanced to describe the fouling rate by suspended or colloidal dissolved particles:

- the silting index (S or SI)
- the plugging index (PI)
- the fouling index (FI) or the silt density index (SDI)
- the modified fouling index or the membrane filtration index (MFI).

These parameters are often used in relation to reverse-osmosis application to obtain a measure for the fouling potential, but in principle they might also be used in microfiltration and ultrafiltration applications to obtain a qualitative indication of the same. A disadvantage of these fouling tests is that they are based on dead-end filtration, whereas commercial applications are applied in a cross-flow mode. This implies that the flow conditions in the module are not taken into account whereas this is a crucial parameter to optimize the process. However, the experimental determination of these parameters is very simple and, therefore, they are frequently used. The silt density index (SDI) is determined with a microfiltration membrane with a diameter of 47 mm and a pore size of 0.45 μm. The feed is pressurized to 210 kPa (2.1 bar) and then the time is measured to collect 500 ml of permeate (Δt_1). Then, 15 minutes after the start of the experiment again the time is measured (Δt_2) to collect 500 ml permeate. The SDI value is calculated according to [51]

$$\mathrm{SDI} = \frac{(1 - \Delta t_1/\Delta t_2)}{15} 100 \tag{2.41}$$

The SDI value is the most commonly used parameter to determine the quality of the feed water in reverse osmosis applications. Because in many cases hollow-fiber membranes with a very small diameter are used, the SDI value should be low. Dupont (Permasep) and Toyobo (Hollosep) indicate maximum values of 3 and 4, respectively. For the spiral-wound modules (Filmtech (DOW), Hydranautics/Toray) SDI values of 5 or less are given. The plugging index (PI) is rather similar to the SDI index, only the measurement time (Δt_2) is variable. The plugging index is defined as follows [52]:

$$\mathrm{PI} = 1 - \frac{\Delta t_1 \, \Delta V_2}{\Delta t_2 \, \Delta V_1} \tag{2.42}$$

The SDI index is used very frequently but as can be seen from the definition, these indices are not based on any fouling mechanism. The silting index (SI) is based on cake or gel filtration [53,54]. The silting index (S) is defined as

$$\mathrm{S} = R_c \frac{A}{V} \tag{2.43}$$

In this measurement the time (t) is measured to collect a certain volume: V_1 (t_1), V_2 (t_2) and V_3 (t_3), respectively. The Silting index (S) is defined as

$$\mathrm{S} = \left[\frac{t_3 - 2t_2}{t_1}\right] \frac{A \, R_m \, V_1}{(V_2)^2} \tag{2.44}$$

The volumes V_1 and V_2 are chosen in such a way that the second term is unity and, therefore, Eq. (2.44) reduces to

$$\mathrm{S} = \frac{t_3 - 2 \, t_2}{t_1} \tag{2.45}$$

Another fouling index is the membrane filtration index (MFI) [55]. The membrane filtration index (MFI) is based on cake filtration ("blocking filtration") as it occurs in colloidal fouling (see also Section 2.5). The flux through the membrane can now be described as the flux through two resistances in series, i.e., the cake resistance (R_c) and the membrane resistance (R_m)

$$J = \frac{1}{A} \frac{\mathrm{d}\, V}{\mathrm{d}\, t} = \frac{\Delta P}{\eta (R_m + R_c)} \tag{2.46}$$

The resistance of the cake (R_c) is assumed to be independent of the applied pressure. When the thickness of the cake is l_c, the resistance of the cake is given by

$$R_c = r_c \cdot l_c \tag{2.47}$$

where r_c, the specific resistance, is assumed to be a constant over the thickness of the cake. For 100% rejection, R_c can be obtained from a mass balance since

$$R_c = \frac{r_c c_b V}{c_c A} \tag{2.48}$$

Now the flux may be written as

$$J = \frac{1}{A}\frac{dV}{dt} = \frac{\Delta P}{\eta\left[R_m + \frac{r_c c_b V}{c_c A}\right]} \tag{2.49}$$

and from Eq. (2.49) it is possible to show

$$\frac{t}{V} = \frac{\eta R_m}{A \Delta P} + \frac{\eta r_c c_b}{2 A^2 c_c \Delta P} V \tag{2.50}$$

A plot of t/V as a function of V should give a straight line after an initial section. The slope of this line is defined as the MFI (see Fig. 2.21). Hence

$$\text{MFI} = \frac{\eta r_c c_b}{2 A^2 c_c \Delta P} \tag{2.51}$$

Although the MFI is based on cake filtration, the other models give a relationship $J \approx t^{-0.5}$ and $V \approx t^{0.5}$ as well. This applies for:

- the gel polarization model [56];
- the osmotic pressure model [25];
- the boundary layer resistance model [57]; and
- the filtration model [58,59].

The use of MFI values can have some advantages:

- by comparing various solutions, different fouling behavior can be observed;
- a maximum allowable MFI value can be given for a specific plant;
- flux decline can be predicted to some extent.

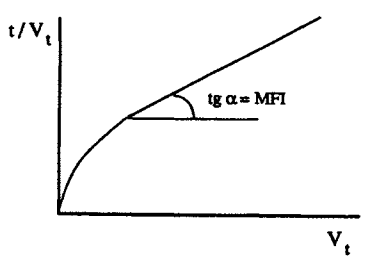

Fig. 2.21. Experimental results obtained with the apparatus depicted in Fig. 2.20.

However, there are also some drawbacks since the MFI values are only qualitative and should not be overstressed. Furthermore, MFI experiments are dead-end experiments whereas membrane filtration is, in practice, carried out in a cross-flow mode. Also, it is assumed that the cake resistance is independent of the pressure, which is not the case in general. Finally, the MFI method is based on cake filtration whereas other factors contribute to fouling as well. Nevertheless, the method is useful as a first estimate of the fouling character of the feed solution.

2.10 FOULING MODELS

The various fouling parameters such as SDI or FI, described in the previous sections, are typically used in reverse osmosis, rather than in microfiltration. But microfiltration is, in fact, the membrane process where fouling phenomena completely determine the efficiency of the separation. Microfiltration has been considered for a long time as an extension of ultrafiltration and the models applied for UF were used for microfiltration. However, flux decline in MF is much more severe and the mechanism is different as well. Therefore other models are needed to describe observed phenomena and a brief summary will be given here. A number of review articles can be found in the literature in which these models are described comprehensively [42,60,61]. The first model [24], given here, is based on the film model (Eq. (2.9)), in which the Lévêque expression is used for the "length-averaged" mass transfer coefficient of the particles

$$J = 0.807 \left(\frac{\gamma_o D^2}{L} \right)^{1/3} \ln \left(\frac{c_m}{c_b} \right) \tag{2.52}$$

The Brownian diffusion coefficient D of a spherical particle be obtained from the Stokes–Einstein relationship.

$$D = \frac{k T}{6 \pi \eta r} \tag{2.53}$$

This simple model, which has been widely applied in ultrafiltration, predicts much lower fluxes than observed from experiments. This is mainly caused by the unrealistic values for the diffusion coefficient as calculated from the Stokes–Einstein equation. Modifications have been proposed by various researchers aimed at taking into account an enhanced back-transport from the wall in so-called continuum models [62,66]. The enhanced back-transport is the result of a shear-induced hydrodynamic diffusion coefficient. Zydney and Colton [62] used the shear-enhanced diffusion coefficient of Eckstein, Bailey and Shapiro

[63] instead of the Stokes–Einstein relationship. With $D = 0.03\,\gamma_o\,r^2$, the following equation for the flux is obtained

$$J = 0.078\left(\frac{r^4}{L}\right)^{1/3}\gamma_o \ln\left(\frac{c_m}{c_b}\right) \tag{2.54}$$

Another model that takes into account an enhanced back-transport of particles from the membrane wall is the inertial lift model [45,64,65]. Due to inertial effects, the particles in the boundary layer are lifted away from the surface towards the bulk. This effect is often referred to as the tubular pinch effect. At steady state the flux is given by

$$J = \frac{v_l}{(1-\delta)^m} \tag{2.55}$$

where $m = 4$ for a two-dimensional channel and $m = 6$ for a tube, d is the dimensionless thickness of the of the deposit layer, and v_l is the lift velocity for a clean tube or channel. For a spherical particle near the wall of a two-dimensional channel the maximum lift velocity is

$$v_l = 0.577\,\frac{\rho\, r^3\,\gamma_o^2}{16\,\eta} \tag{2.56}$$

Altena et al. [64] showed that as long as the permeate flux is higher than the maximum lift velocity a deposition of particles occur and a stagnant cake layer will be formed.

Another model is based on frictional force balances on a particle [67,68]. Drag forces induced by the convective flow will force the particles to deposit on the membrane surface. On the other hand, the drag forces induced by the cross-flow velocity will move the particle along the membrane surface. If the latter force exceeds the former one deposition will not occur. For a tubular membrane the following relationship is given [67]

$$J = 0.22\,\mu^{-1}\,Re^{1.26}\left(\frac{\eta}{\rho\, d_i}\right)\left(\frac{d_p}{d_i}\right) \tag{2.57}$$

in which μ is a proportionality factor which incorporates the drag forces, d_p is the particle diameter and d_i is the diameter of the tube. The last model, the cake filtration model, has been described already in the previous section. Here, the total resistance is composed by two contributions, the membrane resistance, R_m and the cake resistance R_c. A modification of this model was developed by Schulz and Ripperger [69] taking into account the wall shear stress. For turbulent flow the following relationship between flux and velocity v_s has been derived

$$J = \left[\frac{K_2 \Delta P (\rho_p - c_b) \rho}{r_c c_b}\right]^{0.5} \frac{v_s}{\eta} \tag{2.58}$$

where K_2 is a constant and ρ_p the density of the particles. For laminar flow conditions a similar equation has been derived, showing that the flux is proportional to the square root of the velocity.

$$J = \left[\frac{K_3 \Delta P (\rho_p - c_b) v_s}{\eta d_i r_c c_b}\right]^{0.5} \tag{2.59}$$

where d_i is the internal diameter of a capillary and K_3 is a constant.

Futselaar [70] has compared the applicability and limitations of the various models as a function of the particle dimensions based on the microfiltration conditions described in Table 2.3 with a lumen flow capillary module. The flux as a function of the particle diameter for various models is given in Fig. 2.22. The data were calculated for a lumen flow capillary module according to the conditions given in Table 2.3 and using a constant superficial velocity $v_s = 1$ m s^{-1} and a length average shear rate $\gamma_o = 5300$ s^{-1}. For K_2 and K_3 values of $5 \cdot 10^{-9}$ and $1 \cdot 10^{-9}$, respectively, have been taken.

TABLE 2.3

Microfiltration conditions for model comparison [70]

Internal capillary diameter (mm)	1.5
Module length (m)	1.0
Fluid density (kg m^{-3})	1000.0
Fluid viscosity (Pa s)	$1.0\ 10^{-3}$
Particle density (kg m^{-3})	1100.0
Bulk concentration (kg m^{-3})	10.0
Membrane surface concentration (kg m^{-3})	600
Void fraction particle layer (%)	40
Applied pressure (bar)	1.0

A typical flux regime for microfiltration is between 10 and 500 l m^{-2} h^{-1} ($2.8\ 10^{-6}$–$1.4 \cdot 10^{-4}$ m s^{-1}, respectively), indicated by the dashed lines in Fig. 2.22, and it can be seen that the various models predict fairly well the order of magnitude of the permeate flux. It can also be seen that the prediction is better for the relatively large particles, and that the frictional force model (Eq. (2.57)) gives the best result over the entire particle range. On the other hand, the film layer model gives too low values over the whole particle range. It should be realised that the results presented in this figure give only a rough comparison and some

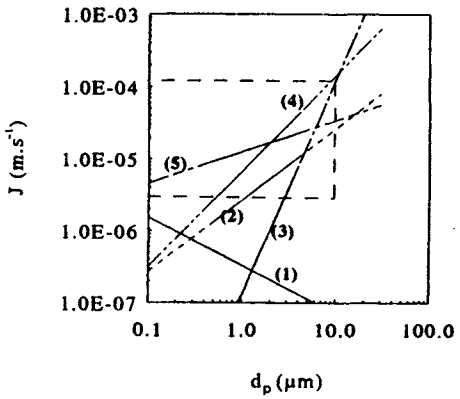

Fig. 2.22. Permeate flux as a function of the particle diameter for various models: (1) film model (Eq. 2.52); (2) cake filtration model (Eqs. 2.58 and 2.59); (3) inertial lift model (Eq. 2.56); (4) continuum model (Eq. 2.54); (5) frictional force model (Eq. 2.57).

models (e.g., frictional force and cake model) include process-dependent 'fitting' parameters. Nevertheless, the predicted 'fouling flux' is in the right order of magnitude and the comparison is useful as a first estimate.

2.11 CONTROL OF FOULING AND CONCENTRATION POLARIZATION

The consequence of concentration polarization and fouling is always a reduction in separation performance. The extent of this reduction is very specific and depends very much on the application. Hence, methods to reduce fouling and concentration polarization can only be described very generally because of the complexity of the phenomenon. Nevertheless, the importance is also evident. The methods to improve the performance can be classified in four categories, which will be discussed separately:

- pretreatment of feed solution;
- adjustment or tailoring of membrane properties;
- membrane cleaning; and
- improvement of operating conditions

2.11.1 Pretreatment

A reduction of fouling and concentration polarization starts in developing a proper pretreatment. Again a classification must be made between porous and nonporous membranes since the concept and extent of fouling is completely different. In the case of pervaporation and gas separation measures are taken to prevent damaging of the membrane by particles or to prevent a reduction of the

separation performance by a specific solute. Sometimes very simple measures can be taken. In the case of gas and vapour permeation a simple 1-μm filter is used to remove particles and sometimes an activated coal column has been installed for the removal of higher hydrocarbons. Also, in the case of pervaporation, clean feed streams are generally used (e.g., from a distillation column). However, when surface water or ground water is treated, as in the removal of trace organics, other measures have to be taken and often a sand filter and candle filter are sufficient. In gas separation the presence of water may change the membrane separation properties (plasticization) and measures must be taken to remove the water. This can be achieved by adsorption on molecular sieves.

In the case of desalination by reverse osmosis there is much experience in pretreatment. Many methods have been used and tested, which depend mainly on the type (seawater, brackish water) and quality of the feed with respect to the type of foulants (suspended solids, bacteria, organics). Typical methods of pretreatment are the addition of Cl_2 (to remove bacteria, algae), flocculants (polyelectrolytes or $FeCl_3$ to remove suspended solids), pH adjustment (H_2SO_4 to prevent scaling), $NaHSO_3$ (Cl_2 removal), heat treatment, UV treatment, activated carbon, and all types of filters such as multi-layer filters and 1–5 μm cartridge filters.

In microfiltration and ultrafiltration many applications are in the field of food, dairy and beverages and care must be taken that no additives are introduced by a pretreatment. Simple measures can already reduce fouling to some extent, for instance, in the case of proteins. Since adsorption of proteins is maximal at the isoelectric point a pH adjustment already gives an improved performance.

2.11.2 Membrane properties

Membrane properties mainly affect the solute–membrane interactions and, consequently, the extent of adsorption and fouling. In the case of proteins, which adsorb more strongly to hydrophobic surfaces rather than to hydrophilic ones the development of hydrophilic membranes (cellulose esters, aliphatic polyamides) can help to reduce fouling. Also chemical modification (e.g., sulfonation of polysulfone) and blending the hydrophobic polymer (polyetherimide, polyvinylidenefluoride) with a hydrophilic one (polyvinylpyrrolidone) can be used to achieve this. Another way to influence the solute–membrane interaction can also be influenced by the pretreatment of the membrane with (hydrophilic) surfactants or enzymes. Conventional ultrafiltration membranes such as polysulfone, polyethersulfone or polyvinylidene fluoride can be made more hydrophilic by surface modification of the membrane. Various methods can be applied [5,42]:

- plasma treatment of the surface;
- polymerization or grafting of the surface initiated by UV, heat or chemicals;
- interfacial polymerization;
- introduction of polar (-OR, -F) or ionic groups ($-SO_3H$) by reaction with reactive agents such as strong bases, bromine or fluorine and strong acids.

Another property is the membrane morphology (pore size, pore size distribution and pore geometry) especially at the surface, which can have a considerable effect on fouling. Because of adsorption onto the pore wall, smaller pores may be blocked and larger pores may become narrower. These adsorption phenomena not only affect the permeation rate but also the selectivity.

2.11.3 Cleaning

Although all the above methods reduce fouling to some extent, cleaning methods will always be employed in practice. The frequency with which membranes need to be cleaned can be estimated from process optimization. Four cleaning methods can be distinguished: *hydraulic cleaning, mechanical cleaning, chemical cleaning,* and *electrical cleaning*. The choice of the cleaning method depends mainly on the module configuration, the chemical resistance of the membrane and the type of foulant encountered.

2.11.3.1 Hydraulic Cleaning

Hydraulic cleaning methods include back-flushing (only applicable to microfiltration and open ultrafiltration membranes), back-shock treatment (back-flushing for only a fraction of a second), alternate pressurizing and depressurizing (pulsation of the flow) and by reversing the flow direction at a given frequency. These latter methods can also be considered to improve the solution hydrodynamics.

2.11.3.2 Mechanical Cleaning

Mechanical cleaning can only be applied in tubular systems using oversized sponge balls.

2.11.3.3 Chemical Cleaning

Chemical cleaning is the most important method for reducing fouling, with a number of chemicals being used separately or in combination. The concentration of the chemical (e.g., active chlorine) and the cleaning time are also very important in relation to the chemical resistance of the membrane. Although a

complete list of the chemicals used cannot be given, some important (classes of) chemicals are: acids (strong, such as H_3PO_4 or weak, such as citric acid), alkali (NaOH), detergents (alkaline, nonionic), enzymes, complexing agents (EDTA), and disinfectants (H_2O_2 and NaOCl).

2.11.3.4 Electric Cleaning

A recent method is the application of a pulsed electric field, which results in the movement of charged particles or molecules away from the membrane [71]. This cleaning method can be carried out without interrupting the process. A drawback of this method is the requirement of electricity-conducting membranes (e.g. metal membranes) and a special module design.

2.11.4 Improvement of Operating Conditions

Improvement of mass transfer is the most important factor in reducing concentration polarization and fouling. Since the mass-transfer coefficient is a parameter that depends both on solution hydrodynamics and module design, both can be optimized independently.

2.11.4.1 Solution Hydrodynamics

Increase of cross-flow velocity

The increase of the cross-flow velocity is the most logical and widely studied method to increase mass transfer. An increase in cross-flow velocity results in a flux increase. However, with increase of the velocity the energy consumption increases as well. The energy consumption is related to the third power of the velocity. Therefore, an (economical) optimal cross-flow velocity must be determined for all kinds of feed streams and module configurations. Other methods related to solution hydrodynamics to improve mass transfer are pulsation of flow and reverse of flow direction.

Turbulence promoters

Other methods that improve mass transfer both in laminar and turbulent systems can be classified in the group of "turbulence promoters": static mixers in tubular membranes, mesh screens in spirals and plate-and-frame systems, attachment of wires at the membrane surface, and fluidized beds in tubular membranes. Although in all cases an improvement in mass transfer is achieved, these methods are not commonly used in industrial systems, except for the spacer materials in spirals and plate-and-frame systems. This might be caused by the resulting pressure drop (static mixers) and damage of the membrane material (fluidized beds) combined with the difficulty of fabrication.

2.11.4.2 Module-related Methods

Concentration polarization is inherently part of the separation process and therefore unavoidable. It can not be eliminated but the effect can also be reduced by a proper module design. From Table 2.1 it can be seen that reduction of the module length results in an improved mass transfer. In most models the flux is proportionally related to the mass-transfer coefficient and a reduction in module length from 1 m to 0.5 m (using two modules of 0.5 m) gives a flux increase of 26% in the case of laminar flow.

The four basic module configurations are tubular, hollow fibers, spirals and plate-and-frame systems and the characteristics of these configurations are widely studied and well known. Within these four basic designs a number of small modifications have been developed. However, it is interesting to see whether progress has been made in developing new module designs. Three different concepts will be considered:

- rotating module;
- corrugated membrane; and
- transversal flow module.

A completely new concept in module design is the rotating module [72–74]. This module consists of two coaxial cylinders in which the inner cylinder, which contains the membrane, is rotating. A schematic drawing of this commercially available module (Sulzer/Switzerland and Membrex/USA) is given in Fig. 2.23. Taylor vortices are generated in the annulus, which results in an improved mass transfer, thereby reducing concentration polarization and fouling. Table 2.4 summarizes some results from Kroner et al. for the concentration of *Saccharomyces cerevisiae* as a function of the rotation speed [72]. Since high shear rates are induced at low axial-flow velocity the system can be operated at low applied pressures.

A drawback should be mentioned: the system is very costly, which will limit a large-scale application. Nevertheless, it is a nice example of a new module design. Another very nice example of reducing concentration polarization and

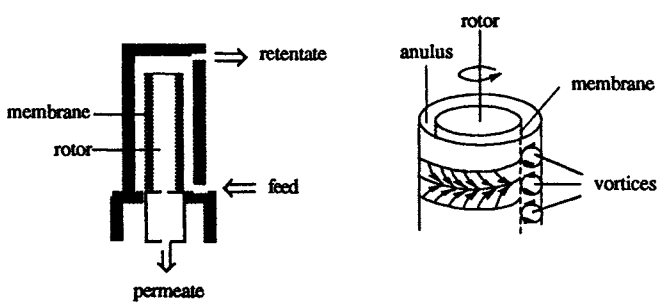

Fig. 2.23. Schematic drawing of a rotating module.

TABLE 2.4

Flux during concentration of *Saccheromyces cerevisiae* (≈ 5 vol%). $\Delta P = 0.15$ bar [72]

Rotation speed (min^{-1})	Flux ($l\ m^{-2}\ h^{-1}$)
20	18.1
200	42.6
2000	121.8

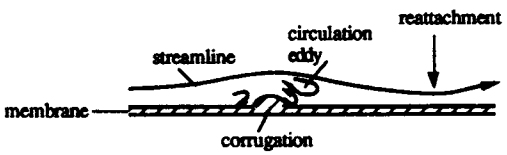

Fig. 2.24. Stream-lines in a corrugated membrane [75].

fouling is the introduction of corrugations at the membrane surface, which act as turbulent promoters. These corrugations are introduced in a flat membrane at a certain distance from each other. An impression of stream-lines for flow over corrugated membranes is given in Fig. 2.24. This figure shows that behind the corrugation a circulation is visible. Probably the local mass transfer is mostly enhanced at the point where the ongoing stream-lines attach again at the membrane surface. As the mutual distance of the corrugates becomes too small the ongoing stream-line will not approach the membrane surface and although circulation flows are still present in between the corrugates — which improve mass transfer — the overall improvement is not that large. On the other hand, when the distance is too large the effect of the corrugation also diminishes. Indeed, an optimal mutual distance has been found as indicated by the critical Reynolds numbers, which have been determined as a function of the mutual distance of the corrugations (see Table 2.5) [75].

This design results in an improvement of mass transfer but the introduction of the corrugations is difficult to apply in practical membrane systems and is only applicable for plate-and-frame systems. This will also limit the commercial applicability. In addition, membrane damage may occur because of the introduction of the corrugates. Although the first experiments did not reveal any damage, this might be a point for further study.

Another very promising design to improve mass transfer is the development of a transversal flow module using hollow fibers or capillary membranes with the top layer outside [76–79]. In this type of module the feed is flowing perpen-

TABLE 2.5

Critical Reynolds numbers for corrugated plates. Corrugations: half-cylinders of 1.5 mm [75]

Mutual distance (mm)	Critical *Re* (–)
None	1850
10	870
15	850
23	600
40	850
80	1230

Fig. 2.25. Schematic drawing of a transversal flow module with fibers arranged parallel-in-line (a) and crossed-in-line (b).

dicular to the fibers, as indicated schematically in Fig. 2.25, and this results in a large enhancement of the mass transfer. In this concept the fibers act as turbulence promoters.

This type of module design is not only of interest for the pressure driven processes microfiltration, ultrafiltration and reverse osmosis, but also for pervaporation, liquid membranes and membrane contactors where the boundary layer resistance can be very severe. A number of research groups are working to improve the performance of this design further and are trying to develop simple preparation procedures. Figure 2.26 is a photograph of such a transverse flow module [70,80].

The transversal flow module may be very suitable in microfiltration where the actual flux is a fraction of the pure-water flux, generally less than 5%. This strong flux decline is caused by the deposition of particles in and/or at the membrane surface. A general description of flux decline is very complex and is very much dependent on hydrodynamic conditions and type of feed solution. The thickness of a stagnant or moving layer of particles can be controlled by changing the hydrodynamic parameters such as flow rate, tube diameter (tubular configurations), channel heights (spiral wound and plate-and-frame configurations), module lengths etc. The membrane surface is here considered as a continuous medium and a continuous build up of a deposition layer will take place. However, the formation of this cake layer can be interrupted by the

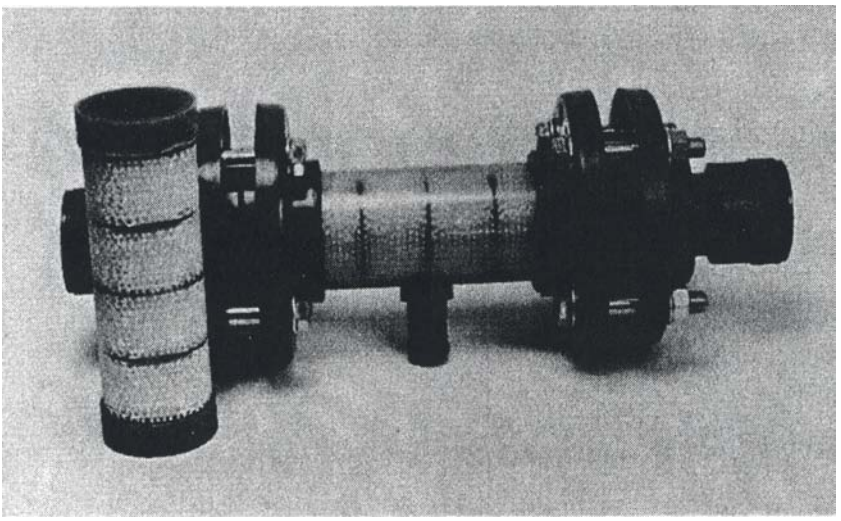

Fig. 2.26. Transverse flow capillary module [70,80].

application of turbulence promoters. In the transversal flow module the membrane itself act as turbulence promoter. Results obtained so far with this transversal flow module are very promising. Experiments performed on oil–water emulsions and also on latex solutions show that, at a given energy consumption (flow rate and pressure difference), the permeation rate has been improved [70,79]. In Fig. 2.27 a stationary flux comparison is given between a transverse flow (TF) module and a lumen flow (LF) module, using a 2% white spirit in

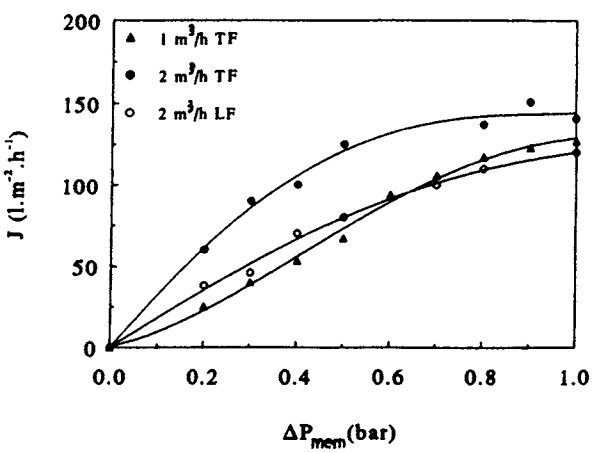

Fig. 2.27. Stationary flux as a function of the applied pressure for transverse flow (TF) and lumen flow (LF) module using a 2% of white spirit in water [70].

water emulsion as feed. The flow rates were 1.0 and 2.0 $m^3 h^{-1}$ for the transverse flow and 2.0 $m^3 h^{-1}$ for the lumen flow module, respectively.

A clear improvement has also been obtained on fermentation broths using the transversal flow module in comparison with the lumen flow module [70]. Development of new modules and modification of conventional modules will be one of the main topics to reduce concentration polarization and fouling. In addition, a further knowledge of the effect of the hydrodynamic parameters in relation to the type of feed solution, cake formation and fouling behaviour is needed.

SYMBOLS

a	constant in Eq. (2.16), Pa $m^3 kg^{-1}$
A	membrane area, m^2
c	concentration, kg m^{-3}
c_b	concentration in the bulk, kg m^{-3}
c_g	gel concentration, kg m^{-3}
c_w	concentration at the membrane wall, kg m^{-3}
c_p	concentration in the permeate, kg m^{-3}
D	diffusion coefficient, $m^2 s^{-1}$
d_h	hydraulic diameter, m
J	flux, $m^3 m^{-2} s^{-1}$
J_w	pure water flux, $m^3 m^{-2} s^{-1}$
J_∞	limiting flux, $m^3 m^{-2} s^{-1}$
k	mass-transfer coefficient, m s^{-1}
k_{ov}	overall mass-transfer coefficient, m s^{-1}
k_L	mass-transfer coefficient in boundary layer, m s^{-1}
k_M	mass-transfer coefficient in membrane, m s^{-1}
l_c	thickness of cake layer, m
m_s	mass of cake, kg
n	exponent in Eq. (2.16), –
p	permeability of boundary layer, m^2
R	gas constant, J/mol K
R	intrinsic retention, –
r_{bl}	specific resistance in boundary layer, m^{-2}
r_c	specific resistance in cake layer, m^{-2}
R_a	adsorption resistance, m^{-1}
R_{bl}	total hydraulic resistance of boundary layer, m^{-1}
R_c	cake layer resistance, m^{-1}
R_g	gel layer resistance, m^{-1}
R_m	membrane resistance, $m^{-1}1$

R_p	pore blocking resistance, m^{-1}
s	sedimentation coefficient, s
T	temperature, K
v_o	partial specific volume, $m^3 kg^{-1}$
v_s	superficial velocity, $m s^{-1}$
x	coordinate perpendicular to membrane surface, m
δ	thickness of the boundary layer, m
ε	porosity, –
γ_o	shear rate, s^{-1}
η	bulk viscosity, Pa s
ΔP	applied pressure, Pa
$\Delta\pi$	osmotic pressure difference, Pa
π	osmotic pressure, Pa
ρ	density, $kg m^{-3}$

REFERENCES

1 M.H.V. Mulder (1991). *Basic Principles of Membrane Technology*. Kluwer, Dordrecht.
2 F. Bellucci (1981). *J. Membr. Sci.*, 9: 285.
3 R.W. Schofield, Fane, A.G., Fell, C.J.D. and Macoun, R. (1990). *Desalination*, 77: 279.
4 E. Matthiasson (1983). *J. Membr. Sci.*, 16: 23.
5 M.H.V. Mulder (1993). In: *Membranes in Bioprocessing. Theory and Applications* (J.A. Howell, V. Sanchez and R.W. Field, Eds.). Chapman and Hall, London, p. 13.
6 P. Aimar, S. Baklouti and Sanchez (1986). *J. Membr. Sci.*, 29: 207.
7 T.B. Choe, P. Masse, A. Verdier and M.J. Clifton (1986). *J. Membr. Sci.*, 26: 17.
8 A. Suki, A.G. Fane and C.J.D. Fell (1986). *J. Membr. Sci.*, 27: 181.
9 A.S. Michaels and S.L. Matson (1985). *Desalination*, 53: 231.
10 J.L. Nilsson (1988). *J. Membr. Sci.*, 36: 147.
11 F.F. Stengaard (1988). *J. Membr. Sci.*, 36: 257.
12 D. Defrise and V. Gekas (1988). *Process Biochemistry*, August: 105.
13 J.H. Hanemaaijer, T. Robbertsen, T. van den Boomgaard and J.W. Gunnink (1989), *J. Membr. Sci.*, 40: 199.
14 T. van den Boomgaard, H.D.W. Roesink, M.A.M. Beerlage, M.H.V. Mulder and C.A. Smolders (1990). *Proceedings Int. Conf. on Membranes and Membrane Processes*, Chicago, Illinois, pp. 219–221.
15 H.D.W. Roesink, M.A.M. Beerlage, M.A.H. Potman, T. van den Boomgaard, M.H.V. Mulder and C.A. Smolders (1991). *Colloids Surfaces*, 55: 231.
16 V. Gekas and B. Hallström (1987). *J. Membr. Sci.*, 30: 153.
17 J.A. Howell and O. Velicangil (1980). In: *Polymer Science and Technology*, Vol. 13. (A.R. Cooper, Ed.). Plenum Press, New York, p. 217.
18 R.J. Baker, A.G. Fane, C.J.D. Fell and B.H. Yoo (1985). *Desalination*, 53.
19 A.G. Fane (1984). *J. Membr. Sci.*, 20: 249.
20 M.W. Chudacek and A.G. Fane (1984). *J. Membr. Sci.*, 21: 145.

21 P.F. Mijnlieff and W.J.M. Jaspers (1971). *Trans. Faraday Soc.*, 67: 1837.
22 H.J. Bixler, L.M. Nelsen and L.W. Bluemle Jr. (1968). *Trans. Am. Soc. Artificial Int. Organs*, 14: 99.
23 W.F. Blatt, A. Dravid, A.S. Michaels and L.M. Nelsen. In: *Membrane Science and Technology* (J.E. Flinn, Ed.). Plenum Press, New York, 1970.
24 M.C. Porter (1972). *Ind. Eng. Chem. Prod. Res. Dev.*, 11: 234.
25 S.I. Nakao, T. Nomura and S. Kimura (1979). *AIChE J.*, 25: 615.
26 P. Dejmek, PhD Thesis, Lund Institute of Technology, Sweden, 1975.
27 J.G. Wijmans, S.I. Nakao and C.A. Smolders (1984). *J. Membr. Sci.*, 20: 115.
28 J.G. Wijmans, S.I. Nakao, J.W.A. van den Berg, F.R. Troelstra and C.A. Smolders (1985). *J. Membr. Sci.*, 22: 117.
29 R.L. Goldsmith (1971). *Ind. Eng. Chem. Fundam.*, 10: 113.
30 V.L. Vilker, C.K. Colton and K.A. Smith (1981). *AIChE J.*, 27: 637.
31 G. Jonsson (1984). *Desalination*, 51: 61.
32 G.B. van den Berg and C.A. Smolders (1989). *J. Membr. Sci.*, 40: 149.
33 J.G. Wijmans. PhD Thesis, University of Twente, The Netherlands, 1984.
34 P. Coté and C. Lipski (1988). In: *Proceedings 3rd Int. Conf. on Pervaporation Processes in the Chemical Industry* (R. Bakish, Ed.). BMC, Englewood, USA, p. 449.
35 R. Psaume, P. Aptel, Y. Aurelle, J.C. Mora and J.L. Bersillon (1988). *J. Membr. Sci.*, 36: 373.
36 H.H. Nijhuis, M.H.V. Mulder and C.A. Smolders (1990). *Proceedings Int. Conf. on Membranes and Membrane Processes*. Chicago, Illinois, pp. 319.
37 H.H. Nijhuis, PhD Thesis, University of Twente, The Netherlands, 1990
38 A.G. Fane and C.J.D. Fell (1987). *Desalination*, 62: 117.
39 E. Matthiasson and B. Sivik (1980). *Desalination*, 35: 59.
40 G. Belfort (1977). *Desalination*, 21: 285.
41 G. Belfort and F.W. Altena (1983). *Desalination*, 43: 105.
42 R.H. Davis (1992). In: *Membrane Handbook* (W.S.W. Ho and K.K. Sirkar, Eds.). Van Nostrand Reinhold, Chapter 33, p. 480.
43 A.G. Fane, In: *Progress in Filtration and Separation, 4* (R.J. Wakeman, Ed.). Elsevier, 1986, p. 101.
44 D.G. Thomas and W.R. Mixon, 1972. *Ind. Eng. Chem. Process Des. Dev.*, 3: 339.
45 G. Green and G. Belfort (1980). *Desalination*, 35: 129.
46 M.C. Porter (1972). Ind. Eng. Chem. Prod. Res. Dev., 11: 234.
47 S. Kimura and S.I. Nakao (1975). *Desalination*, 17: 267
48 M.G. Gutman (1977). *Chem. Eng.*, July: 510.
49 D. Bhattacharyya, A.B. Jumawan and R.B. Grieves (1979). *Sep. Sci. Technol.*, 14: 529.
50 A.B. Suki, A.G. Fane and C.J.D. Fell (1984). *J. Membr. Sci.*, 21: 269.
51 E.I. DuPont de Nemours & Co. (1982). *Permasep Engineering Manual.*
52 K.C. Channabasappa (1975). *Desalination*, 17: 31.
53 Standard Method of Test for Silting Index of fluids for processing electronic and microelectronic devices (1974). *Annual Book of ASTM*, Part 41.
54 Millipore Filter Corporation Silting Index, Apparatus Principles and Operation (1964).
55 J.C. Schippers and J. Verdouw (1980). *Desalination*, 32: 137.
56 D.R. Trettin and M.R. Doshi (1980). *Ind. Eng. Chem. Fundam.*, 19: 189.
57 S.I. Nakao, J.G. Wijmans and C.A. Smolders (1986). *J. Membr. Sci.*, 26: 165.
58 M.W. Chudasek and A.G. Fane (1984). *J. Membr. Sci.*, 21: 145.
59 A.G. Fane (1984). *J. Membr. Sci.*, 20: 249.
60 V. Gekas and B. Hallström (1990), *Desalination*, 77: 195.

61 G. Belfort and N. Nagata (1985), *Desalination*, 53: 57.
62 A.L. Zydney and C.K. Colton (1986), *Chem. Eng. Commun.*, 47: 1
63 E.C. Eckstein, D.G. Bailey and A.H. Shapiro (1977), *J. Fluid Mech.*, 79: 191
64 F.W. Altena and G. Belfort (1984), *Chem. Eng. Sci.*, 39: 343
65 D.A. Drew, J.A. Schonberg and G. Belfort (1991), *Chem. Eng. Sci.*, 46: 3219
66 E.F. Leonard and Vassilieff (1984), *Chem. Eng. Commun.*, 30: 209.
67 R. Rautenbach and G. Schock (1988), *J. Membr. Sci.*, 36: 231
68 H. De Balman, P. Aimar and V. Sanchez (1990), *Sep. Sci. Techn.*, 46: 3219.
69 G. Schulz and S. Ripperger (1989), *J. Membr. Sci.*, 40: 173.
70 H. Futselaar, PhD Thesis, University of Twente, 1993.
71 W.R. Bowen, R.S. Kingdon and H.A.M. Sabuni (1989). *J. Membr. Sci.*, 40: 219.
72 K.H. Kroner, B. Riesmeier, V. Nissinen and M-R. Kula, *Engineering Foundation Conference on Recovery of Bioproducts*. Uppsala, Sweden, 1986.
73 K.H. Kroner and V. Nissinen (1988). *J. Membr. Sci.*, 35: 85.
74 K.H. Kroner, V. Nissinen and H. Ziegler (1987). *Bio/Technology*, 5: 921.
75 M.J. van der Waal and I.G. Rácz (1989). *J. Membr. Sci.*, 40: 243.
76 J. Baudet, US Patent 3,993,816 (1976).
77 R.W. Nichols, US Patent 4,959,152 (1990).
78 M.C. Yang and E.L. Cussler (1986). *AIChE Journal*, 32: 1910.
79 F.N.M. Knops, H. Futselaar and I.G. Rácz (1992), *J. Membr. Sci.*, 73: 153.
80 F.N.M. Knops, Presentation at the International Symposium: Progress in Membrane Science and Technology, 1991, 25–28 June, Enschede, The Netherlands

Membrane Separations Technology. Principles and Applications
Edited by R.D. Noble and S.A. Stern

Chapter 3

Vapor permeation

Y. Cen and **R.N. Lichtenthaler**

Physikalisch-Chemisches Institut, Universität Heidelberg,
Im Neuenheimer Feld 253, 69120 Heidelberg, Germany

3.1 INTRODUCTION

Vapor permeation denotes the transport of matter through a membrane from a vapor feed mixture to a vapor permeate. It is closely related to gas permeation differing only in that a vapor mixture contains compounds that are condensable at standard conditions (1 bar and 0°C), whereas a gas mixture contains only so-called permanent gases. In principle, porous and/or nonporous membranes can be used to separate vapor and gas mixtures depending on the molecular size and shape of their constituents. However, in practice, nonporous membranes are normally used and in that case vapor permeation is very closely related to pervaporation, differing only in that the feed mixture is a vapor and liquid, respectively.

In this chapter the basic principles and the various operating modes of vapor permeation are discussed in general. The dependence of the separation characteristics on the operating conditions (e.g., temperature, pressure, composition, superheating) is demonstrated with experimental results for selected mixtures and membranes. Engineering aspects important for process design are discussed and examples of practical applications are given.

3.2 BASIC PRINCIPLES AND CLASSIFICATION

3.2.1 Vapor Permeation in Comparison with Gas Permeation and Pervaporation

The basic principles and differences of gas permeation, vapor permeation and pervaporation are shown schematically in Fig. 3.1. Feed and retentate are gas, vapor or liquid mixtures, respectively. The permeate is a gas in gas permeation and a vapor in vapor permeation and also in pervaporation. Except for evaporation through porous membranes (often called membrane distillation), pervaporation is the only membrane separation process in which a phase change occurs requiring heat of vaporization. Compared with pervaporation, vapor permeation has the advantage that no phase change occurs during permeation from the feed to the permeate side and, therefore, the problem of supplying the heat of vaporization is avoided. Furthermore, depending on the state conditions of the feed vapor, the annoying problem of concentration polarization on the feed side of the membrane is often not as distinct as in pervaporation. Some disadvantages for separation by vapor permeation, however, are the strong dependence of the separation characteristics on the feed pressure, the sensitivity to friction losses in the feed stream (in addition to the ones on the permeate side) and the possibility of condensation, and hence of the formation of stagnant condensate films, partially covering the membrane on the feed side. Nevertheless vapor permeation is a membrane separation process

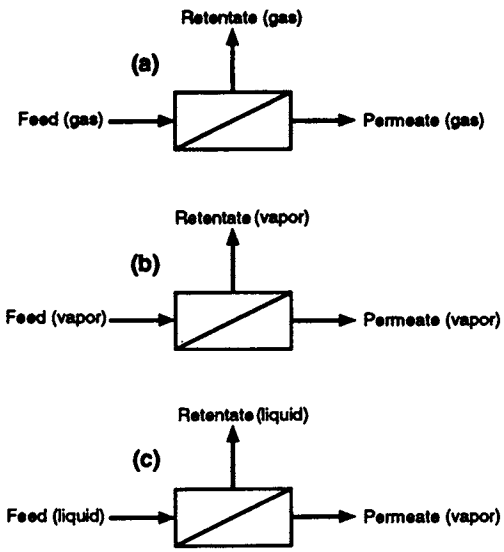

Fig. 3.1. Basic principles of gas permeation (a), vapor permeation (b) and pervaporation (c).

feasible for practical application. It is considered to be especially suitable for the purification of the top stream of rectification columns and for the removal of trace organics from air or other permanent gases.

3.2.2 Classification of Vapor Permeation

There are various possibilities to distinguish between the various types of vapor permeation. It is convenient to classify them according to the operating conditions as summarized in Table 3.1.

TABLE 3.1
Classification of vapor permeation

Category 1				Category 2			
no gases in the feed				with gases in the feed			
vacuum on permeate side		purge gas on permeate site		vacuum on permeate site		purge gas on permeate side	
porous	nonporous	porous	nonporous	porous	nonporous	porous	nonporous

First of all, vapor permeation is divided in two categories. In the first, the feed of the membrane separation process contains only vapor compounds and no permanent gases, e.g., a mixture of alcohol and water vapors. In the second, the feed exists of vapor and gas components, e.g., volatile organic compounds in waste air. Each category is further divided into vacuum and purge gas vapor permeation according to the method by which the permeate is removed from the downstream side of the membrane. Finally vapor permeation with porous and nonporous membranes is distinguished. This classification, although somewhat arbitrary, includes all the different descriptions by which a vapor permeation unit may be designed and operated.

3.3 MATERIAL TRANSPORT THROUGH MEMBRANES

For the development of efficient membranes for vapor permeation and proper design of the separation process, it is essential to understand the transport mechanism through a membrane. Porous and nonporous membranes are discussed separately because there are distinct differences in the transport mechanism. However, it is sometimes difficult to distinguish between porous and nonporous membranes depending on the minimum diameter being accepted as the lower limit for a pore (the range 0.1–0.5 nm is often discussed).

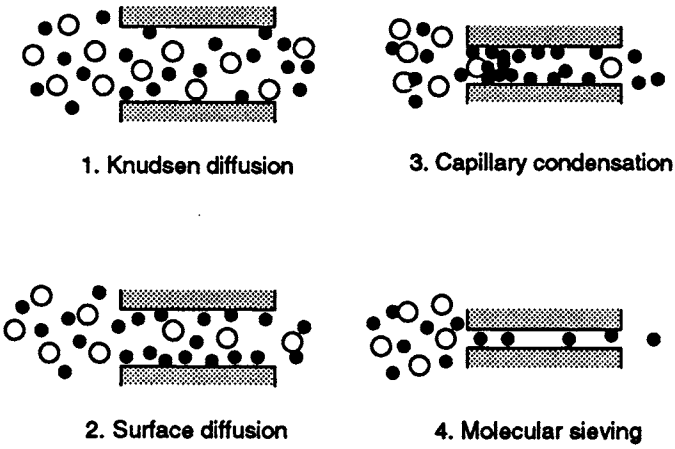

Fig 3.2. Transport mechanisms in porous membranes [1].

3.3.1 Porous Membranes

With porous membranes, usually only molecules differing significantly in their molecular weights, sizes and/or shapes can be separated efficiently. Conventionally four different types of transport mechanism are distinguished as shown schematically in Fig. 3.2 [1,2]: (1) Knudsen diffusion, (2) surface diffusion, (3) capillary condensation with liquid flow and (4) molecular sieving.

It is well known that the application of Knudsen diffusion as a separation processes is limited to systems of large molecular weight ratios as the permeability ratio is inversely proportional to the square root of the molecular weight ratio. Surface diffusion is a mechanism in which the molecules adsorbed on the pore wall diffuse on the surface due to a concentration gradient in the adsorbed phase. This mechanism is probably much more useful for vapor separation than Knudsen diffusion. Separation by condensation with liquid flow in extremely fine pores of a membrane has been shown to be quite efficient in various work for vapor mixtures of which one of the components condenses in the pores due to capillary condensation. In this case, each pore can be blocked with the condensate to prevent the permeation of noncondensable components [3,4]. The last mechanism, i.e., molecular sieving, describes the ideal condition for the separation of vapor compounds of different molecular sizes by porous membranes. The driving force for transport through the pore is usually the difference in pressure between the feed and permeate sides.

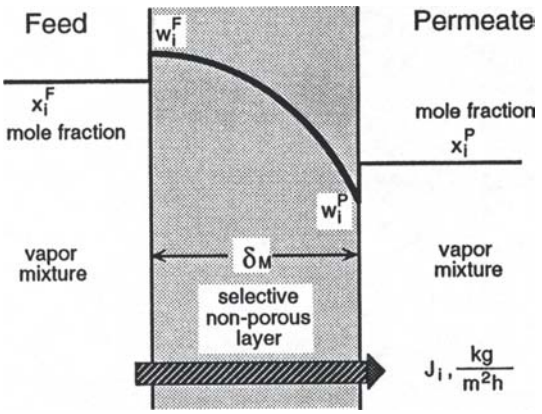

Fig. 3.3. The solution-diffusion model describing mass transport in nonporous membranes.

3.3.2 *Nonporous Membranes*

The separation of vapor mixtures by nonporous membranes is considered to be due to differences in the solubility and diffusivity of the various components of a mixture in the membrane material. Therefore, as long as these differences are significant, even molecules similarly in molecular weight, size and shape can be separated [5]. The driving force for the transport through a nonporous membrane for any permeating compound is given by the difference of its chemical potential between the feed and permeate sides usually achieved with a permeate pressure being much lower than the feed pressure. The so-called solution-diffusion model, schematically illustrated in Fig. 3.3, is widely used to describe the transmembrane material transport [6]. This transport takes place in three consecutive steps:

(1) sorption of components from the feed mixture at the upstream membrane surface;
(2) diffusion of the absorbed components through the membrane matrix;
(3) desorption from the membrane into the vapor phase at the permeate side.

The basic assumptions of this model are the existence of thermodynamic phase equilibrium at both boundary surfaces of the membrane being in contact with the feed and the permeate. The diffusion process inside the membrane is described by Fick's law, which is assumed to be valid for each component i (i = 1, 2,... n):

$$J_i = -D_i(w_1, w_2, \ldots w_n) \cdot \rho_M \cdot dw_i / d\delta_M \tag{3.1}$$

where J_i is the mass flux, D_i is the diffusion coefficient, δ_M is the thickness and ρ_M is the density of the membrane. The concentration of the components i in the

membrane is given by the weight fraction w_i, defined as:

$$w_i = m_i / \left(\sum_{j=1}^{n} m_j + m_M \right) \tag{3.2}$$

with m_i and m_j being the masses of the compounds dissolved and m_M being the mass of the membrane. Under steady-state conditions Eq. (3.1) can be integrated to

$$J_i = \rho_M / \delta_M \cdot \int_{w_i^P}^{w_i^F} D_i(w_1, w_2, \ldots w_n)\, dw_i \tag{3.3}$$

w_i^F and w_i^P are the weight fractions of the component i in the membrane at the feed side and the permeate side boundary, respectively. Generally, D_i depends on the weight fraction of each component, varying locally inside the membrane. As a consequence, the fluxes J_i are mutually dependent. The weight fraction w_i^F and w_i^P depend on the mixture concentration on the feed side and on the permeate side, respectively.

The weight fraction of component i in the permeate is given by

$$w_i = J_i / (J_1 + J_2 + \ldots + J_n) \tag{3.4}$$

If the solubilities and the diffusion coefficients of the compounds in the membrane are known, the flux of each component can be calculated from Eq. (3.3). Equation (3.4) is then used to calculate the concentration of component i in the permeate. Furthermore, the selectivity of the membrane can also be determined, i.e., all properties necessary to describe the separation characteristics of a membrane are determined.

The solubility of pure vapors in the membrane can be obtained from vapor-sorption experiments. The mass absorbed by the membrane is determined with a microbalance at a given temperature as a function of the pressure of solvent vapor, i.e., sorption isotherms are obtained. In recent years such experiments have been performed quite extensively [7–11].

For polymeric membranes three types of sorption isotherms are known, as shown schematically in Fig. 3.4. The amount of solvent vapor absorbed (weight fraction) is shown as a function of solvent vapor activity a_i defined as:

$$a_i = (P_i / P_i^0) \cdot \exp\left[(B_i - V_i') \cdot (P_i - P_i^0) / RT_M \right] \tag{3.5}$$

a_i is more or less the ratio of the vapor pressure (P_i) of the solvent dissolved in the membrane at temperature T_M to the vapor pressure (P_i^0) of pure solvent at temperature T_M. The exponential term in Eq. (3.5) corrects for nonideal behavior of the vapor and usually its value is close to 1 (B_i is the second virial coefficient and V_i' is the molar liquid volume of the solvent at T_M; R = universal gas constant).

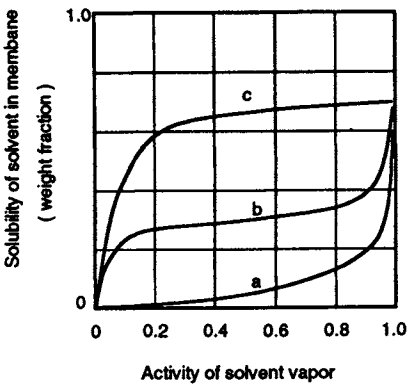

Fig. 3.4 Types of sorption isotherms observed with polymeric membranes: (a) Flory–Huggins type; (c) Langmuir type; (b) combination of (a) and (c).

In Fig. 3.4, curve (a) represents the case normally observed in rubbery polymers. Polymer solution theories such as the Flory–Huggins theory predict this type of sorption isotherms. Curves showing shape (c) are so-called Langmuir-sorption isotherms usually observed for the sorption of vapors in glassy polymers. Curves of type (b) can be considered as a combination of type (a) and type (c). The dependence of w_i as a function of a_i can be described by the equation:

$$w_i = K_i\,(a_i) \cdot a_i \tag{3.6}$$

with $K_i\,(a_i)$ depending itself on the activity a_i. This behavior of K_i is usually observed for the sorption of pure solvent vapors in polymeric membranes used in vapor permeation. An empirical equation for $K_i\,(a_i)$ is given [12] as:

$$K_i\,(a_i) = s_{1i} \cdot [1 + (s_{2i}/s_{1i} - 1) \cdot a_i^{s_{mi}}] \tag{3.7}$$

where s_{1i}, s_{2i} and s_{mi} are adjustable parameters, which have to be fitted to the experimental sorption isotherms using Eq. (3.6).

Figure 3.5 shows sorption isotherms at 333 K for water, methanol, ethanol and *n*-propanol in a poly(vinylalcohol) (PVA) membrane which has been investigated extensively for vapor permeation [11,13]. The results clearly show that at a given activity the solubility of the various compounds decreases in the sequence: water, methanol, ethanol, *n*-propanol; i.e., the more polar solvent molecules are, the better they can be absorbed by a PVA membrane. At 353 K practically the same sorption isotherms are obtained. The sorption isotherms correspond to the type (a) shown in Fig. 3.4 and such behavior is nearly always observed for polymer–solvent vapor systems used in vapor permeation. Only a few examples of type (b) are known [9].

Diffusion coefficients of low-molecular-weight compounds in polymers are usually dependent on the composition. As an example, Fig. 3.6 shows the

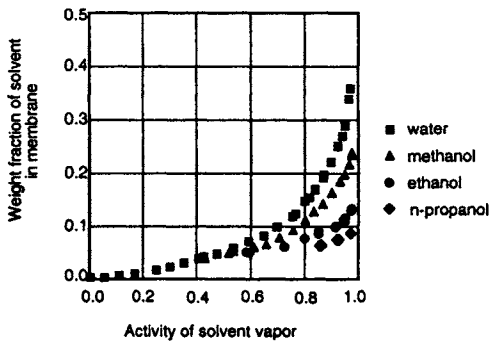

Fig. 3.5. Sorption isotherms for a PVA membrane [13].

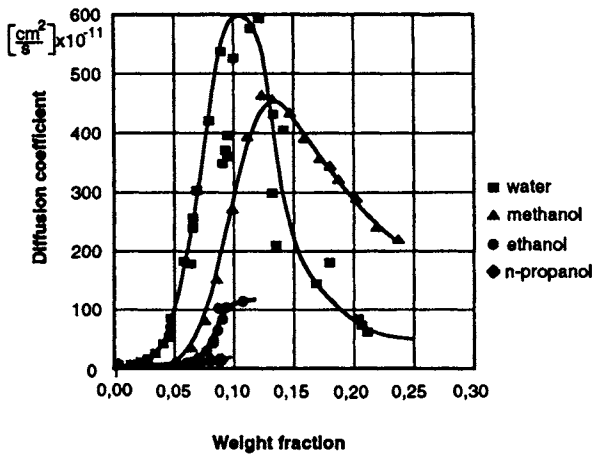

Fig. 3.6. Diffusion coefficients of solvents in a PVA membrane [13].

diffusion coefficients D in PVA obtained from the time dependence of the sorption process for water, methanol, ethanol and *n*-propanol. It is obvious that diffusion coefficients are closely related to the concentration of solvent in the PVA membrane. With an increasing amount of solvent in the membrane, i.e., with increasing degree of swelling of the membrane, D increases. However, for water and methanol, D decreases after having reached a maximum value at a particular value of w_i.

3.4 SPECIFIC INVESTIGATIONS AND APPLICATIONS

Investigations on the permeability of vapor through a membrane date back to the end of the 19th century [14,15]. However, only with the development of new polymers in the 1950s did more materials for membranes become available

and, therefore, studies of vapor permeability gained more and more attention. The mechanism of diffusion of low-molecular-weight compounds in polymers was investigated extensively, partly because of the importance for packing materials [16]. In the last twenty years a continuously increasing number of papers dealing with the permeation of vapors in membranes has been published. It is impossible to include all of them in this chapter. For the sake of simplicity, the papers that are somewhat arbitrarily taken into consideration are divided into the two categories of vapor permeation already discussed (see Table 3.1):

(a) the separation of vapors from gas/vapor mixtures, which is most important for removing volatile organics from waste air in order to eliminate environmental pollution [17–19]. In this case vapor permeability is normally not affected substantially by the gases because the interactions between gases and polymers are usually small. This kind of separation is commonly treated together with gas separation and, therefore, only a short survey and some examples of industrial applications are given here.

(b) The separation of vapors from mixtures containing no permanent gases has been investigated more extensively only in the last ten years, although some work had already been done about 30 years ago [20]. This kind of separation is regarded as a process alternative to pervaporation being, however, more economical and technically more appropriate. So far not very many papers dealing with this separation process have been published. A more detailed discussion is presented here and a few industrial applications are mentioned.

3.4.1 Removal of Vapors from Gas/Vapor Mixtures

3.4.1.1 Specific Investigations

For a long time it has been well known that in appropriate polymeric membranes, vapors show significantly higher permeability than permanent gases. Therefore, it is obvious to use vapor permeation for solvent removal and recovery and for reduction of environmental pollution. Table 3.2 lists quite a number of scientific papers dealing with this problem. With various membrane materials, good selectivities can be obtained for all the different separation problems investigated. Unfortunately the permeabilities obtained are nearly always too low for practical application.

Permeability may be increased with increasing feed pressure as shown in Fig. 3.7. The results of Baker et al. [17] clearly show that the permeability of nitrogen is significantly lower than the organic compounds. Furthermore, it is practically constant in the pressure range investigated, whereas the permeabilities of the organics increase with increasing feed pressure. The same behavior was found for ten different rubbery membranes and it probably reflects the effect of the

TABLE 3.2

Separation of organic solvent vapors from air unless otherwise stated

Solvent	Membrane	Selectivity	Reference
Methanol	Polyimide	221	25
	Silicone	38	25
Ethanol	Polyimide	297	25
Ethanol/N_2	Vycor glass	2–400	4
Acetone	PDMS	11–25	18
		47.7	25
		158	19
Acetone/N_2	Vycor glass	2–300	4
Hexane	Polyimide	32	25
Benzene	Polyimide	51	25
Toluene	Polyimide	180	25
	PDMS	83	19
p-Xylene	Polyimide	460	25
	PDMS	68	19
m-Xylene	Polyimide	513	25
1,2-Dichloromethane	PDMS	142	19
Chloroform	Polyimide	24	25
Carbon tetrachloride	Polyimide	32	25
1,2-Dichloroethane	Polyimide	52	25
	PDMS	103	19
1,2-Dichloropropane	Polyimide	57	25

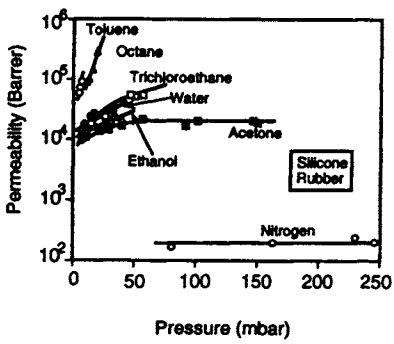

Fig. 3.7. Permeability of pure compounds as a function feed pressure at 40°C and vacuum on permeate side [17]. (1 Barrer = 10^{10} [cm^3 (STP) cm/cm^2 sec cmHg] = 7.50062 · 10^8 [cm^3 (STP) cm/cm^2 sec mbar]).

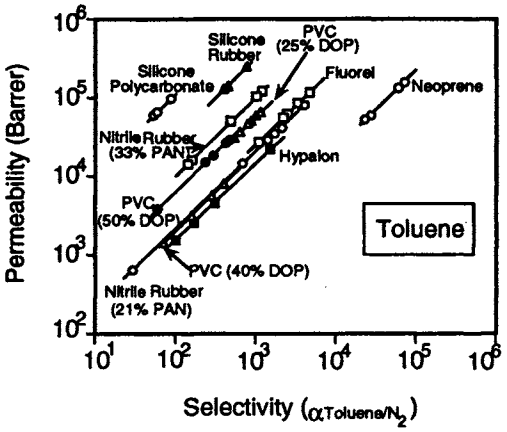

Fig. 3.8. Permeability vs. ideal selectivity for toluene in various rubbery membranes at 40°C and vacuum on permeate side [17].

amount of vapor absorbed on the membrane structure. Higher sorption plasticizes the membrane and increases the diffusion coefficient of the permeating molecules resulting in an increase in permeability. Despite the pressure dependence of the permeabilities, good ideal selectivities are observed, i.e., ratios of the permeabilities of the pure compounds. As an example, Fig. 3.8 shows permeabilities versus ideal selectivities for toluene for membranes made of ten different rubbery polymers. The actual selectivity, however, may be much less than the ideal selectivity, depending on how strongly plasticization is affecting the permeability of nitrogen (it most probably increases and hence, selectivities will decrease). Nevertheless, the few examples discussed clearly show that vapors can be separated from permanent gases using nonporous membranes.

3.4.1.2 Industrial Applications

Compared with vapor permeation, other processes suitable for the removal of vapors from air streams — like absorption, adsorption or chemical sorption — have the disadvantage of being discontinuous processes. Regeneration of the sorption units is required and, therefore, the problem of pollution is usually only transferred from waste air to waste water. Thermal and catalytic burning (700–1000°C) require additional energy and often new hazardous compounds are generated. Biological treatment in many cases is not possible. Vapor permeation avoids further pollution. It is the one most suitable for the reuse of the recovered solvent because it is not destroyed by burning or contaminated with other compounds as in "washing" processes. It seems to be somewhat surprising that vapor permeation is not yet widely used in industry for the treatment of waste air. This is mainly due to the lack of appropriate membranes, i.e.,

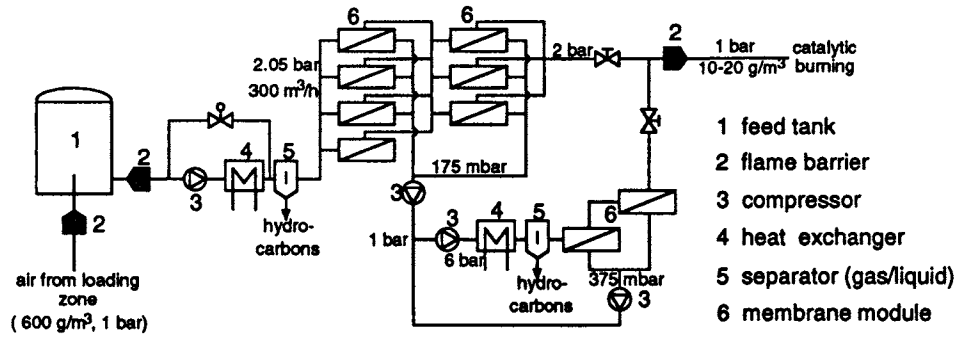

Fig. 3.9. Schematic of a gasoline vapor recovery units [27].

membranes with good separation characteristics and acceptable lifetimes under operating conditions. Many applications are proposed and even have been proven to be reliable in laboratory and/or pilot plant scale [4,5,17,18,21–25]. As an example of the few large-scale applications, Fig. 3.9 shows schematically the process for the recovery of gasoline vapor during loading and/or unloading of gasoline tanks. The process was developed by GKSS GmbH in Germany and five large-scale vapor recovery units combining membrane processes with catalytic final cleaning or gas engines have been installed [26,27]. The process shown in Fig. 3.9 is designed for the treatment of 600 $m^3 h^{-1}$ of air (1 bar, ambient temperature) containing about 20 vol% of hydrocarbon vapors. After compression to about 2 bar and separation of condensate, the air/vapor mixture is fed to the main membrane separation unit operating with a permeate pressure of about 175 mbar. The retentate leaves this unit with such a low content of hydrocarbons that it goes directly to the final catalytic cleaning. The permeate is so rich in hydrocarbons that it can be compressed to about 6 bar and again, after separation of possible condensate, it is fed to a second membrane separation unit operating with a permeate pressure of about 375 mbar. The retentate of this unit also goes directly to catalytic cleaning and the permeate is mixed with the permeate of the main unit after compressing both permeate streams to 1 bar, i.e., it is recycled to the feed of the second unit. Overall about 98% of the hydrocarbons are recovered as condensate, i.e., only about 2% are discharged by catalytic cleaning. A composite membrane is used with a selective layer of polydimethylsiloxane. Although it is still unclear whether such a process is really better with respect to economical and environmental reasons, the successful performance of the plants installed so far is accepted.

3.4.2 Separation of Vapor Mixtures

The separation of vapor mixtures using nonporous membranes was already discussed by Binning et al. [20] in the late 1950s. They investigated the separ-

ation of methanol/benzene with a polyethylene membrane being in contact with a saturated vapor phase of this mixture. More recently, Uragami et al. [28] proposed the term "evapomeation", referring to vapor permeation if the vapor phase is in equilibrium with a liquid feed, i.e., saturated vapors are used as feed. However, this term is strongly discouraged [29]. Vapor permeation includes both the separation of saturated and nonsaturated vapor mixtures.

3.4.2.1 Specific Investigations of the Effect of Operating Parameters

In the early stages, polyethylene and natural rubber were mainly used in vapor permeation experiments because other suitable polymers were not available. In the meantime, however, many other polymeric materials have been studied to solve various separation problems, such as silicone rubber, modified silicone rubber, chitosan derivatives, polystyrene, polyvinylchloride and many others [30–59]. Table 3.3 gives a summary of polymeric materials that have been tested for the separation of particular mixtures by vapor permeation.

Using some selected examples, the influence of operating conditions on the membrane performance in vapor permeation is discussed.

(a) Influence of Feed Composition and Pressure

Figure 3.10 shows the separation diagram for the mixture ethanol/water using a PVA/PAN-composite membrane (GFT mbH — standard). For two different feed pressures p^F up to about 95 w% ethanol in the feed, the content of ethanol in the permeate is small (< 3 w%) and nearly constant. In this composition range, for this membrane permeate composition is almost independent of feed composition. The total flux through the membrane, however, is strongly dependent on the composition and the pressure of the feed as shown in Fig.

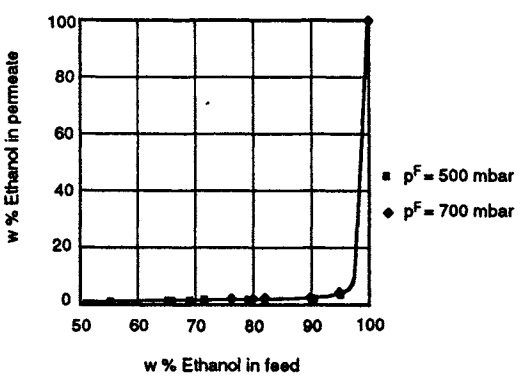

Fig. 3.10. Separation of water from ethanol by vapor permeation using a PVA/PAN-composite membrane (GFT mbH) at 30 mbar permeate pressure [56].

TABLE 3.3
Membrane materials and mixtures tested in vapor permeation

Membrane	Vapor mixture	Reference
Polyvinylalcohol	Water/Methanol	56–58
	Water/Ethanol	49,57,59
	Water/*n*-Propanol	57
	Water/2-Propanol	57–59
	Water/Ethylacetate	56
	Water/Ammonia	57
	Water/Methylamine	57
	Methanol/*n*-Propanol	57
Cellulose acetate	Water/Ethanol	31,40,49
Polysulphonate	Water/Ethanol	49
Polysulphonamid	Water/Ethanol	49
Nafion	Water/Ethanol	59
Polyvinylidene fluoride	Benzene/Cyclohexane	30
Polyimide	Water/Ethanol	43,55
Chitosan derivatives	Water/Ethanol	34
Cellophane	Water/Ethanol	41
PVC	Methanol/Water	35
	Ethanol/Water	35
	2-Propanol/Water	35
Polystyrene	Methanol/Water	37
	Ethanol	Water
Polyacrylonitrile	Ethanol/Water	31
Silicone rubber	Methanol/Water	33
	Ethanol/Water	33,42
	n-Propanol/Water	33
Ceramics	Ethanol/Water	1,2

3.11. As is to be expected with decreasing p^F and decreasing water content in the feed, the transmembrane flux decreases significantly. Similar behavior is often observed and seems to be pretty general.

(b) Influence of Membrane Temperature

The effect of membrane temperature on the total flux and on the separation factor for aqueous feed mixtures with 10 w% and 95.6 w% ethanol (viz. azeotropic composition) through a PVC membrane is shown in Figs. 3.12 and 3.13, respectively. Both flux and separation factor increase with increasing membrane temperature. The increase in flux can be understood from the increase of

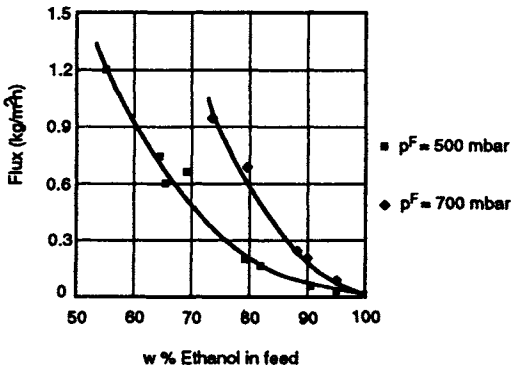

Fig. 3.11. Total permeate flux in vapor permeation for water/ethanol at 75°C and 30 mbar permeate pressure using a PVA/PAN-composite membrane (GFT mbH) [56].

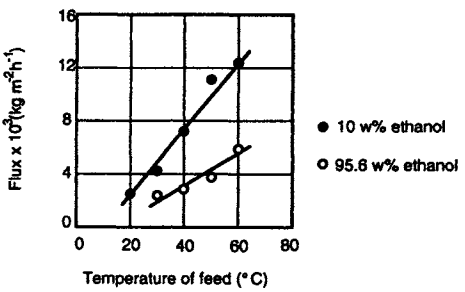

Fig. 3.12. Effect of temperature of ethanol/water feed vapor on the flux through a PVC 400 membrane (p^P = 5 mbar, p^F corresponds to the saturation pressure for any feed temperature and composition) [35].

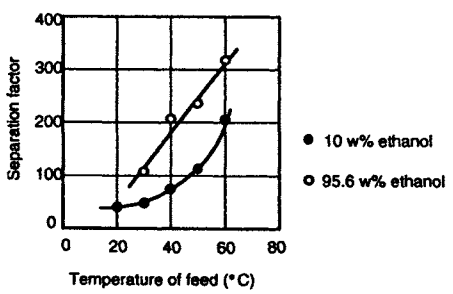

Fig. 3.13. Effect of temperature of ethanol/water feed vapor on the separation factor of a PVC 400 membrane (p^P = 5 mbar, p^F corresponds to the saturation pressure for any feed temperature and composition) [35].

the diffusion coefficients with increasing temperature. The changes in the separation factors with temperature cannot be easily explained. Sometimes they go up with increasing temperature, as shown in Fig. 3.13. But more frequently the α-values go down [49]. So far, no general explanation exists for this behavior.

(c) Influence of Permeate Pressure

The separation characteristics of a membrane are depending strongly on the permeate pressure. This is illustrated in Figs. 3.14 and 3.15 for a PVA/PAN-composite membrane showing the effect of permeate pressure on flux and permeate composition for various feed conditions. With increasing permeate

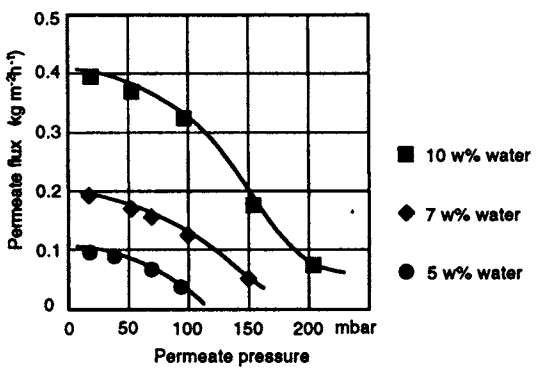

Fig. 3.14. Dependence of permeate flux on permeate pressure for a PVA/PAN-composite membrane (GFT mbH) and saturated 2-propanol/water feed vapor at 80°C and different feed compositions [54].

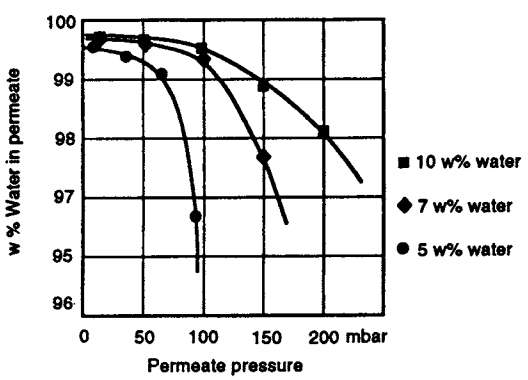

Fig. 3.15. Dependence of permeate composition on permeate pressure for a PVA/PAN-composite membrane (GFT mbH) and saturated 2-propanol/water feed vapor at 80°C and different feed compositions [54].

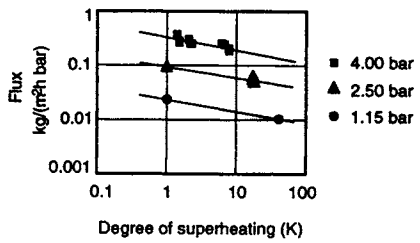

Fig. 3.16. Effect of superheating of ethanol/water feed vapor on the flux through a PVA/PAN-composite membrane at different feed pressures (95 w% ethanol in feed) [49].

pressure, flux and also selectivity decrease. Especially for a feed with a low water content, very low permeate pressures are required in order to obtain a permeate with a low alcohol content. This behavior observed for the PVA/PAN-composite membrane again seems to be quite general.

(d) Superheating of Feed Vapor

In vapor permeation, usually a slightly superheated vapor is used as feed in order to prevent condensation. However, the flux decreases with increasing degree of superheating as shown in Fig. 3.16 for the total flux of an ethanol/water mixture in a PVA/PAN-composite membrane [49]. Obviously, flux can be increased very clearly by decreasing the feed temperature close to the dew point of the vapor mixture. In other words, on the feed side of a membrane module, at any place, the local pressure should be as close as possible to the local saturation pressure in order to obtain a high flux. This is very important with respect to the feed-side pressure losses of a vapor permeation module. Even a small degree of superheating may cause a significant decrease in flux whereas selectivity seems not to be sensitive in this respect.

(e) Flux Puzzle

At saturation conditions of the vapor permeants at the feed-side, vapor permeation is thermodynamically identical with pervaporation, without a phase change. The flux should be the same as the driving force is the same, i.e., the difference in chemical potential across the membrane. Binning et al. [20] observed fluxes that were twofold in pervaporation compared with vapor permeation under saturation conditions. Stannett et al. [60] reported no differences in fluxes measured in pervaporation and saturated vapor permeation. Blackadder et al. [16] identified some important factors to be taken into account in permeability measurements. These are: proper porous support of the actual membrane, reduction of the pressure difference between the feed and permeate sides due to compounds not permeating and the degree of swelling of the membrane before measurements are started. If these factors are taken into consideration, vapor permeation and pervaporation fluxes are the same.

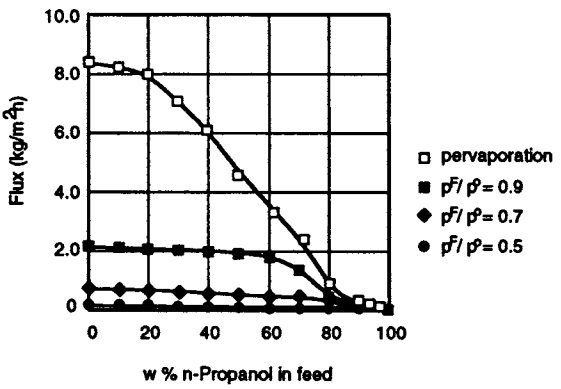

Fig. 3.17. Total flux in vapor permeation of *n*-propanol/water through a PVA/PAN-composite membrane at 80°C for different relative humidities p^F/p^o [57].

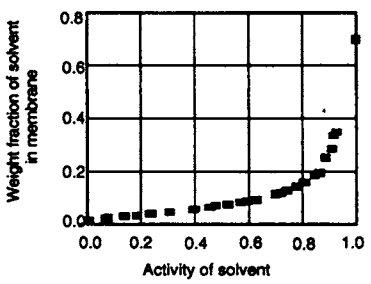

Fig. 3.18. Vapor sorption isotherm of water in PVA at 80°C [13].

Recently, experimental results have been reported [57] for fluxes for various alcohol/water mixtures using a PVA/PAN-composite membrane. As shown in Fig. 3.17, for the mixture of *n*-propanol/water, the flux obtained in pervaporation is much larger than those in vapor permeation for relative humidities $p^F/p^o < 1$, especially for feed mixtures containing a lot of water. This is to be understood from the strong dependence of water solubility in the membrane on relative humidity, i.e., the degree of saturation. From the sorption isotherm of pure water, shown in Fig. 3.18, it can be seen that the solubility of water in PVA changes drastically for solvent activities, becoming a little smaller than 1. For pure compounds, p^F/p^o is equal to the solvent activity, i.e., the solubility changes strongly for values of $p^F/p^o < 1$.

(f) Improvement of Vapor Permeation Performance of Existing Membranes

For a particular mixture, permeability and selectivity are different for different membrane polymers. Even if a membrane is found showing good overall performance with respect to a particular separation problem, improvements

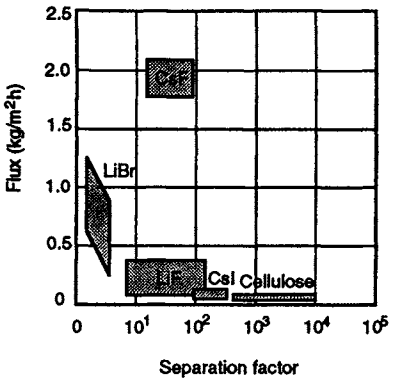

Fig. 3.19. Effect of impregnation of cellulose membranes with various salts on flux and selectivity for vapor permeation of an azeotropic 2-propanol/water mixture [49].

can increase economical efficiency. In this respect investigations have been performed to enhance membrane selectivity and/or flux with nonvolatile additives to the membrane polymer. Such additives cannot leach out because no liquid is in contact with the membrane. According to Jansen et al. [49] homogeneous cellulose films feature high selectivity but low flux for dehydration of alcohol/water mixtures by vapor permeation. By impregnating such films with inorganic salts, fluxes can be raised considerably while selectivity decreases, as shown in Fig. 3.19. Another example is shown in Fig. 3.20 for the dehydration of an ethanol/water mixture with a nonimpregnated (standard) and a CsF-impregnated PVA-composite membrane. Fluxes are increased substantially, while selectivities decrease to still acceptable levels.

This impregnation effect is most probably an increased sorption of water (and to a lesser extent of ethanol) due to specific interactions with the salts. The

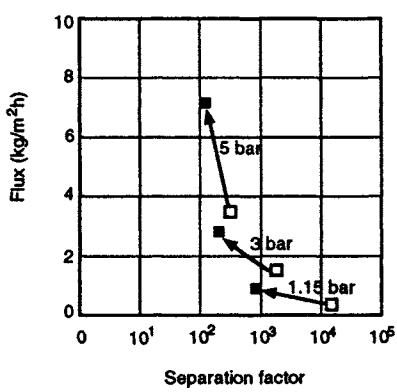

Fig. 3.20. Effect of impregnation of a PVA-composite membrane with CsF on flux and selectivity for ethanol/water vapor separation at different levels of feed pressure (95 w% ethanol in feed) [49].

impregnation technique, although not yet investigated thoroughly, is a possible means of tailoring membranes to specific applications.

3.4.2.2 *Engineering Aspects*

An adequate membrane module is the prerequisite for any technical application of a membrane separation process. Module and process design have to take into account all the factors affecting separation efficiency. In vapor permeation these are, in particular, friction losses at the feed side in addition to those at the permeate side, the challenge to operate as close as possible with saturated vapors as feed and the minimization of concentration polarization by choosing suitable operating conditions. Some of the important features in this respect have already been discussed and therefore only some aspects of technical relevance are now considered additionally.

(a) Membrane Modules

In a vapor permeation module, large volumes have to be handled at the permeate side and also at the feed side, with as little pressure loss as possible. So far, only plate and frame modules have been used in industrial application, such as the one shown schematically in Fig. 3.21. This module has been designed by LURGI GmbH, Germany [44,45] and consists of a number of membrane double cells and a permeate condenser combined into one compact unit.

The vapor feed enters the upper internal distribution channel, passes downwards through the cell across the membranes to both sides of the feed plate and leaves as retentate at the bottom of the cell via the internal retentate collector

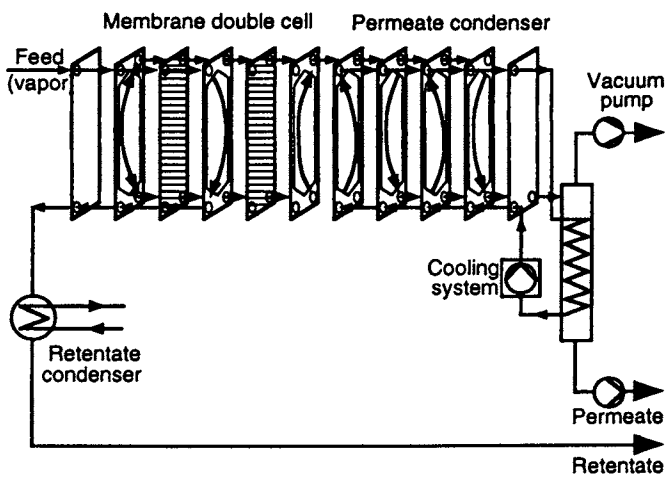

Fig. 3.21. Simplified flow diagram and schematics of the LURGI plate and frame module for vapor permeation [44].

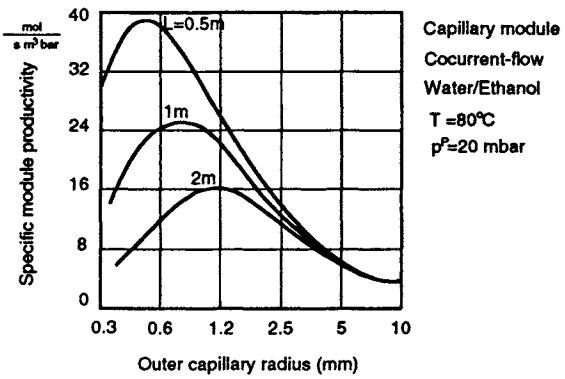

Fig. 3.22. Influence of capillary diameter and capillary length L on specific module productivity [54].

channel. The vapor permeate leaving the backside of the membrane passes through a supporting sieve plate to the profiled permeate collector plate and flows through a short internal heater directly to the permeate condenser cells, where the permeate vapor is liquefied. Commercially available plate-type heat exchanger equipment of stainless steel has been used for the construction. Enlargement of the module size is achieved simply by increasing the number of membrane cells per module unit. Vapor condensation in the feed side of the module cannot be avoided depending on operating conditions. This module has therefore to be installed with the plates arranged vertically. If condensation occurs, the condensate flows downwards to the bottom of permeator instead of accumulating on the surface of the membrane. For a long membrane lifetime this may be essential.

Capillary and hollow-fiber modules are, in principle, more economical mainly because of their higher packing density. Such modules have been tested in vapor permeation pilot plants [43] and model calculations have been performed by Rautenbach et al. [54]. Results of these model calculations clearly reveal that there exists an optimum in specific module productivity depending on the capillary diameter, as shown in Fig. 3.22. The shorter and thinner the capillaries are, the more pronounced is this optimum. The results further show that in vapor permeation there does not exist a very significant difference in separation behavior between co-current and counter-current flow of feed stream and permeate stream.

So far only vacuum vapor permeation has found an application in industry. Purge gas on the permeate side is a disadvantage for permeate condensation and, in addition, circulation of the purge gas requires additional energy.

(b) Concentration Polarization

It is often stated that concentration polarization in vapor permeation is not as important as in pervaporation, because diffusion coefficients D in vapors are

usually up to 10 000 times larger than those in liquids. However, one has to bear in mind that the density ρ of a vapor is up to 1000 times smaller than the one of a liquid. Therefore, the product $D \cdot \rho$ is not very different for a vapor and liquid feed mixture. Rautenbach has recently shown [62] that it is this value $D \cdot \rho$ which is the significant number for calculating the mass-transfer resistance in the laminar boundary layer at the feed side of a membrane. If this resistance is very large compared to the membrane resistance, concentration polarization becomes important in vapor permeation. In such cases, process design must focus on the hydrodynamics of the module and not on membrane improvement.

3.4.2.3. *Industrial Applications*

The straightforward development of vapor permeation from laboratory scale to its first industrial application was realized by LURGI GmbH in Germany [44,45]. The plant was designed for dehydration of 94 w% ethanol to a final composition of 99.9 w% with a capacity of 30 tons/day and is installed at Brüggemann & Co. in Heilbronn, Germany. Figure 3.23 shows a simplified process scheme of this plant. It consists of an evaporator and a three-stage vapor permeation system with two integral vapor compressors. The feed alcohol of subazeotropic concentration is first preheated with the dehydrated alcohol vapor leaving the membrane permeation system. It is then fed to the boiler of the distillation unit where it is evaporated. The saturated vapor of 2.2 bar and 100°C leaving the top of this unit passes directly through the first permeation unit. The slight pressure drop of about 0.5 bar is compensated for by recompression with a single-stage vapor compressor. The vapor enters the second permeation stage as saturated vapor at a temperature of 100°C and is recompressed by a second compressor before passing through the third permeation

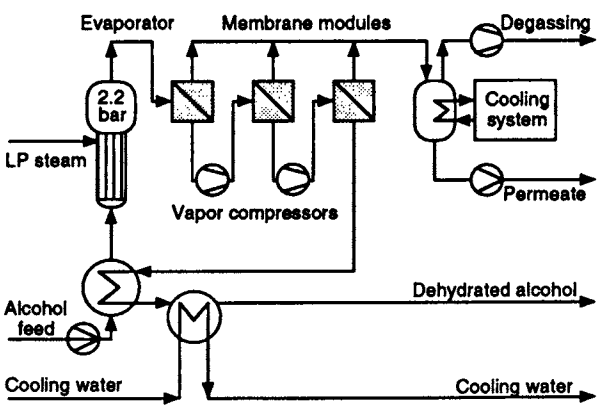

Fig. 3.23. Schematics of an industrial vapor permeation plant for the dehydration of ethanol [44].

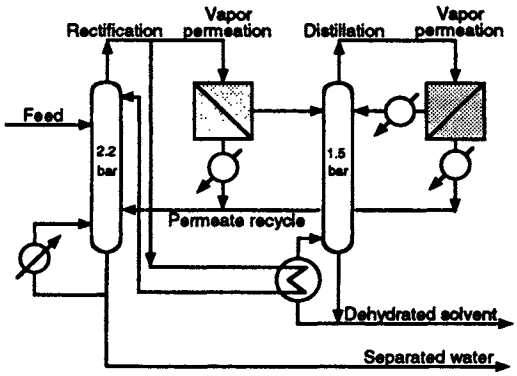

Fig. 3.24. Schematics of a hybrid process for iso-propanol dehydration combining vapor permeation and above-azeotropic distillation [44].

unit. The permeate is condensed by a plate and frame cooler. The permeate pressure is maintained at 10–20 mbar by very efficient permeate condensation. The closed-loop cooling system allows precise temperature control, avoids icing in the condenser and ensures complete condensation of the permeate. Organic vapor emission via the vacuum pump is thus kept to a minimum. The vacuum pump primarily serves to remove uncondensables and inert gases.

Cost analysis indicates that vapor permeation is more economical than pervaporation for this separation problem [44]. It compares favorably with conventional separation processes with respect to economics and it is by far the process to be preferred with respect to reducing environmental pollution.

Similar results concerning costs are expected for the dehydration of iso-propanol from 88 w% IPA to 99 w%. by vapor permeation [44]. Figure 3.24 shows the process scheme of a hybrid process proposed for this separation problem. If vapor permeation is only used to bridge the azeotropic point instead of concentrating directly to the final product, the process is even more economical and a very attractive alternative. This concept is especially advantageous if an extremely high final alcohol concentration is required with a very low residual water content of less than 50 ppm and without any traces of entrainer.

In this hybrid process the water is finally removed from the system at the top of the above-azeotropic distillation column by vapor permeation before condensation. The condensate is just used as reflux. If the two columns are designed as a two-stage pressure system, with some heat transfer, the two single-stage vapor permeation units can be operated without additional vapor compression. Although the process proposed looks very promising it still has to be developed.

3.5 CONCLUSIONS

Vapor permeation is regarded as the membrane process for separating condensable compounds from mixtures containing vapors and permanent gases or only vapors. Therefore, the process is closely related to gas permeation and to pervaporation. Vapor permeation is already used for the separation of volatile organics from waste air and for the dehydration of alcohols. Compared with pervaporation it has the advantage that the membrane is not exposed to a liquid feed. This may be important for the treatment of liquid process streams in industrial plants before and/or after a chemical reaction, especially if these streams contain nonvolatile compounds which are harmful for the membrane material. As no phase change occurs in the membrane separation module, the temperature of the feed does not change as much as in pervaporation where the removal of the heat of evaporation causes a significant decrease of the feed temperature. Usually, the higher the feed temperature the higher the flux and, consequently, the overall membrane area necessary for handling a given process stream is smaller. High temperatures are advantageous, but only if membranes are available that are chemically stable at operating conditions and, in this respect, further development is absolutely necessary (e.g., ceramic membranes). In vapor permeation, the separation characteristics of the membranes are very sensitive to the feed pressure, which at any operating temperature should be kept as close as possible to the saturation pressure. In practical application this requirement is not easy to obtain. Its long-term reliability still has to be proven. Nevertheless, vapor permeation has emerged as a membrane separation process feasible for a wide range of industrial applications, especially if incorporated in hybrid processes.

3.6 FINAL REMARK

As in most fields, a tremendous amount of work has been done in the area of vapor permeation in the past few years. We have tried to present the general advances that have been made. When you judge our efforts we would like you to heed the words of the English lexicographer and author, Samuel Johnson, who in 1755 wrote about his dictionary (one of the first compiled): *"In this work, when it shall be found that much is omitted, let it not be forgotten, that much likewise is performed..."*

ACKNOWLEDGEMENT

The authors are grateful for the financial support of the Bundesministerium für Forschung und Technologie (BMFT) of Germany for their own research in the field of separation processes with nonporous membranes.

REFERENCES

1 M. Asaeda and L.D. Du, Separation of alcohol/water gaseous mixtures by thin ceramic membrane. *J. Chem. Eng. Jpn.*, 19 (1) (1986) 72–77.
2 M. Asaeda, L.D. Du and M. Fuji, Separation of alcohol/water gaseous mixtures by an improved ceramic membrane. *J. Chem. Eng. Jpn.*, 19 (1) (1986) 84–85.
3 J.L. Falconer, R.D. Noble and D.P. Sperry, Catalytic membrane reactors. In: R.D. Noble and S.A. Stern (Eds.), *Membrane Separations Technology*. Elsevier, Amsterdam, 1994.
4 M.M. Qiu and Sun-Tak Hwang, Continuous vapor–gas separation with a porous membrane permeation system. *J. Membr. Sci.*, 59 (1991) 53–72.
5 H. Strathman, B. Bauer and J. Kerres, Polymer membranes with selective gas and vapor permeation properties. *Makromol. Chem., Macromol. Symp.*, 33 (1990) 161–178.
6 Th. Graham, Über die Absorption und dialytische Scheidung der Gase durch kolloidale Scheidewände. *Philosoph. Trans./Annalen der Chemie und Pharmacie*, V. Suppl. (1867) 1–78.
7 B. Will, A. Heintz and R.N. Lichtenthaler, Experimental and theoretical study of vapor permeation. In: R. Bakish (Ed.), *Proc. 3rd Int. Conf. on Pervaporation Processes in the Chemical Industry, Nancy, France*. Bakish Materials Corporation, P.O. Box 148, Englewood, NJ 07631, USA, 1988, pp.37–43.
8 B. Schmittecker and R.N. Lichtenthaler, Selection of polymers for membrane on the basis of sorption measurements. In: R. Bakish (Ed.), *Proc. 1st Int. Conf. on Pervaporation Processes in the Chemical Industry, Atlanta, USA*. Bakish Materials Corporation, P.O. Box 148, Englewood, NJ 07631, USA, 1986, pp. 76–95.
9 J. Hauser, A. Heintz, G.A. Reinhardt, B. Schmittecker, M. Wesslein and R.N. Lichtenthaler, Sorption, diffusion and pervaporation of water/alcohol mixtures in PVA-membranes: Experimental results and theoretical treatment. In: R. Bakish (Ed.), *Proc. 2nd Int. Conf. on Pervaporation Processes in the Chemical Industry, San Antonio, USA*. Bakish Materials Corporation, P.O. Box 148, Englewood, NJ 07631, USA, 1987, pp. 15–24.
10 I. Blume, P.J.F. Schwering, M.H.V. Mulder and C.A. Smolders Vapor sorption and permeation properties of poly-(dimethylsiloxane) films. *J. Membr. Sci.*, 61 (1991) 85–98.
11 A. Heintz, H. Funke and R.N. Lichtenthaler, Sorption and diffusion in pervaporation membranes. In: R.Y.M. Huang (Ed.), *Pervaporation Membrane Separation Processes*. Elsevier, Amsterdam, 1991, Chap. 6, pp. 279–319.
12 R. Rautenbach and R. Albrecht, The separation potential of pervaporation. *J. Membr. Sci.*, 25 (1985) 1–54.
13 B. Schmittecker, Untersuchungen zur Löslichkeit und Diffusion von Wasser und Alkoholhomologen in teilvernetztem Polyvinylalkohol und Polyetherimid. Ph. D. Thesis, Universität Heidelberg, 1990.
14 J.K. Mitchell, On the penetrativeness of fluids. *J. Roy. Inst.*, 2 (1831) 101, 301.
15 Th. Graham, On the absorption and dialytic separation of gases by colloid septa. *Phil. Mag. S.* 4, 32, (218) (1866) 401–420.
16 D.A. Blackadder and J.S. Keniry, The measurement of the permeability of polymer membranes to solvating molecules. *J. Appl. Polym. Sci.*, 16 (1972) 2141–2152.
17 R.W. Baker, N. Yoshioka, J.M. Mohr and A. Khan, Separation of organic vapors from air. *J. Membr. Sci.*, 31 (1987) 259–271.
18 K. Kimmerle, C.M. Bell, W. Gudernatsch and H. Chmiel, Solvent recovery from air. *J. Membr. Sci.*, 36 (1988) 477–488.
19 H. Paul, C. Philipsen, F.J. Gerner and H. Strathmann, Removal of organic vapors from air by selective membrane permeation. *J. Membr. Sci.*, 36 (1988) 363–372.

20 R.C. Binning, R.J. Lee, J.F. Jennings and E.C. Martin Separation of liquid mixtures by permeation. *Ind. Eng. Chem.*, 53 (1) (1961) 45–50.
21 H. Paul, L. Bühler and W. Dahm, Lösungsmittelrückgewinnung durch Gastrennung mittels Membranen. In: *Reprints 1st Aachener Membran Kolloquium, RWTH Aachen* GVD-VDI Gesellschaft Verfahrenstechnik und Chemieingenieurwesen (Ed.), D-4000 Düsseldorf, Germany, 1987, pp. 283–300.
22 W. Dahm, J. Kohlbach, R. Rautenbach, H. Paul and H. Strathmann, Gaspermeation: ein neues Verfahren zur Vorabscheidung und Rückgewinnung von Lösungsmitteln aus Abluft- und Umluftströmen. In: *Reprints 2nd Aachener Membran Kolloquium, RWTH Aachen.* GVD-VDI Gesellschaft Verfahrenstechnik und Chemieingenieurwesen (Ed.), D-4000 Düsseldorf, Germany, 1989, pp. 235–250.
23 R. Rautenbach and R. Ahlers, Rückgewinnung organischer Dämpfe aus Abluft mit Hilfe der Gaspermeation. In: *Reprints 3rd Aachener Membran Kolloquium, RWTH Aachen.* GVD-VDI Gesellschaft Verfahrenstechnik und Chemieingenieurwesen (Ed.), D-4000 Düsseldorf, Germany, 1991, pp. 525–527..
24 R. Pelzer, W. Paulowski, J. Curth, C. Meyer, G. Voss and H.J. Schwefer Betriebserfahrungen mit drei Varianten der Preussag-VapourRed-Anlage zur Kohlenwasserstoffemissionsreduzierung auf Großtanklägern. In: *Reprints 3rd Aachener Membran Kolloquium, RWTH Aachen.* GVD-VDI Gesellschaft Verfahrenstechnik und Chemieingenieurwesen (Ed.), D-4000 Düsseldorf, Germany, 1991, pp. 521–523.
25 X. Feng, S. Sourirajan, H. Tezel and T. Matsuura, Separation of organic vapor from air by aromatic polyimide membranes. *J. Appl. Polym. Sci.*, 43 (1991) 1071–1079.
26 R.D. Behling, K. Ohlrogge and K.V. Peinemann, Rückgewinnung von Kohlenwasserstoffen aus Abluft mit Hilfe von Membranen. In: *Reprints 2nd Aachener Membran Kolloquium, RWTH Aachen.* GVD-VDI Gesellschaft Verfahrenstechnik und Chemieingenieurwesen (Ed.), D-4000 Düsseldorf, Germany, 1989, pp. 251–265.
27 K. Ohlrogge, K.V. Peinemann, J. Wind and R.D. Behling Betriebserfahrungen mit Membranverfahren zur Abtrennung organischer Dämpfe In: *Reprints Aachener Membran Kolloqium, RWTH Aachen.* GVD-VDI Gesellschaft Verfahrenstechnik und Chemieingenieurwesen (Ed.), D-4000 Düsseldorf, Germany, 1991, pp. 197–215.
28 T. Uragami, K. Takigawa and T. Morikawa, Permeation and separation characteristics of aqueous alcohol solutions through hydrophilic and hydrophobic membranes by pervaporation and evaporation. In: R. Bakish (Ed.), *Proc. 3rd Int. Conf. on Pervaporation Processes in the Chemical Industry, Nancy, France.* Bakish Materials Corporation, P.O. Box 148, Englewood, NJ 07631, USA, 1988, pp. 127–133.
29 K.W. Böddeker, Terminology in pervaporation. *J. Membr. Sci.*, 51 (1990) 259–272.
30 F.P. McCandless, D.P. Alzheimer and R.B. Hartman, Solvent membrane separation of benzene and cyclohexene. *Ind. Eng. Chem., Process Des. Develop.*, 13 (3) (1974) 310–312.
31 T. Kataoka, T. Tsuru, S. Nakao and S. Kimura, Membrane transport properties of pervaporation and vapor permeation in ethanol-water system using polyacrylontril and cellulose acetate membranes. *J. Chem. Eng. Jpn.*, 24 (3) (1991) 334–339.
32 T. Kataoka, T. Tsuru, S. Nakao and S. Kimura, Permeation equations developed for prediction of membrane performance in pervaporation, vapor permeation and reverse osmosis based on the solution-diffusion model. *J. Chem. Eng. Jpn.*, 24 (3) (1991) 326–333.
33 T. Uragami and H. Shinomiya, Concentration of aqueous alcoholic solutions through a modified silicone rubber membrane by pervaporation and evapomeation. *Makromol. Chem.*, 192 (1991) 2293–2305.

34 T. Uragami and K. Takigawa, Permeation and separation characteristics of ethanol–water mixtures through chitosan derivative membranes by pervaporation and evapomeation. *Polymer*, 31 (1990) 668–672.
35 T. Uragami and K. Morikawa and H. Okuno, Characteristics of permeation and separation of aqueous alcohol solutions through hydrophobic polymer membranes. *Polymer*, 30 (1989) 1117–1122.
36 T. Uragami and K. Morikawa, Permeation of ethanol through poly(dimethylsiloxane) membranes using temperature differences in membrane permeation processes of the evapomeation method. *Makromol. Chem., Rapid Commun.*, 10 (1989) 287–291.
37 T. Uragami and K. Morikawa, Studies on synthesis and permeabilities of special polymer membranes, 70. Permeation and separation characteristics for aqueous alcoholic systems by evapomeation and pervaporation through polystyrene membranes. *Makromol. Chem.*, 190 (1989) 399–404.
38 T. Uragami and K. Morikawa, Studies on synthesis and permeabilities of special polymer membranes, 69. Comparison of permeation and separation characteristics for aqueous alcoholic solutions by pervaporation and new evapomeation methods through chitosan membranes. *Makromol. Chem., Rapid Commun.*, 9 (1988) 361–365.
39 T. Uragami, T. Morikawa, H. Shinomiya and H. Okuno, Permeation and separation characteristics for organic liquid mixtures through some polymer membranes by pervaporation and evapomeation with control of temperature difference. In: R. Bakish (Ed.), *Proc. 4th Int. Conf. on Pervaporation Processes in the Chemical Industry, Ft. Lauderdale, USA.* Bakish Materials Corporation, P.O. Box 148, Englewood, NJ 07631, USA, 1989, 127–133.
40 H. Suematsu, K. Harada and T. Kataoka, Separation of ethanol-water mixtures by vapor permeation through cellulose membrane. In: R. Bakish (Ed.), *Proc. 3rd Int. Conf. on Pervaporation Processes in the Chemical Industry, Nancy, France.* Bakish Materials Corporation, P.O. Box 148, Englewood, NJ 07631, USA, 1988, pp. 165–171.
41 H. Suematsu, K. Harada and T. Kataoka, Separation of ethanol–water mixtures by vapor permeation through cellophane membrane. *Maku*, 14 (5) (1989) 337–343.
42 H. Suematsu, K. Harada and T. Kataoka, Separation of ethanol–water mixtures using silicone rubber membrane. *Maku*, 12 (2) (1987) 95–100.
43 K. Nagagawa, Y. Kusuki and K. Ninomiya, Separation of water–organic mixtures by vapor permeation through aromatic polyimide hollow fibers. In: R. Bakish (Ed.), *Proc. 4th Int. Conf. on Pervaporation Processes in the Chemical Industry, Ft. Lauderdale, USA.* Bakish Materials Corporation, P.O. Box 148, Englewood, NJ 07631, USA, 1989, pp. 250–260.
44 U. Sander and H. Janssen, Industrial application of vapour permeation. *J. Membr. Sci.*, 61 (1991) 113–129.
45 U. Sander and H. Janssen, Industrial application of vapour permeation. In: R. Bakish (Ed.), *Proc. 4th Int. Conf. on Pervaporation Processes in the Chemical Industry, Ft. Lauderdale, USA.* Bakish Materials Corporation, P.O. Box 148, Englewood, NJ 07631, USA, 1989, pp. 416–427.
46 U. Sander and P.-B. Soukup, Practical experience with pervaporation systems for liquid and vapour separation. In: R. Bakish (Ed.), *Proc. 3rd Int. Conf. on Pervaporation Processes in the Chemical Industry, Nancy, France.* Bakish Materials Corporation, P.O. Box 148, Englewood, NJ 07631, USA, 1988, pp. 508–518.
47 A.E. Jansen, H.F. van Wijk, W.F. Versteeg, J.W. van Heuven Dehydration of alcohols by vapour permeation. In: R. Bakish (Ed.), *Proc. 3rd Int. Conf. on Pervaporation Processes in the Chemical Industry, Nancy, France.* Bakish Materials Corporation, P.O. Box 148, Englewood, NJ 07631, USA, 1988, pp. 338–341.

48 A.E. Jansen, H.F. van Wijk, W.F. Versteeg, J. W. van Heuven Dehydration of alcohols by vapour permeation. In: *Reprints 2nd Aachener Membran Kolloqium, RWTH Aachen.* GVD-VDI Gesellschaft Verfahrenstechnik und Chemieingenieurwesen (Ed.), D-4000 Düsseldorf, Germany, 1989, p. 451.

49 A.E. Jansen, W.F. Versteeg, B. van Engelenburg and J.H. Hanemaaijer Dehydration of alcohols by vapour permeation. In: E.F. Vasant and R. Dewolfs (Eds.), *Gas Separation Technology.* Elsevier, Amsterdam, 1990, pp. 413–427.

50 R. Rautenbach and F. P. Helmus, Dampfpermeation. In: *Reprints 3rd Aachener Membran Kolloquium, RWTH Aachen.* GVD-VDI Gesellschaft Verfahrenstechnik und Chemieingenieurwesen (Ed.), D-4000 Düsseldorf, Germany, 1991, pp. 513–516 .

51 R. Rautenbach and U. Meyer-Blumenroth, Dampfpermeation organischer und organisch-wässeriger Gemische. In: *Reprints 2nd Aachener Membran Kolloquium, RWTH Aachen.* GVD-VDI Gesellschaft Verfahrenstechnik und Chemieingenieurwesen (Ed.), D-4000 Düsseldorf, Germany, 1989, pp. 253–266.

52 R. Rautenbach and U. Meyer-Blumenroth, Verfahrensführung von Dampfpermeationsanlage. In: *Reprints 2nd Aachener Membran Kolloquium, RWTH Aachen.* GVD-VDI Gesellschaft Verfahrenstechnik und Chemieingenieurwesen (Ed.), D-4000 Düsseldorf, Germany, 1989, pp. 375–379.

53 R. Rautenbach and U. Meyer-Blumenroth, Vapor permeation of water–organic mixtures. Module and process design. In: R. Bakish (Ed.), *Proc. 3rd Int. Conf. on Pervaporation Processes in the Chemical Industry, Nancy, France.* Bakish Materials Corporation, P.O. Box 148, Englewood, NJ 07631, USA, 1988, pp. 287–302.

54 Rautenbach and U. Meyer-Blumenroth, Module and process design for vapor permeation. *Desalination,* 77 (1990) 295–322.

55 K. Okamoto, N. Tanihara, H. Watanabe, K. Tanaka, H. Kita, A. Nakamura, Y. Kusiki and Nakagawa, Vapor permeation and pervaporation separation of water–ethanol mixtures through polyimide membranes. *J. Membr. Sci.,* 68 (1992) 53–64.

56 B. Will, Dampfpermeation von Reinstoffen und Mischungen durch Polyvinylalkohol-Composite Membranen. Ph.D. Thesis, Universität Heidelberg, 1992.

57 B. Will and R.N. Lichtenthaler, Comparison of the separation of mixtures by vapor permeation and by pervaporation using PVA composite membranes. I. Binary alcohol–water systems. *J. Membr. Sci.,* 68 (1992) 119–125.

58 B. Will and R.N. Lichtenthaler, Comparison of the separation of mixtures by vapor permeation and by pervaporation using PVA composite membranes. II. The binary systems ammonia–water, methylamine–water, 1-propanol–methanol and the ternary system 1-propanol–methanol–water. *J. Membr. Sci.,* 68, (1992) 127–131.

59 U. Mayer-Blumenroth, Dampfpermeation — Untersuchungen zum Stofftransport und zur Verfahrensführung. Ph.D. Thesis, RWTH Aachen (1989).

60 H. Yasuda and V. Stannett. Permeation, solution, and diffusion of water in some high polymers. *J. Polym. Sci.,* 57 (1962) 907–923.

61 H. Yasuda and V. Stannett. Liquid versus vapor permeation through polymer films. *J. Polym. Sci.,* B1 (6) (1963) 289–293.

62 R. Rautenbach and F.P. Helmus. Considerations on mass-transfer resistance in pervaporation and vapor permeation. *Paper presented at the Int. Symposium Progress in Membrane Science and Technology, University of Twente, Enschede, The Netherlands,* 1991.

Membrane Separations Technology. Principles and Applications
Edited by R.D. Noble and S.A. Stern

Chapter 4

Reverse osmosis

C.J.D. Fell

Centre for Membrane and Separation Technology,
University of New South Wales, Kensington 2033, Australia

4.1 INTRODUCTION

In reverse osmosis, a semipermeable membrane is challenged with a pressurised feed stream containing a solute. The pressure exerted is greater than the osmotic pressure of the feed, causing solvent to flow through the membrane. The technology is also often referred to as hyperfiltration. Figure 4.1 provides a schematic representation of the process.

The most common use for reverse osmosis is in the desalination of water. Here the aim is to remove dissolved salts and organics from water. Both seawater and brackish water are routinely processed. Because of the high osmotic pressure of seawater (2.3 MPa), reverse osmosis plants must frequently operate at high pressures (to 7 MPa) and plant components must be much more

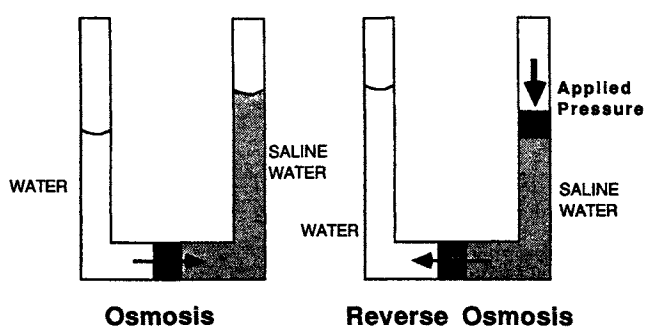

Fig. 4.1. Schematic of the reverse osmosis process.

TABLE 4.1
Osmotic pressures at 25°

Species	Concentration (mg l^{-1})	Osmotic pressure (MPa)
NaCl	35,000	2.79
	5,000	0.39
	1,000	0.12
	500	0.09
Seawater	44,000	3.23
	32,000	2.31
Sucrose	34,000	0.26
	340,000	2.60
Glucose	18,000	0.24
	90,000	1.21

robust than for other membrane based technologies. Table 4.1 provides data on the osmotic pressure of sodium chloride, seawater and sucrose solutions as a function of concentration.

The origins of the industrial application of reverse osmosis can be traced to the observation by Reid and co-workers [1] that dense polymer films could be used for desalination. Shortly afterwards, Loeb and Sourirajan [2] announced the development of a method for preparing anisotropic cellulose acetate membranes, with an active skin layer sufficiently thin to enable industrially interesting desalination fluxes to be obtained.

Since that time, new membranes have appeared and there has been a steady development of modules for efficiently housing the membranes and ensuring sufficient cross flow of feed to limit the buildup of a concentrated layer of solute at the surface of the membrane. This phenomenon, known as concentration polarisation, is responsible for a lowering of the pressure driving force for transfer across the membrane and reduces permeate flux. Since membrane plant is essentially modular, the capital cost of membrane plant is directly reflected in the flux obtained.

Other problems experienced in the industrial application of reverse osmosis are the fouling of the surface of the membrane by particulates in the feed stream or species that become supersaturated and precipitate, and membrane deterioration due to compaction, hydrolysis and chemical attack. Whilst cleaning regimens can be used to restore flux, long term flux decline is often experienced.

The technology has matured to an extent where 25% of the world's capacity

in desalination plant now uses the reverse osmosis process in preference to long established technologies such as multistage flash evaporation. In the USA, the penetration of reverse osmosis into the desalination market is 70%, with the estimated annual sales of desalination membranes being $ 85 million [3]. The technology has also found extensive use in food processing, and, as a result of continually improving module performance, is commencing to appear economically feasible for the environmentally important treatment of secondary sewage effluents and waste streams in industry. Current estimates give an annual growth rate of 20%. Nonetheless, the technology is still considered by some engineers to be problematical, with a risk of process failure due to long-term decline in membrane flux.

This chapter will review the membranes and modules currently available for reverse osmosis, and consider aspects of plant design and operation. The chapter will also consider the likely evolution of the technology over the next decade.

4.2 REVERSE OSMOSIS MEMBRANES

Useful reviews of the present state of membrane development have been provided by Kamiyama et al. [4], Drioli [5], Londsdale [6], Pusch [7] and Baker [8].

Membranes currently used in commercial reverse osmosis installations are asymetric, flat sheet membranes of cellulose acetate or cellulose triacetate, fine hollow fibers of aromatic polyamides or cellulose triacetate and thin film composites where an extremely fine layer of a highly hydrophilic polymer has been placed on a microporous support, usually made from polysulphone.

Asymetric cellulose acetate membranes are typically 100 μm in thickness, with the active surface layer being as thin as 0.3 μm. The preparation of cellulose acetate membranes involves dissolution of cellulose acetate in a solvent (acetone), spreading of the resultant dope in a thin film, an evaporation step to establish a concentration gradient in the film, and quenching of the film in a water bath. The membrane as produced is heat annealed before use to ensure adequate rejection of ions. Cellulose acetate membranes are resistant to chlorine in the feed to 1 mg l^{-1}, but are subject to hydrolysis at high pH. Blends of cellulose acetate and triacetate provide superior performance and a higher salt rejection. Cellulose acetate blend membranes currently account for over 50% of membranes used in water treatment [5].

Asymetric aromatic polyamide hollow fibers were introduced by the DuPont company in the period 1967–72 (Permasep B9 and B10 permeators). The fibers are thin (inside diameter 42 μm, outside diameter 85 μm) and are used in a tightly packed tubesheet configuration with the process flow on the outside of

the fiber. Whilst the permeability of the fiber membrane is significantly less than that of an asymetric cellulose acetate membrane, the packing arrangement allows a high volumetric capacity to be obtained.

Thin film composite (TFC) membranes were developed by Cadotte [9] and Riley et al. [10]. Membranes of this type are produced by interfacial polymerisation at the surface of a finely porous membrane which provides mechanical support for the resultant composite. For example, the PA300 membrane of Fluid Systems/UOP is prepared by the interfacial polymerisation of epiamine (an epichlorohydrin ethylene diamine) with isophthaloyl chloride and has a skin thickness of 0.03–0.05 μ, supported by a permeable hydrogel layer [8]. Similarly, the Filmtec/Dow FT30 membrane is prepared by the interfacial polymerisation of *m*-phenylenediamine with TMC to give a polyamide membrane with a skin thickness of 0.2 μ [3]. Other reactants are used, the aim being to get a thin film composite of good water permability and high salt rejection. Table 4.2 provides data on a range of reverse osmosis membranes now in commercial use [3,4,11].

TABLE 4.2

Properties of Some Commercial Reverse Osmosis Membranes

Type	Manufacturer	Form in which used	pH range	Chlorine tolerance	Oxidation tolerance
Cellulose acetate blend	Various	Spiral wound	3–8	Fair	Fair
Cellulose triacetate	Dow/Toyota	Capillary fiber	4–9	Fair	Good
Aromatic Polyamide	Du Pont	Hollow fiber	4–11	Poor	Fair
Crosslinked polyether TFC	Toray	Spiral wound	1–12	Poor	Fair
Aryl–Alkyl polyetherurea TFC	Fluid Systems/UOP	Spiral wound	3.5–12	Poor	Fair
Cross-linked fully aromatic polyamide TFC	Filmtec/Dow	Spiral wound	1–12	Poor	Fair

Whilst the one-step processing of sea water remains a significant goal for the fabricators of membranes (this requires a salt rejection of 99.4% and an operating pressure of 4–7 MPa), there has been significant recent activity in developing low pressure reverse osmosis membranes suitable for use with brackish water [12–14]. Such membranes are designed to operate at transmembrane pressures of 1–3 MPa rather than the more conventional 2.5–4 MPa.

The chemical and physical properties of the newer membranes remain for the most part proprietary. Direct comparisons of membrane performance are not straightforward because tests are frequently reported for different salt concentrations, different temperatures and transmembrane pressures and under dif-

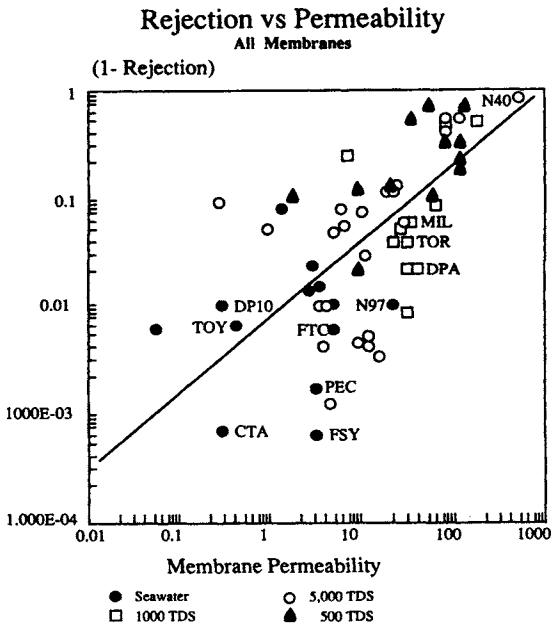

Fig. 4.2. Rejection (fractional) versus permeability (l/m^2 h-MPa) for commercial and experimental membranes reported in recent technical literature (1980–90). Means of reported performance data are plotted. Codes are: CTA, Cellulose triacetate; DP10, Du Pont B10; TOY, Toyobo hollow fibers; FSY, Fluid Systems/UOP; PEC, Toray PEC 1000; FTC, Filmtec; N40, Nitto NTR 7440; N97, Nitto NTR 7197; MIL, Millipore; DPA, DuPont A15; TOR, Toray SU-700.

ferent crossflow conditions on the process side under which significant solute buildup (concentration polarisation) can occur and lead to a reduction in the pressure driving force as the result of osmotic effects.

Figure 4.2 is a first attempt to reconcile available data. The axes are, respectively, fractional solute penetration (P) and apparent membrane permeability (A). Definitions are:

$$P = 1 - \frac{R}{100} \tag{4.1}$$

where R is the percentage rejection of the membrane for solute, and

$$A = \frac{J}{\Delta P - \Delta \Pi} \tag{4.2.}$$

where J is the solute flux and $(\Delta P - \Delta \Pi)$ is the transmembrane pressure when account has been taken of the osmotic pressure of the feed and permeate.

The use of A and P in this way reflects the current wisdom that the mode of solute transfer across the membrane is diffusional (see Section 4.3.1). The units used in expressing A (l/m^2 h-MPa) are those commonly used in the membrane

industry. A table of unit conversions has been provided at the end of this chapter. It should be noted that the calculation of P and ΔP from data in the literature makes no allowance for the possibility of concentration polarisation during the test. However, it is expected that most experimentors will have ensured good feed side mass transfer under membrane test conditions.

The data in Fig. 4.2 suggest that the high salt rejections required for one-step sea water desalination (from 35,000 to 500 mg l^{-1} in one pass) are obtained at the cost of substantially lowered membrane permeability. For the less demanding task of desalinating brackish water (feed 2000–5000 mg l^{-1}) a more permeable membrane can be used and the feed side pressure can be substantially reduced. Where the task is relatively straightforward, as in under-sink units to improve the potability of town water, quite low pressure operation is feasible. The notable feature of Fig. 4.2 is the considerable scatter of data about an apparent mean relationship. This suggests that there is scope for improving the rejection capacity of a membrane without a heavy penalty in permeability. Kamiyama et al. [4] have, for example, suggested that the Toray polyether composite shows superior performance for monovalent ions because of its significant negative charge.

It is not possible to speculate on the ultimate capacity of a reverse osmosis membrane for a given level of solute rejection because of lack of knowledge about the phenomena governing the transport phenomena involved. There will be a limit on skin thickness to retain mechanical integrity. This may well have been approached in those membranes having skin thicknesses of 0.03–0.05 μm. Riley [3] has additionally drawn attention to the need for the support layer to provide a minimum of resistance and has quoted earlier work by Lonsdale in which it is suggested that flow limitations in the microporous support layer limit the solvent capacity of existing membranes to 30% of that feasible. More importantly, it would appear that the best reported rate of water passage is still substantially below that predicted from a diffusion model if it is assumed that a significant proportion of the membrane permits the passage of water molecules.

Other factors determining the choice of a reverse osmosis membrane are its resistance to chlorine (used to prevent biological growth in the membrane system) and oxidising agents. Whilst cellulose acetate blend membranes have a reasonable level of stability to levels of chlorine of 1 mg l^{-1}, the newer thin film composites are less stable, and there is obvious attraction in developing a membrane that can operate effectively at high temperatures and under oxidising conditions.

Membranes not covered in the above discussion are dynamic membranes formed by trapping zirconium oxide and polyacrylics on microporous carriers and those formed by plasma polymerisation. Although experimented with for reverse osmosis applications, neither has yet shown commercial potential.

4.3 THEORY OF REVERSE OSMOSIS

The theoretical development for reverse osmosis includes the prediction of the transport properties of the membrane itself and prediction of the concentration profiles in the feed side flow channel as these give the concentration of solute at the surface of the membrane.

4.3.1 Membrane Transport

It is not yet possible to determine the structure of the skin layer of a reverse osmosis membrane by electron microscopy and there remains some controversy over the possible existence of pores. Current thinking is that the solvent passes through the gaps between polymer chains, which are of the order of 2–5 Å. Studies by Luck [15] and others on the structure of water in the skin layer suggest that the water in membranes with good rejection properties is quite strongly bound. It is therefore not accessible for the hydration of ions attempting to pass the membrane. However, it is noteworthy that high flux, low pressure drop membranes (nanofiltration membranes) are essentially charged ultrafiltration membranes which function by a different mechanism due to Donnan exclusion [16].

Theories used to characterise transport in the skin layer of membranes have been reviewed by Pusch [17]. They include the irreversible thermodynamics approach of Kedem and Katchalsky [18] and Kedem and Speigler [19], the solution–diffusion model [20], and the preferential sorption-capillary flow model of Sourirajan [21].

Irreversible thermodynamics leads to the following expressions for water and solute flow:

$$J_v = L_p \times (\Delta P - \Delta\Pi) \tag{4.3}$$

$$J_s = c_s (1 - \sigma) J_v + D \varepsilon \Delta c \tag{4.4}$$

σ is a measure of the solute–water coupling within the membrane and may often be treated as 1. The theory then characterises the membrane by the parameters L_p and $D\varepsilon$, which may be measured by other than reverse osmosis experiments and then used to quantify the performance of the membrane. A particular strength of this approach is its extension to multicomponent systems, where it can be used to predict membrane behaviour. However, it does not elucidate the actual transfer mechanisms within the membrane.

Parameters in the sorption–capillary flow model have been extensively evaluated by Sourirajan and his co-workers for cellulose acetate membranes. In a recent paper [22], the work has been extended to mixed ionised solutes in aqueous solutions and a solution sequence is developed to allow prediction of

the separation of individual ions from a set of reverse osmosis data taken from a sodium chloride reference solution.

However, the most commonly applied model at present is the solution–diffusion model, which gives the following relationships:

$$J_w = \frac{D_w c_w V_w (\Delta P - \Delta\Pi)}{RT\Delta x} = A(\Delta P - \Delta\Pi) \tag{4.5}$$

for flux of solvent, and

$$J_s = \frac{D_s K_s (C_s^I - c_s^{II})}{\Delta x} \tag{4.6}$$

for the flux of solute. This model successfully predicts the effect of increased pressure on solute rejection, defined as:

$$R = \frac{(c_s^I - c_s^{II})}{c_s^I} \times 100 \tag{4.7}$$

As transmembrane pressure increases, Eq. (4.5) suggests that the solvent flux will increase proportionally. Solute flux (Eq. (4.6)) will rise less rapidly, giving an improvement in solute rejection as is observed experimentally. The model similarly correctly predicts the decrease in rejection that occurs with increased solvent recovery. As a consequence of increased solvent recovery the concentration of retained solute increases, and, by Eq. (4.6), a greater passage of solute (lowered rejection) is expected.

Whilst the solution–diffusion model provides a convenient tool to explain parametric effects in reverse osmosis, methods for the *a priori* prediction of A and D_sK_s are not available and these parameters must be determined by experiment. Nor is it possible, knowing D_sK_s for one ionic species to predict it for another. There also remains some question whether the solution–diffusion equation will hold for high permeability reverse osmosis and nanofiltration membranes where the rejection mechanism may depend on membrane charge.

4.3.2 Concentration Polarisation

The extent of concentration polarisation in reverse osmosis is determined by the effectiveness of feed cross flow in remixing the rejected solute collecting at the surface of the membrane as a result of the flux of solvent through the membrane. The likelihood of feed side concentration polarisation and its adverse effect on the driving force across the membrane conditioned many of the early attempts to develop reverse osmosis equipment. Thus, for example, tubular and relatively high velocity channel flow elements were designed.

The current approach to the design of modules recognises that at low per-

meation rates, the extent of concentration polarisation is likely to be limited. Thus, for example, Du Pont hollow fiber permeators, because of the intrinsic low permeability of the membranes, are said to operate under essentially backmixed conditions on the shell (feed) side [23]. Similarly, the presence of a mesh in spiral wound modules promotes feed side mixing and minimises the effect of concentration polarisation at the membrane surface. However, with the advent of high flux membranes, in which a high recovery per pass is required, the prospect of concentration polarisation again emerges.

The simplest relationship for the membrane surface concentration (c_m) is provided by Eq. (4.8):

$$J = k \ln \frac{(c_m - c_s^{II})}{(c_b - c_s^{II})} \tag{4.8}$$

where k is a mass transfer coefficient, dependent on the extent of cross flow and physical properties prevailing at the surface of the membrane. For example, k may be obtained from the Graetz–Leveque equation for laminar flow, or from a correlation for turbulent flow.

More complete solutions which account for diffusional effects in the axial direction and loss of solvent along the flow channel have been provided by Sherwood et al. [24], Kimura and Sourirajan [25], Derzansky and Gill [26] and Sirkar and Rao [27]. The details of these solutions will not be provided here. However, they broadly show a greater level of polarisation than predicted by Eq. (4.8) and would encourage the use of effective mixing on the feed side of a reverse osmosis membrane. It is unusual, in reverse osmosis, for the membrane surface concentration to exceed twice to three times that of the bulk feed.

4.4 DESIGN OF REVERSE OSMOSIS MODULES

The task in designing a module for reverse osmosis is threefold: (i) to provide mechanical support for the membrane, which must operate at high pressures; (ii) to maximise the efficiency with which flow energy is used in controlling concentration polarisation; and (iii) to provide adequate egress for the permeate.

4.4.1 Conventional Module Types

Two principal designs have evolved to date. These are the hollow fiber and spiral wound configurations. Both tubular [28] and thin channel [29] reverse osmosis units have been developed for food applications where sanitary design is paramount, but would not be considered as efficient designs where costs must be contained as in desalination.

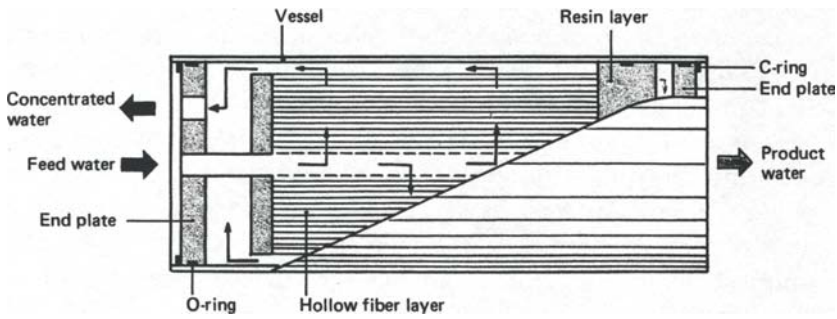

Fig. 4.3. Cut-away view of Toyobo hollow fiber module. Reproduced with permission.

In the DuPont range of Permasep B9 and B10 permeators [30], a bundle of fibers containing millions of individual units is used in a U-tube configuration within a pressure vessel. The fibers are mounted in parallel and fixed into a section of epoxy resin at both ends. One end of the bundle is machined to open the fibers and to provide a path for permeate. Feed to the bundle is provided by a centrally located feed tube, with the feed stream moving radially outwards outside individual fibers. The outer housing is a pressure vessel. The fibers themselves are able to withstand high pressures (to 6.9 MPa) without collapsing, but the bundle, because of its tight packing is prone to fouling if particulates are present in the feed. Broken fibers are said to be self healing. The B9 permeator is designed for use with brackish water, whilst the B10 module is for sea water. Moch [11] reports that the flux for the B9 permeator has been optimised at 5–9 l m^2 h under which conditions process side concentration polarisation is not significant. The productivity of a 200 mm (8 inch) diameter module is 2.5 m^3 h^{-1}, and product recovery per module is 50–60% of feed. Hollow fiber geometry has also been used by Dow Chemical and Toyobo. Figure 4.3 gives a cut-away view of the Toyobo hollow fiber module.

Spiral wound modules date to 1968 [31]. In construction of the spiral wound module, pairs of membranes are separated (active surfaces outside) by a tricot nylon spacer (typical thickness 0.2–0.4 mm) [32] and are glued on three sides. The fourth, open side, is attached to a central permeate collection tube. The membrane pairs are then separated from each other by a plastic net which functions to distribute feed flow and assist feed side mass transfer. The sets of membranes plus spacers are scrolled to give a spiral wound configuration as shown in Fig. 4.4, with the finished roll being provided with anti-telescoping devices and being fixed into a pressure tube using sealing rings. Up to six individual spirals are placed in series within the one pressure tube. Flow of feed takes place across the axis of the scroll. Permeate spirals in to the center permeate collection tube. Whilst early designs of the spiral wound unit used only a pair of membranes, later designs use multiple pairs to avoid too great a

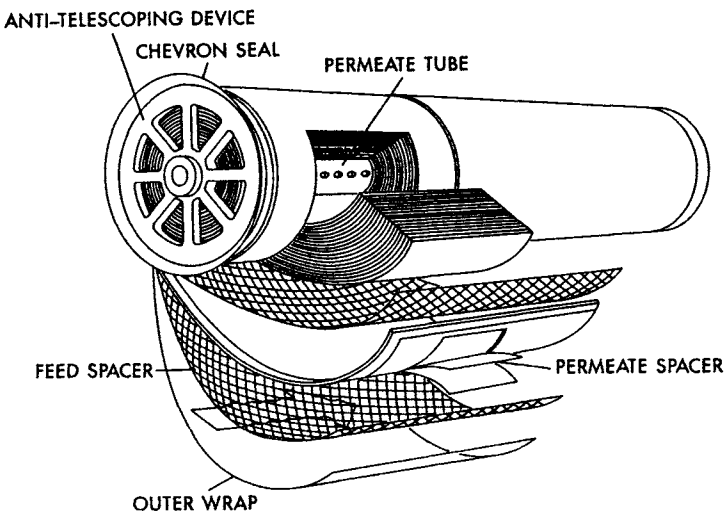

Fig. 4.4. Construction of Millipore spiral wound cartridge. Reproduced with permission.

permeate path length for a given module productivity. Spiral wound modules are now made in diameters to 300 mm and lengths to 1500 mm. Riley [3] reports that spiral wound modules were originally designed to operate at 20–30 l/m^2 h. For high flux, high recovery reverse osmosis of brackish water, considerations like the extent of polarisation reduction on the feed side and pressure drop in the permeate flow path must be considered. It is obviously desirable to choose the spacer to maximise the effectiveness of flow distribution and polarisation reduction at minimum pressure drop. Likewise, it is important to choose a permeate flow path that limits parasitic pressure drop.

Tubular membrane systems incorporating 12 mm diameter tubes of 1000 mm length are currently offered by Paterson Candy. Likewise DDS offer a plate and frame system in which the channel height is 0.3–0.5 mm and the channel width is typically 20 mm. Both designs have a low yield per unit volume and are used principally in food applications where fouling is a major problem.

Table 4.3 compares the productivities and features of different module geometries. The table has been developed from data provided by Belfort [28], Caraccio et al. [30], Eisenberg and Middlebrooks [33], Moch [11], Baker [8] and Riley [3] as indicated. It is noteworthy that an approximate doubling in the reported water output per unit module volume has occurred for spiral wound and hollow fiber units from 1984 to the present. The figures in the table for these modules represent the results of optimisation of module design by manufacturers of spiral and hollow fiber units over the period.

Figure 4.5 (adapted from Birkett [34]) provides a comparison of the productivities of different types of commercial modules. In arriving at Fig. 4.5, permeate

TABLE 4.3

Comparison of module designs

Module design	Packing density (m^2/m^3)	Water flux at 4MPa ($l/m^2\,h$)	Water output per unit ($m^3/m^2\,h$)	Flow channel size (mm)	Ease of cleaning	Estimated manufacturing cost[d] ($/m^2)
Spiral wound	800[a]	21–51[b]	29–35[c]	2	Fair	30–100
Hollow fibers outside feed	20,000[e]	2–10[a,f]	58–74[f,g]	0.05	Poor	5–20
Hollow fibers inside feed[a]	3,000	8	24	6	Fair	20–100
Flat plate[a]	120	17	2	0.5	Good	100–300
Tubular flow inside[a]	150	17	3	12–25	Good	50–200
Tubular flow outside[a]	460	17	8	3	Good	–

a. Ref. [28]; b. Ref. [3]; c. Filmtec literature; d. Ref. [8]; e. Ref. [30]; f. Ref. [33]; g. Ref. [11].

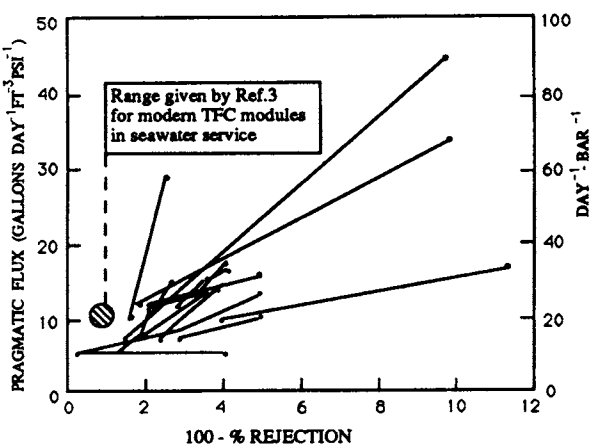

Fig. 4.5. Productivity of different types of commercial modules. Redrawn from Ref. [34].

flux per unit transmembrane pressure has been corrected for the average osmotic back pressure over the feed side of the membrane. The graph includes data for both hollow fiber and spiral wound geometries, including recent data for sea water TFC modules reported by Riley [3]. Whilst mirroring the general interdependence of flux and rejection, Fig. 4.5 shows that there is a considerable variation in the performance of different module designs in service. Modern, one-pass sea water spiral wound modules show higher productivities than would perhaps have been expected, given their excellent salt rejection capabilities.

TABLE 4.4
Commercially available RO membranes and modules

Company	Membrane material	Module type	Sales 1988 (US$ M)
Du Pont (USA)	Composite cellulose acetate	Spiral wound	
	Composite aramid		5
	Asymmetric aramid	Hollow fiber	24
Filmtec/DOW (USA)	Composite polyamide	Spiral wound	26
Fluid Systems/UOP	Composite polyamide	Spiral wound	13
Hydranautics/Nitto Denko (USA/Japan)	Composite polyamide/cellulose acetate	Spiral wound	12
Toray (Japan)	Asymmetric cellulose acetate	Spiral wound	12
	Composite PEC		
Desalination Systems (USA)	Asymmetric cellulose acetate	Spiral wound	5
	Composite polyamide		
Toyobo (Japan)	Cellulose acetate	Hollow fiber	4
Millipore (USA)	Composite	Spiral wound	3
Osmonics (USA)	Cellulose acetate	Spiral wound	3
Sumitomo (Japan)	Asymmetric poly(acrylonitrile)	Spiral wound	n.a.
DDS (Denmark)	Asymmetric cellulose acetate	Plate and frame	n.a.
	Composite polyamide		
Paterson Candy (UK)	Asymmetric cellulose acetate	Tubular	n.a.
	Composite polyamide		

Current suppliers of the different module designs for reverse osmosis are given in Table 4.4 [17] together with an estimate of the 1988 sales commanded by each supplier [3]. Riley [3] has indicated that Hydranautics/Nitto Denko is the only supplier offering a complete design and install service for clients. Other module suppliers provide equipment and advice to contracting companies who design plant to client's specifications and choose the most appropriate configuration of membranes and modules for the purpose at hand.

4.4.2 Optimal Module Design

In the design of a reverse osmosis module a balance is struck between the cost of producing membrane surface and the energy that must be expended to maintain a sufficiently low surface concentration of retained species to ensure membrane productivity. For a given feed and percentage recovery there will be be an optimal configuration of flow channels that will minimise the total

operating cost for a given membrane cost [35]. This may not, of course, be a feasible design as the resultant flow channels may be too narrow to avoid blockage with submicron particulates, or the design may not be able to be constructed economically.

Figure 4.6 gives the result of such an analysis for the desalination of brackish water (NaCl concentration 1500 mg l^{-1}) in a module in which the flow channels consist of multiple channels of rectangular cross section. The lines on Fig. 4.6 are for three different membrane costs per m^2. The least permeate cost is obtained when the transmembrane pressure is low and the percentage recovery is maintained high by keeping the channel height down. To ensure operation under the most favourable conditions (entry zone mass transfer), the channel length should be kept relatively short (100 mm). The channel design arrived at (channel height 0.04 mm, channel width 2200 mm, channel length 100 mm) is not dissimilar from that prevailing in a conventional spiral wound module, when account is taken of the presence of Vexar spacer. The spacer serves to remix the feed site on a regular basis and provides a series of regimes in which developing flow occurs. The analysis would suggest that there is some scope for optimisation of spacer design in spiral wound modules and that a percentage recovery per module of greater than the customary 15% [3] should be aimed for.

Also shown on Figure 4.6 are manufacturers' recommended performance conditions for four commercially available modules having thin channel or tubular geometries. Such geometries, which are used where fouling is high or sanitary design is important, are clearly non optimal.

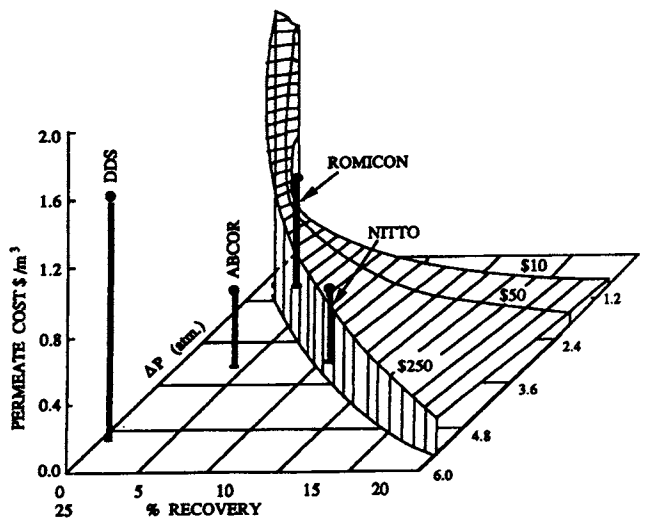

Fig. 4.6. Operating conditions for optimally designed modules for the reverse osmosis of brackish water [35].

Because of uncertainties about the nature of flow on the feed side of hollow fiber modules, it is not possible to extend the analysis to such modules at present. However, it is worth noting that Permasep hollow fiber modules are designed with radial flow of feed through the fiber bundle under conditions said to give essentially backmixed flow with minimal concentration polarisation [23]. As a result, single module recoveries of up to 50% can be obtained.

4.4.3 Spacer Design in Spiral Wound Modules

The spacers used on the feed side of spiral wound modules have dimensions ranging from:

spacer height	0.54–0.82 mm
filament diameter	0.27–0.41 mm
spacer mesh	2.3–3.0 mm

Schock and Miquel [32] have made pressure drop measurements on the feed side of currently available spiral wound modules and report, under manufacturers' recommended flow conditions, feed side pressure drops ranging from 0.02 to 0.08 mPa. This may be compared with a four-fold higher pressure drop for the original Roga module [36], and a pressure drop of 0.04–0.11 mPa for the hollow fiber module of DuPont [30]. The friction factor (λ) may be correlated with flow according to Eq. 4.9

$$\lambda = 6.23\, Re^{-0.3} \tag{4.9}$$

For mass transfer, Schock and Miquel [32] suggest a relationship of the form:

$$Sh = 0.065\, Re^{0.065}\, Sc^{0.25} \tag{4.10}$$

which has been derived from from flat channel experiments.

Using their equations, Schock and Miquel suggest that by optimising spacer design (in particular by adopting a thinner spacer for both the feed and permeate sides), the productivity of conventional spiral wound units could be increased by 35% compared with the conventional Filmtec unit.

4.5 ASSEMBLY OF REVERSE OSMOSIS PLANT

4.5.1 Module Arrangement

Depending on the application and the membranes used, the arrangement in a reverse omosis plant may be staged either on the brine (retentate) side, or on the permeate side. In either case, as the quantity being processed decreases, the membranes are arranged in a cascade so as to maintain a sufficient flow through each module to limit concentration polarisation.

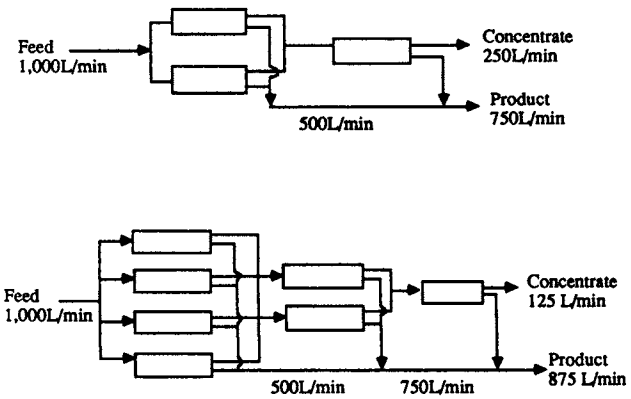

Fig. 4.7. Two- and three-stage cascades for the reverse osmosis of brackish water. Recoveries are 75% and 88% respectively. Redrawn from Ref. [3].

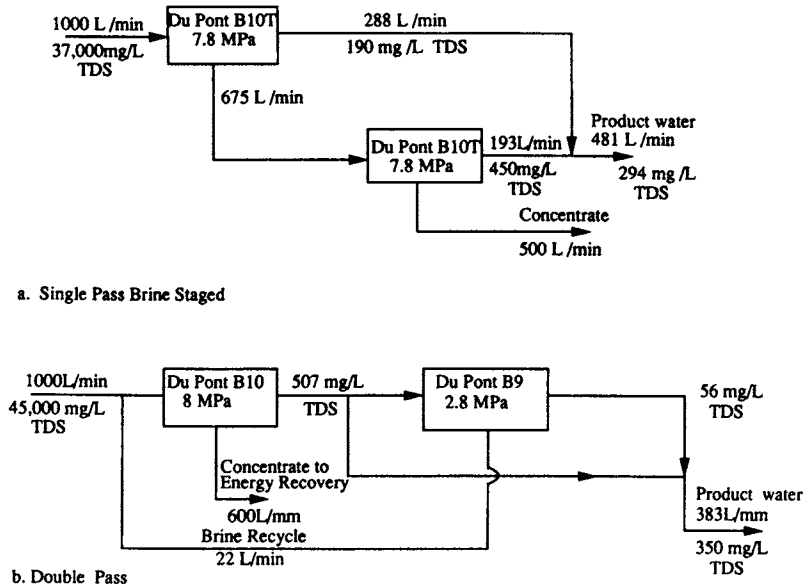

Fig. 4.8. Flow arrangements for two typical sea water installations [37,38].

Figure 4.7 shows two typical flow arrangements for a plant operating on brackish water [3]. Here the individual membranes used have sufficient rejection capability to achieve the desired reduction in salt content and the retentate from the first stage is sent to a second stage and possibly a third stage where it is further concentrated. Such an arrangement is termed "brine side staged".

Characteristic flows are given. Recoveries on brackish water plants can be as high as 95%, depending on the extent of feed pretreatment used, and the presence of dissolved impurities likely to precipitate and cause membrane fouling under the conditions prevailing in the last stage.

Figure 4.8 shows the flow arrangement for two typical seawater installations [37,38]. Two possibilities exist. One-pass desalination may be attempted, using high salt rejection membranes [37]. Brine-side staging is required to maximise recovery, which is 50% in Fig. 4.8a. Alternatively, two-pass desalination may be practised [38]. Here the first bank of membranes produces a brackish water, a portion of which is further desalinated and back blended to give the desired product. Reject from the second stage is passed back to the first stage feed. The advantage of two-pass desalination is that pressure energy stored in the concentrate can be better utilised.

4.5.2 Minimising Energy Costs by Energy Recovery

In large desalination plants, it is usual to recover energy from the reject brine, with power savings of up to 30% being possible when sea water is the feed. Early plants tended to use centrifugal pumps running in reverse to affect energy recovery. Wilson et al. [39] have described the use of a Pelton Wheel turbine having an overall efficiency of 70–80% for this purpose and have indicated a payback period of 0.3–2 years is possible when such a turbine is used on a 250 $m^3\ day^{-1}$ seawater desalination plant.

4.5.3 Plant Process Control

Equipment for adequate process control on reverse osmosis plant is discussed in manufacturers' product bulletins and by Mindler and Epstein [40]. Key parameters to be monitored are: pH, temperature, pressure, flow and permeate conductivity. In addition, there are a range of regular tests necessary on the pretreatment plant to ensure that water entering the reverse osmosis plant meets chemical specification. Figure 4.9 shows the minimum instrumentation necessary for effective plant operation.

4.6 OPERATION OF REVERSE OSMOSIS PLANT

Currently available reverse osmosis membranes are sensitive to chlorine, pH and oxidants, and are liable to fouling either by submicron particulates or microbiological species entering with the feed, or by the precipitation of salts at the surface of the membrane as the feed stream is concentrated.

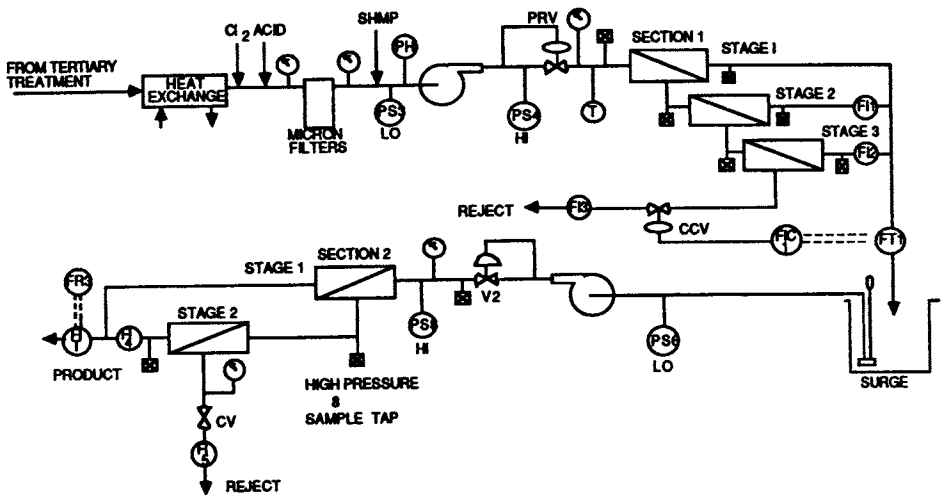

Fig. 4.9. Process control required for a two-step automated reverse osmosis plant for municipal wastewater. Reproduced from Ref. [40] with permission.

Calcium Carbonate Scaling: Mindler and Epstein [40] provide a method to determine whether carbonate scaling will occur for a given feed. The calculation involves a knowledge of the Ca^{++} ion present, the pH of the treated feed, and temperature. If carbonate precipitation is likely at the concentration factor experienced (2–4 times in brackish water plants, 1.3 times in seawater desalination plants) acid must be added to the feed. It is usual to keep the pH of the feed to a reverse osmosis plant at approximately 5.5 by the addition of sulphuric acid.

Calcium Sulfate Scaling: From a knowledge of the Ca^{++} and SO_4^{--} present in the concentrated feed, it is possible to calculate whether the solubility product of $CaSO_4$ will be exceeded. If this is likely to occur, sodium hexametaphosphate (SHMP) must be added to the feed to suppress precipitation. Alternatively, a proprietary sequesterant like Flocon 100 (Pfizer) may be added.

Silt Density Index: Silt density index (SDI) is a measure of the quantity of sub-micron particulates present and is determined by monitoring the flux decline over 15 minutes when the feed water is filtered continuously through a Millipore 0.45 μ membrane at a transmembrane pressure of 207 kPa.

$$\mathrm{SDI} = \frac{\left(1 - \frac{t_i}{t_f}\right) \times 100}{t_e} \tag{10.11}$$

SDI must be kept at 3 or lower for hollow fiber modules.

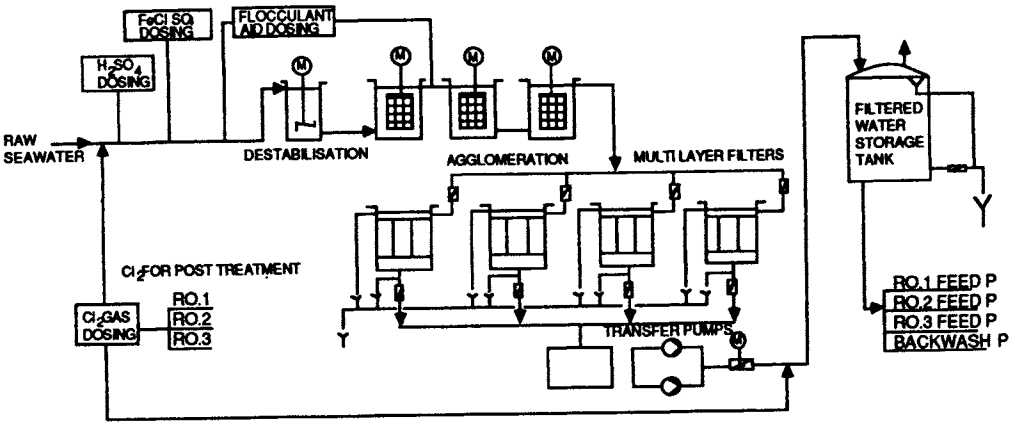

Fig. 4.10. Feed pretreatment scheme used at the Doha reverse osmosis test facility for seawater in Kuwait. Reproduced from Ref. [41] with permission.

4.6.1 Feed Pretreatment

Key to the successful operation of reverse osmosis plant is feed pretreatment. Figure 4.10 gives the pretreatment scheme that was adopted at the Doha reverse osmosis test facility (DROP) for seawater in Kuwait [41]. In this scheme, the SDI for entrant seawater (typically 6.2) was reduced to less than 3, and its pH was adjusted to approximately 5.5. Raw feed and treated water were chlorinated to minimise biological activity.

Before subsequent use in a desalination plant, the chlorine content of the treated water must be lowered by the addition of sodium bisulfite. Sodium hexamethyl phosphate is also usually added to inhibit calcium sulfate scaling. Usages of each of these chemicals for various modules are:

	Usage of Chemicals		
	Fluid Systems/UOP spiral wound	Filmtec Hydranautics	DuPont Hollow Fibers
H_2SO_4 (kg/m^3)	0.36	0.54	0.44
SHMP (g/m^3)	–	21	9
$NaHSO_3$ (g/m^3)	36	22	7

A similar pretreatment scheme has been adopted in the Yuma plant trials [42]. Where there is the possibility of residual organics being present in the feed, the use of an activated carbon filter is recommended.

TABLE 4.5

Comparison of performance of three membrane types

Bank	Membrane type	Output/unit (m^3/h)	Energy (khW/m^3)
1	150 × B10 Permasep	0.31	12.6
	15 × B9 Permasep	1.93	(8.8)*
2	240 × PA UOP spirals	0.20	10.4
	42 × PA 8600 spirals	1.00	
3	Filmtec + other sheet membranes	0.96	12.0
	78 Hydranautics spirals		

*With energy recovery turbine fitted.

4.6.2 Plant Operation

Data from the DROP seawater test facility (Table 4.5) [43,44] allow a comparison of the performance of three different membrane types.

Calculation of Module Performance: For Bank 1 it is possible to estimate module performance from manufacturer's performance data. The nominal capacity of B10 Permasep modules is 788 l/m^2 h for a feed of 30,000 mg/l TDS, a recovery of 30%, a transmembrane pressure of 5.6 MPa and an operating temperature of 25°C. Assuming complete mixing on the feed side, the exit osmotic pressure at design conditions would be 3.4 Mpa. For a brine feed of 45,000 mg/l TDS, the exit osmotic pressure at the same operating conditions will be 4.6 MPa. This leads to a downrating of the capacity of the unit by using Eq. 4.5 equivalent to:

$$(5.6 - 4.6)/(5.6 - 3.4) = 0.45 \times$$

The actual performance of the module is 0.40 ö nominal. The difference may be attributed to a small level of concentration polarisation at the surface of the membrane.

Similarly, for the B9 Permeators, the calculated downrating is 0.98 × compared with 0.72 × in practice. This suggests a higher level of concentration polarisation for these membranes which have a six-fold higher operational flux than the B10 membranes.

4.6.3 Membrane Fouling

Extended tests at the Yuma trial facility [42] have provided data on the long-term flux decline of spiral wound modules used for the desalting of a pretreated surface feedwater. Flux decline can be expressed in terms of Eq. 4.12

$$A(t) = A(1)t^m \tag{4.12}$$

where $A(t)$ and $A(1)$ are the membrane water permeabilities at times t hours and 1 hour respectively, t is the operating time in hours, and m is a coefficient, estimated as –0.02.

After an extended test period, membrane fluxes at the Yuma facility fell below the predictions of Eq. (4.12), and the surface of the membrane was found to be fouled by a layer of colloidal smectite clays. Other factors found to cause flux decline were compaction of the membrane and adsorption by the membrane of organic solutes from the feed.

Although not apparent in the Yuma facility, iron salts and siliceous materials present in the feed can also lead to membrane fouling. Brunelle [45] has drawn attention to the role of charge on the surface of colloidal species in determining fouling rate and comments on the significance of charge on the membrane itself in minimising deposition.

In-service membrane cleaning is usually carried out using cleaning solvents like sodium tripolyphosphate and sodium EDTA, and citric acid. Under ideal conditions it can provide significant restoration of membrane flux. With careful plant operation and regular cleaning, membrane lives in excess of 3 years are possible.

4.7 MAJOR REVERSE OSMOSIS DESALINATION PLANTS

The estimated installed world capacity for desalination is 13.3 million m^3 day^{-1} with reverse osmosis plant accounting for 31% of the total [46]. Two countries USA (30%) and Saudi Arabia (22%) dominate the world reverse osmosis scene. By far the greatest proportion (73%) of the total reverse osmosis capacity is for the desalination of brackish water, with seawater applications (9%) being presently static and the use of reverse osmosis for process water

TABLE 4.6

Large seawater reverse osmosis plants

Location	Nominal capacity '000 m^3/day	Feed	Membranes	Pressure MPa	% Recovery	Overall energy kWh/m^3
Jeddah [47] Saudi Arabia 1989	57	43,300 mg/l TDS	Toyobo CTA hollow fibers	6	35	8.4
Bahrain [48] 1984	46	12,000–30,000 mg/l TDS	Du Pont B10 hollow fibers	6.5	61	5.0
Malta [49] 1983	20	39,200 mg/l TDS	Du Pont B10 hollow fibers	8.1	35	5.9
Las Palmos [46] Spain 1989	24	Seawater	Filmtec spirals			

treatment (18%) growing. Plants are, almost exclusively, designed and built by contractors on a custom basis, using membrane modules supplied by the major membrane manufacturers.

4.7.1 Major Installations

Tables 4.6 and 4.7 give capacity and operating data for some of the world's largest desalination plants for seawater and brackish water respectively. Whilst

TABLE 4.7

Large brackish water reverse osmosis plants

Location	Nominal capacity $m^3/day \times 10^{-3}$	Feed	Membranes	Energy KWH/m^3	% Recovery	Operating pressure MPa
Yuma [3] Arizona USA 1990	274	Brackish 3,000 mg/l TDS	69% Fluid Systems/UOP Cellulose Acetate Blend· 31% Hydranautics Cellulose Acetate Blend			70
Daesan [46] Korea 1990	95	Brackish	Toray Spirals			
Iraq [46] 1983–86	64	Brackish	DuPont Hollow Fibers			
Riyadh [50] Saudi Arabia 1984	60	Brackish	DuPont Hollow Fibers Brine staged 4:2:1		90	2.8
Salboukh [46] Saudi Arabia 1979	60	Brackish 1610 mg/l TDS	DuPont Hollow Fibers		90	
Unayzah [51] Saudi Arabia 1989	52	Brackish 1500 mg/l TDS	Envirogenics Spirals	1.8	90	
Ras Abu Jarjur [52] Bahrain 1984	46	Brackish 19000 mg/l TDS	Du Pont B10 Hollow Fibers	5.0	61	5.8
Cape Coral [53] Florida, USA 1976	46	Brackish 1600 mg/l TDS	42% DOW TCA Fibers 58% Hydranautics Spirals	0.53	75 85	1.4 1.7
Fort Myers [46] Florida, USA 1989	46	Brackish 400–500 mg/l TDS	Hydranautics/ Nitto Denko Spirals		90	0.7
Bayswater [54] Australia 1985	36	CW Blowdown 2500 mg/l TDS	Hydranautics Spirals		82	3.0

capacity data are readily available in the technical literature [45], operating data are frequently not reported. This accounts for the blank entries on Tables 4.6 and 4.7. With the passage of time, there has been a shift from hollow fiber to spiral wound composite modules, with the module replacement market being dominated by spiral wound units able to operate at lower than original design pressures.

4.7.2 Economics of Desalination

Riley [3] has reported the following capital and operating costs for desalination (Table 4.8):

TABLE 4.8

Capital and operating costs for reverse osmosis

Water type	Capital costs (US$ M/^{3}/day)	Operating costs (US$/m^{3}product)
Seawater	2350–5880	1.37–2.35
Brackish	353–941	0.60–0.73

Depending on energy costs and local construction costs, reverse osmosis is now competitive with the more traditional technologies of multistage flash and multiple-effect evaporation in seawater applications.

A detailed breakdown of cost components for a notional seawater desalination plant (capacity 56,500 m^3/day) at a Middle East location is provided by Ericsson et al. [55]. Four typical membrane types and single and double-stage operation are considered. Figure 4.11 reports typical data from this source for FilmTec spiral wound modules. Cheapest water is obtained with a water recovery of approximately 30%. Points worthy of note are the quite small cost attributed to membrane modules in desalination plant (typically 15%) and the high costs associated with feed pretreatment (40%).

A similar analysis by Leitner [56] based on DuPont Permasep modules gives a water cost of $ 1.11/m^3 compared with $1.15/m^3 for multi-stage flash operation. Such estimates are strongly influenced by the cost assigned to energy, which is very location dependent. For large installations, combinations of reverse osmosis and multi-stage flash plant may be attractive, with excess energy from the generation of electrical power for the reverse osmosis system being used in the multi-stage flash plant. An advantage of such an arrangement is the ability to blend product water of different salt contents.

Riley [3] has particularly drawn attention to the lowered costs likely to be obtained in brackish water desalination by the use of the newer, low pressure

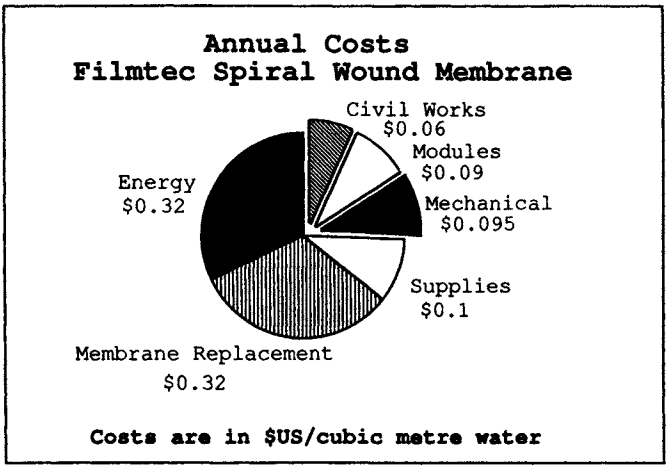

Fig. 4.11. Cost breakdown for Filmtec modules in seawater service [55].

membranes and the advantages if less stringent feed pretreatment could be practised.

4.8 APPLICATIONS OTHER THAN DESALINATION

Although the quantity of reverse osmosis equipment used in applications other than desalination is small (Fig. 4.12), there is a growing market for the application of the technology in the food industry and in other areas where the value of recovered material justifies the processing cost or the technology offers a way of overcoming an effluent problem. Examples include the use of reverse

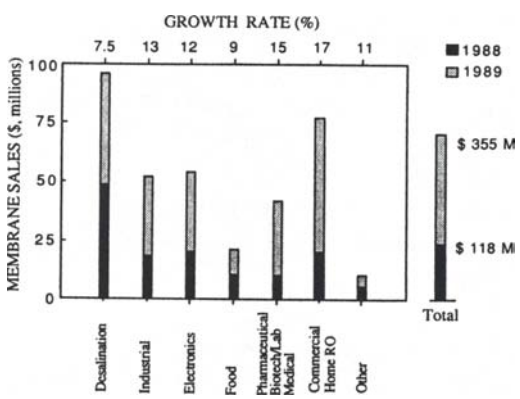

Fig. 4.12. Membrane sales and growth rates for various industrial applications of reverse osmosis.

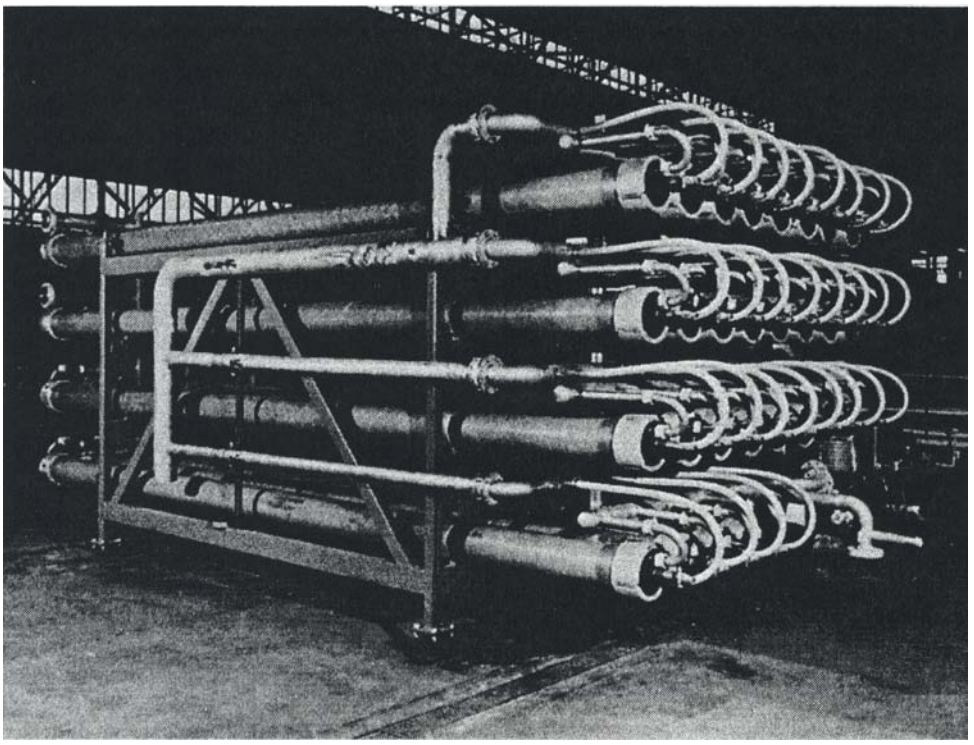

Fig. 4.13. Reverse osmosis plant at the Bayswater Power Station, NSW, Australia [54].

osmosis in the metal finishing, pulp and paper and textile industries. In each of these the permeate from reverse osmosis is recycled. Reverse osmosis also finds use in the preparation of boiler feedwater and the recycle of cooling tower blowdown. Figure 4.13 shows the membrane module assemblies on the cooling tower blowdown plant at the Bayswater 4640 MW power station in New South Wales, Australia. As indicated on Table 4.7, Hydranautics spiral wound modules are used. Permeate is returned to the cooling towers and the brine concentrate is subsequently disposed of by evaporation.

Overviews of the use of reverse osmosis in the food industry are provided by Pepper [57], Paulson et al. [58] and Merson and Ginnette [59]. The technology is well established in the concentration of whey from dairy plants, whole milk and a range of fruit juices. Upper limits on the extent of concentration possible are set either by the osmotic pressure of the concentrate, its viscosity, or the precipitation of components at the surface of the membrane. Tubular and thin channel devices can be operated at much greater feed side Reynolds numbers than hollow fiber or spiral wound devices and offer advantages with viscous feeds containing suspended solids. They are also attractive from the viewpoint

of sanitary design. Spiral wound modules are, however, making increasing inroads in the area of food processing and seem able to cope unexpectedly well with feeds containing colloidal solids. Newer, loose reverse osmosis (nanofiltration) membranes that allow passage of monovalent salts whilst retaining larger species are now finding increasing application in the simultaneous concentration and partial desalting of food products.

Significant markets for reverse osmosis equipment also exist in biotechnology and in the production of pharmaceuticals and injection water [60]. In such applications membrane integrity is a dominant consideration. Pepper [57] has indicated how the production of ultrapure water for semi-conductor manufacturing applications is calling for increasingly tight specifications on the reverse osmosis step as higher capacity chips are developed.

Key to the successful operation of reverse osmosis equipment in food, biotechnological, pharmaceutical and clean water applications is process specific knowledge of feed-membrane interactions and ways to prevent membrane fouling. Little such information is available in the open literature but is frequently available from the membrane manufacturers themselves or from membrane equipment contractors. Pilot scale testing for new applications is obligatory. Because of the modular nature of membrane plant, scaleup from tests on pilot scale equipment is relatively straightforward.

4.9 CONCLUSIONS

Reverse osmosis is the most mature of the industrially applied membrane technologies, with large scale plant for the desalination of brackish water now in routine widespread use throughout the world. Problems of membrane life and flux decline through fouling have largely been solved, but at the cost of extensive feed pretreatment, which must be customised for each feed. There is scope in brackish water desalination for the development of new membranes having both chlorine and oxidant tolerance, and for membranes which can be operated at lower pressures. Some re-engineering of module design is expected to occur.

The technology has also proved successful in the desalination of seawater being economically competitive with multi-stage flash evaporation for large installations. As with brackish water desalination, feed pretreatment remains of paramount importance, particularly if one step-desalination is contemplated.

The greatest opportunities for future growth exist in the food and related industries where concentration by reverse osmosis confers superior properties on the product as thermal damage is avoided. Here there is considerable challenge, both in minimising fouling of the membrane and in coping with highly viscous concentrates that frequently contain solids. Much product spe-

cific wisdom and experience is called for. Module designs for such applications date to the evolution of reverse osmosis as an industrial technology and are probably not optimal either in their usage of energy, required transmembrane pressure called for, or manufacturing cost. Scope for improvement exists.

Faced with the problem of designing or specifying a reverse osmosis plant for a particular application, the process engineer will be obliged to seek advice from the manufacturers of membrane modules and will be able to gain a relatively good estimate of the number of modules and their arrangement to meet the design plant throughput. Uncertainties will exist over the long term flux of the membranes. Membrane manufacturers will place stringent requirements on the nature of the feed stream to avoid premature fouling. Extensive feed pretreatment will generally be necessary and will dominate plant costs.

The long-held dream of reverse osmosis practitioners, that of a module able to produce high quality permeate at a transmembrane pressure just slightly greater than the osmotic back pressure, has yet to be realised. So, too, has the devlopment of a membrane with the ability to resist fouling. Both remain elusive goals for the 1990s. Avoidance of the extensive feed pretreatment that characterises the technology at present would substantially lower processing costs and see reverse osmosis extend into hitherto uneconomic applications in water regeneration and food processing. The challenge is a substantial one.

SOME USEFUL CONVERSION FACTORS

Reverse osmosis has been developed primarily in the USA, Japan and Europe. Units used in describing the performance of reverse osmosis equipment are given in the American Engineering or S.I. systems or variants of these. Some useful conversion factors are provided below:

1 GFD	= 1 US gallon/ft^2 day
	= 1.7 LMH (litres/m^2 h)
	= 0.041 m^3/m^2 day
1000 psig	= 68 Bar = 6.8 MPa = 68 kg$_f$/cm^2
1 l/m^2 h/MPa	= 0.004 GFD/psi

NOMENCLATURE

A	Membrane permeability (Eq. 4.2) [l/m^2 h-MPa]
$A(1)$	Membrane permeability after 1 hour (Eq. 4.12) [l/m^2 h-MPa]
$A(t)$	Membrane permeability at time t (Eq. 4.12) [l/m^2 h-MPa]
c_b	Concentration of solute in bulk feed [mole/l]
$c_m c_s^I$	Concentration of solute at surface of membrane [mole/l]

c_s Average concentration of solute [mole/l]
c_s^{II} Concentration of solute in permeate phase [mole/l]
c_w Concentration of solvent [mole/l]
Δc Solute concentration difference across membrane [mole/l]
D Diffusivity [$m^2 s^{-1}$]
D_s Solute diffusivity in membrane [$m^2 s^{-1}$]
D_w Solvent diffusivity in membrane [$m^2 s^{-1}$]
J, J_v Solvent flux [$l/m^2 h$]
J_s Solute flux [$mole/m^2 s$]
k Mass transfer coefficient [$m s^{-1}$]
K_s Distribution coefficient of solute in membrane [–]
L_p Coefficient in Eq. 4.3 [l/m^2 h-MPa]
P Fractional solute penetration (Eq. 4.1) [–]
ΔP Transmembrane pressure [mPa]
R Percentage rejection (Eq. 4.7) [–]
R Universal gas constant (Eq. 4.5)
Re Reynolds Number [–]
Sc Schmidt Number [–]
Sh Sherwood Number [–]
T Temperature [K]
t Time in Eq. 4.12 [s]
t_i, t_f, t_e Times in SDI test (Eq. 4.11) [s]
V_w Partial molar volume of solvent [l/mole]
Δx Thickness of active layer of membrane [m]
ε Porosity of membrane [–]
σ Reflection coefficient (Eq. 4.4) [–]
$\Delta\Pi$ Osmotic pressure across membrane [MPa]
λ Friction coefficient for spacer (Eq. 4.9) [–]

REFERENCES

1 C.E. Reid and E.J. Breton, *Chem. Eng. Prog. Symp. Ser.*, 55 (24) (1959), 171.
2 S. Loeb and S. Sourirajan, *Adv. Chem. Ser.*, 38 (1962) 117.
3 R.L. Riley, Reverse Osmosis. In: *Membrane Separation Systems: A Research Needs Assessment*. U.S. Department of Energy, DOE/ER/30133-HI, 5-1, Chap. 5.
4 Y. Kamiyama, N. Yoshioka, K. Matsui and K. Nakagome, *Desalination*, 51 (1984) 79.
5 E. Drioli, *Desalination*, 63 (1987) 57.
6 H.K. Lonsdale, *J. Membr. Sci.*, 33 (1987) 121.
7 W. Pusch, *Desalination*, 77 (1990), 35.
8 R.W. Baker, Membrane and Module Preparation. In: *Membrane Separation Systems: A Research Needs Assessment*. U.S. Department of energy, DOE/ER/30133-HI, 1-1, 1990, Chap. 1.

9 J.E. Cadotte, U.S. Patent 4,039,440, August 2, 1977.
10 R.L. Riley, R.L. Fox, C.R. Lyones, C.E. Milstead, M.W. Seroy and M. Tagami, *Desalination*, 23 (1977) 33.
11 I. Moch, *Desalination*, 74 (1989), 171.
12 A.E. Allegrezza, B.S. Parekh, E.J. Parise, E.J. Swiniarski and J.L. White, *Desalination*, 64 (1987) 285.
13 I. Kawada, Y. Inoue, H. Kazuse, H. Ito, T. Shinanti and Y. Kamiyama, *Desalination*, 64 (1987), 387.
14 K. Ikeda, Nakano, H. Ito, T. Kubota and S. Yamamoto, *Desalination*, 68 (1988) 109.
15 W.A.P. Luck, *Desalination*, 62 (1987) 19.
16 R. Rautenbach and A. Groschl, *Desalination*, 77 (1990) 72.
17 W. Pusch, *Desalination*, 59 (1986) 105.
18 O. Kedem and A. Katchalsky, *Biochim. Biophys. Acta*, 27 (1958) 229.
19 O. Kedem and K.S. Speigler, *Desalination*, 1 (1966) 311.
20 U. Merten, in: U. Merten (Ed.), *Desalination by Reverse Osmosis*. M.I.T. Press, Cambridge, Mass, 1966, p. 15.
21 S. Sourirajan, *Reverse Osmosis*. Academic Press, New York, 1970.
22 R. Rangarajan, T. Matsuura and S. Sourirajan, in: *Reverse Osmosis and Ultrafiltration*. ACS Symposium eries 281, ACS, Washington, D.C., 1985, p. 167.
23 W.N. Gill, M.R. Matsumoto, A.L. Gill and Y.T. Lee, *Desalination*, 68 (1988) 11.
24 T.K. Sherwood, P.L.T. Brian, R.E. Fisher and L. Dresner, *Ind. Eng. Chem. Fundam.*, 4 (1965) 113.
25 S. Kimura and S. Sourirajan, *Ind. Eng. Chem. Proc. Des. Develop.*, 7 (1968) 41.
26 L.J. Derzansky and W.N. Gill, *AIChE J.*, 20 (1974) 751.
27 K.K. Sirkar and G.H. Rao, *Desalination*, 48 (1983) 25.
28 G. Belfort, in: Belfort, G. (Ed.), *Synthetic Membrane Processes*. Academic Press, Orlando, 1984, pp. 221–280.
29 R.F. Madsen, *Hyperfiltation and Ultrafiltration in Plate-and-Frame Systems*, Elsevier, New York, 1977.
30 V.P. Caracciolo, N.W. Rosenblatt and V.J. Tomsic, in: S. Sourirajan (Ed.), *Reverse Osmosis and Synthetic Membranes*. National Research Council, Canada, 1977, p. 343
31 D.T. Bray, U.S.Patent 3,417,870, 1968.
32 G. Schock and A. Miquel, *Desalination*, 64 (1987) 339.
33 T.N. Eisenberg and E.J. Middlebrooks, *Reverse Osmosis of Drinking Water*. Butterworths, Boston, 1986.
34 J.D. Birkett, *Desalination*, 46 (1983) 91.
35 D.E. Wiley, C.J.D. Fell and A.G. Fane, *Desalination*, 52 (1985) 249.
36 H. Ohya and Y. Taniguchi, *Desalination*, 16 (1975) 359.
37 H. Winters, *Desalination*, 65 (1987) 189.
38 D.C. Brandt, *Desalination*, 52 (1985) 177.
39 W. Wilson, A. Gruendisch and I. Calder-Potts, *Desalination*, 65 (1987) 231.
40 A.B. Mindler and A.C. Epstein, *Desalination*, 59 (1986) 343.
41 J. Grigoleit and B. Schuttler, *Desalination*, 63 (1987) 209, 217.
42 J.W. Kaakinen and C.D. Moody, in: S. Sourirajan and T. Matsuura (Eds.), *Reverse Osmosis and Ultrafiltration*, ACS Symposium Series 281, 1985, p. 359.
43 R. Nagel, *Desalination*, 63 (1987) 225.
44 A.L.A. Malik, K.M. Mousa, N.G. Younan and B.J.R. Rao, *Desalination*, 63 (1987) 163.
45 M.T. Brunelle, *Desalination*, 32 (1980) 127.

46 K. Wangnick, *1990 IDA Worldwide Desalting Plants Inventory*, Report No. 11, Wangnick Consulting, Germany, 1990.
47 M. Muhurji, G. Faggard, V. Van Der Mast and H. Imai, *Desalination*, 76 (1989) 75.
48 M. Al Arrayedh, B. Ericsson and M. Ohtani, M. *Desalination*, 55 (1985) 319.
49 W.T. Andrews and R.A. Bergman, *Desalination*, 60 (1986) 135.
50 J.M. Rovel and L. Daniel, *Desalination*, 65 (1987) 373.
51 P.J. de Moel, R.F.M. de Gier and G. Onderdelinden, *Desalination*, 55 (1985) 343.
52 M. Al Arrayedh, B. Ericsson, M.A. Saad and H. Yoshioka, *Desalination*, 65 (1987) 197.
53 M. Ashton, *Desalination*, 65 (1987) 277.
54 J. Stuart, T. Bryant, I. Fergus and E. Gabrielli, E., *Desalination*, 75 (1989) 379.
55 B. Ericsson, B. Hallmans and P. Vinberg, *Desalination*, 64 (1987) 459.
56 G.F. Leitner, *Desalination*, 63 (1987) 135.
57 D. Pepper, *Desalination*, 77 (1990) 55.
58 D.J. Paulson, R.L. Wilson and D.D. Spatz, in: S. Sourirajan and T. Matsuura (Eds.), *Reverse Osmosis and Ultrafiltration*. ACS Symposium Series No. 281, ACS, Washington, D.C., 1985, p. 325.
59 R.L. Merson and L.F. Ginnette, (1972) in: R.E. Lacey and S. Loeb, S. (Eds.), *Industrial Processing with Membranes*. Kreiger Publishing, Huntington, N.Y., Chapter X.
60 P.L. Parise, H. Parekh and R. Smith, in: S. Sourirajan and T. Matsuura (Eds), *Reverse Osmosis and Ultrafiltration*. ACS Symposium Series No. 281, ACS, Washington, D.C., 1985, p. 297.

BIBLIOGRAPHY

Belfort, G., *Synthetic Membrane Processes: Fundamentals and Water Applications*, Academic Press, Florida, 1984.

Bungay, P.M., H.K. Lonsdale and M.N. de Pinho, *Synthetic Membranes: Science, Engineering and Applications*, Reidel, Dordrecht, 1986.

Eisenberg, T.N. and E.J. Middlebrooks, *Reverse Osmosis Treatment of Drinking Water*. Butterworths, Boston, 1986.

Lacey, R.E. and S. Loeb, *Industrial Processing with Membranes*, Krieger Publishing, New York, 1979.

Sourirajan, S., *Reverse Osmosis and Synthetic Membranes*. National Research Council, Canada, Ottawa, 1977.

Sourirajan, S. and T. Matsuura, *Reverse Osmosis and Ultrafiltration*. ACS Symposium Series 281, Amer. Chem. Soc., Washington, D.C., 1985.

Turbak, A.F., *Synthetic Membranes; Volume 1: Desalination; Volume 2; Hyper- and Ultrafiltration Uses*. ACS Symposium Series 153 and 154, ACS, Washington, D.C., 1981.

Membrane Separations Technology. Principles and Applications
Edited by R.D. Noble and S.A. Stern

Chapter 5

Pervaporation

J. Néel

Ecole Nationale Supérieure des Industries Chimiques, B.P. 451,
1 rue Grandville, 54001 Nancy Cedex, France

5.1. INTRODUCTION

Pervaporation is a new membrane technique which is used to separate a liquid mixture by partly vaporizing it through a nonporous permselective membrane. The "feed" mixture is allowed to flow along one side of the membrane and a fraction of it (the "permeate") is evolved in the vapor state from the opposite side, which is kept under vacuum by continuous pumping (Fig. 5.1) or is purged with a stream of carrier gas. The permeate is finally collected in the liquid state after condensation on a cooled wall. It is thus enriched in the more rapidly permeating ("faster") component of the feed mixture whereas the retentate is depleted in this component; the "retentate" is the fraction of the feed that does not permeate through the membrane. The membrane is often swelled

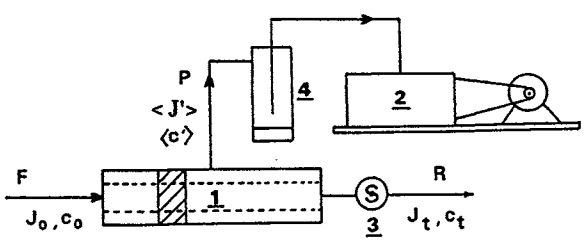

Fig. 5.1. Continuous-flow pervaporation. 1, Permselective tube; 2, vacuum pump; 3, circulating pump; 4, condenser. F, Feed; P, permeate; R, retentate; A, faster component; c, A-content; J_0: feed flow rate; J_t, retentate outlet flow rate; J', permeate flux (prime indicates the permeate). < >, Average value.

(plasticized) by the permeating mixture and the swelling is "vectored" in the direction of the permeate flow, i.e., the swelling decreases from the upstream to the downstream side of the membrane.

Mass transport by pervaporation across permselective membranes involves three successive steps:

1. upstream partitioning of the feed components between the flowing liquid mixture and the swollen upstream surface layer of the membrane.
2. diffusion of the components in the surface layer through the membrane;
3. desorption of these components at the downstream surface of the membrane.

This process is obviously much more complex than simple vaporization, and one can easily understand that the permeate composition is widely different from that of the vapor in direct contact with the liquid feed after establishment of free liquid/vapor equilibrium [1]. The use of a membrane obtained from an appropriate polymeric material generally makes it possible to separate a number of positive binary azeotropic mixtures (Table 5.1).

Due to its high selectivity for liquid mixtures that cannot be efficiently processed by conventional distillation, pervaporation is a useful alternative to distillation and a potential competitor to energy-consuming separation processes such as vacuum and extractive distillation [2].

Mass transport through a dense polymer membrane is a rather slow process and, therefore, pervaporation is not a complete separation technique in itself since pervaporators cannot be assembled in cascade, like plates in a distillation column. Pervaporation is generally used only to complement distillation when the latter process is inefficient, for instance, to pass over the azeotropic composition of a given binary liquid mixture.

If the azeotrope contains unequal proportions of components A and B, pervaporation is carried out through a membrane preferentially permeable to the minor component in order to minimize the amount of permeate required to isolate a pure retentate at the outlet of a pervaporation module (Fig. 5.1). In the case of an azeotropic mixture containing nearly equivalent proportions of A and B (for instance the water–pyridine azeotrope which contains 41.3 wt% water), pervaporation is only used to split the feed into two non-azeotropic fractions, which can each be further separated by distillation (Fig. 5.2).

The specific nature of pervaporation can be recognized by noting the differences that distinguish it from related membrane separation techniques, namely vapor permeation, membrane distillation, fractionation through gas barriers, and perstraction.

Vapor Permeation

This term designates the fractionation of a saturated vapor mixture (emerging from a distillation column) by partial transport through a nonporous permselective membrane, the permeate side of which is kept under low press-

TABLE 5.1

Typical positive azeotropic mixtures (characterized by a minimum boiling temperature) which can be separated by pervaporation through a permselective membrane obtained by grafting polyvinylpyrrolidone onto a thin polytetrafluoroethylene film [1]

A-B Azeotropes (A = Fast component)	T_b (°C)	Azeotrope characteristics		Selectivity		Permeate flux (kg/h m^2)
		T_b (°C)	c (%)	α	β	
A: Chloroform	61.2	60.0	72.0	3.9	1.25	2.65
B: *n*-Hexane	69.0		28.0			
A: Ethanol	78.5	64.9	30.5	16.8	2.89	1.10
B: Cyclohexane	81.4		69.5			
A: Butanol-1	117.4	78.0	10.0	23.5	7.23	0.30
B: Cyclohexane	81.4		90.0			
A: Water	100.0	78.2	4.4	2.9	2.68	2.20
B: Ethanol	82.8		95.6			
A: Water	100.0	79.9	11.8	41.0	7.17	0.35
B: *t*-Butanol	82.8		88.2			
A: Water	100	63.8	5.7	19.1	9.24	0.94
B: Tetrahydrofurane	65.5		94.3			
A: Water	100.0	87.8	18.4	18.1	4.36	1.33
B: Dioxane	101.3		81.6			
A: Ethanol	78.5	71.8	31.0	2.4	1.67	0.95
B: Ethylacetate	77.2		69.0			
A: Methanol	64.7	55.7	12.0	2.9	2.36	0.65
B: Acetone	56.2		88.0			
A: Ethanol	78.5	67.8	32.4	1.3	1.18	2.90
B: Benzene	80.1		67.6			

The selectivities α and β are defined by the following ratios, respectively:

$$\alpha = \frac{(c'_A/c'_B)}{c_A/c_B)} = \frac{c'(1-c)}{c(1-c')}, \quad \beta = \frac{c'}{c}$$

where c and c' are the weight concentrations of the faster permeant (A) in the feed (c) and the permeate (c'), respectively. T_b denotes the normal boiling point of an organic compound or of an azeotropic mixture (at 1 atm). Pervaporation temperature: $T = 25$°C.

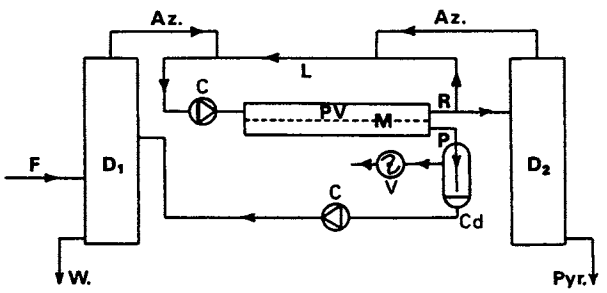

Fig. 5.2. Pervaporation–distillation integrated system designed to separate mixtures of water and pyridine (feed F), richer in water than the azeotropic mixture. (c_{Az} = 41.3 wt% water). F: Feed (water+ pyridine, $c_w > c_{Az}$); D_1,D_2: distillation columns; PV: pervaporator; M: hydrophilic membrane; Cd: condenser; L: recycling loop; V: vacuum pump; C: circulating pump; P: water-rich permeate; R: pyridine-rich retentate; W: water (Blg. T = 100°C); Pyr.: pyridine (Blg. T = 115°C); Az.: azeotropic mixture (c_{Az} = 41.3% of water by weight, Blg. T = 92.6°C).

ure by continuous pumping [3]. A similar technique can be used to separate an easily condensable component, for instance an organic vapor which contaminates a gas stream [4].

In both the above cases, upstream partitioning, which operates in pervaporation, is replaced by sorption of the gaseous feed mixture that flows along the upstream surface of the permselective membrane.

Membrane Distillation

In the membrane distillation process [5], a liquid feed is fractionated after partial vaporization though a porous polymer membrane which is not wetted by the feed. The liquid feed cannot penetrate into the membrane pores as long as the upstream pressure does not exceed the minimum penetration pressure for the pore distribution. To fractionate aqueous mixtures, porous barriers made from hydrophobic polymers, such as polypropylene, polytetrafluoroethylene or polyvinylidene fluoride, can be used.

According to this technique [6], the liquid feed is allowed to flow along one surface of the membrane, whereas the permeated vapor is condensed on a cooled wall, slightly apart from the opposite (downstream) surface of the membrane and parallel to it (Fig. 5.3).

The transport regime is determined by the downstream pressure since the transfer of the vaporized permeate through the pores may take place, depending on this pressure, either by viscous flow or by selective Knudsen diffusion, and may even assume some intermediate mode of transport involving complex phenomena, such as surface flow along the walls of the pores.

Despite the fact that, at first sight, membrane distillation does not basically differ from distillation between a warm liquid surface and a chilled wall, the former process exhibits a slight selectivity towards azeotropic feed mixtures

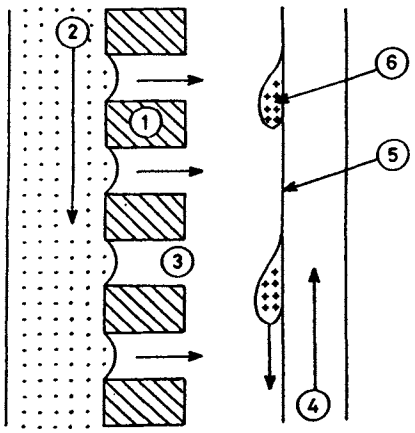

Fig. 5.3. Membrane distillation process. 1. Porous membrane made of hydrophobic polymer; 2. feed mixture; 3. vapor gap; 4. cooling fluid; 5. chilled wall; 6. condensed droplet.

due to the pore transport mechanism mentioned above [7]. In this respect, membrane distillation is somewhat similar to pervaporation. The latter process is generally more selective whereas the former delivers larger amounts of permeate, the vaporization of which often causes a significant temperature drop across the thickness of the operating porous membrane.

Fractionation Through Gas Barriers

In some membrane distillation devices [8], both sides of a porous membrane are in direct contact with liquid phases (Fig. 5.4). In this configuration, a vapor lock is immobilized in each pore of the working membrane, thus forming multiple gas barriers. Vaporization takes place at one liquid–vapor interface of the gas barrier and condensation at the opposite interface. Of course, this process, which is also called "direct contact membrane distillation," only works if the mass transport is driven by an external force. This force is usually induced by keeping the feed mixture at a higher temperature than the condensed permeate. This requirement, therefore, leads to the design of a system in which the permeation module is combined with a heat exchanger. The mass transport through the gas barriers is then apparently driven by a temperature gradient. Obviously, the transport process is strongly affected by the presence of noncondensable gases (air, for instance) which could be dissolved in the feed, since these gases progressively accumulate in the membrane pores. The vapor transport then changes from simple convection to diffusion through a noncondensable gas layer immobilized in the pores and the distillation rate progressively decreases. To avoid this unfavorable effect, direct contact membrane distillation systems are generally equipped with an additional device designed to separate noncondensable gases from the feed prior to its introduction into the module.

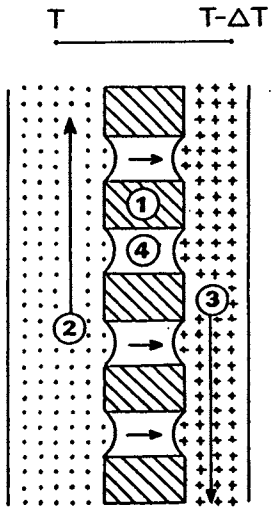

Fig. 5.4. Fractionation by gas membranes (direct contact membrane distillation). 1. Porous membrane made of hydrophobic polymer; 2. liquid feed mixture; 3. condensed distillate; 4. vapor lock (gas membrane).

The term "extraction through gas barriers" more specifically designates a similar process in which mass transport through a gas gap is driven by an activity gradient. For this purpose, the downstream liquid contacting the permeate side of the porous membrane is replaced by a stripping solution which absorbs the volatile component to be extracted from the flowing feed mixture.

By using aqueous sodium hydroxide as a stripping solution and operating with gas barriers immobilized in the walls of porous hollow fibers of polypropylene (Celgard), it is possible to rapidly extract acetic acid from an aqueous or organic liquid mixture [9]. Other typical examples reported in the literature are mentioned below:

- Extraction of bromine generated by oxidation (with chlorine) of bromides dissolved in seawater [10]. This operation is achieved by use of air barriers immobilized in the porous walls of hollow polypropylene fibers. The stripping solution is aqueous sodium hydroxide.
- Extraction of iodine from an aqueous iodine–iodide solution. The stripping solution is aqueous NaOH [11].
- Extraction of ammonia or organic amines contaminating an aqueous effluent by diffusion through gas barriers stripped by a solution of sulfuric acid [11].

Perstraction

Perstraction also makes use of a countercurrent of stripping (purge) liquid, which sets up an activity gradient between the opposite surfaces of a dense

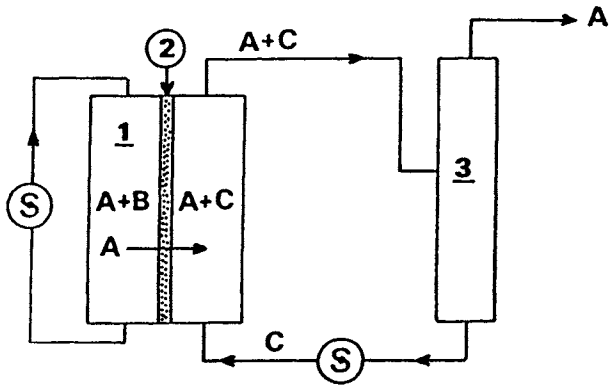

Fig. 5.5. Fractionation by perstraction [12]. 1. Liquid feed (mixture of components A and B); 2. nonporous permselective membrane; 3. distillation column. C: High boiling-temperature leaching solvent. Example: A: Benzene; B: cyclohexane; C: decaline. 2: Permselective membrane made of phosphonated polymer (benzene is the faster permeating component).

permselective barrier (Fig. 5.5). In this case, the barrier is a thin nonporous polymer membrane. Mass transport through the membrane proceeds via a typical three-step solution–diffusion–desorption mechanism which is similar to that involved in pervaporation.

Perstraction has been proposed by Cabasso [12] to separate benzene–cyclohexane mixtures by preferential diffusion of the aromatic component through a membrane made from blends of cellulose acetate and synthetic phosphonated polymers, the stripping liquid being decaline.

5.2 CHARACTERIZATION OF PERVAPORATION MEMBRANES

5.2.1 *Pervaporation Flux and Selectivity*

The behavior of a pervaporation membrane used to separate a binary liquid mixture (components A and B) of given composition is characterized by two experimental parameters, namely, the permeate flux J' (expressed in kg h^{-1} m^{-2} of membrane area) and the selectivity of the barrier, which may be quantified by two alternative dimensionless ratios β and α defined as follows:

$$\beta = \frac{c'}{c} \quad \text{and} \quad \alpha = \frac{c'_A/c'_B}{c_A/c_B} = \frac{c'(1-c)}{c(1-c')}$$

where c and c' are the weight concentrations of the faster permeant (A) in the feed (c) and in the permeate (c'), respectively. To differentiate α from β, the Terminology Commission of the European Society of Membrane Science and

Technology [13] has recommended the designations "separation factor" for α and "enrichment factor" for β. The numerical values of these two parameters can be readily related to one another by means of the following relationships:

$$\alpha = \frac{1-c}{1-\beta c}\beta \qquad \beta = \frac{\alpha}{1+(\alpha-1)c}$$

Parameter α is similar to the membrane selectivity which is widely used in gas permeation, and which is defined as the ratio of the permeabilities of the membrane to two different pure gases under comparable conditions. In the case of pervaporation, the physical meaning of α is not as clear because the two penetrants are no longer transported independently through the membrane due to strong coupling effects [14]. In spite of this difference, α is undoubtedly more significant than β from the physico-chemical point of view since it increases to infinity as the membrane approaches perfect semipermeability (c' then being very close to 1). On the other hand, the use of parameter β makes it easier to formulate the mathematical equations [2] governing the performance (production capacity, operational yield and energy cost) which characterizes a pervaporation module.

A comparison between the ratios α and β clearly shows that the former is larger than the latter, which systematically assumes a rather low value if the feed mixture is rich in the faster-permeating component. For instance, it is quite obvious that β cannot exceed 1.25, even if a perfectly semipermeable membrane is used, when the feed contains 80% by weight of the preferentially transported species.

From the above comments, we can see that no use can be made of α or β values if the feed composition is not specified.

5.2.2 *Concentration Dependence of Pervaporation Flux and Selectivity*

It is worth noting that the flux and selectivity of a membrane used to separate binary mixtures of components A and B depend on the extent to which the permselective film swells under operational conditions and, consequently, on the composition of the facing feed. A complete evaluation of membrane performance, therefore, requires knowledge of the variations of the flux (J') and the selectivity (α or β) with respect to feed composition.

To collect these data, experimental investigations are usually carried out with laboratory pervaporation cells, as described in the literature [15]. The test cell itself is made of stainless steel and the membrane is generally supported by a sintered metal disc. Efficient stirring is ensured by continuous flow of the thermostatted feed mixture in a loop and a downstream pumping system stabilizes the permeate pressure at about 1 mm Hg, in the vicinity of the

membrane. The volume of the liquid feed is approximately 120 ml and the membrane area is about 20 cm^2. The permeate is alternately collected in two cold traps in which it condenses completely. The liquid thus recovered is weighed and titrated by gas chromatography to evaluate permeation rate and selectivity. This analysis only requires the sampling of a small amount of permeate and the composition of the investigated mixture is not significantly changed during the operation. Similar measurements are reiterated with a series of mixtures differing in their composition and the results thus obtained are used to calibrate the representative functions J' vs. c, α vs. c, β vs. c, or c' vs. c.

To accelerate the recognition of these functions, semiautomatic computerized devices, such as that designed by Clément [16], have sometimes been used (Fig. 5.6). Periodically, the permeate is diverted towards a side loop, maintained at low temperature by liquid air, in which it is completely trapped in the frozen state. It is subsequently melted, vaporized and driven into a gas chromatograph by a stream of helium. The resulting chromatogram is instantaneously analyzed

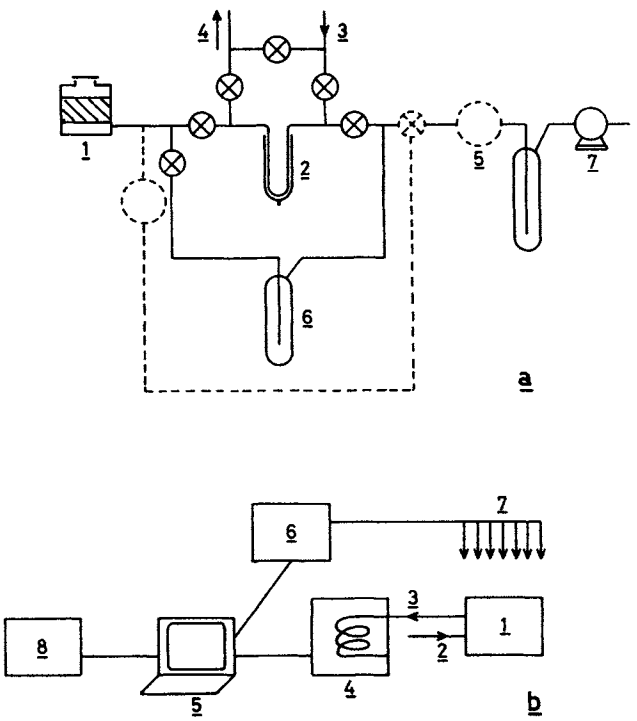

Fig. 5.6. Semiautomatic computerized device designed to characterize pervaporation membranes [16]. (a): 1. Pervaporation cell; 2. sampling of pervaporate; 3. helium stream; 4. to chromatograph; 5. void reservoir; 6. cold trap; 7. vacuum pump. Broken line: pressure control and regulation. (b): 1. Pervaporation device (above); 2. helium inlet; 3. removal of pervaporate; 4. chromatograph; 5. computer; 6. control and regulation of valves; 7. to valves; 8. printer.

by a computer and is compared with that recorded just before the test, with a sample directly extracted from the feed. This comparison permits evaluation of pervaporation rate and selectivity at the known composition of the feed. The experiment is generally carried out, starting from a relatively small volume of liquid mixture, so that the composition of the flowing feed progressively varies as pervaporation is allowed to continue. Reiteration of measurements at regular time intervals thus provides the set of experimental data needed to calibrate the four functions previously mentioned.

It is also worth stressing that selectivity and flux measurements are not equally reliable. In fact, we may consider that experimental errors on selectivity values are rather small provided that measurements are carried out under low downstream pressure, i.e., if there is no significant pressure loss across the sintered metal support. On the other hand, flux values are more questionable because the transfer area is not exactly known, due to contacts between the membrane and its support. In fact, comparative measurements made by Blackadder [17] — investigating the pervaporation transport of pure *p*-xylene at 30°C through a homogeneous sheet of polyethylene (75 μm thick) mounted over five different supports — yielded experimental flux values ranging from 26 to 61 g h^{-1} m^{-2}. It is then clear that the structure of the support may significantly affect the observed transport rate and that experimental flux values measured with a given laboratory pervaporation cell must only be compared between them. Special care must be taken to determine absolute values of permeation rates.

To collect flux and selectivity data which can reliably be used to evaluate the performance of a module working in a continuous way, membrane characterization must be carried out only when the steady-state transport regime is attained. In fact, at the beginning of laboratory tests, the latter regime is generally preceded by a transient period (30 min to several hours, depending on the composition of the feed and on the nature of the membrane), during which flux and selectivity apparently change with time. These variations are governed by the sorption kinetics of the feed mixture by the polymeric barrier material and often involve complex migration phenomena, which may significantly deviate from Fickian diffusion [18]. In practice, these transient behaviors are generally considered as side phenomena which no longer significantly intervene when the steady-state transport regime is established.

At fixed temperature, the selectivity of a given membrane for binary mixtures of components A and B can be completely characterized by the figurative curves α vs. c, or β vs. c. An alternative, more versatile representation, similar to the MacCabe–Thiele diagram used in distillation, is the plot c' vs. c complemented by the reference line illustrating the relevant liquid–vapor equilibrium. To complete this information, it is also useful to depict the influence of feed composition on pervaporation rate, i.e., to report the representative curve J' vs. c.

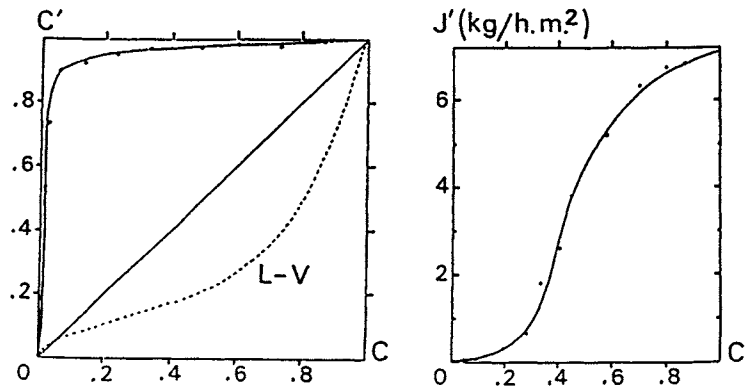

Fig. 5.7. Pervaporation of water–ethanol mixtures through a homogeneous 20 μm-thick polyvinylalcohol membrane. T = 60°C. c, c': Water concentrations (by weight) in feed (c) and in permeate (c'). J': Permeate flux (kg h^{-1} m^{-2}). Dotted line: Free liquid–vapor equilibrium (under atmospheric pressure).

Figure 5.7 shows the two curves characterizing the selectivity and the permeability of a 20 μm-thick homogeneous polyvinylalcohol membrane used, at 60°C, to dehydrate by pervaporation, water–ethanol mixtures of varying composition. The square diagram (c' vs. c) clearly evidences the great selectivity of this membrane to water. Because of its high crystallinity, this material is not very permeable when it is not extensively swollen by the contacting feed, i.e., when it faces mixtures containing less than 20 wt% water. It is also noteworthy that it is virtually impermeable to pure alcohol in which it does not swell at all. The latter feature may be correlated with the high selectivity to water exhibited by the membrane when pervaporation is carried out under very low permeate pressure since the downstream layer of the working membrane is then non-swollen.

By means of similar graphs, Fig. 5.8 characterizes, at 40°C, a 180 μm-thick

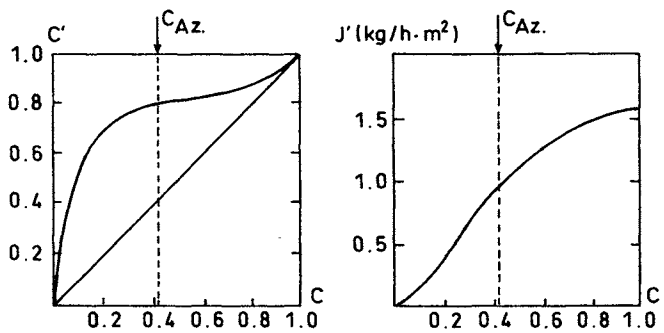

Fig. 5.8. Pervaporation of water–pyridine mixtures through a homogeneous 180 μm-thick membrane made of sulfonic cation–exchange polymer [19]. c_{Az}: Azeotropic composition = 41.3 wt% water. J': Permeate flux (kg h^{-1} m^{-2}).

homogeneous cation-exchange membrane facing water–pyridine mixtures; this binary system exhibits azeotropic behavior when its composition approaches 41 wt% water [19]. Despite its thickness, this hydrophilic polyelectrolyte membrane delivers a satisfactory permeate flux.

Pervaporation rate increases as temperature is raised. Generally, variations of total and individual fluxes are ruled by the Arrhenius equation:

$$J' = J'_0 \exp(-E/RT) \quad J'_i = (J'_i)_0 \exp(-E_i/RT)$$

Considering all systems already studied, it appears that the activation energy E strongly depends on the nature of the membrane and on that of the investigated binary mixture. Data reported in the literature range from 5 to 22 kcal per mole. If both components are characterized by the same activation energy, pervaporation selectivity does not depend on temperature. In such a case, which occurs, for instance, when polyvinylalcohol membranes are used to separate water–ethanol mixtures, pervaporation is the most productive when it is carried out at the highest temperature compatible with the thermal and chemical stability of the barrier material.

Periodicals devoted to membrane science contain a number of experimental results relative to the permeability and selectivity of membranes made of various polymers and used to separate different binary liquid mixtures. These values, which have already been compiled elsewhere [20], mainly concern the dehydration of organic solvents, the separation of hydrocarbons and the extraction of trace amounts of organics contaminating aqueous solutions. Some of them deal with the dehydration of organic acids or bases (amines).

This information can be used, as a first approach, to select an appropriate polymer to manufacture a pervaporation membrane designed for a given separation purpose. Nevertheless, one must keep in mind that these values generally depend strongly on the operational conditions in which they have been measured.

5.2.3 Average Characteristics of Operating Pervaporation Membranes

During continuous pervaporation (Fig. 5.1), the retentate becomes poorer and poorer in the rapidly permeating component (A) as it proceeds along the membrane. Progressively, its concentration c decreases from c_o to c_t as it flows from the inlet to the outlet of the module. In the steady-state regime, the membrane is not faced with a liquid of the same composition over its entire surface. As a consequence, the performance of the system, for instance its production capacity per m^2 of membrane area, is determined by average values of selectivity and permeate flux, defined over the $[c_o, c_t]$ concentration range.

Coming back to the diagrams c' vs. c and J' vs. c, we must therefore focus our attention on the domain comprised between c_o and c_t (Fig. 5.9). To compare the

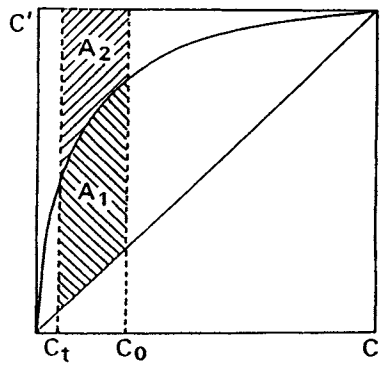

Fig. 5.9. Average selectivity index σ within the [c_o, c_t] concentration range. $\sigma = A_1/A_2$.

selectivity of different membranes and to appreciate their respective abilities to process a mixture of given starting composition (c_0) and to reduce its concentration to a fixed c_t imposed residual value, it has been suggested to refer to an average selectivity index σ defined by the ratio:

$$\sigma = A_1/A_2$$

A_1 and A_2 being the two areas delimited in Fig. 5.9. This ratio has obviously been selected because it equals zero when the membrane is devoid of any selectivity, and approaches infinity in the case of a perfectly semipermeable barrier.

5.2.4 Expected Performance of a Continuous-flow Pervaporator

A simple experimental procedure can also be used to estimate the production capacity of a unit pervaporator equipped with a given membrane and designed to separate a given feed. A laboratory experiment is run after introduction of a known amount (weight = m_0) of the starting mixture (c_0) into a loop comprising a pervaporation cell equipped with the investigated membrane (surface area a) and a circulating pump. The retentate is automatically titrated by a non-destructive method and the experiment is stopped after a lapse of time Δt, when the concentration of the retentate attains the required value (c_t). At the same time, the condensed permeate is weighed (Δm). The production capacity J_t that may be expected from a unit module working in such conditions can then be calculated by means of the following equation:

$$J_t = \frac{1}{a} \frac{m_0 - \Delta m}{\Delta t}$$

The recovery yield R in purified retentate is given by:

$$R = \left(1 - \frac{\Delta m}{m_0}\right)\frac{1 - c_t}{1 - c_0}$$

5.2.5 *Influence of Downstream Pressure on Membrane Performance*

Besides temperature, other external parameters may influence the characteristics of a pervaporation membrane facing a given binary liquid mixture. Downstream pressure being the most determining, it is recommended to measure flux and selectivity under very low permeate pressure (less than 1 mm Hg).

In fact, any rise in this pressure results in an increase of the activities of both permeants dissolved in the downstream layer of the working membrane. Activity gradients across the thickness of the membrane consequently decline and permeation fluxes drop. Regarding selectivity, we have to consider that the resistance opposed by the downstream layer of the membrane becomes less selective as this layer swells more extensively. Moreover, at the membrane/permeate interface, desorption slows down as downstream pressure increases and it progressively becomes the rate-determining step of the process. Accordingly, transport selectivity then undergoes a drastic change, as illustrated in Fig. 5.10.

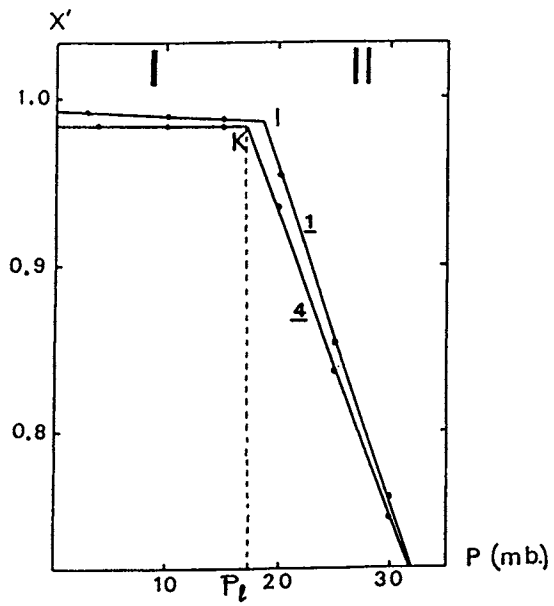

Fig. 5.10. Pervaporation of water–tetrahydrofurane mixtures through a membrane made of regenerated cellulose (Cuprophane), $T = 20°C$. Influence of permeate pressure P (mbars) on pervaporation selectivity [21]. X'. Water concentration in the permeate (mole fraction); X. water concentration in the feed (mole fraction); 1. $X = 0.296$; 4. $X = 0.570$. Boiling temperatures: water, 100°C; THF, 65.4°C.

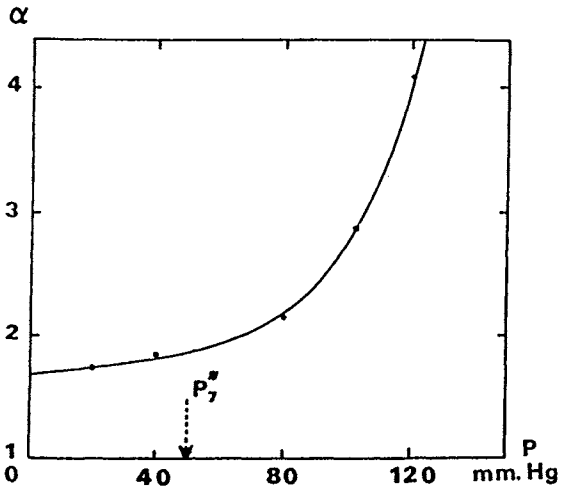

Fig. 5.11. Pervaporation of *n*-hexane–*n*-heptane mixtures through a homogeneous membrane of polyethylene, $T = 30°C$. Influence of downstream permeate pressure on pervaporation selectivity. α (preferential transport of *n*-hexane). Curve deduced from data reported by Greelaw [22]. Hexane content in the processed feed = 74.2 wt%. Boiling temperatures: *n*-hexane, 68.6°C; *n*-heptane, 98.4°C. P_7^* = Saturating vapor pressure of *n*- heptane.

In fact, this graph clearly shows the occurrence of a transition between two distinct transport regimes when downstream pressure exceeds a certain limit which approximates to the saturated vapor pressure of the permeate. Under low downstream pressure, desorption is rapid and diffusion through the membrane is the rate-determining step of the process. Beyond the transition pressure, desorption slows down and progressively governs the selectivity of pervaporation transport. In the latter regime, selectivity is mainly determined by the relative volatilities of the feed components. If the more rapidly permeating species is also the more volatile, selectivity increases as downstream pressure is raised (Fig. 5.11). In the opposite case, a steep decrease in selectivity is observed (Fig. 5.10).

In fact, if one assumes that the permeate behaves as an ideal mixture and does not contain any significant amounts of noncondensable gases (for instance, air entering via leaks in the apparatus), it can be shown [21] that permeate composition X'_A (mole fraction) depends on downstream pressure P, according to the following relationship:

$$X'_A = \frac{P_A^* P_B^*}{P_B^* - P_A^*} \frac{1}{P} - \frac{P_A^*}{P_B^* - P_A^*}$$

where A and B are the fast and the slow permeants, respectively, X' denotes the concentrations (mole fractions) in the permeate; P is the downstream pressure;

and P^* stands for saturated vapor pressures, at operational temperature.

Derivation yields:

$$\frac{dX'_A}{dP} = \frac{P^*_A P^*_B}{P^*_A - P^*_B} \frac{1}{P^2}$$

If the faster component (A) is the less volatile ($P^*_A - P^*_B < 0$), selectivity decreases as P increases, as it is observed when a hydrophilic cellulose membrane is used to dehydrate water–tetrahydrofurane mixtures (Fig. 5.10). In the opposite situation, selectivity increases as P is raised up (Fig. 5.11).

5.3 MECHANISM OF PERVAPORATION MASS TRANSPORT

5.3.1 Mass Transport Through an Unevenly Swollen Polymer Film

At the qualitative level at least, the pervaporation transport of a binary mixture through a non-porous membrane is now elucidated.

When the steady-state regime is established, each penetrant is transported at the same rate through all sections parallel to the surface of the membrane. The permeation flux of A may therefore be evaluated by considering its permeation rate through the non-swollen downstream layer of the membrane (Fig. 5.12).

$$-J'_A = D^*_A \left(\frac{dc_A}{dz}\right)_{z=e}$$

D^*_A = intrinsic diffusivity of A (extrapolated at zero concentration of the penetrant)

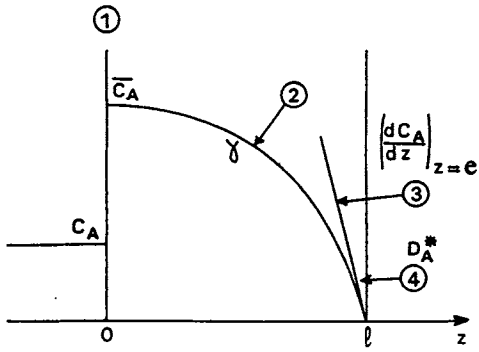

Fig. 5.12. Permeant concentration profile across membrane thickness, during steady-state pervaporation of a pure liquid. 1. Upstream uptake (swelling); 2. convex curvature due to the concentration-dependence of permeant diffusivity [23]; 3. downstream concentration gradient; 4. unswollen downstream layer of the membrane.

$$D_A = D_A^* \exp(\gamma_{AA} c_A + \gamma_{BA} c_B)$$

γ = plasticization parameters; e = membrane thickness.

The latter equation accounts for the fact that, at a given place in the membrane, the diffusivity D_A of component A is concentration-dependent. It generally increases as the polymeric material is more extensively swollen. This dependence is responsible for the curvature of the permeant concentration profile [23] across the thickness of the working membrane. If D_A increases with penetrant concentration, this profile assumes a convex shape as depicted in Fig. 5.12. It follows that the partial flux of component A is determined by the product of two factors:

1. The first is the activity gradient of A in the virtually dry downstream layer of the working membrane. Of course, the higher the upstream starting point of the relevant concentration profile, the greater the gradient, but the downstream slope of the profile also depends on its curvature which is governed by the plasticization of the membrane polymer by the permeants and also by coupling between their flows. In most cases, however, upstream partitioning is the most determining phenomenon and preferential sorption of A in the upstream layer of the membrane favors the rapid transport of this component. It is, therefore, widely admitted [24] that, in a first approach, the selection of a polymer P — suitable for preparing permselective membranes designed to separate A–B mixtures — can be made by referring to the relevant thermodynamical P–A–B phase diagrams.

2. Nevertheless, one should not forget that the intrinsic diffusivities of both A and B permeants are also determining parameters. In fact, in the virtually dry membrane material, the different permeant molecules may migrate with very unequal velocities since their respective mobilities then depend on the relative strength of short-range interactions working between these molecules and specific polar or ionic groupings belonging to the permselective polymer. The downstream layer of the film may therefore oppose unequal resistance to the diffusion of A and B while it is hardly conceivable that the mobilities of these two components could widely differ in the swollen part of the membrane.

5.3.2 Sorption and Diffusion Selectivities

From the above considerations, it follows that the selection of an appropriate membrane polymer P to extract component A from binary mixtures of A and B relies on the fulfilment of the following conditions:

1. Strong preferential sorption of A by polymer P when the latter is contacted with mixtures of A and B. This can be ascertained by referring to the relevant P–A–B phase diagram and by checking that tie-lines intercept the P–A side of this triangular diagram. In fact, this figure and its variation with temperature

provide the most complete information about the partitioning equilibria that take place at the feed/membrane interface. Depending on the solubility of *P* in A and B, and on the mutual miscibility of A and B liquids, different typical ternary diagrams can be distinguished and have been classified by Bode [25]. An alternative way of characterizing the upstream swelling equilibrium is that used by Heintz [26] who establishes "solubility diagrams" by plotting the weight fractions of A and B (c''_A and c''_B) in the swollen polymer as a function of the weight fraction c_A of A in the contacting liquid mixture. It is clear that, for a given *P*–A–B system, the solubility diagram can readily be translated into the corresponding phase diagram since both of them represent the same set of swelling equilibria.

Until now, only few complete *P*–A–B phase diagrams are available in the literature and this does not facilitate the choice of appropriate membrane polymers for pervaporation. To rapidly palliate this lack of data, it is often referred to "preferential solvation" evidenced by contacting each investigated polymer *P* with A-B mixtures of varying composition. For this purpose, a given amount (weight = m_0) of pieces cut out of a film of each tested polymer *P*, is immersed into a fixed volume *V* of a mixture of known concentration (c_0) in component A. Preferential sorption of A obviously provokes a decrease of its concentration (c) in the contacting supernatant liquid mixture. Assuming that this mixture equilibrates a binary adduct represented by the stoichiometry P–$s_A(c)$A and that *P* is insoluble in the facing solution, the so-called "preferential solvation s_A (c)" can be deduced from V, m_0, c_0 and c. The figurative curve s_A vs. c then represents the overall preferential solvation of *P* contacted with mixtures of A and B and the area below this curve roughly quantifies the preferential affinity of polymer *P* for component A, in the presence of component B.

Preferential solvation can also be evidenced and evaluated by means of other experimental techniques, such as analysis of light scattered by *P*–A–B solutions [27].

It is worth noting that the selectivity of upstream partitioning is not governed by the chemical nature of the membrane only; it also depends on the thermodynamical properties of the facing liquid mixture. For instance, it is quite remarkable that the polyvinylpyrrolidone-based pervaporation membrane which readily separates positive azeotropic mixtures (Table 5.1), is not selective when it is faced with negative azeotropes (Table 5.2). In fact, in mixtures exhibiting negative azeotropism, heteromolecular attracting forces A–B are prevailing over self-associating interactions A–A and B–B between like molecules. This feature enhancing mutual drag effects, is unfavorable to the separation of the two components. The same reason also explains why organic contaminants, which are poorly soluble in water, such as hydrocarbons or chlorinated solvents, can be easily extracted from aqueous effluents by pervaporation through silicone-based organophilic membranes [28–30], whereas

these membranes are not very efficient to separate mixtures of ethanol and water, which are completely miscible [28,30]. To support this view, mention may also be made of the observations reported by Böddeker (31) concerning the selectivity of polydimethyl–siloxane membranes used to extract, from water, the four different isomeric butanols (Table 5.3). It clearly appears that pervapor-

TABLE 5.2

Fractionation of negative azeotropic mixtures (characterized by maximum boiling temperature) by pervaporation through a membrane obtained by grafting polyvinylpyrrolidone onto a thin polytetrafluoroethylene film [1]

A-B Azeotropes (A = Fast component	T_b (°C)	Azeotrope characteristics		Selectivity		Permeate flux (kg/h m^2)
		T_b (°C)	c (%)	α	β	
A: Chloroform	61.2	64.7	80.0	1.8	1.10	0.85
B: Acetone	56.2		20.00			
A: Chloroform	61.2	79.9	17.0	1.0	1.0	1.50
B: M.E.K.	79.6		83.0			
A: Butanol-1	117.7	118.7	71.0	1.4	1.09	1.25
B: Pyridine	115.3		29.0			
A: Water	100.0	107.1	22.5	1.0	1.0	2.74
B: Formic acid	100.7		77.5			
A: Acetic acid	118.1	119.5	77.0	2.7	1.17	0.27
B: Dioxane	101.3		23.0			
A: Acetic acid	118.1	159.0	26.0	1.2	1.14	0.04
B: D.M.F	153.0		74.0			
A: Formic acid	100.7	150.0	53.5	2.8	1.31	0.22
B: Pyridine	115.3		36.5			
A: Acetic acid	118.1	139.7	35.0	1.0	1.0	0.09
B: Pyridine	115.3		65.0			
A: Propionic acid	140.9	199.0	74.0	1.7	1.12	0.13
B: Pyridine	115.3		26.0			

A = Faster permeant; T = 25°C.
Parameters α, β, c and c' and T_b are the same as in Table 5.1.
M.E.K. = Methylethylketone; D.M.F. = *N,N*-dimethylformamide.

TABLE 5.3

Extraction of alcohols from water by pervaporation through a homogeneous polydimethylsiloxane film (50 μm thick), $T = 50°C$ (after Böddeker et al. [31]).

Investigated alcohol			Pervaporation performance			
Alcohol	T_b (°C)	c_{max} wt%	J' g/h m^2	c' wt%	β	α
n-Butanol	117.7	7.7	44	37	37	58.1
iso-Butanol	107.9	8.5	52	29	29	40.4
sec-Butanol	99.5	12.5	50	22	22	27.9
tert-Butanol	82.5	100	52	14	14	16.1
Ethanol	78.5	100	190	3	3	3.06

Feed alcohol content: $c = 1\%$, by weight, c' = percent butanol in permeate, c_{max} = solubility of the alcohol in water, at 20°C.
J' = Permeate flux; $\beta = c'/c$; α = selectivity = $[c'/(1-c')]/[c/(1-c)]$.
T_b = Boiling temperature.

ation transport through this membrane is as more selective to the alcohol as the organic component is less soluble in water. As may be expected, salting out by introduction of sodium chloride in the feed increases the separation factor [32,33].

2. The preferential transport of component A can also result from the low mobility of component B in the non-swollen downstream layer of the working membrane, i.e., from a low intrinsic diffusivity D_B^*. The latter value can be determined by extrapolating experimental $D_B(c)$ plots to zero concentration or by studying the diffusion of non-saturated vapor of component B through a thin homogeneous film of polymer *P*. One may also refer to the observation that the membrane appears as virtually impermeable when it is used to process pure B, by pervaporation under low downstream pressure. For instance, the J' vs. c curve represented in Fig. 5.7 shows that polyvinylalcohol is not permeable to dry ethanol, a feature which causes an additional selectivity effect in the dry downstream layer of the membrane. The latter contribution does not exist in the case of the polyvinylpyrrolidone–polyacrylonitrile blend membrane [34] characterized by the permeability curve shown in Fig. 5.13. This difference accounts for the lower selectivity of the polyvinylpyrrolidone-based membrane as compared with that made of polyvinylalcohol.

A number of experimental observations may be mentioned as evidence of the respective contributions of upstream partitioning —or sorption — and downstream diffusion to the overall selectivity of a given membrane.

When polyvinylalcohol (PVA) is used as a permselective material to dehydrate water–ethanol mixtures, pervaporation selectivity is significantly greater

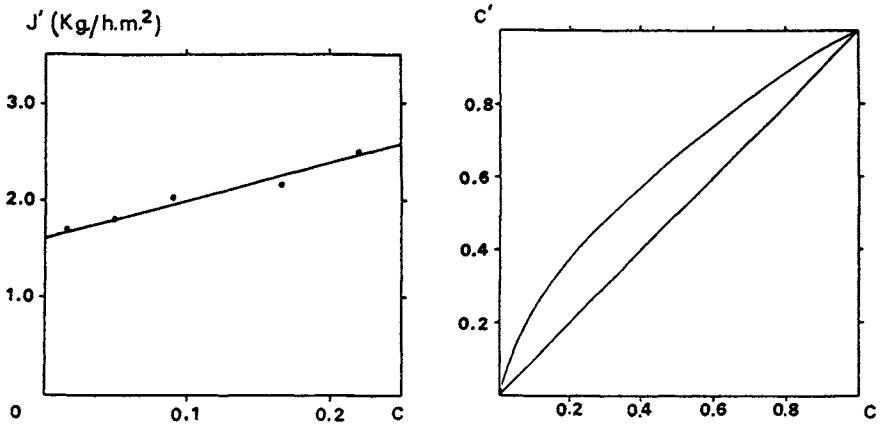

Fig. 5.13. Pervaporation of water–ethanol mixtures through a homogeneous 30 μm-thick membrane made of 58/42 blend of polyacrylonitrile and polyvinylpyrrolidone [34]. Pervaporation temperature: $T = 20°C$.

than sorption selectivity evaluated by analyzing PVA samples swollen after immersion in water–ethanol mixtures of the same composition as the processed feeds (Fig. 5.14). Similar behavior is observed (Fig. 5.15) with other very selective hydrophilic membranes, such as the potassium and cesium salts of ion-exchange membranes obtained by grafting acrylic acid onto thin films of low density polyethylene [35–37].

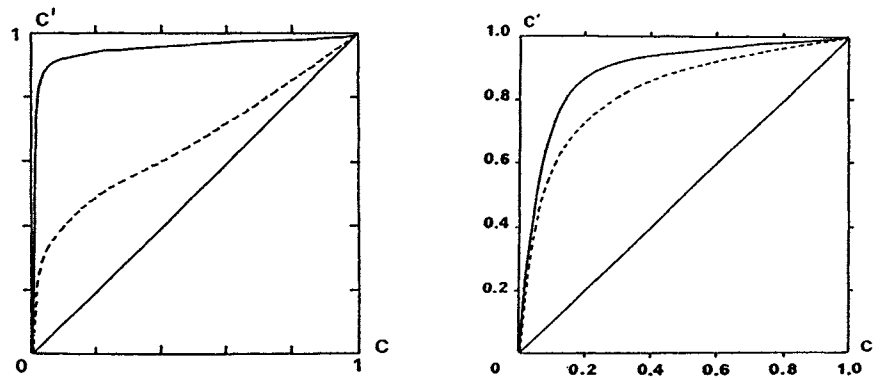

Left: Fig. 5.14. Pervaporation of water–ethanol mixtures through a homogeneous polyvinylalcohol membrane (T = 65°C). Comparison between sorption selectivity and pervaporation selectivity. Dashed line: sorption; solid line: pervaporation.

Right: Fig. 5.15. Pervaporation of water–ethanol mixtures through a homogeneous membrane obtained by grafting acrylic acid onto a thin, low-density polyethylene film and neutralization by immersion in an aqueous solution of potassium hydroxide [35–37] ($T = 35°C$). Comparison between sorption selectivity and pervaporation selectivity. Dashed line: sorption; solid line: pervaporation.

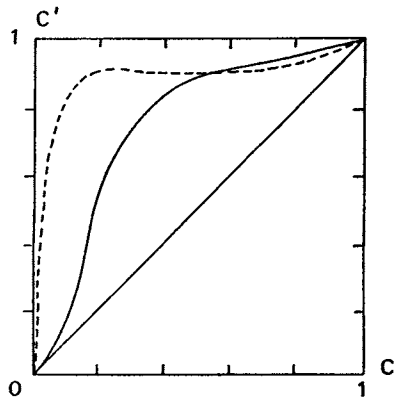

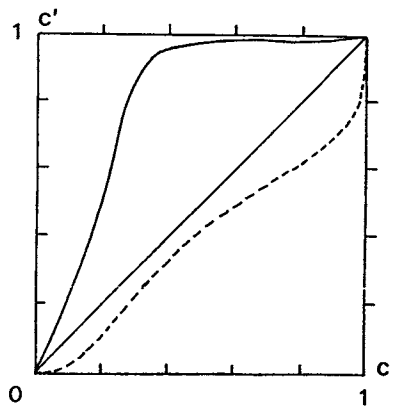

Left: Fig. 5.16. Pervaporation of water–ethanol mixtures through a membrane made of a copolymer butadiene–styrenesulfonic acid, neutralized by immersion into an aqueous solution of sodium hydroxide (Membrane Selemion CMVH from Asahi Glass Co.). Comparison between sorption selectivity and pervaporation selectivity [38], $T = 60°C$. Dashed line: sorption; solid line: pervaporation.

Right: Fig. 5.17. Pervaporation of water–acetic acid mixtures through the CMVH membrane (acid form of that shown in Fig. 5.16). Comparison between sorption and pervaporation selectivities [39]. $T = 60°C$. Water is the preferentially transported component. Dashed line: sorption; solid line: pervaporation.

In the opposite situation, i.e., when sorption and diffusion do not favor the transport of the same feed component [38], competition between the two phenomena results in a rather poor pervaporation selectivity (Fig. 5.16).

In a few cases, it has even been observed that the fast permeant is less extensively sorbed by the membrane material. In this respect, we may mention the results reported by Böddeker [39] concerning the Selemion CMVH membrane from Asahi Glass Co. — shaped from a copolymer involving butadiene and styrenesulfonic acid units — used to dehydrate aqueous solutions of acetic acid (Fig. 5.17). Similar behavior was also observed by Yamada [40] during experiments carried out with membranes made of a copolymer of *N*-vinylpyrrolidone and isobutylmethacrylate. The latter membranes are selective to water although ethanol is preferentially sorbed by the copolymer (Fig. 5.18). According to Uragami [41], the same is observed when poly(vinylchloride) membranes are faced with aqueous solutions of ethanol. Water is the more rapidly permeating component whereas ethanol is preferentially incorporated into the polymer.

The specific influence of diffusion through the downstream layer of a working membrane was also evidenced by using a homogeneous film chemically modified on one side. Such a membrane was obtained by Yamada [42] by reacting, with ethylenediamine, a sheet of polyethylene previously activated by photochlorination. The resulting asymmetrical membrane was used to separate mixtures of aniline and benzene. The experiment consisted in comparing the transport selecti-

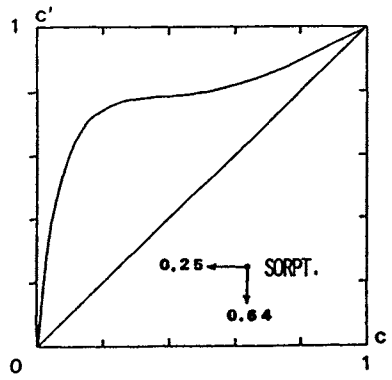

Fig. 5.18. Pervaporation of water–ethanol mixtures through a homogeneous membrane made of a copolymer of *N*-vinylpyrrolidone (20%) and isobutylmethacrylate (80%). $T = 25°C$. Pervaporation selectivity curve (c' vs. c, c and c' are the water contents, by weight, in feed and permeate, respectively). A point belonging to the sorption selectivity curve has been deduced from the experimental data reported in Ref. [40].

vities observed after changing, face-to-face, the orientation of the membrane in the pervaporation cell. The selectivity of the membrane was found to differ noticeably from that of the original polyethylene film only if its modified surface was on the permeate side. In such conditions, pervaporation transport is less favorable to benzene, as may be expected considering that the intrinsic diffusivity of aniline is increased when the membrane material is reacted with the diamine.

5.3.3 Modeling of Pervaporation Mass Transport

Although we have now gained a qualitative understanding of the mechanism of pervaporation transport in the case of a binary feed mixture, the process is nevertheless too complex and involves too many parameters to be elucidated at a quantitative level. A number of experimental data would be needed to achieve a complete analysis and most of them are still lacking.

Relying on simplifying assumptions, quantitative models have however been proposed, which satisfactorily account for the pervaporation transport of a pure liquid. In the case of a binary feed mixture, modeling is much more complex because of possible coupling between the transports of the two components.

5.3.3.1 Vacuum Pervaporation Transport of Pure Liquids

If the permeant is unique, the concentration dependence of its diffusivity in the membrane material may be represented by a relatively simple function of c involving only two parameters. An exponential function is generally used:

$$D(c) = D^* \exp(\gamma c)$$

where D^* is the intrinsic diffusivity, i.e., the diffusivity of the penetrant in the non-swollen membrane material (c approaching zero) and γ represents the so-called plasticization parameter.

Then, assuming that the membrane is homogeneous and isotropic, integration of Fick's first equation over the whole thickness (e) of the film and for boundary conditions ($c = c_w$ for $z = 0$, $c = 0$ for $z = e$) established when the steady-state pervaporation regime is attained, leads to the expression of the permeate flux J' and to the steady permeant concentration profile $c(x)$ across the thickness of the working membrane [14,43].

$$-J' = d(c)\frac{dc}{dz} \qquad D(c) = D^* \exp(\gamma c)$$

$$J' = \frac{D^*}{\gamma e}[\exp(\gamma c_w) - 1]$$

$$c(x) = \frac{1}{\gamma}\ln\left\{x[1 - \exp(\gamma c_w)] + \exp(\gamma c_w)\right\}$$

where x is the relative distance to the upstream interface ($x = z/e$) and c_w is the concentration of the permeant in the swollen upstream layer of the membrane.

The values of D^* and γ are then needed to calculate J'. Several experimental methods such as sorption and desorption kinetics [23,44,45], time-lag techniques [46,47], inverse gas chromatography [48] and analysis of the membrane response to regular forced concentration waves [49] are used to measure directly these two parameters. Relying on the data thus obtained, it is possible to estimate the pervaporation flux that may be expected, at fixed temperature, from the processing of a given pure liquid through a given homogeneous membrane of known thickness. These predictions are generally in rather good agreement with the results of experimental measurements.

5.3.3.2 Vacuum Pervaporation of Binary Liquid Mixtures

It is more difficult to analyze, from a quantitative point of view, the pervaporation transport of binary liquid mixtures. This complexity arises from the fact that, contrary to the situation occurring in gas permeation, the pervaporation transport of a binary mixture of A and B is not additive with respect to those of pure components A and B.

Considering the partitioning at the feed/membrane interface, we must keep in mind that the swelling of a polymer P immersed into binary mixtures of A and B does not vary linearly with respect to the composition of these mixtures [53]. Sometimes, it is observed that the polymer, insoluble in each pure liquid A and B taken separately, readily dissolves in mixtures of A and B. This occurs if the solubility parameter δ_P of this polymer is between those of A (δ_A) and B (δ_B).

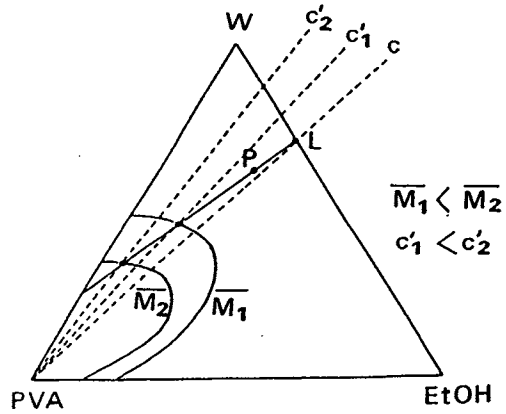

Fig. 5.19. Ternary phase diagram: polyvinylalcohol–water–ethanol. Influence of the molar weight M of the polymeric component.

It is also noteworthy that a ternary system P-A-B involving a polymeric component P is not precisely defined since the swelling extent of P depends on several parameters, such as its molecular weight, its crystallinity and, casually, its degree of crosslinking. For instance, the phase diagram reported in Fig. 5.19, which characterizes the ternary system polyvinylalcohol–water–ethanol, shows that partition between the swollen polymeric phase and the supernatant liquid mixture becomes less selective as the average molecular weight M of the polyalcohol decreases from M_2 to M_1. This is due to the fact that the dissymmetry between the two phases, i.e. the sorption selectivity, progressively vanishes as the polymeric phase is more and more extensively swelled. The permeability of the membrane increasing with its swelling extent, we may expect that the selectivity and the permeability of the membrane should vary contrariwise when the parameters mentioned above are changed.

Apart from these side problems, the major difficulty in accounting for the pervaporation of a binary mixture lies in the fact that the transport of the two permeants are mutually coupled.

In the literature on pervaporation, the term "coupling" is used to designate either the thermodynamical constraint which correlates the flows of the different mobile species, or the mutual drag between the different migrant molecules and which originates from short-range molecular interactions between them. In some cases, the latter effect makes it possible for a given penetrant to move against its own concentration gradient in certain regions of the system.

Thermodynamical coupling has been thoroughly analyzed by Smolders [51,52]. Considering that the individual permeation flux J_i of each permeant is proportional to its local chemical potential gradient, this flux may be expressed as:

$$-J'_i = D_i c_i \frac{d}{dz}\left(\frac{\mu_i}{RT}\right)$$

where D_i = diffusivity of penetrant i within the elementary slice of thickness dz; c_i = concentration of i in the same elementary volume; μ_i = chemical potential of i; R = gas constant; T = absolute temperature (°K).

Then, assuming that the membrane works in virtually isothermal conditions, we obtain

$$-J'_i = \frac{D_i c_i}{RT} \frac{d\mu_i}{dz} \qquad d\mu_i = v_i\, dP + \frac{\partial \mu_i}{\partial a_i} da_i$$

where v_i is the molar volume of component i, a_i its activity and P the operational pressure.

As long as pervaporation is carried out under moderate upstream pressure, the pressure differential between the two opposite surfaces of the membrane is small and the first term of the expansion may be considered negligible as compared with the second. The expression of the flux may, therefore, be reduced to:

$$-J'_i = \frac{D_i c_i}{RT} \frac{\partial \mu_i}{\partial z}$$

Then, referring to the well-known relationship:

$$\mu_i = \mu_i^* + RT \ln (a_i)$$

we deduce:

$$-J'_i = D_i c_i \frac{\partial}{\partial z}\left(\ln (a_i)\right)$$

The main acquisition of the thermodynamics of macromolecular ternary systems resulting from the Flory–Huggins theory [53] is the mathematical function accounting for the variation of $\ln(a_i)$ with respect to the volume fractions of the different components. In the ternary system composed of a polymer 3 and a mixture of solvents 1 and 2, activities vary according to the following functions:

$$\ln(a_1) = \ln(\varphi_1) + (1 - \varphi_1) - \varphi_2 \frac{v_1}{v_2} - \varphi_3 \frac{v_1}{v_3} + (\chi_{12}\, \varphi_2 + \chi_{13}\, \varphi_3)\, (\varphi_2 + \varphi_3) - \chi_{23} \frac{v_1}{v_2} \varphi_2\, \varphi_3$$

where ϕ denotes volume fraction, v: molar volume; χ: Flory interaction parameter; 1, 2: low molecular weight liquids; 3: polymer.

Combining this equation with the preceding one, we obtain the final expression of the individual pervaporation flux J', as follows:

$$-J'_1 = \varphi_1 D_1(\varphi_1, \varphi_2) \frac{d}{dz}\left[\ln(\varphi_1) + (1-\varphi_1) - \varphi_2 \frac{v_1}{v_2} - \varphi_3 \frac{v_1}{v_3} + (\chi_{12}\varphi_2 + \chi_3 \varphi_3)(\varphi_2 + \varphi_3) - \chi_{23} \frac{v_1}{v_2} \varphi_2 \varphi_3\right]$$

where the diffusivity $D_1(\phi_1,\phi_2)$ of penetrant 1 is considered to be composition-dependent.

To calculate the individual flux J'_1 for the steady-state regime, it is necessary to integrate this nonlinear differential equation over the whole thickness of the membrane, considering the boundary conditions at the two opposite surfaces of the barrier. Such a calculation can only be achieved through a numerical method, which requires precise knowledge of the function $D_1(\phi_1, \phi_2)$, accounting for the composition-dependence of the corresponding D_1 diffusion coefficient.

5.3.3.3 The Stefan–Maxwell Approach

The above analysis is based on several assumptions, which have been critically discussed by Bitter [54]. In fact, an objection may be that the solubility of permeants in polymer membranes is inadequately described by the Flory–Huggins equation since this equation is based on a theory that ignores both the crystallinity of the sorbing material and the limited flexibility of macromolecular chains in a polymer network. Moreover, it overlooks the effect of the penetrants on the coordination number of the swollen polymer.

To describe diffusive mass transport in the thickness of the membrane, Bitter suggests relying on Stefan–Maxwell concepts. Let us recall that the Stefan–Maxwell analysis was originally introduced to account for diffusion processes observed in perfect gas mixtures. It was subsequently extended to multicomponent liquid mixtures by Lightfoot [55,55a], who developed the so-called "generalized Stefan–Maxwell theory", and by Mason [56], who examined even more complex systems involving liquids and polymeric species. Recently, attempts have been made to refer to this theory to interpret mass transport through polymer membrane [57]. In contrast to the phenomenological Fickian approach, the Stefan–Maxwell theory deliberately explores the molecular level without differentiating the solvent from the other components. In the multicomponent mixture, each molecule i moves under the influence of a driving force which is a gradient of thermodynamical potential μ_i. As a result, the surrounding molecules exert on it a frictional force f which opposes the driving force and becomes

equal to it after molecule i has reached its steady-state velocity w_i. Then:

$$f = -\text{grad}\,\mu_i$$

Assuming that the frictional force exerted by a molecule j is proportional to the difference in velocities w_i–w_j, we may write:

$$f_{ij} = \frac{RT}{D_{ij}}(w_i - w_j)$$

RT/D_{ij} being the expression of the friction coefficient where D_{ij} is the Stefan-Maxwell mutual diffusivity of i in a mixture of i and j.

Considering all the collisions suffered by i during its movement through the system and averaging the quantities introduced above, we obtain the extended Stefan–Maxwell equations. In the case of a unidirectional mass transport through a membrane and for an isothermal system, these equations reduce to the following forms.

$$\sum_{j=1}^{n} \frac{RT\,c_j}{c\,D_{ij}}\left[\frac{J'_i}{c_i} - \frac{J'_j}{c_j}\right] = -\frac{d\mu_i}{dz} - v_i\frac{dp}{dz}$$

where c is the total molarity of penetrant and polymer species in the membrane and D_{ij} are the generalized Stefan–Maxwell diffusivities. The other symbols have the usual designations: c_i = molarity of i; μ_i = chemical potential of i; v_i = partial volume of i; J'_i = molar flux of i.

Since v_i is generally small for common permeants and since pervaporation is usually carried out under moderate upstream pressure, the pressure term is negligible. If the investigated system only comprises two permeants (1 and 2) and the membrane polymer (m), the preceding equation can be developed as follows:

$$-\frac{c}{RT}\frac{d\mu_1}{dz} = \frac{J'_1}{c_1}\left(\frac{c_m}{D_{1m}} + \frac{c_2}{D_{12}}\right) - \frac{J'_2}{D_{12}}$$

In the derivation of the Stefan–Maxwell equations, it is tacitly assumed that diffusivities D_{ij} are independent of the local composition at each point of the multicomponent system. In mixtures of liquids and polymeric species, however, these diffusivities probably vary with concentration, although much less than Fickian diffusion coefficients and this smaller change is an advantage of the Stefan–Maxwell approach.

Another superiority of this type of analysis is that it involves diffusivity parameters D_{ij}, which, in principle, can be evaluated by separate experiments performed with binary mixtures. Nevertheless, if it is applied to a multicomponent system comprising a polymeric species (a membrane, for instance), those

diffusion parameters can no longer be considered as strictly invariant and equal to separate binary coefficients, and the Stefan–Maxwell theory then leads to approximate results only. It has also been pointed out that Stefan–Maxwell equations do not require particularizing one component as the solvent and therefore look very symmetric. On the other hand, that feature often makes them rather difficult to handle and to combine with mass balances.

In fact, Stefan–Maxwell equations can be exactly integrated in special cases only. A typical example is the pervaporation transport of a single permeant (water, for instance) through a membrane of thickness e. In this binary system, the chemical potential of water is given by:

$$\mu_w = \mu_w^* + RT \ln (a_w)$$

where a_w is the activity of water.

Hence:

$$-\frac{d \ln (a_w)}{dz} = \frac{c_m}{(c_m + c_w) D_{wm}} \frac{J'_w}{C_w}$$

Assuming that the activity coefficient of water γ_w is constant throughout the working membrane,

$$a_w = \gamma_w c_w \qquad c_w = \varphi_w / v_w$$

where c_w is the molarity of water, φ_w its volume fraction and v_w its molar volume.

Consequently we may write

$$\frac{d \ln(a_w)}{dz} = \frac{d\varphi_w}{\varphi_w \, dz}$$

The Stefan–Maxwell equation then reduces to:

$$\frac{(1 - \varphi_w) v_w}{v_w + \varphi_w (v_m - v_w)} \frac{J_w}{D_{wm}} = -\frac{d\varphi_w}{v_w \, dz}$$

Integration between the two opposite surfaces of the working membrane then leads to the formulation of the water permeation rate:

$$J'_w = \frac{D_{wm}}{e \, v_w} \left[\left(1 - \frac{v_m}{v_w} \right) (\varphi_{wo} - \varphi_{we}) - \frac{v_m}{v_w} \ln \frac{1 - \varphi_{wo}}{1 - \varphi_{we}} \right]$$

where φ_{wo} and φ_{we} are the volume fractions of water in the upstream and the downstream layers of the working membrane, respectively.

Moreover, combination of the Stefan–Maxwell equation with that defining the conventional Fickian diffusivity D_w, i.e., $J_w = -D_w \, dc_w/dz$, makes it possible to establish a relationship between D_w and the mutual diffusivity D_{wm}:

$$D_w = D_{wm} \frac{v_w + \varphi_w (v_m - v_w)}{(1 - \varphi_w) v_w}$$

The latter relationship shows that D_w approaches D_{wm} as φ_w goes to zero and we may therefore consider that the mutual diffusivity D_{wm} coincides with the intrinsic diffusivity of water (D_w^*) in the membrane polymer.

In practice, the expression of the flux is often used to estimate the mutual diffusivity D_{wm} of water in a given polymer [58]. For instance, when pure water is processed at 40°C, by pervaporation through a 15 μm-thick homogeneous film of cellulose acetate (Eastman Kodak), the observed permeation rate J'_w equals 1.102 kg/h m^2, i.e., 17 10^{-7} mole cm^{-2} s^{-1}.

This value has been inserted into the theoretical expression of J'_w after being complemented with the following data:

$v_m/v_w = 100$

$\varphi_{wo} = 0.155$ (from measurement of membrane swelling in pure water)

φ_{we} is considered as negligible (vacuum pervaporation).

Calculation then leads to: $D_{wm} = D_w^* = 3.42 \, 10^{-8}$ cm^2 s^{-1} (at 40°C).

This result is in rather good agreement with the value directly deduced from the sorption kinetics of water vapor on the same cellulose acetate film [59].

$$D_w^* = 2.50 \, 10^{-8} \text{ cm}^2 \text{ s}^{-1} \text{ (at 25°C)}$$

with an activation energy equal to 7.9 kcal mole^{-1}.

We may therefore consider that this diffusivity value is reliable enough to be used in calculations aiming at the quantitative interpretation of the pervaporation transport of a binary feed mixture.

5.3.3.4. Pervaporation Mass Transport Through Semicrystalline Polymer films

In the preceding analysis, it was assumed that the membrane was perfectly homogeneous and isotropic. This condition is fulfilled by nonporous membranes made of amorphous polymers (cellulose acetate, polydimethylsiloxane, etc.) whereas it is not when they are made of semicrystalline polymers. For instance, in the case of polyvinylalcohol, comparison of X-ray diffraction patterns recorded with dry and wet fibres, respectively, shows that crystalline domains are virtually impermeable to water molecules. The same is also true for ethanol. It follows that during pervaporation of water–ethanol mixtures through polyvinylalcohol membranes, the permeant molecules migrate through tortuous paths maintained under strain by adjacent crystallites. Since

a macromolecule goes through several crystallites, the latter may be compared to covalent junctions in a crosslinked polymer [60]. Referring then to the classical relationship $P = DS$ between permeability (P), diffusivity (D) and the solubility coefficient (S), we can conceive that the crystallinity of the membrane material influences both S and D.

With respect to penetrant solubility, crystallinity provokes two different effects. Firstly, it reduces the volume of permeable membrane material:

$$S = (1 - X)\, S_{inter}$$

where S_{inter} is the solubility coefficient in the intercrystalline amorphous phase and X the crystallinity of the membrane polymer. Secondly, it perturbs the swelling of intercrystalline amorphous domains. In fact, adjacent crystallites impose restriction on mobility of chain segments comprised in the intermediate amorphous phase. The resulting rain perturbs the thermodynamics of the polymer–penetrant system in this .egion which is not completely relaxed. To account for this strain effect, the classical Flory–Huggins equation, which governs the thermodynamics of unstrained swollen polymeric phases and expresses the activity a_S of the penetrant, has to be complemented with the Flory–Rehner term [53].

Flory–Huggins equation:

$$\ln a_S = \phi_S + \phi_P + \chi\phi_P^2$$

where ϕ denotes molar volumes and χ stands for the Flory interaction parameter.

Flory–Rehner equation:

$$\ln a_S = \ln \phi_S + \phi_P + \chi{\phi_P}^2 + \frac{\langle\alpha\rangle_0^2\, (n/A)\, v_S\, {\phi_P}^2}{v_0}$$

where $\langle\alpha\rangle_0$ is the ratio between the mean distance separating the junctions in the unswollen network and the mean end-to-end distance for the corresponding segment if this segment was unrestricted; n = number of effective segments in the sample; A = Avogadro number; v_S = molar volume of the penetrant; v_0 = volume of the original polymer sample.

Comparison between the two latter equations shows that, for the same ϕ_S value, the activity a_S of the sorbed penetrant is greater in a strained amorphous domain than in a relaxed one. The higher the number of crystalline junctions, the greater is the effect. As a consequence, the penetrant solubility in the intercrystalline amorphous domains is expected to decrease as crystallinity increases. The latter effect may be summarized by the following expression (60):

$$S_{inter} = \frac{S_{am}}{b} \qquad b > 1$$

where b is the so-called "blocking factor", which depends on polymer morphology and on the size and shape of diffusing molecules. This parameter can be deduced from activity measurements by using the Flory–Rehner equation.

The solubility coefficient S may therefore be expressed as:

$$S = \frac{(1 - X)\, S_{am}}{b}$$

where S_{am} is the solubility coefficient characterizing the completely relaxed amorphous phase.

From the above comments, it follows that the transport properties of a membrane made of a semicrystalline polymer should probably depend on its crystallinity X. As a first approach, we may consider that this influence mainly results from the tortuosity τ of amorphous diffusion paths through which the permeant proceeds.

$$D = \frac{D_{am}}{\tau}$$

where D_{am} is the permeant diffusivity in the amorphous polymer.

The tortuosity τ characterizing a two-phase medium comprising an impenetrable phase dispersed in a permeable continuum only depends on the volume fraction X occupied by the non-permeable domains. In this respect, reference is often made to the relationship:

$$\frac{1}{\tau} = (1 - X)^n$$

n ranging from 1.25 to 1.90, depending on the nature of the sample.

We are therefore led to conclude that pervaporation fluxes through a membrane made of a semicrystalline polymer should significantly decrease as the crystallinity of this polymer increases. This prediction is fully consistent with experimental observations made during pervaporation of water–ethanol mixtures through homogeneous polyvinylalcohol (PVA) membranes differing by their crystallinity. The results reported in Fig. 5.20 clearly illustrate the lower permeability of the most crystalline samples [58]. A similar decline was observed by Perrin [59] in the value of the intrinsic diffusivity D_w^* of water in PVA, measured by sorption or desorption kinetics (see table below):

Crystallinity of the PVA sample (%)	28	37	44	56
Intrinsic diffusivity of water at 40°C $10^{11}\, D_w^*$ ($cm^2\, s^{-1}$)	4.2	3.3	2.3	1.5
Plasticization parameter γ_w	7.9	6.9	5.8	4.7

Since pervaporation mass transport only proceeds through the amorphous channels of membranes made of semicrystalline polymers, it would seem that

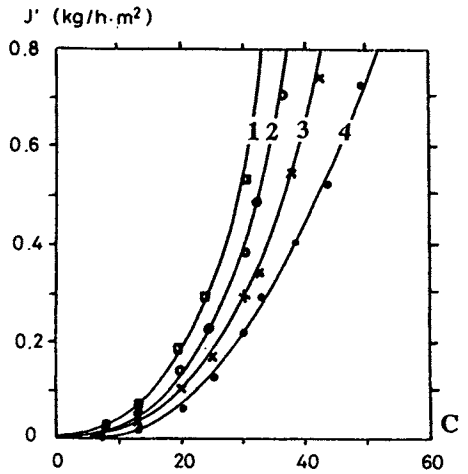

Fig. 5.20. Pervaporation of water–ethanol mixtures through homogeneous, 25 μm-thick polyvinylalcohol membranes differing by their crystallinity X. Percent crystallinity X = 29 (1), 33 (2), 37 (3), 40 (4), deduced from the density of the membrane. T = 45°C. c = Feed water content (wt%). Pervaporation flux J' vs. c.

selectivity should not significantly depend on the crystallinity of the membranes. As shown in Fig. 5.21, where ethanol permeation rates through different PVA membranes used to separate water–ethanol mixtures are plotted vs. feed water content, this is not experimentally corroborated. This discrepancy may be explained by the following side phenomena:

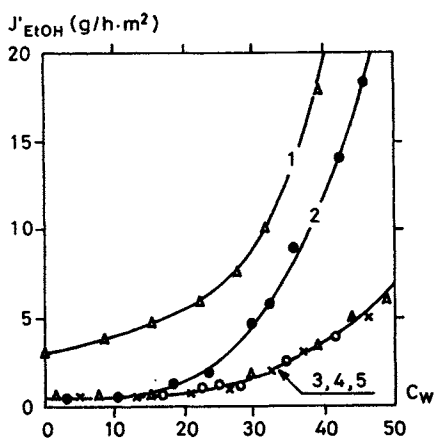

Fig. 5.21. Pervaporation of water–ethanol mixtures through homogeneous, 25 μm-thick polyvinylalcohol films differing by their crystallinity X. Percent crystallinity X = 27 (1), 33 (2), 37 (3), 40 (4), 56 (5). Influence of crystallinity on transport selectivity appreciated by referring to ethanol permeation flux J'_{EtOH}. T = 45°C. J'_{EtOH} vs. c.

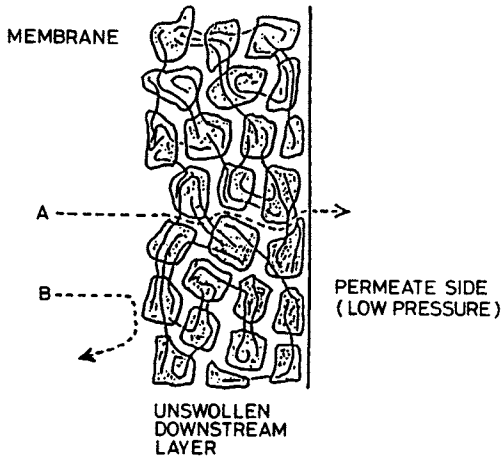

Fig. 5.22. Diffusion selectivity caused by intercrystalline sieving effect in the non-swollen downstream layer of the working membrane.

- Preferential sorption by the strained amorphous intercrystalline phase may be influenced by the crystallinity of the membrane polymer if the blocking factor b is different for the two penetrants.
- We may also conceive that diffusion selectivity in the non-swollen downstream layer of the working membrane could depend on crystallinity. In fact, this selectivity is determined by the relative strength of specific short-range interactions between the permeant molecules and the membrane material and this balance can be influenced by the length and the mobility of intercrystalline chain segments. The latter phenomenon may be visualized as the "downstream intercrystalline sieving effect" illustrated in Fig. 5.22. It could provide an additional contribution making the PVA-based membranes very efficient for dehydration of ethanol.

5.3.3.5 Coupling Effects in Pervaporation

In view of the difficulties entailed in a complete thermodynamical analysis of pervaporation transport, in the case of binary feed mixtures, we understand why the coupling effect has often been reduced to a simple drag effect arising from attractive molecular interactions between the two migrants. Accordingly, Kedem [62] expresses each individual permeation rate as follows:

$$J'_1 = -\mathcal{P}_1 \frac{dc_1}{dz} + k\, c_1 J'_2$$

The first term, proportional to the concentration gradient of component 1, corresponds to diffusional transport while the second accounts for the addi-

tional flux of component 1, which is dragged by the flow of component 2. Parameter k, usually called "drag parameter", quantifies the relative magnitude of the two processes.

This parameter has probably not the same value at any place in the working membrane. In fact, it is hardly conceivable that the mobilities of the two penetrants could greatly differ in the swollen part of the barrier. When it diffuses through this region, the mixed penetrant probably behaves as a unique migrant exhibiting intermediate properties. If such conditions were fulfilled throughout, the drag term would largely prevail and the permeate should have the same composition as the sorbate. Pervaporation and sorption selectivities should be equal. In reality, the influence of the drag effect probably vanishes as contacts between penetrant molecules and the functional groups belonging to the membrane polymer increase in number. Specific interactions between permeant molecules and the membrane polymer progressively prevail over dragging forces between components A and B. It is therefore conceivable that the respective mobilities of the two migrants could be distinctly affected by these interactions with the membrane polymer. In other words, diffusion then contributes to the selectivity of pervaporation transport. It is probable that this situation occurs in the part of the working membrane which is not extensively swollen by the permeants, i.e., in the vicinity of its downstream surface.

These concepts are consistent with the fact that a significant part of the selectivity exhibited by polyvinylalcohol membranes used to dehydrate water–ethanol mixtures is due to selective diffusion in the non-swollen downstream layer of the working membrane (Fig. 5.14). Accordingly, diffusivity measurements carried out by Perrin [59] show that the intrinsic diffusivities of water (D_w^*) and ethanol (D_{EtOH}^*) in polyvinylalcohol largely differ from each other. Comparing, at 40°C, the sorption kinetics of water and ethanol vapors in homogeneous polyvinylalcohol membranes (56% crystalline), this investigator deduces:

$$\text{Water:} \quad D_w^* = 1.49\ 10^{-11}\ \text{cm}^2\ \text{s}^{-1} \qquad \gamma_w = 4.66$$

$$\text{Ethanol:} \quad D_{EtOH}^* = 1.04\ 10^{-13}\ \text{cm}^2\ \text{s}^{-1} \qquad \gamma_{EtOH} = 14.4$$

γ being the parameter included in the expression $D = D^* \exp(\gamma c)$ where the penetrant concentration c is expressed in g g^{-1}. It appears that, in the nearly dry polymer, the diffusivity of water is more than one hundred times as high as that of ethanol.

One may therefore conceive that the magnitude of the drag effect could progressively decrease as the mixed permeant diffuses from the upstream to the downstream interface. This is consistent with the assumption that the additional selectivity provided by diffusion originates from the unequal resistance opposed by the virtually dry downstream layer of the membrane to the

transport of the two migrants. If so, the steady-state concentration profile of the slow permeant may be expected to accommodate a particular shape. In the swollen part of the membrane, both migrants should behave similarly, their concentration profiles showing the usual convex shape starting from an original upstream concentration directly related with the swelling uptake of the relevant component. As permeants approach the downstream surface, their respective mobilities progressively deviate more and more from each other so that the rejected component accumulates in this region. In certain extreme cases, this phenomenon, somewhat similar to concentration polarization, could induce, over a short distance, a reversal in the curvature of the concentration profile of the slow component, which is then dragged against its own concentration gradient, over a very small space interval, by the flow of the fast permeant.

So far, the literature provides only one experimental observation of this effect. It concerns the pervaporation transport of water–acetic acid mixtures through aromatic polyamide membranes and is reported by Matsuura [63]. This experiment, however, is not fully convincing since it makes use of the classical film-stack technique to recognize the steady-state concentration profile of the permeants across the working membrane. According to this procedure, a stack of several identical films is used as pervaporation barrier. When the steady-state transport regime is attained, the cell is disconnected from the vacuum line and the stack of membranes is dismantled. It is then blotted free of surface liquid and is rapidly separated into the individual layers, which are then separately weighed and titrated by gas chromatography technique. It seems clear that, during this operation, concentration profiles are likely to become flat. In fact, their exact recognition would require an improved experimental technique allowing them to be visualized in the thickness of the working membrane.

5.3.3.6 Origin of Downstream Diffusion Selectivity

The additional diffusion selectivity that makes the polyvinylalcohol membranes so efficient for the dehydration of organic liquids was previously taken as a consequence of the so-called "downstream intercrystalline sieving effect". It is clear that this explanation does not hold for other highly performing hydrophilic membranes devoid of any crystallinity, such as ion-exchange membranes.

In fact, homogeneous membranes obtained from macromolecular polyacids prove to be very selective to water after neutralization by immersion into aqueous solutions of various mineral hydroxides [64–66]. A typical example is given by the membranes prepared by grafting acrylic acid onto a thin film of low density polyethylene, used after neutralization by the different alkaline bases [67]. Pervaporation of water–ethanol mixtures through such membranes show that their selectivity depends on the alkaline counterion.

$$H^+ < Li^+ < Na^+ < K^+, Rb^+$$

(Order of increasing selectivity for water)

$$\longrightarrow$$

With respect to permeability, it appears that permeation rate increases according to the same sequence. Surprisingly, the exchange of Li^+ for K^+ ions enhances both permeation rate and selectivity.

In their salt form, all of these membranes are hydrophilic and, after immersion into water–ethanol mixtures, absorb water preferentially. However, they differ by the magnitude of the gap between sorption and pervaporation selectivities. Comparison between lithium and potassium salts shows that the gap which separates the two selectivity curves is greater in the case of the potassium salt, which also ensures the most selective pervaporation transport of water. This suggests that this greater pervaporation selectivity might be due to some particular behavior of water molecules faced with potassium carboxylate ion pairs, enhancing their mobility and, therefore, increasing the D^*_w/D^*_{EtOH} ratio.

IR spectrometry has been successfully used to obtain information about interactions between water, ethanol and this type of membrane material. Reflection spectra have been recorded in the interval between 1300 and 1700 cm^{-1} relevant to vibration modes of carboxylate groupings [68]. The membranes were successively examined in their acid and salt forms.

The most interesting observations were made by comparing the spectra of the resulting membranes after impregnation with water–ethanol mixtures containing 0–20 wt% water. It appeared that, for a given salt, a splitting of the band ascribed to the antisymmetrical vibration of the carboxylate groupings is observed when the proportion of water in the mixture exceeds a definite threshold value called "critical water concentration" (CWC). The CWC depends on the nature of the counterion and it has been shown that the splitting of the band occurs when the vibrations of the carboxylate groupings are perturbed by the insertion of water molecules and the consequential loosening of the ion-pairs. In other terms, the CWC decreases as the relevant ion-pairs are more and more readily penetrated by water molecules.

It is therefore of interest to compare the CWC observed with the different alkaline forms of the investigated ion exchange membrane. Experimental results reported below show a rather good correlation between the CWC measured with each film and its selectivity to water when it is faced with water–ethanol mixtures.

Cation M^+	Li^+	Na^+	Rb^+	K^+
CWC (wt%)	17.5	9	7	5
Increasing selectivity to water	$\longrightarrow$			

Actually, the membrane appears as more selective as the relevant CWC is lower. One can therefore deduce that insertion of water molecules into ion-pairs and their extraction out of their clusters present in the feed mixture, enhances their mobility in the virtually dry membrane material. As a consequence, the intrinsic diffusivity of water in the polyelectrolyte is higher as the relevant ion pairs are more readily penetrated by water molecules. Combined with preferential sorption at the upstream surface of the membrane, this additional effect, which takes place in the non-swollen downstream layer of the working membrane, makes the potassium form more selective.

5.4 ENGINEERING OF PERVAPORATION

To be used at the industrial scale, pervaporation must be designed as a continuous-flow process. The low magnitude of permeate fluxes through non-porous permselective membranes does not favor the use of cascade devices. In this respect, pervaporation cannot advantageously compete with conventional distillation when the latter is selective, since distillation is an iterative process whereas pervaporation is generally confined to one transfer through the permselective membrane used. However, it is worth comparing the respective performances of the two techniques when vaporization selectivity is nil or very low, i.e., in the case of azeotropes or mixtures of close boiling-temperature liquids. Actually, in such cases, distillation is generally replaced by more sophisticated and energy-consuming techniques such as vacuum or extractive distillation and the high selectivity of the membrane process can make it more advantageous.

In itself, pervaporation is not a complete separation technique. It is generally designed as a continuous-flow operation, which makes it possible to alter the composition of a flowing liquid mixture A–B by extracting, through the permselective membrane, a permeate enriched in one of the feed components. For instance (Fig. 5.1), pervaporation can be used to further process an azeotropic mixture emerging from a predistillation column by circulating it through a pervaporator equipped with a membrane preferentially permeable to the minor component (A). Depending on the permeability and on the selectivity of the membrane, the contaminant is more or less rapidly extracted. The residence time required to obtain a refined retentate, in which the residual contaminant content is reduced to a fixed c_t level, is determined not only by the intrinsic characteristics of the membrane used, but also by the required purification ratio $x = c_o/c_t$, c_o and c_t being the A-contents in the feed (c_o) and in the retentate (c_t), respectively. Quite obviously, the more permeable and selective the membrane, the greater is the production capacity of the device.

In a continuous-flow module, the membrane does not work under the same conditions throughout since it is faced with a liquid mixture that becomes

poorer and poorer in contaminant as it approaches the outlet of the device. It is therefore clear that the performance of the system can be predicted only if one knows how the composition of the facing mixture influences the permeability and the selectivity of the membrane, within the $[c_o, c_t]$ concentration range.

It is also noteworthy that pervaporation is far from being an isothermal process, even if the temperature of the incoming feed is carefully controlled. In fact, vaporization of the permeate at the downstream surface of the membrane causes local cooling, which induces a temperature gradient across the barrier. As a consequence, the temperature of the flowing retentate also decreases as it proceeds along the module and, in the steady-state transport regime, a definite temperature profile is established between the two opposite ends of the module.

5.4.1 Equations Governing Continuous-flow Pervaporation

From the above considerations, it clearly appears that pervaporation is a complex multigradient process and that modeling is necessary to evaluate the performance of a module equipped with a membrane of known characteristics [2]. The basic equations governing the process are the three differential equations which formulate mass and heat balances for the elementary volume of flowing liquid comprised, at a given time, within z and z + dz cross-sections (Fig. 5.23).

Overall mass balance

$$dJ = J'(c, T)\, p\, dz$$

where J is the retentate flow rate through the z cross-section, $J'(c, T)$ accounting for the fact that permeation flux J' depends on the composition (c) and on the temperature (T) of the facing liquid mixture, p standing for the perimeter of the module cross-section.

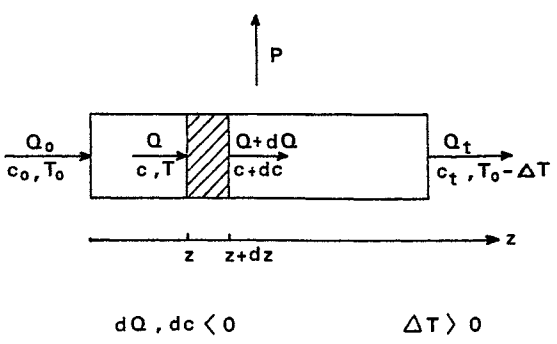

Fig. 5.23. Analysis of continuous-flow pervaporation. Q: Flow rate through the pervaporator; Q_0: inlet flow rate; Q_t: outlet flow rate; P: permeate; J': permeation flux.

Mass balance relative to the faster permeant

$$d(Jc) = c\,\beta(c, T)\,J'(c, T)\,p\,dz$$

which, combined with the preceding equation, yields:

$$J\,dc = [\beta(c, T) - 1]\,c\,J'(c, T)\,p\,dz$$

Heat balance

$$dH = J'(c, T)\,\Delta H'(c')\,p\,dz = J\,k(c)\,dT$$

where the permeate latent heat of vaporization $\Delta H'(c')$ and the retentate heat capacity $k(c)$ are deduced through linear interpolation from the characteristics of the individual components A and B.

This set of differential equations can be numerically integrated by the usual Runge–Kutta method after inserting, into the computer program, the boundary values c_0 and T_0 and all other required data, i.e., the empirical functions $\beta(c, T)$ and $J'(c, T)$ — which were previously experimentally calibrated — and the individual thermal characteristics L_A, L_B (latent heats of vaporization) and k_A, k_B (specific heats) of A and B. Calculations are run after definition of an elementary space interval dz and the results delivered by the computer generate the three functions $J(z)$, $c(z)$ and $T(z)$. The operation is stopped when $c(z)$ attains the required c_t limit. The corresponding z value ($z = \lambda$) can then be used as critical length to estimate the performance which may be expected from a unit module (equipped with 1 m^2 of membrane) working in the imposed conditions.

Production capacity of a unit module

$$J_t = \frac{J(\lambda)}{p\,\lambda}$$

Recovery yield of B in the purified retentate

$$R = \frac{J_t\,(1 - c_t)}{J_0\,(1 - c_0)}$$

Average composition of the permeate

$$\langle c' \rangle = \frac{J_0 c_0 - J_t c_t}{J_0 - J_t}$$

Energy cost of the process

$$E = \frac{(J_0 - J_t)\,\langle L' \rangle}{J_t}$$

where $\langle L' \rangle = \langle c' \rangle\,L_A + (1 - \langle c' \rangle)\,L_B$.

In many cases, it appears that the temperature drop $\Delta T = T_0 - T(\lambda)$ between the feed and the outgoing retentate is too large to be accepted, because a significant part of the membrane would then operate at low temperature and would only deliver a small permeate flux. That means that heat should be supplied to the module to make it work under more isothermal conditions. A practical solution to this problem consists in dividing the pervaporator into several submodules and in reheating the flowing retentate by passing it through intermediate heat exchangers. To account for this external intervention, numerical integration is stopped when $\Delta T = T_0 - T(z)$ attains a fixed allowed magnitude (10°C, for instance). Temperature index is then brought back to T_0 and calculations are resumed, starting now from J and c values given by the preceding run. This operation, which simulates an intermediate reheating between two successive submodules, is reiterated as many times as necessary to keep the temperature of the flowing liquid mixture within the imposed range.

5.4.2 Application to a Typical Case: Dehydration of Ethanol

Relying on the above analysis, it is possible to predict the performance of a pervaporation module equipped with 1 m^2 area of permselective membrane and used to achieve a given separation.

Results below concern the hydrophilic composite membrane produced by Gesellschaft für Trenntechnik mbH (GFT), obtained by coating a porous support film of polyacrylonitrile with a thin layer (4 μm thick) of crosslinked polyvinylalcohol. If it is used to dehydrate, at 90°C, water–ethanol mixtures containing less than 10 wt% water, this membrane is characterized by the graphs reported in Fig. 5.24.

Let us consider the processing of the water–ethanol feed containing 6% water (by weight), to produce dehydrated alcohol in which the water content is reduced to 0.3%. Insertion of these requirements into the computer program leads to the following evaluations:

Productive capacity:

J_t = 2.5 kg of ethanol (99.7%) per hour and m^2 of membrane area

Ethanol recovery yield:

R = 98%

Energy cost of the process:

E = 81 kcal per kg of ethanol (99.7%)

These predictions can be compared with the observations made in pilot-units and in the earliest industrial pervaporation plants.

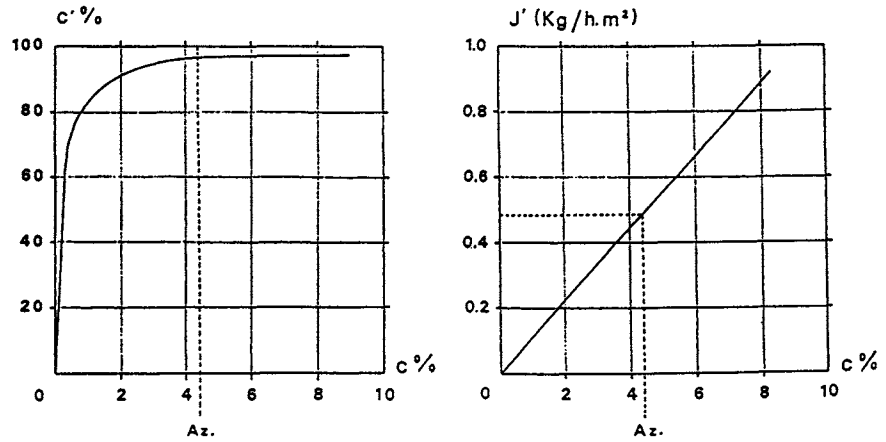

Fig. 5.24. Characteristics (selectivity and permeate flux J') of the PVA-based GFT composite membrane when it is used at 90°C to dehydrate water–ethanol mixtures of low water content. c, c': Feed (c) and permeate (c') water contents (by weight).

With respect to energy cost, some precise data are reported by Sander [69,70]. They concern a test operation carried out by Lurgi Company over a period of two years. Pervaporation was used to produce 6,000 liters per day of water-free ethanol. The feed, emerging from a distillation column, contained 6% water by weight and the process was designed to reduce this concentration to 0.3% in the outgoing retentate. The operation was carried out at 90°C, using Lurgi modules equipped with the GFT membrane. After a working period of two years, the energy cost of the process was estimated as shown in Table 5.4, reproduced from the reports by Sander [69,70]. In this table, the thermal energy consumed by pervaporation is evaluated at 0.126 kg of steam (under 1.5 bar) per kg of refined alcohol. This value, which is roughly equivalent to 80 kcal kg^{-1} of ethanol, is very close to that previously calculated. As stressed by Sander,

TABLE 5.4

Dehydration of the water–ethanol mixture containing 6 wt% water, reducing the residual water content to 0.3%. Comparison between the respective energy costs of entrainer distillation and pervaporation [69,70].

Requisites	Energy cost per kg of ethanol 99.7	
	Entrainer distillation	Pervaporation
Low pressure steam (kg)	1.0–1.6	0.126
Cooling water	76	20
Electrical power	0.016	0.038

pervaporation consumes much less thermal energy than entrainer distillation, but the membrane process requires a little more electrical energy.

These conclusions were further corroborated by observations made in the pervaporation dehydration plant subsequently started by GFT in the sugar refinery of Béthéniville, France. This plant is designed to produce, per day, 150,000 liters of dry ethanol. The modules work at 90°C, to reduce the water content from 7 to 0.2 wt%. In these operational conditions, which are a little more severe than those required in the preceding case, measured thermal and electrical energy costs were found equal to 0.14 kg of steam (under 1.6 bar) and 0.044 kWh kg^{-1} of ethanol, respectively. Considering that the Béthéniville plant needs 2200 m^2 of membrane area to deliver 150,000 liters of dehydrated ethanol every day, one can deduce that the production capacity ensured by 1 m^2 of membrane area is 2.24 kg of alcohol per hour. This result is also in good agreement with the predictions of theoretical calculations.

5.4.3 Side Effects in Pervaporation Engineering

Pervaporation engineering is sometimes faced with side effects casually causing significant reduction in the performance of the process.

5.4.3.1 Concentration Polarization in Pervaporation

As other membrane separation techniques, pervaporation may be disturbed by concentration polarization. Generally, this perturbation is small in that case, compared to that observed in ultrafiltration or other techniques using porous membranes, since mass transport through non-porous membranes is slow. In pervaporation, it is clear that concentration polarization intervenes only on the feed side of the working membrane since permeate desorption under low pressure, at the downstream surface of the membrane, is not selective. Of course, the importance of concentration polarization effects depends on a number of parameters among which are the nature and the composition of the processed mixture, the permeability and the selectivity of the membrane used and the flow hydrodynamics imposed to the processed liquid mixture.

Regarding the influence of feed composition, we must realize that in pervaporation the concentration polarization effect results from depletion of the more rapidly permeating component in the vicinity of the feed/membrane interface. In practice, this component is generally the minor component of the processed mixture and we may consequently consider that concentration polarization is then due to the slow diffusion of this solute from the bulk of the feed to the boundary layer. We may therefore expect that this perturbation is all the more pronounced as the preferentially extracted component is less concentrated in the feed. It should also intensify upon increasing the permeation rate

by using more permeable or thinner membranes. All of these anticipations are corroborated by experimental observation. For instance, let us specify that dehydration of the water–ethanol azeotrope (containing 4.4 wt% water) by pervaporation through the polyvinylalcohol-based GFT membrane, is not significantly disturbed by boundary effects, as long as the residual water content in the processed mixture remains higher than 1% by weight. Below this limit, which is passed in the last modules of an industrial dehydration plant, some care must be taken of the flow hydrodynamics. This sometimes leads to modification of the design of the pervaporation plates or to acceleration of the flowing processed stream by insertion of the modules into a circulation loop. By comparison, more intense concentration polarization effects have been observed [71] during the dehydration of water–isopropanol mixtures by pervaporation through hydrophilic ion-exchange membranes. The latter being more permeable than the conventional GFT membrane, boundary effects are then observed over the entire subazeotropic water concentration range (0–11% by weight).

An elegant demonstration of the influence of concentration polarization in pervaporation was given by Gref [58], who compared the performance of the same membrane successively used to process the two conjugate phases in equilibrium in a binary mixture of partially miscible liquids, such as *n*-octanol and water. In fact, pervaporation being driven by activity gradients, the same permeate should be obtained, at the same rate, in both cases, if no boundary layer phenomena intervene. The curves reported in Fig. 5.25 represent the pervaporation fluxes J' observed at 40°C during experiments comparatively carried out with the two conjugate phases that separate from each other in

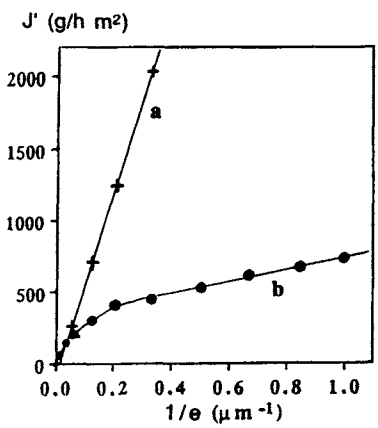

Fig. 5.25. Pervaporation of the two conjugate liquid phases which equilibrate each other in *n*-octanol–water mixtures (T = 40°C). Membranes: Homogeneous cellulose acetate membranes differing by their thickness e. a: Water-rich phase (water content = 99.9 wt%); b: organic-rich phase (water content = 4.7 wt%). Permeation rate vs. $1/e$.

octanol–water mixtures. They contain 4.7 and 99.9 w% water, respectively. A set of experiments was run with a series of homogeneous membranes of cellulose acetate (acetyl content = 39%) differing by their thickness e, which was varied from 2 to 10 μm. It clearly appears that pervaporation of the water-rich phase through those hydrophilic cellulosic barriers is not disturbed by concentration polarization since corresponding plots J' vs. $1/e$ fall perfectly on a straight line starting from the origin of the diagram. On the contrary, pervaporation of the water-poor phase is strongly decelerated by water depletion of the liquid charge, in the vicinity of the upstream surface of the working membrane. The ratio between the two ordinates corresponding to same film thickness virtually equals the polarization factor characterizing the disturbed transport regime. This factor progressively increases as the thickness of the membrane is reduced and as mass transport accelerates.

Of course, concentration polarization is the major impediment that opposes the use of pervaporation through an organophilic membrane made of polydimethylsiloxane (PDMS), ethylene/propylene rubber (EPR) or polyether-block-amide (PEBA) to remove trace organic pollutants contaminating water. In this field, a number of investigators (see table below) came to similar conclusions [72–75]. In most cases, the concentration polarization effect is more determining for the process than permeant diffusion across the membrane and the resistance opposed by the boundary layer governs the contaminant extraction rate. In such an occurrence, it is more important to control the flow hydrodynamics of the processed liquid than to improve the performance of the permselective membrane [76]. The situation is more favorable if the organic component is but sparingly soluble in water since transport selectivity is then enhanced by the thermodynamical non-ideality of the facing liquid mixture.

Organic solute	Concentration	Membrane	Author
Trichloroethylene	0.05–0.25 ppm	Silicone tubing	Psaume and al. [72]
Trichloroethylene	10–50 ppm	PDMS hollow fibers	Coté et al. [73]
Carbontetrachloride	15–30 ppm		
Chloroform	—		
Phenol	40–200 ppm		
Toluene	250 ppm	Ethylene–propylene rubber	Nijhuis [74]
Trichloroethylene	250 ppm		
Toluene	0.4–0.8 ppm	PDMS flat sheet	Hwang et al. [75]
Phenol	50–1200 ppm	PEBA or PDMS	

The same comments also hold for extraction of the aroma compounds dissolved in aqueous media. In this respect, many investigations have been carried

out to evaluate the performance of pervaporation in the processing of fruit juices [77–79], apple essence [80] and fermentation broths in which aroma products are generated [81–84). In these complex mixtures, the solubility of each solute is affected by the presence of all the others and this is also true for its extraction rate through the contacting pervaporation membrane. As a consequence, data obtained through experiments carried out with "model solutions" containing some of the feed components only, cannot be conclusively used to evaluate the applicability of pervaporation to the investigated problem.

5.4.3.2 Residence Time Distribution in Pervaporation Modules

Equations previously established to evaluate the productivity of a unit pervaporator and to predict the yield and the energy cost of a given separation are based on the assumption that the feed assumes a laminar plug-flow. This condition is not fulfilled in every case. In a plate-and-frame module, the flow regime of the processed liquid is not precisely defined and the residence time of the feed in a given plate is somewhat disperse. This can be shown by means of the well-known tracer technique, using a dye or a mineral salt as indicator [85]. The dispersity thus evidenced can cause some heterogeneity in the quality of the emerging retentate since the whole of the flowing mixture is not in contact with the membrane for the same lapse of time. At the exit of each pervaporation plate, some backmixing can therefore take place, reducing the performance of the process.

The only way to palliate those undesirable effects consists in narrowing the residence time distribution of the processed mixture in each plate by an appropriate disposition of the inlet and outlet tubes and a proper geometry of the spacers. Generally, in industrial units, backmixing is practically negligible since, at the two opposite ends of each module, the composition of the entering feed and that of the emerging retentate do not largely differ if the system is designed to keep the corresponding temperature drop within acceptable limits.

5.4.3.3 Pressure Loss in Pervaporation Modules

The reasons why downstream pressure strongly influences pervaporation performance have already been explained. Any rise in permeate pressure provokes a decline in transport rate and a change in selectivity. Both variations become very steep as downstream pressure approaches the saturated vapor pressure of the permeate.

In practice, it is therefore necessary to fix the permeate pressure if one wants to stabilize the working regime of a pervaporator. The major difficulty to overcome is the pressure loss in the downstream part of the module. It results from two successive drops occurring first in the porous material supporting the selective dense layer of the composite membrane and then in the downstream

compartment itself. The latter may be important if the permeate is extracted through the bores of hollow fibers except if special devices equipped with short fibers are used [86]. Until now, hollow fiber pervaporators are not yet developed and the modules so far used in industrial applications are of plate-and-frame or multitubular type. Presently, efforts are being made to manufacture spiral wound modules, safer and less expensive than stacks of plates. In achieving this, the aggressiveness of hot solvents and the necessity to avoid any pressure drop in the permeate channels raise the most difficult problems [87].

5.4.3.4 Pervaporation and Vapor Permeation

Vapor permeation (VP) differs from pervaporation (PV) in that the feed is a mixed vapor instead of a liquid mixture. In both cases, the driving force for mass transport is the difference in the chemical potential of the penetrants between the feed and permeate side of the membrane, the downstream face of which is maintained under low pressure.

At first sight, VP has several theoretical advantages over PV. In the former process, no phase change takes place during the transfer across the membrane and the problems involved with supplying the enthalpy of vaporization are therefore avoided. Furthermore, concentration polarization on the feed side no longer exists since the feed is a vapor.

In practice, however, the situation is far from being so advantageous. In fact, upstream partitioning equilibrium is the same in both processes only if the incoming vapor remains saturated all along the feed channel and if it does not contain noncondensable gases. At the technical level, these requirements are not easily fulfilled because of unavoidable pressure losses in the flowing feed stream. In most experiments carried out with this technique, undesirable condensations were observed in the upstream compartment of the module and a stagnant liquid film appeared on the surface of the membrane.

It is generally reported that, for a given mixture, PV and VP have approximately the same selectivity while mass transport is significantly slower in the latter process [88,89]. On the other hand, Sander [90] claims that both processes ensure the same flux and selectivity and he gives some information concerning an industrial vapor permeation plant used to dehydrate different alcohols (ethanol and isopropanol). This unit was started in 1990 by Lurgi Company at the Sprit und Chemische Fabrik L. Brüggemann KG, in Heilbronn, Germany.

From the economical point of view, it is clear that the processing of liquid mixtures by VP first requires the complete vaporization of the feed. The energy consumed by this preheating is partly recovered only, by heat exchange with the outgoing retentate stream. Vapor permeation may therefore only be advantageous if the feed mixture is available in the vapor state, e.g, if it emerges from the top of a distillation column.

5.4.3.5 Integrated Systems Involving Pervaporation

Quite generally, pervaporation does not operate alone but is combined in so-called "integrated systems" with other conventional separation techniques such as distillation, absorption, phase separation, reverse osmosis and countercurrent washing or extraction. It may also be used to assist reversible chemical reactions or to improve the yield of fermentation processes. In each particular case, the design of the integrated operation must be specifically optimized and, in the following, some illustrative combinations will only be mentioned.

A first example is provided by the recovery of organic solvents (isopropanol, isobutanol, *n*-butanol,...) present as diluted solutes (1–5 w%) in aqueous solutions [91]. It has been suggested to start the processing by partial extraction of water by means of reverse osmosis. In a second step, the organic-enriched retentate is collected in a decantation tank where two liquid phases separate. The alcohol-rich supernatant layer, containing about 30% water, is dehydrated by pervaporation since this technique is perfectly fitted to pass over the azeotropic composition. This hybrid process has been designed to recover valuable alcohols present at a concentration of about 4% in the aqueous layer that separates during decantation of the steam-stripping condensates obtained after regeneration of fixed beds of absorbing charcoal.

In another typical integrated operation, pervaporation through hydrophilic membranes was used to accelerate the esterification of carboxylic acids by alcohols. The feasibility of the process was appreciated at the laboratory scale, by circulating the reacting mixture in a loop passing through a pervaporation cell equipped with the polyvinylalcohol-based hydrophilic GFT membrane [92–94]. Tests were carried out with the pairs propionic acid/propanol-1 and propionic acid/propanol-2 since the membrane used is perfectly impermeable to these reagents and is only passed by water generated by the reaction. Started with original mixtures containing equimolar amounts of acid and alcohol, those experiments showed that assistance by pervaporation makes it possible to pass over the equilibrium conversion limit and to bring the reaction to completion. At the same time, the overall esterification rate increases since the opposite hydrolysis reaction is, at least partly, cancelled. Optimization of the system is realized when the rate of extraction of water through the membrane just equals that of its generation by the chemical reaction. If so, the residual water content in the reacting mixture remains virtually nil during the whole process and the overall kinetics of condensation merge with that of intrinsic esterification (without hydrolysis). For this purpose, the ratio between the membrane surface area and the volume of reacting mixture must be fixed at an optimal value, which can be calculated if all data concerning the condensation kinetics and the membrane permeability are known.

Of course, if the permselective membrane is in direct contact with the reac-

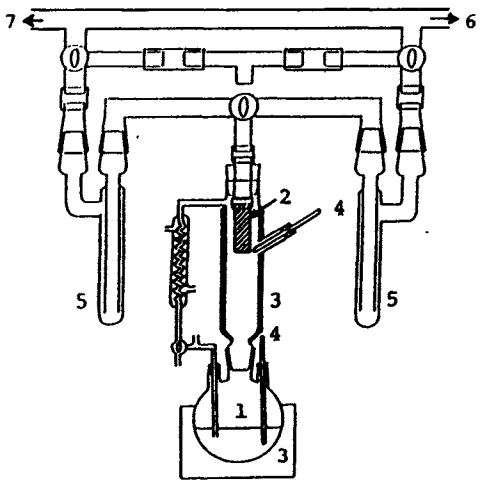

Fig. 5.26. Laboratory device used by Kita et al. [95] to assist esterification by vapor permeation.

tants, one may question about its stability since it is made of a polyalcohol that can also be slowly esterified. It is the reason why an alternative combination has been suggested (Fig. 5.26) in which vapor permeation is used instead of pervaporation to ensure continuous dehydration of the vapor released by the heated reacting mixture [95].

At the industrial level, too, experiments were carried out to evaluate the real advantage resulting from assistance of esterification by pervaporation [96]. Test operations were also run with mixtures of isopropanol and propionic acid. Esterification was started by reacting a mixture containing an excess of alcohol acting as entrainer to extract water generated by condensation of the two reagents (Fig. 5.27). The released vapor was then processed in a distillation column to separate the water–isopropanol azeotrope (11 wt% water), which is too rich in water to be directly recycled into the reactor. Insertion of an intermediate pervaporation module then made it possible to process this azeotropic mixture and to return dehydrated isopropanol to the reactor. Thanks to that slight modification, the residual water content in the reacting mixture was maintained very low and esterification was significantly accelerated. As a result, the production capacity of the system was approximately increased by 30–40%.

It was also suggested to increase the yield of fermentation reactions by means of pervaporation [97]. In most bioreactions, the fermentation product exerts an inhibitory effect on the microorganism used. In the case of ethanolic fermenta-

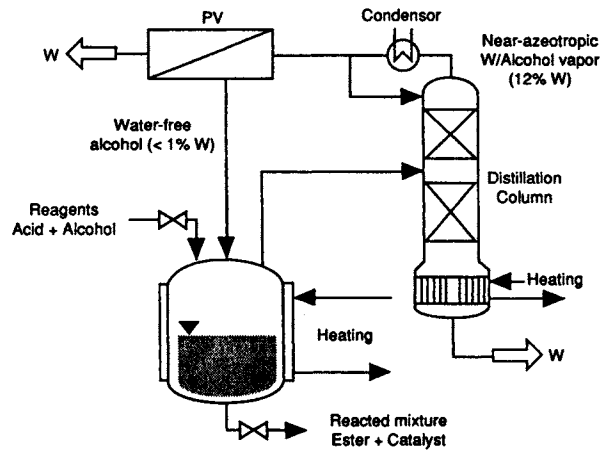

Fig. 5.27. Pilot-scale pervaporation-assisted esterification of isopropanol (according to A. Dams et al., BASF, Germany [96]).

tion, for instance, the reaction slows down when the ethanol content of the broth is higher than 5–6%. Several experiments were carried out with integrated bioreactor–pervaporator systems in which ethanol produced was continuously extracted by pervaporation through an organophilic membrane. In this respect, we may mention the investigations reported by Sodeck [98] and Gudernatsch [99]. In the device designed by the former, ethanol was extracted through a set of permselective silicone-based tubes, while the latter made use of composite hollow fibers with the active layer inside. In both cases, the membrane was of composite type, comprising a porous polysulfone support coated with an organophilic polydimethylsiloxane layer. The conclusions drawn by these two authors are very similar and may be summarized as follows:

1. The heat required to vaporize the permeate can be supplied by the bioreaction itself, since fermentation is an exothermic process.

2. If a sweeping gas is circulated to remove permeated ethanol, oxygen can be supplied to the microorganism by using oxygen-containing mixtures.

However, despite this promising outset, pervaporation is not yet extensively used to assist industrial bioreactions. In fact, several conventional techniques are already available to extract ethanol released during fermentation. For instance, it can be removed by stripping (the major drawback is foaming) or by evaporation under reduced pressure (the microorganisms are then partly deprived of oxygen). As indicated, each of those techniques presents some disadvantage and this is also true for the pervaporation-aided process. In the latter case, difficulties actually arise in the monitoring of the system because it is not easy to keep constant the population of active living cells in continuously working fermenters.

5.5 MANUFACTURE OF PERVAPORATION MEMBRANES

Thin, homogeneous, nonporous membranes can be shaped by evaporation of a polymer solution previously degasified and cast on a horizontal surface. Depending on the nature of the starting polymeric solute (elastomeric, semicrystalline or glassy polymer), membranes produced in this way are smooth, mechanically resistant or brittle, respectively. Of course, materials belonging to the first two categories are preferred since they can easily be deposited as thin dense layers. Investigation of these homogeneous samples has shown that elastomers are more permeable whereas semicrystalline materials are more selective. The latter can therefore be used to shape composite membranes by casting a selective skin layer onto a porous reinforcing support.

5.5.1 Hydrophilic Pervaporation Membranes

The well-known phase inversion process widely used to produce asymmetric reverse osmosis membranes is generally unsuitable to manufacture pervaporation membranes since it does not enable us to adjust the structure of the porous sublayer. Tests performed with commercial reverse osmosis membranes designed for desalination of water showed that these membranes, in spite of their hydrophilicity, do not prove to be very effective when they are used to dehydrate water–organic liquid mixtures by pervaporation.

Membranes used in modules so far working in industrial pervaporation plants are generally of composite type. They are prepared by coating a porous support of definite structure with a thin, dense layer of permselective polymer. During its formation, the superimposed skin is slightly crosslinked to reduce its ability to swell. This reaction is carefully controlled to optimize membrane selectivity and permeability. In the case of polyvinylalcohol, a typically semicrystalline material, crosslinking also prevents any further recrystallization of the deposited polymer, which would cause some instability in the transport properties of the resulting membrane.

In the composite configuration thus obtained, the structure of the porous support exerts a significant influence on the performance of the membrane. Pores must be wide enough to avoid undesirable pressure drop in the permeate stream but not too large to prevent any deep penetration of the coating material during the formation of the membrane. To fulfil these two opposite requirements, it is generally necessary to prepare tailor-made porous supports characterized by sharp pore size distribution, centered on an optimized mean diameter. For that purpose, new techniques such as plasma erosion are often resorted to.

This process has been developed by GFT to manufacture the earliest commercial hydrophilic pervaporation membranes now in use in several plants all over the world [100]. In these membranes, the porous polyacrylonitrile support

film, reinforced by a polyester nonwoven, is coated with a thin, dense, polyvinylalcohol-based, permselective layer. The latter is deposited by evaporation of an aqueous polymer solution containing unsaturated diacids, such as maleic acid, as crosslinking reagents. Of course, various membranes exhibiting slightly different characteristics can be produced from the same starting materials, depending on manufacturing conditions. For instance, the hydrophilic GFT membrane is now available in two variants labelled "High selectivity/Low permeability membrane" and "Low selectivity/High permeability membrane", respectively. They differ only from each other by the structure of the PVA layer, which is more or less tightly crosslinked. By proper selection, it is possible to optimize the performance of all modules involved in a given industrial process. Related membranes were recently developed for dehydration of chemically aggressive liquids, such as organic acids or amines. Contact with acidic feeds disrupts ester linkages in the crosslinked PVA layer of the standard GFT membranes. Resistant membranes were obtained after crosslinking them by more stable ether or carbon–carbon covalent bonds [101]. At high temperature, aliphatic amines simultaneously provoke the breaking of ester linkages, the dissolution of the polyacrylonitrile substrate and the degradation of the reinforcing polyester fabrics. To overcome this difficulty, a special polysulfone support film was developed in which the reinforcing material is made of cellulose or polyphenylenesulfide.

Similar composite membranes can also be produced by other techniques, such as the "film transfer coating" [102] in which the composite structure is obtained by colaminating the porous polyacrylonitrile support with a very thin, dense polyvinylalcohol film. The adhesiveness of the two layers is ensured after lamination, by heat or radiation treatment.

Hydrophilic pervaporation membranes are also manufactured from natural or synthetic polyacids or polybases. For instance, Japanese pervaporation modules Purerator, introduced by Tokuyama Soda Company [103], are equipped with hollow fibers spun from chitosan, a by-product recovered by treatment of lobster shells. One may also classify in this category the pervaporators produced by the British Company Kalsep [104]. They comprise 18 cylindrical permselective elements obtained by coating the inner surface of porous ceramic tubes with a thin layer of potassium polyacrylate. The transfer area corresponding to each bundle is approximately 1.2 m^2. These membranes are very permeable and selective to water, after neutralization by an appropriate alkaline hydroxide, such as potassium or cesium hydroxide. Their high permeability often makes it possible to ensure satisfactory permeation fluxes across 20 μm-thick, homogeneous, dense deposit. Their major disadvantage is the progressive decline of their performance during long-lasting use. This course results from the leaching out of the potassium or cesium counter-ions by exchange with protons from the flowing feed stream. To prevent this unfavor-

able trend, it was suggested to use high molecular weight polybases to neutralize the membrane material [105]. Attempts were therefore made to produce hydrophilic membranes from "polyelectrolyte complexes" by neutralizing polyacids by macromolecular polybases. The resulting membranes called "simplex membranes" were readily obtained on suitable support, by interfacial reaction between anionic and cationic polyelectrolytes. When they are faced with water–ethanol mixtures, they are as selective as polyvinylalcohol membranes and generally exhibit higher permeability [106].

The following table mentions typical polyelectrolytes used as starting materials in this manufacture.

Polyanionic component	Polycationic component
Sodium cellulose sulfate	Poly-(ethyleniminium chloride)
	Poly-(*N,N*-dimethyl-3,5-dimethylene-piperidinium chloride)
	Poly-(dimethyldiallylammonium chloride)

The attempts carried out by the Daicel Research Center [107] concern a typical hydrophilic composite membrane obtained by modifying polyacrylonitrile hollow fibers. A dense polyelectrolyte complex skin layer is generated on the inside wall of the fibers by reaction between the CO_2H-activated surface of the polyacrylonitrile capillaries and a flowing solution of polymeric quaternary ammonium salt.

An alternative way of producing pervaporation membranes is the use of radiation grafting to modify, by insertion of suitable comonomers, inert and resistant films of polyethylene, polytetrafluoroethylene, polyvinylfluoride or polyvinylidenefluoride. In the procedure named "Direct Radiochemical Grafting", the base film is immersed in a solution of the comonomer in a suitable solvent and then irradiated. The modified material is removed and carefully washed to extract the free homopolymer. In the "Delayed Radiochemical Technique", grafting is induced by macroradicals trapped in the preirradiated trunk polymer. The base film is activated by preirradiation under inert atmosphere and then contacted with a solution of the comonomer. A variant of the latter procedure consists in grafting the comonomer onto the starting material preactivated by formation of peroxide or hydroperoxide sites [108]. The support film, slightly peroxidized by irradiation under air, is stored in this state for several months at 5°C. The grafting process consists in contacting this activated material with a solution containing the comonomer and a small amount of ferrous

salt, which prevents rapid homopolymerization [109]. Heating then provokes homolysis of the peroxide linkages and initiates the graft-polymerization.

The common feature to all these grafting techniques is that radiations deeply penetrate into the exposed material and can therefore transform an inert film (polyethylene or polytetrafluoroethylene) into a functionalized permselective membrane. After this operation, the even distribution of comonomer units across the thickness of the film must be ascertained. This control is achieved by staining techniques (complexation with iodine in the case of *N*-vinylpyrrolidone moieties), by Differential Interference Contrast Microscopy or by X-ray scattering if the resulting membrane material contains acidic groupings able to exchange protons for heavy metallic cations. Since the distribution of grafted units is chiefly determined by penetration of the comonomer into the irradiated sheet, obtaining homogeneous membranes is time-consuming. This is the major drawback, which opposes the application of these grafting techniques at the industrial scale.

A more versatile procedure to manufacture appropriate composite pervaporation membranes is electron beam curing [110]. A suitable viscous oligomer containing polymerizable unsaturated end-groups is cast onto a porous support film and is further irradiated by UV light or by electron beams to generate a thin, dense permselective coating.

More recently, promising results were reported concerning the production of pervaporation membranes by plasma polymerization [110,111]. Plasma is a state of matter consisting of molecules, radicals and ionic particles and also comprising electrons and photons. If a solid substrate is exposed to a plasma, the action of all these reactive species results in distinct modifications, either in the substrate or on its surface, depending on the kind of plasma gas used. For the modification of polymer materials, only nonthermal plasmas are applied. These are generated by electrical glow-discharge under reduced pressure of gas (approximately 5 mbar) and application of a high-frequency electrical field. If this plasma is contacted with a microporous film (average pore diameter = 0.1 μm) laid on one of the electrodes, a dense layer settles on the free surface of the film. A precise control of operational conditions then allows this deposition to be adjusted in such a way that it completely covers the surface of the support film without penetrating deeply into the pores.

Actually, the chemical structure of the material deposited by plasma-polymerization is not precisely known. In fact, it is generally obtained from a complex mixture of chemically polymerizable and nonpolymerizable vapors. For instance, a mixture containing hexafluoroethane, perfluoropropane and tetrafluoroethylene can be used to prepare thin organophilic films. Moreover, it appears that the resulting structure depends on many operational parameters among which are the residence time of the vapors in the plasma reactor, the pressure and the power input. Manufacturing conditions are therefore difficult to control and to reproduce.

Among the different effects of plasma on porous substrates, the most beneficial for the preparation of membranes is the formation of a very thin dense coating of functionalized material. This technique therefore appears as an effective means of producing composite membranes for pervaporation. Experience actually shows that plasma-modified porous films can easily be tailor-made for various separation purposes. When a mixture of organic and inorganic gases is brought into low-pressure, high-frequency glow discharge, the plasma-deposited material is strongly functionalized and therefore exhibits good selectivity and enhanced permeability [112]. As a consequence, high permeation fluxes are transported through that permselective layer, the thickness of which generally does not exceed 1 μm. The plasma-deposition technique conclusively appears as a very promising technique for manufacturing composite pervaporation membranes. A close control of plasma parameters allows membranes as selective as those produced by the conventional solution coating process to be obtained and, in most cases, the plasma membrane is significantly more permeable. Being tightly crosslinked, the selective layer does not swell extensively and is therefore more resistant to aggressive mixtures. Plasma membranes obtained by deposition on appropriate porous supports were successfully used to dehydrate acetic acid and water–acetonitrile mixtures, which cannot be processed by pervaporation through the standard GFT membranes.

In certain cases, a very special procedure can be used to produce composite membranes, with an ultrathin permselective skin layer (less than 1 μm thick) made from a definite polymer or polycondensate. If this material is soluble in a volatile organic solvent, nonmiscible with water, the polymer solution is cast on a water surface [113] and the thin film, which then settles on this surface after evaporation of the solvent, is transferred onto an appropriate porous support.

Selective barriers can also be obtained by deposition of a hydrophilic organo-mineral layer onto a suitable porous substrate. For instance, the pores of sintered metal tubes were clogged with zirconium oxide polyacrylate (ZOPA). The resulting composite elements were tested to achieve the complete dehydration of the water–propanol azeotropic mixture [114].

5.5.2 Organophilic Pervaporation membranes

In the last few years, many attempts have been made to develop effective "organophilic membranes" designed for extraction of ethanol or other organic solutes contained in aqueous mixtures. One of the purposes was to integrate such membranes with bioreactors in order to remove, in a continuous way, the fermentation products which exert an inhibitory effect.

For this purpose, silicone-based membranes were extensively investigated. These experiments showed that pervaporation of water–ethanol mixtures through homogeneous films of polydimethylsiloxane (PDMS) results in enrichment of the

permeate in ethanol. A critical analysis of these results, however, shows that pervaporation selectivity does not then significantly exceed that of the liquid–vapor equilibrium under atmospheric pressure [115–119]. The same conclusion also applies to most of the membranes made from polymers usually classified as organophilic in the literature [116,118,120,121]. For instance, pervaporation of water–ethanol feeds containing 5 wt% alcohol, through homogeneous membranes of polytrimethylsilylpropyne (PTSMP) — a material generally considered as the most permeable to ethanol — yields a permeate containing 34% ethanol, whereas free vaporization of the same feeds releases a vapor containing 37% alcohol. Japanese researchers from Sagami Chemical Research Center appear to have recently succeeded in improving significantly the selectivity of PTMSP for ethanol, by grafting various silicon-containing acetylenic comonomers on the side methyl groups of the PTMSP chain [121].

These investigations show that there are very few polymers through which pervaporation of water–ethanol mixtures is more selective to ethanol than a single vaporization step. At present, this seems to be fulfilled only by special membranes [122], such as certain silicalite-filled silicone membranes and some copolymer films obtained by grafting various polyacetylenics on the side methyl groupings of PTMSP [121] or perfluoroalkylacrylates on preactivated styrenemethacrylate trunk copolymers [119].

On the other hand, PDMS-based membranes can be much more effective in processing aqueous solutions of other organic solutes:

1. First, if repulsive forces work between water and the solute molecules, as disclosed by strong deviation from thermodynamical ideality or by the occurrence of a miscibility gap. In such a case, the larger the deviation, the faster is the transport of the organic permeant through the membrane. In other words, a correlation appears between the solubility of the organic component in water and the selectivity of its transport through the silicone film. This correlation was clearly shown by the comparative experiments carried out by Böddeker [31] on the extraction of the four isomeric butanols.

2. The second possible favorable feature is an attractive interaction between the organic solute and the silicone-based membrane. This requires that the solubility parameter of this solute should be close to that of the membrane material, which approximately equals 8.5 (cal per ml)$^{0.5}$. This is fulfilled by chlorinated hydrocarbons, ethers, esters and ketones. Accordingly, experience shows [123] that PDMS films exhibit good selectivity for acetone and dioxane, the solubility parameters of which equal 9.8 and 10.0 (cal per ml)$^{0.5}$, respectively. In the case of ethylacetate (solubility parameter = 9.1), an aqueous feed solution containing 5% ethylacetate yields an 89% ethylacetate permeate while the same feed releases a vapor containing only 78% ester. For the same reason — strong attractive interaction between the solute and the membrane material — and in spite of its low volatility (Blg. T = 182°C), phenol can be readily removed from an aqueous

effluent by pervaporation through a polyether-amide block copolycondensate membrane (PEBA 5533 from ATOCHEM). In fact, a feed containing 1700 ppm phenol yields a 9% phenol permeate that separates into two phases upon condensation [124].

Although they are not very effective for removing ethanol, which is completely miscible with water and is characterized by a solubility parameter equal to 12.7 (cal per ml)$^{0.5}$, silicone-based membranes can, however, be used to extract other organics from aqueous solutions [125,126] or to recover them from polluted air streams. In the USA, Membrane Technology Research Inc. (MTR Inc.) is developing devices equipped with such membranes. They are commercialized under the tradenames Pervap and Vaporsep Systems. In Europe, GFT-Carbone Lorraine Company has recently started the manufacturing of two different silicone-based composite barriers. The standard membrane is obtained by deposition of a functionalized dimethylsiloxane oligomer onto a porous polyacrylonitrile support, followed by curing under electron beam [110]. A more selective but less permeable variant is made by introducing, in the silicone layer, 60% organophilic zeolite-type filler, such as silicalite.

5.5.3 Pervaporation Membranes for Organic–Organic Separation

In the last few years, efforts were made to develop new membranes to separate certain organic–organic liquid mixtures, in order to promote the application of pervaporation in the chemical and petrochemical industries. These investigations mainly concern the separations aromatics/non aromatics, alcohols/alcanes and alcohols/ ethers.

The first problem is raised by refiners who want to recover substituted aromatics contained in the various — heavy, intermediate or light — catalytic naphtha streams and must also reduce the benzene content of the C-6 reformate cuts used in the production of high-grade leadless gasoline. In the chemical industry, potential applications of aromatics/saturates separation could be the removal of aromatics from the feedstock of ethylene plants in order to enhance their production capacity and the separation of benzene and cyclohexane in benzene–toluene–xylene production plants.

The fractionation of alcohols/alcanes and alcohols/ethers mixtures is mainly related with the production of methyltertiobutylether (MTBE) and ethyltertiobutylether (ETBE), which are the antiknock additives recently used, instead of tetraethyl-lead, to improve the octane number of gasoline. These ethers are synthesized through alkylation of the C-4 cut (isobutene + butanes), by reacting it with an excess of methanol or ethanol. The product stream emerging from the reactor then contains saturated C-4, the resulting ether and the unreacted alcohol and this mixture is rather difficult to separate since ether–alcohol mixtures generally exhibit azeotropic behaviour. The objective is therefore to develop an optimized reac-

tion–distillation–pervaporation integrated process in order to achieve the production of the tertiobutylethers in the best economical conditions.

The establishment of corresponding ternary phase diagrams or the systematic measurement of preferential solvation exhibited by a series of polymers contacted with these different liquid mixtures, provides reliable information for selecting an appropriate membrane material. In the development of performing membranes, however, their swelling extent in contact with the processed feeds needs to be adjusted. The crosslinking degree of the membrane must, therefore, be thoroughly controlled and this is rather difficult to ensure when the composite membrane is produced by the usual coating–evaporation technique since the chemical crosslinking reaction is then achieved during the evaporation period. In this respect, plasma deposition from an appropriate gas mixture appears to be a more versatile and reliable procedure.

It was also suggested that definite crosslinked polymer networks of appropriate chemical nature could be realized by means of "physical crosslinking". In this way, promising results concerning the separation of aromatics and saturates by pervaporation have been reported by Exxon [127]. The membranes used were made of linear multiblock copolycondensates comprising alternate flexible (soft) and rigid (hard) sequences, as exemplified by the following chemical formula:

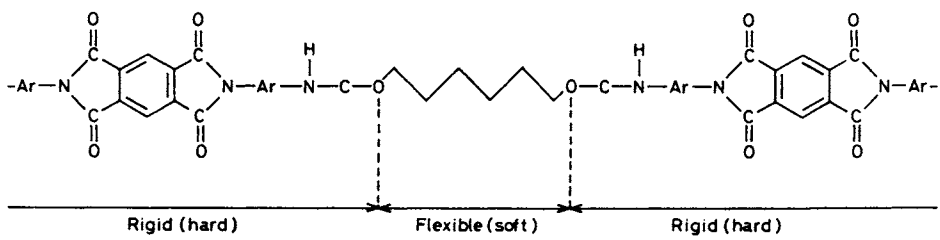

This material, which belongs to the category of polyurethane-imides, can be synthesized by polyaddition of an aromatic dianhydride with a low molecular weight polyoxyethyleneglycol previously end-capped by reaction with an excess of aromatic diisocyanate. The polycondensate thus obtained is soluble in certain organic solvents and it is possible to cast and to evaporate the resulting solution onto appropriate supports. During this operation, the flat polyaromatic moieties are brought in close contact and, due to the strong specific attractive van der Waals forces between them, pile up into stacks of plates. In the deposited film, rigid domains thus nucleate which are bound together by flexible polyoxyethylene links. The resulting network is somewhat similar to chemically crosslinked structures but, in the present case, the parameters of the generated network can be adjusted at will, since they are mainly determined by the chemical nature of the starting reagents and, more specifically, by the molecular weight of the polyoxyethyleneglycol.

Of course, polyoxyethyleneglycol can be replaced by any other flexible hydroxy-ended or amino-ended oligomeric chain, for instance by the low molecular weight polyethylene-adipate obtained by reacting adipic acid with an excess of ethyleneglycol.

Exxon Research and Engineering Co. extensively investigated this type of membranes in order to evaluate their performance in the pervaporation separation of aromatics and saturates. The results obtained with a typical polyurethane-imide membrane are summarized below:

Nature of the membrane

The starting reagents were:
Hydroxy-ended polyethylene-adipate: Molar weight 2,000 g $mole^{-1}$
Diphenylmethanediisocyanate
Pyromellitic-anhydride or (1,2,4,5-benzenetetracarboxylic-dianhydride)
Solvent used to cast the membrane: dimethylformamide.

Operational pervaporation conditions

T = 140°C
Downstream pressure: 5 mbar

Pervaporation results:

Feed: Heavy catalytic naphtha: 51% aromatics (by volume)
Permeate: 84% aromatics
Normalized permeation flux (1 μm-thick membrane): 100 kg/h m^2.

5.6 PRESENT STATE OF ART OF PERVAPORATION

Pervaporation is now widely recognized as an effective technique for fractionating azeotropic mixtures and as a valuable competitor to energy-consuming conventional processes such as vacuum and extractive distillation. The industrial applications of pervaporation are, so far, mainly confined to dehydration of the water–organic liquid azeotropes and to the extraction of volatile trace organics contained in aqueous mixtures.

Most of the currently operational pervaporation plants were started during the last decade by GFT Co. and under license by Mitsui Engineering and Shipbuilding Co. Ltd. (Table 5.5). The major application of the process is the dehydration of water–organic liquid azeotropic mixtures, not only the production of pure ethanol, but also the refining of other organic solvents such as isopropanol, esters, ethers and ketones. In every case, pervaporation is combined with distillation and is mainly used to pass over the azeotropic composi-

TABLE 5.5

Operational pervaporation plants started by GFT Co. and by Mitsui Engineering and Shipbuilding Co., Ltd. (under licence) during 1984–1992

Pervaporation operation	No. of plants
Ethanol dehydration	
Béthéniville sugar refinery, France (150,000 l d^{-1})	1
Provins sugar refinery, France (30,000 l d^{-1})	1
Smaller plants (1,000–12,000 l d^{-1})	11
Isopropanol dehydration	
Production capacity ranging from 5,000 to 15,000 l d^{-1}	5
Dehydration of ethylacetate (1,000–6,000 l d^{-1})	3
Dehydration of ethers (tetrahydrofurane, dimethoxyethane)	
Production capacity ranging from 2,000 to 6,000 l d^{-1}	2
Dehydration of ketones (6,000 l d^{-1})	1
Dehydration of other organic solvents	
Production capacity ranging from 750 to 15,000 l d^{-1}	6
Multipurpose plants (integrated systems)	3
Total number of operational units	33
+ 25 pilot plants (4 m^2 surface area membrane each) installed to test the applicability of the technique to potential fractionation problems	

tion of the mixture, the flow-sheet of the distillation–pervaporation system depending on this composition. More complex integrated process were also developed in which pervaporation is paired with other conventional separation techniques, such as adsorption, phase separation or counter-current extraction. Pilot-scale experiments were also made to insert pervaporation into chemical processes in order to assist a reversible water-generating reaction by continuous removal of water [96,128].

Recently, other European Companies (GKSS, Kalsep, Chemetall GmbH, CM-Celfa, Metallgesellschaft) have begun to develop and install industrial pervaporation systems.

Using organophilic silicone-based membranes, it is also possible to extract by pervaporation organic contaminants contained in aqueous mixtures [129]. This process was developed by the U.S. Centre Membrane Technology Research

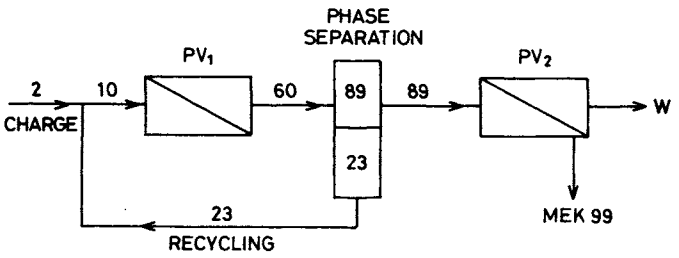

Fig. 5.28. Use of pervaporation to recover methylethylketone (MEK) from an aqueous stream containing 2 wt% ketone. PV_1: Pervaporator equipped with organophilic membranes; PV_2: pervaporator equipped with hydrophilic membranes. Numbers indicate MEK contents (wt%). According to M. Pasternak, Texaco Research Centre [130].

(MTR), which designed the Vaporsep and the Pervap Systems. Both make use of modules equipped with silicone-based membranes to remove organic pollutants contaminating air streams or aqueous effluents. The Vaporsep technique seems to be a successful way to trap hydrocarbon vapors rejected in purge gas streams swept out of oil tanks and to recover volatile fluorinated compounds emerging from large refrigerating plants. The pervaporation recovery of valuable volatile organic solutes contained in aqueous effluents could also be a realistic industrial process if certain requirements were fulfilled concerning the solubility of the contaminant in water, its concentration in the feed and also its affinity for the membrane polymer. A favorable situation occurs when this pollutant is partially miscible with water and when its concentration in the feed is not too low. If it is a ketone, which has some affinity for silicone rubber membranes, pervaporation yields an enriched permeate that spontaneously separates into two liquid phases upon condensation. The dense water-rich layer can be recycled in the feed while the organic-rich supernatant phase is processed in a second pervaporator equipped with hydrophilic membranes to achieve its dehydration. The flowsheet of this process, developed by Texaco Research Centre [130] for the recovery of methylethylketone, is represented in Fig. 5.28.

Of course, this favorable situation would be more frequently encountered if many different organophilic membranes were available on the market. For instance, a potential application of pervaporation is the extraction of phenol contained in industrial waste waters. The process, developed in Germany by GKSS, takes advantage of the strong affinity of this solute for polyamides and polyethers [124]. The pervaporation modules are equipped with PEBA membranes made of polyether–amide block copolycondensates related to the "soft–hard" macromolecular structures already introduced. This decontamination technique is presently being tested in a Japanese Company to design an industrial pervaporation plant sized to treat 530 kg h^{-1} feed flow containing 7% phenol and reduce this content to 300 ppm.

REFERENCES

1 P. Aptel, N. Challard, J. Cuny and J. Néel, Application of the pervaporation process to the separation of azeotropic mixtures, *J. Membr. Sci.*, 1 (1976) 271–287.

2 J. Néel, Q.T. Nguyen, R. Clément and L. Le Blanc, Fractionation of a binary liquid mixture by continuous pervaporation. *J. Membr. Sci.*, 15 (1983) 43–62.

3 R. Rautenbach and U. Meyer-Blumenroth, Module and process design for vapor permeation. *Desalination*, 77 (1990) 295–322.

4 K. Kimmerle, C.M. Bell, W. Gudernatsch and H. Chmiel, Solvent recovery from air. *J. Membr. Sci.*, 36 (1988) 477–488.

5 A.C.M. Franken and S. Ripperger, *Terminology for Membrane Distillation.* Recommendations by the European Society of Membrane Science and Technology, 1988.

6 N. Kjellander, Design and field tests of a membrane distillation system for sea-water desalination. *Desalination*, 61 (1987) 237–243.

7 H. Udriot, *Distillation transmembranaire: Etude d'un procédé de séparation à membrane et développement de nouveaux champs d'application.* Thèse de Doctorat no. 884, Ecole Polytechnique Fédérale de Lausanne, Switzerland, 1990.

8 S. Ripperger, *The ENKA trans-membrane distillation process.* Comm. Workshop on membrane distillation, Rome, Italy, 1986.

9 Ren Qin, A.K. Zander, M.J. Semmens and E.L. Cussler, Separating acetic acid from liquids. *J. Membr. Sci.*, 50 (1990) 51–55.

10 Zhang Qi and E.L. Cussler, Bromine recovery with hollow fiber gas membranes. *J. Membr. Sci.*, 24 (1985) 43–57.

11 M. Imai, S. Furusaki and T. Miyauchi, Separation of volatile materials by gas membranes. *Ind. Eng. Chem., Process Des. Dev.*, 21, (1982) 421–426.

12 I. Cabasso, J. Jagur-Grodzinski and D. Vofsi, A study of permeation of organic solvents through polymeric membranes based on polymeric alloys of polyphosphonates and acetylcellulose. II Separation of benzene, cyclohexene and cyclohexane. *J. Appl. Polym. Sci.*, 18 (1974) 2137–2147.

13 K. W. Böddeker, Terminology in Pervaporation, issued in Nov. 1989 by the Europ. Soc. of Membrane Sci. and Technology, *J. Membr. Sci.*, 51 (1990) 259–272.

14 Sun-Tak Hwang and K. Kammermeyer, Pervaporation. In: *Membranes in Separations*, Techniques of Chemistry, Vol. VII. John Wiley and Sons, 1975, Chap. VII, pp. 99–123.

15 P. Aptel, J. Cuny, J. Jozefowics and J. Néel, Pervaporation through membranes prepared by grafting polar monomers onto polytetrafluoroethylene films, *J. Appl. Polym. Sci.*, 16 (1972) 1061–1076; 18 (1974) 351–364; 18 (1974) 365–378.

16 R. Clément, Appareil automatique programmable destiné à l'acquisition des données caractérisant les membranes de pervaporation. *Actes du Congrès.* Méthodes Informatiques en Chimie. Pau, France, 1989.

17 D.A. Blackadder and J.S. Keniry, The measurement of the permeability of polymer membranes to solvating molecules. *J. Appl. Polym. Sci.*, 16 (1972) 2141–2152.

18 A.H. Windle, Case II sorption. In: J. Comyn (Ed.), *Polymer Permeability.* Elsevier Applied Science Publishers, 1985, pp. 75–118.

19 W. Kujawski, Q.T. Nguyen and J. Néel, Dehydration of water–pyridine mixtures by pervaporation. In: *Proceedings of the International Symposium: Membranes and Membrane Separation Processes*, Torun, Poland. N. Copernicus University, 1989, pp. 67–68.

20 J. Néel, Introduction to pervaporation. In: R.Y.M. Huang (Ed.), *Pervaporation Membrane Separation Process.* Elsevier Science Publishers, Amsterdam, 1991, pp. 1–109.

21 J. Néel, Q.T. Nguyen, R. Clément and D.J. Lin, Influence of downstream pressure on the pervaporation of water–tetrahydrofurane mixtures through a regenerated cellulose membrane (Cuprophan). *J. Membr. Sci.*, 27 (1986) 217–232.
22 F.W. Greenlaw, R.A. Shelden and V. Thomson, Dependence of diffusive permeation rates on upstream and downstream pressures. II. Two-component permeant. *J. Membr. Sci.*, 2 (1977) 333–348.
23 J. Crank, Ch. 9: Some calculated results for variable diffusion coefficients. In: *The Mathematics of Diffusion*, 2nd Ed. Clarendon Press, Oxford, UK, 1975, pp. 160–202.
24 M.H.V. Mulder, T. Franken and C.A. Smolders, Preferential sorption versus preferential permeability in pervaporation. *J. Membr. Sci.*, 22 (1985) 155–173.
25 E. Bode, The use of ternary diagrams for predicting selectivity in pervaporation. In: R. Bakish (Ed.), *Proceedings of the Sixth International Conference on Pervaporation Processes in the Chemical Industry, Ottawa, Canada*. Bakish Materials Corp., P.O. Box 148, Englewood, NJ 07631, USA, 1992, pp. 46–54.
26 J. Hauser, G.A. Reinhardt, F. Stumm and A. Heintz, Non-ideal solubility of liquid mixtures in poly(vinylalcohol) an ts influence on pervaporation. *J. Membr. Sci.*, 47 (1989) 261–276.
27 P. Aptel, J. Cuny, J. Jozefowicz, G. Morel, J. Néel and B. Chaufer, Perméabilité sélective et solvatation préférentielle. *Eur. Polym. J.*, 14 (1978) 595–599.
28 S. Kimura and T. Nomura, Pervaporation of organic substance/water system with silicone rubber membrane. *Maku (Membrane, Japan)*, 8 (3) (1983) 177–183.
29 J. Kaschemekat, J.G. Wijmans, R.W. Baker and I. Blume, Separation of organics from water using pervaporation. In: R. Bakish (Ed.), *Proceedings of the Third International Conference on Pervaporation Processes in the Chemical Industry, Nancy, France*. Bakish Materials Corporation, P.O. Box 148, Englewood, NJ 07631, USA, 1988, pp. 405–412.
30 M. Tanigaki, M. Yoshikawa and W. Eguchi, Selective separation of alcohol from aqueous solution through polymer membrane. In: R. Bakish (Ed.), *Proceedings of the Second International Conference on Pervaporation Processes in the Chemical Industry, San Antonio, Texas, USA*. Bakish Materials Corporation, P.O. Box 148, Englewood, NJ 07631, USA, 1987, pp. 126–145.
31 K.W. Böddeker, G. Bengtson and H. Pingel, Pervaporation of isomeric butanols. *J. Membr. Sci.*, 54 (1990) 1–12.
32 A. Misra, F.W. Kroesser and R.A. Shelden, The effect of solutes on the pervaporation of water–methanol mixtures through cellophane. *J. Polym. Sci.*, 41 (1973) 145–153.
33 A. Mochizuki, Y. Sato, H. Ogawara and S. Yamashita, Pervaporation separation of water/ethanol mixtures through polysaccharide membranes. I. The effects of salts on the permselectivity of cellulose membrane in pervaporation. *J. Appl. Polym. Sci.*, 37 (1989) 3357–3374.
34 Q.T. Nguyen, L. Le Blanc and J. Néel, Preparation of membranes from polyacrylonitrile–polyvinylpyrrolidone blends and the study of their behavior in the pervaporation of water–organic liquid mixtures. *J. Membr. Sci.*, 22 (1985) 245–255.
35 J. Néel, W. Kujawski, Q.T. Nguyen and Z. H. Ping, Mechanism of pervaporation. Selectivity of ion-exchange membranes for the separation of water–ethanol mixtures. In: R. Bakish (Ed.), *Proceedings of the Third International Conference on Pervaporation Processes in the Chemical Industry, Nancy, France*. Bakish Materials Corp., Englewood, NJ, USA, 1988, pp. 21–36.
36 J. Néel, Q.T. Nguyen, R. Clément and R. François, Separation of water–organic liquid mixtures by pervaporation. Mechanism of the process. In: *Proceedings of the International Congress on Membranes and Membrane Processes, I.C.O.M. 87, Tokyo*. 1987, pp. 479–481.

37 Z.H. Ping, Q.T. Nguyen, R. Clément and J. Néel, Pervaporation of water–ethanol mixtures through a poly(acrylic acid) grafted polyethylene membrane. Influence of temperature and nature of the counter-ions. *J. Membr. Sci.*, 48 (1990) 297–308.
38 A. Wenzlaff, K.W. Böddeker and K. Hattenbach, Pervaporation of water–ethanol through ion-exchange membranes. *J. Membr. Sci.*, 22 (1985) 333–344.
39 K.W. Böddeker and A. Wenzlaff, Pervaporation with ion-exchange membranes. In: R. Bakish (Ed.), *Proceedings of the First International Conference on Pervaporation Processes in the Chemical Industry, Atlanta, Georgia, USA*. Bakish Materials Corporation, Englewood, NJ, USA, 1986, pp. 96–110.
40 S. Yamada and T. Nakagawa, Separation of alcohol–water solutions with copolymer membrane. In: R. Bakish (Ed.), *Proceedings of the Second International Conference on Pervaporation Proceses in the Chemical Industry, San Antonio, Texas, USA*. Bakish Materials Corporation, Englewood, NJ, USA, 1987, pp. 176–185.
41 T. Uragami, H. Okuno, T. Nishida and T. Miyata, *Polymer*, 30, (1989) 1117.
42 S. Yamada and T. Hamaya, Liquid permeation and separation by surface-modified polyethylene membranes. *J. Membr. Sci.*, 17 (1984) 125–138.
43 R.B. Long, Liquid permeation through plastic films. *Ind. Eng. Chem., Fundam.*, 4 (1965) 445–451.
44 J. Crank and G S. Park, *Diffusion in Polymers*. Academic Press, 1968.
45 C.E. Rogers, (1985), Permeation of vapors and gases in polymers. In: J. Comyn (Ed.), *Polymer Permeability*. Elsevier Applied Science Publishers Ltd., London, pp. 1–73.
46 P.P. Roussis and J.H. Petropoulos, Permeation time-lag analysis of anomalous diffusion. Part I: Some considerations on experimental methods. *J. Chem. Soc., Faraday Trans. II*, 72 (1976) 737–746.
47 R.A. Pasternak, F.H. Schimscheimer and J. Heller, A dynamic approach to diffusion and permeation measurements. *J. Polym. Sci.*, A2, 8 (1970) 467–479.
48 D.S. Hu and Chang Dae Han, Effect of polymer side chains on the infinite dilution diffusion coefficients of volatile liquids in poly-(methyl-methacrylate) at elevated temperatures. *J. Appl. Polym. Sci.*, 34 (1987) 423–429.
49 R. Paterson and P. Doran, A new method for determining membrane diffusion coefficients from their response to regular forced concentration waves. *J. Membr. Sci.*, 27 (1986) 105–117.
50 O. Kedem, The role of coupling in pervaporation. *J. Membr. Sci.*, 47 (1989) 277–284.
51 M.H.V. Mulder and C.A. Smolders, On the mechanism of separation of ethanol/water mixtures by pervaporation. I. Calculation of concentration profiles. *J. Membr. Sci.*, 17 (1984) 289–307.
52 M.H.V. Mulder, A.C.M. Franken and C.A. Smolders, On the mechanism of separation of ethanol/water mixtures by pervaporation. II. Experimental concentration profiles. *J. Membr. Sci.*, 23 (1985) 41–58.
53 P.J. Flory, Phase equilibria in polymer systems. In: P.J. Flory (Ed.), *Principles of Polymer Chemistry*. Cornell University Press, 1953, pp. 541–593.
54 J.G.A. Bitter, *Transport mechanisms in membrane separation processes*. Koninklijke Shell Laboratorium, Postbus 3003, Amsterdam, The Netherlands.
55 E.M. Scattergood and E.N. Lightfoot, *Trans. Faraday Soc.*, 64 (1968) 1135.
55a E.N. Lightfoot, E.L. Cussler and R.L. Rettig, *AIChE J.*, 8 (1962) 708.
56 E.A. Mason, A.P. Malinauskas and R.B. Evans, *J. Chem. Phys.*, 46 (1967) 3199.
57 P. Schaetzel, E. Favre, Q.T. Nguyen and J. Néel, Mass transfer analysis of pervaporation through an ion exchange membrane. *Desalination*, 90 (1993) 259–276.

58 R. Gref, Fractionnement, par pervaporation, de mélanges liquides partiellement miscibles. Mise en évidence du rôle de la stucture cristalline des membranes denses sur leurs propriérés de transport. Thèse de Doctorat, Nancy, France, 1991.
59 L. Perrin, Etude de la diffusion et de l'équilibre de sorption de corps purs dans des polymères. Application à des systèmes utilisés en pervaporation. Thèse de Doctorat, Nancy, France, 1992.
60 A.S. Michael and R.W. Hausslein, Elastic factors controlling sorption and transport properties of polyethylene. *J. Polym. Sci., C*, 10 (1965) 61–86.
61 R.M. Barrer, *Diffusion In and Through Solids*. Cambridge University Press, 1951.
62 O. Kedem, The role of coupling in pervaporation. *J. Membr. Sci.*, 47 (1989) 277–284.
63 R.K. Tyagi and T. Matsuura, Possibility of concentration polarization inside the membrane during steady state pervaporation. In: R. Bakish (Ed.), *Proceedings of the Fifth International Conference on Pervaporation Processes in the Chemical Industry, Heidelberg, Germany*. Bakish Materials Corp., P.O. Box 148, Englewood, N.J. 07631, USA, 1991, pp. 460–474.
64 I. Cabasso and Zhong-Zhou Liu, The permselectivity of ion-exchange membranes for non-electrolyte liquid mixtures. Separation of alcohol–water mixtures with Nafion membranes. *J. Membr. Sci.*, 24 (1985) 101–119.
65 I. Cabasso, E. Korngold and Zhong-Zhou Liu, On the separation of alcohol–water mixtures by polyethylene ion-exchange membranes. *J. Polym. Sci., Polym. Lett. ed.*, 23 (1985) 577–581.
66 I. Cabasso, Zhong-Zhou Liu and T. Makenzie, The permselectivity of ion-exchange membranes for non-electrolyte liquid mixtures. The effect of counterions. *J. Membr. Sci.*, 28, (1986) 109–122.
67 J. Néel, Q.T. Nguyen, R. Clément and R. François, Separation of water–organic liquid mixtures by pervaporation. Mechanism of the process. *Proceedings of the 1987 International Congress on Membranes and Membrane Processes (ICOM-87, Tokyo)*, 1987, pp. 479–481.
68 G. Zundel and J. Fritsch, In: R.R. Dogonadse, E. Kalman, A.A. Kornyshev and J. Ulstrup (Eds.), *The Chemical Physics of Solvation. Part B*. Elsevier Science Publishers, Amsterdam, 1986, pp. 21–96.
69 U. Sander and P. Soukup, Design and operation of a pervaporation plant for ethanol dehydration. *J. Membr. Sci.*, 36, (1988) 463–475.
70 U. Sander, Application du procédé de pervaporation pour la deshydratation de l'alcool. *L'Actualité Chimique*, 4–5 (1988), 144–150.
71 D.A. Colman and T. de V. Naylor, The influence of operating variables on flux and module design in a high performance pervaporation system. In: R. Bakish (Ed.), *Proceedings of the Fifth International Conference on Pervaporation Processes in the Chemical Industry, Heidelberg, Germany*, 1991, pp. 143–161.
72 R. Psaume, P. Aptel, Y. Aurelle, J. C. Mora and J.L. Bersillon, Pervaporation: Importance of concentration polarization in extraction of trace organics in water. *J. Membr. Sci.*, 36 (1988) 373–384.
73 P. Côté and C. Lipski, Mass transfer limitations in pervaporation for water and waste water treatments. In: R. Bakish (Ed.), *Proceedings of the Third International Conference on Pervaporation Processes in the Chemical Industry, Nancy, France*. Bakish Materials Corporation, Englewood, NJ, USA, 1988, pp. 449–462.
74 H.H. Nijhuis, Removal of trace organics from water by pervaporation. A technical and economic analysis. Ph.D. Thesis, University of Twente, Enschede, The Netherlands, 1990.

75 B. Raghunath and S.T. Hwang, Effect of boundary layer mass transfer resistance in pervaporation of dilute organics. *J. Membr. Sci.*, 65 (1992) 147–161.
76 H.O.E. Karlsson and G. Trägärdh, Pervaporation of dilute organic–water mixtures. A literature review on modelling studies and applications to aroma compound recovery. *J. Membr. Sci.*, 76 (1993) 121–146.
77 E. Bengtsson, G. Trägärdh and B. Hallström, Recovery and concentration of apple juice aroma compounds by pervaporation. *J. Food Sci.*, 10 (1989) 65–71.
78 E. Bengtsson, G. Trägärdh and B. Hallström, Concentration of apple juice aroma from evaporator condensate using pervaporation. *Lebens.-Wiss. -Techn.*, 25 (1992) 29–34.
79 S.Q. Zhang and T. Matsuura, Recovery and concentration of flavour compounds in apple essence by pervaporation. *J. Food Process. Eng.*, 14 (1991) 291–296.
80 A. Voilley, T. Lamer, Q.T. Nguyen and D. Simatos, Extraction of aroma compounds by pervaporation. In: R. Bakish (Ed.), *Proceedings of the Fourth International Conference on Pervaporation Processes in the Chemical Industry, Fort Lauderdale, FL, USA. Bakish Corporation, Englewood, NJ, USA.* 1989, pp. 332–343.
81 A. Voilley, G. Charbit and F. Gobert, Recovery and separation of 1-octen-3-ol from aqueous solutions by pervaporation. *J. Food Sci.*, 55 (1989) 1399–1402.
82 R. Clément, Z. Bendjama, Q.T. Nguyen and J. Néel, Extraction of organics by pervaporation. A novel method for membrane characterization and process design in ethylacetate separation. *J. Membr. Sci.*, 66 (1992) 193–203.
83 T. Lamer and A. Voilley, Influence of different parameters on the pervaporation of aroma compounds. In: R. Bakish (Ed.), *Proceedings of the Fifth International Conference on Pervaporation Processes in the Chemical Industry, Heidelberg, Germany.* Bakish Corporation, Englewood, NJ, USA. 1991, pp. 110–122.
84 A. Voilley, B. Schmidt, D. Simatos and S. Baudron, Extraction of aroma compounds by the pervaporation technique. In: R. Bakish (Ed.), *Proceedings of the Third International Conference on Pervaporation Processes in the Chemical Industry, Nancy, France.* Bakish Materials Corporation, Englewood, NJ, USA., 1988, pp. 429–438.
85 Q.T. Nguyen, B. Wandelt, R. Clément and J. Néel, Fractionation of binary liquid mixtures by pervaporation. Effects of residence time distribution in the pervaporation module. In: *Proceedings of the Fifth World Filtration Congress, Nice, France.* Société Française de Filtration, 1990, pp. 413–419.
86 R.W. Nichols, Standard Oil Company Ohio, Hollow fiber separation module and method for the use thereof. US Patent No. 4,959,152 (Sept. 25, 1990).
87 H.E.A. Brüschke, State-of-art of pervaporation. In: R. Bakish (Ed.), *Proceedings of the Fifth International Conference on Pervaporation Processes in the Chemical Industry, Heidelberg, Germany.* Bakish Materials Corporation, Englewood, NJ, USA, 1991, pp. 2–6.
88 B. Will, A. Heintz and R.N. Lichtenthaler, Experimental and theoretical study of vapor permeation. In: R. Bakish (Ed.), *Proceedings of the Third International Conference on Pervaporation Processes in the Chemical Industry, Nancy, France.* Bakish Materials Corporation, Englewood, NJ, 1988, pp. 37–43.
89 B. Will and R. N. Lichtenthaler, Comparison of the separation of aqueous mixtures by vapor permeation and by pervaporation. In: R. Bakish (Ed.), *Proceedings of the Fifth International Conference on Pervaporation Processes in the Chemical Industry, Heidelberg, Germany.* Bakish Materials Corporation, Englewood, NJ, 1991, pp. 216–229.
90 U. Sander, Development of vapor permeation for industrial application. In: R.Y.M. Huang (Ed.), *Pervaporation Membrane Separation Processes.* Elsevier Science Publishers, Amsterdam, 1991, pp. 509–534.

91 R. Rautenbach, C. Herion and M. Franke, Dehydration of multicomponent organic systems by a reverse osmosis/pervaporation hybrid process. Module, process design and economics. In: R. Bakish (Ed.), Proceedings of the Third International Conference on Pervaporation Processes in the Chemical Industry, Nancy, France, ed. by Bakish Materials Corporation, Englewood, NJ, (1988), pp. 274–286

92 R. Gref, M.-O. David, Q.T. Nguyen and J. Néel, Coupling between pervaporation and chemical reactions: Esterification of carboxylic acids aided by pervaporation. In: R. Bakish (Ed.), *Proceedings of the Fourth International Conference on Pervaporation Processes in the Chemical Industry, Fort Lauderdale, Fl., USA.* Bakish Materials Corporation, Englewood, NJ, 1989, pp. 344–371.

93 M.-O. David, R. Gref, Q.T. Nguyen and J. Néel, Pervaporation–esterification coupling. Part I: Basic kinetic model. *Trans. Inst. Chem. Engineers*, 69A (1991) 335–340.

94 M.-O. David, Q.T. Nguyen and J. Néel, Pervaporation–esterification coupling. Part II: Modelling of the influence of different operating parameters. *Trans. Inst. Chem. Engineers*, 69A (1991) 341–346.

95 H. Kita, K. Tanaka, K. Okamoto and M. Yamamoto, The esterification of oleic acid with ethanol accompanied by membrane separation. *Chem. Lett., Chem. Soc. Jpn.*, (1987) 2053–2056.

96 A. Dams and J. Krug (B.A.S.F., Germany), Pervaporation aided esterification: Alternative in plant extension for an existing chemical process. In: R. Bakish (Ed.), *Proceedings of the Fifth International Conference on Pervaporation Processes in the Chemical Industry, Heidelberg, Germany.* Bakish Materials Corporation, Englewood, NJ, USA, (1991), pp. 338–348.

97 M.H.V. Mulder, Pervaporation in continuous alcohol fermentation. In: R. Bakish (Ed.), *Proceedings of the First International Conference on Pervaporation Processes in the Chemical Industry, Atlanta, USA.* Bakish Materials Corporation, Englewood, NJ, 1986, pp. 187–194.

98 G. Sodeck, H. Effenberger, E. Steiner and W. Salzbrunn, Application of pervaporation membranes in fermentation processes. In: R. Bakish (Ed.), *Proceedings of the Second International Conference on Pervaporation Processes in the Chemical Industry, San Antonio, Texas, USA.* Bakish Materials Corporation, Englewood, NJ, 1987, pp. 157–168.

99 W. Gudernatsch, K. Kimmerle, N. Stroh and H. Chmiel, Recovery and concentration of high vapor pressure bioproducts by means of controlled membrane separation. *J. Membr. Sci.*, 36 (1988) 331–342.

100 H. Brüschke (G.F.T. Ingenieurbüro für Industrianlagenbau), Multilayer membrane and its use in the separation of liquids by pervaporation. Europ. Patent Np. 0,096,339, Dec. 21, 1983.

101 J. Néel, Q. T. Nguyen and H. Brüschke, Composite-Membran zur Abtrennung von Wasser aus organische Komponenten enthalden Fluiden mittels Pervaporation. Europäisches Patentamt, Anmeidung Nz. 90123133.2 (Dec. 21, 1990).

102 W.Heinzelmann, Fabrication methods for pervaporation membranes. In: R. Bakish (Ed.), *Proceedings of the Fifth International Conference on Pervaporation Processes in the Chemical Industry, Heidelberg, Germany.* Bakish Materials Corporation, Englewood, NJ, 1991, pp. 22–30.

103 H. Okusako, Applications of Tokuyama's pervaporation system. In: R. Bakish (Ed.), *Proceedings of the Fourth International Conference on Pervaporation Processes in the Chemical Industry, Fort Lauderdale, Florida, USA.* Bakish Materials Corporation, Englewood, NJ, 1989, pp. 372–385.

104 T. de V. Naylor, F. Zelaya and G. J. Bratton, The BP-Kalsep pervaporation system. Membrane performance and properties. In: R. Bakish (Ed.), Proceedings of the Fourth International Conference on Pervaporation Processes in the Chemical Industry, (1989), Fort Lauderdale, Fl., USA, ed. by Bakish Materials Corporation, Englewood, NJ, pp. 428–454.

105 H. Karakane, M. Tsuyumoto, Y. Maeda, K. Satoh and Z. Honda, Separation of water–ethanol by pervaporation through polyelectrolyte complex composite membrane. In: R. Bakish (Ed.), *Proceedings of the Third International Conference on Pervaporation Processes in the Chemical Industry, Nancy, France.* Bakish Materials Corporation, Englewood, NJ, 1988, pp. 194–202.

106 H. H. Schwarz, R. Apostel, K. Richau and D. Paul, Separation of water–alcohol mixtures through high flux polyelectrolyte complex membranes. In: R. Bakish (Ed.), *Proceedings of the Sixth International Conference on Pervaporation Processes in the Chemical Industry, Ottawa, Canada.* Bakish Materials Corporation, Englewood, NJ, 1992, pp. 233–241.

107 H. Tsuyumoto, H. Karakane, Y. Maeda and H. Tsugaya. Research Center, Daicel Chemical Ind., Ltd., Development of polyion complex hollow fiber membranes for separation of water–ethanol mixtures. In: R. Bakish (Ed.), *Proceedings of the Fourth International Conference on Pervaporation Processes in the Chemical Industry, Fort Lauderdale, Fl., USA.* Bakish Materials Corporation, Englewood, NJ, 1989, pp. 157–168.

108 L. Idier, Préparation de membranes carboxyliques par greffage différé d'acide acrylique sur des polyoléfines, à l'aide d'électrons accélérés. Thèse de Doctorat, Université de Paris XII, 1985.

109 K. Kaji, Distribution of grafted poly-(acrylic acid) in polyethylene film. *J. Appl. Polym. Sci.*, 12, 1986, 4405–4422.

110 G. Ellinghorst, A. Niemöller, H. Scholz, M. Scholz and H. Steinhauser, Membranes for pervaporation by radiation grafting and curing and by plasma processing. In: R. Bakish (Ed.), *Proceedings of the Second International Conference on Pervaporation Processes in the Chemical Industry, San Antonio, Texas, USA.* Bakish Materials Corporation, Englewood, NJ, 1987, pp. 79–99.

111 M. Yamamoto, I. Sakata and M. Hirai, Plasma-polymerized membranes and gas permeability. *J. Appl. Polym. Sci.*, 29, 1984, 2981.

112 G. Ellinghorst, H. Steinhauser and A. Hübner, Improvement of pervaporation plant by choice of PVA or plasma-polymerized membranes. (1992), In: R. Bakish (Ed.), Proceedings of the Sixth International Conference on Pervaporation Processes in the Chemical Industry, Ottawa, Can., ed. by Bakish Materials Corporation, Englewood, NJ, pp. 484–493.

113 E.G. Dubyaga, A.B. Komarova and S.I. Semenova, On surface effects in the process of formation of ultrathin selective polymer layers on liquid support. Preprints of presentations made during the *International Symposium on Membranes for Gas and Vapor Separation*, 1989, Suzdal, USSR, p. 21.

114 C.H. Gooding and F.J. Bahouth, Membrane-aided distillation of azeotropic solutions. Comm., AIChE Spring National Meeting, Houston, Texas, USA, 1983.

115 T. Jopski, H. Strathmann and P. Eyerer, Separation of ethanol–water mixtures by pervaporation with silicon containing polymer membranes. In: R. Bakish (Ed.), *Proceedings of the Fourth International Conference on Pervaporation Processes in the Chemical Industry, Fort Lauderdale, Fl., USA.* Bakish Materials Corporation, Englewood, NJ, 1989, pp. 40–51.

116 V.V. Volkov, V.S. Khotimskii and N. Platé, Organophilic polymers for pervaporation. In: R. Bakish (Ed.), *Proceedings of the Fourth International Conference on Pervaporation Processes in the Chemical Industry.* Bakish Materials Corporation, Englewood, NJ, 1989, pp. 169–176.

117 M.E.F. Garcia, A.C. Habert, R. Nobrega and L.A. Pires, Use of PDMS and EVA membranes to remove ethanol during fermentation. In: R. Bakish (Ed.), *Proceedings of the Fifth International Conference on Pervaporation Processes in the Chemical Industry, Heidelberg, Germany.* Bakish Materials Corporation, Englewood, NJ, 1991, pp. 319–330.

118 P.J. Hickey and C.S. Slater, Pervaporation of dilute ethanol solutions through hydropho-

bic membranes. In: R. Bakish (Ed.), *Proceedings of the Fourth International Conference on Pervaporation Processes in the Chemical Industry, Fort Lauderdale, FL, USA.* Bakish Materials Corporation, Englewood, NJ, 1989, pp. 579–589.

119 K. Ishihara and K. Matsui, Pervaporation of ethanol–water mixture through composite membranes composed of styrene-fluoroacrylate graft copolymers and crosslinked polydimethylsiloxane membrane. *J. Appl. Poly. Sci.*, 34 (1987) 437–440.

120 K. Ishihara, Y. Nagase and K. Matsui, Pervaporation of alcohol–water mixtures through poly-(trimethylsilyl)-1-propyne membrane. *Makromol. Chemie, Rapid Comm.*, 7, 1986, 43–46.

121 T. Inaba, M. Kondo, H. Izawa, Y. Nagase and K. Sugimoto, Pervaporation of ethanol–water mixture with modified substituted polyacetylene. In: R. Bakish (Ed.), *Proceedings of the Fourth International Conference on Pervaporation Processes in the Chemical Industry, Fort Lauderdale, Fl., USA.* Bakish Materials Corporation, Englewood, NJ, 1989, pp. 28–39.

122 H.J.C. Te Hennepe, D. Bargeman, M.H.V. Mulder and C.A. Smolders, Zeolite-filled silicone rubber membranes. Part I: Membrane preparation and pervaporation results, *J. Membr. Sci.*, 35 (1987) 39–55.

123 S. Kimura and T. Nomura, Pervaporation of organic substance/water system with silicone rubber membrane. *Maku (Membrane, Japan)*, 8 (3) (1983) 177–183.

124 K.W. Böddeker, Pervaporation of aqueous phenol. In: R. Bakish (Ed.), *Proceedings of the Second International Conference on Pervaporation Processes in the Chemical Industry, San Antonio, Tex., USA.* Bakish Materials Corporation, Englewood, NJ, 1988, pp. 141–145.

125 J. Kaschemekat, J. G. Wijmans and R. W. Baker, Removal of organic solvent contaminants from industrial effluent streams by pervaporation. In: R. Bakish (Ed.), *Proceedings of the Fourth International Conference on Pervaporation Processes in the Chemical Industry, Fort Lauderdale, Fl., USA.* Bakish Materials Corporation, Englewood, NJ, 1989, pp. 321–331.

126 K.W. Böddeker and G. Bengtson, Selective pervaporation of organics from water. In: R.Y.M. Huang (Ed.), *Pervaporation Membrane Separation Processes.* Elsevier Science Publishers, Amsterdam, 1991, pp. 437–460.

127 B.A. Koenitzer, Exxon Research and Engg. Co., Polyurethane-imide membranes and their use for the separation of aromatics from non-aromatics. U.S. Patent No. 4,929,358, May 29, 1990.

128 C. Herion, L. Spiske and W. Hefner (B.A.S.F., Germany). Dehydration in the synthesis of dimethylurea, by pervaporation. In; R. Bakish (Ed.), *Proceedings of the Fifth International Conference on Pervaporation Processes in the Chemical Industry, Heidelberg, Germany.* Bakish Materials Corporation, Englewood, NJ, 1991, pp. 349–361.

129 J. Kaschemekat, J.G. Wijmans, R.W. Baker and I. Blume, Separation of organics from water using pervaporation. In: R. Bakish (Ed.), *Proceedings of the Third International Conference on Pervaporation Processes in the Chemical Industry, Nancy, France.* Bakish Materials Corporation, Englewood, NJ, 1988, pp. 405–412.

130 M. Pasternak, Texaco Research Centre, Preferential removal of organics by ion-exchange membranes containing organic counterions. *Fourth National Meeting of the North American Membrane Society, San Diego, CA,* Poster No. 13B, 1991.

Membrane Separations Technology. Principles and Applications
Edited by R.D. Noble and S.A. Stern

Chapter 6

Electrodialysis and related processes

H. Strathmann

Faculty of Chemical Technology, University of Twente,
Enschede, The Netherlands

6.1 INTRODUCTION: HISTORICAL DEVELOPMENT

Electrodialysis is a mass separation process in which electrically charged membranes and an electrical potential difference are used to separate ionic species from an aqueous solution and other uncharged components. Electrodialysis is used widely today for desalination of brackish water and in some areas of the world it is the main process for the production of potable water. Although of major importance, water desalination is by no means the only significant application. In Japan, for example, electrodialysis is used on a large scale as a pre-concentration step for the production of table salt. Stimulated by the development of new ion-exchange membranes with better selectivities, lower electrical resistance, and improved thermal, chemical and mechanical properties, other uses of electrodialysis in the food, drug and chemical process industry as well as in biotechnology and wastewater treatment, have recently gained a broader interest. In addition to conventional electrodialysis there are other closely related processes, such as diffusion dialysis, Donnan dialysis, electrodialytic water dissociation, etc. with a multitude of potential large-scale applications. Most of these processes that are utilising standard or special property ion-exchange membranes as key-elements are still in an early stage of development but they are also rapidly gaining commercial and technical relevance [1–3]. Ion-exchange membranes are also used on a large scale in energy storage or conversion systems such as batteries and fuel cells and in electrochemical

production processes, such as the chlorine-alkaline electrolyses. In many applications, electrodialysis and related processes are in direct competition with other separation techniques, such as distillation, ion exchange, reverse osmosis and various chromatographic procedures. In other applications, there are very few technically and economically feasible alternatives to the electro-membrane processes.

Although the large-scale industrial utilization of electrodialysis began about 20 years ago, the principle of the process has been known for about 100 years. The development of electro-membrane processes began in 1890 with the work of Ostwald [4] who studied the properties of semipermeable membranes and discovered that a membrane is impermeable for any electrolyte if it is impermeable either for its cation or its anion. To illustrate this, he postulated the existence of the so-called "membrane potential" at the boundary between the membrane and the solution as a consequence of the difference in concentration. In 1911, Donnan [5] confirmed this postulate for the boundary of an ion-exchange membrane and its surrounding solution. Simultaneously, he developed a mathematical equation describing the concentration equilibrium which resulted in the so-called "Donnan exclusion potential".

The first basic studies related to ion-selective membranes were carried out in 1925 by Michaelis with the homogeneous, weak acid collodium membranes [6]. Around 1940, interest in industrial applications led to the development of synthetic ion-exchange membranes on the basis of phenol-formaldehyde-polycondensation resins [7]. In 1940 Meyer and Strauss proposed an electrodialysis process in which anion-selective and cation-selective membranes were arranged in alternating series to form many parallel solution compartments between two electrodes [8]. With such a multicompartment electrodialyser, demineralization or concentration of solutions could be achieved in many compartments with only one pair of electrodes. Thus the irreversible energy losses represented by the decomposition potentials at the electrodes could be distributed over many demineralizing compartments and therefore minimized. After the importance of the multicell stack arrangement for the economy of the electrodialysis was recognized, and with the development of stable, highly selective ion-exchange membranes of low electric resistance in the late 40s by Juda and McRae of Ionics Inc. [9] and Winger et al. at Rohm and Haas [10], electrodialysis rapidly became an industrial process for demineralizing and concentrating electrolyte solutions. The development of a chemically stable cation-exchange membrane based on sulfonated polytetra-fluorethylene 10 years later led to a large-scale use of this membrane in the chlor-alkali producing industry.

The main use envisaged for electrodialysis in the United States and Europe was the desalination of brackish water and seawater. The membranes to be used in this application should have high selectivity and low electro-osmotic transfer

in contact with very dilute solutions. The electrical resistance, however, was not of the highest priority because it was controlled mainly by the conductivity of the dilute stream. The membranes which fulfilled these requirements were manufactured as so-called heterogeneous structures by the dispersion of a fine ion-exchange resin powder within the solution of a matrix polymer and by the evaporation of the solvent [11].

A completely different use of electrodialysis was envisaged in Japan. Here electrodialysis was used for concentrating sodium chloride from seawater to produce table salt [12]. In this application the electrical resistance of the membrane was of prime importance for the economics of the process. These requirements have led to the development of homogeneous membranes with very low electrical resistance but less mechanical strength.

With the introduction of electrodialysis into the food and drug industry — and especially into the treatment of certain industrial effluents — again, further improvements of both the cell system design and the membrane properties, especially their chemical and thermal stability, became necessary [13]. In the early 80s a completely new area of application of electrodialysis had been opened up. At this time Liu et al. [14] introduced bipolar membranes for the recovery of acids and bases from the corresponding salts by electrical potential induced water dissociation on an industrial scale.

6.2 FUNDAMENTALS OF ELECTROMEMBRANE PROCESSES

As with all mass separation processes, the technical and commercial feasibility of electrodialysis and related processes is determined by the process costs, which are a function of membrane properties, cell system and process design, feed solution composition, etc. To better understand the technical and commercial potential of electrodialysis and related processes in the separation of molecular mixtures — and recognize their limitations — some fundamentals concerning the principle of the processes, the function of the membranes, the mass transport in electrolyte solutions and general energy requirements will be discussed.

6.2.1 Principle of Electrodialysis and Related Processes

The principle of electrodialysis is illustrated in Fig. 6.1, which shows a schematic diagram of a typical electrodialysis cell arrangement consisting of a series of anion- and cation-exchange membranes arranged in an alternating pattern between an anode and a cathode to form individual cells. A cell consists of a volume with two adjacent membranes. If an ionic solution such as an aqueous salt solution is pumped through these cells and an electrical potential is established

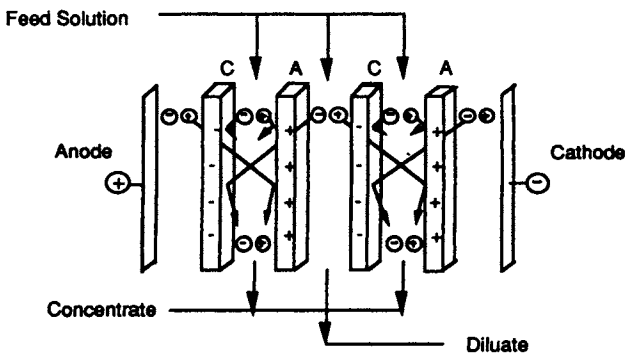

Fig. 6.1. Schematic diagram illustrating the principle of electrodialysis.

between the anode and cathode, the positively charged cations migrate toward the cathode and the negatively charged anions towards the anode. The cations pass easily through the negatively charged cation-exchange membrane but are retained by the positively charged anion-exchange membrane. Likewise the negatively charged anions pass through the anion-exchange membrane and are retained by the cation-exchange membrane. The overall result is an increase in the ion concentration in alternate compartments, while the other compartments simultaneously become depleted. The depleted solution is generally referred to as the diluate and the concentrated solution as the brine or the concentrate. The driving force for the ion transport in the electrodialysis process is the applied electrical potential between the anode and cathode.

Figure 6.1 shows only two cation (C) and two anion-exchange membranes (A). An actual electrodialysis stack may have several hundreds of such membranes [15]. The total space occupied by the diluate solution between two contiguous membranes, the concentrated solution between two contiguous membranes next to the diluate chamber, and the two contiguous anion and cation-exchange membranes make up a cell pair. The cell pair is a repeating unit in an electrodialysis stack.

The schematic diagram described in Fig. 6.1 corresponds to one of the most common forms of electrodialysis used for desalination and deionization purposes. There are, however, several other processes closely related to conventional electrodialysis with various arrangements of ion-exchange or neutral membranes and with or without an electrical potential driving force [16]. Processes such as Donnan-Dialysis, diffusion dialysis, isoelectrodialytic focusing and electrodialytic water dissociation will be discussed in detail later.

The technical feasibility of electrodialysis as a mass separation process, i.e., its capability of separating certain ions from a given mixture with other molecules, is mainly determined by the properties of the membranes used in the system. The economics of the process are determined by the operating costs,

which are dominated by the energy consumption and investment costs for a plant of a desired capacity. Both energy consumption and investment costs are determined to a large extent by membrane properties, but are also affected by various process design parameters such as flow velocities, current density, cell dimensions, etc.

6.2.2 Properties of Ion-Exchange Membranes

Ion-exchange membranes are ion-exchange resins in film form. They consist, therefore, of highly swollen gels carrying fixed positive or negative charges. There are two different types of ion-exchange membranes:

(1) cation-exchange membranes which contain negatively charged groups fixed to the polymer matrix, and

(2) anion-exchange membranes which contain positively charged groups fixed to the polymer matrix.

In a cation-exchange membrane, the fixed anions are in electrical equilibrium with mobile cations in the interstices of the polymer, as indicated in Fig. 6.2, which shows schematically the matrix of a cation-exchange membrane with fixed anions and mobile cations, the latter referred to as counter-ions. In contrast, the mobile anions, called co-ions, are more or less completely excluded from the polymer matrix because of their electrical charge, which is identical to that of the fixed ions. This type of exclusion is called Donnan-exclusion in honor of his pioneering work [17]. Due to the exclusion of the co-ions, a cation-exchange membrane permits transfer of cations only. Anion-exchange membranes carry positive charges fixed on the polymer matrix. Therefore, they exclude all cations and are permeable to anions only. Thus, the selectivity of ion-exchange membranes results from the exclusion of co-ions from the membrane phase.

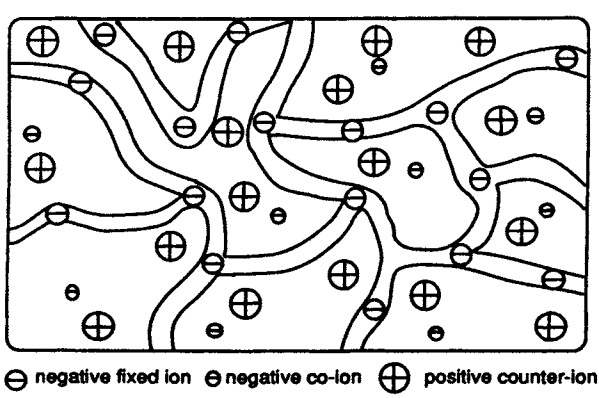

Fig. 6.2. Schematic diagram of the structure of a cation-exchange membrane showing the polymer matrix with the negative fixed charges, the positive counter-ions and the negative co-ions.

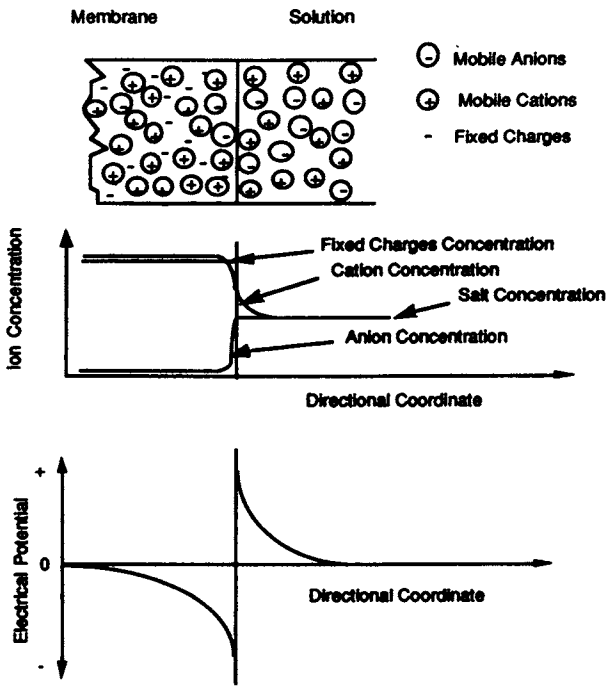

Fig. 6.3. Schematic drawing showing the concentration profiles of mobile cat- and anions in a cation-exchange membrane and the adjacent solution, and illustrating the Donnan potential at the membrane–solution interface.

The exclusion of the co-ions from the membrane phase leads, furthermore, to a build-up of an electrical potential difference between the membrane and the adjacent dilute solution, the so-called Donnan-potential as illustrated in Fig. 6.3. This figure shows the concentration profiles of fixed and mobile ions and the electrical potential gradient, between a cation-exchange membrane and a dilute electrolyte solution. Due to the comparatively high concentration of fixed negative charges, the concentration of the cations which are attracted by the negative fixed charges is higher in the membrane than in the adjacent solution. The concentration of mobile anions, on the other hand, is higher in the solution than in the membrane. This leads to concentration differences of cations and anions between the membrane and the adjacent solution which acts as a driving force for a diffusive mass transport. Since electroneutrality is required at any point in the membrane and the solution, diffusion of individual ions in the opposite direction leads to the build-up of a space charge which counteracts the concentration gradient driving force and equilibrium is established between the attempt of diffusion on one side and the establishment of an electrical potential difference on the other.

The electrical potential difference between the ion-exchange membrane and

an adjacent dilute solution, i.e. the Donnan-potential, cannot be measured directly. It can, however, be calculated [17] if electrochemical equilibrium between the membrane and the adjacent solution is assumed, by:

$$\eta_i^M = \eta_i^O \tag{6.1}$$

where η is the electrochemical potential. The superscripts M and O refer to the membrane and the adjacent outer phase, i refers to an ionic component.

The electrochemical potential can be related to the chemical potential by:

$$\eta_i = \mu_i + z_i F \varphi \tag{6.2}$$

where μ is the chemical potential, z the electrochemical valence (positive for cations and negative for anions), F the Faraday constant, φ the electrical potential and i refers again to an ionic component.

The chemical potential and thus the electrochemical potential is a function of the state variables temperature, pressure and composition [18]. If electrochemical equilibrium and equal temperature between the membrane and the adjacent solution is assumed the Donnan-potential can be expressed by:

$$\Delta\varphi_{Don} = \varphi^M - \varphi^O = \frac{1}{z_i F}\left(RT \ln \frac{a_i^O}{a_i^M} - v_i P_s\right) \tag{6.3}$$

where $\Delta\varphi_{Don}$ is the Donnan-potential, φ^M and φ^O are the electrical potentials in the membrane and in the solution, z_i is the electrochemical valence of the ion i, F the Faraday and R the gas constant, T is the absolute temperature, v_i the partial molar volume of the component i, and P_s the swelling pressure of the membrane.

The exclusion of the co-ions from the membrane can also be derived from the electrochemical equilibrium. If it is assumed that for a dilute solution the co-ion concentration in the membrane is small compared to the fixed ion-concentration, i.e. $C_C^M << C_C^O$, and the electrolyte is a mono-valent salt, then the concentration of the co-ions in the membrane can to a first approximation be expressed by the following relation [19]:

$$C_C^M = \frac{C_C^{O^2}}{C_R^M}\left(\frac{\gamma_\pm^O}{\gamma_\pm^M}\right)^2 \tag{6.4}$$

where C_C^M and C_C^O are the co-ion concentrations in the membrane and in the electrolyte solution, C_R^M is the concentration of the fixed ions in the membrane and $\gamma_\pm^O$ and $\gamma_\pm^M$ are the average activity coefficients of the salt in the electrolyte solution and the membrane.

Equation (6.4) can only describe the Donnan exclusion to a first approximation. In modern ion-exchange membranes considerable deviation of measured co-ion concentrations in the membrane from those calculated by Eq. (6.4) is obtained [20,21]. The differences between the observed and expected membrane behaviour are mainly due to a non uniformity in the distributions of molecular components in the membrane. This results from structural irregularities on a molecular level and from the influence of the electric field. Additionally, the practical application of thermodynamics is rather limited by the difficulties in the experimental measurement of independent interaction, diffusion, resistance and frictional coefficients.

The Donnan exclusion equilibrium and thus the membrane selectivity depend on: (1) the concentration of the fixed ions; (2) the valency of the co-ions; (3) the valence of the counter-ions; (4) the concentration of the electrolyte solution; and (5) the affinity of the exchanger with respect to the counter-ions.

Additional important parameters for the characterization of ion-exchange membranes are the density of the polymer network, hydrophobic and hydrophilic properties of the matrix polymer, the distribution of the charge density, and the morphology of the membrane itself. All these parameters do not only determine the mechanical properties, but also have a considerable influence on the sorption of the electrolytes and the non electrolytes and therefore on the swelling [11].

The most desired properties for ion-exchange membranes are:

- High permselectivity — an ion-exchange membrane should be highly permeable to counter-ions, but should be impermeable to co-ions.
- Low electrical resistance — the permeability of an ion-exchange membrane for the counter-ions under the driving force of an electrical potential gradient should be as high as possible.
- Good mechanical and form stability — the membrane should be mechanically strong and should have a low degree of swelling or shrinking in transition from dilute to concentrated ionic solutions.
- High chemical stability — the membrane should be stable over a pH range from 0 to 14 and in the presence of oxidizing agents.

It is difficult to optimize the properties of ion-exchange membranes because the parameters determining the different properties often have opposing effects. For instance, a high degree of cross-linking improves the mechanical strength of the membrane but also increases its electrical resistance. A high concentration of fixed ionic charges in the membrane matrix leads to a low electric resistance but, in general, causes a high degree of swelling combined with poor mechanical stability. The properties of ion-exchange membranes are determined by two parameters, namely, the basic polymer matrix and the type and concentration of the fixed ionic moiety. The basic polymer matrix determines to a large extent the mechanical, chemical and thermal stability of the

membrane. Very often the matrix of an ion-exchange membrane consists of hydrophobic polymers such as polystyrene, polyethylene or polysulfone. Although these basic polymers are insoluble in water and show a low degree of swelling, they may become water soluble by the introduction of the ionic moieties. Therefore, the polymer matrix of ion-exchange membranes is very often cross-linked. The degree of cross-linking then determines to a large extent the degree of swelling and the chemical and thermal stability, but it also has a large effect on the electrical resistance and the permselectivity of the membrane.

The type and the concentration of the fixed ionic charges determine the permselectivity and the electrical resistance of the membrane, but they also have a significant effect on the mechanical properties of the membrane. The degree of swelling, especially, is affected by the concentration of the fixed charges. The following moieties are used as fixed charges in cation-exchange membranes:

$$-SO_3^- \quad -COO^- \quad -PO_3^{2-} \quad -HPO_2^- \quad AsO_3^{2-} \quad -SeO_3^-$$

In anion-exchange membranes fixed charges may be:

$$-NH_3^+ \quad -RNH_2^+ \quad -R_2NH^+ \quad -R_3N^+ \quad -R_3P^+ \quad -R_2S^+$$

These different ionic groups have significant effects on the selectivity and electrical resistance of the ion-exchange membrane. The sulfonic acid group, e.g., $-SO_3^-$, is completely dissociated over nearly the entire pH-range, while the carboxylic acid group $-COO^-$ is virtually undissociated in the pH range < 3. The quaternary ammonium group $-R_3N^+$, again, is completely dissociated over the entire pH range, while the primary ammonium group $-NH_3^+$ is only weakly dissociated. Accordingly, ion-exchange membranes are referred to as being weakly or strongly acidic or basic in character. Most commercially available ion-exchange membranes have $-SO_3^-$ or $-COO^-$ groups, and most anion-exchange membranes contain $-R_3N^+$ groups [18].

6.2.3 Mass Transfer in Electrodialysis

The mass transfer in electrodialysis can be described by various mathematical relations, most of which are semiempirical. The most comprehensive description is based on a general equation relating the fluxes of heat, electricity, volume and individual components to the corresponding driving forces [22]:

$$J_i = \sum_i L_{ik} X_k (i,k = 1,2,3,\ldots, m) \tag{6.5}$$

where J_i is the flux of individual components, volume, heat or electricity; X_k is the driving force; and L_{ik} is the phenomenological coefficient relating flux and

driving force. For multicomponent systems with heat, volume and electricity fluxes, Eq. (6.5) can be written as a matrix. The diagonal coefficients relate the fluxes to the directly corresponding driving forces, and the cross-coefficients express the coupling of fluxes with indirectly conjugated driving forces.

Transport phenomena can be described rather completely with the aid of Eq. (6.5). Its practical value, however, is rather limited. First of all, Eq. (6.5) is only applicable close to equilibrium because of assumed linear relationships between fluxes and driving forces. Furthermore, the many different coefficients that vary as a function of state variables, such as temperature, composition or pressure, are difficult to determine by independent measurements.

In electrodialysis only mass fluxes and direct electric coupling of individual components are of concern, and the effect of a temperature gradient on the flux of individual components can generally be neglected. Thus, with this approximation, in electrodialysis the mass transport can be described by introducing the proper relations for the chemical potential, the electrical potential and the pressure gradients in Eq. (6.5) [16].

$$J_n = L_{nn} \frac{\mathrm{d}}{\mathrm{d}z} (-s_n T + v_n p + RT \ln a_n) + L_{nv} \frac{\mathrm{d}p}{\mathrm{d}z} + L_{ne} \frac{\mathrm{d}\varphi}{\mathrm{d}z} \tag{6.6}$$

where J is the flux, L a phenomenological coefficient, R the gas constant, T the absolute temperature, v the partial molar volume, p the pressure, s the partial molar entropy, a the activity, φ the electrical potential and p the hydrostatic pressure; z is a directional coordinate perpendicular to the membrane surface and the indexes n, v, and e refer to the components, the volume and the electrical charge, respectively.

When, furthermore, to a very first approximation electroosmotic effects, streaming potential etc. are neglected (i.e., pressure, concentration and temperature gradients are assumed to have no effect on the transport of ions), Eq. (6.6) can be integrated and reduces to:

$$J_n = L_{ne} \frac{\Delta\varphi}{\Delta z} \tag{6.7}$$

Using a mechanistic model for the mass transport in a continuous phase based on molecular diffusion, the phenomenological coefficient can be expressed by the ion mobility and the ion concentration:

$$J_n = C_n^{\mathrm{M}} u_n^{\mathrm{M}} \frac{\Delta\varphi}{\Delta z} \tag{6.8}$$

where J is the transmembrane flux, C the concentration, u the ion mobility, $\Delta\varphi$ the electrical potential gradient, and Δz the thickness of the membrane. The

subscript n refers to an ionic component and the superscript M to the phase, e.g., a membrane.

Equation (6.8) indicates that in electrodialysis, mass transport is caused mainly by an electrical potential difference that acts solely on charged components. Cations and anions move in different directions when subjected to an electrical potential difference and must therefore be considered separately.

Since in electrodialysis the entire transfer of electric charges is due to the transport of ions, the mass flux is directly proportional to the electric current, which is given by [15]:

$$i = F \sum_n z_n J_n \tag{6.9}$$

where i is the current density, F the Faraday constant, z the electrochemical valence and J the ion flux. The subscript n refers to the individual ions.

The relative fluxes of the different ions are denoted by transport number T, which is the ratio of the electric current conveyed by that ion to the total current [23]

$$T_n = \frac{z_n J_n}{\sum_n z_n J_n} \tag{6.10}$$

Combination of Eqs. (6.8) and (6.10) provides a relation between the transport number and the concentration and mobility of the different ions:

$$T_n = \frac{u_n z_n^2 C_n}{\sum_n u_n z_n^2 C_n} \tag{6.11}$$

Here, T is the transport number, z the electrochemical valence, C the concentration and the subscript n refers to the individual components.

The transport number can be related to the transference number by:

$$t_n = \frac{T_n}{z_n} \tag{6.12}$$

where t is the transference number.

For a solution of a univalent salt such as NaCl, the transport number is identical to the transference number. The transference number is $0 > t_n > 1$ and $t_+ + t_- = 1$, where the subscripts + and – refer to cations and anions, respectively.

The transport number or the transference number, respectively, are also a measure of the permselectivity of an ion-exchange membrane. If, for instance, the concentration of the co-ion in the membrane approaches 0, the transference

number of the counter-ion becomes 1 and the entire current through the membrane is transported by the counter-ion.

6.2.4 Membrane Permselectivity

The membrane permselectivity describes the degree to which it passes an ion of one charge and prevents the passage of an ion of the opposite charge. The membrane permselectivity is defined by:

$$\psi^{Mc} = \frac{t_+^{Mc} - t_+}{t_-} \tag{6.13}$$

and

$$\psi^{Ma} = \frac{t_-^{Ma} - t_-}{t_+} \tag{6.14}$$

where ψ is the permselectivity of a membrane, t is the transference number, the superscripts Mc and Ma refer to cation- and anion-exchange membranes and the subscripts + and – to cation and anion respectively.

Thus, the permselectivity of an ion-exchange membrane relates the transport of electric charges by specific counter ions to the total transport of electric charges through the membrane. An ideal permselective cation exchange membrane would transmit positively charged ions only, i.e. for $t_+^{Mc} = 1$ is $\psi^{Mc} = 1$. The permselectivity approaches zero when the transference number within the membrane is identical to that in the electrolyte solution, i.e. for $t_+^{Mc} = t_+$ is $\psi^{Mc} = 0$. For the anion-exchange membrane holds the corresponding relation. The transference number of a certain ion in the membrane is proportional to its concentration in the membrane which again is a function of its concentration in the solutions in equilibrium with the membrane phase, due to the Donnan exclusion as discussed earlier.

6.2.5 Energy Requirements in Electrodialysis

The energy required in an electrodialysis process is the sum of two terms: (1) the electrical energy to transfer the ionic components from one solution through membranes into another solution and (2) the energy required to pump the solutions through the electrodialysis unit. Depending on various process parameters, particularly the feed solution concentration, either one of the two terms may be dominating, thus determining the overall energy costs. The energy consumption due to electrode reactions can generally be neglected since more than 200 cell pairs are placed between the two electrodes in a modern electrodialysis stack [24].

(a) Minimum Energy Required for the Separation of a Molecular Mixture

In electrodialysis as in any other separation process there is a minimum energy required for the separation of various components from a mixture. For the removal of salt from a saline solution this energy is given by [23]:

$$\Delta G = RT \ln \frac{a_w^o}{a_w^s} \tag{6.15}$$

where ΔG is the Gibb's free energy change required to remove water from a solution, R the gas constant, and T the absolute temperature in °K; a_w^o and a_w^s are the water activities in pure water and the solution, respectively. Expressing the water activity in the solution with a monovalent salt by the concentration of the dissolved ionic components the minimum energy required to remove water from a monovalent salt is given by [15]:

$$E_{theo} = \Delta G = 2RT\,(C_o - C_d)\left[\frac{\ln \frac{C_o}{C_c}}{\frac{C_o}{C_c} - 1} - \frac{\ln \frac{C_o}{C_d}}{\frac{C_o}{C_d} - 1}\right] \tag{6.16}$$

where ΔG refers to the Gibb's free energy change required for the production of 1 liter of diluate solution, C is the salt concentration, the subscripts o, d and c refer to the feed solution, the diluate and the concentrate, respectively.

Furthermore,

$$\Delta G = \sum n_i z F \Delta\varphi, \qquad (i = 1,2,3,\ldots n) \tag{6.17}$$

where F is the Faraday's constant (9.652×10^4 A s^{-1} equival.$^{-1}$), z the chemical valence of the ion species i, n the number of moles of species i and $\Delta\varphi$ the potential drop due to the concentration difference in the diluate and concentrate. This potential drop is generally referred to as concentration potential.

(b) Practical Energy Requirements for the Ion Transfer

The total electrical potential drop across an electrodialysis cell consists only partly of the concentration potential, the other part is used to overcome the ohmic resistance of the cell. This ohmic resistance is caused by the friction of the various ions with the membranes and the water while being transferred from one solution to another, resulting in an irreversible energy dissipation in the form of heat generation. The potential drop to overcome the ohmic resistance can be, and generally is, significantly higher than the concentration potential, thus in electrodialysis the energy required in practice is generally significantly higher than the theoretically required minimum energy [25]. Furthermore,

energy is required to pump the feed solution, the diluate and the concentrate through the electrodialysis stack. Depending on various process parameters, particularly the feed solution concentration, either of these three terms may be dominant, thus, determining the overall energy costs.

The energy necessary to remove salts from a solution is directly proportional to the total current flowing through the stack and the voltage drop between the two electrodes in a stack. The energy consumption in a practical electrodialysis separation procedure can be expressed by [22]:

$$E_{prac} = I \, \Delta U \, n \, t \tag{6.18}$$

where E_{prac} is the energy consumption, I the electric current through the stack, ΔU is the voltage drop across a cell pair, n the number of cell pairs in a stack and t the time.

The electric current needed to desalt a solution is directly proportional to the number of ions transferred through the ion-exchange membranes from the feed stream to the concentrated brine. It is expressed as:

$$I = \frac{z \, F \, Q \, \Delta C}{\xi} \tag{6.19}$$

where F is the Faraday constant, z the electrochemical valence, Q the volumetric flow rate of the feed solution, ΔC the concentration difference between the feed solution and the diluate and ξ the current utilisation.

The current utilisation is directly proportional to the number of cell pairs in a stack.

A combination of Eqs. (6.18) and (6.19) gives the energy consumption in electrodialysis as a function of the current applied in the process, the electrical resistance of the stack, i.e., the resistance of the membrane and the electrolyte solution in the cells, the current utilisation and the amount of salt removed from the feed solution:

$$E_{prac} = \frac{n \, \Delta U \, t \, z \, F \, Qf(C_o - C_d)}{\xi} \tag{6.20}$$

Equation (6.20) indicates that the electrical energy required in electrodialysis is therefore directly proportional to the amount of salts that has to be removed from a certain feed volume to achieve the desired product concentration. Energy consumption is also a function of the voltage drop across a cell pair.

The total electrical potential drop across an electrodialysis cell consists of the concentration potential due to the different ion concentrations in the dilute and concentrate solutions and on the voltage drop used to overcome the ohmic resistance of the cell. Figure 6.4 shows the concentration profile in an electrodialysis cell pair. The cell pair contains the concentrated and the depleted feed

solutions, the two membranes and the four boundary layers, in which the concentrations of the salts in the solutions near the membranes may vary considerably from that in the bulk. The total voltage drop across a cell pair consists of three parts: (1) The concentration potential across the membranes between the diluate and concentrate solutions, and between boundary layer and bulk solution concentration, (2) the potential drop due to the ohmic resistance of the solutions, and (3) the potential drop due to the ohmic resistance of the membranes. Thus the total voltage drop is the algebraic sum of the concentration potentials resembling an electromotive force and the voltage drop due to the ohmic resistances. If the cross-section through a cell pair is illustrated by an electric circuit a series of electromotive forces resembling differences in the salt concentrations of the bulk, the boundary and the membrane phase in series with the voltage drop due to the ohmic resistance of the bulk and boundary layer solutions as well as the membranes are obtained. This is also indicated in Fig. 6.4 in which the electromotive forces caused by the concentration differences are indicated by the battery symbols and the ohmic resistances by a resistance symbol.

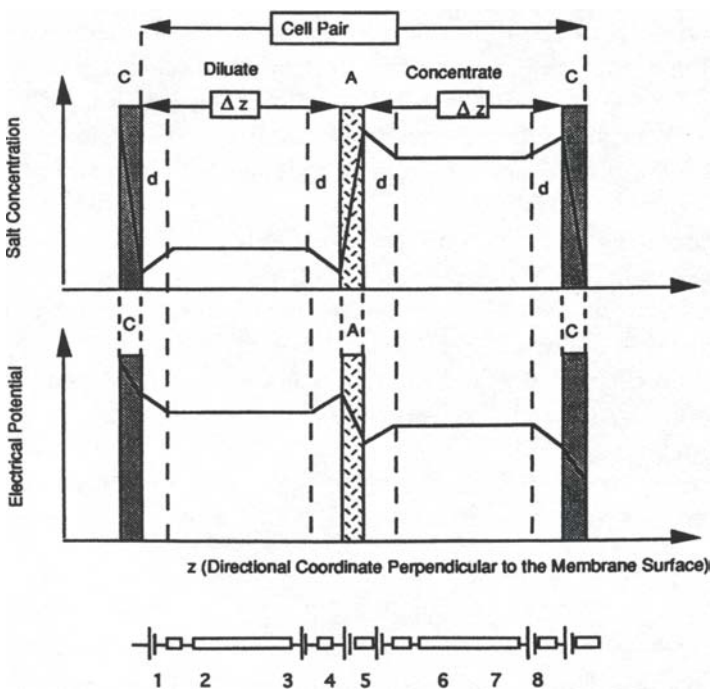

Fig. 6.4. Concentration and electrical potential profiles across an electrodialysis cell pair indicating the various potential drops due to concentration gradients and electrical resistances of the solutions and membranes.

The ohmic resistance is caused by the friction of the various ions with the membranes and the water while being transferred from one solution to another, resulting in an irreversible energy dissipation in the form of heat generation. Moreover, additional energy is also consumed by the electrode processes in the terminal compartiments since these do not contribute to the yield of either diluate or concentrate.

Other parameters being constant, the voltage drop due to the ohmic resistance of the cell pair is increasing with the current density. Electrical resistance, again, is a function of individual resistance of the membranes and of the solutions in the cells. In general the voltage drop due to the ohmic resistance is much larger than the voltage drop due to concentration potential or electrode reaction. It is therefore important to use membranes with low electrical resistance and to space the membranes very closely to reduce the voltage drop and thus the energy losses due to the ohmic resistance of the cell per unit of salt transferred.

An exact calculation of the voltage drop for a given electrodialysis unit takes into account the electrical resistance of the diluate and concentrate solution and of the membranes as well as the concentration potential. Furthermore the concentration polarisation effects in the boundary layers at the membrane surfaces due to a depletion of ion leads to additional voltage drops. An exact calculation of the voltage drop in an electrodialysis stack is rather complex. The calculation of the voltage drop in a practical relevant electrodialysis stack can significantly be simplified by making several approximations:

(1) The equivalent conductivity is independent of concentration over the range of interest.

(2) The concentration potentials are negligibly low, compared to the potential drops caused by the ohmic resistance of the solutions and the membranes.

(3) The concentrate and diluate cells have identical geometry and the flow of the solutions is co-current and of equal velocity.

(4) The inlet concentrations are identical for the diluate and concentrate cell.

(5) Changes in the ohmic resistance of the solutions due to boundary layer effects can be neglected.

With these approximations the voltage drop across a cell pair can be expressed by:

$$U = I\left[\frac{2\Delta}{\Lambda}\left(\frac{1}{C_d}+\frac{1}{C_c}\right)+\rho^{am}+\rho^{cm}\right] \tag{6.21}$$

where Δ is the cell thickness, Λ is the equivalent conductivity of the salt solution, ρ is the resistance, C refers to the salt concentration, the subscripts d and c refer diluate and concentrate and the superscripts am and cm refer to anion and cation-exchange membranes, respectively.

Since the resistance of a solution is inversely proportional to its ion concentration, the voltage drop across a cell pair will in most cases be determined mainly by the resistance of the diluate solution. The concentration in the diluate cell, however, is decreasing during the desalting process and thus its resistance is increasing accordingly. Under the assumption, that the concentration in the diluate is much lower than that in the feed and brine, the energy consumption can be expressed to a first approximation by [2]:

$$E_{pra} = \frac{I\, n\, b\, V \log \frac{C_o}{C_d}}{\xi} \tag{6.22}$$

where I is the electrical current passing through a stack, n the number of cell pairs, V the total volume of the diluate solution, C the concentration, b a constant factor which takes into account the resistance of the membranes, the equivalent conductivity of the solutions, concentration polarisation effects, cell geometry, Faraday constant, etc., and the subscripts o and d refer to the feed and the diluate solution. A typical value for the resistance of an electrodialysis cell pair, i.e., the cation- and anion-exchange membranes plus the diluate and the concentrated solutions (e.g., in the desalination of brackish water), is within the range of 5–500 $\Omega\ cm^2$ [26]. For other applications the electrical resistance of a cell pair might be significantly higher or lower. In applications where extremely low diluate concentrations are required, the conductivity in the diluate cell can be improved by using ion-conductive spacers [27].

(c) Pumping Energy Requirements

The operation of an electrodialysis system requires two or three pumps to circulate the diluate, the brine and eventually the electrode rinse solutions through the stack. The energy required for pumping these solutions is determined by the volumes to be circulated and the pressure drop. It can be expressed by:

$$E_p = k_d Q_d \Delta p_d + k_c Q_c \Delta p_c + k_e Q_e \Delta p_e \tag{6.23}$$

where E_p is the pumping energy, k a constant referring to the efficiency of the pumps, Q volumetric flow rates and Δp the hydrodynamic pressure loss; the subscripts d, c and e refer to diluate, concentrate and electrode rinse solutions, respectively.

The pressure losses in the various cells are determined by the solution flow velocities and the cell design. The energy requirements for circulating the solution through the system may become significant or even dominant for solutions with rather low salt concentration.

Other energy-consuming processes are the electrochemical reactions at the electrodes. In a stack with a multicell arrangement, however, the energy consumed at the electrodes is generally less than 1% of the total energy used for the ion transfer and can therefore be neglected [28].

(d) Energy Consumption in Electrodialysis and Other Separation Processes

In many applications electrodialysis competes with other separation processes. For the desalination of a saline solution, different processes such as reverse osmosis, ion exchange and distillation are used in addition to electrodialysis. All processes require the same theoretical minimum energy. The irreversibly dissipated energy is rather different in the different processes, as can be illustrated by comparing the basic principles of desalination by electrodialysis and reverse osmosis, which are shown schematically in Fig. 6.5.

The basic difference between reverse osmosis and electrodialysis is that in reverse osmosis the water passes through the membrane under a driving force of a hydrostatic pressure difference, whereas in electrodialysis the salt is passing through the membrane under the driving force of an electrical potential difference. The irreversible energy loss in reverse osmosis is caused by friction experienced by water molecules on their pathways through the membrane matrix. This means that the irreversible energy loss in reverse osmosis is independent of the feed water salt concentration. In electrodialysis the irreversible energy loss is caused by the friction of ions on their pathway through the membrane from the diluate to the brine solution. Thus, in electrodialysis the

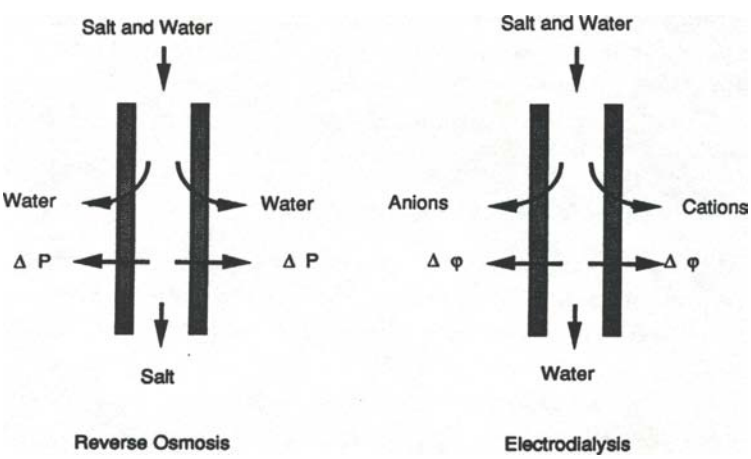

Fig. 6.5. Schematic drawing illustrating the mass transport in reverse osmosis and electrodialysis.

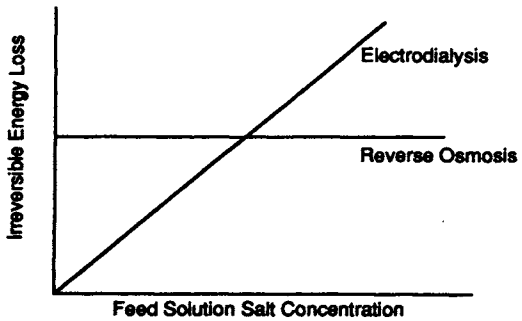

Fig. 6.6. Schematic diagram showing the irreversible energy loss in electrodialysis and reverse osmosis as a function of the feed solution salt concentration.

reversible energy loss is directly proportional to the feed salt concentration. For feed solutions with low salt concentrations, the energy requirements are therefore generally lower in electrodialysis than in reverse osmosis, and at high feed solution salt concentrations the situation is reversed. This is shown schematically in Fig. 6.6 where the irreversible energy consumption versus the feed solution concentration is plotted for electrodialysis and reverse osmosis assuming identical product water concentrations for both cases.

A comparison of mass separation processes concerning their energy consumption must take into account that in electrodialysis the energy is required in the form of electricity, a relatively expensive form, but in distillation a relatively inexpensive form of energy (i.e., heat) can be used. In ion exchange, e.g., very little energy is required directly. However, the chemicals used for the regeneration of the resin require a significant amount of energy for their production.

6.3 PREPARATION AND CHARACTERIZATION OF ION-EXCHANGE MEMBRANES

The technical feasibility and economics of electrodialysis and related processes are determined by the properties of the membranes used in the various applications. The development of efficient membranes with a long useful life under operating conditions is a key issue for the successful application of electrodialytical procedures.

Membranes to be used in electrodialysis and related processes should have a high selectivity for the transport of certain ionic species, while other charged and uncharged components should be more or less completely retained by the membrane. The transport rates for the permeating components in the mem-

brane should be as high as possible. Furthermore, the membrane has to meet certain mechanical requirements and should exhibit good chemical and thermal stability. Due to the importance of the membranes it is not surprising that there are numerous detailed recipes described mainly in the patent literature for the manufacturing of ion-exchange membranes with special application-adjusted properties.

The preparation procedures of ion-exchange membranes are closely related to those of ion-exchange resins. As with resins, there are many possible types with different polymer matrixes and different functional groups to confer ion-exchange properties on the product. Although there are a number of inorganic ion-exchange materials [11], most of them based on zeolites and bentonites, these materials are rather unimportant in today's technically used ion-exchange membranes and will not be discussed further.

Most commercial ion-exchange membranes can be divided, according to their structure and preparation procedure, into two major categories: either homogeneous or heterogeneous membranes.

Homogeneous ion-exchange membranes are produced either by polymerization of functional monomers, for example, by means of polycondensation of phenolsulfonic acid with formaldehyde [29], or by additional functionalizing of a polymer film by sulfonation [30]. For the combination of electrical and mechanical properties, the so-called heterogeneous ion-exchange membranes show many more possible variations. The degree of heterogeneity of ion-exchange membranes increases according to the following scale [31]: (1) homogeneous ion-exchange membranes, (2) interpolymer membranes, (3) microheterogeneous graft- and block-polymer membranes, (4) snake-in-the-cage ion-exchange membranes, and (5) heterogeneous ion-exchange membranes.

From the viewpoint of macromolecular chemistry all the intermediate forms are considered as so-called polymer-blends. As a consequence of the polymer/polymer incompatibility, a phase separation of the different polymers on one hand, as well as a specific aggregation of the hydrophilic and hydrophobic properties is obtained. A classification of the membrane morphology is then possible, depending on the type and the size of the microphase. If membranes are translucent, is this an indication that inhomogeneities, if any, are smaller than the wavelength of visible light (400 nm). Thus, these membranes are called interpolymer or microheterogeneous membranes.

Heterogeneous membranes are produced by melting and pressing of a dry ion-exchange resin with granulated polymers, or by dispersion of the ion-exchange resin in the solution or melting of a matrix polymer [32]. In the same manner, the polymer matrix can be polymerized in situ directly around the resin particles [33]. Microheterogeneous membranes, for example, are produced by means of block-copolymerization of ionogenic and non-ionogenic monomers, or by graft-copolymerization of functional monomers [34]. Inter-

polymer membranes are produced by dissolving compatible, functional polymers in one solvent to form a homogeneous, macroscopically transparent solution, followed by the evaporation of the solvent [35].

6.3.1 Preparation of Ion-Exchange Membranes

As far as their chemical structure is concerned, ion-exchange membranes are very similar to normal ion-exchange resins. The difference between membranes and resins arises largely from the mechanical requirements of the membrane process. Ion-exchange resins are mechanically weak, cation resins tend to be brittle and anion resins are normally soft [36]. They are dimensionally unstable due to the variation in the amount of water imbibed into the gel in different circumstances. Changes in electrolyte concentration, in the ionic form or in temperature may cause major changes in the water uptake and hence in the volume of the resin. These changes can be tolerated in small spherical beads, but in large sheets that have been cut to fit an apparatus they are not acceptable. Thus, it is generally not possible to use sheets of material which has been prepared in the same way as a bead resin. The most common solution to this problem is the preparation of a membrane with a backing of a stable reinforcing material, which gives the necessary strength and dimensional stability [37]. Preparation procedures for making ion-exchange resins and membranes are described in great detail in the patent literature.

(a) Preparation Procedure of Homogeneous Ion-Exchange Membranes

The methods of making homogeneous ion-exchange membranes can be summarized in three different categories:

(1) Polymerization or polycondensation of monomers; at least one of them must contain a moiety that either is or can be made anionic or cationic, respectively.

(2) Introduction of anionic or cationic moieties into a preformed solid film.

(3) Introduction of anionic or cationic moieties into a polymer, such as polysulfone, followed by dissolving the polymer and casting it into a film.

(1) Polymerization and polycondensation of monomers

The first ion-exchange membranes made by polycondensation of monomers were prepared from phenol by polycondensation with formaldehyde according to the following reaction scheme [29]:

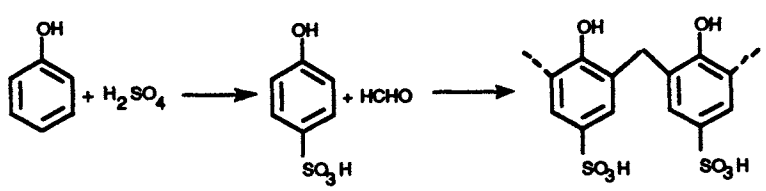

Phenol is treated with concentrated H_2SO_4, which leads to the phenolsulfonic acid in paraform. This acid is reacted with a solution of formaldehyde in water. The solution is then cast into a film, which polymerises at room temperature.

Another method of preparing a cation- and anion-exchange membrane is the polymerization of styrene and divinyl benzene and its subsequent sulfonation and amination. The cation-exchange membrane is obtained according to the reaction scheme [38]:

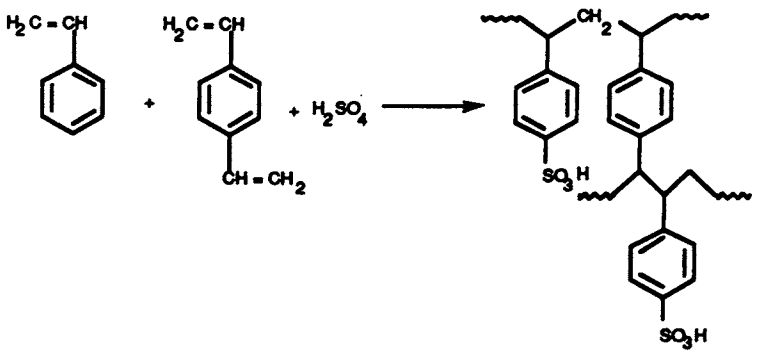

The anion-exchange group is introduced into the polymer by chloromethylation and amination with triamine according to the following reaction scheme:

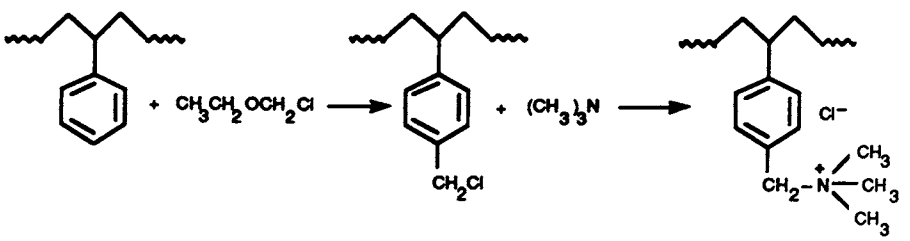

There exist numerous references in the literature for the preparation of ion-exchange membranes by polymerization [38,40–42].

(2) Introduction of anionic or cationic moieties into a solid preformed film

Concerning the introduction of anionic or cationic moieties into a preformed film, the monomer may either contain a cross-linking agent such as divinylbenzene, or alternatively, it may be grafted onto a film by radiation techniques. Starting with a film makes the membrane preparation rather easy. The starting material may be a hydrophilic polymer, such as cellulose or polyvinyl alcohol. More often, however, a hydrophobic polymer such as polyethylene or polystyrene is used.

Ion-exchange membranes made by sulfochlorination and amination of polyethylene sheets, for instance, have low electrical resistance combined with high

permselectivity and excellent mechanical strength. The reaction scheme for the preparation of these membranes is given below [43].

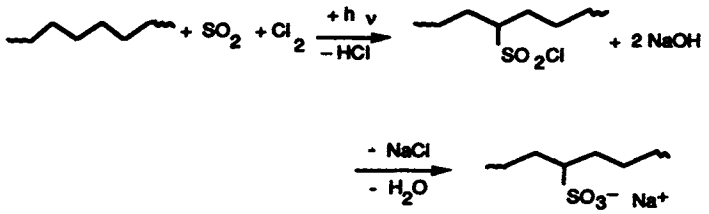

The cation-exchange membrane is prepared by exposing a polyethylene film to a mixture of SO_2 and Cl_2 gases at room temperature under radiation of ultraviolet light.

The anion-exchange membrane is made by amination of the sulfochlorinated polyethylene and reaction with methylbromide.

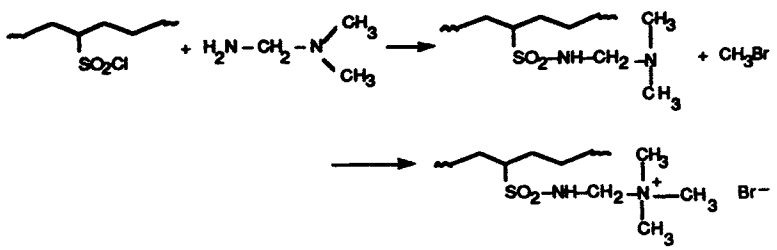

(3) Introduction of anionic or cationic moieties into a polymer chain followed by dissolving the polymer and casting it into a film

Membranes can also be prepared by dissolving and casting a functionalized polymer, such as sulfonated polysulfone, into a film. The reaction which includes (a) a sulfonation procedure followed by (b) a treatment with sodium acetate is illustrated in the following scheme:

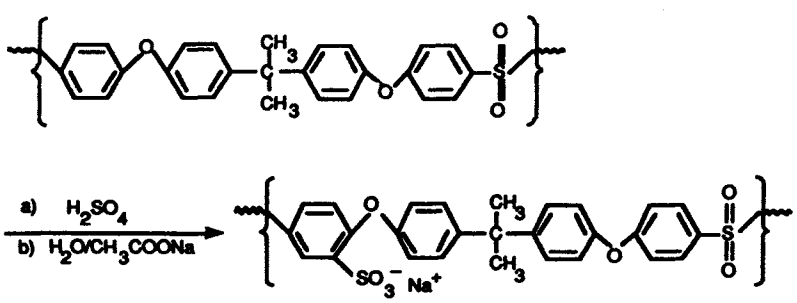

The sulfonated polysulfone can be cast as a film on a screen and precipitated after evaporation of most of the solvent such as dichloroethane. This leads to a reinforced membrane with excellent chemical and mechanical stabilities and good electrochemical properties. [43]

(b) Preparation Procedure of Heterogeneous Ion-Exchange Membranes

These membranes consist of fine colloidal ion-exchange particles embedded in an inert binder such as polyethylene, phenolic resins or polyvinyl-chloride. Such membranes can be prepared simply by calendering ion-exchange particles into an inert plastic film [11]. Another procedure is the dry-molding of inert film-forming polymers and ion-exchange particles and then the milling of the mold stock. Also, ion-exchange particles can be dispersed in a solution containing a film-forming binder, and then the solvent is evaporated to give the ion-exchange membrane. Similarly, ion-exchange particles are dispersed in a partially polymerized binder polymer, and then the polymerization is completed.

However, there are some significant differences between ion-exchange membranes and an ion-exchange resins concerning the details of the polymer structures, which are primarily due to the differences in size. In both cases the fixed, charged ion-exchange groups result in the swelling of the polymer when it is in contact with aqueous solutions. The amount of swelling depends to some degree on the ionic strength of the solution. In the case of granular ion-exchange resins, the extent of swelling is limited by cross-linking and by entanglement of the polymers. Typically, the level of cross-linking is about 10%. Owing to the spherical symmetry of granular ion-exchange resins and to the fact that they are not physically constrained in use, there is generally no functionally important physical damage to the resins from drying and rewetting or from change in ambient ionic strength [36].

Dimensional changes which are tolerable during use in the case of granular ion-exchange resins are not acceptable in ion-exchange membranes due to the large sizes of the latter and the fact that they are physically constrained in the electrodialysis stacks in which they are used. As a result, useful ion-exchange capacities (IEC = 1–3 (mequival/g dry membrane)) tend to be lower than in the case for granular exchangers (IEC = 3–5 (mequival/g resin)) resulting in reduced swelling tendencies. In addition to covalent cross-linking, other strategies are used to limit swelling, such as forming interpenetrating networks between the ion-exchange resin and other mostly semi-crystalline polymers or reinforcing the membrane by a fabric.

Heterogenous membranes with useful low electrical resistances contain more than 65% by weight of the cross-linked ion-exchange particles. Since these ion-exchange particles swell when immersed in water, it has been difficult to achieve adequate mechanical strength and freedom from distortion combined with low electrical resistance. Most heterogeneous membranes that possess adequate

mechanical strength generally show poor electrochemical properties. On the other hand, a membrane that contains ion-exchange particles large enough to show the desired electrochemical performance often exhibits poor mechanical strength.

In general, heterogeneous ion-exchange membranes have relatively high electrical resistances. Homogeneous ion-exchange membranes have a more even distribution of fixed ions and often lower electrical resistances.

(c) Special Property Ion-Exchange Membranes

In the literature, there are numerous methods reported for the preparation of ion-exchange membranes with special properties, for instance, to be used for the production of table salt, as battery separators, as ion-selective electrodes or in the chlor-alkali process. Significant effort has also been concentrated on the development of anion-exchange membranes with low fouling tendencies.

(1) Monovalent Ion Permselective Membranes

Since 1972, Japan has produced table salt by electrodialytic concentration of seawater. For the specific requirements of this process, ion-exchange membranes, which can separate monovalent ions from a mixed solution containing monovalent and multivalent ions, have been developed. Tokuyama Soda for example has commercialized monovalent cation-selective membranes (Neosepta® CMS) prepared by forming a thin cationic-charged layer on the surface. Monovalent anion permselective membranes (Neosepta® ACS), which have a thin, highly cross-linked layer on the membrane surface, have also been developed [44,45]. By such means, the selectivity of sulfate, compared with that of chloride, can be reduced from about 0.5 to about 0.01, and the selectivity of magnesium, compared with that of sodium, from about 1.2 to about 0.1.

(2) Proton Permselective Cation-Exchange Membranes

Amphoteric type ion-exchange membranes are preferentially permeable to hydrogen ions. By coating this membrane with a thin cation charged layer, the selectivity for H^+ versus Na^+ is improved up to [46]:

$$\left(\frac{H^+}{Na^+}\right) = 12$$

(3) Anion-Exchange Membranes with High Proton Retention

By means of traditional membranes, it is not possible to apply electrodialysis in the recovery of acid in order to reuse the acid because of high proton leakage through the anion-exchange membranes. In general, since protons permeate easily through an anion-exchange membrane, acids cannot be concentrated to more than a certain level by electrodialysis with high efficiency. Recently developed membranes exhibit low proton permeabilities and enable efficient acid concentration [45].

(4) Anti-Fouling Anion-exchange Membranes

Significant improvements have been made in the development of anion-exchange membranes with low fouling tendencies. In most conventional electrodialysis plants, the permissible current density in the anion-exchange membrane is smaller than in the cation-exchange membrane largely due to the risk of precipitates [47]. The anion-exchange membrane is more sensitive to fouling. According to some earlier studies concerning the permeability of commercial anion-exchange membranes, the upper molecular weight limit for practical electrodialytical separations is in the range of 100 Da [48]. A molecular weight of 350 Da is to be considered as a maximum size for any electro-transport through, for example, the Ionac MA-3475 membrane. The static permselectivity decreases gradually from 98 to 30% when the molecular weight of the solute increases from 59 Da to 171 Da [49].

Fouling of anion-exchange membranes often occurs when the anion is small enough to penetrate into the membrane structure, but its electromobility is so poor that the membrane is virtually blocked. To overcome this problem, different companies developed membranes that are characterized by a high permeability for large organic anions. In general, the permselectivity of these membranes is lower than that of regular membranes. Since the pore diameter of ion-exchange membranes is in the range of 10 Å, polyelectrolytes of high molecular weight are not harmful to ion-exchange membranes; however, on the other hand, large ionic compounds with molecular weights of several hundreds can cause membrane fouling.

One method to improve the permeability of anion-exchange membranes for large organic acids is based on the adjustment of the degree of cross-linkage and the chain length of the cross-linker in the polymer network [48].

Ionics Inc. produces a macroreticular membrane which is less sensitive to traces of detergents [50]. It is produced by dissolving an organic compound in the membrane-forming system. When the material diffuses from the membrane after the polymerization, large pores are left behind. Alternatively, certain salts, such as potassium iodide, are added to the solvent of the binder polymer, which is mostly dimethylformamide. Through these pores, large anionic molecules can penetrate, thus preventing a steep increase in the electrical resistance. Another type of anti fouling anion-exchange membrane is produced by Tokuyama Soda [44]. The membrane is coated with a thin layer of cation-exchange groups causing electrostatic repulsion of organic molecules. In practice the coating is done by weak sulfonation of the membrane surface, followed by the ordinary chloromethylation and quaternization steps.

Ion-exchange membranes based on aliphatic polymers show reduced organic fouling in natural waters as compared to membranes based on aromatic polymers. The aliphatic membranes also allow operations with solutions containing 0.5 ppm chlorine and for shock chlorination up to 20 ppm free chlorine.

(5) Fluorocarbon-Type Cation-Exchange Membranes

Most conventional hydrocarbon ion-exchange membranes are degraded by oxidizing agents, especially at elevated temperatures. In order to adapt ion-exchange membranes to an application in the chlor-alkali industry, a fluorocarbon-type membrane with excellent chemical and thermal stability was developed first by DuPont as Nafion® [51]. The membrane is produced in a several-step procedure, which starts with the synthesis of an ionogenic perfluorovinyl ether and its copolymerization with tetrafluorethylen (TFE). From the reaction of TFE with sulfur trioxide in the first step a cyclic sulton is formed, which rearranges to 2-fluorsulfonyl-difluoracetylfluoride. This intermediate reacts with hexafluor-propylene-oxide to produce a sulfonyl fluoride adduct.

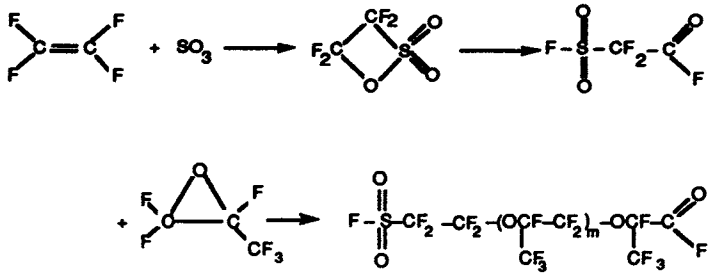

By heating the sulfonyl fluoride with sodium carbonate, the sulfonyl-fluoride-vinyl-ether is formed which is then copolymerized with tetrafluor-ethylene.

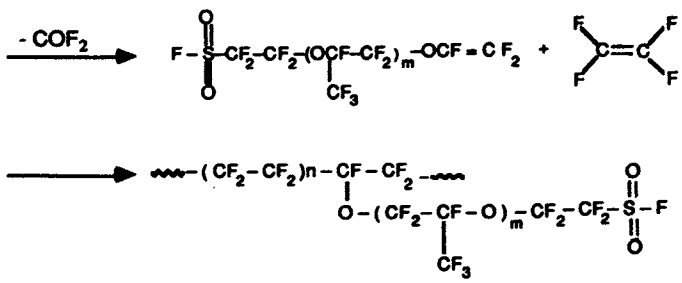

Then the resulting copolymer is extruded as a film of about a 100 μm thickness. Finally the ionogenic moiety is converted to membranes that carry sulfone-groups in the bulk of the membrane phase and carboxyl groups on the surface as the charged moieties. Therefore the $-SO_2F$ groups are reacted with sodium hydroxide to $-SO_3Na$ groups.

The $-CF_2SO_2F$ groups at the surface are converted to $-COOH$ groups in various ways by different manufacturers [44,52–55]. The economic lifetime of chloralkali membranes under the aggressive conditions are in the range of three years. The lifetime is determined in part by morphological changes and in part by loss of carboxylic acid ion-exchange capacity [56].

(6) Alkaline Stable Anion-exchange Membranes

In several technically interesting applications the economics of the process are affected by the limited stability of currently available anion-exchange membranes in strong alkaline solutions. In the case of cation-exchange membranes the chemical stability could be improved by perfluorination of the polymer backbone, resulting in membranes such as the Nafion®, Flemion®, Neosepta®-type structures. Comparable attempts with anion-exchange membranes to overcome the poor alkaline stability have so far been less successful. Due to the fact that the fluorocarbon-type anion-exchange membranes cannot overcome the problem of instability under strong basic conditions, it seems reasonable to assume that the alkaline stability of an anion-exchange membrane is determined by the stability of the incorporated positively charged groups against an attack of hydroxyl ions. By determining the disintegration rate of quaternized amines in alkaline solutions, an anion-exchange membrane with considerable improved alkaline stability was developed [57]. It was shown that due to their higher acidity, the cross-linked *bis*-quaternary structures have a much lower alkaline stability than the mono-quaternary ammonium groups. The highest alkaline stability was obtained with 1-benzyl-1-azonia-4-aza-bicyclo[2.2.2]-octane hydroxide which is obtained by reacting chloromethylated polystyrene with diaza-bicyclo-octane (DABCO).

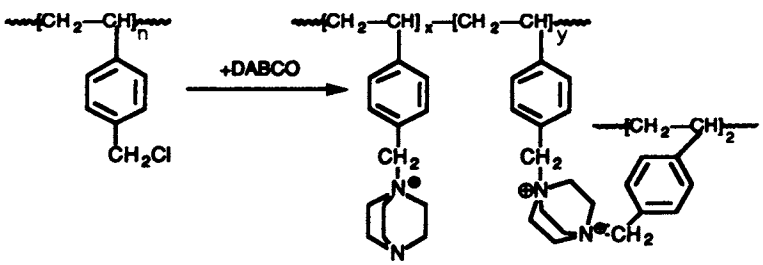

A further advantage arises from the possibility of preparing a well-defined polymer network because exposure to basic solutions does not diminish the degree of cross-linking but it converts the fixed ions to a piperazine system.

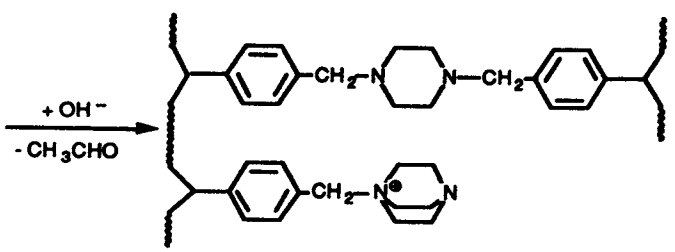

Integrated into a polysulfone or polyethersulfone matrix the anion-exchange membrane shows satisfactory electrical properties and excellent chemical and mechanical stability in strong alkaline solutions even at elevated temperatures.

(7) Bipolar Membranes

Bipolar membranes have recently gained increasing attention as efficient tools for the production of acids and bases from their corresponding salts by electrically enforced accelerated water dissociation. The process, which has been known for many years, is economically very attractive and has a multitude of interesting technical applications [58]. So far, however, large-scale technical use of bipolar membranes has been rather limited by the availability of efficient membranes. The principal structure of a bipolar membrane and its function is illustrated in Fig. 6.7 which shows an anion- and a cation-exchange membrane arranged in parallel between two electrodes similar to conventional electrodialysis. If a NaCl-containing solution is placed between these membranes and an electrical potential gradient is applied, all ionic species are removed from the solution. When there are no sodium and chloride ions left in the solution, the transport of the electrical charges through the membranes is accomplished exclusively by protons and hydroxyl ions, which are available even in pure water in a concentration of ca. 10^{-7} moles per liter due to the dissociation equilibrium of water. The dissociated water is continuously replenished from the outer phases, and thus, an alkaline solution is formed on the anion-exchange side and an acid solution on the cation-exchange side of the bipolar membrane.

Bipolar membranes can be prepared by simply laminating conventional cation- and anion-exchange membranes back to back [59]. The total potential drop depends on the applied current density, the resistance of the two membranes and the resistance of the solution between them. Since the specific

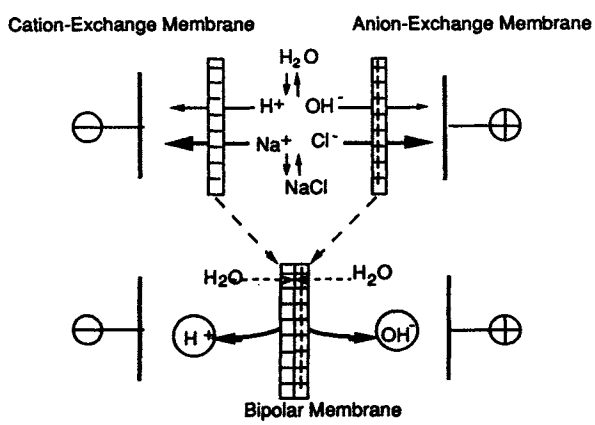

Fig. 6.7. Schematic diagram showing the configuration and basic function of a bipolar membrane.

resistance of deionized water is very high, the distance between the membranes of opposite polarity should be as low as possible. Laminated bipolar membranes often exhibit an unsatisfactory chemical stability at high pH values and sometimes a rather poor water-splitting capability and high electrical resistance. But special surface treatment of commercial ion-exchange membranes and subsequent laminating also may yield bipolar membranes with satisfactory properties. Single film bipolar membranes and multilayer bipolar membranes fulfil most of the practical needs [60]. For example, a bipolar membrane can be prepared by casting a cation selective layer on the top of the previously prepared cross-linked anion-exchange membrane [61]. To minimize the electrical resistance, the thickness of the interphase between the oppositely charged membranes should preferably be less than 5 nm. It could also be shown that in bipolar membranes, the chemical stability is determined to a large extent by the properties of the positively charged anion-exchange moieties and by the properties of the matrix polymer [57]. Furthermore, in practical applications bipolar membranes should not only have good chemical stability but also adequate water-splitting capability. From the ion fluxes observed in practical applications of bipolar membranes in which current densities in excess of 0.1 A cm^{-2} are used, one can calculate that the water dissociation rate in bipolar membranes is by several orders of magnitude faster than in pure water. The reasons for this accelerated water dissociation are not completely verified. There are two possible mechanisms discussed in the literature [61,62]. One is based on the second Wien effect, and the second postulates a catalytical chemical reaction. However, the experimental evidence reported in the literature supports the hypothesis that the water dissociation mechanism is based on a chemical reaction that consists of a reversible proton transfer between the charged groups of the membrane and the water molecules at its surface.

6.3.2 Characterization of Ion-Exchange Membranes

Ion-exchange membranes used in electrodialysis can be classified in terms of their mechanical and electrical properties, their permselectivity and their chemical stability. A microscopic examination yields information on whether or not a membrane is homogeneous or heterogeneous in structure or reinforced and the type of reinforcement used. The electrical charge of an ion-exchange membrane can be determined qualitatively by using indicator solutions. A drop of 0.05% solution of methylene blue and methylorange on a sample stains a yellow on top of an anion-exchange membrane and a blue on top of a cation-exchange membrane, respectively.

(a) Mechanical Properties of Membranes

The mechanical characterization of ion-exchange membranes includes the

determination of thickness, swelling, dimensional stability, tensile strength and hydraulic permeability. All tests should be carried out with pretreated and well-equilibrated membranes. Hydraulic permeability measurements provide information on the transport of components through a membrane under a hydrostatic pressure driving force. The presence of pinholes in ion-exchange membranes will not only lead to a drastically increased hydraulic permeability but will also invalidate any application. Pinholes can be determined by placing a wet membrane sheet on a sheet of white absorbent paper. A 0.2% solution of methylene blue for an anion-exchange membrane or a 0.2% solution of erythrocein-B for a cation-exchange membrane has to be spread over the entire surface. If no spots of the dye can be observed on the paper, the membrane is free of pinholes and can be tested for its hydraulic permeability. The test is carried out at room temperature using deionized water and a hydrostatic pressure driving force. The permeability can then be calculated from the volumetric flow rate.

The swelling capacity of a membrane determines not only its dimensional stability but also affects its selectivity, electrical resistance and hydraulic permeability. The swelling of a membrane depends on the nature of the polymeric material, the ion-exchange capacity and the cross-linking density. Usually, the swelling of a membrane is expressed by the weight difference between the wet and dry membrane. A sample is equilibrated in deionized water. After removing the surface water from the sample, the wet weight of the swollen membrane is determined. Then the sample is then dried at elevated temperature until a constant weight is obtained. The water uptake is determined as weight percent from the weight of the dry and wet sample.

(b) Chemical Stability of Membranes

The economics of electrodialysis and related processes in different applications is determined to a large extent by the chemical stability and the life of the ion-exchange membranes under process conditions. Membrane deterioration — after exposure for certain time periods to various test solutions containing acids, bases, or oxidizing agents — is estimated by visual comparison with new, unexposed samples and by determining changes in their mechanical and electrical properties.

(c) Determination of Membrane Ion-Exchange Capacities

The ion-exchange capacity of charged membranes is determined by titrating the fixed ions, e.g., $-SO_3^-$ or $-R_4N^+$ groups with 1 N NaOH or HCl, respectively. For these tests, cation- and anion-exchange membranes are equilibrated for about one hour in 1 N HCl or NaOH, respectively, and then rinsed free from chloride or sodium with deionized water. The ion-exchange capacity of the samples is then determined by back titration with 1 N NaOH or HCl, respectively. Weak base anion-exchange membranes are characterized by equilibra-

tion in 1 N sodium chloride and titration with standardized 0.1 N silver nitrate solution. The samples are then dried, and the ion-exchange capacity is calculated for the dry membrane.

(d) Permselectivity of Ion-exchange Membranes

As discussed earlier the permselectivity of an ion-exchange membrane relates the transport of electric charges by specific counter ions to the total transport of electrical charge through the membrane. An ideal selective cation exchange membrane would, for example, transmit positively charged ions only. The permselectivity approaches zero when the transference numbers within the membrane are the same as in the electrolyte solution. Due to the Donnan exclusion the permselectivity of a membrane depends also on the concentration of electrolytes in the solution and on the ion-exchange capacity of the membrane. When a membrane separates diluate and concentrate solutions, there will be a concentration gradient across the membrane. In this case the permselectivity can be calculated from the transfer of counter ions (dynamic method) according to the following equation:

$$\psi_n = \frac{t_n^{\mathrm{M}} - t_n^{\mathrm{s}}}{1 - t_n^{\mathrm{s}}} \tag{6.24}$$

where ψ_n the permselectivity of a cation in a cation-exchange membrane and an anion in an anion-exchange membrane, t is the transference number, the superscripts M and s refer to cation- or anion-exchange membranes and to the solution; the subscript n refers to cations and anions, respectively.

The transference numbers are determined by measuring the increase in concentration of certain ions in the feed and the decrease in the diluate solution and by measuring the amount of current passing through the unit during electrodialysis. The current utilization of the ion under consideration will give the transport number for this ion.

A faster method for the determination of apparent permselectivities ψ_n is based on a potential measurement. The experimental set-up of the test procedure is illustrated in Fig. 6.8. In this special case, the transport of water through the membrane is not taken into account and an apparent transference number is obtained. The apparent transference number ${}^{\mathrm{a}}t_n^{\mathrm{M}}$ of an ion (i.e., the water transport is not taken into account) is related to the true transference number by:

$${}^{\mathrm{a}}t_n^{\mathrm{M}} = t_n^{\mathrm{M}} - 0.018 \cdot t_{\mathrm{w}}^{\mathrm{M}} \cdot C_n \tag{6.25}$$

where ${}^{\mathrm{a}}t_n^{\mathrm{M}}$ and t_n^{M} are the apparent and real transference numbers, 0.018 is the molar volume of water in ml mmol^{-1}, $t_{\mathrm{w}}^{\mathrm{M}}$ refers to the water transfer rate and C_n

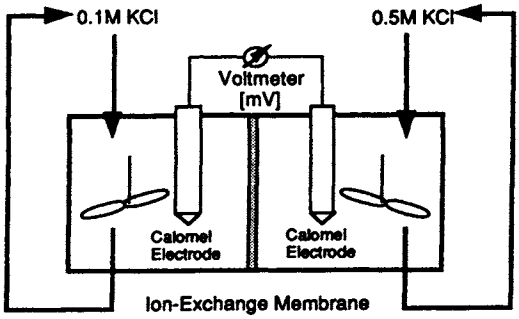

Fig. 6.8. Experimental set-up for determining membrane permselectivities.

to the ion concentration in the solution. The advantage of the determination of the potential between two solutions of different concentrations is that the tests are not obscured by concentration polarisation effects at the membrane surface.

The potential difference between two solutions of the same electrolyte but different concentration can be derived from the general flux equation described earlier and for the boundary conditions $\Delta P = 0$ and $I = 0$ (i.e., $\sum_n z_n F J_n = 0$). By introducing several approximations, such as negligible osmotic flow between the two solutions, constant ion mobilities and small concentration gradients across the membrane phase etc., the potential difference between solutions can be expressed for a monovalent electrolyte by [18]:

$$\Delta\varphi = -\frac{RT}{F}\left(t^{M}_{cou} - t^{M}_{co}\right)\ln\frac{a^{s}_{1}}{a^{s}_{2}} \tag{6.26}$$

where $\Delta\varphi$ is the potential difference between two solutions containing a monovalent electrolyte, t the transference number, a the activity, R the gas constant, T the temperature and F the Faraday constant. The subscripts cou and co refer to the counter- and the co-ion, respectively, and 1 and 2 refer to the two solutions separated by the membrane. The superscripts M and s refer to the membrane and the solution, respectively.

Since, furthermore, $t_{cou} + t_{co} = 1$, Eq. (6.26) reduces to:

$$\Delta\varphi = -\left(2\,t^{M}_{cou} - 1\right)\frac{RT}{F}\ln\frac{a^{s}_{1}}{a^{s}_{2}} \tag{6.27}$$

For a strictly semipermeable membrane, i.e. $t^{M}_{cou} = 1$, the potential difference between the two solutions is given by:

$$\Delta\varphi_{theo} = -\frac{RT}{F}\ln\frac{a^{s}_{1}}{a^{s}_{2}} \tag{6.28}$$

where $\Delta\varphi_{theo}$ the potential difference between two solutions separated by a strictly semipermeable ion-exchange membrane.

By dividing Eqs. (6.27) and (6.28), the counter-ion transference number of an ion-exchange membrane and thus its permselectivity is obtained [2]:

$$\frac{\Delta\varphi}{\Delta\varphi_{theo}} = 2\,t_{cou}^{M} - 1 \tag{6.29}$$

where $\Delta\varphi$ is the potential difference measured with two equal reference electrodes, e.g., calomel electrodes, and $\Delta\varphi_{theo}$ is the theoretically calculated potential difference between two solutions containing a monovalent electrolyte of different concentrations.

The actual test system consists of two cells separated by the membrane sample. The potential difference across the membrane is measured using a set of calomel electrodes. The selectivity is then calculated from the ratio of the experimentally determined to the theoretically calculated potential difference for a 100% permselective membrane.

For a system consisting of standardized aqueous solutions of 0.1 N and 0.5 N KCl at 25°C as an example, this theoretical potential difference amounts to 36.94 mV, as calculated by Eq. (6.24). Under the assumption that the transference number in the solution is approximately 0.5, the apparent permselectivity ψ_n of the membrane is in this case given by:

$$\psi_n = \frac{\Delta\varphi}{36.94} \cdot 100\% \tag{6.30}$$

where $\Delta\varphi$ is the measured potential difference between the two electrolytes. The absolute value of $\Delta\varphi$ is positive for a cation- and negative for an anion-exchange membrane.

(e) Electrical Resistance of Ion-Exchange Membranes

The electrical resistance of ion-exchange membranes is one of the factors that determine the energy requirements of electrodialysis processes. It is, however, in most practical cases considerably lower than the resistance of the dilute solutions, since the ion concentration in the membrane is relatively high. The specific membrane resistance is given as Ω cm. From the engineering point of view, the membrane area resistance in Ω cm^2 is more useful. The resistance of ion-exchange membranes is determined by conductivity measurements in a cell, which consists of two well-stirred chambers separated by the membrane, as indicated in Fig. 6.9.

The actual potential drop across the membrane is measured by calomel electrodes and Haber–Luggin capillaries placed with their tips directly on the membrane surface. The two electrodes used to provide the current flow

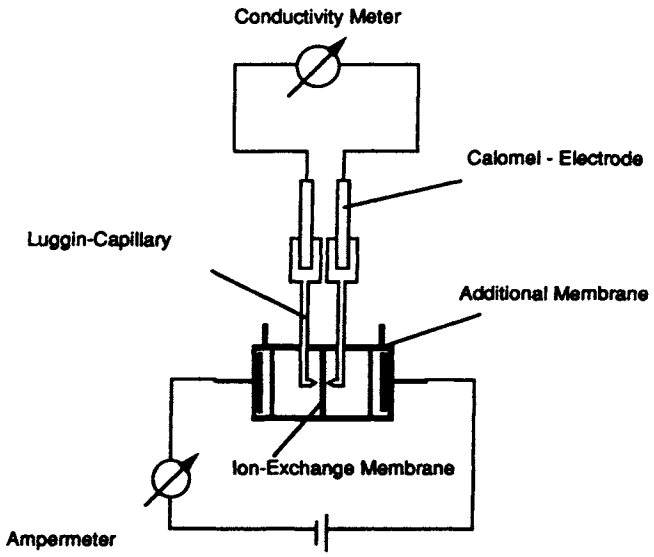

Fig. 6.9. Experimental set-up for determining the electrical resistance of ion-exchange membranes.

through the membrane are usually separated by membranes to avoid gas bubbles that are generated at the electrodes to penetrate into the capillaries and thus obscure the measurement. The potential drop across the membrane is determined as a function of the current density. The membrane resistance is determined from the slope of the current versus the voltage drop curve.

Properties of some commercially available membranes are listed in Table 6.1. This table, however, is far from being complete and subject to rapid change. There are many more special property membranes available on the market today than listed in the table.

TABLE 6.1

Properties of commercial ion-exchange membranes

Membrane	Structure properties	IEC (meq/g)	Thickness (mm)	Gel water (%)	Area resistance** ($\Omega \cdot cm^2$)	Perm-selectivity* (%)
Asahi Chemical Industry Co. Ltd., Hibiya-Mitsui Bldg. 12, 1-chome, Chiyoda-ku, Tokyo, Japan						
K 101	cation PS/DVB	1.4	0.24	24	2.1	91
A 111	anion PS/DVB	1.2	0.21	31	2–3	45
Asahi Glass Co. Ltd., 1-2 Marinouchi, 2-chome, Chiyoda-ku, Tokyo, Japan						
CMV	cation PS/DVB	2.4	0.15	25	2.9	95
AMV	anion PS/butadiene	1.9	0.14	19	2–4.5	92

(continued)

TABLE 6.1 (*continuation*)

Membrane	Structure properties	IEC (meq/g)	Thickness (mm)	Gel water (%)	Area resistance** ($\Omega \cdot cm^2$)	Perm-selectivity* (%)
ASV Flemion®	anion univalent cation perfluorinated	2.1	0.15	24	2.1	91
Ionac Chemical Co., Sybron Corp., Birmingham, NJ 08011, USA						
MC 3470	cation	1.5	0.6	35	6–10	68
MA 3475	anion	1.4	0.6	31	5–13	70
Ionics Inc., 65 Grove Street, Watertown, MA 02172, USA						
61 AZL 386	cation	2.0	0.5	46	4.5	–
103 QZL 386	anion	2.1	0.63	36	6	–
61 CZL 386	cation	2.6	0.6	40	9	–
103 PZL 183	anion	1.2	0.6	38	4.9	–
DuPont Co., Wilmington, DE 19898, USA						
N 117	cation fluorinated	0.9	0.2	16	1.5	–
N 901	cation fluorinated	1.1	0.4	5	3.8	96
RAI Research Corp., 225 Marcus Boulevard, Hauppauge, L.I., NY 117788, USA						
R-5010-L	cation LDPE	1.5	0.24	40	2–4	85
R-5010-H	cation LDPE	0.9	0.24	20	8–12	95
R-5030-L	anion LDPE	1.0	0.24	30	4–7	83
R-5030-H	anion LDPE	0.8	0.24	20	11–16	87
R-1010	cation fluorinated	1.2	0.1	20	0.2–0.4	86
R-1030	anion fluorinated	1.0	0.1	10	0.7–1.5	81
Tokuyama Soda Co. Ltd., 4-5, 1-chome, Nishi-Shimbashi, Minato-ku, Tokyo 105, Japan						
CL-25T	cation	2.0	0.18	31	2.9	81
ACH-45T	anion	1.4	0.15	24	2.4	90
ACM	anion	1.5	0.12	15	4–5	–
AMH	anion	1.4	0.27	19	11–13	–
CMS	cation univalent	>2.0	0.15	38	1.5–2.5	–
ACS	anion univalent	>1.4	0.18	25	2–2.5	–
AFN	anion anti-fouling	<3.5	0.15	45	0.4–1.5	–
AFX	anion dialysis	1.5	0.14	25	1–1.5	–
Neosepta®-F	cation fluorinated					

Measured: *1.0/0.5 N KCl, 25°C; **0.5N NaCl, 25°C

6.4 ELECTRODIALYSIS PROCESS AND EQUIPMENT DESIGN

The performance of electrodialysis and related processes in practical applications is not only a function of membrane properties but is also determined by several process and equipment design parameters, such as feed flow velocities and cell and spacer construction. These parameters affect the cost of the process directly by determining the investment costs, and indirectly by affecting the limiting current density and current utilization. Many of the basic equipment and process design aspects relevant in electrodialysis are also important in other electromembrane processes. But since electrodialysis is the largest industrial-scale electromembrane process it will be discussed here in some more detail.

The basic concept of electrodialysis has been discussed earlier and is shown in Fig. 6.1. This figure depicts the transport of ionic species in a cell arrangement consisting of cation- and anion-exchange membranes in alternating series forming individual cells between two electrodes. A device composed of individual cells in alternating series with electrodes on both ends is referred to as an electrodialysis stack. Although there are many different components necessary for the proper and efficient operation of an electrodialysis plant, such as the electrical power supply, pumps and control and monitoring devices, the stack is the key element.

6.4.1 Electrodialysis Stack Design

There are various stack design concepts described in the literature [63]. In praxis only two different stack designs are used on a large scale. One is the so-called sheet-flow and the other the tortuous path-flow concept.

A typical sheet-flow electrodialysis stack is shown in Fig. 6.10. It is a device to hold an array of membranes between electrodes in such a way that the streams being processed are kept separated. The gaskets not only separate the membranes but also contain manifolds to distribute the process fluids in the different compartments. The supply ducts for the diluate and the brine are formed by matching holes in the gaskets, the membranes and the electrode cells. The distance between the membrane sheets, i.e., the cell thickness, should be as small as possible since the solutions have a relatively high specific electrical resistance.

In industrial-size electrodialysis stacks, membrane distances are typically 0.5–2 mm. A spacer is introduced between the individual membrane sheets both to support the membrane and to help to control the feed solution flow distribution. The most serious design problem for an electrodialysis stack is that of assuring uniform flow distribution in the various compartments. In a practical electrodialysis system, 200–1000 cation- and anion-exchange membranes are installed in parallel to form an electrodialysis stack with 100–500 cell pairs.

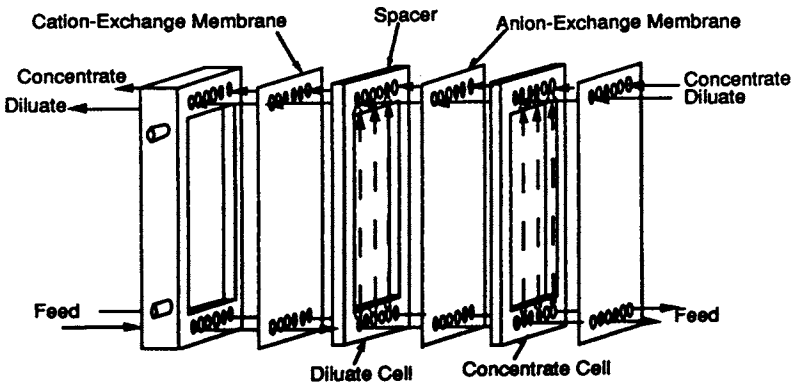

Fig. 6.10. Exploded view of an electrodialysis stack using a sheet-flow cell arrangement.

As other membrane separation processes, electrodialysis is also affected by concentration polarization and membrane fouling. The magnitude of concentration polarization is largely determined by the electrical current density, by the cell and particularly the spacer design and by the flow velocities of the diluate and brine solutions. Concentration polarization effects in electrodialysis lead to the depletion of ions in the laminar boundary layer at the membrane surfaces in the cell containing the diluate flow stream, and to the increase of ions in the laminar boundary layer at the membrane surfaces in the cell containing the brine solution. Concentration polarization is affecting the separation efficiency by decreasing the limiting current density [24].

More difficult to control, and in their consequences much more severe, are membrane fouling effects due to adsorption of polyelectrolytes, such as humic acids, surfactants and proteins. Because of their size, these components often penetrate the membrane only partially, thus resulting in severely reduced ion permeability of the membrane.

In designing an electrodialysis stack, several general criteria concerning mechanical, hydrodynamic and electrical properties have to be considered. Since some of the criteria have opposing effects, the final stack construction is generally a compromise between several conflicting parameters.

A proper electrodialysis stack design should provide a maximum effective membrane area per unit stack volume. The solution-distribution design should ensure equal and uniform flow distribution through each compartment. Any leakage between the diluate, concentrate and the electrode cells has to be prevented. The spacer screen should provide a maximum of mixing of the solutions at the membrane surfaces and cause a minimum in pressure loss.

Most stack designs used in current large-scale electrodialysis plants are one of two basic types: tortuous path or sheet flow. These designations refer to the type of solution flow path in the compartments of the stack. In the tortuous-path

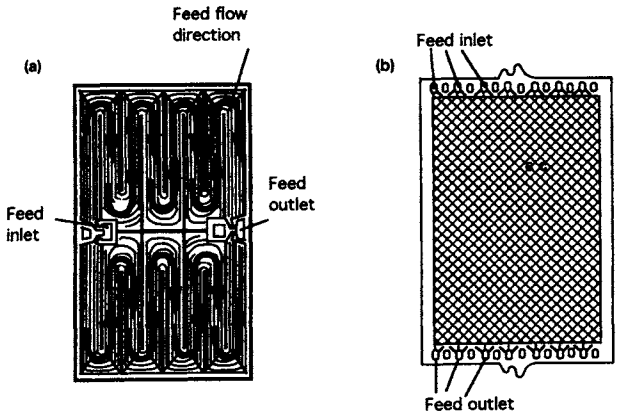

Fig. 6.11. Schematic drawing illustrating (a) the tortuous-path and (b) the sheet-flow spacer gasket.

stack, the membrane spacer and gasket have a long serpentine cut-out which defines a long narrow channel for the fluid path. The objective is to provide a long residence time for the solution in each cell in spite of the high linear velocity that is required to limit polarization effects. A tortuous-path spacer gasket is shown schematically in Fig. 6.11a.

In stack designs employing the sheet-flow principle, a peripheral gasket provides the outer seal and the solution flow is approximately in a straight path from the entrance to the exit ports, which are located on opposite sides in the gasket. This is illustrated in Fig. 6.11b, which shows the schematic diagram of a sheet-flow spacer of an electrodialysis stack.

Solution flow velocities in sheet-flow stacks are typically 3–10 cm s^{-1}, whereas in tortuous-path stacks, solution flow velocities are 15–50 cm s^{-1}. Because of higher flow velocities and longer flow paths, higher pressure drops in the order of 2–3 bars are obtained in tortuous-path stacks than in sheet-flow systems where pressure drops of 0.5–2 bars occur. However, higher velocities help to reduce the deposition of suspended solids and biological materials. There are several other stack concepts described in the literature and most of them provide three or four independent solution flow cycles, which are used, for example, in combination with bipolar membranes.

6.4.2 The Process Design

In addition to the actual stack and the power supply, an electrodialysis plant consists of several other components essential for proper operation, such as pumps, process monitoring and control devices and feed-solution pretreatment

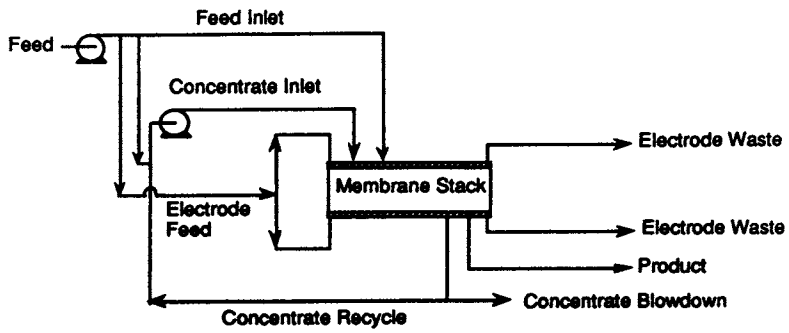

Fig. 6.12. Flow diagram of a typical unidirectional electrodialysis desalination plant.

systems. Again, as in the design of the electrodialysis stack, there are several operating modes for the electrodialytic process described in the literature. However, only two basic concepts are employed in large-scale applications. The first mode of operation is referred to as the unidirectional and the second as electrodialysis reversal (EDR) [64].

A flow diagram of a typical unidirectionally operated electrodialysis plant is shown in Fig. 6.12. After proper pre-treatment, the feed solution is pumped through the actual electrodialysis unit, which generally consists of one or more stacks in series or parallel. A deionized solution and a concentrated brine is obtained. The concentrated and depleted process streams leaving the last stack are collected in storage tanks when the desired degree of concentration or depletion is achieved, or they are recycled if further concentration or depletion is desired. Sometimes acid is added to the concentrated stream to prevent scaling of carbonates and hydroxides. To prevent the formation of free chlorine by anodic oxidation, the electrode cells are sometimes rinsed with a separate solution that does not contain chloride ions. In many cases, however, the feed or brine solution is also used in the electrode cells. Unidirectional-operated electrodialysis plant are rather sensitive to membrane fouling and scaling and often require a substantial feed solution pre-treatment and stack cleaning procedures in form of periodical rinsing of the stack with acid or detergent solutions.

Membrane fouling and scaling can be more or less completely avoided by applying electrodialysis reversal. The flow scheme of an electrodialysis plant operated with reversed polarity is shown in Fig. 6.13. In this operating mode, the polarity of the current is changed at specific time intervals ranging from a few minutes to several hours. In the reverse polarity operating mode, the hydraulic flow streams are reversed simultaneously, i.e., the diluate cell will become the brine cell and vice versa. The advantage of the reversed polarity operating mode is that precipitations in the brine cells will be redissolved when the brine cell becomes the diluate cell in the reverse operating mode [64]. During the reversal, there is a brief period when the concentration of the

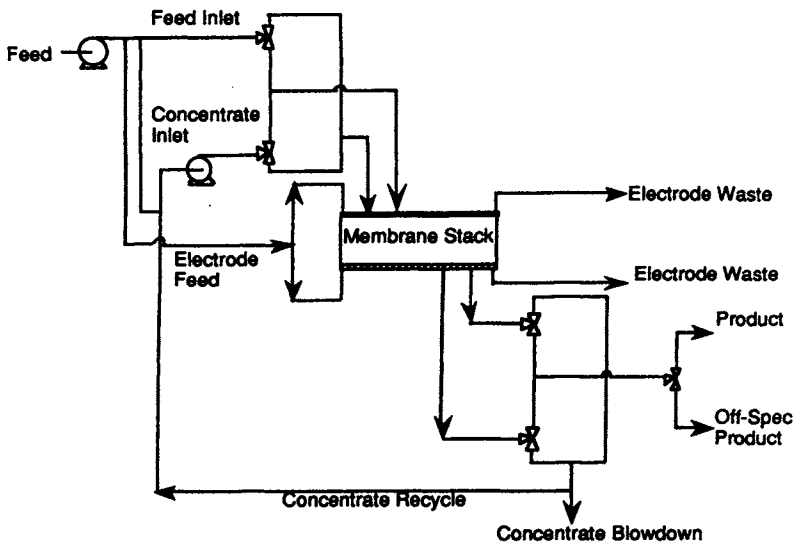

Fig. 6.13. Flow scheme of an electrodialysis reversal plant (operation with reversed polarity).

desalted product exceeds the product quality specification. The product water outlet has a concentration sensor which controls an additional three-way valve. This valve diverts high concentrated product to waste and then, when the concentration returns to the specified quality, directs the flow to the product outlet. Thus, in electrodialysis reversal there is always a certain amount of the product lost to the waste stream. This is generally no problem in desalination of brackish water. It might, however, be not acceptable in certain applications in the food and drug industry when feed solutions with high value products are processed.

6.4.3 Process Parameter Evaluation and Operational Problems

In practical application of electrodialysis there are several major operating parameters that are directly related to the stack and process design and that have a severe influence on technical feasibility and the economics of the process. These are the limiting current density, the current utilization, electrical resistances of the stack and hydrodynamic pressure losses of the liquid-flow streams in the stack. Operational problems may be caused by concentration polarization, membrane fouling and water transport through the membranes due to osmotic and electroosmotic effects or current leakage through the manifold.

(a) Concentration Polarization and Limiting Current Density

In almost all electrodialysis processes the solution to be treated flows between parallel planar ion-exchange membranes. The hydrodynamics of fluids

flowing between flat plates can be discussed on the basis of an idealized model which assumes laminar boundary layers at the membrane surfaces and well-mixed turbulent flow in the bulk solution [65].

The transport of charged species to the anode or cathode through a set of ion-exchange membranes leads to a concentration decrease of counter-ions in the laminar boundary layer at the membrane surface facing the diluate cell and an increase at the surface facing the brine cell.

This tendency for concentration and depletion, respectively, at the membrane surface is referred to as concentration polarization. It can be estimated by a mass balance of the fluxes through the laminar boundary layers at the membrane surface. Employing the very simplified so-called Nernst film model (which neglects all entrance and exit effects and assumes that fluxes parallel to the membrane surface are constant) the transport of different ions and their concentration gradients in the boundary layer can be calculated [66].

The transport of counter ions through an ion-exchange membrane under the driving force of an electrical potential is given by:

$$^{e}J^{M}_{cou} = T^{M}_{cou} \frac{i}{F z_{cou}} \tag{6.31}$$

where J is the flux, T the transport number, F the Faraday constant and z the electrochemical valence; the subscript cou refers to the counter-ion and the superscripts e and M refer to the electrical potential driving force and the membrane, respectively.

The transport of counter-ions in the boundary layer as the result of the electrical potential driving force is given by:

$$^{e}J^{S}_{cou} = T^{S}_{cou} \frac{i}{F z_{cou}} \tag{6.32}$$

where the superscript S refers to the solution.

Since in ion-exchange membranes the transport number in the membrane is always larger than that in the solution, i.e. $T^{M}_{cou} > T^{s}_{cou}$, their flux in the membrane is always larger than in the boundary layer. Therefore, there is a depletion on the side where the counter-ions enter the membrane, i.e., the side facing the diluate solution, while on the other side there is a concentration of ions. This results in a build-up of concentration gradients in the boundary layers. This is indicated in Fig. 6.14, where the concentration profiles of counter-ions in the boundary layers at the surface of an ion-exchange membrane are shown schematically, when an electric current is passing through the membrane.

The concentration gradient in the boundary layer leads to a diffusive flux of salt, which is given by:

$$^{d}J^{S}_{s} = - D_{s} \frac{dCs}{dz} \tag{6.33}$$

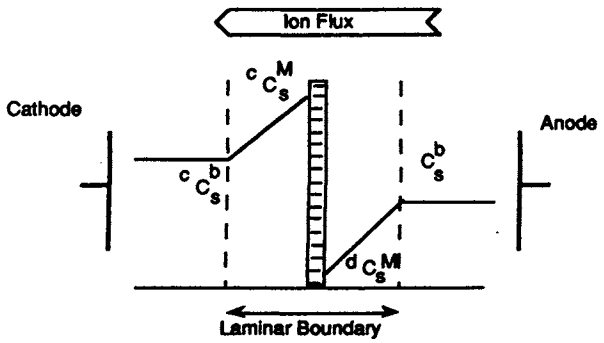

Fig. 6.14. Schematic diagram illustrating concentration polarization in the laminar boundary layer at the surface of an ion-exchange membrane during operation.

where J is the salt flux, D the diffusion coefficient, C the concentration and z a directional coordinate. The superscripts d and s refer to the diffusive flux and the solution, respectively, and subscript s refers to the salt.

At steady state, the combined electrical potential-driven flux and the diffusive flux in the boundary layer solutions equalize the electrical potential-driven flux through the membrane, which is essentially the total electrical flux when diffusion in the membrane is neglected. Thus:

$$J_{cou}^{M} = T_{cou}^{M} \frac{i}{F z_{cou}} = -D_s \frac{dC_s}{dz} + T_{cou}^{S} \frac{i}{F z_+} \tag{6.34}$$

Integration of Eq. (6.34) leads to a simple relation between boundary layer thickness, current density and membrane surface and bulk solution concentration:

$$C_s^{Ms} = C_s^b = C_s^b \pm \left(T_{cou}^{M} - T_{cou}^{S}\right) i \frac{\Delta z}{D_s F z_{cou}} \tag{6.35}$$

where C is the concentration, T the transport number, i the current density, D the diffusion coefficient, F the Faraday constant, z the electrochemical valence and Δz the boundary layer thickness. The superscripts Ms, b, M and S refer to membrane surface, bulk solution, membrane and solution, respectively. The subscripts s and cou refer to salt and counter-ion.

The concentration in the solution at the membrane surface C_s^{Ms} is greater than that of the bulk solution at the membrane surface facing the brine, and smaller at the surface facing the dilute solution, as indicated in the schematic drawing of Fig. 6.14.

If the current is raised above a certain value, the concentration at the membrane surface facing the diluate solution will approach zero. At this stage, there will be no more salt ions to carry the current, and current can only be trans-

ported by protons or hydroxyl-ions, which are formed by dissociation of water due to a large voltage drop as discussed earlier. The current density at which the ion concentration at the surfaces of the cation- and/or anion-exchange membranes in the cells with the depleted solution will become zero, is referred to as the limiting current density: it can be derived from Eq. (6.35), with $C_s^{Ms} = 0$; $i = I_{lim}$ to:

$$I_{lim} = \frac{{}^{d}C_s^b \, D_s \, z_{cou} \, F}{\Delta z (T_{cou}^M - T_{cou}^S)} = \frac{{}^{d}C_s^b \, z_{cou} \, F \, k}{T_{cou}^M - T_{cou}^S} \tag{6.36}$$

where I_{lim} is the current density, C the concentration, z the electrochemical valence, F the Faraday constant, Δz the boundary layer thickness and T the transport number. The superscripts b, M, d, and S refer to the bulk solution, the membrane, the diluate and the solution, respectively. The subscripts s and cou refer to the salt and the counter-ion. The constant k is the mass transfer coefficient, taking into account the influence of the hydrodynamics, flow channel geometry, spacer design, etc.

According to Eq. (6.36) the limiting current density is proportional to the ion concentration in the diluate and the mass transfer coefficient, which is determined mainly by the cell geometry and the feed solution flow velocity. If in electrodialysis the limiting current density is exceeded, the process efficiency will be drastically diminished because of the increasing electrical resistance of the solution and because of water-splitting, which leads to both pH changes and operational problems. The mass transfer coefficient can be expressed by the Sherwood number, which again is a function of the Schmidt and Reynolds numbers [67]. Introducing the proper relations in Eq. (6.36) leads to an expression which describes the limiting current density as a function of the feed–flow velocity in the electrodialysis stack:

$$i_{lim} = {}^{d}c_s^b \, a \, u^b \tag{6.37}$$

where ${}^{d}C_s^b$ is the concentration in the bulk phase of the diluate cell, u is the linear flow velocity of the solution through the electrodialysis cells and a and b are constants whose values are determined by a series of parameters, such as cell and spacer geometry, solution viscosity and ion-transfer numbers in the membrane and the solution.

The constants a and b and, therefore, the limiting current density, are a function of the electrodialysis stack designs and must be determined experimentally. The limiting current density can be determined by measuring the total resistance of a cell pair as a function of the current density. When the total resistance of a cell pair is plotted versus $1/i$ a minimum is obtained at the limiting current density [68]. This is shown schematically in Fig. 6.15.

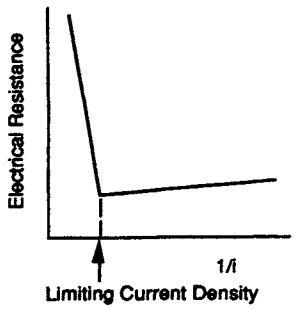

Fig. 6.15. Schematic diagram illustrating the determination of the limiting current density by plotting the total resistance of a cell pair versus $1/i$.

The limiting current density determines the minimum membrane area required to achieve a certain desalting effect.

(b) Process Efficiency and Current Utilization

Another very important parameter for the overall performance of the electrodialysis process is the current utilization. The current utilization determines the portion of the total current that passes through an electrodialysis stack that is actually used to transfer ions from a feed solution. The current utilization, which is always less than 100% is affected by three factors: (1) membrane selectivity, (2) osmosis and ion-bound water transport and (3) current passing through the stack manifold. The current utilization can be expressed by [22]:

$$\xi = \eta_w \, n\eta_s \, \eta_m \tag{6.38}$$

where ξ is the current utilization, η an efficiency term and n the number of cell pairs in a stack. The subscripts w, s and m refer to efficiency loss due to water transfer, efficiency loss due to reduced membrane selectivity and efficiency loss due to current passing through the manifold.

Expressing the efficiency loss due to incomplete membrane permselectivity in terms of co-ions transference numbers in the membrane and in the solution leads to:

$$\eta_s = 1 - \left(t^c_{co} + t^a_{co}\right) \tag{6.39}$$

where t is the transference number, the subscript co refers to co-ions and the superscripts c and a refer to the cation- and anion-exchange membrane. The total current efficiency is obtained by introducing Eq. (6.39) into Eq. (6.38):

$$\xi = n\eta_w \, \eta_m \left(1 - \left(t^c_{co} + t^a_{co}\right)\right) \tag{6.40}$$

The efficiency loss due to current passing through the manifold can be eliminated by proper stack design.

The water transferred due to osmosis and ion hydration can be significant at higher brine salt concentrations. The membrane selectivity also depends on the salt concentration. For a dilute feed and brine solutions, i.e., when the concentration of the feed solution and the brine is much lower than the concentration of the fixed charges in the membrane, an ion-exchange membrane is more or less strictly semipermeable, i.e., the membrane is permeable to counter-ions only. When, however, the ion concentration in the feed solution is of the same order as that of the fixed charges in the membrane, co-ions may also enter the membrane and its selectivity will then be decreased, with the consequence that the current efficiency will also be decreased.

6.4.4 Process Design and Economics

Process design and economics are closely related in electrodialysis. As in most other membrane processes the total cost is the sum of fixed charges associated with amortization of the plant capital cost and operating costs, such as energy and labor costs. Membrane replacement costs are often regarded as a separate item because of the relatively short life of the membrane.

(a) Capital Costs

Capital costs include depreciable items such as the electrodialysis stacks, pumps, electrical equipment and membranes and nondepreciable items such as land and working capital. The capital costs of an electrodialysis plant will strongly depend on the total membrane area required for a certain plant capacity. The required membrane area for a given capacity electrodialysis plant, however, is proportional to the amount of ions removed from a given feed solution and inverse proportional to the current density applied in a stack, as indicated by the following equation:

$$A = \frac{z F Q \Delta C n}{i \xi} \tag{6.41}$$

where A is the effective cell pair area, z the electro-chemical valence, Q the volumetric flow rate of the produced potable water, ΔC the difference in the salinity of feed and product water, n the number of cells in a stack, i the current density (which should be about 80% of the limiting current density), ξ the current utilization and F the Faraday Constant.

It should be noted that the actual membrane area is usually 15–25% higher than the effective membrane area calculated by Eq. (6.41) because of the so-

called shadow effect of spacers. The limiting current density is a function of the diluate concentration. The diluate concentration, however, is changing during the desalting process from the concentration of the original feed to the product solution concentration while it passes from the feed solution entrance of the stack to the product exit. Thus, the limiting current density is decreasing accordingly along the flow path through the stack. The calculation of the minimum membrane area required for a given desalting capacity is based on an average limiting current density, which is a function of the average diluate concentration and can be expressed to a first approximation by:

$$\bar{I}_{lim} = a\,\bar{C}_d = a\,\frac{C_o - C_d}{\log \frac{C_o}{C_d}} \tag{6.42}$$

where $\bar{I}_{lim}$ is an average limiting current density and a is a constant factor, which depends on the cell and spacer geometry and feed flow velocity. $\bar{C}_d$ is the average diluate concentration and C_o and C_d are the feed and diluate concentrations, respectively. Substitution of Eq. (6.42) into (6.41) leads to:

$$A_{min} = a'\,zFQ\,\log \frac{C_o}{C_d} \tag{6.43}$$

where A_{min} is the minimum membrane area required for a certain plant capacity and given feed and product solution concentrations; a' is a constant for a given plant design and operating mode; and the rest of the symbols have the same definition as given above.

For a certain plant capacity, the required membrane area is directly related to the feed water concentration assuming the same product water concentration. This is illustrated in Fig. 6.16, which shows a plot of the required mem-

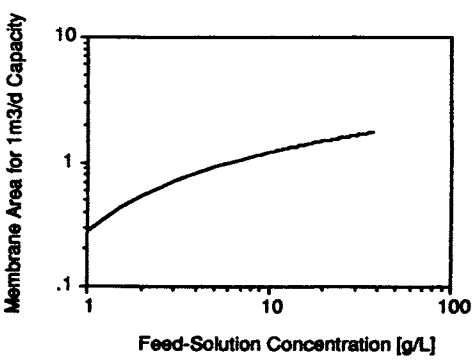

Fig. 6.16. Schematic diagram of the required membrane areas in electrodialysis as a function of the feed water concentration at constant current density and plant capacity and 0.5 g/l product concentration.

brane area to desalt 1 m^3 of a feed solution per day, as a function of the feed solution concentration assuming a product concentration of 0.5 g/l.

For typical brackish water of ca. 3,000 ppm (3 g/l) salt concentration and an average current density of 12 mA cm^{-2}, the required membrane area for a plant capacity of 1 m^3 product per day is ca. 0.4 m^2 of cation and 0.4 m^2 of anion-exchange membranes assuming a product concentration of 500 ppm.

Other items such as pumps, piping and tanks do not depend on feed water salinity but on plant size. For desalination of brackish water with a salinity of ca. 3000 ppm, the total capital costs for a plant with a capacity of 1000 m^3 per day will be in the range of US$ 200–300 per m^3 per day capacity [50]. The cost of the actual membrane is less than 30% of the total capital costs. Assuming a useful life of five years for the membranes (up to seven years is common for many brackish water applications) and 10 years for the rest of the equipment, a feed water salinity of 3000 ppm and a 24-hour operating day, the total amortization of the investment is ca. US$ 0.10–0.15 per m^3 potable water with a salinity of less than 500 ppm.

Capital costs depend not only on the feed solution concentration. Because they are a strong function of the plant size, they depend also on certain operating conditions, such as the current density, as will be discussed later. Certain applications of electrodialysis in the food and drug industry as well as in treating certain industrial effluents require substantial feed solution pretreatment and periodic rinsing of the stack in order to remove scaling and fouling layers from membrane surfaces [69]. The additional equipment needed in these applications of electrodialysis can lead to a substantial increase in the capital costs.

(b) Operating Costs

The operating costs are mainly determined by the required energy. As pointed out before, the energy in electrodialysis is determined by the electrical energy required for the actual desalting process and the energy necessary for pumping the solution through the stack. The energy for the actual desalting process, i.e., the ion transfer from the feed solution to the brine, is proportional to the amount of ionic species to be removed, as indicated in Eqs. (6.20) and (6.22), respectively. The energy requirement for the production of potable water as a function of the feed water concentration is shown in Fig. 6.17. The case considered is a NaCl feed solution with the product having a salt concentration of less than 500 ppm.

The pumping energy is independent of the feed solution salinity, but it does depend on the feed water recovery rate and temperature. Assuming a pressure drop in the unit of ca. 400 KPa (4 bar), a pump efficiency of 70% and 50% recovery, the total pumping energy will be ca. 0.4 kWh per m^3 product water.

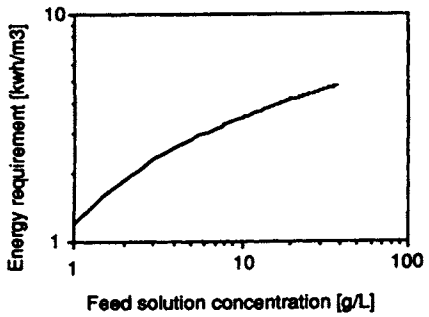

Fig. 6.17. Energy requirements for the production of potable water with a salt (NaCl) content of 500 ppm as a function of the feed solution concentration ($\Delta\varphi$ per cell pair = 0.8 V).

This indicates that at low feed water salt concentrations, the cost for pumping the solution through the unit might become quite significant.

It should be noted that according to Eqs. (6.20) and (6.41), the energy costs increase with increasing current density while the required membrane area decreases with increasing current density. Thus the total desalination cost — which is the sum of capital, energy and operating costs — will reach a minimum at a certain current density as illustrated in Fig. 6.18, where the total cost is shown as a function of the applied current density for a given feed solution.

Furthermore, quite interesting is a comparison of the costs of desalination by various processes as a function of the feed water salinity. At very low feed-solution salt concentrations, ion-exchange is considered to be the most economical process. But its costs are sharply increasing with the feed solution salinity, and at about 500 ppm electrodialysis becomes the more economical process. While between 5000 and 10 000 ppm reverse osmosis is the less costly process. At very high feed solution salt concentrations, in excess of 100 000 ppm, multistage flash evaporation becomes the most economical process. The costs of potable water produced from brackish water sources are in the range of US$ 0.2–0.5 per m^3.

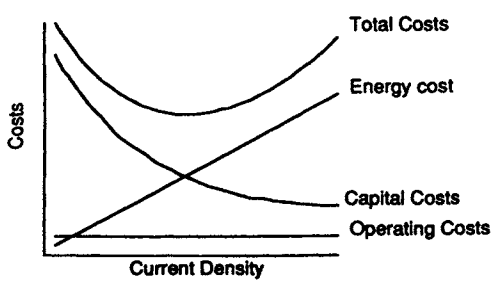

Fig. 6.18. Schematic diagram of the electrodialysis process costs as a function of the applied current density.

The costs of electrodialysis for the production of brackish water given here are only a specific example for a given plant size, location, etc. Costs may vary significantly depending on plant size, plant location, and, of course, feed-solution composition and product-solution requirements. Costs may vary by an order of magnitude depending on the various operating parameters.

6.5 APPLICATION OF ELECTRODIALYSIS

Electrodialysis was developed first for the desalination of saline solutions, particularly brackish water. The production of potable water is still currently the most important industrial application of electrodialysis. But other applications, such as the treatment of industrial effluents, the production of boiler feed water, demineralization of whey and deacidification of fruit juices are gaining increasing importance with large-scale industrial installations. Another application of electrodialysis that is limited regionally to Japan has gained considerable commercial importance. This is the production of table salt from seawater. Diffusion dialysis and the use of bipolar membranes have significantly expanded the application of electrodialysis in recent years. Some of the more important industrial applications of electrodialysis and their state of development are listed in Table 6.2.

TABLE 6.2

Industrial applications of electrodialysis and related processes

Application	Membranes and stack design	Status of the art	Key problems
Brackish water Desalination	anion- and cation- membranes tortuous-path and sheet-flow stacks	commercial	scaling and costs
Boiler feed-water, industrial process water	anion- and cation-exchange membranes	commercial	scaling and costs
Production of table salt	anion- and cation-exchange membranes, sheet-flow stack	commercial	costs
Industrial effluent treatment	anion- and cation-exchange membranes, sheet-flow and tortuous-path stack	commercial	costs
Food and pharmaceutical industry	anion- and cation- exchange membranes, sheet-flow and tortuous-path stack	commercial	membrane fouling, product loss
Ultrapure water	filled-cell stack	commercial	process reliability
Water dissociation	bipolar membranes three cell stack	commercial	performance

6.5.1 Desalination of Brackish Water by Electrodialysis

In terms of the number of installations the most important large-scale application of electrodialysis is the production of potable water from brackish water. Here, electrodialysis is competing directly with reverse osmosis and multistage flash evaporation. For water with relatively low salt concentration (less than 5000 ppm) electrodialysis is generally the most economical process, as indicated earlier. One significant feature of electrodialysis is that the salts can be concentrated to comparatively high values (in excess of 18–20% by weight) without affecting the economics of the process severely. Most modern electrodialysis units operate with so-called reverse polarity, i.e., the anode and cathode, and with that the diluate and concentrate cell systems are exchanged periodically, preventing a scaling due to concentration polarization effects. In brackish water desalination, more than 2000 plants with a total capacity of more than 1 000 000 m^3 of product water per day are installed, requiring a membrane area in excess of 1.5 million m^2 [70]. A substantial number of installations can also be found in Russia and China for the production of potable water. Exact data, however, are difficult to obtain [71].

6.5.2 Production of Table Salt

The production of table salt from seawater by the use of electrodialysis to concentrate sodium chloride up to 200 g l^{-1} prior to evaporation is a technique developed and used nearly exclusively in Japan. More than 350 000 tons of table salt are produced annually by this technique requiring more than 500 000 m^2 of installed ion-exchange membranes. Key to the success of this technology has been the low-cost, highly conductive membrane with a preferred permeability of monovalent ions [12]. However, it should be noted that in Japan this procedure of salt production is highly subsidized.

6.5.3 Electrodialysis in Waste Water Treatment

One of the more important applications of electrodialysis in waste water treatment systems is in processing rinse waters from the electroplating industry. Here, complete recycling of the water and the metal ions can be achieved by electrodialysis in some applications. Compared to reverse osmosis, electrodialysis has the advantage of being able to utilize more thermally and chemically stable membranes, so that processes can be run at elevated temperatures and in solutions of very low or high pH values. Furthermore, the concentrations which can be achieved in the brine can be significantly higher. The disadvantage of electrodialysis is that only ionic components can be removed and additives usually present in a galvanic bath cannot be recovered.

The recovery of nickel salts from electroplating rinse waters is an application which has been pursued by several companies [50]. Here, electrodialysis functions as a "kidney", removing the nickel salts which have been dragged out of the plating tank into a still-rinse. The concentrated nickel salts can often be fed directly back into the plating tank, while the diluate is recycled into the still-rinse.

Dump leach waters containing heavy metal ions have successfully been treated by electrodialysis. The removal of nitrate from drinking water by electrodialysis has been studied extensively and seems to compete well with other treatment procedures, such as ion-exchange or reverse osmosis [72].

An application which has been studied in a pilot plant stage is the regeneration of chemical copper plating baths [73]. In the production of printed circuits, a chemical process is often used for copper plating. The components that are to be plated are immersed into a bath containing (besides the copper ions) a strong complexing agent such as ethylenediamintetraacetic acid (EDTA), and a reducing agent such as formaldehyde. Since all constituents are used in relatively low concentrations, the copper content of the bath is soon exhausted and $CuSO_4$ has to be added. During the plating process, formaldehyde is oxidized to formate. After prolonged use, the bath becomes enriched with Na_2SO_4 and formate and consequently loses its useful properties. By applying electrodialysis in a continuous mode, the Na_2SO_4 and formate can be removed from the solution, without affecting the concentrations of formaldehyde and the EDTA complex. Therefore, the useful life of the plating solution is significantly extended. Several other potential applications of electrodialysis in waste water treatment systems, which have been studied on a laboratory scale, are reported in the literature. While in most of these applications the average plant capacity is considerably lower than that in brackish water desalination or table salt production, there is also a significant number of large plants installed for the treatment of refinery effluents and cooling-tower waste streams [73].

6.5.4 Concentration of Reverse Osmosis Brines

A further application of electrodialysis is the concentration of reverse osmosis brines. Because of the osmotic pressure of concentrated salt solutions, the concentration of brine in reverse osmosis desalination plants can not exceed certain values. Often the disposal of large volumes of brine is difficult, and a further concentration is desirable. This further concentration may be achieved at reasonable costs by electrodialysis [50].

6.5.5 Electrodialysis in the Chemical, the Food and the Drug Industry

The use of electrodialysis in food, drug and chemical industries has been studied quite extensively in recent years. Several applications have consider-

able economic significance and are already well established today. One is the demineralization of cheese whey [50,69]. Normal cheese whey contains between 5.5 and 6.5% of dissolved solids in water. The primary constituents in whey are lactose, protein, minerals, fat and lactic acid. Whey provides an excellent source of protein, lactose, vitamins and minerals, but in its normal form it is not considered a proper food material because of its high salt content. With the ionized salts substantially removed, whey approaches the composition of human milk and therefore provides an excellent source for the production of baby food. The partial demineralization of whey can be carried out quite efficiently by electrodialysis. The process is used extensively and is described in detail in the literature.

The removal of tartaric acid from wine is another possible application. Especially in the production of bottled champagne, it is necessary to avoid the formation of crystalline tartar in the wine and tartaric acid must therefore be reduced to a value which does not exceed the solubility limit. This again can be done efficiently by electrodialysis. Desalting of dextran solutions, another application for electrodialysis, is of technical significance as a large-scale industrial process.

Several other applications of electrodialysis in the pharmaceutical industry have been studied on a laboratory scale [74]. Most of these applications are concerned with desalting solutions containing active agents that have to be separated, purified or isolated from certain substrates [75]. Here, electrodialysis is often in competition with other separation procedures such as dialysis and solvent extraction. In many cases, electrodialysis is the superior process as far as economics and the quality of the product are concerned. The separation of amino acids and other organic acids by electrodialysis seems to be of special interest to the pharmaceutical and chemical industry [76]. However, the deionization of cheese whey is by far the most important application of electrodialysis in the food industry today [50].

6.5.6 Production of Ultrapure Water

More recently, electrodialysis is being used for the production of ultrapure water for the semiconductor industry. A combination with mixed-bed ion-exchange resins seems attractive, since completely deionized water is obtained without a chemical regeneration of the ion exchange resin. This process has been commercialized recently [77].

The electrodialysis industry has experienced a steady growth since it made its appearance as an industrial scale separation process about 20 years ago. Currently, the desalination of brackish water and the production of table salt are still the dominant applications, but new areas of application in the food and chemical industry as well as in waste water treatment are gaining interest rapidly.

6.6 OTHER ELECTRO-MEMBRANE PROCESSES

Today, electrodialysis is by far the most important industrial membrane separation process using ion-exchange membranes. There are, however, several other processes rapidly gaining technical relevance, such as diffusion dialysis, regular electrolysis used for the production of chlorine and caustic soda, the electrodialysis with bipolar membranes used for the production of acids and bases from the corresponding salts, and the combination of conventional electrodialysis with regular ion-exchange techniques to produce ultrapure water. Most of these processes have been developed only recently, and their large-scale industrial utilization is still in the beginning.

6.6.1 Diffusion Dialysis

The process is in principle identical to regular dialysis with the exception that ion-exchange in stead of uncharged membranes are used. The membranes are arranged in parallel in a cell system which is similar to that used in electrodialysis. There are also two flow streams. One containing the feed solution and the other the so-called dialysate which often consists of pure water. The concentration difference between the two solutions separated by the ion-exchange membranes is used as the driving force for the transport of the various components from the feed solution into the dialysate [78].

The process is used on a large scale to recover mineral acids from salt solutions obtained in pickling and etching processes. In this application only anion-exchange membranes are installed in a stack as indicated in Fig. 6.19, which shows the principle of the process. By feeding in alternating cells the salt and acid mixture and a dialysate solution in counter-current flow, the individ-

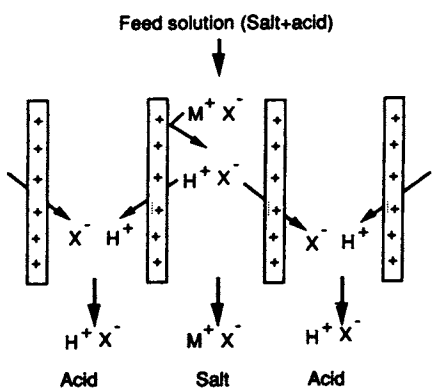

Fig. 6.19. Schematic diagram illustrating the principle of diffusion dialysis.

ual ions will migrate from the feed solution to dialysate following the concentration gradient driving force. While the anion can easily pass the anion-exchange membrane, all cations will be more or less completely rejected, except for protons which also are capable of passing anion-exchange membranes, due to a different transport mechanism. Therefore acids can be separated from salt mixtures by diffusion dialysis using anion-exchange membranes only. When operated in counter-current flow, more than 95% of the acids can be removed from the feed solution.

By using cation- instead of anion-exchange membranes bases can be removed from mixtures with salts, since also the hydroxide ions can permeate cation-exchange membranes much faster than other anions.

6.6.2 Donnan Dialysis

Donnan dialysis is used to exchange ions between two solutions. The stack arrangement is identical to that used in diffusion dialysis. The principle of the process is illustrated in Fig. 6.20, which shows a $CuSO_4$ solution and 1 N H_2SO_4 separated by a cation-exchange membrane.

Since the H^+-ion concentration in the acid solution (') is significantly higher ($p_H = 1$) than the H^+-ion concentration in copper sulfate solution ('') ($p_H = 7$) there will be a driving force for the transport of H^+-ions from solution (') into solution (''). Since the membrane is permeable to cations only, there will be a build-up of an electrical potential, which will counter-balance the concentration difference driving force of the H^+-ions. This electrical potential difference will cause a flux of Cu^{++}-ions against their concentration gradient from solution ('') into solution ('). As long as the H^+-ion concentration difference between the two phases separated by the cation-exchange membrane is maintained, there will be

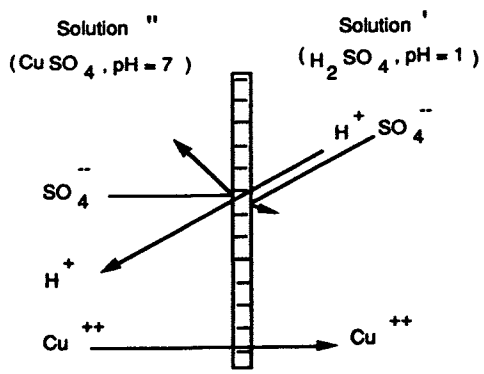

Fig. 6.20. Schematic diagram illustrating the principle of Donnan dialysis using a cation selective membrane and a pH gradient to exchange Cu^{++}-ions against H^+-ions.

the transport of Cu^{++}-ions until their concentration difference is of the same order of magnitude as the H^+-ion concentration difference. The process can be carried out accordingly with anions through anion-exchange membranes. An example of anion Donnan dialysis is the sweetening of citrus juices. In this process hydroxide ions furnished by a caustic solution replace the citrate ions in the juice. Another application of Donnan dialysis is softening of hard water where divalent ions, such as Ca^{++}- and Mg^{++}-, or SO_4^{--}-ions get exchanged for mono-valent ions such as Na^+- or Cl^--ions. Donnan dialysis is competing directly with conventional ion-exchange technology. In some cases, however, it is providing significant advantages in terms reduced waste salts and ease of operation.

6.6.3 Chlorine–Alkaline Electrolysis

The electrolytic production of chlorine and caustic soda by the use of a cation-exchange membrane as a separation medium has gained increasing technical and commercial importance with the development of the chemically very stable Nafion® membrane described earlier. The principle of the process is illustrated in the schematic drawing of Fig. 6.21, which shows an electrolysis cell arrangement consisting of two chambers separated by a cation-exchange membrane. One compartment contains an anode and a sodium chloride feed solution. The other compartment contains the cathode and water at the beginning of the process. When an electrical potential difference between the two electrodes is applied, the positively charged sodium ions will migrate towards the cathode — producing hydrogen and hydroxide ions by an electrochemical reaction at the cathode. The negatively charged chloride ions move towards the anode and will be oxidized to form chlorine. Thus sodium chloride is electrochemically converted into chlorine, caustic soda, and hydrogen. A migration of the hydroxide ions is prevented by the cation-exchange membrane. Therefore, the current utilization in the electrolytic chlorine and caustic soda production is quite high. The compartment containing the produced sodium hydroxide is

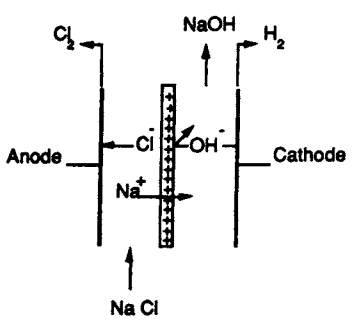

Fig. 6.21. Schematic diagram illustrating the chlorine–alkaline production process.

usually operated in a feed-and-bleed mode and its sodium hydroxide concentration is kept as high as possible. In industrial production processes, sodium hydroxide concentrations in excess of 10% are obtained [79]. Since the sodium chloride concentration is also kept rather high, the electrical resistance of the solutions is comparatively low, and the cell system can be operated at relatively high current densities up to a few thousand A/m^2 [80,81]. The main problem in the electrolytic production of chlorine and caustic soda is the stability of the cation-exchange membrane, which faces a strong caustic environment on one side and a solution containing free chlorine on the other side. Today, the technology is well developed and the membranes used in the process, such as the Nafion®, have demonstrated useful lifetimes of several years in operation, even at elevated temperatures [82].

6.6.4 Acids and Base Production by Electrodialytic Water Dissociation

As indicated earlier, the electrodialytic water dissociation in bipolar membranes is an efficient tool for the production of acids and bases from the corresponding salts [58]. So far, however, the large-scale use of the process has been rather limited because of the shortcomings of current bipolar membranes and of lack of practical experience. But recent advances in the development of efficient bipolar membranes has increased the technical and industrial importance of this process [83,84]. The function of a bipolar membrane has been illustrated earlier in Fig. 6.7.

The electrodialytic production of acids and bases with bipolar membranes has the advantage of being very energy efficient. The theoretical energy required for the process is that for establishing the desired concentration of H^+- and OH^--ions in the outer phases of the membrane from their concentration in the membrane which is approximately 10^{-7} mol l^{-1}. The reversible free enthalpy required for the production of acids and bases in a bipolar membrane at constant temperature and pressure can be calculated by the Nernst Equation for a concentration chain of solutions with different H^+-ion activities, i.e. pH values [85]:

$$\Delta G = F\,\Delta U = 2.3\,RT\,\Delta\mathrm{pH} \tag{6.44}$$

where ΔG is the reversible free enthalpy, ΔU the electrical potential difference between the two solutions, R is the gas constant, T is the absolute temperature, F is the Faraday constant, and ΔpH is the difference between the pH values of the two solutions separated by the bipolar membrane.

For 1 normal acid and base solutions in the two phases separated by the membrane the ΔU is 0.828 V and ΔG is 0.0222 kWh at 25°C. The actual potential drop across the bipolar membrane is higher than the calculated value because of irreversible effects due to the electrical resistance of the bipolar membrane.

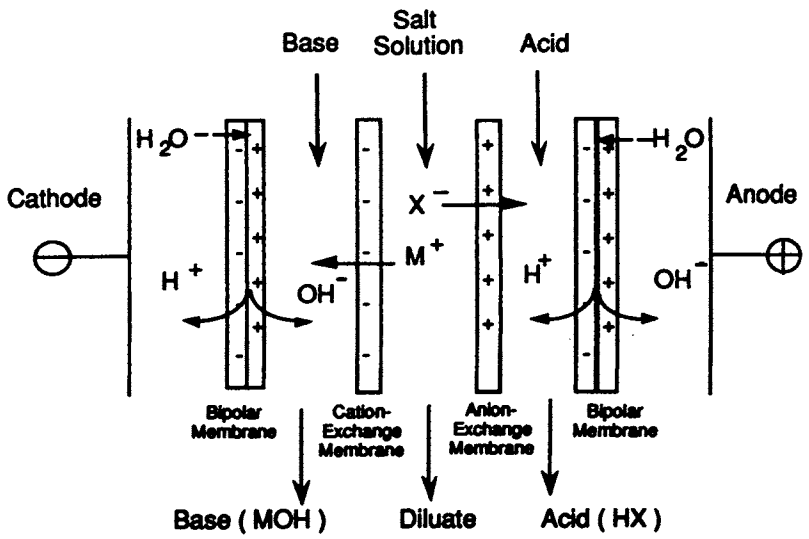

Fig. 6.22. Electrodialysis cell arrangement with bipolar membranes for the production of an acid and a base from the corresponding salt.

In contrast, generation of acid and base via an electrolysis process requires considerably more energy, because of the co-production of H_2 and O_2 [86].

The principle of the electrodialytic acids and bases production with bipolar membranes from the corresponding salts is illustrated in Fig. 6.22. The schematic drawing shows bipolar and cation-exchange and anion-exchange membranes arranged in parallel between two electrodes to form individual compartments.

If a salt solution is introduced in the middle compartment and an electrical potential difference between the electrodes is established, the cations in the salt solution will migrate towards the cathode. They will permeate the cation-exchange membrane and form a base with the hydroxide ions formed within the bipolar membrane. On the other side of the bipolar membrane the protons, which are formed simultaneously with the hydroxide ions, form an acid with the anions migrating from the salt solution through the anion-exchange membrane towards the anode. The net result of the entire process is the production of an acid and a base from the corresponding salt solution in an electrodialysis cell arrangement consisting of 3 individual compartments. As in conventional electrodialysis, the 3 compartment units can be stacked between electrodes.

While the function of a bipolar membrane in electrodialytic water dissociation seems quite obvious, there is considerable controversy as far as the actual mechanism of water dissociation is concerned [85].

The most prominent application of bipolar membranes today is the production of caustic soda. The world wide demand of polyvinyl chloride and other

chlorinated hydrocarbons has lead to the development of a large market for chlorine. Chlorine is generally produced by the chlorine–alkaline electrolysis in which caustic soda is obtained as a by-product that can be offered to the market at a very low price. Caustic soda on the other hand is a bulk chemical which is widely used in the chemical process industry as well as in many other relevant applications. Because of environmental problems caused by chlorinated hydrocarbons and their disposal the demand for chlorine is steadily decreasing and the demand for caustic soda will soon exceed that produced in the chlorine alkaline electrolysis and thus the interest in electrodialytic water dissociation as an alternative process is rapidly increasing.

Although the caustic soda production seems to be today the largest single application of the bipolar membrane technology it is by far not the only one. There are a large variety of potential applications in the chemical industry, in biotechnology and in waste water treatment. Typical processes with bipolar membranes that have been studied on a laboratory or pilot plant scale are [85]:

- The production of alkali hydroxides, such as sodium or potassium hydroxide.
- The production of mineral acids, such as hydrochloric, hydrofluoric or sulphuric acid from the corresponding salt solutions.
- The recovery of organic acids such as formic, acetic, citric, lactic, and itaconic acid or certain amino acids from fermentation broths.
- The adjustment of the pH values in surface and sea water to control scaling in distillation or reverse osmosis water desalination.
- The adjustment of pH values in fermentation or chemical production processes without increasing the ion potential.
- Regeneration of acids and bases from scrubbers used to remove SO_2, NO_x, and amines from waste air streams.

This list of potential applications of the electrodialytic water dissociation with bipolar membranes is far from being complete and with more efficient bipolar membranes becoming available in the future more interesting applications will certainly be identified.

(a) The Production of H_2SO_4 and NaOH from Na_2SO_4

The production of bases and acids such as NaOH and H_2SO_4 from the corresponding salts is by far the most relevant use of electrodialytic water dissociation with bipolar membranes. Acid and base concentrations up to 5 normal solutions can be achieved with a current utilisation of 60–70%. The maximum concentration of the acid and base that can be obtained in this process is limited by the salt leakage into the acid and the base due to the decreasing permselectivity of the bipolar membrane with increasing acid or base concentrations [85]. The relatively low current utilisation is caused mainly

by the low permselectivity of the anion-exchange membranes for protons. Thus to improve the overall efficiency of the electrodialytic water dissociation with bipolar membranes better proton blocking membranes have to be developed in addition to higher permselective bipolar membranes.

(b) Recycling H_2SO_4 and Dimethyl Isopropyl Amine from an Acid Scrubber

Alkaline or acid scrubbers are often used to remove components that are harmful to the environment such as NO_x, SO_2, or amines from waste air streams. In these processes large amounts of acids or bases are consumed and salts are produced. The recovery of a base from scrubbers used to remove SO_2 and NO_x from coal burning power plans has been studied in detail on a pilot plant scale and seems — at least under certain conditions — an economically interesting alternative to the techniques used today [14].

The recovery of dimethyl isopropyl amine removed from a waste air stream by a sulphuric acid scrubber is another interesting application studied on a laboratory scale. A waste air stream is generated when aluminium casting molds are made by mixing sand with an epoxy resin and injecting dimethyl isopropyl amine in a mixture with air as catalyst to cure the resin instantaneously. The amine catalyst is not consumed and emitted in a waste air stream that is scrubbed free of the amine with sulphuric acid. At a pH value of < 1.9 virtually all amine is precipitated as amine sulphate according to the equilibrium between the free amine and the amine sulphate. Complete recycling of the amine and the sulphuric acid can be achieved by combining the electrodialytic water dissociation with distillation. The process is illustrated in Fig. 6.23. The waste air stream containing the amines is fed into an acid scrubber where the free amine is converted into amine sulphate. The effluent of the acid scrubber containing ca. 10% amine sulphate is then fed into to the electrodialytic water dissociation apparatus containing bipolar membranes and anion-exchange membranes in alternating series between two electrodes. In this case there is no cation-exchange membrane in the system so that the salt solution simply loses sulphate ions and gains hydroxide ions, thus raising the pH to a value that the sulphate is converted back to the free amine while the sulphuric acid is recycled to the acid scrubber. The amine water mixture is distilled to recover the amine. The water is recycled to the electrodialysis unit. The process allows a complete recovery of the amine from a waste air stream by combination of an acid scrubber and electrodialytic water dissociation.

(c) The Use of Bipolar Membranes in Biotechnology

Bipolar membranes are used mainly in biotechnology to recover organic acids from a fermentation broth. A typical example is the production of itaconic

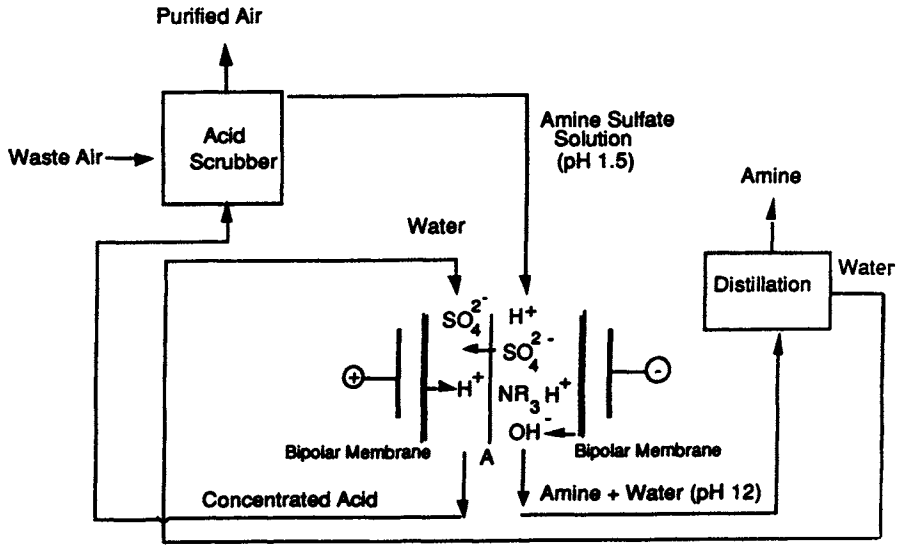

Fig. 6.23. Process scheme for amine recovery from a gas stream using acid scrubbing and a bipolar membrane regeneration system.

acid — an intermediate for the production of poly-acrylonitrile fibres. In the conventional batch-type process the pH value in the fermenter is shifting towards lower values during the acid production and is usually keep constant by adding sodium or ammonium hydroxide. In the conventional production process the free acid is recovered from the spent medium by adding sulphuric acid which generates a significant amount of salts with the desired product and thus requires further purification steps. By applying bipolar membranes the base can be recycled and the itaconic acid recovered continuously. The process scheme is illustrated in Fig. 6.24. The fermenter is fed with substrate. The reactor constituents are passed through a ultrafiltration unit. The product containing filtrate is fed to the middle cell of a three compartment electrodialyser. Here sodium ions, migrate towards the cathode and form with the OH^--ions generated in the bipolar membrane NaOH. Itaconate ions migrates towards the anode and forms itaconic acid with protons generated at the bipolar membrane. The acid is then concentrated and precipitated in a crystallizer. Thus the itaconic acid is produced and continuously removed from the fermenter without the addition of acids or bases, i.e., without the production of additional salts.

(d) Electrodialytic Production of Sodium Methylate by Electrodialytic Methanol Dissociation

Bipolar membranes may not only be used for the electrodialytic dissociation of water, but they can also be applied for the dissociation of alcohols and thus

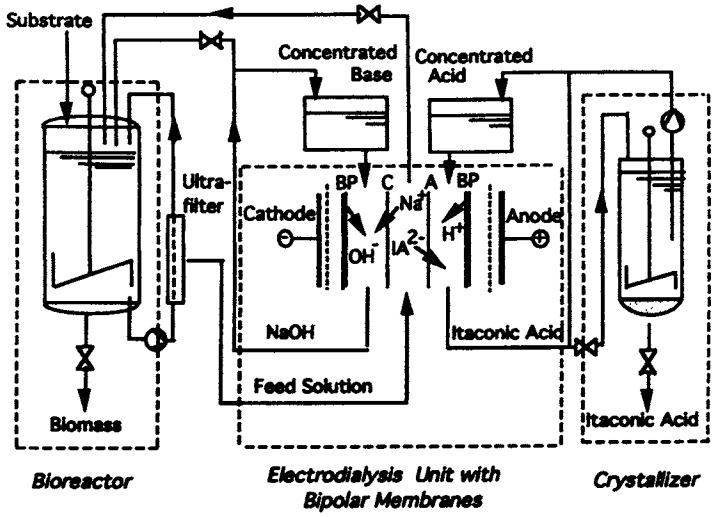

Fig. 6.24. Process scheme for the continuous production of itaconic acid utilising the combination of a fermentation and crystallisation step and electrodialysis with bipolar membranes.

for the production of alcoholates. Methanol, like water, is both a weak base and a weak acid. The dissociation constant, however, is lower than that of water. Therefore, methanol can be converted to its conjugated base typically by a conjugated base of a weaker acid, such as ammonia.

$$CH_3OH + NaNH_2 \leftrightarrow CH_3ONa + NH_3$$

This reaction is not easily carried out. But sodium methylate can also quite efficiently be produced from methanol and sodium acetate in non-aqueous media by the use of bipolar membranes according to the reaction scheme illustrated in Fig. 6.25 which shows a bipolar membranes containing electrodialysis stack consisting of two compartments cell systems in a repeating unit between two electrodes. Water free methanol and sodium acetate are fed into the cell formed by the bipolar and the cation-exchange membrane, while water-free methanol is passed through the other cell. Methanol is split in the bipolar membrane into protons and CH_3O^--ions which form CH_3ONa with sodium ions migrating from sodium acetate-containing cell towards the cathode. The acetate ions recombine on the other side of the bipolar membrane with the protons which were produced simultaneously with the CH_3O^--ions in the bipolar membrane to form acetic acid. Thus in the process sodium acetate and methanol is converted into sodium methylate. Sodium methylate in methanol concentrations of ca. 0.9 mol l^{-1} can be obtained. All in all the process seems to be technical feasible and commercially interesting.

Bipolar membrane have a multitude of potential applications and with

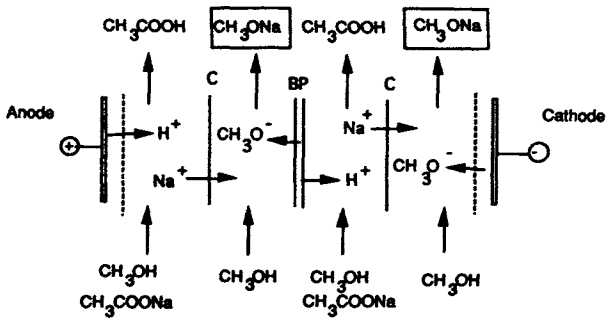

Fig. 6.25. Schematic diagram illustrating the two-compartment cell arrangement with bipolar and anion-exchange membranes only used for generating sodium methylate from methanol and sodium acetate.

efficient bipolar membranes becoming available today the first commercial units have already been installed.

6.7 CONCLUSIONS

Electrodialysis has a long and proven history for the desalination of brackish waters. This traditional role of electrodialysis will certainly continue in future. However, new applications for electrodialysis as well as for related processes are rapidly developing. New challenges in water and waste water treatment as well as in the chemical process and the food and drug industry have had and certainly will also have in future a significant effect on the rapid growth of electrodialysis and related processes. There are, however, still a multitude of problems to be solved. Some are related directly to the properties of the membranes others are caused by the lack of application know-how and practical experience.

NOTATION

A	cell pair area or membrane area
C	concentration
D	diffusion coefficient
E	energy consumption
F	Faraday constant
G	Gibb's free energy
I	electric current through the electrodialysis stack
J	flux

L phenomenological coefficient
P pressure
Q volumetric flow rate
R gas constant
T temperature
T transport number
U voltage
V volume of the solution
X generalized driving force
a activity of a component
a constant
a' constant
b constant
k constant
k mass transfer coefficient
n number of cell pairs in an electrodialysis stack
n number of moles
t transference number
t time
u linear velocity
u ion mobility
z electrochemical valence of ions
z directional coordinate

Greek Letters

Δ difference
μ chemical potential
ξ current utilization
φ electrical potential
η electrochemical potential
η efficiency term
γ activity coefficient
ρ electrical resistance
Λ equivalent conductivity
ψ permselectivity

Superscripts referring to:

$'$ solution separated by the membrane
$''$ solution separated by the membrane

–	average value
M	membrane
Mc	cation-exchange membrane
Ma	anion-exchange membrane
Ms	membrane surface
O	feed solution outside the membrane
a	apparent transfer number
a	anion
b	bulk phase
c	cation
d	diffusive transport
e	electrical potential driving force
o	pure water
s	salt solution

Subscripts referring to:

+	cation
–	anion
Don	Donnan potential
R	fixed ion concentration
c	concentrate solution
co	co-ion
cou	counter-ion
d	diluate solution
e	electrical charges
e	electrode rinse solution
f	feed
i	component
k	component
m	manifold current loss
n	component
o	feed solution
prac	value related to practical experience
s	swelling pressure
theo	theoretical value
v	volume
w	water

REFERENCES

1 T. Sata, Recent trends in ion-exchange research. *Pure Appl. Chem.*, 58 (1986) 1613–1626.
2 E. Korngold, Electrodialysis: Membranes and Mass Transport. In: G. Belfort (Ed.), *Synthetic Membrane Process*. Academic Press, New York, 1984, pp. 192–219.
3 H. Strathmann, Electrodialysis and its application in the chemical process industry. *Sep. Purif. Methods*, 14(1) (1985) 41–66.
4 W. Ostwald, Elektrische Eigenschaften halbdurchlässiger Scheidewände. *Z. Physik. Chemie*, 6 (1890) 71–82.
5 F.G. Donnan, The theory of membrane equilibrium in presence of a non-dialyzable electrolyte. *Z. Electrochem.*, 17 (1911) 572.
6 L. Michaelis and A. Fujita, The electric phenomen and ion permeability of membranes: II. Permeability of apple peel. *Biochem. Z.*, 158 (1925) 28–37.
7 H. Wassenegger and K. Jaeger, Effecting cation-exchange in removing calcium from hard waters. U.S. Patent 2,204,539, 1940.
8 K.H. Meyer, Strauss, *Helv. Chem. Acta*, 23 (1940) 795.
9 W. Juda and W.A. McRae, Coherent ion-exchange gels and membranes. *J. Am. Chem. Soc.*, 72 (1950) 1044.
10 A.G. Winger, G.W. Bodamer and R. Kunin, Some electrochemical properties of new synthetic ion-exchange membranes. *J. Electrochem. Soc.*, 100 (4) (1953) 178–184.
11 F. Helfferich, *Ion-Exchange*. McGraw-Hill Book Co., New York, 1962.
12 T. Nishiwaki, Concentration of electrolytes prior to evaporation with an electromembrane process. In: R.E. Lacey and S. Loeb (Eds.), *Industrial Processing with Membranes*. Wiley & Sons, New York, 1972.
13 H. Strathmann, Ion-exchange membranes in industrial separation processes. *J. Sep. Process Technol.*, 5(1) (1984) 1–13.
14 K.J. Liu, F.P. Chlanda and K.J. Nagasubramanian, Use of bipolar membranes for generation of acid and base: an engineering and economic analysis. *J. Membr. Sci.*, 2 (1977) 109.
15 L.H. Schaffer and M.S. Mintz, Electrodialysis. In: K.S. Spiegler (Ed.), *Principles of Desalination*, Academic Press, New York, 1966, pp. 3–20.
16 H. Strathmann, Membranes and Membrane Separation Processes. In: *Ullmann's Encyclopedia of Industrial Chemistry*, Vol. A 16, Verlag Chemie, Weinheim, FRG, 1990, pp. 187–263.
17 F.G. Donnan and E.A. Guggenheim, Exact thermodynamics of membrane equilibrium. *Z. Phys. Chem.*, A162 (1932) 346–360.
18 F. Bergsma and Ch. A. Kruissink, Ion-exchange membranes. *Fortschr. Hochpolym.-Forsch.*, 21 (1961) 307–362.
19 H.P. Gregor, Gibbs–Donnan equilibria in ion-exchange resin systems. *J. Am. Chem. Soc.*, 73 (1951) 642–650.
20 T.Z. Teorell, *Z. Elektrochem.*, 55 (1951) 460–469.
21 K.H. Meyer and J.F. Sievers, Permeability of membranes. *Helv. Chim. Acta*, 19 (1936) 649–677.
22 H. Strathmann, *Trennung von Molekularen Mischungen mit Hilfe Synthetischer Membranen*. Steinkopff-Verlag, Darmstadt, 1979.
23 K.S. Spiegler, Transport process in ionic membranes. *Trans. Faraday Soc.*, 54 (1958) 1408–1428.
24 M.S. Mintz, Electrodialysis: principles of process design. *Ind. Eng. Chem.*, 55 (6) (1963) 18–28.
25 R.E. Lacey, Basis of electromembrane processes. In: R.E. Lacey and S. Loeb (Eds.), *Industrial Processing with Membranes*. John Wiley & Sons, New York, 1972.

26 J.R. Wilson, *Demineralization by Electrodialysis*. Butterworth, London, 1960.
27 O. Kedem and Y. Maoz. Ion-conducting spacer for improved electrodialysis. *Desalination*, 19(1–3) (1976) 465–470.
28 S.B. Tuwiner, *Diffusion and Membrane Technology*. Reinhold, New York, 1962.
29 B.A. Adams and E.L. Holmes. Brit. Pat. 450 308, 1936.
30 H.Z. Friedlander, Membranes Encycl. *Polym. Sci. Technol.*, 8 (1968) 620–638.
31 G.E. Molau, Heterogeneous ion-exchange membranes. *J. Membr. Sci.*, 8 (3) (1981) 309–330.
32 N.P. Suryanarayana and Krishnaswamy, Ion-exchange membranes based on rubber. *J. Polym. Sci. B*, 1(9) (1963) 491–495.
33 K.M. Joshi and G.M. Ganu, Measurement of ionic activities in aqueous solutions using an epoxy-based ion-exchange membrane electrode. *Indian J. Technol.*, 16 (2) (1978) 52–55.
34 I. Ishigaki, N. Kamiya, T. Sugo and S. Machi, Synthesis of an ion- exchange membrane by radiation-induced grafting of acrylic acid onto poly(tetrafluorethylene). *Polym. J.*, 10 (5) (1978) 513–519.
35 S.R. Caplan and K. Sollner, Influence of the characteristics of the activating polyelectrolyte in the preparation and on the properties of interpolymer ion-exchange membranes: rational principles of membrane preparation and their experimental test. *J. Colloid Interface Sci.*, 40 (1) (1974) 46–66.
36 E.B. Tooper and L.F. Wirth, Ion-exchange resins. In: F.C. Nachod and J. Schubert (Eds.), *Ion-Exchange Technology*. Academic Press, New York, 1956.
37 D.S. Flett, *Ion Exchange Membranes*. E. Horwood Ltd., Chichester, UK, 1983.
38 K. Kusomoto, T. Sata and Y. Mizutani, Modification of anion- exchange membranes with polystyrene sulfonic acid. *Polym. J.*, 8 (1976) 225–226.
40 E.A. Murphy, F.J. Paton and J. Ansell. Apparatus for the electrical treatment of colloidal dispersions. U.S. Patent 2,331,494,1943.
41 W.A. McRae and S.S. Alexander. Sulfonating reagent and its use in preparing cation-exchange membranes. U.S. Patent 2,962,454,1960.
42 A. Eisenberg and H.L. Yeager, *Perfluorinated Ionomer Membranes*. ACS Symp. Ser. No. 180, American Chemical Society, Washington, DC, 1982.
43 P. Zschocke and D. Quellmalz, Novel ion-exchange membranes based on an aromatic polyether sulfone. *J. Membr. Sci.*, 22 (2/3) (1985) 325–332.
44 Tokuyama Soda, Product Bulletin, Tokyo, Japan, 1988.
45 T. Sata, R. Izuo and Y. Mizutani. Study of membrane for selective permeation of specific ions. *Soda to Enso*, 35 (415) (1984) 313–336.
46 R. Yamane, T. Izuo and Y. Mizutani, Ion-exchange membranes, XXIV: Permeability of the amphoteric ion-exchange membranes. *Denki Kagaku*, 33 (8) (1965) 589–593.
47 E. Korngold, F. De Körösy, R. Rahav and M.F. Taboch, Fouling of anion selective membranes in electrodialysis. *Desalination*, 8 (2) (1970) 195–220.
48 W. Gudernatsch, Ch. Krumbholz and H. Strathmann, Development of an anion-exchange membrane with increased permeability for organic acids of high molecular weight. *Desalination*, 79 (1990) 249–260.
49 R. Dohno, T. Azumi and Takashima, Permeability of monocarboxylate ions across an anion-exchange membrane. *Desalination*, 16 (1) (1975) 55–64.
50 Ionics Inc., Product Bulletin, Watertown, MA 02172, 1990.
51 D.J. Connolly and W.F. Gresham, Fluorocarbon vinyl ether polymers. U.S. Patent 3,282,875, 1966.
52 W.G. Grot, Laminates of support material and fluorinated polymer containing pendant side chains containing sulfonyl groups. U.S. Patent 3, 770,567, 1973.

53 Y. Onoue, T. Sata, A. Nakahara and J. Itoh, Process for preparing fluorine-containing polymers having carboxyl groups. U.S. Patent 4,200,711, 1980.
54 Asahi Chemical, Product Bulletin, Tokyo, Japan, 1988.
55 Asahi Glass, Product Bulletin, Tokyo, Japan, 1988.
56 K. Matsui, E. Tobita, K. Sugimoto, K. Kondo, T. Seita and Akimoto, Novel anion-exchange membranes having fluorocarbon backbone: preparation and stability. *J. Appl. Polym. Sci.*, 32 (3) (1986) 4137–4143.
57 B. Bauer, F. Effenberger and H. Strathmann, Anion-exchange membranes with improved alkaline stability. *Desalination*, 79 (1990) 125–144.
58 K.N. Mani, Electrodialysis water-splitting technology. *J. Membr. Sci.*, 58 (2) (1991) 117.
59 F.B. Leitz, Apparatus for electrodialysis of electrolytes employing bilaminar ion-exchange membranes. U.S. patent 3, 654, 125, 1972.
60 F.P. Chlanda, L.T.C. Lee and K.J. Liu, Bipolar membranes and method of making same. U.S. Patent 4, 116,889, 1976.
61 B. Bauer, F.-J. Gerner and H. Strathmann, Development of bipolar membranes. *Desalination*, 68 (1988) 279–292.
62 R. Simons, Electric field effects on proton transfer between ionizable groups and water in ion-exchange membranes. *Electrochimica Acta*, 29 (1984) 151–158.
63 E.L. Huffmann and R.E. Lacey, 1972. Engineering and economic considerations in electromembrane processing. In: R.E. Lacey and S. Loeb (Eds.), *Industrial Processing with Membranes*. John Wiley & Sons, 1972, pp. 39–55.
64 W.E. Katz, The electrodialysis reversal (EDR) process. *Desalination*, 28 (1979) 31–40.
65 K.S. Spiegler, Polarization at ion-exchange membrane–solution interfaces. *Desalination*, 9 (1971) 367–385.
66 G. Jonsson and C.E. Boezen, Polarization phenomena in membrane processes. In: G. Belfort (Ed.), *Synthetic Membrane Processes*. Academic Press, New York, 1984.
67 R.B. Bird, W.S. Stuart and E.N. Lightfoot, *Transport Phenomena*. John Wiley & Sons, New York, 1960.
68 D.A. Cowan and J.H. Brown, Effect of turbulence on limiting current electrodialysis cells. *Ind. Eng. Chem.*, 51 (1959) 1445.
69 R.M. Ahlgren, Electromembrane processing of cheese whey and Electromembrane processes for recovery of constituents from pulping liquors. In: R.E. Lacey and S. Loeb (Eds.), *Industrial Processing with Membranes*. John Wiley & Sons, New York, 1972, pp. 57–81.
70 K. Wangnick, Desalting plant inventory report. International Desalination Association (IDA) Report No 12, 1991.
71 Shi Song, Cheng Yifang and Gao Congjie, Electrodialysis in China. *Desalination & Water Reuse*, 2/4 (1993) 23–25.
72 K. Kneifel, G. Lührs and H. Wagner, Nitrate removal by electrodialysis for brewing water. *Desalination*, 68 (1985) 203–209.
73 E. Korngold, K. Kock and H. Strathmann. Electrodialysis in advanced waste water treatment. *Desalination*, 24 (1–3) (1978) 129–139.
74 Ph.B. Reed, Electrodialysis for the purification of protein solutions. *Chem. Eng. Progress* (Dec. 1984) 47–50.
75 H. Voss, Deacidification of citricacid solutions by electrodialysis. *J. Membr. Sci.*, 27 (1986) 165–171.
76 H. Itoh, T. Yoshizumi and M. Saeki. Sieving effect in electrodialysis with an ion-exchange membrane. *J. Membr. Sci.*, 27 (1986) 155–163.
77 Millipore Corp. Bulletin. No. CJ 001. Bedford, MA, 1987.

78 Y. Kobuchi, H. Motomura, Y. Noma and F. Hanada, Application of ion-exchange membranes to recover acids by diffusion dialysis. *J. Membr. Sci.*, 27 (1987) 173–179.
79 M.V. Coulter, Modern chlor-alkali technology. Ellis Horwood Ltd., Chichester, UK, 1980.
80 M. Seko, S. Ogawa and K. Kimoto, Perfluorocarboxylic acid membrane and membrane chlor-alkali process developed by Asaki Chemical Industry. In: A. Eisenberg and H.L. Yeager (Eds.), *Perfluorinated Ionomer Membranes*. ACS Symp. Ser., 180, American Chemical Society, Washington, 1988.
81 R.L. Dotson and K.E. Woodard. 1982. Electrosynthesis with perfluoronated ionomer membranes in chlor-alkali cells. In: In: A. Eisenberg and H.L. Yeager (Eds.), *Perfluorinated Ionomer Membranes*. ACS Symp. Ser., 180, American Chemical Society, Washington.
82 DuPont Bulletin. Washington, DC, 1988.
83 F. Chlanda, L. Lee and K.J. Lui, US Patent 4,116,889, 1976.
84 Y. Yokoyama, A. Tanioka and K. Miyasaka, Preparation of a single bipolar membrane by plasma-induced graft polymerization. *J. Membr. Sci.*, 43 (1989) 165–175.
85 H. Strathmann, B. Bauer and H.J. Rapp, 1993. Better bipolar membranes. *CHEMTECH* (June 1993) 17–24
86 J. Bockris and A.K.N. Reddy, *Modern Electrochemistry*. Plenum Press, New York, NY, 1970.

Membrane Separations Technology. Principles and Applications
Edited by R.D. Noble and S.A. Stern

Chapter 7

Liquid membranes (liquid pertraction)

L. Boyadzhiev and **Z. Lazarova**

Institute of Chemical Engineering, Bulgarian Academy of Sciences, Sofia, Bulgaria

7.1 INTRODUCTION

Liquid pertraction or liquid membranes appeared as a new and prospective separation method relatively recently. Due to its advantages over solid membranes and liquid–liquid extraction, liquid pertraction attracted the attention of many scientists and engineers. At present this emerging separation operation is the subject of intensive studies in more than 200 laboratories all over the world.

Like most of the new developments, this separation operation has various names, e.g., "liquid membranes", "liquid pertraction" or just "pertraction", "carrier-mediated extraction", "facilitated transport", "two-stage extraction", etc. The most suitable name for the process seems to be "liquid pertraction," proposed by Schlosser and Kossaczky [1]. This name is constructed similar to the name of the closest separation process — liquid–liquid *extraction*. It reflects the transfer process involved as well as the multi-(three) phase structure of the system. The term "liquid membranes" also represents the essential feature of the process, but the conventional image of a membrane — a thin, solid (in this case also semipermeable) barrier — could hardly be adapted to the multiple emulsions for which the term was actually introduced [2,3].

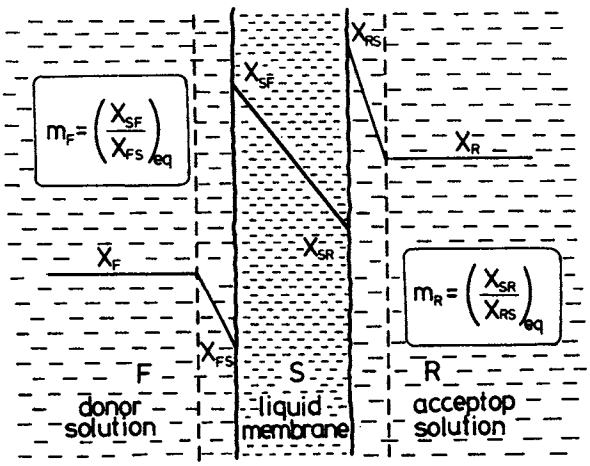

Fig. 7.1. Concentration gradients of transferred solute across the membrane and the boundary layers in donor and acceptor solutions.

7.1.1 Principle of Liquid Pertraction

Liquid pertraction explores a very simple idea: two homogeneous, completely miscible liquids, which may be referred to as *donor* solution (F), and an *acceptor* solution (R) are spatially separated by a third liquid, immiscible and practically insoluble in the former two liquids — the *membrane* phase (S) (see Fig. 7.1). With a few exceptions, F and R are aqueous solutions. Due to the favorable thermodynamic conditions created at the interface between the donor solution F and the organic membrane S, some components are extracted from the donor solution and transported into the membrane liquid. Simultaneously, at the second interface (S/R), conditions are created, which favor the reverse transport, i.e., the extraction of the above-mentioned components from the membrane liquid and their accumulation in the acceptor solution R.

7.1.2 Comparison of Liquid Membranes and Solid Membranes

Liquid membranes have two considerable advantages over solid membranes: as is known, molecular diffusion in the liquids (except in super-viscous ones) is, by several orders of magnitude, faster than that in solids. Furthermore, in some pertraction methods the molecular diffusion in the liquid membrane is replaced by eddy diffusion, which intensifies the transfer process. Hence, it may be stated that solid membranes, even those of submicron thickness, cannot compete with liquid membranes with respect to transfer intensity.

As a general rule, polymer membranes are less selective than liquid ones. They are rather selective towards groups of substances, but not towards indi-

vidual ions or molecules. There is no doubt, however, that polymer chemistry will remove this drawback and, in the future, the selectivity of the solid membranes will reach that of the liquid ones.

These two advantages of liquid membranes cannot, however, compensate for the major superiorities of solid membranes: the simplicity of the devices used and the operation stability.

The realization of a stable pertraction process on an industrial scale is a very difficult task. Conditions excluding each other are to be combined, e.g., the creation of two large liquid interfaces at a minimal but adequate distance to prevent any contact between them. The use of too thin liquid membranes is not recommendable from another point of view also: they have low but measurable solubility in the two aqueous solutions they separate and, in addition, they are very sensitive towards the unavoidable pressure differences created between the two aqueous solutions.

7.1.3 Comparison of Liquid Pertraction and Liquid–Liquid Extraction

It follows from the above that liquid pertraction is a combination in time and space of two well-known separation processes — solvent extraction and solvent stripping [4]. This combination offers two substantial advantages over the classical liquid–liquid extraction:

- Pertraction provides maximum driving force so that the use of multistage and counter-current processes is not required.
- Since the organic liquid is a short-term mediator only, its extraction capacity is of no essential significance. As a result, a great variety of insoluble, inert and harmless organic liquids can be used as an intermediate liquid, containing only a small amount of carriers. As carriers, new, highly selective and also solid extractants can be synthesized.

7.2 TRANSFER MECHANISMS

Like some other membrane processes, mass transfer through the membrane phase in liquid pertraction is based on the difference in the chemical potentials of the solute in the two aqueous solutions, i.e., the intensity of the diffusional flow of the solute is controlled by the concentration difference.

Mass transfer through a liquid membrane can be effected by different mechanisms, two main groups of which may be distinguished:

- the membrane liquid acts as a physical solvent of the permeate;
- the membrane is a liquid substratum containing the selective carrier of the permeate.

The second group of mechanisms is referred to as *facilitated* or *carrier-mediated*

transfer. In this case the carrier reacts reversibly with the permeate, binding it in the donor liquid or at the donor/membrane interface and releasing it in the acceptor liquid or at the membrane/acceptor interface. If one component is coupled to and dependant upon the transfer of other component(s) then the mechanism is called "coupled transfer". It can be "cotransfer" or "counter-transfer", depending on the direction of the coupled fluxes.

7.2.1 Simple Transfer Mechanisms

Two mechanism types of the first group mentioned are presented in Fig. 7.2a and b. In the first case, the permeate A is removed from the donor solution as a result of its solubility in the membrane liquid. Initially the concentration of the permeate in the acceptor equals zero; later it increases in values, which are still lower than those in the donor. This is until why a concentration gradient is created, which is the cause for the transfer of A from F to R. This process continues the equalization of the activities of A in the two solutions of similar nature — F and R. It follows then, that the final result of this process will be the equalization between the concentrations of all transferable components on both sides of the membrane. This simplest case of pertraction does not allow a reasonable recovery or concentration of the permeate. The selectivity of separation in this case is a function of the different transport rates of the components, which in turn depend primarily on the difference between the permeate solubilities in the membrane and to a lower extent on the difference between their diffusion coefficients [5].

Irrespective of the lack of substantial advantages and prospects for practical application, this mechanism has been the subject of many studies, dealing

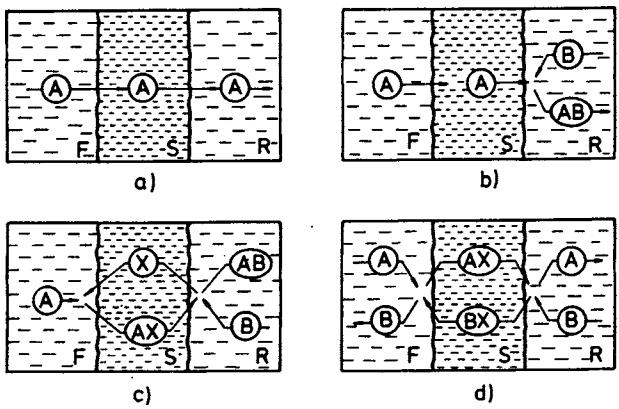

Fig. 7.2. Transfer mechanisms: (a) simple transfer; (b) simple up-hill transfer; (c) facilitated up-hill transfer; (d) counter-current coupled transfer.

mainly with the separation of hydrocarbons using aqueous membranes. More details about this special pertraction system can be found in Section 7.5.

The second mechanism of this group, known as "simple up-hill transport", is shown in Fig. 7.2b. Here, the permeate A is extracted from the donor liquid F due to its selective solubility in the membrane S. Simultaneously, the acceptor solution R containing the reagent B strips and irreversibly binds each molecule of A into the compound AB. The latter or its dissociation products are insoluble in the membrane liquid. In this mechanism the solute A is pumped from the donor F to the acceptor R, apparently counter to its concentration gradient. The term "apparently" is used, since the concentration of the permeate A in the acceptor solution R always remains lower than that in the donor solution F, irrespective of the high concentration of the transformed product AB. By this mechanism, weak organic acids or bases, e.g., phenols, amines, antibiotics, etc., can be transferred and accumulated.

Another possibility of irreversible binding of the solutes transferred through the liquid membrane is offered by enzyme reactions. In the acceptor phase R, the permeate is destroyed by enzymes and is transformed into new products. For example, phenol, recovered from the aqueous solution, is converted by phenolase or UDP-glucoronyltransferase [6,7], nitrogen oxides are reduced to elemental nitrogen [8], cholesterol is separated from blood plasma [9]. More details about this special case can be found in Section 7.5.

7.2.2 *Facilitated Transfer Mechanisms*

As mentioned, the *facilitated* (or *carrier-mediated*) mechanisms do not require a solubility of the permeate A in the membrane liquid. The latter contains an active additive which reacts selectively and reversibly with the substance A, usually by the scheme:

$$A + X \underset{k_f}{\overset{k_f}{\longleftrightarrow}} AX \tag{7.1}$$

where k_f and k_r are the rate constants of the forward and reverse reaction, respectively. As Fig. 7.2c shows, the complex AX is formed in the donor liquid or at the interface F/S, where suitable thermodynamic conditions exist. At the second interface, conditions are created which favor the destruction of the complex AX and the irreversible binding of A as the new product AB, which is insoluble in the membrane liquid S. The active additive X is liberated through the formation of the product AB and, due to its own concentration gradient across the membrane, moves back to the interface F/S, where it is free to bind again with A. In this way, only small amounts of complexing additives to the inert membrane liquid are sufficient for the selective extraction and preconcen-

tration of such various metals as uranium, zirconium, lanthanides, etc. from their very dilute solutions.

The diagram shown in Fig. 7.2d represents the counter-transport case of a coupled transport mechanism. It is an ion-exchange process in which the solute A, recovered from the donor solution F and transported by the active carrier X into the acceptor R, is substituted by an equivalent amount of ions of the same type. A typical example for this type of process is the extraction of metal ions from neutral or slightly acidic media using oleophilic chelating agents, where an equivalent counter-transport of protons takes place.

There is great interest in facilitated membrane transfer, since these kinds of process are considered the ideal separation process for industrial applications.

7.2.3 Other Transfer Mechanisms

Recently, liquid membrane processes based on more complex mechanisms have been developed. They involve redox reactions in the bulk of the liquids F and R or at the two interfaces. The selective transfer through the liquid membrane is a result of the different solubilities of the various oxidation states of the metal ions, e.g., copper, cobalt, iron and manganese [10,244]. It is the task of future studies to reveal the possibilities of the large-scale application of such complex processes and to find out whether or not they have advantages over other liquid membrane separation processes. The reader may find more information on this subject in the excellent publication of Noble and Way [11].

7.3 PERTRACTION TECHNIQUES

The still negligible large-scale application of pertraction separation processes is mainly due to the difficulty of separating two liquids with a liquid membrane of minimal thickness, great area and guaranteed stability. Irrespective of the complexity of this task, much effort and resources have been directed to the development of methods of potential industrial usage during the last 20 years.

Pertraction methods can be classified as follows:

A. Methods without phase dispersion
   1. Bulk (two-cell) methods (BLM)
   2. Supported liquid membranes (SLM)
   3. Liquid film pertraction (LFP)

B. Methods with phase dispersion
   1. Emulsion (surfactant) liquid membranes (ELM)
   2. Other methods with phase dispersion

It should be stressed that this is a conditional classification only, since the methods mentioned cannot be sharply distinguished. Moreover, some of them

are close to classical liquid–liquid extraction. For example, the arrangement of two consecutive multistage extraction columns could be regarded as a pertractor on the same grounds as the two-compartment pulsation column, described below, could be regarded as a coupled extractor–stripper. The same applies to the consecutive extraction–stripping hollow fiber modules each containing two liquids only.

7.3.1 Techniques Without Phase Dispersion

7.3.1.1 Bulk (Two-cell) Techniques

Figure 7.3 shows several types of mass transfer or diffusion cells, which are the simplest design for performing liquid membrane processes. The device is divided in two parts: a common part, containing the membrane liquid S and a second part, in which the donor solution F and the acceptor solution R are separated by a solid impermeable barrier. The liquid S contacts with the two other liquids and effects the transfer between them. All three liquids are stirred with an appropriate intensity avoiding mixture of the donor and the acceptor solution.

The simplest mass transfer cell is the so-called Schulmann bridge (see Fig. 7.3), used by many authors [12–14] for studying the mechanism of liquid–membrane transport of alkaline cations by means of macrocyclic polyether carriers. The other cells are usually shaped as a cylindrical contactor with a solid barrier of flat [15] or cylindrical [17,18] configuration. Burgard et al. [19] proposed an improved modification, supplied with a rotating cylinder (see Fig. 7.3d). The

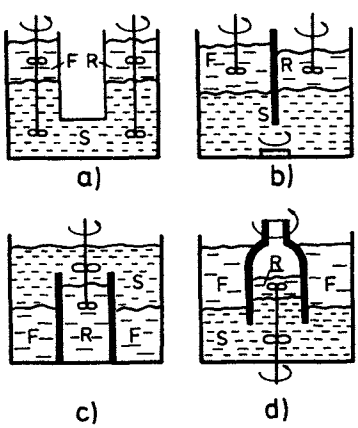

Fig. 7.3. Mass transfer (diffusion) cells: (a) U-tube type (Schulmann bridge); (b) with a flat vertical separating wall; (c) with a cylindrical wall (beaker-in-beaker type); (d) with a rotating inner cylinder.

constant interface areas, the constant hydrodynamic conditions, the simple design of these cells and the easy manipulation are the reasons for their broad use in laboratory studies. These cells are convenient for following the kinetics of the mass transfer process, for studying the reaction mechanisms involved, etc. However, the low specific interface area limits the application of this method to laboratory use.

7.3.1.2 Supported Liquid Membranes (SLM)

The term "supported liquid membranes" usually defines solid (polymer or ceramic) porous membranes, the open pores of which are soaked with the membrane liquid, as is shown in Fig. 7.4a. In a broader sense, this term refers also to much thicker "membranes", supported on both sides by porous solid barriers (Fig. 7.4b) [20–22]. These homogeneous liquid films, supported on both sides, may be termed as a bulk liquid membrane.

The method of impregnated liquid membranes has become more and more popular. By impregnating fine-pore polymer films with a suitable membrane liquid, relatively stable heterogeneous solid–liquid membranes are obtained. These membranes are shaped as thin, flat barriers or as hollow fibers. Usually, they are manufactured from oleophilic polymers, wettable by the membrane liquid. The two interfaces F/S and S/R have equal or close areas which can be made very large by employing modules of spirally wound flat membranes (see Fig. 7.5) or bundles of hollow fibers [23–31].

The studies of pertraction processes using supported liquid membranes are most often performed with simple cells of a vertical or horizontal type depending on the position of the impregnated support (see Fig. 7.6) [32–39]. Gasparini

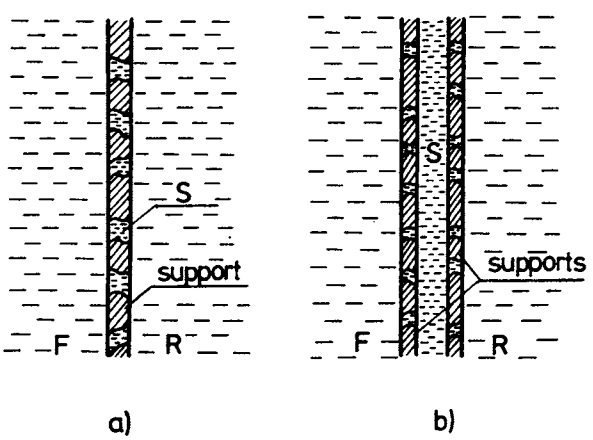

Fig. 7.4. Supported liquid membranes: (a) membrane liquid fills the open pores of a solid support; (b) membrane liquid is "supported" on both sides by two porous solid membranes.

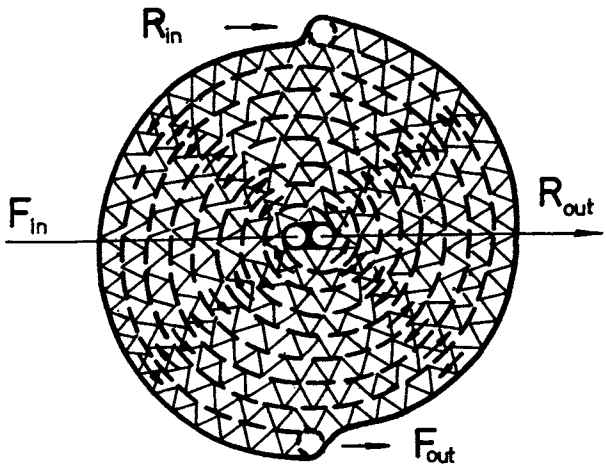

Fig. 7.5. Cross section of a spirally wound module of supported liquid membranes. The distances between the porous supports, impregnated with the membrane liquid S, are fixed by special spacing nets. Donor (F) and acceptor (R) solutions flow between the supports.

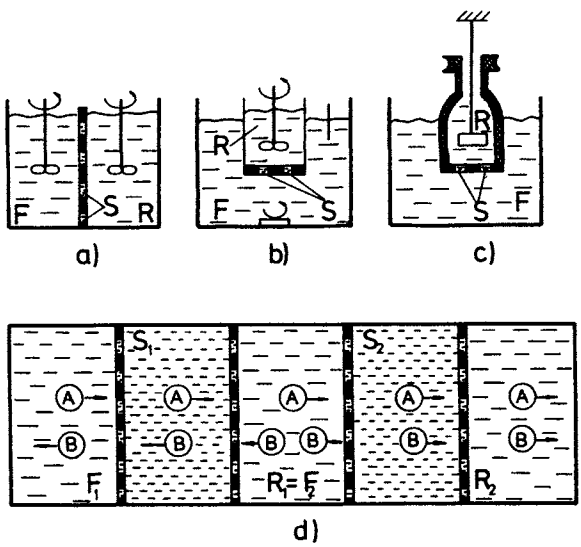

Fig. 7.6. Diffusion (mass transfer) cells with vertical (a), horizontal (b) or rotating (c) supported liquid membrane. Double horizontal diffusion cell (d) in which the acceptor solution R_1 acts as a donor liquid F_2 with respect to the second compartment [41].

et al. [40] and Chiarizia et al. [33] used cells in which the donor phase is placed in a movable inner cylinder serving as an equilibrator of the pressure on both sides of the membrane, thus prolonging its lifetime (Fig. 7.6c). Danesi et al. [41] improved the separation selectivity using a composite SLM cell containing two

different liquid membranes. The acceptor phase R_1 from the first cell acts as the donor phase F_2 of the second cell (see Fig. 7.6). The two-membrane liquids are chosen in a way that they transport selectively the extracted species A between the similar liquids, the initial donor solution F_1 and final acceptor liquid R_2. Flow diffusion cells are also employed [42,43], the aqueous phases in which are flowing in a cocurrent or in a counter-current mode. Cells with recirculation of the donor phase F [44] or of the acceptor phase R [45] were also proposed.

The main advantage of supported liquid membranes is the insignificant amount of membrane liquid required for impregnation of the support matrix. For example, 10 cm^3 of membrane liquid are sufficient to impregnate 1 m^2 of a membrane of 20 μm thickness and 50% porosity.

Regardless of the fact that extremely thin porous supports of the membrane liquid are used, this method cannot provide diffusion fluxes acceptable for practical use intensities. This drawback is compensated for by the large specific area — up to 2000–5000 m^2/m^3 using spirally wound modules or hollow fiber modules, containing thousands of tiny capillaries.

The attempts to improve the mass-transfer process by thinning the polymer barrier below 20 μm sharply increases the risk of membrane rupture and solution intermixing. Besides that, the very low amount of membrane liquid results in a shortened lifetime of the liquid membrane due to its inevitable dissolution and washing out by the aqueous solution [46–50]. The short lifetime of the membrane and the necessity of its periodical or continuous regeneration using the methods proposed for this purpose [44,49,51,52] are the main drawbacks to the large-scale practical use of this technique. In spite of this, there are more and more research laboratories in which the industrial application of this

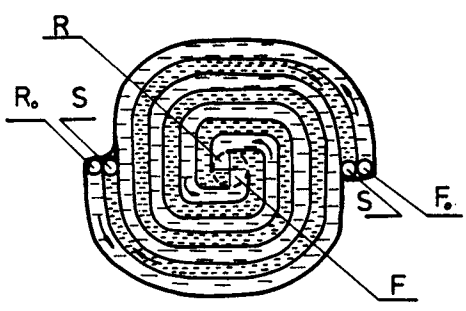

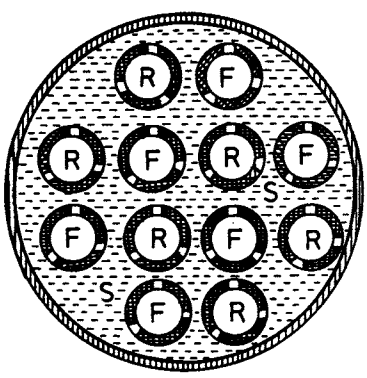

Left: Fig. 7.7. Flowing liquid membranes. Cross section of spirally wound module. Membrane liquid flows between two porous supports.

Right: Fig. 7.8. Cross section of hollow fiber module of contained liquid membranes. There are two bundles of hollow fibers in it: for the donor (F) and, for the acceptor (R) solution, respectively.

method is attempted and in some of them, e.g., in the USA, Japan and Germany, pilot plants exploiting supported liquid membranes are in operation.

The liquid membranes, kept locked between two porous oleophilic membranes (a technique schematically presented on Fig. 7.3b), provide possibilities for eliminating the main disadvantage of supported liquid membranes: the washing out of membrane liquid from the pores. In order to compensate for the high mass-transfer resistance of the motionless, relatively thick membrane layer, Teramoto and coworkers [53,54], following the example of Igawa et al. [55] bring the membrane liquid in motion introducing the term Flowing Liquid Membranes (FLM). To achieve better compactness, the three-layer sandwich is shaped as a coiled cylindrical module (see Fig. 7.7). The so-called Contained Liquid Membranes (CLM), proposed by Sengupta et al. [56,57] exploit the same idea: the membrane liquid flows along a bundle of porous oleophilic hollow fibers, in some of which the donor aqueous solution flows and in the others, the acceptor solution (see Fig. 7.8).

7.3.1.3 Liquid Film Pertraction (LFP)

The principal scheme of liquid film pertraction is shown in Fig. 7.9 [58]. In this technique the three solutions are in continuous motion. The donor solution F and the acceptor solution R flow along vertical solid supports alternately

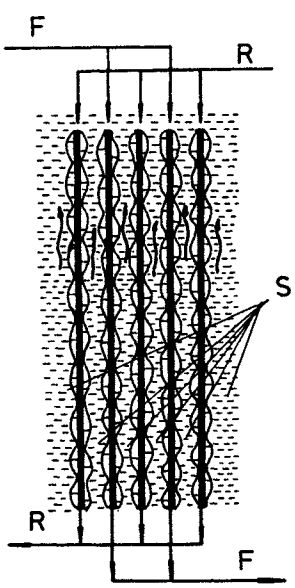

Fig. 7.9. Liquid film pertraction. Donor (F) and acceptor (R) solutions flow down the alternately arranged hydrophilic supports, immersed in the membrane liquid.

arranged at small distances. Each support of a donor film F is placed between two supports of acceptor films R, i.e., the supports with even numbers are intended for the donor liquid F and the odd ones for the acceptor solution R. The hydrophilicity of the supports helps to obtain stable and uniform film flow of the aqueous solutions. The package of film supports is immersed in the organic membrane liquid filling the apparatus, including the narrow interspaces between the alternating supports. This liquid is circulated counterflow to the aqueous solutions by means of a pump. The concentration factor is determined by the flow rate ratio of the F and R solutions.

Alternately arranged flowing films of the donor and acceptor solution on hydrophilic supports can also be created by means of rotating discs partly immersed in the solutions. The discs are mounted on two independent shafts or on a common shaft (see Fig. 7.10) [59].

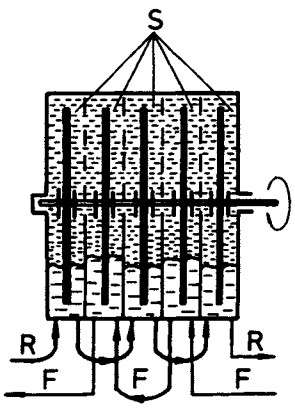

Fig. 7.10. Rotating film pertraction. The alternating rotating hydrophilic discs are partially immersed in the corresponding (donor or acceptor) aqueous solutions.

The continuous motion of the three liquids provides an intense solute transfer since all consecutive steps of mass transfer proceed by the mechanism of eddy diffusion. Under these circumstances, the diffusional resistance of the relatively thick (several millimeter) "membranes" is below that of a motionless membrane liquid filling the pores of supported membranes of only 20 μm thickness [60].

7.3.2 Methods with Phase Dispersion

This group includes pertraction methods in which one or two of the three liquids are dispersed in drops. The most popular among them is the emulsion (surfactant) liquid membrane (ELM) method.

7.3.2.1 Emulsion Liquid Membrane Method (ELM)

In the late 60s and early 70s, N. Li (1971) proposed a method that is now called "Emulsion (Surfactant) Liquid Membranes" (ELM) or "Double Emulsion Method" (DEM). The name reveals that the three-liquid system is stabilized by an emulsifier, the amount of which reaches up to 5% or more with respect to the membrane liquid [9,61–66]. The acceptor solution R, which usually has a smaller volume than the donor solution F of similar nature, is finely dispersed in the intermediate phase S. The consistent (dense) emulsion formed is extremely stable due to the microscopic size of the drops of acceptor liquid (1–10 μm) and to the high content of the properly chosen emulsifier. In the next step, the donor solution F is contacted with the emulsion. For this purpose, the emulsion is dispersed in the donor solution F by gentle mixing (Fig. 7.11). Due to the relatively large interface area between the donor solution and the emulsion globules (0.5–2 mm diameter) and to the extremely large surface area of the microdrops of acceptor solution encapsulated in the globules, the mass transfer process between the two aqueous solutions can be completed within several minutes. After this step, the emulsion is separated and broken. The enriched acceptor solution is further processed and the membrane liquid S is fed back for reuse.

As Fig. 7.11 shows, the ELM method represents a three-stage batch separation process, which may also be performed in a continuous mode using various types of extraction columns [70–76]. As a result of the high emulsifier concentration, the very large interfaces and the different water content in the two aqueous solutions, an intense water swelling as well as occlusion of donor

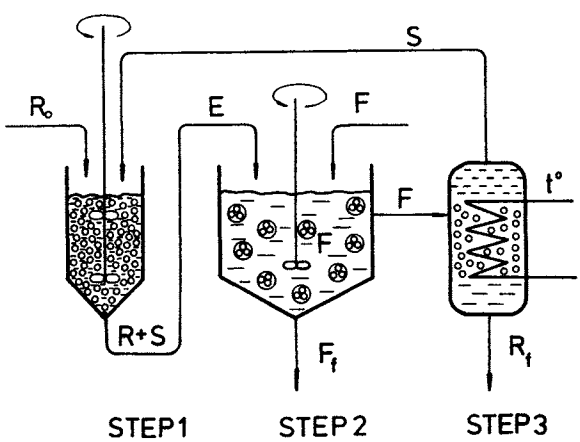

Fig. 7.11. Emulsion Liquid Membrane technique is usually a three-stage operation, which includes: (1) emulsion preparation, (2) contacting the emulsion (E) with donor solution F, and (3) emulsion destruction.

solution in the emulsion often takes place [77,78]. The main disadvantages of ELM are related to emulsion stability: it is far from ideal and during the contact with the donor solution F it partly destructs resulting in a lower extraction efficiency. On the other hand, a too stable emulsion calls forth problems during its destruction in the third stage [79–84]. Regardless of these drawbacks, the ELM method was the first industrially applied method (in China [65] and in Austria [85]).

7.3.2.2 Other Methods with Phase Dispersion

One of the first attempts for separating hydrocarbon mixtures using surfactant-stabilized liquid membranes is performed on equipment schematically presented in Fig. 7.12. As shown, drops of the donor hydrocarbon mixture pass through an aqueous layer containing an emulsifier and are covered with an aqueous membrane. The "dressed" drops further penetrate into the acceptor phase R, where mass transfer of hydrocarbons more soluble in water takes place. Without any prospect of practical realization, this drop column of Li has only historical significance [1,3,62,86]. It is the prototype of the double emulsion method which was later developed and extensively studied.

The two-compartment vertical column supplied with a porous separating wall [88,89] is intended to be an improvement on the two-cell method. The column is separated in two concentric compartments by a vertical hydrophobic porous tube (see Fig. 7.13). The membrane phase S fills the whole device. Both aqueous phases F and R are fed into the top of each compartment; the donor liquid F enters the outer annular space and the acceptor liquid enters the inner

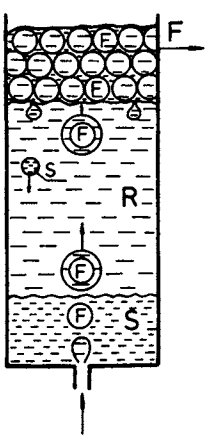

Fig. 7.12. Single drop technique. Drops of donor solution (F) pass up through an aqueous layer S containing an emulsifier. The drops covered with aqueous membrane penetrate into the acceptor liquid (R) and are accumulated in the top part of the column.

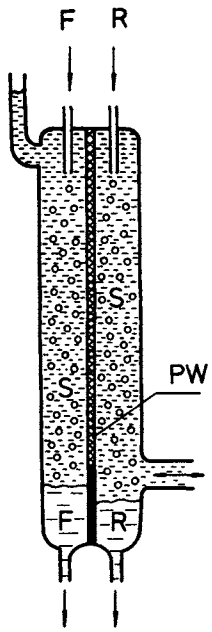

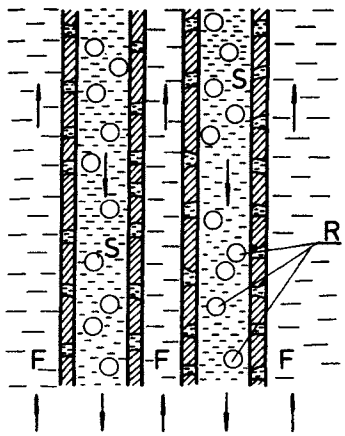

Left: Fig. 7.13. Two-compartment pulsating column [88]. Membrane liquid, filling both compartments oscillates between them at each half stoke passing through the porous wall, wetted by this liquid. Feed (F) and stripping (R) solutions are dispersed at the top with no use of surfactants.

Right: Fig. 7.14. Dispersion and hollow fiber technique [91]. Acceptor solution (R) is dispersed into the organic membrane liquid, flowing in the lumen of porous oleophilic capillaries without a surfactant addition.

tube. The column is equipped with a pulsating device which cyclically transports portions of the organic membrane liquid through the porous filtering wall from one compartment into the other. The method provides intense mass transfer; it uses simple equipment and no surfactants. It has, however, a substantial drawback. Due to the inevitable change in the surface properties of the hydrophobic wall, not only the membrane phase is let through, but also the finest drops of both aqueous solutions F and R. Similar to this is the stirred "double filtration system" proposed by Mitrovic and Wu [90]. The device is complicated by the hydrophilic and hydrophobic filters additionally mounted at the exits of the equipment. These filters reduce entrainment.

Dispersion of one of the aqueous solutions in the membrane liquid without using surfactants and without creating mixing hazards between the two liquids of similar nature is possible if the pertraction scheme, illustrated in Fig. 7.14, is applied [91]. In this case, the acceptor solution R is finely dispersed in the membrane liquid S, which flows in the lumen of the hollow porous fibers. The oleophilic properties of the latter permit the micropores to be filled with the

membrane liquid only, which contacts with the donor solution F flowing outside the fibers.

7.3.3 Comparison of Various Pertraction Techniques

As mentioned, each of the pertraction techniques described has its advantages and disadvantages. For example, ELM provides the highest transfer rates, but the accompanying negative phenomena strongly decrease process selectivity, which is one of the most important characteristics of the separation methods. ELM and SLM are suitable for treating solutions with small content of solid impurities, whereas LFP techniques require a preliminary filtration of the donor and acceptor solution. An important feature of ELM is the extremely high interfacial area between the membrane liquid and the encapsulated solution, in particular, when the second stripping step is controlled by a very slow interfacial chemical reaction. SLM and LFP are, in principle, continuous methods. They yield more predictable, reliable and repetitive results than the three-step ELM method, of which scaling-up is difficult and uncertain. As mentioned, the most severe drawback of supported liquid membranes is the inevitable washing out of membrane liquid from the pores of the support. This drawback imposes a periodical regeneration of the membrane liquid or, its proper formulation by appropriate technique, which is more difficult. The FLM and CLM methods successfully eliminate this drawback, but the limited diffusional fluxes controlled by the membrane liquid immobilized in the pores cannot be ignored. The use of fine hollow fibers or long hollow fiber modules creates a high hydraulic resistance and pressure drops. Besides, working with liquid–liquid systems with a low interfacial tension — below 15 mN/m^2 — is also not recommended due to increased hazards of breakthroughs and aqueous solution intermixing [93]. Breakthrough hazards cannot be predicted in practice since the surface properties, and hence the adhesion of membrane liquid to the polymer surface, is a function of the composition and purity of the aqueous solutions and particularly of the accidental presence of surfactants. In spite of the possibility of creating large specific interfaces, the amount of transferred solute is relatively small owing to the relatively slow molecular diffusion and to its additional reduction by the complex porous structure of the support, which is accounted for by a specific tortuosity factor. In order to achieve the desired extraction efficiency, usually a set of consecutively connected modules is used or the donor solution is recirculated. The same applies to the method illustrated in Fig. 7.14, since the dispersion, of the acceptor solution R, for instance, improves the S–R transfer but not the F–S transfer. The absence of surfactants in this method is a significant advantage. A very attractive feature of the LFP and RFP methods is the continuity of the process and its long-term stability. Scaling-up also presents no problems since the transition from the

laboratory to industrial equipment consists of an increase in the dimensions of the film supports and in their number. An almost unlimited extent of preconcentration of the solute can be achieved by these methods since it is determined by the flow rate ratio of the donor and acceptor solutions. When very high donor-to-acceptor concentration ratios are aimed at, e.g., above 200 — which is the case of using the LFP method for analytical purposes — the acceptor solution may be also recirculated in a closed circle. In this way some valuable or highly toxic substances at a ppm level can be recovered from natural or industrial effluents.

Scrubbing of the extract in liquid–liquid extraction is known to be a very useful operation which may substantially improve both the selectivity of separation and the quality of the final product. It is only the LFP method which permits partial scrubbing or other treating of the organic membrane liquid.

It should be noted that the practical choice of a suitable pertraction method strongly depends on the price of the materials involved. In this respect, the continual reduction in the prices of porous supports and of porous hollow fibers may become a crucial advantage of SLM and LFP methods.

There is still a broad research field for developing new techniques and devices needed in order to realize, in practice, this attractive separation process, i.e., to get it out of its actual embryonic state.

7.4 MATHEMATICAL MODELLING OF PERTRACTION PROCESSES

In the present time of overall computerization there are plenty of mathematical models in each area of scientific research. This hardly compensates, however, for the lack of original ideas or of reliable experimental results. The same relates to pertraction: more than 120 mathematical models or improved versions have been proposed in the last 15 years. In the following, an attempt is made to classify and discuss some of the models developed for designing, scaling-up and for the study of pertraction processes.

According to the mechanisms of solute transfer presented in Section 7.2, the model types can be ordered as follows:

(a) Models describing the simple physical transfer [3,4,64,94–97];

(b) Models describing liquid membrane processes with irreversible chemical reactions taking place in the acceptor phase [80,98–102];

(c) Models describing facilitated transfer mechanisms [61,103–108].

All these models are based on either of two principal approaches [95]. The first is the so-called *membrane approach* which accentuates the analogy to mass transfer through solid membranes. It *a priori* admits that the total resistance of the transport process is located in the liquid membrane S. The processes taking place outside the membrane are completely neglected. No concentration gra-

dients of the transported species in the F and R liquids are considered, which corresponds to the hypothesis of ideal mixing in these solutions. The selectivity and the transfer rate primarily depend on the membrane properties and on the processes taking place on its surfaces or in its bulk. The process is usually reduced to a steady-state (or nonsteady-state) molecular diffusion of solutes through the stagnant liquid membrane with a linear concentration gradient being assumed. The principal drawback of the membrane approach is that attention is focused only on the intermediate membrane phase, with no changes in the other two liquids being considered (e.g., pH, concentration of the solute, volume, etc.) that substantially affect the chemical reactions involved and the rate of mass transfer.

The second approach is the *integral approach* [79,95,109]. It examines the pertraction system as an integrated closed system of three interacting liquids. This approach takes into account, as far as is reasonable and possible, all processes and changes taking place in all three liquids. Besides determining the concentration gradients in the three phases, this approach takes into account the volume changes and the mass balance of the individual components. This approach exploits the idea that liquid pertraction is a combination of two processes which simultaneously take place and affect each other. Models elaborated on this approach account for all changes in the liquid three-phase system, including the modification of the equilibrium conditions at the two interfaces.

7.4.1 Modelling of SLM Processes

The simple geometry of supported liquid membranes significantly simplifies the mathematical description of the transfer process. Many of the models of mass transfer through flat membranes describe the facilitated steady-state membrane processes, the solute A diffusing through the motionless membrane S as a complex with the selective carrier [110–112]. Both the formation and the destruction of the complex takes place in the membrane phase as a result of a reversible chemical reaction. In this case the proposed models accentuate the mechanism of chemical reactions, since the diffusion processes in a stagnant phase are simply described by Fick's laws [98,112]. The flux of solute A (assuming an equality of all diffusion coefficients in the membrane) is expressed as:

$$J = D_A \frac{H_A^o - X_A^\delta}{\delta} (1 + f) \tag{7.2}$$

where f is a factor accounting for the increase in the flux J when a carrier is added to the membrane. Approximate analytical solutions are derived for the factor f in the two extreme regimes — diffusion-controlled and reaction-control-

led [23,108,113–116], which are experimentally confirmed [114]. The intermediate regimes are so far the subject of a numerical solution [118,119]. These models describe processes that could be of interest from a biological point of view or for gaseous mixtures separation using liquid membranes.

The numerous experimental studies of three-phase liquid systems have shown, however, that chemical reactions only rarely take place in the membrane [23]. Hence, these models have only limited application to these cases. It should be further stressed that the diffusion coefficients D_A and D_X are actually apparent owing to the microporous structure of the solid support. In order to obtain the total mass flux of A through the membrane, Eq. (7.2) should be multiplied with the "effective" interfacial area which differs from the geometrical one. The product of the interfacial area a and the diffusion coefficient D_A in each case must be obtained by preliminary experimental studies.

The later models used the integral approach and considered also phenomena taking place outside the membrane as well as some second-order phenomena [25,41,120,121]. It was found in this way that in a number of cases the hydrodynamics in the donor liquid and the rates of reactions taking place in it have a primary effect on mass transfer efficiency. For example, the analytical solution of Noble et al. [121], valid for reactions of the type

$$\text{A (solute)} + \text{X (carrier)} = \text{AX (complex)} \tag{7.3}$$

at steady-state conditions, accounts for the mass-transfer resistance in the liquids F and R.

According to this solution, the factor f in Eq. (7.2) is:

$$f = \frac{\left[1 + \dfrac{\alpha k_f x_F/k_r}{(1 + k_f x_F/k_r)}\right]\left(1 + \dfrac{1}{Sh_F} + \dfrac{1}{Sh_R}\right)}{1 + \dfrac{\alpha k_f x_F/k_r}{(1 + k_F x_F/k_r)}\dfrac{\tanh\lambda}{\lambda} + \left[1 + \dfrac{\alpha k_F x_F/k_r}{(1 + k_F x_F/k_r)}\right]\left(\dfrac{1}{Sh_F} + \dfrac{1}{Sh_R}\right)} \tag{7.4}$$

where

$$\lambda = \frac{1}{2}\left[\frac{1 + (\alpha + 1)\, k_f x_F/k_r}{(D_{AX}/k_r\, \delta_S^2)\,(1 + k_f x_F/k_r)}\right]^{0.5} \tag{7.5}$$

$$\alpha = D_{AX}\, y_S^0 / D_A\, c_F \tag{7.6}$$

and

$$Sh_W = k_W \delta_W / D_A, \quad \text{where} \quad W \equiv F \text{ or } R \tag{7.7}$$

For the case of a steady-state transfer process of an ion-exchange reaction mechanism of the type

$$A\ (solute) + 2HX\ (carrier) = AX_2\ (compl.) + 2H\ (subst.) \tag{7.8}$$

Danesi [25] proposed a solution considering both the reaction and mass-transfer rates in the donor and membrane liquid:

$$J = \frac{k_f y_S^2 x_F}{\delta_S k_r z_F^2 / D_{AX} + k_f y_S^2 / k_F + z_F y_S} \tag{7.9}$$

Provided a very rapid chemical reaction and ideal mixing in the donor solution, Eq. (7.9) is reduced to:

$$J = \frac{D_{AX} k_f y_S^2 x_F}{\delta_S k_r z_F^2} \tag{7.10}$$

7.4.2 Modelling of ELM Processes

The first models of this type of liquid membrane processes neglected the complex structure of the emulsions. In accordance with the membrane approach, the concept of the hypothetical membrane — a thin film of the membrane phase enveloping the uniform globules — was developed. All acceptor-phase microdrops were assumed to form one big and homogeneous internal drop covered with the membrane (see Fig. 7.15a). The transfer process is thus reduced to diffusion through a motionless spherical liquid shell of hypothetical thickness δ_S, experimentally evaluated using a calculated molecular diffusion coefficient. Some models do not consider the spherical geometry and use equations for a steady-state flow through a flat membrane [2,70,98,103,122]. The second group of models of "spherical shell" type accounts for the spherical geometry of the emulsion globule. These models are used to describe transport processes based on the first two transfer mechanisms [95,123], as well as on the facilitated transport concept [124–126].

Later on, the acceptor phase was not considered as a homogeneous drop constituting the core of the globule, but as a dispersion of drops of negligible size and of equal absorbing capacity, uniformly distributed in the globules. It is assumed in this case that the dispersion is stagnant and a reaction front advances to the center of the globule until the reagent B dissolved in the acceptor R is completely consumed, i.e., the solute diffuses forth to the center of the globule, irreversibly reacting with the reagent of the acceptor liquid in each concentric layer of the regular dispersion mentioned (see Fig. 7.15b). This model applies only to systems with a constant solute concentration at the F/S interface [127]. On this much more realistic concept, a series of the so-called "advancing front" models are created, elements of which can be found in former theoretical

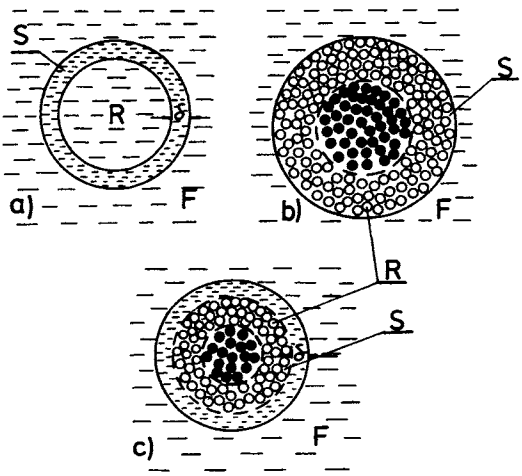

Fig. 7.15. Models of ELM processes. (a) Shell concept. The acceptor solution microdrops are assumed to form one large ideally mixed internal drop covered with the membrane (S). The hypothetical membrane thickness δ_s and solute diffusivity D_s are the rate-controlling parameters. (b) Advancing front concept. The acceptor solution microdrops of negligible size and equal absorbing capacity are uniformly distributed in the membrane liquid (S). A hypothetical reaction front advances towards the globule center consuming the reagent B dissolved in the dispersed acceptor solution R. (c) Combined "advancing front–shell" model concept [70,132].

studies [105,128]. Many authors improved and employed this model type [80,99,100,126,129–131]. The model of Kim [132] suggests an additional globule envelope of membrane liquid which imposes an extra diffusional resistance (Fig. 7.15c). A similar idea was earlier proposed by Cassamatta et al. [70], simply adding an "immobilized spherical shell" to the advancing front model. The model of Stroeve and Varanasi [126] follows the integral approach and, in contrast to the model of Ho et al. [100], takes into account the mass transfer resistance in the donor solution F. Some of the improved models of this type manage with a "front" with undefined location in the bulk of the globule and with a reversible chemical reaction, the later being the most often encountered case [73,80,133–135].

The integral approach permits the consideration of the processes taking place in the donor solution F, as well as some second-order phenomena — e.g., the spontaneous emulsion break-up,donor liquid occlusion, water osmosis and swelling, equilibrium condition changes caused by the transfer, etc. — all of which significantly affect the separation selectivity and should not be neglected [64,79,109,112,131]. It should be stressed that emulsion break-up may drastically change the course of the transfer process. Boyadzhiev et al. [79] developed a model involving a two-direction solute transfer: from the donor to the acceptor and back from R-phase to F-phase. The transfer is controlled by two mechanisms, diffusion and intermixing, respectively, the latter being due to the

spontaneous emulsion break-up. The total solute flux in this case is:

$$J = \frac{k_{F,i}\, k_{S,i}\, k_{R,i}\, a_{F/S}\, a_{S/R}\, (m_{F,i}\, x_{F,i} - m_{R,i}\, x_{R,i})}{k_{F,i}\, a_{F/S}\, (k_{R,i} + m_{R,i}\, k_{S,i}) + k_{R,i}\, a_{R/S}\, (K_{F,i} + m_{F,i}\, k_{S,i})} - \gamma\, x_{R,i}\, V_R \quad (7.11)$$

where the first term on the right side denotes the diffusional flux of the i-th component and the second term, the flux caused by emulsion break-up.

When phenol or other solutes of low solubility in the membrane liquid are consecutively transferred and "swallowed" in the acceptor solution — by a fast irreversible reaction — the following simplifications may be assumed:

$$m_{R,i} = m_{F,i} = m_i << 1 \quad (7.12)$$

$$a_{F/S} << a_{S/R} \quad \text{and} \quad V_S\, x_{S,i} << V_{R,i}\, X_{R,i} \quad (7.13)$$

$$k_{F,i} > k_{S,i} > k_{R,i} \quad (7.14)$$

Then Eq. (7.11) transforms into:

$$J = \frac{d(V_F\, x_{F,i})}{dt} = k_{S,i}\, m_i\, a_{F/S}\, (x_{R,i} - x_{F,i}) + \gamma\, x_{R,i}\, V_R \quad (7.15)$$

The parameters γ and k_S are evaluated from experimental data of laboratory tests. The drawback of this model is that it does not include the rate of the chemical reactions and yields no *a priori* information about the parameters γ and k_S. It should be kept in mind, however, that no theoretical, even rough, predictions of these parameters are possible owing to process complexity.

Later, more complicated models were developed, involving non-linear equilibria, water osmosis, etc. [53,82,136,137], as well as models considering the polydispersity of the acceptor solution drops [73]. Interesting from a practical point of view are the models describing continuous multistage separation processes based on the double emulsion method. Such models are proposed by Hatton et al. [99,130], Gladek et al. [94], Wankat and Noble [108], Reed et al. [138] and other authors.

7.4.3 Modelling of LFP Processes

The first models of liquid–film pertraction assumed that mass transfer should be controlled by the convective diffusion in all the three liquids involved. The mass-transfer coefficients, however, were obtained from the experimental data [139]. Later on, an analytical solution for these parameters, based on the theory of mass transfer to falling films was proposed [140]. Solutions for mass transfer accompanied by a slow chemical reaction or mass transfer with recirculated membrane liquid are still not available.

Finally, it should be mentioned that irrespective of the great number of mathematical models proposed, part of which was reviewed above, modelling of liquid membrane processes cannot provide a reliable design of a real separation process based only on published reference data. The only advisable way to avoid risks is to perform laboratory or pilot-plant tests. The use of correct and realistic models provides, however, good opportunities to get knowledge about the nature of the phenomena and to save valuable materials and time.

7.5 APPLICATION OF LIQUID PERTRACTION

7.5.1 Separation of Hydrocarbons

The first attempt to separate hydrocarbons with an aqueous membrane, stabilized by surfactants, was made by N.N. Li [141]. He used a single-drop diffusion column and a double-emulsion technique and examined a great variety of hydrocarbon mixtures, the separation of which is an important step of many processes in the petrochemical and chemical industries [2,3].

Most of the studies in this field aim at the separation of aromatic hydrocarbons from hydrocarbon mixtures containing normal paraffins, isoparaffins, olefins, and naphthenic hydrocarbons (cycloparaffins) among others [142–148].

As is seen from Table 7.1, which summarizes the data for many of the examined oil-in-water-in-oil (OWO) systems, the transferred component is usually benzene or toluene. This choice can be related to the higher solubility of the aromatic hydrocarbons in water. For example, the solubility of benzene in water is 187.5 times higher than that of *n*-hexane. Thorough studies have been performed by Casamatta and coworkers [4,149,150], which used emulsion liquid membranes for the separation of hydrocarbons with solubilities in water ranging from 3 to 1800 ppm. Recently, there has been an enhanced interest towards the separation of hydrocarbons from natural or industrial products, e.g., naphtha, kerosene, benzine, xylene fraction, etc.

The systems mentioned are separated using single-drop diffusion columns [1,2,86,94,122] or using the double-emulsion technique, usually as a batch process. Attempts are made to apply continuous DE processes. Casamatta et al. [150] used a perforated plate-pulsed column; Jeong [75] carried out similar continuous experiments in a larger Oldshue–Rushton extraction column.

The stable emulsion of hydrocarbon mixture F, encapsulated in the aqueous, membrane S, is destructed afterwards by heating [149,151] or by freezing [152]. The oil-in-water dense emulsions are stabilized by various water-soluble surfactants; the membrane solution further contains additives for correcting its viscosity, density and other properties.

In some cases, the aqueous membrane contains an additive which selectively

TABLE 7.1

Use of liquid membranes for the separation of hydrocarbon mixtures

Solute	Donor (F)	Acceptor (R)	Ref.
Toluene	heptane/toluene	hexane;S-100N	[2,3]
		kerosene, trichlorobenzene	[4,5,79,149, 150]
		kerosene	[159]
		decahydronaphthaline	[1,64]
		o-xylene	[96]
		isooctane+carbon tetrachloride + oil	[86]
		butane;dodecane	[160,415]
	chlorobenzene/toluene	kerosene	[4]
	cyclohexane/toluene		[4,5]
	hexane/toluene		[3,157,161]
	dimethylpentane/toluene		[2,161]
	p-xylene/toluene	hexane	[414]
benzene	benzene	trimethylpentane, carbon tetrachloride	[162]
	cyclohexane/benzene	kerosene, trichlorobenzene	[150]
		dodecane	[54]
	hexane/benzene	chlorobenzene	[122,163]
		hexane	[2,3]
		isooctane, carbon tetrachloride	[94,97,164]
		mineral oil	[155,157]
		isooctane + add.	[151,165]
		mineral oil	[166]
	heptane/benzene	kerosene, pentanol	[167]
	toluene/benzene	*o*-xylene	[96]
ethylbenzene	octane/ethylbenzene	hexane, nitrogen	[87,154]
	ethylcyclohexane/ethylbenzene	pentane	[154]
	styrene/ethylbenzene		[62,154]
methylnaphthol	dodecane/methylnaphthol	*n*-heptane	[167]
o-xylene	*m*-xylene/*o*-xylene	organic solvent	[154]
o-xylene + *p*-xylene	*o*-xylene		[154]
benzene/cyclohexane	hexane/benzene/cyclohexane	hexane	[3]
hexene/hexadiene	hexane/hexene/hexadiene		[3]
aromatic hydrocarbons	paraffins/cycloparaffins/ aromatic hydrocarbons		[3]
benzene/toluene	hexane/benzene/toluene		[3]

(continued)

TABLE 7.1 (*continuation*)

Solute	Donor (F)	Acceptor (R)	Ref.
benzene/toluene	dimethylbutane/ dimethylpentane/ benzene/toluene	hexane	[3]
hexene	hexane/hexene	S100N	[2]
hexadiene	hexane/hexadiene		[2]
heptene	hexane/heptene	hexane	[161]
cyclohexane	hexane/cyclohexane		[2,3,157,161]
styrene	ethylbenzene/styrene	pentane	[62]
ethylcyclohexane	octane/ethylcyclohexane		[62]
carbon tetrachloride	heptane/carbon tetrachloride	kerosene	[4,5]
hexane	hexane/heptane	*n*-octane	[102]
methylpentane	octane/methylpentane	S100N	[2]
1-methylnaphthalene	dodecane/1-methyl-naphthalene	–	[413]

reacts with the transferred component. For instance, Matulevicius and Li [102] separated hexene from heptane by adding copper-ammonium acetate to the aqueous membrane. The additive reacts only with the olefin by forming a weak complex which is soluble in the membrane liquid S. This mechanism increased the apparent solubility of hexene in the aqueous membrane and to facilitate its transport into the acceptor phase R. In the separation of benzene from cyclohexane Teramoto et al. [54] used silver nitrate as a carrier. The silver cation reacts reversibly with benzene but not with cyclohexane.

The separation effect of the aqueous membrane is based primarily on the different solubilities of the hydrocarbons in the aqueous membrane and on the difference in their diffusivities. According to Casamatta et al. [4,5], solubility difference is a more important factor than diffusivity difference, since the coefficients of molecular diffusion of hydrocarbons in water have close values and, in addition, their exponents in the mass transfer relationships are in the range $0.5 < n < 1$. Other authors propose more complex transfer mechanisms this take into account the permeation rate of hydrocarbons both through the bulk of the aqueous membrane and through the surfactant monolayers adsorbed on the two interfaces [2,3,152,154–156].

There are contradictory opinions in the literature about the role of surfactants on the transfer rate and the separation selectivity [3,62,97,157]. Casamatta et al. [149] claim that surfactants indirectly influence the transfer rate and the separation efficiency through emulsion structure, its hydrodynamics and stability. The question about the contribution of surfactant as a component that improves

or inhibits the solubility of hydrocarbons, or as a carrier facilitating the transfer, remains open. Recently, some authors proposed the idea that the surfactant micelles solubilize the hydrocarbons and transport them through the aqueous membrane as do typical carriers [156].

Kato and Kawasaki [158] developed a new way of increasing the rate of mass transfer and of improving membrane stability by adding oleophilic surfactants to the acceptor phase R. The method is applied to benzene–hexene mixtures, as well as to intermediate products of oil refinery. SPAN 20 (0.3 wt.%) is added to the acceptor phase consisting of isooctane. According to the authors, this additional surfactant dissolved in the R phase accumulates on the emulsion globule surface decreasing the size of emulsion globules and therefore increasing the emulsion contact area. This leads to a five- to six-fold increase in the rate of mass transfer in hydrocarbon mixtures like naphtha and kerosene [157].

Teramoto et al. [54] separated benzene and cyclohexane, using an aqueous membrane supported on both sides by hydrophobic-coiled polymer membranes. In some studies, conducted using the SLM technique, the outer acceptor phase is a gas, e.g. nitrogen [153,154]. These cases must be regarded as a link between the liquid pertraction and pervaporation.

In conclusion, it should be noted that the use of liquid aqueous membranes for the separation of hydrocarbon mixtures is less advantageous compared to the systems of the reverse type, i.e., water-in-oil-in-water (WOW) systems. This statement is based on the fact that the apparent uphill transport scheme cannot be applied (so far) to systems of the OWO type. With these systems, the transferred solute is only partially removed from the initial mixture F, but it is not concentrated in the R phase. Irrespective of these restrictions, there is still pronounced interest towards this group of processes.

7.5.2 Pertraction of Metals

There is a broad application of all pertraction methods in the separation and concentration of metal ions, e.g., for selective recovery of valuable metals, for environmental purposes, etc.

The chronological sequence of the studies of metal pertraction is hard to follow. However, the studies of Bloch et al. [168] who extracted uranyl ions from aqueous solutions by means of a polyvinyl chloride membrane plastified with TBP, may be among the oldest studies.

7.5.2.1 Alkaline and Earth Alkaline Metals

It is known that various membrane systems with built-in selective carriers are functioning in living organisms, transporting substances of vital importance like sodium, calcium, glucose and phosphates, etc. The principles on which

these processes were based were applied by Cussler [23], who attempted to pump sodium ions from their aqueous solutions apparently against to their concentration gradient. These studies dealt with the creation of *in vitro* models of the natural membrane systems and with the simulation of the transport processes involved.

Reuch and Cussler [12] paid attention to the cyclic polyethers, known as selective carriers of alkaline and earth alkaline metal ions. As the main factor controlling selectivity, they considered the ratio of the radius of the nonsolvated metal ion to the radius of the central polyether ring. Even very small differences between the radii of two metal cations affect process selectivity: a 0.2 Å change in the cationic radius causes a 500-fold change in the flux of solute transferred through the membrane. The polyether D18C6 is referred to as the most appropriate carrier for K^+ of the monovalent metal ions and for Pb^{2+} of the divalent ones. The selectivity of this crown ether strongly depends on the diluent of the carrier as well [169].

Later on, many macrocyclic compounds were used for this purpose: crown ethers [55,170–176,416,418,421]; carboxylic acids of crown ethers [13,178,179, 417,419,420] and aminoderivatives of crown ethers [180]. Anzai et al. [189] examined the liquid membrane transfer of alkaline metal ions by means of photosensitive crown ethers. Various noncyclic polyether compounds, selective for alkaline ions, were also synthesized and applied to liquid membrane transfer. For example, it was difficult to develop selective carriers for Li^+ separation from its aqueous solutions since Li^+ has the smallest ionic radius but the largest and most stable hydrate among the alkaline metals. Hiratani et al. [181] overcame this obstacle by means of noncyclic polyether compounds. The spectroscopic and other analyses revealed that these compounds form a cavity in which only a specified cation fits. The selectivity of these compounds is controlled by the chain structure and particularly by the composition of the terminal functional groups. Sakamoto et al. [182] successfully separated Li^+ from Na^+ by means of a supported liquid membrane using the nitrophenol derivative of 14-crown-4 as an active carrier. Inokuma et al. [183] successfully separated Mg^{2+}, Ca^{2+} and Ba^{2+}. The carrier they used was a mixture of a crown ether and an alkanoid acid.

Separations of membranes of alkaline picrates [171,184] or alkaline perchlorates [185] were also reported.

7.5.2.2 Noble Metals

There are only a few publications on the recovery of silver and gold by liquid pertraction [422,423]. Izatt et al. [186] studied the mechanism of silver transfer as $AgBr_2^-$ by means of ELM using as a carrier the macrocyclic ether DC18C6. Besides the $AgBr_2^-$ species, several cations present in the donor solution: Li^+,

Na^+, K^+ or Mg^{2+} can be also transferred. The acceptor R was a solution of $Li_2S_2O_3$.

Munoz et al. [187] separated silver from aqueous solutions using a mixture of D2EHPA and CYANEX®471 on a porous teflon support. More than 90% of the silver was removed from the treated solution in two hours. In order to find a suitable stripping reagent, EDTA, thiosulphate, thiocyanate and ammonia were tested, but the 0.25 M ammonia solution may be used only as an acceptor phase.

Diluent selection for the membrane phase was decisive for the efficient separation of $AuCl_4^-$ from aqueous solutions in some cases. Burgard et al. [172] established that the use of dichloroethane as a diluent of the carrier chosen — a polyethylene oxide derivative — leads to a saturation of the membrane phase with the complex being formed and the transfer into the acceptor phase sharply decreasing. When chloroform was used instead, $AuCl_4^-$ was quantitatively transferred into the acceptor solution R.

In hydrometallurgical leach solutions, gold and silver are present as dicyanoaurate or dicyanoargentate anions, respectively. Their recovery by means of quaternary ammonium salts leads to a strongly hampered stripping step; the use of amines yielded the highly toxic HCN. Therefore, Tromp et al. [188] proposed the macrocyclic complexing reagent Kryptofix®22DD for the extraction of these metals. In this case, stripping may be effected with water.

Nishiki and Bautista [190] extracted Pt^{4+} from hydrochloric solutions by means of SLM, achieving a concentration factor of 60. The membrane consisted of TOA dissolved in xylene, the acceptor phase was a solution of Na_2CO_3.

In order to improve the stripping of platinoid metals from the organic phase, Purin et al. [191] combined liquid membranes with electrochemical processes: stripping was carried out in an electric field. Moskvin and Shmatko [192] used a similar approach, combining liquid membranes with electrodialysis.

Pd and Pt have very close properties. Only Pd^{2+} forms, however, hydrate in acidic solutions [193], which may be bound by special carriers like the sulphur-containing macrocyclic compounds, e.g., T18C4 (thio-18-crown-6).

Hidalgo et al. [194] used a SLM module impregnated with a CYANEX®471 solution for separation of Pd^{2+} from Pt-containing chloride solutions as well as for the recovery of Pd^{2+} from waste catalysts.

7.5.2.3 Rare-earth and Radioactive Metals

Most attention was paid to uranium in this group of metals [195–198,424–426]. Macasek et al. [199] optimized the recovery of this metal from waste aqueous solutions and its preconcentration for analytical purposes. The ELM method was applied using TOPO, TBP, KELEX®100 and D2EHPA as carriers. The best results were obtained with D2EHPA.

Akiba et al. [200,201] developed a liquid–membrane process for the recovery of uranium, contained in wet process phosphoric acid (WPPA). For this purpose they used both ELM and SLM techniques with various carriers: D2EHPA alone or mixed with 1-octanol, TOPO.

Sifniades et al. [202] transferred U(VI) from a 5–6 M phosphoric acid solution, simulating a WPPA waste solution, through a membrane consisting of a mixed extractant (D2EHPA/TOPO) solution in kerosene. The acceptor solution was phosphoric acid containing Fe^{2+} as a reducer.

Other authors also studied uranium recovery from phosphoric acid solutions with the mixed extractant D2EHPA/TOPO [203–208].

For uranium extraction by the scheme

$$[UO_2^{2+}]_F + 2[(HX)_2]_S + [R]_S \longleftrightarrow [UO_2\,X_2(HX)_2R]_S + 2[H^+]_F \qquad (7.16)$$

where

$$HX = D2EHPA, \quad R = TOPO,$$

U^{4+} has to be previously oxidized to U^{6+}. For this purpose, $NaClO_4$ is added to the donor solution F containing 500 ppm U^{4+}. The complex stripping into the 5 M phosphoric acid acceptor solution most often takes place by reduction with Fe^{2+} as follows:

$$[UO_2^{2+}]_S + 2[Fe^{2+}]_R + 4[H^+]_R \longleftrightarrow [U^{4+}]_R + 2[Fe^{3+}]_R + 2[H_2O]_R \qquad (7.17)$$

The technical and economic comparative analysis of pertraction and conventional liquid–liquid extraction processes [209], performed within the joint program of Exxon Research & Engineering and Davy McKee for uranium recovery from WPPA, revealed the following advantages of pertraction:

- lower operation costs;
- direct treatment of "black" acids containing organic admixtures, no cooling steps for their separation being needed;
- processing of concentrated solutions of phosphoric acid (up to 45% of P_2O_5);
- the only preliminary step required is the separation of solids.

When a mixture of mono- and di-octylphenylphosphoric acids (OPAP) is used as a carrier, U^{4+} can be directly, without preoxidation, transferred through the organic membrane.

Akiba and Kanno [210] used SLM impregnated with TOA for the separation and concentration of U^{6+} from dilute sulfuric acid solutions. Their acceptor solution contained Na_2CO_3. The temperature of the treated solution should not exceed 50°C, since the rate of the transfer process strongly decreases above this value.

The effect of other metals on uranium extraction from sulfate solutions with TAA was studied, also [211]. Except for VO_3^- and MoO_4^{2-}, the ions of iron, aluminum, silicon and magnesium do not affect the process. $Fe_2(SO_4)_3$ suppresses the Mo(VI) coextraction.

Babcock et al. [212] tested a SLM unit consisting of four hollow fiber modules for continuous treatment of waste water from the uranium mines in Wyoming. The uranium concentration was reduced from 125 to less than 5 ppm for 50 days. The final acceptor solution R (150 g l^{-1} of Na_2CO_3) contained about 1% of uranium. In a later study [213] these authors used the same technique for the separation of uranyl cations from the accompanying vanadate ions in the leaching solutions.

Akiba and Hashimoto [31] extracted U(VI) from sea water by means of the SLM method using a 0.1 M solution of KELEX®100 as a carrier. In approximately 20 hours, 99% of the uranium was extracted.

Zhu et al. [214] extracted lanthanides from leaching solutions in the presence of NaCl by the ELM method in an Oldshue–Rushton column. The carrier was D2EHPA and the acceptor — an aqueous solution of HCl. As a result of the ion-exchange process pH of the donor solution changed along the column and had to be corrected by intermediate alkalization.

Sourougy et al. [215] separated lanthanides from nitric media by the ELM method also using D2EHPA as a carrier. The extraction efficiency decreased in the order: Sc > Sm > Er > Gd > La > Y. Zhang et al. [216] carried out a similar separation of lanthanides from $(NH_4)_2SO_4$ aqueous solutions.

Teramoto et al. [217] separated and concentrated the lanthanides La, Nd, Sm, Eu, Gd, Dy and Yb using as a carrier 2-ethylhexylphosphoric acid mono-2-ethylhexyl ester (PC®88A). Ninety-eight percent of the metal ions cited were removed from the initial solution in five minutes. After stirring of the emulsion for 20 minutes, an enrichment factor of about 50,000 was achieved. Pertraction offered additional advantages in the case of Yb^{3+} removal. In contrast to the conventional extraction, where insoluble in the organic phase complexes of Yb^{3+} are formed, here the organic membrane is continuously regenerated, keeping the concentration of the metal complex in the membrane at low levels.

Lanthanides and actinides can be successfully separated by means of the SLM technique [218–220,427,428]. Danesi et al. [221] separated actinides and lanthanides from acidic radioactive waste water using modules of flat membranes and hollow fibers. The extraction of actinides is more complete. Some of the experiments were performed in three-compartment cells supplied with two supported liquid membranes of different composition. The first membrane (between F_1 and R) was a solution of octyl (phenyl) -*N*, *N*-diisobutyl-carbamoylmethylphosphine oxide + TBP in decaline. The second membrane (between R and F_2), was a solution of Primene®JMT in decaline, also continuously removed the nitric acid, transferred simultaneously with the metal ions into the

acceptor solution R. In this way, a constant concentration of the nitric acid was maintained, which contributed to the process stabilization and the membrane lifetime. Danesi and Cianeti [41] achieved, by means of a SLM of "acidic type" (D2EHPA in dodecane), a complete removal of Am^{3+} from the initial aqueous solution F_1.

Novikov and Myasoedov [223] established the optimum conditions for the separation of the lanthanide/actinide couples: Am/Cm, Eu/Tb, and Eu/Am, achieving separation factors of 5.0, 10.8 and > 100, respectively.

Instead of D2EHPA, Nakamura and Akiba [224] used diisodecyl-phosphoric acid (DIDPA) as a carrier of Eu^{3+} due to its better hydrophobic and extraction properties. Brown et al. [18] transferred Eu^{3+} in the system water-$CHCl_3$-water by means of the 18C6 crown ether. A preliminary reduction of $Eu(NO_3)_3$ to $Eu(NO_3)_2$ was necessary in this case due to the instability of the Eu^{3+} complex. It was for the same reason that the experiments were performed in an argon atmosphere.

Gasparini et al. [40] demonstrated a direct SLM extraction of Pu(IV) and Zr(IV) from alkaline media without preliminary acidification of the aqueous solution. Ninety-five percent of the plutonium and zirconium ions are transferred into the acceptor liquid — an aqueous solution of oxalic acid — by tributylacetohydroxamic acid (TBAH), dissolved in diethylbenzene and 2-octanol for approx. 250 minutes.

Rajec et al. [225] and Mikulai et al. [226] preconcentrated pertechnetates with a liquid membrane containing Aliquat®336.

7.5.2.4 Copper

Copper is the most often-encountered subject of pertraction studies. This priority can be explained not only with the practical significance of this metal, but also with the availability of various highly selective commercial extractants suitable for the treatment of the acidic or alkaline copper solutions [429–431,465,470]. Table 7.2 lists many of the publications devoted to the problems of copper pertraction. It can be seen that the majority of the authors prefer chelating extractants, e.g., of the LIX®, ACORGA®, KELEX® or other series, as carriers, of copper ions. Organophosphorus acids or aliphatic acids are rarely applied to this purpose.

As inert diluents of the selective extractants various hydrocarbons with a low solubility in the treated copper solutions are used, e.g., kerosene [89,128,227, 228], normal paraffins as *n*-heptane [229,230], *n*-dodecane [191], isoparaffins [231], cycloparaffins as cyclohexane [232,233], aromatic hydrocarbons as xylene [36], toluene [39,106] and benzene [234].

Synthetic mono- or polycomponent aqueous solutions of copper salts and industrial solutions or waste waters are used as donor solutions. As a rule, the

TABLE 7.2
Pertraction of copper

Carrier	Method	References
LIX®64N	ELM	[43,63,66,107,128,231,309,396–401,407,432]
	SLM	[9,24,35,43,44,227,245,402,408]
LIX®65N	ELM	[43,229,241,247,248,403–407,433]
	SLM	[36,43–45]
	LFP	[466,467]
LIX®54	SLM	[236]
	LFP	[467]
LIX®70	ELM	[304]
LIX®34	ELM	[404]
	SLM	[246]
ACORGA®P5050	ELM	[78,412]
ACORGA®P5100	ELM	[66,85,399]
	SLM	[26,227]
	LFP	[243,467]
ACORGA®P5300	ELM	[58,66]
	SLM	[58,227]
KELEX®100	ELM	[304,404]
	SLM	[227]
SME®529	ELM	[61,124,237]
	SLM	[44]
benzoilacetone	ELM	[109,234,238,404]
fatty acids	ELM	[89,128,232,235,242,409,410]
	SLM	[411]
D2EHPA	ELM	[13,232,309]
	SLM	[9,191,402,434]

latter are of acidic type, but in some cases alkaline solutions, e.g., ammoniacal copper solutions [235,236] are treated. Aqueous solutions of sulfuric acid with concentration in the range 50–270 g l^{-1} are used as acceptor phases. Sulfuric acid is preferred to other strong mineral acids due to its practical insolubility in the membrane liquid and furthermore, to the availability of a well-established process of copper electrowinning from concentrated sulfate solutions. There are also data on the usage of acceptor solutions of nitric acid [36,232,237], hydrochloric acid [33,124,232,238,239], or perchloric acid [240]. In all these cases the donor solutions contained copper salts with the corresponding anionic part, e.g., nitrate or chloride, Cu^{2+} being transferred between two aqueous phases F and R of various pH values but of the same anionic composition. Nakashio et

al. [241] used the ELM method and stressed on the role of the emulsifier in copper pertraction. They produced a series of surfactant derivatives of glutamic acid dialkyl esters, which exhibited better properties than sorbitan oleates or polyamines used so far.

It is of interest to compare the copper fluxes transported under the same experimental conditions by various carriers. For instance, Marr et al. [242] compared the data of copper pertraction with stearic acid and LIX®64N. They found that the emulsion formed by LIX®64N is more stable and thus provides a higher copper accumulation in the encapsulated acceptor solution. Teramoto and Tanimoto [44] impregnated hollow polymer fibers with organic solutions of SME®529, LIX®64N or LIX®65N.

Largman and Sifniades [227] tested the transfer intensity with the carriers ACORGA®P5100, KELEX®100 and LIX®64N and ordered the fluxes of copper which are transferred across the liquid membranes as follows:

$$J_{\text{ACORGA}^{\circledR}\text{P5100}} > J_{\text{KELEX}^{\circledR}\text{100}} > J_{\text{LIX}^{\circledR}\text{64N}}$$

Schugerl et al. [66] compared the data about copper preconcentration from its dilute aqueous solutions (initial Cu^{2+} concentration from 1 to 100 mg l^{-1}) by the ELM technique using the carriers ACORGA®P5100, ACORGA®P5300 or LIX®64. Regardless of the close distribution coefficients in all three cases, the results strongly differed, which was attributed to the various kinetics of chelate complex formation and destruction. For example, the intense fluxes with the carriers of the ACORGA series are related to the higher stripping rate, i.e., to the higher rate of chelate destruction. The authors did not, however, account for the more pronounced adsorption properties or the higher solubilities both of chelate complex and extractant in the aqueous phase as possible causes of this phenomenon.

Lee et al. [43] compared the results of copper pertraction applying the ELM and SLM methods. The conclusion was drawn that supported membranes are more advantageous since they yield more reproducible results, the transferred fluxes being of comparable magnitude. Boyadzhiev et al. [58,243] included one more pertraction method in their comparative study: liquid film pertraction. The obtained results gave evidence for the applicability of all three methods to copper pertraction with ACORGA®P5300. Some results on copper pertraction from acidic (pH = 2) waste waters, containing 1 g l^{-1} copper obtained by means of a Rotating Film Pertractor are shown in Fig. 7.16. The carrier in this case was LIX®860.

In the general case, the driving force of the pertraction process is generated by the pH gradient between the aqueous phases on both sides of the organic membrane. It is also possible for copper transport to be generated by redox reactions [39]. The treated solution contains a reducer, the acceptor phase an

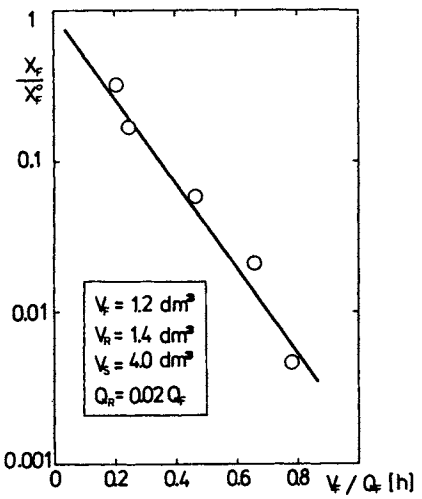

Fig. 7.16. Removal of copper from waste water by RFP technique. Initial copper content in the feed: 1 g l^{-1}. The membrane liquid is a 5% (vol.) solution of LIX®860 in dodecane; the acceptor is 3 N sulfuric acid.

oxidizer. The transfer is based on the different extractability of the various valent states of copper ions [Cu(II) and Cu(I)]. Ohki et al. [10] proposed the idea of using photoinduced reactions also for liquid–membrane separations.

An explicit assessment of the effect of various parameters on the efficiency of copper pertraction is hard to give. There are data about the effect of initial copper concentration in the treated solutions [33,245], their pH value [109,246], the carrier concentration [35,107,238], the emulsifier concentration [233,241,247, 248], the membrane viscosity [107] and the composition of the acceptor liquor [35,124]. The temperature effect [72,250] as well as hydrodynamic parameters like mixing velocity or flow rate of the phases are also studied [124,238,249].

The experimental data are subjected to mathematical modelling in order to draw conclusions about the process mechanism and about the rate-controlling step using various carriers. According to Yagodin et al. [9], when D2EHPA is used as a carrier, the process is diffusion-controlled, since the reactions of copper complex formation and destruction are faster than mass transfer, the latter being actually rather intense when applying the ELM method. The substitution of D2EHPA for the oxime LIX®64N leads to a sharp decrease in the flux of transferred Cu^{2+} ions since the control passes to chemical kinetics. In this case the flux strongly depends on the presence of catalysts in the system, this being considered as evidence for the decisive role of chemical reactions taking place.

It is generally accepted that copper interaction with the chelating carrier, summarized as:

$$[Cu^{2+}]_W + 2[HR]_S \longleftrightarrow [CuR_2]_S + 2[H^+]_W \quad (7.18)$$

proceeds in two steps:

$$[Cu^{2+}] + [HR] \longleftrightarrow [CuR^+] + [H^+] \quad (7.19)$$

$$[CuR^+] + [HR] \longleftrightarrow [CuR_2] + [H^+] \quad (7.20)$$

The second reaction step is considered as the slower and hence as the rate-controlling one.

The experiments of O'Hara et al. [236], performed with alkaline aqueous solutions and LIX®54 as a carrier, showed that diffusion in the liquid membrane is the rate-controlling step, provided both the mixing intensity and initial copper concentration in the F solution are high enough. Using LIX®54 as a carrier, Yoshizuka et al. [246] found that the rate-controlling step at pH values above 5 is the diffusion of copper in the donor phase or the diffusion of the complex in the membrane. At low pH values, however, the interfacial chemical reaction is the rate-controlling step. According to Chiarizia et al. [33] the process is controlled by the diffusion in the membrane or in the aqueous layers adhering to it. Komasawa et al. [36] considered the chemical reactions taking place at the F/S interface as the rate-controlling step. Bart et al. [251] also confirmed that chemical kinetics controls the overall pertraction rate, assuming low copper concentration in the donor solution. Lorbach et al. [252] examined three cases: the resistance is located in the F phase (low concentrations of copper ions and protons); the resistance is located at the F/S interface (low concentration of copper ions, high proton concentration); and the resistance is located in the membrane S (high concentration of copper ions, low proton concentration). Using the SLM method with the carrier ACORGA®P5100, Flett and Pearson [42] assumed a diffusional control both in the bulk of the aqueous phase and in the aqueous layers adhering to the membrane. Danesi et al. [25] concluded that copper pertraction with a carrier LIX®64N is simultaneously controlled by the chemical reactions and complex diffusion. Applying the LFP method, Boyadzhiev and Lazarova [253] pointed to the important role of donor and membrane liquid hydrodynamics on the mass transfer.

According to the studies of Ivakhno et al. [254], the rate of copper pertraction with chelating extractants is controlled by the rates of the forward and reverse chemical reaction. These authors declined the general opinion that chemical reactions take place at the F/S and S/R interfaces. By analyzing the corresponding kinetic equations, they established that the reaction occurring in the aqueous layers close to the interfaces significantly contributes to the overall process resistance. This hypothesis is supported by other authors as well [255,256].

7.5.2.5 Other Valuable or Toxic Metals

Waste water purification from chromates is a severe environmental problem [26,42,257,258,435–438]. Frankenfeld and Li [259] examined the relationship between the various mechanisms of extraction and stripping chromate ions from the waste waters of galvanic production. The extraction may be performed by means of two carrier types: tertiary amines or quaternary ammonium salts. In the first case, the extraction process may be expressed as amine neutralization:

$$[R_3N]_S + [2H^+ + Cr_2O_7^{2-}]_F \longleftrightarrow [(R_3NH)_2Cr_2O_7]_S \tag{7.21}$$

whereas in the second one, the process is accompanied by a salt formation:

$$[(R_3NH)_2X]_S + 2H^+ + Cr_2O_7^{2-}]_F \longleftrightarrow [(R_3NH)_2Cr_2O_7]_S + [2H^+ + X^{2-}]_F \tag{7.22}$$

where $X = SO_4$ or Cl_2.

The destruction mechanism of the chromate–amine complex depends on the composition of the regenerating solution R. With an alkaline R solution, the stripping scheme is:

$$[(R_3NH)_2Cr_2O_7]_S + 4(Na^+ OH^-]_R \longleftrightarrow [R_3N]_S + [2(2Na^+ + CrO_4^{2-}]_R + [3H_2O]_R \tag{7.23}$$

whereas with an acidic R solution the scheme is:

$$[(R_3NH)_2Cr_2O_7]_S + [H_2SO_4]_R \longleftrightarrow [(R_3NH)_2SO_4]_S + [2H^+ + Cr_2O_7^{2-}]_R \tag{7.24}$$

Both mechanisms are successfully applied in a number of liquid membrane studies.

Kitagawa et al. [260] developed a pilot plant involving one or two pertraction steps: the unit treats 45 l of waste waters containing 100 ppm of Cr^{6+} with 1 l of emulsion for 5 hours. As a result, chromium concentration is brought down below 1 ppm with up to 65 g l^{-1} of Cr^{6+} being accumulated in the alkaline acceptor solution (10% NaOH).The two-step version uses a 20% solution of NaOH as an acceptor and chromium concentration in this liquor finally reaches up to 182 g l^{-1}.

The liquid membrane transfer of chromium is most often performed with TOA or TAA, e.g., Alamine®336 [196,261–267]. Mori et al. [268] pointed out that treating sulfuric solutions of Cr(VI) with a membrane of tridodecyl- or trioctylamine dissolved in kerosene yields a stable, gel-like complex in the organic

phase, which may be avoided by adding 2-ethylhexyl alcohol to the membrane liquid S.

Fuller and Li [269] carried out a simultaneous separation of Cr(VI), Cr(II) and Zn(II) from a cooling blow-down stream by using a mixture of two carriers: TBP and Aliquat®336. Using also quaternary ammonium salts, Strzelbicki et al. [270] separated chromium and rhenium present in the donor solution as NH_4ReO_4 and K_2CrO_4. The emulsion containing rhenium is finally destructed by the addition of *n*-butanol.

A potential application field of pertraction is the removal of the highly toxic mercury from waste waters or physiological liquors and the registration of traces of mercury in various solutions [429,439,440]. For example, mercury is present as a soluble HgI_4^{2-} complex, which can be extracted by means of high-molecular amines or quaternary ammonium salts [259] according to the scheme:

$$[2(R_4NX)]_S + [HgCl_4^{2-}]_F \longleftrightarrow [(R_4N)_2HgCl_4]_S + [2X^-]_F \qquad (7.25)$$

Stripping is performed with an aqueous solution of a strong acid, inorganic or organic base like ethylenediamine.

Kitagawa et al. [260] successfully applied the ELM technique for mercury extraction: the concentration of Hg^{2+} was reduced from 1100 ppm to below 0.2 ppm in approximately 10 minutes. This corresponds to more than 99.98% removal efficiency.

Baba et al. [271] tested various carriers and emulsifiers for a preconcentration of Hg^{2+} from nitrate and chloride solutions. The combination of tributylphosphine sulfide as a carrier and L-glutamic acid dioleyl ester as a surfactant was found to be the most advantageous one.

Boyadzhiev and Bezenshek [272] established the optimum conditions for treating nitrate aqueous solutions containing from 0.07 to 0.35 g l^{-1} of mercury ions at a pH value of about 3. The membrane phase was a 10% solution of a technical mixture of long-chain fatty acids (linolic and oleic) in normal paraffins C_{11}–C_{13} containing 1% emulsifier: SPAN®80. The stripping was carried out with 2 M sulfuric acid. Figure 7.17 presents the effect of the agitation intensity on the efficiency of the Hg^{2+} transfer.

Weis and Grigoriev [273] gave preference to another extractant: dibutylbenzoylthiourea (DBBT), which reacts with Hg^{2+} according to:

$$2[R^2NCSNHCOR^1]_S + [Hg^{2+}] \longleftrightarrow 2[H^+]_F + [Hg(R^2NCSNCOR^1)_2]_S \qquad (7.26)$$

where $R^1 = C_6H_5$ and $R^2 = (n\text{–}C_4H_9)_2$

Stripping into the hydrochloride solution R is accompanied by an irreversible chemical reaction with urea present in this phase:

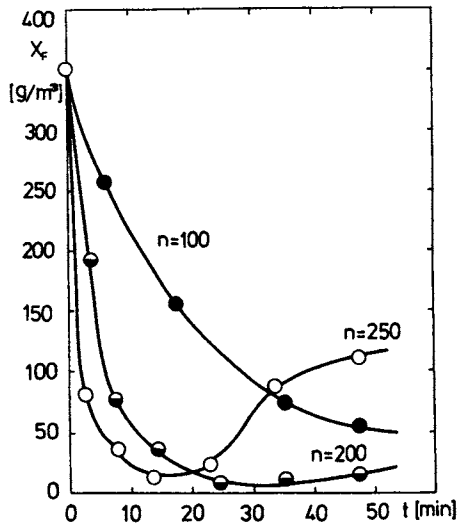

Fig. 7.17. Mercury removal from slightly acidic aqueous solutions. Stirring intensity during the second (contacting) process stage influences both the rate of transfer and emulsion break-up.

$$[Hg^{2+}]_R + 2[HCl]_R + 4[(NH_2)_2CS]_R \longleftrightarrow [Hg(NH_2)_2CS)_4Cl_2 + 2[H^+]_R \quad (7.27)$$

Bivalent mercury may be selectively separated from other cations such as K^+, Cd^{2+}, Tl^+, Sr^{2+}, Ag^+ and Pb^{2+} by means of macrocyclic ethers functioning as carriers [274]. Bacon and Jung [15] used the ability of some macrocyclic ligands to extract mercury ions from model solutions without transferring other cations of biological importance. It is known that chemodialysis does not function as a treatment for mercury intoxications. An improved method using liquid membranes could significantly contribute to the rapid removal of this toxic metal from the human organism.

Pertraction processes may be applied for removing the highly toxic cadmium from waste waters, e.g., of galvanic production [441–445]. The cyanide complex $[Cd(CN)_4]^{2-}$ is extracted with Aliquat®336. The destruction of the extracted species and the liberation of the cadmium ion is a difficult task [260] that can be solved by means of the disodium salt of EDTA, provided pH of the acceptor solution is maintained in the range between 4 and 6. Danesi et al. [275] used the SLM method to elucidate the transfer mechanism of the cadmium complex with the carrier TLAHCl. Takahashi et al. [276] also published a study on this subject, using D2EHPA as a carrier.

According to Zhang and Huang [277] the combination of two extractants (D2EHPA and alkylphosphine oxime) allows the simultaneous separation of Cd^{2+} and CN^- from galvanic bath waste waters. The concentrate obtained may

be directly used in the process.

Izatt et al. [278] tested 14 various macrocyclic compounds for the membrane extraction of $Pb(NO_3)_2$. Satisfactory results (extraction efficiency of 91%) are obtained with didecyl-1,10-diazo-18-crown-6. Biel et al. [279] removed 90% of the lead in the presence of lithium and potassium from a nitrate solution by using a similar compound, dicyclohexano-18-crown-6.

In a number of liquid membrane studies the experimental data about the selective separation and concentration of zinc are analyzed [280–283,432,446–450]. Usually, Zn^{2+} is extracted with D2EHPA from sulfuric, perchloric or other acidic media by the cation exchange mechanism as follows:

$$[Zn^{2+}]_W + 2[(HR)_2]_S \longleftrightarrow [ZnR_2(HR)_2]_S + 2[H^+]_W \quad (7.28)$$

$$[Zn^{2+}]_W + 1.5[(HR)_2]_S \longleftrightarrow [ZnR_2(HR)]_S + 2[H^+]_W \quad (7.29)$$

According to Tanagaki et al. [284] $ZnCl_2$ may be transferred from a hydrochloric solution by means of TOA. A complex between TOA and HCl is initially formed, to which, subsequently, $ZnCl_2$ is added.

The first large-scale equipment for zinc recovery from the waste waters of rayon production was built in Austria as a result of long-term thorough studies [85]. It has the following technical parameters: flow rate of waste waters, 75 m^3 h^{-1}; flow rate of membrane phase, 5 m^3 h^{-1}; flow rate of sulfuric acid solution, 0.5 m^3 h^{-1}. The removal of 400–600 ppm of Zn^{2+} from the waste water containing calcium, 5–8 g l^{-1} of sulfuric acid, 25 g l^{-1} of sodium sulfate and various modifiers and solids was achieved by means of di-2-ethyl-hexyl dithiophosphoric acid (D2EHDTPA) — an efficient extractant for metals, which finds a rare use in liquid–liquid extraction due to the hampered stripping of the loaded organic phase. Irrespective of the slow stripping kinetics, the ELM method yields a satisfactory pertraction rate due to the extremely large S/R interface. D2EHDTPA extracts Zn^{2+} at a pH about 0.5, whereas D2EHPA cannot be used at pH values below 2. Sulfuric acid of minimum 2 M concentration is required for stripping. The average process efficiency is 99.5%; zinc concentration in the final acceptor liquor is about 60 g l^{-1}.

Draxler and Marr [285] used a combined ELM procedure for the simultaneous separation and concentration of zinc, cadmium and lead from the waste waters of zinc production with D2EHDTPA as a carrier. The three metal cations cannot be simultaneously stripped by the sulfuric acceptor solution so that part of the membrane phase is separately regenerated with a hydrochloric solution. The purification of the waste waters in zinc production after copper cementation is performed by Schugerl et al. [66], which applied a continuous ELM process in a Kuhni-type column using LIX®51 as a carrier. This extractant is preferred for separating metal ions from ammonia or other alkaline solutions. Harada et al. [286] separated zinc and iron from their mixtures by making use

of the different reaction mechanisms of the two extractants, TOA and D2EHPA, present in the membrane liquid. The two aqueous solutions F and R are of various HCl concentration: 1 M HCl and 0.05 M HCl, respectively. TOA transfers both zinc and iron ions from the F to the R solution. D2EHPA transfers the Fe^{3+} ions back to the F solution. The final result of this "two-way" transport is the efficient one-step separation of the two metal ions.

Verhaege et al. [287] successfully used D2EHPA for the separation of zinc from nickel. The concentration of zinc ions in the donor solution was 600 ppm and that of nickel ions is 58 g l^{-1}. Zinc is separated by the SLM technique using a membrane phase containing 30 vol.% of D2EHPA. The treated solution is maintained in continuous motion inside the hollow fibers, the acceptor solution circulated outside. Finally the whole amount of zinc and only 1% of the nickel present in the donor solution are transferred to the acceptor solution. Poa et al. [288] also developed a SLM process for the separation of zinc from nickel using octylamine as a carrier.

Loiacono et al. [239] developed an interesting approach for the separation of zinc from copper by the three-compartment SLM technique. One of the two membranes is impregnated with a D2EHPA solution, the other with a LIX®64N solution. The treated solution is placed in the middle compartment, i.e., between the two membranes. The zinc ions are transferred through the membrane containing D2EHPA, the copper ions through the LIX-containing membrane.

Couples of metal ions can be separated by an appropriate combination of carriers, the donor and acceptor solution. For example, Melzner et al. [16] selectively separated zinc from solutions containing copper and cobalt. Danesi et al [289] separated Zn(II) and Cd(II) from chloride solutions using TLAHCl as a carrier. The separation is based on the strong effect of Cl^- concentration on the liquid membrane transfer of the two metal ions. Izatt et al. [290] separated cadmium from mercury by means of crown ethers.

Various liquid membrane methods are used for the separation of cobalt and nickel [291–300,451–454]. D2EHPA was the carrier most often used [92,301–303]. The comparative studies of Strzelbicki and Charewicz [304] on ELM systems showed that D2EHPA is an efficient carrier for Co^{2+} and Ni^{2+} from nitrate and chloride media. Sulfates usually inhibit this separation process, in which case other extractants like KELEX®100 or LIX®70 should be employed.

A good separation of cobalt and nickel is achieved by means of another commercial organophosphorus compound, CYANEX®272 [41,305]. Reichley-Yinger and Danesi [306] found out that the presence of glycine in the treated solution favors the separation of Co^{2+} from Ni^{2+}. Glycine is a hydrophilic ligand that forms more stable complexes with Ni^{2+}, thus retaining its ions in the donor solution F.

There is only limited information about the treatment of solutions containing Fe^{2+} ions [307–309,455]. This could be related to the fact that iron is a wide-

spread and nontoxic metal. It is usually separated from solutions by means of supported liquid membranes impregnated with TOA [310,311]. The electrodialysis of Fe^{3+} through a supported liquid membrane impregnated with TBP was also studied [312]. This kind of process, however, lies beyond the scope of this chapter.

Guerriero and Meregali [313] developed a SLM process for the recovery of indium from sulfuric leaching solutions containing many other ions besides indium (Cu, As, Zn, Fe, Sb, Bi). D2EHPA is used as a carrier. A separation factor of the couple In^{3+}/Cu^{2+} of 10^4–10^6 and a concentration factor of indium of about 400 was achieved, the copper content exceeding by 70 times that of indium.

An analogous SLM process using a membrane of TBP dissolved in cumene is proposed by Valiente [314] for the separation of titanium(IV) from chloride solutions.

Charewicz et al. [315] separated indium(II) and strontium(II) by the ELM technique using carboxylic acids (caprylic and linolic) as carriers. Liquid membranes are applied by Wang and Liu [316] and Zeng and Chan [317] to separate vanadium and by Hozawa et al. [318] to concentrate gallium and indium. In order to achieve a selective extraction of Ga^{3+} from a gallium–aluminum solution, Shimidzu and Okushita [319] impregnated their porous support with alkylated cupferron (ammonium salt of *N*-(alkylphenyl)-*N*-nitrosohydroxylamine).

Gutknecht and Schugerl [320] successfully separated germanium from fly ash leaching solutions by means of an ELM method. A practically complete germanium recovery from a 9 M hydrochloric solution is achieved in several minutes. The donor phase contained other metal ions (Cu, Ag, Fe, Mo, Si, among others) in much higher concentrations. These were not detected in the acceptor solution (1 M NaOH). The organic membrane was a mixture of carbon tetrachloride, xylene and a surfactant.

Izatt et al. [321] separated thallium from donor solutions containing various thallium salts: cyanides, carbonates, nitrates, etc., by means of the crown ether DC18C6. In this study valuable results about the role of the coanion on the pertraction of thallium ions are presented.

7.5.3 Pertraction of Inorganic Substances

The elevated concentration of nitrogen compounds, e.g., ammonia, in waste waters causes a severe ecological problem. After Li's patent [322] for ammonia recovery by means of ELM was published, a number of studies appeared on this subject [99,146,323,324,456]. Kitigawa et al. [260] studied NH_4^+ pertraction from waste water. It is known that in alkaline solutions (pH > 9) the equilibrium:

$$NH_3 + H_2O \longleftrightarrow NH_4OH \longleftrightarrow NH_4^+ + OH^- \qquad (7.30)$$

is shifted to undissociated ammonia molecules, which are soluble in the oil membrane S. When an acidic acceptor solution R is used, NH_3 transferred through the membrane is irreversibly transformed into NH_4^+ and is thus removed from the waste water. The membrane liquid in this case consists of isoparaffins, polyamines or sorbitan monooleate as emulsifiers. The acceptor liquid is an aqueous solution of HCl or H_2SO_4. Under the optimum conditions, these authors reduced the NH_4^+ content from 50 to 0.37 ppm within 20 minutes of contact time.

Rautenbach et al. [325,397] used the same technique for the removal of ammonia from waste waters in a broad concentration range. The initial ammonia concentration varied from 50 to 1000 ppm, the H_2SO_4 concentration in the acceptor solution from 0.5 to 20 wt.%. They found that in all cases more than 99% of ammonia present in the outer, donor phase were extracted in 40 minutes. As a liquid membrane, paraffin oil containing a surfactant was used. The amount of extracted ammonia increases on raising the H_2SO_4 concentration in the R solution. With 20 wt.% of H_2SO_4, however, a pronounced phase inversion takes place. A tendency for emulsion inversion is observed at low ammonia concentrations in the donor solution F as well. This undesirable phenomenon is caused by the lower osmotic pressure of the R solution. A more significant difference between the osmotic pressures on both sides of the membrane gives rise to a transfer of water from F to R, swelling and emulsion break-up.

Schlosser and Kossaczky [326] studied a similar pertraction system, using a four-mixer cascade ending with a settler. They studied the effect of various surfactants and other additives on pertraction efficiency and the de-emulsification kinetics in an electrical field. Among the surfactants tested were: SPAN®80, TWEEN®80, the polyamine ECA® and the oxime LIX®64N. The acceptor phase was an aqueous solution of H_3PO_4, the liquid membrane *n*-alkanes. The use of additives modifying the structure of the adsorption film between the emulsion and the donor phase is considered by the authors to favor both the pertraction and the subsequent emulsion break-up.

Takuma Co. (Osaka, Japan) in cooperation with Exxon Research and Engineering Company [327] proposed a liquid membrane technology for ammonia extraction from wastes (night soil) and utilization. It competes with the anaerobic biological denitrification, which imposes a preliminary extra dilution of the treated waters, to reduce the ammonia content below 200 ppm, and addition of methanol. In this case, ammonia is converted to nitrogen and cannot be further utilized. The process permits to extract 90% of the ammonia present in a donor solution at pH 10.2 in less than 20 minutes. An ammonium sulfate solution of 15% final concentration is obtained, which may be applied as a fertilizer.

By combining ELM with steam regeneration, Cahn et al. [328] extracted $(NH_4)_2S$ from waste waters.

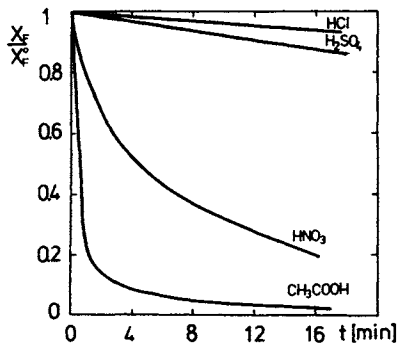

Fig. 7.18. ELM removal of nitric, hydrochloric, sulfuric and acetic acids. Membrane liquid is carbon tetrachloride.

The pertraction of inorganic acids (HNO_3, HCl, H_2SO_4) from aqueous solutions is described [104,329,330]. Boyadzhiev and Bezenshek [331] attempted the separation of the acids mentioned by means of the ELM technique. As a membrane liquid carbon tetrachloride, containing 1 vol.% of TBP as a carrier, is used. As Fig. 7.18 shows, the distribution coefficient of the acid between the organic membrane and water ($m_{HNO_3} = 5 \cdot 10^{-3}$, $m_{H_2SO_4} < 10^{-4}$, $m_{HCl} < 10^{-4}$, respectively) is the factor controlling the rate of acid extraction and separation. In the same figure the removal of acetic acid ($m_{CH_3COOH} = 6.15 \cdot 10^{-2}$), effected within a few minutes, is shown.

Ivakhno et al. [332] compared the results of HNO_3 pertraction obtained in a diffusion cell with supported or unsupported bulk membrane of *n*-decane using two carriers, TBP and TAA. An aqueous suspension of calcium hydroxide is used as the acceptor phase R. They found that TAA yields better results.

Membrane pertraction of HNO_3 using the SLM technique was performed by Danesi et al. [333]. The authors studied the effect of various carriers dissolved in diethylbenzene. According to this study, the most appropriate proved to be the aliphatic amines TLA and Primene®JM-T, followed by TOPO and other mono- or bifunctional organophosphorus carriers.

Special attention was paid to the liquid pertraction of anions, hardly extractable by other methods [259]. The phosphate ion PO_4^{3-} is a typical example. It is extracted from aqueous solutions by means of oil-soluble amines or quaternary ammonium salts. The acceptor phase contains $CaCl_2$ and $Ca(OH)_2$, so that $Ca_3(PO_4)_2$, insoluble in the organic membrane, is obtained. The two steps of the transfer are illustrated by the following chemical reactions:

$$3(R_3N\text{–}HCL) + PO_4^{3-} \longleftrightarrow (R_3NH)_3PO_4 + 3Cl^- \tag{7.31}$$

$$2(R_3N\text{–}H)_3PO_4 + 3CaCl_2 \longleftrightarrow 6(R_3NHCl) + Ca_3(PO_4)_2 \tag{7.32}$$

The final result is the exchange of PO_4^{3-} and Cl^- between the two aqueous phases F and R. The transfer of PO_4^{3-} through liquid membranes containing a selective carrier was also studied by other authors [334,335].

Kataoka et al. [34] studied the mechanism of Cl^- transport through a supported liquid membrane using as a carrier Amberlite®LA-2. They found that the rate of Cl^- transfer from the F to the R solution depends on the NaOH concentration in the acceptor solution R. This fact is related to the slower back-transfer of OH' from R to F.

Boyadzhiev and Bezenshek [336] extracted and concentrated iodine from its synthetic aqueous solutions or brine by means of the LFP method. Besides iodine, the treated brine contained bromine, NaCl, $CaCl_2$ and $MgCl_2$ as well as suspended solid particles. As the organic membrane, a mixture of *n*-paraffins (C_{10}–C_{13}) was used. The acceptor phase was alkalized with a NaOH aqueous solution of Na_2SO_3 and a pH value of 12. The transfer of iodine is due to the fact that iodine molecules, transferred through the organic membrane S into the alkaline acceptor solution R, are converted into ions (I^-) insoluble in S according to the reaction:

$$I_2 + Na_2SO_3 + 2NaOH \longleftrightarrow Na_2SO_4 + 2NaI + H_2O \qquad (7.33)$$

In the experiments with brine, the solids are removed by filtration, then the anion I^- is converted into elemental iodine by the addition of $NaNO_2$ at pH = 2–3. This method allows the decrease of iodine concentration in the donor solution F from 0.034 kg m^{-3} down to 0.0006–0.0008 kg m^{-1}. Simultaneously, a 100-fold accumulation of iodine in the acceptor solution, with no other ions transferred from the feed, is achieved.

7.5.4 Pertraction of Organic Substances

Liquid membranes have a broad potential application for purification of industrial effluents from toxic organic compounds. The donor liquids usually represent dilute aqueous solutions of weak organic acids or bases. When present in an undissociated molecular form, these organic species are relatively soluble in the oil membrane S. Their transport through the membrane is usually based on their concentration gradient across the membrane, maintained by means of an irreversible chemical reaction of the solute with a strong base or a strong acid, respectively, dissolved in the acceptor phase R. The resulting salt is usually a strong electrolyte dissociated into ions, which are insoluble in the oil membrane S. In this way, irrespective of the high salt concentration in the acceptor phase R, the apparent concentration of solute in this liquid is practically zero.

The system most thoroughly studied is aqueous solution of phenol-hydrocarbon(s)-aqueous solution of sodium hydroxide [71,98,122,337,341,353,457–464,468,469]. It results from many branches of industry, e.g., coal coking, oil

refinery, production of synthetic resins, etc., that yield waste waters containing the highly toxic phenol. The concentration of phenol in these waters varies within a broad range, from several ppm or even parts of ppm to several percent. Biochemical dephenolization is known to work well only at low concentrations (below 100–200 ppm), whereas conventional liquid–liquid extraction can be applied in a broader range: from 100 to 10,000 ppm [337]. Liquid–liquid extraction has, however, a severe drawback: the solubility of the used polar organic solvents in the dephenolized raffinate imposes an additional treatment of the latter in order to remove the dissolved solvent. This drawback can be eliminated by using nontoxic organic solvents with very low water solubility, e.g., below 1 ppm. Normal paraffins of nine or more carbon atoms meet this requirement. However, they cannot be used as solvents in liquid–liquid extraction, since the distribution coefficients of phenol between the paraffins and water are far below one. In this particular case, liquid membranes offer a specific advantage over the liquid–liquid extraction processes [139,338].

Many other hydrocarbons or their mixtures of various composition are used as membrane liquids: isoparaffins S100N [80,98,102,337,339], hydraulic and transformer oils, naphtha [340], normal paraffins [272,341–343], mono-*n*-alkylbenzenes [341], silicon oil [343], benzene [396], kerosene [73,90,340,344–347], a mixture of diethyl ether and kerosene [90] and mineral oil [101].

Schlosser and Kossaczky [341] pointed out that the solute flux strongly depends on the distribution coefficient of phenol between the solvent used and the donor liquid. But in the case of the ELM technique, the use of solvents providing higher distribution coefficients does not always help in improving the transfer process. For example, alkylbenzene better dissolves phenol than *n*-paraffins, but the viscosity of the obtained emulsions is about five times higher than that of *n*-paraffin emulsions. As a result, phenol pertraction with alkylbenzene has a lower rate, irrespective of the higher distribution coefficient.

A great number of surfactants are employed for emulsion stabilization. The most often used is sorbitan monooleate (SPAN®80) [73,98,102,122,337,339,341, 344,345], but amine-based surfactants such as ECA® provide better emulsion stability when strong alkaline solutions (pH > 13) are used as acceptor phase. Yu et al. [348] and Zhang et al. [349] developed new surfactants of a succinimide type especially for this process.

The effluents to be treated contain from 100 to 1000 ppm of phenol. In some studies more concentrated donor solutions containing above 2000 ppm of phenol are also used [101,344,349,350]. Cahn and Li [98] claim that phenol in the acceptor phase can be equilibrated with phenol in the treated effluent (F phase) even if its concentration in the R phase exceeds that in the F phase by 10,000 times.

The existing results reveal that the ELM method is quite successful for the dephenolization of waste waters. Provided an appropriate emulsion formula-

tion, phenol concentration in the donor solution can be sharply reduced in a few minutes. For instance, in the studies of Li and Shrier [337], phenol concentration decreased from 1740 ppm to below 10 ppm in 5 minutes, which corresponds to 99.4% recovery. Schlosser and Kossaczky [341], as well as Li [351], obtained similar results for the same pertraction time: 97% and 99.6% recovery, respectively, at an initial phenol content of 1000 ppm. Stirred tank contactors as well as various extraction columns were used [94]. Zhu et al. [352] and Ihm et al. [353] published the results of their studies on water dephenolization with a two-step, mixer-settler cascade. The continuous countercurrent column of Li and Zhang [71] of 120 cm height and 6.2 cm diameter removed 99% of the phenol present in waste waters at an initial concentration of 500 ppm. The height of a theoretical stage is about 160–190 cm [354]. Wang et al. [76] treated phenol-containing waters in a rotating-disc extraction column.

Other pertraction techniques are also applied to remove phenols from dilute aqueous solutions. Their advantage is that no surfactants complicating the process are used. For example, Boyadzhiev compared three different liquid membrane methods to this purpose: ELM, SLM and LFP [338]. All techniques provided successful water dephenolization, the membrane phase consisting of a mixture of *n*-paraffins (C_{10}–C_{13}), irrespective of the relatively low values of the distribution coefficients ($m = 0.10$–0.15). The ELM method offers a much higher mass-transfer coefficient. The alkaline acceptor solution decreases the SLM lifetime. When a concentrated solution of sodium phenolate is desired, LFP is the more appropriate method.

Both the relatively low distribution coefficients and the necessity for processing of phenol-containing waters with strongly alkaline acceptor solution are probably the reason that supported liquid membranes are rarely employed for this purpose [355].

Pertraction processes are suitable for treating phenolic waste waters, which also contain large amounts of chlorides, ammonia and amines [98]. The tentative economic estimation of Cahn and Li confirmed the superiority of the ELM over the classical liquid–liquid extraction with respect to phenol recovery from water at a concentration level of about 1000 ppm. Later, Schlosser and Kossaczky [341] confirmed this assertion following another calculation scheme.

Many studies are devoted to recovery of various phenol derivatives and other organic acids [76,80,459,474–479]. Teramoto et al. [73] separated *o*-, *m*- and *p*-cresol applying the DE technique, the acceptor phase being an aqueous solution of lithium hydroxide. Borwankar et al. [84] studied the pertraction of *o*-chlorophenol, Yu and Zhang [357] 2-, 3- and 4-methylphenol, and Araki et al. [358] nitrophenol with *n*-butanol as a carrier. Wang et al. [76] and Yan et al. [359] performed a successful pertraction of aliphatic and other organic acids. Cahn and Li [98] and Terry et al. [80] recovered acetic acid using a liquid membrane consisting of an isoparaffinic mixture. Boyadzhiev [79] employed a mixture of

carbon tetrachloride and TBP for the same purpose; Nuchnoi et al. [381] separated the aliphatic acids by means of a supported liquid membrane soaked with a mixture of TOPO and kerosene. The pertraction of lactic acid, acetic acid, propionic acid and acrylic acid has drawn the attention of O'Brien [360]; citric acid in fermentation liquids was the transported component in the studies of Boey et al. [361], Basu and Sirkar [480], Friesen et al. [481], Sirman et al. [482]. Ishikawa et al. [30] separated and preconcentrated fumaric acid and L-malic (hydroxysuccinic) acid from acidic aqueous solutions (pH = 2.0) using a 1-decanol supported liquid membrane.

The studies of Kikic et al. [153] on the separation of mixtures of xylene isomers by means of double emulsions and a gaseous acceptor phase (nitrogen) are also of interest.

The transfer processes of various aromatic acids are examined as well, e.g., benzoic acid [89,459,483], amino acids like phenylalanine [362,484,485], ω-aminosulphonic acids [363], optical isomers of the acids like D- and L-phenylglycine [364] and other related compounds [364–369,469,473,486–488,].

Methods were developed for the separation of weak organic bases like aromatic and aliphatic amines from aqueous solutions [98,133,135,357,370,469, 471,472]. The acceptor phase R in this case is a solution of a strong mineral acid, e.g., HCl or H_2SO_4. In this way the amine transported through the membrane is transformed in the acceptor solution into a salt that is not oil-soluble and therefore cannot be back-transported.

It is known that sensitive methods for the analysis of trace quantities of toxic amines in the atmosphere, waste waters and physiological liquids are strongly needed. Audunsson [371,372] successfully applied the SLM technique for analytical purposes, preconcentrating amines from very dilute donor solutions.

Liquid membranes are used also for the selective transfer of electroneutral species like saccharides. The monosaccharides fructose, galactose and glucose were recovered from alkaline donor solutions (pH = 10) and were concentrated in an acidic acceptor solution (pH = 3). The selective transfer of these solutes is effected by means of phenylboric acid dissolved in a solution of TOMAC in dichloroethane. Simultaneously with the transfer of saccharides from the donor to the acceptor solution, an equivalent transfer of chloride ions in the opposite direction takes place [373].

7.5.5 Biotechnological and Medical Applications

Biotechnology and medicine are among the application fields of liquid membranes with the most prospects. There are numerous laboratory studies employing liquid pertraction [83,161,379,489–493]. Yagodin et al [9,374] used liquid membranes to extract toxins from biological liquors. By means of a liquid membrane of paraffin oil stabilized with sorbitan monooleate, they extracted

cholesterol — the main cause for atherosclerosis — from blood. The valuable blood components — proteins, glucose, calcium, inorganic phosphorus compounds, blood cells, etc. — are not transported through the membrane and remain unaltered in the treated blood sample. Yurtov et al. [83] separated cholesterol and aminoacids, e.g., lysine, using the ELM technique. The membrane liquid is vaseline oil and the acceptor solution is a mixture of ethyl alcohol and diethyl ether in a phosphate buffer (an isotonic solution) or a suspension of glucosides in the isotonic solution. The first kind of acceptor solution is appropriate for the separation of lipids, the second for a selective isolation of free cholesterol from aterogenic lipoproteins.

Liquid pertraction has a potential medical application in the case of drug or chemical poisoning. It is known that the poisoning hazards most often encountered are those with salicylates (e.g., Aspirin®) and barbiturates (e.g., Luminal®). Both types of medicines are organic acids, so the acceptor phase capsulated (if the ELM method is considered) contains a strong base. This approach yields promising results: about 95% of the two preparations are isolated and neutralized within five minutes from a medium simulating the stomach liquid [380]. Frankenfeld and Li [161] proposed other reagents — proteins, active carbon and specific medical antibodies — to be encapsulated in the membrane liquid in order to provide for an irreversible binding of the transferred compounds.

Chiang et al. [376] demonstrated a possibility of *in vitro* separation of six different barbiturates, among which are amobarbital and phenobarbital, the donor solution having a pH of 2. Panaggio and Rhodes [377] gave more attention to the theory of liquid membrane transfer of some medical preparations (acetylsalicylic acid, salicylic acid etc.) using as a donor a 0.1 N solution of hydrochloric acid containing the corresponding substance and as an acceptor, an alkaline solution of pH 10.

Majumdar and Stroeve [378] studied the application of SLM technique to curative purposes: removal of local anesthetics as methyl-, ethyl-, 2-ethyl-, butyl-*p*-aminobenzoate etc., from various aqueous donor liquors.

The review of Davies [379] covers the usage of ELM for the therapy of some diseases by applying special treatment with pharmaceuticals. No removal of substances from physiological liquids is aimed in this case, but a controlled release of the drug encapsulated in the oil membrane. The preparation is dissolved in the capsulated liquid and after the emulsion has been swallowed, the medicine slowly penetrates through the membrane liquid into the acceptor medium, which has to be cured. In this way the concentration level of the drug, required to achieve the medicinal effect, is maintained for a long time. Results of animal treating *in vivo* with insulin, with the antitumorous preparation, Bleomycin®, with anticancerogenic and with antinarcotic substances are published. Recently, much of information has appeared in specific medical lit-

erature concerning this new approach in medicinal treatment known as "controlled release".

Li and Asher [161, 380] proposed a liquid membrane device for artificial oxidation of blood, as required, for example e.g. in surgical intervention. Halwachs and Schugerl [163] called this device an "artificial lung". It aims to enrich blood with oxygen and to remove carbon dioxide without harming blood proteins and cells, as conventional blood oxygenators do. The principal schemes of the liquid-membrane oxygenators are shown in Fig. 7.19. In the first case (Fig. 7.19a) a SLM method is used. Liquid fluorocarbons, indifferent to blood, transport oxygen to venous blood and simultaneously remove carbon dioxide. In the second case the oxygen is capsulated in liquid fluorocarbons using an emulsifier and the single-drop technique. Oxygen dissolves in the membrane and diffuses through it into the blood. Carbon dioxide is transferred in the opposite direction and is removed from the system. The liquid-membrane oxygenators are successfully tested both *in vitro* and *in vivo* on dogs.

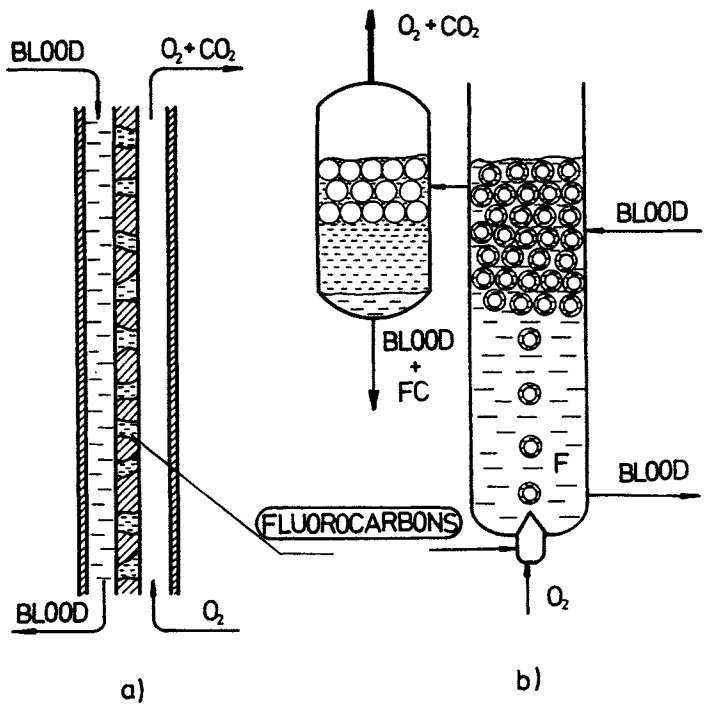

Fig. 7.19. Blood oxygenators. (a) SLM concept. Oxygen and carbon dioxide are counter-transported across a porous impregnated with liquid fluorocarbons solid membrane. (b) Single-drop technique. Oxygen bubbles, enveloped with liquid fluorocarbon films, enrich the surrounding medium in oxygen and remove the carbon dioxide. Bubbles are collapsed in the second apparatus and the gas and the liquid mixtures are separated.

Recently, a series of biotechnological studies using liquid membranes were published. The term "pertractive fermentation", a combination of fermentation and of liquid pertraction, was introduced. Nuchnoi et al. [381] combined the acidogenic fermentation with the selective transfer of some of the products through a supported liquid membrane. In this way the products inhibiting the fermentation process or reducing the efficiency of microorganisms are continuously removed. The membrane is a thin, porous support of polytetrafluorethylene impregnated with a solution of TOPO in kerosene. The donor solution F, which is the fermentation medium (broth), circulates on one side of the membrane. On the other side is the acceptor solution containing NaOH. The metabolic products like acetic acid and butyric acid are selectively removed from the fermentation medium and are irreversibly bound in the acceptor solution. The total yield of volatile aliphatic acids from this fermentation system is about five times higher than that from conventional acidogenic fermentation.

Del Cerro and Boey [382] separated citric acid from fermentation broth applying the emulsion liquid membrane technique. The membrane contains 5 vol.% of ALAMINE®336. The acceptor phase is an aqueous solution of sodium carbonate.

Marchese et al. [383] isolated benzylpenicilline from cultural solutions using the SLM method. The antibiotic is transferred through the organic membrane as an ionic couple with a tetrabutylammonium cation. Yamaguchi et al. [364] studied the separation of optical isomers of aminoacids with supported liquid membranes. They separated D- and L-glycine with a membrane phase containing crown ethers as selective carriers for the second isomer. A macrocyclic carrier of this type, dibenzo-18-crown-6 (DB18C6), was used also by Sugiura and Yamaguchi [384] for separation of the L-leucine and L-tryptophan esters applying the SLM method.

7.5.5.1 Special Case: Liquid–Membrane Enzyme Reactors

A special case of selective removal of substances, mainly toxins from physiologic liquids, is the use of enzymes in the acceptor liquid R. The ELM method represents an alternative technique to the enzymes immobilization in a gel matrix or to their covalent bonding to inert supports [493,495]. Frankenfeld and Li [161] listed several advantages of liquid membrane techniques over those formerly used: cofactors can be included without taking any special measures; multienzyme systems can be applied; and the enzymes encapsulated in the organic membrane are protected against deactivation by substances not transferred and remaining in the donor solution or physiological liquid. Artificial detoxification of blood using pertraction takes place in the same way as the living organism eliminates the lipophilic metabolites and helps in the self-regeneration of the liver [385].

May and Li [6] encapsulated purified phenolase in the emulsified acceptor liquid. The phenols, dissolved in the outer donor phase, diffuse through a hydrocarbon membrane and are oxidized by the enzyme present in the acceptor liquid. The oxidized products cannot diffuse back to the outer physiologic solution F. The authors assert that after 90 minutes of contact time only a small part (about 20%) of the enzymes diffuse through the membrane into the outer solution F. There are also other studies on the usage of encapsulated enzymes for separation of toxic phenolic derivatives from blood or blood plasma [7,122, 386]. Volkel et al. [385] encapsulated the enzyme uridine diphosphoglucoronyl transferase (UDPGT) and the cofactor uridine diphosphoglucoronic acid (UDPGA). The liquid membrane consists in this case of *n*-paraffins, *n*-dodecanol and lecithin. Unlike SPAN-80, the most often used emulsifier, lecithin does not deactivate the enzyme. Lecithin yields water soluble products, which can be removed by the excretory system of the organism.

Asher et al. [356,387] proposed that liquid membranes be applied for uremia treatment: urea is hydrolysed by urease capsulated in the emulsion. After three hours of contact time, the urea concentration decreases from 2000 to 600 mg l^{-1}. The hydrolysis of urea yields ammonia and carbon dioxide. The latter can be easily removed by the respiratory system, whereas ammonia can accumulate to a toxic level if no artificial removal is undertaken. In order to "catch" ammonia, the authors developed a liquid membrane system adding tartaric acid in the acceptor liquid. Thus, ammonia is transformed in an ammonium cation (NH_4^+), which is insoluble in the oil membrane. Tartaric acid is preferred to sulfuric acid since the former is biodegraded. In this way ammonia concentration is reduced from 10 to 2 mg l^{-1}. The stability of the liquid membrane emulsion is tested on rats and on dogs both *in vitro* and *in vivo* [388]. It should be stressed, however, that a higher rate of toxin removal is required for a potential clinical usage; for a daily removal of 12 g of urea, a stoichiometric amount of 112 g of emulsion is needed.

Urea removal through the gastrointestinal tract can be a valuable complement to chemodialysis. In this way, urea concentration in blood can be maintained at a harmless level for a longer time, thus relieving crisis states and prolonging the intervals between chemodialysis procedures. The enzyme degradation of urea is studied by other authors as well [389].

Chronic uremia leads to the accumulation not only of urea in the organism, but also of creatine, uric acid, phosphates, etc. Maugh [380], Frankenfeld and Li [161], Trouve et al. [389] proposed pertraction systems for the removal of these substances.

Purified enzymes, bacterial homogenates and whole cells of *Micrococcus denitrificans* are used for the selective removal of nitrates and nitrites by means of liquid membranes [8]. Nitrates and nitrites are transferred through the organic membrane liquid by means of various amine carriers. The most efficient

proved to be the secondary amine AMBERLITE®LA-2 [259]. Applying the ELM technique, the whole amount of nitrates and 90% of the nitrites are reduced, the cells remaining intact and active for about five days. Nitrites are the intermediate product of nitrate reduction and the final product is nitrogen. The conversion of nitrates and nitrites by avoiding ammonia formation, affected by means of liquid membranes, is a prospective way of purifying solutions from these nitrogen compounds and, what is more, strong enzyme inhibitors like $HgCl_2$ cannot affect the cells encapsulated in the acceptor liquid.

Enzyme liquid membrane reactors may be applied not only to the simplest type of bioconversion — hydrolysis, which requires only one enzyme dissolved in water — but also to more complex syntheses and transformations of biologically active natural products, e.g., racemate separation, synthesis of amino-acids, etc. [390].

To achieve the synthesis of L-leucine from α-ketoisocaproate, Makryaleas et al. [391] encapsulated three substances in the emulsion phase: L-leucine dehydrogenase (LEUDH), the cofactor reduced nicotinamid-adenine-dinucleotide (NAD-H) and the regenerating enzyme formate dehydrogenase (FDH). The substrata α-ketoisocaproate and ammonium formate are transferred by the selective carrier ADOGEN®464 from the donor solution F through the liquid membrane containing *n*-paraffins and SPAN®80. The same carrier transfers back to the donor solution F the reaction products obtained in the acceptor phase R: L-leucine and carbonic acid. With an enzyme concentration of 30 units ml^{-1}, 84% of the substrata are converted to L-leucine for 105 minutes. L-alanine is obtained in a similar way from D-and L-lactate [392].

Penicillin G, produced by fermentation, is converted into 6-aminopenicillanic acid (6-APA) in a continuous liquid–membrane reactor 2.5 m height and with a volume of 10.5 l [390]. Penicillin is transferred through the kerosene membrane into the acceptor phase by the AMBERLITE®LA-2 carrier. The enzyme penicillin-G-acylase, present in the acceptor solution, converts the substratum (penicillin G) to phenylacetic acid and 6-APA. The latter is a source substance for the production of acid-resistant and stable penicillin-type antibiotics. In this way, extraction of penicillin G from the fermentation broth, enzyme reaction and accumulation of the desired product in the acceptor phase simultaneously take place. For the practical application of enzyme liquid–membrane reactors, however, further improvements of the integrated operations involved are still required.

7.5.6 Process Economics and Industrial Application of Liquid Pertraction

Liquid pertraction is generally considered one of the cheapest separation methods. Being a membrane operation, the separation does not involve phase transitions. Consequently, the power consumption is only a small part of the

total expenses even in the case of the ELM method. Unlike other membrane processes, however, there is a loss of membrane liquid and, therefore, the treated solution in many cases should be purified from this liquid. As a result, the total cost of the separation rises. On the other hand, the liquid membranes in some pertraction techniques are not too delicate so that some procedures for solution pretreatment, typical for other membrane processes, may be omitted.

Most of the available economic information concerns processes, employing SLM and ELM operations. However, this rather scarce information, based on laboratory or pilot tests, should be regarded only as tentative.

One of the first economic estimations considering the application of supported liquid membranes in copper hydrometallurgy [24] pointed out that this operation is considerably cheaper than the solvent extraction process used for the same purpose. The capital costs are reduced with a factor of two, the maintenance costs are reduced even further. The main advantage, however, exists in the fact that there are practically no losses of extractant caused by drop entrainment, whereas, for example, in conventional copper extraction process, these are found to be about 10–15 US cents per kg copper, thus constituting 40–59% of the annual operation costs of the extraction equipment. These data should be considered with some reservations since the authors cited underestimate the cost of the porous supports and assume an unrealistic (five years) membrane lifetime.

It was shown in the detailed study of Pearson [26] that the question of how much supported liquid membranes are more profitable for removing copper and chromium from waste waters, compared to solvent extraction or ion exchange, cannot be explicitly answered due to the relatively high price of polypropylene porous supports and to the lack of an efficient method of membrane regeneration. This study, as well as the later one of Flett and Pearson [42], reveals that in the case of recovery of more valuable metals like chromium and nickel, the value of the final product — chromic acid or nickel sulfate, respectively — exceeds the production costs. Their calculations relate to the case of 4000 m^3 waste waters per year, containing approximately 1 g l^{-1} of chromium or nickel.

Supported liquid membranes become unprofitable when strongly diluted solutions (below 100 ppm) are to be treated. Therefore, this pertraction technique is not appropriate for removal of traces of toxic or valuable metals from waste waters [93].

Data about the economics of a process for zinc recovery from waste waters applying the ELM technique are provided by Yu et al. [393]. The material operational costs for the purification of 1 m^3 of water, containing 1 g l^{-1} of zinc, are assessed at 1.57 yuans (1 yuan = 21 US cents). The essential part (64%) of the costs can be attributed to hydrochloric acid, used as acceptor solution, to sodium hydroxide used for the neutralization of the donor solution to pH 2

(18%) and to the extractant HDEHP (13%). The energy expenses are relatively low at 14%. No mention is made of labor costs, overheads or capital investments. According to the authors, treatment of solutions containing above 150–200 ppm of zinc is still economically profitable, provided the concentrated solution of $ZnCl_2$ is reused.

Similar are the data published by Draxler et al. [78]. According to them, the operational costs for producing 1 kg of zinc (as a concentrated solution of $ZnSO_4$) amount to 52 US cents. In this case, the initial metal content in the donor solution was 0.5 g l^{-1}, the acceptor was a sulfuric acid solution of 250 g l^{-1} and the carrier was D2EHDTPA. The data are a result of a one-year test on a pilot plant with 1 m^3 h^{-1} capacity. They are later confirmed on a full-scale plant designed to treat 75 m^3 h^{-1} waste waters.

The ELM technique, which proved particularly efficient for the selective recovery of zinc from waste waters of rayon production, manifests superior economic parameters, compared to other processes used for this purpose such as precipitation with H_2S and $Ca(OH)_2$, ion exchange or liquid–liquid extraction [78,394].

There are also studies dealing with the economic comparison of the various pertraction techniques. According to Ivakhno et al. [395], which compared the costs of waste water purification from aromatic amines, the bulk pertraction methods, especially these of the LFP group, are 1.5 times cheaper than the ELM and more than three times cheaper than the corresponding SLM processes. The calculations refer to a price of the porous polymer supports of 50 US \$/m^2 having a lifetime of 4000 h and to equal extractant (carrier) losses for all pertraction techniques. It should be mentioned, however, that both the price and the lifetime of the supports in this study exceed the values provided by other sources. Besides, pertraction techniques with phase dispersion always show much higher losses of the membrane liquid.

7.6 CONCLUSION

The numerous theoretical and experimental studies, as well as the economic tests, support liquid membrane techniques as very prospective separation operations. The pertraction systems, functioning as highly efficient chemical "pumps" selectively separating and concentrating substances, can be applied in a number of industrial branches, e.g., hydrometallurgy, chemical and pharmaceutical industries, galvanic technologies, etc. One of the most attractive application fields is biotechnology. On the basis of described pertraction techniques, various processes for selective extraction of valuable components from cultural solutions and highly efficient enzyme reactors–separators can be created. Liquid–membrane processes have vast potential applications for environ-

mental purposes as well. The use of an electrochemical or photochemical driving force of the transmembrane process is also of special interest.

On the other side, the study of pertraction processes yields a lot of information about the nature and mechanism of transport phenomena taking place in physiological systems.

Although liquid membrane processes are still in the research or development stage, they hold a deserving position in the large family of membrane separation processes due to their indisputable advantages over conventional separation operations.

LIST OF SYMBOLS AND ABBREVIATIONS USED

Symbols

a	interfacial area
D	diffusivity
f	facilitation factor
J	interfacial flux of species
k	mass transfer coefficient
k_f	rate constant of forward reaction
k_r	rate constant of reverse reaction
m	distribution coefficient
t	time
u	linear velocity
V	volume
x	concentration of solute
y	carrier concentration
z	concentration of hydrogen ions
δ	membrane thickness
Sh	Sherwood number $k_F \cdot d/D$

A	denotes the transfered solute
B	denotes the reagent in the stripping phase
F	denotes the feed (donor) solution
R	denotes the stripping (acceptor) solution
S	denotes the liquid membrane

Pertraction methods

BLM	bulk liquid membranes
CLM	contained liquid membranes

DEM	double emulsion method
ELM	emulsion (surfactant) liquid membrane
FLM	flowing liquid membranes
LFP	liquid film pertraction
SLM	supported liquid membrane

Carriers and solvents

D2EHPA	di(2-ethyl-hexyl)phosphoric acid
DBBT	1,1-di-*n*-butyl-3-benzoyl-thiourea
DB18C6	dibenzo-18-crown-6 (2,3,11,12-dibenzo-1,4,7,10,13,16-hexa-oxacyclooctadeca-2,11-diene)
DC18C6	dicyclo-18-crown-6
DIDPA	diisodecylphosphoric acid
DTPA or D2EHDTPA	bis(2-ethylhexyl) dithiophosphoric acid
EDTA	ethylendiaminetetraacetic acid
TAA	trialkylamine
TBAH	tributyl aceto hydroxamic acid
TBP	tri-*n*-butylphosphate
TIOA	tri-iso-octylamine
TLAHCl	trilaurylammonium chloride
TOA	tri-*n*-octylamine
TOPO	tri-*n*-octylphosphine oxide

Carriers and solvents (trade names)

ACORGA®	5-nonylsalicylaldoxime + nonylphenol (ICI)
Adogen®464	tri-alkylmethylammonium chloride (Shering)
Alamine®336	tri-octyl amine (Henkel)
Aliquat® 336	methyl-tri-octylammonium chloride (Henkel)
Amberlite®LA2	*N*-lauryl-1,1,3,3,5-hexamethyl-hexyl amine (Rohm & Haas)
CYANEX®272	bis(2,4,4-trimethylpentyl) phosphinic acid (Cyanamid)
KELEX®100	7-dodecenyl-8-hydroxyquinoline (Shering)
LIX®34	*n*-8-quinolyl-*p*-dodecylbenzenesulfonamide
LIX®54	phenyl-alkyl-β-diketone (Henkel)
LIX®64N	mixture of two oxime compounds LIX®63 and LIX® 65N (Henkel)
LIX®65N	2-hydroxy-5-nonylbenzophen oxime (Henkel)
LIX®70	5,8-diethyl-7-hydroxy-6-dodecanone oxime + 3-chloro-5-nonane-2-hydroxyphenone oxime
S 100N®	isoparaffinic neutral oil (Exxon)
SME®529	2-hydroxy-5-nonylacetophenone oxime (Shell)

REFERENCES

1 Schlosser, S. and Kossaczky, E. (1975). Procs. 5th Int. Congress CHISA'75, Pertraction through liquid membrane. Prague, Czechoslovakia, I 3.12.
2 Li, N.N. (1971). *Ind. Eng. Chem. (Proc. Des. Devel.)*, 10: 215.
3 Li, N.N. (1971). *AIChE J.*, 17: 459.
4 Casamatta, G., Boyadzhiev, L. and Angelino H. (1974). *Chem. Eng. Sci.*, 29: 2005.
5 Casamatta, G., Angelino, H. and Boyadzhiev L. (1977). *Teor. Osn. Khim. Technol.*, 11: 825.
6 May, S. and Li, N.N. (1974). *Enzyme Engineering* (E.K. Pye and L.B. Wingrad, eds.), Plenum Press, New York, 2, p. 77.
7 Poppe, W., Halwachs, W. and Schuegerl, K. (1984). *Chem. Ing. Techn.*, 56: 70.
8 Mohan, R. and Li, N.N. (1974). *Biotech. Bioeng.*, 16: 513.
9 Yagodin, G., Lopukhin, Y., Yurtov, E., Gusseva, T. and Sergienko, V. (1983). Extraction of cholesterol from blood using liquid membrane. Procs. ISEC'83, Denver, Colorado, Pharmaceutical and Biological Extraction Processes, I, pp. 385–386.
10 Ohki, A., Takeda, T., Takagi, M. and Ueno, K. (1983). *J. Membr. Sci.*, 15: 231.
11 Noble, R.D. and Way, J.D., (1987). *Liquid Membranes. Theory and Applications* (R. Noble and J.D. Way, eds.) ACS Symposium Series No. 347, ACS, Washington, DC, p. 1.
12 Reusch, C.F. and Cussler, E.L. (1973). *AIChE J.*, 19: 736.
13 Strzelbicki, J. and Bartsch, R.A. (1982). *J. Membr.Sci.*, 10: 35.
14 Izatt, R.M., McBride, D.W., Brown, P.R., Lamb, J.D. and Christensen, J.J. (1986). *J. Membr. Sci.*, 28: 69.
15 Bacon E. and Jung, L. (1985). *J. Membr. Sci.*, 24: 185.
16 Melzner D., Tilkowski, J., Mohrmann, A., Poppe, W., Halwachs, W. and Schuegerl, K. (1984). *Hydrometallurgy*, 13: 105.
17 Christensen J.J., Lamb, J.D., Brown, P.R., Oscarson, J.L. and Izatt, R.M. (1981). *Sep. Sci.Technol.*, 16: 1193.
18 Brown P.R., Izatt, R.M., Christensen, J.J. and Lamb, J.D. (1983). *J. Membr. Sci.*, 13: 85.
19 Burgard, M., Elisoamiadana, P. and Leroy, M.J.F. (1983). Liquid Membrane studies: Transport against the concentration gradient of $AuCl_4^-$. Procs. ISEC'83, Denver, Colorado, Solid-Supported Liquid Membranes, II, pp. 399–400.
20 Rosano, H.L., Schulman, J.H. and Weisbuch, J.B. (1961). *Ann. N.Y. Acad. Sci.*, 92: 457.
21 Moore, J.H. and Schlechter, R.S. (1973). *AIChE J.*, 19: 741.
22 Vorob'ev, A.V., Krykin, M.A., Popkov, Yu.M. and Timashev, S.F. (1985). *Teor. Osn. Khim. Tekhnol.*, 19: 544.
23 Cussler E.L. (1971). *AIChE J.*, 17: 1300.
24 Baker, R.W., Tuttle, M.E., Kelly, D.J. and Lonsdale, H.K. (1977). *J. Membr. Sci.*, 2: 213.
25 Danesi, P.R., Horwitz, E.P., Vandegrift, G.F. and Chiarizia, R. (1981). *Separ. Sci. Technol.*, 16: 201.
26 Pearson, D. (1983). *Ion Exchange Membranes* (D.S. Flett, ed.). Ellis Horwood, Publ., London, p. 55.
27 Nakashio, F. (1984). *Kemikaru Enjiniyaru*, 29: 58.
28 Zhang, X., Meregalli, L. and Guerriero, R. (1985). *J. Nonferrous Metals*, 37: 64.
29 Loiacono, O. and Drioli, E. (1985). *Chim. Oggi*, No 7/8:11.
30 Ishikawa, H., Murakami, T., Hata, M. and Hikita, H. (1985). *Chem. Eng. Comm.*, 34: 123.
31 Akiba, K. and Hashimoto, H. (1985), *Talanta*, 32, 8B: 824.
32 Harada, M., Yamazaki, F., Adachi, M. and Eguchi, W., (1983). Enrichment and Separation of Metals by Liquid Membrane with Tri-*n*-Octylamine. Procs. ISEC'83, Denver,

Colorado, Solid-Supported Liquid Membranes, I, pp. 376–377.
33 Chiarizia, R. and Castagnola, A. (1983). *J. Membr. Sci.*, 14: 1.
34 Kataoka, T., Nishiki, T., Tamura, Y. and Ueyama, K. (1980). *J. Chem. Eng. Jpn.*, 13 (1): 35.
35 Kataoka, T., Nishiki, T. and Ueyama, K. (1982). *Bull. Chem. Soc. Jpn.*, 55 (4): 1306.
36 Komasawa, I., Otake, T. and Yamashita, T. (1983). *Ind. Eng. Chem. (Fund.)*, 22 (1): 127.
37 Danesi, P.R., Horwitz, E.P. and Rickert, P. (1982). *Sep. Sci. Technol.*, 17, 9: 1183.
38 Danesi, P.R., Chiarizia, R. and Castagnola, A. (1983). *J. Membr. Sci.*, 14 (2): 161.
39 Takagi, M., Ohki, A. and Ueno, K. (1983). A Liquid Membrane Separation of Ionic Species Using a Redox Reaction as a Driving Potential. Procs. ISEC'83 Denver, Colorado, pp. 60–61.
40 Gasparini, G.M., Grossi, G.G., Casarci, M. and D'Andrea, A. (1983). The Recovery of Plutonium by Means of Solid Supported Liquid Membrane. Procs. ISEC'83, Denver, Colorado, Solid-Supported Liquid Membranes, II, pp. 395–396.
41 Danesi, P.R. and Cianeti, C. (1984). *J. Membr. Sci.*, 20 (2): 215.
42 Flett, D. and Pearson, D. (1985). Role of Hollow Fibre Supported Liquid Membranes in Hydrometallurgy. Procs. Extraction Metallurgy '85, Institution of Mining and Metallurgy, London, p. 1.
43 Lee, K.H., Evans, D.F. and Cussler, E.L. (1978). *AIChE J.*, 24, 5: 860.
44 Teramoto, M. and Tanimoto, H. (1983). *Sep. Sci. Technol.*, 18, 10: 871.
45 Takahashi, K. and Takeuchi, H., (1985). *J. Chem. Eng. Jpn.*, 18, 3: 205.
46 Danesi, P.R., Reichley-Yinger, L. and Rickert, P.G. (1987). *J. Membr. Sci.*, 31, 2–3: 117.
47 Fabiani, C., Merigiola, M., Scibona, G. and Castagnola, A.M. (1987). *J. Membr. Sci.*, 30: 97.
48 Neplenbroek, A.M., Bargaman, D. and Smolders, C.A. (1988). SLM — Degradation by Emulsion Formation. Procs. ISEC'88, Moscow, 3, pp. 61–63.
49 Fujinawa, K., Akiyama, M., Akiba, I., Adachi, H., Shono, A., Imaishi, N. and Hozawa, M. (1989). *Kagaku Kogaku Ronbunshu*, 15 (1): 159.
50 Takeuchi, H. and Nakano M. (1989). *J. Membr. Sci.*, 42 (1/2): 183.
51 Danesi, P.R. and Rickert, P.G. (1986). *Solv. Extr. Ion. Exch.*, 4 (1): 149.
52 Tanigaki, M., Ueda, M. and Eguchi, W. (1988). *Sep. Sci. Technol.*, 23 (10/11): 1161.
53 Teramoto, M., Matsuyama, H., Takaya, H. and Asano, S. (1987). *Sep. Sci. Technol.*, 22: 2175.
54 Teramoto, M., Matsuyama, H., Takaya, H., Yonehara, T. and Miyake,Y. (1988). Separation of Benzene from Cyclohexane by Flowing Liquid Membrane and Removal of Heavy Metal Ions by Spiral-Type Flowing Liquid Membrane Module. Procs. of ISEC'88, Moscow, 3, pp. 110–113.
55 Igawa, M., Saitou, K., Monoe, F., Nishida, K., Tanaka M. and Yamabe, T. (1985). *Nippon Kagaku Kaishi*, 5: 825.
56 Sengupta, A., Basu, R., Prasad, R. and Sirkar, K. (1988). *Sep. Sci. Technol.*, 23 (12/13): 1735.
57 Sengupta, A., Basu R. and Sirkar, K. (1988). *AIChE J.*, 34 (10): 1698.
58 Boyadzhiev, L., Lazarova, Z. and Bezenshek, E. (1983). Mass Transfer in Three-Liquid Phase Systems. Procs. ISEC'83, Denver, Colorado, p. 391.
59 Schlosser, S., Kossazky, E. and Porubensky, V. (1984). Pertraction of Ammonia. Procs. CHISA'84, Prague, Czechoslovakia, Separation Processes, 2.
60 Boyadzhiev, L. (1984). *Isotopenpraxis*, 20 (9): 345.
61 Martin, T.P. and Davies, G.A. (1977). *Hydrometallurgy*, 2 (4): 315.
62 Alessi, P., Canepa, B. and Kikic, I. (1979). *Can. J. Chem. Eng.*, 57 (1): 54.
63 Marr, R. and Kopp, A. (1980). *Chem. Ing. Techn.*, 52 (5): 399.
64 Schlosser, S. and Kossaczky, E. (1978). Comparison of Pertraction through Liquid Mem-

brane and Liquid–Liquid Extraction. Procs. CHISA'78, Prague, Czechoslovakia.
65 Zhang R., (1984). *Separation Techniques by Liquid Membranes*, Jiangxi Renmin Publ., Nanchang.
66 Schuegerl, K., Mohrmann, A., Gutknecht, W. and Hauertmann, H. (1985). *Desalination*, 53: 197.
67 Kato, S. and Kawasaki, J. (1987). *J. Chem. Eng. Jpn.*, 20: 140.
68 Marr, R., Bart, H. and Siebenhofer, M. (1980). A New Concept for Mass Transfer in Liquid Surfactant Membranes. Procs. ISEC'80, Lion.
69 Marr, R., Bart, H. and Bouvier, A. (1981). *Industrie Anzeiger*, 28: 16.
70 Casamatta, G., Bouchez, D. and Angelino, H. (1978). *Chem. Eng. Sci.*, 33: 145.
71 Li, X. and Zhang, Y. (1981). *Mo Fenli Kexue Yu Jishu*, 1, 21(1981).
72 Melzner, D., Mohrmann, A., Poppe, W., Halwachs, W. and Schuegerl, K. (1982). Continuous Extraction of Metals with Liquid Membrane Emulsions in a Kueni Extractor. Procs. 3rd Chem. Eng. Conf., Graz, pp. 358–366.
73 Teramoto, M., Sakai, T., Yanagawa, K. and Miyake Y. (1983). *Sep. Sci. Technol.*, 18: 985.
74 Goswami, A.N., Rawat, B.S. and Krishna, R. (1985). *J. Membr. Sci.*, 25 (1): 101.
75 Jeong, Y., Ihm, S. and Won, Y. (1987). *J. Membr. Sci.*, 32: 47.
76 Wang, J., Wang, B., Cui, Z., Sun, Y., Liu, Z. and Guen, J. (1988). *Shuichuli Jishu*, 14 (2): 69.
77 Colinart, P., Delepine, S., Trouve, G. and Renon, H. (1984). *J. Membr. Sci.*, 20: 167.
78 Draxler, J., Furst, W. and Marr, R. (1988). *J. Membr. Sci.* 38: 281.
79 Boyadzhiev, L., Sapundzhiev, T. and Bezenshek, E. (1977). *Sep. Sci.*, 12: 541.
80 Terry, R.E., Li, N.N. and Ho, W.S. (1982). *J. Membr. Sci.*, 10: 305.
81 Way, J.D., Noble, R.D., Flynn, T.M. and Sloan, E.D. (1982). *J. Membr. Sci.*, 12: 239.
82 Lorbach, D. and Marr, R. (1987). *Chem. Eng. Process.*, 21: 83.
83 Yurtov E.V., Korolyova, Golubkov, A.S. and Grigoriev, V.B. (1988). *Dokl. AN SSSR*, 302 (5): 1164
84 Borwankar R.P., Chan, C.C., Wasan, D.T., Kurzeja, R.M., Gu, Z.M. and Li, N.N. (1988). *AIChE J.*, 34 (5): 53.
85 Draxler, J. and Marr, R. (1986). *Chem. Eng. Process.*, 20: 319.
86 Stelmaszek, J. and Borkowska, B. (1975). *Inzynieria Chemiczna*, 5, 4: 869.
87 Alessi, P., Canepa, B., Costa, P. and Kicic, I. (1979). *Riv. Combust.*, 33: 189.
88 Boyadzhiev, L. and Kyuchoukov, G. (1978). Further Development of Carrier Mediated Extraction. Procs. CHISA'78, Prague, Czechslovakia.
89 Boyadzhiev, L. and Kyuchoukov, G. (1980). *J. Membr. Sci.*, 6: 107.
90 Mitrovic, M. and Qiulin, W. (1982). Carrier Mediated Extraction in a Mixer-Dual Filter System. Procs. 3rd CEC'82, Graz, pp. 367–372.
91 Schneider, K. and Rintelen, T.H. (1986). *Chem. Ing. Techn.*, 58, 10:800.
92 Nakano, M., Takahashi, K. and Takeushi, H. (1987). *J. Chem. Eng. Jpn.*, 20, 3: 326.
93 Schulz, G. (1988). *Desalination*, 68: 191.
94 Gladek, L., Stelmaszek, J. and Szust, J. (1981). *Recent Devel. Separ. Sci.*, 6: 29.
95 Kremesec, V.J. (1981). *Sep. Purif. Methods*, 10: 117.
96 Kremesec, V.J. and Slattery, J.C. (1982). *AIChE J.*, 28, 3: 492.
97 Stelmaszek, J. (1977). *J. Membr. Sci.*, 2, 197.
98 Cahn, R.P. and Li, N.N. (1974). *Sep. Sci.*, 9, 6: 505.
99 Hatton, T.A., Lightfoot, E.N., Cahn, R.P. and Li, N.N. (1983). *Ind. Eng. Chem. (Fund.)*, 22: 27.
100 Ho, W.S., Hatton, T.A., Lightfoot, E.N. and Li, N.N. (1982). *AIChE* J., 28, 4: 662.
101 Kim, K., Choi, S. and Ihm, S. (1983). *Ind. Eng. Chem. (Fund.)*, 22: 167.

102 Matulevicius, E. and Li, N. (1975). *Sep. Purif. Methods*, 4, 1: 73.
103 Hochhauser, A. and Cussler, E. (1975). *AIChE Symp. Ser.*, 71, 152: 136.
104 Kopp, A., Marr, R. and Moser, F. (1978). *Inst. J. Chem. Eng. Symp. Ser.*, 54: 279.
105 Kopp, A., Marr, R. and Moser, F. (1978). Liquid Membranes with Pump — A Classification of Emulsion Behavior and Consequences for Theories. Procs. CHISA'78, Prague, Czechoslovakia.
106 Nakashio, F. and Kondo, K. (1980). *Sep. Sci. Technol.*, 15, 4: 1171.
107 Voelkel, W., Halwachs, W. and Schuegerl, K. (1980). *J. Membr. Sci.*, 6: 19.
108 Wankat P.C. and Noble, R.D. (1984). *Ind. Eng. Chem. (Fund.)*, 23: 137.
109 Kondo, K., Kita, K., Koida, I., Irie, J., Otake, T. and Yamashita, T. (1979). *J. Chem. Eng. Jpn.*, 12: 203.
110 Goddard, J., Schultz, J. and Suchdeo, S. (1974). *AIChE J.*, 20, 4: 625.
111 Goddard, J. (1977). *Chem. Eng. Sci.*, 22: 487. (1977)
112 Schulz, G., Goddard, J. and Suchdeo, S. (1974). *AIChE J.*, 3, 20: 417.
113 Goddard, J., Schultz, J. and Basset, R., (1970). *Chem. Eng. Sci.*, 25, 5: 665.
114 Smith, K., Meldon, J. and Colton, C. (1973). *AIChE J.* 19, 1: 102.
115 Stroeve, P. and Varanasi, P. (1982). *Sep. Purif. Methods*, 11: 29.
116 Suchdeo, S. and Schultz, J. (1974). *Chem. Eng. Sci.*, 29: 13.
117 Chaudry, M., Noor ul Islam, Mohammad, D. (1987). *Nucleus* (Karachi), 23: 7.
118 Smith, D.R. and Quinn, J.A. (1979). *AIChE J..*, 25: 197.
119 Hoofd, L. and Kreuzer, F. (1979). *J. Math. Biol.*, 8: 1.
120 Babcock, W., Baker, R., Lachapelle, E. and Smith, K. (1980). *J. Membr. Sci.*, 7: 71.
121 Noble, R., Way, J. and Powers, L. (1986). *Ind. Eng. Chem. (Fund.)*, 25: 452.
122 Halwachs, W., Flaschel, E. and Schuegerl, K. (1980). *J. Membr. Sci.*, 6: 33.
123 Gladek, L., Stelmaszek, J. and Szust J. (1982). *J. Membr. Sci.*, 12: 153.
124 Teramoto M., Takihana, H., Shibutani, M., Yuasa T., Hara, N. (1983). *Sep. Sci. Technol.*, 18: 397.
125 Noble, R. (1983). *Ind. Eng. Chem. Fund.*, 22: 139.
126 Stroeve, P. and Varanasi, P. (1984). *AIChE J.*, 30: 1007.
127 Draxler, J. and Marr, R. (1983). *Chem. Ind.*, 106:698.
128 Marr, R., Kopp, A. and Wilhelmer, J. (1979). *Ber. Bunsenges. Phys. Chem.*, 83: 1097.
129 Fales, J. and Stroeve, P. (1984). *J. Membr. Sci.*, 21:35.
130 Hatton, T. and Wardius, D. (1984). *AIChE J.*, 30: 934.
131 Park, H., Yoo, J., Suh, I., Han, P., Kang W., Burgard, M. and Leroy M. (1983). Analytical and Experimental Studies of Mass Transport through Liquid Membranes. Procs. ISEC' 83, Denver, Colorado, pp. 288–289.
132 Kim, J. and Stroeve, P. (1989). *J. Membr. Sci.*, 45: 99.
133 Teramoto, M., Takihana, H., Shibutani, M., Yuasa, T., Miyake, Y. and Teranishi, H. (1981). *J. Chem. Eng. Jpn.*, 14, 2: 122.
134 Bunge, A.L. and Noble, R.D., (1984). *J. Membr. Sci.*, 21: 55.
135 Baird, R.S., Bunge, A.L. and Noble, R.D. (1987). *AIChE J.*, 33, 1: 43.
136 Wardius, D., Hatton T. (1985)., *Chem. Eng. Comm.*, 37:159.
137 Yagodin, G. and Ivakno, S. (1986). *Teor. Osnov. Khim. Technol.*, 20: 291.
138 Reed, D., Bunge, A. and Noble R. (1987). *ACS Symp. Ser. Liquid Membranes*, 62: 83.
139 Boyadzhiev, L., Bezenshek, E., Lazarova, Z. (1984). *J. Membr. Sci.*, 21: 137.
140 Kholpanov, L., Awetisjan, K., Maljusov, W. (1988). *Teor. Osn. Khim. Technol.*, 22: 299.
141 Li, N.N. (1968). *U.S. Patent 3,410,794.*
142 Ward, W. (1972). *Recent Dev. Sep. Sci.*, 1: 151.

143 Cahn, R. and Li, N.N. (1976). *J. Membr. Sci.*, 1: 129.
144 Alessandrini, A., Alessi, P., Kikic, I., Visalberghi, M. (1978). Adv. Sep. Sci. Univ. Trieste, 234.
145 Nam, S. (1979). *Hwahak Konghak*, 17: 377.
146 Kataoka, T. and Nishiki, T. (1981). *Kemikaru Enjiniyaringu*, 26, 9:723.
147 Lagoo, C., Shankar, H., Murthy, S., Narayana, S. (1985). *Indian Chem.* Eng., 27: 52.
148 Plucinski, P. (1986). The Influence of the Surfactants on the Permeation of Hydrocarbons through Liquid Membranes. Procs. Europ. Jap. Congress on Membr., Membr. Proc., pp. 475–481.
149 Casamatta, G., Boyadzhiev, L. and Angelino, H. (1975). Mixture Separation through Two-Stage Extraction. Procs. CHISA'75, Prague, Czechoslovakia.
150 Casamatta, G., Chavarie, C., Angelino, H. (1978). *AIChE J.*, 24: 345.
151 Kawasaki, J., Suzuki, T., Kato, S., Kondou, I.(1986). Separation of Hydrocarbons by Liquid Membrane Instability and Rates of Permeation. Procs. 3th World Congr. Chem. Eng., Tokyo, Japan, pp. 220–223.
152 Plucinski, P. (1985). *Tenside Deterg.*, 22: 18.
153 Kikic, I., Alessi, P. and Vissalberghi, M. (1978). *Inst. Chem. Eng. Symp. Ser.*, 54: 139.
154 Alessi, P., Kikic, I. and Visalberghi, M. (1980). *Chem. Eng. J.*, 19: 221.
155 Shah, N.D. and Owens, T.C. (1972). *Ind. Eng. Chem. (Proc. Res. Develop.)*, 11: 1.
156 Plucinski, P. and Szust, J. (1988). *J. Membr. Sci.*, 38: 261.
157 Lieberwirth, I., Moehle, L. and Pfestorf, R. (1986). *Wiss. Z.*, 35: 451.
158 Kato, S. and Kawasaki, J. (1987). *J. Chem. Eng. Jpn.*, 20, 6: 585.
159 Ihm, S., Jeong, Y., Won., Y. (1987). *J. Membr. Sci.*, 32: 31.
160 Cahn, R. and Li, N.N. (1976). *Membrane Separation Processes*, (Ed. P.Meares). Elsevier, Amsterdam, p. 327.
161 Frankenfeld, J.W. and Li, N.N. (1982). *Treatise Anal. Chem.*, 5: 251.
162 Steele, R.D. and Halligan, J.E. (1974). *Sep. Sci*, 9, 4: 299.
163 Halwachs, W., Schuegerl, K. (1978). *Chem. Ing. Techn.*, 50, 10: 767.
164 Stelmaszek, J. (1981). *Recent Dev. Sep. Sci.*, 6: 11.
165 Kawasaki, J., Suzuki, T., Kato, S., Toyoda, I. and Kondou, I. (1987). *Kagaku Kogaku Ronbunshu*, 13: 487.
166 Alieva, R., Kuliev, A., Mekhtieva, Z., Akhundova, T. (1980). *Azerb. Khim. Zh.*, 3: 95.
167 Krishna, R., Goswami, A. and Sharma, R. (1987). *J. Membr. Sci.*, 34: 141.
168 Bloch, R., Kedem, O. and Vofsi, D. (1963). *Nature*, 199: 802.
169 Zhang, Q. and Cussler, E. (1984). *J. Membr. Sci.*, 19:259. 170. Bartsch , R., Charewicz, W., Kang, S. and Walkowiak, W. (1987). ACS Symp. Ser., Liquid Membranes, 347: 86.
171 Yoshida, S. and Hayano, S. (1986). *J. Am. Chem. Soc.*, 108: 3903.
172 Burgard, M., Jurdy, L., Park, H. and Hembureg R. (1983). *Nov. J. Chim.*, 7: 575.
173 Nakatsuji, Y., Sakamoto, M. and Okahara, M. (1988). *J. Chem. Soc., Chem. Comm.*, 1101.
174 Sakim, M., Hayashita, T., Yamabe, T. and Igawa, M. (1987). *Bull. Chem. Soc. Jpn.*, 60: 1289.
175 Ramadan A. and Danesi, P. (1988). *Solv. Extr. Ion Exch.*, 6: 157.
176 Christensen, J., Lamb, J., Brown, P., Oscarson J. and Izatt, R. (1981). *Sep. Sci. Technol.*, 16: 1193.
177 Strzelbicki, J. and Charewicz, W. (1978). *J. Inorg. Nucl. Chem.*, 40: 1415.
178 Fyles, T. (1986). *J. Chem. Soc. Faraday Trans. 1*, 82: 617.
179 Yamaguchi, K., Negi, S., Kozakai, S. and Negano, R. (1988). *Bull. Chem. Soc. Jpn.*, 61: 2047.
180 Nakatsuji, Y., Kobayashi, H. and Okahara, M. (1986). *J. Org. Chemistry*, 51: 3789.
181 Hiratani, K., Taguchi, K., Sugihara, H. and Iio, K. (1987). *J. Membr. Sci.*, 35: 91.

182 Sakamoto, H., Kimura, K. and Shono, T. (1987). *Anal. Chem.*, 59: 1513.
183 Inokuma, S., Hayase, T. and Kuwamura, T. (1987). *Yukagaku*, 36: 340.
184 Xenakis, A. and Tondre, C. (1987). *J. Colloid Interface Sci.*, 117: 442.
185 Stolwijk T., Sudhoelter, E. and Reinhoudt, D. (1987). *J. Am. Chem. Soc.*, 109: 7042.
186 Izatt, R., Clark, G. and Christensen, J. (1985). *J. Membr. Sci.*, 24: 1.
187 Munoz M., Valiente, M. and Freiser, H. (1988). Facilitated Transport of Ag(I) through Supported Liquid Membranes Containing CYANEX 471 and DEHPA Mixtures. Procs. ISEC'88, Moscow, 3: 93.
188 Tromp, M., Burgard, M. and Leroy, J. (1988). *J. Membr. Sci.*, 38: 295.
189 Anzai, J., Suzuki, Y., Ueno, A. and Osa, T. (1985). *Isr. J. Chem.*, 26: 60.
190 Nishiki, T. and Bautista, R. (1983). AIChE Meeting, Denver' 83.
191 Purin B., Chibizov, V. and Kulikova L. (1988). Liquid Membrane Transport Systems for Metal Extraction. Procs. ISEC'88, Moscow, 3, pp. 13–14.
192 Moskvin, L. and Shmatko, A. (1988). Electrodialysis through Extraction Membrane. Procs. ISEC'88, Moscow, 3, p. 19.
193 Izatt, R., Eblerhardt, L., Clark, G., Bruening, R., Bradshaw, J., Cho, M. and Christensen, J. (1987). *Sep. Sci. Technol.*, 22 (2/3): 701.
194 Hidalgo, N., Masana, A., Valiente, M., Freiser, H., and Sargon, J. (1988). The Use of Catalyzed Extraction in the Separation of Palladium (II) by Supported Liquid Membranes Containing CYANEX 471. Procs. ISEC'88, Moscow, p. 94.
195 Huang, C. and Huang, T. (1988). *Ind. Eng. Chem. Res.*, 27: 1681.
196 Kobuke, Y., Tabushi, I., Oh, K. and Aoki, T. (1988). *J. Org. Chem.*, 53, 25: 5933.
197 Chaudry, M., Noor ul Islam and Mohammad, D. (1987). *J. Radioanal. Nucl. Chem.*, 109: 11.
198 Ivakhno, S. and Rogatinski, A. (1986). *Izv. Mosk. Khim. Inst.*, 43: 17.
199 Macasek, F., Rajec, P., Rehacek, A., Vu, N. and Popovnakova, T. (1985). *J. Radioanal. Nucl. Chem.*, 96: 529.
200 Akiba, K., Takashi, T. and Kanno, T. (1984). *Tohoku Daigaku Senko Seiren Kenkyusho Iho*, 40: 11.
201 Akiba, K. and Hashimoto, H. (1987). *Chem. Aspects Down Stream Thorium Fuel Cycle*, pp. 65–70.
202 Sifniades S., Largman T., Tunick, A. and Koff F. (1981). *Hydrometallurgy*, 7: 201.
203 Flett, D., Melling, J. and West, D. (1982). Investigation of Supported Liquid Membrane Process for Uranium Recovery from Wet-Process Phosphoric Acid. Procs. Oslo'82 Ion Exch. Solv. Extr. Symp., I, pp. 16–18.
204 Bock, J., Klein, R., Valint, P. and Ho, W. (1982). Liquid Membrane Extraction of Uranium from Wet-Process Phosphoric Acid. Procs. Symp. Sulfric/Phosphoric Acid Plant Oper., 1981, pp. 175–83.
205 Hayworth, H., Ho, W., Burns, W. and Li, N.N. (1983). *Sep. Sci. Technol.*, 18: 493.
206 Dickens, N., Rose, M. and Davies, G.A. (1984). *Trans. Inst. Chem. Eng. Symp. Ser.*, 88: 69.
207 Kim, K., Yoo, J. and Park, H. (1985). *Hwahak Konghak*, 23: 263.
208 Yoo, J., Kim, K. and Park, H. (1988). A Study on the Recovery of Uranium in Phosphoric Acid by Liquid Surfactant Membrane. Procs. ISEC'88, Moscow, 3, p. 101.
209 Lunt, D. and Naden, D. (1981). Liquid Membrane Extraction of Uranium from Wet Process Phosphoric Acid — A New Process. Procs. Hydrometallurgy'81, Manchester.
210 Akiba, K. and Kanno, T. (1983). Active Transport of Uranium(VI) through Supported Liquid Membrane Containing TOA. Procs. Symp. Solv. Extr., 1983, Hamamatsu, pp. 63–68.
211 Zhang, Y. (1983). *Mo Fenli Kexue Yu Jishu*, 3: 10.

212 Babcock, W., Kelly, D. and Friesen, D. (1983). Uranium Recovery with Coupled-Transport Membranes. Procs. ISEC'83, Denver, Colorado, Solid-Supported Liquid Membrane, I, p. 373.
213 Babcock, W., Friesen, D. and Lachapelle, E. (1986). *J. Membr. Sci.*, 26: 303.
214 Zhu, Y., Jiang, C., Wang, S., Liu, Z. and Yu, J. (1983). Extraction of Rare Earth by Liquid Surfactant Membranes. Procs. ISEC'83, Denver, Colorado, Emulsion Liquid Membranes, I, pp. 58–59.
215 Sourougy, M., Khalifa, S., Zaki, E. and Aly, H. (1988). Lanthanide Extraction by Liquid Emulsion Membrane Based on Di-(2-Ethylhexyl) Phosphoric Acid. Procs. ISEC'88, Moscow, 3, p. 96.
216 Zhang,Z., Zhang, R., Wang, D. and Huang, B. (1986). *Mo Fenli Kexue Yu Jishu*, 6: 41.
217 Teramoto, M., Sakuramoto, T., Koyama, T., Matsuyama, H. and Miyake, Y. (1986). *Sep. Sci. Technol.*, 21: 229
218 Eguchi, W., Tanigaki, M. and Mori, Y. (1986). *Asahi Found. Ind. Technol.*, 49: 237.
219 Muscatello, A., Navratil, J., Killion, M. and Price, M. (1987). *Liquid Membranes*, ACS Symp. Ser., 347: 182.
220 Akiba, K. and Nakamura, S. (1987). *Chemical Aspects Down Stream.* pp. 85–90.
221 Danesi, P., Chiarizia, R., Rickert, P. and Horwitz, E. (1985). *Solv. Extr. Ion Exch.*, 3: 111.
222 Danesi, P. and Cianetti, C. (1984). *J. Membr. Sci.*, 20: 201.
223 Novikov, A. and Myasoedov, B. (1987). *Solv. Extr. Ion Exch.*, 5: 117.
224 Nakamura, S. and Akiba, K. (1989). *Sep. Sci. Technol.*, 24: 673.
225 Rajec, P., Macasek, F. and Belan J. (1986). *J. Radioanal. Nucl. Chem.*, 101: 71.
226 Mikulai, V., Kopunec, R., Svec, A. and Macasek, F. (1988). The Membrane Extraction — A Suitable Method for the Preconcentration of Metals. Procs. ISEC'88, Moscow, 3, p. 14.
227 Largman, T. and Sifniades, S. (1978). *Hydrometallurgy*, 3: 153.
228 Strzelbicki, J. and Charewicz, W. (1980). *Chem. Stosow*, 2: 239.
229 Kondo, K., Nakashio, F. and Funatsu, K. (1983). Extraction Kinetics of Copper with Liquid Surfactant Membranes Containing Hydroxyoxime in a Stirred Transfer Cell. Procs. ISEC'83, Denver, Colorado, Emulsion Liquid Membranes, II, pp. 286–287.
230 Nakashio, F. and Kondo, K. (1982). *Kenkyu Hokoku-Asai Garasu Kogyo Gijitsu Shoreikai*, 41: 289.
231 Frankenfeld, J., Cahn, R. and Li, N.N. (1981). *Sep. Sci. Technol.*, 16: 385.
232 Strzelbicki, J. and Charewicz, W. (1978). *Sep. Sci. Technol.*, 13: 141.
233 Mikucki, B. and Osseo Asare, K. (1986). *Hydrometallurgy*, 16: 209.
234 Kondo, K., Takahashi, S., Tsuneyuki, T. and Nakashio, F. (1978). *J. Chem. Eng. Jpn.*, 11: 193.
235 Schlosser, S., Kubicarova, E. and Kossaczky, E. (1981). Pertraction of Copper from Ammoniacal Solutions. Procs. CHISA'81, Prague, Czechoslovakia.
236 O'Hara, P. and Bohrer, M. (1989). *J. Membr. Sci.*, 44: 237.
237 Fujinawa, K., Morishita, T., Hozawa, M. and Ino, H. (1985). *Kagaku Kogaku Ronbunshu*, 11: 293.
238 Kondo, K., Kita, K. and Nakashio, F. (1981). *J. Chem. Eng. Jpn.*, 14: 20.
239 Loiacono, O., Drioli, E. and Molinari, R. (1986). *J. Membr. Sci.*, 28: 123.
240 Brunette, J., Lakkis, L., Lakkis, M. and Leroy, M. (1983). Metal Extraction with 4-Acylpyrazol-5-ones: Synergetic Effects with Liphophilic Ammonium Salts; Application to Liquid Membrane Transport. Procs. ISEC'83, Denver, Colorado, pp. 284–285.
241 Nakashio, F., Goto, M., Matsumoto, M., Irie, J. and Kondo, K. (1988). *J. Membr. Sci.*, 38: 249.

242 Marr, R., Bart, H. and Bouvier, A. (1981). *Chem. Ing. Techn.*, 53: 208.
243 Lazarova, Z. and Boyadzhiev, L. (1988). Solutes Recovery from Aqueous Solutions by Creeping Film Pertraction. Procs. ISEC'88, Moscow, 3, p. 23.
244 Ohki, A., Hinoshita, H., Takagi, M. and Ueno, K. (1983). *Sep. Sci. Technol.*, 18: 969.
245 Cox, J., Bhatnagar, A. and Franois, R. (1986). *Talanta*, 33: 713.
246 Yoshizuka, K., Kondo, K. and Nakashio, F. (1986). *J. Chem. Eng. Jpn.*, 19: 312.247.
247 Goto, M., Kondo, K. and Nakashio, F. (1989). *J. Chem. Eng. Jpn.*, 22: 79.
248 Kriechbaumer, A. and Draxler, J. (1982). *Osterr. Chem. Z.*, 83: 275
249 Marr, R., Protsch, M., Bouvier, A., Draxler, J. and Kriechbaumer, A. (1983). *Chem. Ing. Techn.*, 55: 328.
250 Teramoto, M. (1983). *Kagaku Kogo*, 27: 20.
251 Bart, H., Baker, A., Lorbach, D. and Marr, R. (1988). *Chem. Ing. Techn.*, 60: 169.
252 Lorbach, D., Bart, H. and Marr, R. (1986). *Chem. Ing.Techn.*, 58: 156.
253 Boyadzhiev, L. and Lazarova, Z. (1987). *Chem. Eng. Sci.*, 42: 1141.
254 Ivakhno, S., Tarassov, V. and Yagodin, G. (1985). Mezhfaznie Jawlenija pri Membrannoi Extraczii Metallov. Procs. SIS'85, Czechoslovakia, pp. 21–24.
255 Whewell, R.J., Huges, M.A. and Hanson, C. (1977). Aspects of the Kinetics and Mechanism of the Extraction of Copper with Hydroxyoximes. Procs. ISEC'77, Toronto, pp. 185–192.
256 Hanson, C., Hughes, M.A. and Whewell, R.J. (1978). *J. Appl. Chem. Biotech.*, 28: 426.
257 Yan, Z., Ding, X. and Lin, F. (1982). *Huanjing Kexue*, 3: 1.
258 Molinari, R., Drioli, E. and Pantano, G. (1989). *Sep. Sci. Technol.*, 24, 1015.
259 Frankenfeld, J.W. and Li, N.N. (1977). *Rec. Dev. Sep. Sci.*, 3: 285.
260 Kitagawa, T., Nishikawa, Y., Frankenfeld, J. and Li, N.N. (1977). *Environ. Sci. Technol.*, 11: 602.
261 Li, X. and Zhang, Y. (1982). Extraction of Chromium Ions from Aqueous Solution with Liquid Surfactant Membranes. Procs. Joint Meet. Chem. Eng., Chem. Ind. Eng. Soc. China Am. Inst. Chem. Eng., 2, p. 571.
262 Lee, H., Yoo, J. and Ihm, S. (1983). *Hwahak Konghak*, 21:119.
263 Ivakhno, S., Yagodin, G., Rogatinski, A., Gusev, V. and Afanasiev, A. (1987). *Zh. Fiz. Khim.*, 61: 649.
264 Malik, T., Chaudry, A., Husain, K. and Ahmed, B. (1987). *Nucleus*, 24: 25.
265 Weiss, S. and Castaneda, A. (1988). Mass Transfer of Chromium through a Liquid Membrane. Procs. ISEC'88, Moscow, 3, p. 88.
266 Ando, K., Masaoka, S., Akiyoshi, M. and Obata, E. (1988). *Kagaku Kogaku Ronbunshu*, 14: 417.
267 Teramoto, M. Matsuyama, H., Yamashiro, T. and Okamoto, S. (1989). *J. Membr. Sci.*, 45: 115.
268 Mori, Y., Uemae, H., Hibito, S. and Eguchi, W. (1987). *Kagaku Kogaku Ronbunshu*, 13: 412.
269 Fuller, E.J. and Li N.N., (1984). *J. Membr. Sci.*, 18: 251.
270 Strzelbicki, J., Charewicz, W. and Mackiewicz, A. (1984). *Sep. Sci. Technol.*, 19: 321.
271 Baba, Y., Inoue K., Nakashio, F., Matsumoto M. and Goto, M. (1987). *Nippon Kagaku Kaishi*, 8: 1623.
272 Boyadzhiev, L. and Bezenshek, E. (1983). *J. Membr. Sci.*, 14: 13.
273 Weiss, S., Grigoriev, V. and Muehl, P. (1982). *J. Membr. Sci.*, 12: 119.
274 Izatt, R., Johnes, M. Lamb, J., Bradshaw, J. and Christensen, J. (1986). *J. Membr. Sci.*, 26: 241.
275 Danesi, P., Cianetti, C. and Violante, V. (1983). *J. Membr.Sci.*, 14: 175.

276 Takahashi, M., Ohta, T., Nishiguchi, M., Katayama, Y. and Takeuchi, H. (1988). *Kagaku Kogaku Ronbunshu*, 14: 549.
277 Zhang, X. and Huang, P. (1988). *J. Chem. Ind. Eng. China*, 39: 570.
278 Izatt, R., Bruening, R., Clark, G., Lamb, J. and Christensen, J. (1986). *J. Membr. Sci.*, 28: 77.
279 Biel, M., Izatt, R., Lamb, J. and Christensen, J. (1982). *Sep. Sci. Technol.*, 17: 289.
280 Boyadzhiev, L. and Bezenshek, E. (1982). *Chem. Ing. Techn.*, 54: 506.
281 Fernandez, L., Aparicio, J. and Muhammed, M. (1986). *J. Membr. Sci.*, 27: 77.
282 Huang, T. and Yuang R. (1987). *J. Membr. Sci.*, 31: 209.
283 Uribe, I., Wongswan, S. and Perez de Ortiz, E. (1988). *Ind. Eng. Chem. Res.*, 27, 9:1696.
284 Tanigaki, M., Shiode, T., Ueda, M. and Eguchi, W. (1988). *Sep. Sci. Technol.*, 23: 1145.
285 Draxler, J. and Marr, R. (1988). Extraction of Zinc, Cadmium, Lead by Emulsion Liquid Membranes. Procs. ISEC'88, Moscow, 3, p. 4.
286 Harada, M., Shiomi, N. and Yamazaki, F. (1984). *J. Chem. Jpn.*, 17: 567.
287 Verhaege, M., Ryckeboer, M. and Vanhullebusch, M. (1988). Elimination of Zinc from a Nickel Sulphate Solution by Liquid Membranes. Procs. ISEC'88, Moscow, 3, p. 78.
288 Poa, D., Miller, J. and Yao, N. (1985). Development of a Supported Liquid Membrane as a Nickel–Zinc Secondary Battery Separator. Report No. D3REP3, Argonne Natl. Lab., USA.
289 Danesi, P., Horwitz, E. and Rickert, P. (1983). Permeation Rate of Metal Species through Supported Liquid Membranes: Diffusional and Chemical Resistances with Cationic and Anioinic Carriers. Procs. ISEC'83, Denver, Colorado, p. 378.
290 Izatt, R., Bruening, R., Wu, G., Moon, H. and Christensen, J. (1987). *Anal. Chem.*, 59: 2405.
291 Gu, Z., Wasan, D. and Li, N.N. (1985). *Sep. Sci. Technol.*, 20: 599.
292 Gu, Z., Wasan, D. and Li, N.N. (1986). *J. Membr. Sci.*, 26: 129.
293 Zhang, R., Xie, G., Liu, Y., Huang, Y. and Wang, W. (1984). *Huanjing Kexue*, 5: 30.
294 Pemsler, P. and Dempsey, M. (1984). The Application of Supported Liquid Membrane Separators to Alkaline Secondary Batteries. Proc. Electrochem. Soc. 84-4. (Adv. Battery Mater. Processes), p. 187.
295 De Santa G., Di Casa, M., Seghi, B. and Fabbrizzi, L. (1989). *J. Am. Chem. Soc.*, 111: 2422.
296 Osseo-Asare, K. and Chaiko, D. (1989). *J. Membr. Sci.*, 42: 215.
297 Lee, K. (1977). *Diss. Abstr. Int.* B 1978, 38, 7:3305.
298 Narebska, A., Wodzki, R. and Wyszynska, A. (1989). *Makromol. Chem.*, 190: 1501.
299 Chiarizia, R. and Castagnola, A. (1984). *Solv. Extr.Ion Exch.*, 2: 479.
300 Matsuyama, H., Katayama, Y., Kojima, A., Washijima, I., Miyake, Y. and Teramoto, M. (1987). *J. Chem. Eng. Jpn.*, 20: 213.
301 Huang, T. and Yuang, R. (1988). *J. Chem. Techn. Biotechn.*, 42: 3.
302 Nam, S. and Kim, B. (1986). *Nonmunjip Sanop Kwahak Kisul Yonguso*, 14: 371.
303 Strzelbicki, J. and Charewicz, W. (1984). *Hydrometallurgy*, 13: 89.
304 Strzelbicki, J. and Charewicz, W. (1980). *Hydrometallurgy*, 5: 243.
305 Danesi, P. and Reichley, Y. (1986). *J. Membr. Sci.*, 27: 339.
306 Reichley, Y. and Danesi, P. (1985). *Solv. Extr. Ion Exch.*, 3: 49.
307 Beg, M. and Kidwai, M. (1985). *J. Membr. Sci.*, 24: 97.
308 Yatsimirskii, K., Talanova, G. and Rybak Akimova, E. (1986). *Dokl. AN SSSR*, 288: 646.
309 Ujita, G., Shibata, J. and Nishimura, S. (1984). *Technol. Rep. Kansai Univ.*, 25: 81.
310 Tanigaki, M., Hashiguchi, Y., Yoshinori, H., Shode, T., Mori, Y. and Eguchi, W. (1987). *Solv. Extr. Ion Exch.*, 5: 325.
311 Harada, M., Yamazaki, F., Adachi, M. and Eguchi, W. (1984). *J. Chem. Eng.*, 17: 527.
312 Moskvin, L., Shmatko, A. and Krasnoperov, V. (1987). *Elektrokhimiya*, 23: 30.

313 Guerriero, R., Meregalli, L. and Zhang, X. (1988). *Hydrometallurgy*, 20: 109.
314 Valiente, M., Munoz, M. and Fernandez, A. (1988). Study of the Mass Transfer Process on the Separation of Ti(IV) by a SSLM using Tributylphosphate (TBP) in Cumene as a Carrier. Procs. ISEC'88, Moscow, 3, 95.
315 Charewicz, W., Hendrychowski, A. and Strzelbicki, J. (1984). *Chem. Stosow.*, 28: 497.
316 Wang, Y. and Liu, G. (1985). *Xiangtan Daxue Ziran Kexue Xuebao*, 2: 122.
317 Zeng P. and Chan S. (1987). *Wuji Huaxue*, 3: 122.
318 Hozawa, M., Shono, A., Akiyama, M., Imaishi, N. and Fujinawa, K. (1987). Separation and Concentration of Gallium and Indium Using Liquid Membrane. Proc. Symp. Solv. Extr., Hamamatsu, Japan, pp. 95– 100.
319 Shimidzu, T. and Okushita H., (1986). *J. Membr. Sci.*, 27: 349.
320 Gutknecht, W. and Schuegerl, K. (1988). Recovery of Germanium from Model and Fly Ash Leaching Solutions by the Emulsion Liquid Membrane Technique. Procs. ISEC'88, Moscow, 3, 68.
321 Izatt, R., Bruening, R., Clark, G., Lamb, J. and Christensen, J. (1986). *J. Membr.* Sci., 28: 77.
322 Li, N.N. (1974). *U.S. Patent* 482592.
323 Rautenbach, R. and Albrecht, R. (1979). *Wiss. Umwelt*, 2: 97.
324 Downs, H.H., Li, N.N. (1981). *J. Sep. Process Technol.*, 2, 4: 19.
325 Rautenbach, R. and Machhammer, O. (1988). *J. Membr. Sci.*, 36: 425.
326 Schlosser, S. and Kossaczky, E. (1987). *Synthetic Polymeric Membranes* (B. Sedlacek and J. Kahovec, eds.). Walter de Gruyter & Co., Berlin, p. 571.
327 Hayworth, H. (1981). *CHEMTECH*, 342.
328 Cahn, R.P., Li, N.N. and Minday, R.M. (1978). *Environ. Sci. Technol.*, 12, 9: 1051.
329 Nishiki, T. and Kataoka, T. (1985). *Bull. Univ. Osaka Prefecture*, Series A, 34, 1: 7. (1985)
330 Fernandez, L.A., Elizalde, M.P. and Aparicio, J.L. (1989). *J. Membr. Sci.*, 44 (2–3): 213.
331 Boyadzhiev, L. and Besenshek, E. (1976). *Comptes Rendus Acad. Bulg. Sci.*, 29, 4: 559.
332 Ivakhno, S., Kadasov, D. and Varlamov, V. (1988). Membrane Extraction of Nitric Acid. Procs. ISEC'88, Moscow, 3, p. 71.
333 Danesi, P.R., Cianetti, C. and Horwitz, E.P. (1983). *Solv. Extr. Ion Exch.*, 1 (2): 299.
334 Trouve, G., Malher, E., Colinart, P. and Renon, H. (1982). *Chem. Eng. Sci.*, 37, 8: 1225.
335 Zeng, P. and Cheng, R. (1986). *Xiangtan Daxue Ziran Kexue Xuebao*, 4: 54.
336 Boyadzhiev, L. and Bezenshek, E. (1988). *J. Membr. Sci.*, 37: 277.
337 Li, N.N. and Shrier, A. (1972). *Rec. Dev. Sep. Sci.*, 1: 163.
338 Boyadzhiev, L. (1984). *Teor. Osn. Khim. Technol.*, 18, 6: 735.
339 Ho, W.S., Hatton, T.A., Lightfoot, E.N. and Li, N.N. (1981). Extraction with Liquid Surfactant Membranes: A Diffusion-Controlled Model with Advancing Reaction Front. Procs. 2nd World Congress of Chem. Eng., Montreal, Canada.
340 Stelmaszek, J. (1979). *Inzynieria Chemiczna*, 9: 211.
341 Schlosser, S. and Kossaczky, E. (1978). Emulsion Properties Influence on Pertraction of Phenol from Water. Procs. CHISA'78, Prague, Czechoslovakia.
342 Boyadzhiev, L. (1981). Carrier Mediated Extraction: A Comparative Study on Supported Liquid Membranes and Double Emulsion Technique. ProcS. CHISA'81, Prague, Czechoslovakia.
343 Halwachs, W., Voelkel, W. and Schuegerl, K. (1980). Removal of Toxins from Plasma and Blood with Liquid Surfactant Membranes. Procs. ISEC'80, Liege, Belgium, 2, p. 80.
344 Shu, R., Chang, Y., Liu, Y., Chemg, J., Tao, C. and Lu, H. (1980). *Huan Ching K'o Hsueh*, 1, 4: 4.
345 Teramoto, M. and Matsuyama, H. (1986). *J. Chem. Eng. Jpn.*, 19, 5: 469.

346 Yang, P., Yang, X., Shen, L. (1987). *Shanghai Huanjing Kexue*, 6, 3: 13.
347 Zhang, Y., Liu, Y., Su, R. (1988). *Water Treat.*, 3, 1: 79.
348 Yu, J., Jiang, C., Liu, Z., He, P. (1982). *Mo Fenli Kexue Yu Jishu*, 2 (1): 9.
349 Zhang, X., Zang, X., Fan, J. and Liu, Z. (1982). *Huanjing Huaxue*, 1 (4): 320.
350 Bargeman, D. and Smolders, C. A. (1986). *Synthetic Membranes: Science, Engineering and Applications* (P.M. Bungay et al., eds.). D. Reidel Publ. Company, p. 567.
351 Li, N.N. (1978). *J. Membr. Sci.*, 3: 265.
352 Zhu, C., Wang, Q., Wu, W. and Wu, X. (1981). *Zhejiang Daxue Xuebao*, 4: 64.
353 Ihm, S.K., Kim, K.S. and Choi, S.J. (1981). *Hwahak Konghak*, 19, 3: 217.
354 Zhang, Y. and Li, X. (1983). *Desalination*, 47: 351.
355 Du, Q., Cheng, W. and Yu, T. (1987). *Huanjing Kexue*, 8 (2): 49.
356 Voelkel, W., Poppe, W., Halwachs, W. and Schuegerl, (1982). *J. Membr. Sci.*, 11: 333.
357 Yu, W. and Zhang, L. (1986). *Fenxi Ceshi Tongbao*, 5 (6): 59.
358 Araki, T., Kubo Y., Takata M., Gohbara S. and Yamamoto, T. (1987). *Chem. Lett.*, 6: 1011.
359 Yan, N.X., Huang, S.A., Shi, Y.J. (1987). *Sep. Sci. Technol.*, 22 (2–3): 801.
360 O'Brien, D. and Senske, G. (1989). *Sep. Sci. Technol.*, 4 (9–10): 617.
361 Boey, S.C., Garcia del Cerro, M.C. and Pyle, D.L. (1987). *Chem. Eng. Res. Des.*, 65 (3): 218.
362 Thien, M.P., Hatton, T.A. and Wang, D.I. 1988). *Biotechn. Bioeng.*, 32: 604.
363 Takeshima S., Sakurai, H. and Horisaka, K. (1986). *Ganryu Aminosan*, 9: 143.
364 Yamaguchi, T., Nishimura, K., Shinbo, T. and Sugiura, M. (1985). *Chem. Lett.*, 10: 1549.
365 Bryjak, M., Wieczorek, P., Kafarski, P. and Lejczak, B. (1988). *J.Membr. Sci.*, 37: 287.
366 Woo, I.S. and Kang, A.S. (1988). *Hwahak Konghak*, 26 (4): 435.
367 Kafarski, P., Skrzypinski, W., Bryjak, M., Plucinski, P. and Wieczorek, P. (1988). *Pept. Chem. Date*, 717.
368 Rebek, J., Askew, B., Nemeth, D. and Parris, K. (1987). *J. Am. Chem. Soc.*, 109, 8: 2432.
369 Scrimin, P., Tonellato, U. and Zanta, N. (1988). *Tetrahedron Letters*, 29 (39): 4967.
370 Baird, R., Reed, D. and Bunge, A., (1986). *NATO ASI*, Ser. E, 107: 585.
371 Audunsson, G. (1986). *Anal.Chem.*, 58: 2714.
372 Audunsson, G. (1988). *Anal.Chem.*, 60 (13): 1340.
373 Shinbo, T., Nishimura, K., Yamaguchi, T., Sugiura, M. (1986). *J. Chem. Soc., Chem. Commun.*, 350.
374 Yagodin, G., Yurtov, E. and Gusseva, T. (1987). *Vopr. Med. Khim.*, 33: 66.
375 Yagodin, G., Ivakhno, S., Levkin, A. and Solov'ev, S. (1983). Kinetics of Membrane Extraction of Copper. Procs. All Union Conf. Extract., Riga, p. 98.
376 Chiang, C. and Fuller, G., Frankenfeld, J. and Rhodes, C. (1978). *J. Pharm. Sci.*, 67: 63.
377 Panaggio, A. and Rhodes, C. (1984). *Drug Dev. Ind. Pharm.*, 10: 637.
378 Majumdar, A. and Stroeve, P. (1986). *J. Membr. Sci.*, 26: 329.
379 Davis, S. (1981). *Chem. Ind.*, 3, 683.
380 Maugh, T. (1976). *Science*, 193: 134.
381 Nughnoi, P., Yano, T., Nishio, N. and Nagai, S. (1987). *J. Ferment. Technol.*, 65, 3: 301.
382 Del Cerro, C. and Boey, D. (1988). *Chem. Ind.*, 21: 681.
383 Marchese, J., Lopez, J. and Quinn J. (1989). *J. Chem. Techn. Biotechnol.*, 46: 149.
384 Sugiura, M. and Yamaguchi, T. (1984). *Sep. Sci. Technol.*, 19: 623.
385 Voelkel, W., Bosse, J., Poppe, W., Halwachs, W. and Schuegerl, K. (1984). *J. Membr. Sci.*, 30: 55.
386 Asher, W., Bovee, K., Frankenfeld, J., Hamilton, R. and Lee, H. (1975). *Kidney Int.*, 3: 409.
387 Asher, W., Vogler, T., Bovee, K., Holtzapple, P. and Hamilton, R. (1977). *Trans. Am. Soc. Artif. Internal Organs*, 23: 673.

388 Asher, W., Bovee, K., Vogler, T., Hamilton, R., and Holtzapple, P. (1979). *Clin. Nephrology*, 11: 92.
389 Trouve, G., Jore, D., Duranel, C. and Renon, H. (1982). *Innov. Techn. Biol. Med.*, 3: 635.
390 Schuegerl, K. and Scheper, T. (1988). Biotransformation in Enzyme Liquid Membrane Reactors. Chem. and Biotechnol. Biol. Act. Nat. Products, Proc. 4th Int. Conf., Budapest, 1987, p. 133.
391 Makryaleas, K., Scheper, T., Schuegerl, K. and Kula, M.R. (1985). *Chem. Ing. Tech.*, 57, 4: 362.
392 Barenschee, T., Dullau, R., Meyer, E.R., Scheper, T., Schuegerl, K., Hustedt, H. and Schuette, H. (1989). *Chem. Ing. Techn.*, 61, 5: 426.
393 Yu, J., Wang, S., Ma, N. and Jiang, C. (1987). *Desalination*, 62: 315.
394 Marr, R. and Draxler, J. (1988). *Chem. Ing. Techn.*, 60: 8.
395 Ivakhno, S., Gusev, V., Kadasov, D. and Rogatinski, A. (1989). *Khim. Tekhnol.*, Kiev, 57.
396 Schlosser, S. and Kossaczky, E. (1980). *J. Membr. Sci.*, 6: 83.
397 Rautenbach, R., Albrecht, R. and Machhammer, O. (1981). *Maschinen-markt*, Wuerzburg 87, 78: 1610.
398 Bouvier, A. and Marr, R. (1981). Metal Ion Separation with the Help of Liquid Membrane. Procs. CHISA'81, Czechslovakia.
399 Li, N.N., Cahn, R., Naden, D. and Lai, R. (1983). *Hydrometallurgy*, 9: 277.
400 Liu, Y., Su, R., Zhang, Y., Zhang, G., Tao, Z., Tong, P. and Zhang, X. (1983). *Mo Fenli Kexue Yu Jishu*, 3:37.
401 Chang, C., Tai, J., Hoh, Y. and Wang, W. (1984). *J. Chim. Inst. Chem. Eng.*, 15: 151.
402 Ge, D. and Drioli, E. (1983). *Mo Fenli Kexue Yu Jishi*, 3: 1.
403 Takahashi, K. Othsubo, F. and Takeuchi, H. (1983). *Kagaku Kogaku Ronbunshu*, 9: 409.
404 Matsumoto, M., Kondo, K. and Nakashio, F. (1983). Extraction of Copper with Liquid Surfactant Membranes Containing Chelating Reagent in a Stirred Tank. Proc. Solv. Extr. Conf., Denver.
405 Bunge, A., Reed, D. and Noble, R. (1988). Encapsulated-Phase Leakage during Emulsion Liquid Membrane Extraction. Proc. ISEC'88, Moscow, 3, p. 57.
406 Sakai, N., Chida, T. and Simoiizaki, J. (1986).*Nippon Kogyo Kaishi*, 102: 97.
407 Fujinawa, K. Komatsu, T., Hozawa, M., Imashi, N. and Ino, H. (1984). *Kagaku Kogaku Ronbunshu*, 10: 75.
408 Kim, B. (1984). *J. Membr. Sci.*, 21: 5.
409 Marr, R., Bart, H. and Bouvier, A. (1981). *Ger. Chem. Eng.*, 4: 209.
410 Marr, R. and Kopp, A. (1982). *Intern. Chem. Eng.*, 22: 44.
411 Boyadzhiev, L. (1981). Carrier Mediated Extraction or Liquid Membrane. Int. Symp. Hydrometallurgy'81, Manchester, UK.
412 Lorbach, D., Bart, H. and Marr, R. (1986). *Ger. Chem.Eng.*, 9: 321.
413 Sharma, A., Goswami, A. and Krishna, R. (1989). *J. Membr. Sci.*, 40: 329.
414 Hung, T., Chen, C. and Lee, C. (1989). *J. Chin. Inst. Chem. Eng.*, 20: 319.
415 Ulbrich, M., Marr, R. and Draxler, J. (1991). *J. Membr. Sci.*, 59: 189.
416 Izatt, R., Roper, D., Bruening, R. and Lamb, J. (1989). *J. Membr. Sci.*, 45: 73.
417 Yamaguchi, K., Kuboniwa, H., Murakami, N., Hirao, A., Nakahama, S. and Yamazaki, N. (1989). *Bull. Chem. Soc. Jpn.*, 62: 1097.
418 Lamb, J., Bruening, R., Linsley, D., Smith, C. and Izatt R. (1990). *Sep. Sci. Technol.*, 25: 13.
419 Wakita, R., Matsumoto, M., Nakatsuji, Y. and Okahara, M. (1991). *J. Membr. Sci.*, 57: 297.
420 Brown, P., Hallman, J., Whaley, L., Desai, D., Pugia, M. and Bartsch, R. (1991). *J. Membr. Sci.*, 56: 195.

421 Wienk, M., Stolwijk, T., Sudholter, E. and Reinhoudt D. (1990). *J. Am. Chem. Soc.*, 112: 797.
422 Meifang, J. and Yuangi Z. (1990). Study on Extraction of Gold and Cyanide Solution by Liquid Membrane. Proc. Int. Congr. ICOM'90, Chicago, USA, pp. 676–678.
423 Sirlin, C., Burgard, M., Leroy, M. and Prevost, N. (1990). *J. Membr. Sci.*, 54: 299.
424 Chiarizia, R. and Horwitz, E. (1990). *Solv. Extr. Ion Exch.*, 8: 65.
425 Chiarizia, R., Horwitz, E., Rickert, P. and Hodgson, K. (1990). *Sep. Sci. Technol.*, 25: 1571.
426 Hirato, T., Kishigami, I., Awakura, Y. and Majima, H. (1991). *Hydrometallurgy*, 26: 19.
427 Zhu, C. and Izatt, R. (1990). *J. Membr. Sci.*, 50: 319.
428 Nakamura, S., Ohashi, S. and Akiba, K. (1992). *Sep. Sci.Technol.*, 27: 863.
429 Kardiwarenko, L., Bagreev, V. and Zolotov, Y. (1990).*Zh. Neorg. Khim.*, 35: 2160.
430 Wodzki, R., Wyszynska, A. and Narebska, A. (1990). *Sep. Sci. Technol.*, 25: 1175.
431 Matsumoto, M., Matsuo, K., Kondo, K. and Nakashio, F. (1990). *J. Membr. Sci.*, 53: 287.
432 Kataoka, T., Nishiki, T., Kimura, S. and Tomioka, Y. (1989). *J. Membr. Sci.*, 46: 67.
433 Matsumoto, M., Ema, K., Kondo, K. and Nakashio, F. (1990). *J. Chem. Eng. Jpn*, 23: 402.
434 Takigawa, D. (1992). *Sep. Sci. Technol.*, 27: 325.
435 Zhong, Y., Siya, L., Ying, C. and Bojun, L. (1990). Treatment of the Wastewater Containing High Concentration of Cr(VI) Using Liquid Membrane. Proc. Int. Congr. ICOM'90, Chicago, USA, pp. 718–720.
436 Salazar, E., Ortiz, M. and Irabien, J. (1990). *Inst. Chem. Eng.Symp. Ser.*, 199: 279.
437 Chiarizia, R., Horwitz, E. and Rickert P. (1990). *Sep. Sci.Technol.*, 25: 1571.
438 Mori, Y., Hibino, S., Uemae, H., Tanigawa, M. and Eguchi, W. (1991). *Kagaku Kogaku Ronbunshu*, 17: 1104.
439 Ikeda, I., Yamazaki, H., Konishi, T. and Okahara, M. (1989). *J. Membr. Sci.*, 46: 113.
440 Ikeda, I., Yamazaki, H., Kurosawa, H. and Okahara, M. (1991). *Nippon Kagaku Kaishi*, 5: 612.
441 Drioli, E., Loicano, O., Molinari, R. and Pantano, G. (1989). *Chim. Oggi*, 7: 25.
442 Kaprantchik, V., Proyaev, V., Kopirin, A. and Slatennikov, Y. (1989). *Radiokhimia*, 6: 100.
443 Izatt, R., Bruening, R., Bruening, M., Lindh, G. and Christensen, J. (1989). *Anal. Chem.*, 61: 1140.
444 Kardiwarenko, L., Shkinev, V., Spivakov, B., Bagreev, V., Yurtov, E. and Koroleva, M., *Zh. Inorg. Chem.* (Russ), 36: 1887.
445 Takahashi, S. (1991). *Sep. Sci. Technol.*, 26: 1495.
446 Sato Y., Kondo K. and Nakashio F. (1990). *J. Chem. Eng. Jpn.*, 23: 23.
447 Teramoto, M., Tohno, N., Ohnishi, N. and Matsuyama, H. (1989). *Sep. Sci. Technol.*, 24: 981.
448 Saito, T. (1990). *Sep. Sci. Technol.*, 25: 581.
449 Goto, M., Yamamoto, H., Kondo, K. and Nakashio, F. (1991). *J. Membr. Sci.*, 57: 161.
450 Shiau, C. (1991). *Sep. Sci. Technol.*, 26: 1519.
451 Yang, C. and Peng, X. (1990). *Membr. Sci. Technol.*, 11: 102.
452 Matsuyama, H., Boku, J. and Teramoto, M. (1990). *Water Treatment*, 5: 237.
453 Li, J. and Yang, X. (1990). *Youse Jinshu*, 42: 55.
454 Huang, T. and Tsai, T. (1991). *J. Chem. Eng. Jpn.*, 24: 126.
455 Bulavchenko, A. and Torgov, V. (1991). *Kolloidn. Zh.* (Russ), 53: 1017.
456 Lee, C. and Chan, C. (1990). *Ind. Eng. Chem. Res.*, 29: 96.
457 Pfeiffer, R. and Bunge, A. (1990). Breakage and Swelling in Emulsion Liquid Membrane. Procs. Intern. Congr. ICOM'90, Chicago, USA, pp. 703–705.
458 Urtiaga, A., Ortiz, M. and Irabien, A. (1990). *Inst. Chem. Eng. Symp. Ser.*, 199: 35.
459 Wang, C. and Bunge, A. (1990). *J. Membr. Sci.*, 53: 71.

460 Wu, B. and Wu, Q. (1990). *Membr. Sci. Technol.*, 10: 16.
461 Uramoto, H., Kawabata, N. and Teramoto, M. (1990). *J. Membr. Sci.*, 62: 219.
462 Urtiaga, A., Ortiz, M., Inmaculada, S., Ernesto, I. and Angel, J. (1992). *Ind. Eng. Chem. Res.*, 31: 877.
463 Dai, Y., Wang, X. and Yang, Y. (1992). *Membr. Sci. Technol.*, 12: 37.
464 Bart, H., Ramaseder, E., Haselgruebler, T. and Marr R. (1992). *Hydrometallurgy*, 28: 253.
465 Boyadzhiev, L. (1990). *Sep. Sci. Technol.*, 25: 187.
466 Jin, M., Lazarova, Z. and Boyadzhiev L. (1991). *Water Treatment*, 6: 219.
467 Lazarova, Z. (1991). *Chem. Techn.*, 9: 333.
468 Boyadzhiev, L. and Alexandrova, S. (1992). *Sep. Sci.Technol.*, 27: 1307.
469 Lazarova, Z. (1993). *Solv. Extr. Ion Exch.*, 11.
470 Lazarova, Z., Sapundshiev, T. and Boyadzhiev, L. (1992). *Sep. Sci. Technol.*, 27: 493.
471 Lazarova, Z. and Boyadzhiev, L. (1992). *Intern. J. Environ. Anal. Chem.*, 46: 233.
472 Lazarova, Z. and Boyadzhiev, L. (1992). *Talanta*, 39: 931.
473 Boyadzhiev, L. and Atanasova, I. (1991). *Biotechnol. Bioeng.*, 38: 1059.
474 Gadekar, P., Mukkolath, A. and Tiwari, K. (1991). *Sep. Sci. Technol.*, 27: 427.
475 Yang, P., Shen, L. and Feng, H. (1992). *Membr. Sci. Technol.*, 12: 39.
476 Nuchnoi, P., Nashio, N. and Nagai, S. (1989). *J. Ferment. Bioeng.*, 67: 195.
477 Reisinger, H., Marr, R. and Preitsehopf, W. (1990). Liquid Membrane Permeation in the Field of Biotechnology. Procs. Intern. Congr. ICOM'90, Chicago, pp. 715–716.
478 Chaudhuri, J. and Pyle, D. (1992). *Chem. Eng. Sci.*, 47: 41.
479 Hano T., Matsumoto M., Ohtake T., Sasaki K., Hori F. and Kawano Y. (1992). Application of Liquid Membrane Technique to the Recovery of Fermented Organic Acid. *Solvent Extraction 1990* (T. Sekune, ed.), Elsevier Sci. Publ., pp. 1887–1892.
480 Basu, R. and Sirkar, K. (1990). Citric Acid Extraction with Microporous Hollow Fibers. Procs. Int. Congr. on Membrane and Membrane Processes ICOM'90, Chicago, USA, 1, pp. 641–643.
481 Frisen, D., Babcock, W., Brose, D. and Chambers, A. (1991). *J. Membr. Sci.*, 56: 127.
482 Sirman, T., Pyle, D. and Grandison, A. (1990). *Separation in Biotechnology*, 2: 245.
483 Wang, C. and Bunge, A. (1990). *J. Membr. Sci.*, 53: 105.
484 Bryjak, M., Wieczorek, P., Kafarski, P. and Lejczak, B. (1991). *J. Membr. Sci.*, 56: 167.
485 Teramoto, M., Yamashiro, T., Inoue, A., Yamamoto, A., Matsuyama, H. and Miyake, Y. (1991). *J. Membr. Sci.*, 58: 11.
486 Deblay, F., Delepine, S., Minier, M. and Renon, H. (1991). *Sep. Sci. Technol.*, 26: 97.
487 Luka, C., Mitihac, L. and Constantinescu, T. (1990). *Rev. Roum. Chim.*, 35: 467.
488 Hano, T., Ohtake, T., Matsumoto, M., Kitayama, D., Hori, F. and Nakashio, F. (1990). Separation and Enrichment of Amino Acids with Liquid Surfactant Membrane. *Solvent Extraction 1990* (T. Sekune, ed.), Elsevier Sci. Publ., pp. 1881–1886.
489 Srivastava, R., Raju, D., Singh, V. and Upadhyay, S. (1991). *J. Membr. Sci.*, 58: 211.
490 Paradkar, V. and Dordick, J. (1991). *Biotechnol. Prog.*, 7: 330.
491 Sorenson, B. and Callahan, R. (1990). Penicillin Separations with Contained Liquid Membranes. Proc. Int. Congr. ICOM'90, Chicago, USA, pp. 695–696.
492 Scheper, T. (1990). Enzyme immobilization in liquid surfactant membrane emulsions. *Adv. Drug Delivery Revs.*, 4: 209.
493 Hano, T., Othake, T., Matsumoto, M., Ogawa, S. and Hori, F. (1990). *J. Chem. Eng. Jpn.*, 23: 772.
494 Barenshee, T., Dullau, R., Meyer, E., Scheper, T., Schuegerl, K., Hustedt, H. and Schuette, H. (1989). *Chem. Ing. Techn.*, 61: 426.

Membrane Separations Technology. Principles and Applications
Edited by R.D. Noble and S.A. Stern

Chapter 8

Membrane bioseparations

Stephen L. Matson

Arete Technologies Inc., 15 Withington Lane, Harvard, MA 01451, USA

8.1 INTRODUCTION

8.1.1 Historical Perspectives

As recently as a decade ago, the potential of membrane technology was frequently underestimated by biochemical engineers dealing with conventional fermentation processes. Membrane separations — in particular, microfiltration (MF), ultrafiltration (UF), and reverse osmosis (RO) — played only modest roles in recovering and purifying the products of classical fermentation processes. Porous MF and UF membranes found limited application in the separation and/or concentration of particulate, colloidal, and macromolecular species, and reverse osmosis was only rarely employed in downstream processing.

In truth, the great majority of bioseparation tasks were and still are accomplished by a small group of more conventional "workhorse" unit operations; these include centrifugation and vacuum filtration for solid/liquid separations, chromatography for protein recovery and purification, and solvent extraction for antibiotic purification [1–5]. Prior to about 1980, relatively few practicing biochemical engineers had enjoyed much successful experience with membranes. More often than not, prior operating history with many membrane bioseparations could be characterized as either nonexistent or unsatisfactory.

At first blush, this limited penetration of the fermentation process market by membranes seems surprising, given that certain inherent characteristics of membranes would appear to recommend them for many bioprocessing tasks:

- gentleness (e.g., avoidance of chemical separating agents and phase changes);

- low-temperature operating capability;
- energy-efficiency (e.g., in dewatering);
- ability to be isolated and contained (i.e., closed-system operation);
- scalability; and
- simplicity.

However, several factors made for a relatively poor early showing of membranes in bioseparation applications:

- Membrane suppliers had relatively little pertinent experience with the particulars of downstream bioprocessing.
- Flux decline and fouling — problems encountered to some extent in most membrane applications — proved particularly severe with bioseparations.
- Many membranes pressed into service in this field had initially been developed for other purposes and were not optimized for bioprocess applications.
- A lack of membrane industry standards and discipline (e.g., regarding the specification and significance of molecular-weight cut-offs) caused much user confusion and disappointment.
- Bioprocess engineers were loathe to risk loss of high-value products with as-yet-unproven membrane process technology, especially when existing bioseparation needs were being served more or less adequately if inelegantly by conventional technologies.

Happily, recent developments on several fronts have done much to alter this state of affairs. At the very least, membrane technology is today regarded as providing credible competition for more conventional bioseparation unit operations. While some understandable skepticism lingers on in the industry, membranes are increasingly becoming the technology of choice in certain downstream bioprocessing applications.

8.1.2 Current Status

The improved circumstances of membrane bioseparations result from a confluence of several factors. For one thing, much valuable operating experience has been gained within the past two decades by consumers and suppliers alike of membrane technology and equipment. Moreover, along with an appreciation of the market potential has come the tailoring of existing membranes and membrane processes — as well as the invention of new ones — capable of better addressing specific market needs.

Equally important to the emergence of membranes as viable bioseparation technology, however, has been the sea change that has taken place in the nature of downstream bioprocessing itself. Modern biotechnology has created certain particularly critical, value-added separations — e.g., the recovery and purifica-

tion of therapeutic proteins produced by via recombinant techniques — for which membranes are well suited. As of early 1993, seventeen biotechnology-derived drugs and vaccines had been approved by the Food and Drug Administration [6]. In 1992, the sales of these drugs by ten so-called "biotechnology" companies alone exceeded two billion dollars [7] — excluding sales by established pharmaceutical companies of such products as Eli Lilly's recombinant human insulin [8]. Looking ahead, the number of biopharmaceuticals in various stages of regulatory review or nearing submission to the FDA is certainly an order of magnitude larger than those already approved and on the market.

Numerous membrane bioseparation market surveys exist, but their conclusions are generally too unreliable and/or short-lived to warrant further comment here. Suffice it to say that ample economic incentive now exists to induce membrane technologists to address the scale-up challenges presented by the modern biotechnology industry.

8.1.3 Chapter Organization

An appreciation of the special considerations and constraints involved in the recovery and purification of biologically-derived products is essential to anyone who would contemplate applying membranes in this arena. It is thus inevitable that this chapter begins with some rather tutorial material dealing with the principal bioproduction methods and their commercial products.

Beyond this, however, a discussion of membrane bioseparations could conceivably follow a number of possible lines, as suggested by the organizational framework in Table 8.1. This chapter is organized primarily according to the particular type of component being separated. Fortunately, there exists a reasonably good correspondence between the nature of this bioproduct, the unit operation required to separate and/or purify it, and the type of membrane and membrane process best suited to accomplishing this task. This chapter attempts to treat each of these aspects of membrane bioseparations in parallel, in a manner that is complementary to the somewhat different organizational approaches taken by other reviewers [9–14].

8.2 BIOTECHNOLOGY AND BIOSEPARATIONS: AN OVERVIEW

Biotechnology can be defined as the technological exploitation or manipulation of biological systems for the production of a useful economic or therapeutic result [15]. This rather broad definition encompasses activities as diverse as the extraction of valuable components from plant and animal sources (even human plasma), the biomedical application of membrane separations (e.g., hemodialysis), and the production of many foods and beverages. However, our focus here is on the manufacture of biologically-derived compounds under the con-

TABLE 8.1
Dimensions of membrane bioseparation technology

Type of bioprocess/ bioreactor	Microbial fermentation
	Cell culture
	Animal (e.g., mammalian, insect)
	Plant
	Extraction from native sources
	Recovery from plants and animals
	Plasma processing
	Biocatalysis (e.g., enzyme bioreactors)
Nature of bioproduct being separated	Particulate
	Intact cells
	Intracellular components (e.g., inclusion bodies)
	Protein precipitates
	Macromolecular
	Intracellular proteins
	Extracellular proteins
	DNA
	Low-molecular-weight solutes
	Primary metabolites (e.g., citric acid, amino acids, vitamins)
	Secondary metabolites (e.g., antibiotics)
	Contaminants (e.g., virus)
Unit operation	Bioreactor support
	Media pretreatment (e.g., sterilization)
	Productivity enhancement (e.g., cell recycle)
	Solid/liquid separation
	Cell harvesting
	Clarification
	Protein recovery and purification
	Microsolute recovery and concentration
	Contaminant removal
	Product finishing and formulation
Nature of membrane separation process	Microfiltration
	Ultrafiltration
	Reverse Osmosis
	Other

trolled conditions of biochemical processes, where a production bioreactor of some sort is followed by a separation train designed to recover and purify a component produced therein.

8.2.1 Representative Bioproducts

The size and complexity of biologically produced materials runs the gamut from simple organic solutes (e.g., ethanol) at one extreme to macromolecular, colloidal, and particulate species (e.g., proteins and whole cells) at the other. Each category of bioproduct demands its own type of separation technology.

8.2.1.1 Low-Molecular-Weight Products

Low-molecular-weight organic compounds, referred to here as "microsolutes", are derived principally from conventional fermentation processes. Certain microsolutes like ethanol and simple organic acids (e.g., citric, acetic, and lactic) are derived from the catabolic processes of cellular metabolism that break down energy-rich nutrients into simpler components; these products tend to be rather inexpensive. Still other compounds result from biosynthetic rather than degradative bioprocesses. Among these, the amino acids and vitamins are examples of so-called primary metabolites, characterized by modest unit values of about ten dollars per kilogram or less. More complex and higher value secondary metabolites like antibiotics command prices of up to several dollars per gram [1,2,4,5]. Table 8.2 shows a representative few of the 200 or so fermentation-derived microsolutes of commercial significance.

TABLE 8.2
Representative low-molecular-weight fermentation products

Amino acids	glutamic acid
	lysine
Organic acids	citric acid
	acetic acid
	lactic acid
	gluconic acid
Ketones and alcohols	acetone
	butanol
	ethanol
Vitamins	
Antibiotics	penicillins
	cephalosporins
	cyclosporin
	thienamycin
Other secondary metabolites	

8.2.1.2 Macromolecular Products

Table 8.3 illustrates the great variety of macromolecular products that can be produced by microbial fermentation and/or mammalian cell culture. Unit values vary significantly but are generally high compared to those of their lower-molecular-weight counterparts discussed above. For instance, the production cost of a purified therapeutic monoclonal antibody may have a value of the order of $1,000/g even before being packaged in final dosage form. Yet another calibration point is provided by recombinant tissue-type plasminogen activator (t-PA), which is administered at a cost of approximately $2000 per 100 mg dose or $20,000/g.

TABLE 8.3
Classes of macromolecular products from fermentation and cell culture

Therapeutic proteins	enzymes
	monoclonal antibodies
	interleukins
	interferons
	recombinant plasma proteins
	vaccines
Peptide hormones	recombinant human insulin
	bovine and human growth hormones
Diagnostic enzymes and antibodies	
Polysaccharides and biopolymers	xanthan gums
	dextrans
	polyhydroxybutyrate
Industrial enzymes	proteases
	amylases
	glucose isomerase

Clearly, we associate the "biotechnology revolution" of the past two decades principally with the production of therapeutic proteins and peptides by recombinant DNA and hybridoma technologies. It is indisputable that biotechnology has become a cost-effective technology for the creation of new therapeutic drugs and novel treatment modalities. Human insulin (Eli Lilly), human growth hormone (Genentech), alpha interferon (Biogen/Schering Plough), and hepatitis B vaccine (Chiron/Merck) were the first genetically engineered pharmaceuticals to reach the market in the 1980s [8,16]. Table 8.4 summarizes

TABLE 8.4

Representative products from mammalian cell culture and their therapeutic indications (from Ref. [16] with permission)]

Product	Disease/condition
Lymphokines	Viral infections
Erythropoietin	Anemia, hemodialysis
Recombinant insulin	Diabetics, insulin dependent
Beta cells	Diabetics
Urokinase	Blood clots
Granulocyte stimulating factor	Wounds, severe
Tissue plasminogen activator	Heart attacks, survive to hospital
Transfer factor	Multiple sclerosis
Protein C	Hip surgery, protein C deficiency
Epidermal growth factor	Burns
Factor VIII	Hemophilia
Human growth hormone	Pituitary deficiency
Orthoclone	Kidney transplant rejection
Alpha interferon	Hairy-cell leukemia

several other biotechnology-derived therapeutic proteins already on the market or pending final FDA approval, along with their clinical indications.

8.2.1.3 Cell Biomass

In the interest of completeness, it should be noted that occasionally it is the cell biomass in its entirety — as distinct from one of its components — that constitutes the product of commercial value. Representative products range from such ancient commodities as bakers' and brewers' yeasts to decidedly non-traditional products like single cell protein. Still other examples include the production of intact microorganisms for use in whole-cell-catalyzed bioconversions.

The economics of producing cell biomass are typically dominated either by the cost of feedstock or the cost of its bioconversion, rather than by the cost of subsequent product recovery [17]. These latter operations can be quite simple, amounting in some instances to little more than filtration, washing, and drying of the cell biomass.

8.2.2 Principal Bioproduction Systems

Most bioproduction processes fall into either of two categories: fermentation or mammalian cell culture. Production technologies based on extraction of

products from sources such as plant and animal tissues are not specifically discussed in this chapter, although many of the bioseparation principles and practices described below will be applicable.

8.2.2.1 Fermentation

Figure 8.1 shows a block diagram of a classical fermentation process comprised of the following process steps [1,2,4,5,18]:

- steam sterilization of the fermenter vessel and materials charged to it;
- feedstock pretreatment (e.g., solubilization, screening, etc.);
- addition of essential nutrients;
- adjustment of temperature and pH;
- heating and/or filtration of process air to combat contaminating microorganisms and phage;
- growth of an inoculum from a seed culture;
- inoculation of the fermenter; and, finally,
- the fermentation itself.

The types of microorganisms most frequently used in fermentations (i.e., bacteria, yeast, and fungi) are typically hardy, shear-resistant (with the exception of mycelial cultures), and quite demanding of oxygen — at least as compared to the types of mammalian cells more commonly exploited in cell culture operations (see below).

Fermenters take several physical configurations, all of which are designed to vigorously agitate and aerate their contents, to facilitate maintenance of aseptic operation, and to provide close temperature control. Most fermenters are sim-

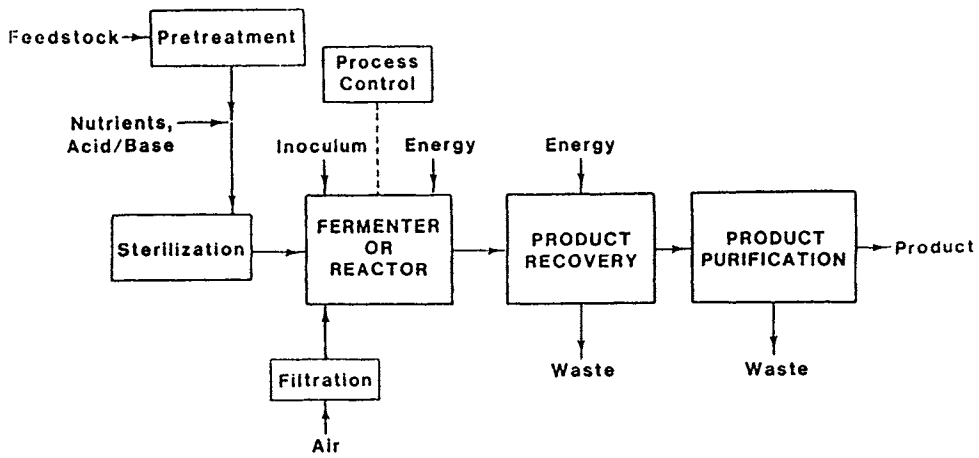

Fig. 8.1. Classical fermentation process diagram.

ply baffled and sparged stirred-tank reactors fitted with impellers, although very large airlift fermenters have been operated with good results within the past decade [19–21]. While continuous fermentation holds considerable promise and has recently met with some success, the vast majority of fermentations are still conducted batchwise with cultivation times ranging from a few days to a week or longer.

Whereas the comparatively low-value microsolutes of Table 8.2 are invariably made by microbial fermentation (at least when manufactured by biochemical routes at all), the comparatively high-value macromolecular products such as the therapeutic proteins of Tables 8.3 and 8.4 can be and are produced commercially by more than one method — i.e., by microbial fermentation, animal cell culture, or both techniques. That is, the choice of production process depends not so much on the identity of the desired product as it does on the nature of the biological host that produces it. For instance, recombinant Factor VIII:c, the blood-clotting protein that is lacking in hemophiliacs, is currently being produced competitively by two very different production technologies. One company relies on microbial fermentation, while a competitor employs mammalian cell culture. The same can be said of tissue plasminogen activator or t-PA. The various advantages and disadvantages of animal cell culture *vis-a-vis* microbial fermentation are examined in Section 8.2.2.2 below.

Fermentation media are generally complex, as illustrated by the list of typical media ingredients provided in Table 8.5, and fermentation product mixtures are necessarily even more complex. Table 8.6 summarizes the types of particu-

TABLE 8.5

Typical fermentation media ingredients (adapted from Ref. [39])

Carbon Source	Glucose
	Starch or flour
	Vegetable oils
	Molasses
	Lactose
	Sucrose
Nitrogen Source	Ammonium ion
	High protein sources (soy flour, corn gluten)
	Specialized sources (cornsteep liquor, yeast extract)
Phosphorus	Inorganic/organic phosphates
Calcium ($CaCO_3$)	
Magnesium ($MgSO_4$)	
Potassium	
Trace metals	

TABLE 8.6
Fermentation broth components

Class	Examples	Molecular weight	Size range (nm)
Particulates	Suspended solids	–	10,000–1,000,000
	Colloidal materials	–	100–1,000
Microorganisms	Yeasts	–	1,000–10,000
	Bacterial cells	–	500–3,000
	Viruses	–	30–300
Macromolecular solutes	Proteins and polysaccharides	10^4–10^6	2–10
	Enzymes	10^4–10^5	2–5
Microsolutes	Common antibiotics	300–1000	0.6–1.2
	Mono- and di-saccharides	200–400	0.–1.0
	Organic acids	100–500	0.4–0.8
	Inorganic ions	10–100	0.2–0.4
	Water	18	0.2

late, colloidal, macromolecular, and low-molecular-weight components that are commonly found in unclarified or "whole" fermentation broths, also referred to as fermentation beers. Each of these general categories of materials encompasses a large number of individual species. For example, a simple bacterium such as *E. coli* can contain of the order of 5000 distinct proteins.

As discussed further in Section 8.2.3 below, the complexity and considerable size range of materials present in unclarified fermentation broths present quite a downstream processing challenge, particularly for membrane-based processes. Other factors contributing to the difficulty of handling fermentation beers are their high solids contents and sometimes high viscosities (especially when mycelial cultures derived from molds and fungi are used). Given that even the plugging of valves and steam traps can be problematic in fermentation operations, it comes as no surprise that relatively fouling-prone membranes and membrane equipment face particular problems in this arena.

Aqueous fermentation broths are also typically fairly dilute (see Table 8.7). In the most favorable cases (e.g., the fermentation of simple organics like ethanol and citric acid), concentrations can approach values of moles per liter. However, the titer of the antibiotic penicillin G is typically only 30–40 mM — a level achieved only after some four decades of strain improvement boosted penicillin G concentrations by more than a hundred-fold [5]. Other important antibiotics are less than one-tenth as concentrated in their fermentation broths. Finally, we note that vitamin B_{12} is typically present in the fermenter effluent at a concentration of just 20 ppm by weight or so (i.e., about 15 μM). Many

TABLE 8.7
Component concentrations in fermentation broths

Fermentation product	Concentration in broth (%)
Ethanol	7–12
Organic acids	4–10
SCP biomass	3–5
Enzymes	2–5
Penicillin G	3–4
Lipids	1–3
Acetone/butanol/ethanol	1.8–2
Riboflavin	1–1.5
Erythromycin	0.4–0.6
Vitamin B_{12}	0.002

therapeutic proteins can be produced by dilute mammalian-cell suspension culture at concentration levels this high and higher.

Given the attention showered upon the so-called "new biotechnology" in the popular, scientific, and financial press of recent years, it might be tempting to dismiss classical fermentation processes as being rather archaic. However, this would be a serious mistake. Some of the first genetically engineered therapeutic proteins to reach the market were produced by microbial hosts harnessed in classical fermentation processes; examples include human growth hormone, hepatitis B vaccine, and t-PA. Furthermore, the past decade has witnessed a number of impressive advances in fermentation technology, including the operation of sizable airlift fermenters, large-scale continuous culture, and improved techniques for fermenter analysis and control. Fermentation remains a cost-effective technology, particularly for production of relatively simple biomolecules. It will continue to hold an important place in bioprocessing.

8.2.2.2 Cell Culture

Having said this, many recombinant therapeutic proteins — especially the larger and more complex ones — are produced by mammalian cell culture rather than fermentation despite the fact that fermentation is the more established and less expensive bioproduction technology. Bioreactor productivity explains much of this, with two factors operating to make the volumetric productivity of fermenters higher than that of cell culture reactors. In the first place, microorganisms like *E. coli* exhibit doubling times of the order of tens of minutes rather than the tens of hours more characteristic of animal cells in culture. Additionally, mam-

malian cells in suspension culture are generally much more dilute, typically growing only to cell densities that are lower by one to three orders of magnitude than those characteristic of their microbial counterparts in fermentation.

Notwithstanding these considerable advantages of fermentation, the greater versatility of mammalian cells makes them preferred hosts for the production of many recombinant proteins. Our focus here is on mammalian cell culture, although other types of animal cells, e.g., insect cells, have also been exploited in bioproduction. On the one hand, mammalian cells are generally capable of secreting their protein products into the media, in contrast to the situation with simpler cells like bacteria that often retain high levels of recombinant proteins within their cells in the form of insoluble protein precipitates or "inclusion bodies". The formation of inclusion bodies in microbial hosts necessitates additional bioprocessing steps — e.g., cell disruption, resolubilization, and protein refolding — that cannot always be accomplished successfully. In contrast, mammalian cells are not only more adept at correctly folding and processing recombinant proteins, but they also typically possess the machinery required to transport those proteins out of the cell. Finally, the therapeutic activity of many an important glycoprotein depends critically on the association of particular carbohydrate sequences with that protein. Mammalian cells are capable of effecting such post-translational protein modifications as glycosylation and proper disulfide bond formation.

Simple flasks and roller bottles are commonly used for laboratory-scale cell culture; indeed, roller bottles even suffice for the limited-scale production of certain vaccines. Viviculture, i.e., the use of whole animals as bioreactors, is frequently employed for the small-scale production of diagnostic monoclonal antibodies. In this technique, hybridoma cells are cultured within and ultimately harvested from the ascites cavity of the mouse. Technology is just now emerging to produce recombinant proteins in quantity with the help of transgenic animals capable of expressing desired proteins in the milk of such species as cows, sheep, pigs, and goats [22–24].

At larger production scales, equipment for the suspension culture of mammalian cells is strikingly similar to that used in fermentation. Stirred-tank and air-lift bioreactors are employed that range in size from a few hundred liters to a maximum capacity of about 10,000 L [20,21,25,26]. Indeed, it is not uncommon for conventional fermenters to be modified and pressed into service as mammalian cell bioreactors. Since mammalian cells exhibit greater sensitivity to shear and since they grow much more slowly than microorganisms, these modifications generally involve reducing the intensity of mixing and the rate of oxygen supply to the culture. Anchorage-dependent cells are typically grown in immobilized-culture systems that are based on microcarriers or microcapsules suspended in stirred-tank or fluidized-bed reactors, although packed-column and membrane bioreactors are also used to some extent in culturing

anchorage-dependent cells.

The cell types used in cell culture operations can be termed either "normal" or "permanent" depending on their source and lifespan. The former, generally used in manufacturing human vaccines, have finite lifetimes and complex nutritional requirements, and they are anchorage dependent. In short, they are difficult to work with in large-scale bioprocesses. On the other hand, the so-called "permanent" cell lines — e.g., newborn hamster kidney (BHK), Chinese hamster ovary (CHO), Vero, and hybridoma cells — can divide indefinitely and are more readily grown in suspension culture. Accordingly, they constitute the "workhorse" cell lines for cell culture. Well over two hundred different animal cell lines have now been employed in hybridoma and recombinant DNA work, and each has its own particular requirements for media, growth conditions, etc. The production of therapeutic proteins from potentially tumorigenic cells obviously demands that particular care be taken to ensure substantially complete removal of such potentially dangerous contaminants as viruses and cellular DNA.

Not surprisingly, the media used in mammalian cell culture are even more complex than those used in fermentation. Major components include perhaps a dozen amino acids at concentrations of ≈0.1–0.2 mM, several vitamins at ≈0.1 μM, inorganic salts, glucose at ≈5–10 mM, antibiotics such as penicillin and streptomycin to suppress bacterial growth, and phenol red as a pH indicator.

Traditionally, most cell culture media have also been supplemented with up to 10 vol.% of serum derived from the horse or calf — e.g., fetal bovine serum. Serum is obtained by allowing freshly collected blood to clot and then removing the complex liquid that remains [27]. In addition to containing numerous low-molecular-weight components (e.g., sugars, amino acids, vitamins, and metabolites), peptide hormones, and growth factors, serum also contains plasma proteins (e.g., albumin and the gamma globulins) as well as contaminants like bacterial endotoxins introduced after blood collection. The presence of these serum proteins considerably complicates the task of purifying recombinant proteins from serum-supplemented cell culture supernatants. For that reason — and in the interest of using better defined, more reproducible, and less expensive media — a major dynamic in the practice of mammalian cell culture involves eliminating or at least minimizing the amount of serum employed, replacing its essential components through the use of various defined media.

Table 8.8 illustrates the impact that the choice of bioreactor and amount of serum can have on the difficulty of separating and purifying an IgG immunoglobulin — in this instance, a monoclonal antibody — from cell culture supernatant [28]. The growth of hybridoma cells in mouse ascites fluid produces the highest antibody titer, but the product is present at low protein purity by virtue of its contamination with significant amounts of other murine (i.e., mouse-derived) proteins; moreover, ascites culture does not scale up readily. In con-

TABLE 8.8

Typical protein concentrations and purities obtained in various cell culture systems (from Ref. [53] with permission)

Source	Protein (mg/ml)	Total IgG (mg/ml)	Specific IgG (mg/ml)	Purity (%)
Ascites	20.0	6.0	6.0	30.0
Suspension culture				
10% FBS[1]	4.0	0.8	0.03	0.6
5% FBS	2.0	0.4	0.03	1.2
1% FBS	0.4	0.1	0.03	6.0
Serum-free	0.08	0.03	0.03	40.0
Hollow fiber culture				
10% FBS	6.5	5.2	5.0	75.0
Serum-free	5.3	5.0	5.0	95.0

[1]Fetal bovine serum.

trast, suspension culture is more scalable and controllable, but it typically produces much lower levels of the desired antibody — e.g., ≈30 mg L^{-1} in this instance. Moreover, at least when serum is employed, antibody purity is also rather low due to the presence of contaminating serum proteins (including other IgGs) that can be difficult to separate from the particular IgG antibody of interest. The advantage of a serum-free medium is thus readily apparent. Finally, Table 8.8 shows results obtained with an immobilized cell culture system based on entrapment and compartmentation of cells by protein-retentive hollow-fiber membranes. Relatively high antibody concentrations and purities are, in principal, attainable via such engineering approaches, which can be augmented by equally powerful biochemical techniques involving manipulation of cell growth conditions [29–31].

8.3 IMPLICATIONS FOR MEMBRANE BIOSEPARATIONS

8.3.1 Feedstream Characteristics and Process Constraints

The difficult nature of fermentation broths and cell culture supernatants presents a number of challenges in the recovery and purification of the various components contained within them.

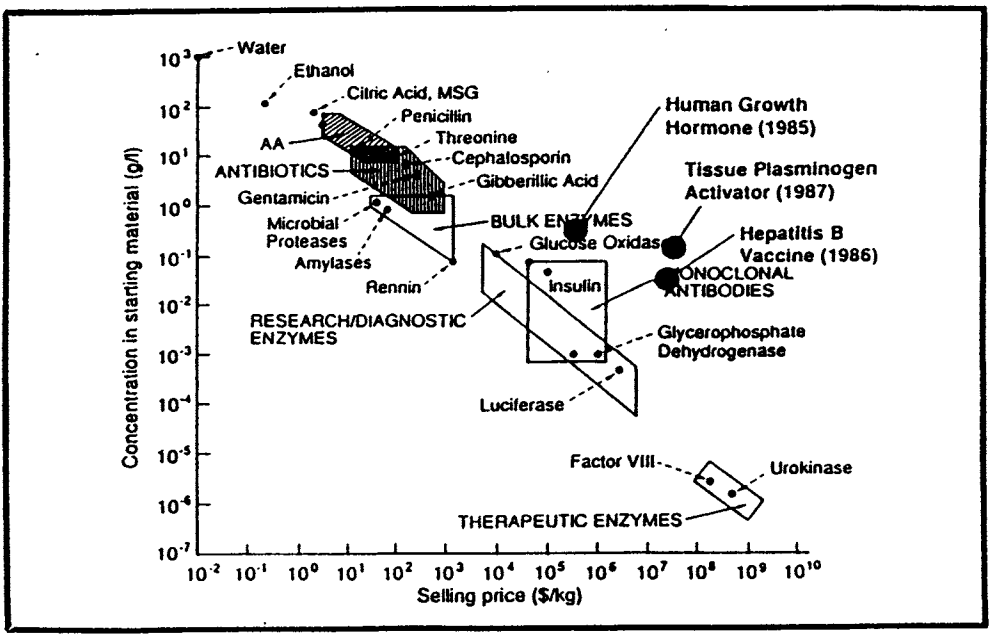

Fig. 8.2. Selling prices of various compounds versus initial concentrations (from Ref. [50] with permission).

8.3.1.1 Diluteness

As mentioned above, biological products are frequently present in fermentation broths and cell culture supernatants at concentrations of the order of a fraction of a millimole per liter or even less; thus, substantial dewatering is invariably required early on in most bioseparation process trains. The relationship between the ultimate selling price of a biologically derived substance and its initial concentration is shown in Fig. 8.2 [32–34]. This particular modification of the ubiquitous "Sherwood plot", well known to chemical engineers, makes it clear that the work (and cost) of separation correlates fairly well with the diluteness of the desired component in the starting mixture. However, low concentration alone cannot explain the particularly high costs of the three representative recombinant proteins included in Fig. 8.2 (i.e., human growth hormone, tissue plasminogen activator, and hepatitis B vaccine). Other factors obviously come into play where therapeutic proteins are concerned.

8.3.1.2 Mixture Complexity

One of these factors is mixture complexity (see Table 8.7). The combination of insoluble particulate and colloidal material, along with dissolved macro-

molecular and low-molecular-weight solutes, practically guarantees that a number of different types of downstream processing steps will be required.

8.3.1.3 Molecular Complexity and Instability

Proteins and glycoproteins are particularly complex chemical entities, characterized by a hierarchy of primary, secondary, tertiary, and quaternary structure. Retention of the biological activity of these proteins depends upon maintenance of a precise structure on all of these levels. An extreme example of the subtlety of these structural differences is provided by glycoprotein isoforms, which may differ from one another only in the particular sequence of residues on the carbohydrate moiety [35]. Bioassays aside, it can be extraordinarily difficult even to detect such differences by standard analytical methods, let alone base an efficient separation process upon them. More often than not, however, the physicochemical and biochemical richness of proteins leads to property differences that *can* be exploited for the purposes of protein selection and separation [36].

The tendency of many proteins to undergo denaturation must also be considered when choosing bioprocess operating conditions. It goes without saying that purification processes must not entail extremes of pH or temperature; however, other aspects of a protein's environment can be equally important to its stability. For example, chaotropic agents such as thiocyanate salts and detergents are widely used to displace sorbed proteins of certain classes from chromatographic media, but they must be used with great care since they are potentially denaturing. Other possible causes of protein denaturation include high concentrations of organic solvents (generally greater than about ten percent), traces of heavy metals (e.g., lead, iron, and chromium), the stripping of stabilizing cofactors from a protein, the presence of proteolytic contaminants in crude mixtures, adsorption at gas/liquid or liquid/solid interfaces, fluid shear, and oxidative cleavage of disulfide bridges. An advantage of membrane bioseparations is avoidance of chemical separating agents altogether.

With therapeutic proteins, even state-of-the-art analytical methods may be incapable of assessing whether the chemistry and structural integrity of a protein has been maintained during the course of its purification. In such cases, determination of therapeutic efficacy may be the only meaningful measure of a successful bioseparation.

Therapeutic proteins are not the only type of fragile bioproduct. It is well-known that many low-molecular-weight antibiotics are degraded at acidic pH values and/or at "high" temperatures (i.e., ambient and above). For this reason, the recovery of heat-labile antibiotics is frequently conducted at low temperatures (e.g., 4°C), and even then yield losses of 10% and more must sometimes be tolerated. Membrane processing can address certain of these yield issues.

8.3.1.4 High In-Process Value

The in-process value of a therapeutic protein may be extremely high — e.g., upwards of a thousand dollars per gram for a monoclonal antibody at or near the end of its purification train. This is a consequence of low bioreactor productivities (e.g., low antibody titers and cultivation times of a week and more), coupled with the difficulty of multistep downstream processing. Indeed, purification of a batch of cell culture supernatant can itself require two to three days of work with equipment that is itself expensive. As a consequence, purification mistakes can be costly. One industry anecdote centers on a process-scale immunoaffinity purification column worth some half a million dollars which was based on a $5000/kg antibody; this ligand and its support were rendered worthless when a process upset irreversibly fouled the column. Understandably, risk-averse biochemical engineers respond conservatively when presented with unproven membrane separation technologies.

Finally, overall product recovery is at a premium when unit values are high. Bioseparation processes comprised of five separate steps are not at all uncommon, and even more steps are necessary in some instances [37]. Single-step yields generally range from 80 to 90%. Figure 8.3 shows overall product yield expressed as a function of the number of separation and purification steps and

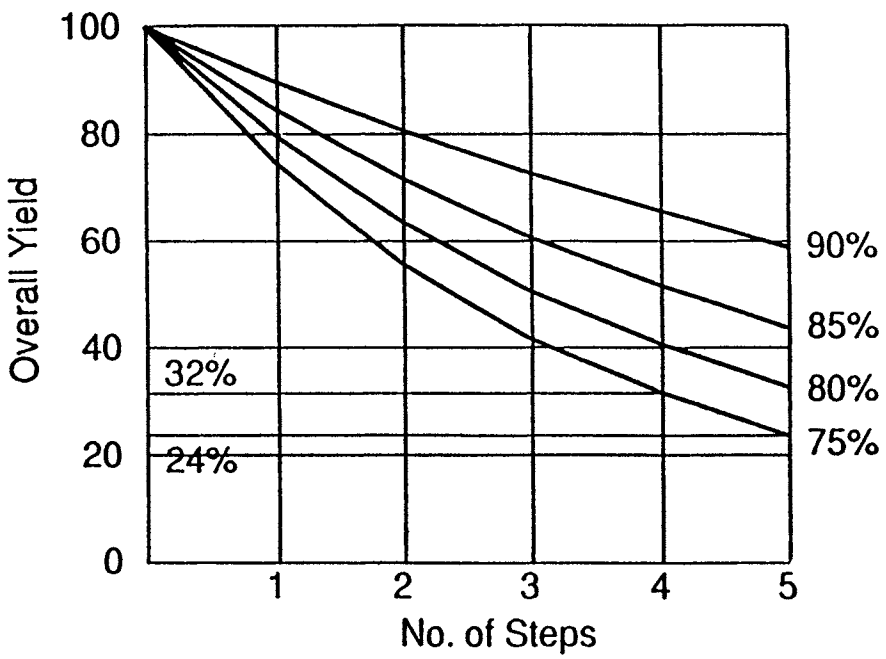

Fig. 8.3. Product yield in a multistep purification process.

the average fractional recovery obtained in each of those steps. It is painful to recover only one-fourth to one-third of the total amount of protein initially present, particularly after having invested a week or more of bioreactor time in production of the crude material. Hence, separation technologies like membranes that permit integration or elimination of purification steps can be highly leveraged.

8.3.1.5 Scale of Bioprocessing

While a few fermenters and mammalian cell culture bioreactors used in producing recombinant proteins have capacities as large as ten thousand liters, most cell culture is conducted on a considerably smaller scale — e.g., a few hundred liters or so. Small production scales contribute to high product costs. Indeed, annual production volumes correlate inversely with bioproduct prices in much the same fashion as concentration and price were shown related in Fig. 8.2 [38]. Buckland [27] has pointed out that a million doses (at 0.01–0.1 mg per individual dose) of an immunomodulator or vaccine translates to an annual production volume of just 10–100 g of protein. This quantity is comparable to the production scale of many diagnostic monoclonal antibodies. Production volumes are perhaps a hundred-fold larger for hormone drugs, but even so the annual production amounts only to a few kilograms per year per million doses — miniscule by the standards of more conventional chemical operations. Even antibiotics, some of which are administered at dosages of the order of a gram, require the annual production of just a metric ton or so of product per million doses. It is inescapable, then, that the production of high-value biologicals will seldom benefit from significant economies of scale.

8.3.1.6 Nature of Bioreactor Operation

The precise nature of the product stream that emerges from a bioreactor depends on a host of factors that inevitably vary somewhat from one production run to the next. Biological processes are incompletely understood at best, and the scope and effectiveness of on-line bioprocess analysis and control techniques are limited. The situation is further complicated by the inherent instability and unpredictability of many cell lines in cell culture operations.

The batchwise nature of fermentation and cell culture — coupled with lot-to-lot product stream variability — necessitates the adoption of batch as opposed to continuous separation protocols. Individual bioreactor lots may be pooled into larger lots to facilitate downstream processing and to ensure quality control.

The opportunity for the molecular biologist and bioreactor engineer to impact the nature and difficulty of downstream processing operations cannot be

overestimated. We have already noted the trend toward the use of reduced-protein or protein-free serum supplements for mammalian cell culture, which significantly reduces the burden of contaminating proteins that must be dealt with downstream. By the same token, molecular biologists have considerable freedom in the selection and engineering of host organisms or cell lines to be used for a particular bioproduction task. By selecting a host that is capable of producing an *extra*cellular product (ideally having undergone all appropriate post-translational modifications), one can avoid the need to recover, resolubilize, and renature a protein that might otherwise have been produced in the form of *intra*cellular inclusion bodies.

8.3.1.7 Purity Requirements

The purity demanded of a biological product clearly depends on its ultimate use. For instance, the standard of purity of a crude food-grade, industrial, or detergent enzyme may be quite low. Similarly, the acceptable purity of an enzyme or antibody used in a diagnostic device might also be rather low — e.g., 75% or so — although complete removal of interfering or cross-reactive proteins might be necessary.

In contrast, "several nines" protein purity may be required where therapeutic-grade proteins are concerned, thereby requiring several log reduction of contaminants. Not surprisingly, required protein purity has also been shown to correlate well with selling price [40]. Moreover, substantially complete removal of endotoxins, DNA, proteolytic degradation products, protein mutants, deamidated protein forms, microbial contaminants, viruses, and mycoplasma is generally necessary for therapeutic products [41]. Indeed, the question is not so much what should be removed as it is what it is possible to remove. If the presence of a particular contaminant can be detected by available analytical methods, it will often be a matter of concern to regulatory agencies such as the FDA, which may then dictate its removal to near limits of detection — assuming that the technology required to achieve this level of purification exists.

The issue of ultrapurification is particularly germane to the use of membranes, since membrane-based separations are generally more effective in performing crude or bulk separations than they are in achieving high purities or removing trace contaminants. However, all separation technologies — even such high-resolution procedures as chromatography and the various electrophoretic methods — can be severely challenged by certain difficult bioseparations.

8.3.1.8 Nature of Bioprocess Development and Regulatory Issues

Speed and reliability often take precedence over elegance and efficiency in bioseparation process development. Initially, the investigation of a new bio-

pharmaceutical proceeds slowly, with at least five to seven years often being required to prove out the potential of a promising drug in preclinical and clinical trials. However, once this potential is established, the pressure to scale up production technology and to "freeze" the chosen process for final product/process approval by regulatory authorities becomes immense. Because biopharmaceuticals are largely defined by the process used to make them, a therapeutic product and its production process are essentially indistinguishable. Thus, FDA approval is quite specific to a given manufacturing process. Once the Drug Master File (DMF) for a product has been submitted to the FDA, subsequent process changes are only rarely and grudgingly made, inasmuch as process modifications must be validated from the point of view of not affecting the product in any significant way. Hence, process changes are time-consuming, risky, and expensive. The objective, then, is to develop an acceptable bioproduction/bioseparation process in a reasonably short time, even if this involves sacrificing some process efficiency or economy. The winning process is sometimes the one that works first — not necessarily best. All in all, these circumstances bode well for membranes, since their scalability facilitates rapid and reliable process development.

8.3.1.9 Contamination Control and Containment

Contamination control relates to protection of bioreactors and their products from inadvertent contamination by microorganisms, phages (bacterial viruses), and bacterial endotoxins. Containment refers to protection of bioprocess personnel from exposure to pathogenic organisms. Humphreys [8] has noted that, while accomplishing either one or the other of these objectives is relatively easy, accomplishing both at the same time is quite another matter.

Membranes are attractive because they are closed systems, unlike centrifuges that compete with membranes for various cell harvesting and clarification tasks. Membranes serve as effective barriers — both to the intrusion of potentially harmful species into bioreactors and to the escape of such species from them and into the environment [42].

8.3.1.10 Economic Considerations

Although economics may not drive the design of a bioseparation process for a high-value biopharmaceutical, lowering purification costs obviously improves profitability. Indeed, minimization of product recovery and purification costs can be all-important to a product's competitiveness where many of the lower-unit-value commodities derived by fermentation are concerned (e.g., antibiotics and organic acids).

Dogma has it that the costs of separation and purification typically represent about 50–90% of "total" pharmaceutical production costs [43–46]. Purification costs as a fraction of the total production costs are generally lower for bulk fermentation products like the penicillins [47] and considerably higher for more complex therapeutic proteins. Cost of goods sold (COGS) represents roughly 5–25% of the sales price of traditional pharmaceuticals like antibiotics, and as much as 10–40% of the selling price of the large glycoprotein biopharmaceuticals. Application of these rules of thumb suggests, for instance, that the COGS for a $200 million/year therapeutic protein like tissue plasminogen activator might be of the order of $50 million/year — with separation and purification accounting for most of that cost. The market for cost-effective membrane technology is evident.

8.3.2 Bioseparation Process Design

8.3.2.1 Process Flowsheets

While they may differ in detail, most bioseparation processes have certain key elements in common. Most bioseparation processes include one or more of the following steps [3,33,48]:

(i) *removal of insolubles* (e.g., cell harvesting or clarification);
(ii) *product recovery and isolation* (e.g., concentration and partial enrichment of products);
(iii) *purification*, frequently multi-step; and
(iv) *product polishing* (e.g., final contaminant removal, product formulation, and sterile filtration).

Traditionally, membranes have played important roles in product recovery and product polishing operations (e.g., sterile filtration). Only recently have membrane-based processes been developed which possess sufficient resolution to permit them to tackle purification tasks. The emerging technology of affinity membranes provides an example of this [49].

Figure 8.4 shows a generalized process flowsheet that illustrates three alternative bioseparation pathways that are appropriate to cellular, extracellular, and intracellular products. The most straightforward situation results when the desired product is the cell mass itself (e.g., single cell protein, bakers' or brewers' yeast); here, little more than cell washing and drying may be required. Where the product is extracellular, the crude bioreactor effluent must be clarified by removal of insolubles prior to recovering the product from the resulting solution. Finally, where the desired product is intracellular, several intermediate steps are required to free the entrapped product. After the cells are harvested, washed, and dewatered, the cell walls are disrupted by mechanical or

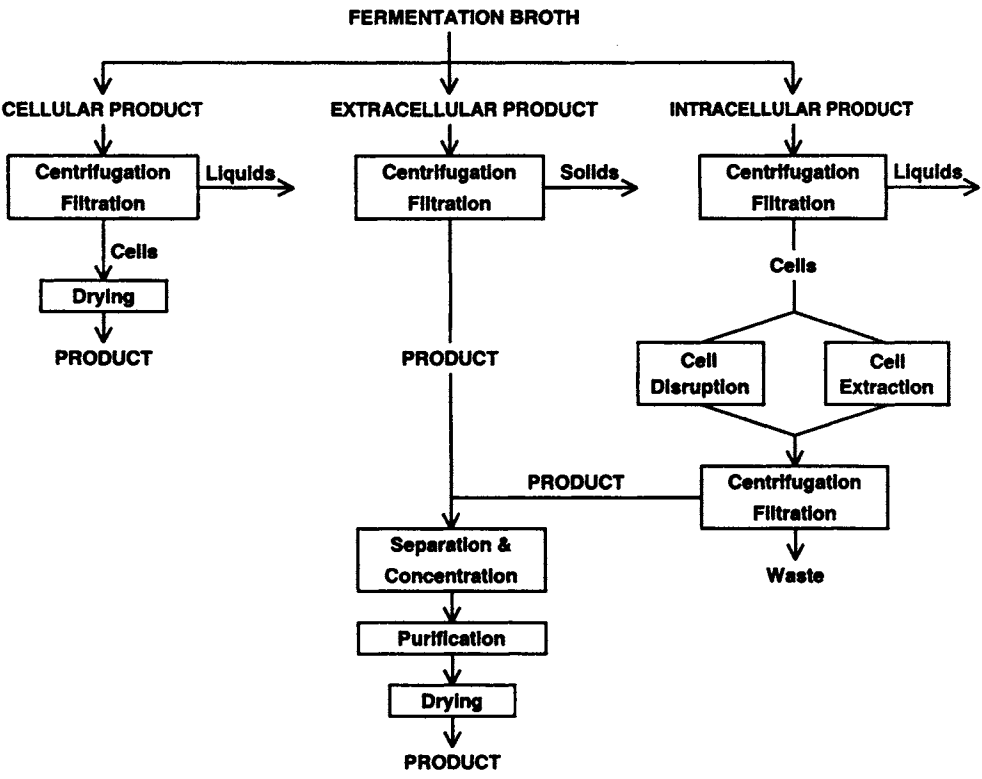

Fig. 8.4. Generalized biochemical separation process flowsheet.

chemical means in order to release their intracellular contents into what becomes an exceedingly complex mixture. Hopefully, filtration or centrifugation then produces a "clear" liquid that can then be treated in the same manner as a clarified stream containing an intracellular product.

Detailed but representative process flowsheets are provided in various references for each of these three principal bioproduct types — specifically, for antibiotics [50], for intracellular enzymes [50], and for monoclonal antibodies produced from various sources [51–53].

8.3.2.2 General Principles and Guidelines

Previous authors have presented various heuristics and general strategies for the design of bioseparation processes [3,40,54–56]. A few of the more important ones follow:

- Characterize the product and its major contaminants as thoroughly as possible prior to bioprocess design.

- Encourage the molecular biologist and bioreactor engineer to plan ahead for product purification.
- Choose steps that exploit the biggest differences in properties of the product and its contaminants.
- Use a separation based on a given physicochemical or biochemical principle only once in the separation train (i.e., employ "orthogonal" techniques).
- Dewater early and follow dilution by volume reduction.
- Schedule the most effective separation step(s) early (i.e., those with high capacity and selectivity).
- Separate the most plentiful impurities at the earliest opportunity.
- Schedule the most expensive and arduous step last to take advantage of volume reduction upstream, since capital and operating costs generally scale with solution volume.
- Where possible, keep it simple.

Obviously, these general rules are frequently broken; indeed, they sometimes conflict with one another. Nonetheless, the application of these principles often dictates precisely how and even whether membranes will be considered for a given bioseparation step.

8.4 MICROFILTRATION AND ULTRAFILTRATION IN CELL HARVESTING AND CLARIFICATION

Historically, microfiltration (MF) and ultrafiltration (UF) have been the most prominent membrane bioseparations. Below, we consider their application to the solid/liquid separations involved in the harvesting of cells and in the clarification of whole fermentation broths and cell culture supernatants. Since some downstream processing operations like chromatography demand "gin clear" feedstreams [54], this can be a tall order.

8.4.1 General Considerations

8.4.1.1 Rationale for Cross-Flow Filtration

As shown in Fig. 8.4, the first operation to be accomplished in most any bioseparation process is removal of insoluble material. The separation of cells and cell debris presents several difficulties, especially where the conventional approaches of centrifugation and rotary drum vacuum filtration are concerned [1,2].

On the one hand, the "solids" present in fermentation beers and cell culture supernatants vary widely in size, ranging from fractions of a micron (e.g., colloidal cell debris and cell fragments) up to tens of microns in size (e.g., whole cells). Specifically, microorganisms such as the bacterium *E. coli* are approximately 1 μm in diameter and 2 μm long, and yeasts (e.g., *S. cerevisiae*) are somewhat larger at about 8 μm by 5 μm. Mammalian cells are significantly larger yet; for instance, CHO cells in suspension culture have an effective diameter of ≈14 μm, while hybridoma cells range in size from about 12 to 20 μm [57]. Moreover, these cells, comprised as they are of about 80–85% water, differ little in density from the liquid medium in which they are suspended. Accordingly, the efficiency of centrifugation suffers from the fact that sedimentation velocities for these materials are generally low and wide-ranging; "clean" solid/liquid separations are sometimes unattainable. Prior to the development of a membrane alternative, however, centrifugation was the only viable approach to cell harvesting.

The application of conventional rotary drum vacuum filters for cell removal and clarification is similarly problematic. Cells, which are frequently glutinous, tend to form cohesive, poorly draining, and compressible filter cakes. Such cakes generally have low hydraulic permeabilities, thus limiting the productivity of conventional filtration. Additionally, the need to employ filter aids (e.g., diatomaceous earth) introduces additional complications. Diatomaceous earth disposal costs are high and ever increasing.

In recent years, cross-flow MF and UF have emerged as effective and economical competitors to centrifugation and conventional filtration processes in these applications [12,44,58–60]. The advantages of cross-flow filtration are several:

- potential for high solids recovery and production of a relatively clear permeate;
- simple product washing, since the need to resuspend centrifuged solids is avoided;
- avoidance of filter aid purchase and disposal costs; somewhat lower capital costs;
- biological containment and avoidance of aerosols; and
- simple temperature control.

Disadvantages include the following:

- significant membrane replacement and pumping costs;
- higher water content in the recovered solids — i.e., dense slurries as opposed to pastes; and
- time-dependent, hard-to-control operation.

Generally speaking, cross-flow membrane filtration will be most competitive where one of the following conditions exist:

- the cells are shear-sensitive (e.g., mammalian cells as opposed to microorganisms);

- the solid/liquid density difference is small (e.g., less than 0.1 g/cm^3);
- the scale of operation is small (e.g., batch sizes under several thousand liters); and
- the initial solids concentration is relatively high (e.g., greater than ≈15%).

8.4.1.2 Membrane Characteristics

Both microfiltration membranes and ultrafiltration membranes (especially those with MWCOs greater than about 100–300 kD) are equally capable of retaining cells, since the pores of both types of membranes are orders of magnitude smaller than cells [59,61,62]. Thus, both membrane types can be used in cell harvesting, cell washing, and clarification operations. The choice between them is dictated by such considerations as relative transmembrane fluxes, fouling rates, and the overall process objective.

For example, only MF membranes have the potential (albeit not always the ability) to pass macromolecular solutes like proteins into the permeate while retaining cells. This permselectivity recommends MF membranes where recovery of an extracellular protein is the ultimate objective. In other contexts, it is desired that the membrane retain proteins as well as cells and cell debris — e.g., in the clarification of an antibiotic-containing fermentation broths. Here, the clarified permeate should be devoid of proteinaceous impurities, and ultrafiltration is the membrane process of choice. Examples of each of these situations and membrane choices are provided in Section 8.4.2 below.

Membrane and module materials for use in bioprocess applications should at minimum be chemically sanitizable (e.g., with sodium hydroxide and/or hypochlorite solutions). In particular, fouled membranes should be capable of being cleaned or regenerated after use. (Typical sanitization and cleaning solutions — along with strategies for minimizing membrane fouling in the first place — are discussed in Section 8.6 below.) In certain applications, it may be desirable that the membrane, module, and system be sterilizable, but many membranes and modules are incapable of surviving contact with live steam or withstanding the severe conditions involved in autoclaving (e.g., 121°C for 30 minutes). One interesting approach to this problem involves the development of hollow-fiber membrane modules which are sufficiently inexpensive to be disposed of after a few uses [63]. Such a strategy is obviously unthinkable with systems based on difficult-to-replace and expensive flat-sheet cassettes constructed of stainless steel.

Much of the process equipment used in fermentation and cell culture operations is designed for "steam-in-place" sterilization, and this capability (or at least "clean-in-place" design) may be demanded of membrane systems. Where sterility and/or containment are issues, membranes, modules and system connections must pass various integrity tests (e.g., the pressure hold, diffusion, and

bubble point tests) to insure that housing seals and membranes are free of leaks or defects. Finally, membranes and membrane devices must not shed particles or contribute leachables or pyrogens to the process stream. The configuration of the membrane module is not critical, although feed channel dimensions must clearly be large enough to permit aggregates of suspended solids to pass. Module design and operating conditions (in particular, feed flow rate and pressure drop) must be chosen to avoid potentially damaging fluid shear rates. Shear-induced damage, while generally of little concern with proteins and microbial cells, can be a problem with relatively fragile mammalian cells (see below).

In the following sections, we present some general operating guidelines for and several examples of the application of MF and UF membranes in cell harvesting and in the clarification of fermentation broths and cell culture supernatants. We have emphasized the experience of fermentation and biotechnology industry personnel with real applications — as opposed to the experience of membrane proponents with "model" separations.

8.4.2 Separation of Microbial Cells

8.4.2.1 Microfiltration

Where available, past experience is undoubtedly the best guide to predicting membrane performance (i.e., flux, selectivity, and fouling rate) in a given bioprocess application. At this writing, theory and equations are of limited practical use. Defrise and Gekas [64] and Hanisch [59] provide tables that summarize a considerable body of experience with the application of both MF and UF membranes in microbial and mammalian cell systems. Generally speaking, it is easier to separate microorganisms with membranes than it is to separate mammalian cells, since the former are less shear sensitive. Where microorganisms are concerned, relatively large yeast cells like *S. cerevisiae* are more readily separated than smaller bacteria like *E. coli* [65].

Merck investigators [65] recently evaluated three types of microporous membranes for the harvesting and diafiltration of low- and high-cell-density fermentations of a recombinant yeast (*S. cerevisiae*) and a recombinant bacteria (*E. coli*). Hollow-fiber and flat-sheet modules containing about 0.5–2.5 m^2 of various 0.05 to 0.45-μm pore-size membranes were operated at feed pressures of 70–230 kPa (10–33 psig) in a test system designed to process whole, unconditioned fermentation broth (see Fig. 8.5). Yeast and bacteria cells were first concentrated four-fold, diafiltered with cold (4°C) buffer (see Section 8.5), and then concentrated once again to a final cell density of about 50% — thereby producing cell suspensions some ten to twenty times more concentrated than

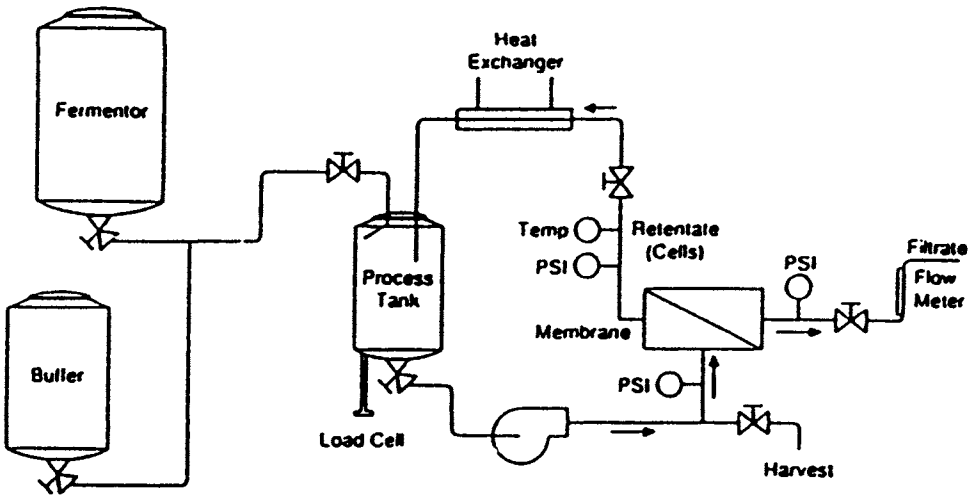

Fig. 8.5. Cell harvesting and diafiltration by cross-flow microfiltration (from Ref. [65] with permission).

the initial fermentation broths. The intermediate diafiltration step served to wash the cells and remove soluble components that might otherwise have interfered with other downstream processing operations.

Two-hundred liter batches of fermentation broth (corresponding to five hundred liters of filtrate in some cases) could be successfully processed in this manner in two hours or less. Short processing times are desirable since these minimize the potential for product degradation.

Filtrate fluxes varied considerably among the membranes and fermentation systems considered, with typical values ranging from about 25 to 100 $L/m^2 h^{-1}$. *E. coli* harvests were generally slower and somewhat more sensitive to cell density than harvests of the yeast *S. cerevisiae*. Kroner and co-workers [66–69] have also investigated cross-flow microfiltration for bacterial harvests, and they conclude that filtrate fluxes should be at least 100 $L/m^2 h^{-1}$ to be competitive with centrifugation at large scales.

Cross-flow microfiltration occupies a particular niche in harvesting cells characterized by densities very near those of the fermentation broths containing them. A case in point is provided by oleaginous yeast cells (e.g., *A. curvatum*) which, by virtue of their high fat content, exhibit a cell-vs.-broth density difference less than one-third that seen with *S. cerevisiae* [70]. Cross-flow MF and UF successfully concentrate such low-density yeast cells under conditions where centrifugation suffers from poor volumetric productivity (see Fig. 8.6). Interestingly, an ultrafiltration membrane (Romicon PM50) provided

somewhat higher average fluxes and concentration factors than the single microfiltration membrane tested. Indeed, a number of investigators have observed that higher fluxes may be realized with small-pore-size as opposed to large-pore-size membranes in cell harvesting and clarification applications [64,65,71,72] — or at least that filtrate flux is surprisingly independent of pore size and pure water flux [61,73]. Such observations are easily misinterpreted, however, and so we return to elaborate on this point in Section 8.6.1 below.

Wichmann and co-workers have published a particularly thorough comparison of centrifugation and cross-flow microfiltration for the harvesting of microbial cells [60]; their objective was assessment of alternative methods for enhancing the productivity of an amino-acid-producing fermenter by means of cell recycle. While both centrifugation and microfiltration were deemed competitive in this application, centrifugation was ultimately recommended on the basis of its greater reliability and higher volumetric productivity. The greatest advantage of membranes was their ability to produce a relatively clear filtrate; however, membrane fouling was problematic.

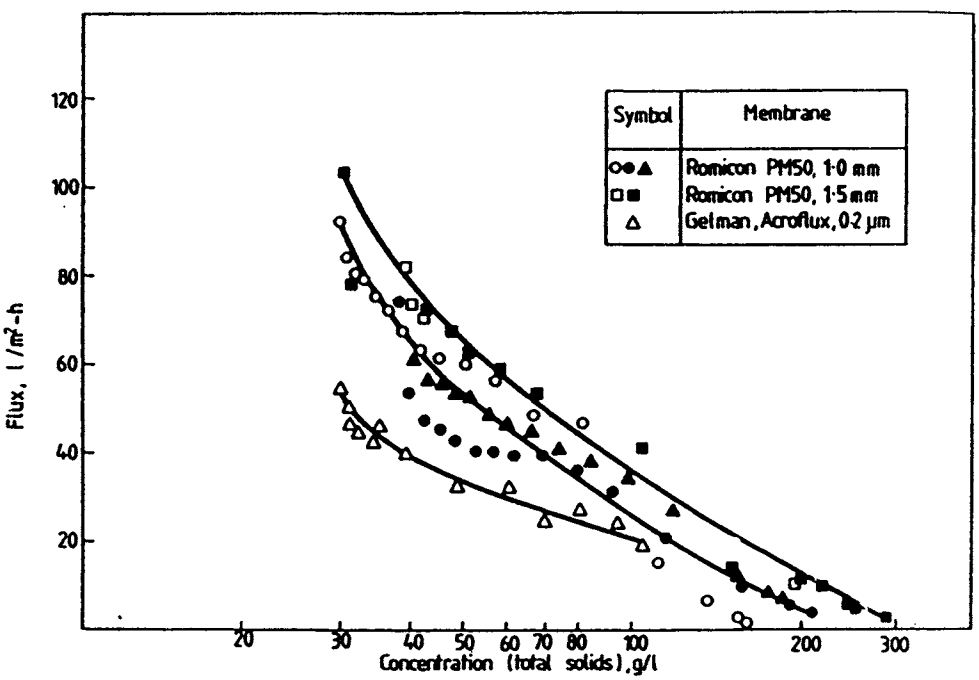

Fig. 8.6. Concentration of low-density yeast by cross-flow MF and UF (from Ref. [70] with permission).

8.4.2.2 Ultrafiltration

Since the filtrate fluxes obtained when ultrafilters are used to process fermentation broths and cell culture supernatants are often comparable to those afforded by microfilters, it comes as no surprise that ultrafiltration has also been used in cell harvesting and clarification operations. However, where it is desirable to retain proteins and other macromolecular species (e.g., polynucleotides) as well as cells, ultrafiltration is the membrane clarification process of choice. Such instances arise, for example, where low-molecular-weight fermentation products like antibiotics are to be recovered and purified.

Ultrafiltration membranes useful in cell harvesting will typically have molecular-weight cut-off (MWCO) values of at least 100–300 kD. Zahka and Leahy [61] have compared cross-flow MF and UF (referred to as "tangential flow" operations) in the separation and concentration of three types of microorganisms. Parameters examined in their study included operating pressures and feed flow-rates (i.e., fluid shear rates), temperature, cell concentration, medium components, antifoam concentration, and membrane cleaning techniques. As shown in Fig. 8.7, a 100 kD MWCO UF membrane and a 0.2-μm MF membrane gave similar permeate fluxes in processing an *E. coli*-containing fermentation broth.

In their production-scale tests, a 400-L batch of cell suspension was processed with 2.3 m^2 of this 100 kD MWCO UF membrane housed in a flat-sheet cassette-type module. Inlet and outlet pressures were controlled at about 275 and 170 kPa (40 and 25 psig) respectively, and the cell suspension was recirculated through the unit at a flow rate of 800 L h^{-1} by means of a screw pump. Cells were

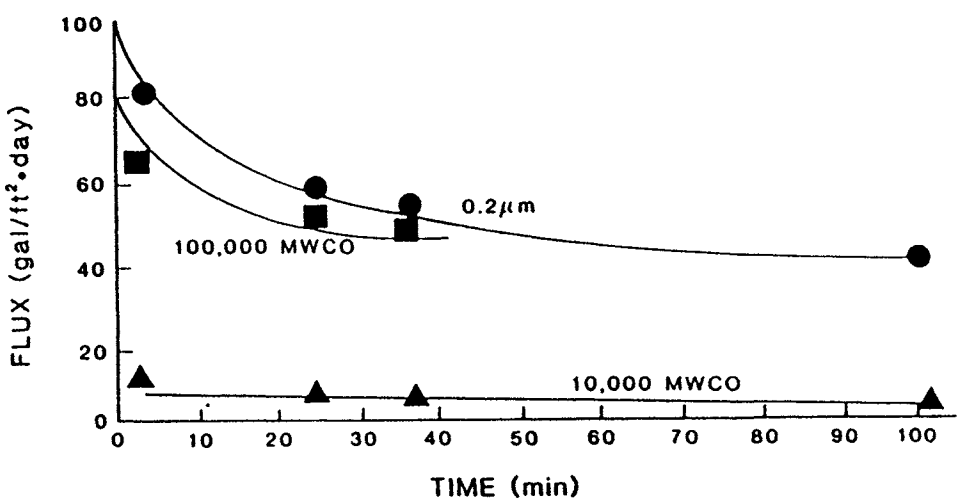

Fig. 8.7. Effect of membrane pore size on permeate flux: *E. coli* cell harvest (from Ref. [61] with permission).

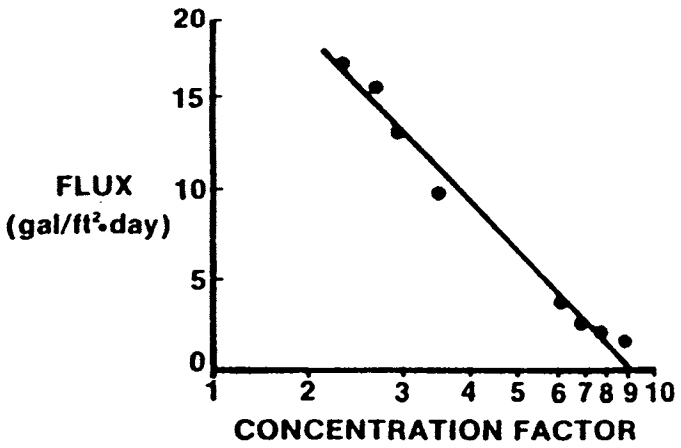

Fig. 8.8. Effect of cell concentration on flux: *B. thuringiensis* cell harvest (from Ref. [61] with permission).

concentrated by a factor of twenty in six hours at an average filtrate flux of 26 $L/m^2\ h^{-1}$. Figure 8.8, obtained for the harvest of *B. thuringiensis* cells, exhibits precisely the inverse dependence of filtrate flux on cell concentration that is expected from theory.

A rather early and courageous large-scale application of ultrafiltration for clarification involved processing an *N. lactamdurans* broth containing the antibiotic cephamycin C, an extracellular fermentation product [74]. This Merck facility produced twenty-eight 55,000-L batches weekly of a difficult-to-clarify broth that required extensive pretreatment prior to recovery and purification of cephamycin C by ion exchange. Preliminary experiments showed that rotary drum vacuum filtration suffered from low filtration rates even with added filter aid; moreover, cephamycin C recovery was poor despite attempts to improve it by reslurrying the cake and filtering for a second time. Centrifugal separation was also problematic due to slow sedimentation rates and the formation of a dilute sludge that retained a considerable amount of the product; several resuspension/centrifugation cycles were required to achieve adequate yields. Given the limitations of both of these conventional approaches to the separation of fermentation solids, UF membranes were evaluated and found attractive.

Spiral-wound and hollow-fiber module designs were tested but rejected due to their tendency to become clogged with broth solids, either at the flow-channel inlet or within the module as dewatering proceeded. Dorr-Oliver thin-channel flat-leaf Ioplate modules (now available from the Amicon Division of W.R. Grace) were specified that contained a total of about 1070 m^2 of a 24 kD MWCO Dynel (PVC/PAN copolymer) membrane. Pretreatment upstream of the bank of UF modules consisted of chilling the fermentation broth and passing it through a 30-mesh screen.

The unclarified feed was supplied to the UF modules at an inlet pressure of 414 kPa (60 psig), and the system was operated at a feed-to-permeate flow rate ratio of 10-to-1. Each batch was initially concentrated to about one-third of its original volume by ultrafiltration. As the filtrate flux began to fall due to the increasing solids content, the batch was then diafiltered with water (see Section 8.5) until the desired objective of 98% cephamycin C recovery was achieved, albeit at the expense of dilution of the antibiotic with the diafiltrate. Protein retention was not measured but was probably very high. Membrane lifetime ranged from 600 to 1000 batches. Additional useful information on operating conditions, cleaning protocols, process control techniques, and other practical matters is provided in the original reference [74].

In summary, ultrafiltration was found superior to rotary drum vacuum filtration in this application for several reasons:

- UF afforded 98% antibiotic recovery as compared to the 96% recovery attained with the conventional reslurry–refiltration process;
- UF system materials costs (including membrane replacement) were one-fourth those of precoat filtration;
- UF required one-third the operating labor; and
- the UF system capital cost was 20% lower than that of the additional rotary drum vacuum filtration capacity required, even disregarding the additional burden that filter aid disposal would have placed on waste treatment facilities.

For a design and cost analysis of an antibiotic clarification process based on cross-flow microfiltration as opposed to ultrafiltration, the reader is referred to another recently published membrane handbook [75].

8.4.3 Separation of Mammalian Cells

As compared to the separation of microbial cells, relatively little information has been published on the large-scale application of cross-flow membrane filtration to the more difficult task of separating mammalian cells from cell culture supernatants. Typically, this operation is conducted for the purpose of producing a clarified stream suitable for recovery of an extracellular product, usually a therapeutic protein. Because of the macromolecular nature of these products, microfiltration rather than ultrafiltration is generally required in these applications.

The fragility of mammalian cells distinguishes them from bacteria and yeast and makes separation of the former much more challenging. In processing mammalian cells, particular care must be taken not to stress them beyond the point at which sublethal cell damage or even cell lysis can occur. The lysis of cells and the accompanying release of their contents into the supernatant can introduce particularly troublesome contaminants. For example, even trace

amounts of foreign DNA constitute an unacceptable impurity in therapeutic proteins, and the lipid components of cell membranes and organelles are particularly severe foulants of synthetic polymeric membranes. To complicate matters still further, the sensitivity of mammalian cells to interfacial and fluid stresses is exacerbated by the use of low-protein and serum-free media. Elucidation of safe yet productive membrane system operating conditions is a preoccupation of biochemical engineers responsible for developing bioseparation processes downstream of mammalian cell culture operations.

In this regard, Maiorella et al. at Cetus Corp. (now Chiron) have practiced a systematic and instructive methodology for the determination of conditions at which to operate MF systems for the clarification of cell culture suspensions [76]. They evaluated five laboratory- and pilot-scale membrane systems varying in size from a few hundred square centimeters to several square meters — namely, Millipore's Minitan and Prostak flat-sheet cassettes, Dorr-Oliver's Ioplate thin-channel system, and Microgon's MiniKros and KrosFlo hollow-fiber systems. Four factors with the potential to cause cell damage were considered: (i) fluid shear, (ii) TMP-induced deformation and lysis of cells within membrane pores, (iii) fluid turbulence, and (iv) damage in pumps. The third and fourth of these potential causes of cell damage were deemed relatively unimportant. Specifically, turbulent flow conditions characterized by Reynolds numbers up to 71,000 did not measurably affect cell viability. Neither did cells suffer significant damage in positive displacement rotary lobe pumps when impeller tip speeds were kept below 350 cm s^{-1}. However, fluid shear and TMP-induced cell deformation and lysis were determined to be matters of legitimate concern.

Various investigators have shown that the viability and integrity of mammalian cells can be affected by shear and the attendant cell distortion experienced in laminar flow fields [77–83]. The lysis of animal cells occurs when the shear stress imposed on them exceeds some critical value which depends on the type of cell, its growth conditions and solution environment, and the particular measure of cell damage employed. Lysis-free operation dictates that a membrane system be operated so as to keep the maximum fluid shear rate comfortably beneath that value which, when multiplied by the fluid viscosity, corresponds to the critical shear stress of the type of cell at hand. This critical cell shear stress (and associated fluid shear rate) is probably best determined on a case-by-case basis, since published values vary widely. In the above-cited Cetus study, appreciable damage to the five animal cell lines investigated began to occur at wall shear rates in excess of about 3000 s^{-1}.

A second operating limit is associated with the TMP-induced deformation of cells into the pores of microporous membranes bridged by them — a phenomenon quite capably addressed by Zydney and Colton [84] in the context of membrane plasmapheresis. Simply stated, the Zydney/Colton theory relates

red blood cell hemolysis to the time-dependent strain experienced by the membrane of a viscoelastic red cell as it resides at the mouth of an MF membrane pore. The magnitude of this strain is a function of two factors: (i) the transmembrane pressure, and (ii) the shear-rate-dependent residence time of a cell at the membrane pore mouth. Cell lysis occurs when the critical strain for lysis is exceeded before a cell is swept away from the pore opening by the tangential flow field. Given a value for the wall shear rate, the Zydney/Colton model predicts the critical cell membrane tension at which lysis just begin to occur; this critical cell membrane tension can be related, in turn, to a more pragmatic parameter — namely, the product of microfiltration membrane TMP and pore diameter. The net result is a map of MF membrane operating conditions that delineates regions where the wall shear rate, membrane pore size, and transmembrane pressure are such that erythrocyte suspensions can be safely processed without hemolysis.

Maiorella et al. assumed that cell lysis induced by this mechanism of pore deformation would be no more severe for their cultured animal cells than for erythrocytes. Thus, they resolved to operate their clarification membrane system at conditions beneath the solid line of Fig. 8.9, which corresponds to the predictions of the Zydney/Colton model and corroborating experimental data for erythrocyte hemolysis. By the same token, Maiorella et al. resolved to

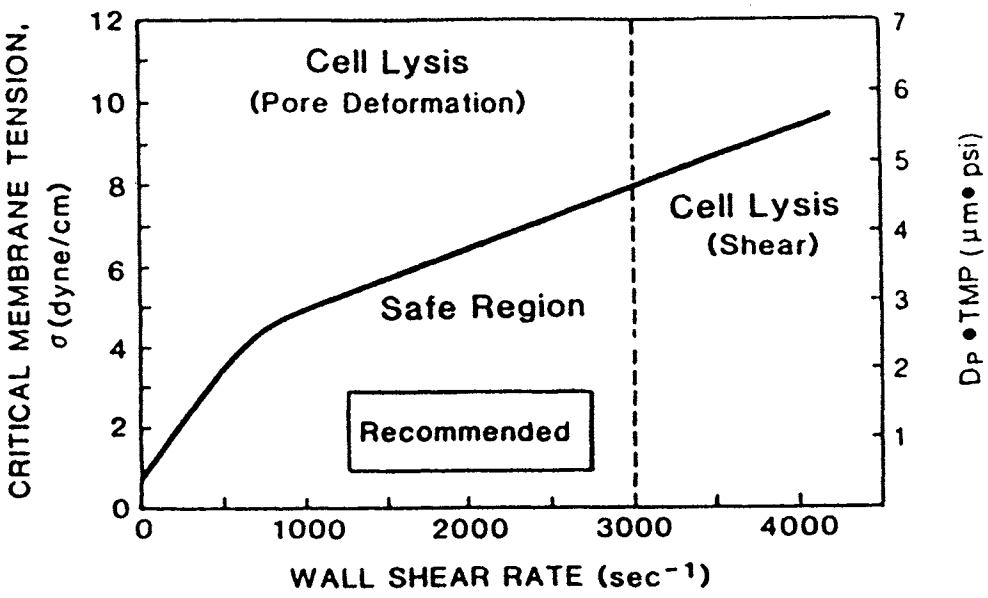

Fig. 8.9. Operating regimes for the cross-flow microfiltration of mammalian cells (from Ref. [76] with permission).

operate at wall shear rates lower than 3000 s^{-1} (i.e., in the region to the left of the vertical dashed line of Fig. 8.9), since this was the critical shear rate found to induce lysis of their cultured animal cells.

At this point the reader must be cautioned not to rely too much on the quantitative aspects of Fig. 8.9 — i.e., on the numerical value of the critical shear rate capable of inducing cell lysis — since these features of Fig. 8.9 depend on the particulars of the type of cell at hand. Rather, it is the general approach to the problem of determining safe membrane operating conditions that we wish to bring to the reader's attention and recommend.

After operating conditions have been identified at which a cell suspension can be filtered safely, maximizing permeate flux becomes the next priority. The most effective system designs and operating protocols control the filtration rate directly, while the transmembrane pressure is permitted to "float" within preset limits, seeking that value which produces the predetermined flux [75,76,85,86]. This strategy, which evolved in the context of membrane plasmapheresis [87,88], generally gives higher sustained fluxes than afforded by the more conventional control strategy wherein membrane module inlet and outlet pressures are fixed and the filtrate flux varies in response to the changing membrane and boundary-layer resistances. By limiting the initial high flux and rapid accumulation of solids at the membrane surface that would otherwise take place upon start-up, accompanied by excessive membrane fouling and pore blocking, permeate flux control maximizes membrane throughput averaged over the duration of a run. The most straightforward means of executing the strategy of permeate flux control is to install a positive displacement pump (e.g., a peristaltic pump) in the filtrate line.

The effect of permeate flux control is illustrated in Fig. 8.10, which shows transmembrane pressures experienced across a 0.65-μm microfilter — namely, Millipore's hydrophilic Durapore polyvinylidene fluoride membrane — during the clarification of suspensions of a murine myeloma cell line at fixed filtrate rates between 50 and 100 $L/m^2\,h^{-1}$. At the highest permeate flux, TMP climbed rapidly as cell concentration proceeded, whereas TMP remained fairly constant at the lower permeate flux of 50 $L/m^2\,h^{-1}$ up to cell densities of $20 \cdot 10^6$ cells/cm^3. Accordingly, within the so-called "safe" operating region depicted in Fig. 8.9, the Cetus investigators further identified a smaller region of "recommended" operating conditions for their MF system operation. This "recommended" operating region was characterized by moderate TMP and moderately high shear rate — conditions that minimized concentration polarization and thus maximized long-term flux and protein passage.

Larger mammalian cells were separated more readily than smaller ones, as evidenced by the lower and more nearly constant TMPs experienced during filtration of the larger cells. This observation is consistent with considerable experience in separating microorganisms with membranes as discussed above.

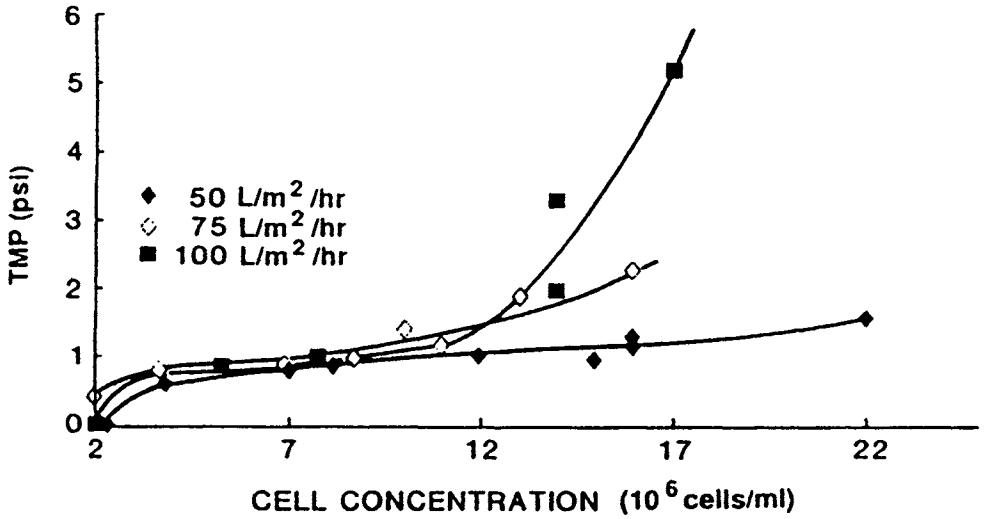

Fig. 8.10. Effect of permeate flux on transmembrane pressure in recovering a monoclonal antibody from cell culture supernatant (from Ref. [76] with permission).

Finally, it was noted that cell suspensions containing significant levels of cell debris were unfilterable at reasonable TMPs.

A good example of a successful clarification run is provided in Fig. 8.11, which shows a mammalian cell suspension being concentrated twenty-fold in less than an hour at an average permeate flux of 53 $L/m^2\ h^{-1}$ by means of a Microgon 0.2-μm cellulosic (CA/CN) hollow-fiber membrane. Here, the overall process objective was recovery of a monoclonal antibody secreted into the medium by a hybridoma. Over 95% of the antibody was recovered in the permeate at the indicated operating conditions, chosen to be consistent those deemed "recommended" in Fig. 8.9.

An outstanding scale-up study of cross-flow microfiltration as applied to the clarification of a CHO cell culture supernatant containing recombinant t-PA has been published by van Reis et al. of Genentech [85]. These investigators sought to operate their MF membrane system at high wall shear rates (2000–8000 s^{-1}) — but at modest pressure drops (≤ 35 kPa or 5 psi), in the laminar flow regime (Re < 2100), and at a reasonably high permeate-to-feed flow rate ratio or "conversion" (i.e., $Q_f/Q > 0.1$). These objectives were simultaneously met by their choice of a relatively open-channel (0.6-mm ID), 0.2-μm polypropylene hollow-fiber membrane — specifically, Akzo's Microdyn membrane.

Pilot-scale experiments were performed with 1200-L batches of cell culture suspension under conditions of constant filtrate flux in order to assess the effect of operating parameters on process capacity, achievable cell concentration factors, and yield of t-PA recovered in the filtrate. Representative results are

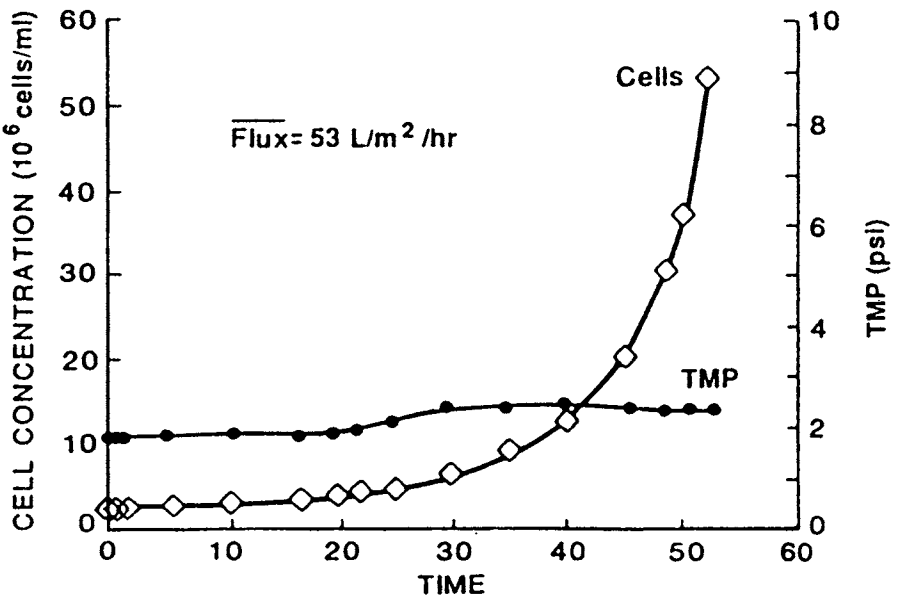

Fig. 8.11. Hybridoma cell separation by hollow-fiber membrane microfiltration (from Ref. [76] with permission).

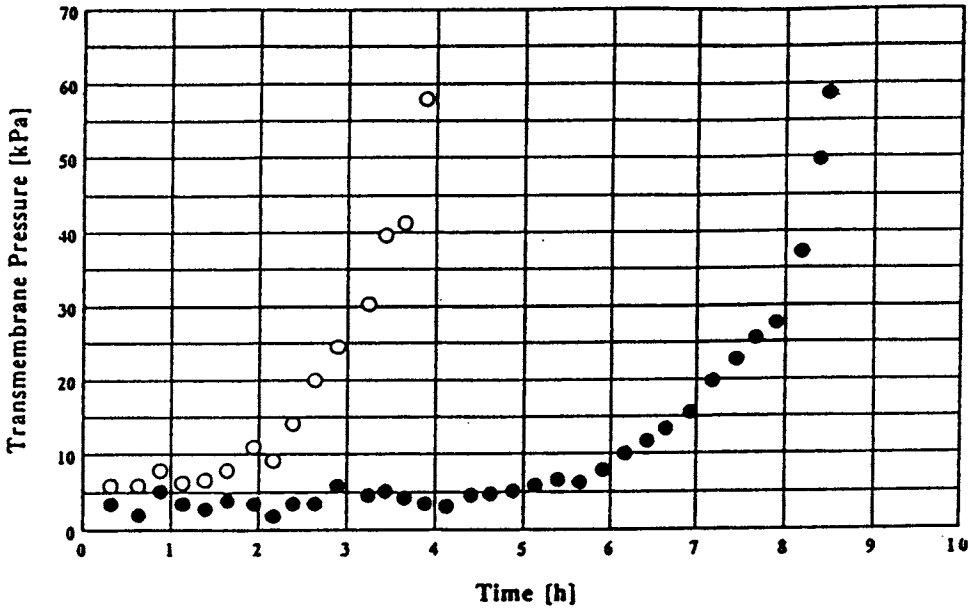

Fig. 8.12. Effect of permeate flux and shear rate on transmembrane pressure in t-PA recovery (from Ref. [85] with permission).

shown in Fig. 8.12. The open circles refer to operating conditions of high inlet wall shear rate (8000 s^{-1}) and high flux (50 $L/m^2\ h^{-1}$), while the closed circles represent operation at low-shear (4000 s^{-1}), low-flux (27 $L/m^2\ h^{-1}$) conditions.

The behavior exhibited in Fig. 8.12 is qualitatively consistent with that shown previously in Figure 8.10. Strikingly, a cell concentration factor of 9.5 was attained in the run conducted at low-shear, low-flux conditions before the TMP increased to its limit value of 70 kPa (10 psi). In contrast, a concentration factor of only 2.8 was reached at the more aggressive operating conditions. Ultimately, a concentration factor of fifteen was realized in routine, full-scale t-PA production.

Achieving high yield is a matter of paramount importance in the recovery of a high-unit-value therapeutic protein like t-PA. In principal, several factors may tend to reduce protein yields in microfiltration: (i) adsorption of protein onto the membrane, (ii) rejection of protein due to membrane sieving, (iii) denaturation of protein, and (iv) loss of protein in the cell concentrate. The first three factors proved insignificant in this particular application. However, nearly 7% of the t-PA protein (i.e., ≈1/15 of the product) would have been discarded with

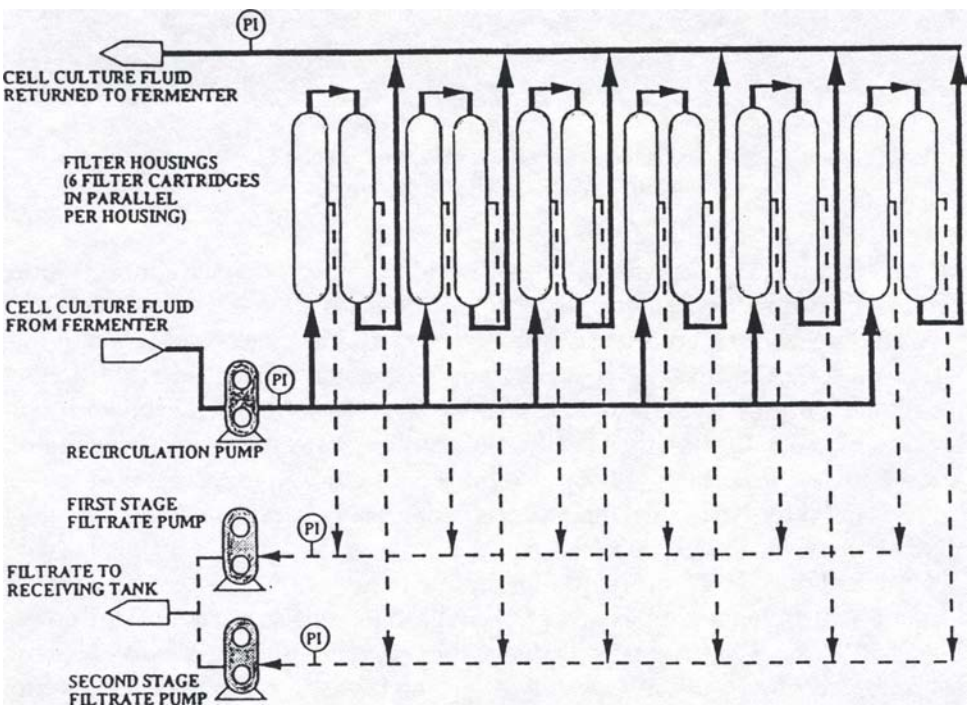

Fig. 8.13. Flow diagram for cross-flow microfiltration system for t-PA recovery (from Ref. [85] with permission).

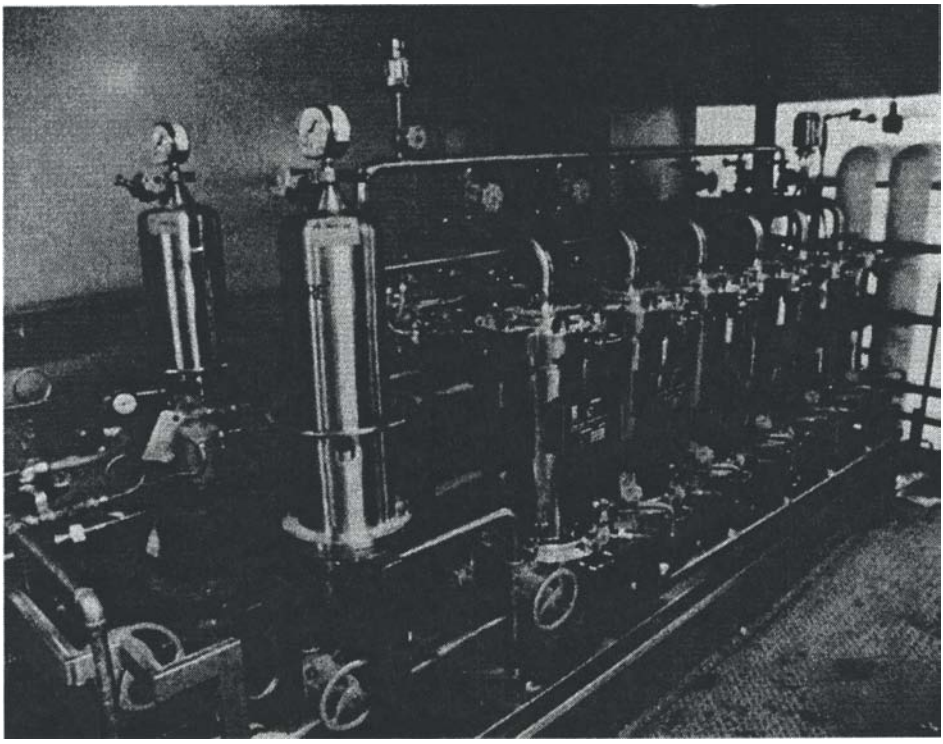

Fig. 8.14. Photograph of 180 m^2 cross-flow microfiltration system for t-PA recovery from cell culture (from Ref. [85] with permission).

the cell concentrate if Genentech's system had been operated at a concentration factor of fifteen without taking steps to avoid this loss.

Accordingly, a staged process was designed and implemented wherein the initial cell concentration step was followed by constant-volume diafiltration to improve t-PA recovery. Product yields in excess of 99% were achieved with less than 7% product dilution by initially concentrating fifteen-fold and then diafiltering with two volumes of phosphate-buffered saline. The reader is referred to Section 8.5.1.3 for additional discussion of diafiltration and equations useful in predicting its impact on product recovery.

A process flow diagram and photograph of the 180-m^2 cross-flow MF system ultimately installed and operated at Genentech for this application are shown in Figs. 8.13 and 8.14, respectively. Since the late 1980s, this impressive system has operated efficiently and reliably at an inlet wall shear rate of 4000 s^{-1} to process t-PA-containing cell suspensions at a feed flowrate of about 33,000 L h^{-1} and a permeate rate of 4800 L h^{-1} (i.e., 27 L m^2 h^{-1}). Kilogram quantities of t-PA are routinely recovered at yields in excess of 99%.

8.4.4 Generalizations and Design Guidance

Cross-flow MF and UF can now be considered established technologies for the concentration of both microbial and mammalian cell suspensions. The same can be said of their application to the clarification of fermentation broths and cell culture supernatants containing either macromolecular or low-molecular-weight bioproducts (e.g., recombinant therapeutic proteins and antibiotics, respectively). As the above examples demonstrate, the unique characteristics of membranes practically guarantee that cross-flow membrane filtration will be adopted in certain "niche" applications where the nature of cells and/or supernatant precludes the use of centrifugation or rotary drum vacuum filtration. Beyond these special cases, however, cross-flow MF and UF filtration will also be competitive with more conventional techniques where transmembrane fluxes approach or exceed about 100 $L/m^2 h^{-1}$ [66] — fluxes that are achievable under reasonably favorable circumstances.

The clarification of fermentation broths and cell culture supernatants that contain significant levels of cell debris remains a much more formidable objective, however. No existing separation technique — including membrane filtration [58,76] — really excels at this difficult task. In fact, the lipids associated with disrupted cell membranes and intracellular organelles are particularly troublesome to membranes by virtue of their propensity to cause severe and irreversible membrane fouling (see Section 8.6).

For the separation of intact microbial and mammalian cells, however, filtration rates ranging from about 25 to 100 $L/m^2 h^{-1}$ may be assumed for preliminary design purposes. Flux estimates may be refined further by taking into account the particular type of cell and the density of the cell suspension to be handled, as well as the pertinent experience (if any) of others with related systems.

Membrane system capital costs are notoriously difficult to gauge *a priori* in cell separation applications. However, it has been estimated that the capital-related costs of clarifying a mammalian cell culture supernatant might range from about \$0.05 to \$0.15/L of filtrate based on a plant capital investment of \$5,000/m^2 of membrane area [75]. Generalizations regarding operating costs are even riskier to make, but processing costs of the order of about \$0.01 to \$0.10/L of permeate might be expected with relatively simple-to-handle feed-streams characterized by low solids and/or low protein contents [75,89]. The operating costs associated with "problem" streams characterized by high solids and/or protein concentrations and requiring frequent membrane cleaning and/or replacement due to fouling may be several times higher [89].

Permeate fluxes in the range of 25–100 $L/m^2 h^{-1}$ have been documented for both MF and UF membranes used to treat process streams derived from various microorganisms and cell lines. As noted in Section 8.4.1.2, the "correct" type of

membrane to use depends largely on the nature of the product to be recovered. Several early studies [64,65,71,72] indicated that higher fluxes could be realized with UF membranes than with MF membranes — a counterintuitive observation sometimes attributed to the presumed blocking of relatively large MF membrane pores by deformable cells. Now, however, it is appreciated that MF membranes can function just as well as UF membranes if the former are operated under conditions of permeate flux control [76,85,86]. We subscribe to the notion that the better performance of ultrafilters as compared to microfilters in these early studies is probably attributable to their operation under "free-flow" conditions wherein transmembrane pressures (TMPs) were fixed and permeate fluxes were allowed to "float" [85]. Under these operating conditions, polarization and secondary membrane formation are inherently less severe with relatively low-flux UF membranes than is the case with relatively open, high-flux MF membranes. The steep initial flux loss invariably experienced with MF membranes operated at fixed TMPs can be minimized by controlling the permeation rate rather than the TMP as discussed above, thus leveling the playing field for MF membranes.

Because process performance can be highly dependent on the particulars of the biological system being processed, it is important that laboratory and pilot experiments be performed early in the design process to validate key assumptions. Once optimal operating conditions have been established for a particular bioseparation, it then becomes critical that membrane module scale-up be accomplished as faithfully and rigorously as possible — e.g., maintaining a fixed fluid path length as one proceeds from laboratory to pilot to production-scale membrane modules. Indeed, the scalability of membrane bioseparations is one of the principal benefits of using membrane technology in this arena.

8.5 PROTEIN RECOVERY AND CONCENTRATION BY UF

Ultrafiltration, and the related process of diafiltration, have a long history of use in the recovery and concentration of proteins from aqueous solutions [90–93]. Eykamp discusses the fundamentals of UF in another chapter in this book, and the application of this technology in the food and beverage industry is the subject of yet another chapter by Cheryan and Alvarez. The use of UF in the production of de-ashed whey protein concentrates and various other cheese products are among the most economically important industrial-scale applications of ultrafiltration today. Clearly, much of what the food processing industry has learned about using UF to concentrate the severely fouling proteinaceous solutions encountered there translates directly to bioprocessing applications. Accordingly, the interested reader is referred to these other two chapters for additional information.

8.5.1 Design Equations

8.5.1.1 Concentration by Ultrafiltration

Design equations for ultrafiltration-based processes are obtained by combining the material balance equations for the solute of interest with an expression relating permeate and retentate concentrations [50,94–97]. The extent of protein concentration in batch ultrafiltration is readily estimated from the initial volume of the feed solution (V_o), the final volume of retentate (V_r), and the membrane rejection coefficient σ for the particular protein of interest, defined as

$$\sigma = 1 - C_p/C_r$$

In a typical molecular-weight cut-off curve, the rejection coefficient σ is plotted as a function of solute molecular weight. Given these definitions and a minimal amount of algebra, final and initial protein concentrations can be related to one another as follows:

$$C_r = C_o \cdot (V_o/V_r)^{\sigma}$$

In the limit of complete protein rejection (i.e., $\sigma = 1$), the protein is obviously concentrated by the same factor by which the solution volume is reduced.

8.5.1.2 Purification by Ultrafiltration

Less obvious but no less important is the ability of ultrafiltration to purify proteins by effecting their separation from lower-molecular-weight contaminants. Contaminating microsolutes consist of salts, simple sugars, and other metabolites that are either initially present in the fermenter feed or cell culture media or that are produced in the bioreactor. In other instances, contaminants may be introduced in the course of subsequent downstream processing steps. For example, salts and simple organic solvents are frequently used both as protein precipitating agents and as eluents in column chromatography.

Because UF membranes exhibit very small rejection coefficients for low-molecular-weight contaminants (i.e., $\sigma_\mu \approx 0$), while they exhibit very high rejection coefficients for macromolecular solutes like proteins (i.e., $\sigma_M \approx 1$), ultrafiltration can separate a protein from low-molecular-weight contaminants at the same time as the protein is concentrated. The degree of removal of membrane-permeable microsolutes relative to membrane-retained macromolecular solutes during batch ultrafiltration may be estimated as follows:

$$(C_\mu/C_M)_r = [(C_\mu/C_M)_o] \cdot [(V_o/V_r)]^{-(\sigma_m - \sigma_\mu)}$$

where C_μ and C_M represent the concentrations of micro- and macro-solutes, respectively. In producing protein concentrates from cheese whey (the liquid

fraction separated from the curd in cheesemaking), protein purity expressed as a fraction of total solids content is typically increased several-fold during concentration, as a consequence of the permeation of low-molecular-weight contaminants (chiefly lactose and inorganic salts) across the UF membrane. This process is known as "de-ashing".

8.5.1.3 Purification by Diafiltration

The extent to which a protein can be purified by ultrafiltration alone is rather limited. As UF-mediated concentration of a proteinaceous solution proceeds, the viscosity of the feed solution rises sharply, and concentration polarization becomes flux-limiting. Boosting protein purity still further by ultrafiltration alone is no longer viable; additional enrichment of protein must rely on depleting contaminating microsolutes rather than concentrating the macromolecular solute.

The feed-and-bleed process of diafiltration, which combines some of the elements of dialysis and ultrafiltration, can accomplish this objective. Several examples of the use of diafiltration in bioprocessing have already been encountered in Sections 8.4.2.2 and 8.4.3 above. In its simplest embodiment, diafiltration is a constant-feed-volume process wherein protein-containing solution is recirculated past a protein-impermeable, contaminant-permeable UF membrane. Water or fresh buffer is continually added to the feed tank at the same rate as permeate is withdrawn, thereby maintaining constant feed/retentate volume — and, where $\mu_M \approx 1$, a fixed concentration of protein in the retentate ($C_{M,r}$). Membrane-permeable microsolutes are selectively washed through the UF membrane and away from the desired macromolecular product.

The concentration of microsolutes (e.g., salts or solvent) in the retentate ($C_{\mu,r}$) falls off exponentially with diafiltrate volume as given by the following expression:

$$C_{\mu,r} = C_{\mu,o} \cdot \exp\,[-(V_d/V_o) \cdot (1 - \sigma_\mu)]$$

where V_d is the volume of water or buffer added to the feed solution during diafiltration, and (V_d/V_o) is typically referred to as the diafiltration or dilution ratio. A similar expression can obviously be written for the concentration of retained macrosolute ($C_{M,r}$). The following equation for the ratio of retained micro- and macro-solute concentrations results from combining the two expressions:

$$(C_\mu/C_M)_r = (C_\mu/C_M)_o \cdot \exp\,[-(V_d/V_o) \cdot (\sigma_M - \sigma_\mu)]$$

Because purity depends exponentially on the dilution ratio, diafiltration is quite a powerful purification technique. Practically speaking, it is rare to resort to

diafiltration ratios greater than about two or three in order to achieve a desired degree of separation of protein from low-molecular-weight contaminants.

Finally, it should be noted that diafiltration is equally effective in increasing the recovery of membrane-permeable solutes in clarification operations (e.g., antibiotic recovery). The equations developed above are useful in estimating the improvement in product yield attainable in this manner.

8.5.2 Typical Applications

As discussed in Section 8.3.2, concentration is a ubiquitous operation in downstream bioprocessing. The opportunity to concentrate proteins by ultrafiltration arises in several contexts:

- immediately following clarification, particularly where the total protein concentration is below about 60 g L^{-1} [54];
- immediately following any purification step that significantly dilutes the protein (e.g., column chromatography); and
- as a post-purification, terminal concentration step just prior to product isolation and formulation.

The particular benefits of ultrafiltration as applied to protein concentration are several. On the one hand, the diluteness of fermentation broths and cell culture supernatants makes it important that the method of concentration be energy-efficient and productive; ultrafiltration is both. Moreover, the relatively gentle nature of ultrafiltration minimizes the tendency of many proteins to denature. The objective, after all, is recovery of protein activity, not just mass.

With regard to the gentleness of ultrafiltration, it should be noted that concerns were raised early on in the application of UF in bioseparations that the fluid shear fields encountered in pumping protein solutions through UF systems might be generally damaging to proteins [96,98,99]. It has since been demonstrated, however, that proteins — while readily undergoing denaturation at gas/liquid interfaces (e.g., at free liquid surfaces in contact with air in vessels) — are, in fact, quite resistant to very high shear rates in the absence of other threats to their stability [100–102]. Sensitivity to fluid shear during UF is now regarded as an issue only for the most fragile proteins or insofar as shear exacerbates other mechanisms of protein denaturation such as deposition on membrane pore surfaces [103].

A more serious concern regarding the use of ultrafiltration in downstream processing is that this technique generally concentrates macromolecular contaminants along with the particular protein of interest. Accordingly, undesirable contaminants like cellular DNA and bacterial endotoxins may be concentrated many-fold during ultrafiltration, whereas alternative unit operations like ion-exchange chromatography may actually reduce DNA and/or endotoxin levels while achieving some modest degree of protein concentration.

Many of the early large-scale applications of ultrafiltration in concentrating proteins involved the recovery of fermentation-derived enzymes, an application that continues to be economically important [96,104–107]. Substantial purification of high-molecular-weight enzymes can be achieved along with concentration by ultrafiltration under favorable circumstances. For example, a 26-fold increase in enzyme specific activity (corresponding to 97% removal of bulk protein contaminants) has been reported in one instance [108], and 50% removal of proteinaceous contaminants from enzyme has been documented in another [105]. For the most part, however, ultrafiltration must be regarded as a non-selective concentration process where mixtures of proteins are concerned. Instances where significant protein purification is also accomplished remain the exceptions to the rule.

The selection of particular ultrafiltration membranes for use in concentrating proteins is a matter of some importance. As part of a protocol designed to screen and evaluate candidate membranes, one group of investigators measured membrane sieving coefficients in the ultrafiltration of thymosin fraction 5 [15]. Their intention was to purify this bovine thymus extract by effecting a relatively tight molecular-weight "cut" with UF. Their data demonstrated quite convincingly that actual membrane sieving coefficients correlated quite poorly with nominal MWCO values reported by membrane manufacturers — a result that probably would have surprised few of the latter.

As the biotechnology industry has emerged, the focus has shifted somewhat to the use of ultrafiltration for the concentration of higher-unit-value therapeutic proteins derived either from fermentations using genetically engineered microorganisms or from mammalian cell culture. An important use of UF is in concentrating protein solutions both before the crude solutions are loaded onto chromatography columns and after the purified protein is eluted from them. On the one hand, the throughput of column chromatography is frequently flow-rate-limited; thus, preconcentration can increase the productivity and reduce the size of chromatography columns. At the same time, the elution of proteins from these purification columns is frequently accompanied by significant dilution, thus necessitating a "post-elution" concentration step.

An example of the use of ultrafiltration both upstream and downstream of chromatography has been thoroughly documented for the case of the recovery and purification of a monoclonal antibody produced in batch suspension cell culture [109]. In the "large-scale" process depicted in Fig. 8.15, a 100 kD MWCO polysulfone UF membrane housed in a plate-and-frame cassette was first used to concentrate the IgG_{2a} antibody (molecular weight ≈146 kD) approximately ten to twenty-fold; 280-L batches of clarified supernatant were processed with better than 95% antibody recovery. Preconcentration by UF in this manner facilitated the antibody's subsequent purification on an affinity chromatography column by avoiding throughput limitations associated with the soft gel

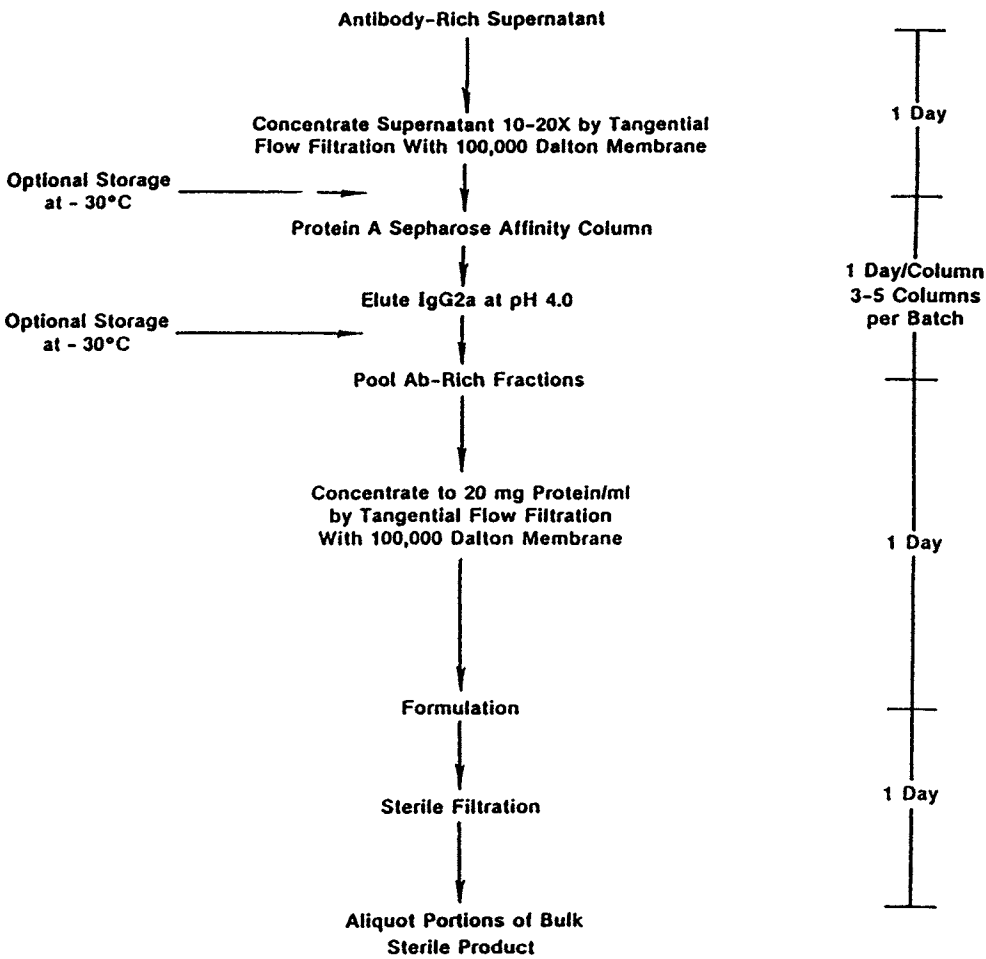

Fig. 8.15. Antibody purification processes with UF for pre- and post-column concentration.

media employed (Protein A immobilized on Sepharose CL-4B). Following affinity purification, the pooled antibody-containing eluent fractions were concentrated for a second time using the same 100 kD MWCO ultrafilter. This "post-elution" concentration step increased the total protein concentration to 20 g L^{-1}.

Quite apart from its role in post-elution concentration of proteins, ultrafiltration also finds frequent use in buffer, salt, and solvent removal or exchange operations conducted downstream of column chromatography. As noted above, the elution of proteins from chromatographic media is frequently

brought about by using elution buffers that have pH values, ionic strengths, and/or concentrations of specific ions or organic solvents that differ substantially from those used in loading the media and that are occasionally extreme. Indeed, elution buffers are sometimes quite hard on eluted protein, designed as they are to disrupt the normal binding of protein to the chromatographic sorbent. Accordingly, the eluted (and frequently diluted) protein finds itself in a solution of buffer, salts, and/or solvents that may be denaturing or that may be incompatible with the next bioprocessing step. Another opportunity to desalt protein solutions via diafiltration arises in the context of the use of concentrated solutions of electrolytes (e.g., ammonium sulfate) to selectively precipitate or "salt out" proteins.

Diafiltration is employed to transfer proteins into more suitable solution environments — e.g., perhaps into a solution with a pH or salt concentration adjusted for a subsequent ion-exchange purification step, or perhaps into the final formulation buffer. Buffer exchange or solvent switching are accomplished by diafiltering the protein-containing solution with several "diavolumes" of whatever solution into which it is desired to put the protein.

Diafiltration competes in these buffer exchange and desalting applications with gel filtration, a column chromatography operation based on size-exclusion gels like Sephadex. The advantages of ultrafiltration include minimal loss of purified protein and avoidance of dilution. In fact, diafiltration is often combined with ultrafiltration to desalt and concentrate proteins simultaneously.

In principle, the desalting of biotechnology-derived proteins can also be accomplished with membrane electrodialysis or ED [110]. Indeed, ED has been used for years to desalt cheese whey. Apart from its large-scale use in desalting dextran solutions [111], however, electrodialysis is infrequently used at present in bioprocessing.

Yet another important bioprocess objective achievable with diafiltration — namely, reduction of product losses suffered in clarification operations — has already been encountered in Section 8.4 above. Specifically, we refer the reader to our discussion there of two large-scale diafiltration processes designed to increase the yield of a soluble and membrane-permeable product by washing it away from membrane-retained solids, thereby permitting the product to be recovered in the permeate in high yield. In the first instance, cephamycin C was recovered in high yield from a fermentation broth by a combined UF/diafiltration process conducted at Merck (see Section 8.4.2.2); in the second, t-PA was recovered in high yield from cell culture supernatant at Genentech employing a diafiltration process based on a protein-permeable but cell-impermeable microfilter (see Section 8.4.3). The latter example involving MF membranes nicely illustrates that the use of diafiltration is not restricted to UF membranes capable of discriminating between macromolecules and microsolutes. Rather, diafiltration can be conducted with any type of permselective membrane (e.g.,

MF membranes) capable of separating one class of materials (e.g., suspended solids) from another (e.g., dissolved solutes).

Finally, an interesting alternative to the recovery of soluble proteins by ultrafiltration has been pursued by the group at University College London. These investigators have considered the merits of isoelectric precipitation of soya protein prior to its concentration by cross-flow MF [112,113] or UF [114,163]. The separation of precipitated protein particles by MF or UF membranes with pores ranging from 0.1 to 10 μm in diameter promised to be faster than concentrating the soluble protein by UF. However, membrane fouling was severe at these conditions of low protein solubility (see Section 8.6.2), and the scope of the technique is presumably limited to stable proteins.

Given the wide range of specific applications encountered and the spectrum of behaviors exhibited by protein solutions (which range from being relatively straightforward to nearly impossible to process), it is perhaps foolhardy to cite a "typical" value for the flux of an ultrafiltration membrane in a downstream bioprocessing application. Because of the dominant role of concentration polarization and membrane fouling in determining transmembrane fluxes, permeation rates in bioprocess applications typically have little to do with intrinsic membrane permeability and everything to do with the particulars of the system involved (i.e., membrane, protein, other foulants and contaminants, and operating conditions.) Having said this, flux values in the range of 5 to 40 $L/m^2\,h^{-1}$ can reasonably be expected in many bioprocessing applications. Additional guidance may be found in the numerous references cited in this chapter as well as in those written by Eykamp, Mulder and Smolders, and Cheryan and Alvarez.

8.6 FLUX-LIMITING PHENOMENA IN MEMBRANE BIOSEPARATIONS

The topics of concentration polarization and membrane fouling are treated quite capably and thoroughly elsewhere in this volume in chapters by Mulder and Smolders ("Polarization Phenomena and Membrane Fouling") and by Eykamp ("Microfiltration and Ultrafiltration"). However, no discussion of membrane bioseparations would be complete without recognizing the particular significance of these phenomena in processing feedstreams of biological origin [64,115–120].

8.6.1 Concentration Polarization in MF and UF

In previous sections of this chapter, we provided several examples of the effect of concentration polarization in reducing MF and UF filtrate fluxes in bioseparation applications. In particular, we have seen that MF and UF membranes afford surprisingly similar filtrate fluxes in cell harvesting operations

and in the clarification of fermentation broths and cell culture supernatants (see Sections 8.4.2 and 8.4.3). Indeed, typical ultrafiltration fluxes realized in the concentration of proteins are generally not all that different from typical microfiltration fluxes realized in the separation of cell suspensions. The vastly different intrinsic permeabilities of MF and UF membranes to pure water would seem to have little bearing on the permeate fluxes observed in actual bioseparations.

While several factors contribute to this situation, concentration polarization is surely the greatest "equalizer" of membrane permeation rates. Considerable progress has been made in recent years toward a better appreciation of the fundamentals of concentration polarization. The theory of concentration polarization has been most completely and successfully developed for the case where solutions of macromolecules (e.g., proteins) are concentrated by ultrafiltration [91,121–127]. The classical gel-polarization model describes the accumulation and back-diffusion of macromolecular solutes within the stagnant boundary layer at the membrane surface, along with the effect of this polarization on membrane flux. Here, one often finds fairly good agreement between the predicted and observed effects on flux of the key variables — namely: (i) protein concentration, (ii) solution-phase mass transfer coefficients, and (iii) transmembrane pressure.

Unfortunately but understandably, the acceptance of corresponding theories for the membrane filtration of particulate and colloidal suspensions (e.g., cells and cell debris) has been much slower in coming. Separate camps and alternative hypotheses still persist to some extent, and a common mechanism and model capable of rationalizing a majority of the flux data obtained in the cross-flow microfiltration of cells still eludes us [128]. The situation is even more complicated when polarizable solutes like proteins are present in the feed stream along with particulates.

Having said this, a reasonably well-developed, semi-quantitative theoretical foundation has emerged within recent years [126,129,130], reducing some of the confusion that has persisted in this area. For example, membrane scientists were puzzled at one time by the observation that their gel-polarization model, which had been applied so successfully to describe the ultrafiltration of proteins, substantially underpredicted the fluxes observed during the microfiltration of cell suspensions — in fact, by more than an order of magnitude in some instances. This so-called "flux paradox" has now been rationalized by invoking various other transport phenomena (e.g., shear-induced diffusion and inertial lift forces) capable of assisting in the back-transport of particulate and colloidal species away from the membrane surface.

In addition to many of these theoretical issues having been resolved in recent years, applications engineers have also been developing a much better understanding of how operating procedures and module and system design can affect the severity of these polarization phenomena. For example, in Section

IV.D several early studies were cited that suggested that UF membranes might exhibit higher fluxes than MF membranes in cell separation and clarification [64,65,71,72]. However, it is now generally appreciated that MF membranes can provide sustainable high fluxes if the filtration rate (as opposed to the transmembrane pressure) is controlled directly [76,85,86]. With permeate flux control, the initial period of severe MF membrane flux decline associated with polarization and pore blocking can be avoided, with the result that higher average transmembrane fluxes are achieved over the longer term. Mention should also be made here of several innovations in membrane module design that promise to provide better control over solution hydrodynamics and to reduce membrane polarization [69,131–134).

8.6.2 Membrane Fouling

Control of membrane fouling is an all-too-frequent preoccupation of those who would apply porous membrane filtration in bioseparations. While fouling is encountered to some degree in most membrane separations, it is particularly severe in downstream bioprocessing. Moreover, pretreatment of the feedstream to the membrane is not a viable option in bioseparation applications, whereas extensive pretreatment may be conducted to minimize fouling in other applications of membranes (e.g., in the production of potable water by reverse osmosis).

The prevalence and severity of membrane fouling in bioprocess applications is largely a consequence of the fouling-prone nature of many of the components present in fermentation broths and cell culture supernatants — namely, cell debris, proteins, and lipids derived from cell membranes and organelles. We first discuss approaches for minimizing the severity of membrane fouling and then turn to the matter of regenerating membranes once they become fouled.

The interactions of particulate, colloidal, and macromolecular species of biological origin with membrane pores and pore-wall surfaces are complex and almost always undesirable. Not surprisingly, attempts to avoid or minimize membrane fouling often center on minimizing the extent of such interactions. For example, many proteins are notorious for their tendency to adsorb or deposit on membrane surfaces, with monolayers building to multiple layers and eventually leading to protein denaturation. (It should be noted that some membrane scientists reserve the term "protein adsorption" to describe membrane/protein interactions that occur at zero-flow or low-shear conditions; they use the term "protein deposition" to describe protein/protein interactions induced by flow through membrane pores [119]. We make no such distinction here.)

Membrane fouling by protein adsorption may be reduced to some degree by processing proteinaceous solutions at conditions that maximize the solubility of the protein. In particular, amphoteric protein molecules exhibit their mini-

mum solubility at pH values corresponding to the point of zero net charge — i.e., at their isoelectric point or pI. Thus, it is generally advisable to process a protein solution at a pH value far removed from its pI, consistent of course with its stability [113,135]. Unfortunately, since any given protein is invariably encountered in a complex mixture containing many other proteins with different pI values, this strategy for avoiding fouling is more simply stated than executed.

Another approach to controlling protein/membrane interactions involves manipulation of the membrane surface chemistry so as to reduce protein deposition thereon. This generally involves modifying membrane surfaces to be as hydrophilic and minimally charged as possible [12]. Hydrophobic membranes — in particular, polysulfone ultrafilters — are notorious for engaging in hydrophobic-hydrophobic interactions with the hydrophobic "patches" present on the exterior surfaces of many proteins; rendering a membrane surface hydrophilic by appropriate surface chemistry clearly eliminates this cause of protein adsorption. However, membrane hydrophilicity cannot be achieved simply by incorporating electrically charged groups on the membrane surface; if present, such moieties could then interact electrostatically with either positively or negatively charged "patches" that coexist in the manner of a mosaic on the surfaces of proteins.

Ideally, the membrane surface should present polar but electrically neutral functional groups to protein-containing solutions. These polar groups can either belong to the membrane polymer or polymer blend itself [107,136], or they may be added by some appropriate surface treatment such as coating, grafting, or other suitable chemical modification of the membrane surface [137–143]. Careful fundamental studies of the causes and control of protein adsorption on MF and UF membranes will undoubtedly aid in the development of strategies to minimize and cope with membrane fouling in the future [144].

Other troublesome membrane foulants frequently found in bioprocess streams are the antifoams traditionally used in fermentation operations [59,61,66]. These hydrophobes (e.g., silicones, polypropropylene glycols, etc.) severely fouled polysulfone UF membranes when the latter were first used with antifoam-containing streams. The result was that UF membranes quickly earned a bad reputation in the bioprocessing industry. However, it is now appreciated that this type of fouling can be minimized or avoided in several ways: (i) by reducing the quantity of antifoam used, (ii) by relying on mechanical foam breakers, (iii) by operating at temperatures well removed from an antifoam's cloud point [67,145], and (iv) by using antifoams specifically designed to be with compatible with membranes (e.g., Pluronic F-68 and Dow Corning 1920).

Having just emphasized the importance of membrane surface chemistry, it is humbling to note that one of the more visible and successful large-scale

applications of MF membranes in biotechnology, the clarification of t-PA-containing cell culture supernatants at Genentech, is conducted with a hydrophobic polymeric membrane — namely, Akzo's Microdyn polypropylene MF membrane. It is conceivable that proteins deposit on the initially hydrophobic membrane surface upon first exposure to cell culture supernatant, thus rendering the surface hydrophilic and limiting further protein deposition. This is consistent with the fact that periodic cleaning of the membrane renders its surface hydrophobic once again, making it necessary to wet the pores in the dry membrane with alcohol prior to its subsequent use.

Once a membrane is fouled, various physical and chemical techniques may be used to restore at least some fraction of its initial permeability. The approaches of back-flushing and permeate closure (wherein cross flow is maintained in the absence of transmembrane flow) are examples of hydraulic cleaning techniques. More effective methods for membrane cleaning involve chemical agents. Solutions that have been found useful in membrane sanitization and/or cleaning include the following [65,74–76,85]:

- alkaline solutions such as dilute sodium hydroxide at concentrations up to about 2 to 5% (w/v);
- disinfectants such as sodium hypochlorite (≈250 ppm), hydrogen peroxide (≈0.01 %), and formaldehyde;
- detergents including alkaline phosphates (≈1% sodium tripolyphosphate), sodium dodecylbenzenesulfonate (≈0.05%), and various non-ionic detergents;
- chelating agents such as tetrasodium ethylenediaminetetraacetic acid (0.05%); and
- acidic solutions (e.g., phosphoric, acetic, and citric) at concentrations up to about 1 M.

These chemicals are often used in combination or in a sequence of sanitization and cleaning steps.

8.7 OTHER MEMBRANE BIOSEPARATIONS

8.7.1 Microsolute Concentration and Purification

Given the diluteness of typical fermentation broths, dewatering is a particularly common bioprocessing task. Several membrane technologies — most notably, reverse osmosis (RO) and pervaporation (PV) — can accomplish this operation.

The energy efficiency with which reverse osmosis can separate water from low-molecular-weight solutes is, of course, well established where seawater and brackish water desalting are concerned. In bioprocessing, this benefit can

be particularly significant — especially in the recovery and concentration of certain heat-labile fermentation products like antibiotics that require processing at ambient temperature or below. Reverse osmosis competes in such applications with vacuum evaporation, a particularly energy- and capital-intensive unit operation [146–148]. Some years ago, a pioneering study at Merck concluded that a heat-sensitive antibiotic could be concentrated by RO at higher yield and with one-thirtieth the energy requirement of vacuum evaporation [146].

Other bioproducts that have been concentrated by RO include various amino acids and organic acids [149–151]. In at least one instance, RO has been shown to have the potential for purifying (as opposed to simply concentrating) a fermentation-derived solution of itaconic acid. At sufficiently low pH, this low-molecular-weight organic acid becomes preferentially membrane-permeable [152].

Despite these potential advantages, however, the application of RO in bioprocessing remains limited for several reasons:

- membrane fouling can be severe, and extensive pretreatment is not a viable option;
- RO membrane fluxes are frequently inadequate as a consequence of intrinsically low membrane permeability and/or appreciable osmotic pressures generated by nutrient sugars and salts present in fermentation broths; and
- more traditional unit operations like solvent extraction compete effectively in many applications.

Although little used to date, the process of nanofiltration (NF) or "loose RO" based on the like of Dow/FilmTec's NF-40 or NF-70 membranes has potential in bioprocessing applications by virtue of the high water fluxes afforded by these thin-film-composite membranes [153]. The lower selectivities afforded by nanofiltration membranes are of little consequence since bioproducts like antibiotics are fairly easily rejected.

Although they find limited use in bioprocessing today, other membrane technologies which show promise for the recovery and concentration of low-molecular-weight bioproducts include pervaporation [154], membrane solvent extraction or MSX [155,156], and liquid membranes [12]. Pervaporation, by far and away the most important of these processes, finds use in dehydrating a number of solvents produced by fermentation — most notably, ethanol. Indeed, the 150,000 L/day ethanol dehydration plant at Betheniville, France, which went on stream in 1988, represents the largest application of pervaporation to date; it houses some 2400 m^2 of PV membrane area [157]. Membrane solvent extraction has been investigated for the dispersion-free isolation of mevinolinic acid (a precursor to the cholesterol-lowering drug mevinolin) from an emulsion-prone fermentation broth [158].

8.7.2 Sterile Filtration and Contaminant Removal

The removal of potentially harmful contaminants from therapeutic products is a constant preoccupation at all stages in downstream processing. The task begins even upstream of the bioreactor with the production of contaminant-free water for cell culture media and of sterile feed air for fermentation, and it extends to sterile filtration of the final product itself. The list of contaminants that are unacceptable in therapeutic drugs is long, but microorganisms, viruses, foreign DNA, immunogenic proteins, and bacterial endotoxins are the primary offenders [159].

The sterile filtration by MF of pharmaceutical preparations like small-volume parenterals ranks as one of the highest-value-added membrane separations in existence, especially on the basis of the mass of contaminants removed. Where there is a substantial difference in size between the pharmaceutical and the contaminant to be removed, microfiltration or ultrafiltration can be employed. For example, solutions of small-molecule drugs (e.g., antibiotics) are routinely and reliably microfiltered to remove microbial contaminants. Sterile filtration is perhaps the only instance in bioprocessing in which microfiltration systems are operated in a dead-ended as opposed to cross-flow mode [160].

One might also expect it to be a relatively straightforward matter to exclude viruses from cell culture fluids using ultrafiltration, but this is hardly the case. Although viruses are large (e.g., tens to hundreds of nanometers) and thus are readily rejected by most UF membranes, the problem lies in the extraordinary degree of virus removal required. Twelve-log reduction of viral contaminants is routinely specified and sought via the application of multiple, "orthogonal" approaches. Unfortunately, the presence of the occasional defect or very large pore prevents most ultrafilters from performing well in this application. Recently, Millipore has developed a composite membrane with improved virus-rejection characteristics which promises to make one- or two-stage ultrafiltration viable in these applications [161,162].

Finally, we note that certain contaminant removal problems are not amenable to membrane separation technology at all — or, for that matter, to more conventional methods. For example, while a number of approaches (including membranes) are effective in removing bacterial endotoxins from water, their removal from therapeutic proteins is extraordinarily difficult. Affinity techniques, a membrane-based version of which is discussed briefly in the following section, have some potential for accomplishing this.

8.7.3 Affinity Membranes

Affinity separation processes for the recovery and purification of proteins are conventionally carried out using adsorbent particles (e.g., agarose or silica)

packed in columns. However, despite the high selectivity that affinity processes provide, their application on the process scale has been hampered by the inability of affinity columns to handle high fluid flow rates at reasonable ligand utilization efficiencies.

Affinity membrane devices are based on microporous hollow-fiber membranes activated by covalent attachment of affinity ligands to their interior pore-wall surface area [49]. On the one hand, affinity membranes are capable of processing high volumetric flow rates of dilute protein solutions by virtue of their uniquely small aspect ratio as compared to columns — that is, membranes provide very short fluid-flow path lengths in comparison to the superficial area provided for flow. Thus, pressure drop does not limit the feed flow rate during the loading step as it can with conventional chromatography columns. Moreover, convection of protein-containing solution through ligand-activated membrane pores nearly eliminates diffusional resistances associated with the porous or gel-type adsorbent particles normally used in affinity column separations, because the diffusion distance of a target protein molecule to a nearby ligand-activated pore wall is always short.

As a consequence, the speed and scalability of affinity-based bioseparations can be improved significantly with membrane supports, and ligand turnover numbers can be increased. Pressure drop and intraparticle diffusion cease to be flow-rate-limiting, as other factors such as adsorption kinetics place new but less restrictive limits on performance [164].

These conceptual arguments for adopting affinity membranes in protein capture applications are powerful ones, and ambitious attempts to commercialize this technology have been made within the last few years [165]. Emphasis has been placed on the introduction of products based on (i) membrane-bound Protein A (for the capture of therapeutic monoclonal antibodies) and (ii) immunoaffinity membranes activated with monoclonal antibodies for the capture of various recombinant proteins [166]. Affinity membranes have had a slow start in large-scale bioprocess applications, largely because of the ambitious specifications that the membranes must meet in order to perform to their potential. Ligand binding capacity (i.e., the mass of target protein bound per unit volume of membrane matrix) must be reasonably high despite the fact that affinity membranes are cycled rapidly in use, and the rate and extent of membrane fouling cannot be excessive. These problems in affinity membrane surface chemistry and morphology are gradually being solved, however, with the result that the promise of affinity membranes comes closer to being realized. Indeed, affinity membrane technology may afford a paradigm for future trends in the development of ever more selective membrane bioseparations.

LIST OF SYMBOLS

BHK	Cell line from newborn hamster kidney
CA/CN	cellulose acetate/cellulose nitrate
CHO	cell line from Chinese hamster ovary
C_M	macrosolute concentration
C_μ	microsolute concentration
C_o	initial concentration (mol L^{-1})
C_r	concentration in retentate (mol L^{-1})
DMF	drug master file
DNA	deoxyribonucleic acid
ED	electrodialysis
IgG	immunoglobulin
IgG_{2a}	immunoglobulin of subclass 2a
MF	microfiltration
MSX	membrane solvent extraction
MWCO	molecular-weight cut-off
PAN	polyacrylonitrile
PBS	phosphate-buffered saline
P_f	filtrate pressure (kPa)
pI	isoelectric point
P_{in}	feed channel inlet pressure (kPa)
P_{out}	feed channel outlet pressure (kPa)
PV	pervaporation
PVC	polyvinylchloride
PVDF	polyvinylidine fluoride
Q	feed flow rate (L s^{-1})
Q_f	filtrate flow rate (L s^{-1})
RO	reverse osmosis
TMP	transmembrane pressure (kPa); $[(P_{in} - P_{out})/2] - P_f$
t-PA	tissue plasminogen activator
UF	ultrafiltration
V_d	volume of diafiltrate (L)
V_o	initial volume (L)
V_r	volume of retentate (L)

Greek letters:

σ	solute rejection coefficient; critical cell membrane tension (dyne/cm)
σ_μ	microsolute rejection coefficient
σ_M	macrosolute rejection coefficient

REFERENCES CITED

1 *Fermentation and Biochemical Engineering Handbook* (1983). (H.C. Vogel, ed.), Noyes Publications, Park Ridge, New Jersey.
2 Atkinson, B. and Mavituna, F. (1991). *Biochemical Engineering and Biotechnology Handbook*, 2nd Ed., Stockton Press, New York.
3 Belter, P.A., E.L. Cussler, and Hu, W.-S. (1988). *Bioseparations: Downstream Processing for Biotechnology*, John Wiley & Sons, New York.
4 Bailey, J.E. and Ollis, D.F. (1986). *Biochemical Engineering Fundamentals*, 2nd Ed., McGraw-Hill, New York.
5 Wang, D.I.C., Cooney, C.L., Demain, A.L., Dunnill, P., Humphrey, A.E. and Lilly, M.D. (1979). *Fermentation and Enzyme Technology*, John Wiley & Sons, New York.
6 Borman, S., FDA approves 32 new drugs, biologics in 1992. *C&E News*, Jan. 18, 1993, p. 8.
7 Thayer, A.M., Poor 1992 Earnings, Shaky Stocks Plague Biotechnology Firms. *C&E News*, Mar. 29, 1993, pp. 17–19.
8 Humphrey, A. (1990). Problems and Challenges in the Production and Processing of Biologically Active Materials. In: *Frontiers in Bioprocessing* (S.K. Sikdar, M. Bier and P. Todd, eds.). CRC Press, Inc., Boca Raton, Florida, pp. 1–13.9. Strathmann, H. (1985). *Trends in Biotechnol.*, 3: 112.
10 Cussler, E.L. (1989). Bioseparations, Especially by Hollow Fibers. *Ber. Bunsenges. Phys. Chem.*, 93: 944.
11 *Membrane Separations in Biotechnology* (1986). W.C.McGregor, ed., Marcel Dekker, Inc., New York.
12 Michaels, A.S. and Matson, S.L. (1985). *Desalination*, 53: 231.
13 Fane, A.G. and Radovich, J.M. (1990). Membrane Systems. In: *Separation Processes in Biotechnology* (J.A. Asenjo, ed.). Marcel Dekker, New York, pp. 209–262.
14 Drioli, E. (1986). Membrane Processes in the Separation, Purification, and Concentration of Bioactive Compounds from Fermentation Broths. In: *Separation, Recovery, and Purification in Biotechnology* (J.A. Asenjo and J. Hong, eds.). ACS Symp. Ser. 314, American Chemical Society, Washington, DC, pp. 52–66.
15 McGregor, W.C. (1986). *Membrane Separations in Biotechnology*, Marcel Dekker, Inc., New York, pp. xvii–xix, 1–36.
16 Ratafia, M. (1987). *Biotechnology*, 5: 692.
17 Cooney, C.L. (1983). *Science*, 219: 728.
18 Gaden, E.L. (1981). *Sci. Amer.*, 245: 180.
19 Chisti, M.Y. (1989). *Airlift Bioreactors*, Elsevier Applied Science, London.
20 Nelson, K.L. (1988). *Biopharm. Manuf.*, 1: 42.
21 Rhodes, M. and Birch, J.R. (1988). *Bio/Technology*, 6: 518.
22 Glover, J.F. (1991). *Genetic Engr. Biotechnol.*, 11: 18.
23 Hennighausen, L., Ruiz, L. and Wall, R. (1990). *Current Opinion in Biotechnol.*, 1: 74.
24 Gannon, F., Powell, R., Barry, T. and McEvoy, T.G. (1990). *J. Biotechnol.*, 16: 155.
25 *Animal Cell Biotechnology* (1985). R.E. Spier and J.B.Griffiths, eds., Academic Press, New York.
26 *Large-Scale Mammalian Cell Culture* (1985). J. Feder and W.J. Tolbert, eds., Academic Press, New York.
27 Darnell, J.E., Lodish, H.F. and Baltimore, D. (1990). *Molecular Biology of the Cell*, 2nd Ed., Scientific American Books, New York.
28 Hopkinson, J. (1985). *Bio/Technology*, 3: 225.

29 Inlow, D., Maiorella, B. and Shauger, A. (1992). U.S. Patent No. 5,156,964.
30 Maiorella, B., Shauger, A., Poulhazan, M., Howarth, B., and Inlow, D. (1992). Paper presented at the 203rd ACS National Meeting, Abstract No. BIOT-112, American Chemical Society, Washington, DC.
31 Schneider, Y.J. and Lavoix, A. (1990). *J. Immunol. Methods*, 129: 251.
32 Van Brunt, J. (1988). *Bio/Technology*, 6: 479.
33 Dwyer, J.L. (1984). *Bio/Technology*, 2: 957.
34 Dunnill, P. (1983). *Biochem. Soc. Symp.*, 48: 9.
35 Builder, S.E., van Reis, R., Paoni, N. and Ogez, J. (1988). Process Development and Regulatory Approval of Tissue-Type Plasminogen Activator. Proceedings of the 8th International Biotechnology Symposium, Paris, France, July 17–22, 1988.
36 Belfort, G. (1989). *Ber. Bunsenges. Phys. Chem.*, 93: 939.
37 Fish, N.M. and Lilly, M.D. (1984). *Bio/Technology*, 2: 623.
38 Rosen, C.G. (1987). *Chemtech*, 17: 612.
39 Buckland, B.C. (1990). Industrial Fermentation Processes. Biochemical Engineering Summer Course, University College London, London.
40 Horvath, C. (1988). Protein Chromatography Systems. ASME Short Course on Process Equipment Technology for Biopharmaceutical Manufacturing. Univ. of Virginia, Charlottesville, Virginia.
41 Garg, V.K., Costello, M.A.C., and Czuba, B.A. (1991). Purification and Production of Therapeutic Grade Proteins. In: *Purification and Analysis of Recombinant Proteins* (R. Seetharam and S.K. Sharma, eds.). Marcel Dekker, New York, pp. 29–54.
42 Schultz, J.S. (1987). *J. Membr. Sci.*, 30: 239.
43 Fulton, S.P., Shahidi, A.J., Gordon, N.F., and Afeyan, N.B., (1992). *Bio/Technology*, 10: 635.
44 Martin, N., and Luker, M. (1987). *Chemical Engineer (London)*, 434: 14.
45 Lightfoot, E.N. (1990). Separations in Biotechnology: The Key Role of Adsorptive Separations. In: *Protein Purification: Molecular Mechanisms to Large-Scale Processes* (M.R. Ladisch et al., eds.). ACS Symp. Ser. 427, American Chemical Society, Washington, DC, pp. 35–51.
46 *Separation and Purification: Critical Needs and Opportunities* (1987). National Academy Press, Washington, DC.
47 *Penicillin G and Penicillin V*, (1986). Chemica Medicinal Chemical Monograph No. 1, M. Barber and Associates, Coulsdon, England.
48 Bonnerjea, J., Oh, S., Hoare, M., and Dunnill, P. (1986). *Biotechnology*, 4: 954.
49 Klein, E. (1991). *Affinity Membranes*, John Wiley & Sons, New York.
50 Atkinson, B. and Mavituna, F. (1991). *Biochemical Engineering and Biotechnology Handbook*, 2nd Ed., Stockton Press, New York, pp. 873–904, 964–991.
51 Ostlund, C. (1986). *Trends in Biotechnol.*, 4: 288.
52 Garg. V.K. (1990). Large-Scale Purification of Monoclonal Antibodies for Therapeutic Use. In: *Targeted Therapeutic Systems* (P. Tyle and B.P. Ram, eds.). Marcel Dekker, New York, pp. 45–73.
53 Fulton, S.P. (1989). *The Art of Antibody Purification*, Amicon/W.R. Grace & Co., Danvers, Massachusetts.
54 Prokopakis, G.J. and Asenjo, J.A. (1990). Synthesis of Downstream Processes. In: *Separation Processes in Biotechnology* (.A. Asenjo, ed.). Marcel Dekker, NewYork, pp. 571–601.
55 Wheelwright, S.M. (1987). *Biotechnology*, 5: 789.
56 Asenjo, J.A. (1990). Selection of Operations in Separation Processes. In: *Separation Processes in Biotechnology* (J.A. Asenjo, ed.). Marcel Dekker, NewYork, pp. 3–16.

57 Griffiths, J.B. and Riley, P.A. (1985). In: *Animal Cell Biotechnology* (R.E. Spier and J.B. Griffiths, eds.). Academic Press, New York, pp. 17–48.
58 Mackay, D. and Salusbury, T. (1988). *Chemical Engineer (London)*, 447: 45.
59 Hanisch, W. (1986). Cell Harvesting. In: *Membrane Separations in Biotechnology* (W.C. McGregor, ed.). Marcel Dekker, Inc., New York, pp. 61–88.
60 Wichmann, R., Wandrey, C. and Grosse-Wiesmann, J. (1990). *Appl. Microbiol. Biotechnol.*, 32: 373.
61 Zahka, J. and Leahy, T.J. (1985). Practical Aspects of Tangential Flow Filtration in Cell Separations. In: *Purification of Fermentation Products* (T. Leahy and D. LeRoith, eds.). ACS Symp. Ser. 271, American Chemical Society, Washington, DC, pp. 51–69.
62 Ludwig, K. and O'Shaughnessey, K. (1989). *American Biotechnology Laboratory*, 7: 41.
63 Conversion of Bioreactors to Continuous Perfusion Using Hollow Fiber Cell Separators. (1990). Microgon, Inc., Laguna Hill, California.
64 Defrise, D. and Gekas, V. (1988). *Proc. Biochem.*,23: 105.
65 Bailey, F.J., Warf, R.T. and Maigetter, R.Z. (1990). *Enzyme Microb. Technol.*, 12: 647.
66 Kroner, K.H., Schutte, H., Hustedt, H. and Kula, M.-R. (1984). *Proc. Biochem.*, 19: 67.
67 Kroner, K.H., Schutte, H., Hustedt, H. and Kula, M.-R. (1984). In *Third European Congress on Biotechnology*, Verlag Chemie, p. III-549.
68 Kroner, K.H., Nissinen, V., and Ziegler, H. (1987). *Bio/Technology*, 5: 921.
69 Kroner, K.H., Nissinen, V. (1988). *J. Membr. Sci.*,36: 85.
70 Bell, D.J. and Davies, R.J. (1987). *Biotechnol. Bioeng.*, 29: 1176.
71 Cheryan, M. (1979). *Ultrafiltration Handbook*, Technomic Publishing, Lancaster, Pennsylvania, p. 279.
72 Gatenholm, P., Paterson, S., Fane, A.G., and Fell, C.J.D. (1988). *Proc. Biochem.*, 23: 79.
73 McDonogh, R.M., Bauser, H., Stroh, N. and Chmiel, H. (1992). *Chem. Eng. Sci.*, 47: 271.
74 Gravatt, D.P. and Molnar, T.E. (1986). Recovery of an Extracellular Antibiotic by Ultrafiltration. In: *Membrane Separations in Biotechnology* (W.C. McGregor, ed.). Marcel Dekker, Inc., New York, pp. 89–97.
75 Mir, L., Michaels, S.L., and Goel, V. (1992). Cross-Flow Microfiltration: Applications, Design, and Cost. In: *Membrane Handbook* (W.S. Ho and K.K. Sirkar, eds.). Van Nostrand Reinhold, New York, pp. 571–594.
76 Maiorella, B., Dorin, G., Carion, A. and Harano, D. (1991). *Biotech. Bioeng.*, 37: 121.
77 Born, C., Zhang, Z., Al-Rubedai, M. and Thomas, C.R. (1992). *Biotech. Bioeng.*, 40: 1004.
78 Papoutsakis, E.T. (1991). *Trends in Biotechnol.*, 9: 427.
79 Petersen, J.F., McIntire, L.V. and Papoutsakis, E.T. (1988). *J. Biotechnol.*, 7: 229.
80 Kretzmer, G. and Schugerl, K. (1991). *Appl. Microbiol. Biotechnol.*, 34: 613.
81 Smith, C.G., Greenfield, P.F. and Randerson, D.H. (1987). *Biotechnol. Tech.*, 1: 39.
82 Abu-Reesh, I. and Kargi, F. (1989). *J. Biotechnol.*, 9: 167.
83 Tramper, J., Williams, J.B., Joustra, D. and Vlak, J.M. (1986). *Enzy. Microb. Technol.*, 8: 33.
84 Zydney, A.L. and Colton, C.K. (1984). *Chem. Eng. Commun.*, 30: 191.
85 van Reis, R., Leonard, L.C., Hsu, C.C. and Builder, S.E. (1991). *Biotech. Bioeng.*, 38: 413.
86 Automated, Scalable Cell/Protein Separations (1991). Product brief, Sepracor Inc., Marlborough, MA.
87 Werynski, A., Malchesky, P.S., Sueoka, A., Asanuma, Y., Smith, J.W., Kayashima, K., Herpy, E., Sato, H. and Nose, Y. (1981). *Trans. Am. Soc. Artif. Intern. Organs*, 27: 539.
88 O'Connor, J.L. and Kessler, S.B. (1983). *ASAIO Abstracts*, 12: 59.
89 Colton, C.K. (1991). Private communication.
90 Blatt, W.F., Feinberg, M.P., Hopfenberg, H.P., and Saravis, C.A. (1965). *Science*, 150: 224.

91 Michaels, A.S. (1968). Ultrafiltration. In: *Progress in Separation and Purification*, Vol. 1 (E.S. Perry, ed.). Wiley-Interscience, New York, pp. 297–334.
92 Wang, D.I.C., Sinskey, A.J., and Butterworth, T.A. (1970). Enzyme Processing Using Ultrafiltration Membranes. In: *Membrane Science and Technology* (J.E. Flinn, ed.). Plenum Press, New York, pp. 98–119.
93 Porter, M.C. and Nelsen, L. (1972). Ultrafiltration in the chemical, food processing, pharmaceutical, and medical industries. In: *Recent Developments in Separation Science*, Vol. 2 (N.N. Li, ed.). CRC Press, Cleveland, Ohio, pp. 227–267.
94 Eykamp, W. and Steen, J. (1987). Ultrafiltration and Reverse Osmosis. In: *Handbook of Separation Process Technology* (R.W. Rousseau, ed.). Wiley-Interscience, New York, pp. 826–839.
95 Breslau, B.R. (1982). Ultrafiltration, Theory and Practice. Paper presented at the 1982 Corn Refiners Association Scientific Congress, Lincolnshire, Illinois, June 16–18, 1982.
96 Flashel, E., Wandrey, C., and Kula, M.-R. (1983). Ultrafiltration for the Separation of Biocatalysts. In: *Advances in Biochemical Engineering/Biotechnology, Vol. 26: Downstream Processing* (A. Fiechter, ed.). Springer-Verlag, New York, pp. 73–142.
97 Kulkarni, S.S., Funk, E.W., and Li, N.N. (1992). Ultrafiltration: Module and Process Configuration. In: *Membrane Handbook* (W.S. Ho and K.K. Sirkar, eds.). Van Nostrand Reinhold, New York, pp. 432–445.
98 Charm, S. and Wong, B. (1970). *Biotechnol. Bioeng.*, 12: 1103.
99 Charm. S. and Wong, B. (1980). *Enzyme Microb. Technol.*, 3: 111.
100 Narendranathan, T.J. and Dunnill, P. (1982). *Biotechnol. Bioeng.*, 24: 2103.
101 Virkar, P.D., Narendranathan, T.J., Hoare, M., and Dunnill, P. (1981). *Biotechnol. Bioeng.*, 23: 425.
102 Truskey, G.A., Gable, R., DiLeo, A. and Manter, T. (1987). *J. Parenter. Sci. Technol.*, 4: 16.
103 Bowen, W.R. and Gan, Q. (1992). *Biotechnol. Bioeng.*,40: 491.
104 Kerkhof, P.J.A.M. (1988). *Chem. Biochem. Eng. Quart.*,2: 192.
105 Neubeck, C.E. (1980). U.S. Patent No. 4,233,405.
106 Hummel, W., Schutte, H., and Kula, M.-R. (1982). *Eur. J. Appl. Microbiol. Biotechnol.*, 12: 22.
107 Levy, P.F. and Sheehan, J.J. (1991). *BioPharm*, 4: 24.
108 Barbaric, S., Kozulic, B., Ries, B. and Mildner, P. (1980). *Biochem. Biophys. Res. Commun.*, 95: 404.
109 Lee, S.M., Gustafson, M.E., Pickle, D.J., Flickinger, M.C., Muschit, G.M. and Morgan, A.C. (1986). *J. Biotechnol.*, 4: 189.
110 Jain, S.M. (1983). *Ann. N.Y. Acad. Sci.*, 413: 290.
111 Strathmann, H. (1992). Electrodialysis: Applications. In: *Membrane Handbook* (W.S. Ho and K.K. Sirkar, eds.). Van Nostrand Reinhold, New York, pp. 255–262.
112 Devereux, N., and Hoare, M. (1986). *Biotechnol. Bioeng.*, 28: 422.
113 Bentham, A.C., Ireton, M.J., Hoare, M. and Dunnill, P. (1988). *Biotechnol. Bioeng.*, 31: 984.
114 Devereux, N., Hoare, M. and Dunnill, P. (1986). *Chem. Eng. Commun.*, 45: 255.
115 Zeman, L.J. (1983). *J. Membr. Sci.*, 15: 213.
116 Le, M.S. and Gollan, K.L. (1989). *J. Membr. Sci.*, 40: 231.
117 Nilsson, J.L. (1990). *J. Membr. Sci.*, 52: 121.
118 Chmiel, H., Bauser, H., Schulenberg-Schell, H. and Weber, H. (1990). *Pharm. Ind.*, 52: 223.
119 Bowen, W.R. and Gan, Q. (1991). *Biotechnol. Bioeng.*,38: 688.
120 Suki, A., Fane, A.G. and Fell, C.J.D. (1984). *J. Membr. Sci.*, 21: 269.
121 Blatt, D.F., Dravid, A., Michaels, A.S., and Nelsen, L. (1970). Solute Polarization and

Cake Formation in Membrane Ultrafiltration: Causes, Consequences, and Control Techniques. In: *Membrane Science and Technology* (J.E. Flynn, ed.). Plenum Press, New York, pp. 47–97.
122 Vilker, V.L., Colton, C.K. and Smith, K.A. (1981). *AIChE J.*, 27: 620.
123 Jonsson, G. (1984). *Desalination*, 51: 61.
124 Porter, M. (1986). Concentration Polarization in Reverse Osmosis and Ultrafiltration. In: *Synthetic Membranes: Science, Engineering, and Applications* (P.M. Bungay et al., eds.). D. Reidel Publishing Co., pp. 367–388.
125 Wijmans, J.G., Nakao, S., van den Berg, G.B., Troelstra, F.R., and Smolders, C.A. (1985). *J. Membr. Sci.*, 2: 117.
126 Belfort, G. (1987). Membrane Separation Technology: An Overview. In: *Advanced Biochemical Engineering* (H.R. Bungay and G. Belfort, eds.). John Wiley & Sons, New York, pp. 187–218.
127 Aimar, P., Howell, J.A., Clifton, M.J. and Sanchez, V. (1991). *J. Membr. Sci.*, 59: 81.
128 Hodgson, P.H., Leslie, G.L., Schneider, R.P., Fane, A.G., Fell, C.J.D. and Marshall, K.C. (1993). *J. Membr. Sci.*, 79: 35.
129 Zydney, A.L. and Colton, C.K. (1986). *Chem. Eng. Commun.*, 47: 1.
130 Davis, R.H. (1992). Theory for Crossflow Microfiltration. In: *Membrane Handbook* (W.S. Ho and K.K. Sirkar, eds.). Van Nostrand Reinhold, New York, pp. 480–505.
131 Shmidt, I. and Badiali, M. (1988). U.S. Patent No. 4,790,942.
132 Waal, van der M.J. and Racz, I.G. (1989). *J. Membr. Sci.*, 40: 243.
133 Knops, F.N.M., Futselaar, H. and Racz, I.G. (1992). *J. Membr. Sci.*, 73: 153.
134 Nichols, R.W. (1990). U.S. Patent No. 4,959,152.
135 Norde, W., MacRitchie, F., Nowicka, F.G. and Lyklema, J. (1986). *J. Colloid Interface Sci.*, 112: 447.
136 Degen, P.J., Martin, J., Schriefer, J., and Shirley, B. (1987). U.S. Patent No. 4,693,985.
137 Dalven, P.I., Hildebrandt, J.R., Shamir, A., Laccetti, L.T., Hodgins, L.T. and Gregor, J.P. (1985). *J. Appl. Poly. Sci.*, 30: 1113.
138 Kim, J., Saito, K., Furusaki, S., Takanobu, S. and Okamoto, J. (1991). *J. Membr. Sci.*, 56: 289.
139 Steuck, M.J. (1986). U.S. Patent No. 4,618,533.
140 Sternberg, S. (1982). U.S. Patent No. 4,340,482.
141 Henis, J.M., Tripodi, M.K. and Stimpson, D.M. (1988). U.S. Patent No. 4,794,002.
142 Azad, A.R.M. and Goffe, R.A., (1990). PCT International Patent Application No. WO 90/04609.
143 Stengaard, F.F. (1988). *Desalination*, 70: 207.
144 Robertson, B.C. and Zydney, A.L. (1990). *J. Colloid Interface Sci.*, 134: 563.
145 McGregor, W.C., Weaver, J.F. and Tansey, S.P. (1988). *Biotechnol. Bioeng.*, 31: 385.
146 Datta, R., Fries, L. and Wildman, G.T. (1977). *Biotechnol. Bioeng.*, 19: 1419.
147 Kalyanpur, M., Skea, W. and Siwak, M. (1985). *Dev. Ind. Microbiol.*, 26: 455.
148 Trieber, L.R., Gullo, V.P. and Putter, I. (1981). *Biotechnol. Bioeng.*, 23: 1255.
149 McGregor, W.C. (1989). *J. Biotechnol.*, 10: 277.
150 Nielsen, W.K. and Kristensen, S. (1983). *Process Biochem.*, 18: 8.
151 Schlicher, L.R. and Cheryan, M. (1990). *J. Chem. Tech. Biotech.*, 49: 129.
152 Adams, F., Rice, L.F., Ferry, G. and Taylor, R.J. (1970). U.S. Patent 3,544,455.
153 Cadotte, J., Forester, R., Kim, M. Petersen, R., and Stocker, T. (1988). *Desalination*, 70: 77.
154 Baker, R.W. (1990). Pervaporation in *Membrane Separation Systems: A Research Needs Assessment* (Vol. II), U.S. Dept. of Energy Report No. DOE/ER/30133-H1.

155 Kiani, A., Bhave, R.R. and Sirkar, K.K. (1984). *J. Membr. Sci.*, 20: 125.
156 Kim, B.M. (1984). *J. Membr. Sci.*, 21: 5.
157 Fleming, H.L. (1992). *Chem. Eng. Progr.*, 88: 46.
158 Prasad, R. and Sirkar, K.K. (1989). *J. Membr. Sci.*, 47: 235.
159 Garg, V.K., Costello, M.A.C. and Czuba, B.A. (1991). Purification and Production of Therapeutic Grade Proteins. In: *Purification and Analysis of Recombinant Proteins* (R. Seetharam and S.K. Sharma, eds.). Marcel Dekker, New York, pp. 29–54.
160 Goel, V., Accomazzo, M.A., DiLeo, A.J., Meier, P., Pitt, A. and Pluskal, M. (1992). Deadend Micro-filtration: Applications, Design, and Cost. In: *Membrane Handbook* (W.S. Ho and K.K. Sirkar, eds.). Van Nostrand Reinhold, New York, pp. 506–570.
161 DiLeo, A.J. and Allegrezza, A.E. (1991). *Nature*, 351: 420.
162 DiLeo, A.J., Allegrezza, A.E. and Burke, E.T. (1992). U.S. Patent No. 5,096,637.
163 Devereux, N., Hoare, M. and Dunnill, P. (1986). *Biotechnol. Bioeng.*, 28: 88.
164 Suen, S.Y., Caracots, M. and Etzel, M.R. (1993). *Chem. Eng. Sci.*, 48: 1801.
165 Brandt, S., Goffe, R.A., Kessler, S.B., O'Connor, J.L. and Zale, S.E. (1988). *Bio/Technology*, 6: 779.
166 Garg, V.K., Zale, S.E., Azad, A.R.M. and Holton, O.D. (1992). Role of Functionalized Membrane Separation Technology in Downstream Processing of Biotechnology-Derived Proteins. In: *Frontiers in Bioprocessing II* (P. Todd, S.K. Sikdar and M. Bier, eds.). American Chemical Society, Washington, DC, pp. 321–330.

Membrane Separations Technology. Principles and Applications
Edited by R.D. Noble and S.A. Stern

Chapter 9

Food and beverage industry applications

Munir Cheryan and **Jose R. Alvarez**[a]

Department of Food Science, 103 Agricultural Bioprocess Laboratory, University of Illinois, Urbana, IL 61801, USA
[a]Department of Chemical Engineering, University of Oviedo, Oviedo, Spain

9.1. INTRODUCTION

The application of membranes in the food and allied industries increased dramatically in the 1980s. This is a remarkable achievement, considering that food manufacturers are traditionally quite conservative in their approach to innovation and utilization of "new, improved" technology. Indeed, membrane technology, from its birth in the early 1960s to the early 1980s, was viewed by the food industry with a mixture of interest and suspicion. The principles and concepts behind the science of membrane separations were quite alien at that time compared to the traditional unit operations prevailing in their plants. Since the food industry operates on a smaller margin of profit than most other process industries, it was difficult to justify the expense of discarding what had always worked (e.g., thermal evaporation) and installing a new unit operation (e.g., reverse osmosis) that had not yet been completely proven to "work" in other industries, let alone the food industry.

Regulatory agencies, such as the Food and Drug Administration (FDA) and the U.S. Department of Agriculture, were unsure of how to treat this new technology, resulting in further reluctance by the food industry to adopt membrane separations. This explains why, for example, although cheese-making by ultrafiltration (UF) had been developed and patented in France in 1969, it was

only in the early 1980s that the U.S. dairy industry accepted it as a serious alternative to the traditional method. Today, there are probably few large-scale cheese operations that are not involved with membranes in some way, either for cheese-making, whey treatment, salt brine recovery or other allied processes.

The acceptance of membrane technology by such a conservative industry is due in no small part to (a) advances in the material science of membranes (which have resulted in more robust membranes better suited to sanitation standards and cleaning regimes used by the industry), (b) improved module design, (c) a better understanding of the fouling phenomena, and (d) increased awareness by food industry managers of the science and technology of membranes. The 1990s will continue to see a major penetration of membrane technology in all its facets in the food and kindred industries. Some applications that are already commercial or near commercial are listed in Table 9.1. This includes reverse osmosis (for concentration, to complement or replace evaporation), nanofiltration (for desalting and deacidification), ultrafiltration (for fractionation, concentration and purification), microfiltration (for clarification instead of centrifuges, sterilization instead of heat, and fractionation of macromolecules), electrodialysis (for demineralization instead of ion-exchange) and possibly even pervaporation for specialized applications instead of extraction and/or distillation.

As Table 9.1 shows, the existing and potential applications of membranes in the food industry are vast and varied, and it is beyond the scope of this chapter to cover all applications in detail. We instead focus on the two largest applications to date: dairy products and fruit juices. Information on other food applications is available elsewhere [1]. Much of the research and development has been largely done by companies and the operating parameters may be somewhat specific to a particular application. Nonetheless, there is sufficient knowledge about these applications to make some general observations about the practice and art of membrane separations in the food industry.

9.2 DAIRY INDUSTRY

Among the food industries, diary processing probably accounts for the largest share of installed membrane capacity. Figure 9.1 shows trends in the use of membranes since 1970. Present usage is weighted towards reverse osmosis (RO) and ultrafiltration (UF), although there are expectations of a dramatic growth in the utilization of ceramic membranes for specialized applications. Figures 9.2 and 9.3 are general schematics of the possible applications of membranes in the dairy industry. Processing cheese whey, a by-product of cheese manufacture, was the first successful commercial application. "Nanofil-

TABLE 9.1
Food industry applications of membrane technology

Dairy	RO:	(Pre)Concentration of milk and whey prior to evaporation
		Bulk transport
		Specialty fluid milk products (2–3X/UHT)
	NF:	Partial demineralization and concentration of whey
	UF:	Fractionation of milk for cheese manufacture
		Fractionation of whey for whey protein concentrates
		Specialty fluid milk products
	MF:	Clarification of cheese whey
		Defatting and reducing microbial load of milk
	ED:	Demineralization of milk and whey
Fruits and Vegetables	Juices:	Apple (UF,RO), apricot, citrus (MF/UF,RO,ED), cranberry, grape (UF,RO), kiwi, peach (UF,RO)
	Pigments:	anthocyanins
	Wastewater:	apple, potato (UF,RO)
Animal Products	Gelatin:	concentration and de-ashing (UF)
	Eggs:	concentration and reduction of glucose (UF,RO)
	Animal by-products:	blood, wastewater treatment (UF)
Beverages	MF/UF:	Wine, beer, vinegar — clarification
	RO:	Low-alcohol beer
Sugar refining	Beet/cane solutions, maple syrup, candy wastewaters — clarification (MF/UF), desalting (ED), preconcentration (RO)	
Grain Products	Soybean processing:	Protein concentrates and isolates (UF)
		Protein hydrolyzates (CMR)
		Oil degumming and refining (UF,NF)
		Recovery of soy whey proteins (UF,RO)
		Wastewater treatment
	Corn refining:	Steepwater concentration (RO)
		Light-middlings treatment: water recycle (RO)
		Saccharification of liquefied starch (CMR)
		Purification of dextrose (MF/UF)
		Fermentation of glucose to ethanol (CMR)
		Downstream processing (MF,UF,NF,RO,ED,PV)
		Wastewater treatment
Biotechnology	Production of high quality water (MF,UF,RO,ED)	
	Downstream processing (MF,UF,RO,ED): cell harvesting, protein fractionation, desalting, concentration	
	Bioreactors:	enzyme hydrolysis
		tissue culture
		plant cells

ED: electrodialysis, MF: microfiltration, CMR: membrane reactor, NF: nanofiltration, PV: pervaporation, RO: reverse osmosis, UF: Ultrafiltration, UHT: ultra-high temperature.

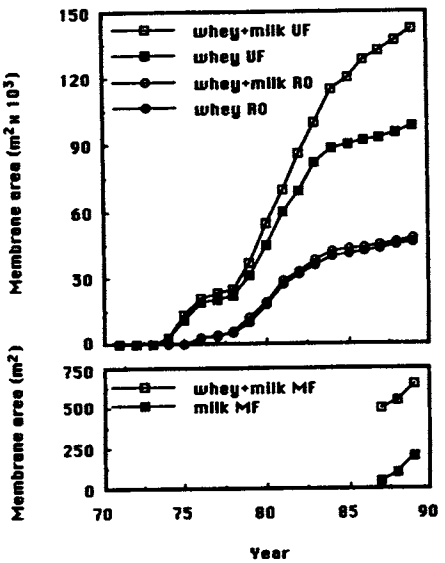

Fig. 9.1. Membrane area installed in the dairy industry worldwide. Estimated by Maubois [92].

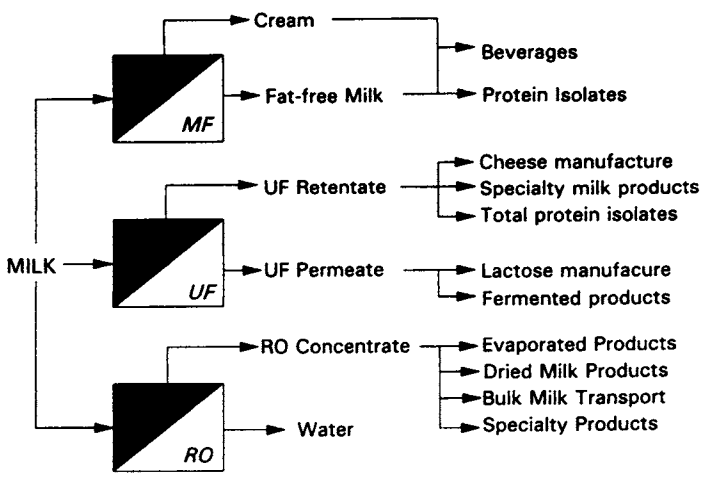

Fig. 9.2. General schematic of possible membrane applications in milk processing.

tration" or "loose RO" has a specialized application in the dairy industry. Reverse osmosis usage is dependent on prevailing energy costs, since it is used primarily as a substitute for thermal evaporation. Not shown in Fig. 9.1 are electrodialysis and pervaporation; the former has major commercial application (although not on the scale of the pressure-driven membrane processes), but the latter has yet to make its presence felt in the dairy industry.

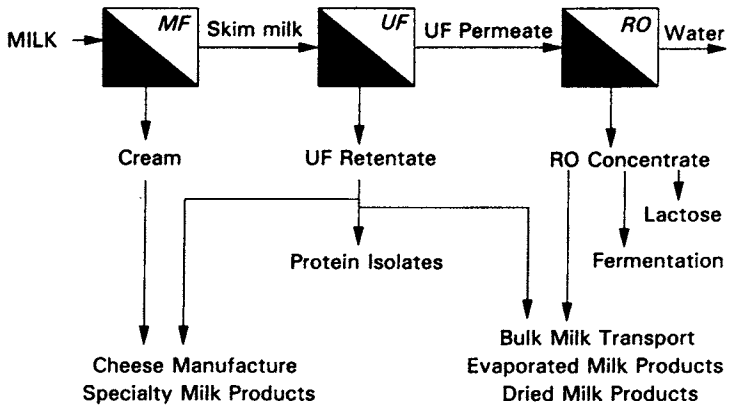

Fig. 9.3. Membrane processing of milk by sequential operations.

9.2.1 Milk

9.2.1.1 Concentration by Reverse Osmosis

The use of reverse osmosis for concentration of milk has been studied since the early 1960s. The major attraction to the dairy industry (apart from the obvious savings in energy) was that, unlike thermal evaporation or freeze concentration, moisture removal was accomplished without a change of phase or having to use extremes of temperatures. The milk is exposed to minimum heat during concentration, which avoids protein denaturation, development of the "cooked" flavor and other heat damaging effects on the constituents of milk. Initial trials with first generation cellulose acetate membranes were discouraging because of the limitations in cleaning, temperature and pH. Sanitation in the early modules also left much to be desired. The development of second generation thin-film composites was a major advancement that largely overcame many of the obstacles, except for their zero-chlorine tolerance (dairy plant operators use chlorine liberally in day-to-day operations as a sanitizer). Figure 9.4 compares the operating parameters of commercially available composite and cellulose acetate membranes.

The osmotic pressure of milk is about 600–700 kPa, due largely to the lactose and dissolved salts (Table 9.2). Figure 9.5 shows typical data obtained for the concentration of milk in a spiral wound thin-layer composite membrane. Figure 9.6 shows the contribution of osmotic pressure and concentration polarization to the reduction in flux compared to water. The asymptotic relationship between applied transmembrane pressure and flux is due to concentration polarization of proteins and fat, giving rise to increased hydrodynamic resistance to permeate flow and/or to higher osmotic pressure. The decrease in flux at higher pressures is probably due to a compaction of the polarized/fouling layer,

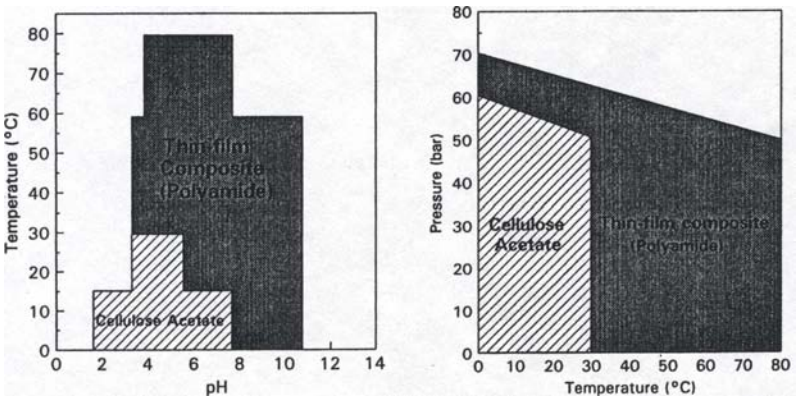

Fig. 9.4. Comparison of operating limits of thin-film composite (polyamide) and cellulose acetate membranes.

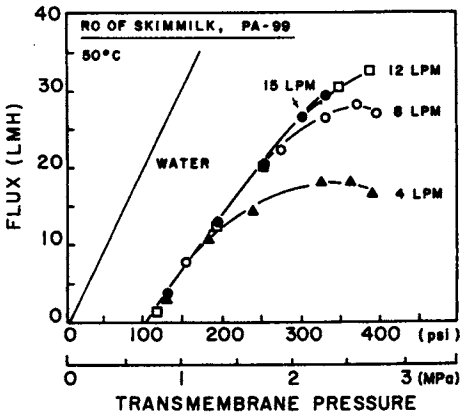

Fig. 9.5. Reverse osmosis of skim milk with a polyamide composite membrane. The variable is flow rate through a 50 mm diameter spiral module. From Cheryan et al. [2].

TABLE 9.2

Composition of selected dairy products

Component	Milk	Cheese whey	Cottage cheese	Feta cheese	Mozzarella cheese	Cheddar cheese
Total solids	12.5	6.0	20.3	44.8	45.8	63.3
Protein (NX6.38)	3.3	0.6	17.3	14.2	19.4	24.9
Fat	3.5	0.1	0.4	21.3	21.6	33.1
Lactose	4.9	5.0	1.9	4.1	2.2	1.3
Ash	0.7	0.6	0.7	5.2	2.6	3.9

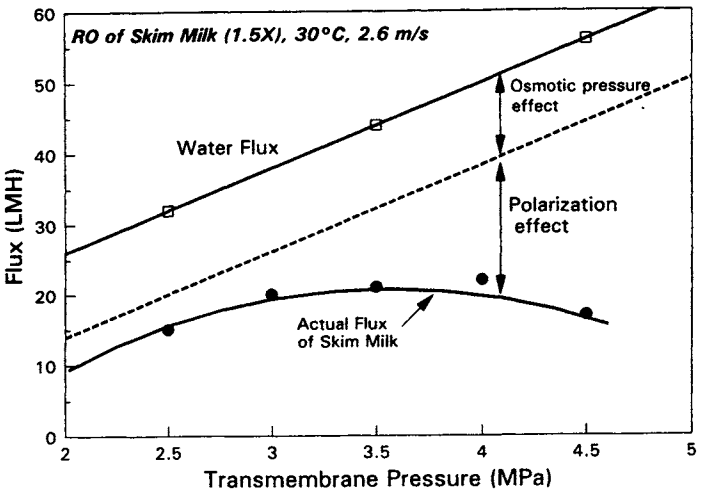

Fig. 9.6. Effect of various phenomena on reverse osmosis of skim milk. Adapted from Hiddink et al. [94].

giving rise to increased resistance, or to a much higher osmotic pressure [2].

Fouling (which is a decrease in flux with time under constant operating conditions) is generally much less with milk than with whey. The nature of the deposit is mostly protein, but inorganic salts such as calcium phosphate play an important role [3]. This salt could act as a bridge between the membrane and the protein, leading to a higher hydraulic resistance of the protein layer.

Operating conditions should be carefully controlled, especially with RO of whole milk. RO of raw milk will give concentrates of poor bacteriological quality and increased free fat content [4]. Suitable preheat treatment at a subpasteurization level ("thermization") can usually avoid such problems, as will operating the RO plant at temperatures of 50–55°C. Although the high pressures *per se* pose no problem, the sudden release of pressure at the outlet of the module can damage fat globules [5]. This can be overcome by proper design of the outlet high-pressure valve. The maximum solids concentration in the retentate is limited largely by the osmotic pressure. Most commercial modules have a limit of about 3–4 MPa, which means a maximum of 3–4X concentration before the flux drops too low to be economical. Some specific applications of reverse osmosis for milk concentration are discussed below:

Reduction of milk transport costs

Perhaps the greatest potential for RO in the dairy industry is in bulk milk transport, especially in those countries which have large distances between producing and consumption areas. Considering that milk is more than 85% water, preconcentration of the milk prior to shipment to central dairies should

result in considerable savings in transportation costs, as well as reducing chilling and storage costs [6]. RO-milk products, when reconstituted with good quality water, are indistinguishable from unconcentrated milks in flavor and other quality attributes. If accepted by the regulatory authorities in the countries concerned, this would result in several large RO plants in USA, Australia, Canada, India, China and possibly even the European common market, among others.

Fluid and frozen milk products

Milk concentrates produced by RO followed by ultra-high temperature (UHT) sterilization and homogenization may have some market value as such, especially for use in cooking applications. Its viscosity and other sensory qualities may not make it acceptable as a beverage for direct consumption; UF-milk may be better (see later). Ice cream prepared using RO concentrated skim milk has been prepared successfully [7–9].

Savings in dairy plant operations

The removal of water from milk during the production of dried milk powder accounts for a significant portion of the product's final cost. Milk (either whole or skimmed) is usually concentrated to 45–50% total solids before spray drying. Because of the upper solids limitation mentioned above, RO cannot be used by itself as a complete substitute for conventional evaporation. RO, however, can be used as a preconcentration step ahead of the evaporators to reduce the time and energy demands of evaporation, or as a means to increase capacity of existing evaporators. Figure 9.7 shows the relative amounts of water to be

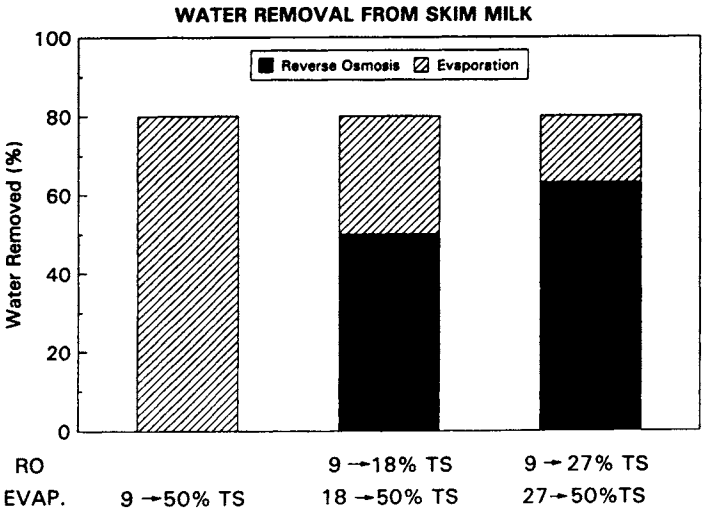

Fig. 9.7. Relative amounts of water removed by reverse osmosis and evaporation during concentration of skim milk.

TABLE 9.3

Comparison of energy consumption and surface areas for RO-concentration of milk 2.5X at a feed rate of 1000 kg per hour [100]

Process	Area (m^2)	Energy (kcal/kg milk)
Thermal concentration	10.4	455
Open-pan boiling	10.4	455
Evaporator:		
Double-effect evaporator	25	209
Mechanical Vapor Recompression	32	136
Membrane Process*		
Batch, single-pump	65	80
Batch, dual-pump	65	7
Continuous, one-stage	206	16
Continuous, three-stage	93	7

* Spiral-wound cellulose acetate membrane. A spiral-wound thin-film composite membrane would use about half this energy [2].

removed by evaporation and reverse osmosis to achieve a 50% total solids (TS) concentrate. Table 9.3 compares the energy consumption of RO and thermal evaporation for a 2.5X concentration of milk.

Although the feasibility of concentrating milk by RO has been demonstrated for many years, it is surprising that there are few such installations in the world. There is ample evidence that, for equivalent capital costs, the operating cost of a RO plant is much less than a thermal evaporation plant [2]. The potential energy savings are enormous. In 1986, there were 680,000 metric tons of dried milk products and 864,000 tons of condensed and evaporated milk products produced in the United States alone. This represents potentially about 5.5 million tons of water that can be removed by incorporating a 2.5X RO process in the evaporation plants. Even if only 25% of the condensed, evaporated or dried milk products was processed with RO in this fashion, it represents a savings of at least 300 million MJ per year.

Feeding RO-concentrated whole milk into a centrifugal separator can increase the capacity of the separator, with little or no effect on the skimming efficiency. However, when used to make butter, fat losses were higher than normal, and the curd content greatly increased in the butter. The manufacture of "khoa", a heat-desiccated milk product in the Indian subcontinent, has great potential [10].

Fermented products

RO-milk concentrates (13–17% total solids) can be used directly in the manu-

facture of yogurt. Several investigators [11–13] founded that the culture growth, acid production, acetaldehyde concentration, viscosity, flavor, and other desirable attributes of the product did not differ greatly from yogurt prepared the conventional way with added milk powder. Protein enriched cultured milk products, such as "Ymer", a traditional Danish cultured product, can be prepared by RO concentration of skim milk to 15% TS. This reportedly increases yield by 50%. However, although there has been considerable research on the manufacture of hard cheese by RO [14], ultrafiltration seems to be the preferred method (discussed later).

9.2.1.2 Milk Fractionation by Ultrafiltration

Ultrafiltration membranes allow the passage of the lactose and soluble salts while retaining the protein and fat and some of the insoluble or bound salts. Polysulfone-type membranes (e.g., polyethersulfone) are most popular even though they foul more than cellulosic membranes. However, polysulfone has the advantage that higher temperatures can be used (generally 50–55°C to keep the viscosity low, flux high and the growth of microorganisms under control), they can better tolerate extremes of pH (thus making cleaning much easier) and chlorine (for sanitation). It is interesting that milk tends to foul membranes much less than cheese whey despite its higher concentration of solids (Table 9.2).

Typical data for UF of milk are shown in Figure 9.8. Permeate flux increases as the pressure increases, but becomes independent of pressure at a level that

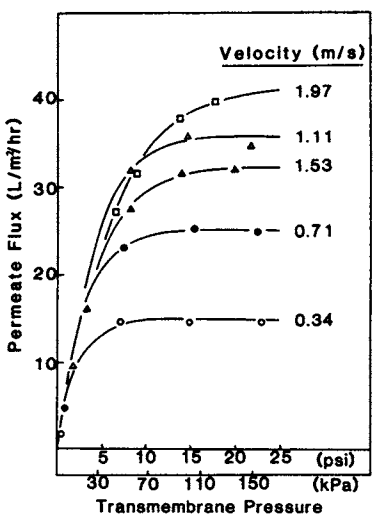

Fig. 9.8. Ultrafiltration of skim milk in a hollow fiber module [95].

TABLE 9.4

Composition of whole milk and PRO-CAL, a low-cholesterol, low-fat, high-calcium milk produced by ultrafiltration [15]. Values are per 100 g serving

Component	Regular whole milk	PRO-CAL One	PRO-CAL Zero
Fat (g)	3.5	0.87	0.1
Protein (g)	3.5	6.1	6.1
Carbohydrate (g)	4.8	4.8	4.9
Sodium (mg)	52	52	52
Potassium (mg)	161	161	161
Calcium (mg)	130	217	217
Cholesterol (mg)*	14	3.5	0.5
Calories	65	52	49
Calories from fat	48	15	4

* Calculated assuming 0.40% of the fat is cholesterol.

depends primarily on the recirculation velocity of the retentate. Concentration polarization is quite severe with milk, and thus it is best to operate at the highest velocity possible. In most cases, maximum total solids obtainable with UF is about 38–42%. Some specific applications are discussed below:

Fluid milk products

There is considerable potential in the manufacture of specialty milk-based beverages. Milk is the major source of calcium in the average American diet and a significant source of high-quality protein and other nutrients. In addition, as shown in Table 9.4, while whole milk provides a large number of nutrients, it also contains the undesirable fat and cholesterol. Removal of the fat will reduce these compounds, but the resulting milk has poor texture and taste.

To compensate for the poor taste and to maximize the concentration of the desirable protein and calcium, a process has been developed [15] using ultrafiltration as shown in Fig. 9.9. Since calcium in milk is mostly in the insoluble or bound form, or associated with impermeable casein micelles, concentrating skim milk by UF will simultaneously concentrate the calcium and protein, while leaving the concentration of sodium, potassium and lactose unchanged, as shown in Table 9.4 for the PRO-CAL products. Fat can be added back to improve sensory quality if desired. The taste and texture of the UF-milk (called PRO-CAL, to reflect its higher protein and calcium contents) is superior to regular skim milk, even skim milk with added milk solids. The low cholesterol product, with 1% added fat, can be used to make soft-serve ice cream and milk shakes. Processes for the reduction of lactose in skim milk have been proposed by Watters et al. [16] and Rajagopalan and Cheryan [103,104].

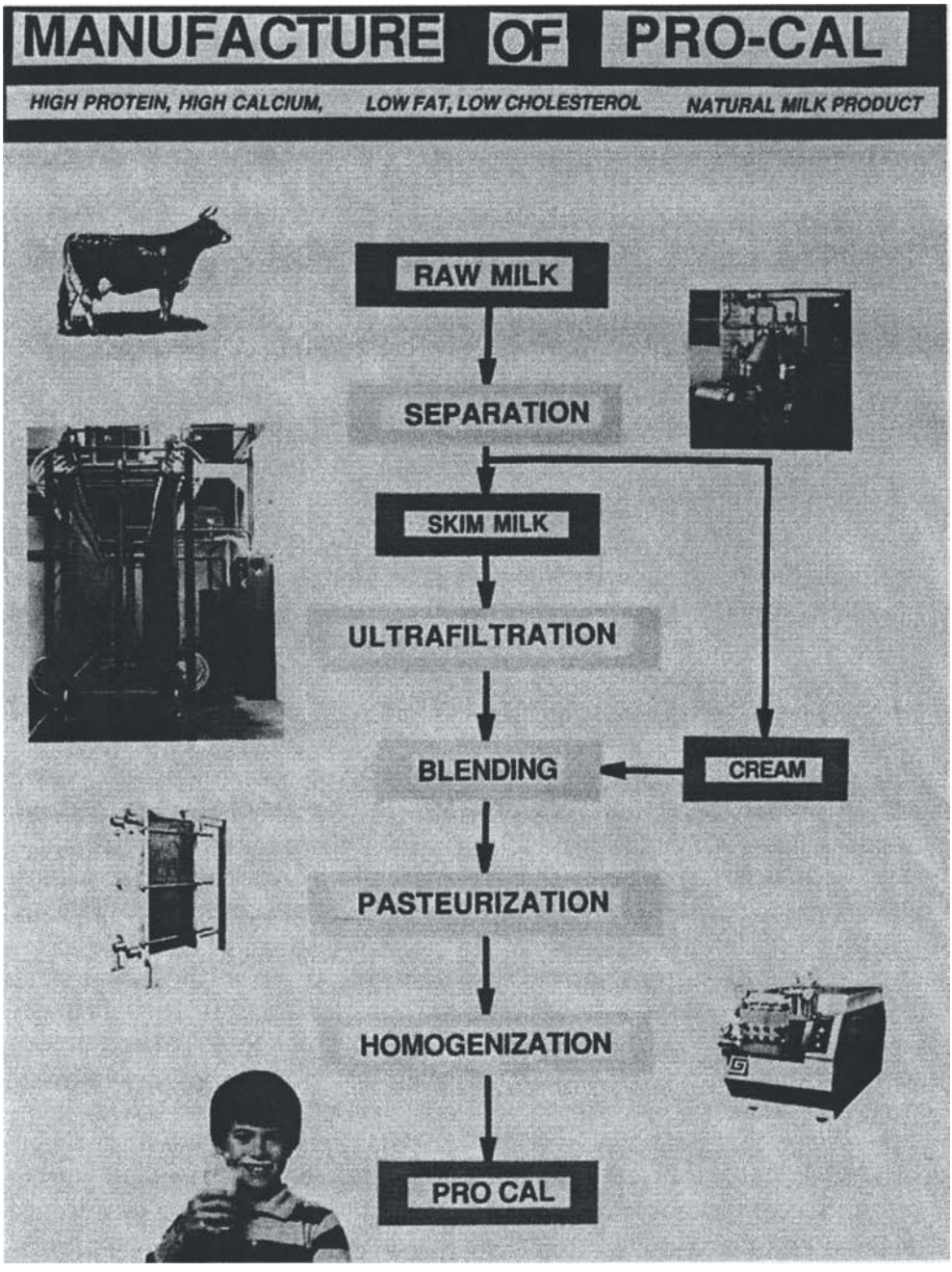

Fig. 9.9. Manufacture of PRO-CAL, a high-protein, high-calcium low-fat milk product by ultrafiltration [15].

When used for the production of yogurt, UF milk gave a product with better viscosity and firmness than yogurt made from evaporated, milk powder-added or RO-concentrated milks, although organoleptic scores were lower than the others, due most likely to the loss of lactose and salts [17].

"Ymer" has also been manufactured from UF milk. After 2X concentration by UF, cream is added if necessary, followed by homogenization and pasteurization. The concentrate is acidified by the addition of microbial culture. UF Ymer is generally much better in overall quality; furthermore, a 15–20% increase in yield is obtained due to the inclusion of whey proteins.

On-farm ultrafiltration of milk

This has been studied in the United States and France with a view to reducing transportation and refrigeration costs. The general consensus from several studies is that, while it is technically feasible for large dairy herds and when the concentrated milk is used for the manufacture of cheese, regulatory and marketing problems would inhibit application of the process. Stability of ultrafiltered milk is satisfactory [18], but there are doubts about the heat treatment given before UF ("thermization" at 65–70°C for 10–20 seconds) and the problem of health and safety compliance requirements on the farm. Nevertheless, the day may come when milk will be processed and packaged on site at dairy farms, leading to decentralization of processing operations [19]. Thus producers will be able to ship value-added finished products rather than raw milk. This will open up new opportunities for UF on the dairy farm.

9.2.1.2.1 Cheese manufacture

The principal use of milk ultrafiltration in the dairy industry today is the manufacture of cheese. The pioneering work of Maubois and coworkers in 1969 that resulted in the "MMV" process for the manufacture of cheese has revolutionized the dairy industry. From a membrane technologist's point of view, cheese can be defined as a fractionation process whereby protein (casein) and fat are concentrated in the curd, while lactose, soluble proteins, minerals and other minor components are lost in the whey [1]. Thus one can readily see the application of ultrafiltration: concentrate milk to a protein/fat/solids level normally found in cheese (Table 9.1). This "pre-cheese" is then converted to cheese by conventional or modified cheesemaking methods, as shown in Fig. 9.10. Some cheesemaking options with ultrafiltration are shown in Fig. 9.11.

Some of the benefits of using UF in cheesemaking are:

- An increase in yield of 10–30% with soft and semi-soft cheeses due to the inclusion of the whey proteins. Figure 9.12 shows the potential savings in milk in the manufacture of different cheeses depending on the degree of concentration of the retentate.
- A lower requirement of the enzyme (rennet). There is conflicting scientific

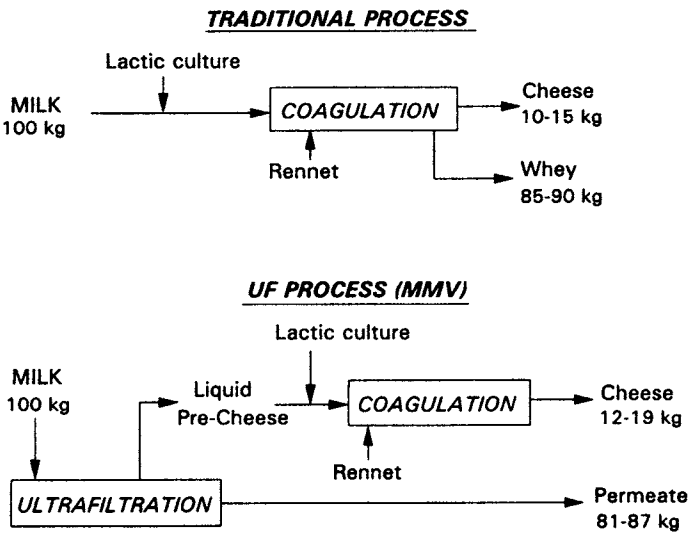

Fig. 9.10. Traditional and UF methods for the manufacture of cheese [92].

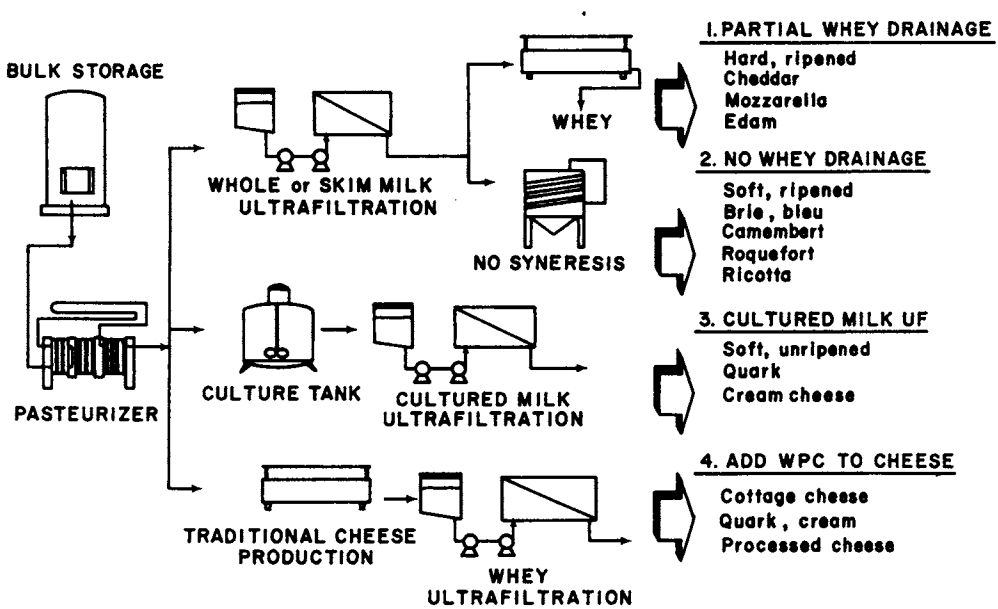

Fig. 9.11. Cheese-making options with ultrafiltration [50].

evidence in the literature [20]; in some cases it has reduced enzyme requirements by 70–85%.

- A reduced volume of milk to handle, reducing the number of cheesemaking vats.

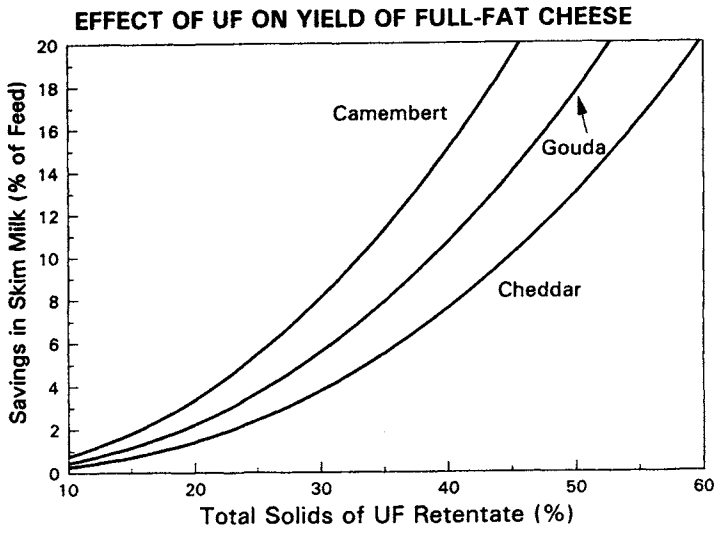

Fig. 9.12. Potential savings in milk usage by using ultrafiltration, expressed as a percentage of the total solids (TS) of the UF concentrate [96].

- Little or no whey is produced because most of the water and lactose has been already removed [21–23].
- Uniformity in the quality of the product. Protein levels can be standardized and the product suffers less from seasonal variations [22,24].
- Ability to use a continuous and automated process, which improves quality control, especially of moisture in the final product. This also results in improved sanitation and environmental conditions [22–24].

There are some technical difficulties with this process:

- The increase in viscosity is dramatic when the protein content of milk exceeds 12–14%. Therefore, it is more difficult to mix the starter culture and rennet. This may lead to texture problems in the cheese. This can be partially overcome by addition of NaCl, citrate or acid before UF [21,25].
- The buffer capacity of the retentate is increased, so even if there is a higher lactic acid production, pH does not drop to the desired value, which is usually pH 4.6 [26].
- Recirculation of retentate, even at the relatively low pressures encountered in UF, may lead to a partial homogenization of fat and reduce texture of hard cheeses. In addition, exposure of retentate to heat and air may damage whey proteins, which may affect water content and texture of the cheese.
- Semi-hard and hard cheeses have a low moisture content and consequently a high solids content. A true "pre-cheese" cannot be made for these products. However, even a partial pre-concentration can have significant benefits.

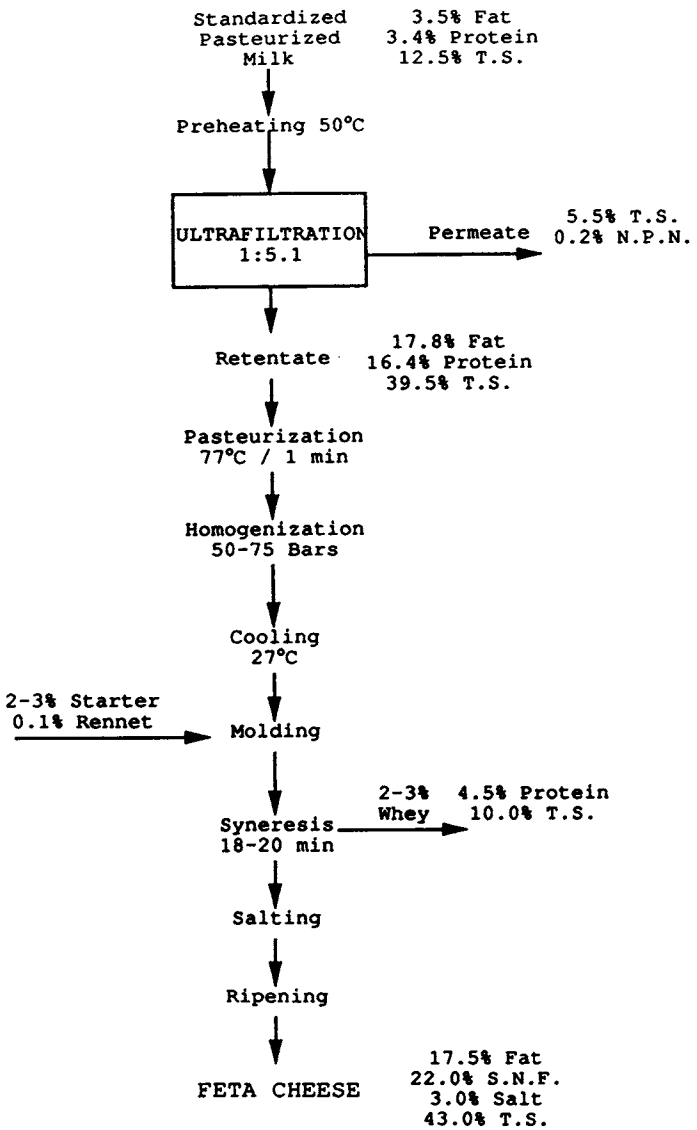

Fig. 9.13. Manufacture of feta cheese by ultrafiltration [92].

Some specific examples of UF cheese are presented below:

Feta Cheese. The advantages of ultrafiltration in the production of feta cheese are especially remarkable (Fig. 9.13). The inclusion of whey proteins makes the cheese smoother in texture than the traditional product. The heat treatment denatures the whey protein, giving smoothness to the cheese, as well as higher moisture. If the Feta cheese is required to have similar texture to the traditional

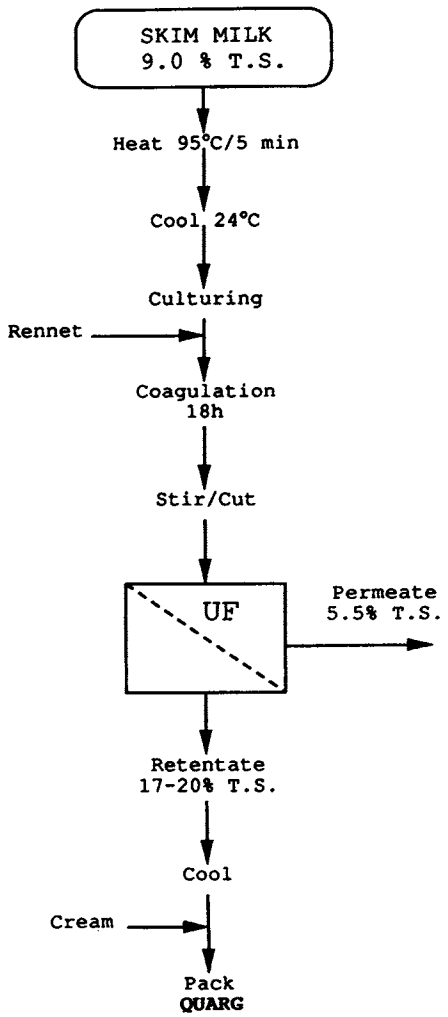

Fig. 9.14. Manufacture of quarg by ultrafiltration [93].

one, some whey drainage has to be considered, and less UF is done (typically only to 2.5X rather than the 5X shown in Fig. 9.13).

Quarg is an unripened, soft, smooth curd cheese, produced from skim milk. It is low in calories and high in protein, similar to the shrikhand popular in the Indian subcontinent. Quarg is another UF success story (Fig. 9.14). To minimize possible bitterness due to high residual minerals in the product, ultrafiltration should be done at a low pH (which will solubilize the minerals and allow them to permeate). If the UF is done at the end of fermentation, a UF system capable of handling this coagulated product has to be used.

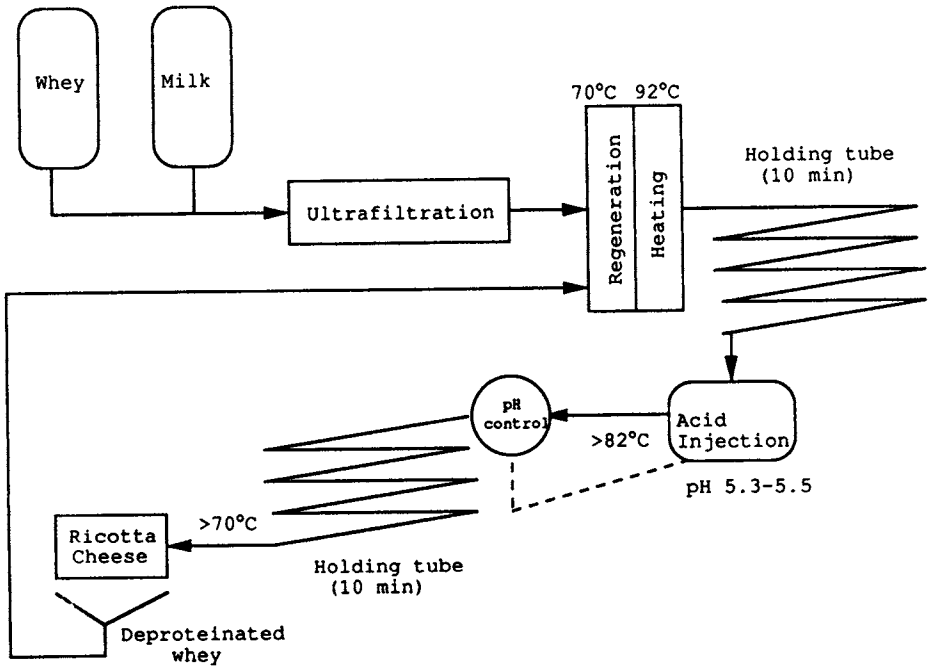

Fig. 9.15. Manufacture of ricotta cheese by ultrafiltration [29].

Camembert is another variety of soft cheese with a special surface ripening. The internal part remains soft mainly due to the migration of lactic acid, along with minerals, to the surface. This explains the need to control the mineral content of the retentate in order to ensure good quality in the final product. Whey proteins do not significantly affect the texture of the cheese, and so its inclusion has no detrimental effect; in fact, it helps to increase the yield.

Ricotta manufacture by UF has been developed by Maubois and Kosikowski [28]. More recently, Modler [29] proposed a continuous method (Fig. 9.15) where coagulation takes place in 30 m of heavy wall tygon tubing of 3.8 cm diameter. The coagulated curd is separated from the deproteinated whey by a conveyor belt.

Mozzarella cheese was another challenge for UF (Fig. 9.16), because whey proteins affect stretchability and meltability of the cheese. When cheese is made from low-concentrate retentates, it has stretching and melting characteristics similar to the regular mozzarella. Most UF processes for mozzarella include reduction of calcium by acidification of the milk to about pH 5.8 before ultrafiltration, followed by diafiltration of the retentate. This is considered essential for the development of stretching properties of the cheese. Homogenization of milk is known to reduce the stretchability of the cheese; therefore, skim milk is ultrafiltered, and the fat content is adjusted later by adding cream. High whey

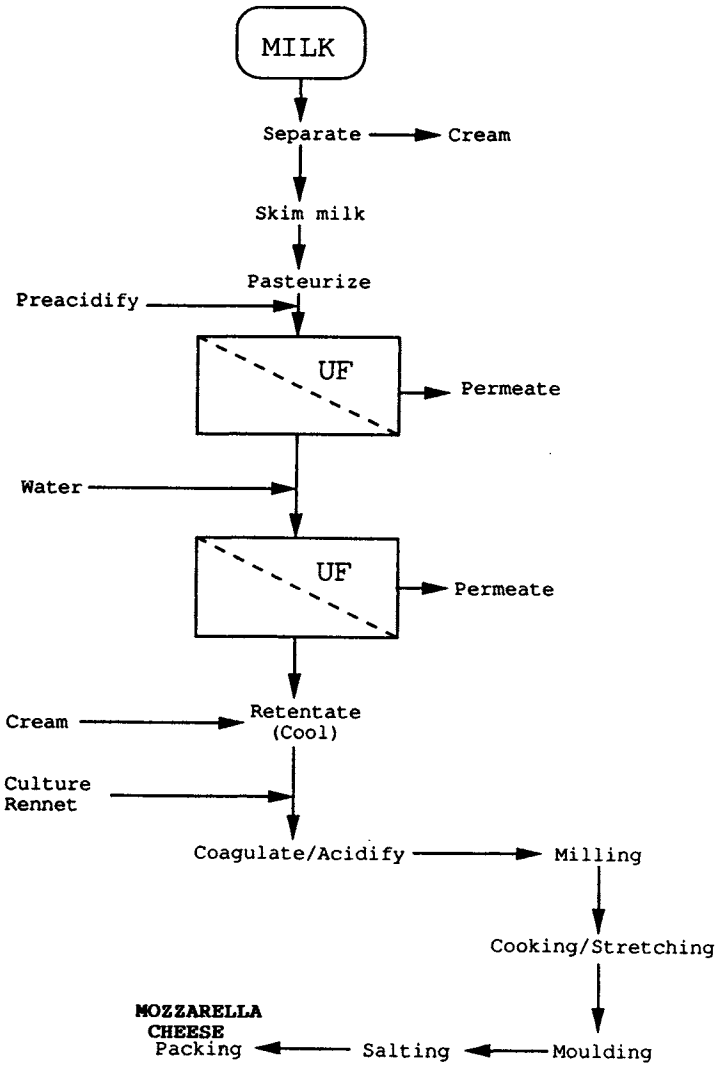

Fig. 9.16. Manufacture of mozzarella cheese by ultrafiltration [92].

protein in the mozzarella results in poorer melting quality. Denaturated whey proteins allow the entrapment of moisture, lowering the melting quality; complexes between whey protein and casein are also likely to be responsible.

Cheddar by UF has long been considered the ultimate challenge for the cheesemaker. Most semi-hard cheeses require a relatively long period of maturation (aging) in order to achieve the desired texture and flavor. The proteolytic activity of the coagulant is a key factor in ripening. Slow proteolysis reported in early studies of UF hard and semihard cheeses was due to the low levels of

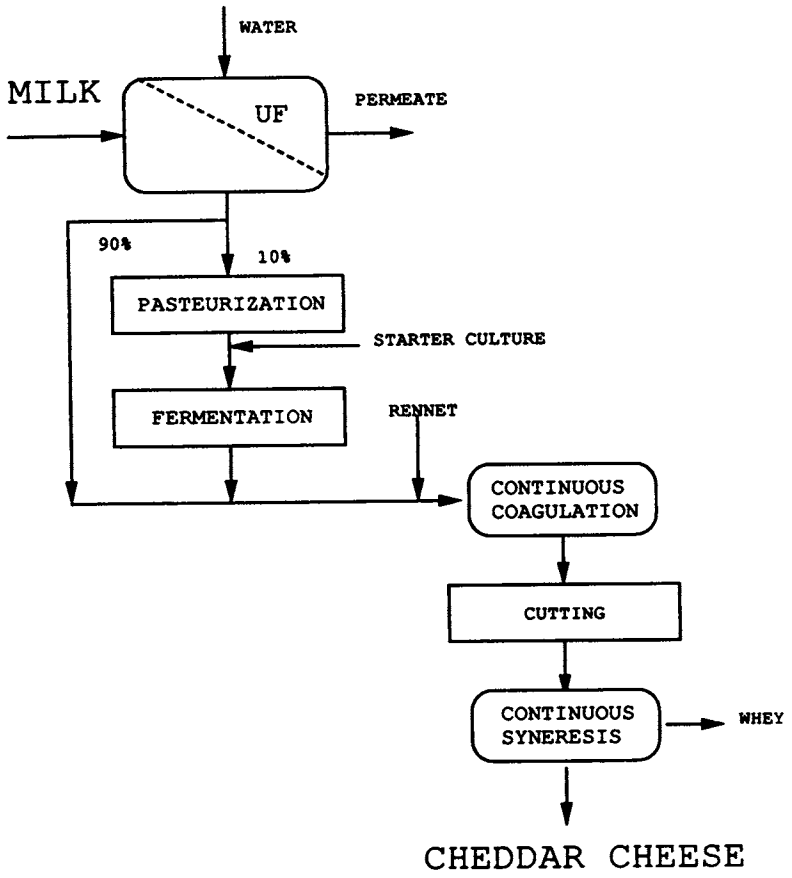

Fig. 9.17. Manufacture of cheddar cheese by ultrafiltration using the APV Sirocurd process [24,31].

residual rennet. Therefore, more residual rennet is required in the UF cheese to obtain the same rate of ripening.

There are numerous publications on the problems of making cheddar cheese by ultrafiltration [1,30]. Perhaps the only successful solution comes from CSIRO in Australia, after more than a decade of development. A schematic of the process is shown in Fig. 9.17. In order to obtain a "pre-cheese" of the same total solids content (62%), a nine-fold concentration has to be done. This is not possible with most common UF equipment. Some expulsion of moisture during curd handling (instead of during UF) is necessary to reach that solids level. The effect of whey proteins on the properties of UF cheeses is still a matter of debate. Undernaturated whey proteins appear to be resistant to the action of rennet, starter and plasmin. Whey proteins could act as an inert filler, giving the cheese a smoother texture or have a diluting effect which limits the accessibility of enzymes to the casein micelles.

Cheddar cheese yields are not as high as those of soft cheeses. If a 5X milk concentrate is used, inclusion of whey proteins would increase yield by 2.5%. If the water of hydration is included, yield should increase by 5%. If there are no losses of casein, it raises yield up to 6%. Furthermore, if 95% fat retention is obtained, then yield increase should go up to 8%, which has been reported in commercial manufacture [24,31].

By 1986, the first commercial cheddar cheese plant using the "APV Sirocurd" process was installed at the Murray Golburn dairy in Cobram (in Victoria, Australia) producing cheddar cheese reportedly indistinguishable from that produced by the conventional batch process. A larger plant designed to handle 42,000 liters of whole milk per hour was installed in 1990 at Land O'Lakes, Minnesota. Whole milk is standardized and pasteurized before being concentrated 5X in a nine-stage UF system utilizing polyethersulfone spiral modules (not all nine stages are used at start-up; a few are kept in reserve to be brought online during the processing day to compensate for flux decline). The final three stages include diafiltration to reduce the lactose content of the retentate (this is necessary for proper texture and flavor development of the finished cheese).

The retentate (38–40% total solids) is split into two streams. About 10% is repasteurized and is fermented with the starter culture; this is then mixed with the rest of the retentate and enzyme (rennet) in a continuous coagulator. The coagulum is then cut and cooked in two syneresis drums where generation of curd and whey occurs. The curd–whey mixture is then pumped to a draining and matting conveyor and a standard cheddaring system before packaging. The permeate from the UF plant is sent to a RO plant to produce sterile water for cleaning and diafiltration. From a commercial viewpoint, the Sirocurd process is attractive because of its continuous nature, higher yields and better control of moisture in the final cheese.

9.2.1.3 Milk Microfiltration

The development of inorganic/ceramic membranes has opened up a new set of applications of membranes in milk processing. Although a relatively small application today in terms of installed membrane area (Fig. 9.1), this is expected to increase rapidly in this decade. It is interesting that, although several studies have shown that these inorganic membranes also suffer from typical fouling problems caused by interactions between the membrane, protein and/or minerals [32–35], it has not prevented them from being used for separations of milk components by a mechanism that is not fully understood.

The main applications of microfiltration in milk processing are fat separation, bacterial removal and caseinate concentration. As shown in Fig. 9.18, casein micelles (milk protein in suspension) are considerably smaller than the bacteria and fat. A membrane with pores around 0.3–1.0 microns should be able

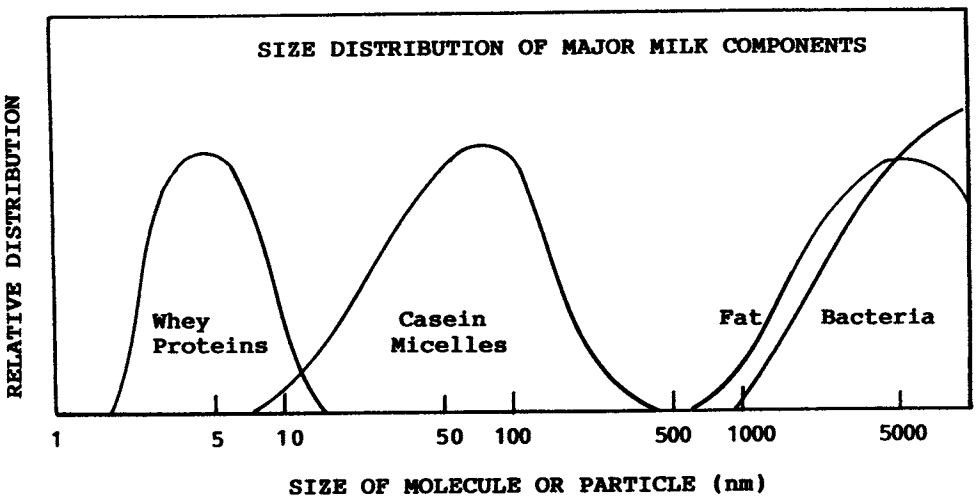

Fig. 9.18. Size distribution of major milk components. Not shown are the carbohydrate (lactose) and soluble salts, which are much smaller than the components shown.

to separate the fat and bacteria from the rest of the milk components, provided the membrane had a fairly uniform and narrow pore size distribution and the appropriate physical and chemical properties to minimize fouling. However, attempts with polymeric membranes failed, due to the formation of a "dynamic" or secondary membrane of polarized solutes that quickly caused MF membranes to behave like UF membranes, i.e., the caseins and whey proteins were also rejected. To minimize the formation of this secondary membrane, the modules had to be operated at extremely high velocities (over 6 m s^{-1}) and low transmembrane pressure (less than 5 psig or 40 kPa) to minimize compaction of the polarized layer.

This appears to be a contradiction, since high velocities, especially in narrow-diameter tubes (e.g., < 3 mm), result in high pressure drops. A pressure profile along the length of a tubular module is shown in Fig. 9.19 (top left). Typically, the permeate channel is operated at low (close to atmospheric) pressures. The retentate side is operated with a high inlet pressure and low outlet pressure to maintain high velocity. This results in severe fouling (by compaction of polarized solutes) at the inlet of the module; on the other hand, the low pressure at the outlet means that some of the available membrane area towards the outlet was not being utilized effectively. The resulting performance would be as shown in Fig. 9.19 (bottom left): a rapid drop in flux and an increase in protein rejection to the extent that the microfilter behaves as an UF membrane.

The key to the eventual successful development of the "Bactocatch" process (a trade name for the system developed by Alfa-Laval) is the "constant pressure" or "high-flux, low-fouling (HFLF)" mode of operation [36]. As shown in

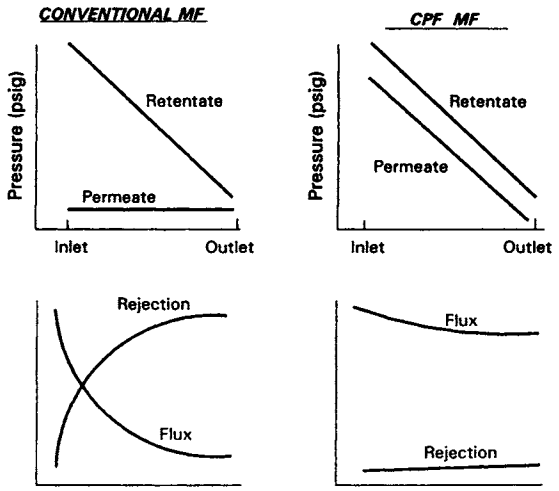

Fig. 9.19. Pressure profiles (top) and flux (bottom) during microfiltration of milk. Left: Conventional microfiltration. Right: Constant-pressure or HFLF microfiltration, as shown in Fig. 19.20.

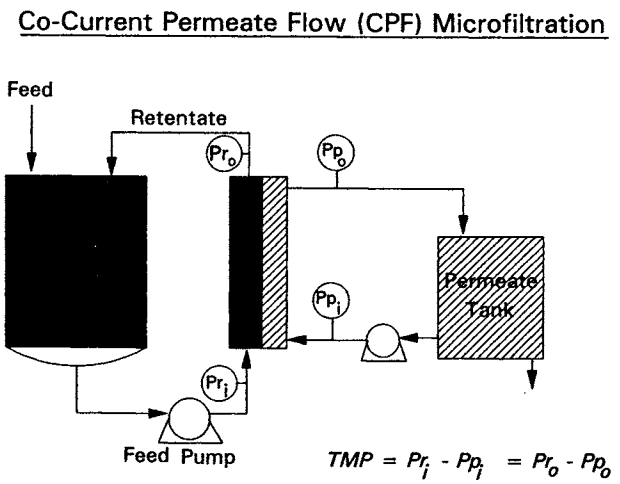

Fig. 9.20. Constant-pressure or high-flux, low-fouling (HFLF) microfiltration. The feed is pumped through retentate channels at high velocity. The permeate is pumped through the shell side of the module with the same pressure drop as the retentate.

Fig. 9.20, this requires the simultaneous operation of a retentate pumping loop and a permeate pumping loop, to simulate a pseudo-"backwashing" operation, but in a continuous manner rather than the periodic or intermittent manner practiced traditionally. With two parallel flows adjusted so that the pressure DROP was the same on the permeate and retentate sides of the module, the

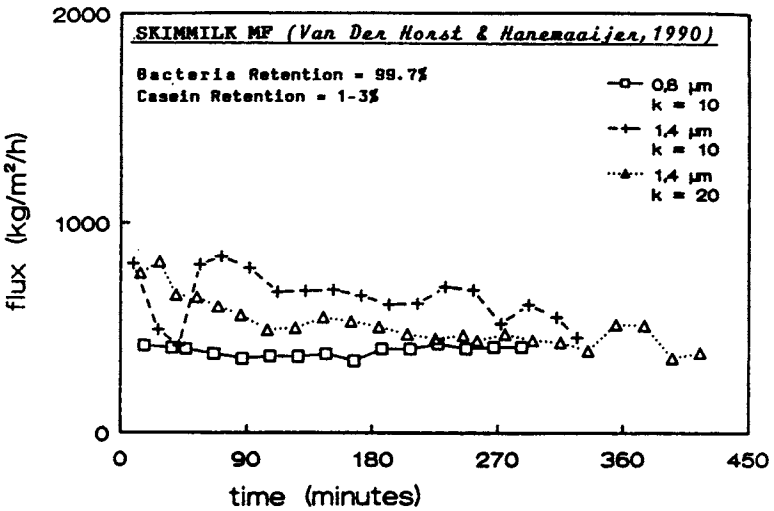

Fig. 9.21. Microfiltration of skim milk in a ceramic MF membrane [34].

pressure profile would be more like that shown in Fig. 9.19 (top right). The performance would then be much better (Fig. 9.19, bottom right).

This combination of tubular ceramic membranes (Bactocatch uses Membralox membranes) and the double loop, constant-pressure operation has produced dramatic results. Fluxes of 500–700 liters $m^{-2} h^{-1}$ can be achieved over a period of 6 hours (Fig. 9.21). If needed, the transmembrane pressure can be increased slightly by 0.05–0.1 bar (0.75–1.5 psi) to compensate for fouling (Fig. 9.22).

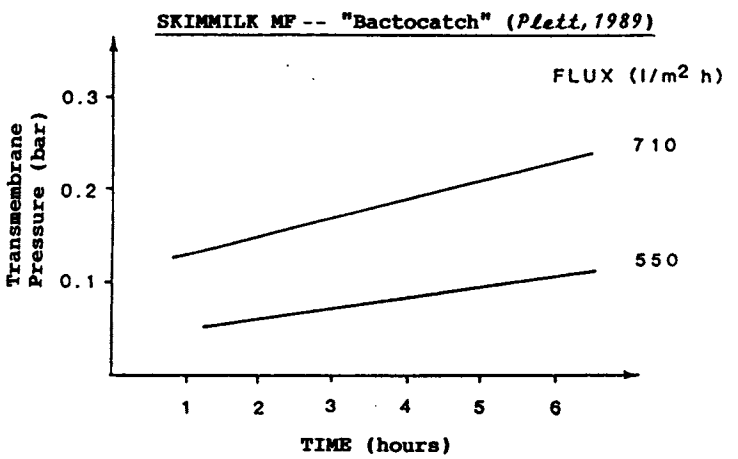

Fig. 9.22. Microfiltration of skim milk in a ceramic MF membrane (the "Bactocatch" process). From Plett [37].

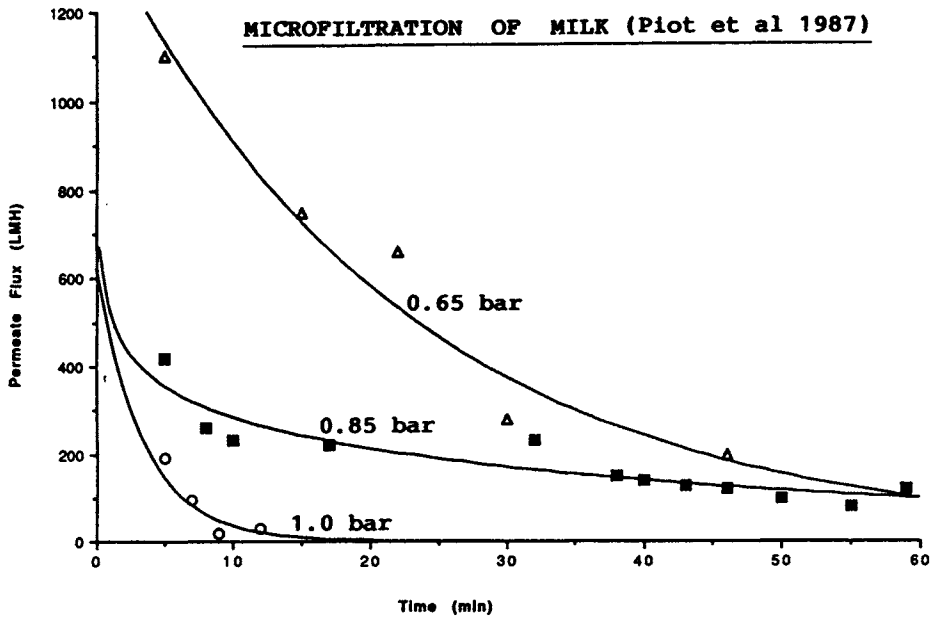

Fig. 9.23. Microfiltration of milk: effect of transmembrane pressure on flux. From Piot et al. [32].

Under these operating conditions of high velocity and low transmembrane pressures, performance is very sensitive to operating pressures (Figs. 9.22 and 9.23). Bacterial retention is 99% with the microbial load usually found in milk [37]. On the other hand, there is no significant change in the concentration of other components, so the permeate is essentially bacteria-free skim milk.

The Bactocatch process became commercial in 1988–89 in Sweden. Its application is supposed to result in more stable pasteurized and refrigerated milk products. Perhaps it could be most useful in subtropical and tropical countries, where inadequate refrigeration and transportation facilities results in high microbial loads in the milk coming in to dairy plants. A Bactocatch system on the receiving dock to lower the microbial load can significantly improve the quality of the milk products in these countries.

The production of enriched casein by MF has been studied by Fauquant et al. [33]. If 0.02 micron microfiltration membranes are used, it will separate out the caseins and allow the whey proteins to be isolated.

9.2.2 Cheese Whey

Whey is the liquid fraction that is drained from the curd in cheese making. Every 100 kg of milk used in cheese manufacture results in 10–20 kg of cheese and 80–90 kg of whey. The general composition of whey is shown in Table 9.2. Even though individual components of cheese whey (proteins and lactose) have

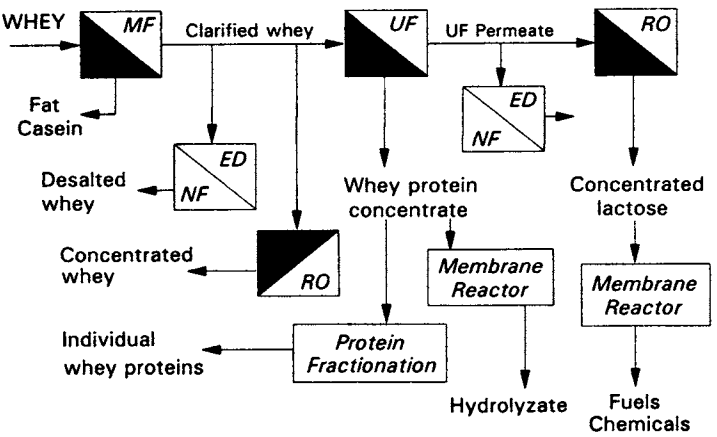

Fig. 9.24. Membrane processing of cheese whey.

uses by themselves, whey itself was difficult to dispose of or utilize, due to its unfavorable lactose-to-protein ratio and high biological oxygen demand of 30,000–50,000 ppm. Ultrafiltration offered a way to improve the ratio in favor of the protein. In fact, whey processing is one of the first successful industrial applications of membranes. Figure 9.24 shows a general schematic of possible applications of membranes in whey treatment.

There are two kinds of cheese whey: sweet whey (resulting from cheeses that are produced by enzyme action, and thus the pH is above 5.6) and acid whey (which results from cheeses made by acidification, with a pH of about 4.6). The latter generally has twice the amount of calcium phosphate and more lactic acid. Calcium phosphate is more soluble at low pH and low temperature. Thus the operating conditions of temperature and pH are selected based on the behavior of calcium salts, in addition to considerations of viscosity, protein denaturation and microbial growth.

9.2.2.1 Concentration by Reverse Osmosis

Cheese whey was the first liquid food to be concentrated on a commercial scale using membrane technology. Early designs utilized 25 mm diameter tubular cellulose acetate membranes. Modern operations focus more on spiral-wound modules using thin-film composite membranes, although many plants successfully continue to use cellulose acetate membranes, sometimes because of excessive fouling with polyamide-based composites. The degree of concentration done by RO depends on prevailing energy costs: if it is to be used as a pre-concentrator, it is probably best to do a 2X concentration to 12% total solids (TS) by RO, and the rest (12–45% TS) by evaporation. However, concentration to 18–27% TS may be justified if bulk transport of whey is the primary goal. This

could explain why many plants in the United States still remain at the 12% TS level of concentration, while in Europe, probably due to higher energy costs, the TS concentration has been raised to 24%. The limiting factors to high concentration by RO are osmotic pressure, viscosity and solubility of the lactose and calcium salts, which may precipitate out at high concentrations, especially if temperature and pH are not regulated.

9.2.2.2 Whey Fractionation by Ultrafiltration

Today, whey protein concentrates produced by ultrafiltration are well-established in the food and dairy industries [38]. Owing to the relatively mild process conditions of temperature and pH, the functionality of the whey proteins remain good, giving rise to a wide range of applications (Table 9.5). The initial protein content of 10–12% (dry basis) can be increased by ultrafiltration to result in 35, 50 or 80% protein products, with a concomitant decrease in lactose and some salts. Further fractionation of the components into beta-lactoglobulin and alpha-lactalbumin fractions can be done as shown in Fig. 9.25.

Whey is a very severe foulant of ultrafiltration membranes. It appears to foul hydrophobic membranes (e.g., polysulfone) much more than hydrophilic membranes (e.g., cellulose acetate). Numerous studies [1,39–44] have shown that membrane fouling in whey ultrafiltration is due to proteins and salts. Interestingly, it appears that α-lactalbumin is the principal foulant, even though it is

TABLE 9.5

Reported uses of whey protein concentrates [101]

Baked custard	Coffee whitener	Meat analogs
Beverages	Cream fillings	Meat extenders
Acid—clear	Cream icings	Meat loaf
Acid—turbid	Cream sauces	Meringues
Neutral	Cream desserts	Noodles
Biscuits	Cultured beverages	Pasta
Breads	Doughnuts	Potato flakes
Cakes	Egg white replacer	Puddings
Cake fillings	Egg yolk replacer	Hot dogs
Candy	Gravies	Sausage
Caramel	Hot dogs	Sherbet
Milk chocolate	Ice cream	Snack foods
Nougats	Imitation cream cheese	Tortillas
Canned refried beans	Imitation milk	Whipped toppings
Chocolate drinks	Macaroni	Yogurt

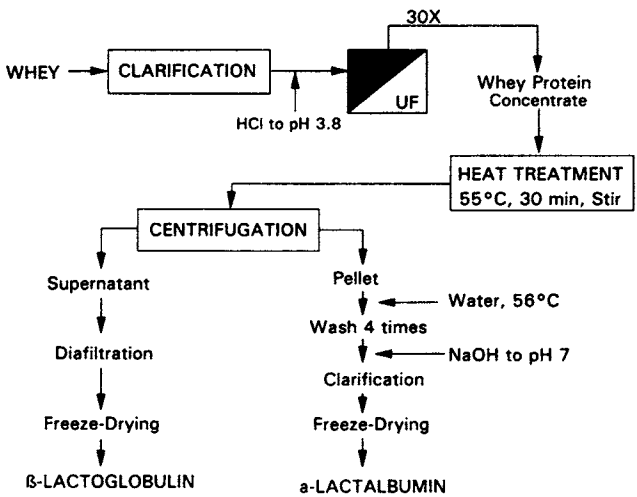

Fig. 9.25. Fractionation of whey proteins using membranes [38,92].

present in the lowest concentration among the major proteins in milk [1,39]. The minerals and salts, primarily calcium phosphate, also play a very important role by themselves, e.g., they can precipitate on the membrane or within the pores, and/or they can enhance protein fouling by interacting with the membrane, perhaps forming "bridges" between the membrane and proteins.

The appropriate pretreatment is important for high fluxes. Heat treatment at about 55°C for about 30–90 minutes appears to improve flux, perhaps by forming protein–mineral complexes that cannot interact with the membrane [1]. Kuo and Cheryan [40] proposed lowering pH to increase solubility of the salts so that they would remain soluble (Fig. 9.26). Patocka and Jelen [41] suggested pretreatments with citric acid and EDTA at pH 2.5 to sequester the calcium; this resulted in a 25% increase in flux. Addition of calcium chloride decreased flux. On the other hand, Kim et al. [42] proposed the addition of calcium chloride after cooling to 0–5°C, followed by pH adjustment to 7.3 and heating to 50°C. The precipitate formed was then removed by centrifugation or decantation. The UF flux almost doubled. However, these pretreatments could reduce the functionality of the whey protein concentrates. A sequential combination of centrifugal clarification and microfiltration, or microfiltration alone, are also effective [40,43,44] and will probably have less detrimental effects on the product, and indeed, may even improve them by removing the fat. Salt and protein deposition have also been implicated with fouling of ceramic membranes by whey [45,46].

The operating conditions also have a serious effect on the fouling. In general, the pH should be far away from the isoelectric point of the proteins and the

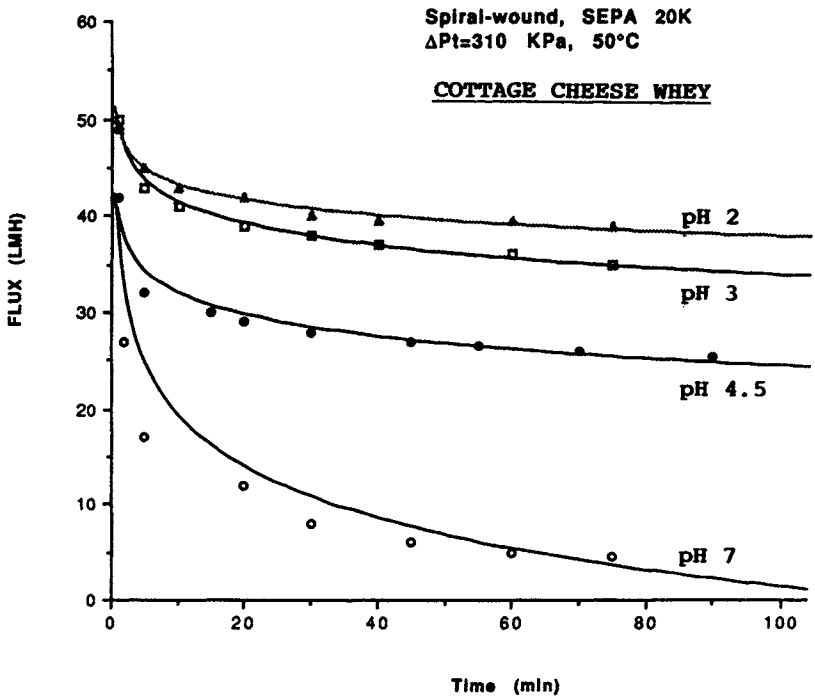

Fig. 9.26. Effect of pH of acid whey on flux with a polysulfone spiral-wound membrane [40].

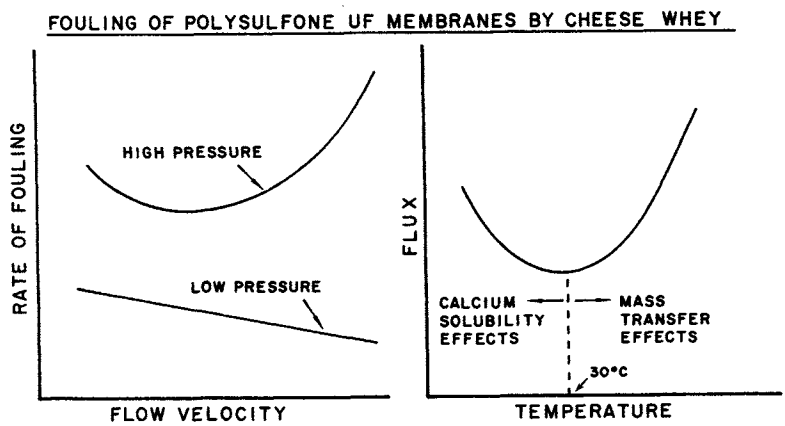

Fig. 9.27. Fouling of polysulfone UF membranes by cheese whey. Left: Effect of transmembrane pressure and flow velocity on rate of fouling. Right: Effect of temperature on flux.

temperature should be far away from 30°C. As shown in Fig. 9.27, low temperatures will result in higher flux because of improved calcium solubility, while temperatures above 30°C improve flux because of the favorable effect on vis-

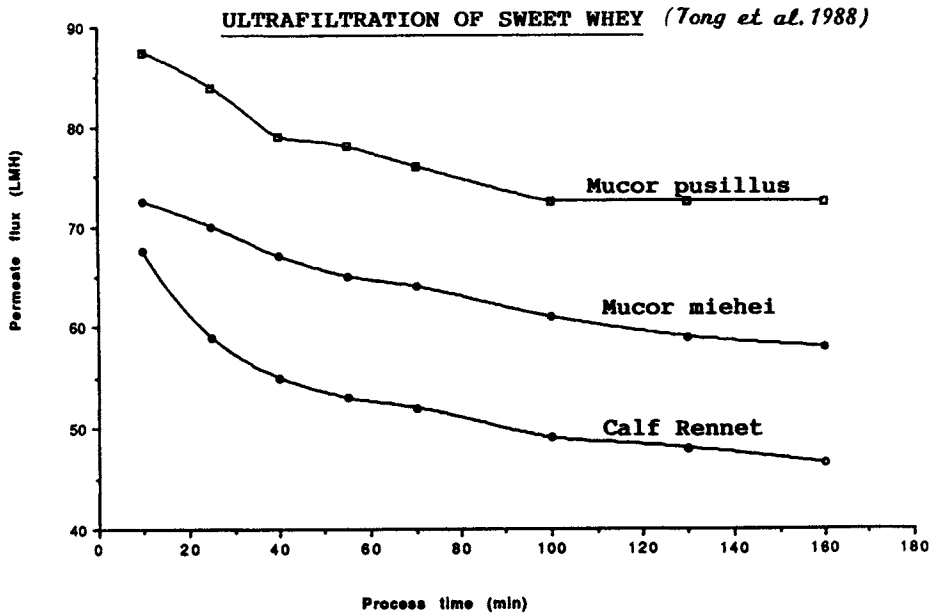

Fig. 9.28. Effect of enzyme coagulant used in the manufacture of cheese on flux of the whey during ultrafiltration [47].

cosity and diffusivity, which leads to improved mass transfer and flux [1]. There is an optimum combination of pressure and velocity to minimize fouling (Fig. 9.27); high velocities decrease rates of surface fouling and polarization if the net transmembrane pressure is low. However, at high operating pressures, high velocities seem to aggravate fouling, even though initial fluxes may be much higher [40].

Even the coagulant used in cheese-making can have an effect on membrane fouling (Fig. 9.28). *Mucor pusillus* rennet gave the highest permeate flux, while the traditionally used calf rennet had the worst effect [47]. It is interesting that whey produced from cheese made with calf rennet, when subjected to the action of *Mucor pusillus*, resulted in increased flux almost to the level of the whey obtained with the *Mucor pusillus* whey.

9.2.2.3 Microfiltration of Whey

The major application of MF is as a pretreatment for UF of whey. Whey usually contains small quantities of fat (in the form of small globules of 0.2–1 microns) and casein (as fine particulates of 5–100 microns). Centrifugal separation of whey does not completely remove the fat and casein fines. Thus when the whey is ultrafiltered, these components can have detrimental effects on the functional properties of the whey protein concentrates, especially the lipid-con-

taining components. A process similar to the HFLF or "Bactocatch" described earlier, with tighter membranes of about 0.2 microns, can effectively remove substantial quantities of these undesirable components. Fat-to-protein ratios of 0.07–0.25 in whey can be reduced to 0.001–0.003 by microfiltration [34]. In addition, some of the precipitated salts may be removed, and there is a considerable reduction in microbial load.

9.2.2.4 Demineralization

There are currently three ways to obtain demineralized whey: ion exchange, electrodialysis and nanofiltration. Owing to the high salt content of whey, ion exchange is operated for short periods of time, with frequent regeneration of the resin, which involves large amounts of regeneration chemicals and water to rinse excess chemicals from the weak anion resin. There may also be a wide variation in pH which can cause the proteins to destabilize.

Electrodialysis (ED) could be an attractive alternative. Since the demineralization rate and efficiency, as well as costs, depend on the conductivity of the solutions, whey is usually concentrated prior to electrodialysis. This also reduces the processing volume. However, electrodialysis cannot complete a 100% demineralization because of the rapid increase in resistance as the ions are being depleted. It appears that the best option is to use ED to obtain 50–70% demineralization, followed by ion exchange up to the required amount. Typical composition of partially demineralized whey is shown in Table 9.6.

TABLE 9.6
Composition of demineralized lactose whey [102]

Component	Delactosed whey powder (%)	55% Demineralized delactosed whey powder (%)
Protein	26	30.2
Lactose	48	54
Fat	1.5	1.8
Ash	16	7
Moisture	2.5	2.5
Organic milk salts	6	4.5
Potassium	4.5	1.2
Sodium	1.6	0.7
Calcium	1.1	0.8
Magnesium	0.3	0.2
Phosphate	4.2	2.6
Chloride	3.2	0.6

The term "nanofiltration" is used for membranes with more open pores than RO membranes. In general, compounds with a molecular weight of 200–500 daltons are completely rejected. This corresponds hypothetically to pores of 10 Å (1 nm). The idea of "loose" reverse osmosis membranes is not new, but with the improvement in performance of thin-film composites, it opens up a new range of applications in whey processing as a means of demineralization instead of electrodialysis or ion exchange.

The "Ultra-Osmosis" process developed by Filtration Engineering (United States) is used to treat "salty" whey. These cheese whey drippings may be 6% NaCl out of a total solids concentration of 12%. At present, cheese plants are not permitted to process salt drippings or blend with sweet whey, due to its high salt content (48). Membranes such as the Film-Tec NF-40 or Desal-5 operated at 1.5–2.5 MPa and 40–55°C can reduce the Na, K and Cl contents significantly without loss of other minerals and components. The salty whey is collected throughout the day and held at 52°C until the cheese-making process is completed. After centrifugation, the salty whey is concentrated to 50% of its original volume, followed by diafiltration at constant volume until conductivity reaches about 10–20% of the initial value, indicating that 80–90% removal of K or Na ions has taken place. The desalted whey is now further concentrated to 25% of its original volume, resulting in a net 95% removal of the salt. At this point the whey resembles sweet whey and it may be reintroduced into the regular whey stream for handling.

To overcome flux decline during the above process, a single-step process can be done, where diafiltration is carried out adding water at half the rate that permeate is removed. This results in 90% demineralization when the initial volume is reduced to 22.5% of the original. USDA guidelines are now available for the "Ultra-Osmosis" process [48].

9.3 FRUIT JUICES AND EXTRACTS

There are three primary areas where membranes can be applied to the processing of fruit juices:

(1) Clarification, e.g., in the production of sparkling clear beverages using microfiltration or ultrafiltration;

(2) Concentration, e.g., using reverse osmosis to produce fruit juice concentrates of greater than 42°Brix;

(3) Deacidification, e.g., electrodialysis to reduce the acidity in citrus juices.

9.3.1 Clarification

Clear single-strength fruit juices (e.g., from apples, pears, grapes, cranberries, pineapples, etc.) have traditionally been produced in batch operations,

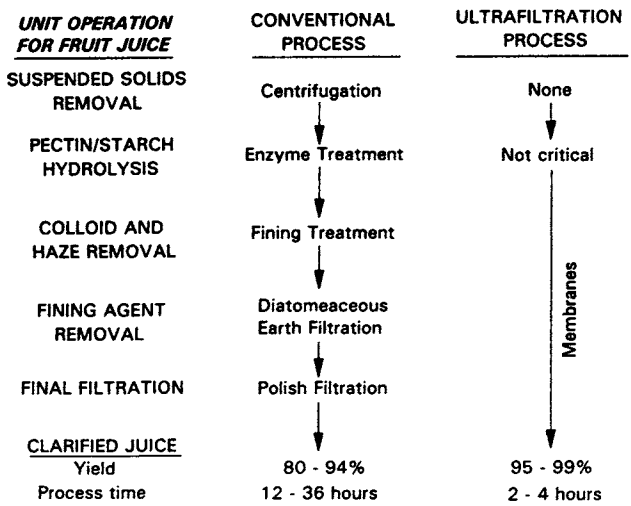

Fig. 9.29. Manufacture of apple juice by the traditional process (left) and the UF process (right).

with a series of filtration/separation steps designed to remove suspended solids, colloidal particles, proteins and condensed polyphenols. This usually involved filter presses and large amounts of filter-aids such as bentonite and/or diatomaceous earth (DE). Research in the late 1970s indicated that MF or UF could be used successfully to replace several of these operations [1]. Figure 9.29 compares traditional and UF processes for producing clear juices and Fig. 9.30 shows a typical schematic.

UF has several advantages:

- Clarification and fining is done in one step. While traditional juice requires the use of fining agents (bentonite, gelatin, etc.), enzymes (pectinase, amylase), centrifugation and diatomaceous earth filtration that may take 12–36 hours, membrane cross-flow filtration avoids these steps to produce a clear and satisfactory product in 2–4 hours.
- Increased juice yield. Juice recovery of 96–98% is typical without diafiltration or predilution. In contrast, conventional processes recover only 80–94%. This increased recovery comes from the elimination of the DE and fining agent loss. A nominal 1% increase in recovery in a plant processing 350,000 liters per day can increase revenue by $150,000 per season.
- Elimination of filter-aid and filter presses. This alone can save about $0.02–0.06 per gallon of juice, and save the processing plant the troublesome disposal of the DE and fining agents.
- Better product quality. The reliable and consistent removal of haze-forming components (suspended solids, colloidal particles, proteins and polyphenols) eventually translates into superior juice quality, typically less than 0.1–0.3 NTU (Nephelometric Turbidity Units) compared to the

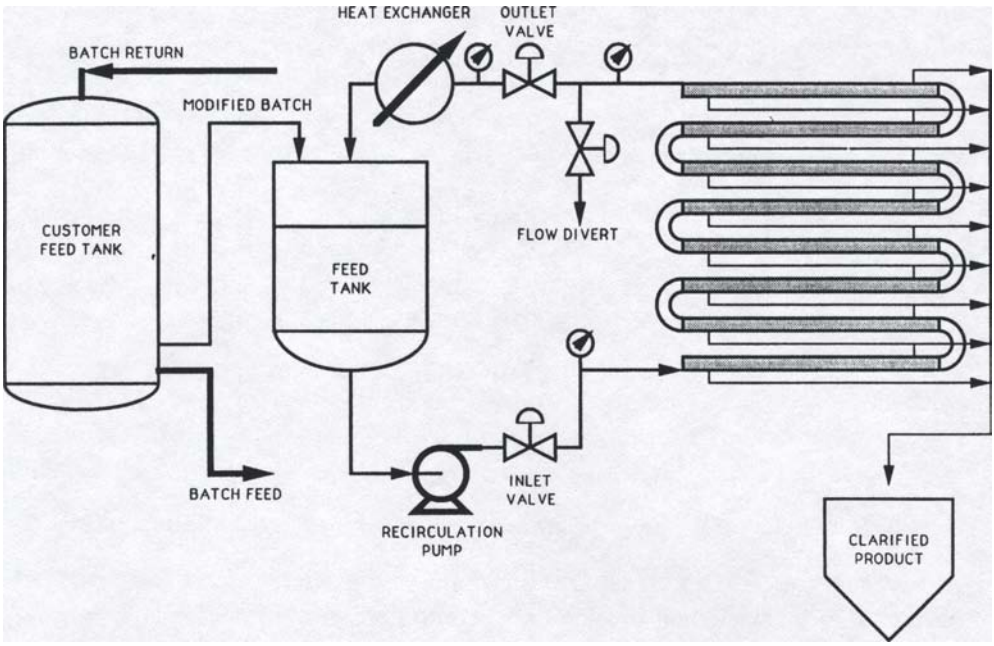

Fig. 9.30. Typical schematic of a UF fruit juice plant producing clear apple juice [50].

2–5 NTU from conventional processing. However, higher flavor losses have been observed with polysulfone and polyamide UF membranes compared to conventional plate-and-frame filter presses for apple juice [49].

- Enzyme usage is reduced 50–75%, depending on the juice. It can be eliminated altogether, although some pretreatment with enzymes help reduce membrane fouling and viscosity, resulting in higher flux and lower pumping energy.

All these advantages result in higher profits for the UF process (Fig. 9.31). For example, a Cadbury–Schweppes' apple juice plant processing over 500,000 liters per day reported savings of $350,000 per year, due to the elimination of more than 350,000 kg per year of DE, a major reduction in labor costs and a 4% increase in yield [50].

9.3.1.1 Apple Juice

The most work has been done with apple juice, starting with the pioneering work of Heatherbell et al. [51]. The method used for extraction has a profound effect on the suspended solids, and thus the yield (Fig. 9.32). After pressing, a depectinization step is recommended to decrease viscosity of the fluid and

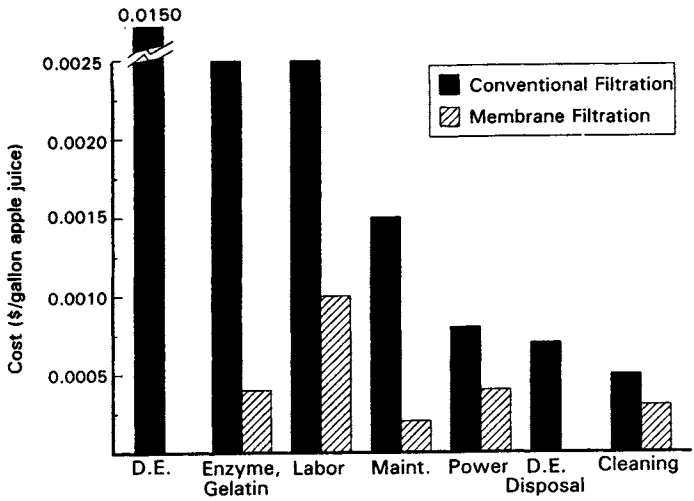

Fig. 9.31. Cost advantages of cross-flow membrane filtration versus conventional filtration using diatomaceous earth (D.E.). Based on 1988 estimates [50].

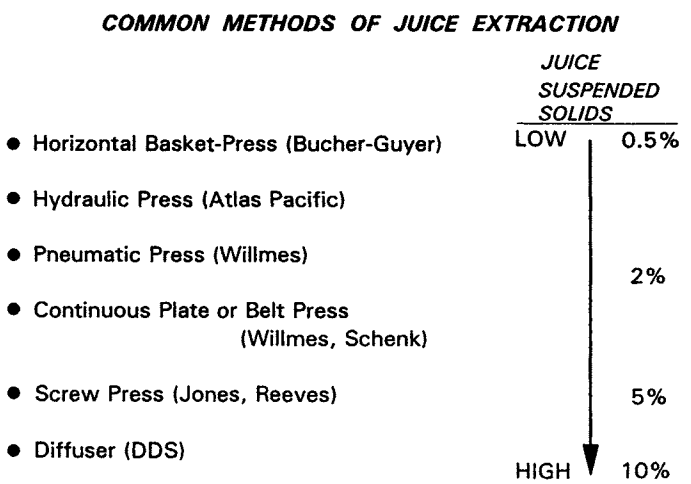

Fig. 9.32. Common methods of juice extraction [50].

allow higher permeate flux. Figure 9.33 compares the effect of depectinization on flux for apple juice. Rao et al. [49] also observed almost a doubling of the flux as a result of depectinization with a Romicon 50K MWCO polysulfone hollow fiber membrane.

The two most common modes of operation are batch and modified-batch (Fig. 9.30). Operation in batch mode is carried out until the centrifuged solids level in the retentate is 50–80%. If maximum sugar recovery is desired (e.g., if

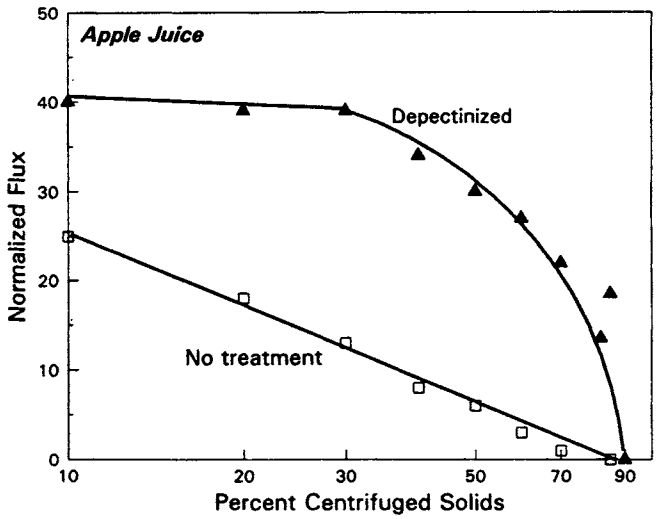

Fig. 9.33. Effect of pectinase enzyme treatment on apple juice flux with Romicon hollow fiber membranes [98].

juice is going to be concentrated), diafiltration may be done at constant volume until there is a volume of permeate with a solids content equal to the volume of the 50% solids concentrate obtained with UF. Padilla and McLellan [52] studied the influence of membrane pore size on flux and other quality factors of UF apple juice (Table 9.7). In general, steady-state flux increased with pore size. However, turbidity and polyphenolic concentration also increased. After six months storage at 18°C, the UF juices processed with the 100K and 500K MWCO membranes showed large increases in turbidity. Permeate total solids and Hunter L values (a measure of the color) were not affected by pore size.

TABLE 9.7

Effect of membrane molecular weight cut-off (MWCO) on ultrafiltration of apple juice [52]

	Molecular weight cut-off of membrane			
	10K	50K	100K	500K
Initial flux (LMH)	28	100	210	280
Permeate solids (%)	12.39	12.53	12.57	12.57
Turbidity (NTU):				
Initial	0.4	0.6	2.2	2.3
After 6 months	–	–	4.0	6.0
Total phenolics (mg l^{-1})	350	366	377	369
Hunter L values	51.6	51.0	50.4	50.4

Wu et al. [53] compared two polysulfone ultrafilters of 5,000 and 50,000 MWCO with a ceramic 0.1 micron microfilter. Flux was much higher with the ceramic membrane (110 LMH vs 28 LMH for the 5000 MWCO UF membrane). Although there was no appreciable sensory difference between MF and UF apple juice permeates, the MF juice was considerably darker and was slightly preferred by taste panelists.

The metallic membrane developed by CARRE (Seneca, South Carolina) has been used for apple juice with an interesting variation [54]. The membrane (30K–40K MWCO) is zirconia "formed-in-place" on a porous sintered stainless steel substrate in tubes of 25 mm or more in diameter. Membranes can be created with varying molecular weight cutoffs or pore diameters. This "Ultra-press" process combines juice pressing and filtration in one step. Whole apples are pureed and treated with cellulase and pectinase at 50°C for 2 hours to reduce the viscosity of the feed. The resultant slurry is pumped through the tubular membrane system (over 70 m long) designed as a single-pass, once-through process. Pressures are typically 200–350 psi (1.3–2.4 MPa) with 1.25-inch diameter tubes, and 700–800 psi (4.5–5.4 MPa) with 1-inch tubes. Yields obtained were 80–85% with a single pass, which can be increased with multiple passes. The system has reportedly reduced processing costs by $0.026–$0.04 cents per liter [55].

9.3.1.2 Other Juices

Among other juices, passion fruit juice has been studied by Yu et al. [56]. Surprisingly, even though they used a UF membrane (PCI BX6, 25K MWCO), over 80% of the flavor compounds were retained. Sugars and organic acids had a retention of 10–40%. Perhaps the high pressures (12 bar) and low temperature (20°C) created a dynamic fouling layer that increased retention during processing. Retentivities of these compounds increased with the concentration ratio. Foulants on the membrane were identified as cellulose, hemicellulose, sugars, citric acid and pectin.

Kirk et al. [57] studied the ultrafiltration of pear juice with hollow fibers. Membranes of different MWCOs (10K, 30K and 50K) had little influence on permeate juice color. Optimum operating conditions were 157 kPa pressure, 0.15 m/s, 50°C. Permeate flux declined with the logarithm of the concentration.

Kiwi fruit juice processing has been reported by Wilson and Burns [58]. A dramatic improvement in clarity was obtained, and it allowed the non-thermal sterilization of kiwi fruit juice. Storage for 6 months at 15°C resulted in only very slight deterioration as browning and ascorbic acid loss.

Ultrafiltration of strawberry juice apparently has a detrimental effect on color and appearance of the product, due perhaps to a loss of anthocyanins by adsorption on the membrane [59]. Pouliot and Goulet [60] reported that maple

sap could be clarified with a 10K membrane, using pressures of 190–200 kPa.

Hart et al. [61] used 0.45-micron ceramic microfilters with enzyme-treated apricot puree to obtain a sparkling, clear apricot juice at fluxes of 90–190 LMH. Concentrating the permeate subsequently by vacuum evaporation resulted in a concentrate with good retention of clarity, flavor and aroma.

9.3.2 Concentration

Fruit juice concentration by reverse osmosis is potentially one of the largest applications of membrane technology. The major benefit of RO is that it diminishes thermal damage of delicate aroma components while reducing the amount of energy needed for removal of water.

9.3.2.1 Apple Juice.

Early work by Merson and Morgan [62] with apple juice showed that cellulose acetate membranes showed good sugar retention, but aroma/flavor compounds permeated the membrane, which lowered the quality of the concentrate [63]. Aroma is determined by C_2–C_6 alcohols, C_4–C_8 esters and C_2–C_6 aldehydes. Three compounds are especially important in providing apple-like characteristics: ethyl 2-methylbutyrate, hexanal and 2-hexenal. High osmotic pressure limits concentration to 20–25°Brix with conventional RO. Pectins contributed to fouling and viscosity which also affect plant performance. Thus apple juice RO is usually preceded by depectinization by enzymes and clarification (usually by UF), which then makes it one of the easiest liquids to process by RO [64]. Cleaning and restoration of capacity at the end of a process cycle is no problem. This suggests that spiral modules are probably the best design for this application.

Polyamide RO membranes retained more of the flavors than cellulose acetate (Fig. 9.34; an overall 45% versus 23%) and also resulted in higher flux (Fig. 9.35). Conventional cellulose acetate membranes (with 97% salt rejection) had much higher flux than high-retention (99% salt rejection) CA membranes, but the flavor retention was much poorer. Table 9.8 shows typical feed and permeate analyses for apple juice concentrated by a polyamide composite membrane.

9.3.2.2 Orange Juice

With orange and other citrus juices, many of the flavor compounds reside in an oil phase present in the juice in the form of an emulsion. Since they are sparingly soluble in water, flavor retention should be much better with orange juice than apple juice. Orange juice concentrates are today produced mostly by conventional multi-stage evaporation. Most of the citrus essences are stripped in the first effect, and in the later stages other compounds are destroyed or

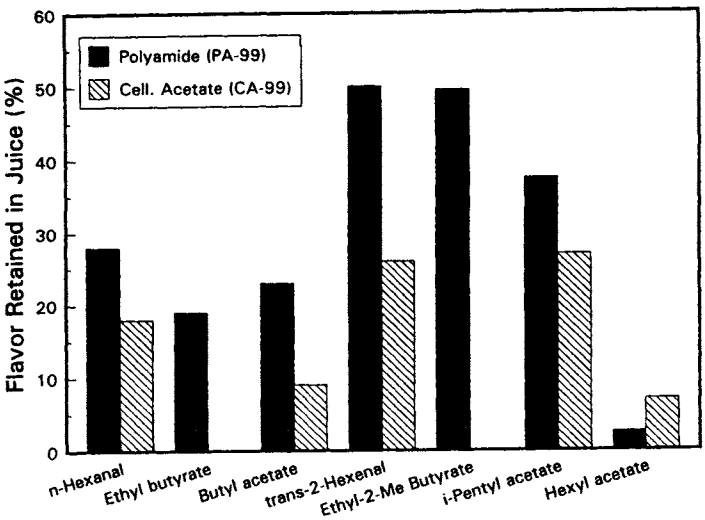

Fig. 9.34. Retention of flavor compounds after reverse osmosis of apple juice with a polyamide composite membrane (PA-99, Osmonics) and cellulose acetate membrane (CA-99, Osmonics). The retention index values indicate various flavor compounds: see Chua et al. for details [99].

TABLE 9.8

Analysis of apple juice feed and permeate from RO through a PCI AFC-99 tubular thin-film composite membrane [64]

	Feed (ppm)	Permeate (ppm)	Retention (%)
Dry matter	122,700	327	99.7
Sucrose	12,100	20.7	99.8
Glucose	28,700	57.5	99.6
Fructose	65,400	130	99.8
Malic acid	3,910	21.2	99.5
Citric acid	341	0.9	99.8
Free amino acids	276.4	<0.1	
Methyl-ethyl butyrate	0.97	<0.04	
Butyl butyrate	0.1	<0.04	
Hexyl acetate	0.04	<0.04	
Total acidity (meq/l)	46.1	0.38	99.2
pH	3.95	5.13	

transformed into another undesirable compounds (e.g., furfurals).

The mid-1970s saw intense research activity in this area [65,66] primarily with cellulosic membranes. Peri [67] first centrifuged the juice, then concen-

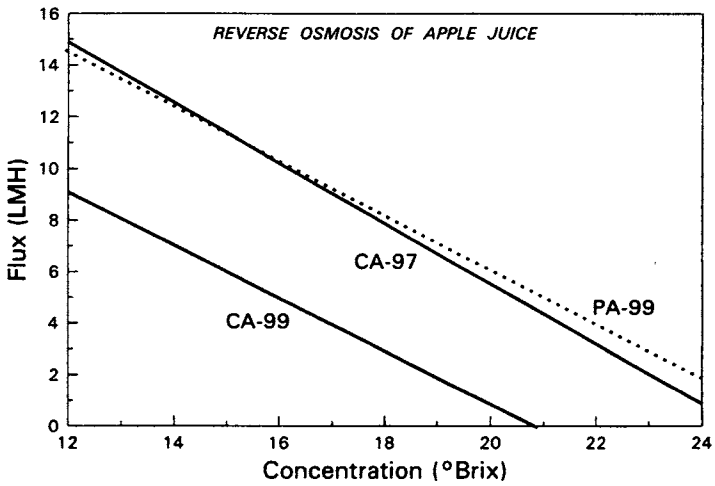

Fig. 9.35. Reverse osmosis of apple juice: effect of membrane on flux [99].

trated it up to 25°Brix at 5–7°C using pressures of 30–70 bar. There was a high retention of sugars, acids,phenolics, nitrogen compounds and ash, but only 30–100% of the volatile aroma compounds was retained.

Reverse osmosis with a polyamide composite membrane can concentrate orange juice without a significant loss of aroma, sugar or acids [68]. However, conventional RO is limited by osmotic pressure and viscosity considerations to less than 30°Brix. Therefore RO can be used as a preconcentration step, with thermal evaporation completing the required concentration to 42°Brix. Using RO ahead of the evaporators can increase evaporator capacity and reduce thermal damage to the product.

Braddock et al. [69] used a tubular thin-film composite membrane at 6 MPa and 30°C to concentrate orange juice from 12 to 25.3°Brix (with an initial flux of 45 LMH), grapefruit juice from 9 to 25.1°Brix (flux of 50 LMH) and lemon juice from 8 to 22.5°Brix (flux of 35 LMH). No losses of acids, vitamin C, limonene or pectin were observed. Glucose and fructose amounts in permeate were 0.02–0.4% and there was no loss of sucrose. There were more aroma losses by vaporization than by permeation through the membrane.

The first commercial RO plant used PCI's AFC-99 membranes with a feed rate of 4200–9200 l h^{-1} and a water removal rate of 2000 l h^{-1}. The feed was pasteurized orange juice with a dissolved solids content of 10–12°Brix, pH 3.2–3.7 and a pulp content of 2–7.5%. It was necessary to do a quick flush with alkali every 4–6 hours to remove the hesperidin that fouled the membranes [64]. Flavor of the concentrate has been judged to be very good and comparable to single-strength fresh juice when rediluted.

Perhaps the most significant development in recent years is the production

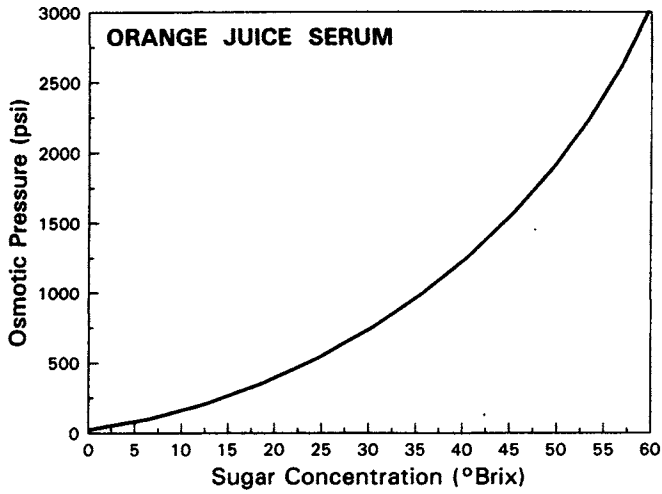

Fig. 9.36. Osmotic pressure of orange juice serum as a function of sugar concentration (1 psi = 6.89 kPa). Adapted from Cross [70].

of highly concentrated (42–60°Brix) fruit juices using a combination of high- and low-retention RO membranes. The osmotic pressure of orange juice containing 10–12% soluble solids (10–12°Brix) is about 250–300 psi (Fig. 9.36). It increases to 1500 psi at 42°Brix and 3000 psi at 60°Brix. The resulting high viscosity and osmotic pressures would result in very high energy consumption and require modules capable of pressures beyond present-day state of the art.

The "FreshNote" process was developed by SeparaSystems, a joint venture of Du Pont and Food Machinery Corporation, to overcome these limitations [70,71]. As shown in Fig. 9.37, the basic concept is a two-stage process. Ultrafiltration is first used with the juice to separate out the pulp (the "bottom solids") from the serum which contains the sugars and flavor compounds. The bottom solids contains some soluble solids, all the insoluble solids, pectins, enzymes, orange oils and the microorganisms that would affect the stability of the concentrate. The UF retentate, about 1/10 to 1/20th the feed volume, is subjected to a pasteurization treatment that destroys spoilage microorganisms and improves stability of the finished product when blended back with the concentrated UF permeate.

The serum (UF permeate), which amounts to about 90–95% of the feed volume, is concentrated by reverse osmosis using hollow fine fibers made of aromatic polyamide. Pressures are typically 1000–2000 psi. A multi-stage system is used with high-retention membranes in the early stages and low-retention membranes (i.e., leaky "loose" membranes) in later stages. When the serum concentration reaches so high as to make the effective driving force too low, the concentrate is pumped through low-retention membranes. Some of the sugars

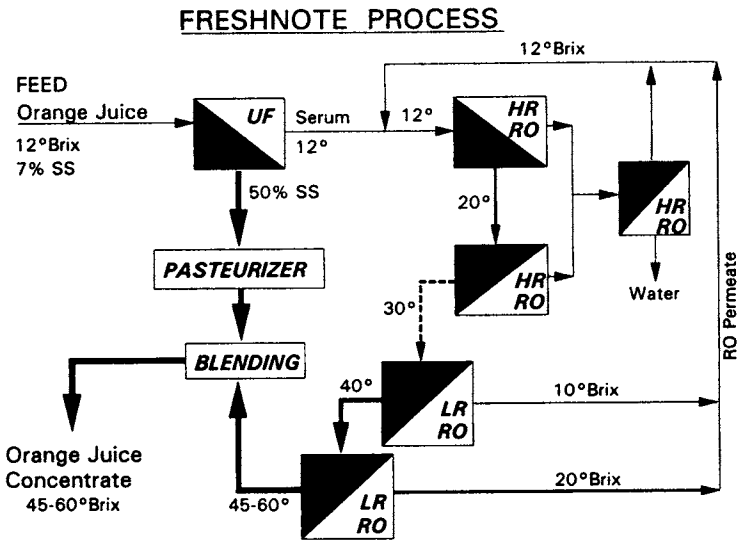

Fig. 9.37. FreshNote process developed by SeparaSystems for fruit juice concentrates using a combination of UF and high-retention (HR) and low-retention (LR) reverse osmosis membranes. The Brix values for various retentates and permeates are for illustrative purposes only. Exact values depend on the application and process design. Adapted from Cross [70] and Walker [71].

leak through, but this results in a lower osmotic pressure difference across the membrane, which allows lower pressures to be used. Permeate with a non-zero sugar or flavor content is returned to stages containing high-retention membranes. For particularly demanding applications, the water removed from the RO modules can be sent to a separate high-retention RO module to remove any traces of sugar or flavor compounds. The concentrated serum can then be blended back with the pulp or bottom solids stream.

SeparaSystems reports fruit juice concentrates of 45–55°Brix have been obtained commercially, and up to 70°Brix has been obtained in pilot trials [71]. Careful control of operating conditions is necessary. For example, the freshly extracted juice is blanketed with nitrogen and its temperature is controlled below 10°C throughout the remainder of the process. The flavor compounds in the serum are not subjected to any heat during processing, which also explains the high flavor scores this product receives. The flavor and cost comparisons shown in Fig. 9.38 indicate very good market potential for this process.

Watanabe et al. [72] have used a similar combination of high and low-retention membranes (Nitto-Denko spirals NTR-7199 and NTR-7450 respectively) to concentrate 11°Brix apple juice to 45°Brix, using pressures of 7.5 MPa and 9.5 MPa respectively. Similar concepts were used by Koseoglu et al. [73] to produce concentrated and/or sterilized single-strength orange juice using hollow fiber UF and tubular membrane RO.

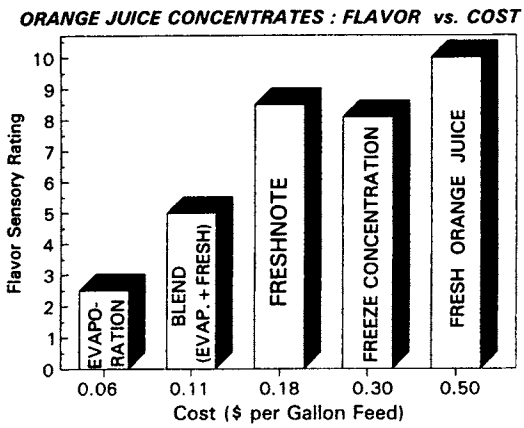

Fig. 9.38. Flavor-cost comparisons of orange juice manufactured by various processes [70].

An interesting variation of this theme (to reduce the net osmotic pressure difference across the membrane) is "direct osmosis". Milleville [74] describes a system which uses 2-inch diameter tubes, each 10 feet long, with RO membranes of 100 MWCO. The fruit juice flows in the tubes at 31°C, while the osmotic agent (concentrated sugar solution) flows in the shell side at 45°C. The difference in concentration on either side of the membrane results in a chemical potential difference that will cause the water to flow from the dilute side to the concentrated side. It is claimed that concentrates of 42–60°Brix can be produced by this method. The reported advantage of this system is that no transmembrane pressure is applied, which reduces energy consumption and reduces fouling. The diluted osmotic agent (sugar syrup on the shell side) can be reconcentrated or used within the plant. The economics of this process will, of course, depend heavily on the latter factor.

9.3.2.3 Tomato Juice

Concentration of tomato juice presents a difficult problem, because it has a high pulp content (25% fiber) and a high viscosity (which behaves in a non-Newtonian manner). The rheological properties of the juice are affected by the method of juice manufacture. The break temperature, which is the temperature to which tomatoes are exposed after chopping, can give different levels of enzyme inactivation which, in turn, affects final viscosity. A cold break (at 65°C) results in less inactivation of the natural enzymes, which results in high viscosity. Thus, RO-concentration of tomato juice is limited by both the osmotic pressure and the viscosity. If the fibers were separated, the remaining serum would behave as a water-like liquid.

The usual concentration of natural tomato juice is 4.5–5°Brix. Commercial

tomato sauces are 8–12°Brix, and tomato pastes are 28–29°Brix. Because of the fiber content and particle size, tubular modules are probably best; for example, little fouling has been reported with the PCI AFC-99 tubular membrane [75,76]. In addition, flux was unaffected by the feed velocity in the range 0.3–4 m s^{-1}. This has been attributed to a "tubular pinch" effect, i.e., the solids are suspended in the middle of the flow channel, and thus away from the wall where the membrane is located. Rejection of natural tomato soluble solids was 94–99%. Flux is 39.7 LMH at 72°C and 55.2 bar after 52 hours of operation, and 41 LMH at 78°C and 41.4 bar after 717 hours [76]. Tomato juice concentration using a dynamically formed zirconia membrane has been reported by Watanabe et al. [77].

The first RO plant for tomato juice has operated since 1984 with PCI AFC-99 tubular membranes, processing more than 250 tons per hour (during the season) of 4.5°Brix juice to 8°Brix. Retention of organic acids (citric and L-malic), sugars (glucose, fructose), mineral ions (K, Mg, Na, PO_4, Cl) and free amino acids was excellent [78]. Some loss of low molecular weight volatiles (methanol, ethanol) were observed. The color was very good, and showed none of the browning normally associated with evaporation. This color quality is retained when the RO juice was evaporated to 28–30°Brix paste because of the reduced time in the evaporator. Despite aggressive cleaning regimes, this plant has operated in Italy for five seasons with the same set of membranes [64].

The original work was stimulated by potential energy savings. Thus further development work has been done to reach 15–20°Brix, although direct RO may not be the most economical way of reaching this concentration. Using the combination of HR (high retention) and LR (low retention) membranes as with the "FreshNote" process has not been successful so far because the reblended pulp and serum concentrate separate out on standing [64].

9.3.2.4 Maple Syrup

The interest in RO of maple syrup grew in the 1970s in response to increasing energy prices. Reverse osmosis is able to remove about 60% of water from the maple sap. The concentrate is then boiled in a conventional open pan evaporator to develop the characteristic color and flavor. For 90,000 gallons of maple sap, this results in a decrease of 33% in the processing cost compared to the all-thermal process [79]. The number of installations increased from less than 5 in 1980 to more than 100 today [80].

9.3.2.5 Other Juices

Demeczky et al. [63] reported concentration of some other fruit juices. Sour cherries concentrated 2.6-fold at 6.0 MPa showed some losses of acid (14–24% depending on the membrane used); nevertheless, the taste and smell of product

was superior to that obtained by vacuum evaporation. Peach juice could be concentrated from 11 to 30.7%, with some losses of aroma components, acids and sugars. However, RO resulted in better taste than evaporation. Red currant concentration was carried out in two stages. Permeate of first stage was subsequently concentrated to give a final product of 27% solids. In this case, the re-diluted juice did not show any difference from the original single-strength juice, while the juice obtained by evaporation was of lower quality. Black currant juice gave the same sensory results as red currant; it could be concentrated from 11 to 30% (2.6-fold). Strawberry juice was concentrated in two stages to give a final product of 25.4% solids. In spite of color, aroma and sugars losses, panelists could not find significant differences between the rediluted concentrate and the original juice.

9.3.3 Electrodialysis

Electrodialysis has potential applications in the deacidification of fruit juices but its commercial practice remains small. Conventional electrodialysis has been investigated by Adhikary et al. [81]. A special configuration of only anion-exchange membranes has been used [82], with alternating compartments containing the citrus juice and KOH. Since only anions are able to pass through the membranes, the net effect is the extraction of citrate ions from the juice and their replacement by OH ions from the KOH solution [83]. Energy requirements vary between 0.02–0.1 kWh/equivalent. Audinos et al. [84] studied the use of ED for manufacturing sweetening products from grapes.

9.4 PIGMENTS AND COLORANTS

Natural colorants extracted with water from plant sources are usually about 0.1% concentration and are contaminated with a wide variety of dissolved compounds. Two major classes of water-soluble natural colorants used in foods are anthocyanins and betalaines. Anthocyanins are intensely colored, water soluble compounds responsible for almost all the red and blue colors of flowers and fruits. Woo et al. [85] describe a process for extracting anthocyanins from cranberry pulp waste and recovering it by UF and RO. Perilla anthocyanins have been recovered from spent brine by UF [86] and electrodialysis [87].

Betalaines are the red betacyanin and the yellow betaxanthin found in red beet, which is the source for commercial betanins. They are very heat-sensitive. Betacyanin (molecular weight 560) accounts for 75–95% of the total colorants. Red beet extracts contain 8–10% dissolved solids with 0.1–0.2% of betacyanin. Membrane applications with red beet juice have been reported by Bayindirli et al. [88], Behr et al. [89] and Lee et al. [90].

Water extracts of grape skins contain 4–6% dissolved solids and 0.08–0.150% anthocyanins, the major anthocyanin being 3,5-diglycoside (molecular weight 655). Water extracts are treated by ultrafiltration to separate sugars and pectins. Diafiltration is carried out if higher recovery is desired, and the permeate is then concentrated by RO [91].

9.5 CONCLUSIONS

Membrane technology will continue to be applied on a large scale in the food industry. Although this review focused on selected industries, the potential is vast as shown in Table 9.1. For example, reverse osmosis has not yet made a major penetration into the fruit juice industry. However, the United States harvest of oranges in the 1985–86 season was 7.5 million metric tons, of which approximately 82% was processed and marketed as frozen concentrate orange juice. Over 700,000 metric tons of apple juice is marketed every year in the United States alone. Annual tomato production in United States is 3,300,000 tons; about 80% is processed into tomato products. Some industries, e.g., wet corn refining and oilseeds, have only recently begun to apply this technology in their operations. Considering the vast amounts of water used, these industries may experience the greatest growth of membrane applications in this decade.

REFERENCES

1 Cheryan, M. 1986. *Ultrafiltration Handbook.* Technomic, Lancaster, PA.
2 Cheryan, M., Veeranjaneyulu, B.V. and Schlicher, L.R. 1990. Reverse osmosis of milk with thin-film composite membranes. *J. Membr. Sci.*, 48: 103–114.
3 Kulozik, U. and Kessler, H.G. 1988. Permeation rate during reverse osmosis of milk influenced by osmotic pressure and deposit formation. *J. Food Sci.*, 53: 1377–1347.
4 Abbot, J., Glover, F.A., Muir, D.D. and Skudder, P.J. 1979. Application of reverse osmosis to the manufacture of dried whole milk and skim milk. *J. Dairy Res.*, 46: 663.
5 De Boer, R. and Nooy, P.F.C. 1980. Concentration of raw whole milk by reverse osmosis and its influence on fat globules. *Desalination*, 35: 201–211.
6 Cox, G.C. and Langdon, I.A. 1985. Economic evaluation of reverse osmosis for reduction in milk transport costs. *Australian J. Dairy Technol.*, 40 (3): 113–117.
7 Bundgaard, A.G. 1974. Hyperfiltration of skim milk for ice cream manufacture. *Dairy Industries*, 39 (4): 119–122.
8 Iversen, E.K. 1980. *Dairy Sci. Abstr.*, 42: 3326.
9 Sorbensen, J.J. 1980. *Dairy Sci. Abstr.*, 42: 3382.
10 Pal, D. and M. Cheryan. 1987. Application of reverse osmosis in the manufacture of khoa. Process optimization and product quality. *J. Food Sci. Technol.*, 24: 233–238.
11 Davies, F.L., Shankar, P.A. and Underwood, P.A. 1977. The use of milk concentrated by reverse osmosis for the manufacture of yoghurt. *J. Soc. Dairy Technol.*, 30 (1): 23–28.

12 Guirguis, N, Versteeg, K. and Hickey, M.W. 1987. The manufacture of yoghurt using reverse osmosis concentrated skim milk. *Australian J. Dairy Technol.*, 42(3): 75–78.
13 Dixon, B.D. 1985. Dairy products prepared from reverse osmosis concentrate. Market milk products, butter, skim milk powder and yoghurt. *Australian J. Dairy Technol.*, 40(3): 91–95
14 Pal, D. and Cheryan, M. 1987. Membrane technology in dairy processing. Part 1. Reverse osmosis. *Indian Dairyman*, 39: 251–267.
15 Cheryan, M. 1989. PRO-CAL: a high-calcium, low-cholesterol milk produced by ultrafiltration. Unpublished report, University of Illinois, Urbana.
16 Watters, J.C., Rezvani, R. and Klein, E. 1989. Reduction of the lactose content of skim milk by continuous countercurrent cascade ultrafiltration. *Separ. Sci. Technol.*, 24(5/6): 369–382.
17 Abrahamsen, R.K. and Holmen, T.B. 1980. Yogurt from hyperfiltrated, ultrafiltrated and evaporated milk and from milk with added milk powder. *Milchwissenschaft*, 35: 399–402.
18 Kosikowski, F.V. 1986. New cheese-making procedures utilizing ultrafiltration. *Food Technol.*, 40 (6): 71–77, 156.
19 Honer, C. 1990. Does ultrafiltration have a place on the farm? *Dairy Field Today*, 173 (3): 52.
20 Mehaia, M.A. and Cheryan, M. 1983. Coagulation studies of ultrafiltration-concentrated skim milk. *Milchwiss.*, 38: 708–710
21 Lawrence, R.C., Creamer, L.K. and Gilles, J. 1987. Texture development during cheese ripening. *J. Dairy Sci.*, 70: 1748–1760.
22 Ryder, D.N. 1985. Use of membranes in the manufacture of hard and semi-hard cheeses. *Desalination*, 53: 129–133.
23 Agbevavi, D.R and Mayer, R. 1983. Production and quality of cheddar cheese manufactured from whole milk concentrated by reverse osmosis. *J. Food Sci.*, 48: 642–643.
24 Parrott, D.L. 1990. The application of spiral-wound ultrafiltration membranes in the APV Sirocurd process for the continuous production of cheddar cheese. *Proceedings, 1990 International Congress on Membranes and Membrane Processes, Vol. 1*, pp. 265–266.
25 Qvist, K.B., Thomsen, D. and Höier, E. 1989. Effect of ultrafiltered milk and use of different starters on the manufacture, fermentation and ripening of Havarti cheese. *J. Dairy Res.*, 54: 437–446.
26 Mistry, V.V. and Kosikowski, F.V. 1984. Growth of lactic acid bacteria in highly concentrated ultrafiltered skim milk retentates. *J. Dairy Sci.*, 68: 2536–2543.
27 Patel, R.S., Reuter, H. and Prokopek, D. 1986. Production of quarg by ultrafiltration. *J. Soc. Dairy Technol.*, 39: 27–31.
28 Maubois, J.L. and Kosikowski, F.V. 1978. Making Ricotta cheese by ultrafiltration. *J. Dairy Sci.*, 61: 881.
29 Modler, H.W. 1988. Development of a continuous process for the production of ricotta cheese. *J. Dairy Sci.*, 71: 2003–2009.
30 Pal, D. and Cheryan, M. 1987. Membrane technology in dairy processing. Part II. Ultrafiltration. *Indian Dairyman*,. 39 (8): 373–391.
31 Jameson, G.W. 1987. Manufacture of cheddar cheese from milk concentrated by ultrafiltration: The development and evaluation of a process. *Food Technol. Australia*, 39 (12): 560–564.
32 Piot, P., Vachot, J.V., Veaux, M., Maubois, J.L. and Brinkman, G.E. 1987. Ecremage et epuration bacterienne du lait entier cru par microfiltration sur membrane en flux tangentiel. *Technique Laitiere & Marketing*. 1016: 42–46.

33 Fauquant, J., Maubois, J.L. and Pierre, A. 1988. Microfiltration du lait sur membrane minerale. *Technique Laitiere & Marketing*, 1028: 21–23.
34 Van der Horst, H.C. and Hanemaaijer, J.H. 1990. Cross-flow microfiltration in the food industry. State of the art. *Desalination*, 77: 235–258.
35 Vetier, C., Bennasar, M. and Tarodo de la Fuente, B. 1988. Study of the fouling of a mineral microfiltration membrane using scanning electron microscopy and physico-chemical analyses in the processing of milk. *J. Dairy Res.*, 55: 381–400.
36 Malmberg, R. and Holm, S. 1988. Low bacteria skim milk by microfiltration. *North European Food Dairy J.*, 1: 75–78.
37 Olesen, N. and Jensen, F. 1988. Microfiltration. The influence of operating parameters on the process. *Milchwissenschaft*, 44: 476–479
38 Maubois, J.L., Pierre, A., Fauquant, J. and Piot, M. 1987. Industrial fractionation of whey proteins. *Int. Dairy Fed. Bull.*, 212: 154–159.
39 Merin, U. and Cheryan, M. 1980. Factors affecting the mechanism of flux decline during ultrafiltration of cottage cheese whey. *J. Food Process. Preserv.*, 4: 183–198.
40 Kuo, K.P. and Cheryan, M. 1983. Ultrafiltration of acid whey in a spiral-wound unit: Effect of operating parameters on membrane fouling. *J. Food Sci.*, 48: 1113–1118.
41 Patocka, J. and Jelen, P. 1987. Calcium chelation and other pretreatments for flux improvement in ultrafiltration of cottage cheese whey. *J. Food Sci.*, 52: 1241–1244.
42 Kim, S.H., Morr, C.V., Seo, A. and Surak, J.G. 1989. Effect of whey pretreatment on composition and functional properties of whey protein concentrate. *J. Food Sci.*, 54: 25–29.
43 Rinn, J.C., Morr, C.V., Seo, A. and Surak, J.G. 1990. Evaluation of nine semi-pilot scale whey pretreatment modifications for producing whey protein concentrate. *J. Food Sci.*, 55: 510–515.
44 Hanemaaijer, J.H. 1985. Microfiltration in whey processing. *Desalination*, 53: 143–155.
45 Taddei, C., Aimar, P., Daufin, G. and Sanchez, V. 1986. Etude du transfert de natiere lors de l'ultrafiltration de lactoserum doux sur membrane minerale. *Le Lait*, 66 (4): 371–390.
46 Aimar, P., Taddei, C., Lafaille, J.P. and Sanchez, V. 1988. Mass transfer limitations during ultrafiltration of cheese whey with inorganic membranes. *J. Membr. Sci.*, 38: 203–221.
47 Tong, P.S., Barbano, D.M. and Jordan, W.K. 1988. Permeate flux during ultrafiltration of whey: Influence of milk coagulant used for cheese manufacture. *J. Dairy Sci.*, 71: 2342–2348.
48 O'Shea, D.P. 1990. Filtration Engineering, USA. Personal communication.
49 Rao, M.A., Acree, T.E., Cooley, H.J. and Ennis, R.W. 1987. Clarification of apple juice by hollow fiber ultrafiltration: fluxes and retention of odor-active volatiles. *J. Food Sci.*, 52: 375–377.
50 Koch Membrane Systems. 1988. Product literature.
51 Heatherbell, D.A., Short, J. and Struebi, P. 1977. Apple juice clarification by ultrafiltration. *Confructa*, 22(5/6): 157.
52 Padilla, O.I. and McLellan, M.R. 1989. Molecular weight cut-off of ultrafiltration membranes and the quality and stability of apple juice. *J. Food Sci.*, 54: 1251–1255.
53 Wu, M.L., Zall, R.R. and Tzeng, W.C. 1990. Microfiltration and ultrafiltration for apple juice clarification. *J. Food Sci.*, 55: 1162–1163.
54 Thomas, R.L., Westfall, P.H., Louviere, Z.A. and Ellis, N.D. 1986. Production of apple juice by single-pass metallic membrane ultrafiltration. *J. Food Sci.*, 51: 559–563.
55 Swientek, R.J. 1987. Metallic membrane filtration. *Food Processing*, 46 (1): 74–75.
56 Yu, Z.R., Chiang, B.H. and Hwang, L. 1986. Retention of passion fruit juice compounds

by ultrafiltration. *J. Food Sci.*, 51: 841–844.
57 Kirk, D.E., Montgomery, M.W. and Kortekaas, M.G. 1983. Clarification of pear juice by hollow fiber ultrafiltration. *J. Food Sci.*, 48: 1663–1666.
58 Wilson, E.L. and Burns, D.J.W. 1983. Kiwifruit juice processing using heat techniques and ultrafiltration. *J. Food Sci.*, 48: 1101.
59 Rwabahizi, S. and Wrolstad, R.E. 1988. Effect of mold contamination and ultrafiltration on the color stability of strawberry juice and concentrate. *J. Food Sci.*, 53: 857–861.
60 Pouliot, G. and Goulet, J. 1987. Hollow fiber ultrafiltration of maple sap: a performance study. *J. Food Sci.*, 52: 1394–1396.
61 Hart, M.R., Ng, K.C. and Huxsoll, C.C. 1989. Microfiltration of enzyme-treated apricot puree. *ACS Symp. Ser.*, 405: 355–367.
62 Merson, R.L. and Morgan, A.I. 1968. Juice concentration by reverse osmosis. *Food Technol.*, 22 (5): 97–100.
63 Demeczky, M., Khell-Wicklein, M. and Godek-Kerek, E. 1981. The preparation of fruit juice semi-concentrates by reverse osmosis. In *Developments in Food Preservation.* pp. 93–119.
64 Pepper, D. 1990. RO for improved products in the food and chemical industries and water treatment. *Desalination*, 77: 55–71.
65 Matsuura, T., Baxter, A.G., Sourirajan, S. 1974. Studies on reverse osmosis for concentration of fruit juices. *J. Food Sci.*, 39: 704–711.
66 Watanabe, A., Kimura, S. and Kimura, S. 1978. Flux restoration of reverse osmosis membranes by intermittent lateral surface flushing for orange juice processing. *J. Food Sci.*, 43: 985–988.
67 Peri, C. 1974. Concentration of orange juice by reverse osmosis. *Sci. Tec. Degli Alimenti*, 4 (1): 43–47.
68 Medina, B.G. and Garcia, A. 1988. Concentration of orange juice by reverse osmosis. *J. Food Process Engr.*, 10: 217–230.
69 Braddock, R.J., Nikdel, S., and Nagy, S. 1988. Composition of some organic and inorganic compounds in reverse osmosis-concentrated citrus juices. *J. Food Sci.*, 53: 508–512.
70 Cross, S. 1988. Achieving 60°Brix with membrane technology. Presented at the 49th Annual Meeting, Institute of Food Technologists, New Orleans, June 19–22.
71 Walker, J.B. 1990. Membrane process for the production of superior quality fruit juice concentrates. *Proceedings, 1990 International Congress on Membranes and Membrane Processes, Vol. 1*, pp. 283–285.
72 Watanabe, A., Nabetani, H., Nakajima, M., Ohmori, T., Yamada, Y. and Isiguro, Y. 1990. Development of multi-stage RO combined system (MRC) for high concentration of apple juice. *Proceedings, 1990 International Congress on Membranes and Membrane Processes, Vol. 1*, p. 282.
73 Koseoglu, S.S., Lawhon, J.T. and Lusas, E.W. 1990. Use of membranes in citrus juice processing. *Food Technol.*, 44 (12): 90–97.
74 Milleville, H.P. 1990. Direct osmosis concentrates juices at low temperature. *Food Processing*, 51 (1); 70–71.
75 Pepper, D., Orchard, A.C.J. and Merry, A.J. 1985. Concentration of tomato juice and other fruit juices by reverse osmosis. *Desalination*, 53: 157–166.
76 Merlo, C.A., Rose, W.W., Petersen, L.D., White, E.M. and Nicholson, J.A. 1986. Hyperfiltration of tomato juice. Pilot-scale high temperature testing. *J. Food Sci.*, 51: 403–407.
77 Watanabe, A. Ohtani, T., Kimura, S., Kimura, S. 1982. Performance of dynamically formed zirconia-PAA membrane during concentration of tomato juice. *Nippon Nogei*

Kagaku Kaishi, 54: 339–344.
78 Gherardi, S., Bazzarini, R., Trifiro, A., Voi, A.L. and Palamas, D. 1986. Pre-concentration of tomato juice by reverse osmosis. *Int. Fruchtstaft-Union, Wiss.-Tech. Komm.* (Berlin),. 19:241–252.
79 Sendak, P.E. and Morselly, M.F. 1984. Reverse osmosis in the production of maple syrup. *Forest Products J.*, 34(7/8): 57–61.
80 Gekas, V., Hallstrom, B. and Tragardh, G. 1985. Food and dairy applications: The state of the art. *Desalination*, 53: 95–127.
81 Adhikary, S.K., Harkare, W.P., Govindan, K.P. and Nanjundaswamy, A.M. 1983. Deacidification of fruit juices by electrodialysis. *Ind. J. Technol.*, 21 (March): 120–123.
82 Smith, R.N. and Lacey, R.E. 1982. Electromembrane process for the food industry. *Proc., Scientific Conference, Corn Refiners Association, Lincolnshire, Illinois, June 16–18.* pp. 91–118.
83 Lopez-Leiva, M.N. 1988. The use of electrodialysis in food processing. Part 2. Review of practical applications. *Lebens. Wiss. Technol.*, 21: 177–182.
84 Audinos, R., Lurton, L. and Moutounet, M. 1985. Advantage of electrodialysis for manufacturing sweetening products from grapes. *Csi. Aliments*, 5 (4): 619–637.
85 Woo A., Von Elbe, J., and Amundson, C.H. 1980. Anthocyanin recovery from cranberry pulp wastes by membrane technology. *J. Food Sci.*, 45: 875–879.
86 Chung, M.Y., Hwang, L.S. and Chiang, B.H. 1986. Concentration of perilla anthocyanins by ultrafiltration. *J. Food Sci.*, 51: 1494–1496.
87 Lin, S.S., Chiang, B.H. and Hwang, L.S. 1989. Recovery of perilla anthocyanins from spent brine by diafiltration and electrodialysis. *J. Food Engr.*, 9: 21–34.
88 Bayindirli, A., Yildiz, F. and Ozilgen, M. 1988. Modelling of sequential batch ultrafiltration of red beet extract. *J. Food Sci.*, 51: 369–372.
89 Behr, N., Goebel, G. and Pfeiffer, H. 1984. Red beet juice concentrate with improved neutrality and stability. *Ger. Offenbach.* DE 3,229,345.
90 Lee, Y.N., Wiley, R.C., Shen, M.J. and Schlimme, D.V. 1982. Purification and concentration of betalaines by ultrafiltration and reverse osmosis. *J. Food Sci.*, 47: 465–471.
91 Philip, T. 1984. Purification and concentration of natural colorants by membranes. *Food Technol.*, 38 (12): 107–108.
92 Maubois, J.L. 1989. Paper presented at North American Membrane Society annual meeting, Austin, TX. June 1989.
93 Phillips, D.J. 1989. Application of membrane processing to cheese manufacture. In: *Process Engineering in the Food Industry: Developments and Opportunities* (R.W. Field and J.A. Howell, eds). Elsevier, New York. pp. 249–257.
94 Hiddink, J., R. De Boer and P.F.C. Nooy. 1980. Reverse osmosis of dairy liquids. *J. Dairy Sci.*, 63: 204–214
95 Chiang, B.H. and M. Cheryan. 1986. Ultrafiltration of skimmilk in hollow fibers. *J. Food Sci.*, 51: 340–344.
96 Dejmek, P. 1986. Milk saving in cheesemaking by ultrafiltration. *Milchwissenschaft*, 41: 686–688.
97 Plett,E. 1989. The constant pressure difference method for microfiltration. Presented at the Third International Conference on Fouling and Cleaning in Food Processing, Prien, Bavaria, W.Germany, June 4–7.
98 Romicon,Inc. 1988. Personal communication.
99 Chua, H.T., Rao, M.A., Acree, T.E. and Cunningham, D.H. 1988. Reverse osmosis concentration of apple juice; flux and flavor retention by cellulose acetate and polyamide membranes. *J. Food Process Engr.*, 9: 231–245.

100 Cheryan, M., Sarma, S.C. and Pal, D. 1987. Energy considerations in the manufacture of khoa by reverse osmosis. *Asian J. Dairy Res.*, 6: 143–153.
101 Marshall, K.R. and Harper, W.J. 1988. Whey protein concentrates. *Int. Dairy Fed. Bull.*, 233: 22–32.
102 Batchelder, B.T. 1987. Electrodialysis applications in whey processing. *Int. Dairy Fed. Bull.*, 212: 84–90.
103 Rajagopalan, N. and Cheryan, M. 1991. Total protein isolates from milk by ultrafiltration: Factors affecting product composition. *J. Dairy Sci.*, 74: 2435–2440.
104 Rajagopalan, N. and Cheryan, M. 1991. Process optimization in ultrafiltration. Flux-time considerations in the purification of macromolecules. *Chem. Engr. Comm.*, 106: 57–69.

Membrane Separations Technology. Principles and Applications
Edited by R.D. Noble and S.A. Stern

Chapter 10

Membrane contactors

Bradley W. Reed, Michael J. Semmens and **Edward L. Cussler**

Hoechst Celanese Corporation, Separations Products Division,
Charlotte, NC 28273, USA

10.1 WHAT ARE MEMBRANE CONTACTORS?

Membrane contactors are a new way to accomplish separation processes like gas absorption and liquid–liquid extraction. They promise dramatically improved performance over conventional dispersed-phase contactors. They typically reduce the volume of equipment required for gas absorption by more than twenty times, and the volume of equipment for liquid extraction by more than five hundred times.

In this section, we first want to describe what these contactors are and how they work. In Section 10.2, we want to give a basic mathematical description of the contactors, stressing the simple case of dilute solutions. We discuss the practical issues to be considered in contactor design, and the advantages and disadvantages of membrane contactors in Section 10.3. In Section 10.4, we catalogue specific examples as a guide to future designs, and finally, in Section 10.5, we present a bibliography of published applications.

What are membrane contactors? The easiest way to see is by means of the specific example of antibiotic extraction. Conventionally, antibiotics are produced by fermentation. The fermentation beer, which is the feed, originally contains the antibiotic and the microorganisms. The beer is filtered to remove the microorganisms; the filtrate is then extracted with an organic solvent, frequently a higher alcohol, an alkyl acetate or methylene chloride. The organic extract contains more concentrated antibiotic. This valuable solute is often further purified by additional extraction, by adsorption and by crystallization. The extractions can often be the most expensive step in this chain.

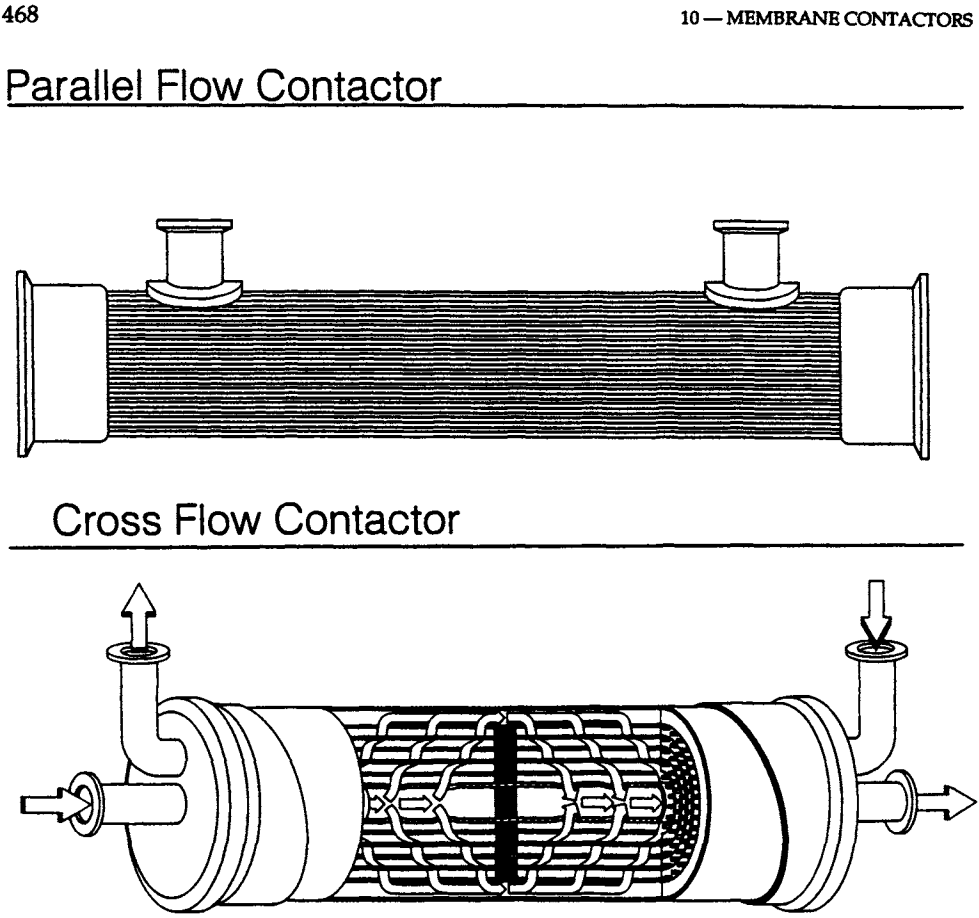

Fig. 10.1. Commercial hollow-fiber membrane contactors.

A membrane contactor can be used effectively for this extraction. Membrane contactors are typically hollow-fiber modules like those shown schematically in Fig. 10.1. Filtered beer is fed to the module; and fresh solvent is fed countercurrently. Antibiotic is extracted from the beer, diffuses across the membrane and into the bulk solvent phase. The result is an extract containing much of the antibiotic.

The contactors in Fig. 10.1 have three major advantages and one potential disadvantage over conventional equipment. The advantages are:

(1) *High surface area per volume.* Membrane contactors can supply twenty to one hundred times more surface area per volume than conventional equipment.

(2) *Complete loading.* Membrane contactors give this large area even at small flow rates where conventional packed towers are compromised.

(3) *No flooding.* Membrane contactors can reduce or avoid solvent and raffinate entrainment, which can inhibit both packed towers and mixer-settlers.

The disadvantage is potentially serious:

(4) *Slower mass-transfer.* The membrane may retard mass-transfer between the feed and the solvent. This typically occurs only when the resistance of the contained phase in the membrane pores is significant compared to the bulk phase resistances.

The success of membrane contactors depends on the three advantages being more important than the disadvantage.

This discussion shows that the membrane must be carefully chosen to retard the mass-transfer as little as possible. In practice, this choice has not been a major problem. The choice has suggested two heuristics. First, choose the membrane so that it is wet by the fluid in which the solute of interest is "more" soluble. For example, if the antibiotic partitions more strongly into the solvent vs. water, then choose a membrane wet by the solvent. If the antibiotic partitions more strongly into the aqueous feed than into the solvent, then choose a membrane wet by water.

The second heuristic is to choose a membrane which hinders solute diffusion as little as possible. In many cases, this has been realized by choosing a microporous membrane. Such a membrane is wet by either the solvent or the feed; in either case, solute diffuses easily through the pores. Such a microporous membrane does risk convective flow through the pores. Such flow, a significant risk, can usually be eliminated either by applying a static pressure or by using gel coated hollow-fibers, solutions described in Section 10.3.

Thus membrane contactors are usually hollow-fiber modules offering fast mass-transfer because of their large surface area per volume. They avoid problems of loading and flooding, but can slow mass-transfer in some applications. Their performance and design are detailed in the remaining sections of this chapter. Before beginning this section, we want to make two more points about these devices.

First, membrane contactors are unusual in this book in that the membrane's chemistry is relatively unimportant. In reverse osmosis, the membrane's chemistry controls salt rejection, flux rates and chlorine resistance, factors which dominate performance. In gas separation, membrane chemistry controls oxygen/nitrogen selectivity, which drives the economic potential of this most important of membrane separations. But for membrane contactors, the membrane's chemistry should "not" influence mass-transfer. The goal for contactors is a membrane whose effect is not negative, rather than a membrane whose effect is positive because it is selective.

The second interesting point about membrane contactors involves their comparison with conventional separation equipment. This conventional equipment usually aims at achieving some kind of fluid–fluid contact. Most commonly, this contact tries to achieve a large surface area per volume. In all these conventional cases, the shape of the fluid–fluid contact is an accident of nature;

we accept these accidental interfaces between fluids because we have no choice.

Membrane contactors open a new horizon because they can give us any shape of fluid–fluid interface that we want. They can provide large surface area per volume which has been our past goal. This interfacial contact area is achieved without dispersion and, as a result, is controllable. New designs entering the marketplace utilize a "crossflow" configuration on the shellside (outside the hollow-fiber) of the device, nurturing Taylor vortices to accelerate mass-transfer. This raises a new question: what shape of fluid–fluid interface is best for mass-transfer? We do not know, but we look forward to using membrane contactors to find out.

10.2 QUANTITATIVE DESCRIPTION OF CONTRACTORS

In this section, we present the basic mathematical description of membrane contactors. This description is common with separation equipment grouped as "differential contactors". As such, the general equations and appropriate coefficients are given in most textbooks on unit operations. We do not re-derive the equations here; instead, we give basic results specifically useful for membrane contactors. We will restrict our presentation to dilute solutions because the equations are much simpler algebraically and because the concentrated parallels are in those same textbooks.

10.2.1 Key Equations

When we consider using a membrane contactor, we often want to know how large a unit we need for a specific job, or how good a separation we can achieve with a particular module. Answering these questions commonly depends on the basic equation for any dilute absorption or extraction

$$L = \text{HTU} \cdot \text{NTU} \tag{10.1}$$

where L is the module length, HTU is the height of a transfer unit, and NTU is the number of transfer units. The NTU are roughly parallel to the number of equilibrium stages in distillation, or the number of mixer-settlers in extraction. However, the NTU do not refer to the equilibrium limit commonly approached in staged distillation or extraction.

In the same sense, the HTU roughly parallel the length of a distillation stage, or the depth of a mixer-settler. The HTU are even more parallel to the "height of an equivalent theoretical plate" often used to describe analytical chromatography. Alternatively, one can think of the NTU as signaling the difficulty of the separation and the HTU as measuring the efficiency of the equipment. This way of thinking has dominated the design of separation processes for fifty years.

Commonly, Eq. (10.1) is expressed in terms of the operating parameters in the following form:

$$L = \left[\frac{v_o}{ka}\right]\left\{\left(\frac{\frac{Q_S K}{Q_F}}{\frac{Q_S K}{Q_F} - 1}\right)\ln\left(\frac{y_o - Kx_o}{y_1 - Kx_1}\right)\right\} \tag{10.2}$$

The quantity in square brackets is the HTU, that in braces is the NTU and: v_o is the superficial feed velocity; k is the overall mass-transfer coefficient; a is the surface area of membranes per volume of bed; Q_S,Q_F are the solvent and feed flows, respectively; K is the partition coefficient, the concentration at equilibrium in the solvent phase divided by that in the feed; and x, y are the solute mole fractions in the feed and solvent, respectively.

The subscripts "o" and "1" refer to the feed inlet and the raffinate outlet, respectively. The quantity ($Q_S K/Q_F$) often appears in expressions like these, and is sometimes called the "absorption factor" or the "extraction factor".

Expressions like Eq. (10.2) are the cornerstone of any analysis of mass-transfer. Equation (10.2) is limited to dilute solutions undergoing countercurrent contacting. In countercurrent contacting, the feed and solvent flow past each other in opposite directions. Because countercurrent contacting gives the most complete separation, it is most frequently used. Occasionally, crossflow is used, in which solvent flows perpendicular to the feed. Newer designs utilize a baffled design to couple crossflow with a countercurrent flow profile. Rarely is cocurrent processing used, in which feed and solvent flow in the same direction. We will not discuss crossflow and cocurrent contacting here, although relations similar to Eq. (10.2) are easily derived for these cases.

One limit of Eq. (10.2) that is especially useful occurs when the extracting solvent flow is in excess. In this case, Eq. (10.2) becomes

$$L = \left[\frac{V_o}{ka}\right]\left\{(1)\ln\left(\frac{y_o}{y_1}\right)\right\} \tag{10.3}$$

or

$$\frac{y_1}{y_o} = \frac{c_1}{c_o} = e^{-kaL/v_o} \tag{10.4}$$

in which c_o and c_1 are the inlet and outlet concentrations of solute in, for example, moles/(dm)^3. While this limit occurs infrequently in industrial practice, its algebraic simplicity makes it an easy way to learn about contactor design. We will use it in the simplest examples given in Section 10.4.

Equations (10.1)–(10.4) allow the design of membrane contactors for separating solutes from dilute solutions. In most cases, most of the quantities in these

equations will be specified. For example, we may know how much we want to extract and how much feed and solvent flow we want to use. We can then discover how big a membrane contactor we need if we know how to find the mass-transfer coefficient k.

But what is the mass-transfer coefficient? We need its value to design our contactor. As a result, we next turn to its estimation.

10.2.2 Mass-Transfer Correlations

Mass-transfer coefficients describe how fast membrane contactors function. An engineering concept, they are buried within mass-transfer textbooks and so can be a hard concept for many to understand. As such, they have an undeserved reputation for being difficult. Mass-transfer coefficients can be tricky because they sometimes involve messy unit conversions, but they are not inherently difficult.

The easiest way to understand mass-transfer coefficients is to return to Eq. (10.3) given above. This equation gives the concentration in a membrane contactor as a function of the residence time (L/v_o) in that contactor. As a result, the product (ka) is just a rate constant characterizing absorption or extraction. As such, this product is much like a first order chemical reaction rate constant, with the familiar units of reciprocal time. As such, (ka) is closely related to the idea of a reaction half-life in nuclear chemistry or to the idea of a decimal reduction time in microbiology.

These characteristics of the mass-transfer coefficient have two implications. The first, less important implication is that membrane contactors separate with a declining efficiency. If 1 m of contactor can extract 90% of the solute, then 2 m will extract 99%, 3 m, 99.9%, and so on. Strictly speaking, such behavior is predicted only by the limit represented by Eq. (10.3); in practice, such behavior is qualitatively characteristic.

The second, more important implication of these mass-transfer coefficients is the hidden difference from chemical reaction rate coefficients. Chemical reaction rate coefficients obviously depend on chemistry but are independent of fluid flow. For example, the chlorination of benzene and of hexane proceed with very different rates, but both rates are independent of stirring velocity. In contrast, mass-transfer coefficients depend on fluid mechanics as well as on chemistry. The air stripping of benzene and hexane from water depends not only on their vapor pressures, but also on the air and water velocities. This dependence on physical quantities is why in medicine, a mass-transfer coefficient is sometimes called "the velocity of diffusion".

To estimate mass-transfer coefficients, we must first recognize that the overall coefficient k in Eqs. (10.2) and (10.3) includes contributions from the fluids flowing on either side of the membrane and the membrane itself.

$$\frac{1}{k} = \frac{1}{k(\text{feed})} + \frac{1}{k(\text{membrane})} + \frac{1}{Kk(\text{solvent})} \tag{10.5}$$

This relation is usually justified by drawing an analogy with Ohm's law. The first term $(1/k)$ represents the overall resistance to mass-transfer. This equals the sum of the resistances due to the fluid inside the feed, the membrane itself, and the solvent, which are the three terms on the right hand side. Thus Eq. (10.5) says that the overall resistance is the sum of the three resistances in series. The expression is slightly complicated by the partition coefficient K, which defines the distribution of the solute between the feed and the solvent at equilibrium. K is incorporated so that the mass-transfer may be expressed in terms of the solute concentration in the phase of interest. In this case Eq. (10.4) is written in terms of the concentrations in the feed.

We must now estimate the three terms in Eq. (10.5). Correlations for doing so, given in Table 10.1, are best known for hollow-fibers, which are the form of membrane contactor used most commonly and stressed in this review. These correlations are sometimes based on theory, but are more commonly determined from collections of experimental results. They are best grouped as those without chemical reaction and those with chemical reaction.

If the membrane is porous the membrane resistance will depend upon which phase wets the membrane; and if it is nonporous, the partition coefficient between the phase of interest and the membrane must be incorporated. The equations in Table 10.1 for the membrane give the effective mass-transfer coefficient when mass-transfer is expressed in terms of feed concentration. Corresponding relations for the opposite case are easily found by switching the definition of the feed and the solvent. In doing so, however, we must be careful to also change the definition of the partition coefficient.

(a) Correlations Without Chemical Reaction

The correlations summarized in Table 10.1 merit discussion: Eq. A, given for inside the hollow-fiber, is by far the best established. Originally derived theoretically, it has been accurately checked with a wide variety of experiments in liquids. It is also consistent with related heat transfer experiments, which differ only in replacing the factor of 1.62 with the factor of 1.86; we suspect the higher heat transfer factor is due to free convection. Equation E, derived experimentally, has not been as completely checked for gases, and shows some sign of failing at low flow.

Equations B, C and D, given for transport across the membrane, represent three different possible membranes. In Eq. B, the membrane is nonporous; past examples of such membranes include those used for kidney dialysis. Such membranes are unusually stable, even when feed and solvent flows are erratic. Their disadvantage is that their diffusion coefficient and their partition coefficient may be small and cause an unnecessarily high membrane resistance. Still,

TABLE 10.1

Mass-transfer correlations for membrane contactors

Basic situation	Correlation	Definitions	Remarks
Without Chemical Reaction			
(A) Inside Fiber	$\frac{kd}{D} = 1.62\left(\frac{d^2v}{LD}\right)^{1/3}$	D = diffusion coefficient d = fiber diameter v = actual feed velocity L = module length	The most accurate estimate
(B) Across nonporous membrane	$k = \frac{DK'}{l}$	K' = equilibrium concentration in membrane divided by that in feed l = membrane thickness	D is the value in the membrane
(C) Porous membrane wet by feed	$k = \frac{D}{l}\left(\frac{\varepsilon}{\tau}\right)$	l = membrane thickness ε/τ = void fraction/tortuosity	The factor ε/τ is often about 0.1
(D) Porous membrane wet by solvent	$k = \frac{KD}{l}\left(\frac{\varepsilon}{\tau}\right)$	l = membrane thickness K = partition coefficient (cf. Eq. 10.2) ε/τ = void fraction/tortuosity	The key is often the value of K
(E) Outside Fiber Parallel Flow	$\frac{kd_e}{D} = 1.3\left(\frac{d_e^2 v_o}{L\nu}\right)^{0.80}\left(\frac{\nu}{D}\right)^{0.33}$	d_e = equivalent diameter v_o = superficial velocity L = module length ν = kinematic viscosity	
(F) Perpendicular Flow "Crossflow"	$\frac{kd}{D} = 1.4\left(\frac{dv_o}{D}\right)^{1/3}$	d = fiber diameter v_o = superficial velocity	Probably reliable if no channeling across fibers
With Chemical Reaction			
(G) Fast Reaction	$k = \sqrt{k_R D}$	k_R = reaction rate coefficient	Can often apply to non-first order reactions
(H) Instantaneous Reactions	$k' = k\left(1 + \frac{[\text{reagent}]}{n[\text{solvent}]}\right)$	k' = coefficient with reaction k = coefficient without reaction	Reaction so fast that reactants do not coexist

they merit more attention than they have received to date.

Equations C and D are for fluid-filled porous membranes and thus are affected by the membrane's void fraction ε and tortuosity τ. Void fractions range from 0.2 to 0.9 and cluster around 0.35; tortuosities are commonly around 2 to 3, but can range as high as ten. Thus the factor (ε/τ) is usually around 0.1, though values as high as 0.8 and as low as 0.03 occasionally occur.

Decreases in mass-transfer due to void fraction and tortuosity can often be avoided by carefully choosing a membrane wet by feed or by solvent. For gas transfer applications using an aqueous feed, a hydrophobic membrane is preferred. Diffusion resistance in gas-filled pores is negligible compared to the liquid-phase resistance. For a hydrophilic solute in solvent extraction applications, we choose a hydrophilic membrane, hoping that k(membrane) will be much larger than k(solvent), and so leave the mass-transfer unaltered (cf. Eq. (10.4)). For a hydrophobic solute, we choose a hydrophobic membrane, hoping that a larger K will increase k(membrane) beyond k(feed). These hopes, based on the choice of membrane properties, frequently are justified by experiment.

In passing, we should note that the size of any membrane pores does not explicitly appear in Eqs. B, C and D. It does appear implicitly through the diffusion coefficient. The effects on the diffusion coefficient can be large for large solutes in nonporous membranes, and may be significant for diffusion in gas-filled pores where Knudsen diffusion is important. In many cases with liquid-filled membrane pores, the effect of pore size is minor.

We next return to mass-transfer outside the fibers, described by Eq. E. This equation is the least reliable of any in Table 10.1 because the experiments on which it is based are often compromised by channelling and backmixing outside the fibers for "parallel-flow" (axial flow along the outside of the fibers) contactors. Quarrels over the factor 1.3, especially its variation with void fraction, will probably continue to be fruitless. At present, we can only recommend that this result be used for initial estimates. Eq. F, for flow perpendicular to the fibers, is a sound start, but it needs extension to modules with helically and spirally arranged fibers. Such promising fiber bundle designs will certainly receive close attention in the future.

(b) Correlations with Chemical Reaction

Two final equations in Table 10.1 deal with the effect on mass-transfer of chemical reactions. Because this difficult subject is detailed elsewhere, we include these equations largely as a reminder of the increases in mass-transfer which reaction can cause. Still, we want to make two points about these equations which help understand both the literature and the examples given below.

Chemical reactions affect mass-transfer when their kinetics are rapid. These rapid kinetics are commonly discussed in terms of two limits, "fast" and "instantaneous". At first glance, these two limits might seem redundant: after all, surely an "instantaneous" reaction is "fast". While this may be true in popular usage, it is not true in this case.

A "fast" reaction is one in which the chemical kinetics influence mass-transfer, but are not so rapid that the reagents can not coexist. In this case, the Hatta number must be large, i.e.:

$$\frac{\sqrt{k_R D}}{k} >> 1 \tag{10.6}$$

One common example occurs during the mass-transfer of chlorine into water, where the chlorine reacts to produce hypochlorous and hydrochloric acids. In this case, dissolved chlorine and water can locally coexist, even though they later react.

In contrast, an instantaneous reaction is so rapid that the reagents can not coexist. One good example is the absorption of hydrogen sulfide in aqueous sodium hydroxide to produce sodium bisulfide. Near the gas–water interface, dissolved H_2S is present, but hydroxide is not. In the bulk aqueous solution, hydroxide exists, but dissolved H_2S does not. Between these two regions, there is a reaction front at which the reaction occurs; but away from this front, both reagents never coexist. Many acid-base reactions are instantaneous, but not all. Carbon dioxide absorption is often an exception.

To see how these limits can be distinguished experimentally, we again turn to a specific example, detailed in one of the problems below. Imagine air containing hydrogen cyanide gas (prussic acid) is being fed on the shell side of hydrophobic hollow-fibers and an aqueous sodium hydroxide solution is fed to the fibers' lumen. The prussic acid will diffuse out of the air and across the fibers' gas-filled pores to react in the aqueous stream:

$$HCN + NaOH \rightarrow NaCN + H_2O \tag{10.7}$$

We want to use Table 10.1 and some experiments to determine the step controlling this process.

We expect the mass-transfer in the liquid will be the slowest step and hence control the process. In other words, we expect the overall coefficient k will approximately equal that within the fiber lumen. Without reaction, this coefficient would be, from Eq. A,

$$k = 1.62 \frac{D}{d}\left(\frac{d^2 v}{DL}\right)^{1/3} \tag{10.8}$$

If the reaction is instantaneous, it will be

$$k = 1.62 \frac{D}{d}\left(\frac{d^2 v}{DL}\right)^{1/3}\left\{1 + \frac{[NaOH]}{[HCN]}\right\} \tag{10.9}$$

where [NaOH] is the concentration of sodium hydroxide in the bulk liquid, and [HCN] is the concentration of prussic acid in pure water at equilibrium with the local prussic acid partial pressure. Because this concentration ratio is often much greater than one, the correction for instantaneous reaction, given in the braces of Eq. (10.9), is often major.

Alternatively, if the reaction is fast, the results are very different. The reaction rate r for the reaction in Eq. (10.7) is

$$r = \{k_R[\text{NaOH}]\}\,[\text{HCN}] \tag{10.10}$$

When the hydroxide is in excess, the quantity in braces is nearly constant and the reaction is effectively first order. From Eq. G, we then have

$$k = \sqrt{k_R[\text{NaOH}]D} \tag{10.11}$$

This result is a sharp contrast with that for the instantaneous reaction given in Eq. (10.9). For that case, k depends on the velocity v, varies linearly with the hydroxide concentration and is unaffected by chemical kinetics. In the fast reaction case in Eq. (10.11), the mass-transfer coefficient is independent of the velocity (v) and varies with the square root of the hydroxide concentration and is a function of chemical kinetics.

These mass-transfer correlations, both with and without chemical reactions, can serve as a basis for analyzing and designing membrane contactors. How this is done is discussed in detail in the next two sections.

10.3 PAST EFFORTS

Applications utilizing membrane contactors, which are covered in this section, fall in one of four basic categories:

(i) gas/liquid mass-transfer using porous membranes;
(ii) gas/liquid mass-transfer using nonporous membranes;
(iii) liquid/liquid mass-transfer using porous membranes;
(iv) liquid/liquid mass-transfer using nonporous membranes.

Such processes are referenced in literature using a variety of terms such as membrane gas transfer, pervaporation, immobilized gas membranes, membrane distillation, membrane extraction, perstraction, immobilized liquid membranes, supported liquid membranes, contained liquid membranes and facilitated transport membranes.

A catalogue of published applications is presented in the bibliography at the conclusion of this chapter. The bibliography is not intended to be exhaustive, but provides a listing to assist the reader in locating prior work related to a specific separation of interest. The advantages and disadvantages of using membrane contactors in these separations are discussed at length below.

10.3.1 Advantages of Membrane Contactors

Membrane contactors provide a novel means of accomplishing gas/liquid

and liquid/liquid separations. Separation may be accomplished readily without having to mix the two phases intimately. In contactors using a porous membrane, the membrane simply acts as a barrier between the phases and does not impart any additional selectivity to the separation beyond that dictated by the equilibrium chemistry between the two phases. This equilibrium is typically quantified by the Henry's Law constant for gas/liquid systems or a distribution coefficient for liquid/liquid systems. In contactors using a nonporous membrane, the membrane may be selective because the solutes must partition into, and diffuse through, the solid membrane barrier. Both the partition coefficient K' and the diffusion coefficient in the membrane phase can determine the rate of solute transport across the membrane. The requirement of the solute to "permeate" the polymer membrane is evidenced by the name given to such processes as pervaporation and pertraction. Just as in gas separations, a nonporous polymer membrane which enhances selectivity decreases the flux across the membrane.

Aside from the enhanced selectivity possible with nonporous membranes, when should one consider the use of membrane contactors? The advantages of using membrane contactors are:

(a) High Surface Area per Volume

The efficiencies of conventional dispersed-phase contactors are typically expressed by their overall mass-transfer coefficient multiplied by the surface area per volume $k{\cdot}a$. The area is key. The more interfacial area a contactor provides between phases, the more efficient the contactor becomes, and the smaller its required size for a given separation. Typical values for surface area per volume supplied by various contacting devices are listed below:

TABLE 10.2

The specific surface areas of different contactors

Contactor	Surface area per volume (ft^{-1})
Free dispersion columns	1–10
Packed/trayed columns	10–100
Mechanically agitated columns	50–150
Membranes	500–2000

Clearly, membrane contactors provide up to several orders of magnitude more surface area per volume than conventional contactors. For hollow-fiber contactors, the surface area provided per volume is directly influenced by the fiber diameter. As the hollow-fiber diameter is decreased, the surface area that may be housed within a given volume of contactor increases.

(b) No Loading and Flooding Limitations

As membrane contactors operate without phase dispersion, independent adjustment of the feed and solvent fluids is possible without constraint. The membrane provides a fixed interfacial area that is independent of fluid mechanics. Thus flooding, the entrainment of the dispersed phase at high continuous phase flows, is eliminated and much higher capacities are possible. Conversely, complete loading is achieved even at low flow conditions.

(c) Reduction of Dispersed Phase Backmixing

Backmixing has long plagued the operation of dispersed phase contactors by limiting the number of transfer units, or NTUs, achievable. This limitation with conventional equipment is partially overcome by redistribution at various stages in the device.

In the membrane contactor, if the phase flowing within the fibers is considered equivalent to the dispersed phase in a conventional mixer-settler, then the continuous phase flows countercurrently outside of the fibers. The flow of each phase is forced inside or between the hollow-fibers, and the opportunity for backmixing is reduced. By reducing dispersed phase backmixing, higher NTUs and lower solvent/feed ratios can be realized.

(d) Accommodates Near-Identical Phase Densities

One of the first requirements in selecting a solvent for use in liquid/liquid extraction is a density different from the feed. If the two densities are similar, phase separation after dispersion may be difficult. As membrane contactors operate without dispersion, near-identical feed and solvent phase densities are possible without operating problems.

(e) Direct Scale-up

Membrane contactors are modular in design. When an application requires several contactors in series or parallel, this modular design allows a given process to be tested on a reduced scale. For instance, assume design calculations indicate that a particular separation will require a system of 24 contactors, 6 parallel streams of 4 contactors in series. The full scale process can be simulated using a single set of 4 contactors in series at one-sixth the total flow.

(f) Coupling of Process Steps

The ability of membrane contactors to facilitate mass-transfer between phases without dispersion leads to interesting possibilities for combining what are typically distinct process steps. Such coupled processes are referred to as gas membranes, immobilized liquid membranes and contained liquid membranes (see Fig. 10.2).

Take, for example, the recovery of ammonia from waste water. If the desired process is ammonia removal without ammonia release into the air, two packed towers are required: one to selectively strip free ammonia from the aqueous

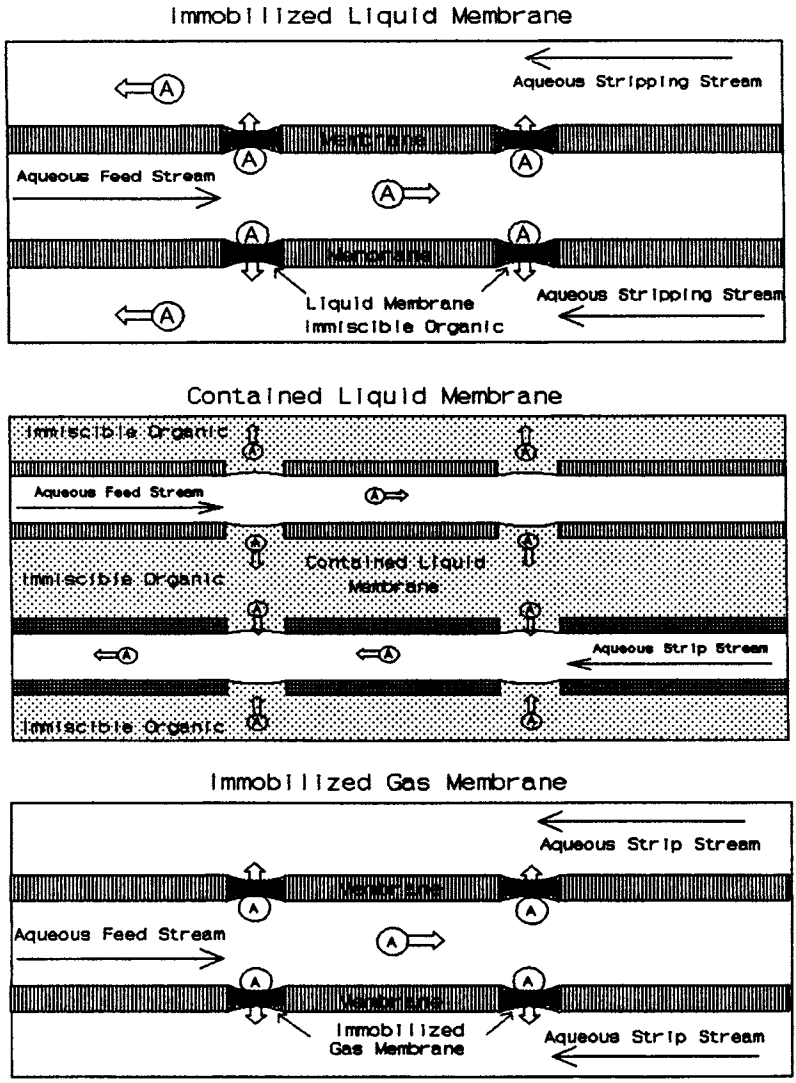

Fig. 10.2. Coupled processes using membrane contactors.

feed into an air stream, and a second to acid scrub the ammonia from the air. If sulfuric acid is used for the scrubbing, the ammonium is recovered as an ammonium sulfate solution. This two-step process is highly inefficient since ammonia has a low Henry's constant and large volumes of air are needed to effectively strip the ammonia from the wastewater. Capital and operating costs for the air blowers are high. In addition, large columns are needed for air stripping because the desired removal efficiency can only be achieved with very low hydraulic loading rates.

Using a membrane contactor can reduce the complexity, size and cost of the equipment needed. A hydrophobic microporous membrane is used in this application. The ammonia-containing water is pumped on one side of the membrane while sulfuric acid is pumped on the other side. The hydrophobic membrane is not wetted, so the pores of the membrane remain dry and gas-filled between the two liquid streams; hence the term "gas membrane". The ammonia partitions from the wastewater feed into the gas membrane, diffuses through the air-filled pores and is absorbed into the acid on the opposite side of the membrane. This neutralization by acid drives mass-transfer.

Similar coupled process advantages are possible for liquid/liquid extractions with the use of immobilized liquid membranes. Consider the example of two stage solvent extraction used for the purification and concentration of metals and pharmaceutical products. The first solvent phase can be immobilized in the pores of a microporous membrane support between feed and the second solvent (strip) phase. In this manner the immobilized solvent phase transports the solute from the feed phase to the strip phase within the same device, eliminating the need for two contacting devices. The lifetime of such a "membrane" is dependent on the solubility of the solvent in the feed and strip streams. In time the solvent is leached from the membrane, and the process must be interrupted to refill the membrane pores with fresh solvent. This major disadvantage led to the contained liquid membrane concept using two bundles of hollow-fiber membranes within the same contactor. The feed solution is pumped through one set of fibers and the strip phase is pumped through the second set while the first solvent is circulated on the shell-side of the fibers. The "contained liquid membrane" provides a reservoir between the feed and strip flows, which can be continuously regenerated.

10.3.2 Disadvantages of Contactors

Just as we must understand the advantages of membrane contactors when considering equipment options, we must understand their limitations. The disadvantages of using membrane contactors are as follows:

(a) The membrane resistance can be significant

Conventional contactors, including packed towers, have two resistances to mass-transfer, one in the feed and one in the receiving phase. The overall resistance to mass-transfer depends on the sum of the resistances in these two phases. In membrane contactors, the membrane provides a third resistance. While this third membrane resistance is often negligible, it can sometimes contribute significantly to the overall mass-transfer resistance.

The membrane resistance can be easily estimated as the membrane's thickness divided by its permeability. The thickness can sometimes be measured

directly; for microporous membranes, it is often around 30 μm, but for nonporous membranes, it can be as small as 0.01 μm. The membrane permeability, often described as P, depends on whether the membrane is porous or nonporous. If the membrane is porous, its permeability is just the diffusion coefficient in the pores times the membrane's void fraction divided by its tortuosity. If the membrane is nonporous, its permeability will be the product of the membrane's diffusion coefficient and a partition coefficient. The particular partitions coefficient is between the membrane and the adjacent phase, and is completely discussed in this book's chapter on pervaporation.

(b) Transmembrane pressure limitations

Axial pressure drops are usually modest in membrane contactors. Transmembrane pressures need not be high, as in reverse osmosis or ultrafiltration. The reason is that membrane contactors depend on "diffusion" across the membrane. Unlike reverse osmosis and ultrafiltration, they do not depend on convection across the membrane.

Transmembrane pressures are not usually important for nonporous membrane contactors. They are important for porous membrane contactors because they may cause accidental flow across the membrane, causing unwanted froth, foam or emulsion. Such accidental flow, or "breakthrough", can be controlled by applying a higher pressure on the phase which does not wet the pores. This higher pressure must not exceed a critical value, or the nonwetting fluid will penetrate the pores and contaminate the other fluid stream. This critical transmembrane pressure ΔP resulting in breakthrough is approximately defined by the Young–Laplace equation:

$$\Delta P = \frac{2\,\sigma\cos\theta}{r} \qquad \text{(gas/liquid)} \qquad (10.12)$$

$$\Delta P = \frac{2\,\gamma\cos\theta}{r} \qquad \text{(liquid/liquid)} \qquad (10.13)$$

where: σ = surface tension (dynes/cm); γ = interfacial tension (dynes/cm); θ = contact angles; and r = pore radius (cm).

The maximum transmembrane pressure for maintaining a stable interface between two phases is a function of the membrane pore size and the contact angle between the phases. Because this contact angle can be depressed by traces of surfactant, this can sometimes be a serious problem, cured by coating the microporous fibers with a thin layer of gel. In most cases, it is not severe, and can be solved by using the generalizations in Table 10.3.

(c) Available material of construction

Conventional contactors may be fabricated from a wide range of materials, including metals, polymers, ceramics and glass, whose chemical resistance is

TABLE 10.3
Influence of application on maximum transmembrane pressure

Case membrane	Wetting fluid	Nonwetting fluid	ΔP Tolerance
Gas/Liquid			
1. hydrophobic	gas	aqueous	function of σ, θ, r
2. hydrophobic	gas	organic	unstable
3. hydrophobic	aqueous	gas	function of σ, θ, r
4. hydrophobic	organic	gas	function of σ, θ, r
5. hydrophilic	gas	aqueous	unstable
6. hydrophilic	gas	organic	unstable
7. hydrophilic	aqueous	gas	function of σ, θ, r
8. hydrophilic	organic	gas	function of σ, θ, r
Liquid/Liquid*			
1. hydrophobic	organic	aqueous	function of γ, θ, r
2. hydrophobic	aqueous	organic	unstable
3. hydrophobic	nonpolar organic	polar organic	lower than #4
4. hydrophobic	polar organic	nonpolar organic	higher than #3
5. hydrophilic	organic	aqueous	lower than #6
6. hydrophilic	aqueous	organic	higher than #5
7. hydrophilic	nonpolar organic	polar organic	higher than #8
8. hydrophilic	polar organic	nonpolar organic	lower than #7

*Taken from: Prasad, R., S. Khare, A. Sengupta and K.K. Sirkar (1990). Studies on novel configurations of liquid-in-membrane pore in membrane solvent extraction. *AIChE J.*, 36, No. 10.

suitable for many operating environments. By contrast, membrane contactors generally employ polymeric membranes and an adhesive resin, used to bond the membranes into the modular casing. Although many polymers and resins have chemical resistance to acid and base, they often have limited resistance in aggressive organic solvents. The chemical compatibility of the materials of construction must be carefully assessed in advance for each application.

(d) Ability to handle solids

Unlike typical membrane filtration operations, membrane contactors do not foul due to an accumulation of particulates at the surface of the membrane. Membrane contactors operate on the principle of diffusion flux through the pores, not a convective flux which leads to gel polarization. Although particulates do not typically lead to surface fouling of the membranes, they can plug the flow, particularly at the inlet of the hollow-fibers. For this reason, prefiltration is recommended.

(e) Capacity

When determining the scale-up cost for conventional contacting equipment with higher capacity, the logarithmic relationship known as the "six-tenths factor" is typically applied:

$$C_{(n)} = r^{0.6} \cdot C$$

where: $C_{(n)}$ = new plant cost; r = ratio of new to previous capacity; C = previous plant cost.

The principle of this relationship is quite simple. A single contactor to handle twice the capacity will not cost twice as much to produce; there is an economy of scale. However, a membrane system to handle twice the capacity will cost approximately twice as much if the same basic module size is used. This lack of an economy of scale for membrane systems has inhibited their acceptance in large-scale gas separation.

While the "six-tenths factor" may apply to the cost of larger individual contactors, there will always be a practical upper limit on the manufactured size of membrane contactors. The ability to manufacture devices large enough to compete on a cost basis with conventional contactors will define the upper limits on capacity where membrane contactors find acceptance.

10.4 SPECIFIC EXAMPLES

The design of hollow-fiber membrane contactors is readily accomplished using the simple theory presented above in Section 10.2. The approach used in each of the following examples is as follows:

(i) Evaluate the individual resistances to mass-transfer using the appropriate correlations such as those presented in Table 10.1.

(ii) Add the individual resistances to determine the overall mass-transfer coefficient, k, for the conditions considered. In most cases it becomes clear on inspection that one resistance is much greater than the others and, therefore, limits the rate of mass-transfer.

(iii) With the value of k known, Eq. (10.3) may be used to size hollow-fiber contactors for a given application. As noted above, in the special case where one solvent is present in excess, and it is reasonable to assume that the concentration in equilibrium with the solvent changes very little, Eq. (10.4) may be used.

Example 1 — Drug Recovery

The first example is based on mevinolinic acid, a precursor of Merck's product, Mevinolin (Prasad and Sirkar, *J. Membr. Sci.*, 1990). We want to estimate the percent of the drug extracted from water into isopropyl acetate at pH

7.4. The water flow to a hollow-fiber module has a superficial velocity of 0.14 cm s^{-1}, which corresponds to an actual velocity within the fibers of 0.5 cm s^{-1}. Each module is 15 cm long and has a surface area per volume of 48 cm^2/cm^3 bed. The partition coefficient, K, is 800. Other values are estimated from the literature.

We can estimate the extraction using Eq. (10.4) if we can calculate each quantity involved. In particular, from correlation A in Table 10.1

$$\frac{k(\text{feed})\, d}{D} = 1.64 \left(\frac{d^2 v}{DL}\right)^{1/3}$$

$$\frac{k(\text{feed})\, 240 \cdot 10^{-4}\ \text{cm}}{0.8 \cdot 10^{-5}\ \text{cm}^2/\text{sec}} = 1.64 \left(\frac{(240 \cdot 10^{-4}\ \text{cm})^2 \cdot 0.5\ \frac{\text{cm}}{\text{sec}}}{0.8 \cdot 10^{-5}\ \frac{\text{cm}^2}{\text{sec}} \cdot 15\ \text{cm}} \right)^{1/3}$$

$$k(\text{feed}) = 7 \cdot 10^{-4}\ \text{cm/sec}$$

$$k(\text{membrane}) = \frac{D \varepsilon K}{(\text{thickness})\,(\text{tortuosity})}$$

$$= \frac{\left(0.5 \cdot 10^{-5}\ \frac{\text{cm}^2}{\text{sec}}\right)(0.57)\,(800)}{(25 \cdot 10^{-4}\ \text{cm})\,(3)}$$

$$= 0.3\ \text{cm/sec}$$

Using Eq. (10.5), we find

$$\frac{1}{k} = \frac{1}{k(\text{feed})} + \frac{1}{k(\text{membrane})} + \frac{1}{k(\text{receiving})}$$

$$= \frac{1}{k(\text{feed})}$$

Now we can use Eq. (10.4):

$$\frac{c}{c_0} = e^{-kaL/v_0}$$

$$= \exp\left[\frac{-7 \cdot 10^{-4}\ \frac{\text{cm}}{\text{sec}} \left(\frac{48\ \text{cm}^2}{\text{cm}^3}\right)(15\ \text{cm})}{0.14\ \frac{\text{cm}}{\text{sec}}} \right]$$

$$= 0.03$$

In other words, 97% of the mevinolinic acid is recovered. The experimental value is about 98%, in reasonable agreement. Similar results are possible for any weak acid or base.

Example 2 — Ammonia Stripping

As a second example, imagine we want to use a fiber module to strip ammonia from a waste water which is at pH 11.2 (Semmens et al., 1990). The waste water flows at a superficial velocity of 1.0 cm s^{-1}, corresponding to a lumen velocity of 3.3 cm s^{-1}. The module is 1 m long, has a surface area per volume of 35 cm^2/cm^3 bed, and has fibers measuring 400 μm in internal diameter. The membrane wall is 25 μm thick and, under these conditions, the membrane's pores are air-filled. The Henry's law constant is $1.8 \cdot 10^{-3}$. A strong acid is pumped over the outside of the fibers and the ammonia gas that crosses the membrane reacts rapidly with the excess acid to form nonvolatile ammonium sulfate.

Our solution parallels that given above. From Eq. A in Table 10.1

$$\frac{k(\text{feed})\, d}{D} = 1.64 \left(\frac{d^2 \upsilon}{DL}\right)^{1/3}$$

$$\frac{k(\text{feed})\, 400 \cdot 10^{-4}\ \text{cm}}{1.8 \cdot 10^{-5}\ \text{cm}^2/\text{sec}} = 1.64 \left(\frac{(400 \cdot 10^{-4}\ \text{cm})^2 \cdot 3.3\ \frac{\text{cm}}{\text{sec}}}{1.8 \cdot 10^{-5}\ \frac{\text{cm}^2}{\text{sec}} \cdot 100\ \text{cm}}\right)^{1/3}$$

$$k(\text{feed}) = 1 \cdot 10^{-3}\ \frac{\text{cm}}{\text{sec}}$$

We again use Eq. D in Table 10.1 to calculate the membrane resistance but in this case the Henry's constant is used since the pores are air-filled.

$$k(\text{membrane}) = \frac{D_P}{l}\left(\frac{\varepsilon}{\tau}\right) \cdot H$$

$$= \frac{0.04\ \text{cm}^2/\text{sec}(0.5) 1.8 \cdot 10^{-3}}{25 \cdot 10^{-4}\ \text{cm}\ (3)}$$

$$= 5 \cdot 10^{-3}\ \frac{\text{cm}}{\text{sec}}$$

where D_p, the pore diffusion coefficient, is the Knudsen value in the small, gas-filled pores (Cussler, 1984). Since an excess of strong acid is provided, the external resistance is negligible and from Eq. (10.5):

$$\frac{1}{k} = \frac{\text{sec}}{1{\cdot}10^{-3}\ \text{cm}} + \frac{\text{sec}}{5{\cdot}10^{-3}\ \text{cm}} = 8{\cdot}10^{-4}\ \text{cm/sec}$$

Now from Eq. (10.4),

$$\frac{c}{c_o} = e^{-kaL/v_o}$$

$$= \exp\left[-8{\cdot}10^{-4}\ \frac{\text{cm}}{\text{sec}}\left(\frac{35\ \text{cm}^2}{\text{cm}^3}\right)100\ \text{cm}/1.0\ \frac{\text{cm}}{\text{sec}}\right]$$

$$= 0.06$$

This 94% recovery is consistent with experiment. In contrast, *conventional packed bed technology requires a 13 m bed and an air flow of 300 ft³ air/gal feed for the same recovery.* Utilizing membrane contactors, we have a 1 m bed which requires no air flow.

Example 3 — Oxygen Transfer

This example illustrates how hollow-fiber membranes can be used to transfer oxygen into water without bubble formation. In this application, sealed fibers are used and the lumen side of the fibers is pressurized with pure oxygen. Water flows over the outside of the fibers and oxygen diffuses across the membrane and dissolves into the water. The mass-transfer behavior of sealed fibers was characterized by Ahmed (1992) and the correlations used in this example are drawn from this reference.

Assume 3000 fibers measuring 61 cm × 280 μm are housed in a 5-cm diameter pipe. The water flow rate through the pipe is 151 l min^{-1}, which gives a water velocity of 142 cm s^{-1} past the fibers. If the water is at a temperature of 15°C and the influent dissolved oxygen (DO) concentration is 0.5 mg l^{-1}, calculate the effluent DO from the module when it is operated at an oxygen pressure of 60 psi inside the fibers.

In this application the mass-transfer is controlled by liquid film diffusion on the outside of the fibers. The mass-transfer coefficient can be calculated from the correlation of Ahmed et al.

$$Sh = 0.018 \cdot Re^{0.83} \cdot Sc^{0.33}$$

Calculating Reynolds Number

$$Re = \frac{v d_e}{\nu}$$

where

$$d_e = \text{equivalent diameter} = \frac{d_p^2 - nd^2}{d_p + nd}$$

$$= \frac{(5.0\text{ cm})^2 - (3000 \cdot 0.028\text{ cm})^2}{5.0\text{ cm} + 3000 \cdot 0.028\text{ cm}}$$

$$= 0.25\text{ cm}$$

$$Re = \frac{(142\text{ cm/sec} \cdot 0.25\text{ cm})}{0.01142\text{ cm}^2/\text{sec}}$$

$$= 3157$$

$$Sc = \frac{\nu}{D} = \frac{0.01142\text{ cm}^2/\text{sec}}{1.688 \times 10^{-5}\text{ cm}^2/\text{sec}}$$

$$= 676$$

Calculating *Sh* from Ahmed's Correlation

$$Sh = 124$$

$$k = \frac{124\ D}{de}$$

$$= \frac{124 \cdot 1.688 \cdot 10^{-5}\text{ cm}^2/\text{sec}}{0.25\text{ cm}}$$

$$k = 0.0082\text{ cm/sec}$$

The interfacial area/volume, *a*, is next calculated.

The increase in oxygen concentration in the water may now be calculated

$$a = \frac{4\pi nd}{\pi d_p^2 - n\pi d^2}$$

$$= \frac{4.3000 \cdot 0.028\text{ cm}}{(5\text{ cm})^2 - 3000(0.028\text{ cm})^2}$$

$$a = 14.84\text{ cm}^{-1}$$

using an equation similar to Eq. (10.4):

$$\left(\frac{C^* - C_o}{C^* - C}\right) = e^{kaL/\upsilon}$$

In this equation, C^* is the concentration of dissolved oxygen at equilibrium with the gas inside the fiber, and is related to the pressure of the gas by the Henry's Constant. At 15°C the value of C^* is 220 mg L^{-1} for pure oxygen at 60 psi.

Now we can calculate C

$$\frac{(220\ \text{mg/L} - 0.5\ \text{mg/L})}{(220\ \text{mg/L–C})} = e^{\left(0.0082\ \frac{\text{cm}}{\text{s}}\ \text{cdot}\ 14.8\ \text{cm}^{-1} \cdot \frac{61\ \text{cm}}{142\ \text{cm/s}}\right)}$$

$$\frac{219.5}{220 - C} = 1.053$$

$$\therefore\ C = 12.6\ \text{mg/L}$$

The module can, therefore, raise the dissolved oxygen content of the water by more than 12 mg L^{-1}.

This result agrees very well with experimental data and has the interesting property of being insensitive to water flow rate. This is because the mass-transfer coefficient is almost linearly dependent upon the water velocity. Doubling the water flow rate therefore doubles the mass-transfer coefficient but the amount of mass-transferred remains approximately constant because the residence time in the reactor (L/υ) is halved.

The ability to use hollow-fibers in this way for gas transfer exploits the energy that has already been expended in separating and compressing the pure oxygen. The approach appears to have merit in the aeration of warm, shallow waters and for applications where a high dissolved oxygen concentration must be maintained.

Example 4 — Nitrogen Stripping of Oxygen from Water

In this example water is pumped through the inside of hollow fibers and nitrogen is applied to the shell-side of the membrane module. Ninety-five percent of the oxygen must be removed from a 10 gal min^{-1} stream of water. We wish to calculate the number of commercial membrane modules required to treat this flow rate. The design of the commercial shell and tube modules is summarized below in Table 10.4. A sufficiently high flow rate of nitrogen is assumed to drive the oxygen partial pressure to near zero in the exiting nitrogen stream. The dimensionless Henry's constant, *H*, for oxygen in water is 32.37.

TABLE 10.4

Design information for commercial hollow-fiber contactors*

Overall dimensions	2-in diameter × 24-in length
Number of fibers	9000
Internal fiber diameter	240 μm
Fiber wall thickness	30 μm
Membrane Porosity	30%
Effective membrane pore size	0.05 μm
Fiber material	polypropylene
Membrane tortuosity	2.6
Effective fiber length	54.6 cm

*Commercial contactor (Cat #5PCM-105) available from Hoechst Celanese Corporation.

We assume that the flow is treated by three modules in parallel, and the feed resistance inside the fibers can be calculated using the now familiar correlation:

$$\frac{k(\text{feed})d}{D} = 1.62\left(\frac{d^2\upsilon}{LD}\right)^{1/3}$$

The water flow rate per module is first calculated

$$= \frac{(10\ \text{gal/min})\ (3.78\ \text{L/gal})\ (1000\ \text{cm}^3/\text{L})}{3 \cdot 60\text{s/min}}$$

$$= 210\ \text{cm}^3/\text{s}$$

from which the velocity inside the fibers, υ, is determined:

For the membrane resistance we consider Knudsen-hindered diffusion through the small gas-filled pores of the equation. Equation D from Table 10.1 is used.

The pore diffusion coefficient, D_p, may be estimated at 25°C (Cussler, 1984).

The mass-transfer resistance in the nitrogen phase may be calculated using a modified version of Eq. E in Table 10.1 and is found to be negligible (Prasad and Sirkar, 1988):

$$\upsilon = \frac{210\ \text{cm}^3/\text{s} \cdot 4}{\pi \cdot (0.024\ \text{cm})^2 \cdot 9000}$$

$$\upsilon = 51.6\ \text{cm/s}$$

$$\frac{k(\text{feed}) \cdot (0.024\ \text{cm})}{2.5 \cdot 10^{-5}\ \text{cm}^2/\text{s}} = 1.64 \left(\frac{(0.024\ \text{cm})^2 \cdot 51.6\ \text{cm/s}}{2.5 \times 10^{-5}\ \text{cm}^2/\text{s} \cdot 54.6\ \text{cm}} \right)^{1/3}$$

$$k(\text{feed}) = 4.7 \cdot 10^{-3}\ \text{cm/s}$$

$$D_p = 4850\, d_p = \sqrt{\frac{T}{MW}}$$

$$= 4850(5 \cdot 10^{-6}\ \text{cm}) \sqrt{\frac{298}{29}}$$

$$D_p = 0.078\ \text{cm}^2/\text{s}$$

$$k_{\text{membrane}} = \frac{D_p\, \varepsilon\, H}{\tau\, l}$$

$$= \frac{0.074\ \text{cm}^2/\text{s} \cdot 0.3 \cdot 32.37}{2.6 \cdot 0.003\ \text{cm}}$$

$$= 96.8\ \text{cm/s}$$

$$\frac{k_{\text{receiving}}\, d_e}{DH} = 5.85 \left[\frac{d_e(1-\phi)}{L} \right] \left[\frac{\rho v_s\, d_e}{\mu} \right]^{0.6} \left[\frac{\nu}{D} \right]^{0.3}$$

thus

$$\frac{1}{k} = \frac{1}{4.7 \times 10^{-3}} + \frac{1}{96.8}$$

$$k = k_{\text{feed}} = 4.7 \times 10^{-3}\ \text{cm/s}$$

Using Eq. (10.4), for 95% removal

$$\frac{C}{C_o} = 0.05 = e^{-kaL/v}$$

Substitute and solve for L using $a = 4/d$ where d = internal fiber diameter.

$$-\ln(0.05) = -(4.7 \times 10^{-3}\ \text{cm/s}) \left(\frac{4}{0.024\ \text{cm}} \right) L/51.6\ \frac{\text{cm}}{\text{s}}$$

$$\therefore\ L = 198\ \text{cm}$$

Since each module is 54.6 cm in length, 4 modules in series are required. In all, 12 modules are needed to treat the 10-gpm flow.

By comparison, newer membrane contactors utilizing a more efficient, crossflow design are now available which offer larger capacity than previous contactors (Table 10.5).

TABLE 10.5
Design information of commercial crossflow contactor*

Overall dimensions	4-in diameter × 27-in length
Number of fibers	35,500
Internal fiber diameter	240 μm
Fiber wall thickness	30 μm
Membrane porosity	30%
Effective membrane pore size	0.05 μm
Fiber material	polypropylene
Membrane tortuosity	2.6
Effective fiber length	63 cm

*Commercial contactor (Cat #5PCM-113) available from Hoechst Celanese Corporation.

Using similar calculation techniques and crossflow correlations shown in Table 10.1, the total number of contactors required is reduced from twelve to one. For these crossflow devices, the aqueous phase (limiting resistance) flows outside the hollow fibers (shellside) and the nitrogen flows inside the hollow fibers (tubeside).

Example 5 — Phenol Extraction

Compare the effectiveness of a reciprocating plate extraction column with hollow-fiber membrane modules for extracting phenol from solution using MIBK. Data for the example are drawn from Karr and Ramanujan (1988).

These authors pilot tested a 3.8 m × 5.2 cm diameter column to treat a water containing 440 ppm of phenol. The conditions tested and relevant data are shown below:

Influent phenol concentration	$= 440\ mg\ l^{-1}$
Effluent phenol concentration	$= 1\ mg\ l^{-1}$
The partition coefficient K for MIBK	$= 40$
Water flow rate	$= 24\ ml\ s^{-1}$
MIBK flow rate	$= 27.9\ ml\ s^{-1}$
Temperature	$= 105°C$
Diffusivity of phenol in water	$= 1 \cdot 10^{-5}\ cm^2\ s^{-1}$
Diffusivity of phenol in MIBK	$= 3 \cdot 10^{-5}\ cm^2\ s^{-1}$

The experiments on the reciprocating plate extraction column showed that the NTU = 6.61 and the HTU = 55.4 cm.

How many modules are required if modules as described in Table 10.4 are used in this application?

The water velocity υ within the fibers may be calculated

$$v = 24\ \text{cm}^3\ \text{s}^{-1} \cdot 4/\pi \cdot (0.024\ \text{cm})^2 \cdot 7500$$
$$= 7.1\ \text{cm}\ \text{s}^{-1}$$

We may also calculate a superficial water velocity, υ_o, for the module and the solvent velocity, υ_s.

$$\upsilon_o = 24\ \text{cm}^3\ \text{s}^{-1} \cdot 4/\pi\ (4\ \text{cm})^2$$
$$= 1.9\ \text{cm}\ \text{s}^{-1}$$

$$\upsilon_s = 27.9\ \text{cm}^3\ \text{s}^{-1} \cdot 4/\pi \times (4\ \text{cm})^2 \cdot 0.43$$
$$= 5.2\ \text{cm}\ \text{s}^{-1}$$

The mass-transfer coefficients are calculated:

$$k_{\text{feed}} = 1.64 \cdot \left(\frac{D}{d}\right) \cdot \left(\frac{d^2\upsilon}{DL}\right)^{1/3}$$

$$= 1.64 \left(\frac{1{\cdot}10^{-5}\ \text{cm}^2/\text{s}}{0.024\ \text{cm}}\right)\left(\frac{(0.024)^2\ (7.1\ \text{cm/s})}{(1{\cdot}10^{-5}\ \text{cm}^2/\text{s})\ (54.6\ \text{cm})}\right)^{1/3}$$

$$= 1.3{\cdot}10^{-3}\ \text{cm/s}$$

$$k_{\text{membrane}} = \frac{D\,\varepsilon\,K}{l\,\tau} = \frac{(3{\cdot}10^{-5}\ \text{cm}^2/\text{s} \cdot 0.3 \cdot 40)}{0.003\ \text{cm} \cdot 2.6}$$

$$= 4.6{\cdot}10^{-2}\ \text{cm/s}$$

$k_{\text{receiving}}$ is estimated using the equation of Prasad and Sirkar (1988):

$$k_{\text{receiving}} = 5.85 \left(\frac{HD}{d_e}\right)\left[\frac{d_e(1-\phi)}{d_e}\right]\left[\frac{\rho\upsilon_s d_e}{\mu}\right]^{0.6}\left[\frac{\nu}{D}\right]^{0.3}$$

$$= 5.85 \cdot \left(\frac{40 \cdot 3{\times}10^{-5}\ \text{cm}^2/\text{s}}{0.53\ \text{cm}}\right)\left(\frac{0.53\ \text{cm}(1{-}0.43)}{54.6\ \text{cm}}\right)\left(\frac{5.2\ \text{cm/s} \cdot 0.53\ \text{cm}}{0.75\ \text{cm}^2/\text{s}}\right)^{0.6}$$
$$\times\left(\frac{0.75\ \text{cm}^2/\text{s}}{3{\times}10^{-5}\ \text{cm}^2/\text{s}}\right)$$

$$= 3.33 \cdot 10^{-3}\ \text{cm/s}$$

Summing the resistances:

$$\frac{1}{k} = \frac{1}{1.3\times10^{-3}} + \frac{1}{3.33\times10^{-3}} + \frac{1}{4.6\times10^{-2}}$$

$$k = 9.4 \times 10^{-4} \text{ cm/s}$$

Therefore,

$$\frac{c}{c_o} = 0.023 = e^{\left(\frac{-9.4\cdot10^{-4}\text{ cm/s} \times 166\text{ cm}^{-1} \times L}{7\text{ cm/s}}\right)}$$

$$L = 272 \text{ cm}$$

and five modules are needed in series.

The HTU is then calculated for the membrane module:

$$\frac{272}{6.61} = 41.3 \text{ cm}$$

The results of this analysis are summarized in Table 10.6.

TABLE 10.6
Comparison of contactors

	a (cm^{-1})	HTU (cm)	Volume required (cm^3)
Membrane Contactors	167	41.3	3430
Recip. Plate Contactor	2–4?	55.4	7777
Membrane/Column Ratio	~80/1	0.75/1	0.44/1

Example 6 — Oil Extraction of Volatile Organic Compounds (VOCs) from Water

In this example we consider the use of an externally coated hollow-fiber membrane that allows the fibers to be immersed in oil without wetting. Water is pumped through the fibers while oil is recirculated outside the fibers and the pores of the membrane remain dry and air-filled. In this three-phase system, VOCs can readily diffuse across the membrane and into the oil as described by Zander et al, (1989).

Tetrachloroethylene (TCE)-contaminated water is treated in a membrane module under the following conditions:

external fiber diameter	= 450 μm
internal fiber diameter	= 400 μm

shellside equivalent diameter	= 0.12 cm
fiber length	= 30 cm
water velocity	= 2.65 cm s^{-1}
superficial oil velocity	= 0.7 cm s^{-1}
K_d (oil/water partition coefficient)	= 1000 dimensionless
H (Henry's constant)	= 0.753 dimensionless
D_{air}	= 7.54×10^{-2} cm^2 s^{-1}
D_{oil}	= 9×10^{-7} cm^2 s^{-1}
D_{water}	= 8.9×10^{-6} cm^2 s^{-1}
oil viscosity	= 4.88×10^{-5} cm^2 s^{-1}

Evaluate the resistances:

(i)

$$k_{water} = 1.62 \left(\frac{d^2 \upsilon}{LD}\right)^{0.33} \cdot \frac{D}{d}$$

$$= 1.62 \cdot \left[\frac{(0.04 \text{ cm})^2 \cdot 2.65 \text{ cm/s}}{8.9\times10^{-6} \text{ cm}^2/\text{s} \cdot 30 \text{ cm}}\right]^{0.33} \cdot \frac{8.9\times10^{-6} \text{ cm}^2/\text{s}}{0.04 \text{ cm}}$$

$$k_{water} = 9\times10^{-4} \text{ cm/s}$$

(ii)

$$k_{membrane} = \frac{D \cdot H}{l} \cdot \frac{\varepsilon}{\tau}$$

$$= \frac{7.54\times10^{-2} \text{ cm}^2/\text{s} \cdot 0.753 \cdot 0.3}{0.0025 \text{ cm } 2.6}$$

$$k_{membrane} = 2.62 \text{ cm/s}$$

(iii)

$$k_{oil} = 1.3 \left(\frac{d^2 \upsilon_o}{L\nu}\right)^{0.8} \left(\frac{\nu}{D}\right)^{0.33} \frac{D}{d} \cdot K_d$$

$$= 1.3 \left(\frac{(0.045 \text{ cm})^2 \, 0.7 \text{ cm/s}}{30 \text{ cm} \cdot 4.88\times10^{-5} \text{ cm}^2/\text{s}}\right)^{0.8} \left(\frac{4.88\times10^{-5} \text{ cm}^2/\text{s}}{9\times10^{-7} \text{ cm}^2/\text{s}}\right)^{0.33}$$

$$\cdot \left(\frac{9\times10^{-7} \text{ cm}^2/\text{s}}{0.045 \text{ cm}}\right) \cdot 1000$$

$$k_{oil} = 1.37 \text{ cm/s}$$

Inspection reveals that mass-transfer is limited by aqueous diffusion to the membrane wall and not by the volatility of the compound. Indeed, much less volatile organic compounds can be removed with equal efficiency. Only when H is small enough to raise the membrane resistance to a value comparable with

the resistance in the aqueous phase does it begin to influence VOC removal performance.

We may calculate the overall removal of TCE in the module

$$\frac{C}{C_o} = e^{-kaL/v}$$

$$= e^{-(9\times10^{-4}\ \text{cm/s})\cdot\left(\frac{4}{0.04\ \text{cm}}\right)\cdot\frac{30\ \text{cm}}{2.65\ \text{cm/s}}}$$

$$\therefore \frac{C}{C_o} = 0.36$$

i.e. 67% TCE removal.

10.5 BIBLIOGRAPHY OF MEMBRANE CONTACTOR APPLICATIONS

1 Prasad, R. and Sirkar, K.K. (1989). Hollow fiber solvent extraction of pharmaceutical products: a case study. *J. Membr. Sci.*, 47: 235–259.
Application: Liquid/liquid (meviolinic acid).

2 Kang, W. et al. (1988). Evaluation of O_2 and CO_2 transfer coefficients in a locally integrated tubular hollow fiber bioreactor. *Appl. Biochem. Biotech.*, 18: 35–51.
Application: Gas Transfer (O_2, CO_2)

3 Fournier, R.L. (1988). Mathematical model of microporous hollow-fiber membrane extractive fermentor. *Biotech. Bioeng.*, 31: 235–239.
Application: Gas Transfer, Liquid/liquid Extraction (O_2, ethanol)

4 Fleischaker, R. (1988). Review of membrane oxygenation of bioreactors. *Bioprocess Engineering Symposium, ASME Winter Meeting.*
Application: Gas Transfer (O_2)

5 Prasad, R. and Sirkar, K.K. (1990). Hollow fiber solvent extraction: performances and design. *J. Membr. Sci.*, 50: 153–175.
Application: Liquid/liquid Extraction (4-methylthiazole, 4-cyanothiazole)

6 Dahuron, L. and Cussler, E.L. (1988). Protein extractions with hollow fibers. *AIChE J.*, 34 (1): 130–136.
Application: Liquid/liquid Extraction (myoglobin, αchymotrypsin, cytochrome-c, catalase, urease)

7 Frank, G.T. and Sirkar, K.K. (1986). An integrated bioreactor-separator: *in situ* recovery of fermentation products by a novel membrane-based dispersion-free solvent extraction technique. *Biotech. Bioeng. Symp. No. 17*, pp. 303–316.
Application: Gas Transfer, Liquid/liquid Extraction (O_2, ethanol)

8 Yang, M.C. and Cussler, E.L., Designing hollow-fiber contactors. AIChE J., 32 (11): 1910–1916.
Application: Gas Transfer (O_2, CO_2)

9 Servas, F.M. et al. (1983). High efficiency membrane oxygenator. *Trans. Am. Soc. Artif. Intern. Organs*, XXIX: 231–236.
Application: Gas Transfer (O_2, CO_2)

10 Yang, M.C. and Cussler, E.L. (1989). Artificial gills. *J. Membr. Sci.*, 42: pp. 273–284.
Application: Gas Transfer (CO_2)

11 Qi, Z. and Cussler, E.L. (1985). Hollow fiber gas membranes. *AIChE J.*, 31 (9): 1548–1553.
Application: Gas Trnasfer (H_2S, SO_2, NH_3)

12 Qi, Z. and Cussler, E.L. (1985). Microporous hollow fibers for gas absorption. *J. Membr. Sci.*, 23: 321–345.
Application: Gas Transfer (CO_2, NH_3, H_2S, SO_2)

13 Semmens, M.J. et al. (1989). Using a microporous hollow-fiber membrane to separate VOCs from water. *J. AWWA, Research and Technology* (April 1989): 162–167.
Application: Gas Transfer (VOCs)

14 Basu, R. et al. (1990). Nondispersive membrane solvent back extraction of phenol. *AIChE J.*, 36 (3).
Application: Liquid/liquid Extraction (phenol)

15 Sengupta, A. et al. (1990). Liquid membranes for flue gas desulfurization. *J. Membr. Sci.*, 51: 105–126.
Application: Gas Transfer (SO_2)

16 Kenfield, C.F. et al. (1988). Cyanide recovery across hollow fiber gas membrane. *Environ. Sci. Tech.*, 22: 1151–1155.
Application: Gas Transfer (cyanide)

17 Callahan, R.W., Novel Uses of Microporous Membranes: A Case Study. *AIChE Symposium Series*, 84, No. 261, pp. 54–63.
Application: Gas Transfer (O_2, H_2S, SO_2, NH_3 CO_2) Liquid/liquid Extraction (Gold)

18. D'Elia, N.A. et al. (1986). Liquid–liquid extractions with microporous hollow fibers. *J. Membr. Sci.*, 29: 309–319.
Application: Liquid/liquid Extraction (*p*-nitrophenol, acetic acid)

19 Sengupta, A. et al. (1988). Separation of liquid solutions by contained liquid membranes. *Sep. Sci. Tech.*, 23 (12/13): 1735–1751.
Application: Liquid/liquid Extraction (phenol, acetic acid)

20 Prasad, R. and Sirkar, K.K. (1988). Dispersion-free solvent extraction with microporous hollow-fiber modules. *AIChE J.*, 34 (2): 177–188, 1988.
Application: Liquid/liquid Extraction (succenic acid)

21 Kiani, A. et al. (1984). Solvent extraction with immobilized interfaces in a microporous hydrophobic membrane. *J. Membr. Sci.*, 20: 125–145.
Application: Liquid/liquid Extraction (acetic acid)

22 Prasad, R. et al. (1986). Further studies on solvent extraction with immobilized interfaces in a microporous hydrophobic membrane. *J. Membr. Sci.*, 26: pp. 79–97.
Application: Liquid/liquid Extraction (acetic acid)

23 Qi, Z. and Cussler, E.L. (1985). Bromine recovery with hollow fiber gas membranes. *J. Membr. Sci.*, 24: 43–57.
Application: Gas Transfer (bromine)

24 Sengupta, A. et al. (1988). Separation of solutes from aqueous solutions by contained liquid membranes. *AIChE J.*, 34 (10).
Application: Liquid/liquid Extraction (phenol, acetic acid)

25 Alexander, P.R. and Callahan, R.W. (1987). Liquid–liquid extraction and stripping of gold with microporous hollow fibers. *J. Membr. Sci.*, 35: 57–71.
Application: Liquid/liquid Extraction (gold)

26 Yang, M.C. and Cussler, E.L. (1987). A hollow-fiber trickle-bed reactor. *AIChE J.*, 33 (10): pp. 1754–1756.

Application: Gas Transfer ($SO_2 \rightarrow H_2SO_4$)

27 Danesi, P.R. and Reichley-Yinger, L. (1986). A composite supported liquid membrane for ultraclean co-ni separations. *J. Membr. Sci.*, 27: 339–347.
Application: Liquid/liquid Extraction (Co, Ni)

28 Danesi, J.R. and Cianetti, C. (1983). Induction time in metal permeation processes through supported liquid membranes. *J. Membr. Sci.*, 14: 175–186.
Application: Liquid/liquid Extraction (Cd)

29 Inloes, D.S. et al. (1983). Ethanol production by saccharamyces cerevisiae immobilized in hollow-fiber membrane bioreactors. *Appl. Environ. Microbiol.*, July: 264–278.
Application: Gas Transfer (O_2) Liquid/liquid Extraction (ethanol)

30 Fabiani, C. et al. (1987). Degradation of supported liquid membranes under a osmotic pressure gradient. *J. Membr. Sci.*, 30: 97–104.
Application: Liquid/liquid Extraction (trilaurylamine hydrochlorate)

31 Majumdar, S. et al. (1988). A new liquid membrane technique for gas separation. *AIChE J.*, 34 (7): 1135–1145.
Application: Gas Transfer (Co_2)

32 Evren, V. and Piskin, E. (1985). Membrane oxygenators embodying silicone-coated microporous membranes. *Progr. Artif. Organs*: 566–569.
Application: Gas Transfer (O_2)

33 Yamaguchi, T. et al. (1988). Amino acid transport through supported liquid membranes: mechanism and its application to enantiomeric resolution. *Bioelectrochem. Bioenerg.*, 20; 109–123.
Application: Liquid/liquid Extraction (amino acids)

34 Tromp, M. et al. (1988). Extraction of gold and silver cyanide complexes through supported liquid membranes containing macrocyclic extractants. *J. Membr. Sci.*, 38: 295–300.
Application: Liquid/liquid Extraction (gold & silver cyanide)

35 Johnson, B. et al. (1987). Liquid membranes for the production of oxygen-enriched air. *J. Membr. Sci.*, 31: 31–67.
Application: Gas Transfer (O_2)

36 Shukla, R. et al. (1989). ABE Production in a novel hollow fiber fermentor–extractor. *Biotech. Bioeng.*, 34: 1158–1166.
Application: Gas Transfer (O_2) Liquid/liquid Extraction (acetone, butanol, ethanol)

37 Lee, K.H. et al. (1978). Selective copper recovery with two types of liquid membranes. *AIChE J.*, 24 (5): 860–868.
Application: Liquid/liquid Extraction (Cu)

38 Chaundry, M.A. et al. (1989). Transport study of V(V), Zn(II) and Be(II) using supported liquid membranes. *J. Radioanal. Nucl. Chem.*, 129 (2): 409–423.
Application: Liquid/liquid Extraction (V, Zn, Be)

39 Callahan, R.W. (1989). Liquid/liquid extraction with Celgard microporous membranes and component products. *Filtration News*, 7 (1).
Application: Liquid/liquid Extraction (Pd, Cu, Au)

40 Wickramasinghe, S.R. et al. (1991). Better hollow fiber contactors. *J. Membr. Sci.*, 62: 371–388.
Application: Gas Transfer (O_2)

Membrane Separations Technology. Principles and Applications
Edited by R.D. Noble and S.A. Stern

Chapter 11

Analysis and design of membrane permeators for gas separation

Amitava Sengupta[a] and **Kamalesh K. Sirkar**[b]

[a]Hoechst Celanese Corporation, Charlotte, NC 28273, USA
[b]New Jersey Institute of Technology, Newark, NJ 07102, USA

11.1 INTRODUCTION

Compared to other membrane technologies like reverse osmosis and ultrafiltration, commercial gas separation using membranes is relatively new [1]. However, the rate of growth of this technology has been phenomenal. Progress was made based on development of new materials, new membrane fabrication processes and new application developments. The growth is expected to continue through the 1990s, making it perhaps a 100-million-dollar industry by the end of this decade [2–4].

Like its sister technologies, membrane gas separation is commercially appealing for many reasons. These include higher energy efficiency, generally lower capital and operating costs, compact modular construction, low maintenance cost, ease of installation and operation, mechanical simplicity and ease of scale-up. Over the years, a large range of applications has been developed [3]. Membranes are used commercially for separation of H_2 from refinery off-gases, ammonia purge gas and syn-gas [5–7], CO_2 removal from natural gas — including the enhanced oil recovery (EOR) applications [8–11], acid gas separation [12], air separation and N_2 generation [13–15], recovery of solvent from air [16–18] and compressed air-drying [2].

As membrane gas separation technology matures, the need to understand

the performance of membrane separators in a process configuration becomes increasingly important. The separation characteristics of permeators will directly affect the process economics. The capability of performance analysis and prediction is, therefore, an essential part of the technology development. The performance analysis also aids directly in designing membrane modules for a given separation requirement. Furthermore, membrane separations are often used in hybrid processes, i.e., as processes in conjunction with other separation processes, or other unit operations [19]. Analysis and design of membrane permeators are, therefore, essential tools even in the preliminary process design stage.

11.2 SCOPE OF THIS CHAPTER

Over the years, a great variety of different types and classes of membranes have been developed and reported. Membranes can be classified in various ways [20–22]. For gas separation, membranes can be solid (polymeric or inorganic or metallic) or liquid. Solid membranes can be nonporous, microporous, asymmetric, or composite. Liquid membranes can have different structures, e.g., immobilized or supported liquid membranes, emulsion liquid membranes and contained liquid membranes. Other variations, e.g., solvent-swollen membranes, ion-exchange membranes, etc., have also been developed. Besides these variations, the membrane can be packaged in the permeator module in different forms. The two forms commercially used are hollow fiber and spirally wound flat sheet. The analysis and design of the permeator may depend strongly on this choice.

The actual mechanism of gas transport and separation can also vary. Different postulated mechanisms are solution–diffusion, facilitation, Knudsen diffusion, surface diffusion and molecular sieving. Incorporating such phenomena in a single analytical framework is beyond the scope of the present chapter. The strategy here is to keep the permeator performance analysis as generally applicable as possible. Mechanistic aspects of transport are not considered. It is assumed that the membrane transport and permeation properties are known. The goal is to compute and predict the overall macroscopic separation in a separator 'module' based on known 'local' rates of transport, or to design the module for a required extent of separation. However, as discussed later, the analysis framework developed here can be built upon and extended to simulation of more complex cases.

Additionally, a steady-state operation is assumed. Although there have been studies reported in literature on transient response of membrane modules [23], at this time it is likely to be only of academic interest. Therefore, no temporal variation inside the membrane module has been considered here.

11.3 GOVERNING EQUATIONS AND USEFUL DEFINITIONS

In case of simple permeation, the rate of permeation across a membrane at a given point in a permeator is governed by the following equation:

$$\begin{bmatrix}\text{RATE OF}\\ \text{PERMEATION}\\ \text{OF SPECIES } i\end{bmatrix} = \begin{bmatrix}\text{PERMEABILITY OF SPECIES } i\\ \hline \text{EFFECTIVE MEMBRANE THICKNESS}\end{bmatrix}\begin{bmatrix}\text{MEMBRANE}\\ \text{AREA}\end{bmatrix}\begin{bmatrix}\text{EFFECTIVE PARTIAL}\\ \text{PRESSURE DIFFERENCE}\\ \text{OF } i \text{ ACROSS MEMBRANE}\end{bmatrix} \tag{11.1a}$$

The rate of permeation is a 'point function', much as the local rate of reaction in a reactor. For nonreactive permeation, the permeability is a quantity unique to the permeant–membrane combination and is a function of temperature. For permeation through rubbery membranes, it can be shown to be the product of the diffusivity and the solubility of the permeant in the membrane [24]. For glassy polymers, the 'dual-mode' model has been used [25].

Most commercial gas separation membranes are asymmetric in nature. The permeation is modelled by assuming the membrane has a dense 'skin' backed by an integral porous support with graded porosity. It may not be possible to measure the effective membrane thickness physically. For this reason, and for ease of analysis, the permeability and the effective membrane thickness are often combined together, and their ratio is called the permeance:

[PERMEATION RATE] = [PERMEANCE] [AREA] [EFFECTIVE PARTIAL PRESSURE DIFFERENCE] (11.1b)

or

[PERMEATION FLUX] = [PERMEANCE] [EFFECTIVE PARTIAL PRESSURE DIFFERENCE] (11.1c)

The commonly reported units of these quantities and the appropriate conversion factors are shown in Table 11.1.

For a differential permeation area dA, Eq. (11.1b) can be expressed for species i as:

$$dR_i = (P_i/t_m)\,(dA)\,(\Delta p_i) = (Q_i)\,(dA)\,(\Delta p_i) \tag{11.2a}$$

In the case of a nonporous homogeneous membrane, Δp_i is the partial pressure difference between the feed gas phase and the permeate gas phase (Fig. 11.1) and can be expressed in terms of the total phase pressures and the corresponding mole fractions at every location inside the permeator:

$$dR_i = (Q_i)\,(dA)\,(P_F\,x_i - P_P\,y_i) \tag{11.2b}$$

$$= (Q_i)\,(dA)\,P_F\,(x_i - \gamma\,y_i) \tag{11.2c}$$

where γ is the permeate to feed pressure ratio, defined as

$$\gamma = P_P / P_F \tag{11.2d}$$

TABLE 11.1

Definitions, units and conversion factors

Quantity	Engineering unit	Scientific units	
Permeation rate	Std ft^3/day	Mole/sec	Std cm^3/sec
Permeation flux	Std ft^3/(day)(ft^2)	Mole/(sec)(m^2)	Std cm^3/(sec)(cm^2)
Permeance	Std ft^3/(day)(ft^2)(psi)	Mole/(sec)(m^2)(Pa)	Std cm^3/(sec)(cm^2)(cm Hg)
Permeability	(Std ft^3)(ft)/(day)(ft^2)(psi)	(Mole)(m)/(sec)(m^2)(Pa)	(Std cm^3)(cm)/(sec)(cm^2)(cm Hg)

Notes:

1. Standard condition implies 0°C and 1 atm.
2. A common unit of permeability is Barrer, defined as 1 Barrer = 10^{-10} (Std cm^3)(cm)/(sec)(cm^2)(cm Hg).
3. The conversion factors for permeance are: 1 Mole/(sec)(m^2)(Pa) = 2.986×10^{13} Barrer/cm; 1 Std ft^3/(day)(ft^2)(psi) = 6.824×10^5 Barrer/cm.

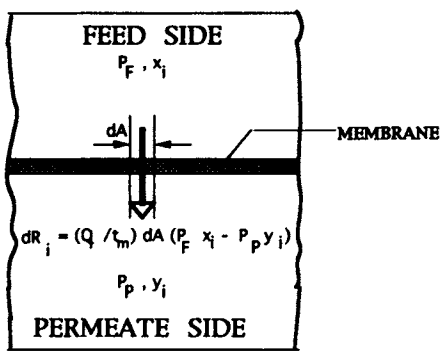

Fig. 11.1. Permeation across a differential membrane area.

For permeation to take place, a positive Δp_i is required. There are three ways of ensuring it: (i) a high-pressure feed gas can be used (high P_F); (ii) a vacuum can be maintained on the permeate or product side (low P_P); and (iii) a sweep or carrier gas can be used on the permeate side to reduce y_i. For commercial gas separation processes, only the first two options are viable since use of a sweep or carrier would be generally counterproductive to separation. A sweep gas may be used, however, if the permeated fraction is of no value.

Equations (11.2a) and (11.2b) apply to any species i. The relative rates of permeation of two species i and j can, therefore, be expressed as

$$dR_i/dR_j = (Q_i/Q_j)\,(\Delta p_i/\Delta p_j) = \alpha\,(\Delta p_i/\Delta p_j) \tag{11.3}$$

The quantity $\alpha(= Q_i/Q_j)$ is called the selectivity of species i over species j for the given membrane. The selectivity and the permeance are the two most important characteristics of commercial membranes. In practice, the permeance of the faster permeating species is used in the numerator to define the selectivity so that α is always greater than or equal to unity. The higher the value of α, the better is the separation capability of the membrane. A value of $\alpha = 1$ means no separation at all.

Equations (11.2a)–(11.3) show that the permeation rate increases with increases in permeability and feed pressure, and decreases with increase in the membrane thickness and the permeate pressure. The permeability of a given polymer material is generally constant. The feed and the permeate pressures are process variables which are often fixed also. Therefore, a most commonly sought-after goal in membrane processes is to have an extremely thin membrane. However, a very thin membrane would not be able to withstand high trans-membrane pressure. That is why successful gas permeation membranes have almost always been the asymmetric type or the thin-film composite type [26].

It is important to recognize that as different species permeate at different rates, the effective partial pressure of each species will change *along* the bulk gas-flow direction. The overall separation, therefore, depends not only on selectivity, but on various other factors as well. Figure 11.2a shows the flow rates and compositions for a so-called membrane separation stage, where L and V are the molar flow rates. An overall material balance can be written as:

$$L_F = L_R + V_P \tag{11.4a}$$

A component material balance for species i can be written as:

$$L_F x_{iF} = L_R x_{iR} + V_P y_{iP} \tag{11.4b}$$

Three terms are often employed to characterize a membrane separation stage — stage cut (θ), component recovery in the permeate (Ψ_i) and the component recovery in the residue (Φ_i):

$$\theta = V_P/L_F \tag{11.5a}$$

$$\Psi_i = y_{iP}\, V_P/x_{iF}\, L_F \tag{11.5b}$$

$$\Phi_i = x_{iR}\, L_R/x_{iF}\, L_F = 1.0 - \Psi_i \tag{11.5c}$$

Another term, the enrichment factor (e_i), is also used sometimes:

$$e_i = y_{iP}/x_{iF} \tag{11.5d}$$

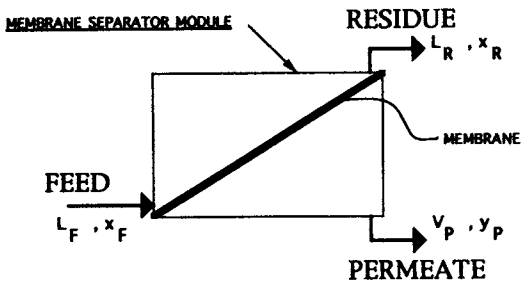

(a) GENERAL SCHEMATIC OF A MEMBRANE SEPARATION STAGE

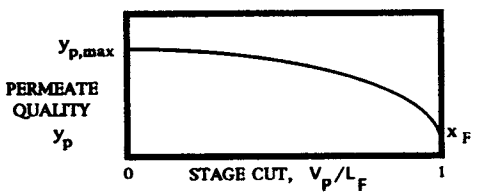

(b) GENERAL PERFORMANCE OF A MEMBRANE SEPARATION STAGE FOR A BINARY SYSTEM

Fig. 11.2. A membrane separation stage.

Using these definitions, the mass balance equations can be reformulated:

$$\theta = (x_{iF} - x_{iR} / (y_{iP} - x_{iR}) \tag{11.6a}$$

$$\Psi_i = 1.0 - \Phi_i = e_i\,\theta = 1 - (1 - \theta)\,(x_{iR} / x_{iF}) \tag{11.6b}$$

The above terms are used extensively in the literature on membrane gas permeator analysis.

The theoretical maximum value of θ can be 1.0. However, the permeator would not achieve any effective separation when θ is 1, and in that case y_{iP} would equal x_{iF}. The magnitude of the permeate composition is largest when θ approaches zero and normally decreases monotonically as θ increases, especially for binary separation. In an actual permeator, y_{iP} would be somewhere between the above mentioned maximum y_{iP} and x_{iF}. These facts are illustrated in Fig. 11.2b.

11.4 PROCESS DESIGN OPTIONS AND SEPARATION SCHEMES

As in other unit operations, there are two cost elements involved in membrane processes — the capital cost and the operating cost. Sometimes the cost

of pretreating the feed gas stream before it enters the membrane processing stage may have to be added to these costs since the membrane may be damaged by an impurity in the feed stream, e.g., H_2O, NH_3, etc. The capital cost for the membrane process is determined primarily by the permeation area required for the necessary separation, whereas the operating cost is influenced essentially by the power requirement for the fluid moving equipment, e.g., compressors.

Two major factors in process design are the product purity and the product recovery. The product from a membrane separation step can be either the unpermeated residue stream or the permeate stream. Examples of the former category are nitrogen generation from air (remove O_2 from air), dehydration of natural gas (remove H_2O from hydrocarbons), sour gas treating (remove CO_2 and H_2S from hydrocarbons), landfill gas upgrading (remove CO_2 from CH_4), syngas ratio adjustment (partially remove H_2 from H_2-CO mixture), etc. Examples of the latter category are hydrogen recovery from refinery streams, production of oxygen enriched air, helium recovery, recovery of CO_2 for enhanced oil recovery applications, etc.

The process design is influenced very strongly by the separation goal. For example, in nitrogen generation from air, the goal is to remove as much oxygen as possible from the feed air. Along with O_2, N_2 also permeates since membranes have finite selectivities. Therefore, for a membrane with a given selectivity, the higher the purity of the N_2 desired, the larger is the fraction of the feed to be permeated, i.e., the larger the stage cut (and the larger the membrane area required). The quality of the permeate is of no consequence here. However, as stage cut increases, more and more N_2 is lost in the permeate, and the fraction of feed N_2 that is recovered as the high-purity N_2 product is reduced. Thus, in this case, high product purity leads to large membrane area, and low recovery.

On the other hand, for producing oxygen-enriched air, it is the O_2 level in the permeate that is important. A lower stage cut will produce higher oxygen quality in the permeate. However, that implies a very low oxygen recovery, and most of the feed air will be lost in the residue. If the air is compressed prior to feeding the membrane unit, considerable power is also lost in the residue unless some other uses are found for this residue stream.

In the air separation example, the loss of N_2 or O_2 may not be crucial since the feed is essentially free. In separation of process streams the situation is likely to be quite different. Consider H_2 recovery from refinery streams. It would be preferable to have a very high H_2 quality in the permeate stream as well as a very high H_2 recovery (and negligible loss in the residue stream). However, both objectives may not be achievable with a membrane of moderate selectivity. An optimum has to be developed by including the cost of membrane area, the value of high quality product and the price of lost H_2 in the residue in any cost analysis.

The permeation process is also influenced strongly by the operating condi-

tions, e.g., the temperature, the feed pressure and the permeate pressure. An increase in temperature will generally increase the permeability but reduce the selectivity. However, all membrane modules have upper limits of operating temperature. The choice of temperature sometimes depends also on the presence of condensibles in the residue stream. The feed and the permeate pressures are in some cases predetermined by existing process conditions. At other times, they can be used as optimizing parameters. A higher feed pressure increases the rate of permeation, and so the required stage cut can be achieved with less membrane area. However, higher feed pressure means higher compression costs, both capital and operating. On the other hand, a low permeate pressure will also increase the permeation rate, but the permeate may have to be recompressed before it can be used further.

It is also important to recognize that high selectivity is not always economical. As the selectivity of the membrane increases, the permeate quality (the faster component mole fraction) increases. However, this, in effect, reduces the permeation driving force by increasing the faster component partial pressure in the permeate. Thus more membrane area may be required to achieve a fixed stage cut [16]. For a given range of operating variables, there is an optimum range of membrane selectivity beyond which the separation becomes cost prohibitive.

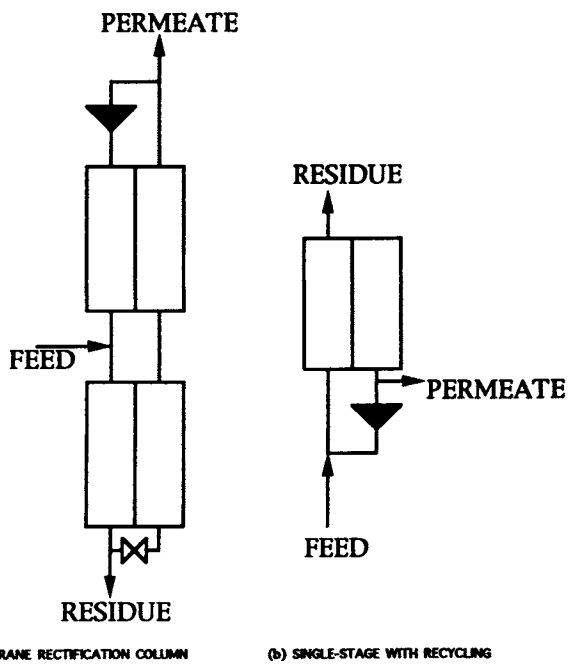

Fig. 11.3. Novel separation schemes.

These examples illustrate that there is a complex interplay between the design variables, the process variables, the system properties and the operating conditions. A number of factors have to be weighed against one another. Many process design decisions need to be based on the separation goals, and one has to do a permeation analysis before an economic assessment can be made and an optimum process can be designed.

The above discussion also suggests that in actual industrial practice, a single-stage membrane separation may often be inadequate. To achieve the target separation at the lowest possible cost, frequently a *separation scheme* needs to be configured. Staging is a classical example where the unpermeated stream from one stage is introduced (after repressurization, if necessary) as the feed to a subsequent stage. Recycling between stages is also a common practice. If a large number of stages with front and back recycling is used it may resemble a multistage distillation column [27]. Using one enricher and one stripper, Hwang and Thorman [28] introduced the novel concept of a 'continuous membrane column' or the membrane rectification column. On the other hand, a single-stage separation with partial permeate recycling has been studied by Teslik and Sirkar [29] and Majumdar et al. [30]. These two separation schemes are shown in Fig. 11.3. Comparisons between these schemes have been con-

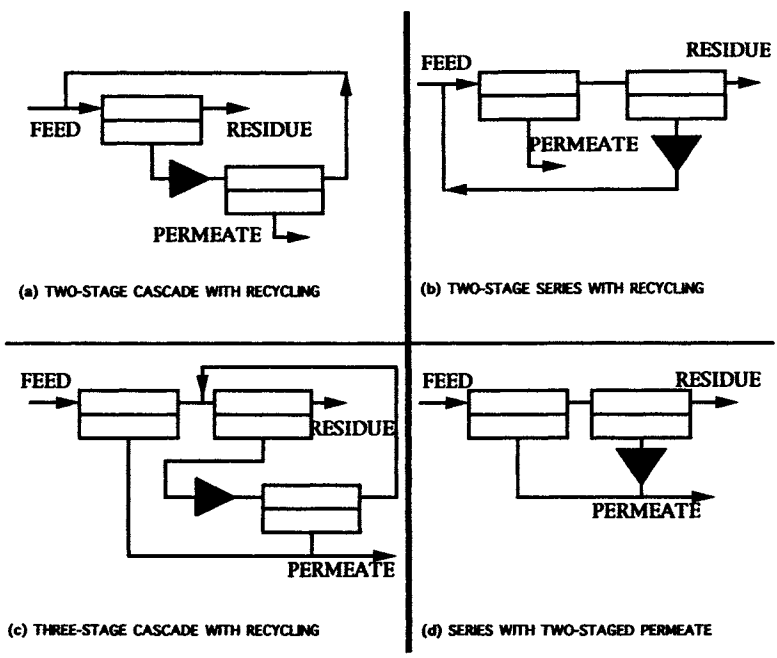

Fig. 11.4. Examples of commercial separation schemes.

sidered by Matson et al. [20], Teslik and Sirkar [29] and Qiu et al. [31].

In industrial practice, a number of variations are possible. A few examples are:

(a) two-stage cascade with recycling [32,33];
(b) two-stage series with recycling [33];
(c) three-stage cascade with recycling [32,12];
(d) series with two-staged permeates [32].

These four schemes are shown in Fig. 11.4. The extent of separation and the membrane area in each stage will depend on cost considerations. Regardless of the separation configuration, for a given stage the permeation analysis or design approach will always be the same.

11.5 IMPORTANT CONSIDERATIONS IN PERMEATION ANALYSIS

A number of aspects need to be addressed for a thorough understanding and analysis of actual membrane gas separation processes. Some of them are briefly considered below.

Membrane Selectivity vs. Stage Separation Factor

The term 'separation factor' is often used in separation analyses to characterize the extent of separation in a separator. For example, for a binary system like the one shown in Fig. 11.2a, a separation factor between the faster permeating species #1 and the slower permeating species #2 can be defined, with respect to the feed and the permeate, as

$$\alpha_{S,1-2} = [y_{1P}\, x_{2F}] / [x_{1F}\, y_{2P}] \tag{11.7}$$

The separation factor characterizes the actual overall macroscopic separation in the permeator and will depend on the stage cut. This should be distinguished from the membrane selectivity, which is normally constant irrespective of the permeator size. As pointed out in Section 11.3, the permeation rate changes along the permeator length. At a very low stage cut, the permeate quality is always the highest, and so is the separation factor. As further permeation occurs, the permeation driving force for the faster permeating species decreases. Therefore, the permeate mole fraction of the faster species and the separation factor both decrease.

For differential permeation at the inlet of the permeator, the permeate concentrations at this location are determined by the local permeation rates, i.e.,

$$\begin{aligned} y_{1P} / y_{2P} = dR_1 / dR_2 &= [Q_1(x_{1F} - \gamma\, y_{1P})] / [Q_2(x_{2F} - \gamma\, y_{2P}] \\ &= \alpha(x_{1F} - \gamma\, y_{1P}) / (x_{2F} - \gamma\, y_{2P}] \end{aligned} \tag{11.8}$$

So

$$\alpha_{S,1-2} = [y_{1P}\, x_{2F}] / [x_{1F}\, y_{2P}] = \alpha \{[1 - \gamma(y_{1P}/x_{1F})]/[1 - \gamma(y_{2P}/x_{2F})] \qquad (11.9)$$

Thus, as $\gamma \rightarrow 0$, $\alpha_{S,1-2} \rightarrow \alpha$ in this case. For any nondifferential separation with nonzero γ, the separation factor $\alpha_{S,1-2}$ will always be less than α.

Passive vs. Active Transport

The preceding analyses assumed constant gas permeabilities and considered gas permeation controlled by the partial pressures of the permeants. This is characterized as the *passive transport*. There can also be *active transport* or *facilitated transport* across the membrane in which case the total transmembrane flux is enhanced by the use of a carrier in the membrane, which complexes reversibly with the permeant. The active transport membranes can have either fixed carriers or mobile carriers [34]. The total permeant flux is the sum of the fluxes for the noncomplexed and the complexed permeants for mobile carriers. Very large facilitation can be achieved by using appropriate carriers.

The ratio of the species permeance through a membrane with carrier (Q_i) to that with no carrier (Q_{iD}) is called the facilitation factor, F_i, defined as:

$$F_i = Q_i/Q_{iD} \qquad (11.10)$$

The facilitation factor is generally a complex nonlinear function of the local feed and permeate gas phase concentrations, the carrier concentration in the membrane, and the complexation parameters. Equations (11.2a)–(11.3) are still generally valid, but the permeabilities and selectivities are only local values and will change from location to location inside the permeator module. The effective permeabilities have to be computed or estimated at each point along the permeator.

Sometimes, even for passive transport, the permeability of a species may depend on the feed pressure due to phenomena modelled as dual sorption–dual transport. Polymer plasticization by the permeant may also contribute to such a behavior [35]. Independent permeability measurements or prediction techniques over the range of feed and permeate pressures are required in these cases, and the permeability variations may have to be incorporated in the permeation analysis [36].

Module Configurations

Two configurations used in commercial modules are the spirally wound flat sheets and hollow fibers (Fig. 11.5). Spiral-wound modules are easier to make, but compared to hollow-fiber modules, they pack less membrane permeation area per unit volume, and take up more space for a given application. Also, in

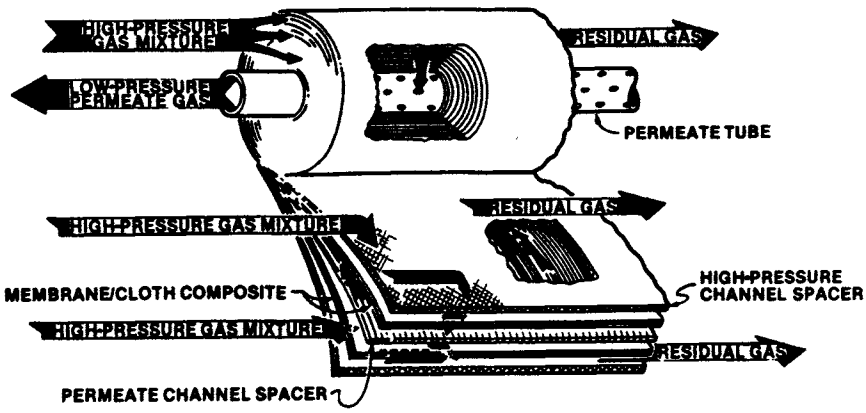

(a) SPIRALLY WOUND PERMEATOR MODULE

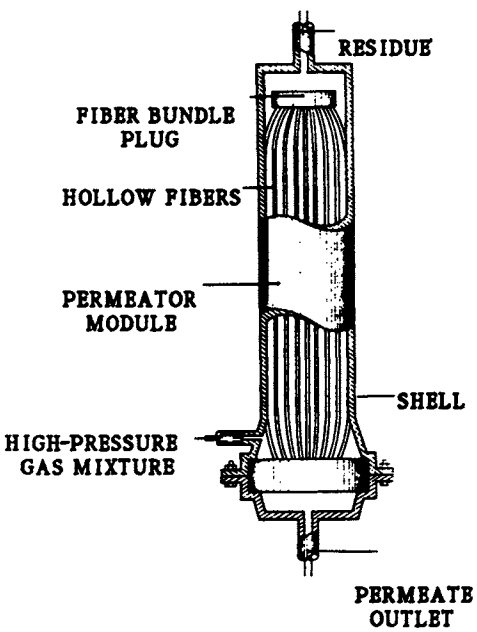

(b) HOLLOW-FIBER PERMEATOR MODULE

Fig. 11.5. Two types of commercial membrane modules.

spiral-wound modules, the membrane needs backing or support, which are not required by hollow fibers. As shown in Fig. 11.6, the flow patterns inside these

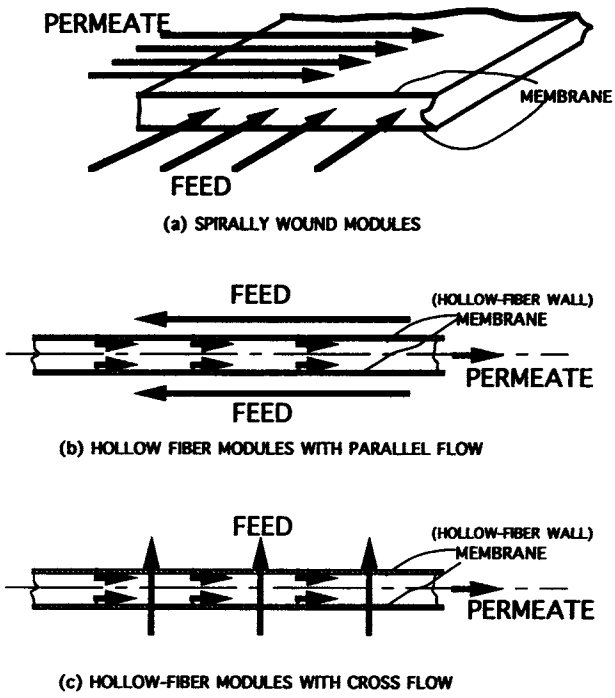

Fig. 11.6. Flow paths in various module configurations.

two classes of modules are quite different. The spiral-wound modules have skew flow. The hollow-fiber modules generally have parallel flow, but some devices also have flow perpendicular to the fiber length, or 'cross flow', as shown in Fig. 11.6.

Pressure Drop Inside the Permeator

As gas flows through the membrane modules, there would inevitably be some pressure loss in the bulk flow directions. This is because the *flow cross sections* often have to be small in order to achieve a high membrane permeation area per unit module volume (the so-called specific permeation area) leading to compact modules. Depending on the flow situation, the pressure drop can be either in the feed side and/or in the permeate side. It also depends on module geometry, e.g., the channel length and thickness for spiral wounds, the fiber diameters and the packing density for hollow fibers and the module length. Pressure drop is always detrimental to separation. If the pressure drop takes place in the feed side, the actual average feed pressure becomes less than the feed inlet pressure. If the pressure drop is in the permeate side, the actual average permeate pressure is higher than the permeate outlet pressure. In either case, the permeation driving force is reduced. The module designer has to settle

always for optimum values of module geometry parameters, which give a high specific area while avoiding excessive pressure drop.

In a hollow-fiber permeator, whether the feed will be introduced in the shell or the tube side sometimes depends on the pressure drop considerations. If the stage cut is small, it is almost always preferable to have the feed in the shell side where the pressure drop is relatively small compared to that in the fiber lumen. Conversely, for a high stage cut situation, it may be better to have the feed in the fiber lumini, since most of it will eventually permeate into the shell, and the overall cost associated with pressure drop may be less with tube-side feed.

Effect of Membrane Asymmetry

The commercial basis for membrane gas separation technology was created by the preparation of dense asymmetric membrane which had a 'skin' on one side with a backing of graded porosity underneath. However, this structure is difficult to model. In practice, it is modeled by assuming a distinct nonporous layer, which offers all the permeation resistance backed by a highly open porous structure through which there is no permeation resistance at all [37,38]. In this case, the composition inside the pores in the backing will be different from that in the bulk permeate (y' as opposed to y, Fig. 11.7). The permeate inside the porous backing is considered to be unaffected by the bulk permeate composition and unmixed with that from any adjacent layers. This composition y' is essentially controlled by the relative local permeation rates, which in turn are dictated by the local feed composition and local total pressures only:

$$dR_i = Q_i\, dA\, (P_F\, x - P_P\, y') \tag{11.11a}$$

where

$$y' = dR_i / \sum_i dR_i \tag{11.11b}$$

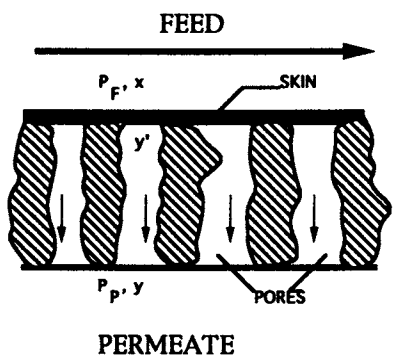

Fig. 11.7. Cross-flow model for asymmetric membranes.

The bulk permeate at any point along the permeator represents the accumulated effect of all permeation prior to that point. However, it does not affect the local permeation rate. This is called the 'cross-flow' model and should be distinguished from the cross-flow pattern inside the permeator module discussed earlier and shown in Fig. 11.6. Similar models can be used for a truly composite membrane, which has a thin, distinct selective layer backed by a nonintegral porous support. Note, however, that the above model for dense asymmetric or composite membranes is insufficient for describing the permeation if the flux is very high or the membrane is extremely thin because the permeation resistance of the porous backing starts becoming important under these situations.

Effect of Membrane Elastic Deformation

Since separation is caused by a pressure difference across the membrane, the membrane has to withstand a high transmembrane pressure differential in all practical separation problems. If the membrane is a rubber at room temperature, this pressure differential may cause significant elastic deformation in the membrane, which in turn may alter its permeance. A deformation analysis should be carried out in this case involving the elastic properties of the membrane material to properly account for this phenomenon.

Flow Patterns Inside the Permeator

The existence of the skew flow, the parallel flow and cross flow have already been identified. The parallel flow may be cocurrent, or countercurrent or even a combination of the two (Fig. 11.8). For membranes without any so-called cross-flow permeation due to an asymmetric structure, the countercurrent flow pattern will always produce better separation [39,40], much as in any other continuous-contact separation like distillation, absorption or extraction. In case of cross-flow permeation, the difference between cocurrent and countercurrent bulk flow patterns are much less pronounced [37,38]. The permeator modeling will depend on the flow pattern because the boundary conditions are different.

Gas Phase Mass Transfer Resistances

Normally, diffusion rates in gases are much higher than those in solid or liquid membranes. Therefore, it is frequently, and justifiably, assumed that there is negligible gas-phase concentration gradient in a membrane permeator [41]. However, this assumption may be erroneous in special situations where the permeation flux is very high. This is true for very thin membranes or for highly facilitated transport. In these cases the membrane resistance to mass transfer is so small that it is of the same order of magnitude as the gas-phase

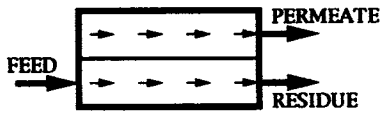

(a) COCURRENT

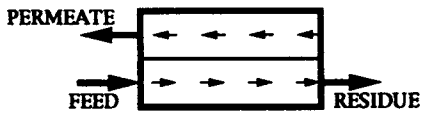

(b) COUNTERCURRENT

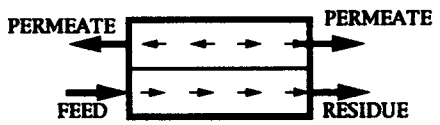

(c) COCURRENT-COUNTERCURRENT

Fig. 11.8. Possible parallel flow patterns.

mass transfer resistance on either side of the membrane. Here, the analysis and modeling becomes complicated since the effective permeance K_{iO} for species i will be controlled by the actual membrane permeability as well as the feed and permeate gas-phase film transfer coefficients k_F and k_P, respectively:

$$K_{iO} = [1/k_F + 1/k_P + t_m / P_i]^{-1} \tag{11.12}$$

The effective permeance depends now on the gas-phase flow rates, flow geometries, etc.

11.6 LITERATURE REVIEW OF PERMEATOR ANALYSIS AND DESIGN

Membrane permeation analysis, staging and permeator simulation and design issues have been addressed by various authors using a variety of structures and forms. The earliest work was done by Weller and Steiner [42,43] who analyzed membrane gas permeation of binary mixtures for two different cases: Case I for perfect mixing in both the feed and the permeate side, and Case II for no mixing. They derived analytical expressions for enrichment in a single stage in the form of permeate outlet concentration as a function of the residue concentration. Case II of their analysis was essentially what has been defined in

Section 11.5 as the cross-flow permeation.

Subsequently, the perfect mixing case was extended by Huckins and Kammermeyer [44,45] and Brubaker and Kammermeyer [46] to ternary and quaternary mixtures. Naylor and Backer [47] provided multistage enrichment calculations for gaseous diffusion separation, and derived the required number of theoretical stages using a McCabe–Thiele type graphical method. Stern et al. [48] extended the Weller and Steiner Case II calculations to a multicomponent system.

Stern and Walawender [49] and Walawender and Stern [39] established a comprehensive framework of single-stage permeator analysis and design by considering different flow patterns inside the pemeator, and identifying the effects of different key separation parameters. They also illustrated alternate approaches of using either the membrane area, or the permeate or residue composition as the independent variable. Blaisdell and Kammermeyer [40] also provided a useful approach to modeling countercurrent and cocurrent separations.

Pan and Habgood [50] derived a unified mathematical formulation for all possible flow patterns for binary mixture separation without flow pressure drop, and included cases where the feed had a nonpermeable component and the permeate had a sweep or purge gas, which could permeate back to the feed side. They also carried out a thorough parametric analysis, considering the effect of sweep gas, permeate to feed pressure ratio, variations of permeabilities and/or selectivities, etc. Pan and Habgood [51] analyzed single- and multistage permeation of a multicomponent mixture and provided a parametric analysis of the permeation cascade. Pan and Habgood [52] addressed the issues of permeate pressure drop in hollow-fiber modules, and discussed the choice of permeate pressure for optimum performance of cascades.

Antonson et al. [53] considered hollow-fiber permeators with homogeneous membranes and analyzed both tube-side feed and shell-side feed. They discussed the effects of a number of variables including broken fibers on the permeator performances. Chern et al. [36] also simulated a hollow fiber gas separator and incorporated the effect of pressure on the gas permeabilities. Rautenbach and Dahm [54] analyzed four flow patterns, e.g., completely mixed, cross flow, cocurrent and countercurrent for multicomponent gas mixture separation. Schulz [55] provided simplified performance predictions for some of the separation schemes introduced in Section 11.4.

Along with conventional permeation analysis, Stern et al. [56] and Thorman and Hwang [57] incorporated the effect of membrane deformation on separation. Pan [37,38] extended the cross-flow model for asymmetric membranes to simulate actual commercial-scale permeators employing dense-skinned cellulose acetate membranes. Chen et al. [58] incorporated axial diffusion terms in permeator analysis.

A close look at different permeation models over the last forty years reveals that analysis and design problems can be formulated in various ways depending on what the authors consider relevant and important. As the simulation objectives differ, so do the methods of solving the resulting equations. The two main problem classifications are, of course, the rating and the design. In the former, one considers a permeator device or module of known dimensions and permeation area. The module is used to separate a feed-gas mixture at a known flow rate and composition. The goal of the analysis would be to predict the performance of this module in terms of the residue composition, the permeate composition and the stage cut. The independent variable in this case would be simply the membrane area.

On the other hand, in the design problem, the goal is to calculate the total membrane permeation area required for a desired extent of separation. One may wish to calculate the area required to achieve a certain mole fraction of the faster permeating component in the residue. This is a purification problem where the product of interest in the separation step is the residue. Alternately, one may wish to calculate the area required to achieve a certain permeate quality, i.e., the faster component mole fraction. This is the so-called recovery problem where the product is the permeate. The two design problems need to be formulated differently.

In both design problems the goal is to calculate the total area. However, the area in turn depends on the module geometry. If the number of hollow fibers (for hollow-fiber modules) or the number of permeate channels (for spiral-wound modules) is fixed based on module manufacturing considerations, one has to calculate the module length. Conversely, if the module length is fixed from other design considerations, one needs to calculate the number of fibers or the number of channels (or the number of windings in case of spiral-wound modules) required. If commercially available permeator modules are of fixed length and total area, the design calculation goal would be to determine the total number of modules to be used in series or in parallel configuration.

11.7 COMPLETELY MIXED FLOW FOR A MULTICOMPONENT SYSTEM

In this section permeator analysis will be introduced by considering the simplest possible scenario, i.e., a permeator where the gas phases on either side of the membrane are completely mixed. As a result, there are no spatial gradients of concentrations, and only algebraic equations need to be solved. Examples of such a permeator used in practice would be rare, possible exceptions being small membrane modules used as diagnostic tools or sensors. However, this analysis provides a baseline for more complex ones introduced later.

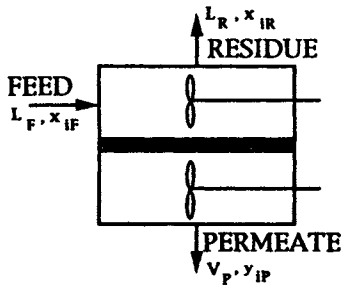

Fig. 11.9. A membrane module with completely mixed flow.

Figure 11.9 depicts a mixed-flow situation inside a permeator module for a general multicomponent gas mixture. The mole fraction of component i on the feed side of the membrane is constant throughout the module and is the same as the residue mole fraction x_{iR}. This assumption is analogous to that used commonly for the continuous-flow stirred tank reactor (CSTR) in reactor design. Similarly, the mole fraction on the permeate side is constant, and the same as the permeate outlet composition. The total membrane area is A_T, and the feed and permeate pressures, P_F and P_P, are constant.

In case of a multicomponent feed mixture containing n species, individual component balances have to be addressed. Unlike the binary system, no single selectivity term can be defined here. One possible approach would be to use a reference component with respect to which the selectivities of the other components can be defined as follows:

$$\alpha_i = Q_i / Q_{Ref} \tag{11.13}$$

A component balance on i can be written as:

$$L_F\, x_{iF} - L_R\, x_{iR} = V_P\, y_{iP} = Q_i\, A_T [P_F\, x_{iR} - P_P\, y_{iP}],\ i=1,2,...n \tag{11.14}$$

Summing up Eq. (11.14) for components 1 through n, one can get

$$L_F - L_R = V_P = Q_{Ref}\, A_T\, P_F \left[\sum_i \alpha_i x_{iR} - \gamma \sum_i \alpha_i y_{iP} \right] \tag{11.15a}$$

$$= A_T^*\, L_F \left[\sum_i \alpha_i x_{1R} - \gamma \sum_i \alpha_i y_{iP} \right]$$

or

$$1 - L_R/L_F = V_P/L_F = A_T^* \left[\sum_i \alpha_i x_{1R} - \gamma \sum_i \alpha_1 y_{iP} \right] \tag{11.15b}$$

where

$$\alpha_i = Q_i/Q_{Ref}\,, \quad \text{and} \quad A_T^* = Q_{Ref}\, A_T\, P_F\, /L_F \tag{11.16}$$

Eliminating L_R from Eqs. (11.14) and (11.15a) one can write

$$x_{iF} - x_{iR} = A_T^* \left[\alpha_i (x_{iR} - \gamma\, y_{iP}) - x_{iR} \left\{ \sum_i \alpha_i x_{iR} - \gamma \sum_i \alpha_i y_{iP} \right\} \right] \qquad i = 1,2,\ldots(n-1) \tag{11.17}$$

The quantities y_{iP} are obtained directly from Eqs. (11.14) and (11.15a):

$$y_{iP} = \alpha_i [x_{iR} - \gamma\, y_{iP}] \Big/ \left[\sum_i \alpha_i x_{iR} - \gamma \sum_i \alpha_i y_{iP} \right]; i = 1,2,\ldots(n-1) \tag{11.18}$$

Only $(n-1)$ components are considered in Eqs. (11.17) and (11.18) since the sum of the mole fractions is always 1.0 and the reference component balance is not needed.

Equations (11.15b), (11.17) and (11.18) are $(2n-1)$ algebraic equations to be solved simultaneously for $(n-1)$ $x_i - s$, $(n-1)$ y_i–s, and L_R. The solution would directly provide the residue mole fractions, the permeate mole fractions, and would also allow the calculation of the stage cut, i.e., V_P/L_F.

11.8 COMMON ASSUMPTIONS IN ANALYSIS AND DESIGN

Some of the common assumptions employed in membrane gas separation analysis in hollow-fiber modules are listed below:

1. Concentration gradients in the gas phase at any cross section of the module are negligible for permeators not having a bulk cross-flow pattern. Hence, only the concentration changes *along* the permeator need to be considered.
2. Flows are evenly distributed. The so-called 'end effects' resulting from flow direction change, undeveloped velocity profiles, etc., are negligible.
3. Permeance of each species is constant for the given range of operating conditions.
4. There is negligible pressure drop on the shell side of the module.
5. Pressure drop inside the fiber lumen can be described using the Hagen–Poiseuille equation, i.e., the flow is always laminar.
6. Gas viscosities are independent of pressure.
7. The membrane does not undergo any physical deformation.

For spirally wound permeators the following assumptions are commonly used:

1. The feed phase concentration varies along the permeator axis, and the permeate phase concentration varies along the permeator axis as well as along

the length of the membrane leaf. There is no concentration gradient perpendicular to the membrane surface.

2. There is no end effect.

3. Permeance of each species is constant for the given range of the operating conditions.

4. Feed-side pressure drop is negligible. On the permeate side there is pressure drop along the length of the membrane leaf, which can be described by equations governing pressure drop in a channel with spacer screens. There is no pressure variation in any cross section of the membrane leaf.

5. Gas viscosities are independent of pressure.

6. The membrane does not undergo any physical deformation.

11.9 HOLLOW-FIBER PERMEATORS FOR BINARY SYSTEM

A simple rating problem is considered first. Let there be a hollow-fiber permeator of given length containing a given number of fibers with known inside and outside diameters. Assume that the fibers are plugged at one end, and the permeate is collected at the other end of the module. A feed-gas mixture of known flow rate, pressure and composition is introduced to the shell side of this module from one end. The objective is to set up a modeling framework to predict how much of the feed gas will permeate through the membrane, and what would be the residue and the permeate compositions and flow rates.

Assume initially that the membrane is homogeneous (i.e., no cross-flow permeation). The flow pattern inside the module can be cocurrent or countercurrent, as shown in Fig. 11.10. *Under cocurrent flow condition* (Fig. 11.10a), a component material balance for the faster permeating species (identified here as species #1, i.e. $i = 1$) over a differential permeator length dz can be written as:

$$-\mathrm{d}[Lx] = Q_1 (\pi D_{LM} \, \mathrm{dz} \, N_T) (P_F x - P_P y) = \mathrm{d}(Vy] \tag{11.19}$$

Here D_{LM} is the logarithmic mean of the fiber's inside and outside diameters and N_T is the total number of hollow fibers. Based on a diffusion analysis in the tubular homogeneous membrane it can be shown that D_{LM}, rather than the inside or outside diameters, should appear in the permeation equation (much as in case of heat conduction across cylindrical tubes).

A similar material balance for the slower permeating component ($i = 2$) can be written as:

$$-\mathrm{d}[L(1-x)] = Q_2(\pi D_{LM} \, \mathrm{dz} \, N_T) [P_P(1-x) - P_P(1-y)] = \mathrm{d}[V(1-y)] \tag{11.20}$$

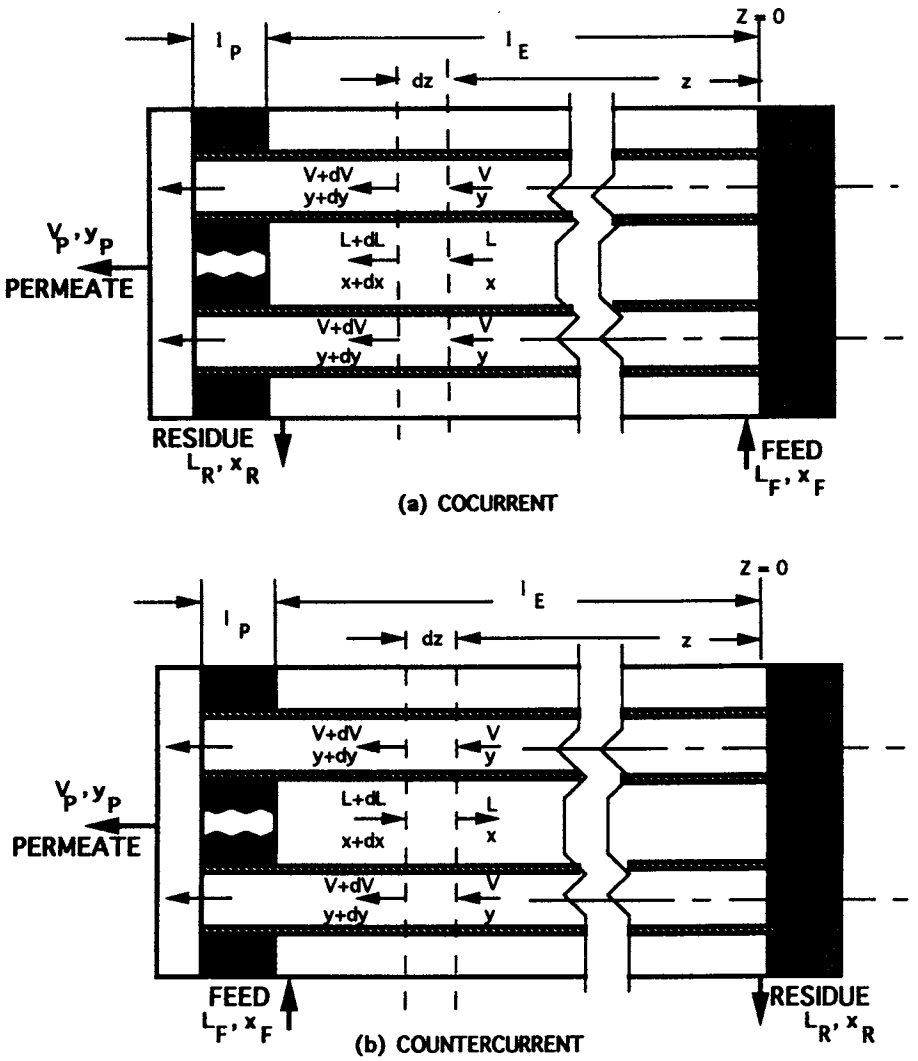

Fig. 11.10. Differential mass balance for shell-side feed in hollow-fiber permeators.

Since the feed is in the shell side, P_F can be assumed to be constant. The permeate pressure will change, however, and a pressure drop equation can be written as:

$$dP_P / dz = -128\mu\, q/(\pi D_i^4 N_T) \tag{11.21}$$

where q is the actual volumetric flow rate on the permeate side at any axial location. It can be related to the local molar permeate flow rate V using ideal gas law:

$$q = R_g\, T\, V/P_P \tag{11.22}$$

Equations (11.21) and (11.22) can be combined to:

$$dP_P^2/dz = -256\,\mu\,R_g\,T\,V/(\pi\,D_i^4\,N_T) \tag{11.23}$$

It is preferable to make the above equations dimensionless. The following definitions are normally used:

$$\alpha = Q_1/Q_2\,;\ \gamma = P_P/P_F\,; \tag{11.24a}$$

$$z^* = z/l_E\,;\ L^* = L/L_F\,;\ V^* = V/L_F\,; \tag{11.24b}$$

$$K_1 = \pi\,D_{LM}\,l_E\,N_T\,P_F\,Q_2/L_F\,; \tag{11.24c}$$

$$K_2 = 128\,\mu\,R_g\,T\,l_E\,L_F/(\pi\,D_i^4\,N_T\,P_F^2) \tag{11.24d}$$

Equations (11.19), (11.20) and (11.23) can, therefore, be rewritten as:

$$-d[L^*x]/dz^* = K_1\,\alpha(x - \gamma y) = d[V^*y]/dz^* \tag{11.25}$$

$$-d[L^*(1-x)]/dz^* = K_1[(1-x) - \gamma(1-y)] = d[V^*(1-y)]/dz^* \tag{11.26}$$

$$d\gamma/dz^* = -K_2\,V^*/\gamma \tag{11.27}$$

Adding up Eqs. (11.25) and (11.26) leads to

$$-dL^*/dz^* = K_1[\alpha(x - \gamma y) + \{(1-x) - \gamma(1-y)\}] = dV^*/dz^* \tag{11.28}$$

An overall material balance would relate L^* and V^* at every axial location inside the permeator module:

$$L_F = L + V \tag{11.29a}$$

or,

$$L^* = 1 - V^* \tag{11.29b}$$

Based on the following identities

$$dx/dz^* = [d\{L^*x\}/dz^* - x\,dL^*/dz^*]\ /\ L^* \tag{11.30a}$$

and

$$dy/dz^* = [d\{V^*y\}/dz^* - y\,dV^*/dz^*]\ /\ V^* \tag{11.30b}$$

one can formulate a set of four differential equations involving x, y, V^* and γ which will conveniently describe the permeation process. The equations are listed in Table 11.2.

In order to describe the problem completely, the boundary conditions need to be specified. For x and V^*, these are straightforward:

$$\text{at } z^* = 0,\ x = x_F; \tag{11.31a}$$

TABLE 11.2

Governing equations for hollow-fiber permeators: binary system and shell-side feed

Cocurrent flow:

$$dx/dz^* = -K_1[\alpha(1-x)(x-\gamma y) - x\{(1-x)-\gamma(1-y)\}]/(1-V^*)$$

$$dy/dz^* = K_1[\alpha(1-y)(x-\gamma y) - y\{(1-x)-\gamma(1-y)\}]/V^*$$

$$dV^*/dz^* = K_1[\alpha(x-\gamma y) + \{(1-x)-\gamma(1-y)\}]$$

$$d\gamma/dz^* = -K_2\, V^*/\gamma$$

Boundary conditions: at $z^* = 0$, $x = x_F$; $y = \phi_1(x,\gamma)$; $V^* = 0$
at $z^* = 1$, $\gamma = \phi_2(\gamma_o, V^*)$

Countercurrent flow:

$$dx/dz^* = K_1[\alpha(1-x)(x-\gamma y) - x\{(1-x)-\gamma(1-y)\}]/L^*$$

$$dy/dz^* = K_1[\alpha(1-y)(x-\gamma y) - y\{(1-x)-\gamma(1-y)\}]/V^*$$

$$dV^*/dz^* = K_1[\alpha(x-\gamma y) + \{(1-x)-\gamma(1-y)\}]$$

$$dL^*/dz^* = K_1[\alpha(x-\gamma y) + \{(1-x)-\gamma(1-y)\}]$$

$$d\gamma/dz^* = -K_2\, V^*/\gamma$$

Boundary conditions: at $z^* = 0$, $y = \phi_1(x,\gamma)$; and $V^* = 0$
at $z^* = 1$, $\gamma = \phi_2(\gamma_o, V^*)$, $x = x_F$; and $L^* = 1$

Here $K_1 = \pi D_{LM} l_E N_T P_F Q_2 / L_F$, $K_2 = 128\,\mu R_g T l_E L_F/(\pi D_i^4 N_T P_F^2)$ and ϕ_1 and ϕ_2 are functionalities described by Eqs. (11.32) and (11.31c), respectively.

$$V^* = 0 \tag{11.31b}$$

For γ and y the boundary conditions are more complicated. The permeate outlet pressure is a given quantity, designated by γ_o ($= P_{Po}/P_F$). There would be some pressure drop along the potted section of the hollow fiber. The correct boundary condition would, therefore, be:

$$\text{at } z^* = 1,\ \gamma = [\gamma_o^2 + 2\,K_2\,V^*\,l_P/l_E]^{1/2} = \phi_2\,(V^*) \tag{11.31c}$$

Note that this is a coupled boundary condition, since V^* is not known *a priori* at $z^* = 1$.

The value of y at the plugged end of the hollow fibers will be determined by the local relative rates of permeation, i.e.

$$\text{at } z^* = 0,\ y = \{d[Vy]/dz\}/\{dV/dz\} = \{d[V^*y]/dz^*\}/\{dV^*/dz^*\}$$

or,

$$\text{at } z^* = 0,\ y = \alpha(x-\gamma y)/[\alpha(x-\gamma y) + \{(1-x)-\gamma(1-y)\}] \tag{11.31d}$$

The above is a quadratic in y, which can be solved to calculate y at $z^* = 0$ as a function of x and γ at $z^* = 0$. The solution is

$$y = \{1 + (\alpha-1)(x_F + \gamma) - [\{1 + (\alpha-1)(x_F + \gamma)\}^2 - 4\alpha(\alpha-1)\gamma x_F]^{1/2}\}/\{2(\alpha-1)\gamma\}$$
$$= \phi_1(x_F, \gamma) \tag{11.32}$$

Note that γ is not known at $z^* = 0$. Thus, we need to solve a split boundary value problem here. At the feed end, two explicit conditions and one coupled condition are specified, whereas at the residue end, one coupled condition is specified. The solution of the above set of equations would provide us with the following quantities of interest: (a) V^* at $z^* = 1$, which is the stage cut; (b) x and y at $z^* = 1$, which are the residue and permeate mole fractions of the faster component; and (c) γ at $z^* = 0$, which indicates the extent of permeate pressure buildup inside the fiber lumen.

For the countercurrent flow condition, shown in Fig. 11.10b, the governing equations can be set up in a similar manner with a few changes. The integration is still carried out from the closed fiber end. The differential equation for y, V^* and γ in this case are identical to those for cocurrent; only the equation for x has an opposite sign. The material balance is necessarily different, and Eqs. (11.29a) and (11.29b) may be replaced by:

$$L = V + L_R = V + L_F - V_P \tag{11.33a}$$

or,

$$L^* = V^* + L_R^* = V^* + 1 - V_P^* \tag{11.33b}$$

Since L_R^* and V_P^* are not known *a priori,* it is advisable not to express L^* in terms of these quantities. Instead, it is preferable to include L^* as an extra variable like V^*. The governing equations and the boundary conditions are listed in Table 11.2.

Because $V^* = 0$ at $z^* = 0$, the differential equation for y becomes indeterminate at that location for either flow pattern. It is necessary to employ L'Hospital rule in this case. Thus, at $z^* = 0$,

$$dy/dz^* = K_1[d/dz^*[\alpha(1-y)(x-\gamma y) - y\{1-x) - \gamma(1-y)\}]]/[dV^*/dz^*] \tag{11.34a}$$

The above equation can be rearranged as

$$\frac{dy}{dz^*} = \frac{[\alpha - (\alpha-1)\,y]\,dx/dz^*}{2\{\alpha(x - \gamma y) + (1 - x) - \gamma(1-y)\} + \gamma[\alpha - (\alpha-1)\,y]} \tag{11.34b}$$

The dimensionless constants K_1 and K_2 incorporate all the system parameters and operating variables. For a given rating problem with given pressures, flow

rates and module dimensions, K_1 and K_2 have unique values. However, a single set of K_1 and K_2 actually represents a family of solutions, since there are numerous possible combinations of the parameters that may yield the same values of K_1 and K_2. This is the advantage of making the equations dimensionless.

If the viscosities of the individual gaseous components are markedly different and if there is significant composition change along the permeator, the gas mixture viscosity, used in evaluating K_2, may change appreciably. The best way to handle this is to express mixture viscosity as a function of pure component viscosities and the mixture composition [59]. A sample expression is given below for an n-component mixture:

$$\mu_{\text{mixture}} = \sum_i y_i \mu_i \left(\sum_j \delta_{ij} y_j \right) \tag{11.35a}$$

where

$$\delta_{ij} = \frac{\left[1 + (\mu_i/\mu_j)^{1/2} (M_{wj}/M_{wi})^{1/4}\right]^2}{\left[8(1 + M_{wi}/M_{wj})\right]^{1/2}} \tag{11.35b}$$

In the above case, the dimensionless constant K_2 should be defined for the viscosity at a reference composition, e.g., the feed composition. In the governing equations, K_2 should then be replaced by a product of (a) K_2 defined at reference composition, and (b) the ratio of actual viscosity to the reference viscosity.

The analysis so far was restricted to the basic configuration of shell-side feed with homogeneous hollow-fiber membranes. The effects of some variations on the governing equations are discussed next.

Tube Side Feed

In this case the feed pressure P_F would decrease as the feed flows through the hollow fibers (Fig. 11.11). However, the permeate pressure can be taken as a constant. The following modifications are required in the governing equations. The dimensionless constants K_1 and K_2 and other variables should be defined using P_{Fi}, the feed inlet pressure, instead of P_F

$$\gamma = P_P/P_{FI}\,; \quad K_1 = \pi\, D_{LM}\, l_E\, N_T\, P_{FI}\, Q_2/L_F\,;$$

and

$$K_2 = 128\, \mu\, R_g\, T\, l_E\, L_F\, /\, (\pi\, D_i^4\, N_T\, P_{FI}^2) \tag{11.36}$$

The quantity γ now becomes a constant, and should be replaced by γ_o, based on outlet permeate pressure P_{Po}. A new dimensionless feed pressure, β, should preferably be defined as

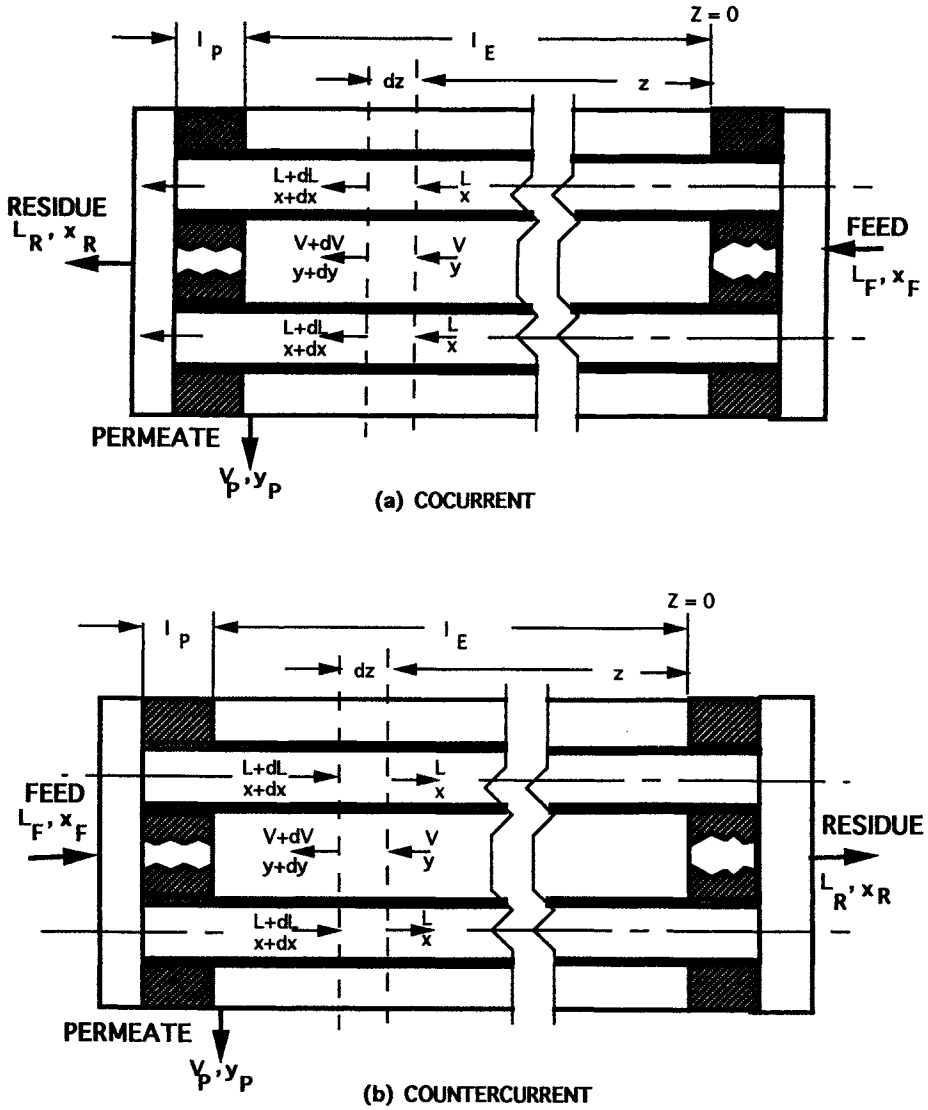

Fig. 11.11. Differential mass balance for tube-side feed in hollow-fiber permeator.

$$\beta = P_F/P_{Fi} \tag{11.37}$$

The governing equations will now incorporate the change of β, instead of γ, with length. Table 11.3 shows the dimensionless differential equations for tube-side feed, as well as the modified boundary conditions. Note that under cocurrent flow conditions, this becomes an initial value problem, unlike the case with shell-side feed.

TABLE 11.3

Governing equations for hollow-fiber permeators: binary system and tube-side feed

Cocurrent flow:

$$dx/dz^* = -K_1\left[\alpha(1-x)(\beta x - \gamma_o y) - x\{\beta(1-x) - \gamma_o(1-y)\}\right]/L^*$$

$$dy/dz^* = K_1\left[\alpha(1-y)(\beta x - \gamma_o y) - y\{\beta(1-x) - \gamma_o(1-y)\}\right]/(1-L^*)$$

$$dL^*/dz^* = -K_1\left[\alpha(\beta x - \gamma_o y) + \{\beta(1-x) - \gamma_o(1-y)\}\right]$$

$$d\beta/dz^* = -K_2\, L^*/\beta$$

Boundary conditions: at $z^* = 0$, $x = x_F$; $y = \phi_1(x_F, \gamma')$; $L^* = 1$; $\beta = [1 - 2\,K_2\,(l_P/l_E)]^{1/2}$

where $\gamma' = \gamma_o/\beta$

Countercurrent flow:

$$dx/dz^* = K_1\left[\alpha(1-x)(\beta x - \gamma_o y) - x\{\beta(1-x) - \gamma_o(1-y)\}\right]/L^*$$

$$dy/dz^* = K_1\left[\alpha(1-y)(\beta x - \gamma_o y) - y\{\beta(1-x) - \gamma_o(1-y)\}\right]/V^*$$

$$dL^*/dz^* = K_1\left[\alpha(\beta x - \gamma_o y) + \{\beta(1-x) - \gamma_o(1-y)\}\right]$$

$$dV^*/dz^* = K_1\left[\alpha(\beta x - \gamma_o y) + \{\beta(1-x) - \gamma_o(1-y)\}\right]$$

$$d\beta/dz^* = K_2\, L^*/\beta$$

Boundary conditions: at $z^* = 0$, $y = \phi_1(x, \gamma_o)$; and $V^* = 0$

at $z^* = 1$, $\beta = [1 - 2\,K_2\,(l_P/l_E)]^{1/2}$; $x = x_F$; and $L^* = 1$

Here $K_1 = \pi\, D_{LM}\, l_E\, N_T\, P_{Fi}\, Q_2/L_F$, $K_2 = 128\,\mu\, R_g\, T\, l_E\, L_F/(\pi\, D_i^4\, N_T\, P_{Fi}^2)$, and ϕ_1 is a function defined by Eq. (11.32) in the text.

Asymmetric Membrane

Since the bulk permeate composition and the composition of the local permeate emerging from an asymmetric membrane are not identical, there would be some minor changes in the governing equations. Table 11.4 shows the equations for an asymmetric membrane. Note that K_1 is defined with D_o instead of D_{LM}. Here we assume that the selective skin is on the outside surface of the hollow fiber. If the skin is on the inside, D_i would be used instead. Equations are given for the shell-side feed (Fig. 11.10) and the tube-side feed (Fig. 11.11), both for a countercurrent flow pattern only.

Elastic Deformation of Membrane

When the hollow fiber gets deformed under outside or inside pressure due to the elastic nature of the membrane material, the permeation analysis is more involved [56]. An example is considered here. The measured inside and outside

TABLE 11.4

Governing equations for asymmetric hollow fiber: binary system and countercurrent flow

Shell-side feed

$$dx/dz^* = K_1[\alpha(1-x)(x-\gamma y') - x\{(1-x)-\gamma(1-y')\}]\ /L^*$$

$$dy/dz^* = K_1[\alpha(1-y)(x-\gamma y') - y\{(1-x)-\gamma(1-y')\}]\ /V^*$$

$$dV^*/dz^* = K_1[\alpha(x-\gamma y') + \{(1-x)-\gamma(1-y')\}]$$

$$dL^*/dz^* = K_1[\alpha(x-\gamma y') + \{(1-x)-\gamma(1-y')\}]$$

$$d\gamma/dz^* = -K_2\ V^*/\gamma$$

Boundary conditions: at $z^* = 0$, $y = \phi_1(x,\gamma)$; and $V^* = 0$

$$\text{at } z^* = 1,\ \gamma = \phi_2(\gamma_o,\ V^*),\ x = x_F;\ \text{and } L^* = 1$$

Here $K_1 = \pi\ D_o\ l_E\ N_T\ P_F\ Q_2/L_F$, and $K_2 = 128\ \mu\ R_g\ T\ l_E\ L_F/(\pi\ D_i^4\ N_T\ P_F^2)$

Tube-side feed

$$dx/dz^* = K_1\Big[\alpha(1-x)(\beta x-\gamma_o y') - x\{\beta(1-x)-\gamma_o(1-y')\}\Big]/L^*$$

$$dy/dz^* = K_1\Big[\alpha(1-y)(\beta x-\gamma_o y') - y\{\beta(1-x)-\gamma_o(1-y')\}\Big]/V^*$$

$$dL^*/dz^* = K_1\Big[\alpha(\beta x-\gamma_o y') + \{\beta(1-x)-\gamma_o(1-y')\}\Big]$$

$$dV^*/dz^* = K_1\Big[\alpha(\beta x-\gamma_o y') + \{\beta(1-x)-\gamma_o(1-y')\}\Big]$$

$$d\beta/dz^* = K_2\ L^*/\beta$$

Boundary conditions: at $z^* = 0$, $y = \phi_1(x,\gamma)$; and $V^* = 0$

$$\text{at } z^* = 1,\ \beta = [1 - 2\ K_2\ l_P/l_E]^{1/2};\ x = x_F;\ \text{and } L^* = 1$$

Here $K_1 = \pi\ D_o\ l_E\ N_T\ P_{Fi}\ Q_2/L_F$, and $K_2 = 128\ \mu\ R_g\ T\ l_E\ L_F/(\pi\ D_i^4\ N_T\ P_{Fi}^2)$

In this Table, y' is given at every point as $y' = \phi_1(x,\gamma)$, and ϕ_1 and ϕ_2 are functionalities defined by Eqs. (11.32) and (11.31c) in the text.

diameters in the unstressed condition, D_i and D_o are going to be different from the actual diameters during permeation under pressure, D_i' and D_o'. The fiber would either contract or expand depending on whether the high-pressure feed is outside or inside of the fiber. A stress-strain analysis for elastic materials can be applied here to calculate D_i' and D_o' for any outside and inside pressure. The analysis is facilitated by using dimensionless contraction ratios, ε_i and ε_o, defined as

$$\varepsilon_i = D_i'/D_i\ ; \qquad \varepsilon_o = D_o'/D_o \tag{11.38}$$

and a elastic deformation factor ζ, defined as

$$\zeta = [\ln (D_o/D_i)]\ /\ [\ln (D_o'/D_i')] = \ln (\eta)\ /\ \ln [\eta\ \varepsilon_i\ /\ \varepsilon_o] \tag{11.39}$$

where

$$\eta = D_i / D_o \tag{11.40}$$

Table 11.5 shows the differential equations for the case of elastic deformation. Only a countercurrent flow pattern and a shell-side feed have been considered.

TABLE 11.5

Governing equations for hollow fibers under elastic deformation: binary system, countercurrent flow and shell-side feed

---

$dx/dz^* = \zeta K_1[\alpha(1-x)(x-\gamma y) - x\{(1-x) - \gamma(1-y)\}] / L^*$

$dy/dz^* = \zeta K_1[\alpha(1-y)(x-\gamma y) - y\{(1-x) - \gamma(1-y)\}] / V^*$

$dV^*/dz^* = \zeta K_1[\alpha(x-\gamma y) + \{(1-x) - \gamma(1-y)\}]$

$dL^*/dz^* = \zeta K_1[\alpha(x-\gamma y) + \{(1-x) - \gamma(1-y)\}]$

$d\gamma/dz^* = K_2[\lambda_1/\lambda_2 + 1]\ V^*/\gamma + [K_3\ V^*/\gamma - (\varepsilon_i^4/K_2)(\gamma/V^*)]^{-1}$

Boundary conditions: at $z^* = 0$, $y = \phi_1(x,\gamma)$; and $V^* = 0$

at $z^* = 1$, $\gamma = \phi_2(\gamma_o, V^*)$, $x = x_F$; and $L^* = 1$

ϕ_1 and ϕ_2 are functionalities described by Eqs. (11.32) and (11.31c).

Here: $K_1 = \pi\ D_{LM}\ l_E\ N_T\ P_F\ Q_2/L_F$

$K_2 = 128\ \mu\ R_g\ T\ l_E\ L_F/(\pi\ D_i^4\ N_T\ P_F^2)$

$K_3 = L_F\ M_{W,avg}/(6\ \pi\ l_E\ \mu\ N_T)$

$\lambda_1 = 8(-1.0 - 0.75\ Re_w + 0.0407\ Re_w^2)$

$\lambda_2 = 8(1.0 - 0.056\ Re_w + 0.0154\ Re_w^2)$

$Re_w = [V^*(M_{w1} - M_{w2})\ dy/dz^* + M_{w,avg}\ dV^*/dz^*]\ [L_F/2\ \pi\ N_T\ \mu\ l_E]$

M_{w1}, M_{w2} and $M_{w,avg}$ are molecular weights of component 1, 2 and the average.

The quantity ζ is calculated at each location as follows: first, the following two algebraic equations are solved simultaneously for ε_i and ε_o

$$\gamma = P_A/P_F - 2\ \Gamma/3\ [\chi/\varepsilon_i - \chi^{-1}]$$

$$1 = P_A/P_F - 2\ \Gamma/3\ [\chi/\varepsilon_o - \chi^{-1}]$$

where P_A is the atmospheric pressure, $\Gamma = Y_M/P_F$ where Y_M is the Young's modulus for the elastic material under consideration, $\chi = [\varepsilon_o^2 - \eta^2\ \varepsilon_i^2]/[1 - \eta^2]$, and $\eta = D_i/D_o$

From ε_i and ε_o, ζ is calculated: $\zeta = \ln(\eta) / \ln[\eta\ \varepsilon_i / \varepsilon_o]$

11.10 SPIRALLY WOUND PERMEATORS FOR BINARY SYSTEM

Figure 11.12 shows an unwound membrane leaf from a spirally wound membrane permeator. There are two membrane sheets in the leaf, and permeation occurs from both sides into the leaf. The permeation analysis is more complicated here since the local feed composition and the local permeate composition vary both along the module axis (l-direction) and the length of the leaf (w-direction). The feed composition profile (x vs l) itself would depend on w.

Pan [37] has carried out a useful analysis of permeation in spirally wound modules assuming the membrane to be asymmetric. The approach is described here with appropriate changes in notation. A new quantity u, the feed gas flow rate per unit membrane leaf length, is used in the analysis. The component balances on the feed side along the module axis at any w-location can be described as:

$$[\delta(ux)/\delta l]_w = -2\, Q_1(P_F x - P_P y') \tag{11.41}$$

$$[\delta\{u(1-x)\}/\delta l]_w = -2\, Q_2\{P_F(1-x) - P_P(1-y')\} \tag{11.42}$$

The factor 2 appears in the above equations since each feed channel is exposed to two membranes. On the permeate side, the pressure P_P is always assumed to depend only on w, and not on l. It is also preferable to define a local permeate flow rate V_a and a local permeate mole fraction y_a, which are essentially averaged over the l-dimension, and therefore change only in the w-direction. The differentials of V_a, y_a and P_P can be expressed as:

$$dV_a/dw = u_F - u_R \tag{11.43}$$

$$d(V_a y_a)/dw = u_F x_F - u_R x_R \tag{11.44}$$

$$d(P_P^2)/dw = -2\, R_g\, T\, \mu\, V_a/(l_T\, t_L\, B) \tag{11.45}$$

The last equation is equivalent to Darcy's law, and B is the flow coefficient of the permeate channel with spacer screen. The quantities u_R and x_R are them-

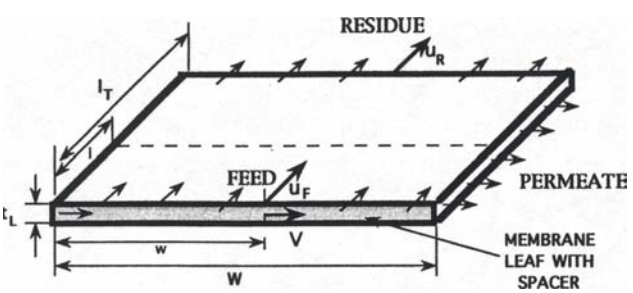

Fig. 11.12. Mass balance in spirally wound permeators.

selves functions of w. The above equations can be made dimensionless as follows:

$$dV_a^*/dw^* = 1 - u_R/u_F \tag{11.46}$$

$$d(V_a^* y_a)/dw^* = x_F - x_R(u_R/u_F) \tag{11.47}$$

$$d\gamma_2/dw^* = -K_S V_a^* \tag{11.48}$$

where

$$V_a^* = V_a/L_F;\ w^* = w/W;\ \gamma = P_P/P_F$$

and

$$K_S = 2 R_g T \mu W L_F/(l_T t_L B P_F^2) \tag{11.49}$$

Since P_P is a constant along l, Eqs. (11.41) and (11.42) can be integrated along l. For cross-flow permeation across the membrane, the following equation has been derived [37] to relate local u_R and x_R:

$$1 - u_R/u_F = (y_R'/y_F')^a [(1 - y_R')/(1 - y_F')]^b [\alpha - (\alpha - 1)y_R'] / [\alpha - (\alpha - 1) y_F'] \tag{11.50a}$$

where

$$a = [\gamma(\alpha - 1) + 1] / [(\alpha - 1)(1 - \gamma)] \tag{11.50b}$$

$$b = [\gamma(\alpha - 1) - \alpha] / [(\alpha - 1)(1 - \gamma)] \tag{11.50c}$$

and

$$2 l_T Q_2 (P_F/u_F)\, \alpha(1 - \gamma) = \alpha - (\alpha - 1)y_F' - \{\alpha - (\alpha - 1)y_R'\}(u_R/u_F) - (\alpha - 1) \int_{y_F'}^{y_R'} (u/u_F)\, dy' \tag{11.51}$$

Here, y_F' and y_R' are functions of x_F and x_R, respectively, given by the functionality of Eq. (11.32). Equations (11.50a) and (11.51) can be solved for u_R and x_R for a given γ. Equations (11.46) through (11.48) constitute the main governing equations for V_a^*, $(V_a^* y_a)$ and γ. These are to be solved at each location in conjunction with Eqs. (11.50a) and (11.51). The boundary conditions are:

$$\text{at } w^* = 0,\ V_a^* = 0, \text{ and } (V_a^* y_a) = 0$$

$$\text{at } w^* = 1,\ \gamma = \gamma_o \tag{11.52}$$

11.11 DESIGN APPROACHES FOR HOLLOW-FIBER PERMEATORS

The permeator design involves the calculation of the membrane area required for a given extent of separation. As discussed before, for a feed of given composition, the extent of separation can be defined with respect to either a specified residue composition, or a specified permeate composition. In mathematical terms, this means that the independent variable would be x or y, respectively. Unlike the rating problem, the preferred approach here would be to use a dimensionless area A^*, defined as

$$A^* = \pi D_{LM} z N_T P_F Q_2/L_F = K_1 z^* \tag{11.53}$$

If the membrane is asymmetric, with the skin on the outside, D_{LM} should be replaced by D_o. When x is the independent variable, a set of four differential equations can be developed describing change of y, A^*, V^* and γ as functions of x. These equations can be obtained simply from the corresponding rating problem equations by suitable inversion or division of one equation by the other. For example, consider Table 11.2. By inverting the first equation for the cocurrent flow situation, one gets a direct expression for the derivative dA^*/dx. Dividing the second equation by the first, one gets an expression for dy/dx, and dividing the third by the first, one gets an expression for dV^*/dx, etc. The boundary conditions will be defined at $x = x_F$, and at $x = x_R$, the latter being the known quantity now. The design governing equations are listed in Table 11.6 for shell side feed.

A relatively simple design method has been developed by Pan [38] that can be employed when the system is binary, the permeate pressure is constant, and the membrane is asymmetric so that cross-flow permeation in the membrane can be assumed. If the residue composition x_R is specified, the dimensionless membrane area A_T^* can be expressed as a function of x_R, the constant permeate pressure ratio γ_o and the stage cut θ as follows:

$$A_T^* = \left[\{x_F - (1-\theta)x_R\}/\alpha + (1-x_F) - (1-\theta)(1-x_R)\right]/(1-\gamma_o) \tag{11.54}$$

where

$$A_T^* = \pi D_{LM} l_E N_T P_F Q_2 \tag{11.55}$$

The stage cut θ can be expressed in terms of the local permeate mole fractions y_F' and y_R' in the same way as shown in Section 11.10 for a spiral-wound permeator:

$$1-\theta = (y_R'/y_F')^a \left[(1-y_R')/(1-y_F')\right]^b \left[\alpha-(\alpha-1)y_R'\right]/\left[\alpha-(\alpha-1)y_F'\right] \tag{11.56}$$

where

$$y_F' = \phi_1(x_F, \gamma_o) \text{ and } y_R' = \phi_1(x_R, \gamma_o) \tag{11.57}$$

TABLE 11.6

Design equations for hollow-fiber permeators: cocurrent flow, binary system and shell-side feed

Residue concentration as the independent variable:

$$dA^*/dx = -(1 - V^*)/[\alpha(1-x)(x-\gamma y) - x\{(1-x) - \gamma(1-y)\}]$$

$$dy/dx = -[(1 - V^*)/V^*]\,[\alpha(1-y)(x-\gamma y) - y\{(1-x) - \gamma(1-y)\}] \,/$$
$$[\alpha(1-x)(x-\gamma y) - x\{(1-x) - \gamma(1-y)\}]$$

$$dV^*/dx = (1 - V^*)[\alpha(x-\gamma y) + \{(1-x) - \gamma(1-y)\}] \,/[\alpha(1-x)(x-\gamma y) - x\{(1-x) - \gamma(1-y)\}]$$

$$d\gamma/dx = -K_3\, V^{*2}/\{\gamma[\alpha(1-x)(x-\gamma y) - x\{(1-x) - \gamma(1-y)\}]\}$$

Boundary conditions: at $x = x_F$, $A^* = 0$; $y = \phi_1(x,\gamma)$; $V^* = 0$

at $x = x_R$, $\gamma = \phi_2(\gamma, V^*)$

Permeate concentration as the independent variable:

$$dA^*/dy = -V^*/[\alpha(1-y)(x-\gamma y) - y\{(1-x) - \gamma(1-y)\}]$$

$$dx/dy = -\,[V^*/(1 - V^*)]\,[\alpha(1-x)(x-\gamma y) - x\{(1-x) - \gamma(1-y)\}] \,/$$
$$[\alpha(1-y)(x-\gamma y) - y\{(1-x) - \gamma(1-y)\}]$$

$$dV^*/dy = V^*[\alpha(x-\gamma y) + \{(1-x) - \gamma(1-y)\}] \,/[\alpha(1-y)(x-\gamma y) - y\{(1-x) - \gamma(1-y)\}]$$

$$d\gamma/dx = -K_3\, V^{*2}/\{\gamma[\alpha(1-y)(x-\gamma y) - y\{(1-x) - \gamma(1-y)\}]\}$$

Boundary conditions: at $y = y_F$, $A^* = 0$; $x = x_F$; and $V^* = 0$

at $y = y_o$, $\gamma = \phi_2(\gamma_o, V^*)$

Here $K_3 = 128\,\mu\, R_g\, T\, L_F^2/(\pi^2\, D_i^4\, D_{LM}\, N_T^2\, P_{Fi}^3\, Q_2)$, and ϕ_1 and ϕ_2 are functionalities described by Eqs. (11.32) and (11.31c).

Here ϕ_1 represents the functionality shown in Eq. (11.32), and exponents a and b are given by Eqs. (11.50b) and (11.50c).

11.12 HOLLOW-FIBER PERMEATORS FOR MULTICOMPONENT SYSTEMS

As pointed out in Section 11.7, the selectivities in multicomponent systems are defined with respect to a reference component, as shown in Eq. (11.13). The choice of the reference component depends on the system. It may be the slowest permeating component in the mixture. However, sometimes that may not be the ideal choice. For example, the mixture may contain a group of compounds with very small and similar permeances (e.g. hydrocarbon mixtures with minor amounts of high-C compounds). Choosing one among this group as the reference component may not be useful, and it may be preferable to use some other component with permeance somewhere in the middle range. Note also that if

there are a number of components with similar permeances, it is actually better to treat them together as a pseudo-single component.

The component balance for the i-th component in a hollow-fiber permeator can be written for a countercurrent flow pattern as

$$d[Lx_i] = d[Vy_i] = \pi D_{LM}\, dz\, N_F\, Q_i[P_F x_i - P_P y_i],\ i=1,2,3,\ldots n \qquad (11.58)$$

As in binary systems, one can deduce from the above the dimensionless governing equations for total flow rates L^* and V^*:

$$dL^*/dz^* = dV^*/dz^* = [\pi D_{LM} N_F Q_{Ref} P_F l_E/L_F]\left[\sum_i \{\alpha_i(x_i - \gamma y_i)\}\right]$$

$$= K_{1,M}\left[\sum_i \{\alpha_i x_i - \gamma \sum_i \alpha_i y_i)\}\right] \qquad (11.59)$$

where

$$K_{1,M} = \pi D_{LM} N_F Q_{Ref} P_F l_E/L_F \qquad (11.60)$$

Note that when i corresponds to the reference component, $\alpha_i = 1$. The complete set of differential equations involving the flow rates, the permeate pressure ratio and the mole fractions x_i–s and y_i–s for an n-component system is given in Table 11.7 for shell-side feed operation. For an n-component system, and counter-

TABLE 11.7

Governing equations for hollow-fiber permeators: multicomponent system, shell-side feed and countercurrent flow

$$dx_i/dz^* = K_1\left[\alpha_i(x_i - \gamma y_i) - x_i\left\{\sum_i \alpha_i x_i - \gamma \sum_i \alpha_i y_i\right\}\right]/L^*;\ i=1,2,\ldots,(n-1)$$

$$dy_i/dz^* = K_1\left[\alpha_i(x_i - \gamma y_i) - y_i\left\{\sum_i \alpha_i x_i - \gamma \sum_i \alpha_i y_i\right\}\right]/V^*;\ i=1,2,\ldots,(n-1)$$

$$dL^*/dz^* = K_1\left[\sum_i \alpha_i x_i - \gamma \sum_i \alpha_i y_i\right]$$

$$dV^*/dz^* = K_1\left[\sum_i \alpha_i x_i - \gamma \sum_i \alpha_i y_i\right]$$

$$d\gamma/dz^* = -K_2\, V^*/\gamma$$

Boundary conditions: at $z^* = 0$, $V^*=0$; $y_i = \phi_1(x_i,\gamma)$, $i=1,2,\ldots(n-1)$

at $z^* = 1$, $\gamma = \phi_2(\gamma_o, V^*)$; $L^* = 1$; $x = x_{iF}$, $i=1,2\ldots(n-1)$

Here $\alpha_i = Q_i/Q_{Ref}$

$K_1 = \pi D_{LM} l_E N_T P_F Q_{Ref}/L_F$

$K_2 = 128\, \mu R_g T l_E L_F/(\pi D_i^4 N_T P_F^2)$

and ϕ_1 and ϕ_2 are functionalities described by Eqs. (11.32) and (11.31c).

current flow, a total of $(2n + 1)$ simultaneous differential equations are involved. They include $(n - 1)$ equations for x_i, $(n - 1)$ equations for y_i, two equations for L^* and V^*, and one for γ. No equations for the reference component need to be considered since the sum of the mole fractions is always unity in both the feed and the permeate.

11.13 PERMEATION IN PRESENCE OF SWEEP GAS

A sweep or purge gas is sometimes used on the permeate side of a hollow-fiber permeator to reduce the permeate partial pressure and thereby increase the permeation driving force. Figure 11.13 shows a module with a sweep gas in countercurrent mode. The sweep gas itself will generally have some permeability through the membrane, and hence, will appear on the feed side as well.

The governing differential equations will remain essentially the same as those developed before for a no-sweep situation. The only addition is that the mole fractions of the sweep component in the feed and the permeate have to be considered also. For an n-component feed gas mixture, it becomes a $(n + 1)$ component system, and a total of $(2n + 3)$ simultaneous differential equations need to be solved. The exception occurs when the feed mixture itself contains the sweep gas species. The boundary conditions will be different, too. At the inlet, the sweep may or may not contain some species present in the feed gas mixture. For an n-component feed and countercurrent flow, the $(2n + 3)$ boundary conditions will be:

$$\text{at } z^* = 0,\ V^* = V_I^*(= V_I/L_F);\ y_i = y_{iI},\ i=1,2,\ldots n \tag{11.61a}$$

$$\text{at } z^* = 1,\ L^* = 1;\ \gamma = \phi_2(\gamma_o, V^*);\ x_i = x_{iF},\ i=1,2,\ldots n \tag{11.61b}$$

It is to be noted that the indeterminate boundary conditions encountered at the closed fiber ends for a no-sweep condition (Eqs. (11.34a) and (11.34b)) no longer apply here since V is not zero at that location.

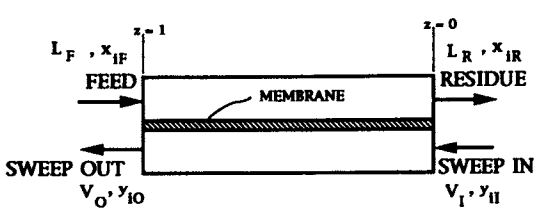

Fig. 11.13. Permeation in presence of sweep gas.

11.14 NUMERICAL TECHNIQUES FOR SOLUTION

Almost all the equations formulated so far need to be solved numerically, using computers. Three distinct classes of numerical solutions are needed most frequently. They are: (1) solution of simultaneous nonlinear algebraic equations; (2) solution of a set of simultaneous nonlinear ordinary differential equations with all values specified at one boundary (the so-called initial-value problems); (3) solution of a set of simultaneous nonlinear ordinary differential equations with values specified on both boundaries (the so-called split-boundary value problems).

The preferable numerical technique or algorithm used for each class of problem depends on the nature of the specific problem at hand, e.g., the extent of nonlinearity, the stiffness of the differential equations, difficulties of convergence, etc. Based on the experiences of the present authors, Newton–Raphson type algorithms are most useful as algebraic equation solvers, Runge–Kutta type algorithms work quite well with the initial value problems, and finite difference algorithms work best with the boundary-value problems.

As an example, the finite difference method for solving the boundary- value problem is considered. The system of differential equations for a given problem can be represented in vector form as:

$$\mathbf{dy}/dv = \mathbf{f} \tag{11.62}$$

where v designates the independent variable here, **y** is the vector of the dependent variables and **f** is the vector containing the derivatives. Each of the differential equations can be replaced by the corresponding finite difference expression at every grid point of a chosen domain. Central difference formulas can be used at the internal grid points, whereas forward or backward difference formulas can be used at the two boundaries. The resulting set of equations for any i-th variable can be represented in matrix notation as:

$$\mathbf{Ai\ yi} = \mathbf{bi} \tag{11.63a}$$

Here, **Ai** is a matrix of constants. The elements of **bi** are mostly proportional to the derivative of the i-th component at the chosen grid points, except perhaps the end elements, which will likely be obtained from the boundary conditions. If an estimate of **yi** at every grid point 1,2,...n are known for iteration (k), the new values of the elements of **yi** for iteration ($k + 1$) can be obtained by solving Eq. (11.63a). The general form can be represented as follows:

$$\begin{bmatrix} a_{i1} & d_{i1} & & & & & \\ c_{i1} & a_{i2} & d_{i2} & & & & \\ & c_{i2} & a_{i3} & \cdot & & & \\ & & \cdot & \cdot & \cdot & & \cdot \\ & & & \cdot & \cdot & \cdot & \\ & & & & \cdot & \cdot & \\ & & & & a_{n-1} & d_{n-1} & \\ & & & & c_{n-1} & a_n & \end{bmatrix} \begin{bmatrix} y_{i1}^{(k+1)} \\ y_{i2}^{(k+1)} \\ y_{i3}^{(k+1)} \\ \cdot \\ \cdot \\ \cdot \\ y_{i,n-1}^{(k+1)} \\ y_{i,n}^{(k+1)} \end{bmatrix} = \begin{bmatrix} b_{i1}^{(k)} \\ b_{i2}^{(k)} \\ b_{i3}^{(k)} \\ \cdot \\ \cdot \\ \cdot \\ b_{i,n-1}^{(k+1)} \\ b_{i,n}^{(k+1)} \end{bmatrix} \tag{11.63b}$$

It is to be noted that $y_1, y_2, \ldots y_n$, etc., are the values of just one variable y_i at the grid points #1,2,...n, and similarly $b_1, b_2, \ldots b_n$ are the values of the functions at the corresponding grid points. One such matrix expression is written for each of the dependent variables involved in the set of differential equations.

The matrix **Ai** is almost always tridiagonal, and in many cases most of the diagonal elements are also zero. This is especially true here since no second derivatives are involved in the system of differential equations, and also since central difference formulas are used for the derivatives at the internal grid points. The solution of the above matrix equations is therefore not complex, and starting with an estimate of all the dependent variables at all the grid points, one can proceed with successive iterations till convergence is achieved. The split boundary conditions generally appear as boundary elements in **bi**.

Very frequently, library subroutines (e.g. IMSL routines) are available commercially for each class of algorithm, which can be used very effectively to solve the specific problem. It is not necessary for the user to write his/her own program based on the chosen algorithm. Sengupta and Sirkar [60,61] have reported on this approach. However, it may sometimes be necessary to tailor these subroutines to suit one's need most effectively.

For example consider the boundary value problems. As mentioned above, finite difference techniques work well with these kinds of problems. However, in order for the technique to converge rapidly, or sometimes to converge at all towards a stable solution, it is essential to provide the subroutine with the initial estimates of all the variables at the chosen grid points inside the domain. An approach that has been used with success many times by the present authors is to solve the specific problem first *as if* it is an initial value problem to generate profiles of each variable over the domain. The profiles of some of the variables are then turned around in a chosen way (the easiest method is to use a mirror image of the original profile) to generate the initial estimates for the actual boundary value problem, and then proceed with successive iterations until the target variable(s) converge within a preset tolerance.

11.15 MULTIMEMBRANE MODULE CONFIGURATIONS

It has been shown by a number of authors [60–66] that in some cases the separation can be improved significantly if two membranes of opposing selectivities are used in the same module instead of only one membrane. This is called a two-membrane permeator. The advantages have been rationalized in terms of improved driving force for each of the two membranes in the module because of synergy. These kinds of permeators have been studied for both binary as well as ternary gas-mixture separation.

Figure 11.14a shows the schematic of such a module for ternary separation. The two membranes A and B have opposing selectivities with respect to components #1 and #2 of the ternary feed-gas mixture, respectively, whereas component #3 has the least permeance through both membranes. Three product streams may be obtained from this two-membrane separator, as shown in Fig. 11.14. The merits of this type of multimembrane separator vis-a-vis a series configuration, e.g. a permeator containing only membrane A followed by a permeator containing only membrane B, have been discussed in Sengupta and Sirkar [67].

In another variation of the multimembrane module concept, Sidhoum et al. [68,69] have introduced the internally staged permeator, shown schematically in Fig. 11.14b. The permeate from membrane A acts as the local feed to mem-

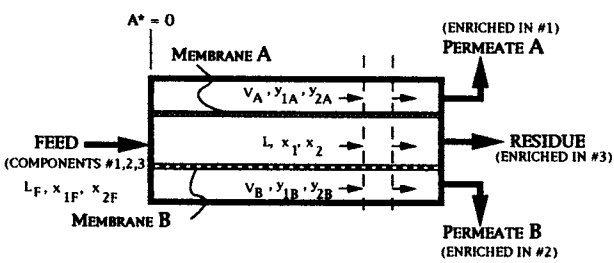

(a) TWO-MEMBRANE PERMEATOR

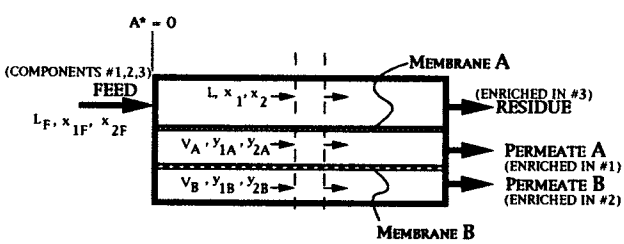

(b) INTERNALLY STAGED PERMEATOR

Fig. 11.14. Membrane permeators with two different types of membranes.

brane B all along the permeator length. Membranes A and B need not be of opposing selectivities; they can even be the same membrane, the only difference being the sequence in which they are exposed to the feed gas.

No commercial application exists for the two-membrane permeator or the internally staged permeator. However, it is useful to develop the permeation analysis for these situations since they establish the pattern in which the analysis can be built upon to accommodate complexities in permeator module configurations. Only cocurrent flow is considered here and pressure drop in the bulk-flow direction is neglected. For each differential area of membrane A, dA_A, there would be a corresponding differential membrane B area dA_B. The permeance for each permeant-membrane combination needs to be considered now, e.g., Q_{iA} is the permeance of i-th species through membrane A, etc. A total of $2n$ permeances are involved for two membranes and an n-component system. For the *two-membrane permeator*, the mass balance for component i can be written as

$$-\mathrm{d}(Lx_i) = Q_{iA}\,\mathrm{d}A_A(P_F x_i - P_{PA}y_{iA}) + Q_{iB}\,\mathrm{d}A_B(P_F x_i - P_{PB}y_{iB}) \quad (11.64a)$$

$$\mathrm{d}(V_A y_{iA}) = Q_{iA}\,\mathrm{d}A_A(P_F x_i - P_{PA}y_{iA}) \quad (11.64b)$$

$$\mathrm{d}(V_B y_{iB}) = Q_{iB}\,\mathrm{d}A_B(P_F x_i - P_{PB}y_{iB}) \quad (11.64c)$$

The above equations can be made dimensionless as follows:

$$-\mathrm{d}(L^* x_i)/\mathrm{d}A^* = Q_{iA}^*(x_i - \gamma_A y_{iA}) + \Omega\, Q_{iB}^*(x_i - \gamma_B y_{iB}) \quad (11.65a)$$

$$\mathrm{d}(V_A^* y_{iA})/\mathrm{d}A^* = Q_{iA}^*(x_i - \gamma_A y_{iA}) \quad (11.65b)$$

$$\mathrm{d}(V_B^* y_{iB})/\mathrm{d}A^* = \Omega\, Q_{iB}^*(x_i - \gamma_B y_{iB}) \quad (11.65c)$$

where

$$L^* = L/L_F;\ V_A^* = V_A/L_F;\ V_B^* = V_B/L_F$$

$$\gamma_A = P_{PA}/P_F;\ \gamma_B = P_{PB}/P_F;\ \Omega = A_B/A_A$$

$$Q_{iA}^* = Q_{iA}/\sum_i (Q_{iA} + Q_{iB});\ Q_{iB}^* = Q_{iB}/\sum_i (Q_{iA} + Q_{iB})$$

and

$$A^* = A_A\, P_F \sum_i (Q_{iA} + Q_{iB})/L_F \quad (11.66)$$

The overall mass balance is

$$L^* + V_A^* + V_B^* = 1 \quad (11.67)$$

Table 11.8 shows the differential equations involving V_A^*, V_B^*, x_i, y_{iA} and y_{iB}.

TABLE 11.8

Governing equations for two-membrane permeators and internally staged permeators: multicomponent system and cocurrent flow with no pressure drop

Two-membrane permeator

$$dV_A^*/dA^* = \sum_i Q_{iA}^* x_i - \gamma_A \sum_i Q_{iA}^* y_{iA}$$

$$dV_B^*/dA^* = \Omega\left[\sum_i Q_{iB}^* x_i - \gamma_B \sum_i Q_{iB}^* y_{iB}\right]$$

$$-dx_i/dA^* = \Big[Q_{iA}^*(x_i - \gamma_A y_{iA}) + \Omega\, Q_{iB}^*(x_i - \gamma_B y_{iB}) - x_i\left\{\sum_i Q_{iA}^* x_i - \gamma_A \sum_i Q_{iA}^* y_{iA} + \Omega\left(\sum_i Q_{iB}^* x_i - \gamma_B \sum_i Q_{iB}^* y_{iB}\right)\right\}\Big]/(1 - V_A^* - V_B^*)$$

$$dy_{iA}/dA^* = \left[Q_{iA}^*(x_i - \gamma_A y_{iA}) - y_{iA}\left(\sum_i Q_{iA}^* x_i - \gamma_A \sum_i Q_{iA}^* y_{iA}\right)\right]/V_A^*$$

$$dy_{iB}/dA^* = \Omega\left[Q_{iB}^*(x_i - \gamma_B y_{iB}) - y_{iB}\left(\sum_i Q_{iB}^* x_i - \gamma_B \sum_i Q_{iB}^* y_{iB}\right)\right]/V_B^*$$

Internally staged permeator

$$dV_A^*/dA = \sum_i Q_{iA}^* x_i - \gamma_A \sum_i Q_{iA}^* y_{iA} - \Omega\left[\gamma_A \sum_i Q_{iB}^* y_{iA} - \gamma_B \sum_i Q_{iB}^* y_{iB}\right]$$

$$dV_B^*/dA^* = \Omega\left[\gamma_A \sum_i Q_{iB}^* y_{iA} - \gamma_B \sum_i Q_{iB}^* y_{iB}\right]$$

$$-dx_i/dA^* = \left[Q_{iA}^*(x_i - \gamma_A y_{iA}) - x_i\left\{\sum_i Q_{iA}^* x_i - \gamma_A \sum_i Q_{iA}^* y_{iA}\right\}\right]/(1 - V_A^* - V_B^*)$$

$$dy_{iA}/dA^* = \Big[Q_{iA}^*(x_i - \gamma_A y_{iA}) - \Omega\, Q_{iB}^*(\gamma_A y_{iA} - \gamma_B y_{iB}) - y_{iA}\left\{\sum_i Q_{iA}^* x_i - \gamma_A \sum_i Q_{iA}^* y_{iA} - \Omega[\gamma_A \sum_i Q_{iB}^* y_{iA} - \gamma_B \sum_i Q_{iB}^* y_{iB}]\right\}\Big]/V_A^*$$

$$dy_{iB}/dA^* = \Omega\left[Q_{iB}^*(\gamma_A y_{iA} - \gamma_B y_{iB}) - y_{iB}\left\{\gamma_A \sum_i Q_{iB}^* y_{iA} - \gamma_B \sum_i Q_{iB}^* y_{iB}\right\}\right]/V_B^*$$

For the *internally staged permeator*, the dimensionless mass balance for component i can be written as

$$-d(L^* x_i)/dA^* = Q_{iA}^*(x_i - \gamma_A y_{iA}) \tag{11.68a}$$

$$d(V_A^* y_{iA})/dA^* = Q_{iA}^*(x_i - \gamma_A y_{iA}) - \Omega\, Q_{iB}^*(\gamma_A y_{iA} - \gamma_B y_{iB}) \tag{11.68b}$$

$$d(V_B^* y_{iB})/dA^* = \Omega\, Q_{iB}^*(\gamma_A y_{iA} - \gamma_B y_{iB}) \tag{11.68c}$$

The differential equations involving V_A^*, V_B^*, x_i, y_{iA} and y_{iB} are given in Table 11.8.

11.16 RECYCLE AND REFLUX

In case of recycle or reflux operation, the differential equations for a permeator module do not change, but the boundary conditions do. In fact, the unique nature of a recycle and/or reflux situation is that the boundary conditions become coupled. This is illustrated by the following examples. The flow schematics are shown in Figs. 11.15a and 11.15b. Only a binary system is considered, and pressure drop in bulk-flow direction is neglected. The quantity η_R designates the recycle ratio or the reflux ratio. This is the fraction of the permeate stream leaving the permeator module that is mixed with the incoming fresh feed (in case of recycle), or the fraction that is recompressed and sent back to the enricher (in case of reflux).

For recycle operation (Fig. 11.15a), the actual flow of feed into the permeator module, L_I, and the mole fraction of the faster permeating component in that stream, x_I, are not known *a priori* since V_O and y_O are not known. However, the net feed flow to the stage, L_F, and the corresponding x_F are known, just as in a non-recycle case. The following boundary conditions are, therefore, applied for a recycle ratio ϕ_R:

$$\text{at } z^* = 0;\ V^* = 0; \quad \text{and} \quad y = \phi_1(x, \gamma)$$

$$\text{at } z^* = 1,\ L^* = 1 + \eta_R V^*; \quad \text{and} \quad x = (x_F + \eta_R V^* y)/(1 + \eta_R V^*) \quad (11.69)$$

The functionality ϕ_1 is given by Eq. (11.32).

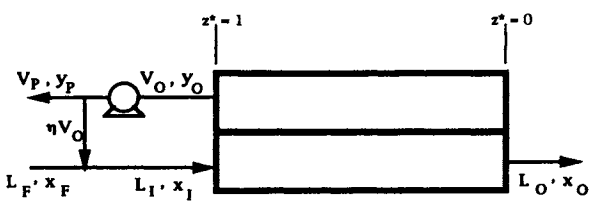

(a) PARTIAL PERMEATE RECYCLE

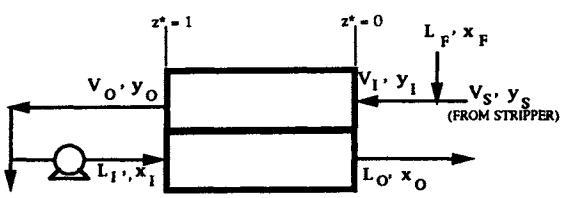

(b) ENRICHER SECTION OF MEMBRANE RECTIFICATION COLUMN

Fig. 11.15. Mass balance for recycle and reflux operations.

Figure 11.15b shows the enricher section of a membrane rectification column. It is assumed that V_S and y_S, entering from the stripper section, are known quantities (actually, while simulating the whole column, both the enricher and the stripper sections have to be solved simultaneously, and the quantities V_S, y_S, L_O and x_O will actually couple the two solutions). Considering the enricher section, the quantities V_I and y_I are, therefore, known. However, L_I and x_I are not known. The following boundary conditions can be written for reflux ratio η_R:

$$\text{at } z^* = 0,\ V^* = 1 + V_S^*,\ \text{and}\ \ y = (x_F + y_S V_S^*) / (1 + V_S^*)$$

$$\text{at } z^* = 1,\ x = y,\ \text{and}\ \ L^* = \eta_R V^*$$

where

$$V_S^* = V_S / L_F \tag{11.70}$$

11.17 SHORTCUT ANALYSIS AND DESIGN METHODS

So far, we have discussed analysis and design techniques involving the so-called 'exact' numerical solutions. In some instances, it may be preferable to have quick 'first approximations' of some of the quantities like stage cut, residue and permeate outlet composition, the membrane area requirement, etc., without going through rigorous numerical calculations. Under certain simplifying conditions and assumptions, it is possible to develop analytical expressions for these quantities, and therefore, to compute their values much more quickly. While these approaches can never be the substitutes for the exact numerical solutions, they can be useful for making quick estimates during the initial design decisions. This is especially true where the membrane separator unit is only part of a large process.

One of the earliest approaches to approximate solutions was proposed by Boucif et al. [70] for a binary mixture. They expressed the residue and the permeate outlet compositions from a permeator module as power series expansions in terms of a dimensionless total membrane area A_T^*, the series being truncated after the third power of area. For example, *for cocurrent flow*, one may write:

$$x_R = a_0 + a_1 A_T^* + a_2 A_T^{*2} + a_3 A_T^{*3} \tag{11.71}$$

$$y_P = b_0 + b_1 A_T^* + b_2 A_T^{*2} + b_3 A_T^{*3} \tag{11.72}$$

where

$$A_T^* = Q_2 P_F A_T / L_F \tag{11.73}$$

The series expansions contain unknown coefficients a_0, a_1, a_2, a_3, b_0, b_1, b_2, and b_3. When the above expressions are substituted in the differential equations governing permeation and the boundary conditions, and the terms containing the same order of A^* on both sides of the equations are equated, one can get explicit algebraic expressions for these unknown coefficients in terms of the membrane selectivity α, the permeate pressure ratio γ, and the feed mole fraction x_F. For cocurrent flow in this case the *rating problem*, therefore, becomes very simple. For any given membrane area A_T, and for known feed-flow rate and feed pressure, one calculates A_T^* from Eq. (11.73), and then x_R and y_P from Eqs. (11.71) and (11.72). Subsequently, one can calculate the stage cut θ as follows:

$$\theta = (x_F - x_R) / (y_P - x_R) \tag{11.74}$$

For the *design problem* under cocurrent flow, one has to solve first a cubic algebraic equation for A_T^* using either Eq. (11.71) or (11.72), depending on whether x_R or y_P is specified in the design problem, respectively. Once A_T^* is known, one then calculates the unknown quantity y_P (or x_R, as the case may be), and then θ, using Eq. (11.74).

For countercurrent flow, the expansion is carried out in terms of a dimensionless area A_T' as follows:

$$x_F = x_R + c_1 A_T' + c_2 A_T'^2 + c_3 A_T'^3 \tag{11.75}$$

$$y_P = d_0 + d_1 A_T' + d_2 A_T'^2 + d_3 A_T'^3 \tag{11.76}$$

where

$$A_T' = Q_2 P_F A_T / L_R \tag{11.77}$$

Note that A_T' is defined with L_R, which is not known *a priori*. The constants c_1, c_2, c_3, d_0, d_1, d_2, and d_3 are obtained as functions of α, γ, and x_R. For a *design problem where x_R is specified*, one first solves Eq. (11.75) for A_T', and then calculates y_P, and subsequently θ, using Eqs. (11.76) and (11.74), respectively. For a *design problem where y_P is specified*, one solves Eqs. (11.75) and (11.76) simultaneously for x_R and A_T', and then calculates θ. The *rating problem* for countercurrent flow is more involved. Here, one expresses A_T' in terms of A_T^*, x_R and y_P as follows:

$$A_T' = A_T^* (y_P - x_R) / (y_P - x_F) \tag{11.78}$$

Equations (11.75) and (11.76) are then solved simultaneously for x_R and y_P.

Boucif et al. [71] extended the series solution for the case where the pressure drop on the permeate side varies along the permeator length. In either of these two analyses, the series solutions has been found to match quite well with the exact numerical solutions up to practical values of the component cut for the faster permeating component. A wide range of parametric variations have been explored, including variations in α, γ and x_F. At very high stage cut, however,

the series solution can deviate significantly from the exact numerical solution. The point at which the deviation starts depends on the three above parameters.

Shortcut analysis and design approaches employing techniques other than the power series solution have also been developed. Rautenbach and Dahm [72] developed a series of analytical expressions for some limiting cases. They considered three distinct models. The first model assumes an ideal semipermeable membrane, which means α is infinitely large, or $\alpha^{-1} = 0$. The second model assumes additionally that the permeate partial pressure is negligible, i.e., $\gamma y = 0$. The third model assumes that the permeate pressure is constant inside the module, i.e. $\gamma y = \gamma_o y_P$. Algebraic expressions have been developed for each model to calculate the membrane area requirement and θ. These expressions are presented in Table 11.9.

Basaran and Auvil [73] carried out an asymptotic analysis on membrane permeator modeling to develop algebraic expressions that are applicable in certain limiting regimes of operation. They used perturbation expansions in terms of a very small parameter in the governing equations. Two limiting cases are considered. For the limit where a approaches unity, the perturbation parameter ε is $(\alpha - 1)$, whereas for the limit where a approaches infinity, the perturbation parameter is $(\alpha^{-1} - 1)$. As expected, the solutions match well with the exact numerical solutions under limiting conditions, but may deviate considerably at other conditions.

A simple graphical method has been presented by Jain [74] for calculating the stage cut and the membrane area requirement for specified residue composition. The method uses the Blaisdell and Kammermeyer model [40] to generate a series of parameterized graphs. The calculations are based on the following governing equation:

$$\frac{dL'}{dx} = \frac{-L'}{x + \dfrac{\alpha}{(1-\alpha) + (\gamma - 1)/(x - \gamma y)}} \tag{11.79}$$

where

$$L' = L/L_R; \text{ and } y = (L'x - x_R)/(L' - 1) \tag{11.80}$$

Equation (11.79) is solved subject to the following conditions:

$$\text{at } x = x_R,\ L' = 1; \text{ and at } x = x_F,\ L' = 1/(1-\theta) \tag{11.81}$$

Also

$$\frac{y_R}{1 - y_R} = \frac{\alpha(x_R - \gamma y_R)}{(1 - x_R) - \gamma(1 - \gamma_R)} \tag{11.82}$$

The solution for L' thus yields the value of θ directly.

TABLE 11.9

Analytical expressions for permeator performance under simplifying assumptions

Model #1

$$L^* = \frac{1 - x_F}{1 - x}$$

$$\alpha z^* A_T^* = \frac{1 - x_F}{(1 - \gamma)^2}\left[\ln\left\{\frac{1 - x}{1 - x_F} - \frac{x_F - \gamma}{x - \gamma}\right\} - \frac{(1 - \gamma)(x_F - x)}{(1 - x)(1 - x_F)}\right]$$

Model #2

$$L^* = \left(\frac{x}{x_F}\right)^{1/(\alpha-1)} \left(\frac{1 - x_F}{1 - x}\right)^{\alpha/(\alpha-1)}$$

$$\alpha z^* A_T^* = (1 - x_F)\left[1 + \frac{x_F}{\alpha(1 - x_F)} - \left(\frac{x}{x_F}\frac{1 - x_F}{1 - x}\right)^{1/(\alpha-1)}\left\{1 + \frac{x_F}{\alpha(1 - x_F)}\left(\frac{x}{x_F}\frac{1 - x_F}{1 - x}\right)^{\alpha}\right\}\right]$$

Model #3

$$L^* = \left(\frac{x_F - h_1}{x - h_1}\right)^{\frac{h_1+a_1}{h_1-h_2}} \left(\frac{x - h_2}{x_F - h_2}\right)^{\frac{h_2+a_1}{h_1-h_2}}$$

$$\alpha z^* A_T^* = \alpha \frac{(h_1 - x_F)(h_1 - h_2)}{(\alpha - 1)(h_2 + a_1)}\left[\left(1 + \frac{(h_2 + h_1)(x_F - h_2)}{(h_1 + a_1)(h_1 + x_F)}\right) - \left(\frac{x - h_2}{x_F - h_2}\frac{x_F - h_1}{x - h_2}\right)^{\frac{h_1+a_1}{h_1-h_2}}\right.$$

$$\left. \times \left\{1 + \frac{(h_2 + a_1)(x_F - h_2)}{(h_1 + a_1)(h_1 - x_F)}\left(\frac{x - h_2}{x_F - h_2}\frac{x_F - h_1}{x - h_1}\right)^{\frac{h_1+a_1}{h_2+a_1}}\right\}\right]$$

where $h_1 = \frac{a_2}{2} + \sqrt{\left(\frac{a_2}{2}\right)^2 - a_3}$, $\quad h_2 = \frac{a_2}{2} - \sqrt{\left(\frac{a_2}{2}\right)^2 - a_3}$

$a_1 = (1 - \gamma_w)/(\alpha - 1) - (\gamma y)_w$; $a_2 = 1 + (\gamma y)_w + \gamma_w/(\alpha - 1)$; and $a_3 = \alpha(\gamma y)_w/(\alpha - 1)$

The membrane area requirement is subsequently calculated from the following integral:

$$A_T = \frac{L_F}{Q_1 P_F} \int_{\frac{1}{1-\theta}}^{1} \frac{-(1 - \theta)\, dL'}{(x - \gamma y) + \dfrac{(1 - x) - \gamma(1 - y)}{\alpha}} \tag{11.83}$$

A series of graphs can be generated for the stage cut and the membrane area requirement as functions of the different parameters, e.g., x_F, x_R, γ, etc. Once

these parameterized graphs are available, the performance of the system under consideration can be predicted for a wide range of conditions.

11.18 GENERAL COMMENTS ON SEPARATION BEHAVIOR

As mentioned in Sections 11.4 and 11.5, a large number of variables and parameters affect the separation in a membrane permeator. They include process variables like feed-flow rate, feed composition, desired product recovery and/or product purity; system properties like permeabilities and selectivity; module properties like membrane area, flow cross-section geometry, flow-path length and membrane thickness; and operating variables like temperature, feed pressure and permeate pressure. Prediction of the separation behavior under specific circumstances is, therefore, very difficult without a quantitative analysis. However, some general qualitative conclusions can be arrived at, based on the pattern of performance. These conclusions, many of which are discussed in Refs. [19], [32], [37] and [38], are summarized below:

1. Membrane gas separators are most efficient for bulk separation. If the purity requirement is too high for either the residue stream or the permeate stream, then a point of diminishing return is reached when increasing membrane area does not gain corresponding improvement in separation, and so is economically prohibitive.

2. Hybrid processes where membranes are used for bulk separation, followed by other more conventional separation processes for final purification, are likely to be more economically successful than processes employing only conventional separation or only membranes.

3. In a single membrane stage, higher product purity is generally associated with low product recovery, and vice versa.

4. A larger membrane area generally increases the purity of the residue stream, whereas a smaller membrane area increases the purity of the permeate stream.

5. A high membrane selectivity is not always beneficial to the overall membrane process economics since it can actually increase the membrane area requirement.

6. A higher feed pressure and/or a lower permeate pressure increases the purity of the residue and reduces the membrane area requirement.

7. Both the pressure differential between the feed and the permeate stream and the permeate-to-feed pressure ratio are important in separation.

8. For a given membrane area, a higher feed-flow rate reduces residue purity but does not significantly affect the permeate-flow rate.
9. In a binary separation, the permeate mole fraction of the faster gas always decreases monotonically with an increase in stage cut.
10. In permeators employing homogeneous or nonasymmetric membranes, countercurrent feed-permeate flow pattern is always more efficient than the cocurrent flow pattern.
11. In permeators employing asymmetric membranes, the effect of the flow pattern on separation is greatly attenuated. The countercurrent flow may or may not produce better separation.
12. In hollow-fiber permeators where significant pressure buildup occurs in the fiber lumini, operation with shell-side feed is likely to be more efficient for low stage cuts, whereas tube side feed is likely to be more efficient for high stage cuts.
13. In ternary mixture separation, the residue mole fraction of the component with intermediate permeability goes through a maximum as a function of the stage cut.

11.19 NOTATION

a	Constant, Eq. (11.50b)
a_0,a_1,a_2,a_3	Coefficients in series expansion, Eq. (11.71)
$a_{i1},a_{i2},\ldots a_{in}$	Elements of matrix **Ai**, Eq. (11.63b)
A	Membrane area, m^2
A^*	Dimensionless membrane area, Eq. (11.53)
A_T	Total membrane area, m^2
A_T^*	Dimensionless total membrane area, Eq. (11.16) for multicomponent system, and Eq. (11.73) for binary system
A_T'	Dimensionless total membrane area based on residue-flow rate, Eq. (11.77)
A_A,A_B	Area of membranes A and B, respectively, for permeators containing two different membranes
Ai	Matrix of constants for component i, Eq. (11.63b)
b	Constant, Eq. (11.50c)
b_0,b_1,b_2,b_3	Coefficients in series expansion, Eq. (11.72)
$b_{i1},b_{i2},\ldots b_{i,n}$	Elements of array **bi**, Eq. (11.63b)
B	Darcy's permeability of the porous permeate channel in a spiral-wound permeator

bi	Array containing current values of the derivatives and the boundary conditions for the *i*-th component, Eq. (11.63b)
c_0,c_1,c_2,c_3	Coefficients in series expansion, Eq. (11.75)
$c_{i1},c_{i2},\ldots c_{in}$	Elements of matrix **Ai**, Eq. (11.63b)
d_0,d_1,d_2,d_3	Coefficients in series expansion, Eq. (11.76)
$d_{i1},d_{i2},\ldots d_{in}$	Elements of matrix **Ai**, Eq. (11.63b)
D_i,D_o	Hollow-fiber inside and outside diameter, respectively, m
D_i',D_o'	Hollow-fiber inside and outside diameter under elastic deformation, respectively, m
D_{LM}	Logarithmic mean of the inside and outside diameters of hollow fiber, m
e_i	Enrichment factor for component *i*
F_i	Facilitation factor for component *i*
f	Array containing the derivatives, Eq. (11.62)
k_F,k_P	Gas phase mass transfer coefficients on the feed side and the permeate side of the membrane, respectively, mole/(sec)(m^2)(Pa)
K_1,K_2	Dimensionless constants, Eqs. (11.24c), (11.24d)
$K_{1,M}$	Dimensionless constant, Eq. (11.60)
K_3	Constant defined in Table 11.5
K_{iO}	Effective overall permeance for component *i*, mole/(sec)(m^2)(Pa)
K_S	Dimensionless constant, Eq. (11.49)
l_E,l_P	The effective length and the potted length, respectively, of hollow fiber in a permeator, m
l_T	Total module length for a spiral-wound module, m
L	Total gas-flow rate at any permeator location on the high-pressure side of the membrane, mole/sec
L_F,L_R	Value of L at the feed inlet stream and the residue stream, respectively, mole/sec
L^*	Dimensionless L, Eq. (11.24b)
M_{wi}	Molecular weight of component *i*
$M_{w,avg}$	Average molecular weight
N_T	Total number of hollow fibers in a hollow-fiber permeator
P_F	Total pressure on the high-pressure side of the membrane, Pa
P_{Fi}	Value of P_F at the feed inlet point
P_P	Total pressure on the low-pressure side of the membrane, Pa
P_i	Permeability of component *i*, (mole)(m)/(sec)(m^2)(Pa)
Δp_i	Effective partial pressure difference of component *i* across membrane, Pa
q	Actual volumetric flow rate on any side of the membrane, m^3/sec
Q_i	Permeance of component *i*, mole/(sec)(m^2)(Pa)
Q_{iD}	Permeance of component *i* due only to molecular diffusion, mol/(sec)(m^2)(Pa)

Q_{iA}, Q_{iB} Permeance of component i through membranes A and B, respectively, in case of a permeator containing two membranes, mole/(sec)(m^2)(Pa)

Q_{iA}^*, Q_{iB}^* Dimensionless values of Q_{iA} and Q_{iB}, respectively, Eq. (11.66)

Q_{Ref} Permeance of a reference component in case of a multicomponent system, mole/(sec)(m^2)(Pa)

R_i Permeation rate of component i, mole/sec

R_g Universal gas constant, (Pa)(m^3)/(Mole)(K)

Re_w Wall Reynolds number, defined in Table 11.5

t_L Permeate leaf thickness in a spiral-wound permeator, m

t_m Effective membrane thickness, m

T Temperature, K

u Gas-flow rate per unit membrane leaf length on the high-pressure side of the membrane in a spiral-wound permeator, mole/(sec)(m)

u_F, u_R Value of u at the feed inlet stream and the residue stream of the permeator, respectively, mole/(sec)(m)

v Independent variable in matrix notation, Eq. (11.62)

V Total gas-flow rate at any permeator location on the low-pressure side of the membrane, mole/sec

V^* Dimensionless V, Eq. (11.24b)

V_A, V_B Value of V for permeates A and B, respectively, in case of a permeator containing two different membranes, mole/sec

V_a Local average permeate-flow rate in spiral-wound permeators, mole/sec

V_a^* Dimensionless V_a, Eq. (11.49)

V_A^*, V_B^* Dimensionless values of V_A and V_B, respectively, Eq. (11.66)

V_I Sweep inlet-flow rate, mole/sec

V_I^* Dimensionless V_I, Eq. (11.61a)

V_P Value of V at the permeate outlet, mole/sec

V_S Flow rate from the stripper entering the enricher section of a membrane rectification column, mole/sec

V_S^* Dimensionless V_S, Eq. (11.70)

w Permeate flow direction in a spiral-wound permeator

w^* Dimensionless w, Eq. (11.49)

W Total leaf length in a spiral-wound permeator, m

x Mole fraction of the faster permeating component of a binary mixture on the high-pressure side of the membrane

x_F Value of x at the feed inlet stream of the permeator

x_i Mole fraction of component i of a multicomponent mixture on the high-pressure side of the membrane

x_{iF} Value of x_i at the feed inlet stream of the permeator

x_{iR} Value of x_i at the residue stream

y	Mole fraction of the faster permeating component of a binary mixture on the low-pressure side of the membrane
y_P	Value of y at the permeate outlet stream
y_a	Local average permeate mole fraction y in a spiral-wound permeator
y_S	Mole fraction y in the stream entering the enricher section of a membrane rectification column, mole/sec
y_i	Mole fraction of component i of a multicomponent mixture on the low-pressure side of the membrane
y_{iA}, y_{iB}	Value of y_i for permeates A and B, respectively, in a permeator containing two membranes
y_{iI}	Value of y_i at the sweep inlet stream
$y_{i,n}$	Value of dependent variable i at the n-th grid point of the solution domain
y_{iP}	Value of y_i at the permeate outlet stream
Y_M	Young's modulus of the membrane material
y'	Local permeate mole fraction based on cross flow, Eq. (11.11b)
yi	Array containing the values of the i-th dependent variable at all the grid points inside the solution domain
z	Axial location in a permeator, m
z^*	Dimensionless z, Eq. (11.24b)

Greek Symbols:

α	Membrane selectivity for a binary system, Eq. (11.3)
α_i	Selectivity of component i with respect to a reference component, Eq. (11.13)
$\alpha_{S,1-2}$	Stage separation factor, Eq. (11.7)
β	Dimensionless feed pressure, Eq. (11.37)
χ	Quantity defined in Table 11.5
δ_{ij}	Interaction parameters for calculating gas mixture viscosity, Eq. (11.35b)
$\varepsilon_i, \varepsilon_o$	Contraction ratios, Eq. (11.38)
ϕ_1	Functional form, Eq. (11.32)
ϕ_2	Functional form, Eq. (11.31c)
Φ_i	Component i recovery in the permeate
γ	Ratio of permeate pressure to feed pressure, Eq. (11.2d)
γ_A, γ_B	Values of γ for permeates A and B, respectively, in permeators containing two different membranes
γ_o	Value of γ at the permeate outlet stream
Γ	Dimensionless Young's modulus, defined in Table 11.5
η	Diameter ratio, Eq. (11.40)

η_R	Recycle ratio
λ_1,λ_2	Constants defined in Table 11.5
μ	Gas mixture viscosity, Pa-sec
μ_i	Viscosity of pure gas *i*, Pa-sec
θ	Stage cut, Eq. (11.5a), Eq. (11.74)
Ω	Ratio of the areas of membrane B to that of membrane A in case of permeator modules containing two different membranes
Ψ_i	Component *i* recovery in the residue
ζ	Elastic deformation factor, Eq. (11.39)

REFERENCES

1 Lonsdale, H.K. (1982). *J. Membr. Sci.*, 10: 81.
2 Haggin, J. (1988). *Chem. Eng. News*, June 6, p. 7.
3 Spillman, R.W. and Sherwin, M.B. (1989). Presented at the *1989 Membrane Technology/Planning Conference*, October 17, 1989, Boston, MA.
4 Smith, R. (1990). Process Economics Program Report No. 190A, SRI International, Menlo Park, California.
5 Bollinger, W.A., MacLean, D.L. and Narayan, R.S. (1982). *Chem. Eng. Progress*, October '90, p. 27.
6 Yamashiro, H., Hirajo, M., Schell, W.J. and Maitland, C.F. (1984). Presented at the *Europe–Japan Congress on Membranes and Membrane Processes*, June 18–21, Stressa, Italy.
7 Schott, M.E., Houston, C.D., Glazer, J.L. and DiMartino, S.P. (1987). Presented at the *American Institute of Chemical Engineers 1987 National Meeting*, Houston, Texas, April 1, 1987.
8 Schendel, R.L. (1984). *Chem. Eng. Progress*, May 1984, p. 39.
9 Schell, W.J. and Houston, C.D. (1982). *Chem. Eng. Progress*, October 1982, p. 33.
10 Cooley, T.E. and Dethloff (1985). *Chem. Eng. Progress*, October 1985, p. 45.
11 Mazur, W.H. and Chan, M.C. (1982). *Chem. Eng. Progress*, October 1982, p. 38.
12 Kulkarni, S.S., Funk, E.W., Li, N.N. and Riley, R.L. (1983). *Tutorial Lectures in Electrochemical Eng. and Tech. II*, AIChE Symposium Series No. 229, 79: 172.
13 Golan, A. (1989). Presented at the *1989 Membrane Technology/Planning Conference*, October 17, 1989, Boston, MA.
14 Beaver, E.R. (1989). Presented at the *1989 Membrane Technology/Planning Conference*, October 17, 1989, Boston, MA.
15 Fleischman, R.F. (1989). Presented at the *1989 Membrane Technology/Planning Conference*, October 17, 1989, Boston, MA.
16 Peinemann, K.V., Mohr, J.M. and Baker, R.W. (1987). *Recent Advances in Separation Techniques III*, AIChE Symposium Series No. 250, 82: 19.
17 Paul, H., Philipsen, C., Gerner, F.J. and Strathmann, H. (1988). *J. Membr. Sci.*, 36: 363.
18 Kimmerle, K., Bell, C.M., Gudernatsch, W. and Chmiel, H. (1988). *J. Membr. Sci.*, 36: 477.
19 Gottschlich, D.E., Roberts, D.L. (1990). *Energy Minimization of Separation Processes Using Conventional/Membrane Hybrid Systems*, U.S. Department of Energy Final Report No. DOE/ID-10301, September 28, 1990, EG&G Idaho, Inc., Idaho Falls, Idaho.
20 Matson, S.L., Lopez, J. and Quinn, J.A. (1983). *Chem. Eng. Sci.*, 38: 503.

21 Hwang, S.T. and Kammermeyer, K. (1984). *Membranes in Separations*, Robert E. Krieger Publishing Company, Inc., Malabar, Florida, p. 2.
22 Sengupta, A. and Sirkar, K.K. (1986). *Progress in Filtration and Separation, Vol. 4* (R.J. Wakeman, Ed.), Elsevier, Amsterdam, p. 289.
23 Kao, Y.K. and Yan, Z. (1987). *Chem. Eng. Communications*, 59: 343.
24 Stern, S.A. and Frisch, H.L. (1981). *Ann. Rev. Mater. Sci.*, 11: 523.
25 Koros, W.J., Paul, D.R. and Rocha, A.A. (1976). *J. Membr. Sci.*, 14: 687.
26 Lonsdale, H.K. (1987). *J. Membr. Sci.*, 33: 121.
27 Schulz, G., Michele, H. and Werner, U. (1982). *J. Membr. Sci.*, 11: 311.
28 Hwang, S.T. and Thorman, J.M. (1980). *AIChE J.*, 26: 558.
29 Teslik, S. and Sirkar, K.K. (1986). *Recent Developments in Separation Science Vol IX* (N.N. Li and J. Calo, Eds.), CRC Press, Cleveland, p. 245.
30 Majumdar, S., Heit, L.B., Sengupta, A. and Sirkar, K.K. (1987). *Ind. Eng. Chem. Res.*, 26: 1434.
31 Qiu, M.M., Hwang, S.T. and Kao, Y.K. (1989). *Ind. Eng. Chem. Res.*, 28: 1670.
32 Spillman, R.W. (1989). *Chem. Eng. Progress*, January 1989, p. 41.
33 Gottschlich, D.E., Roberts, D.L., Wijmans, J.G., Bell, C.M. and Baker, R.W. (1989). *Gas Sep. Purif.*, 3: 170.
34 Cussler, E.L., Aris, R. and Bhown, A. (1989). *J. Membr. Sci.*, 43: 149.
35 Jordan, S.M., Koros, W.J. and Fleming, G.K. (1987). *J. Membr. Sci.*, 30: 191.
36 Chern, R.T., Koros, W.J. and Fedkiw, P.S. (1985). *Ind. Eng. Chem. Process Des. Dev.*, 24: 1015.
37 Pan, C.Y. (1983). *AIChE J.*, 29: 545.
38 Pan, C.Y. (1986). *AIChE J.*, 32: 2020.
39 Walawender, W.P. and Stern, S.A. (1972). *Separation Sci.*, 7: 553.
40 Blaisdell, C.T. and Kammermeyer, K. (1973). *Chem. Eng. Sci.*, 28: 1249.
41 Breuer, M.E. and Kammermeyer, K. (1967). *Separation Sci.*, 2: 319.
42 Weller, S. and Steiner, W. (1950). *J. Appl. Phys.*, 21: 279.
43 Weller, S. and Steiner, W. (1950). *Chem. Eng. Progress*, 46: 585.
44 Huckins, H.E. and Kammermeyer, K. (1953). *Chem. Eng. Progress*, 49: 180.
45 Huckins, H.E. and Kammermeyer, K. (1953). *Chem. Eng. Progress*, 49: 295.
46 Brubaker, D.W. and Kammermeyer, K. (1954). *Ind. Eng. Chem.*, 46: 733.
47 Naylor, R.W. and Backer, P.O. (1955). *AIChE J.*, 1: 95.
48 Stern, S.A., Sinclair, T.F., Gareis, P.J., Vahldieck, N.P. and Mohr, P.H. (1965). *Ind. Eng. Chem.*, 57: 49.
49 Stern, S.A. and Walawender, W.A. (1969). *Separation Sci.*, 4: 129.
50 Pan, C.Y. and Habgood, H.W. (1974). *Ind. Eng. Chem. Fund.*, 13: 323.
51 Pan, C.Y. and Habgood, H.W. (1978). *Can. J. Chem. Eng.*, 56: 197.
52 Pan, C.Y. and Habgood, H.W. (1978). *Can. J. Chem. Eng.*, 56: 210.
53 Antonson, C.R., Gardner, R.J., King, C.F. and Ko, D.Y. (1977). *Ind. Eng. Chem. Process Des. Dev.*, 16: 463.
54 Rautenbach, R. and Dahm, W. (1985). *Chem. Eng. Process.*, 19: 211.
55 Schulz, G. (1985). *Chem. Eng. Process.*, 19: 235.
56 Stern, S.A., Onorato, F.J. and Libove, C. (1977). *AIChE J.*, 23: 567.
57 Thorman, J. and Hwang, S.T. (1978). *Chem. Eng. Sci.*, 33: 15.
58 Chen, S., Kao, Y.K., and Hwang, S.T. (1986). *J. Membr. Sci.*, 26: 143.
59 Reid, R.C., Prausnitz, J.M. and Sherwood, T.K. (1977). *The Properties of Gases and Liquids*, 3rd Ed., McGraw-Hill, New York, p. 411.

60 Sengupta, A. and Sirkar, K.K. (1984). *J. Membr. Sci.*, 21: 73.
61 Sengupta, A. and Sirkar, K.K. (1987). *AIChE J.*, 33: 529.
62 Ohno, M., Ozaki, O., Sato, H., Kimura, S. and Miyauchi, T. (1977). *J. Nucl. Sci. Tech.*, 14: 589.
63 Ohno, M., Morisue, T., Ozaki, O. and Miyauchi, T. (1978). *J. Nucl. Sci. Tech.*, 15: 376.
64 Stern, S.A., Perrin, J.E. and Naimon, E.J. (1984). *J. Membr. Sci.*, 20: 25.
65 Perrin, J.E. and Stern, S.A. (1985). *AIChE J.*, 31: 1167.
66 Perrin, J.E. and Stern, S.A. (1986). *AIChE J.*, 32: 1889.
67 Sengupta, A. and Sirkar, K.K. (1988). *J. Membr. Sci.*, 39: 61.
68 Sidhoum, M., Sengupta, A. and Sirkar, K.K. (1988). *AIChE J.*, 34: 417.
69 Sidhoum, M., Majumdar, S. and Sirkar, K.K. (1989). *AIChE J.*, 35: 764.
70 Boucif, N., Majumdar, S. and Sirkar, K.K. (1984). *Ind. Eng. Chem. Fund.*, 23: 470.
71 Boucif, N., Sengupta, A. and Sirkar, K.K. (1986). *Ind. Eng. Chem. Fund.*, 25: 217.
72 Rautenbach, R. and Dahm, W. (1986). *J. Membr. Sci.*, 28: 319.
73 Basaran, O.A. and Auvil, S.R. (1988). *AIChE J.*, 34: 1726.
74 Jain, R. (1988). Presented at the *North American Membrane Society Meeting*, June 1–3, 1988, Syracuse, NY.

Membrane Separations Technology. Principles and Applications
Edited by R.D. Noble and S.A. Stern

Chapter 12

Gas separation using inorganic membranes

Klaas Keizer, Robert J.R. Uhlhorn and **Ton J. Burggraaf**

University of Twente, Faculty of Chemical Technology, Laboratory of Inorganic Chemistry, Materials Science and Catalysis, P.O. Box 217, 7500 AE Enschede, The Netherlands

12.1 INTRODUCTION

There is a wide variety of inorganic membranes on the market. Table 12.1 shows a number of the commercial membranes available. Materials include metals, glasses and ceramics; the pore size in these materials ranges from 4 to 5000 nm. Dense metals are also available commercially and dense ceramics are in development. At present, these materials are mainly applied in the field of micro- and ultrafiltration. The housing of all the commercial materials is based on rubber sealing and the membrane modules cannot withstand a temperature higher than 200°C. According to the manufacturers, the main advantages of inorganic membranes compared with organic membranes are:

- high pressures up to 10 MPa can be applied;
- possibilities of cleaning with steam;
- good backflushing possibilities to remove fouling.

Historically, the use of inorganic membranes started in the gas separation of nuclear fuels and this is still the largest application. There is not much literature available about this separation process in the open literature, but the process is based on the separation of $U^{235}F_6/U^{238}F_6$ by Knudsen diffusion. Knudsen diffusion occurs if the mean free path λ of the molecules is much larger than the average pore dimension d_p of a porous material through which the molecule diffuses. A Knudsen number *KN* can be defined, which is:

$$KN = \frac{\lambda}{d_p} \text{ with } \lambda = \frac{16\eta}{5\,\pi\,P_m}\sqrt{\frac{\pi RT}{2M}} \tag{12.1}$$

In this equation d_p is the pore size of the porous material; η is the viscosity of the gas; P_m is the average pressure in the membrane; R is the Gas constant (= 8.31 J/mol·K); T is the absolute temperature (K); and M is the mass of the diffusing molecule.

In Table 12.2, Knudsen separation factors α^* of some typical gas mixtures are shown. For nuclear fuel, the value of α^* is extremely small, but the value added to the product is large and in other types of nuclear fuel separations, small separation factors also occur. The Knudsen separation factor represents the separation obtainable with this mechanism. The effective separation factor in a real process is considerably smaller. For pores larger than about 50 nm non-selective diffusion [1] and laminar flow [2,3–5] results in a smaller separation factor. Process parameters, such as the pressure ratio across the membrane and the concentration polarization, also play an important role in decreasing the separation factor [6–9]. The separation factor is also affected by using the process of counter- or cocurrent flow instead of cross flow.

For O_2/N_2 or CO_2/CH_4 as important commercial separation processes, α^* is also rather small and commercially not very attractive. Only hydrogen can be separated from other components with a relatively large separation factor because of the small molecular mass of hydrogen.

TABLE 12.1

Commercially available porous inorganic membranes [62,90]

Membrane material	Support material	Membrane pore diameter (nm)	Geometry of membrane element	Manufacturer
Ni,Au		>500	tube	Mott,Pall
Ag,Pt				Osmonics
Ag/Pd		0	tube	
ZrO_2	C	4	tube	SFEC
ZrO_2	C	4–14	tube	UC
ZrO_2	metal	dynamic	tube	Carre
ZrO_2	Al_2O_3	10	tube	TDK
SiC	SiC	150–8000	tube	Ceram Filters
SiO_2 (glass)		4–120	tube capillary	Asahi,Fuji,Schott
Al_2O_3	Al_2O_3	4–5000	monolith/tube	Alcoa/SCT
Al_2O_3	Al_2O_3	200–1000	tube	Norton/Millipore
Al_2O_3	Al_2O_3	200–5000	tube	NGK
Al_2O_3	Al_2O_3	200	tube	Hoogovens
Al_2O_3	Al_2O_3	25–200	disk	Anotec/Alcan

TABLE 12.2

Knudsen separation factor α^* of some typical gas mixtures

Gas mixture	α^*
$U^{235}F_6/U^{238F6}$	1.0036
O_2/N_2	0.94
CO_2/CH_4	0.60
H_2/CH_4	2.83
He/CH_4	2.00
H_2/N_2	3.74
H_2/C_3H_8	4.69
H_2/C_6H_{12}	6.48

From the definition given above for Knudsen diffusion it can be stated that it is not the *type* of material that is important but the *structure* in comparison with the *pressure* and *temperature* of the gas mixture to separate. Therefore, an exact pore size regime for Knudsen diffusion behavior cannot be given, but the pores have to be larger than 2 nm, and for nuclear fuel separation, smaller than 200 nm. Near standard conditions (100 kPa and 20°C), the upper limit is in the order of 50 nm.

Under standard conditions, porous inorganic membranes with pores in the range of 2 to 50 nm have, in gas separation processes, *no* particular advantages over organic membranes with the *same* structure. Inorganic membranes have advantages, however, if radiation occurs, the pressure is great, or if the temperature is higher than 100°C.

A large advantage of Knudsen diffusion transport is the high value of the permeability. For an alumina membrane top layer with a thickness of 5 μm and a pore diameter of 50 nm on a porous support with large pores, the permeability is 200×10^{-6} mol m^{-2} s^{-1} Pa^{-1} for hydrogen. This SI-related unit can be translated to units used in commercial applications like Nm^3 H_2 m^{-2} bar^{-1} day^{-1}. In the above mentioned membrane, this value will be 45,000 Nm^3 H_2 m^{-2} bar^{-1} day^{-1} at room temperature or 3600 kg H_2 m^{-2} bar^{-1} day^{-1} [10] (Section 12.3.2).

Another possible method of enhancing the separation factor is to use an extra transport mechanism for one of the gases, for example, surface diffusion, multilayer diffusion and capillary condensation. For surface diffusion, it is difficult to predict in which direction the separation factor will change, and the changes are never larger than a factor of 2 to 3 (Section 12.3.2). For multilayer diffusion, and especially capillary condensation, separation factors can increase greatly up to 1000. These types of separations are only possible if *one* condensable gas is present. The separation process can be optimized by choosing a good combination of pressure and temperature (Section 12.3.2).

If more selective *membranes* are necessary for an actual separation process, the pore size has to be decreased to values smaller than 2 nm or dense materials have to be used (Sections 12.3.3 and 12.3.4).

In Section 12.2, possible inorganic membrane structures, types of membranes and membrane preparation and modification are described. In Section 12.3, inorganic membrane separation mechanisms will be considered together with their potential for gas separation. Section 12.4 of this chapter will consider why — and in which cases — gas separation with inorganic membranes can have an advantage over other separation possibilities. In Section 12.5, an evaluation and conclusions will be given concerning the application possibilities of gas separation with inorganic membranes.*

12.2 MEMBRANE STRUCTURE, PREPARATION AND MODIFICATION

12.2.1 Membrane Structure

Before treating the membrane structure it is necessary to make some agreement concerning the terminology of pore diameter used in this paper. From a materials science and catalysis point of view, the terminology is standardized by the IUPAC definitions [11] as shown in Table 12.3. The corresponding types of filtration, as used in membrane and filtration literature, are also shown is this table. For gas transport through porous or dense materials this classification also makes sense, as shown in Section 12.3.

Possible structures of inorganic membranes are shown in Fig. 12.1. Structure A is a homogeneous structure, which can be found in porous metal sheets, in porous glass capillaries of the Vycor-type [12], or in alumina prepared by anodization [13,14]. Pore sizes found in these types of materials are at least 3

TABLE 12.3

Terminology of pore diameters d_p according to IUPAC definitions [11] and the type of filtration belonging to that pore size

Terminology	Pore diameter (nm)	Type of filtration
macropores	$d_p > 50$	microfiltration
mesopores	$2 < d_p < 50$	ultrafiltration
micropores	$d_p < 2$	nanofiltration/gas separation
dense	$d_p = 0$	solution/diffusion

* The unit of permeability throughout this chapter will be mol m^{-2} s^{-1} Pa^{-1}, the actual amount which permeates through a membrane; the membrane thickness will be mentioned separately; Barrer will *not* be used, this is not a SI-unit and the membrane thickness is not always known. For some separation mechanisms the diffusion through the membrane is not proportional to the pressure difference between feed and permeate, the used unit will then be mentioned separately.

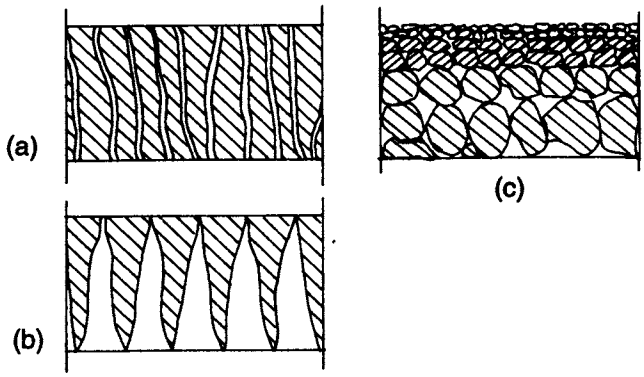

Fig. 12.1. The possible porous structures of inorganic membranes: (a) homogeneous structure; (b) asymmetric structure; (c) composite structure as realized in ceramic membranes.

nm (glass) up to values larger than 1 μm for metal sheets. Homogeneous membranes should be as thin as possible, because otherwise the permeability is too small for practical applications. A more attractive structure for membranes is the asymmetric structure, shown in Fig. 12.1b. However, it is rather difficult to obtain such a structure in inorganic materials. At present there is only *one* commercial ceramic system with such a structure, the anodized alumina of Anotec/Alcan (Table 12.1). This structure is shown in Fig. 12.2. The support side has pores in the order of 200 nm, the top side pores being in the order of 25 nm. Thus far, large tubular surfaces cannot be obtained with this method.

12.2.2 Membrane Preparation

For ceramic or partly ceramic membranes, composite types of structures are easiest to fabricate. Tubes or monolithic elements with several channels can be fabricated by slip-casting, extruding or other ceramic shaping methods. For carbon supports, pyrolysis of polymeric precursor or pressing of carbon material are common techniques. The pore size obtained in these materials can be typically 5–15 μm after sintering at 1400–1600°C (for alumina). The porosity is typically 40–50% or somewhat higher for carbon.

These tubes, multichannels or plates can act as a support for a microfiltration layer with pores of 0.2–1 μm [15,16], a thickness of 10–50 μm and a porosity of 40–50 percent. Terpstra et al. use a suspension of α-Al_2O_3 powder particles for film-coating an alumina layer on a porous support. The thickness of the coated layer can be adjusted by changing the suspension viscosity. This can be done,

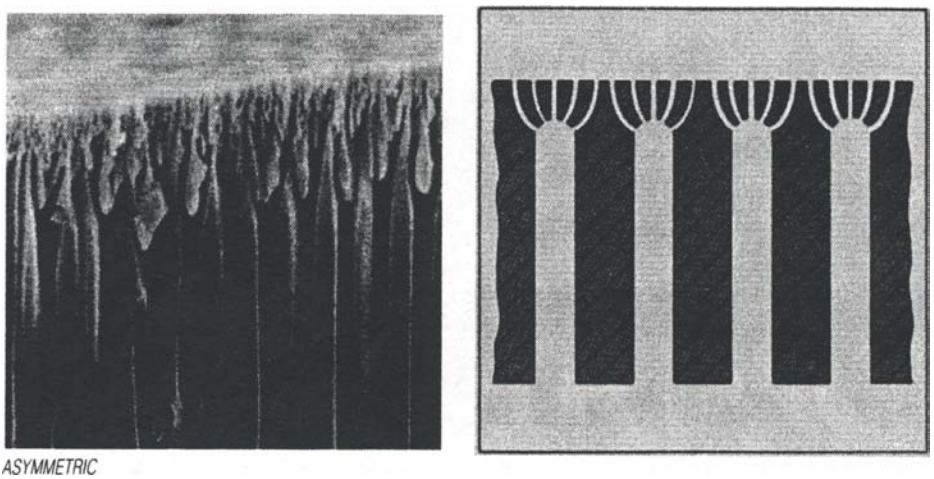

Fig. 12.2. An anodized alumina membrane with an asymmetric structure (picture courtesy of Alcan International Ltd., Banbury, UK).

for instance, by changing the solid contents of the suspension. To prevent the formation of pinholes in the layer, the capillary suction of the pores of the support is suppressed. These types of layers have to be sintered at a temperature between 1200 and 1450°C depending on the powder particle size used and the resulting pore structure.

It is possible to prepare more than one layer on the support, as shown in Fig. 12.3, and, in principle, the number of layers is not limited. The preparation of a second and third layer is based on the same principle. In general, the pore size of the ultimate layer is the smallest, as also holds for the layer thickness. This is obvious, because this layer determines selectivity and the permeability of the total membrane system.

This technique is suitable to apply layers with pore sizes ranging from 50 to 5000 nm. On carbon tubes, very fine ZrO_2 suspensions are used which results in pore sizes in the order of 10 nm [17].

The above-mentioned suspensions are prepared by milling standard powders but even finer particles can be obtained by the hydrolysis of salts or alkoxides of, e.g., Al(III), Ti(IV), Zr(IV), Si(IV) or other ions. By good control of the physical and chemical parameters, colloidal suspensions (sols) are then obtained.

With these suspensions, so-called sol–gel techniques can be applied using the capillary force of the support [18] or suppressing the capillary force of the support (see, e.g., Ref. [19]). The advantage of using the support capillary force is that the adherence between top layer and support is very good, a sharp pore size distribution is obtained and a layer thickness up to 10 μm can easily be achieved within 10 seconds with this cake filtration (slip casting) process. A

Fig. 12.3. SEM picture of an all-alumina membrane consisting of a macroporous support, two film coating layers with pores of 0.2 and 1 μm and an sol–gel top layer with a thickness of 8 μm and with pores of the order of 3 nm.

difficulty is that the support quality should be very good and that the pore size in the top of the support should not be larger than 1 μm because otherwise, the capillary force at the beginning of the slip-casting process is too weak. It is obvious from Fig. 12.3 that not only can the macroporous support be used as a carrier for the top layer but that also multilayer supports with some microfiltration layers can act as a support for the top layer.

The disadvantage of suppressing the capillary force is that the adherence is less strong, the pore size distribution is less sharp and the layer thickness is more difficult to control. Also in this case, the viscosity of the *colloidal* suspension is the most important parameter in controlling the thickness. For thicknesses more than 10 μm, multiple dipping procedures are necessary.

To obtain crack-free membrane top layers in this way, process parameters like drying, calcining and sintering have to be carefully controlled. In most cases organic additives are used as drying-controlled chemical agents (DCCA) or to adjust the viscosity of the colloidal suspension. These additives are burned out during the calcination and sintering process. The pore size and pore size distribution in the final product are more or less affected by the use of the additives.

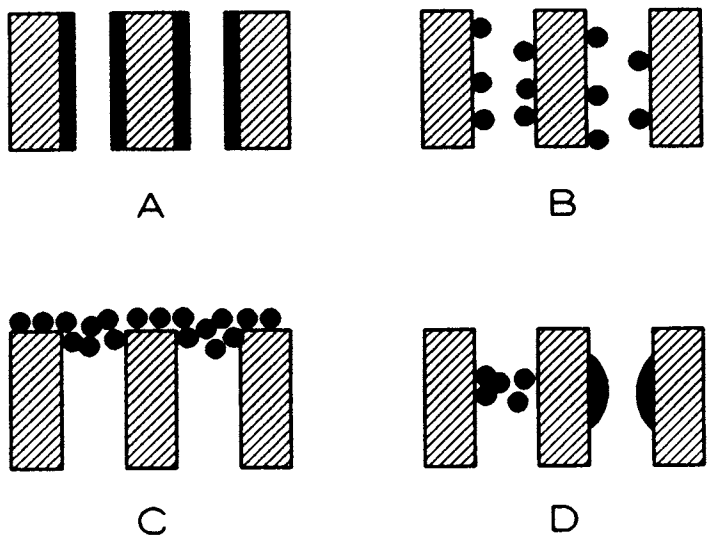

Fig. 12.4. Schematic representation of the modified membrane toplayer structures: (A) monolayer or multilayer deposit; (B) nanoparticles within pore, partial plugging; (C) plugs in the pore entrance, film on top of the membrane; (D) plugs or constrictions at a certain site in the top layer.

In this way, alumina and titania top layers are prepared on porous oxides or glass supports [18–21]. ZrO_2 top layers are prepared on carbon [22] and on alumina supports [19] and silica top layers on alumina supports [23,24]. The porous structure of all these top layers with thicknesses less than 10 μm ranges from mesoporous to macroporous ($d_p > 3$ nm). Microporous systems ($d_p < 2$ nm) cannot be achieved with the technique using colloidal suspensions. These structures are suitable for gas separation by Knudsen diffusion transport, as shown in Table 12.2, surface diffusion, multilayer diffusion and capillary condensation. Effective transport by surface diffusion, multilayer diffusion or capillary condensation is only possible in pores smaller than 10 nm.

Furthermore, the mesoporous membrane systems (obtained commercially or in laboratory experiments) can be modified, as shown in Fig. 12.4, in order to obtain microporous or dense systems in a very thin layer (< 100 nm, Fig. 12.4C).

12.2.3 Membrane Modification

In Fig. 12.4, the nanostructures of modified inorganic membrane top layers are shown. Structure A is obtained by depositing a monolayer or a multilayer on the surface of the top layer pores. This type of modification can bring the pore size into the microporous range or gives the internal top layer surface a catalytic activity in nonseparative applications (see following sections). The same holds for structure B in which nanoparticles are deposited instead of a

continuous layer. There are techniques in which only the top layer is modified and even the site of the modification within the top layer can be controlled [25–27]. Structure C is obtained by depositing a polymeric gel on top or partly in the membrane top layer [10,28–33]. By controlling pH and temperature, tetraethylorthosilicate or other alkoxide components can be polymerized with a distinct amount of water and the inorganic polymer chain length and chain branching can be controlled. Inorganic polymers with a molecular weight smaller than 1000 and having straight chains can be obtained and packed thoroughly on top or partly in the membrane top layer. A pore size of 1 nm or less can be obtained in a layer of about a 50 nm thickness. The thermal stability of silica chains is high and the structure can be maintained up to 700°C. The water sensitivity of silica can be suppressed by using inorganic copolymers.

Structure D is realized by Chemical Vapor Deposition (CVD) techniques in which a metal organic component enters from one side of the membrane and a reactant (like water) enters from the other side of the membrane. The membrane can be homogeneous (Vycor glass [34–37] or a composite system [92]. Depending on the structure of the material and the process parameters the deposition will be dense or (micro)porous and will be located somewhere within the membrane or the membrane top layer. Thicknesses can vary between 100 nm and several microns, but the process itself is not completely established at present.

The conclusions from this section are that, based on materials science principles, all kinds of structures in the macroporous/mesoporous, microporous or dense regimes can be obtained. There are some limits in the thickness of the selective layer obtained which are related to the material process parameters but also to the quality of the support structure.

In ceramic composite membrane systems modification techniques, which result in microporous systems and dense structures, are possible. The research and development of micropore systems and ultrathin, dense systems with controlled properties is, however, in its infancy.

12.3 TRANSPORT OF GASES THROUGH MEMBRANES

Abundant literature has been published concerning transport of gases and vapors through porous and dense materials. Graham (1833) published early quantitative data in one of the first issues of *Philosophical Magazine*, and since that time, the amount of papers has increased steadily. For membrane applications it is, however, appropriate to restrict ourselves to the transport regimes that can be related to the membrane structures which are obtainable. An additional approach is that equations for gas and vapor transport are simplified to useful equations for process engineers, materials scientists and engineers and

membrane experts. In this chapter gas transport through porous media is related to the pore size classification shown in Table 12.3.

12.3.1 Pore size $d_p > 50$ nm

In this regime, Knudsen diffusion, bulk diffusion and laminar flow occur (we exclude turbulent flow at pore sizes larger than 5 μm). These transport mechanisms hold for a single gas. If a pressure gradient is applied in this regime where laminar flow is present, the bulk diffusion is less than 1% of the laminar flow, so bulk diffusion is omitted in the transport equation.

The transport equation then becomes [28–31,38–40]:

$$F_o = \frac{2\varepsilon\mu_k \bar{v}\, \bar{r}}{3RT} + \frac{\varepsilon\mu_p r^2}{8\eta RT}\bar{P} \tag{12.2}$$

where F_o is the total permeability (mol m^{-2} s^{-1} Pa^{-1}), ε is the porosity, r is the modal pore radius of the medium (m), μ_k and μ_p are shape factors — which are both, in general, equal to the reciprocal tortuosity of the medium (which may vary between 2 and 10), R is the gas constant (= 8.31 J mol^{-1} K^{-1}), T is the absolute temperature (K), P is the mean pressure (Pa), η is the viscosity of the gas (in Pa s^{-1}) and v is the average molecular velocity (m s^{-1}), which is:

$$\bar{v} = \sqrt{\frac{8RT}{\pi M}} \tag{12.3}$$

where M is the molecular mass of a gas molecule.

The first term on the right-hand side represents the Knudsen diffusion, the second term is the laminar-flow contribution. In Fig. 12.5 the N_2 permeability of a 2-mm-thick homogeneous support is shown with pores of 120 nm and a porosity of 45% (see arrow). From this curve the Knudsen diffusion contribution is easily found at an average pressure $P = 0$. The laminar-flow contribution is represented by the slope of the curve and increases with increasing average pressure as expected from Eq. 12.2. This is easily understood, because the mean free path of the molecules — as well as the Knudsen number — becomes smaller with increasing pressure (Eq. 12.1).

If the permeability of one gas is measured for a certain membrane material, the permeability of a second gas (e.g., He or Ar) can be calculated quite accurately (to within 5%). The only parameters are the molecular mass and the viscosity of the gas. At $P = 0$ the permeability ratio between two gases A and B is:

$$\alpha^* = \frac{F_o^A}{F_o^B} = \sqrt{\frac{M_B}{M_A}} \tag{12.4}$$

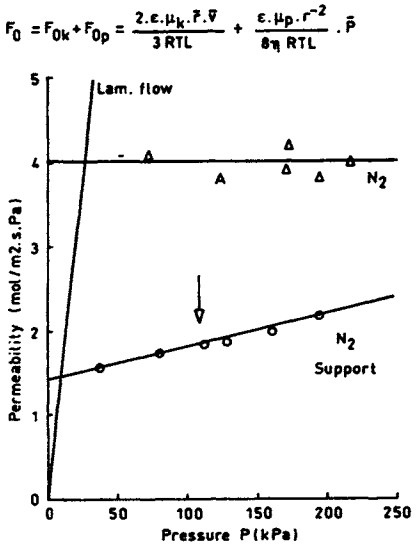

Fig. 12.5. The N_2 permeability of an alumina porous support (see arrow) with a pore size of 120 nm, a thickness of 2 mm, a porosity of 45%, and a shape factor of 0.4. Curve A represents the permeability of the top layer with a pore size of 3 nm, a thickness of 3 μm, a porosity of 50% and a shape factor of 0.16. The laminar-flow curve is shown as an example.

where M_A and M_B represent the masses of molecules A and B respectively.

At higher pressures the viscosity η of gas B (viz. He or Ar) should be taken into account. In this way it is possible to determine the permselectivity of several gases for this membrane material by measuring only *one gas* as a function of the average pressure. This permselectivity is always smaller than α^* mentioned in Table 12.2 because of the laminar-flow contribution.

However, the measurement of pure gas permeability *cannot* be used for *multigas* transport through the same membrane. There are several reasons for the differences in measuring single gas or multigas transport through membranes with pores larger than 50 nm. The three main reasons for this are:

(a) There will be a momentum exchange between the molecules of different masses. In that case gas transport is described with complex models [1] or the dusty gas model [41].

(b) The pressure ratio P_r (defined as the back pressure divided by the feed pressure). The actual separation factor α will then be

$$\alpha = 1 + \frac{(1 - P_r)(\alpha^* - 1)}{1 + P_r(1 - y)(\alpha^* - 1)} \tag{12.5}$$

where

$$\alpha = \frac{y}{1-y} \cdot \frac{1-x}{x}$$

where y is the mole fraction of the faster permeating component in the permeate and x is the mole fraction of this component in the feed. At $P_r = 0$, α is equal to α^* if other factors in the change of α are omitted. Haraya et al. [3–5] have shown some experimental data of this phenomenon.

(c) Concentration polarization, which occurs rather quickly in a cross-flow situation because of the high permeabilities of these porous membranes [4].

Reasons (b) and (c) are related to process parameters and, therefore, also occur in membrane systems with pores smaller than 50 nm.

In all these cases the multigas transport selectivity is smaller than the selectivity defined by the ratio of single gas permeability. Optimization of process parameters is therefore one of the major research goals in gas transport through pores larger than 2 nm and, for this reason, a lot of effort is applied in the UF_6 separation.

12.3.2 Pore Size 2 nm < d_p < 50 nm

In this pore region the laminar-flow contribution becomes less important and at pressures smaller than 1 MPa the gas transport through the porous membrane becomes independent of the average pressure, as shown in Fig. 12.5 (curve A). This curve represents the calculated permeability of an alumina top layer with a thickness of 3 μm, a porosity of 50% and a tortuosity of 0.16 on a porous support (see arrow). The pore size of the top layer is 3 nm. The calculation method is shown elsewhere [38]. For this situation the laminar-flow term, as presented in Eq. 12.2, is negligible. In this pore regime, two other transport mechanisms become more important; surface diffusion and multilayer diffusion/capillary condensation.

Surface diffusion occurs if one or several of the gases in a mixture, which transport through the membrane, experiences an interaction with the material of the pore wall. There are at least three models to describe the transport of these types of gases along the surface: the hydrodynamic model, the hopping model and the random walk model.

The last one is based on a two-dimensional form of Fick's law:

$$|F_s| = A\,\rho_{app}\,D_s\,\mu_s\,\frac{dq}{dl} \tag{12.7}$$

where F_s is the surface transport (kg m^{-3}), A the outer surface area (m^2), ρ_{app} the apparent density (kg/m^3), D_s the surface diffusion coefficient (m^2 s^{-1}) and dq/dl the gradient in surface occupation.

In rewriting the surface diffusion transport [28–31], one finds that:

$$F_{oS} = \frac{|F_s|}{\Delta P} = \frac{2\varepsilon \mu_s D_s}{\bar{r} A_o N_{AV}} \frac{dx_s}{dP} \tag{12.8}$$

where μ_s is the surface diffusion shape factor, A_o is the surface area occupied by one molecule (m^2), N_{AV} is Avogadro's number, and x_s is the fractional occupation of the surface in relation to a monolayer.

Surface diffusion and Knudsen diffusion can be treated as a combined transport, so for pores with $2 < d_p < 50$ nm the total permeability F_o is:

$$F_o = F_{oK} + F_{oS} = \frac{2\varepsilon \mu_k v \bar{r}}{3RT} + \frac{2\varepsilon \mu_s D_s}{\bar{r} A_o N_{AV}} \cdot \frac{dx_s}{dp} \tag{12.9}$$

If the nonmaterial parameters are lumped together, it follows that:

$$F_o = \varepsilon\mu\left(A\bar{r} + B\frac{1}{\bar{r}}\right) \tag{12.10}$$

under the assumption that $\mu = \mu_k = \mu_s$ and that the effective r is not changed by the amount adsorbed.

The surface diffusion *contribution* increases, then, with decreasing pore size. However the effectiveness of surface diffusion is dependent on the value of D_s times dx_s/dP (amount adsorbed as a function of pressure). These two parameters conflict with each other. On a given surface the amount of physically/chemically adsorbed molecules can be increased by increasing the adsorption/interaction energy. The energy of diffusion/migration, which is coupled to the energy of adsorption, is then also increased, which results in a lower mobility over the surface. The reverse is also true.

The disadvantage of *physical* adsorption is that it is not very selective for a distinct gas and therefore generally does not increase the separation efficiency.

The ratio between surface diffusion and gas diffusion is limited, i.e., for CO_2 on alumina or for Vycor-type glass this value is about 0.4 to 2. For CH_4 this value on the same materials is smaller than 0.3. This means, for instance, that CH_4/CO_2 surface diffusion has a negative effect on the separation of CH_4/CO_2 in mesoporous systems. CH_4 transport according to Knudsen diffusion is faster than that of CO_2 (Table 12.2: $\alpha^* = 1.65$), according to surface diffusion it is slower. The total effect is that there is almost *no* separation. The same holds for the separation of hydrocarbons like C_2H_6, C_3H_6 or i-butane from low-mass molecules [42–44]. The trend is that heavier molecules show larger surface diffusion, which *counteracts* the separation efficiency by Knudsen diffusion. Oxygen and nitrogen show *no* measurable surface diffusion on oxides and *some* surface diffusion on carbon types of materials.

Almost all literature data are shown at pressures between 0–100 kPa and temperatures between 0 and 100°C. At higher pressures and temperatures the surface diffusion *contribution* in relation with gas diffusion is smaller (e.g. Ref. [30]).

TABLE 12.4
Critical constants and saturated vapor pressure at 20°C for a number of gases [93,94]

Gas	T_c(°C)	P_c (MPa)	P_o(20°C)* (10^{+5} Pa)
CO_2	31	7.3	57.1
NH_3	132.5	11.3	8.7
H_2S	100.4	8.9	17.9
SO_2	157.8	7.8	3.6
H_2O	374	21.8	0.023
CH_4	–82	4.6	–
O_2	–118	5.0	–
N_2	–147	3.4	–
C_2H_6	32	4.8	37.5
C_2H_4	9.9	5.1	–
C_3H_8	96.8	4.2	8.40
C_3H_6	92	4.5	10.17
n-C_4H_{10}	152	3.8	2.08
n-C_4H_8	146	4.0	2.51

One exception is H_2 surface diffusion. It can occur at some higher temperatures (up to 300°C [30]) in the presence of precious metals (Pt, Pd or Ag). The pressure should, however, be low ($P < 50$ kPa) for a contribution in relation with gas diffusion of over 100%. Uhlhorn et al. [30] found that the surface diffusion of H_2 could be two times the gas diffusion in a silver modified alumina membrane. The advantage is that Knudsen diffusion for H_2 is faster than for any other gas. In this way a H_2-to-N_2 transport ratio of about 9 could be found.

In summary, surface diffusion seems to be less suitable for enhancing gas separation with mesoporous materials with the possible exeption of a H_2/other gas separation on precious metal modified membranes.

If the temperature is decreased and the pressure is increased multilayer diffusion and capillary condensation in mesoporous systems can occur. The gas (vapor) should in those cases be near or under the critical temperature. In Table 12.4 critical parameters and the vapor pressure at room temperature are shown for a number of gases. Near room temperature most of those gases are condensable except for O_2, N_2 and CH_4 and will show surface/multilayer diffusion by physical adsorption in oxidic or carbon types of membranes.

At a certain pressure at the high pressure side of the membrane the vapor will condense in the porous structure of the membrane according to the Kelvin equation:

$$\ln \frac{P_t}{P_o} = \frac{2\gamma V_m \cos\theta}{r' RT} \tag{12.11}$$

where P_t is the capillary condensation pressure (Pa), P_o the saturated vapor pressure (Pa), γ the interfacial tension (N m^{-1}), θ the contact (wetting) angle, r' the actual radius of a cylindrical-shaped pore and V_m the molar volume of the *liquid* component (m^{-3} mol^{-1}).

It should be noted that r' is effectively smaller than the pore radius itself because of adsorption of vapor before condensation (t-layer).

In most cases capillary condensation takes place at 0.5–0.8 of the saturated vapor pressure P_o. Although a number of regimes can be distinguished with this kind of transport [45] two regimes are most important:

(a) multilayer adsorption across the entire pore surface so the actual pressure in the membrane is always smaller than the capillary condensation pressure. This adsorption can introduce an extra transport of a larger vapor molecule along the surface in comparison with a smaller gas molecule. As an example, the transport of N_2 and C_3H_6 molecules through mesoporous membranes is shown. The Knudsen gas diffusion ratio for N_2 and C_3H_6 is 0.82 and is valid for low relative pressures of propene (see also Eq. 12.11). At higher relative pressures of propene this ratio increases to 1 and changes to 1.5 at a relative pressure of 0.42 for C_3H_6 as shown in Fig. 12.6A. This means that propene, as the larger molecule, permeates *faster* through the membrane than the smaller nitrogen molecule.

In a N_2-C_3H_6 gas mixture the separation factor α as defined in Eq. 12.6 is 2.0. This value is larger than the ratio of 1.5 for pure gas permeabilities because of a partial blockage of the pores for N_2. For the gas phase transport of N_2 a smaller effective pore size is available (see previous sections).

(b) capillary condensation at the feed side and multilayer diffusion at the permeate side.

Now a part of the pores is filled with *liquid* and the pore is blocked for any gas transport. Then the permselectivity increases further. At a relative pressure of 0.78 at the feed side, the C_3H_6/N_2 in pure gas permeation is 7.1 [10,46]. In a gas mixture the separation factor is 13 as shown in Fig. 12.6B due to blocking of the pore for N_2 transport and the low solubility of N_2 in a C_3H_6 *liquid*. However this value should be larger, as shown by Barrer [47], for a H_2/SO_2 mixture through a carbon plug. He found enrichment factors of 1000 for SO_2 at P/P_o of 0.75. It can therefore be concluded that some pores of the alumina top layer are not filled with liquid. This can be due to the presence of some larger pores (order 10 nm) and to an incomplete wetting of propene on alumina.

Permeabilities are extremely large (3×10^{-5} mol m^{-2} s^{-1} Pa^{-1} is equal to 6500 Nm^{-3} m^{-2} day^{-1} bar^{-1} for propylene) as shown in Fig. 12.6A. The actual separation can be increased to 75 at the same relative pressure by modification of the

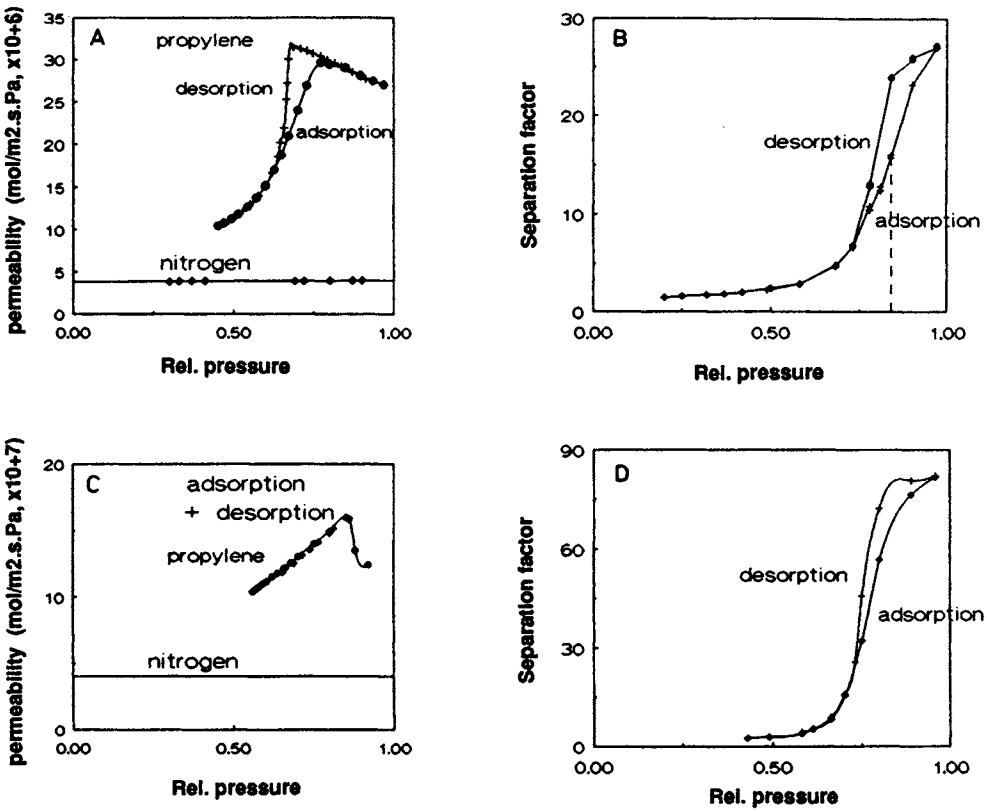

Fig. 12.6. (A) Permeability of a supported γ-alumina thin film for nitrogen and propylene at 263 K as a function of the relative vapor pressure of propylene. (B) The separation factor of a propylene-nitrogen mixture with the same membrane, where propylene is the preferentially permeating component; dashed line gives the relative pressure at which the maximum in the permeability of Fig. 12.6A occurs. (C) As (A) but for a magnesia-supported γ-Al_2O_3 thin film. (D) As (B) but for a magnesia supported γ-Al_2O_3 thin film.

top layer with magnesia (Fig. 12.6D). Then larger pores are also blocked. The permeability then decreases to 15×10^{-7} mol m^{-2} s^{-1} Pa^{-1}, which is equal to 300 Nm^3 m^{-2} day^{-1} bar^{-1} propene (Fig. 12.6C).

It should be noted the value of α drops to less than 5 if the capillary condensation disappears ($P_t/P_o < 0.5$ in this case). Another interesting example of capillary condensation is the separation of water with an alumina/silica composite membrane from hydrocarbons, alcohols or solvents like acetone or DMF at slightly elevated temperatures (~ 100°C). The values of α can be considerably high (α > 100 [48,49]). The water permeability is dependent on the water content in the vapor mixture. At 20% of water this permeability is $1.3.10^{-2}$ mol m^{-2} s^{-1} or 20 l H_2O (liquid) m^{-2} day^{-1} for a water/alcohol (solvent) mixture at atmospheric pressure. The permeate concentration of water is close to zero.

The exact mechanism is not known, but perhaps preferential adsorption of water and good wetting plays an important role. Azeotropic points can be easily bypassed by this separation mechanism.

In summary: with pore size in the range of 2–50 nm the optimal Knudsen factor α^* as shown in Table 12.2, can be reached if appropriate process parameters are chosen. Surface diffusion is *not* an effective mechanism for increasing the Knudsen separation factor. An exception holds for H_2 at low pressures (< 50 kPa) if the membrane is modified with a large amount of metals like Pd, Pt, Ag. Capillary condensation can be an effective separation mechanism for gas mixtures containing a condensable component.

12.3.3 Pore Size d_p < 2 nm

It is extremely difficult to characterize pore diameters quantitatively in the range 0–2 nm. Capillary condensation does not take place in such small pores, and models on gas transport through these types of pores are still in their infancy.

In carbon molecular sieve membranes, Koresh and Soffer [50,51] tried to develop a model based on analysis of potential energy profiles of a molecule in very small pores. Uhlhorn [10] tried to develop such a qualitative model for a silica-type material. In Fig. 12.7 the potential energy E of a molecule of radius r is shown as a function of the distance d between the walls. If the walls are far apart (Fig. 12.7A), potential minima near the wall occur due to attractive forces of the molecule–wall interaction. These potential minima start to overlap when the walls are brought together (Fig. 12.7B) and finally overlap completely (Fig.

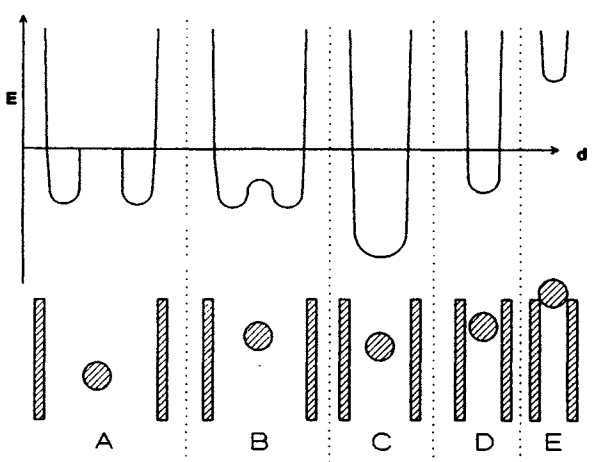

Fig. 12.7. Potential energy E of a molecule of radius r as a function of distance d between the pore walls: (A) distance > 2 nm; (B) distance 1–2 nm; (C) distance 2–3 molecule diameters; (D) distance 1–2 molecule diameters; (E) distance < 1 molecular diameter.

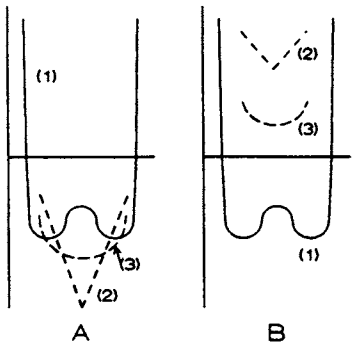

Fig. 12.8. Interaction energy plotted against the distance d between the pore walls for the case of Fig. 12.7B with an additional attractive potential (A) or repulsive potential (B); 1 = potential of Fig. 12.7B, (2) specific interaction, (3) resultant curve.

12.7C). This gives rise to one potential minimum due to attractive interaction between the molecule and *both* walls (see also Refs. [36,37]). As the walls come even closer to each other, the minimum is raised due to the overlap of the repulsive part of the energy potential of the molecule–wall interaction until the pore becomes impermeable (Fig. 12.7E). Figure 12.7 takes only the size effects of the molecule into account. Also attractive and repulsive forces of a different nature can exist. The specific interactions (e.g. dipole–dipole interactions) should be added to the potential energy curves as shown in Fig. 12.8. In Fig. 12.8 a random attractive force is added to the situation presented in Fig. 12.7B. In Fig. 12.8 it is shown that specific interactions can lower the potential minima (Fig. 12.8A) as well as increase these minima (Fig. 12.7B). In this way it is possible to make a pore effectively impermeable to a molecule even if the size of the molecule permits its entrance in the pore. The qualitative picture of Figs. 12.7 and 12.8 shows that in *pores* with *molecular dimensions* the *size of the molecules* and *specific molecule–wall interactions* can lead to distinct differences in potential energy *barriers* and therefore the *transport rate*. These short-range interactions become important, when the pore diameter is not larger than approximately 3 times the molecule diameter.

As shown in Table 12.5, surprising effects can take place for the separation of O_2/N_2 in molecular sieve carbon membranes [50] with a reasonable permeability at room temperature. A permeability ratio for O_2-to-N_2 of 7 is found with a permeability of oxygen of 12 $m^3\,m^{-2}\,bar^{-1}\,day^{-1}$.

Most reported results with microporous membranes concern the permeability of hydrogen in comparison with the transport of other gases. In Table 12.6, data concerning some of these separations are shown. There is a wide variety of separation factors and permeabilities. Very high separation factors can be achieved (> 1000) but the permeability is lower for the more selective membranes. The separation factor can increase as well with a decrease in

TABLE 12.5

Permeabilities and permselectivities at room temperature of 3 gases through a molecular sieve carbon membrane according to Ref. [50]

Gas	Permeability $m^3\ m^{-2}\ bar^{-1}\ day^{-1}$	permeability $mol\ m^{-2}\ s^{-1}\ Pa^{-1}\ (10^{-8})$	Selectivity mixture
O_2	12	5.4	$O_2/N_2 = 7$
N_2	1.6	0.8	$He/N_2 = 21$
He	35	16.4	$He/O_2 = 3$

Thickness of carbon membrane is 6 μm; an organic hollow fiber membrane is pyrolized at 800°C and activated two times by slight oxidation at 600°C.

TABLE 12.6

Separation factors α and permeabilities of H_2 in comparison with other gases by diffusion through microporous and dense membranes

Gas mixture	α	Permeability $m^3\ m^{-2}\ bar^{-1}\ day^{-1}$	$mol\ m^{-2}\ s^{-1}\ Pa(10^{-8})$	Temp. (°C)	Material	Ref.
H_2/C_3H_6	160	300	160	200	SiO_2	[10]
H_2/CH_4	200	300	160	150	SiO_2-TiO_2	
H_2/N_2	2000	3	1.6	450	$SiO_{2\text{-glass}}$	[34]
H_2/N_2	12	0.8	0.4	200	SiO_2-glass	[36,37]
H_2/CH_4	56	21	11	200	carbon	[51]
	32	35	18	200	carbon	
	35	16	8	25	carbon	
H_2/any	>1000	0.1–2*	–	200	Pd metal	[54]

* The feed and permeate pressure are 1 and 0 resp.; the membrane thickness is 200 and 1 μm respectively.

temperature depending on the activation transport for a distinct molecule. This is one of the criteria used to discriminate between micropores and mesopores. The transport rate in mesopores *decreases* with temperature, in micropores *increases* with temperature. The activation energies in porous sytems are in most cases small (< 10 kJ mol^{-1}), which is smaller than in dense systems. Activation energies for H_2 transport in dense materials are at least 20 kJ mol^{-1}.

In silica systems all kind of structures and layer thicknesses (50–200 nm) can be obtained with sol–gel and vapor deposition techniques but because of the small scale of the structure at present process control is difficult and still a matter of research. A second problem with the use of silica is the sensitivity of the structure to water. The microporous silica structure densifies in the

presence of water and the permeability decreases. In several groups including ours, research is carried out to suppress this chemical instability.

To optimize process control it is necessary to know the microporous structure as a function of the process parameters. Physical and chemical characterization is then a must and gas adsorption, as a function of pressure and temperature, is a good possibility in combination with the transport properties of several gases. A problem is that pore size calculations in the microporous region are not easy and the theories are still in development. Physical adsorption and permporometry can, however, be used as a finger print characterization method for the actual structure.

With more structural information, gas separation can be better controlled and directed to gas mixtures not including H_2. Uhlhorn [10,32] has already found a preferential transport of CO_2 over CH_4 with leads to a separation factor of a gas mixture 50 CO_2–50 CH_4 of 60 at a temperature of 100°C. These kinds of results change drastically, however if the preparation procedure is not carefully controlled. Furthermore it seems that elevated temperatures (100°C–300°C) are necessary for more optimal separation properties.

In activated carbon [50,51] the structure can also be varied from dense to microporous in all varieties by partial oxidation (activation) at a temperature of at least 400°C. It seems that room temperature gas transport properties are somewhat better than in silica but at elevated temperatures the properties do not improve as is the case for silica-type membranes.

The conclusion is that with microporous structures, which are obtained by modification of mesoporous/macroporous structures, high H_2 separation selectivities can be obtained while good possibilities exist for other gases. Selectivities, but especially permeabilities, are better at elevated temperatures. The structural sensitivity of silica systems to water should, however, be improved. Physical and chemical characterization of the microporous structure during preparation is a must for better control of that microporous structure and thus a control of the separation properties.

12.3.4 Dense Membranes; Pore Size d_p = 0 nm.

The transition from microporous to dense materials is a gradual one especially in silica systems (e.g., from microporous silica to silica glass). This is especially true for ultrathin- and/or ultrafine-grained materials where grain boundaries can hardly be distinguished from micropores and where nanoparticles and microdomains in glass have similar dimensions. A criterium to distinguish between dense and microporous material can probably be found in the activation energy of the transport and in the adsorption capacity. In denser materials the transport (diffusion) is more strongly activated than in microporous systems. Besides dense silica (only for H_2 and He transport) other dense

inorganic materials can act as membrane materials. In this chapter three types of materials are mentioned:

(a) immobilized inorganic liquids (LIM) incorporated in porous structures;
(b) dense metal sheets based on palladium (Pd);
(c) dense ceramics with oxygen ion conduction.

(a) Immobilized Inorganic Liquids

Inorganic salts with relatively low melting points can be immobilized as a liquid in porous solids due to the capillary forces of the porous solid [52,53]. The porous solid is a metal or a ceramic. The wetting of the liquid should be good, otherwise the immobilization becomes poor. The Young–Laplace equation can be used to determine the blow-out pressure ΔP:

$$\Delta P = \frac{2\,\gamma \cos\theta}{r} \tag{12.12}$$

where γ is the interfacial tension (N m^{-1}), θ is the wetting angle and r is the equivalent spherical pore radius.

In two patents Pez and Carlin [52,53] give some results for the transport properties that can be achieved, and some examples are shown in Table 12.7. In immobilized liquid $LiNO_3$ (mp 270°C) O_2/N_2 separation is possible with a

TABLE 12.7

Gas separation properties with dense membrane materials

Membrane material	Gas	Permeability (mol m^{-2} s^{-1})	Permeability (mol m^{-2} day^{-1})	Temp. (°C)	Ref.
$LiNO_3$/porous metal	O_2	3.5×10^{-7}/Pa	70/bar	429	[52,53]
	N_2	2.0×10^{-9}/Pa	0.4/bar	429	
$ZnCl_2$/porous metal	NH_3	4.9×10^{-6}/Pa	950	311	[52,53]
	H_2	1.5×10^{-9}/Pa	0.3	311	
	N_2	–	–	311	
Pd (200–1 μm) dense	H_2	–	0.1–2	200	[54]
ZrO_2-Y_2O_3*	O_2	$(3–20)\times10^{-6}$	0.006–0.04	1200	[95]
Bi_2O_3-Er_2O_3*	O_2	8×10^{-5}	0.15	800	[55]
$La_{0.6}Sr_{0.4}CoO_3$*	O_2	2.5×10^{-3}	5	850	[56]
$SrCo_{0.8}Fe_{0.2}O_3$*	O_2	2.3×10^{-2}	45	850	[56]

* The pressure on feed and permeate side are 100 kPa and 10 Pa, respectively. The permeability is in this case proportional to ln (P_f/P_p) where P_f and P_p are feed pressure and permeate pressure, respectively.

** The pressure on feed and permeate side are 3 kPa and 1 Pa respectively. The membrane thickness is 0.5 μm.

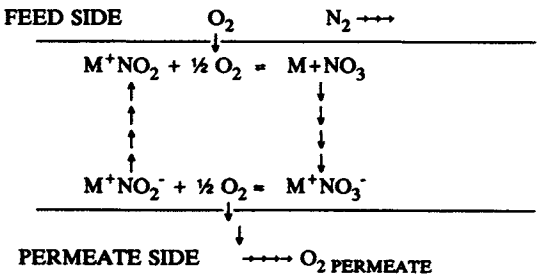

Fig. 12.9. Simplified transport scheme of nitrate and nitrite ions through a molten $LiNO_3$ to permeate oxygen.

largest observed separation factor α equal to 170 and a permeability for oxygen of 70 $m^3\ m^{-2}\ bar^{-1}\ day^{-1}$.

The transport mechanism includes interconversion between nitrate and nitrite ions according to the reaction:

$$2\ NO_3^- \rightleftharpoons 2\ NO_2^- + O_2 \tag{12.13}$$

In the liquid nitrite and nitrate, ions are transported according to the scheme shown in Fig. 12.9. Some oxygen and nitrogen molecules are transported by solution/diffusion but only a minor amount.

$ZnCl_2$ (mp 283°C) can transport ammonia by the formation of a zinc ammoniate complex. The formation of this complex is very fast and the permeability of ammonia can be very high (about 1000 $m^3\ m^{-2}\ bar^{-1}\ day^{-1}$, Table 12.7). For the transport mechanism there is also a simplified scheme, shown in Fig. 12.10. The separations factors (NH_3/N_2 and NH_3/H_2) are both over 1000.

Of course these reactions are also possible with other types of low- melting immobilized salts. In practice, serious problems arise. In the first place, the solid/liquid transition of the salt can be a problem because of expansion or

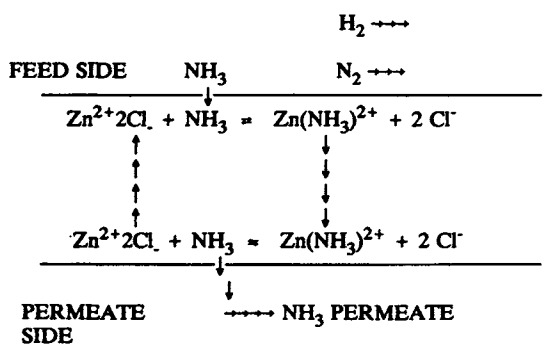

Fig. 12.10. Simplified scheme of zinc–ammonium complexes through an immobilized $ZnCl_2$ molten salt.

shrinkage of the liquid. Secondly, the salt should wet the porous solid structure; thirdly, the salt should *not* react with the basic porous structure, and in the fourth place, side reactions with present impurities as well as a slow decomposition of the salt can take place. Water is one of the components that can destroy the given reaction path. It is, however, worthwhile to do more research in this direction.

(b) Dense Metal Sheets

Atomic hydrogen can easily dissolve in palladium and palladium alloys (with Ag, Ru, Ni, etc.). Sheets and sheets in tubular form can be prepared easily in thicknesses of 20 μm or less. Therefore these sheets can act as membranes for selective transport of H_2. At 200°C the permeability is relatively low (Table 12.6 and 12.7). At higher temperatures (400–500°C) transport can be of the order of 10–20 $m^3\ m^{-2}\ day^{-1}$. The permeability is *not* proportional to the partial pressure difference of H_2 but one may approximate the permeation by a half-power pressure law [54]. The selectivity is, in principle, infinite.

The problems with dense Pd films arise from the α–β phase transition of palladium and the dissolving mechanism of H_2 in the metal. Both are coupled with volume changes (expansion) of the metal sheet. The sheet becomes brittle and can crack or even disintegrate. The price of these precious metals for large-scale applications can also be a problem.

(c) Dense Ceramics (Oxygen Ion Conductors)

Dense ceramic systems are in principle impermeable for gas molecules. However, some oxide materials can transport oxygen as oxygen ions or hydrogen as protons at elevated temperatures. Oxygen ion transport becomes substantial at temperatures higher than 600°C. Some data are shown in Table 12.7 for oxygen transport through dense oxygen ion conductors. These figures are for *pressure*-driven transport. If an electrical potential difference is applied these figures are higher especially for stabilized ZrO_2 and stabilized Bi_2O_3. This occurs because only *neutral* species can be transported in the membrane, i.e. a combination of an negative oxygen ion and a positive electron hole (or a positive oxygen ion vacancy and an electron both in the opposite direction). With electrical potential, permeation holes or electrons are delivered by the electrical charge.

Perovskites with high electronic (hole or electron) conductivity are reported to have a good high-temperature O_2 permeability. Bouwmeester et al. [55] found, however, a permeability of a factor of 20 lower than the values reported by Teraoka [56], Table 12.7).

Dense metals and inorganic membranes are very selective for H_2 or O_2

transport but permeability is in most cases relatively low and elevated temperatures are needed. With some materials permeability values come close to those obtained in microporous sytems have been obtained. Further improvements might be obtained by making ultrathin membranes of mixed conducting materials.

Liquid immobilized membranes can permeate such distinct gases as O_2 or NH_3 very selectively by facilitated transport, but the membrane performance in these cases is still a matter of research.

12.4 GAS SEPARATION USING INORGANIC MEMBRANES

12.4.1 Types of Gas Separation

In gas separation a number of regimes can be distinguished:

1. Separation of permanent gases at room temperature. Examples are O_2/N_2, H_2/N_2, H_2/CO, H_2/CH_4 or He/CH_4. The requirements for these separations are that selectivities and permeabilities be as high as possible. There are no special requirements for the thermal and chemical stability of membranes used in this type of separation except that the structure has to be stable at high pressures.

2. Separation of condensable gases at room temperature. Examples are CO_2/CH_4, CO/CO_2, H_2O/air,(C_3 and C_4)/(C_1 and C_2), removal of acid gases (HCl, H_2S, SO_2), ammonia or hydrocarbons/air. Chemical stability can play an important role in the choice of the material. Inorganic materials can better stand up to organic environments than can organic materials; the reverse is also true.

3. Separations of condensable gases at higher temperatures (up to 300°C) This is the main field of fractional distillation, e.g., hydrocarbon separation. However, steam/hydrocarbon separation can also be important. Another possibility is water/alcohol separation, for instance, to break an azeotrope and water/solvent separation.

4. Separation of such permanent gases as H_2 or O_2 at higher temperatures up to about 1000°C. The separation becomes more interesting if it is combined with a reaction.

5. A unique case is nonseparative gaseous diffusion and flow through inorganic membranes at higher temperatures for distinct types of reactions. For instance, air with a NO_x impurity can be treated with ammonia in a membrane reactor. The contact between NO_x and NH_3 can be mediated and controlled by a means of a catalytically active membrane in such a way that in the exhaust gas, no NO_x nor NH_3 are present [57]. Even if the concentration of NO_x or other types of impurities change with time, these impurities can be removed in a membrane reactor [58].

The question is, in which cases can an inorganic membrane be applied for one of the five above mentioned gas separation regimes. One should be careful to introduce inorganic membranes in an arbitrary way. Because of market inertness and also because of the typical properties of inorganic membranes, not all gas separation applications are obvious.

12.4.2 Separation of Permanent Gases at Room Temperature

Separations of permanent gases like O_2,CO_2 or H_2 at room temperature (regime 1) are *not* the strongest properties of inorganic membranes. Only in the development of molecular sieve carbon (MSC) membranes some remarkably high values in selectivities and permeabilities of oxygen/nitrogen separation at room temperature have been found compared with other types of membranes [50]. Other types of separation processes like cryogenic distillation or (pressure swing) adsorption are, however, more accepted and also applied in commercial separations.

A very good control of the porous structure of silica can lead to a separation factor α at room temperature for instance a CO_2/CH_4 separation of about 50 with 75 $m^3\ m^{-2}\ bar^{-1}\ day^{-1}$ [10]. This separation factor is comparable with those found in polysulfone membranes, although the permeability is greater in this case. Large surface areas of the microporous silica structure are not prepared yet and a careful control of the preparation procedure is an absolute necessity. Separation of permanent gases with ceramic membranes for use at *room* temperature is commercially problematic due to the existence of well-established efficient techiques.

12.4.3 Separation of Condensable Gases at Room Temperature

The separation of condensable gases at *room* temperature can be of some value. By capillary condensation, a condensable gas can be separated from a less condensable gas or a permanent gas. There are two restrictions for selective separation; the non-condensable or permanent gas should not be soluble in the condensed liquid, and minor components can only be separated by capillary condensation in a limited number of cases. Uhlhorn [10] showed that hydrocarbon separation from permanent gases is possible with high selectivities but only in the capillary condensation regime.

Water removal at room temperature and atmospheric pressure is also possible up to about 60% relative humidity (= 1.4 kPa; see Table 12.4) with mesoporous systems. With microporous systems lower values can be achieved under the condition that the membranes are not sensitive to water. Acid gases can also be removed with a mesoporous membrane but *not* as a minor component (< 1000 ppm). In the case of a minor component, a dense-type membrane is required (e.g., immobilized liquid) which is not yet on the market.

12.4.4 Separation of Condensable Gases at Temperatures between 100 and 300°C.

At elevated temperatures (up to 300°C) capillary condensation for vapor separation has good potential. Asaeda and Du [48,49] and Sakohara et al. [59] have already shown that near 100°C water can be separated from alcohols and solvents with a high separation factor. This application has already been commercialized by NGK/Mitsubishi.

An interesting option in this temperature region is that membrane separation processes replace a part of the fractional distillation, especially for heavy oil fractionation. Although some papers show applications of inorganic membranes in refining processes of petroleum residues [60], not much research has yet started in hydrocarbon separation. It should, however, be interesting to carry out membrane distillation with some of the membrane structures already obtained. The structural resistance of inorganic membranes in organic liquids and vapors is *excellent*.

12.4.5 Separation of H_2 or O_2 at Temperatures Above 250°C

At present, most applications of inorganic membranes point to separation of H_2 from gas mixtures in the temperature regime of 250–700°C ([34,61–73] and others). The reason for this type of separation is quite obvious. Saturated hydrocarbons are of less value than unsaturated ones, so reactions such as:

$$C_n H_{2n+2} \rightleftharpoons C_n H_{2n} + H_2\uparrow \tag{12.14}$$

are important in preparing unsaturated hydrocarbons. The first problem with these types of reactions is that the one-step conversion of this reaction is small (thermodynamically determined), because two molecules are formed from one molecule. High temperatures and low pressures are needed to obtain some conversion with the disadvantage of carbon formation. The second problem is the separation of H_2 with a cryogenic technique (distillation) by cooling to –100°C. Both problems make the already developed processes technically and economically unattractive [73].

The second problem can be solved by using an inorganic membrane separator instead of cryogenic distillation (Fig. 12.11). The separation can be carried out at the same temperature as the reaction. Most authors mentioned are using mesoporous membranes (Al_2O_3 or Vycor glass) with only a limited selectivity according to Knudsen diffusion (Eq. 12.4). Real separation problems, then, are not solved but the conversion per cycle of the reaction is higher also because of high permeability of the porous membrane. As really selective membranes dense-stabilized, Pd (Pd/Ag) or silica-composite membranes can be used as

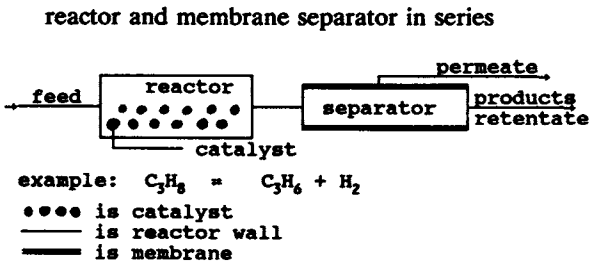

Fig. 12.11. Schematic representation of a reactor and membrane separator for the dehydrogenation of hydrocarbons (or alcohols) in series.

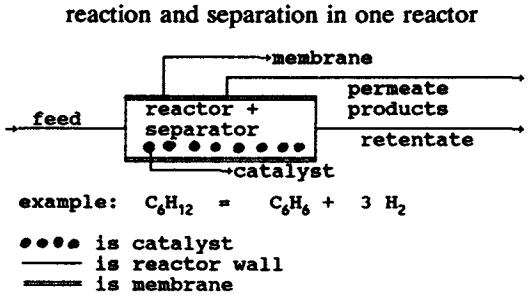

Fig. 12.12. Schematic representation of a single membrane reactor for the dyhrogenation of hydrocarbons (or alcohols) and the separation of H_2.

both have separation factors over 200. However, it makes more sense to incorporate the catalyst in the membrane reactor itself (Fig. 12.12). H_2 formed at the catalyst can then be immediately removed from the reaction side. This can drive the reaction, shown in Eq. 12.14 to completion even at a lower temperature and a higher pressure. The flow conditions in the reactor have to be optimized, however, to remove hydrogen as fast as possible, and the permeability of the membrane for hydrogen should be at least as large as the hydrogen formation. Perhaps a better option is to bring the catalyst on top of the membrane itself. Then the problem arises that the amount of catalyst is limited. The shape and flow properties of the membrane reactor thus become of main importance and the surface area-to-volume ratio of the membrane reactor should be as high as possible.

Fukuda et al. [74] and Kameyama et al. [75–77] tried to use membranes in reactors for the decomposition of H_2S to H_2 and S_2 for increasing the conversion. The used membranes (Al_2O_3 and Vycor glass) had, again, a limited selectivity and were not stable (Vycor glass) at temperatures of 800°C, so conversion improvement was limited.

Until now a combination of dehydrogenation reactions and a highly selective membrane is rarely demonstrated. The main exception is represented by the papers of Gryaznov and coworkers [78,79]. They used (stabilized) Pd membranes with a very high H_2-selectivity for a combination of hydrogenation and dehydrogenation reactions of complex hydrocarbons. The Pd film itself is also the catalyst. On one side of the membrane a dehydrogenation reaction is carried out, the hydrogen diffuses through the Pd(Ag) membrane and, on the other side, the hydrogen is used for a hydrogenation reaction. Because of the low permeability of Pd(Ag) only small-scale reactions seem suitable to use in such a reactor. The problem of heat control is solved, however, in such a reactor because of the coupling of endothermic and exothermic reactions and a large heat transfer over the membrane.

Another type of selective membrane applications in a high temperature reactor is the use of solid electrolyte chemical cells. In Section 12.3.4c permeability properties of solid electrolytes are shown. The oxygen pumped through the membrane (as oxygen ions) can be used in the partial (selective) oxidation of alkanes/alkenes or for other reactions like methane coupling, steam reforming reactions and SO_2 oxidation. The oxygen transport can either be pressure driven in which case a catalyst is needed, or can be driven by an electrical potential where the (metal) electrodes can act as a catalyst. In both cases oxygen ions are transported which can be a very active process in distinct selective oxidation reactions. A review on this type of reactions, which occur in the temperature region of 500–1100°C, is given by Gellings et al. [80].

12.4.6 Nonseparative Applications in High-Temperature Membrane Reactors

A previous type of membrane reactor is applied to avoid nonselective total oxidation in the gas phase in a mixture O_2/feed. It is not necessary to use a *highly selective* membrane for avoiding nonselective gas phase reactions. A mesoporous or even a macroporous membrane can also be applied. The component, which has to be partially oxidized (or oxidative dehydrogenated or otherwise), is supplied from one side of the membrane and oxygen from the other side as shown before. The catalyst is a part of the membrane system (catalytically active membrane) either on top of the membrane or inside the membrane. The amount of catalyst surface area in a 'heat-exchanger' type of module is about 8000 m^2 considering a module of a 10 cm diameter and 1 m length with about 200 membrane tubes and a membrane top layer thickness of 10 μm. The total outer membrane area in this module is 2 m^2.

A precise dosage of oxygen is necessary at the actual *site* of the reaction on the surface of the catalyst. This dosage depends on the process parameters applied in relation with the ceramic *structure* of the membrane/catalyst. Fleming [61] already suggested using these types of membranes in a reactor and

recently, a number of papers were published on this subject. Omata et al. [81] used this concept for the oxidative coupling of methane. They provide an alumina tube (50 nm pores) with a PbO/MgO catalyst on top.

Zaspalis et al. [57,82–86] and Keizer et al. [87] used the concept of a catalytically active membrane for the oxidative dehydrogenation of methanol to formaldehyde (Ag-catalyst *in* the membrane).

This concept can also be applied for other types of reactions like the Claus reaction [58] or the denox reaction using ammonia [57].

In the Claus process the following reaction takes place:

$$2H_2S + SO_2 \rightarrow \frac{3}{8} S_8 + 2H_2O \tag{12.15}$$

The catalyst for this reaction is γ-Al_2O_3, which is impregnated in the α-Al_2O_3 membrane. At the end of the reactor neither H_2S nor SO_2 should be present and S_8 should be present on only one side of the membrane. All these requirements can be realized with this reaction in a reactor with a membrane (+ catalyst) having a pore diameter not larger than 1000 nm. Boundary conditions are that the reaction is fast (as is the Claus reaction) and the feed concentrations are not too high (< 5%). For the denox reactions the same conditions hold, as shown by Zaspalis [57,88]. The catalyst used for this reaction is V_2O_5/TiO_2. The membrane consists of a TiO_2 top layer modified with a monolayer of V_2O_5 (about 5–10 μm thick with 6 nm pores) on an alumina support. The membrane top layer, therefore, acts as the catalyst.

12.5 CONCLUSIONS AND EVALUATION

Gas separation using inorganic membranes is not an established field. At present no large-scale applications are realized, except perhaps for the application of dense metals in the separation of hydrogen at high temperatures [89]. With extended effort in research and development it can, however, become of major importance in the membrane technology.

Inorganic membranes can be prepared from all types of materials (metal, glass, ceramic, etc.) and with all kinds of structures. For highly selective gas separation, porous membranes with pores larger than 2 nm are not very suitable. Only the capillary condensation mechanism can achieve selective separations for vapors, in a distinct pressure/temperature regime.

Microporous (pore diameter < 2nm) and dense inorganic membranes can be highly selective, but application near room temperature is limited because of low permeability.

The situation changes drastically if higher temperatures are taken into account. At temperatures of 100–300°C, vapor separation is possible. Interesting

examples are water/alcohol or solvent separations with water as the faster-permeating component and probably hydrocarbon mixtures with sufficiently molecular different weight. The last example has not been proven yet.

It is also shown that permanent gas separation with microporous silica-based membranes is straight forward with H_2, He and CO_2 as fast-permeating components and hydrocarbons, N_2 and O_2 as slow-permeating gases. Carbon membranes are also selective for H_2 separation from hydrocarbons.

At temperatures higher than 300°C, dense membranes (metal sheets, immobilized inorganic liquids, dense glass films and oxygen ion conductors, etc.) can start to play a role in separation with almost infinite selectivity but limited permeability. Permeability improvements seem to be possible. The separation potential of silica-based composite membranes is also very good in this region. The structure is stable up to at least 700°C. The water sensitivity still has to be improved.

The attention of using inorganic membranes at high temperatures is not, however, directed only to separation but also to high-temperature membrane reactors in which reaction and separation are combined. By selective separation of H_2, a dehydrogenation reaction of hydrocarbons for example can be driven to completion instead of the very limited (thermodynamically determined) conversion in a conventional reactor.

It is also possible to change the reactor path of typical reactions so that nonselective gas phase reactions are avoided or new products are formed. For this application low-selective, porous membranes can be used, which are modified with catalytically active phases.

This whole consideration of commercial inorganic membrane applications becomes unsettled if high-temperature modules are not developed in time. The connections and sealings between membrane and housing are completely different from those applied in low-temperature (organic) membrane modules. A second problem that has to be solved is the difference in the expansion coefficient between the membrane and housing, which can generate stresses of several 100 MPas (thousands of bars) and, of course, causes cracks.

A number of companies recognize the problems but only a limited number of (small) companies are actually trying to solve them. In 1991–1992 some (small) high temperature membrane modules were introduced on the market (Velterop BV), which are now tested in practical processes.

However, the membrane *material* development is at present two to four years ahead of the high temperature *module* development. Therefore, more effort must be put towards the development of high-temperature modules to give inorganic membranes a real chance in high-temperature gas separations and membrane reactor applications.

LIST OF SYMBOLS

A	outer surface area of membrane (m^2)
A_o	surface area occupied by one adsorbed molecule (m^2)
d_p	pore diameter (m)
D_s	surface diffusion coefficient ($m^2\ s^{-1}$)
F_o	total permeability (mol $m^{-2}\ s^{-1}\ Pa^{-1}$)
F_{oK}	permeability by Knudsen diffusion (mol $m^{-2}\ s^{-1}\ Pa^{1961}$)
F_{oS}	permeability by surface diffusion (mol $m^{-2}\ s^{-1}\ Pa^{-1}$)
F_S	surface transport (kg m^{-3})
M_A,M_B	mass of a diffusing molecule A or B, respectively (kg)
N_{AV}	Avogadro's number (= 6.022×10^{23})
P	mean pressure (Pa)
P_r	pressure ratio across the membrane (–)
ΔP	pressure difference across the membrane (Pa)
P_t	capillary condensation pressure (Pa)
P_o	saturated vapor pressure (Pa)
dq/dl	gradient in surface occupation (mol $kg^{-1}\ m^{-1}$)
r	modal pore radius (m)
r'	actual radius of cylindrical capillary ($< r$ because of adsorbed gas (m)
R	Gas constant (J $mol^{-1}\ K^{-1}$)
T	absolute temperature (K)
V_m	molar volume of *liquid* component ($m^3\ mol^{-1}$)
v	average molecular velocity (m s^{-1})
x_s	fractional occupation of the internal membrane surface in relation with a monolayer (–)
x	the mole fraction of the faster-permeating component in the feed (–)
y	the mole fraction of the faster-permeating component in the permeate (–)
α	actual separation factor (–)
α^*	ideal separation factor according to the inverse ratio of the square root of molecular masses
γ	interfacial tension (N m^{-1})
ε	porosity (–)
η	viscosity of a gas (N $s^{-1}\ m^{-2}$)
θ	contact (wetting) angle (–)
μ_k	shape factor for Knudsen diffusion
μ_p	shape factor for laminar flow
μ_s	shape factor for surface diffusion
ρ	the apparent density of a membrane (kg m^{-3})

REFERENCES

1 Present, R.D. and de Bethune, A.J. (1949). *Phys. Review*, 13: 1050.
2 Marcel, R. (1984). Summerschool on Membrane Science and Technology, Cadarache, France.
3 Haraya, K., Shindo, Y., Hakuta, T. and Yoshitome, H. (1986a). *J. Chem. Soc. Jpn.*, 19: 186.
4 Haraya, K., Obata, K., Hakuta, T. and Yoshitome, H. (1986b). *J. Chem. Eng. Jpn.*, 19: 431.
5 Haraya, K., Shindo, Y., Hakuta, T. and Yoshitome, H. (1986c). *J. Chem. Eng. Jpn.*, 19: 461.
6 Haraya, K., Hakuta, T., Yoshitome, H. and Kimara, S. (1987). *Sep. Sci. Techn.*, 22: 1425.
7 Shindo, Y., Obata, K., Hakuta, T., Yoshitome, H., Todo, N. and Kato, J. (1981). *Adv. Hydr. Energy*, 2: 325.
8 Shindo, Y., Hakuta, T., Yoshitome, H. and Inoue, H. (1983). *J. Chem. Eng. Jpn.*, 16: 120.
9 Shindo, Y., Hakuta, T., Yoshitome, H. and Inoue, H. (1984). *J. Chem. Eng. Jpn.*, 17: 650.
10 Uhlhorn, R.J.R. (1990). Ceramic Membranes for Gas Separation, Synthesis and Transport Properties. Ph.D. Thesis, University Twente.
11 Sing, K.S.W. et al. (1985). *Pure Appl. Chem.*, 57: 603.
12 Schnabel, R. and Vaulont, W. (1978). *Desalination*, 24: 249.
13 Smith, A.W. (1974). U.S. Patent 3,850,762, 5 pp.
14 Furneaux, R.C., Rigby, W.R. and Davidson, A.P. (1986). EPA 0178,831, 8 pp.
15 Terpstra, R.A., Bonekamp, B.C., van Veen, H.M., Engel, A.J.G., de Rooy, R. and Veringa, H.J. (1988a). *Science of Ceramics*, 14: 557.
16 Terpstra, R.A., Bonekamp, B.C. and Veringa, H.J. (1988b). *Desalination*, 70: 395.
17 Veyre, R. (1985). *Ann. Chim. Fr.*, 1985: 359.
18 Leenaars, A.F.M. and Burggraaf, A.J. (1985a). *J. Coll. Interface Sci.*, 105: 27.
19 Cot, L., Guizard, Ch. and Larbot, A. (1988). *Industrial Ceramics*, 8: 143.
20 Anderson, M.A., Gieselman, M.J. and Xu, Q.Z. (1988). *J. Membr. Sci.*, 39: 243.
21 van Praag, W., Zaspalis, V.T., Keizer, K., Ommen, J.G.van, Ross, J.R.H. and Burggraaf, A.J. (1989). *Proceedings ICIM'89, Montpellier, France.* pp. 397–401.
22 Cacciola, A. and Leung, P.S. (1981). EPE 040,282, 20 pp.
23 Larbot, A., Fabre, J.-P., Guizard, C. and Cot, L. (1989a). *J. Am. Ceram. Soc.*, 72: 257.
24 Larbot, A., Julbe, A., Guizard, C. and Cot, L. (1989b). *J. Membr. Sci.*, 44: 289.
25 Burggraaf, A.J. and Keizer, K. (1990a). Concise Encyclopedia of Advanced Ceramic Materials, (R.W. Cahn, editor), Pergamon press, Oxford, p 769–74.
26 Burggraaf, A.J., Keizer, K. and Uhlhorn, R.J.R. (1990b). EPA 90201069.3.
27 Uhlhorn, R.J.R., Zaspalis, V.T., Keizer, K. and Burggraaf, A.J. (1992b). *J. Mater. Sci.*, 27: 538.
28 Uhlhorn, R.J.R., Huis in't Veld, M.B.J.H., Keizer, K. and Burggraaf, A.J. (1989a). *J. Mater. Sci. Lett.*, 8: 1135.
29 Uhlhorn, R.J.R., Huis in't Veld, M.B.J.H., Keizer, K. and Burggraaf, A.J. (1989b). *Proceedings of FICIM'89, Montpellier, France.* pp. 323–28.
30 Uhlhorn, R.J.R., Keizer, K. and Burggraaf, A.J. (1989c). *J. Membr. Sci.*, 46: 225.
31 Uhlhorn, R.J.R., Keizer, K. and Burggraaf, A.J. (1989d). In: *Advances in Reverse Osmosis and Ultrafiltration* (T. Matsuura and S. Sourirajan, Eds.). pp. 239–59.
32 Uhlhorn, R.J.R., Keizer, K. and Burggraaf, A.J. (1992d). *J. Membr. Sci.*, 66: 271.
33 Huis in't Veld, M.B.J.H., Uhlhorn, R.J.R., Keizer,K. and Burggraaf, A.J. (1989). *Proceedings FICIM'89, Montpellier, France.* pp. 383–7.
34 Gavalas, G.R., Megiris, C.E. and Nam, S.W. (1989). *Chem. Eng.*, 44: 1829.
35 Megiris, C.E., Nam, C.W. and Gavalas, G.R. (1989). *Proceedings ICIM'89, Montpellier, France*, pp. 355–61.

36 Okubo, T. and Inoue, H. (1989a). *J. Membr. Sci.*, 42: 109.
37 Okubo, T. and Inoue, H. (1989b). *AIChE J.*, 35: 845.
38 van Vuren, R.J., Bonekamp, B.C., Keizer, K., Uhlhorn, R.J.R., Veringa, H.J. and Burggraaf, A.J. (1987). *Mater. Sci. Monogr.*, 38c: 2235.
39 Keizer, K. and Burggraaf, A.J. (1988a). *Science of Ceramics*, 14: 83.
40 Keizer, K., Uhlhorn, R.J.R., Vuren, R.J.van, and Burggraaf, A.J. (1988b). *J. Membr. Sci.*, 39: 285.
41 Mason, F.A., Malinauskas, A.P. and Evans, R.B. (1967). *J. Chem. Physics*, 46: 3199.
42 Tamon, H., Kyotani, S., Wada, N., Okazaki, M. and Toei, R. (1981a). *J. Chem. Eng. Jpn.*, 14: 136.
43 Tamon, H., Okazaki, M. and Toei, R. (1981b). *AIChE J.*, 27: 271.
44 Tamon, H., Okazaki, M. and Toei, R. (1985). *AIChE J.*, 31: 1226.
45 Lee, K.H. and Hwang, S.T. (1986a). *J. Coll. Interface Sci.*, 110: 544.
46 Uhlhorn, R.J.R., Keizer, K. and Burggraaf, A.J. (1992c). *J. Membr. Sci.*, 66: 259.
47 Barrer, R.M. (1965). A.I.Ch.E. Symp.Series, 1: 112.
48 Asaeda, M. and Du, L.D. (1986a). *J. Chem. Eng. Jpn.*, 19: 72.
49 Asaeda, M., Du, L.D. and Fuji, M. (1986b). *J. Chem. Eng. Jpn.*, 19: 84.
50 Koresh, J.E. and Soffer, A. (1983). *Sep. Sci. Techn.*, 18: 723.
51 Koresh, J.E. and Soffer, A. (1986). *Chem. Soc. Faraday Trans. I*, 82: 2057.
52 Pez, G., and Carlin, R.T. (1986a). EPA 0194,493, 34 pp.
53 Pez, G., and Carlin, R.T. (1986b). U.S. patent 4,617,029, 8 pp.
54 Ilias, S., and Govind, R. (1989). *AIChE Symp. Series*, 268: 18.
55 Bouwmeester, H.J.M., Kruidhof, H., Burggraaf, A.J. and Gellings, P.J. (1992). *Solid State Ionics*, 53–56: 460.
56 Teraoka, Y., Zhang, H., Furukawa, S. and Yamazoe, N. (1985). *Chem. Lett.*, 1985: 1743.
57 Zaspalis, V.T. (1990). Catalytically Active Membranes: Synthesis, Properties and Reactor Applications, Ph.D Thesis, University Twente.
58 Swaay, W.P.M., Sloot, H.J. and Kreulen, H. (1989). *Proceedings Summerschool on New Membrane Processes, Enschede, Netherlands.*
59 Sakohara, S., Kitao, S., Ishizaki, M. and Asaeda, M. (1989). *Proceedings ICIM'89, Montpellier, France.* pp 231–6.
60 Deschamps, A., Walther, C., Bergez, P., and Charpin, J. (1989). *Proceedings of FICIM'89, Montpellier, France.* pp 237–42.
61 Fleming, H.L. (1987). *1987 BCC Membrane Planning Conference*, Cambridge, Mass.
62 Hsieh, H.P. (1989). *AIChE Symp. Series*, 268: 53.
63 Itoh, N., Shindo, Y., Hakta, T. and Yoshitome, H. (1984). *Int. J. Hydrogen Energy*, 9: 835.
64 Itoh, N., Shindo, Y., Haraya, K., Obata, K., Hakuta, T. and Yoshitome, H. (1985). *Int. Chem. Eng.*, 25: 138.
65 Itoh, N. (1987). *AIChE J.*, 33: 1576.
66 Itoh, N. and Govind, R. (1989). *AIChE Symp. Series*, 268: 10.
67 Mohan, K. and Govind, R. (1986). *AIChE J.*, 32: 2083.
68 Mohan, K. and Govind, R. (1988a). *Sep. Sci. Techn.*, 23: 1715.
69 Mohan, K. and Govind, R. (1988b). *AIChE J.*, 34: 1493.
70 Nam. S.W. and Gavalas, G.R. (1989). *AIChE Symp. Series*, 268: 68.
71 Shinji, O., Misono, M. and Yoneda, Y. (1982). *Bull. Chem. Soc. Jpn.*, 55: 2760.
72 Sun, Y.M. and Khang, S.J. (1988). *Ind. Eng. Chem. Res.*, 27: 1136.
73 Bitter, J.G.A. (1986). Brit. Patent Appl. 8629135, 15 pp.
74 Fukuda, K., Dokiya, M., Kameyama, T. and Kotera, Y. (1978). *Ind. Eng. Chem. Fundam.*, 17: 243.

75 Kameyama, T., Dokiya, M., Fukuda, K. and Kotera, Y. (1979). *Sep. Sci. Techn.*, 14: 953.
76 Kameyama, T., Fukuda, K., Fushisige, M., Yokokawa, H. and Dokiya, M. (1980). *Proceedings 3rd World Hydrogen Energy Conference, Tokyo, Japan.* pp. 2.325–2.333.
77 Kameyama, T., Dokiya, M., Fujishige, M., Yokokawa, H. and Fukuda, K. (1981). *I&EC Fundam.*, 20: 97.
78 Gryaznov, V.M. and Smirnov, V.S. (1977). *Kin. Cat.*, 3: 579.
79 Gryaznov, V.M. (1986). *Z. Phys. Chemie*, 147: 123.
80 Gellings, P.J., Koopmans, H.J.A. and Burggraaf, A.J. (1988). *Appl. Catal.*, 39: 1.
81 Omata, K., Hashimoto, S., Tominaga, H. and Fujimoto, K. (1989). *Appl. Catal.*, 52: L1.
82 Zaspalis, V.T., Keizer, K., van Ommen, J.G., van Praag, W., Ross, J.R.H. and Burggraaf, A.J. (1989a). *AIChE Symp. Series*, reprint (unpublished).
83 Zaspalis, V.T., Keizer, K., van Ommen, J.G., van Praag, W., Ross, J.R.H. and Burggraaf, A.J. (1989b). *Brit. Ceram. Soc. Proc.*, 43: 103.
84 Zaspalis, V.T., Keizer, K., van Ommen, J.G., van Praag, W., Ross, J.R.H. and Burggraaf,A.J. (1989c). *Proceedings FICIM'89, Montpellier, France.* pp. 367–72.
85 Zaspalis, V.T., van Praag, W., van Ommen, J.G., Ross, J.R.H. and Burggraaf, A.J. (1991a). *Appl. Catal.*, 74: 205.
86 Zaspalis, V.T., van Praag, W., van Ommen, J.G., Ross, J.R.H. and Burggraaf, A.J. (1991b). *Appl. Catal.*, 74: 235.
87 Keizer, K., Zaspalis, V.T. and Burggraaf, A.J., (1990). *Proceedings CIMTEC'90, Montecatini Terme, Italy.*
88 Zaspalis, V.T., van Praag, W., van Ommen, J.G., Ross, J.R.H. and Burggraaf, A.J. (1991c). *Appl. Catal.*, 74: 249.
89 Kammermeyer, K. (1976). *Chem. Ing. Techn.*, 48: 672.
90 Hsieh, H.P. (1988). *AIChE Symp. Series*, 261: 1.
91 Hsieh, H.P., Bhave, R.R. and Fleming, H.L. (1988). *J. Membr. Sci.*, 39: 221.
92 Lin, Y.S., Vries, K.J. de, Brinkman, H.W. and Burggraaf, A.J. (1992), *J. Membr. Sci*, 66: 211.
93 Smith, B.D. and Srivastava, R. (1986), Thermodynamic Data for Pure Compounds. Elsevier, Amsterdam.
94 Landolt-Börnstein (1960), Zahlenwerte und Funktionen aus Physiek, Chemie, Astronomie, Geophysik und Technik. 2. Teil, Bandteil 2a, Gleichgewichte Dampf-Condensat und Osmotische Phänomene. Springer-Verlag. Berlin.

BIBLIOGRAPHY

Abe, F. (1987). EPA 0228885, 22 pp.
Aimar, P., Taddei, C., Lafaille, J.P. and Sanchez, V.(1988). *J. Membr. Sci.*, 38: 203.
Anderson, M.A., Gieselman, M.J., Xu,Q., Moosemiller, M., Knaebe, M. and Bischoff, B. (1987). DOE/ID/12626-T1, DE 87 012714: 60 pp.
Armor, J.N. (1989). *Appl. Catal.*, 49: 1.
Asaeda, M., Watanabe, J., Matono, Y., Kojima, K., and Toei, R. (1981). *J. Chem. Eng. Jpn.*, 14: 13.
Ash, R., Barrer, R.M., and Foley, T. (1976). *J. Membr. Sci.*, 1: 355.
Ash, R., Barrer, R.M., and Sharma, P. (1976). *J. Membr. Sci.*, 1: 17.
Baker, R.W., and Blume, I. (1986). *Chemtech*, April: 232
Bakiewicz, J.L., Keizer, K., and Burggraaf, A.J. (1989). Euroceramics (G. de Wit, R.A. Terpstra, R. Metselaar, eds.), Elsevier Applied Science, London, pp.3–610.

Bein, T., Brown, K., Enzel, P., and Brinker, C.F. (1986). Better Ceramics through Chemistry III (C.J.Brinker, D.E.Clark, D.R.Ulrich, eds.), p.425.

Bein, T., Brown, K., and Brinker, C.J. (1989). Zeolites: Facts, Figure, Future (Jacobs, P.A., van Santen, R.A., eds.), Elsevier Science Pub., Amsterdam, p. 887.

Bonekamp, B.C., Terpstra, R.A., and Veringa, H.J. (1989). Euroceramics 1 (de Wit, G., Terpstra, R.A., and Metselaar, R,. eds.), Elsevier Applied Science, London, p. 218.

Brautigam, U., Burger, H., and Vogel, W. (1989). *J. Non-Cryst. Solids*, 110: 163.

Brinker, C.J., Hurd, A.J., Frye, G.C., Ward, K.J., and Ashley, C.S. (1991) *J. Non-Cryst.Solids*, 112: 253

Burggraaf, A.J., and Keizer, K. (1989) Proceedings of ICIM '89, Montpellier, France, pp.311–22.

Burggraaf, A.J., Keizer, K., and Hassel, B.A. van (1989). *Solid State Ionics*, 32/33: 771.

Callahan, R.W. (1988). *AIChE Symp. Series*, 261: 54

Charpin, J., Bergez, P., Valin, F., Barnier, H., Maurel, A., and Martinet, J.M. (1988). Industrial Ceramics, 8: 23.

Dellefield, R.J. (1990) AIChE Symp.Series, preprint (not published)

Freilich, D., and Tanny, G.B. (1978). *J. Colloid Interface Sci.*, 64: 362.

Gallagher, D., and Klein, L.C. (1986). *J. Colloid Interface Sci.*, 109: 40.

Gieselman, M.J., Moosemiller, M.D., Anderson, M.A., and Hill. C.G. (1988). *Sep. Sci. Techn.*, 23: 1695.

Gieselman, M.J., and Anderson, M.A. (1989). *J. Am.Ceram. Soc.*, 72: 980.

Gilliland, E.R., Baddour, R.F., Perkinson, G.P., and Sladek, K.J. (1974). *Ind. Eng. Chem.Fundam.*, 13: 95.

Gilliland, E.R., Baddour, R.F., Whang, H.Y., and Sladek, K.J. (1972). *J. Electroanal.Chem Interf. Electrochem.*, 37: 361

Guizard, C., Legault, F., Idrissi, N., Larbot, A., Cot, L., and Gavach, C. (1989). *J. Membr. Sci.*, 41: 127.

Haggin, J. (1989). *C&EN*, July: 198.

Harold, M.P., Cini, P., Patenaude, B., and Venkataraman, P. (1989). *AIChE Symp.Series*, 268: 26.

Hennepe, H.J.C.ten, Bargeman, D., Mulder, M.H.V., and Smolders, C.A. (1987). *J. Membr. Sci.*, 35: 39.

Higashi, K., Ito, H., and Oishi, J. (1964). *J. Nuclear Sci. Techn.*, 1: 298

Hwang, S.T. (1976). *Sep.Sci. Techn.*, 11: 17

Itaya, K., Sugawara, S., Arai, K., and Saito, S. (1984). *J. Chem. Eng. Jpn.*, 17: 514.

Kaiser, A., and Schmidt, H. (1984). *J. Non-Cryst. Solids*, 63: 261.

Kammermeyer, K. (1968) in: Progress in Separation and Purification 1, New York Inet, pp.335-72.

Klein, L.C., and Gallgher, D. (1988). *J. Membr. Sci.*, 39: 213.

Klemetson, S.L., and Scharbow, M.D. (1978). *Prog. Water Technol.*, 10: 193.

Konno, M., Shindo, M., Suguwara, S., and Saito, S. (1988). *J. Membr. Sci.*, 37: 193.

Larbot, A., Alary, J.A., Fabre, J.P., Guizard, C., and Cot, L. (1986). *Mat. Res. Soc. Symp. Series*, 73: 659.

Larbot, A., Alary, J.A., Guizard, C., and Cot, L. (1987a). *Int. J. High Techn. Ceramics*, 3: 143.

Larbot, A., Alary, J.A., Guizard, C., Fabre, J.-P., Idrissi, N., and Cot, L. (1987b). *Mat. Sci. Monogr.*, 38c: 2259.

Larbot, A., Fabre, J.-P., Guizard, C., and Cot, L. (1988). *J. Membr. Sci.*, 39: 203.

Lee, E.K. (1987). *Encycl. Phys.Science*, 8: 20.

Lee, K.H., and Khang, S.T. (1986). *Chem. Eng. Comm.*, 44: 121.
Leenaars, A.F.M., Keizer, K., and Burggraaf, A.J. (1984). *J. Mat. Sci.*, 19: 1077.
Leenaars, A.F.M., and Burggraaf, A.J. (1985b). *J. Membr. Sci.*, 24: 245.
Leenaars, A.F.M., and Burggraaf, A.J. (1985c). *J. Membr. Sci.*, 24: 261.
Leenaars, A.F.M.,Keizer, K. and Burggraaf, A.J. (1986). *Chemtech*, Sept.: 560.
Li, D., Seok,D .R., and Hwang, S.T. (1988). *J. Membr. Sci.*, 37: 267.
Loeb, S., and Sourirajan, S. (1962). *Adv. Chem. Ser.*, 38: 117.
Mohnot, S., and Cussler, E.L. (1984). *Chem.Eng. Sci.*, 39: 569.
Niwa, M., Ohya, H., Tanaka, Y., Yoshikawa, N., Matsumoto, K., and Negishe, Y. (1988). *J. Membr. Sci.*, 39: 301.
Noble, R.D. (1987). *Sep. Sci. Techn.*, 22: 731.
Okazaki, M., Tamon, H., and Toei, R. (1978). *J. Chem. Eng. Jpn.*, 11: 209.
Okazaki, M., Tamon, H., and Toei, R. (1981) *AIChE J.*, 27: 262.
Ollis, D.F., Thompson, J.B., and Wolynic, E.T. (1972). *AIChE J.*, 18: 457.
Rowell, R.L., Carrano, S.A., deBethune, A.J., and Malinauskas, A.P. (1971). *J. Colloid Interface Sci.*, 37: 242.
Schmidt, H. (1984). Mat.Res.Symp.Proc., 32: 327.
Sladek, K.J., Gilliland, E.R., and Baddour, R.F. (1974). *Ind. Eng. Chem. Fundam.*, 13: 100.
Suzuki, H. (1986). EPA 0,180,200, 27 pp.
Suzuki, H. (1987). U.S. Patent 4,699,892, 10 pp.
Suzuki, K., Kiyozumi, Y., Sekine, T., Obata, K., Shindo, Y., and Shin, S. (1989). Zeolites: Facts, Figures, Future (Jacobs, P.A., van Santen, R.A., eds.), Elsevier Science Pub., Amsterdam, p. 65.
Uhlhorn, R.J.R., Huis in't Veld, M.B.J.H., Keizer, K., and Burggraaf, A.J. (1988). *Sci. Ceramics*, 14: 551.
Uhlhorn, R.J.R., Huis in't Veld, M.H.B.J., Keizer, K. and Burggraaf, A.J. (1992a). *J. Mat. Sci.*, 27: 527
Veen, H.M., Terpstra, R.A., Tol, J.P.B.M., and Veringa, H.J. (1989). Proceedings of FICIM'89, Montpellier, France, pp. 329–35.
Vinek, H. (1980). *Z. Phys. Chem. Neue Folge*, 120: 119.
Way, J.D., Noble, R.D., Flynn, T.M., and Sloan, E.D. (1982). *J. Membr. Sci.*, 12: 239.
Xu, Q., and Anderson, M.A. (1989). *Mat. Res. Soc. Symp. Series*, 132: 41.
Yoldas, B.E. (1975). *Ceram.Bull.*, 54: 289.
Zeltner, W.A., and Anderson, M.A. (1989). Proc.FICIM'89, Montpellier, France, pp. 213–24.

Membrane Separations Technology. Principles and Applications
Edited by R.D. Noble and S.A. Stern

Chapter 13

Economics of gas separation membrane processes

Robert Spillman

Amicon, Inc., Beverly, MA, USA

13.1 INTRODUCTION

Gas separation via membranes is one of the most exciting and significant new unit processes to have appeared in many years. The first commercially significant gas separation membranes were introduced only in late 1979 but within a span of ten years this technology found its way into a wide range of industries and applications. The future promises to be equally exciting as new membrane materials, processes and innovations make their way to the marketplace.

A gas separation membrane separates gas species (gas/gas separation) and is distinctly different from gas filtration (gas/solid separation). A gas separation membrane preferentially removes one or more components of a gas mixture that is passed across a membrane surface. The fact that no mechanical or chemical processes are involved makes the membrane process simple and easy to operate.

The simplicity of the gas separation membrane process gives it special appeal when one considers the complexity of competing processes. Gas separation membranes, however, do not offer a separation solution that is particularly unique over the more traditional gas separation processes. Gas separation membrane processes compete with cryogenics and a wide variety of chemical and physical adsorption and absorption processes (e.g., amine absorption, pressure swing adsorption, carbon bed adsorption, etc.). In the case of air separation, membranes compete with the on-site production or delivery of oxygen and nitrogen liquids or gases. Since alternative processes achieve the

same separation, membranes must compete on the basis of overall economics, convenience and safety.

It is traditionally very difficult for new technologies to displace the old and in the case of gas separation membranes the challenges are immense. Most of the conventional gas separation processes have been used for decades and all have undergone continual improvements in design and energy efficiency. Introduction was further impeded by the fact that the initial membrane applications were in the oil, gas and petrochemical industries where process innovations come at a slower rate due to the size and costs of the gas streams involved. Even more importantly, timing of the market development unfortunately coincided with the depression of the oil and gas industries in the 1980s.

In spite of the market and technical obstacles, gas separation membrane processes have penetrated a wide variety of markets and applications. This penetration is due to the inherent advantages of these membranes in many applications; low capital investment, ease of operation, low energy consumption, safety and good weight and space efficiency.

Gas separation membranes do have practical and theoretical limitations, however, and there exists considerable confusion and disagreement about the preferential use of membranes over alternative processes. This confusion is aggravated by the fact that membrane technology is not well understood by many of the potential benefactors of this new process. Engineering courses have only recently begun to include gas separation membranes in their curriculum but even so, the information base and mathematical tools required to properly assess their performance are not readily available. As a result, potential users of membrane technology must rely on vendors for assistance. This can sometimes inhibit creative application of the technology.

The purpose of this contribution is to provide some perspective as to where gas separation membranes offer significant potential and where there still remain considerable obstacles. This author feels that this is best accomplished by focusing on the key considerations in membrane process design followed by economic illustrations of how membranes compare with competing processes. This is a risky undertaking since economic comparisons of processes are highly site-specific and are never easily extended to other cases. This difficulty is greatly compounded due to the fact that membrane technology is rapidly changing in terms of membrane performance and in terms of vendor pricing. Current membrane technologies offer a price/performance ratio that is an order of magnitude better than some of the earlier systems that were first introduced. Membrane innovation will continue, albeit at a slower rate, and economic comparisons made today may not be valid in the near future.

Throughout this chapter the terms "gas separation membrane" and "membrane" are used interchangeably, unless noted.

13.2 APPLICATIONS AND TECHNOLOGY BACKGROUND

13.3.1 Commercial Applications and Suppliers

Although a variety of companies had offered gas separation membranes on a limited scale as early as 1968, these earlier membrane systems were not widely accepted as viable gas separation processes. A variety of technical and market entry barriers combined to make commercial success an expensive and difficult reality. Only after Monsanto introduced their Prism membrane system in 1979 did gas separation membranes really take hold. Since that time gas separation membranes have slowly but steadily penetrated a wide range of applications.

Table 13.1 provides an overview of the major commercial application areas for gas separation membrane processes along with some of the major suppliers. Many new applications are under development. Membrane gas separations have attracted the interest of many companies and there are now over twenty

TABLE 13.1

Gas membrane applications and suppliers

Common gas separations	Application	Suppliers
O_2/N_2	Nitrogen generation, oxygen enrichment	Permea (Air Products), Linde (Union Carbide), A/G Technology, Generon (Dow Chemical/BOC), Asahi Glass, Osaka Gas, Oxygen Enrichment Co.
H_2O/Air	Air dehumidification	Permea, Ube Industries, Perma Pure
H_2/Hydrocarbons	Refinery hydrogen recovery	Permea, Grace Membrane Systems (W.R. Grace)
H_2/CO	Syngas ratio adjustment	As above
H_2/N_2	Ammonia purge gas	As above
CO_2/Hydrocarbons	Acid gas treating, landfill gas upgrading	Grace Membrane Systems, Cynara (Dow Chemical), Separex, (Hoechst Celanese), Permea
H_2O/Hydrocarbons	Natural gas dehydration	As above
H_2S/Hydrocarbons	Sour gas treating	As above
He/Hydrocarbons	Helium separations	As above
He/N_2	Helium recovery	As above
Hydrocarbons/Air	Pollution control, hydrocarbon recovery	Membrane Technology and Research, Aluminium Rheinfelden/GKSS, NKK

suppliers. Many additional companies have initiated R&D efforts to develop their own systems. Although the current market for membrane-based gas separation is small relative to the level of developmental activity, many companies see a potentially large future market as new innovations are developed.

13.2.2 Gas Separation Membrane Technology

Membrane technology for the separation of liquid/liquid and liquid/solid streams has been practiced in industry for many years (e.g., reverse osmosis, ultrafiltration and microfiltration). While gas separation membranes are a logical extension of these other membrane technologies, gas separation environments are quite unlike those seen in other applications. For example, pressures of 2000 psi and temperatures of 70°C are possible and which greatly exceed the conditions typically experienced in other membrane applications. These harsh conditions delayed the commercial introduction of gas separation membranes until advances in membrane technology gradually led to the development of membranes suitable for such difficult environments [1,2].

A summary of gas separation membrane technology and principles is provided for perspective. Cited references should be consulted for more in-depth treatment of the following subjects.

13.2.2.1 Membrane Classes

There are three basic types of membranes that can be used for gas separation. The vast majority of commercial membranes are based on technology termed "nonporous" membranes. These membranes contain no holes or pores in the conventional sense of the word as would typically be found in ultrafiltration or microfiltration membranes. Instead, they rely on the principle that gases dissolve in and diffuse through solid materials [3]. This principle is often observed in a negative sense, for example, with respect to the plasticization and swelling of gaskets and seals in certain gas environments. Gas separation membranes take advantage of this phenomenon and polymers are specifically chosen that are highly permeable to the gases of interest. A separation of two gases is possible due to the fact that gases exhibit differing rates of transport through the polymer. For example, oxygen will pass though a typical polymeric membrane two to seven times faster than nitrogen, depending on the membrane and the conditions of the separation. The ratio of the permeation rates of two gases defines the selectivity of the membrane for those gases.

A second class of gas separation membranes is based on the use of a "porous" membrane in which the gases are literally separated on the basis of their molecular weight (Knudsen diffusion) or size (molecular sieving) by small pores through the membrane. This type of membrane is not yet generally

employed in commercial gas membrane applications due to fabrication, durability and cost issues. Additionally, Knudsen diffusion membranes provide only low separation factors. It might be noted, however, that the world's first and largest gas membrane separation plant, in fact, was based on Knudsen diffusion separation using inorganic porous membranes [4]. The Department of Energy operated the Oak Ridge Gaseous Diffusion Plant since the mid-40s using these membranes to enrich the ^{235}U isotope for national defense purposes. The original plant covered some 270 acres and was upgraded with new membranes in the late 70s/early 80s at a cost of $1.5 billion! Development of porous membranes for industrial gas separation is still underway with recent efforts centered on taking advantage of other separation mechanisms (e.g., molecular sieving) that provide significantly higher selectivities [5,6].

A third general class of gas separation membranes is often termed facilitated transport or immobilized liquid membranes [7]. These membranes operate on the principle that a carrier fluid in the membrane acts as the primary gas solubilization agent. The advantage is that gases have higher solubilities in liquids than in solids and the addition of "carrier species" can substantially increase the separation factors. The most common configuration for such membranes is to impregnate the carrier liquid into a microporous membrane. Another approach involves the use of solvent-swollen ion exchange membranes. An analysis of the benefits and problems of such membranes illustrates that they are most attractive for treating gas streams having low partial pressures of the permeating gas [8]. These membranes, however, have not yet achieved the stability and lifetime required for widespread use. These types of membranes have been evaluated for a number of applications, including paraffin/olefin separations and sulfur dioxide removal from flue gas.

The earliest commercial membranes were based on polysulfone and cellulose acetate. These polymer types still predominate but have been joined by polyimides, polyamides, polycarbonates, polyetherimide and sulfonated polysulfone [9]. In general, membrane technology is moving away from the reverse osmosis technology from which it evolved. In addition to the move to new polymers, there has been developed a large amount of know-how developed with respect to module construction and gas pretreatment.

Current gas separation membranes are formed as dense films, asymmetric membranes or as composites [10]. A major focus of membrane development is the elimination of "pinholes" or minor defects in the separating layer. Such defects can dramatically affect the apparent selectivity of a membrane due to the high mobility of gases and the high pressure differences that are usually employed in a separation. Compatibility of the membrane polymers with the gas stream environment is also a key technical requirement.

13.2.2.2 Principles

Membrane-based gas separation is a relatively straightforward process concept. A typical gas separation is schematically diagrammed in Fig. 13.1. Air is separated into its nitrogen and oxygen components by passing the feed air stream across a membrane surface. Membrane separation of gases is a concentration-driven process which, for gases, is directly related to the pressures of the feed and permeate streams.

In this example, the air feed is compressed to provide the driving force for the separation. This air stream is then passed across the membrane surface in a "cross-flow" arrangement (as opposed to "dead-end" as with particulate filters). The membrane is more permeable to oxygen than to nitrogen and thus the oxygen permeates through the membrane to the low-pressure permeate side. The remaining stream is enriched in nitrogen and exits as the high pressure "residue" stream. Although the diagram shows complete separation, membrane permeation, in fact, is a rate-controlled process and complete separation is not achieved. The degree of separation is defined by the selectivity of the membrane and by the conditions of the separation (pressure, temperature, flow rate, membrane area, etc.).

Polymeric membranes are most often characterized by the "solution-diffusion" mechanism, which states that the transport of gas molecules through a solid polymer film is governed by the solubility and diffusivity of the gas in the polymer [3]. The product of these two factors determines the "permeance" of that gas through a certain material. Permeance is defined as the volume of gas permeating a unit area of membrane per unit time per unit pressure differential and normalized to a unit thickness. A common measurement unit is called the Barrer (1 Barrer = 10^{-10} cm^3-cm/cm^2-sec-cmHg). The actual "permeability" of a membrane is the permeance of the membrane material divided by the effective

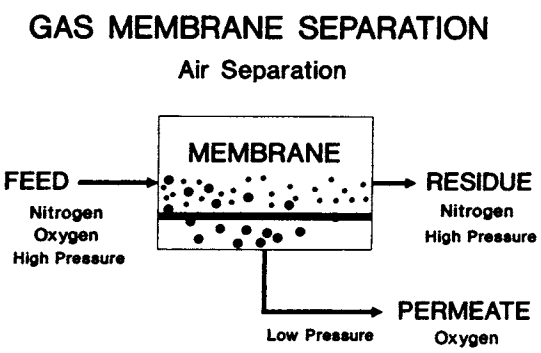

Fig. 13.1. Schematic of a membrane-based air separation process.

thickness of the separation layer, which typically ranges from 0.1 to 5 microns. A wide variety of units are used to express permeability ($cm^3\ cm^{-2}\ sec^{-1}\ cmHg^{-1}$, $ft^3\ ft^{-2}\ hr^{-1}\ 100\ psi^{-1}$, $m^3\ m^{-2}\ hr^{-1}\ atm^{-1}$, etc.).

A second theory covers the "porous" class of membranes (e.g., glass or ceramic membranes). This model assumes that membranes contain physical pores (on the order of Angstroms) and that the separation is based on a combination of molecular sieving, Knudsen diffusion, surface diffusion and capillary condensation. Molecular sieving, as the name suggests, separates molecules by their effective size. This class of membranes generally exhibits rather low separation factors for most applications and is therefore not widely employed. Work continues in this area since high selectivities are possible under the right conditions of membrane fabrication [11].

It should be noted that controversy exists over whether, in fact, the porous model theory also applies to nonporous polymeric membranes [12,13]. The exact nature of the transport mechanism is relevant to membrane R&D but the permeability characteristic of either membrane type sufficiently describes the end performance of that membrane to allow meaningful performance comparisons without regard to mechanism.

13.2.2.3 Module Configurations

The vast majority of commercial gas separation membranes are based on polymers that are formed as either flat sheets or as hollow fibers and assembled into modules. A membrane module is defined here as a the smallest practical unit containing a set membrane area and any supporting structures. Individual membrane modules are assembled into pressure vessels to form the membrane unit or "stage" which includes the necessary piping and pretreatment equipment.

Flat sheet membrane is manufactured in long rolls and then assembled into plate-and-frame or spiral wound configurations. Hollow fibers are small tubes that have outer diameters ranging from as little as 50 microns to over 500 microns. In many, but not all, cases the high-pressure feed gas is introduced to the outer shell of the fiber and the low pressure permeate travels through the bore. Hollow fibers provide higher packing densities than spirals but the small size of the internal bore (40 to 300 microns) can often present a problem when large quantities of gas are permeating the membrane (high pressure drop down the fiber bore). In some low-pressure air separation membranes the high-pressure gas is passed through the fiber lumen and this eliminates the back-pressure problem. The limitation of this approach is the burst pressure of the membrane.

The choice of either a spiral-wound or hollow fiber approach is not a decision that necessarily has to be made by the end user. It is more of a decision by the membrane manufacturer how best to package a particular membrane technology to be able to offer the most cost-effective process to the final customer. The

user should evaluate first the overall performance and cost-effectiveness of the options. Both designs coexist in the market and one may be preferred over the other depending on the specific application.

13.3 PRINCIPLES OF MEMBRANE PROCESS DESIGN

This section presents some of the basic considerations of how the design of a membrane gas separation process affects the economics of that process. Very few publications currently exist that cover the design of such membrane processes. This void stems largely from the nature of the membrane unit separation and the need for sophisticated computer programs to model the system. The problem is further compounded by one of the inherent advantages of membranes — their versatility. This versatility allows the design engineer to tailor a membrane process that is very specific to the application. This can only be accomplished, however, with computer programs not generally available at present. As membrane unit operations are included in process design packages some of these problems will be alleviated but not necessarily overcome. There are a number of not-so-obvious factors to be considered in membrane process design that greatly impact the economics of the process. A few of these factors will be illustrated in this section. Furthermore, it is nearly impossible to make broad generalizations about process design. What may be true for a membrane system from one supplier may not apply to one from another supplier.

13.3.1 Basic Performance Principles

Based on a *single-stage* membrane, several generalizations can be made to highlight what's important in optimizing a membrane process. Membrane separation of gases is a concentration-driven process, which for gases is directly related to the partial pressures of the gas species. It is the pressure differential between the feed and permeate streams that has by far the greatest impact on a particular membrane's effective performance. This pressure differential will impact *both* the amount of membrane area required and the volume and composition of the residue and permeate streams. It is also important to note that the desired product stream may be either the residue or permeate stream (or both in some cases). In natural gas treating, for example, the high-pressure methane residue is the "product" gas. In hydrogen separations, on the other hand, the hydrogen "product" exits the process as the lower-pressure permeate stream. As will be demonstrated, this difference results in some quite different conclusions regarding process optimization. The following analyses are based on representative membrane performance data that have appeared in the literature.

13.3.1.1 Product is the Residue Gas Stream

Relative membrane requirements and methane recovery are presented as a function of feed pressure, permeate pressure, feed gas purity and product purity in Figs. 13.2a–d for the case of a two-component feed stream (90% CH_4/10% CO_2). The product gas is 97% CH_4 and is delivered as the high-pressure residue stream. Although the figures would change for different separation problems the trends would still be the same for cases wherein the product gas is the residue stream.

Figure 13.2a illustrates the importance of pressure differential on both membrane area requirements and product recovery. It may be economically justified in some circumstances to add additional compression to the feed stream to

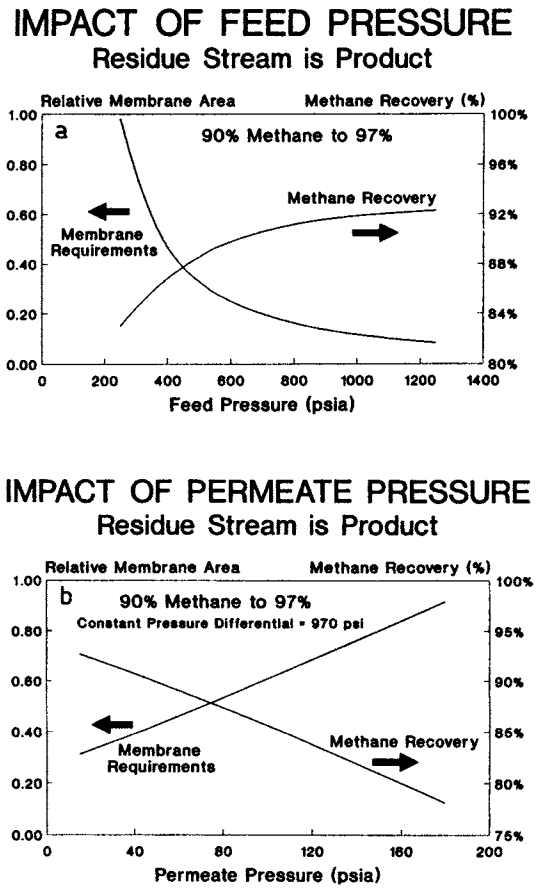

Fig. 13.2. Impact of selected process variables on single-stage membrane performance for a case in which the residue stream is the product gas. (a) Impact of feed pressure. (b) Impact of permeate pressure when the total pressure differential is kept constant. See overleaf for (c) and (d)

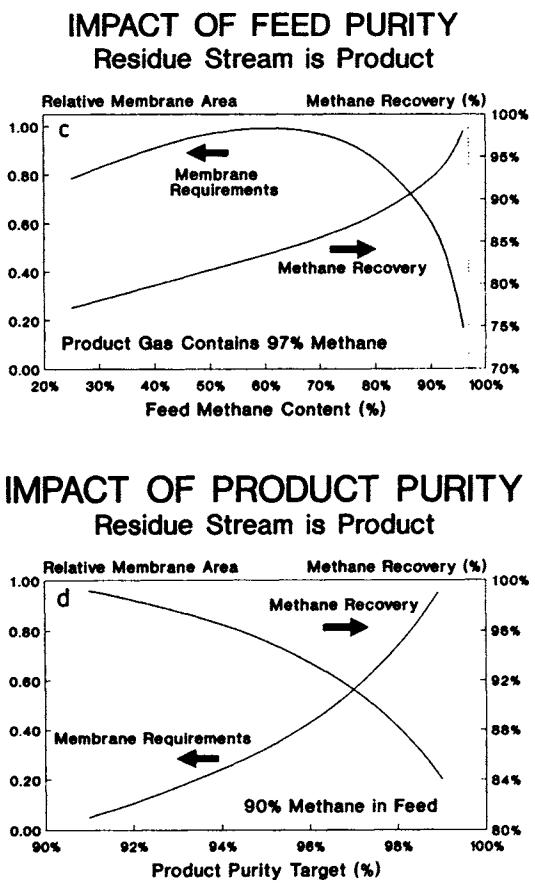

Fig. 13.2 *continued.* (c) Impact of feed stream purity. (d) Impact of product purity requirements.

reduce membrane costs and to improve recovery. At the lower pressures, the high packing density advantage of hollow fiber membranes becomes increasingly important due to the high membrane area requirements.

Figure 13.2b demonstrates that even with the same pressure differential between the feed and permeate sides, overall performance is also a significant function of the permeate pressure. It is illustrative to think of this effect in terms of the ratio of the feed and permeate pressures. A vacuum pump on the permeate side can significantly increase the pressure ratio (and membrane separation efficiency) without greatly impacting the pressure differential.

The impact of feed stream purity on membrane area requirements and product recovery is shown in Fig. 13.2c. The surprising feature of this graph is the appearance of a maximum membrane area requirement at the 60% feed methane concentration. Gas separation membranes are highly efficient at high CO_2 loadings and the membrane area requirements decrease as shown. This occurs because the initial membranes remove enough CO_2 that the resulting

size of the gas stream is greatly reduced towards the latter stages of the separation. The smaller flow requires less membrane and this more than offsets the additional membrane area required for the higher initial CO_2 loading.

Figure 13.2d demonstrates that as one approaches a 100% purity target for the membrane separation, the costs of the separation rise rapidly. Although this is true for any separation, the rate of rise for membrane separations is generally sharper. For this reason membranes are not often employed as the final process step in cases where ultrahigh purity is required. They are best utilized to achieve purities of 99% and below. Some exceptions exist such as the dehumidification of air.

13.3.1.2 Product is the Permeate Stream

In most hydrogen applications the permeate stream is the product gas of interest. Membranes are highly permeable to hydrogen and this gas is most often the component sought in a separation. A typical example involves the separation of hydrogen from methane (and higher hydrocarbons) for recovery and recycle to a refinery process. This situation results in a quite different set of graphs from those presented in Fig. 13.2. These are displayed in Figs. 13.3a–d. In this case it is important to realize that the first gas permeating a membrane is enriched in the most permeable component (e.g., hydrogen). The concentration of hydrogen in the permeate stream is highest at the point that the feed first contacts the membrane. The feed gas at this point has the highest hydrogen concentration that the membrane will see and the driving force is at a maximum. As the feed gas travels down the membrane it is depleted of hydrogen and the driving force is correspondingly reduced.

In the following examples, the permeate stream pressure is set at a slightly elevated pressure (50 psia) since most applications require that this stream be recompressed for use. The higher pressure reduces recompression cost. Figure 13.3a illustrates the importance of feed pressure on this separation. This plot is similar in appearance to Fig. 13.2a and reaffirms the general importance of pressure differential in membrane separation performance.

Figure 13.3b analyzes the impact of permeate pressure on performance. Unlike corresponding Fig. 13.2b, this plot demonstrates that lower permeate pressures will actually result in an increase in membrane area requirements *to achieve the same product purity*. This seemingly contradictory result occurs only because the product purity target was kept the same. The lower permeate pressure would have resulted in a purer permeate if the membrane area had been kept constant. Since the purity target was fixed, however, more membrane area was required so that additional permeate gas would "dilute" the stream to achieve the targeted purity (the first permeating gas is enriched in hydrogen as was discussed above). The benefit is that product recovery is substantially

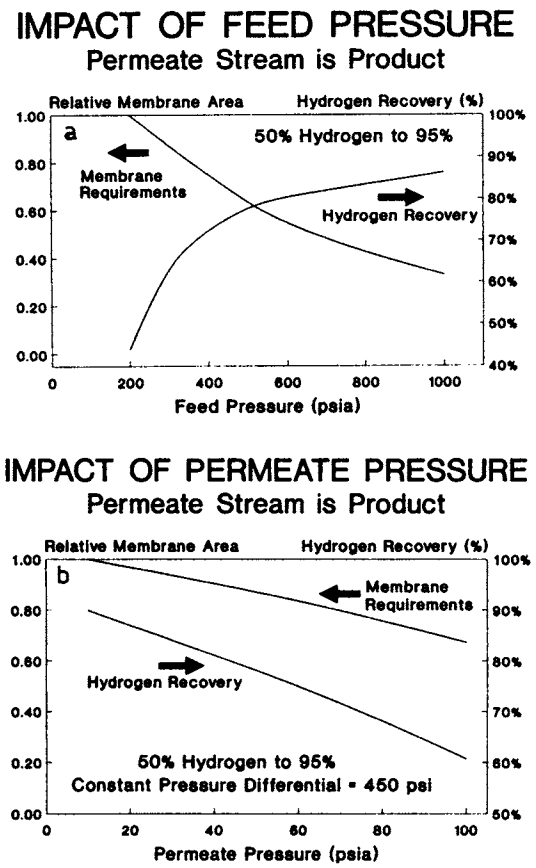

Fig. 13.3. Impact of selected variables on membrane performance in the case where the membrane permeate is the product gas. (a) Impact of feed pressure. (b) Impact of permeate pressure when the total differential is kept constant. See opposite for (c) and (d).

enhanced. Lower permeate pressures actually provide a better separation and the membrane area increase is more a result of the improved hydrogen recovery. If the recovery rate was fixed (instead of the product purity) membrane area requirements would decrease with decreasing permeate pressure.

Figure 13.3c illustrates that membrane area requirements increase with higher purity feed-gas streams. This relationship is again due to the fact that the product purity requirement remains constant. Since hydrogen is the permeating gas more membrane is required as the volume of hydrogen increases. Membrane area requirements also increase with higher recovery rates.

Figure 13.3d demonstrates that the highest purity permeate is achieved with the lowest membrane area — but with a significant recovery penalty. This outcome is again a function of the fact that the initial permeate is most concentrated in hydrogen. Thus, if high hydrogen purity is desired then only a

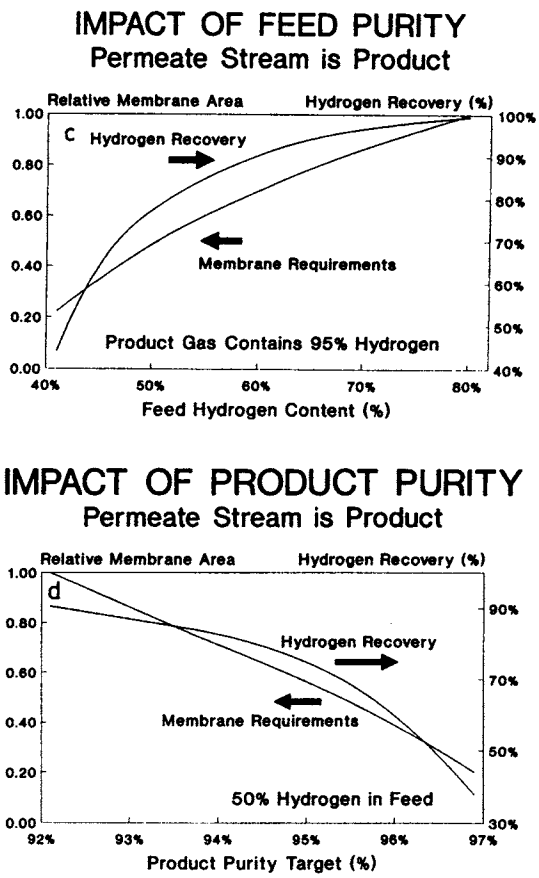

Fig. 13.3 *continued.* (c) Impact of feed stream purity. (d) Impact of product purity requirements.

relatively small amount of membrane is required. This figure demonstrates the trade-off between purity and recovery which must be considered in an economic optimization.

13.3.1.3 General Conclusions

Some generalizations for a *single-stage* membrane process can be made:

- Membrane area requirements are reduced and product recoveries are increased as the pressure differential increases.
- The absolute permeate pressure (or pressure ratio) is also important. Higher pressure ratios lead to improved separation performance. Pressure differential alone does not define membrane performance.
- Increasing membrane area leads to a purer residue but a less pure permeate.
- Product recoveries tend to drop rapidly as the purity requirement is increased.

The last point brings us to a general observation for single-stage membrane processes. Membranes are very efficient concentrators. They become increasingly efficient as the product requirements are relaxed from a 100% purity target. Single-stage systems find good application as bulk concentrators prior to a second purification process such as amine, PSA, other molecular sieve or cryogenic treatment.

As will be demonstrated in Section 13.4.4, multistage membrane systems can overcome some of the problems and limitations demonstrated for the single-stage systems. These multistage approaches usually require additional equipment but the costs often are small relative to the process improvements.

A final important note is that gas separation membranes scale linearly with gas feed volumes. The advantage is that scale-up of a process is quite simple — just add more membrane area. There are no nonlinearities that are often associated with other separation processes. If the membrane separation works for a small gas stream then it will provide the same performance upon scale-up. The disadvantage is that the cost of scale-up is also more linear than some competing processes. Significant improvements have been made in this area, however, as innovations in membrane housing design are reducing the scale-up factor to values not much greater than traditional process equipment [14]. This is due to the fact that the membrane area cost component is generally far smaller than the associated housings and support equipment.

13.3.2 Design Trade-offs

Careful analysis of Figs. 13.2 and 13.3 reveals the various trade-offs inherent in single-stage membrane process design. Optimization of a particular process can result in considerable economic benefits once the variables are understood. If constraints such as product purity and recovery are fixed, variables such as feed compression or permeate vacuum can be adjusted for process optimization. Given a specific application, there are three important elements to be considered in an economic assessment: (1) the cost of the membrane plant (membrane elements and pressure housings), (2) the capital and operating expenses of the compression requirement, and (3) any product losses (e.g., methane in the permeate stream). This is diagrammed in Fig. 13.4. The objective of an economic optimization is to design a process that will balance these trade-offs for a particular application.

References occasionally appear in the literature that suggest that product loss for membrane separation is high in comparison with competing processes. This is a misleading statement that is often based on a single-stage membrane design, often with a poor choice of operating conditions. As will be illustrated in the following sections, much higher recovery rates can be achieved with multistage designs. These processes are rarely analyzed in the literature, however, since they are more difficult to design. It is generally true that the most

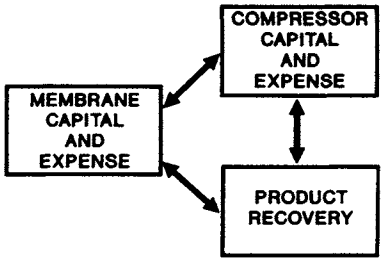

Fig. 13.4. Trade-offs in membrane process design.

efficient membrane process will likely be one in which the product loss will be somewhat higher than that of an "equivalent" nonmembrane process. It is important, however, not to make process comparisons on just one parameter. Product loss should simply be counted as another operating expense. The advantage of membrane processing often comes in the lower capital investment and lower operating expenses. If these advantages offset the product loss expenses then membrane processing should be the preferred approach.

13.4 MEMBRANE PROCESS DESIGNS

If membrane processing were limited to single-stage designs then economic optimization would not be too difficult. However, a single-stage system may not allow the process engineer to meet preselected performance and process criteria. This limitation can be overcome with additional membrane stages and recycle loops.

A wide variety of possible membrane process designs exist that can be employed with great benefit to solve a particular problem. The following discussion takes the reader step by step through a series of process design options to illustrate the importance of various factors. Several gas separation examples are presented to illustrate the practical importance of these designs.

13.4.1 Definitions

A membrane stage is defined as one or more membrane modules assembled into an operating unit that provides a specific function different from any other membrane stages that may be utilized in the same process. A membrane plant is comprised of one or more membrane stages but the plant as a whole has a single inlet (feed) and two outlets (residue and permeate). Although the term "membrane stage" connotates a significant additional investment, this is not often the case. As will be seen, adding a membrane stage can be highly cost-effective.

A good set of terminology for characterizing the various membrane process designs has not yet been established. The terms "two-stage" and "three-stage"

membrane processes do not adequately define the nature of the configuration (i.e., whether any recycle streams are employed). This discussion draws on existing terminology and adds descriptive terms where appropriate.

13.4.2 Assumptions

No one particular membrane type was selected for these analyses but the performance characteristics are reasonably representative of what can be found in the literature. Figures for membrane performance and pricing are particularly difficult to ascertain owing to the large number of systems and the wide range of applications. For example, although similarly priced membranes could be used for both air separation and hydrogen applications, the actual installed cost of both systems is radically different. This difference arises from the cost of high-pressure housings, pretreatment, controls and supporting infrastructure. In fact, the cost of the membrane element is often a very small percentage of the overall unit cost. This percentage can run under 5% for small, high pressure units.

An added problem is the wide range of membrane performance that can be found. For example, it is difficult to compare a low permeability, hollow fiber membrane to a high permeability, spiral-wound membrane. The effective performance difference between the two is minimized due to the fact that the hollow fiber membrane makes up for the lower permeability through higher packing densities. Membrane costs, when expressed as $/membrane area, are also misleading since they do not take into account the permeability or effectiveness of the membrane. In the above example the hollow fiber membrane would cost less per unit area than the spiral but the net price/performance of the two units would still be the same.

For the purpose of the economic optimization analyses in Section 13.3, a Membrane Performance Figure (MPF) is established, which eliminates the membrane area and permeability variables. Membrane performance is characterized by the normalization of the gas flow (flux) of the membrane under fixed conditions to the *installed* membrane cost to achieve that performance. Thus, MPF is expressed as $ft^3\ \$^{-1}\ hr^{-1}\ 100\ psi^{-1}$ or $cm^3\ \$^{-1}\ sec^{-1}\ cmHg^{-1}$. This is simply the division of the membrane permeability (defined earlier) by the membrane price-per-unit area ($\$/ft^2$ or $\$/cm^2$). The values selected for this analysis do not necessarily correlate with commercial values owing to the wide range of membrane performance, pricing and installed costs that accompany any particular installation. These analyses also assume that the permeability of each component through the membrane is independent of composition, pressure and temperature. All membranes are influenced by these variables, however, and they must be considered in actual design. The numbers presented here may therefore not be representative of actual membrane units. Operating conditions were selected to illustrate a point and no attempt was made to optimize the

design for the case studied.

Table 13.2 lists some of the major assumptions employed in this Section. The MPF values are broadly representative of membrane technology but they should not be used for judging economic viability of a particular process. Any number of factors could substantially increase or decrease these figures. The same caveats clearly apply to compressors and operating expenses. High-pressure oil field compressors cost far more per unit of horsepower than low-volume, low-pressure systems. These variables are fixed for the following discussion so as to provide a basis of reference that allows consistent conclusions about membrane process design without interference from dislocations in membrane cost variables.

TABLE 13.2

Membrane performance and economic assumptions

A. Membrane Performance

Membrane Type	Application
A	Hydrogen and Carbon Dioxide Separations
B	Air Separations
C	Solvent Vapor Recovery

	Membrane Performance Factor (scf $\$^{-1}$ hr^{-1} 100 psi^{-1})		
Gas	Type A	Type B	Type C
H_2	2.8×10^{-1}	–	–
N_2	5.7×10^{-3}	3.8×10^{-2}	1.0
CO	7.5×10^{-3}	–	–
CO_2	1.4×10^{-1}	–	–
CH_4	6.7×10^{-3}	–	–
O_2	–	2.0×10^{-1}	–
Toluene	–	–	80

Selectivities	Type A	Type B	Type C
H_2/N_2	50	–	–
H_2/CO	37	–	–
CO_2/CH_4	21	–	–
H_2/CH_4	42	–	–
O_2/N_2	–	5.2	–
Tol/N_2	–	–	80

Notes: To convert units to cm^3 $\$^{-1}$ sec^{-1} cm Hg^{-1} multiply the Membrane Performance Factor by 1.43×10^{-2}. Gas pair selectivities are calculated by dividing the respective MPFs.

(continued)

TABLE 13.2 (*continuation*)

B. Membrane Process Assumptions

- Solution-diffusion mechanism
- Permeate backpressure 1–10 psi
- Negligible pressure drop on residue stream
- Membrane life two to five years depending on application
- Membrane Performance Factor is independent of temperature, pressure and gas composition
- Compressor and vacuum pump efficiency set at 70%

C. Cost Assumptions

Item	Installed Cost
Gas-fired Compressors, High Pressure	$1,000/HP
Electrical Compressors, High Pressure	$500/HP
Air Compressors	$250/HP
Vacuum Pumps	$1,000/HP
Electricity	$0.06/kWhr
Natural Gas, at Wellhead	$1.50/MM Btu
Natural Gas, Utility	$5.00/MM Btu
Hydrogen Gas	$3.50/Msçf

D. Cost Calculations

Total Capital is the sum of installed membrane and compressor (or vacuum pump investment). No Working Capital is assumed.

Yearly expenses are the sum of the following items:

- product losses (calculated as the amount of product gas not recovered in the separation times the value of the purified gas).
- power expenses for operating compressors or vacuum pumps.
- membrane replacement expenses calculated at 20% of the total installed membrane capital per year, or less, depending on the application.
- maintenance expenses calculated as 5% of the installed compressor cost.

The Process Cost is calculated as the sum of Yearly Expenses and Capital Charges divided by the product gas flow to arrive at a process cost expressed in $/unit volume.

E. Conversion Factors

1 hp (horsepower) = 0.746 kW

1 psi = 6.9×10^{3} Pa

1 psi = 6.89×10^{-2} bar

1 psi = 0.07 kg/cm^2

1 scf ft^{-2} hr^{-1} 100 psi^{-1} = 1.55×10^{-5} cm^3 cm^{-2} sec^{-1} cm Hg^{-1}

1 ft (foot) = 0.305 m

1 lb = 0.454 kg

1 MMscfd (million standard cubic feed per day)* = 1.12×10^{3} Nm^3/hr

*Industry convention is such that "standard cubic foot" (scf) is measured at 60°F, 1 atm.

All stream flows are normalized to the feed flow rate except for applications involving the production of nitrogen or enriched oxygen. In the latter cases the flows are normalized to the product gas since this flow is what determines the size of this membrane application. Process costs ($/Mscf) are based on the product gas flow. Capital is the sum of installed membranes and compressors. Yearly expenses include membrane replacement, any product gas losses, power for the compressors and maintenance.

13.4.3 Single-Stage Membrane Processes

13.4.3.1 Single-Stage with Feed Compression

This design has already been discussed in depth in Section 13.3.1.1. Although this design allows the least flexibility, it is by far the most common arrangement currently found in commercial applications. Given that the feed and product compositions are fixed, the design engineer can only work with the pressure ratio between the feed and permeate streams. In membrane separation it may be economically justified to increase the feed gas pressure to above that required for the product gas (or reduce the permeate pressure). This both improves the separation efficiency of the membrane and reduces the amount of membrane area required. Figure 13.5 illustrates the benefit of feed gas compression for the case of separating carbon dioxide from natural gas (methane).

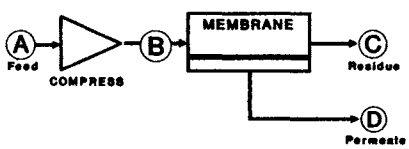

CASE A: No Feed Compression

		A	B	C	D
CH4	%	90.0	90.0	97.0	55.6
CO2	%	10.0	10.0	3.0	44.4
RATE	Ratio	1.00	1.00	0.81	0.19
PRESS	psia	300	300	300	15

CASE B: With Feed Compression

		A	B	C	D
CH4	%	90.0	90.0	97.0	49.5
CO2	%	10.0	10.0	3.0	50.5
RATE	Ratio	1.00	1.00	0.85	0.15
PRESS	psia	300	800	800	15

Process Comparison Ratios

	MEMB AREA	TOTAL CAPITAL	YEARLY EXP	PROCESS COST	PROD REC (%)
CASE A	1.00	1.00	1.00	1.00	87.7%
CASE B	0.24	0.53	0.58	0.56	91.9%

Fig. 13.5. The impact of compression on membrane process performance and cost. This process employs a type A membrane and gas-fired compressors.

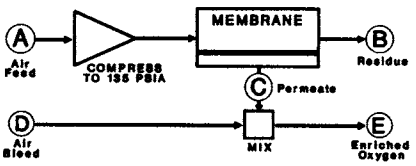

Flows normalized to product stream E.

CASE A: No Bleed Air

		A	B	C	D	E
O2	%	21.0	3.0	30.0	21.0	30.0
N2	%	79.0	97.0	70.0	79.0	70.0
RATE	Ratio	1.52	0.52	1.00	---	1.00
PRESS	psia	15	135	15	15	15

CASE B: With Bleed Air

		A	B	C	D	E
O2	%	21.0	10.5	40.0	21.0	30.0
N2	%	79.0	89.5	60.0	79.0	70.0
RATE	Ratio	0.93	0.60	0.33	0.67	1.00
PRESS	psia	15	135	15	15	15

Process Comparison Ratios

	MEMB AREA	TOTAL CAPITAL	YEARLY EXP	PROCESS COST	PROD REC (%)
CASE A	1.00	1.00	1.00	1.00	94.4%
CASE B	0.30	0.32	0.42	0.36	89.3%

Fig. 13.6. Production of oxygen-enriched air in a single-stage membrane blending the permeate with an air bleed provides the lowest cost for producing a 30% enriched oxygen stream. Process uses a type B membrane with electrical compressors.

The added compression cost is more than offset by the reduction in product gas loss and in the size and cost of the membrane plant. Product recovery is increased to 91.9%.

In applications where the product gas is the permeate stream, the membrane area may be reduced through the use of feed gas bypass [15]. Figure 13.6 illustrates a possible design for producing 30% enriched oxygen. Case A uses a straight membrane process to generate the enriched oxygen stream. Case B uses the membrane to produce a stream of 40% oxygen, which is then blended with air to achieve a 30% concentration. Since less membrane area is required to achieve a higher purity there is a membrane capital cost savings. Compression savings are also achieved since a large portion of the final product volume comes from the bleed air.

13.4.3.2 Single-Stage with Permeate Vacuum or Diluent Gas

Instead of compressing the feed gas one could also apply a vacuum to the permeate stream. While this does not change the pressure differential by a significant amount, it does impact the pressure ratio (feed to permeate pressures). As was demonstrated earlier, the pressure ratio is very important to membrane process economics. Another alternative is to use a "flushing" gas stream (e.g., nitrogen) to dilute the permeate gas. In effect, this reduces the partial pressure of the permeating components and increases the apparent pressure ratio. The draw-

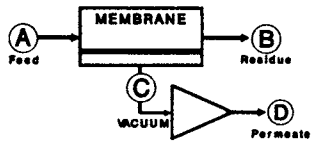

CASE A: No Permeate Vacuum

		A	B	C	D
CH4	%	90.0	97.0	55.6	55.6
CO2	%	10.0	3.0	44.4	44.4
RATE	Ratio	1.00	0.81	0.19	0.19
PRESS	psia	300	300	15	15

CASE B: With Permeate Vacuum

		A	B	C	D
CH4	%	90.0	97.0	46.9	46.9
CO2	%	10.0	3.0	53.1	53.1
RATE	Ratio	1.00	0.86	0.14	0.14
PRESS	psia	300	300	5	15

Process Comparison Ratios

	MEMB AREA	TOTAL CAPITAL	YEARLY EXP	PROCESS COST	PROD REC (%)
CASE A	1.00	1.00	1.00	1.00	87.7%
CASE B	0.57	0.62	0.60	0.58	92.7%

Fig. 13.7. Removal of carbon dioxide from natural gas using a vacuum on the permeate. Process employs a type A membrane.

back is that the use of a diluent stream is expensive and some back-flow of the flush gas into the high-pressure residue stream does occur.

These approaches are generally most useful when the feed gas pressure or the permeate volume are low. Permeate vacuum is occasionally used in the production of enriched oxygen from ambient air, in solvent vapor recovery or in certain gas dehydration applications (the volume of permeate is small). Figure 13.7 illustrates the advantage of this design for a natural gas separation. The base case is the same as was presented in Fig. 13.5. Operating at a reduced permeate pressure of 5 psia is shown to provide significant benefits.

In the case of an oxygen/nitrogen separation the highest purity level of oxygen is achieved with the minimum membrane area (which also leads to minimal recovery). Under these conditions the use of a vacuum pump would generally be preferred since the permeate volume is much smaller than the feed gas volume. In this situation the volume of gas pumped by the vacuum pump is much smaller than the amount of feed gas that would have to be compressed.

Solvent vapor recovery applications also involve the use of low feed pressures and low permeate volumes. Figure 13.8 compares the use of a compressor with the use of a vacuum for the separation of toluene vapor from air. The use of a vacuum provides much improved economics.

13.4.3.3 Single-Stage with Recycling

One way to improve product recovery is through the use of a recycle loop. This improvement is illustrated in Fig. 13.9 for a case in which the feed gas is

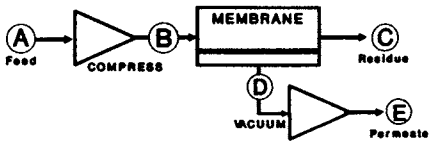

CASE A: Feed Compression Only

		A	B	C	D	E
Toluene	%	2.0	2.0	0.5	7.0	7.0
N2	%	98.0	98.0	99.5	93.0	93.0
RATE	Ratio	1.00	1.00	0.77	0.23	0.23
PRESS	psia	15	135	135	15	15

CASE B: Permeate Vacuum Only

		A	B	C	D	E
Toluene	%	2.0	2.0	0.5	14.3	14.3
N2	%	98.0	98.0	99.5	85.7	85.7
RATE	Ratio	1.00	1.00	0.89	0.11	0.11
PRESS	psia	15	16	16	1	15

Process Comparison Ratios

	HP	MEMB AREA	TOTAL CAPITAL	YEARLY EXP	PROCESS COST*	PROD REC (%)
CASE A	1.00	1.00	1.00	1.00	1.00	80.5%
CASE B	0.19	3.30	0.44	0.28	0.33	78.7%

Fig. 13.8. Solvent vapor recovery membrane system for the removal of toluene from nitrogen. Operating with the vacuum on the permeate side reduces process cost. This process employs a type C membrane and electric compressors.

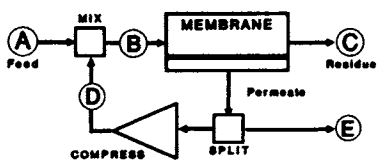

CASES B and E: 30% Permeate Recycle

		A	B	C	D	E
CH4	%	90.0	87.5	97.0	45.3	45.3
CO2	%	10.0	12.5	3.0	54.7	54.7
RATE	Ratio	1.0	1.06	0.87	0.06	0.13
PRESS	psia	800	800	800	800	15

Process Comparison Ratios

		PERM* RECYCLE	MEMB AREA	TOTAL CAPITAL	YEARLY EXP	PROCESS COST	PROD REC (%)
$1.75/MMBtu Product Value	CASE A	0%	1.00	1.00	1.00	1.00	91.9%
	CASE B	30%	1.21	1.52	0.98	1.09	93.2%
	CASE C	50%	1.43	2.10	1.00	1.23	94.3%
$8.00/MMBtu Product Value	CASE D	0%	1.00	1.00	3.73	3.08	91.9%
	CASE E	30%	1.21	1.52	3.28	2.81	93.2%
	CASE F	50%	1.43	2.10	2.92	2.66	94.3%

*Permeate Recycle is the percentage of the membrane permeate that is recycled to the feed side.

Fig. 13.9. Single-stage membrane with recycle. Recycling improves product recovery but this process design is not cost-effective unless high product values are involved. Type A membrane with gas-fired compressors.

already at high pressure. A portion of the permeate stream is recompressed and recycled to the feed stream. The percentage of the stream recycled is adjusted to provide the desired performance. In this case, the overall product recovery is greatly enhanced but at the expense of the recycle compression and additional membrane requirements. For the case studied, no benefits were found when the product gas was valued at $1.75/MMBtu. The added recovery did not pay for the added capital costs and expenses. Benefits were found for recycle when the product gas was valued at $8.00/MMBtu as is shown (Case F vs Case D).

Although this design has been discussed often in the literature it offers no real benefits even at higher product values. As will be seen later, multistage designs are superior for improving product recovery. A two-stage recycle membrane can achieve higher recoveries at lower cost than a single-stage with recycle.

13.4.3.4 Single- vs. Multistage Processes

The single-stage membrane process shown in Fig. 13.5 has a methane product loss that is moderately high for the example chosen. Unfortunately, since this design is the simplest it is the one most often used in many process comparisons. An objective of much membrane R&D is to increase the separation factors for membranes so that higher recoveries can be achieved without having to compress or to recycle gas streams. However, gas separation membranes are easily staged to provide much higher product recoveries and it can be even be demonstrated in some cases that multistaging is a better approach than simply employing higher selectivity membranes in a single stage design.

Single-stage membranes do represent the lowest capital investment option. A multistage membrane process entails additional compression and membrane investment. Process design involves tradeoffs between higher product recovery and increased equipment and utility costs. In situations where investment payback is important then a single-stage design will often prevail. Investments based on discounted cash flow analyses, however, will tend to favor multistage membrane systems. The following examples of multistage processes will illustrate these points.

13.4.4 Two-Stage Membrane Processes

13.4.4.1 Two-Stage Membrane Series

The single-stage membrane process depicted in Fig. 13.5 can consist of any number of individual membrane modules. By splitting the modules into two stages, as shown in Fig. 13.10, one can take advantage of the differences in permeate composition that are produced by each stage. Although the final

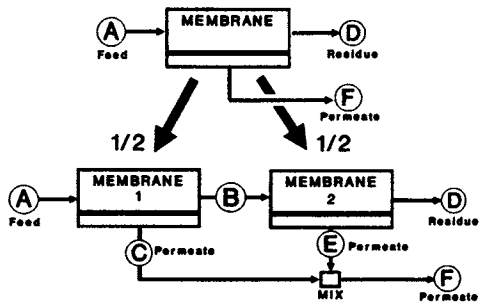

		A	B	C	D	E	F
CO2	%	7.0	3.8	43.9	2.0	27.3	36.6
CH4	%	93.0	96.2	56.1	98.0	72.7	63.4
RATE	Ratio	1.00	0.92	0.08	0.86	0.06	0.14
PRESS	psia	860	860	15	860	15	15

Even though the membrane is split into two stages the resulting residue and permeate streams (D and F, respectively) have the same composition and flow rates. The composition of the individual permeate streams (C and E) are quite different, however. Stream E could be used as compressor fuel because of its higher BTU content.

Fig. 13.10. Two-stage membrane series. Membrane area can be split in any proportion to form separate stages. The permeate compositions from each stage are different but the overall separation remains the same. Type A membrane.

permeate composition is the same when remixed (Stream F) the compositions of the individual permeate streams (C and E) are quite different. This can be advantageous in this case since the permeate from the second membrane has a higher methane content and could be used as a reduced-BTU fuel for compressors or boilers.

If the feed gas stream must be compressed then a two-stage series design could be used to reduce compression costs. Instead of compressing the entire feed gas stream one could place a compressor between the two stages as shown in Fig. 13.11. In this case the first stage membrane is operated at a lower pressure to bulk remove the carbon dioxide impurity. This substantially reduces the size of the second-stage compressor since the gas volume is now reduced.

The recovery of hydrogen from a variety of refinery and petrochemical streams with membranes poses a special design problem. Unfortunately, hydrogen is the more permeable gas and exits as the low-pressure permeate. For most uses the hydrogen must be recompressed and this cost is quite significant both in terms of capital and operating expenses. In most cases compressors already exist but the engineer may not have control over the suction pressures of these compressors and one having the optimum operating parameters may not exist. For the case illustrated in Fig. 13.12 the problem was to design a process that produced hydrogen at 91% purity with 85% recovery. This can be accomplished with a single-stage unit with a permeate pressure of 550 psia

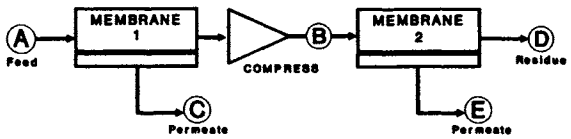

CASE A: Without Membrane 1

		A	B	C	D	E
CH4	%	50.0	50.0		90.0	11.7
CO2	%	50.0	50.0		10.0	88.3
RATE	Ratio	1.00	1.00		0.49	0.51
PRESS	psia	200	600		600	15

CASE B: With Membrane 1

		A	B	C	D	E
CH4	%	50.0	75.0	9.5	90.0	22.0
CO2	%	50.0	25.0	90.5	10.0	78.0
RATE	Ratio	1.00	0.62	0.38	0.48	0.14
PRESS	psia	200	600	15	600	15

Process Comparison Ratios

	MEMB AREA*	TOTAL CAPITAL*	YEARLY EXP	PROCESS COST	PROD REC (%)
CASE A	1.00	1.00	1.00	1.00	88.0%
CASE B	1.29	0.75	0.94	0.87	86.8%

*Membrane 1 relative cost is set to 1/2 that of Membrane 2 due to low pressure operation.

Fig. 13.11. Two-stage membrane series with intermediate compression. Bulk removal of gas impurities reduces compression costs and allows the use of a lower cost first-stage membrane system. Type A membrane with gas-fired compressors.

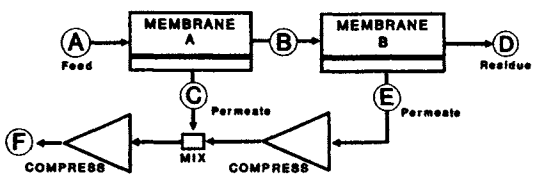

CASE A: Single Stage

		A	B	C	D	E	F
H2	%	60.0			20.0	91.0	91.0
N2	%	40.0			80.0	9.0	9.0
RATE	Ratio	1.00			0.44	0.56	0.56
PRESS	psia	2000			2000	550	2000

CASE B: Two Stage

		A	B	C	D	E	F
H2	%	60.0	45.0	89.8	20.0	92.8	91.0
N2	%	40.0	55.0	10.2	80.0	7.2	9.0
RATE	Ratio	1.00	0.66	0.34	0.44	0.23	0.56
PRESS	psia	2000	2000	1000	2000	300	2000

Process Comparison Ratios

	MEMB AREA	TOTAL CAPITAL	YEARLY EXP	PROCESS COST	PROD REC (%)
CASE A	1.00	1.00	1.00	1.00	85.4%
CASE B	1.24	1.09	1.00	1.01	85.4%

Fig. 13.12. Two-stage membrane series for hydrogen separation. Membranes can be staged with different permeate pressures and yet still achieve the overall separation performance of a single-stage system. The process can therefore be designed around existing compressors. Type A membrane with electrical compressors.

(Case A). But if existing compressors had suction pressures of 1000 and 300 psia, the entire stream would have to be recompressed from 300 psia. Alternatively, the two-stage process illustrated in Case B matches the membrane permeate pressures to existing compressors with no increase in process cost or performance.

13.4.4.2 Two-Stage Membrane Series with Recycling

Most multistage membrane designs incorporate some sort of recycle to improve product separation and recovery. Such designs are easily implemented from a membrane standpoint but always require compression for the recycle stream. Gas compression is expensive but recycling generally improves the overall process efficiency.

The air separation process shown in Fig. 13.13 is an example of a membrane series with a recycle step. This design can improve product recovery (nitrogen in this case) and at the same time reduce membrane capital costs. This arrangement is simply a two-stage series wherein the permeate from the second stage is recycled back to the feed gas compressor. The membranes are split so as to produce a permeate from the second stage that has a higher nitrogen content than the feed air. Recycling this high-nitrogen permeate stream to the feed side increases the nitrogen recovery rate and reduces the compression and membrane area re-

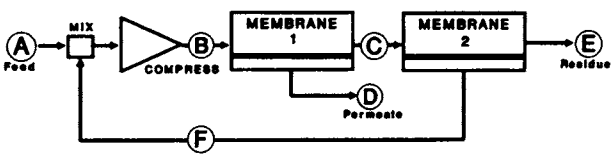

Flows normalized to product streams C or E.

CASE A: No Recycle

		A	B	C	D	E	F
N2	%	79.0	79.0	98.0	71.3		
O2	%	21.0	21.0	2.0	28.7		
RATE	Ratio	3.45	3.45	1.00	2.45		
PRESS	psia	15	125	125	15		

CASE B: With Recycle

		A	B	C	D	E	F
N2	%	79.0	80.9	94.0	66.7	98.0	88.1
O2	%	21.0	19.1	6.0	33.3	2.0	11.9
RATE	Ratio	2.50	3.18	1.65	1.53	1.00	0.65
PRESS	psia	15	125	125	15	125	15

Process Comparison Ratios

	MEMB AREA	TOTAL CAPITAL	YEARLY EXP	PROCESS COST	PROD REC (%)
CASE A	1.00	1.00	1.00	1.00	35.6%
CASE B	0.91	0.91	0.91	0.91	48.9%

Fig. 13.13. Two-stage membrane series with recycle for inert gas production. Type B membrane with electrical compressors.

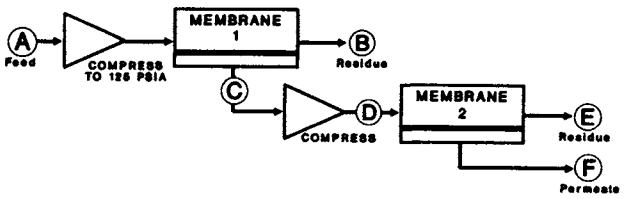

Flows normalized to product streams C or F.

CASE A: Single-Stage

		A	B	C	D	E	F
N2	%	79.0	80.0	48.4			
O2	%	21.0	20.0	51.6			
RATE	Ratio	33.0	32.3	1.00			
PRESS	psia	15	125	15			

CASE B: Two-Stage Cascade

		A	B	C	D	E	F
N2	%	79.0	90.0	42.0	42.0	70.0	28.5
O2	%	21.0	10.0	58.0	58.0	30.0	71.5
RATE	Ratio	10.0	6.60	3.40	3.40	2.40	1.00
PRESS	psia	15	125	15	125	125	15

Process Comparison Ratios

	O2 CONC	MEMB AREA	TOTAL CAPITAL	YEARLY EXP	PROCESS COST*	PROD REC (%)
CASE A	51.6%	1.00	1.00	1.00	1.00*	7.9%
CASE B	71.5%	4.67	1.78	0.67	0.64*	34.0%

*Process cost adjusted for O2 concentration difference.

Fig. 13.14. Two-stage membrane cascade for production of oxygen from air. Additional membrane cascades can be added to achieve the desired oxygen purity. Type B membrane with electrical compressors.

quirements. For cases in which the feed gas is already at high pressure the permeate would be compressed prior to mixing with the feed gas stream.

This type of design is useful when the impurity level is high and a bulk removal step (first-stage membrane) is warranted. This design could also be used for cases in which the permeating gas (from the first stage) is the product gas. The recycle step substantially improves recovery for those cases in which the permeate must have a relatively high purity.

13.4.4.3 Two-Stage Membrane Cascade

The nature of membrane gas separation makes it more difficult to achieve a specified product purity in a single-stage process when the product gas exits as the permeate stream (as was demonstrated in Section 13.3.1.2). This can be overcome via a cascade membrane process as shown in Fig. 13.14. Note the difference in oxygen purity between Case A (51.6%) and Case B (71.5%).

13.4.4.4 Two-Stage Cascade with Recycling

The addition of a recycle loop to a two-stage cascade membrane process results in the process shown in Fig. 13.15. This example illustrates the dramatically improved methane recovery such a design can offer in the case of natural

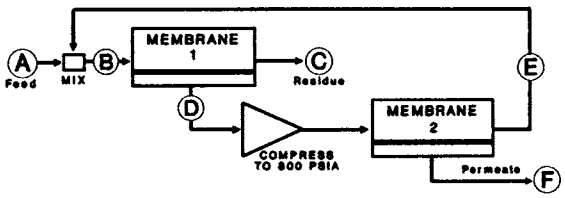

CASE A: Single-Stage

		A	B	C	D	E	F
CH4	%	90.0	90.0	97.0	49.5		
CO2	%	10.0	10.0	3.0	50.5		
RATE	Ratio	1.00	1.00	0.85	0.15		
PRESS	psia	800	800	800	15		

CASE B: Two-Stage Cascade With Recycling

		A	B	C	D	E	F
CH4	%	90.0	89.6	97.0	50.9	85.0	10.0
CO2	%	10.0	10.4	3.0	49.1	15.0	90.0
RATE	Ratio	1.00	1.10	0.92	0.18	0.10	0.08
PRESS	psia	800	800	800	30	800	15

Process Comparison Ratios

	MEMB AREA	TOTAL CAPITAL	YEARLY EXP	PROCESS COST	PROD REC (%)
CASE A	1.00	1.00	1.00	1.00	91.9%
CASE B	1.40	2.21	0.56	0.89	99.2%

Fig. 13.15. Two-stage membrane cascade with recycling for natural gas treating. The second stage enhances methane recovery. Type A membrane with gas-fired compressors.

gas treating. The additional membrane expenses are minimal but the compression cost can be significant and the attractiveness of such a process depends on the value of the product gas. Optimization of the process involves selection of the stage two membrane area (affects the recycle product purity and recovery rate), the stage one permeate pressure (higher pressure reduces the recompression cost but lowers membrane efficiency), and selection of an operating pressure for the stage two membrane (a second compressor could be used afterwards to bring the recycle product stream back to the feed gas pressure).

This two-stage cascade recycle process is analogous to the single-stage stream splitting process (Fig. 13.9) except that the stream splitting step is now replaced with a membrane. The membrane in effect defines the proportion of the stream that is to be recycled, but in so doing it provides an additional degree of separation that dramatically improves product recovery and the overall process economics. This process is also useful for applications in which the permeate stream from the second stage is the product gas.

Economic comparisons of the single-stage (Fig. 13.5), single-stage with recycling (Fig. 13.9), and the two-stage cascade with recycling (Fig. 13.15) shows that the recycle cascade offers the best economics. The "cost" of the lost product (e.g. methane in the permeate) is included in the process cost. This comparison clearly illustrates the economic benefits of membrane process optimization. It also demonstrates that properly designed membrane systems can achieve high product recoveries.

13.4.4.5 Ideal Two-Stage Cascade with Recycling

If the composition of the recycle stream shown in Fig. 13.15 is set to that of the feed stream, the configuration is known as an ideal cascade [16]. By matching the compositions of these streams there are no efficiency losses due to mixing. The impact of excessive mixing losses on membrane process economics can be significant. These inefficiencies can be analyzed via an "availability loss" or "exergy" analysis on a particular membrane process to determine whether improved configurations are possible [17]. An interesting application of this analysis was performed for a two-stage membrane cascade involving hydrogen recovery from a syngas stream [18]. This analysis demonstrated it was actually more economical to first design an ideal two-stage cascade that resulted in a higher-than-required hydrogen product gas and then to dilute that gas stream (the second stage permeate) to a lower purity by running a direct partial bypass of the feed gas to the permeate stream.

13.4.5 Three-Stage

As should already be evident, many design permutations are possible with gas separation membranes. There are many possible three-stage designs and only two will be illustrated here. The staging of membranes is not particularly expensive or difficult. Several three-stage designs are in commercial use.

13.4.5.1 Two-Stage Recycle Cascade with Premembrane

The two-stage cascade shown in Fig. 13.15 can be easily improved with the addition of a premembrane to form the process shown in Fig. 13.16. The function of this premembrane is for bulk separation of the gas mixture prior to the two-stage recycle cascade. This arrangement is quite useful for reducing the compression requirements of the cascade recycle compressor. This design is used for treating natural gas wherein the feed carbon dioxide content is high. Note that the recycle stream from the third stage membrane could also be recycled to the feed of the second stage.

This type of design could also be employed for cases in which the combined permeate streams from stages 1 and 3 form the product stream as in hydrogen separations. In this application the two-stage recycle cascade would provide increased hydrogen recovery.

13.4.5.2 Two-Stage Cascade with Postmembrane

Most air separation membrane systems are utilized just for their nitrogen or oxygen enriched streams. The three-stage design shown in Fig. 13.17 allows efficient production of both streams. Membrane stages one and three provide a

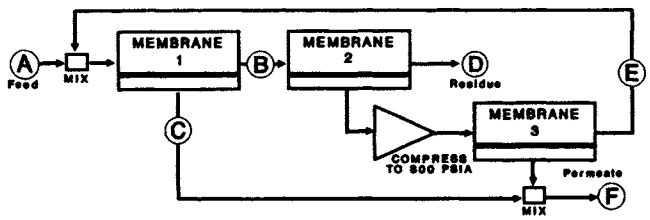

CASE A: Two-Stage Cascade With Recycling

		A	B	C	D	E	F
CH4	%	70.0	70.0		97.0	70.0	4.0
CO2	%	30.0	30.0		3.0	30.0	96.0
RATE	Ratio	1.00	1.17		0.71	0.17	0.29
PRESS	psia	800	800		800	800	15

CASE B: Three-Stage With Recycling

		A	B	C	D	E	F
CH4	%	70.0	85.0	15.7	97.0	70.0	13.3
CO2	%	30.0	15.0	84.3	3.0	30.0	86.7
RATE	Ratio	1.00	0.88	0.24	0.68	0.12	0.32
PRESS	psia	800	800	15	800	800	15

Process Comparison Ratios

	HP	MEMB AREA	TOTAL CAPITAL	YEARLY EXP	PROCESS COST*	PROD REC (%)
CASE A	1.00	1.00	1.00	1.00	1.00	98.4%
CASE B	0.41	0.85	0.64	1.02	0.84	93.8%

Fig. 13.16. Two-stage recycle cascade with premembrane for treating natural gas. The use of a premembrane to bulk remove highly contaminated gases reduces overall process costs. Type A membrane with gas-fired compressors.

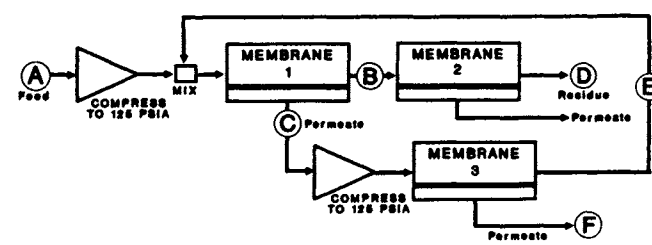

CASE A: Two-Stage Cascade With Recycling

		A	B	C	D	E	F
N2	%	79.0	90.0	58.0	97.0	96.0	30.0
O2	%	21.0	10.0	42.0	3.0	4.0	70.0
RATE	Ratio	2.12	1.71	0.90	1.00	0.41	0.49
PRESS	psia	15	125	15	125	15	125

Fig. 13.17. Production of both nitrogen and oxygen streams using a three-stage membrane process. Type B membrane with electrical compression.

70% purity oxygen product stream (Stream F). The stage two membrane is used to provide a nitrogen product purity of 97%. The residue stream from stage three is recycled to the feed of stage one to increase recovery and to reduce compression costs. The balance of membrane area between stages one and two depends on the targeted oxygen purity and recovery.

13.4.6 Other Membrane Process Designs

13.4.6.1 Continuous Membrane Columns

The membrane processes discussed thus far operate in a mode wherein the permeate gas comes entirely from gases crossing the membrane from the high-pressure to the low-pressure side. In fact, modules can be constructed in which a separate gas stream can be introduced on the permeate side of the membrane. The advantage of such a design is that a "flush" gas can be used to effectively reduce the partial pressure of the permeating gas by simple dilution of the permeate stream. A simple implementation of this concept would be to use a nitrogen flush gas to sweep the permeating CO_2 in a natural gas-treating separation (Fig. 13.7). The nitrogen dilutes the permeate gas stream and therefore reduces the partial pressure of the CO_2. The disadvantage is that nitrogen will pass to the high pressure side and contaminate the residue stream.

Another design, termed a Continuous Membrane Column (CMC), can also be employed to improve separation recoveries over what could be achieved with a simple single-stage system [19,20]. Figure 13.18 illustrates the general operation of such a membrane system.

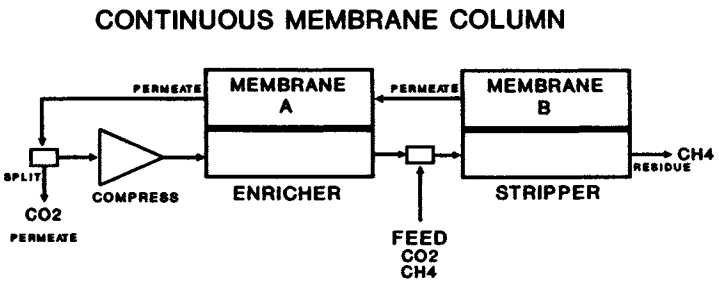

Fig. 13.18. Continuous membrane column. (From Ref. [19]).

13.4.6.1 Designs Utilizing Different Membranes

All of the above examples, assume that all stages of a membrane process utilize the same membrane. Different membrane types can be employed for each stage to either increase efficiency or to achieve a different type of separation. The example in Fig. 13.19 illustrates the use of a lower selectivity but higher permeability membrane in the second stage for the recovery of hydrogen from a refinery stream. As can be seen the lower selectivity (Case B) results in a product stream (Stream F) of slightly lower purity but the recoveries in both cases are still the same. The process benefit comes from the lower capital

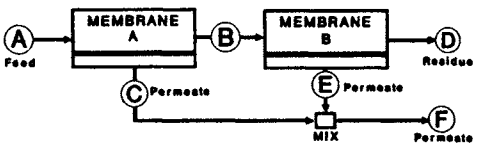

CASE A: Same Membrane

		A	B	C	D	E	F
H2	%	70.0	40.0	96.4	20.0	75.9	91.5
CH4	%	30.0	60.0	3.6	80.0	24.1	8.5
RATE	Ratio	1.00	0.47	0.53	0.30	0.17	0.70
PRESS	psia	800	800	250	800	250	250

Membrane B has same performance as Membrane A.

CASE B: Different Membranes

		A	B	C	D	E	F
H2	%	70.0	40.0	96.4	21.0	71.8	90.3
CH4	%	30.0	60.0	3.6	79.0	28.2	9.7
RATE	Ratio	1.00	0.47	0.53	0.29	0.18	0.71
PRESS	psia	800	800	250	800	250	250

Membrane B has 2X the permeability and 1/2X the selectivity of Membrane A.

Process Comparison Ratios

	MEMB AREA*	TOTAL CAPITAL*	YEARLY EXP	PROCESS COST	PROD REC (%)
CASE A	1.00	1.00	1.00	1.00	91.4%
CASE B	0.78	0.78	0.96	0.91	91.4%

Fig. 13.19. Two-stage membrane series in which membrane B has twice the permeability and half the selectivity of membrane A.

requirement in Case B. This results in a lower process cost compared to Case A. This example illustrates why in some cases membrane selectivities are not as important as membrane permeability.

A second example involves the use of membranes having opposite selectivities and is sometimes referred to as a "Two-Membrane Column" [21]. This design is similar to the Continuous-Membrane Column and is claimed to provide good efficiencies for applications with high product purity requirements. The example in Fig. 13.20 is for a helium/hydrocarbon separation in which Membrane A permeates methane more readily than the helium. As was noted in earlier discussions, it is easier to achieve a certain product purity when

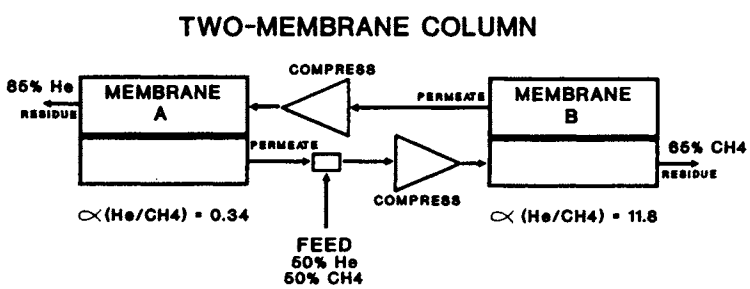

Fig. 13.20. Two Membrane Column. Membrane A has the opposite selectivity of membrane B for a helium/methane separation. (From Ref. [21]).

the gas of interest exits as the residue (in this case helium from the second stage). The added advantage is that the helium is delivered at high pressure from Membrane A.

The applicability of the Two-Membrane Column design is dependent on the availability of suitable membranes having the desired separation performance. This design must also compete with several of the two-stage options mentioned earlier.

13.4.7 Hybrid Systems

Gas separation membranes can and have been combined with other traditional gas separation processes to yield hybrid processes with cost/performance advantages that neither process could achieve individually. These processes generally take advantage of the bulk separation properties of membranes or of a certain gas/gas separation that otherwise is difficult to achieve. The number of potential hybrid processes is limitless and many require little imagination. Those involving recycle loops or membrane staging are more interesting.

13.4.7.1 Membrane/Solvent Treating

The removal of carbon dioxide from methane (natural gas) has traditionally been accomplished via solvent washing processes such as amine treating. Amine processing costs escalate rapidly with increasing carbon dioxide content. Membranes, on the other hand, are very effective CO_2 concentrators. By bulk-separating the feed gas with a membrane the subsequent amine plant can be downsized. A more common scenario is that a membrane unit can be used to increase the capacity or reduce the operating costs of an existing amine plant. If the membrane permeate stream has enough BTU value it can be used for amine plant fuel.

13.4.7.2 Membrane/Cryogenic Distillation

Membranes can also be used to downsize cryogenic units via a preseparation step in many applications. One process claims that the addition of a membrane reduces the size of the cryogenic unit by 65% to achieve the required separation [22]. Another process claimed in the patent literature withdraws a low purity nitrogen by-product stream from an air liquefaction unit, removes the oxygen from the stream via a membrane and returns the nitrogen residue stream back to the cryogenic unit [23]. Operating savings are claimed.

Another process separates high levels of carbon dioxide from methane via liquefaction and passes the methane-rich overhead stream to a membrane separator for final purification [24]. The CO_2-rich membrane permeate is re-

cycled to provide enhanced recovery. A separate design is illustrated for cases in which the feed gas stream has lower levels of carbon dioxide. The latter process employs a two-stage membrane to increase the CO_2 content of the feed gas to the cryogenic unit.

13.4.7.3 Membrane/Pressure Swing Adsorption (PSA)

A number of process designs have appeared involving pressure swing adsorption units and membranes. As before, gas separation membranes can always be used to downsize a PSA unit for a variety of applications [25]. The more interesting applications involve recycle loops.

Membranes can be used to recover product from the waste purge gas used to flush the spent PSA column [26]. A PSA unit is used to recover hydrogen from an H_2/CO stream. At the end of the PSA cycle the adsorbed carbon monoxide must be flushed from the column. The feed gas stream is commonly used for this operation but substantial product losses can result. A membrane can be used to recover this hydrogen for recycle back to the feed gas. This process reduces the size of the PSA unit and includes a second membrane stage for enhanced product recovery [27].

13.4.7.4 Membrane/Condensers

Higher hydrocarbons are often found in many natural gas and refinery gas streams. The dew point of these gas streams can be relatively low due to the presence of diluent gases such as carbon dioxide or hydrogen. In many processes cryogenic temperatures are required to condense these higher hydrocarbons at great capital and operating expenses. Membranes could be used to remove the carbon dioxide or hydrogen and in so doing raise the hydrocarbon dew point of the gas stream. This would allow easier separation of the higher hydrocarbons since simple condensors could now be used in place of expensive cryogenic units [28]. Some membrane systems are specially designed to tolerate hydrocarbon condensation directly in the membrane unit for this application.

13.4.7.5 Membrane/Inert Gas Combustors

At present, gas separation membranes do not have especially high selectivities for oxygen/nitrogen separations since oxygen is not nearly as permeable a gas as, for instance, carbon dioxide. If an air stream is first burned (e.g., with natural gas) the resulting carbon dioxide is easily separated from the nitrogen. This process is being used to produce nitrogen for oil field platforms [29]. The efficiency of the CO_2/N_2 separation also makes it interesting for flue gas CO_2 recovery.

13.4.7.6 Other

A process has been proposed [30] in which a hydrogen/nitrogen mixture produced by the dissociation of ammonia can be adjusted or purified using a membrane. This process was claimed to be economically favorable to the delivery of liquid hydrogen.

As can be seen there are an infinite number of possible process combinations involving gas separation membranes. A number of additional process combinations will be shown in following examples and case studies.

13.4.8 Membrane Process Optimization

It should be clear from the previous examples that although membrane separation is a relatively simple process, the design and optimization of membrane processes can, in fact, be complex. Process optimization can be rather difficult once one moves away from the simple one-stage design. Considering the three-stage process in Fig. 13.16, there are a total of nine major variables that must be evaluated and most of these variables directly impact each other. Even with the aid of computer programs multistage processes can be very difficult to evaluate and optimize. Optimization programs have been developed but they are not generally accessible to the engineering community [31].

Unfortunately, many past publications compared nonoptimized single-stage systems with other separation processes and in so doing reached incorrect or misleading conclusions. Single-stage designs do provide a low capital investment but they can result in higher than necessary product losses. As was illustrated in several examples, high product losses can be avoided with proper design. The flexibility of membranes allows the design of processes that fall in a wide range between the low-capital, single-stage design and the high recovery, multistage designs. The process engineer has great latitude with gas separation membranes to balance the membrane costs, compression costs and product losses to a design that best meets the specific needs of a process.

13.5 CASE STUDIES OF MEMBRANE APPLICATIONS

13.5.1 Overview

Comparing the costs of various processes is complex and generally very dependent on the specific situation. Comparing membrane processes with the more traditional gas separation processes is complicated by three factors. First, the technology of gas separation membranes has improved dramatically over the past several years. These technical advances, combined with increased

competition in the industry, have greatly improved the price/performance of membrane processes. Publications are sometimes out of date within two years with respect to membrane cost comparisons. For example, air separation membranes are 300–400% more efficient in 1990 than they were in 1985. This trend will continue (but at a slower rate) and this makes process comparisons difficult.

The second problem in making comparisons is that membranes do not neatly replace existing separation processes in many situations. The nature of the membrane separation is different and this often results in having to make other operating or process changes to accommodate the membrane package. It is impossible to assess these impacts on a broad basis. One example of this problem is in the separation of hydrogen in refinery streams. Hydrogen will exit as the low-pressure membrane permeate. However, most applications require hydrogen at high pressures and thus the gas must be recompressed. The cost of recompression varies greatly depending on the situation and this added cost will usually make the difference in whether a membrane is economically attractive as opposed to a separation that does not result in such a pressure loss.

A third problem in judging membrane economic competitiveness from published information is that the bases for such calculations are rarely given. Differing methods of accounting for depreciation and membrane replacement costs will often cloud the situation. Furthermore, economic comparisons are not common and many are presented in conferences but never published in journals. Only recently have publications appeared that attempt to place some perspective on membrane economics [32].

The following sections attempt to place some perspective on the economic attractiveness and limitations of using membranes for a variety of applications based on published cost comparisons. However, due to the problems discussed above it is important to take these analyses as guidelines only.

13.5.2 Oxygen/Nitrogen Separation

Although air separation membranes were not well established prior to 1986, these membranes have become one of the fastest growing segments of the gas separation membrane market. New membrane developments brought the cost of air separation down to levels where it can be competitive in some applications with on-site delivery of liquified gases. The availability of inexpensive nitrogen is also creating some markets where the less expensive gases provide utility.

Membranes separate air into oxygen (permeate) and nitrogen (residue) streams. The present state of membrane technology is such that high separation factors are not possible, however. The practical impact is that high-purity oxygen streams are not economically viable and a typical one-stage separation has an upper oxygen purity limit of 30–45%. Relatively high purity nitrogen is possible but recovery rates are somewhat low.

At present, the vast majority of membrane applications are for the production of nitrogen. An "inert gas" stream (predominately nitrogen with some argon) can be economically produced with purities up to 99.5%. (Suppliers usually quote this stream as having less than 0.5% oxygen). Low selectivity makes production of higher purity nitrogen relatively expensive. Membranes are most efficient for producing nitrogen with purities less than 98%.

13.5.2.1 Nitrogen Production

Nitrogen production from membranes competes with both delivery of liquified nitrogen and with on-site PSA (pressure swing adsorption) generators. In general, membrane separation is not competitive with liquid delivery when the gas volume is high or when high purity nitrogen is required. It is also obviously not competitive when liquid nitrogen is utilized for its cooling properties. For the smaller volume applications membranes compete directly with small PSA units. PSA units are capable of producing a higher purity gas than membranes. Monsanto prepared an overview of where membranes compete for this application [33]. This is shown in Figure 13.21 with some shading added to reflect advances in membranes since the original figure was prepared.

Membrane air separation is growing rapidly for applications requiring inert gas blanketing. Inert gas is used to blanket flammable materials, to preserve foods and to prevent oxidation. Membranes offer special promise in applications involving transportation. For instance, fresh fruits, vegetables and flowers are sometimes shipped via air when spoilage is rapid; membrane separators are being added to cargo containers to produce an inert atmosphere during shipment. PSA and liquified nitrogen are not suitable for this application due to their bulk. Membranes are far more weight- and space-efficient (even with the compressor) and the gas blanket typically does not have to exceed 95% nitrogen

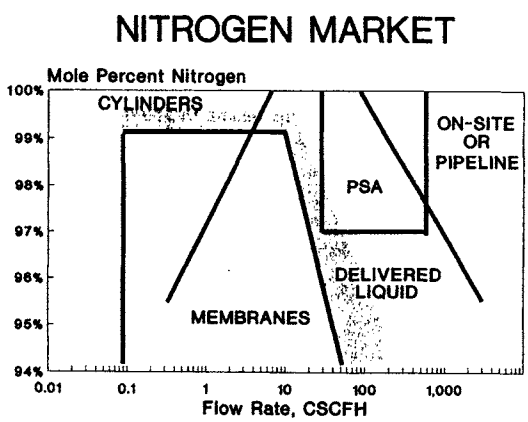

Fig. 13.21. Air separation technologies and sources for nitrogen gas. (From Ref. [33]).

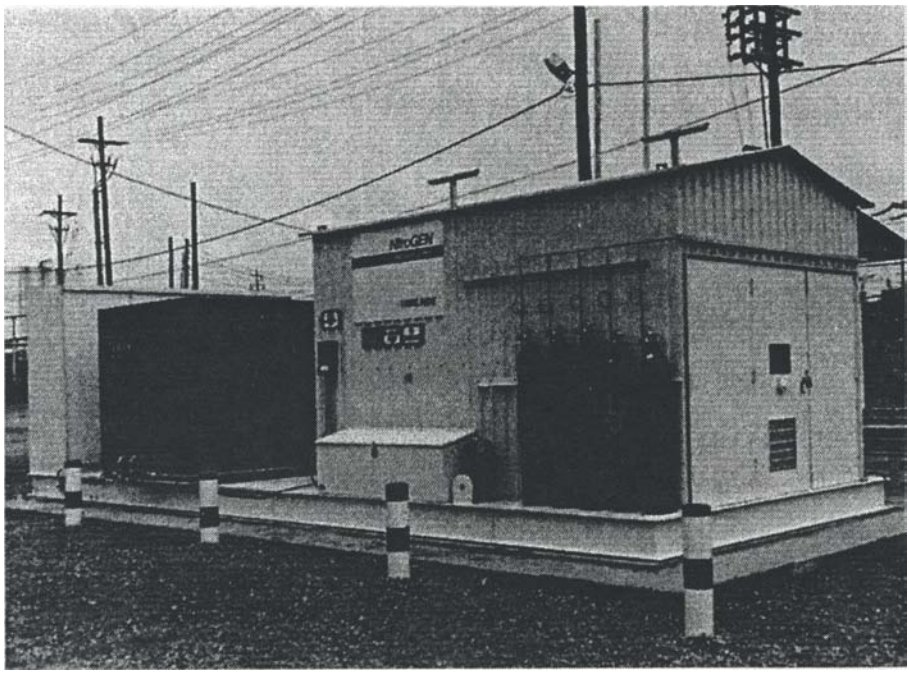

Fig. 13.22. NitroGen™ membrane system for nitrogen production from air. (Courtesy of Linde Division, Union Carbide Industrial Gases, Inc., Danbury, CT).

purity for optimum performance. Membranes also compete with "inert gas generators", which combust a hydrocarbon fuel to produce a nitrogen and carbon dioxide inert gas stream.

Although most commercial membrane separators utilize a single-stage design, Union Carbide's NitroGen system employs a two-stage series with recycle process design [34,35]. As was illustrated in Section 13.4.4.2 this design can provide some improvement in process efficiency. A NitroGen system is shown in Fig. 13.22.

Monsanto has published cost comparisons of their Prism Alpha air separation membrane system versus delivered liquid nitrogen [30,33]. A powder metal company was using delivered liquid nitrogen at a cost $0.40 per hundred standard cubic feet (CSCF). An additional charge for tank rental was $370/ month. At a monthly usage of 286,000 standard cubic feet (scf) this resulted in a total cost of $0.53 per CSCF of nitrogen. A Prism Alpha unit is shown in Fig. 13.23.

A membrane system producing the same volume of 99% nitrogen gas (1% oxygen) was calculated to have a compressor power requirement of 7.05 KW and a monthly capital and compressor maintenance charge of $475/month. Assuming a power cost of $0.07/KWH the membrane approach provides nitrogen at a cost of $0.26 per CSCF. This represents more than a 50% saving over delivered liquid nitrogen.

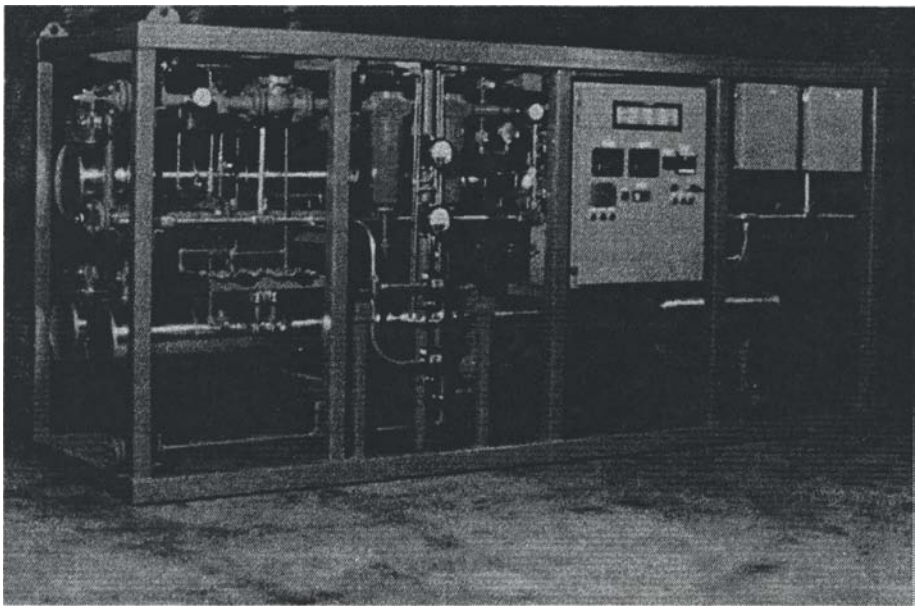

Fig. 13.23. A Prism Alpha air separation membrane from Permea. (Courtesy of Monsanto, St. Louis, MO).

The above example shows a clear cost advantage for membrane-produced nitrogen at the 550-scfh level. Lower volume nitrogen requirements would benefit the membrane approach even more since the cost of delivered liquid nitrogen begins to escalate rapidly at the lower volumes. Prices vary depending on location but delivery of 100,000 scf of nitrogen would cost approximately 50% more per cubic foot while delivery at the 50,000 scf-level would raise the cost by nearly 150%.

The cost savings for the membrane approach would also improve for lower nitrogen purities. As was demonstrated in Section 13.3.1.1 membrane area requirements decrease rapidly when the residue product purity requirements are relaxed. A membrane unit and compressor rated at 1,500 scfh of 99% nitrogen could be operated at a higher feed flow rate to deliver over 3000 scfh of 97% nitrogen with only a 30% increase in compressor requirements. Thus, a lower purity product could be produced at even greater cost savings.

A/G Technology developed an economic comparison of their system with PSA [36,27] (Table 13.3). This analysis showed the membrane unit to be of equivalent overall cost to PSA for the size of plant analyzed (3400 SCFH). However, the PSA unit has a 33% higher capital cost. The lower capital cost of a membrane unit becomes more of an advantage as the utilization rate decreases (less gas over which to amortize the investment).

Dow Chemical (Generon) provided an assessment of the economic perfor-

TABLE 13.3

Cost comparison for 95% nitrogen-enriched air generation

	A/G Technology Membranes	PSA
Capacity (ton/day)	3.0	3.0
Installed capital cost ($ 000)	90.00	120.00
Expenses ($/day)		
Membrane replacement	16.00	–
Power	35.00	41.00
Capital charges	33.00	44.00
Depreciation	13.00	17.00
Other	9.00	10.00
Total ($/day)	106.00	112.00
Total ($/ton)	35.00	37.00
Total ($/100 SCF)	0.13	0.13

From Ref. [36].

mance of membranes with their product literature [38]. Good savings are demonstrated for membranes versus delivered nitrogen. A membrane system designed to deliver 3000 scfh of 95% N_2 in continuous operation results in a total gas cost of $0.089 per CSCF. This includes all utilities and maintenance but no capital charges. In contrast, delivered nitrogen is expected to cost $0.387 per CSCF to provide 95% purity gas (blended with air). A payback period of 16.6 months is calculated for the membrane system.

Various publications highlight specific air separation membrane applications and contrast their utility with nonmembrane alternatives. Advantages over liquid nitrogen include no tank rental, no vaporizer, less cost, no evaporation loss, no future price increases and elimination of vendor dependence. Advantages over PSA units include no moving parts, minimal air pretreatment, instant start-up, no after filters and no cooling water. Compared to inert gas generators membranes are safer (no combustion), produce higher quality gas (no carbon dioxide or moisture), and are more reliable. A number of key factors would have a significant impact on the economical operating region of nitrogen separation membranes. Typical systems operate at 100–150 psia. Higher pressures would decrease the size and cost of the membrane system at the expense of higher compression costs. If higher pressure nitrogen is needed, the membrane option becomes even more attractive. In some foreign countries or remote areas where liquid delivery is unavailable membranes provide a new solution to an expensive problem. In applications where portability, size and weight become important or where low maintenance is a factor, membranes would again extend their range of applicability.

13.5.2.2 Oxygen Production

Membranes are not currently capable of producing high purity oxygen. Single-stage membranes are limited to producing oxygen purities in the 30–45% range and multistage membrane systems are too expensive to compete with alternative techniques. Membranes are well-suited for applications requiring "enriched" oxygen, however [39].

One large potential application is for enriched oxygen production for home medical use. This is a large application that is currently served by liquids, cylinders or PSA units that mix a high purity oxygen stream with air to achieve the desired purity. Membrane separators provide some significant advantages in that the desired purity is directly produced from the membrane (no mixing equipment required), the oxygen stream is effectively filtered (it is the permeate stream), and the product stream is already humidified by virtue of the fact that moisture permeates along with the oxygen (no humidification step is needed). In spite of these advantages the acceptance of membranes into this application has been slow.

A second large potential application revolves around the concept of enhanced combustion for all types of furnaces and engines. Oxygen enrichment of up to 30% has been demonstrated to provide benefits in combustion efficiency and pollution reduction. Progress here is limited not so much by membrane performance but rather by combustion system development and acceptance. The level of oxygen consumption also plays a major role in determining whether a membrane process is economic.

A typical single-stage membrane system that produces 97% nitrogen would deliver at the same time a permeate stream having an oxygen concentration of 30%. Higher oxygen concentrations can be achieved by increasing the feed flow rate, reducing the membrane area or by increasing the pressure differential. All of these actions increase the separation cost. An analysis of how membrane performance impacts economics was conducted by the BOC Group [40].

An economic assessment of membrane oxygen production cost was performed by Sepracor [41] in which several different membrane types and membrane processes were evaluated. The present cost of oxygen from conventional sources varies dramatically with usage level with prices ranging from a low of $25/ton for dedicated cryogenic plants up to $250/ton for small-scale deliveries. Oxygen cylinders cost over $500/ton of delivered oxygen. An analysis was made of a high permeability, low selectivity (alpha = 2.2) membrane in a single stage permeator. Membrane performance was quoted at 11 scf/$-hr-100 psi (for oxygen) and the product produced was 33% oxygen in a plant sized at 25 tons of equivalent pure oxygen per day. Equivalent pure oxygen (EPO) is defined as the amount of pure oxygen that would be blended with air to make

the same concentration of oxygen-enriched air. The calculated cost was \$98/ton of EPO. The same process based on a membrane performance of 55 scf/\$-hr-100 psi results in a cost of \$55/ton EPO. Energy consumption was shown to contribute \$30/ton EPO in large part due to the relatively low selectivity of the membrane.

Higher selectivity membranes are available but generally have lower permeabilities which lead to higher capital costs. The same authors evaluated a membrane having a selectivity of 4.8 (O_2/N_2) but with an oxygen permeability one-tenth that of the first case (1.1 scf/\$-hr-100 psi). Although energy requirements are reduced to \$13/ton EPO and the oxygen purity is raised to 43%, the capital costs explode and dominate the final cost of nearly \$500/ton EPO. The authors note that if the above membrane could be simply made thinner by a factor of 10 and the membrane cost reduced to one-half, the resulting cost would be \$49/ton EPO. The authors also evaluated different schemes for producing a 90% purity oxygen stream including recycle processes (single-stage with recycling, continuous membrane column, and two-stage series with recycling) and a new "super" membrane with a selectivity of 60. Their conclusion was that only the advanced membrane would offer attractive economics (at \$49/ton EPO) for large-scale applications.

The conclusions of this paper were that membranes were competitive for oxygen enrichment at rates up to 10 tons/day at purities of 30–50% O_2. Lower installed membrane costs would expand this market. However, the authors assumed membrane lives of only two years and also assumed that the entire membrane unit would be replaced in the change-out. This results in a significant addition to the operating cost that is probably overly pessimistic for membranes in this type of service. Nonetheless, this paper provides a good overview of the issues surrounding membrane performance and process design relatively to their impact on economics.

Figure 13.24 illustrates the competitiveness of membranes for oxygen production according to Monsanto's calculations [33]. The competitiveness of PSA at low flow rates combined with the purity limitations of the membrane system greatly reduce the competitiveness of the membrane approach. As will be demonstrated later, however, other publications suggest that membranes are more competitive than what this figure indicates. Also, this analysis does not reflect situations in which both the oxygen and nitrogen products are utilized. Membranes may prove especially useful for these applications.

A cost comparison of A/G Technology membranes (AVIR) with PSA is presented in Table 13.4. Membranes are shown to provide a capital cost advantage of almost half that of PSA. Power consumption for PSA is also higher and the result is a marked advantage for the membrane unit. Reported production costs of \$28 per ton of oxygen are significantly lower than values discussed earlier. This advantage is claimed for capacities up to 20 tons/day with an

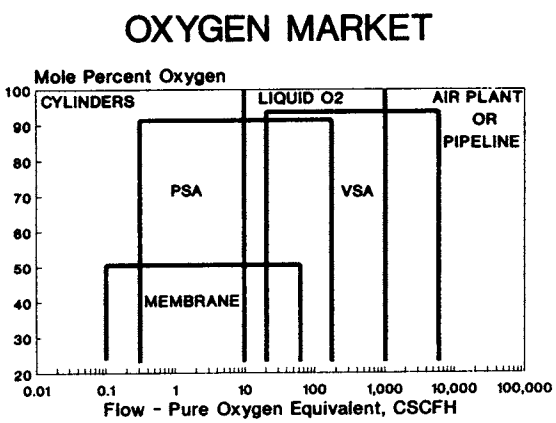

Fig. 13.24. Technology comparison for oxygen production/separation. (From Ref. [33]).

oxygen purity of 35% (all calculations are based on the volume of available oxygen). An AVIR oxygen generation unit is pictured in Fig. 13.25. Other comparisons show similar performance advantages for the membrane system [42].

A/G Technology also published an analysis of costs for small, lab-scale, oxygen-enriched air systems [43]. The application was to utilize an AVIR membrane unit to supply 35% oxygen to fermentor units at a rate of 25 l/min. A unit with a design capacity of 50 l/min operating off of 115 psia compressed air sells for $8300. A cost comparison with delivered gas cylinders (at $0.155/scf) reveals that the membrane separator has a simple payback of only 1.1 years. Operating costs of $450/year are assumed for the compressed air supply.

TABLE 13.4

Cost comparison for 35% oxygen-enriched air (10 tons/day available oxygen)

	A/G Technology Membranes	PSA
Installed capital cost ($000)	288.00	552.00
Expenses ($/Day)		
Membrane replacement	38.00	–
Power	86.00	131.00
Capital charges	105.00	202.00
Depreciation	33.00	63.00
Other	18.00	27.00
Total ($/day)	280.00	423.00
Total ($/ton)	28.00	42.00

From Ref. [36].

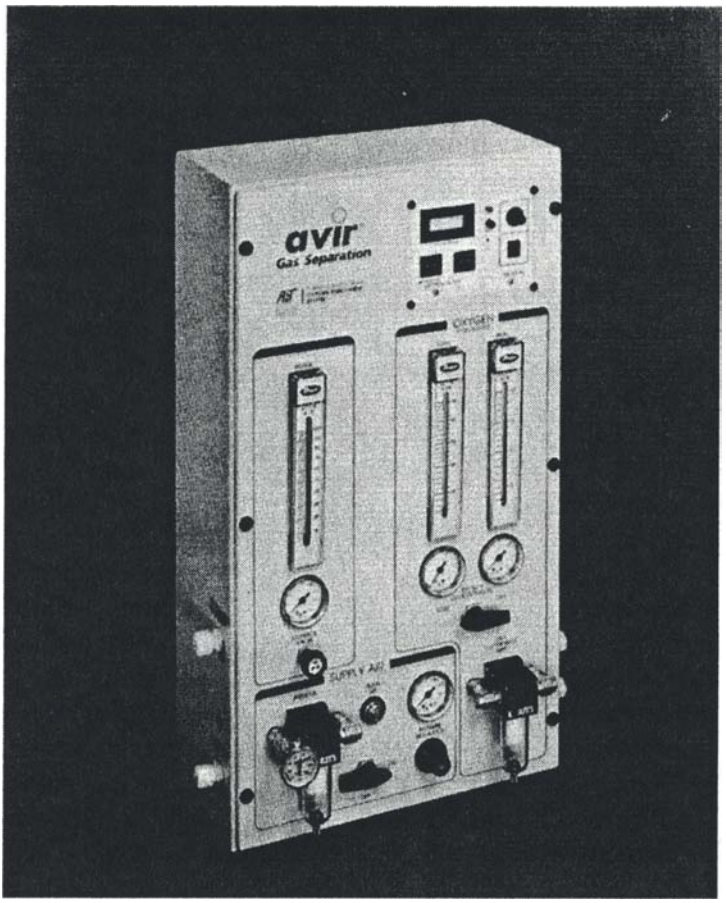

Fig. 13.25. AVIR oxygen separation membrane system supplied by A/G Technologies. (Courtesy of A/G Technologies, Needham, MA).

13.5.3 Hydrogen Separations

Membrane processes for the separation of hydrogen are now widespread in the ammonia and refinery industries and to a lesser extent in the petrochemical industry. Membranes have been demonstrated to provide an especially effective separation for the recovery of hydrogen from waste gas streams.

Membrane hydrogen separation processes compete primarily with cryogenic distillation, pressure-swing adsorption (PSA) and catalytic processes. Catalytic purification removes impurities from gas streams by reacting the impurity to form another compound that is either subsequently separated or is tolerated in the product gas [44]. A general overview of how membrane pro-

cessing compares with cryogenics in both ammonia plant and refinery operations summarizes the key operational differences [45].

13.5.3.1 Ammonia Purge Gas

Hydrogen and ammonia are reacted at high pressure and temperature over a catalyst to produce ammonia. Hydrogen is produced by the steam-reforming of natural gas and nitrogen is supplied from air. The conversion to ammonia is incomplete and the unreacted gases are recycled to the reactor after the ammonia is removed. A constant purge stream is maintained to prevent the buildup of inert gases such as argon and unreacted methane. Historically, plant operators simply burned this purge stream for its fuel value since separation was prohibitively expensive. Membranes were demonstrated to provide a cost-effective separation that resulted in both energy savings and an effective capacity increase. This application provided an excellent entry opportunity for membranes since the membrane process was very cost-effective and there was little process risk. Membrane failure would not disrupt the operation of the plant since membranes were only added to improve efficiency. Their use could be easily justified with a simple payback analysis. Success in these applications eventually led to the incorporation of membranes into more critical process applications. An Ube Industries hollow fiber membrane unit is depicted in Fig. 13.26.

In one reported case a 1000 ton per day ammonia plant in Mississippi installed a single-stage membrane recovery process to recover hydrogen from the purge gas stream. In addition to the hydrogen savings, the plant reported a 5% capacity increase of 50 tpd of ammonia [46]. At $200/ton this amounts to a $10,000 per day increase in product value (over $3 million per year). Ammonia scrubbers placed in front of the membrane unit recover an additional $200,000/year of ammonia. The purge gas previously was sent to the plant fuel system. Additional natural gas was now required to make up for the loss of the hydrogen fuel and, thus, the hydrogen cost savings was the difference of the value of hydrogen as a feedstock versus its value as a fuel. This difference is usually large enough to easily justify the membrane recovery process.

Commercial membranes separate hydrogen as the low-pressure permeate. The hydrogen usually must be recompressed for use in most applications as is the case with an ammonia plant. The cost of recompression can be minimized by raising the permeate pressure but the membrane separation will then suffer, as was demonstrated in Section 13.3.1.2. Higher permeate pressures reduce the hydrogen purity and recovery and increase the size of the membrane unit. The trade-off between recompression costs and membrane separation efficiency must be considered in any process optimization.

A two-stage series design can be employed to reduce total process costs as shown in Fig. 13.27. The first stage is operated at a high permeate pressure

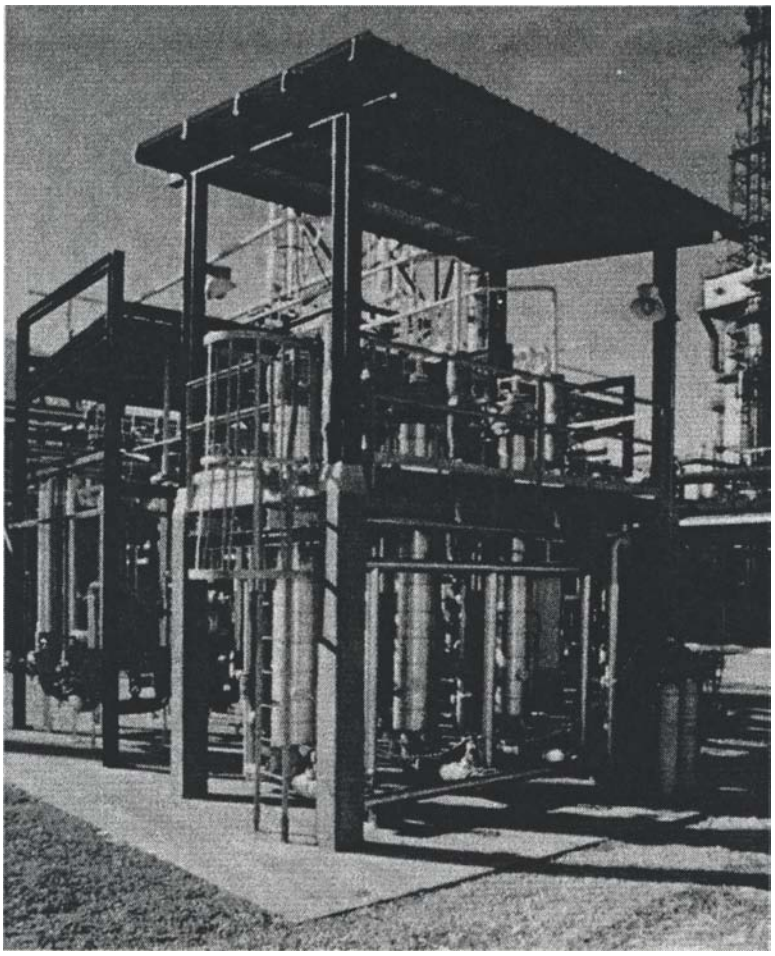

Fig. 13.26. Ube Industries hollow fiber hydrogen recovery unit. (Courtesy of Ube Industries, Tokyo, Japan).

under conditions where the hydrogen driving force is still high (the feed hydrogen partial pressure is high). The second stage permeate is operated at a lower pressure to achieve additional hydrogen recovery at about the same hydrogen purity as the first-stage permeate. The permeate pressures are selected to match the suction pressures of existing compressors. This eliminates separate compressor requirements and reduces overall recompression costs. This process increased production at a 600 tpd Louisiana ammonia plant by 4% [47].

An economic comparison of membrane and cryogenic separation was conducted in 1983 which showed membrane and cryogenic distillation as equally competitive [48]. The analysis studied the separation of a 15 million standard cubic feet per day (MMscfd) feed stream containing 60.8% hydrogen, 20%

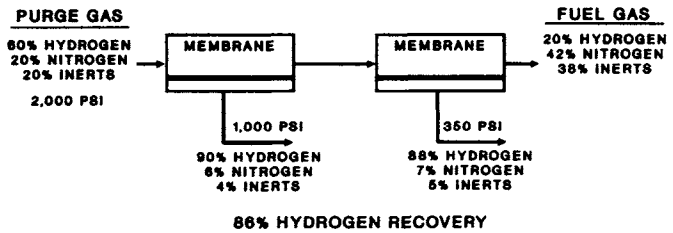

Fig. 13.27. Two-stage membrane series for hydrogen recovery from an ammonia purge gas stream. (From Ref. [47]).

nitrogen and 19.2% inerts. Both processes had comparable hydrogen recovery (95%) and purity (90%). The membrane unit was operated in two stages to minimize recompression cost. Capital costs for the two options were nearly identical (approximately $1.35 million). Subsequent advances in membranes have reduced this investment figure substantially, however, and a new analysis would be expected to be clearly favorable to membranes. The membrane process was found to have the added advantages of lower maintenance costs (greater simplicity, no moving parts), operation at near-ambient temperatures, lower weight and space requirements and lower installation costs.

13.5.3.2 Refinery Hydrogen Recovery

Hydrogen is utilized throughout refineries in a wide variety of unit processes. Hydrogen is either consumed or produced in a variety of processes [49]. The number of potential sources and applications of hydrogen in a refinery make general process comparisons impossible since flow rates, purity requirements, stream pressures and product values are all highly site dependent. A series of publications have analyzed a range of specific applications, however, and the general advantages and constraints of membranes can be illustrated. The use of hydrogen in refineries is expected to grow rapidly over the next decade in response to poorer quality crude oil and the growing demand for higher quality petroleum products. Hydrogen is supplied by direct production (e.g., steam-methane reforming) and by recovery of hydrogen from process off-gases, especially from those processes that generate hydrogen as a by-product. Membranes compete with oil scrubbing, PSA and cryogenic distillation.

Liquid Air Engineering analyzed the economic payback of an operating membrane unit at a Conoco refinery for recovering hydrogen from a gas oil hydrotreator purge [50]. The feed stream contained 71% hydrogen at 1065 psig at a flow rate of 12 MMscfd. The hydrogen permeate product contained 95% hydrogen at 445 psia at a flow rate of 7 MMscfd (75% hydrogen recovery) which was used in a hydroprocessing unit. The membrane unit was claimed to provide several inherent benefits including improved product quality, increased catalyst life, greater feedstock flexibility, higher productivity, in-

cremental hydrogen economy and reduced power consumption. These advantages led to yearly credits of $512,000 for the membrane process. Expenses included steam consumption, lost hydrogen fuel value and maintenance for a yearly total of $126,000 leaving a net earnings of $312,000/yr. The total investment was $662,000, which resulted in a simple payback period of 1.7 years. The refinery concluded that no other process could have offered better economics. A number of intangible advantages were also claimed.

The Fluor Corporation also compared membranes with two modes of PSA operation for reclaiming hydrogen from hydrotreator purge gas [48]. Unreacted hydrogen from the hydrotreator effluent is recycled back to the reactor to improve recovery but a portion of this stream must always be purged to prevent buildup of inerts. The purge gas stream was sent to the plant fuel system, which in this case operated at 85 psia. A 7 MMscfd purge stream at 815 psia containing 72% hydrogen was upgraded to 93% with membranes and 99.5% with PSA (Fig. 13.28). The membrane provided a hydrogen recovery of 81% when operated with a permeate pressure of 265 psia. Two PSA options were analyzed; the first produces a product at 465 psia with a desorption pressure of 75 psia and the second produces a product at 265 psia with 20 psia desorption. The advantage of the second PSA approach is that hydrogen recovery is increased by 34% over the higher desorption pressure. However, the lower pressure desorption

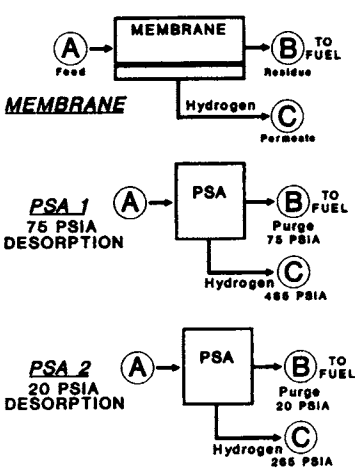

		A	B	C
H2	%	72.0	36.0	93.0
H.C.	%	28.0	64.0	7.0
RATE	MMscfd	7.00	2.90	4.10
PRESS	psia	815	785	265

		A	B	C
H2	%	72.0	51.0	99.5
H.C.	%	28.0	49.0	0.5
RATE	MMscfd	7.00	3.96	3.04
PRESS	psia	815	75	465

		A	B	C
H2	%	72.0	34.0	99.5
H.C.	%	28.0	66.0	0.5
RATE	MMscfd	7.00	2.95	4.05
PRESS	psia	815	20	265

	HYDROGEN PURITY	HYDROGEN % REC.	FUEL PRESS.	CAPITAL ($000)	COSTS ($/MSCF) EXPENSE	COSTS ($/MSCF) TOTAL
MEMB	93.0%	81.3%	785	630	0.11	0.20
PSA 1	99.5%	60%	75	1,225	0.05	0.29
PSA 2	99.5%	80%	20	1,025	0.29	0.24

Fig. 13.28. Comparison of membrane and PSA separation of hydrogen from a hydrotreater purge gas stream. (From Ref. [48]).

stream could not be directly added to the 85 psia fuel system.

There are several major differences in the performance results of the three processes. First, the hydrogen is delivered at a relatively low pressure (265 psia) from the membrane system and second PSA unit. The first PSA system provides the gas at a higher pressure (465 psia). The cost of recompressing the hydrogen for use is an added expense for the first two processes. The second difference is that the membrane system has the highest hydrogen recovery (81%) compared to the PSA processes (60% and 80%, respectively). The third difference is that the membrane hydrogen purity at 93% is lower than either PSA option (99.5%). Membranes cannot economically achieve the high purities provided by a PSA unit. Lower hydrogen purities may reduce the effective capacity of the reactor.

Figure 13.28 summarizes the cost and performance factors for all three options. The installed capital cost for the membrane system is 51% and 62% of the two PSA processes, respectively. The preferred PSA option is to run at a 20 psia desorption pressure but this would mean that a use for the low-pressure fuel gas would have to be found. If hydrogen purity is not a major issue then the membrane unit offers the best combination of installed cost, total process cost and ease of operation. Another company, Perry Gas Processors, also compared membranes with PSA for a hydrotreator purge gas application and concluded that membranes were 25% less expensive than the PSA process [51].

Conoco made a detailed cost comparison of membrane, PSA, and cryogenic processes for recovering hydrogen from a hydrodesulfurization unit [52]. The stream analyzed was 15 MMscfd, 800 psig and contained 75% hydrogen. A product stream was sought at 315 psia, 98% hydrogen purity and at least 75% hydrogen recovery. Costs for direct hydrogen product via steam-methane reforming were also calculated as a reference. The results of this analysis are shown in Fig. 13.29. Capital costs are installed battery limits including any required pretreatment and recompression. A value of $1.07/Mscf was placed on the raw purge stream (fuel value). Return on investment was placed at 25% pretax IRR. Other expenses included 10% depreciation, operating labor, taxes, overheads, cooling water at $0.10/gal, power at $0.034/kWh and natural gas at $3.25/MMBtu. The hydrogen production cost does not include depreciation or return on investment in order to clearly show just the cost of incremental reforming (assumes that additional capacity is available).

The membrane option was clearly shown to be the most economic. Total production costs for the membrane unit were $1.40/Mscf with a capital investment of approximately $1 million (1986). Superior economics over incremental hydrogen production demonstrate the cost effectiveness of purge gas recovery by membranes.

Ube Industries compared membranes with adsorption and cryogenic processes for the recovery of hydrogen from refinery off-gas [53,54]. Their comparison, summarized in Table 13.5, showed that membranes have 50–70% of the

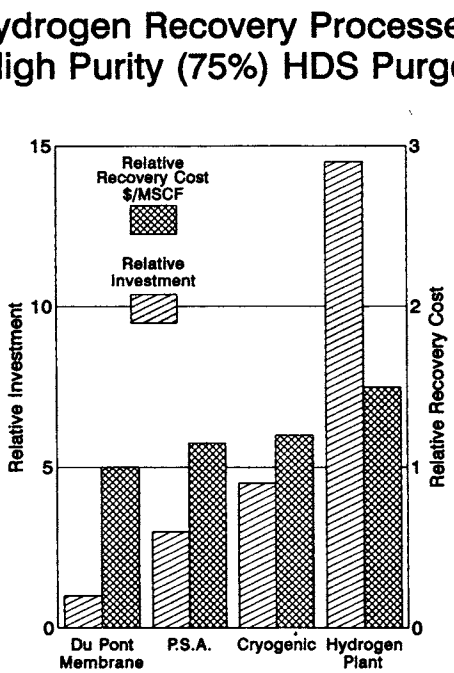

Fig. 13.29. Process economic comparisons for hydrogen recovery from a hydrosulfurization purge gas stream. (From Ref. [52]).

capital cost of PSA or cryogenic units. Relative ease of operation and versatility were also noted for membranes. Comparison of the plot area requirements for the three processes demonstrates the significant space and weight advantages that membrane processes can sometimes offer. Operation of the polyimide membrane at higher temperatures reduces cost and improves recovery.

Grace Membrane Systems (W.R. Grace & Co.) developed a membrane system that can recover purge gas hydrocarbon values as well as hydrogen. The higher hydrocarbons in purge gas streams have values greater than that of fuel gas but recovery is not usually economic. As hydrogen is removed from the purge gas stream the dew point of these hydrocarbons is reduced. Hydrogen can be removed until hydrocarbon condensation occurs. Although liquid condensation on the membrane may affect gas removal efficiency it will not damage membranes designed for this service. A special membrane unit recovers the condensed hydrocarbons and the remaining gas residue stream can be cooled to easily condense additional quantities [28]. This approach is useful both for refinery and natural gas processing applications. A spiral wound membrane system from Grace Membrane Systems is shown in Fig. 13.30. Spiral membranes are usually mounted horizontally but limited space in an existing refinery dictated the vertical design.

TABLE 13.5

Comparison of membranes with adsorption and cryogenic processing (hydrogen recovery from refinery off gas)

	Membrane Process			
	80°C	120°C	Adsorption	Cryogenic
Hydrogen recovery (%)	87	91	73	90
Recovery H_2 purity (%)	97	96	98	96
Product gas flow rate (MMscfd)	2.76	2.86	2.24	2.86
Power (kW)	220	220	370	390
Steam (kg/h)	230	400	–	60
Cooling water (t/h)	38	38	64	79
Investment ($ millions)	1.12	0.91	2.03	2.66
Installation area (ft^2)	86	52	651	1292

From Ref. [53].

In 1983 Air Products made a comparison of membrane, PSA and cryogenic processes for upgrading a catalytic reformer off-gas stream containing 75–85% hydrogen at 265 psia [55]. Their results are presented in Table 13.6. Details on each process were not given, however, and it is impossible to judge process conditions and the cost assumptions. Although the membrane system was judged to have 17% higher operating costs over the PSA system, its capital cost was by far the lowest of the three options. Dramatic improvements in membrane price/performance ratios since the time the study was done should have improved the membrane economics.

TABLE 13.6

Product purity, recovery, relative operating, capital and product costs to treat a catalytic reformed off-gas stream

Purification process	Product purity (%)	Product recovery (%)	Relative capital cost	Relative operating cost	Relative product cost
Cryogenic	97.5	96.0	1.44	1.22	1.06
Membrane	96.9	89.4	1.00	1.17	1.09
PSA	99.9	86.0	1.40	1.00	1.00

From Ref. [55].

Many additional papers and presentations on the use of membranes in refinery applications have appeared and all illustrate the benefits and ease of operation that membranes provide in this application [56–58].

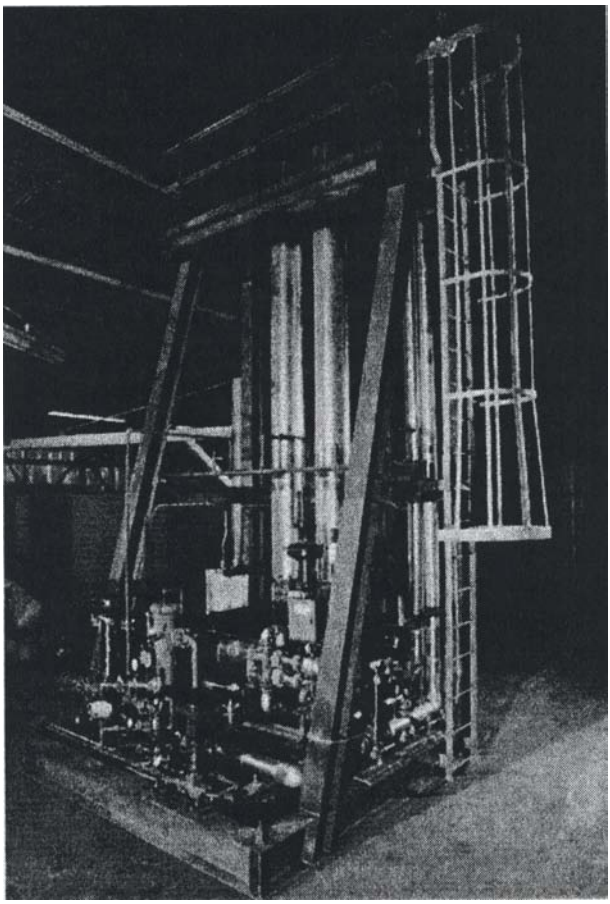

Fig. 13.30. A Grace Membrane Systems hydrogen recovery unit. (Courtesy of Grace Membrane Systems, Houston, TX).

13.5.3.3 Petrochemical Applications

Synthesis gas is a mixture of hydrogen and carbon monoxide that is used in a variety of petrochemical and metallurgical processes. It is produced from natural gas, oil or coal via different processes. Syngas can be used for the production of methanol and other oxygenated chemicals such as acetic acid, ethylene glycol and ethanol. The stoichiometry of the feed gas must be adjusted depending on the process. Table 13.7 illustrates some of the possible chemical products and the corresponding H_2/CO ratio required for the syngas feedstock.

Membranes can be used to adjust the syngas stoichiometry by selectively removing hydrogen. Traditional methods for separating synthesis gas have been cryogenic separation and blending or PSA to provide the desired hy-

TABLE 13.7
Chemicals from synthesis gas

Product	Reaction stoichiometry	H_2/CO ratio in syngas
Raw syngas	Produced via steam-methane reforming	3.0
Acetic acid	$2H_2 + 2CO \rightarrow CH_3C(O)OH$	1.0
Ethylene glycol	$3H_2 + 2CO \rightarrow HOC_2H_4OH$	1.5
Acetic anhydride	$CH_3C(O)OCH_3 + CO \rightarrow CH_3C(O)OC(O)CH_3$	0.0
Acetaldeldehyde	$3H_2 + 2CO \rightarrow CH_3CH_2OH + H_2O$	1.5
Ethanol	$4H_2 + 2CO \rightarrow CH_3CH_2OH + H_2O$	2.0
Ethylene	$4H_2 + 2CO \rightarrow CH_2CH_2 + 2H_2O$	2.0

Gas separation membranes remove the excess hydrogen from the syngas to provide the proper H_2/CO ratio for the product of interest.

drogen purity. However, these traditional processes produce carbon monoxide at low pressure while membranes provide this gas at high pressure. This contrasts with the refinery separations discussed earlier wherein it is the hydrogen that is required at high pressure.

Air Products reported an economic and performance comparison of membranes for this application [59]. A feed stream containing 73% hydrogen and 24% carbon monoxide (ratio of 3.0) was treated with a membrane to produce a syngas stream of 64% hydrogen and 32% carbon monoxide (ratio of 2.0) for an oxo-alcohol process. The feed gas flow was 18.5 MMscfd and the pressure was 340 psia. The product gas flow was 13 MMscfd with a pressure slightly below that of the feed. The permeate contained 98% hydrogen and less than 2% carbon monoxide. The membrane cost for this system was found to be less than one-half the cost of a PSA system. The PSA system has the added disadvantage of requiring compression for the product gas. The same paper discusses a two-stage membrane system to produce a 98% pure carbon monoxide stream.

In another application membranes were used to treat the purge gas from a methanol reactor [60]. Methanol reactor purge streams contain hydrogen, carbon dioxide, carbon monoxide, methane, nitrogen, methanol and water. The reported application had a purge gas stream of 58% hydrogen at a pressure of 697 psia. Before the membrane process was introduced this stream was sent to the fuel gas system. A membrane system was installed at a point after the methanol was scrubbed from the purge gas. The permeate stream pressure was set at 395 psia, which resulted in a hydrogen purity of 80% and a recovery of 48%. This hydrogen stream was recompressed using the existing syngas compressors and recycled to the reactor.

This membrane operation was reported to provide an incremental increase in methanol production of 2.57 million gal/year in a 100 million gal/year plant.

If the permeate stream pressure were lowered to 95 psia the hydrogen recovery increases to 91% and the incremental plant production rises by 3.87% *with half the membrane investment required* compared to the first case. Site-specific constraints prevented this mode of operation in this particular application.

Incremental costs associated with the membrane process included a debit for loss of the fuel gas value of the purge stream, the incremental cost of compression and utility charges. Nonetheless, the use of membranes provided a 13% reduction in variable costs to produce a gallon of methanol, although specific numbers were not presented. Current membrane system performance would improve these economics even further.

Hybrid membrane/PSA systems have been designed that offer lower costs and improved reliability in some applications. Process options for producing the proper ratio of hydrogen and carbon monoxide in the synthesis gas include (1) production of carbon monoxide via partial oxidation of CO_2, (2) separation of the syngas stream with PSA, (3) separation with a membrane unit, and (4) separation with a membrane/PSA hybrid process. These various options were compared and detailed economics presented on the PSA and membrane/PSA cases [61]. Results are presented in Table 13.8.

As was discussed earlier, a key advantage of the membrane system is that the carbon monoxide exits the membrane as the high-pressure residue stream and thus greatly reduces recompression costs compared to the PSA unit. The disadvantage of the membrane-only process is that the hydrogen permeate stream is contaminated with 2–10% carbon monoxide. If the hydrogen is to be used in a subsequent processing step (e.g., hydrogenation) then the carbon monoxide must be removed. The membrane/PSA hybrid solves this problem by adding a PSA unit to treat the membrane permeate stream. The size of the PSA unit is significantly reduced compared to the PSA-only process option since the size of the permeate stream is smaller and since it now contains only a low level of carbon monoxide to be removed. Carbon monoxide recovered from the PSA unit is recompressed and returned to the treated syngas stream (after the membrane). The membrane unit size is also reduced since the proper ratio is made after the carbon monoxide is returned to the stream from the PSA unit. Finally, the hydrogen from the PSA unit is sufficiently purified for later use. Another benefit of this design is that production of the syngas feed could continue, at reduced capacity, if either the membrane or PSA unit shut down.

13.5.3.4 Hydrogen Production

The Department of Energy has supported research into the use of membranes to purify hydrogen from coal gasifiers [62]. A thorough analysis of a variety of membrane process designs was undertaken to analyze the costs for this hydrogen/nitrogen separation [63]. Membrane process configurations

TABLE 13.8
Comparison of PSA and membrane/PSA hybrid processes for syngas ratio adjustment

Basis			
Feed flow rate (MMscfd)	20.0		
Feed pressure (psia)	435		
Hydrogen use pressure (psia)	165		
Gas compositions (%)	Raw feed	H_2 Product	Synthesis gas
H_2	63%	99.99+%	49.1%
CO	35	–	49.1
Other	2	–	1.8
Comparison	PSA only	Membrane + PSA	
Compression (BHP)	1080	415	
Capital ($MM)			
– Separation Equipment	$1.43	$1.38	
– Installation	0.17	0.22	
– Compressors	0.86	0.33	
Total	$2.46	$1.93	
Compressor Operating Cost over 3 Years ($MM)	$0.97	$0.37	
Total Capital Cost + 3 Years Operation ($MM)	$3.43	$2.30	

From Ref. [61].

evaluated included single-stage, single-stage with feed bypass, single-stage with recycling, two-stage series with recycling and two-stage cascade with recycling. The impact of employing two different membranes for the two-stage cascade was also evaluated. Economics were presented for a wide range of feed and product hydrogen concentrations.

The conclusions were that the single-stage approaches were best for the easiest separations (where little separation is required to meet the product targets). The two-stage series with recycling is best for intermediate separation difficulty and the two-stage cascade is best for the most difficult separations. No advantages were seen for the single-stage with a recycling process. Optimized processing costs for upgrading a 34% hydrogen stream to product purities between 80% to 98% ranged from $0.85 to $1.20 per Mscf for designs that provided a 95% hydrogen recovery.

On a much lower scale, gas mixtures of hydrogen and nitrogen are employed in certain metallurgical processes for high-temperature sintering. These mixtures can be provided via the blending of pure delivered gases. Ammonia

dissociators, which produce a blend of 25% nitrogen and 75% hydrogen, can also be used but higher hydrogen purities are generally required in many applications. Ammonia dissociators provide a lower cost source of hydrogen compared to delivered gases, however.

A test demonstrated the economic feasibility of using a membrane system to upgrade the output of an ammonia dissociator so as to achieve the required hydrogen purity [30]. A metallurgical company was spending a total of $123,000/ year on delivered compressed hydrogen. Hydrogen was costing approximately $1.43/100 scf and equipment rental added another $450/month. In contrast, a dissociator/membrane system was evaluated and determined to cost a total of $56,000/year. This included the cost of ammonia (at $0.12/lb), power costs and depreciation on the system ($670/month). No details were provided on the capital costs on the membrane unit.

The net savings for this application amounted to $67,000/year, even after depreciation. Additionally, the plant in this situation had a use for the residual nitrogen stream resulting from the separation. An additional credit of $19,000/ year was claimed for this stream, bringing the total savings to $86,000/year.

13.5.4 Carbon Dioxide Separations

Membranes have shown promise in a variety of applications related to the processing of natural gas streams. Some natural gas contains impurities such as carbon dioxide and hydrogen sulfide that require removal prior to delivery to a pipeline. Both are corrosive to the pipeline and hydrogen sulfide is also toxic. Almost all natural gas contains moisture that must be removed to prevent pipeline corrosion and hydrate formation. Membranes are attractive in principle for this type of application since (1) the feed gas is already at high pressure, (2) the gas impurities readily permeate membranes, and (3) the methane stream exits as the high pressure residue which means no recompression is necessary. This is a tough environment for membranes, however, as pressures can be quite high (e.g., up to 2,000 psi) and each gas stream has a different composition.

13.5.4.1 Natural Gas Treating

The most common process for removing carbon dioxide and hydrogen sulfide is amine absorption. A wide variety of amine systems exists and there are many other nonamine processes (physical solvents, solid bed adsorbents, etc.) that offer advantages in certain situations. In amine treating, contaminated natural gas is flowed up a packed column while an aqueous amine solution contacts the gas in a countercurrent flow. The amine absorbs the "acid" or "sour" gas components and is removed by a heat regeneration step. This technology accounts for some 70% of natural gas treatment processes and is a

sophisticated, mature technology. Amine plants are efficient and, combined with the diverse gas-treating environment (every gas stream is different), this makes natural gas-treating one of the toughest applications for membranes.

Amine plants have some limitations, however, that invite the introduction of new technology. These units are large and heavy and the need for tall structures presents problems for their use on offshore platforms or in environmentally sensitive areas. Continuous supervision and maintenance are required due to their complexity. The amine regenerator consumes a moderate amount of gas and its presence on an offshore platform represents a fire safety hazard.

Membrane units can be used to treat gas right at the wellhead instead of at a central plant. Small units are far more cost-effective than an amine plant and wellhead treatment can reduce corrosion and safety problems when transporting gas to centralized amine treating plants. Membrane units can treat gas to pipeline specifications right at the wellhead to meet typical U.S. specifications such as <2% CO_2 and <140 ppm H_2O. Depending on the application, membranes can also remove H_2S to meet pipeline specs of <4 ppm but this separation is economically difficult if the feed H_2S concentration is too high. A Grace Membrane Systems unit for wellhead treating is shown in Fig. 13.31.

A cost comparison of amine absorption (both DEA and MDEA) and membrane treating was reported, which included capital costs, utilities, labor, maintenance and lost product value (methane lost to the permeate stream) in the calculations [64,65]. The membrane processes were optimized to provide the lowest cost. The need for proper membrane process design was clearly demonstrated. Two- and three-stage membrane processes were found to be much more cost-effective than the simpler one-stage membrane plants in many situations. Single-stage membranes were cost-effective for low flow rate applications but at the higher flow rates staging was justified to reduce product losses and overall process costs. The designs presented in Figs. 13.15 and 13.16 are the most common multistage designs for the applications analyzed.

Figure 13.32 summarizes the resulting cost comparison between DEA amine, optimized MDEA and membrane processing for a 60 MMscfd feed stream with CO_2 compositions ranging from 5 to 90%. Processing costs are based on the amount of feed gas processed and included 10-year depreciation, an 11% after tax return on investment, utilities, labor, maintenance, membrane and amine replacement, plant overhead and charges for any lost product due to incomplete separation (assumed to be essentially zero for the amine case). Membranes were found to offer significant advantages under many conditions in spite of the higher product gas losses. Part of the reason for this is that amine processes have substantial utility requirements (fuel gas) to regenerate the rich amine solutions.

Figure 13.32 also illustrates an interesting aspect of membrane performance in that costs go through a maximum at a carbon dioxide content of 30%. This fact leads to some useful membrane/amine process hybrid designs discussed

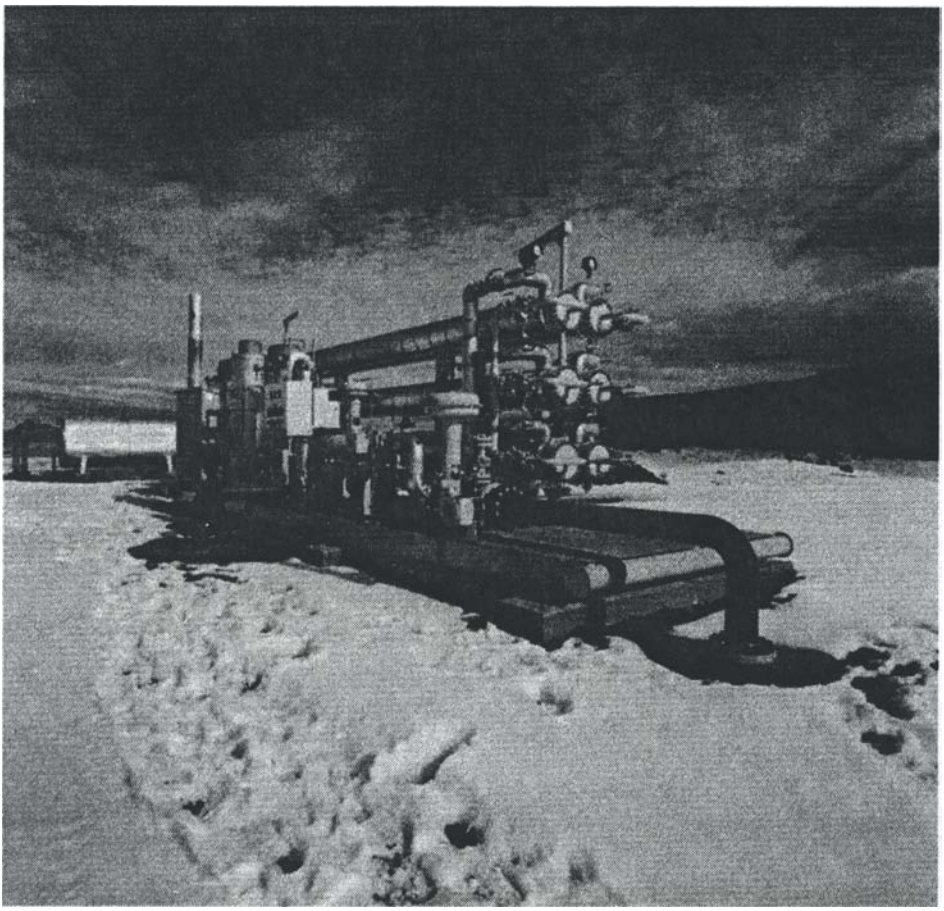

Fig. 13.31. A Grace Membrane Systems membrane unit for wellhead natural gas treating. (Courtesy of Grace Membrane Systems).

in an earlier section.

A breakdown of DEA amine and membrane costs for a feed stream of 37 MMscf, 1,000 psia, 10% CO_2 is presented in Table 13.9. Membrane processing shows advantages in all key categories except lost product value (loss of hydrocarbons into the permeate stream). Higher recoveries were possible with membranes but the additional capital requirements were not considered cost-effective for this particular application. Hydrocarbon losses can be minimized through proper process design but there will exist a balance between the additional capital requirement and product losses. Hydrocarbon losses should be considered as another operating expense. These losses would be effectively eliminated in cases where the low BTU permeate stream could be used for process heating or gas-fired compressor operation.

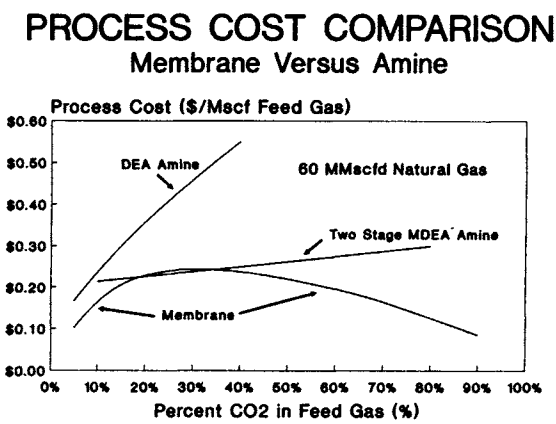

Fig. 13.32. Cost comparison between DEA amine, optimized MDEA and membrane processing for a 60 MMscfd feed stream with carbon dioxide concentrations ranging from 5 to 90%. (From Ref. [64]).

TABLE 13.9

Comparison of amine and membrane processing for the treatment of 10% CO_2 natural gas

Amine	
Capital ($ millions)	4.54
Expenses ($ millions/year)	1.81
Lost product ($ millions/year)	0.04
Capital charge ($ millions/year)	1.23
Processing cost ($/MSCF Feed)	0.24
Membrane (Multistage process)	
Capital ($ millions)	3.33
Expenses ($ millions/year)	0.85
Lost product ($ millions/year)	0.69
Capital charge ($ millions/year)	0.90
Processing cost ($/MSCF Feed)	0.19

From Ref. [64].

A second study that evaluated a similar natural gas stream concluded that membranes were not attractive for some of the cases studied [66]. However, this paper only compared single-stage membrane designs and based the cost calculations on older membrane technology. The conclusion was that methane losses in the permeate led to high processing costs for high gas flow rates. The use of multistage recycling designs for natural gas-treating applications significantly reduces hydrocarbon losses, however. Proper design would reverse many of the observations made in that study.

Grace Membrane Systems compared amine (30% DEA) and two-stage membrane processes for a specific gas stream (3 MMscfd, 8% carbon dioxide). This analysis concluded that membranes offered both capital and operating cost advantages [67]. The membrane installed capital was 26% less than the amine system and operating costs were 62% less. Although the methane loss for the membrane system was greater (even with the second stage), this analysis demonstrated that the fuel requirements for the amine unit were far greater. This analysis did not consider the economic benefits of unattended operation for membranes. It did demonstrate the effectiveness of membranes for even the low-flow applications.

A similar study was conducted by Perry Gas Companies (Houston, TX) for a 10 MMscfd, 12.2% carbon dioxide stream compared single-stage membranes with DEA and with a hybrid membrane/DEA system [68]. Their results are presented in Table 13.10. In this case the use of a single-stage membrane reduces the capital cost significantly (no compressors required) but the increase in operating costs is due to the lost methane gas in the permeate. The hybrid system utilizes membranes for bulk removal and a DEA system for final cleanup to reduce methane loss. It is obvious that the selection of a process will depend heavily on the specifics of the situation. Methane value of $3.50/MMBtu was used for these calculations. However, wellhead natural gas prices have plunged since the oil glut and field prices of $1.50–$2.00/MMBtu are more common as of 1990. Under these circumstances the relative importance of hydrocarbon loss becomes less significant. Cost comparisons were explored in some additional detail in a subsequent papers [69,70].

TABLE 13.10

Comparison of amine and membrane processes for natural gas treating

	DEA amine	Membranes	Membrane/DEA hybrid
Relative capital cost	1.0	0.26	0.72
Relative operating cost	1.0	1.51	1.14
Relative net present cost @ 15%	1.0	0.76	0.89

From Ref. [68].

Membranes have been considered for offshore platforms where advantages of weight, space and safety make membrane processing particularly attractive. A comparison of an offshore MDEA amine plant with membranes was made for treating a 96 MMscfd feed stream containing 16.5% CO_2 at 1000 psia [71]. The amine plant was found to require over two times the area and over three times the weight of an equivalent membrane plant for this particular application. A detailed analysis of costs and equipment was presented. Major cost

TABLE 13.11

Process comparison for natural gas treating

Option	Description	Overall operating cost	Overall capital cost	Overall space	Overall weight
1	Single-stage membrane	1	1	1	1
2	Membrane plus DEA	0.44	4.6	1.19	5.39
3	Two-stage membrane plus compression	0.85	1.43	1.65	1.47
4	Selexol	0.13	6.18	1.74	7.79
5	DEA	0.087	6.36	1.96	8.1
6	Act. MDEA	0.068	6.25	1.58	7.91

From Ref. [72].

advantages for the membrane unit resulted from the skid-mounted nature of the membrane system. The reduction in engineering and fabrication costs resulted in a 40% cost advantage for the membrane unit. This cost-saving did not include any savings on the platform construction that would result from the reduced weight and space requirements of the membrane unit. An additional significant advantage is that the membrane system is much safer and easier to operate than an amine plant. These factors are especially important for an offshore platform. A separate study by John Brown Engineers and Constructors, Ltd. illustrates the relative merits of membranes for a specific gas treating application (Table 13.11) [72]. As can be seen, the weight and space savings are again demonstrated to be quite significant for membranes.

The Ralph Parsons Company reported on the capital cost savings of a two-stage membrane unit compared to DEA, MDEA and activated MDEA processing [73]. This paper also describes a membrane/Selectox process for removal and treating of hydrogen sulfide. A number of other papers have appeared discussing the advantages of membranes in natural gas treating [74–76].

13.5.4.2 Carbon Dioxide Enhanced Oil Recovery

Carbon dioxide is pumped into dying oil reservoirs to extend the life of an oil field. The CO_2 is pumped into the ground on the periphery of the field at high pressures. The CO_2 then diffuses through the formation to drive residual oil towards existing oil wells. This technique has proven to be quite successful in West Texas and many more projects are now being considered. Over time, the CO_2 also arrives at the well and begins to "contaminate" the natural gas associated with the well. Carbon dioxide contents can reach as high as 95% as the project matures. Levels of 40–90% of CO_2 may be achieved in as few as three years.

The objective of the gas separation is to claim both the natural gas and the CO_2 (for reinjection). Since both the volume and composition of the gas change with time it is difficult to economically design and operate a conventional amine treatment plant for this application. Membrane systems can be quite useful due to their effectiveness at the high carbon dioxide contents and a number are in field use. The recovered carbon dioxide stream is often reinjected at high pressures back into the reservoir. This stream must therefore be recompressed. The membrane permeate pressure must be carefully selected to minimize the recompression requirements without excessively reducing the efficiency of the separation since the pressure ratio is lowered. However, a higher permeate pressure reduces membrane efficiency and an optimization is required to find the best operating condition.

One of the first detailed case studies involving membranes for EOR applications was performed by Amoco Production Company [77]. The study involved a 148 MMscfd, 90% carbon dioxide EOR stream at 285 psia pressure. In this analysis membranes were used as a "topping" process for bulk removal of carbon dioxide prior to a "polishing" step with a conventional DEA unit. Unfortunately, total membrane treating was not considered. The hydrocarbon gas product and carbon dioxide-enriched streams had pressure requirements of 650 and 450 psia, respectively. This detailed analysis summarized investment costs and operating expenses for treating the gas at several stages in the project (the carbon dioxide content and flow rate increase over time from 1.9% CO_2/ 14.8 MMscfd at the start to 90% CO_2/148 MMscfd at maturity). DEA amine, cryogenic, combined TEA/DEA amine and membrane/DEA processes were compared. The results are summarized in Table 13.12. The membrane/DEA case showed the most favorable economics. An examination of this paper provides an excellent overview of the factors that must be considered and the complexity of the analysis.

A similar analysis was conducted by Monsanto in comparing membranes with hot potassium carbonate and cryogenic separation processes [78]. The analysis assumed a 100 MMscfd, 80% carbon dioxide stream. The results are shown in Table 13.13. In this case the feed gas stream was available at a very low pressure (40 psia) and is compressed to 250 psig for the amine and membrane systems and to 500 psig for the hot potassium carbonate process. The cost of compression tends to obscure the capital cost benefit of the membrane approach. This design utilized a recycle stream to increase separation efficiency.

An optimization study was conducted by United Engineers and Constructors [79] for an EOR project in which a variety of process designs were considered. For the specific problem considered, it was found that a combined membrane/DEA amine process offered the best economics when the membrane was used to remove carbon dioxide down to 15% before delivery to an

TABLE 13.12

Gas separation process comparison for CO_2-enhanced oil recovery

	Process			
	DEA amine	Cryogenic	TEA/DEA amine	Membrane/ DEA
Capital investment ($ millions)	103.6	73.5	65.0	47.0
Operating expenses ($ millions/year)				
Ex. utilities	10.8	7.8	6.9	8.8
Utilities	29.4	18.0	15.9	10.7
Product losses	0.1	2.6	0.1	0.9
Capital charge ($ millions/year)	28.0	19.9	17.6	12.7
Total cost ($ millions/year)	68.2	48.2	40.4	33.1

From Ref. [77].

TABLE 13.13

Process comparison for CO_2-enhanced oil recovery

	Process		
	Hot Potassium Carbonate	Cryogenic/DEA	Membrane DEA
Capital Investment ($ millions)			
CO_2 removal unit	21.1	24.2	16.1
DEA treating	–	4.0	4.9
Compression	19.1	17.3	18.1
Other	4.0	–	4.0
Total	45.0	46.4	43.1
Operating expenses ($MM/yr)	11.8	8.5	6.5
Capital charge ($MM/yr)	12.2	12.5	11.6
Total ($MM/yr)	24.0	21.0	18.1

From Ref. [78].

amine plant (Fig. 13.33). This combination was cheaper than either process by itself. A sensitivity analysis revealed a wide range of optimum carbon dioxide concentrations, ranging from 7 to 35%. The availability of membranes that tolerate hydrocarbon condensation plus improved price/performance would tend to move the curve in Fig. 13.33 to the left.

Fluor Engineers compared membranes with membrane/Benfield and straight amine treating for a 104 MMscfd, 40% carbon dioxide stream but found

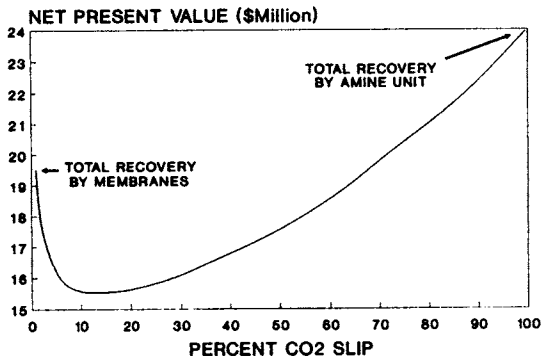

Fig. 13.33. Optimization of a combined membrane/DEA amine process for a carbon dioxide-enhanced oil recovery project. (From Ref. [79]).

an advantage for the amine-only system for the situation under study [80]. Details of their cost calculations were not available and the conclusions were only expressed as ratios (Table 13.14). A simple TEA amine system provided the best economics for this case. The large volume of gas to be processed contributed to the high investment cost of membranes for this application. Also, the CO_2 content of 40% also falls nearly on top of the cost curve for membrane separations. In a separate study of a 140 MMscfd EOR stream containing 90% carbon dioxide, Fluor concluded that membranes offered a 5% operating cost advantage over a competing distillation system [48]. No capital investment comparison was made, however. A subsequent comparison of membrane/distillation and distillation-only treating of an EOR stream gave the hybrid membrane process savings of 25% in capital and 20% in utilities [81].

TABLE 14

Process comparison for CO_2-enhanced oil recovery

	TEA amine	Membrane/hot potassium carbonate	Membrane only
Capital cost	1.0	1.0	1.6
Operating cost	1.0	1.3	1.9
Evaluated cost	1.0	1.1	1.7

From Ref. [80].

13.5.4.3 Landfill Gas and Digester Gas Upgrading

Landfills and sewage treatment digesters produce methane-rich biogas that is contaminated with approximately 50% carbon dioxide. Although biogas is an

interesting energy source, its energy content is too low for economic transport by a pipeline even for a short distance. Biogas is produced at low pressure (atmospheric) and is available only at low flow rates (generally 3 MMscfd and below). Although biogas is expensive to upgrade the gas is essentially free and collection satisfies certain environmental interests. Also, such gas is usually located near industrialized areas where energy values are much higher. Several landfills currently use membranes to provide a high-quality gas. In this application membranes compete directly with water-scrubbing, amine treatment and PSA and indirectly with use of the untreated contaminated gas as a low Btu fuel. The competitiveness of membranes for biogas applications is strongly dependent on the pressure requirements of the product gas. Low pressures penalize membrane economics. If a high-pressure gas is required, then membranes offer clear advantages.

A comparison of membrane, water and amine processes was conducted [82] in which the membrane process provided superior performance over amine and marginal improvements over water-scrubbing. A subsequent study [83] performed a more detailed analysis of the water-scrubbing process and determined that the membrane approach offered a 4% performance advantage for the conditions selected.

A pilot plant has been in operation for several years in which the performance and economics of membrane-treating are being evaluated [84]. Membrane performance was monitored as a function of feed gas and operating conditions and variables were adjusted to provide optimum performance. Costs were evaluated for both one-stage and two-stage series with membrane recycle processes. The two-stage unit was judged to have the best economics. Alternative processes were evaluated including water wash, amine-treating (MEA), and pressure-swing adsorption (PSA). The conclusion was the membrane processing was superior for gas flows below 0.8 MMscfd. PSA becomes more attractive at higher flows. The authors felt that the membrane option will dramatically improve as new membranes are introduced.

13.5.4.4 Flue Gas Recovery

There has been great interest in the recovery of carbon dioxide from flue gas streams both for the product value of CO_2 (e.g., enhanced oil recovery) and for environmental reasons (reducing the "greenhouse" effect). Although the separation factors for CO_2 and N_2 are high for many membranes, the low pressure of the feed gas makes membrane separation rather expensive. Japan's Ministry of International Trade and Industry (MITI) has initiated a multiyear project that will examine the recovery of CO_2 from flue gas and some portion of the effort will cover membrane separation options. A number of membrane process designs have been proposed but it seems likely that hybrid membrane systems

will show greater promise than membrane-only designs. The results of MITI's study will more clearly illustrate the potential for membranes in this application.

13.5.5 Water Vapor Removal

13.5.5.1 Air Dehumidification

Membranes are used for the dehydration of process air streams. Conventional processes involve the use of desiccants or PSA systems. A membrane system will remove moisture very effectively from a pressurized air stream. Dew points of –35°C can be reached. This process is similar to that proposed for natural gas treating. Dehydration is achieved with some loss of feed air to carry the moisture out through the permeate. In contrast to natural gas dehydration the feed air generally has a value of only the cost of compression. The membrane approach eliminates regeneration cycles, eliminates dust and noise and can operate without power.

Permea introduced a product called Prism Cactus that is designed as a point-of-use air dehumidification system [85]. The membrane is connected to a compressed air line and replaces the more bulky and complex desiccant dryers. A unit weighing only 3.2 kg can treat an air feed of 27,000 scfd at 150 psia and reduce the dew point to 0°C. Due to the low driving forces, however, membrane driers do lose a fair amount of the compressed air feed to the permeate. Special membrane designs help to minimize this problem by deliberately using some percentage of the feed gas stream as a "flush" gas to reduce the moisture partial pressure in the permeate. This gas loss can still be significant as the dew point is lowered. The cost of the process is almost entirely attributable to the cost of the compressed air that is lost in the permeate. The membranes themselves are rather inexpensive.

13.5.5.2 Dryer Exhaust Dehumidification

Dryers are used throughout industry in various applications requiring the removal of moisture from a product. These processes generally heat a feed air stream and the hot, dry air is passed over the product. Example applications include drying of fertilizer, sugar, paper or coal in fluid bed or rotary dryers. The heat in the moisture-laden exhaust air is lost when the air is vented to the atmosphere. Approximately 90% of the original energy is contained in the latent heat of the water vapor. Bend Research developed a membrane that removes the hot water vapor from the exhaust air and concentrates the water vapor in the permeate stream [86,87]. Compressing the water-laden permeate stream allows for an efficient transfer of the energy in a subsequent condenser so that a substantial amount of the original energy is recovered.

Bend Research determined that such a process could be economic in cases where the cost of energy is high. In an economic calculation in which the cost of steam was assumed to be $5.00 per million Btu, Bend determined that the membrane process could recover the steam at a cost of $4.50 per million Btu. This is not judged to be a significant advantage for the membrane process, however. The membrane allows recovery of 10.2 times the energy that must be added to the process (to operate the compressor). The major limitation is the cost of capital for the compressor which accounts for over 90% of the entire capital cost. In situations with higher fuel costs or lower compressor costs the membrane system could be quite promising. In a coal dryer application the membrane system was able to recover 30% of the energy. It was calculated that this would reduce the temperature of the feed air to 665°F from the original 1000°F.

13.5.5.3 Natural Gas Dehumidification

Natural gas is typically moisture saturated when it is produced at a well. Such saturation can cause problems such as hydrate formation and corrosion and must be removed before being delivered to a pipeline. At present this is accomplished with glycol dehydration or with solid desiccants depending on the amount of water that must be removed. Many membranes have very high water permeability and their use in dehydrating natural gas has often been suggested as a possible application. Selectivities of over 400 (water to methane) are available. However, the cost and performance constraints are quite tough for this application. The concentration of water in a high-pressure natural gas stream is low (less than 0.2 mole% in many cases). Pipeline requirements are typically less than 0.014 mole% depending on the country or pipeline. This results in a rather low driving force for a membrane separation and the pressure on the permeate side becomes crucial in making this an economic process. When gas streams contain carbon dioxide, dehydration of the gas is greatly simplified since the carbon dioxide acts as a "carrier" gas to bring the moisture across the membrane. However, if carbon dioxide is not present methane will effectively take its place and the resulting hydrocarbon losses can make this approach relatively expensive.

One study compared conventional glycol dehydration with membrane dehydration for a quite large (255 MMscfd) natural gas stream on an offshore platform [88]. The membrane performance was not divulged and the design was a straightforward single-stage system. The feed pressure was high (1785 psia) but the product moisture specification was quite low (0.006%). Under these conditions the size of the membrane unit was quite large and the amount of hydrocarbon loss was also very high since no process optimization (recycling, permeate vacuum, etc.) was attempted. Not surprisingly, the membrane

unit installed cost was 50% higher than the comparable glycol unit and was 25% heavier. The biggest problem, however, was that the operating costs for the membrane unit were some 16 times higher than the glycol unit due to the hydrocarbon losses. Improved membrane performance and a different process design are both required to make the membrane process competitive under these conditions. Not considered in the analysis, however, are any benefits that may accrue due to the simplicity of the membrane operation. The high cost of platform manpower would improve the comparison for the simple membrane process.

Membrane dehydration economics are vastly improved with different process designs, lower gas feed flows, applications wherein the hydrocarbon-rich permeate stream can be used, and/or improvements in membrane permeability and selectivity. One possible process is the single-stage recycle. In this application the moisture-saturated permeate is recompressed to the feed pressure. The excess water condenses out at the high pressures and is removed in a liquid separator prior to the stream being recycled to the feed. In effect this eliminates all hydrocarbon losses but increases compression expenses.

13.5.5.4 Vehicle Exhaust Moisture Recovery

The U.S. military has had an interest in dehydration membranes for collection of water from vehicle exhaust in areas where water is scarce or possibility contaminated. The membrane unit would concentrate moisture from the exhaust in the permeate which would then be condensed and collected.

13.5.6 Other Applications

13.5.6.1 Helium Separations

Membranes can be used for the separation of helium from natural gas or in the reclamation of spent helium gases from dirigibles or deep sea diving atmospheres. Reclamation involves separating the helium from nitrogen and oxygen for recovery and recycling. Membranes provide a very effective recovery option for the extremely low flows involved for this latter application and several units are in operation.

Helium is currently extracted from natural gas using a cryogenic process in which the gas stream is cooled to condense all constituents besides helium. The concentration of helium in natural gas typically ranges between 0.3 and 1% in deposits that supply U.S. helium recovery plants. A company called Alberta Helium Limited was established in 1973 to pursue commercial development of membrane technology for this application [89]. The Alberta Research Council also played a key role. A four-stage membrane pilot plant was constructed that

could process 3 MMscfd of gas containing 0.05% helium. The membrane unit produced a helium concentration of 72 to 90%. Further on-site processing produced a final helium purity of 99.997%.

A preliminary cost analysis was prepared in 1981 for a commercial plant to produce 25 million cubic feet per year of gaseous helium from feed gas containing between 0.05 to 0.1% helium. The capital and operating costs for a plant to treat 0.05% helium feedstock were $50 million and $2.8 million (Canadian), respectively. A higher helium concentration in the feedstock (0.1%) would lower these costs to $36 million and $2.7 million/yr, respectively. These calculations suggested that the membrane approach would cost substantially less than the comparable cryogenic approach. At a feed helium concentration of 0.2% the process costs are estimated at $100 per 1,000 cubic feet of pure helium assuming a 15% rate of return (1980 cost estimate).

A number of membrane/cryogenic process hybrids have been proposed, which greatly reduce the overall costs. Additionally, improvements in membrane performance since 1981 should favorably impact the capital costs, although a significant portion of these costs are due to the compression requirements, which would not have dropped.

13.5.6.2 Solvent Vapor Recovery

Many industrial processes that handle hydrocarbons produce waste air streams containing hydrocarbon vapors. In addition to there being a loss of valuable hydrocarbons these emissions represent health, environmental and safety problems. Membranes can be utilized to remove and concentrate these vapors. NKK (Japan) markets a system for use with the filling of industrial gasoline storage facilities (tanks, railroad cars, etc.) and Membrane Technology and Research (California) markets a system for smaller industrial applications such as web drier emissions. Considerable R&D has been conducted at the research institute GKSS in Germany and commercialization is being undertaken by Aluminium Rheinfelden (Germany). The type of membrane generally used in this application readily permeates hydrocarbons while retaining air.

The economic advantages of such systems have not been clearly established as of yet. Competing processes (condensation, incineration, adsorption) can be rather low-cost, depending on the specifics of the application. The driving force for solvent vapor recovery is largely environmental and the resulting regulations concerning emission levels play a key role in the decision of whether or not solvent vapor recovery membranes are economically attractive. Factors working against the use of membranes in such applications include (1) feed streams are not pressurized (compressors are required), (2) emission requirements are sometimes quite low (low driving force), and (3) membrane performance varies with each vapor constituent. Membrane separation does work

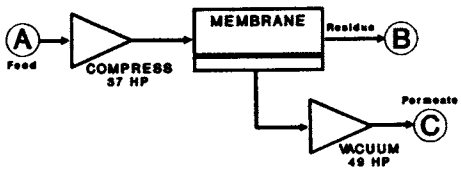

		A	B	C
BUTANE	PPM	300	70	1,700
AIR	%	BAL	BAL	BAL
RATE	SCFM	500	430	70
PRESS	psia	15		15

Membrane Selectivity = 30
Membrane Area = 233 m^2
Capital Cost = $282,000
Operating Costs = $113,000/yr (includes depreciation)

Operating Cost = $0.52/1000 scf feed
Operating Cost = $0.68/lb solvent recovered

Fig. 13.34. Solvent vapor recovery membrane process for the removal of butane from air. (From Ref. [90]).

well in those situations where feed gas solvent concentration and removal efficiencies match the strengths of the membrane process.

Membrane Technology and Research has conducted the greatest number of economic analyses that have been published to date. In one application a membrane system is used to remove 80% of the butane from an industrial off-gas for pollution control [90]. The example is based on treating a 300 ppm butane stream produced during the production of polystyrene packaging materials. Butane is reduced to 70 ppm, which meets EPA standards. The economics of this separation are shown in Fig. 13.34. The cost was calculated to be $0.68 per pound of butane removed.

The permeate stream from the above example is rather dilute, which complicates any actual recovery efforts for recycling the solvent. Two-stage cascade designs provide a much improved separation wherein the permeate is compressed and treated with a second membrane. The retentate from the second-stage unit is recycled to the first stage. The same paper calculated the economics of a system for reducing the level of 1,1,1-trichloroethane (TCE) to 0.1% from a feed concentration of 1.0%. The permeate stream from the second membrane was recovered as a pure TCE liquid. The cost was calculated to be $0.76/1000 scf of feed or $0.21/lb of recovered solvent.

A three-stage system was designed to recover freon (CFC-113) at 3.0% in air and reduce it to 0.075%. The final permeate product was pure CFC-113 liquid. The feed flow rate was 500 scfm and the capital cost, including compressors was estimated at $650,000. Energy costs were calculated at $63,500/year. The process cost, including depreciation, was $1.25 per 1000 scf feed or $0.21/lb of CFC-113 that was recovered. The value of recovered freon far exceeds the process costs.

MTR also calculated the cost of a system designed to recover 1000 l/day of solvent from a stream with a solvent concentration of 0.5 vol% [91]. A vacuum is generated on the permeate side to provide the pressure difference. If the fuel value of the recovered solvent were $0.20/liter a yearly credit of $73,000 is obtained. If the solvent could be reused a higher credit would be available. However, the costs presented did not seem to include the cost of a cooling unit for such recovery. If the solvent is to be recovered then the cost difference between a cooling unit and a membrane/cooling hybrid should be compared. This process still results in a waste stream containing 0.1 vol% of solvent. Depending on the application this stream could possibly be recycled. Additional analyses of the economics of solvent recovery membranes are provided in DOE reports [92].

Nippon Kokan (now NKK) produced a nonquantitative comparison of membrane-based solvent vapor recovery for gasoline vapor applications [93]. Membranes were compared with a variety of absorption, adsorption and chilling condensation processes. Membranes were claimed to offer advantages in cost, safety, space and operability. The NKK system is designed for higher levels of vapor in the feed (15–50 vol%). Their process includes a recovery column for gasoline recovery. The vapor composition of the residue gas is less than 5 vol%.

GKSS has issued several detailed reports concerning the operation of their system in reducing emissions from a gasoline loading facility [94,95]. Detailed operating data are provided on a system that recovered 95–99% of the feed stream hydrocarbons. Economics were not provided, however.

More recent work has centered on combining membranes with chillers to provide an optimized hybrid process for the recovery of freon [96]. A chiller is commonly used to liquify high concentration freon streams but due to economics the temperature is set such that a 5% freon waste stream is still released from the chiller. A small solvent vapor recovery membrane can treat this residual stream to reduce the freon content to 0.5%. The membrane permeate contains 11% freon which is then recycled to the chiller. This substantially reduces the emission problem and improves the overall recovery of freon. The membrane area requirement is low and this type of arrangement offers good possibilities for reducing the energy consumption that would otherwise be necessary to meet stricter emission standards. A two-stage membrane plus chiller was demonstrated to reduce the freon to 0.05%.

MTR prepared a rough analysis of costs for removing 95% of halocarbons in a feed air stream as a function of feed solvent concentration. Figure 13.35 compares these costs for carbon adsorption and compression/condensation. As can be seen solvent recovery membranes are currently most useful when treating solvent concentrations in the 1 to 10% range. This graph also illustrates the potential of a hybrid process. Condensation can be used prior to a membrane and carbon adsorption can be used afterwards as needed to meet the desired emission specification.

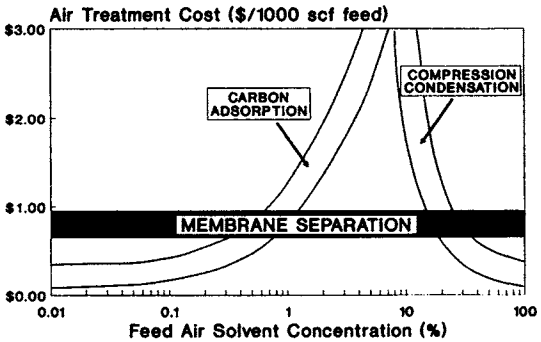

Fig. 13.35. Comparison of competing methods for 95% halocarbon recovery. (Courtesy of Membrane Technology and Research, Menlo Park, CA).

13.5.6.3 Hydrocarbon Dew Pointing

Membranes similar to the type used for solvent vapor recovery could, in principle, be used to remove heavier hydrocarbons from a natural gas stream. Some natural gas streams require some sort of treatment to reduce the hydrocarbon dew point of the gas so as to prevent hydrocarbon condensation in the pipeline. Some limited work has been done in this area but no economic analyses have yet been published [97].

13.5.6.4 Hydrocarbon Condensation

Membranes can also be employed for separating heavier hydrocarbons from a gas stream by condensing these hydrocarbons on the feed side of the membrane [28]. Condensation of hydrocarbons occurs when their partial pressure increases (at constant temperature) until the hydrocarbon dew point is reached. Gas separation membranes can achieve this condition via the removal of a diluent gas such as carbon dioxide or hydrogen and thereby raising the partial pressure of the hydrocarbon gases. The resulting condensed liquid can be separated from the gas stream using specially designed membrane units and liquid separators. Such a membrane process can be economical compared to conventional adsorption, absorption and cryogenic processes currently being used in chemical and petroleum industries for removal of condensable hydrocarbons from a gas stream.

13.5.6.5 Other Separations

Membranes have also been proposed for the removal of nitrogen from natural gas. No commercial membrane yet exists with a sufficient separation

factor to make this a viable process. Membranes for adjusting the carbon dioxide/hydrogen sulfide ratio for Claus plant use are also sought but none yet exist that are of economic significance. Many other applications are under evaluation or development.

13.5.7 Other Information Sources

Considerable additional effort to quantitate the economic performance of membranes versus conventional separation processes has been undertaken by a variety of consulting and engineering firms. Such studies are generally not available to the public as they are typically done under confidential contracts as single- or multiclient studies. SRI International (Menlo Park, CA) has performed a wide range of membrane performance and market analyses for different membrane types and applications.

13.6 SUMMARY AND CONCLUSIONS

Gas separation membranes are still a young technology and new products and processes are continually appearing. The growth of this technology has brought with it a better appreciation of the advantages of these membranes, where they can compete and what improvements are necessary to expand their applicability. Such progress has been painful and expensive. Industrial process development requires a heavy investment in manpower, time and facilities. However, this effort has produced a much clearer understanding of what is required for new membranes and how their performance impacts the economics of a particular process.

The topics covered in this chapter were designed to provide the reader an introduction to some of the more important membrane process design concepts. The case analyses also provide an appreciation for the issues involved in designing a cost-effective process. Although single-stage membrane systems are useful in many applications, it was demonstrated that membrane staging can provide dramatic performance improvements in many situations. Optimizing multistage processes can sometimes be complex but the basic process models presented here should cover many types of applications.

The basic purpose for membrane staging is to achieve higher product recoveries than what are achievable with single-stage systems. Higher selectivity membranes can reduce product losses but, regardless of the separation factor, the nature of membrane separation dictates that staging will often be the most cost-effective design. The key membrane performance variables are selectivity, permeability and durability. Although the objective of membrane research has been to develop membranes with improvements in all three of these properties,

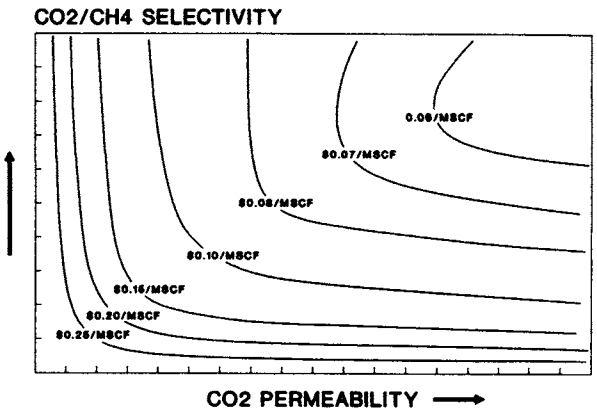

Fig. 13.36. Impact of membrane selectivity and permeability on the cost of treating a specific natural gas stream.

there are always trade-offs that must be resolved. Figure 13.36 illustrates the impact of membrane permeability and selectivity on the costs for treating a specific natural gas stream. As can be seen, technical targets that emphasize selectivity increases over permeability may not necessarily provide any economic improvements. This kind of analysis provides insights as to what membrane improvements are the most beneficial, whether such improvements will result in a competitive product versus a nonmembrane process and what the value of any improvement would be. This latter point has a direct impact on the amount of R&D that is warranted for a particular application. This figure can be redrawn for different applications (e.g., carbon dioxide-enhanced oil recovery, hydrogen recovery, etc.) and for different values of the variables (e.g., natural gas value, membrane costs, etc.).

Gas separation membrane processes are now employed in a wide range of industries and applications. New processes are under development and as new membranes are introduced their use will continue to expand. The cost comparison cases presented in this chapter confirm that membrane separation of gases can provide economic benefits in many applications. Competition from the more traditional gas separation processes is strong and there are many areas where membranes cannot compete at present. Membrane technology is improving at a faster rate than these other processes, however, and the gap will continue to shrink for the foreseeable future. Clear conclusions on the cost effectiveness of membranes are not possible since each application is very site dependent. There are also many intangible factors that impact a process selection. For example, environmental laws concerning chemical usage and waste disposal give membrane-processing some advantage over liquid-based processes. Factors such as equipment size and weight also can heavily influence process selection.

The availability of gas separation membranes is creating opportunities that were not conceived of just a few years ago. Many industries are finding that the low-purity, low-cost nitrogen available from a membrane unit provides valuable benefits that normally could not be justified on the basis of delivered nitrogen. Discovery of new applications and the introduction of new membranes will continue to drive this market. Some of the greatest barriers to commercialization, however, are due to commercial factors such as the depression in the energy industry in the 80s, unfamiliarity and suspicion of new processes, and the aggressive response of nonmembrane competition. These factors have all combined to make market penetration a long and difficult process [98]. As a knowledge base for membrane-based gas separation processes is developed and is taught in engineering courses, the growing application of gas separation membranes to industrial processes is certain to continue for many years.

REFERENCES

1 Spillman, R.W. and Sherwin, M.B. (1990). *CHEMTECH*, 20 (6): 378.
2 Baker, R.W. and Blume, I. (1986). *CHEMTECH*, 16 (4): 232.
3 Rautenbach, R. and Albrecht, R. (1989). *Membrane Processes*. Otto Salle Verlag GmbH & Co., Frankfurt, Germany, p. 422.
4 Fain, D.E. (1988). Gas Separation Processes: Technology/Business Review. Presented at the 1988 BCC Membrane Technology/Planning Conference, Boston, MA, Nov. 2.
5 Fleming, H.L. (1989). Molecular Sieving Inorganic Membranes. Presented at the 1989 BCC Membrane Technology/Planning Conference, Cambridge, MA, Oct. 17–Nov. 2.
6 Hammel, J.J., Robertson, W.J., Marshall, W.P., Barch, H.W., Das, B., Smoot, M.A. and Beaver, P. (1989). U.S. Patent 4,842,620 issued Jun. 27, 1989.
7 Pellegrino, J.J. (1989). An Overview of Facilitated Transport Membranes: Technology and Applications. Presented at the 1989 BCC Membrane Technology/Planning Conference, Cambridge, MA, Oct. 17.
8 Gottschlich, D.E., Roberts, D.L. and Way, J D. (1988). *Gas Sep. Purif.*, 2: 65.
9 Fritzsche, A.K. and Narayan, R.S. (1987). *Chem. Econ. Eng. Rev.*, 19 (205): 19.
10 Puri, P.S. (1990). *Gas Sep. Purif.*, 4: 29.
11 Fleming, H. (1989). Molecular Sieving Inorganic Membranes. presented at the 1989 Seventh Annual Membrane Technology/Planning Conference, Cambridge, MA, Nov. 17.
12 Yong, C., Fouda, A.E. and Matsuura, T. (1989). Effect of Drying Conditions on the Performance and Quality of Synthetic Membranes Used for Gas Separation. *AIChE Symposium Series* 272, 85, p. 18.
13 Sourirajan, S. (1989). A Unified Approach to Membrane Separations. Presented at the 1989 Annual Membrane Technology/Planning Conference, Cambridge, MA, Nov. 17–19.
14 Cooley, T.E. (1988). U.S. Patent 4,746,430, issued May 24, 1988.
15 Kimura, S.G. and Browall, W.R. (1986). *J. Membr. Sci.*, 29: 69.

16 Hwang, S.T. and Kammermeyer (1965). Operating Lines in Cascade Separation of Binary Mixtures. *Can. J. Chem. Eng.*, 43 (1): 36–39.
17 Chu, C.-H. (1990). Exergy Analysis for Membrane Gas Separation. Presented at the 1990 AIChE Spring National Meeting, Orlando, FL, March 20.
18 Gottschlich, D.E. and Roberts, D.L. (1990). The Use of Thermodynamics in Designing Membrane Systems for Gas Separation. Presented at the March 1990 AIChE Meeting, Orlando, FL, paper 78a.
19 Hwang, S-T. and Ghalchi, S. (1982). *J. Membr. Sci.*, 11: 187.
20 Sengupta, A. and Sirkar, K. (1986). Membrane Gas Separation. In: *Progress in Filtration Separation IV*. Elsevier, Amsterdam, p. 289.
21 Yan, Zhiquan and Kao, Yuen-Koh (1989). Analysis and Design of Two-Membrane Column for Gas Separation. *AIChE Symposium Series 272*, 85, p. 41.
22 Linde, G., Schmid, W., Boelt, M. and Burr, P.S. (1985). U.S. Patent 4,548,618, issued Oct. 22, 1985.
23 Agrawal, R. and Auvil, S.R. (1986). U.S. Patent 4,595,405, issued Jun. 17, 1986.
24 Duckett, M. and Limb, D.I. (1987). U.S. Patent 4,639,257, issued Jan. 27, 1987.
25 Doshi, K.J. (1983). U.S. Patent 4,398,926, issued Aug. 16, 1983.
26 Perry, E. (1980). U.S. Patent 4,238,204, issued Dec. 9, 1980.
27 Choe, J.S., Auvil, S.R. and Agrawal, R. (1987). U.S. Patent 4,701,187, issued Oct. 20, 1987.
28 Minhas, B.S., Spillman, R.W. and Cooley, T.E. (1990). Membranes for Hydrocarbon Liquid Recovery from a Gas Stream. presented at the 1990 Spring National Meeting of the American Institute of Chemical Engineers, Orlando, Florida, March 21, 1990.
29 Bhat, P.V. and Beaver, E.R. (1987). Innovations in Nitrogen Generation Using Membrane Systems. Presented at the 1987 Summer AIChE Meeting, Minneapolis, MN, Aug, 17.
30 McGinn, K. (1988). Producing a Sintering Atmosphere Through a Hollow Fiber Membrane. Presented at the 1988 Metal Powder Industries Federation Meeting, Orlano, FL, June 10.
31 Spillman, R.W., Barrett, M.G. and Cooley, T.E. (1988). Gas Membrane Process Optimization. presented at the 1988 AIChE Spring Annual Meeting in New Orleans, March 9.
32 Spillman, R.W. (1989). *Chem. Eng. Progr.*, 85 (1): 41.
33 Beaver, E.R., Bhat, P.V. and Sarcia, D.S. (1988). Integration of Membranes with Other Air Separation Technologies. *AIChE Symposium Series 261*, 84, p. 113.
34 Prasad, R., Haas, O.W. and Schaub, H.R. (1990). High Purity N_2 via Membrane Air Separation. Presented at the 1990 AIChE Spring National Meeting, Orlando, FL, March 21.
35 Thompson, D.R., Prasad, R. and Van Lente, T.S. (1990). Operating Experience Using Membranes to Produce Nitrogen. Presented at the 1990 AIChE Spring National Meeting, Orlando, FL, March 21.
36 Gollan, A. and Kleper, M.H. (1986). Membrane-Based Air Separation. *AIChE Symposium Series 250*, 82, p. 35.
37 Gollan, A. and Kleper, M.H. (1987). State-of-the-Art: Permeable Membrane Gas Separation. Presented at the 1987 Fifth Annual Membrane Technology/Planning Conference, Boston, MA, Oct.
38 Technical Bulletins 174-474-85, 174-472-85, 174-469-85, 174-473-85, and 174-467-86, Dow Chemical Company, Midland, MI.
39 Sulpizio, T.E. (1985). Oxygen Enrichment — Markets and Economics. Presented at the 1985 Membrane Technology/Planning Conference, Cambridge, MA, Oct. 30.
40 Jain, R. (1988). Graphical Method for the Economic Evaluation of Membrane Based Air

Separation. Presented at the North American Membrane Society Meeting, Syracuse, New York (June).
41 Matson, S.L., Ward, W.J., Kimura, S.G. and Browall, W.R. (1986). J. Membr. Sci., 29L 79.
42 Enriching Air with Oxygen — Cheaply. *Chem. Week*, July 1984: 36.
43 Gollan, A. and Kleper, M.H. (1989). Point-of-Use Air Separation Systems. Presented at the 1989 Seventh Annual Membrane Technology/Planning Conference, Cambridge, MA, Nov. 17–19.
44 Wang, S.I., Nicholas, D.M. and DiMartino, S.P. (1983). Selection and Optimization of Hydrogen Purification Processes. AIChE Meeting, Denver, CO Aug. 29.
45 Tomlinson, T.R. and Finn, A.J. (1990). *Oil Gas J.*, (Jan 15): 35.
46 Shirley, J. and Borzik, D. (1982). *Chem. Proc.*, 42: 30.
47 MacLean, D.I., Prince, C.E. and Chae, Y.C. (1980). *Chem. Eng. Progr.*, 76 (March): 98.
48 Schendel, R.L., Mariz, C.L. and Mak, J.Y. (1983). *Hydrocarbon Proc.*, 62 (Aug.): 58.
49 Stookey, D.J., Patton, C.J. and Malcolm, G.L. (1986). *Chem. Eng. Progr.*, 82 (11): 36.
50 Grotewold, D.R. (1990). The Application of Medal's Hydrogen Membrane Separation Technology in Petroleum Refinery Hydroprocessing Systems. Presented at the 1990 AIChE Spring National Meeting, Orlando, FL, March 1990.
51 Schell, W.J. and Houston, C.D. (1985). Refinery Hydrogen Recovery with Separex Membrane Systems. Presented at the 1985 National Petroleum Ref. Assoc., March.
52 Heyd, J. (1986). Hydrogen Recovery Using Membranes in Refining Applications. 1986 National Petroleum Refiners Association, March.
53 Nakamura, A., Hotta, M. and Kusuki, Y. (1987). *Nippon Kagaku Kyokai Geppo*, Oct.: 31.
54 Nakamura, A. (1987). Gas Separation with Polyimide Membranes. Presented at the Energy Conservation Meeting by AFME & MITI, Paris, France, March 25.
55 Wang, S.I., Nicholas, D.M. and DiMartino, S.P. (1983). Selection and Optimization of Hydrogen Purification Processes. Presented at the 1983 AIChE Summer Meeting, Denver, CO, Aug. 29.
56 Lane, V.O. (1983). *Hydrocarbon Proc.*, 62: 56.
57 Bollinger, W.A., MacLean, D.L. and Narayan, R.S. (1982). *Chem. Eng. Progr.*, 78, p. 27.
58 Bollinger, W.A., Long, S.P. and Metzger, T. (1984). *Chem. Eng. Progr.*, 80: 51.
59 Schott, M.E., Houston, C.D., Glazer, J.L. and DiMartino, S.P. (1987). Membrane H_2/CO Ratio Adjustment. AIChE National Meeting, Houston, TX, April 1.
60 Burmaster, B.M. and Carter, D.C. (1983). Increased Methanol Production Using Prism Separators. AIChE National Meeting, Houston, TX, March.
61 Doshi, K.J., Werner, R.G. and Mitariten, M.J. (1989). *AIChE Symposium Series 272*, 85, p. 62.
62 Bell, C., Pinnau, I., Wijmans, J., Baker, R., Gottschlich, D. and Roberts, D.L. (1989). *Low Cost Hydrogen/Novel Membrane Technology for Hydrogen Separation from Synthesis Gas.* Final Report to the U.S. Dept. of Energy (Contract # DE-AC21-85MC22130).
63 Gottschlich, D.E., Roberts, D.L., Wijmans, J.G., Bell, C.-M. and Baker, R.W. (1989). *Gas Sep. Purif. J.*, 3: 172.
64 Babcock, R.E., Spillman, R.W., Goddin, C.S. and Cooley, T.E. (1988). *Energy Progress*, 8 (3): 135. (Note: Figure 1 is switched with Fig. 2 and Fig. 3 is switched with Fig. 4 due to publisher's error).
65 Spillman, R.W. and Dethloff, W.L. (1988). Membrane Gas Treatment is Economic. *Am. Oil Gas Reporter*, Oct.: 36.
66 Fournie, F.J. and Agostini, J.P. (1987). *J. Petrol. Technol.*, June: 707.
67 Cooley, T.E. and Dethloff, W.L. (1985). *Chem. Eng. Progr.*, Oct.: 45.

68 Purgason, R.S. and Houston, C.D. (1983). Purification of Carbon Dioxide-Containing Gas Streams with Membranes. 1983 AIChE National Meeting, Denver, CO (Aug.).
69 Miller, B.D., Richards, R. and Schott, M.E. (1984). Separex System Makes Hydrocarbon Recovery Feasible. 1984 AIChE National Meeting, Anaheim, CA, May.
70 Markiewicz, G. (1988). Separex Membrane Systems: The Economical Solution to Gas Treating Problems. Gas Processors Association, New Orleans, LA, Jan.
71 Cooley, T.E. (1990). The Use of Membranes for Natural Gas Purification. Presented at the 1990 Gas Processors Association Meeting, European Chapter, Biarritz, France, May 17.
72 Personal communication, Ian Johnson, John Brown Engineers and Constructors, Ltd., October 24, 1988.
73 Meissner, R.E., Cumare, F.E. and Steppe, R.J. (1986). Application of Membrane Technology for Treating Acid Gas-Bearing Natural Gas. 1986 AIChE National Meeting, New Orleans, LA, April.
74 Cooley, T.E. and Spillman, R.W. (1989). Membrane Gas Treating. Presented at the 68th Annual Gas Processors Association Convention, San Antonio, TX, March 14.
75 Spillman, R.W., Cooley, T.E. and Yearout, J.P. (1989). Experience with Membrane-Based Natural Gas Treating. Presented at the 1989 Laurance Reid Gas Conditioning Conference, Norman, OK, March 7.
76 Youn, K.C., Blytas, G.C. and Wall III, H.H. (1982). Role of Membrane Technology in the Recovery of Carbon Dioxide: Economics and Future Prospects. Gas Processors Association, November 18.
77 Goddin, C.S. (1982). Comparison of Processes for Treating Gases with High Carbon Dioxide Content. Gas Processors Association, Dallas, TX, March 19.
78 Boustany, K., Narayan, R.S., Patton, C.J. and Stookey, D.J. (1983). Economics of Removal of Carbon Dioxide from Hydrocarbon Gas Mixtures. Gas Processors Association, San Francisco, CA, March.
79 Ryan, B.F. and Anderson, M.D. (1988). Hybrid Membrane — Solvent Process Optimization. *AIChE National Meeting, New Orleans, LA*, March.
80 Schendel, R.L. and Seymour, J.D. (1984). Integration of Membranes with other Separation Processes. Membrane Technology R&D Workshop, Clemson, South Carolina, Oct.
81 Schendel, R.L. (1984). *Chem. Eng. Progr.*, 80 (May): 39.
82 Finken, H. and Kratzig (1984). *Chemie-Technik*, 13 (8): 75.
83 Werner, U. (1984). Refinement of Biological and Natural Gases by the Membrane Process. Presented on the occasion of the Exchange of Information of Chemists and Engineers of the Gas Industry, Bad Kissingen, West Germany, Sept.
84 Rautenbach, R. and Ehresmann, H.E. (1989). Upgrading of Landfill Gas by Membranes — Process Design and Cost Evaluation. *AIChE Symposium Series 272*, 85, p. 48.
85 Murphy, M.K., Beaver, E.R. and Rice, A.W. (1989). *AIChE Symposium Series 272*, 85, p. 34.
86 *Research on an Energy-Efficient Drying Process.* DOE Final Report DOE/ID/12293-1 (DE86013369), Feb. 26, 1986.
87 Gienger, J.K. and Ray, R.J. (1988). Membrane-Based Hybrid Processes. *AIChE Symposium Series 261*, 84, p. 168.
88 *Study on Membrane Technology.* Final Report (October 1988). Prepared by Global Engineering for the Offshore Supplies Office, Department of Energy, UK (GEL 1419).
89 *Helium Recovery from Natural Gas* (1986). Published by Alberta Energy, Scientific and Engineering Services Division, Publication I/172 (ISBN 0-86499-413-3).
90 Wijmans, J.D. and Helm, V.D. (1989). *AIChE Symposium Series 272*, 85, p. 74.
91 Peinemann, K.V., Mohr, J.M. and Baker, R.W. (1986). The Separation of Organic Vapors

from Air. *AIChE Symposium Series 250*, 82, p. 19.
92 Baker, R.W., Hibino, K., Mohr, J. and Kuroda, T. (1985). Membrane Research in Energy and Solvent Recovery Systems from Industrial Effluent Streams. U.S. Dept. of Energy, DOE/ID/12379-T2 (DE85 014583).
93 Technical Bulletin, *Hydrocarbon Vapor Recovery with Membrane Technology*. Nippon Kokan, Tokyo, Japan, p. 9 (1987).
94 Behling, R.-D., Ohlrogge, K., Peinemann, K.-V. and Wind, J. (1990). Experimental Results of Field Experiments for the Separation of Gasoline Vapors by Means of Membranes. Presented at the 1990 Spring National Meeting of the AIChE, Orlando, FL, March.
95 Behling, R.-D., Ohlrogge, K., Peinemann, K.-V. and Kyburz, E. (1989). *AIChE Symposium Series 272*, 85, p. 68.
96 Personal communication, Dr. Richard Baker, Membrane Technology and Research (MTR), May 8, 1990.
97 Watler, K.W. (1989). U.S. Patent 4,857,078, issued Aug. 15.
98 Spillman, R.W. (1987). Bringing New Technology to a New Market. Presented at the 1987 Membrane Technology/Planning Conference, Boston, MA, October.

Membrane Separations Technology. Principles and Applications
Edited by R.D. Noble and S.A. Stern

Chapter 14

Catalytic membrane reactors

John L. Falconer, Richard D. Noble and **David P. Sperry**

Department of Chemical Engineering, University of Colorado, Boulder, Colorado 80309-0424, USA

14.1 INTRODUCTION

A catalytic membrane reactor (CMR) is a combination of a heterogeneous catalyst and a permselective membrane, which is a thin film or layer that allows one component of a mixture to selectively permeate through it [1]. A CMR usually operates at higher yields, better reaction selectivity (as opposed to separation selectivity), or lower cost than a separate catalytic reactor and downstream separation units. Though the use of CMRs is not widespread at present, the development of new membranes, particularly porous ceramic and zeolite membranes, creates the potential to significantly improve yields of many catalytic processes. Hsieh [2] and Armor [1] recently reviewed inorganic membrane reactors.

Roth [3], in a review of the future opportunities in industrial catalysis, indicated that we are at a threshold of major changes in separation technology (particularly in a shift from distillation to separation by synthetic membranes), and these changes will have substantial impact on chemical process technology. He stated that membranes will be of importance in the emerging area of catalytic membrane reactors. He referenced a quote by Gryaznov of the former Soviet Union: "Priority in our country should be given to the use of membrane catalysis in all plants that utilize the selective hydrogenation of acetylenic alcohols to ethylenic alcohols, nitro compounds to amines, and the hydrogenation of cyclopentadiene to monomer for synthetic rubber." Roth further pointed out a number of opportunities for CMRs for equilibrium limited reactions, such as the production of ethylene from ethane, ammonia synthesis, methanol syn-

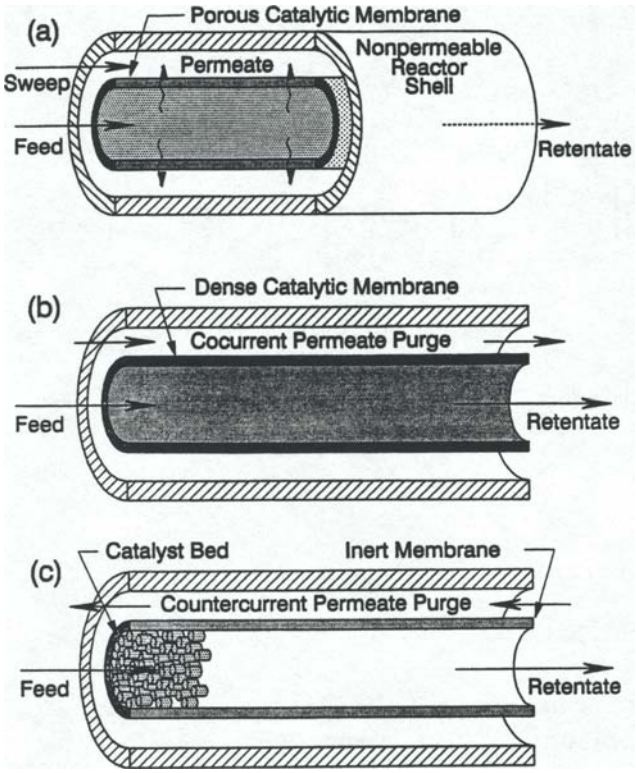

Fig. 14.1. Schematic representations of three arrangements of catalytic membrane reactors: (a) a porous membrane on which a catalyst is impregnated, (b) a nonporous (dense) membrane whose surface is a catalyst, and (c) a porous membrane with a high surface area catalyst located inside the tube.

thesis, and the water gas shift reaction. Itoh [4] stated recently, however, that for practical applications of membrane reactor technology, further developments of technology to manufacture membranes that possess high selectivity, high permeability, and high temperature durability are necessary.

This chapter will discuss the advantages and potential applications of CMRs, and review laboratory studies and theoretical models. Membranes have been used in the form of tubes, disks, and monoliths; the tube arrangement will be used to illustrate the processes. A permselective membrane tube separates two gaseous regions. Reaction takes place on a heterogeneous catalyst that is located in the porous structure of the membrane, on the surface of the membrane, or in one of the two regions. The three arrangements that have been used are shown in Fig. 14.1.

- A porous membrane that is also a catalyst or a catalyst is impregnated on its internal surface (Fig. 14.1a).
- A nonporous (dense) membrane that is also a catalyst or on whose surface

a catalyst is deposited (Fig. 14.1b).

- A porous or nonporous membrane tube, in the center of which is located a high surface area catalyst (Fig 14.1c), or a recycled catalyst entraining feed stream circulates through the tube [5]). The third arrangement has been referred to as a membrane enclosed reactor [6,7], but for the purposes of this chapter, all three types will be labeled as catalytic membrane reactors (CMRs). The permeate stream can flow countercurrent, cocurrent, or perpendicular (crossflow, with ports at the center of the impermeable shell) to the feed stream. Though shown in Fig. 14.1 with the reactants fed to the tube side, the reactants could instead be fed to the shell side. Another arrangement is to locate the catalyst on the shell side and feed reactants to the tube side. In this arrangement the membrane can control the molecules that contact the catalyst.

For the porous membrane (Fig. 14.1a), in which the catalyst is part of the membrane, the reactants diffuse from the feed stream (tube side) to the permeate stream (shell side) while simultaneously being converted to products. The products will diffuse in both directions because their concentrations will be highest inside the membrane.

A CMR can have many advantages over a separate catalytic reactor and downstream separation units. One distinct advantage is that combining two processes, which are normally carried out separately, will lower capital costs, since separations can account for 70% of a chemical plant's cost [8]. The appropriate reactor design can improve yield or reaction selectivity, and this can also decrease downstream separation costs. Several possible applications of CMRs to improve yield or selectivity are:

- Removal of one of the reaction products as it forms (Fig. 14.2a). If one product preferentially permeates through the membrane, then a reaction that is limited by thermodynamic equilibrium can obtain higher overall conversion (than could be obtained in a conventional catalytic reactor), or operate at a lower temperature to obtain the same conversion. The equilibrium constant is not changed, but the product is removed from further contact with the catalyst so that it cannot react by the reverse reaction. This has been the approach used most often in CMR studies. The conversion that can be obtained is limited by permeation of the reactant(s) unless a highly selective membrane is used. Another advantage, when the membrane selectivity is infinite, is that a pure product is produced on the permeate side of the membrane [9].
- Removal of one of the reaction products before it can further react to undesirable products or before it can decompose and poison the catalyst (for example, carbon deposition). In a series reaction, preferential removal of an intermediate product can significantly improve selectivity (Fig. 14.2b).

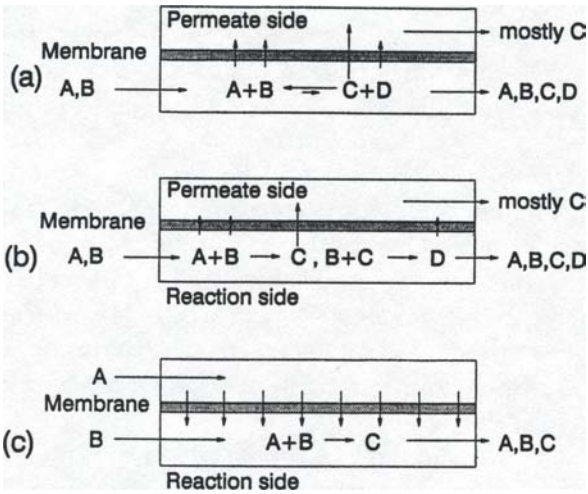

Fig. 14.2. Schematics of various applications of CMRs: (a) Preferential removal of product C in equilibrium-limited reaction, (b) Preferential removal of a desired intermediate C to prevent further reaction to D, (c) Controlled addition of reactant A through the membrane.

- Controlled addition of one of the reactants through the membrane to maintain its concentration low, and thus limit side reactions or subsequent reactions of the product (Fig. 14.2c). Controlled addition can also be used to prevent catalyst deactivation [10].
- Addition of one reactant through the membrane so that a higher concentration of that reactant can be obtained on the catalyst surface (Fig. 14.3a). This may yield higher conversions when the concentration of that reactant on the catalyst surface is limited because of competitive adsorption. A more uniform concentration can be obtained on the catalyst surface than in a standard tubular reactor.
- Locating the catalyst on the opposite side of the membrane from the reactant feed or from one of the reactants, or locating the catalyst within the membrane. The membrane then controls which reactants reach the catalyst. The membrane could prevent a poison from reaching the catalyst or preferentially allow certain species to diffuse through the membrane and react (Fig. 14.3b). For example, an impure reactant could be on one side of the membrane without adding diluents or poisons to the rest of the reacting gas stream. The impure reactant could be much less expensive. In a mixture of reactants, only one reactant could be hydrogenated and removed, so that both selective reaction and separation are obtained.
- Carrying out two reactions in the same CMR. The membrane separates the two reactions, and only one component (one of the products of reaction 1) can permeate through the membrane to serve as a reactant for reaction 2.

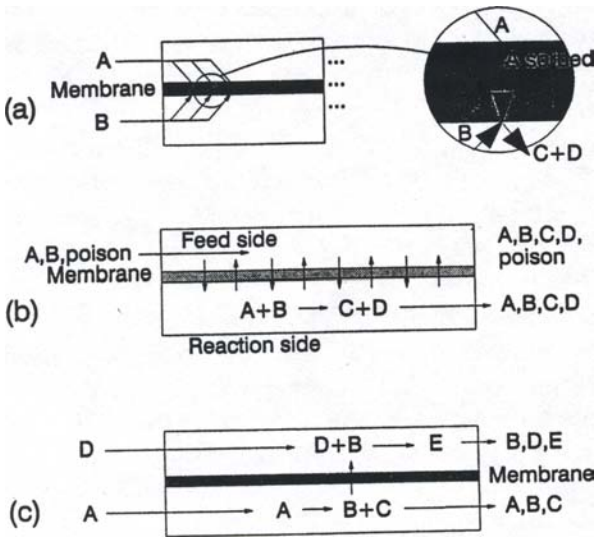

Fig. 14.3. Schematics of various applications of CMRs. (a) Reactant permeation through the membrane to obtain an enhanced adsorbed concentration of A on the other side of the membrane. (b) Separating the catalyst from the feed by a membrane. The reactants and products can pass through the membrane, but the poison cannot. (c) Two reactions in the same CMR. One of the products of reaction 1 is a reactant for reaction 2.

Heat can transfer across the membrane from the exothermic to the endothermic reaction (Fig. 14.3c).

Though not all these approaches have been successfully demonstrated, they show that the potential of catalytic membrane reactors is much broader than shifting equilibrium limited reactions to higher conversions, which has been the main application to date.

The types of membranes available for CMRs, their properties, and their advantages will be presented first in this chapter. The separations mechanisms that occur in these membranes will then be discussed. Specific examples of CMR laboratory studies will then be reviewed to demonstrate the effectiveness of these concepts. Finally, theoretical models of CMRs will be presented.

This chapter will focus on gas phase reactions that take place on metal or metal oxide catalysts. Gas–liquid reactions will not be emphasized, though ceramic tubes have been proposed as a means of increasing gas–liquid contact in catalytic reactors [11]. Biochemical applications are discussed in another chapter. Other systems, which combine reaction and separation but are not considered CMRs for this chapter, include facilitated transport and phase transfer catalysis. In facilitated transport, a complexing agent (which is impregnated in the membrane) reacts reversibly with one or more components of a solution that is on one side of a membrane. The resulting complex, after passing through the membrane due to a concentration gradient, releases the solute on

the other side [12]. No net reaction takes place in this arrangement. In phase transfer catalysis [13], the reversible reaction occurs at an interface, not in the bulk. This process usually occurs with liquid/liquid systems; for example, a membrane is used to stabilize an organic/aqueous interface. Reaction can be promoted between these immiscible phases without dispersing them. Ionic species, which are normally insoluble in the organic phase, can be transferred across the interface by an ion-exchange agent that is soluble in the organic phase. Noncatalytic reactors have also been combined with semipermeable membranes. For example, H_2O and CO_2 have been decomposed homogeneously in the gas phase near 2000 K, and the O_2 product preferentially removed through a zirconia membrane in order to increase equilibrium conversion [14,15]. For CO_2 decomposition, conversion was increased from 1.2% (equilibrium) to 21.5% with the membrane. Similarly, the water gas shift reaction has been carried out using a $SrCe_{0.95}Yb_{0.05}O_{3-\alpha}$ membrane, which is a protonic conductor, to separate H_2 at 1075–1175 K. The rate of H_2 extraction was directly proportional to the current [16].

14.2 MEMBRANES

A suitable membrane for a CMR should have high permeability and good separation selectivity. It also must be stable at reaction temperatures in the presence of reactive gases and able to withstand a significant pressure drop. In general, for the same pressure drop, higher permeabilities are obtained with thinner membranes because permeation rate is inversely proportional to thickness. However, the membrane must be thick enough to avoid formation of cracks and pinholes during its preparation and to prevent rupture from mechanical stresses that occur during use. Also, for porous membranes, an optimal thickness exists because as the membrane becomes too thin, the increasing permeation of the other components (for example, the reactants in an equilibrium-limited process) results in a decrease in conversion [4,17].

Two general types of membranes, nonporous (dense) and porous, have been used in catalytic membrane reactors. Nonporous metal membranes such as Pd alloys, which absorb hydrogen atoms and then transport them by diffusion, were the first type used to combine heterogeneous catalytic reaction and separation [18,19]. Virtually complete reaction conversion is possible with these membranes because they allow only one component to permeate. Nonporous oxide membranes have also been used. The porous membranes are glasses with small pores, composite ceramics, and zeolites. The recent improvements in ceramic membranes, which are usable at high temperatures, have opened up many possibilities for CMRs. The selectivities of porous membranes, however, are much lower than those of Pd alloys unless the pores are of molecular dimen-

sions (zeolite membranes). Polymeric membranes could be used in CMRs, but polymers are not suitable for use at elevated temperatures, nor can they be used in the corrosive environments encountered in many chemical reactions.

In the following sections, the membranes will be divided into two classes, porous and nonporous, since this is a convenient division for discussing the transport mechanisms. Another way to classify these membranes is uniform structures (Pd or Ag foils, porous Vycor glass) and layered or composite structures (ceramic and zeolite membranes). Only brief descriptions of membranes and transport mechanisms that are potentially suitable for CMR use are given in the following sections. Armor [1] presented extensive descriptions of preparations of a wide variety of inorganic membranes, and Hsieh [2] presented tables of membranes and suppliers. In addition, another chapter in this book discusses inorganic membranes.

14.2.1 Nonporous Metallic Membranes

Many of the CMRs studied to date have used Pd alloy membranes, which allow completely selective permeation of H_2. Commercial Pd/Ag alloys are used to obtain high purity H_2 at 575–675 K [20]. Alloying is necessary to prevent embrittlement; pure Pd undergoes a structural change from an α to β phase as the temperature cycles, and the Pd becomes brittle [9,21–23]. Hydrogen also has higher fluxes through some Pd alloys [20], and the catalytic activities of some alloys are higher than that for pure Pd for hydrogenation and dehydrogenation reactions [9]. Group V, VI, or VIIIB metals are the best choice for increased permeation and resistance to embrittlement [9]. The most commonly used alloying components are Ag, Ru, Rh, Ni, and Au [2].

Thin alloy foils have often been used as membranes, but higher fluxes have been obtained by depositing a thin, dense metal film onto a porous support [24–26]. Such membranes have higher permeabilities than foils because the metal layer is thinner [25–26]. A number of techniques (chemical vapor deposition, sputtering, and electroplating) have been used to create thin metal films [2,27–29].

Armor [1] stated that little progress has been made in large scale CMRs with metal membranes because of cost, fabrication durability, and catalyst poisoning. Carbon and sulfur compounds can potentially poison the membranes. Others [30,31] have also indicated that the low permeabilities, high cost, and metal sintering have hindered widespread use of metal membranes. The small surface area of the membrane, which is also the catalyst in many cases, can also limit the reaction rate [4]. The specific area can be increased by depositing a porous catalyst layer on the nonporous alloy [32].

The only other metal membrane used to date in CMRs is silver, through which oxygen selectively permeates. Silver membranes have been used to a much smaller extent than Pd alloy membranes [33].

14.2.2 Nonporous Oxide Membranes

Nonporous oxide membranes have seen only limited use in CMRs, though some oxides exhibit high separation selectivities for H_2 or O_2. For example, silica is permeable to H_2, which moves through the openings in the silica network. Solid electrolyte membranes, such as Ca-stabilized zirconia, are semipermeable to O_2 but not to other gases [4], and PbO has been used to selectively permeate O_2 [34].

Gavalas et al. [35] developed a method for depositing a thin layer of silica within a porous Vycor glass tube (4-nm average pore diameter) by reacting SiH_4 on the tube side of the membrane with O_2 on the shell side. The reactant gases diffuse to each other and react. A thin (0.1 μm) nonporous silica films forms before the reaction limits itself. The solid matrix of the Vycor prevents formation of large pinholes and protects the deposited film from loss of adhesion or other mechanical damage. These membranes were highly selective to H_2 permeation, and ratios of H_2/N_2 fluxes between 2000 and 3000 were measured at 725 K. In contrast, at 300 K the fluxes of H_2 and N_2 were at the ratio of their Knudsen diffusion coefficients. With increasing temperature, the N_2 flux decreased slightly, but the H_2 flux increased rapidly so that large ratios were obtained at 725 K. The H_2 flux was one-third of that for an untreated Vycor tube. These membranes were stable at 725 K, but densification took place at 875 K.

14.2.3 Porous Ceramic and Glass Membranes

Uniform, microporous Vycor glass membranes can be prepared with pores as small as 4 nm. For 4.5 nm diameter pores, in a Vycor glass membrane, 86% of the pores have been reported to have a diameter within ±1 nm of the average [36]. They are made by acid leaching one of the phases that form in Vycor glass. These glass membranes may be limited in their applications, however, because they are brittle [20]. Moreover, when microporous glass is heated above 575 K for long periods, or to much higher temperatures for shorter periods, it loses its microstructure [20]. Some glasses are stable above 1075 K, however [36,37].

The development of composite ceramic membranes, with pore diameters as small as 2.5 nm, may also limit the use of microporous glass membranes because higher fluxes can be obtained through microporous ceramic membranes. The large number of pores per cm^2 and the thin permselective layer in ceramic membranes result in high flux/volume ratios. Porosities as high as 59% have been reported for the permselective layer [38,39]. The ceramics are also stable to high temperatures; Al_2O_3 membrane can be used to 1075 K without degradation of the pore structure [37]. The ceramics are also mechanically stable and can withstand pressure drops of 1.5 MPa, and they are resistant to corrosive chemicals.

Ceramic membranes have other advantages. They have controlled, stable, and narrow pore-size distributions. Catalytic materials that are deposited by impregnation can also be dispersed on ceramics and thus they can have high catalyst surface/volume ratios [40]. Since the same materials used for ceramic membranes are also used as catalyst supports, ceramics are ideally suited for dispersing metals and oxides. The ceramic may catalyze undesirable reactions and modifications may be necessary. For example, alumina surfaces have acidic sites that can catalyze reactions.

Most ceramic membranes consist of a layered or graded structure with a thin (few μm) permselective layer deposited onto a thicker (several mm) macroporous layer. For example, a thin γ-alumina layer with 4-nm diameter pores is deposited onto an α-alumina layer with 120 nm pores. The γ-alumina layer, which can have BET surface area of 240 m^2/g [41], acts as the membrane and the α-alumina is essentially a high temperature support. Because the final layer is thin, it allows for rapid diffusion. Though most of the composite ceramic membranes used in CMRs or for separations have been Al_2O_3, the same procedures can be used to make the top layers of ceria, titania, zirconia, or mixtures of these oxides [38]. Layers from 0.2 to 8 μm have been prepared, and for some binary oxides, pores have been stable up to 1025 K [38].

Detailed preparation procedures and characteristics of ceramic membranes are described elsewhere [10,38,39,41–51]. The membranes are often prepared by slip casting [2]. A thin layer of particles is deposited from a stable dispersion of small particles by contacting a dry support with the dispersion. Capillary pressure forces the liquid to flow into the pores of the support [2]. Controlled drying and calcination yield a membrane without pinholes or cracks. Because the small particles needed for a selective membrane can seep into the macroporous support during manufacture, a thin intermediate layer or layers is required. Typically, 40–80% of the pressure drop occurs in the permselective top layer [10,52]. Specific surfaces areas of 120 m^2/m^3 [53] have been reported for monoliths and 50–80 m^2/m^3 for bundles of single tubes. Ceramic membranes have been modified with MgO and SiO_2 to obtain better separation selectively, and SiO_2 modification has been reported to decrease pore sizes below 1 nm [54].

14.2.4 Zeolite Membranes

More widespread applications of CMRs may take place when zeolites can be readily made into membranes. Only a few cases of zeolite membranes have been reported [55,56]. Ishikawa et al. [56] prepared an inorganic zeolite on porous glass (4 nm average pore diameter) by dipping the glass tube into liquid solutions. Though they had no direct evidence of permeation through a zeolite structure, they obtained high separation factors for water/alcohol liquid solu-

tions; separation factors of 2700 were reported for a water/butanol mixture. Fluxes through the glass-supported zeolite membrane were a significant fraction of the fluxes through the porous glass, which by itself exhibited a separation factor of one.

A patent by Suzuki [55] reported the preparation of a large number of zeolite membranes. These were ultrathin layers (1 nm to tens of nm thick) that were prepared by forming a thin gel film by gentle sedimentation from a mixture. The patent claimed that A, X, Y, L, FU-1, ZSM-5, and silicalite-type zeolite membranes can be prepared in this manner. X-ray diffraction was used to verify that the desired zeolite was formed. The zeolites were deposited on various supports, including Vycor (4 nm diameter pores), stainless steel, Ni, and Al_2O_3. Ion exchange was used to change the catalytic properties of the zeolites by substituting rare earth and transition metals into the zeolites.

Jia et al. [57] reported that adding silicalite zeolite to silicone rubber membranes created a zeolite membrane, but the high temperature limit of silicone rubber probably limits its applications in CMRs. They defined a term called a facilitation ratio, which is a measure of the increased permeability due to zeolite addition. This parameter correlated with the kinetic diameter of gases transported through the membrane. Smaller gases had a larger enhancement due to the relative ease of movement through the pores. Also, this parameter increased with more zeolite present in the membrane.

14.3 SEPARATION MECHANISMS

While only one mechanism controls separation in nonporous metal membranes and their use is restricted to H_2 and O_2 permeation, four diffusion mechanisms can take place in porous membranes, which can be used for a wider variety of compounds. The four mechanisms are Knudsen diffusion, surface diffusion, capillary condensation, and molecular sieving (shape selectivity). Most of the porous membranes used for gas phase CMRs to date have been operated at sufficiently low pressure that Knudsen diffusion predominated, but all four mechanisms will be described. Viscous flow can be present in porous membranes if the pressure or the pressure drop is too high, but viscous flow does not yield a separation and thus will not be discussed.

The flux of component i through the membrane is a product of the permeability and the driving force, which is usually a pressure gradient for gases. Flux is a measure of the productivity of a membrane for transporting a given component. Permeability is also a measure of productivity and is often reported in the barrer units:

$$1 \text{ barrer} = 10^{-10} \text{ cm}^3 \text{ (STP) cm/cm}^2 \text{/s (cm Hg)}$$

The various transport mechanisms affect the fluxes of each component, and this affects the separating ability. Though the permeability is the term most often used to describe transport of a component across the membrane, another measure of productivity is the permeance, which is the ratio of flux of a component to its concentration change. The permeance is thus the ratio of the permeability to the effective membrane thickness.

The separation selectivity of a membrane is characterized by the separation factor, α_{ij}, which is a measure of the ability of a membrane to selectively separate two components. The separation factor is greater than one when the mole fraction of component i is increased relative to component j on the permeate side of the membrane. The separation factor is defined as:

$$\alpha_{ij} = (F_{iy}/F_{ix})/(F_{jy}/F_{jx}) = (f_{iy}/f_{ix})/(f_{jy}/f_{jx}) \tag{14.1}$$

where F is a molar flow rate, f is a mole fraction, and the subscripts refer to permeate (y), the low pressure side, and feed (x), the high pressure side.

Separation is a function of the flow configuration and the pressure drop across the membrane [38]. If the pressure ratio (low pressure/high pressure) is close to one, then back diffusion will decrease the separation factor. As the pressure ratio decreases, the amount of back diffusion decreases and separation factors approach those predicted by theory [38]. As the flux through the membrane becomes a significant fraction of the feed flow rate, the configuration of the reactor determines the separation factor. As shown in Fig. 14.4 for separation flow where a vacuum was maintained on the permeate side, countercurrent flow was the most efficient configuration. The ideal separation factor

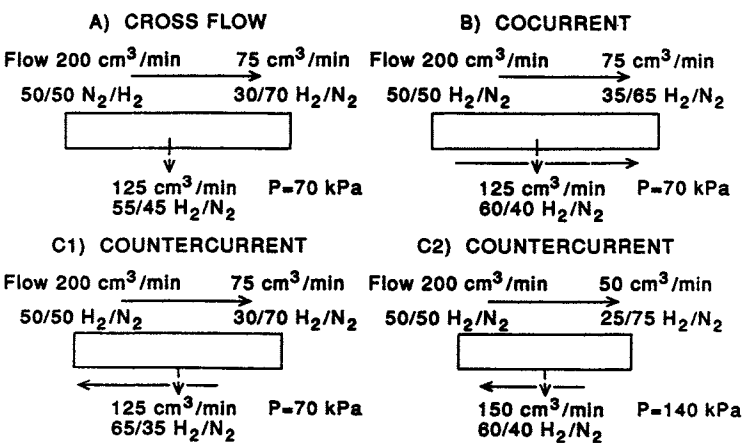

Fig. 14.4. H_2/N_2 separation in a Ag-modified γ-Al_2O_3 composite membrane at different process modes (A) crossflow; feed pressure is 70 kPa, (B) cocurrent; feed pressure is 70 kPa, (C1) countercurrent; feed pressure is 70 kPa, (C2) countercurrent; feed pressure is 140 kPa. (Reproduced from Ref. [38] by permission of Elsevier Science Publishers.)

corresponds to separation based on transport mechanisms only, and neglects effects from flow configurations or concentration changes. For gases it is equal to the ratio of permeabilities.

Table 14.1 presents a brief comparison of permeabilities and separation factors that have been observed for various mechanisms in inorganic membranes. The following sections describe these mechanisms.

TABLE 14.1

Permeabilities of membranes suitable for CMRs

Membrane	Separation mechanism	Representative permeability[a] (barrers)	Typical separation factors	Ref.
Nonporous				
Ag, 100 μm thick	O atom diffusion	1.6 at 675 K; 600 at 1075 K	∞	20
Pd alloys	H atom diffusion	10^4–10^5	∞	19,58,59
10% CaO/90% ZrO_2	ionic diffusion of O^{2-}		∞	60
SiO_2 in porous Vycor	activated diffusion of H	5×10^5 at 723 K	2000	35
Porous				
Vycor glass	Knudsen	10^4–10^5	1–6	20
Ceramic composite	Knudsen	10^5–10^6	1–6	38,46
Ceramic composite	Surface diffusion + Knudsen	$>10^5$	1–9	20,38
Ceramic composite	Capillary condensation	10^4–10^5	80–1000	41–43,54
Zeolite on Vycor	Molecular sieve separation	not reported	>700	29,55

[a]Based on total membrane thickness.

14.3.1 Nonporous Membranes

Palladium alloys are the nonporous membranes used most often in CMRs. Hydrogen adsorbs and dissociates into atoms on the metal surface, and the atoms then diffuse through the metal membrane because H atoms are soluble in Pd. At the other side of the membrane, hydrogen atoms recombine and desorb from the surface (Fig. 14.5a). Though other gases can dissociate on Pd, none have a significant solubility in Pd and thus essentially infinite separation factors can be obtained when separating H_2 from other gases.

When H_2 in the gas phase is in equilibrium with hydrogen in Pd, the solubility of H_2 in the α phase of the Pd/H system is almost directly proportional to $P_{H_2}^{1/2}$:

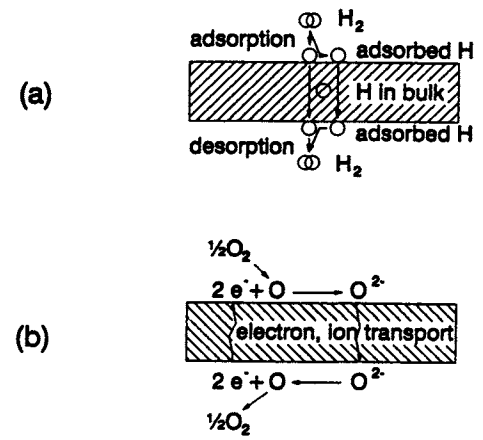

Fig. 14.5. Schematic presentations of transport mechanisms in nonporous membranes: (a) H_2 transport through a Pd alloy by dissociative adsorption, dissolution, diffusion, and associative desorption, and (b) oxygen transport through a zirconia membrane by dissociative adsorption and ion diffusion.

$$C_{H_2} = S(P_{H_2})^{1/2} \tag{14.2}$$

where S is the Sievert constant [4]. The square-root pressure dependency is a result of H_2 dissociation. The flux of H_2 through a metal membrane increases exponentially with temperature,

$$P_{er} = P_o\, e^{-E/RT} \tag{14.3}$$

while the solubility decreases with temperature [22]. In this equation, E is the activation energy and P_o is a constant. The activation energy is 4.6 kcal/mol for Pd [61]. The flux is related to the permeability, P_{er} and the pressure of H_2 as follows:

$$J = \frac{SD_H(P_{H_{2x}}^{1/2} - P_{H_{2y}}^{1/2})}{l} = \frac{P_{er}(P_{H_{2x}}^{1/2} - P_{H_{2y}}^{1/2})}{l} \tag{14.4}$$

where D_H is the diffusivity of H in Pd. The diffusion coefficient for the α phases in the range 415–585 K is given by [62]:

$$D_\alpha\,(cm^2/s) = 2.3\times10^{-3}\, e^{-21{,}700/RT} \tag{14.5}$$

where the activation energy is in J/mol. As for most membrane processes, the flux is inversely proportional to the membrane thickness. Though other metals also permeate H_2, the flux is highest for Pd and Pd alloys [61].

Oxygen permeation through Ag membranes is similar to H_2 permeation through Pd alloy membranes. Apparently oxygen atoms diffuse, and the per-

meability into vacuum is proportional to $P_{O_2}^{1/2}$ [33]. The limiting stage of O_2 transport has been reported to be at the side where O_2 desorbs, and depositing a high surface area Ag film on that side of a Ag membrane increased the O_2 permeability by an order of magnitude [33]. In CMRs where controlled addition of O_2 through a Ag membrane was used, the O_2 permeability was affected significantly by other gases, which adsorb on the Ag [33]. For example, C_3H_6 decreased O_2 permeability by an order of magnitude relative to the value obtained for diffusion into vacuum, apparently because of competitive adsorption, but NH_3 and alcohols reacted with oxygen and increased O_2 permeability significantly. As shown in Table 14.1, the O_2 permeability in Ag is much lower than the H_2 permeability in Pd.

Nonporous silica glass is also highly selective to H_2 permeation, and large separation factors can be obtained (Table 14.1). This selectivity is due to the small openings in the glass network. The permeation is activated and an activation energy of 34.7 kJ/mol has been measured [35]. Permeation is through adsorption and a solution/diffusion mechanism. Reaction of H_2 with oxygen in the silica may be important for this process [35]. Figure 14.6 shows that other

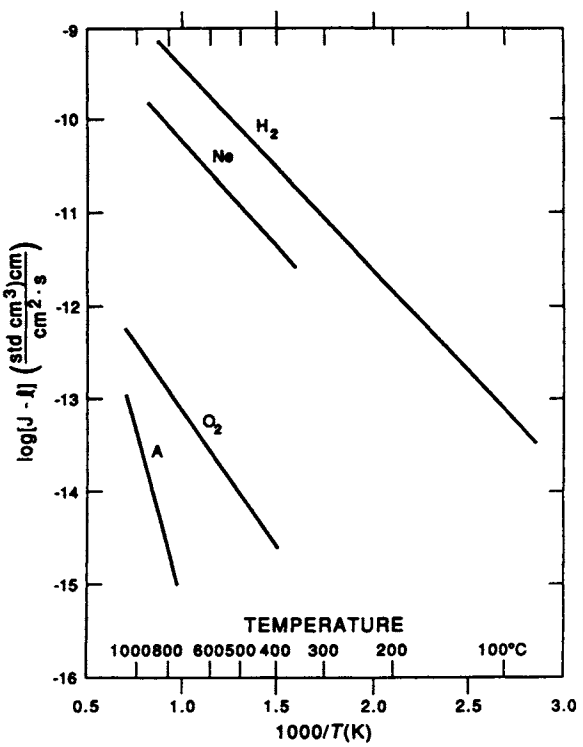

Fig. 14.6. Permeation of gases through vitreous SiO_2 as a function of inverse temperature. (Reproduced from Ref. [20] with permission.)

gases also diffuse through vitreous SiO_2, but at much lower rates than H_2. The fluxes depend exponentially on temperature.

Calcium-stabilized zirconia permeates O_2 by dissociation on the surface and O_2 conduction through the structure. Electron conduction in the opposite direction maintains charge neutrality (Fig. 14.5b). External electrodes are not needed. For a large range of pressure and temperature, ionic conductivity is larger than electronic conductivity. The flux of oxygen is proportional to the difference in $P_{O_2}^{1/4}$ [4]. Similarly, PbO deposited on MgO in a ceramic membrane has been reported to transport oxide ions selectivity [34].

14.3.2 Porous Membranes

Four types of diffusion mechanisms can be utilized to effect separation in porous membranes. In some cases, molecules can move through the membrane by more than one mechanism. These mechanisms are described below. As shown in Table 14.1, Knudsen diffusion gives relatively low separation selectivities compared to surface diffusion and capillary condensation [41]. Shape selective separation can yield high selectivities. The separation factor for these mechanisms depends strongly on pore size distribution, temperature, pressure, and interactions between the gases being separated and the membrane surfaces. Thus, the actual separation will depend on the treatments to the surfaces and the specific gases to be separated [42].

14.3.2.1 Knudsen Diffusion

Under viscous flow (Poiseuille flow), the mean free path of fluid molecules is small compared to the pore diameter, and molecules undergo many more collisions with each other than with the walls of the membrane. The molecules in a mixture do not behave independently in viscous flow and no separation is possible [20]. Thus, viscous flow is not desirable in CMRs. As the pressure is lowered, the mean free path (λ) of the molecules becomes longer than the pore diameter (Fig. 14.7a). As a result, the molecules undergo far more collisions with the pore walls than with each other, and the molecules flow through the pores independently of each other. The mean free path of a gas molecule can be calculated by

$$\lambda = \frac{\bar{k}T}{\sqrt{2}\sigma P} \tag{14.6}$$

where: $\bar{k}$ = Boltzmann's constant; T = absolute temperature; P = absolute pressure; and σ = molar average collision diameter.

Table 14.2 indicates some representative values of the mean free path of several gases at pressures and temperatures that might be encountered in a CMR.

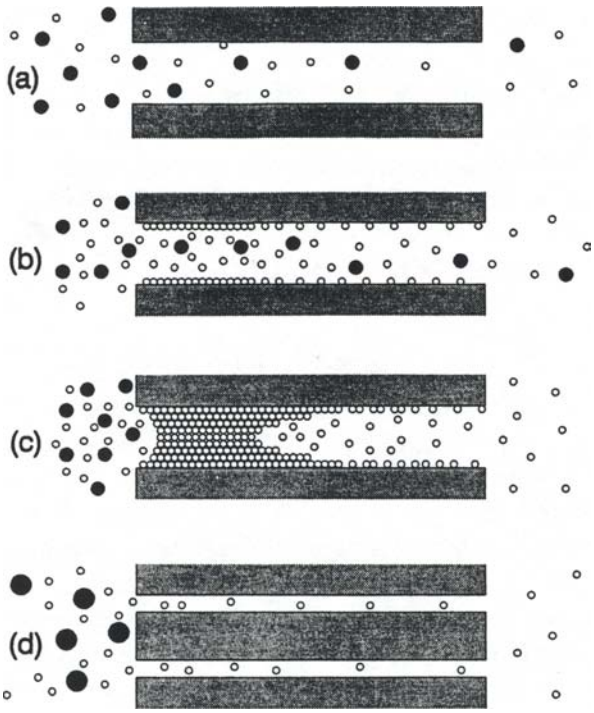

Fig. 14.7. Schematic representations of transport mechanisms in porous membranes: (a) Knudsen diffusion, (b) surface diffusion, (c) capillary condensation, and (d) molecular sieving.

For a circular capillary of radius r and length l, the molar flux of component i in the Knudsen diffusion regime is given by,

$$J_i = \frac{8\pi r^3}{3\sqrt{2\pi M_i RT}} \frac{\Delta P_i}{l} \tag{14.7}$$

where ΔP_i is the pressure drop of component i across the membrane and M_i is the molecular weight of component i. The flux through a microporous membrane of thickness l is given by:

$$J_i = \frac{GS}{\sqrt{2\pi M_i RT}} \frac{\Delta P_i}{l} \tag{14.8}$$

where G is a geometric factor that takes into account tortuosity and porosity. Note that the flux is independent of the average pressure as long as the pressure is in the Knudsen diffusion regime.

An equimolar mixture of feed gas, diffusing across a membrane in the Knudsen diffusion regime, will have a separation factor $\alpha_{ij} = \sqrt{M_i / M_j}$ when the

TABLE 14.2

Mean free paths for various gases

Gas	σ_{ij} (nm)	Mean free path (nm) at					
		Temp. 500 K			Temp. 800 K		
		0.1 MPa	1.0 MPa	5.0 MPa	0.1 MPa	1.0 MPa	5.0 MPa
He	0.2576	234	23	4.7	375	37	7.5
H_2	0.2915	183	18.3	3.7	293	29	5.9
Ar	0.3465	129	12.9	2.6	207	20.7	4.1
CO	0.3706	113	11.3	2.3	181	18.1	3.6
N_2	0.3749	111	11.1	2.2	177	17.7	3.5
CO_2	0.3897	102	10.2	2.0	164	16.4	3.3
Butane	0.4997	62	6.2	1.2	100	10.0	2.0
Cyclohexane	0.6093	42	4.2	0.8	67	6.7	1.3

σ_{ij} values taken from Hirschfelder, J.O., C.F. Curtiss and R.B. Bird (1954). *Molecular Theory of Gases and Liquids*. John Wiley & Sons, Inc., NY.

permeate side is a vacuum. Otherwise, the separation factor will be smaller, as shown in Fig. 14.8 for a H_2/N_2 mixture permeating through a γ-Al_2O_3 membrane. The narrow pore size distributions and the small pores of ceramic and glass membranes allow separation due to Knudsen diffusion (for the appropriate pressure range) by preferential diffusion of the lighter component through the membrane. In composite membranes, the thin permselective layer can be in the Knudsen diffusion regime and thus be responsible for all the separation. The support layers, with their larger diameter pores, are usually in the viscous flow regime [41].

Separation by Knudsen diffusion has some limitations because only the lighter component can be preferentially removed. The best separation in the Knudsen diffusion regime is thus obtained for H_2. When the molecular weight difference between components to be separated is small, an economical separation probably cannot be obtained by Knudsen diffusion. Also, it is impossible for a reaction to proceed to completion without recycling the unreacted feed gas because some of the feed gas passes through the membrane to the permeate side [63].

14.3.2.1 Surface Diffusion

A process that can occur in parallel with Knudsen diffusion is surface diffusion (Fig. 14.7b). A gas can chemisorb or physisorb on the pore walls and migrate along the surface. Surface diffusion increases the permeability of the

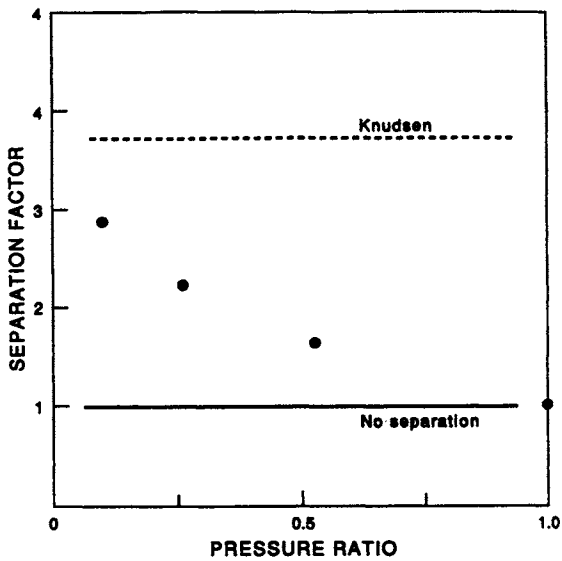

Fig. 14.8. Separation of H_2 and N_2 over a -$A1_2O_3$ membrane. The separation factor is shown as a function of the pressure ratio on the low and high pressure sides of the membrane. (Reproduced from Ref. [38] by permission of Elsevier Science Publishers.)

more strongly adsorbed components in a diffusing mixture while simultaneously reducing the permeability of the gas diffusing components by decreasing the effective pore diameter. Thus, this diffusion mechanism is more important for membranes with small pores. For example, the number of molecules in a monolayer on the wall of a 5-nm diameter pore can be over 200 times larger than the number of molecules in the gas phase of that pore at 0.1 MPa. As the temperature increases, species desorb from the surface, surface diffusion becomes less important, and Knudsen diffusion predominates. When surface diffusion occurs, competitive adsorption must also be considered.

Many examples of surface diffusion transport through porous membranes have been reported in the literature [17,20,38,58,64–69]. Surface diffusion of C_6H_{12} during C_6H_{12} dehydrogenation lowered the efficiency of separation of the H_2 product (relative to Knudsen diffusion) [17,58]. The permeability ratio of N_2/CO_2 in a ceramic membrane under Knudsen diffusion conditions should be 0.8 from molecular weights, but values of 1.05–1.15 have been measured due to the surface diffusion of CO_2 [38]. In a γ-alumina membrane the H_2/N_2 flux ratio was measured as 3.74; this is the value predicted by Knudsen diffusion. However, when the membrane was modified with Ag, surface diffusion of H_2 increased the ratio to as high as 8 because H_2 chemisorbed on the Ag. The ratio decreased with higher pressures because the Knudsen diffusion component became more dominant at higher pressures [38], as shown in Fig. 14.9. Ulhorn et al. [54] also referred to multilayer diffusion to explain the high separation

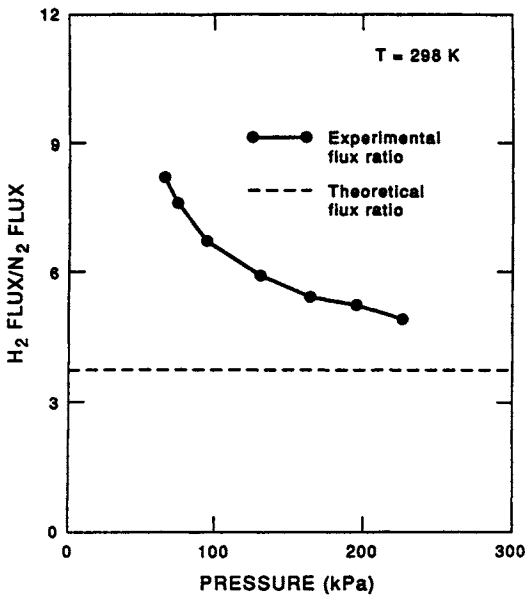

Fig. 14.9. H_2/N_2 flux ratio as a function of pressure on a γ-Al_2O_3 membrane top layer (dashed line) and on a Ag-modified γ-Al_2O_3 top layer (solid line) in an isothermal and isobaric counterdiffusion experiment. (Reproduced from Ref. [38] by permission of Elsevier Science Publishers.)

factors for a C_3H_6/N_2 mixture. For γ-Al_2O_3, they reported separation factors of 5.6 (C_3H_6/N_2).

The surface flow has been reported to obey the following relation [38]:

$$J_s = -\rho(1-\varepsilon) D_s \mu_s \frac{dq}{dl} \tag{14.9}$$

where ρ is the true density of the adsorbed layer, D_s is the surface diffusion coefficient, μ_s is the tortuosity of the surface, and dq/dl is the surface concentration gradient. Surface diffusion must usually be determined experimentally.

14.3.2.3 Capillary Condensation

When one of the components in a mixture is a condensible vapor and the pores are small enough, the condensate can block gas-phase diffusion through pores [41]. This condensate will evaporate on the low partial pressure side of the membrane. The Kelvin equation predicts that condensation can occur in small pores even though the partial pressure of that component is below its vapor pressure. The Kelvin equation represents thermodynamic equilibrium between the gas phase and fluid in the pore:

$$\frac{P}{P_s} = \exp\left(\frac{-2\gamma\cos\theta}{r\rho RT}\right) \tag{14.10}$$

where P = vapor pressure in bulk phase in the presence of capillary pores; P_s = normal vapor pressure in the bulk phase; γ = surface tension of the condensed fluid in the pore; θ = contact angle between the condensed fluid and the pore wall; ρ = molar density of the condensed liquid; and r = mean pore radius.

As a result of capillary condensation, the pores can completely fill with that component (Fig. 14.7c). For a narrow distribution of pore sizes, all pores will be filled and the fluxes of the other components through the membranes will be quite small and limited by their solubility in the condensible component. Thus, extremely high separation factors are possible.

High separation factors were reported for C_3H_6/N_2 mixtures as C_3H_6 condensed in the pores of modified γ-Al_2O_3 membranes [54]. As the relative pressure of C_3H_6 increased, the separation factors increased as high as 80. When the relative pressure of C_3H_6 decreased, hysteresis was observed and the separation factor did not follow the same curve as during the pressure increase. In other studies involving capillary condensation, separation factors as high as 460 were reported for H_2O/air separation, 120 for CH_3OH/H_2O (gas phase) separation [42], and 1000 for SO_2/H_2 separation [43].

14.3.2.4 Molecular Sieve Separation

Molecular sieve membranes can yield high separation factors by permitting small molecules to diffuse while essentially excluding larger molecules (Fig. 14.7d). This type diffusion, where the pores are of molecular size, has been referred to as shape selective or configurational diffusion. Suzuki [56] presented examples of the selective separation that can be obtained with shape-selective zeolite membranes. A zeolite layer with 0.4-nm diameter pores was deposited onto a stainless steel support. For an equimolar feed mixture of CH_4, C_2H_6, and C_3H_8 at 15 atm pressure, the permeate consisted of 73.5% CH_4, 26% C_2H_6, and only 0.5% C_3H_8. Thus the zeolite membrane was extremely selective for diffusion of the smaller molecules. This is much greater separation than can be obtained by Knudsen diffusion. Suzuki [55] claimed that zeolite membranes with pore sizes from 0.3 to 1.2 nm could be prepared so larger molecules could also diffuse. Fluxes were not reported for these zeolites, so comparisons cannot be made to other membranes.

Another example of what may be shape-selective separation was also reported for SiO_2-modified Al_2O_3 membranes [54]. The pores were less than 1 nm, and H_2/C_3H_6 separation factors greater than 100 were obtained at 475 K. Transport of He was measured to show that transport was activated, and an activation energy of 4 ± 2 kJ/mol was obtained.

14.4 EXPERIMENTAL STUDIES OF CMRs

The reaction systems that have been studied with CMRs are summarized in tables based on the type of reaction and the advantage obtained by using CMRs. These tables are not comprehensive. In some cases, a reference to a particular reaction was not included because sufficient detail was not presented in the publication. Thus, these tables should be considered as a representative sample of published studies. A short summary of the results of these studies is presented below for each type of system. A typical experimental CMR system is shown in Fig. 14.10.

14.4.1 Equilibrium-Limited Reactions

The majority of the reactions studied in CMRs have taken advantage of the ability of membranes to selectively remove a product, usually H_2, either by diffusion through Pd alloys or by Knudsen diffusion through microporous glass or ceramic membranes. Thus reversible dehydrogenation reactions have been extensively studied because the removal of H_2 from the reaction zone shifts equilibrium conversion to higher values. Most of the studies in the tables for equilibrium-limited reactions show that the overall conversion is significantly higher in a

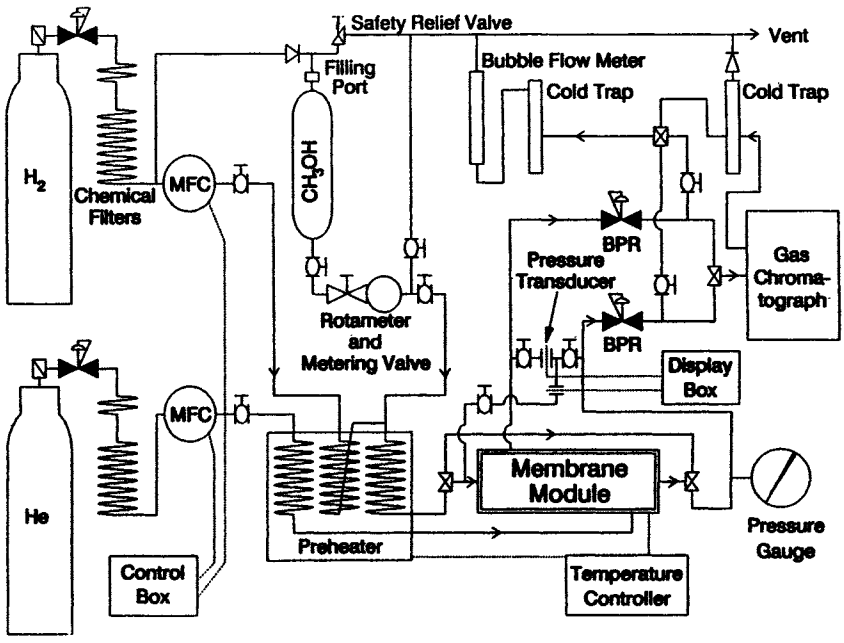

Fig. 14.10. Schematic of laboratory apparatus to study catalytic membrane reactors.

CMR than in a conventional catalytic reactor. In some cases, when a Pd alloy membrane was used, almost complete conversion was reported.

14.4.1.1 Organic Reactions

As shown in Tables 14.3 and 14.4, perhaps the most-studied reaction in CMRs is the catalytic dehydrogenation of cyclohexane to benzene:

$$C_6H_{12} \leftrightarrow C_6H_6 + 3H_2 \tag{14.11}$$

or to cyclohexene:

$$C_6H_{12} \leftrightarrow C_6H_{10} + H_2 \tag{14.12}$$

These are endothermic reactions and are limited by equilibrium under most reaction conditions. The selective removal of H_2 through the membrane results in higher equilibrium conversions. Early studies in CMRs [18,19] involved dehydrogenation to cyclohexene. When Wood [19] pumped H_2 out through a Pd/Ag alloy membrane, C_6H_{10} formed. When H_2 was added through the membrane, C_6H_{12} formed. Benzene was observed only for dehydrogenation at longer residence times. The many subsequent studies of these reactions used pressures below 300 kPa because high pressures decrease equilibrium conversion. For Pd alloy membranes, conversions of almost 100% have been reported [4]. High conversions were only obtained at low cyclohexane feed rates. The Pd alloy serves as both the membrane and the catalyst for this reaction. An added benefit of the Pd alloy membrane is that pure H_2 is produced.

Itoh [4] ran cyclohexane dehydrogenation over a Pd membrane in two modes: (1) an inert sweep gas removed H_2; (2) 0_2 in the sweep gas reacted away the H_2. Both methods kept the H_2 concentration low in the permeate side of the membrane and thus provided a driving force for diffusion. The heat liberated by oxidation could also be transferred across the membrane and used to provide the endothermic heat of dehydrogenation.

In porous membranes, the yield of benzene increases as the feed gas flow rate decreases or the sweep gas flow rate increases [2], but at some point, higher sweep gas flow rates do not change the conversion [4]. That is, with increased sweep flow, the system becomes permeation controlled: the flux cannot be increased any more because of the resistance of the membrane [4]. In the porous membranes, the reactants also diffuse through the membrane and thus the conversion that can be obtained is limited. A thinner membrane allows more permeation, but an optimal thickness exists and if the membranes is too thin, too much C_6H_{12} passes through it [17].

With a Vycor membrane, both a membrane impregnated with catalyst and an inert membrane tube with catalyst inside the tube gave conversions that were better than equilibrium. The impregnated membrane had a 64% conver-

sion, versus 48% for the inert membrane and catalyst. Equilibrium conversion was 31%.

Seok and Hwang [73] studied the metathesis of propene to ethylene and 2-butene as an example of an equilibrium-limited reaction. They used a rhenium oxide catalyst supported on both an alumina and Vycor glass membrane. For the reaction conditions studied, the equilibrium conversion was 34%, and they were able to obtain conversion up to 40%. The limitation on conversion enhancement was the membrane selectivity. Since the reactants and products are similar in size and weight, the separation efficiency due to Knudsen diffusion was small.

For several other equilibrium-limited reactions, both Pd alloy membranes (Table 14.3) and porous membranes (Table 14.4) have been used in CMRs to increase conversion above that obtained in a standard plug flow reactor.

TABLE 14.3

Reactions in nonporous Pd or Pd-alloy CMRs

Membrane; Catalyst	Reactant/Product	Temp. (K)	Ref.	Result
Pd/25% Ag	ethane/ethylene	644–727	14	Ethylene conversion increased from 0% to 0.7%.
Pd/23% Ag	cyclohexane/cyclohexene	400	19	Removal of H_2 through membrane caused cyclohexene and benzene to form.
Pd; 0.5% Pt on Al_2O_3	cyclohexane/benzene	473	4,59	Conversion increased from 18.7% to 99.7%.
Pd/24% Ag; zeolite	alkanes/aromatics (dehydrocyclo-dimerization)	823	71	Selectivity to aromatics increased from 53% to 64%.
Pd/Rh	*n*-heptane/benzene, toluene (dehydrocyclization)	—	9	Yields of aromatics were doubled by the membrane heat treatment.
Pd/Ni	isopentenes/isoprene (dehydrogenation) toluene/benzene (hydrodealkylation)	683	72	Yield of isoprene increased from 14% to 21%. Rates of both reactions are increased. The two reactions are coupled by H transport through the membrane.
Pd	methylnaphthoquinone, acetic anhydride/vitamin K	—	9	CMR allows 4 steps to be combined into 1 step. Yield increased from 80% to 95%.
Pd/Ni	1,4- and 1,5-dimethyl-naphthalenes / α-methyl-naphthalene (hydrodealkylation)	< 873	72	Undesired isomerization to β-methylnaphthalene is suppressed by removing H_2 through membrane.
Pd	CH_4, H_2O/CO, H_2 (steam reforming)	973–1073	60	Methane conversion increased from equilibrium (77%) to 96%.

TABLE 14.4

Organic reactions in porous membrane reactors

Membrane; Catalyst	Reactant/Product	Temp. (K)	Ref.	Result
Vycor glass; 0.38% Pt on Al_2O_3 beads	cyclohexane/ benzene	488	73	CMR conversion (80%) higher than equilibrium conversion (35%) at 488 K and equal to equilibrium conversion at 528 K.
Porous glass; 0.5% Pt on Al_2O_3 pellets	cyclohexane/ benzene	453–493	64	Conversion increased in some cases to 2.5 times equilibrium conversion. Surface diffusion of C_6H_6 enhanced conversion.
0.34 wt % Pt on Vycor glass	cyclohexane/ benzene	553,573	6,74	Compared CMRs and a plug flow reactor. Slow flows through a catalytic membrane are required for improved conversion over either a membrane-enclosed packed bed reactor or a plug flow reactor.
γ-Al_2O_3	$CH_3OH/(CH_3)_2O$, CH_2O, CH_4, CO	473–773	10	Different product distributions were obtained at each side of membrane.
Al_2O_3; 20% Cr_2O_3 on Al_2O_3 pellets	propane/propene	848	21	Conversion increased from 40% to 59%, with 90% selectivity to propene.
Al_2O_3; Pt, Sn promoted $ZnAlO_4$	isopentenes/ isoprene	823	21	Conversion increased from 27% to 37%, with 85% selectivity to isoprene.
Al_2O_3; 4:1 K_2O/V_2O_5 on $Li_{0.5}Fe_{2.4}Cr_{0.1}O_4$ (a spinel)	ethylbenzene/ styrene	898	21	Conversion increased from 51% to 65%, with 94% selectivity to styrene.
Vycor glass; ReO_3 impregnated	C_3H_6/C_2H4, C_4H_8 (methathesis)	295	74	Conversion increased from 34% to 40%. Butene was the most permeable component (surface diffusion dominated total permeation).

14.4.1.2 Inorganic Reactions

One of the inorganic reactions that has generated interest for CMRs is the dehydrogenation of hydrogen sulfide, which has a low equilibrium conversion below 1075 K:

$$xH_2S \leftrightarrow xH_2 + S_x \tag{14.13}$$

Raymont [74] suggested using a CMR to increase H_2 production from H_2S.

Kameyama et al. [36] used a porous glass membrane tube with MoS_2 catalyst on the shell side and obtained H_2S conversions that were about twice equilibrium conversions. The separation factors were small (1.2–2.3) and less than ideal (4.1), apparently due to viscous flow.

Seok and Hwang [73] used a CMR for the water–gas shift reaction. Since the reaction is exothermic, the equilibrium constant increases with decreasing temperature, but the reaction rate decreases with decreasing temperature. Thus, for lower temperatures the residence time in the reactor must increase to provide sufficient reaction time. They were able to obtain up to 85% conversion at 430 K. The conversion decreased with increasing permeation rate because the reactants also permeated through the membrane and had shorter residence times in the catalytic region.

Table 14.5 summarizes the CMR results for inorganic reactions. Only a few

TABLE 14.5

Inorganic dehydrogenations in ceramic CMRs

Membrane; Catalyst	Reactant/Product	Temp.(K)	Ref.	Result
Porous glass; MoS_2 pellets	H_2S/H_2, S_x	873–1092	36,37	Conversions were 1.5 to 4 times higher than the equilibrium yield.
Al_2O_3; MoS_x	H_2S/H_2, S_x	1073	27	Conversion increased from 4.8% to 14%.
ZrO_2 / 5.2% CaO	H_2O/H_2, O_2	1673–2073	15	Low permeability of O^{2-} in membrane limits H_2 production.
$SrCe_{0.95}Yb_{0.05}O_{3-\alpha}$ with porous Pt and Pd coatings	H_2O/H_2, O_2	1023	16	Stable operation at 1023 K. Energy efficiency is low due to the resistance of the ceramic tube.
$SrCe_{0.95}Yb_{0.05}O_{3-\alpha}$ with porous Pt and Pd coatings	C_2H_6/C_2H_4, H_2	1073–1173	16	H^+ conductivity fits Arhenius type temperature dependence.
$SrCe_{0.95}Yb_{0.05}O_{3-\alpha}$ with porous Pt and Pd coatings	H_2O, CO/H_2, CO_2 (water–gas shift)	1073–1173	16	H^+ pumped away from the reaction electrically to drive the reaction.
Vycor glass; $RuCl_3 \cdot 3H_2O$ (impregnated)	H_2O, CO/H_2, CO_2 (water–gas shift)	403–438	74	Conversion (maximum 85%) decreased with increased flow through the glass. The CMR allowed operation at 200 K lower than needed in a plug flow reactor.
Pd on porous glass; Fe_2O_3/ Cr_2O_3 (packed)	H_2O, CO/H_2, CO_2 (water–gas shift)	673	25	Conversion increased above equilibrium and 100% conversion obtained under some conditions.

inorganic reactions have been carried out in CMRs, but the CMRs exhibited significant advantages.

14.4.1.3 Controlled Addition of Reactants

Many CMRs have been run with one reactant fed to the tube side of the membrane and a second reactant fed to the shell side. Table 14.6 summarizes the studies that used controlled addition of a reactant through the membrane. These studies demonstrated significant advantages for this mode of operation. In many cases in Table 14.6 the reaction selectivity was increased. For example, the controlled addition of H_2 through a Pd alloy membrane has several potential advantages for the hydrogenation of olefins [62,75];

- Subsequent separation of unreacted H_2 from the products can be eliminated.
- The reaction rate can be controlled by changing the permeation rate. Increasing the pressure of H_2 increases the permeation rate.
- Reaction using permeate H_2, instead of mixing H_2 with the olefin, is much faster when the olefin adsorbs strongly and decreases hydrogen coverage. The surface concentrations of both reagents may be controlled independently, thus suppressing adsorption competition that can be detrimental in some catalytic reactions [9].
- The negative temperature dependence of dissolved H_2 concentration can prevent temperature overrun.
- Hydrogen-rich gases (from refineries, for example) can be used instead of more expensive pure H_2, since only H_2 permeates through the membrane [9].
- Hydrogenation can be more selective because side reactions can be repressed at lower H_2 pressures [1].
- The desired hydrogen atom concentration can be maintained along the entire length of the reactor [9]. Such a uniform concentration would be more difficult to obtain in a standard tubular reactor, where the H_2 concentration in the gas phase decreases with distance down the reactor. Gryaznov [9] pointed out that this advantage is particularly important for incomplete hydrogenation reactions with products that are thermodynamically unstable in excess H_2.

Nagamoto and Inoue [62,75] demonstrated the differences between mixing H_2 and an olefin before feeding them to a catalytic reactor and permeating H_2 through a 50-μm thick Pd membrane. The surface of the membrane was coated with a Pd black deposit to increase the catalyst surface area. For C_2H_4 hydrogenation [75], they identified two distinct reaction regimes as a function of C_2H_4 pressure, as shown in Fig. 14.11. At lower C_2H_4 pressures, the overall rate of reaction was approximately proportional to the C_2H_4 pressure, because the

TABLE 14.6

CMRs with controlled addition of reactant

Membrane; Catalyst	Reactant/Product	Temp. (K)	Ref.	Result
Pd	propene/propane	373	63	Adsorption of olefin on the reaction surface interfered with H_2 adsorption from the reaction side. Feeding H_2 from the opposite side of membrane.
Pd	1-butene/butane	373	63	Reaction by permeate H_2 was much faster than by gaseous H_2 when the other reactant affected H_2 adsorption strongly.
Pd	1,3-butadiene/butene	373	63	Hydrogenation rate for butadiene was much larger when H_2 permeated than when premixed with butadiene.
Pd	butynediol/butenediol	—	9	In CMR, only partial hydrogenation of triple bond occurs; otherwise triple bond hydrogenated to single bond.
Pd; Pd black deposit	ethylene/ethane	325–375	76	Two regimes — limited by reaction rate or by H_2 permeation.
Pd/Ru and Pd/Rh; Pd alloy + Ga, Zn	pentadiene-1,3 → cyclopentene, cyclopentane	573–723	77	Cyclopentene forms when no H_2 feed. Cyclopentene and cyclopentane form with H_2 fed through membrane. Membrane eliminates simultaneous formation of cyclopentadiene.
Ag	partial oxidation of CH_3OH, C_2H_5OH	519–651	33	Selectivity to aldehydes increased from 56% to 83% when O_2 fed through Ag.
Ag	partial oxidation of NH_3	523–655	33	Selectivity to NO increased when O_2 feed through Ag, and NO was not detected without membrane.
PbO/MgO	CH_4, O_2/C_2H_6	970–1075	34	Both reaction rate and selectivity to C_2 hydrocarbons higher in CMR. Selectivity greater than 90% observed.
$Bi_{1.7}La_{0.3}O_2$	C_3H_6, O_2/C_6H_6, C_6H_8 (oxidative dehydrodimerization)	875	78	Feed through membrane to increase selectivity to C_6 dimers (instead of carbon oxides) from 39% to 77%.
Silicone rubber capillaries; aqueous $PdCl_2$ on shell side	C_2H_4, O_2/CH_3CHO (Wacker process)	298–348	74	Higher conversions were obtained than in a bubble column reactor.
Pd/Y, Pd/Ag	CO, H_2/hydrocarbons	373–673	79	Significantly more higher hydrocarbons when H_2 fed through membrane than when CO + H_2 premixed.
γ-Al_2O_3	CH_3OH, $O_2/(CH_3)_2O$, CH_2O, CH_4, CO	473–773	10	Oxygen supplied from permeate side increased the catalyst lifetime.

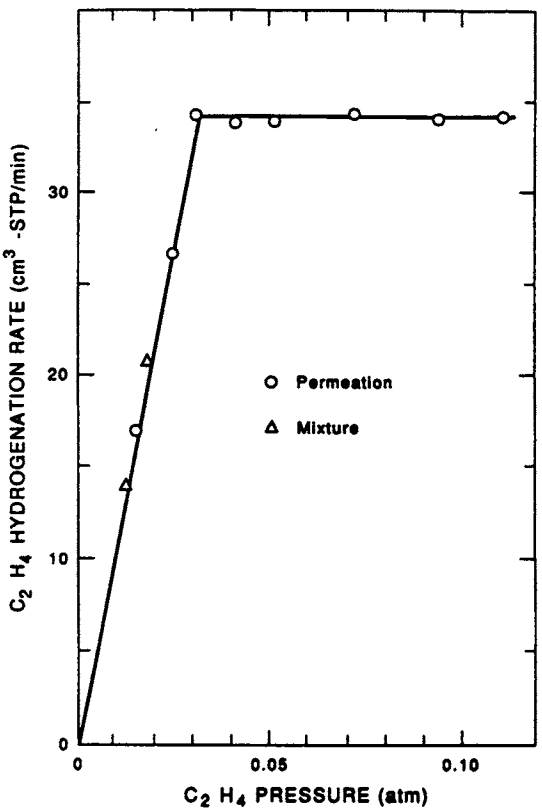

Fig. 14.11. Overall hydrogenation rate of C_2H_4 as a function of C_2H_4 pressure. Reactant H_2 is permeating a 50-μm Pd membrane at a constant flow rate at 373 K. (Reprinted from Ref. [75] by courtesy of Marcel Dekker, Inc.)

C_2H_4 coverage was low and the hydrogen surface coverage was high; thus, the catalytic reaction limited the rate of product formation. At higher C_2H_4 pressures, the overall rate of reaction was equal to the permeation rate of H_2 through the Pd membrane. Thus, the rate of reaction depended on the H_2 pressure on the other side of the membrane and can be controlled by controlling the pressure of H_2.

Nagamoto and Inoue [75] found that permeate H_2 was no more reactive than when gas phase H_2 was used for C_2H_4 hydrogenation. However, for olefins that strongly adsorb and preferentially compete with H_2 for sites on the Pd catalyst, the CMR yielded a higher conversion at 375 K. For 1,3-butadiene hydrogenation, the rate under H_2 permeation limitation was over ten times higher than for the same composition of reactants premixed and fed to the reactor. Hydrogen sorption was strongly affected by reaction or adsorption of 1,3-butadiene, even when 1,3-butadiene only partly covered the surface [62]. Thus, for the premixed

reactants, the rate was limited by H_2 adsorption, but for the permeation system, the rate of transfer of H_2 through the membrane was so fast that the reaction was limited by the permeation rate. That is, the coverage of adsorbed hydrogen was larger for the permeation system than for the reactor with premixed reactants.

Gryaznov [9] reported controlled hydrogenation of butynediol by the addition of H_2 through a Pd membrane. When H_2 was fed through the membrane, the carbon–carbon triple bond in butynediol was not completely hydrogenated to the single bond and thus no butanediol was formed. In contrast, when H_2 was bubbled through the butynediol, butanediol was formed.

Controlled addition of O_2 through a Ag membrane (100 μm thick) has been used to carry out oxidation of NH_3, CH_3OH, C_2H_5OH, and mixtures of these alcohols [33]. For NH_3 oxidation, the selectivity to NO increased when a CMR was used. For reaction of a NH_3/O_2 mixture (without using a CMR), N_2 and N_2O were formed, but NO was not detected. When O_2 was fed through the Ag membrane instead, N_2 (40%) and NO (15%) were the products. Similarly, when O_2 diffused through the Ag membrane, the yield of acetaldehyde from C_2H_5OH oxidation was 83%; for premixed gases, the yield was only 56%. The authors concluded that it was possible that O_2 supplied by diffusion through the membrane created a higher surface concentration of the form of oxygen necessary for reaction than was obtained by adsorption from the gas phase.

One of the interesting aspects of this study was that during oxidation of NH_3, CH_3OH, and C_2H_5OH, the rate of O_2 transfer through the Ag exceeded the O_2 permeability of Ag measured during diffusion into vacuum. Ratios of fluxes during reaction to those for diffusion into vacuum were as high as 8.3. Apparently the reaction removed oxygen from the surface faster than desorption into vacuum. Indeed, during reaction with oxygen diffusing through the membrane, O_2 appeared in the gas phase only above 597 K.

Perhaps one of the more dramatic examples of the advantages of controlled addition of a reactants was the study of selective oxidative coupling of CH_4 by Omata et al. [34]. They used a PbO catalyst supported by MgO, which was deposited on a ceramic membrane. The formation of C_2 hydrocarbons was carried out near 1000 K by feeding air to the tube side of the membrane and CH_4 to the shell side. The catalyst was on the shell side. They reported three advantages of this arrangement:

- Air could be used instead of O_2 as the reactant without introducing large amounts of N_2 into the exit stream. Neither N_2 nor O_2 was detected in the gas phase in the CH_4 stream.
- The rate of C_2 formation per unit surface area was higher.
- The selectivity increased significantly. As can be determined from the rates shown in Fig. 14.12, selectivities greater than 90% were measured in the CMR, while for a supported catalyst selectivities were as low as 50%.

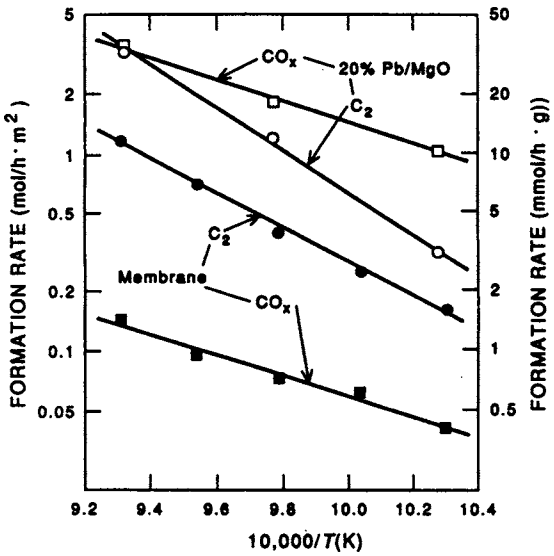

Fig. 14.12. The formation rate of C_2 hydrocarbons and carbon oxides, during the oxidative coupling of CH_4, as a function of inverse temperature. The solid points correspond to values measured in a CMR with air fed on one side of the membrane and CH_4 on the other. The open points correspond to reaction on a supported Pb/MgO catalyst. (Reproduced from Ref. [34] with permission of author.)

These examples of controlled addition of reactants all utilize nonporous membranes. Zaspalis et al. [10] reported for a microporous ceramic membrane that O_2 could be supplied from the permeate side to increase the catalyst lifetime by diminishing carbon deposition, without O_2 emerging on the reactant side. In this case, the O_2 is not a reactant in the overall reaction; instead, it effects catalyst regeneration. Zaspalis et al. [40] also found for oxidative dehydrogenation of CH_3OH by controlled addition of O_2 that the product distribution was significantly different on each side of the membrane, and selective oxidation products (CH_2O, CH_3OCH_3) were at higher concentrations on the CH_3OH feed side. As the thickness of the permselective membrane increased, conversion increased and selectivity to CH_2O decreased because of increased contact time with the catalyst surface.

14.4.2 Simultaneous Reactions

A unique use of nonporous Pd alloy membranes is to carry out a hydrogenation reaction on one side of the membrane and a dehydrogenation reaction on the other side [79]. Basov and Gryaznov [80] coupled the dehydrogenation of cyclohexanol with the hydrogenation of phenol to cyclohexanone using a Pd/Ru membrane. This approach has several advantages:

- The hydrogen formed as a product in one reaction is used as a reactant in the other reaction.
- Removal of H_2 by reaction creates a low concentration of H_2 on the permeate side of the membrane and thus increases the driving force for diffusion.
- The reactants from the two reactions are not mixed.
- The heat of reaction from the exothermic hydrogenation reaction is transferred across the membrane to supply energy for the endothermic dehydrogenation reaction.

Similarly, Gryaznov et al. [28] combined the dehydrogenation of isoamylene on one side of a Pd alloy membrane with the hydrodealkylation of toluene on the other side of the membrane.

14.4.3 Zeolite Membrane Reactors

Suzuki [55] presented a large number of examples of catalytic membranes with ultrathin zeolite membranes. He added reactants to one side of the zeolite and removed products from the other side. A list of the types of reactions he studied is given in Table 14.7. A good example of the potential of CMRs using a zeolite membrane is for a feed of $H_2 + C_3H_6 + i\text{-}C_4H_{10}$ over a Pt-Ca A zeolite

TABLE 14.7
CMRs with zeolites [56]

Membrane; Catalyst	Reactant/Product	Temp.(K)	Comment
Na Y-zeolite	cumene cracking	524–723	Only products (ethylene, propylene) on permeate side.
Re Y-zeolite	hexane cracking		
Rb Y-zeolite	CH_3OH toluene, styrene, ethylbenzene	673	Styrene and ethylbenzene on permeate side.
PdCu Y-zeolite	C_3H_6, steam/acetone	393	Acetone on permeate side.
HY-zeolite	1-hexene/benzene	—	C_6H_6 on permeate side
Pt-Ca A zeolite	H_2, C_3H_6, isobutene/C_3H_8	—	Only H_2 and C_3H_8 on permeate side. Membrane does selective hydrogenation and separation.
Pt-Ca A zeolite	H_2, 2-butenes/butane	—	Only *trans*-butene-2 hydrogenated and separated.
Pd-Ca Y zeolite	*n*-hexane, methylcyclohexane, H_2/C_2H_4, C_3H_6	543	Hexane selectively separated and converted to C_2H_4 and C_3H_6.

membrane. Only H_2 and C_3H_8 appeared on the permeate side because the zeolite did not transport isobutane. That is, this mode of operation allowed selective hydrogenation and separation at the same time. Similarly, only *trans*-butene-2, and not *cis*-butene-2, was hydrogenated and separated through the same zeolite membrane. Unfortunately the patent did not include information on fluxes or stabilities of the zeolite membranes. However, if such membranes can be prepared reproducibly with high permeabilities, they would significantly expand the potential applications of CMRs.

14.5 THEORETICAL ANALYSIS AND OPERATION OF CMRs

14.5.1 Analysis

To model a steady-state CMR requires mass balances for each component, an energy balance, and the appropriate boundary conditions. A separate set of equations is needed for both the reaction and separation sides of the membrane. These equations are coupled by the flow of mass and energy across the membrane. A typical steady-state mass balance is:

(change in molar flux with axial position) = (reaction generation) – (loss due to membrane permeation)

$$\frac{dF_i}{dz} = \bar{r}_i - \frac{A}{V} J_i \tag{14.14}$$

where F_i = molar flux of component i; z = axial distance; $\bar{r}_i$ = reaction rate of component i; A = membrane surface area (m^2); V = volume of appropriate zone (m^3); J_i = flux of component i through membrane ($mol/m^2 \cdot s$); (+ for permeation out of zone, – for permeation into zone).

The energy balance is:

Energy change with axial position due to convection	=	Heat generated by the reaction	–	Heat losses due to sensible heat flow with membrane permeation, membrane conduction, and exchange with the external environment

The exact form of these terms depends on the specific reaction(s) and the equation describing each heat loss term.

All the models to date have assumed plug flow on both the feed and permeate side of the membrane and many have assumed isothermal operation. Several models will be reviewed; comparisons to experimental data indicate these models can effectively predict experimental conditions for the systems studied. Most of the models are for equilibrium-limited reactions because these have been the systems most studied experimentally.

As mentioned, the dehydrogenation of cyclohexane

$$C_6H_{12} \leftrightarrow C_6H_6+3H_2$$

has been extensively studied. Microporous ceramic or glass membranes with pore sizes less than 100 nm were used. Knudsen diffusion, the dominant transport mechanism, favored H_2 permeation and thus the reaction proceeded to higher conversions than obtained at thermodynamic equilibrium. This enhancement of conversion (X) of reactant i due to product removal in the above reaction scheme is given by the following equation (subscript for reactant i dropped for convenience):

$$X = 1 - \frac{F'_r + F'_s}{F_r} \tag{14.15}$$

where F_r = inlet molar flow rate of reactant i on reaction side; F'_r = outlet molar flow rate of reactant i on reaction side; F'_s = outlet molar flow rate of reactant i on separation side.

When F'_s equals zero, this equation corresponds to a conventional plug flow reactor or product removal by a completely selective membrane.

Equation (14.15) illustrates the main features of a catalytic membrane reactor for equilibrium limited reactions. As the *product* permeates through the membrane, the outlet molar flowrate F'_r of reactant on the reaction side decreases due to a shift in equilibrium, and the conversion increases. As the *reactant* permeation increases, the outlet molar flowrate on the separation side, F'_s, increases and the conversion decreases. Thus, the product permeation rate and the separation factor between product and reactant are important factors.

Itoh et al. [17] used a plug flow, isothermal model for C_6H_{12} dehydrogenation to demonstrate the effect of permeation rate on conversion. They varied the permeation rate by varying the membrane thickness. Figure 14.13 shows the conversion versus membrane thickness for various reaction rates, as measured by the preexponential factor for the reaction rate constant. As the reaction rate increases, the maximum conversion takes place at a smaller value of membrane thickness. It is an important result because if the permeate rate is too low (large membrane thickness), the product cannot escape from the reaction (feed) zone fast enough and the conversion is reduced. Conversely, a high permeation rate relative to reaction rate is inefficient because both reactant and product permeate through the membrane. Therefore, a maximum occurs in conversion as the membrane thickness changes for a given reaction rate. Secondly, a higher reaction rate produces a higher conversion for a given membrane thickness.

In an additional study, Itoh [58] modeled cyclohexane dehydrogenation in a Pd membrane reactor. Figure 14.14 shows the effects of the flow rate on each side of the membrane on conversion. As the permeate side (purge) flow rate increases, the concentrations (and partial pressures) of permeating components

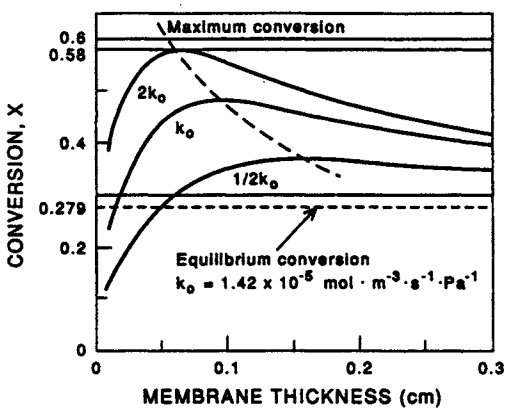

Fig. 14.13. Conversion (X) for cyclohexane dehydrogenation in a Vycor glass CMR versus membrane thickness for several values of the preexponential factor (k_o). (Reproduced from Ref. [17] with permission of AIChE.)

decrease. This increases the driving force for diffusion through the membrane and the conversion increases. Decreasing the feed-side flow rate of reactants increases the residence time in the reactor, and thus the conversion increases. As shown in Fig. 14.14, complete conversion was obtained at low feed flow rates and high purge flow rates. Note also the excellent agreement between the model and the experimental data.

Sụn and Khang [6] modeled the above system for two types of membrane reactors: (1) the catalyst placed within the porous membrane and no reaction in

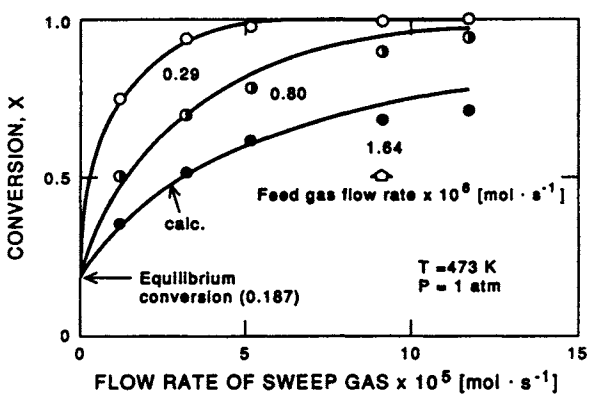

Fig. 14.14. Conversion for cyclohexane dehydrogenation in a Pd membrane reactor versus flow rate of sweep gas. The effect of feed gas flow rate is shown for three feed gas flow rates (0.29, 0.80 and 1.64 mol s^{-1}). The circles are experimental data points and the lines are calculated from the reactor model. (Reproduced from Ref. [58] with permission of AIChE.)

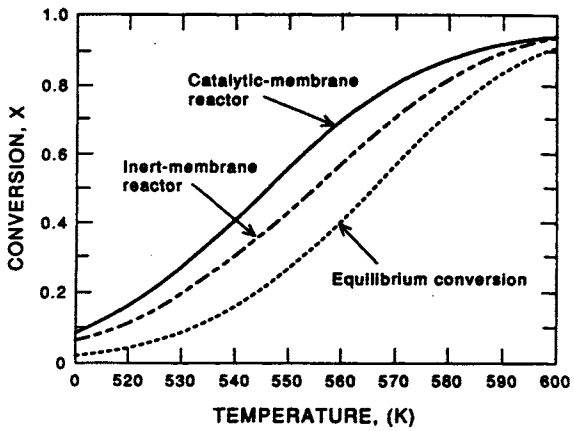

Fig. 14.15. Calculated values of conversion (X) versus temperature for long residence time operation of two CMRs. Cyclohexane dehydrogenation and a porous membrane were used for the model. The equilibrium conversion is also shown. (Reprinted with permission from Ref. [6]. Copyright (1988) American Chemical Society.)

the feed or permeate zone, (2) a packed catalyst bed in the feed zone with an inert, permselective membrane surrounding it. An equimolar feed of C_6H_{12} and H_2 was assumed. For long residence times (Fig. 14.15), the catalyst in the membrane was superior to the inert membrane reactor over the entire temperature range studied. The effects of simultaneous reaction and separation in the catalytic membrane were concluded to cause the difference. For short residence times, the relative advantages of a particular reactor configuration are less obvious [6]. Short residence times tend to limit reaction times and lead to lower conversion, so the improvements over equilibrium conversion were small; and in some cases equilibrium was not reached.

The most extensive analysis and simulation of CMRs was done by Mohan and Govind [81–83]. They modeled three reactions: C_6H_{12} dehydrogenation, HI decomposition, and C_3H_6 disproportionation in a porous membrane reactor [82]. The cyclohexane dehydrogenation is highly endothermic and requires high temperatures for reasonable conversion. The HI decomposition suffers from low equilibrium conversion. Propylene disproportionation is an industrial process requiring elevated temperatures, 500 K. The latter reaction is reversible at room temperatures, but a CMR could provide enhanced conversion below 500 K and thus save energy.

Figure 14.16 shows the ratio of calculated to equilibrium conversion (X/X_e) versus the ratio of the maximum permeation rate of the fastest gas to the maximum reaction rate δ. The porous membrane is permeable to both reactants and products and operated in cocurrent mode. Increasing δ increases the rate of *reactant* permeation in addition to product permeation. Reactant loss event-

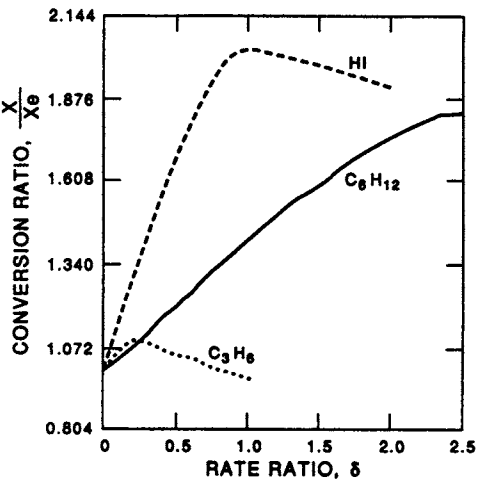

Fig. 14.16. Ratio of calculated conversion, X, to equilibrium conversion, X_e, as a function of the ratio, δ, of the maximum permeation rate of the fastest gas to the maximum reaction rate for C_6H_{12} dehydrogenation, HI dehydrogenation, and C_3H_6 disproportionation. (Reprinted from Ref. [82] by courtesy of Marcel Dekker, Inc.)

ually outweighs the gain from product removal, so that at some value of δ, a maximum in X/X_e occurs, as shown in Fig. 14.16. The reactant loss is especially acute in C_3H_6 disproportionation to C_2H_4 and C_4H_8 since the Knudsen diffusion rates of the various components are similar. Because the optimal value of δ is quite low for C_3H_6 disproportionation, some modification to the reactor design is necessary.

One modification is the flow directions of feed and purge streams: cocurrent or countercurrent. The usual preference is countercurrent operation since the driving force across the membrane is larger. With reactive systems, however, the concentrations of reactants and products on each side of the membrane affect the reaction and the permeation rates. In Fig. 14.17, ΔX_R is the difference in conversion enhancement when cocurrent operation is used instead of countercurrent operation. For C_6H_{12} dehydrogenation, cocurrent operation works better. Most of the reaction occurs near the feed end and the large driving force at that point increases product permeation. Countercurrent operation suffers from back permeation of H_2 at the feed end as δ increases. For C_3H_6 disproportionation, countercurrent operation is best. This is due to the fact that reactant loss due to permeation is the rate determining variable.

Two additional means are available to reduce reactant permeation to the permeate side [82]. The first method is back permeation of the reactant from the permeate side to the reaction side. For this approach, two conditions are necessary. First, the reactor has to be operated cocurrently. In this operating mode, the reactant concentration on the permeate side can exceed the feed side

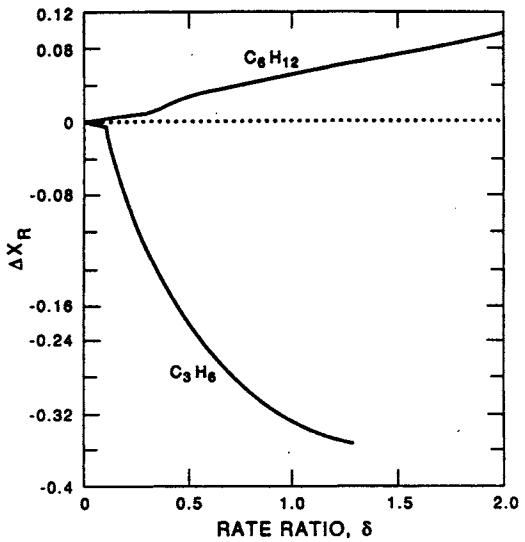

Fig. 14.17. Difference in conversion enhancement (ΔX_R). Conversion in cocurrent operation minus conversion in countercurrent operation, versus the ratio δ of the maximum permeation rate of the fastest gas to the maximum reaction rate for cyclohexane dehydrogenation and propylene disproportionation. (Reprinted from Ref. [82] by courtesy of Marcel Dekker, Inc.)

as one moves down the length of the reactor. Secondly, the total pressure on each side of the membrane should be the same so that the driving force for back permeation is minimized The second approach is recycle of the unreacted feed. Recycle can work if the permeation of reactants is intermediate to the permeation of products. In this manner, the unreacted feed is enriched in the reactants relative to at least one of the products. Product accumulation in the recycle, however, can limit the extent of conversion.

The three reactions studied by Mohan and Govind [82] are endothermic. However, for the HI and C_3H_6 reactions, heat of reaction values are low and the conversion change with temperature is small. Cyclohexane dehydrogenation is highly endothermic and a temperature drop of 40 K decreases the equilibrium constant by a factor of a hundred. Thus, for this reaction, nonisothermal conditions have a significant effect on conversion.

External heat has to be supplied to achieve high conversions for endothermic reactions. A large amount of inert gas diluents should not be used for this purpose since they would decrease permeation rates and mask the effect of an equilibrium shift. In Fig. 14.18 the conversion, X, is plotted as a function of the rate ratio, δ, for different amounts of external heat input for cyclohexane dehydrogenation. A problem with using CMRs for endothermic reactions is that heat is lost due to permeation. As a result, a decrease in heat input decreases the extent of any equilibrium shift. There is an optimum rate ratio δ

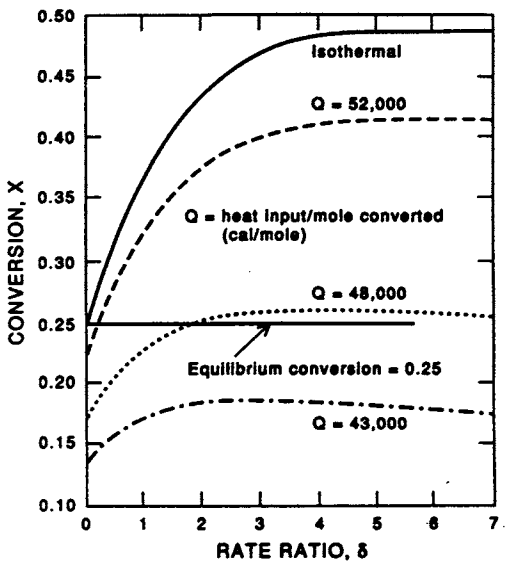

Fig. 14.18. Conversion versus the ratio of the maximum permeation rate of the fastest gas to the maximum reaction rate, as a function of the heat input (Q) for cyclohexane dehydrogenation. (Reprinted from Ref. [82] by courtesy of Marcel Dekker, Inc.)

beyond which the extent of shift is negated by heat loss by permeation. This result indicates that increases in permeation rate through the membrane affect *both* the mass and heat transfer in the system.

Recently, Itoh and Govind [83] presented simulation results for two reactions in a palladium membrane CMR. They modeled 1-butene dehydrogenation to butadiene on the feed side of the membrane and hydrogen oxidation on the permeate side. Their modeling results showed that an adiabatic reactor provided increased conversion over an isothermal reactor for a large range in the heat transfer coefficient. The reason for this improvement in the adiabatic case is the transport of heat generated in the exothermic reaction to the endothermic reaction zone. Complete conversion of butene was possible for short reactor lengths and adiabatic operation.

The modeling efforts to date have been limited mainly to equilibrium-limited reactions. New models will need to incorporate changes in transport mechanisms through the membrane (capillary condensation, for example) and different membrane applications (enhanced conversion of an intermediate, for example).

14.5.2 Additional Factors Affecting CMR Operation

As indicated in the results from the experimental studies and the models, a number of factors affect the operation of CMRs. Among the factors are flow

directions of feed and purge, membrane selectivity and permeability, reactor temperature, feed and purge gas flow rates, reactant concentrations, and the reaction being carried out. Other factors are also important. The pressure drop across the membrane determines the flux through the membrane, but is also limited by the mechanical properties of the membrane. The location of the catalyst within the membrane can influence the residence time of reactants and the reaction selectivity [10]. In a porous membrane, the catalyst can be distributed in the pores, on top of the pores, or the pores can be made of the catalytic material. The presence of other gases can affect permeabilities significantly, and thus values obtained for individual components may not be applicable for CMR operation. For example, O_2 permeability in Ag decreased an order of magnitude in the presence of C_3H_6 [33]. In microporous membranes, surface diffusion will be significantly affected by adsorption of other species.

Physical processes also need to be considered. Membrane operation can degrade due to fouling as small particles in the feed (or produced by catalyst degradation) build up on the membrane and obstruct reactant or product flux. Coke, from secondary reactions, may accumulate on catalytically active membranes and block small pores and decrease permeability. Cracks and pinholes can also develop and decrease selectivity. This possibility can limit how thin a membrane can be because these openings can be paths for viscous transport. Seals between the membrane and the reactor shell can also be a source of reduced selectivity, and seals for high temperature operation in reactive gases may be a problem when the coefficients of expansion are significantly different, as for ceramics and metals.

14.6 SUMMARY

A review of catalytic membrane reactors (CMRs), which combine heterogeneous catalytic reaction with membrane separation, was presented. A number of possible advantages, in addition to shifting equilibrium conversion and reducing cost by combining two processes, are presented. These include preferential removal of an intermediate product, controlled addition of a reactant, controlling which gases contact a catalyst, and combining two reactions in the same system. The major separating mechanisms were discussed, as were their advantages and limitations. Some description of the membranes that can be used in a CMR was included. An extensive discussion of published experimental and modeling studies was presented. Though large scale use has not been made of CMRs, the recent laboratory studies and the improvements in materials properties (such as composite ceramic and zeolite membranes) opens up many application possibilities. A review of laboratory studies and the simulation studies of CMRs indicate some of the possibilities.

A few references were located after this review was completed. They are worthy of inclusion and are noted here. Ito et al. [84] studied the decomposition of HI. Champagnie et al. [85] studied ethane dehydrogenation. Lee and Hwang [86] and Aseda and Du [87,88] studied capillary condensation in microporous membranes. Ilias and Govind [89] provided an overview of high temperature membrane reactors. Recently, the *Journal of Membrane Science* and the *Journal of Applied Catalysis* published a joint issue on membrane catalysis [90,91].

ACKNOWLEDGMENTS

We gratefully acknowledge support by the National Science Foundation, Grant CBT-8900248, the Department of Energy, Grant DE-FG21-9OMC27115, and the Center for Separations using Thin Films at the University of Colorado. We also thank Margy Lanham for typing the many versions of this chapter and Dr. Steve C. Gebhard for his valuable comments.

NOTATION

A	area (m^2)
C	concentration (mol m^{-3})
D	diffusion coefficient (m^2 s^{-1})
E	activation energy (J mol^{-1})
f	mole fraction
F	flow rate (mol s^{-1})
G	geometric factor
J	flux (flow rate/unit area) (mol s^{-1} m^{-2})
k	rate constant ($k_o e^{-E/RT}$) (mol s^{-1} m^{-3} Pa^{-1})
$\bar{k}$	Boltzmann constant (J mol^{-1} K^{-1})
l	thickness (m)
M	molecular weight
P	pressure (Pa)
q	surface concentration (mol m^{-2})
Q	permeability (flux/pressure gradient) (mol s^{-1} m^{-1} Pa^{-1})
r	radius [m]
R	gas constant (J mol^{-1} K^{-1})
$\bar{r}$	reaction rate (mol s^{-1} m^{-1})
S	Sievert constant (mol m^{-3} $Pa^{-1/2}$)
T	temperature (K)
V	volume (m^3)
X	reactant conversion
z	axial distance (m)

Greek letters

α	separation factor
γ	surface tension (Pa · m)
δ	ratio of maximum permeation rate of fastest gas to maximum reaction rate
ε	porosity
θ	contact angle
λ	mean free path (m)
μ	tortuosity
ρ	density (mol m^{-3})
σ	molar average collision diameter (m)

Subscripts

e	equilibrium
ij	represent various gas components
r	reaction side
R	difference from equilibrium
s	separation side

Superscripts

	outlet

REFERENCES

1 Armor, J.N. (1989). *Appl. Catal.*, 49: 1.
2 Hsieh, H.P. (1989). *AIChE Symp. Ser. 268*, 85: 53.
3 Roth, J.F., (1990). *Studies in Surface Science and Catalysis*, Vol. 54 (Eds. M. Misano, Y. Moro-oka and S. Kimura) Elsevier, p. 3.
4 Itoh, N. (1990). *Studies in Surface Science and Catalysis*, Vol. 54 (Eds. M. Misano, Y. Moro-oka and S. Kimura) Elsevier, p. 268.
5 Closset, G.P., J.T. Cobb and Y.T. Shah (1974). *Biotech. Bioeng,*. 16: 345.
6 Sun, Y.-M. and S.-J. Khang(1988). *Ind. Eng. Chem. Res.*, 27: 1136.
7 Bednarski, M.D., H.K. Chenault, E.S. Simon and G.M. Whitesides (1987). *J. Am. Chem Soc.*, 109: 1283.
8 AIChE Statement on U.S. Energy Problems with Recommended Actions, *Chem. Eng. Prog.* 48 (Nov. 1977).
9 Gryaznov, V.M. (1986). *Platinum Metals Rev.*, 30: 68.
10 Zaspalis, V.T., K. Keizer, J.G. van Ommen, W. van Praag, J.R.H. Ross and A.J. Burggraaf (1988). *AIChE Symp. Ser.*, Summer 1988, Denver meeting.
11 Harold, M. P., P. Cini and B. Patenaude, *AIChE Symposium Series No. 268*, (R. Govind and N. Itoh, eds.) New York, Vol. 85, p. 26.
12 Noble, R.D. and J.D. Way (1987), *Liquid Membranes: Theory and Applications*, ACS Symposium Ser. No. 347.

13 Dehmlow, E.V. and S.S. Dehmlov, *Phase Transfer Catalysis. 2nd Ed.*, Verlag-Chemie Publ. Co., Monographs in Modern Chemistry (1983) Vol. II.
14 Pfefferle, W.C. (1966). U.S. Pat. 3290406.
15 Cales, B. and J.F. Baumard (1982). *High Temperature–High Pressures*, 14, 681.
16 Iwahara, H., T. Esaka, H. Uchida, T. Yamaguchi, and K. Ozaki (1986). *Solid State Ionics*, 18 & 19: 1003.
17 Itoh, N., Y. Shindo, K. Haraya, K. Obata, T. Hakuta and H. Yoshitome (1985). *Int. Chem Eng.*, 25: 138.
18 Wood, B.J. and H. Wise (1966). *J. Catal.*, 5: 135.
19 Wood, B.J. (1968). *J. Catal.*, 11: 30.
20 Hwang, S.-T. and K. Kammermeyer (1975). *Techniques of Chemistry: Membranes in Separations*. Wiley Interscience, NY.
21 Bitter, J.G.A. (1988). UK Pat. App. GB 2201159 A.
22 Philpott, J. and D.R. Coupland (1988). *Chemical Industries*, Vol. 31, p. 679. Marcel Dekker.
23 Gryaznov, V.M., V.S. Smirnov, and M.G. Slinko (1977), *Proc. of 6th International Congress Catal.*, The Chemical Society London, Vol. 2: 894.
24 Mikhalenko, N.N., E.V. Khrapova, and V.M. Gryaznov (1986). trans. *Kinet. Katal.*, 27: 138.
25 Kikuchi, K., S. Uemiya, N. Sato, H. Inoue, H. Anio and T. Matsuda (1989). *Chem. Lett.*: p. 489.
26 Uemiya, S., Y. Kude, K. Sugino, N. Sato, T. Matsuda and E. Kikuchi (1988). *Chem. Lett.*: p. 1687.
27 Abe, F. (1987). Eur. Pat App. 0228885 A2.
28 Gryazrov, U.M., L. Gory, V.S. Smirnov and A.P. Mischenko (1973). US Pat. 3,876,555.
29 Grazrov, U.M., V.S. Smirnov, V.M. Udovir, M.M. Ermilova, L.D. Gogua and N.A. Pritula (1977). US Pat. 4,132,668.
30 Govind, R. and N. Itoh (1989). *AIChE Symposium Series No. 268* (R. Govind and N. Itoh, eds.), New York, Vol. 85, p. 10.
31 Nourbakhsh, N., A. Champagnie, T.T. Tsotsis, and I.A. Webster (1989). *AIChE Symposium Series No. 268* (R. Govind and N. Itoh, eds.), New York, Vol 85, p 75.
32 Campbell, C.T. (1988). *Studies in Surface Science and Catalysis*. Vol. 38, (Ed. J.W. Ward), Elsevier, p. 783.
33 Gryaznov, V.M., V.I. Vedernikov, and S.G. Gul'yanova (1986). trans. *Kinet. Katal.* 27: 142.
34 Omata, K., S. Hashimoto, K. Asami and K. Fujimoto (1989). Abstracts, PACIFI-CHEM '89, 1989 International Chemical Congress of Pacific Basin Societies, Honolulu, HI, Dec. 1989, p. 139.
35 Gavalas, G.R., C.E. Megiris and S.W. Nam (1989). *Chem. Eng. Sci.*, 44: 1829.
36 Kameyama, T., M. Dokiya, M. Fujishige, H. Yokokawa and K. Fukuda (1981). *Ind. Eng. Chem. Fund.*, 20: 97
37 Kameyama, T., M. Dokiya, M. Fujishige, H. Yokokawa and K. Fukuda (1983). *Int. J. Hydrogen Energy*, 8: 5.
38 Uhlhorn, R.J.R., K. Keizer and A.J. Burggraaf (1989). *J. Membr. Sci.*, 46: 225.
39 Gieselmann, M.J., M.A. Anderson, M.D. Moosemiller, C.G. Hill (1988). *Sep. Sci Tech.*, 23: 1695.
40 Zaspalis, V.T., K. Keizer, W. van Praag, J.G. van Ommen, J.R.H. Ross and A.J. Burggraaf (1989). *Brit. Ceram. Soc. Proc.*, 43: 103.
41 Terpstra, R A., B.C. Bonecamp, H.M. van Veen, A.J.G. Engel, R. de Rooy and H.J. Veringa (1988). *Sci. Ceram.*, 14: 557.
42 Hsieh, H.P., R.R. Bhave and H.L. Fleming (1988). *J. Membr. Sci.*, 39: 221.

43 Keizer, K., A F.M. Leenaars and A.J. Burggraaf (1982). *Eur. Coll. on Ceramics in Adv. Energy Tech.*, 367.
44 Keizer, K., A.F.M. Leenaars and A.J. Burggraaf (1985). *J. Colloid Interface Sci.*, 105: 367.
45 Keizer, K. and A.J. Burggraaf (1988). *Sci. Ceram.*, 14: 83.
46 Keizer, K., R.J.R. Uhlhorn, R.J. van Vuren and A.J. Burggraaf (1988). *J. Membr. Sci.*, 39: 285.
47 Leenaars, A.F.M., K. Keizer and A.J. Burggraaf (1984). *J. Matl. Sci.*, 19; 1077.
48 Terpstra, R.A., B.C. Bonecamp and H.J. Veringa (1988). *Desalination*, 70: 395.
49 Uhlhorn, R.J.R., K. Keizer and A.J. Burggraaf (1989). *Advances in Reverse Osmosis and Ultrafiltration* (T. Matsuura, ed.) ACS Symp. Ser., p. 239.
50 Uhlhorn, R.J.R., M.H.B.J. Huis in't Veld, K. Keizer and A.J. Burggraaf (1989). *J. Matl. Sci. Lett.*, 8: 1135.
51 van Swaaij, W.P.M., H.J. Sloot and H. Kreulen, (1989). Presented at the 7th Europ. Summer School in Membr. Sci. New Membr. Proc., Univ. of Twente, Enschede, The Netherlands, June 5–9.
52 Fleming, H.L. and K.P. Goodboy (1987). *Handbook of Sci. Tech. Alumina Chemicals*, preprint.
53 Fleming, H.L. (1987). BBC Membr. Planning Conf., Oct. 20–22, Cambridge, MA.
54 Uhlhorn, R.J.R., K. Keizer and A.J. Burggraaf (1990). Presented at the 1990 International Congress on Membranes and Membrane Processes (ICOM '90), Chicago, IL, Session 25, p. 451.
55 Suzuki, H. (1987). U.S. Pat. 4,699,892 (1987)
56 Ishikawa, A., T.H. Chiang and F. Toda (1989). *J. Chem. Soc. Chem. Commun.*: 764.
57 Jia, M.D., K.V. Penemann and R.D. Behling (1990). Presented at the 1990 Intemational Congress on Membranes and Membrane Processes (ICOM '90), Chicago, IL, Session 25, p. 448.
58 Itoh, N. (1987). *AIChE J.*, 33: 1576.
59 Oertel, M., J. Schmitz, W. Weirich, D. Jendryssek-Neumann and R. Schulten (1987). *Chem. Eng. Technol.*, 10: 248.
60 Nigara, Y. and B. Cales (1986) *Bull. Chem. Soc. Jpn.*, 59: 1997.
61 Barrer, R.M. (1941). *Diffusion in and through Solids*, Cambridge University Press, London.
62 Nagamoto, H. and H. Inoue (1985). *Chem. Eng. Comm.*, 34: 315.
63 Itoh, N., Y. Shindo, K. Haraya and T. Hakuta (1988). *J. Chem. Eng. Jpn.*, 21: 399.
64 Hwang, S.-T. and K. Kammermeyer (1966). *Can. J. Chem. Eng.*, 44: 82.
65 Kameyama, T., M. Dokiya, K. Fukuda and Y. Kotera (1979). *Sep. Sci. Tech.*, 14: 953.
66 Weaver, J.A. and A.B. Metzner (1966). *AIChE J.*, 12: 655.
67 Sladek, K.J., E.R. Gilliland and R.F. Baddour (1974). *Ind. Eng. Chem. Fund.*, 13: 100.
68 Gilliland, E.R., R.F. Baddour, and J.I. Russell (1958). *AIChE J.*, 4: 90.
69 Barrer, R.M. and J.A. Barne (1952). *Proc. Roy. Soc. A*, 211: 250.
70 Clayson, D.M. and P. Howard (1987). Br. Pat. Appl. 2 190 397A.
71 Gryaznov, V.M., V.S. Smimov and M.G. Slinko (1973). *Proceedings 5th International Congress Catalysis.* North Holland Publishing Co., Amsterdam, Vol. 2, p. 1139.
72 Shinji, O., M. Misano and Y. Yoneda (1982). *Bull. Chem. Soc. Jpn.*, 55, 2760.
73 Seok, D.R. and Hwang, S.T. (1990). *Studies in Surface Science and Catalysis*, Vol. 54, (Eds. M. Misano, Y. Moro-oka, and S. Kimura) Elsevier, p. 248.
74 Raymont, M.E.D. (1975). *Hydrocarbon Proc.*, 54: 139.
75 Nagamoto, H. and H. Inoue (1981). *J. Chem. Eng. Jpn.*, 14: 377.
76 Gryaznov, V.M., A P. Mischenko and M.E. Sarylova (1987). UK Pat. App. GB 2187758 A.

77 DiCosimo, J.D. Burrington and R.K Grasselli (1986). U.S. Patent 4,571,443.
78 Caga, I.T., J.M. Winterbottom and I.R. Harris (1989). *Catal. Lett.*, 3: 309
79 Gryaznov, V.M. (1969). *Dokl. Akad. Nauk SSSR*, 189: 794
80 Basov, N.L. and V.M. Gryaznov (1985). *Membr. Katal.*, 117.
81 Mohan, K. and R. Govind (1986). *AIChE J.*, 32: 2083.
82 Mohan, K. and R. Govind (1988). *Sep. Sci. Tech.*, 23: 1715.
83 Itoh, N. and R. Govind (1989). *Ind. Eng. Chem. Res.*, 28: 1544.
84 Ito, N., Y. Shindo, T. Hakuta and H. Yoshitome (1984). *Int. J. Hydrogen Energy*, 9: 835
85 Champagne, A.M., T.T. Tsotsis, R.G. Minet and I.A. Webster (1990). *Chem. Eng. Sci.*, 45: 2423.
86 Lee, K-H. and S.-T. Hwang (1986). *J. Colloid Interface Sci.*, 110: 544.
87 Asaeda, M., L.D. Du and M. Fuji (1986). *J. Chem. Eng. Jpn.*, 19: 84.
88 Asaeda, M. and L.D. Du (1986). *J. Chem. Eng. Jpn.*, 19: 72
89 Ilias, S. and R. Govind (1989). *AIChE Symposium Series No. 268*, (R. Govind and N. Itoh, eds), New York, Vol. 85, p. 18.
90 *J. Membr. Sci.*, 77 (2 & 3) (1993).
91 *Appl. Catal.*, 96 (1) (1993).

Subject index